SEISMIC VULNERABILITY OF THE CONTEMPORARY LOADBEARING MASONRY BUILDING TYPOLOGY

A thesis submitted to the University of Malta

for the degree of Doctor of Philosophy

in the Faculty for the Built Environment

by

PETRA SAPIANO

Supervisor: **Dr Marc A. Bonello**, Department of Civil and Structural Engineering, Faculty for the Built Environment, University of Malta, Malta

Co-supervisor: **Prof. Alex Torpiano**, Department of Architecture and Urban Design, Faculty for the Built Environment, University of Malta, Malta

Department of Civil and Structural Engineering,

Faculty for the Built Environment

JULY 2019

To my big and little P’s

L-Università ta' Malta

FACULTY/INSTITUTE/CENTRE/SCHOOL FACULTY FOR THE BUILT ENVIRONMENT

DECLARATION OF AUTHENTICITY FOR DOCTORAL STUDENTS

Student's I.D. /Code 399979(M)

Student's Name & Surname PETRA SAPIANO

Course DOCTOR OF PHILOSOPHY

Title of Dissertation/Thesis
SEISMIC VULNERABILITY OF THE CONTEMPORARY LOADBEARING MASONRY BUILDING TYPOLOGY

(a) Authenticity of Thesis/Dissertation

I hereby declare that I am the legitimate author of this Thesis/Dissertation and that it is my original work.
No portion of this work has been submitted in support of an application for another degree or qualification of this or any other university or institution of higher education.
I hold the University of Malta harmless against any third party claims with regard to copyright violation, breach of confidentiality, defamation and any other third party right infringement.

(b) Research Code of Practice and Ethics Review Procedure

I declare that I have abided by the University's Research Ethics Review Procedures.

☑ As a Ph.D. student, as per Regulation 49 of the Doctor of Philosophy Regulations, I accept that my thesis be made publicly available on the University of Malta Institutional Repository.

☐ As a Doctor of Sacred Theology student, as per Regulation 17 of the Doctor of Sacred Theology Regulations, I accept that my thesis be made publicly available on the University of Malta Institutional Repository.

☐ As a Doctor of Music student, as per Regulation 24 of the Doctor of Music Regulations, I accept that my dissertation be made publicly available on the University of Malta Institutional Repository.

☐ As a Professional Doctorate student, as per Regulation 54 of the Professional Doctorate Regulations, I accept that my dissertation be made publicly available on the University of Malta Institutional Repository.

[redacted]
Signature of Student

PETRA SAPIANO
Name in Full (in Caps)

28/07/2019
Date

*Tick applicable paragraph

ACKNOWLEDGEMENTS

My sincere gratitude goes to my supervisors, Dr. M.A. Bonello B.E.&A.(Hons)(Melit.), M.Sc.(Lond.), Ph.D.(Lond.), D.I.C., Eur.Ing.(FEANI), Perit and Prof. A. Torpiano B.E.&A. (Hons) (Melit.), M.Sc. (Lond.), Ph.D. (Bath), D.I.C., M.I.Struct.E., C.Eng., Eur.Ing., Perit for encouraging me to further my studies, for their support and guidance, and for sharing their wealth of knowledge throughout the years.

My sincere thanks also go to Prof. Pauline Galea B.Sc., Ph.D. (Wellington) (Head of the Department of Geosciences in the Faculty of Science of the University of Malta), for carrying out the ambient noise measurements of a building in Xemxija, for providing the simulated ground motion record which was used as input to the numerical models analysed using ELS® and for extracting the frequency spectrum of this simulated earthquake record for use in this study. I also thank Perit Melissa Giordmaina for allowing access into the building in Xemxija for the recording of these ambient noise vibrations.

My gratitude also goes to Prof. Liberato Camilleri B.Ed. (Hons), M.Sc., Ph.D. (Lanc.) (Head of the Department of Statistics and Operations Research in the Faculty of Science of the University of Malta) for his guidance and assistance in the selection of the statistical analysis tools, in the use of the computer program 'IBM SPSS Statistics' (version 23) and in the interpretation of the results obtained.

I wish to thank also Perit Adrian Mifsud B.E.&A. (Hons) (Melit.), M.Sc. (Lond.), D.I.C. with respect to his guidance on the properties of local clay subsoils.

Furthermore, my thanks go to Prof. Ruben P. Borg B.E.&A. (Hons) (Melit.), Spec.Struct.Eng.(Milan), Ph.D.(Sheff.), Eur.Ing., C.Eng., M.I.C.E., C.Env., M.I.E.D., M.A.S.C.E., M.I.C.T., M.C.S., Perit for his guidance, particularly with respect to the work carried out under the SIMIT Project (Integrated Civil Protection System for the Italo-Maltese Cross-border area, Sistema Integrato di Protezzione Civile Transfrontaliero Italia-Malta, Italia – Malta Operational Programme, Project Code: B1-2.19/11).

The help of the following Research Support Officers on the SIMIT Project with respect to the acquisition of the approved planning permit drawings of the buildings in the Test Sites from the Malta Planning Authority and the completion of the FEMA 154 and GNDT second level assessments is also being acknowledged: Perit Godwin Abela, Perit Charlo' Briguglio, Perit Ann Marie Delicata, Perit Kim Cassar Torreggiani and Perit Yanica Zammit. Furthermore, the financial backing of the SIMIT Project for the purchase of the computer equipment and the ELS® software licence required for the first stage of numerical modelling carried out in this study, in addition to the financial backing of the Faculty for the

Built Environment for the purchase of an additional month of software licence and the extensive data storage devices required to save and backup these analyses is also being gratefully acknowledged.

Furthermore, I wish to thank Applied Science Inc. and Mr. Steven Scoba for granting the use of a 1 year licence of the software package, ELS (Extreme Loading® for Structures, version 3.1), at a reduced cost, and Dr. Huda Helmy from the Consultation Department for her valuable help in answering my queries regarding the use of this software program. My gratitude also goes to S.T.A.DATA srl for allowing me to use the software package 3Muri® at no charge and to Ing. Davide Seni and Ing. Sonia Pastore from the S.T.A.DATA srl technical department for their assistance and support in the use of this software program.

My thanks are also extended to the Malta Planning Authority for allowing access to the approved permit drawings of the buildings in the Test Sites of Msida, Xemxija (Malta), and Nadur (Gozo); the Malta Resources Authority for allowing access to reports on geological investigations carried out in Xemxija and Nadur during the British period; the Institute for Climate Change and Sustainable Development - GIS Laboratory of University of Malta for the elaboration of thematic maps based on the results of the seismic vulnerability assessments carried out as part of this study; and the Department of Physics of the University of Malta for allowing the use of one of their workstations for the processing of the numerical analyses carried out using ELS®.

Special thanks also go to Dr Reuben Grima B.A. (Melit.), M.A. (R'dg), Ph.D. (Lond.), F.S.A., Ms. Jennifer Porter B.A. (Ann Arbor), M.A. (Courtauld), Dr. Rebecca Dalli Gonzi B.E.&A. (Hons) (Melit.), A.& C.E., M.Sc. (Edin.), Ph.D. (Glas.) and Perit Alexia Mercieca B.E.&A. (Hons) (Melit.), M.Sc. AAD (Edin.) for making me feel welcome when working in their offices and for unconsciously tutoring also me while guiding their respective students.

My thanks also go to Prof. Peter Fajfar from the University of Ljubljana, Slovenia, for answering the repeated questions of a Ph.D. candidate from Malta, whom he never met.

Finally, my most sincere gratitude goes to my closest friends - Svet, Sean, Rosanne, Lorna, Fleur and Christa for their prayers and encouragement, and my family - my sisters, parents and in-laws for taking care of my boy even when they were completely exhausted, and for their support, help, prayers, and encouragement to hold on, without which I would not have reached this day. A special thanks also goes to my sister Elisa, for helping me out with the conversion of the data extracted from 3Muri® to the UK number format. My last words of thanks go to my husband, Pierre, for encouraging me to extend my studies and for putting up with me even through all this, and to our Paolo, for somehow making it a point to be part of this journey, from the very start.

I take full responsibility for any shortcomings in this thesis.

ABSTRACT

No major earthquake has been recorded in the Maltese Islands since the emergence of the contemporary loadbearing unreinforced masonry building typology around 50-60 years ago, so the behaviour of this typology under seismic excitations is unknown. Notwithstanding the low-to-moderate seismicity of the region, seismic considerations are ignored in the structural design of most residential buildings pertaining to this construction category. This, in conjunction with the prevalence of specific building characteristics (such as, a soft basement storey) and construction details which could potentially impair the seismic resistance of this building typology, highlights the necessity of a deeper understanding of the building response to seismic actions. This thesis investigates the seismic vulnerability of this masonry building typology through the identification of building characteristics which affect its seismic response. Hence, a preliminary assessment form for the estimation of the seismic vulnerability of this building typology is developed in this study and is applied in the evaluation of 183 buildings in two Test Sites, including the comparison of the resulting ratings to those obtained from three existing assessment methods. The statistical analysis of the data collected in the Test Sites results in the identification of eleven characteristics as significant predictors of the final rating. Furthermore, the examination of the variation in dynamic properties and seismic response parameters, resulting from non-linear time-history analyses of numerical models, investigating the influence of six characteristics on the seismic response through the Applied Element Method, indicates, in particular, the impairment of the seismic resistance of this building typology in the presence of a soft storey, higher building heights and clay-predominant subsoils. The adequacy of a non-linear static analysis which, by default, assumes a box-like behaviour of the analysed structures, for the seismic assessment of the masonry building typology under study is also investigated. While further detailed studies are required, the conclusions from this study provide a clear indication of the seismic vulnerability of the URM building typology under investigation and the applicable numerical analysis methods.

Keywords: seismic vulnerability, loadbearing masonry, statistical analysis, significant predictors, applied element method, non-linear time-history analysis; non-linear static analysis.

TABLE OF CONTENTS

LIST OF TABLES

LIST OF FIGURES

GLOSSARY OF TERMS / ABBREVIATIONS

α_{cc} coefficient taking account of long term effects on the compressive strength and of unfavourable effects resulting from the way the load is applied

β_{NC} dispersion measure with respect to ground motion record and numerical modelling

γ_c partial safety factor for concrete

γ_m partial safety factor for materials

γ_{im} risk-targeted safety factor for the limit state seismic intensity

γ_s partial safety factor for steel reinforcement

σ_{fv} standard deviation of probability density function describing variation in shear strength of masonry units (N/mm^2)

σ_{fv} standard deviation of probability density function describing the variation in yield strength of steel reinforcement (N/mm^2)

$\phi \infty$ final creep coefficient

$\psi_{E,I}$ combination coefficient for the variable actions

ψ_{2i} combination coefficient for the quasi permanent value of variable actions

Ω; ω angular frequency (rad/s)

B width of the foundation (mm)

CF confidence factor

c.o.v. coefficient of variation

c_k score of k^{th} deficiency (Form for the assessment of deficiencies in masonry buildings)

c_{vi} scores corresponding to classes A to D (GNDT second level assessment form)

DPC damp proof course

DPM damp proof membrane; damage probability matrices

d_{et}* target displacement of the equivalent single-degree-of-freedom system with period T* and unlimited elastic behaviour (m)

d_t* target displacement of the equivalent single-degree-of-freedom system with period T* and exhibiting a non-linear response (m)

E Young's Modulus (N/mm^2)

EDP engineering demand parameter

E_s Young's Modulus of the subsoil material (N/mm^2)

F frequency (Hz)

F_{el} capacity of the structure when the first wall reaches its maximum flexural of shear strength in (N)

F_{elmax} maximum capacity of the structure assuming an unlimited elastic behaviour (N)

FEMA Federal Emergency Management Agency

F_{ri} enhanced factors (damage probability matrix for the Maltese Islands)

F_y* yield force of the single-degree-of-freedom system (N)

f_b normalised mean compressive strength of masonry units in the direction of the applied action effect (N/mm^2)

f_{ck} characteristic compressive cylinder strength of concrete at 28 days (N/mm^2)

f_{cm} mean value of concrete cylinder compressive strength (N/mm^2)

f_k characteristic compressive strength (N/mm^2)

f_m mean compressive strength (N/mm^2)

f_n frequency (Hz)

f_{vlim} shear strength limit (N/mm^2)

f_{vmo} mean shear strength (N/mm^2)

f_{vk} characteristic shear strength of masonry (N/mm^2)

f_{yk} characteristic yield strength of reinforcement (N/mm^2)

f_{ym} mean yield strength of reinforcement (N/mm^2)

G Shear Modulus (N/mm^2)

G_{kj} characteristic permanent load

GNDT Gruppo Nazionale per la Difesa dai Terremoti

HCB hollow concrete blockwork

I second moment of area (mm^4); macroseismic intensity

i_c deficiency index (Form for the assessment of deficiencies in masonry buildings)

IDA incremental dynamic analysis

IM_{PL} maximum intensity measure corresponding to a performance level

k parameter related to hazard curve; sway stiffness (N/m)

m mass (kg)

m* mass of equivalent single-degree-of-freedom system (kg)

N poisson's ratio

NC limit state of Near Collapse

OSR overstrength factor

P density (kg/m^3)

p_i parameter weightings (GNDT second level assessment form)

p_{1k} weighting of the k^{th} deficiency (Form for the assessment of deficiencies in masonry buildings)

p_{2j} weighting of the j^{th} category (1 of 5) under which the present deficiency falls (Form for the assessment of deficiencies in masonry buildings)

p.g.a. peak ground acceleration

P_{NC} probability of exceeding the Near Collapse limit state (equivalent to the probability of failure)

Q_{ki} characteristic variable load

q behaviour factor for estimation of design seismic action

q_o 'basic' behaviour factor

q_u reduction factor with respect to the limit state of Near Collapse

S soil factor

S_{aD} design spectral acceleration

S_{aNC} spectral acceleration at failure

SD limit state of Significant Damage

SDAP seismic adapted pushover method

$S_e(T^*)$ elastic acceleration response spectrum for a single-degree-of-freedom system with period T* (m/s^2)

$S_d(T^*)$ design acceleration response spectrum for a single-degree-of-freedom system with period T* (m/s^2)

SMRU Seismic Monitoring and Research Unit (University of Malta)

T_B lower limit of the period of the constant acceleration part of the elastic response spectrum (s)

Tc upper limit of the period of the constant acceleration part of the elastic response spectrum (s)

T_D the value of the period defining the start of the constant displacement part of the elastic response spectrum (s)

T_{De} return period of the design ground motion (years)

T_{NC} return period corresponding to the Near Collapse limit state (years)

T* fundamental period of equivalent single-degree-of-freedom system (s)

UCL upper coralline limestone

UOM University of Malta

URM unreinforced masonry

μ_D mean damage grade

V vulnerability index

v_s Poisson's ratio of the subsoil material

Vs shear wave velocity (m/s)

W self-weight (kg/m^3)

Chapter 1 INTRODUCTION

1.1 Background

On the 17th August 2016 an earthquake, measuring a magnitude of 3.6 on the Richter scale with its epicentre to the North East of Malta [1], between Malta and Sicily, was felt in a number of areas around the Maltese Islands. However, given the low magnitude, it did not result in any reported structural damages. Barely a week later, on the 24th August 2016, a magnitude 6.0 earthquake hit Central Italy. The latter was only one of a series of earthquakes to hit the area, which totalled over 3000 localised seismic events by the 31st August 2016 [2] and resulted in around 300 victims. Further significant seismic events hit the same region in October of the same year and in January 2017.

Numerous low magnitude earthquakes are identified on the Maltese Islands by the Seismic Monitoring and Research Unit (SMRU) of the University of Malta every year, with most events going completely un-noticed by the local population. Since the last major earthquake reported to have caused significant damages in the Maltese Islands was the 7.4 magnitude earthquake of the 11th January 1693, with an epicentre in South East Sicily, the lack of damaging events in the current population's recollections or those of the previous generation has led to a general perception in the general public and in the construction sector that the Islands have a minimal earthquake risk [3]. Furthermore, the lack of knowledge on the use of precast prestressed concrete slab constructions, required for the distinction between static and dynamic actions leads to the public's general feeling of reassurance that these structural elements were correctly sized to cater for the applied (static) actions. This factor, while undisputed, does not preclude the adoption of construction practices, and construction connection details, to prevent the impairment of the seismic resistance of local constructions. Concern on the earthquake which hit the Maltese Islands in August 2016 was understandably minor. However, a temporary increase in the level of unease on the seismic resistance of the local constructions was perceivable following the events on the Italian peninsula. *Would our buildings resist an earthquake of similar intensity?*

Since 2010, the use of the Eurocodes became mandatory in the Maltese islands, for public procurement projects. However, there are currently no Building Regulations which require that specific building typologies are designed to resist seismic action. The requirement to design to any seismic standard remains solely a client decision. Even in the design of structures of national importance, such as the Marsaxlokk Power Station, and Mater Dei Hospital, the aseismic requirement was a client decision and not a regulation. Hence, while the recommendations of Clause 3.2.1(4) in

Eurocode 8: Part 1 [4], with respect to the application of simplified seismic design procedures for the structural design of new structures in areas of low-to-moderate seismicity, would be applicable to the scenario of the Maltese Islands, (which are located in a seismic zone with a design peak ground acceleration of 0.10g), it is very likely that, in the case of residential buildings constructed both before and after 2010, no particular seismic design considerations would have been taken into account.

a) Double height spaces at lower levels;
b) Adjacent buildings with different heights;
c) Unrestrained party walls – vacant sites;
d) Misalignment of slab levels;
e) Misalignment between planes of facade;
f) Setbacks – sloping sites;
g) Projecting rooms;
h) Large areas of openings on facades.

Figure 1-1 Examples of building characteristics commonly found in the contemporary loadbearing URM building typology and which could impair the seismic resistance of this construction typology ([5]p. 137, 138; [6] p.289).

The contemporary loadbearing unreinforced masonry (hereinafter referred to as 'URM') building typology, which developed in the Maltese Islands around 50-60 years ago, and which is the most widespread construction typology in the newer urban areas, consists mainly of apartment blocks in row developments, of around four to five residential floors, over an open plan garage at semi-basement level. This level is generally roofed over by precast prestressed concrete slabs with a cast in-situ topping. The horizontal structural system at the other levels typically consists of cast in-situ concrete slabs, while walls are constructed in either local stone masonry blocks or hollow concrete blockwork walls (with a ratio of net to gross area of around 0.60 to 0.72). Front facades typically consist of double leaf stone walls with a cavity in between, with the two leaves connected through stone

bondstones distributed throughout the wall area, while all other walls usually consist of a single leaf of masonry having a thickness ranging between 153 mm to 228 mm. Party walls between blocks are commonly constructed in a single 228 mm stone wall thickness and could be either a) shared throughout the height of the buildings, b) shared only throughout the residential levels, or c) completely independent with either a minimal gap or no gap between the two walls [5] [6]. However, 228 mm thick hollow concrete blockwork party walls have also started being used in recent years.

International published studies and manuals on existing seismic vulnerability assessment methods in use in other countries, reviewed in Chapter 2 of this thesis, suggest that the contemporary loadbearing masonry construction typology present in the Maltese Islands includes a number of building characteristics which could influence its seismic resistance (some of these are indicated in Figure 1-1). These include, but are not limited to,

- the presence of soft storeys at the lowermost level/s;
- the presence of large open plan living areas with no internal cross-walls in the residential levels;
- the narrow and long plan layouts, which lead to a plan configuration with a long corridor directly adjacent to one of the party walls and rooms on the other side;
- the slender elevation proportions;
- the large opening areas on the facades;
- the sharing or unsharing of party walls (where, in the latter case, the minimum gap between the buildings to avoid the risk of damage due to pounding is not provided);
- the presence of rooms projecting from facades (which, in the case of newer developments, are starting to have significant proportions which go beyond those of a 'closed balcony');
- the presence of setbacks; and
- the presence of double height spaces, which are typically located either in the first two levels above ground for commercial uses, or at higher storey levels in duplex residential units.

The presence of misaligned floors in adjacent buildings is also very common, not only on sloping sites, but also in level locations because of the gradual development of urban areas, and the changes in planning regulations over the years. In addition, the revision of the allowable building heights by planning regulatory authorities leads to the increase in number of floors over originally lower constructions, even in cases where party walls are shared, with little or no concern as to whether the bearing capacity of the walls or the foundations is exceeded, and with respect to the change in resistance of these walls to actions. Moreover, significant differences in heights of abutting constructions give rise to a reduced restraint of the party walls and the structure in the upper storeys of the higher blocks when the adjacent structures are still lower in height [5] [6].

Furthermore, low mortar quality, the typical absence of mortar in the vertical wall joints, the relatively thin single wall sections and the use of construction details, which do not provide an adequate connection between horizontal diaphragms and the vertical loadbearing system, also tend to impair the seismic response of this building typology. Examples of such details include the simple seating of cast in-situ slabs and precast prestressed concrete slabs over the underlying walls, with no provision

of a positive (reinforced) connection to these walls, to ensure a 'box-like' behaviour of the different storeys. In addition, the limited bearing provided in the case of slabs which are added in as a result of subsequent alterations, and the general practice of not providing ring beams at the perimeter of every storey or peripheral ties and horizontal ties above internal walls within slab construction systems, result in a further reduction of the structural resistance to seismic actions. Moreover, in the case of double leaf wall construction, the bearing of slabs only on the inner leaf leads to an uneven distribution of seismic actions over the wall area and the possible 'hammering action' with respect to the outer leaf at the bondstone positions [7].

The lack of occurrence of damaging events has not permitted the knowledge of the behaviour of the existing building stock during seismic excitations from experience. Considering the widespread presence of the contemporary loadbearing building typology under study in the Maltese Islands, and the particular seismic vulnerability associated with the characteristics and construction details of this class of buildings, a detailed study of the influence of particular characteristics on the seismic resistance of this building typology and on the applicable analysis methods in order to achieve a reliable seismic assessment, was deemed as an important contribution of this study in the local construction scenario.

1.2 Context of Study: Geology, Seismicity of the Maltese Islands and Previous Local Studies

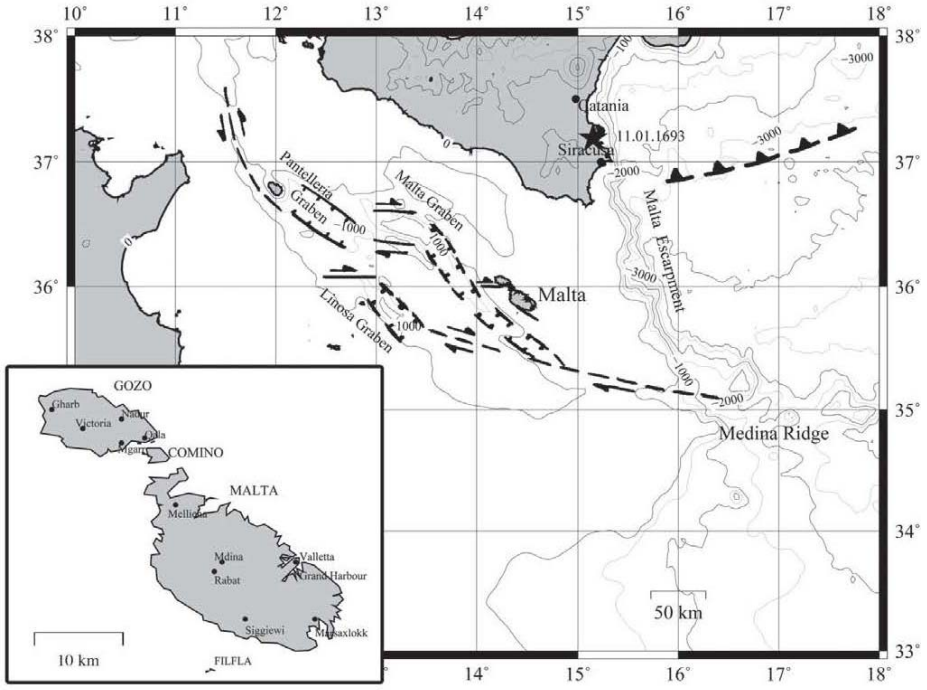

Figure 1-2 Bathimetry of the Sicily Channel and main tectonic features of the Sicily Channel Rift Zone ([3] p.726).

The geological sequence of the Maltese Islands, consisting mainly of sedimentary rocks of marine origin includes the following five main layers (from the bottom upwards): a) the lower coralline limestone, which is the oldest rock formation layer, b) globigerina limestone, c) blue clay, d) greensand, and e) upper coralline limestone [8] [9] . Only lower coralline limestone and globigerina limestone are present

in most of the eastern part of Malta, whereas upper coralline limestone outcrops over blue clay slopes characterise the western part of Malta and most of Gozo, hence indicating that the full geological sequence is present at these locations [10]. The presence of the softer blue clay layer, whether as an outcrop or as a second underlying layer beneath the stiffer upper coralline limestone formation, can give rise to amplifications of seismic vibrations which can cause increased damages to buildings in a seismic event.

As explained by Galea [3], the Maltese Islands are positioned on the Pelagian Platform in the Sicily Channel, around 200 km away from the 'Europe – Africa plate boundary'. Figure 1-2 shows that the 'Pantelleria rift' includes three grabens (Pantelleria Graben, Malta Graben and Linosa Graben), which include a system of faults which span from 'southern Sicily to Tunisia', and to which the Maltese Islands owe their formation [3]. Furthermore, while Malta and Gozo are affected even by earthquakes with epicentres in the south of Greece, Galea identifies the main seismic source around the Maltese Islands as the faults on 'the northern end of the Malta escarpment' in the seabed outside Siracusa, which is likely to correspond with the epicentre of the 1693 earthquake. A second major source is the system of faults in the Pantelleria Rift grabens which extend to the south of Malta, and could be located even just 20 km away from the island [11].

A seismic risk assessment for the Maltese Islands was carried out prior to the design of the Delimara power station in 1990. Though the author of this thesis did not have access to a copy of the original report, a detailed overview is given by Blackman [12]. As explained by Torpiano [13] and Blackman [12], the report suggested the design of the power station to be based on a design life of 40 years and a 6.5 magnitude earthquake with a probability of exceedance of 10%. This corresponds to a peak ground acceleration of 0.12g, hence placing Malta in seismic zone 2A according to the 1988 Uniform Building Code (UBC). Blackman [12], on the other hand, carried out a study of the different factors which affect the level of seismic risk of the Maltese Islands, giving particular attention to the influence of particular geological formations and the seismic resistance of buildings.

While, as discussed in further detail in Section 2.5 of this thesis, a damage probability matrix for buildings in the Maltese Islands was proposed by Camilleri [7], the studies carried out by Galea [14] and Mangion [15] investigated the seismic resistance of historical constructions through numerical modelling. The seismic resistance of the contemporary loadbearing URM building typology present in the Maltese Islands with respect to isolated structures was studied by Farrugia [16], Galdes [17], Marmara' [18], Tong [19] and Borg [20], while, the influence of the location of such unreinforced masonry structures within an aggregate on their resulting seismic resistance was studied by Bonello [21], Zammit [22] and Azzopardi [23]. Farrugia [16] carried out a FEMA 310 (where, hereinafter 'FEMA' refers to the 'Federal Emergency Management Agency') assessment of two alternative plan layouts of this construction typology (with overall heights of three and five storeys, respectively) under a seismic action with a design peak ground acceleration of 0.12g. Galdes [17] applied the elastic response spectrum method of Eurocode 8: Part 1 [4] on three different plan layouts and on the five-storey layout investigated by Farrugia [16], for a seismic event with a design peak ground acceleration of 0.10g, studying also the effect of different geologies (rock or clay) on the seismic resistance of the latter plan

configuration. Marmara' [18] and Tong [19], on the other hand, studied the variation in seismic resistance of the three main layouts considered by Galdes [17], with and without a soft storey at semi-basement level, for two different mortar strengths (2 N/mm^2 and 5 N/mm^2), and considering a rock or a clay subsoil, under a seismic excitation with a maximum peak ground acceleration of 0.10g. Borg [20] furthered the studies carried out by Galdes [17], Marmara' [18], and Tong [19] by investigating the seismic resistance of the contemporary loadbearing unreinforced masonry building typology with a steel frame at semi-basement level of equivalent stiffness as the overlying levels for: a) six different plan proportions (for plan length-to-width ratios of 1:1 to 6:1); b) three mortar strengths (2 N/mm^2, 3.5 N/mm^2 and 5 N/mm^2); c) two different masonry construction materials (softstone masonry or hollow concrete blockwork); d) rock (Eurocode 8: Part 1 Table 3.1 [4]: Type A ground) or clay (Eurocode 8: Part 1 Table 3.1 [4]: Types B and C ground); and e) overall building heights of three to six storeys. Bonello [21], Zammit [22] and Azzopardi [23] subsequently extended the investigations carried out on three of the plan proportions (for plan length-to-width ratios of 2:1, 4:1 and 6:1) considered by Borg [20] to study the variation in seismic resistance (in terms of the interaction ratio of the main loadbearing walls and the maximum allowable safe building height) when the buildings are incorportated in two-, three- and four-building aggregates for the subsoil cases and the mortar strengths considered by Borg [20]. Bonello [21] also investigated the effect of mirroring the plan layout of the structures in the aggregate system on the resulting seismic resistance. Zammit [22], on the other hand, investigated the influence of the presence of setbacks at the topmost storey and a double height space between ground and first floor first individually, then in combination, on the seismic resistance of the URM building typology under study. In addition, Zammit [22] studied the difference in the seismic resistance of the two-building aggregate case including setbacks at the topmost level and a double height space between ground and first floor, resulting when the common party wall is shared throughout all levels and when separate party walls are present at basement level while a shared party wall is present in the rest of the storeys above ground. Moreover, Azzopardi [23] investigated the influence on the seismic resistance of the unreinforced masonry structures in two-, three- and four-building aggregates when the abutting structures were displaced in the longitudinal direction by 0.2 times the width of the single units forming the respective aggregates, such that the transverse walls of the adjacent structures resulted as misaligned on plan by this same distance. Furthermore, Said [24] used a similar procedure based on the Equivalent Frame Method as adopted by Marmara' [18], Tong [19], Borg [20], Bonello [21], Zammit [22] and Azzopardi [23] to calibrate the seismic vulnerability ratings proposed by the author of this thesis with respect to the preliminary seismic vulnerability assessment form for the contemporary loadbearing unreinforced masonry typology present in the Maltese Islands (a copy of which is presented in Figures 1 to 11 of Appendix A) which was developed as part of the study presented herein, as outlined in Section 3.2 of this thesis and Documents (i) [5], (ii) [25] and (iii) [6] in Appendix B.

The outcomes of these studies are summarised in Tables 2-2 and 2-3 in Section 2.2.2 and in Section 2.6 of this thesis. The studies carried out by Galdes [17], Marmara' [18], Tong [19], Borg [20], Bonello [21], Zammit [22], Azzopardi [23] and Said [24] were all based on the assumption of a design seismic action which has a surface wave magnitude not exceeding 5.5 (hence, considering a Type 2 response

spectrum in accordance with Table 3.3 of Eurocode 8: Part 1 [4] for the evaluation of the design response spectrum, the base shear and the horizontal seismic forces acting at every storey level), which could be debatable, particularly when considering the magnitude of the last major earthquake to cause severe damage in the Maltese Islands. Nevertheless, the type of subsoil, the mortar strength, the presence of a soft storey, the overall plan proportions and the masonry construction material of the isolated buildings (and, if located within an aggregate, the building characteristics of the structures within the aggregate), the size of the aggregate, the position of the building within the aggregate and the alignment of the transverse walls of adjacent structures within the aggregate, were all shown to have a significant influence on the seismic resistance of the masonry building typology under study.

1.3 Research Focus: Aims and Objectives

The main aim of the study presented herein is the investigation of the seismic vulnerability of the contemporary loadbearing masonry building typology through the identification of the main building characteristics which influence its seismic behaviour, and the evaluation of their relative bearing on the seismic vulnerability of this building typology, following a detailed examination of the variation in dynamic properties and the resulting response parameters obtained from numerical analyses of a typical six-storey structure. This is achieved through:

a) a detailed review of published studies investigating the seismic response of masonry buildings, which incorporate particular building characteristics, which are commonly present in the contemporary loadbearing URM building typology, in addition to a thorough analysis of existing seismic vulnerability assessment methods, the failure mechanisms and parameters considered, together with the relative weightings assigned to the different parameters;
b) the development of a preliminary seismic vulnerability assessment form, which includes all the identifiable building characteristics, which could potentially alter the seismic response of this building typology, in addition to a corresponding rating system for the evaluation of the seismic vulnerability rating of the building typology under study through this form;
c) the seismic evaluation of the buildings in two Test Sites in Malta and Gozo, using the preliminary seismic vulnerability assessment form, and the comparison of the resulting seismic vulnerability ratings with the corresponding ratings obtained through a GNDT (Gruppo Nazionale per la Difesa dai Terremoti) second level assessment [26], a FEMA 154 [27] check and an extended GNDT second level check including the five additional parameters proposed by Formisano et al. [28] [29] [30] [31] for the consideration of the 'aggregate effect' in the seismic vulnerability assessment;
d) a statistical analysis of the data collected through the use of the preliminary seismic vulnerability assessment form, and the resulting seismic vulnerability outcome, for the identification of the parameters which are the most significant predictors of the seismic vulnerability rating of the building typology under study;
e) the study of the influence of six building characteristics, selected mainly following the evaluation of the statistical analysis results, on the seismic resistance of the contemporary loadbearing masonry URM building typology, through the detailed assessment of the response

parameters resulting from the non-linear time-history analysis of numerical models, including the presence of the six characteristics, first in isolation, and then in combination.

In addition, the present study aims to determine whether a non-linear static pushover analysis method, which assumes (by default) a 'box-like' structural behaviour of all analysed structures, can predict, with reasonable accuracy, the resistance to seismic actions of the contemporary loadbearing masonry building typology. This is investigated through the direct comparison of the exhibited seismic resistance and the response parameters obtained through a non-linear static pushover analysis of numerical models of the URM building typology under study, with the results obtained from the non-linear time-history analysis of corresponding numerical models.

In view of the lack of knowledge on the actual response of the contemporary loadbearing URM building typology to seismic excitations from past earthquake events, the last stages of the study involving the numerical simulations of the seismic behaviour of this construction typology using the non-linear dynamic and the non-linear static pushover analysis methods, and the detailed review of the resulting response parameters is considered to be the main knowledge contribution of the study presented herein.

1.4 Outline Structure

This thesis is subdivided into six Chapters including this introductory chapter. In Chapter 2 (Seismic Vulnerability of Buildings: code requirements, building characteristics, assessment methodologies and numerical analysis), as the title suggests, includes a review of the recommendations found in Eurocode 8: Part 1 [4] with respect to the design of structures, which are intended to resist seismic actions, the results of published studies regarding the influence of particular seismic characteristics on the seismic response of buildings, in addition to a detailed study of existing seismic vulnerability assessment methods in use in other countries, alternative automated procedures and studies evaluating the influence of the 'aggregate effect' on the seismic vulnerability rating. The main characteristics of four numerical modelling methods are also reviewed and compared.

Chapter 3 (Methodology and its Application) gives an overview of the unpublished or background information related to the work carried out by the author for the development of the preliminary seismic vulnerability assessment form and the corresponding rating system, the description of the Test Sites and the aggregates on which the developed form was applied, the comparisons of the resulting seismic vulnerability ratings with those obtained for the same buildings through the use of existing methods, and the statistical analysis of the results. However, the reader is also referred to Appendix B for the published work (or the work which is pending publication) concerning these parts of the research study carried out for this thesis. Chapter 3 also includes a detailed review of the numerical models analysed using the two software packages utilised in this study, namely ELS® and 3Muri®, including the investigated parameters, particular numerical modelling techniques used, the modelling simplifications adopted, the material properties, the inertial loads specified, the representation of the subsoil scenarios investigated and the design seismic action considered in both analyses methods carried out in this research study. Furthermore, Appendix A includes information pertaining to the

preliminary assessment form, its development, the Test Sites where this form was applied, and the comparison of the seismic vulnerability outcomes obtained from the use of this form, the original GNDT second level assessment, and the extended GNDT second level assessment on the same sample of buildings. Appendix C includes information on the material properties defined in the numerical models, and the corresponding references to the studies from where these properties were obtained, in addition to the results of verification checks carried out on modelling techniques, model restraints, and model parameters defined in the analysed models. Details of the inertial loads considered, and the corresponding revised slab densities, plots of the simulated scaled seismic record applied to all models, together with the plan layouts of the analysed cases are also included.

Chapter 4 (ELS® Numerical Analysis: Examination of Results and Discussion) includes a detailed evaluation of the variation in the dynamic properties of the analysed numerical models, and the seismic response parameters extracted from these models. Based on the results of international studies reviewed in Chapter 2, an attempted interpretation of these variations with respect to the structural behaviour under seismic actions is put forward, and the relative influence of the investigated characteristics is derived. Appendix D includes tables with the main response parameters extracted from the analysed models.

Chapter 5 (3Muri® Numerical Analysis: Examination of Results and Discussion) reviews and evaluates the response resulting from the 3Muri® non-linear static pushover analysis of control numerical models and numerical models including one additional seismic vulnerability characteristic to that obtained from an ELS® non-linear dynamic analysis of corresponding numerical models for the determination of the validity of the former method of analysis for the seismic assessment of the URM building typology under study. The main basis of comparison considered is the building height at which an adequate seismic resistance is exhibited by the corresponding numerical models for the equivalent limit state. However, the natural frequency with respect to the first (fundamental) mode of vibration in the x- and y-plan orientations, the modes of displacement for the dominant frequencies of vibration and the maximum displacement resulting from load distributions acting in the transverse x-x plan orientation of the analysed numerical models are also compared, when applicable. A comparison of the seismic resistance exhibited by the analysed control numerical models to the closest corresponding cases considered by Borg [20] is also carried out. Furthermore, this Chapter also reviews the response parameters resulting from the investigation of four additional cases of the URM building typology under study through a 3Muri® non-linear static pushover analysis. The applicability of the presence of shear failure in the longitudinal walls and the main transverse walls and the maximum allowable limit of the reduction factor 'q_u' throughout all the analysed numerical models, as possible additional capacity criteria to be used in a non-linear static assessment is also examined. Appendix E includes tables with the main non-linear static pushover analysis results, the maximum building heights at which an adequate seismic resistance was exhibited by the cases investigated using 3Muri®, the modal analysis results, and wherever applicable, the corresponding results obtained from the equivalent numerical models analysed using ELS®.

Chapter 6 (Conclusions and Recommendations For Future Research Work) gives an overview of the main conclusions derived from the various studies carried out in this research study, while including an assessment of the inherent limitations, and a critical evaluation of the possible sources of error and potential improvements. A number of studies which could build upon the knowledge gained from this thesis, or address identified gaps, particularly in the current knowledge of the local construction and geological material properties, the seismic response of different construction scenarios, the associated seismic resistance and possible structural strengthening techniques, are also proposed.

Chapter 2 SEISMIC VULNERABILITY OF BUILDINGS: CODE REQUIREMENTS, BUILDING CHARACTERISTICS, ASSESSMENT METHODOLOGIES AND NUMERICAL ANALYSIS

2.1 Introduction

Coburn and Spence [32] and Karbassi [33] classify seismic vulnerability evaluation methods into two main categories, namely the 'observed' and the 'predicted' procedures. The former is based on the statistical analysis of earthquake damage recorded after the occurrence of seismic events, and can result in the formulation of damage probability matrices (DPM), from which the probability of occurrence, associated with different damage levels, for a particular building typology, in different hazard scenarios, can be obtained. On the other hand, in the 'predicted' procedures, the evaluation of the seismic vulnerability of a structure is carried out through design specifications and calculations using analytical models which could vary in complexity, depending on the ultimate objective behind the assessment. The latter method is more applicable to engineered buildings where the resistance to earthquake excitations can be evaluated with higher accuracy. Karbassi [33] classifies score assessment methods and the development of fragility curves under this assessment category.

Calvi et al. [34], on the other hand, categorise seismic vulnerability assessment methods as either 'empirical' or 'analytical', a combination of which results in 'hybrid methods'. While the 'empirical methods' category seems to be similar to the 'observed' damage category mentioned by Coburn and Spence [32], since Damage Probability Matrices fall under this classification, Calvi et al. [34] include also vulnerability index methods, such as the GNDT second level assessment method [26], under this category. There therefore appears to be some degree of overlap between the categorisations referred to by Coburn and Spence [32] and Calvi et al. [34]. Analytical methods involve the use of computational analysis for the investigation of the behaviour of structures during a seismic event (studies by Valente and Milani [35], Furukawa et al. [36], Casolo [37]), and for the derivation of fragility or capacity curves (studies by Karbassi and Nollet [38] [39] [40] and Karbassi and Lestuzzi [41]), and damage probability matrices (study carried out by Kappos et al. [42]).

The following sections include a detailed review of the requirements of Eurocode 8: Part 1 [4] for the design of structures which are intended to resist earthquake actions, existing empirical seismic vulnerability assessment methods and pre- and post-earthquake survey methods, with particular consideration of the building characteristics which are identified in these methods as influencing the

structural behaviour during seismic actions and the corresponding variation in this building response. Numerical analysis methods for the investigation of the response of masonry structures under seismic loads are also reviewed and compared.

2.2 Building Characteristics and Seismic Resistance

2.2.1 Eurocode 8 requirements

Table 2-1 Eurocode 8 (EN 1998-1:2004) [4] recommendations for the design of buildings to resist seismic actions, including particular recommendations for unreinforced masonry buildings.

Eurocode 8: Part 1 Clause	Requirement	Prevented scenario
4.2.1.1(1); 4.2.1.5(2); 4.2.3.2(8a); 4.2.3.3(2)	Provision of uninterrupted load paths in slabs and throughout building height up to foundation level	Stress concentrations; increased storey displacements
4.2.1.2; 4.2.1.3; 4.2.3.2(2); 4.2.3.3(3); 4.4.2.3(3)	Uniformity and symmetry in lateral stiffness, wall layouts and resistance to horizontal actions in both orthogonal plan directions, hence similar mass and lateral stiffness of individual storeys	Eccentricities between centre of mass and centre of stiffness resulting in generation of torsional forces; sudden changes in lateral storey stiffness resulting in stress concentrations and increased displacements
4.2.1.4	Provision of adequate resistance to torsional effects to ensure resistance to generated torsional actions	Torsional rotations which give rise to stress concentrations
4.2.1.5; 4.2.3.2	Provision of rigid diaphragms at all intermediate floor and roof levels with enough in-plane stiffness and adequate connection to the underlying structural walls	Buckling or deflection of slabs under horizontal earthquake actions resulting in loss of contact of part of slab from walls leading to unequal distribution of forces to structural walls
4.2.1.6	Uniform transfer of seismic actions to all primary structural walls through the foundation system and its connection to the overlying structure	Non-uniform distribution of seismic forces in different areas of the same structure, such as due to slipping of walls on foundations
4.2.3.2(3) and (5)	Compact plan shape; ratio of longer to shorter plan orthogonal dimension not exceeding 4	Stress concentrations; torsional effects
4.2.3.2(6)	At every level and in both orthogonal directions, the ratio of the distance between the centre of stiffness and the centre of mass (perpendicular to direction of analysis) to the torsional radius (in the direction of analysis) is not to exceed 0.3	Generation of torsional forces which exceed the torsional resistance of every respective storey
4.2.3.3(5)	Limits on the proportions of setbacks	Stress concentrations and sudden changes in lateral storey stiffness of overlying floors
9.2.2(1); 9.2.3(1)	Minimum strength for masonry units and mortar	Crushing of masonry walls
9.5.1(2)P; 9.5.2(1)	Provision of continuous concrete tie beams or steel ties directly above all walls at every slab level and aligned with the respective walls	Inadequate connection between slabs and walls, hence non-uniform distribution of earthquake forces to primary structural walls; failure of storeys to ensure a box-like behaviour under horizontal actions

An adequate seismic vulnerability assessment method should identify all those characteristics in a structure which could alter its collapse resistance under seismic excitations, and/or hinder its energy dissipation capacity, hence leading to premature failure. Unreinforced masonry structures are intrinsically vulnerable when exposed to earthquake forces, mainly due to the fact that their main lateral load-resisting members are composed of discrete blocks bound by mortar, which, in the Maltese Islands, tends to be very weak. In addition, the horizontal structural systems generally in use, and the typical connection details present between the roofing structures and the walls, often fail to ensure an adequate transfer of forces between these systems and a box-like behaviour. However, the presence of particular building characteristics can cause a further reduction of this box-like behaviour, the setting up of torsional forces, the creation of high stiffness gradients between overlying floors, therefore leading to higher stress concentrations at localised positions in the building and, consequently, increased displacements, all of which aggravate the seismic vulnerability of these structures.

The Eurocode 8: Part 1 [4] recommendations for buildings which are designed to resist seismic actions are summarised in Table 2-1. A number of recommendations specific to the construction of unreinforced masonry are included in this table. Furthermore, regularity criteria on plan and in elevation are also included in Table 2-1. In Eurocode 8: Part1 [4] , the regularity on plan and elevation of a structure are determining factors in the allowable structural model (simplified planar model along at least two orthogonal directions or three-dimensional model), the allowable analysis method (response spectrum analysis through the application of a system of lateral forces at the slab levels, or a modal analysis) and the applicable behaviour factor in the structural design of structures for the resistance to seismic actions. These requirements are summarised in Table 4.1 of Eurocode 8 [4].

Eurocode 8: Part 1 [4] also takes into account the alteration of seismic vibrations acting on a structure resulting from the characteristics of the underlying ground through the soil factor 'S' and the alternative values of periods 'T_B', 'T_C' and 'T_D' defined in Tables 3.2 and 3.3 for different ground types, corresponding to Type 1 and Type 2 elastic response spectra, respectively. Furthermore, Clauses 4.4.2.7(2) and (3) give the minimum recommended gaps for the avoidance of impact from pounding.

2.2.2 Influence of particular building characteristics on the seismic response of structures

During an earthquake, the excitations of the ground beneath a structure are transferred to the structure through its foundations. The resistance of the building mass to these forced, random vibrations results in the generation of inertia forces. Hence, the inertia forces and the structural lateral stiffness (together with the variation of these two properties throughout the height of the building) control the displacement of the building, and the consequent stresses generated through this random motion, since they influence directly the duration of the oscillation, and the magnitude and mode of the displacement. Furthermore, every mode of oscillation of a structure corresponds to the deformed shape the building takes when vibrating at its corresponding natural period.

Tables 2-2, 2-3, 2-4 and 2-5 summarise the knowledge gained from international and local studies with respect to the influence which the dynamic properties and particular building and ground

characteristics have on the seismic response of structures. The characteristics reviewed in these tables were limited to the construction scenario of the contemporary loadbearing masonry building typology in the Maltese Islands. The influence of other building features, which are not directly applicable to the building typology under study, such as, the presence of plan configurations with re-entrant corners, the presence of flexible diaphragms, the irregular distribution of masonry infill walls in the facades of reinforced concrete frames, the eccentric positioning of the infill walls with respect to the centre-line of the beams, the variations in the stiffness of columns along the perimeter of a building (resulting from the 'shortening' effect on columns of infill walls which do not reach up to the top of the columns) and the effect of unresisted side thrusts from arches or pitched roofs, were not considered in this review.

Table 2-2 Results from studies investigating the influence of ground and building characteristics on the seismic response of structures -1.

Characteristic	Referenced study	Effect on seismic response of structure
a)Natural frequency	Chopra [43]	The reduction in the natural frequency of a structure following a seismic event can be attributed to the structural deterioration and, hence, the loss in stiffness as a result of cracking.
	Calvi et al. [44]	
	Mucciarelli et al. [45]	
	Mangion [15]	
b)Ground material	Galdes [17]	Amplification of seismic actions in the presence of clay result in the resistance to collapse under seismic excitations with a maximum peak ground acceleration (p.g.a.) of 0.10g of a contemporary loadbearing URM building, which includes a soft storey at the lowermost level, at three storeys if built on rock, and two storeys if built on clay.
	Borg [20]	In the six building configurations studied (plan length: width ratios ranging from 1:1 to 6:1), for the same masonry construction material and the same mortar strength, a reduction in the total number of storeys at which collapse was resisted, resulted with reduction in stiffness of the subsoil material when comparing Type A, Type B and Type C ground (EC8-1, Table 3.1 [4]).
	Gueguen et al. [46]	When buildings are constructed over more flexible ground (corresponding to shear wave velocities lower than 600 m/s), a complex interchange of seismic vibrations (soil-structure interaction) between the ground and the building occurs, with the building reflecting back into the ground some of the energy resulting from its vibration. In the case of stiffer, heavier buildings constructed over flexible ground, soil-structure interaction effects are more pronounced.
	Lou et al. [47]	
	Farghaly et al. [48]	
	Reza Tabatabaiefar et al. [49] [50]	
	Xiong et al. [51]	
	Gutenberg [52]	Amplification of seismic vibrations identified in sites located on alluvium depths of more than 500 feet when compared to sites located on a rock outcrop in the vicinity.
	Lang [53]	A high impedance contrast resulting from the presence of a softer ground layer over a stiffer ground layer or bedrock, gives rise to amplifications of the earthquake vibrations.
	Murty et al. [54]	Increased rotational flexibility at foundation level in structures constructed on individual foundations over a flexible ground leads to higher displacements in the lower floors of these structures.

Table 2-3 Results from studies investigating the influence of ground and building characteristics on the seismic response of structures -2.

Characteristic	Referenced study	Effect on seismic response of structure
c)Building height	Murty et al. [54]	The increase in height of a building results in increase in mass, but also an overall reduction in its stiffness which causes a decrease in its natural frequency.
d)Plan proportions	Borg [20]	In masonry loadbearing structures constructed in softstone masonry, with a rock subsoil (Type A, EC8-1 Table 3.1 [4]) and mortar strength of 5 N/mm^2, a decrease in seismic resistance was only reported for plan length-to-width ratios higher than 4:1. However, with lower mortar strengths (3.5 N/mm^2 and 5 N/mm^2) and / or less stiff subsoils (ground Types B and C, EC8-1 Table 3.1 [4]), or in the case of hollow concrete blockwork constructions (on any subsoil type and any mortar strength), a decrease in seismic resistance with increased rectangularity of plan ratios was identified in plan ratios higher than 1:1.
e)Construction materials	Borg [20]	Loadbearing masonry structures constructed in softstone masonry result in a resistance to collapse at a higher number of storeys than equivalent structures constructed in hollow concrete blockwork. The increase in the compressive strength of mortar is also reflected in a higher seismic resistance.
f) Soft storey	Farrugia [16]	The three storey layout with a soft storey at the lowest level does not resist an earthquake with a maximum p.g.a. of 0.04g.
	Galdes [17]	As in (b) Ground material in Table 2-2
	Marmara' [18]	[18] and [19] studied the resistance to a seismic action with a maximum peak ground acceleration of 0.10g of three plan configurations of the contemporary loadbearing URM building typology with assumed mortar compressive strengths of 2 N/mm^2 and 5 N/mm^2, respectively, with/without the presence of a soft storey and considering a rock or clay subsoil. The presence of a soft storey resulted in a significant reduction in the number of floors resisting collapse on both ground types and for all three plan configurations. However, in the absence of a soft storey, structures analysed on rock resisted collapse at an overall height of one storey higher than the corresponding structures analysed on clay. The higher mortar compressive strength considered by Tong [19] also resulted in the resistance to collapse at a higher number of storeys in both subsoil scenarios.
	Tong [19]	
	Arnold and Reitherman [55]	The discontinuity in the load paths at the slab above a soft storey gives rise to stress concentrations at the junction between the soft storey and the overlying structure.
	Guevara-Perez [56]	The reduced stiffness and higher flexibility of a soft storey when compared to the overlying levels results in the attraction of a higher proportion of seismic forces, which cause higher displacements in the vertical structural elements at this level.
	FEMA 454 [57]	
	Murty et al. [54]	

Table 2-4 Results from studies investigating the influence of ground and building characteristics on the seismic response of structures -3.

Characteristic	Referenced study	Effect on seismic response of structure
g) Setbacks	Al-Ansari [58] [59]	Setbacks at penthouse level result in the localised reduction in mass and stiffness at that floor (cantilevered beam simplification).
	Parisi [60]	When setbacks of limited proportions are distributed throughout the height of a building, the lower position of the centre of mass results in a lower overturning moment, and therefore, an increased stability.
h) Voids in slabs	ASCE/SEI 31-03 [61]	The presence of a void in a slab results in stress concentrations and the setting up of secondary moments in the slab as the seismic force is re-routed around the void.
	Öztürk [62]	Voids in slabs larger than one third of the slab plan area result in impairment of the rigid diaphragm action due to a non-uniform transmission of seismic forces to the primary structural elements, hence causing larger displacements.
i) Pounding	Anagnostopoulos [63]	Damage due to impact during the seismic vibration of adjacent structures, which are not adequately far apart depends on the dynamic characteristics of the respective structures, the size of the gap between the buildings, and the degree of restraint of the structures (whether all the structures are bounded by a structure on both sides or whether a structure occupies an end position in an aggregate). Structures at the end of a row construction experience higher induced displacements due to the lack of restraint to motion from the 'free' side. Large mass discrepancies between adjacent buildings result in higher damages on the lighter structure in the row.
	Mahmoud et al. [64]	Pounding of adjacent, equal height buildings on a flexible subsoil results in a decrease in maximum displacements, 'hammering' forces and inelastic shear forces, particularly for the more flexible structure due to soil-structure interaction effects. Maximum acceleration values at every floor, however, increase.
j)Projecting rooms	D'Ayala [65]	A 'cumba', which is typical of the buildings present in Fener and Balat in Istanbul, Turkey, is similar to the 'projecting room' found in the contemporary loadbearing URM building typology in the Maltese Islands. However, it has a lower self-weight and different connection details to the Maltese version. A heavier form of this 'closed balcony' would have induced overturning moments on the facade since a ‘cumba’ is supported by C-shaped iron members supported onto the facade walls. On the other hand, the construction of the projecting room in the local scenario, supported by a cantilevered reinforced concrete slab, which is continuous with the internal slab of the adjacent room, together with its limited proportions ensures that no, or minor overturning effects result in the main facade wall.

Table 2-5 Results from studies investigating the influence of ground and building characteristics on the seismic response of structures -4.

Characteristic	Referenced study	Effect on seismic response of structure
k)Large or irregularly distributed openings on facades	Formisano et al. [28] [29] [30] [31]	A high percentage difference of area of openings to total façade area in adjacent structures within an aggregate results in an increased seismic vulnerability of the structures in question in view of the resulting high stiffness gradient between adjacent facades.
	Ferreira et al. [66]	Higher seismic vulnerability is associated with buildings positioned within an aggregate with increased percentage of cases, where a horizontal misalignment of openings in adjacent buildings is present.
	Parisi and Augenti. [67]	The irregular positioning of openings on facades (openings of different sizes, misalignment in the vertical or horizontal direction or difference in the number of openings per floor) result in stress concentrations, which lead to an increased displacement, and a significant reduction of the in-plane resistance (in terms of ultimate displacement capacity, displacement ductility, and force reduction factor) of the facade wall to seismic actions, particularly when openings of different heights are present in the same floor.
	Parisi et al. [68]	The increase in the misalignment of lintel levels of openings on a building facade results in a reduction of its minimum seismic resistance parameters (elastic stiffness, ultimate resisting force, and ultimate displacement).

2.3 Seismic Vulnerability Assessment Methods Developed in Italy

The incidence of a number of devastating earthquakes in Italy (from the 1976 Friuli earthquake to the August/October 2016 and January 2017 seismic events in Central Italy, and the less severe earthquake of December 2018 in Sicily) has motivated the development of a number of seismic vulnerability assessment methodologies, in addition to methods intended for the pre-event planning of emergency operations, and the post-event methods for the assessment of safety for use. Furthermore, the succession of seismic occurrences throughout the years ensured that these developed methods remain in use up to the present day, which hence guarantees their regular updating.

2.3.1 GNDT first and second level seismic vulnerability assessment methods

The GNDT first level assessment form [69] (also referred to as GNDT level 1 method) records information which is more useful for the estimation of exposure and a first level of seismic risk assessment of the urban building stock. It is intended mainly for use with residential building typologies constructed in masonry, reinforced concrete, steel or a combination of more than one main structural material. The data collected in this assessment form includes information required for the identification of the building, the number of floors, their respective floor area and the floor-to-ceiling heights, the minimum and maximum height of the topmost roof above street level, the width of the road along the main façade, the number of units and their respective uses, the degree of occupancy of every unit, the age of the structure and the year when the last major works were carried out on it, the current state of the finishes, and the mechanical and electrical systems, the main structural

typology of the building and the degree and extent of damages in the vertical and horizontal structural members, the staircases and the infill masonry walls (if present). While a seismic vulnerability rating cannot be determined directly from the GNDT first level assessment form, the statistical analysis of the data collected in an urban area can be used to obtain an approximate indication of the variation in seismic vulnerability of the surveyed building stock, particularly in a post-earthquake scenario.

The vulnerability index method for masonry buildings proposed by Benedetti and Petrini [70], which was the forerunner of the GNDT second level assessment method [26] [71] (also referred to in this thesis as the GNDT level 2 assessment method), involves the allocation of a seismic vulnerability class from A to D (which correspond to an increasing seismic vulnerability) to the ten parameters listed in Table 2-6 which describe:

a) the structural system (Parameter 1: assesses the presence of adequate interlocking of courses at the junctions between perpendicular walls and tie beams around the external perimeter of the building at all levels, to ensure a 'box-like' behaviour; Parameter 2: assesses the type and quality of the wall construction, the shape and material of the masonry blocks and the presence of bondstones or ties when more than one leaf is present; Parameter 4: provides a simplified estimate of the seismic resistance of the building, by equating the seismic resistance of the building in its weaker orientation to that of an equivalent shear wall, and presenting the result as a ratio of the resulting seismic resistance to the seismic resistance required by the current (Italian) regulations; Parameter 6: records the regularity of the plan layouts, and, hence, the lateral storey stiffness, throughout the height of the building, and the presence of setbacks; Parameter 7: assesses the function of the slabs in ensuring a box-like behaviour of the buildings, and the transfer of seismic forces to the supporting walls through the presence of a rigid diaphragm and adequate ties between the slab and the vertical structural elements; Parameter 8: considers the construction typology of the topmost roof with respect to its weight, the exertion or otherwise of side thrusts onto the underlying structural walls, and the presence of perimeter tie beams in order to assess the influence which the roofing system at this level has on the seismic behaviour of a structure);
b) the stability of the ground with respect to the risk of differential settlement, the topography of the site where the building under assessment is located and the presence of adequate ties at foundation level (Parameter 3);
c) the regularity of the plan layout (Parameter 5: assesses the influence of the overall plan shape and any deviations from the square or from the rectangular plan layouts, up to a maximum acceptable ratio of shorter side dimension to longer side dimension of 0.8, taking into consideration not only elongated rectangular layouts, but also plan shapes which include re-entrant corners such as T-, C-, L- and cross-shaped configurations);
d) the presence of non-structural elements attached to the facades which, if dislodged, could damage nearby buildings or injure people (Parameter 9);
e) the current state of repair of the building, with particular emphasis on the presence of cracks and the condition of the structural walls (Parameter 10).

Table 2-6 Parameters considered in the Benedetti and Petrini ([70] p.68) seismic vulnerability assessment method, scenario classes, weightings and corresponding parameters in the GNDT level 2.

Parameter number	Parameter description	Classes (C_{vi})				Weighting (p_i)	Corresponding GNDT level 2 Parameter number
		A	B	C	D		
1	Organisation of the vertical structural system	0	5	20	45	1	1
2	Quality of the vertical structural system	0	5	25	45	0.25	2
3	Position of building and type of foundations	0	5	25	45	0.75	4
4	Distribution of the main structural elements	0	5	25	45	1.5	3
5	Plan regularity	0	5	25	45	0.5	6
6	Regularity of building throughout its height	0	5	25	45	0.5 or 1	7
7	Slabs	0	5	15	45	var (formula)	5
8	Roofing system (topmost roof)	0	15	25	45	var (formula)	9
9	Nonstructural elements	0	0	25	45	0.25	10
10	Current state of repair	0	5	25	45	1	11

Benedetti and Petrini [70] explain that Class A represents a situation which is in accordance with current regulations, whereas Class B represents situations which include deviations from current regulations, but which however, do not result in a significant loss of seismic resistance. Classes C and D, on the other hand, include situations which result in significant deviations from the regulations and, hence, are associated with a pronounced increase in seismic vulnerability. The weightings assigned to the ten parameters take into consideration the bearing which every parameter has on the seismic resistance of a building and were, therefore, divided into three main categories: elements of primary importance, corresponding to a weighting of 1.5 (Parameter 4); important elements, to which a weighting of between 0.5 to 1.0 was assigned (Parameters 1, 3, 5 and 10); and secondary elements which were assigned weightings lower than 0.5 (Parameters 2 and 9). The masonry typologies considered by Benedetti and Petrini [70] are mainly related to traditional masonry residential buildings found in older town centres of Italy. The relative degree of importance of the different parameters, with respect to the seismic resistance of these typologies, as reflected in the parameter weightings and the construction scenarios considered in the definition of Classes A to D for every parameter, is conditioned by the structural systems, construction methods and building characteristics present in these specific typologies. As in the case of the GNDT second level assessment method, the vulnerability index, *V*, is obtained from [72]:

$$V = \sum_i C_{vi} p_i$$

Equation 2-1

where C_{vi} and p_i are the scores corresponding to Classes A to D for every parameter, and the parameter weightings, respectively, as summarised in Table 2-6. The vulnerability index is normalised by expressing it as a ratio of the maximum possible vulnerability score.

The GNDT second level assessment method [26] [71], whose list of parameters and corresponding scores and weightings are reported in Table 2-7, retained the basic structure and methodology of the method developed by Benedetti and Petrini [70]. However, apart from the general re-arrangement of the sequence of the assessed parameters and the modification of the weightings corresponding to Parameters 5 (Slabs) and 9 (Roofing system), the GNDT level 2 method includes the consideration of an additional parameter (Parameter 8) where the degree of restraint of main walls, subjected to out-of-plane seismic actions provided by the adequate interlocking of perpendicular walls, is assessed. This parameter is assigned a weighting of 1.0, hence denoting the 'important' contribution which this parameter is considered to have with respect to the overall seismic resistance of a structure. Furthermore, Lemme et al. [73] clarify that the class scores and parameter weightings proposed in the GNDT level 2 method can vary depending on the particular construction characteristics of the different parameters in the building typology under assessment in a particular region. While the level of reliability of the information, upon which the class is selected for every parameter, must be recorded in the form, this does not have a bearing on the partial (for the respective parameters) or final seismic vulnerability index.

Table 2-7 Parameters, scores and weightings considered in the GNDT level 2 assessment method [26], including comparison to the Benedetti and Petrini method [70].

Parameter number	Parameter description	Classes (C_{vi})				Weighting (p_i)	Benedetti and Petrini (1984)	
		A	B	C	D		Correspond-ing Parameter number	Weighting (p_i)
1	Type and organisation of structural system	0	5	20	45	1	1	1
2	Quality of the structural system	0	5	25	45	0.25	2	0.25
3	Seismic resistance of the building	0	5	25	45	1.5	4	1.5
4	Position of building and foundations	0	5	25	45	0.75	3	0.75
5	Slabs	0	5	15	45	0.5	7	var (formula)
6	Plan configuration	0	5	25	45	0.5	5	0.5
7	Configuration throughout height	0	5	25	45	0.5 or 1	6	0.5 or 1
8	Maximum distance between main walls	0	5	25	45	1	N/A	N/A
9	Roofing system (topmost roof)	0	15	25	45	0.5, 0.75, 1.0	8	var (formula)
10	Non-structural elements	0	0	25	45	0.25	9	0.25
11	Current state of repair	0	5	25	45	1	10	1

Additional deviations from the Benedetti and Petrini [70] method are summarised below. In a number of cases, these variations are not present in the original version of the manual for the GNDT level 2 assessment method [26], but they are included in the modified version of the manual by Regione Toscana [71]. The authors of the latter version explain that these alterations / additions are the result

of the observations made on the damaged buildings, and the failure modes, in extensive seismic vulnerability assessment campaigns carried out in Tuscany between 1982 and 1990, as part of regional and national initiatives, and between 1987 and 2001 after the occurrence of a number of seismic events, including the 1997 Umbria-Marche earthquake. The observed deviations include:

a) Parameter 2 (Quality of the structural system): while the general version of the GNDT level 2 assessment method manual [26] does not present any variations in the interpretation of this parameter, when compared to the Benedetti and Petrini [70] equivalent, in the GNDT second level assessment manual modified by the Regione Toscana [71], this parameter takes into consideration also the influence of the quality of the mortar on the contribution provided by the walls to the seismic resistance of the building under assessment;
b) Parameter 4 (Position of building and foundations): this parameter is given a similar description in the GNDT second level assessment method [26] and in the corresponding parameter (Parameter 3) in the method proposed by Benedetti and Petrini [70]. However, the description of the scenarios for Classes A to D differs between the two methods. Instead of distinguishing between stable or unstable ground, and the presence of tie beams at foundation level, in the GNDT level 2 assessment method [26], this parameter considers buildings erected directly on rock and the exertion or otherwise of a side thrust by cohesionless soils, depending on the inclination of the terrain. In the case of sloping terrain, it also takes into consideration whether the foundations of the building are constructed all at the same level or stepped. No consideration of the presence of ties at foundation level is made in the GNDT level 2 method [26], and the degree of inclination of the ground associated with every Class A to D differs from the ranges attributed to the respective classes in the Benedetti and Petrini [70] proposal.
c) Parameter 5 (Slabs): when comparing the construction scenarios corresponding to the different classes considered for this parameter in the GNDT level 2 method [26], and the equivalent parameter in the Benedetti and Petrini method [70] (Parameter 7), while the general version of the GNDT level 2 manual [26] does not present any variations, the Regione Toscana modified version of this document [71] takes into consideration two additional slab construction typologies under Class D. These include: i) the presence of (heavy) reinforced concrete slabs in buildings with weak wall construction systems, and ii) the presence of slabs which include poorly reinforced perimeter tie beams, which, therefore, do not constitute adequate ties between the slab and the walls, or reinforced concrete tie beams which are cast in a recess in the wall and, hence, do not encompass the whole wall thickness.
d) Parameter 6 (Plan configuration): while the general version of the GNDT level 2 assessment method manual [26] reproduces faithfully the irregular plan configurations considered by Benedetti and Petrini [70], the Regione Toscana modified version [71] of the latter method considers an additional type of T-shaped plan irregularity, where the projecting part of the building is very small when compared to the rectangular section. In these cases, the manual suggests that such projections can be ignored and the building can be assumed to have a rectangular layout.

e) Parameter 9 (Roofing system): when this parameter is compared to the corresponding parameter in the Benedetti and Petrini proposal [70] (Parameter 8), the GNDT second level assessment method [26] takes into consideration also the presence of steel ties, and includes additional construction scenarios to Classes B and C, which consider varying degrees of connection between the roofing structure and the vertical structural elements, and different roof typologies, which vary in the extent of side thrust exerted onto the underlying structure. A further extended list of additional construction scenarios for Classes B to D is presented in the Regione Toscana modified version of the GNDT level 2 manual [71].

f) Parameter 10 (Non-structural elements): the GNDT level 2 method [26] includes a consideration of the damage which could be caused by the collapse of false ceilings. This was not included in the corresponding Benedetti and Petrini parameter [70] (Parameter 9).

In their correlation between the vulnerability index (V), resulting from the GNDT second level assessment method [26], and the seismic vulnerability ratings (reproduced in Table 2-8), Lemme et al. [73] indicate how a more refined rating, which was based on the definition of the scenarios for Classes A to D as set originally by Benedetti and Petrini [70], was obtained. This refined rating covers a whole range of possible seismic vulnerability situations from 'Adequate', 'Low', 'Medium-low', 'Medium', 'Medium-high' to 'High'.

Table 2-8 Correlation between vulnerability index (V) and seismic vulnerability ratings in the GNDT second level assessment method. Lemme et al. ([73] p.III-6).

Class	Score	Seismic vulnerability index (V)	Basic seismic vulnerability rating	Vulnerability index (V) ranges	Refined seismic vulnerability rating
A	0	0.00	Adequate	0.00-0.10	Adequate
B	52.5	0.13	Low	0.10-0.20	Low
				0.20-0.40	Medium-low
C	203.75	0.51	Medium	0.40-0.60	Medium
				0.60-0.80	Medium-high
D	393.75	1.00	High	0.80-1.00	High

The Regione Toscana version of the GNDT second level assessment manual compiled by Ferrini et al. [71] presents a number of tables, with images intended to explain the construction scenarios corresponding to the description of Classes A to D considered by the manual, with respect to the parameters, which assess the influence of walls (Parameters 1 and 2), slabs (Parameter 5), roofing systems (Parameter 9) and non-structural elements (Parameter 10) on the seismic resistance of masonry buildings, in the context of the masonry construction typology considered in this second level assessment method. With the exception of the more contemporary wall construction typologies G, H-I, L, M, U, V considered under Parameter 2 and the reinforced concrete slab typologies presented with respect to Parameter 5, these images (particularly in the case of the double leaf wall construction typologies, the construction details of the wall – slab junctions and the horizontal construction systems as evidenced in Figures 2-1, 2-2 and 2-3 respectively) seem to suggest that, similarly to its forerunner, the GNDT level 2 assessment method is mainly intended for the seismic vulnerability assessment of traditional masonry building typologies in older urban centres. This typology would, hence, very likely

include buildings, which would rarely exceed four storeys in height and predominantly consist of modular layouts with large wall cross-sectional areas at every level. The restriction of this method to the seismic vulnerability assessment of residential buildings precludes its use for the assessment of larger masonry constructions such as palaces or stately residences. Hence, apart from reductions in lateral storey stiffness arising from the presence of porticos at ground floor level, this building typology would very likely not include characteristics such as large open plan spaces, soft storeys, projecting floors and double height spaces, which are more common in more contemporary typologies, unless these characteristics are the result of more recent conversions.

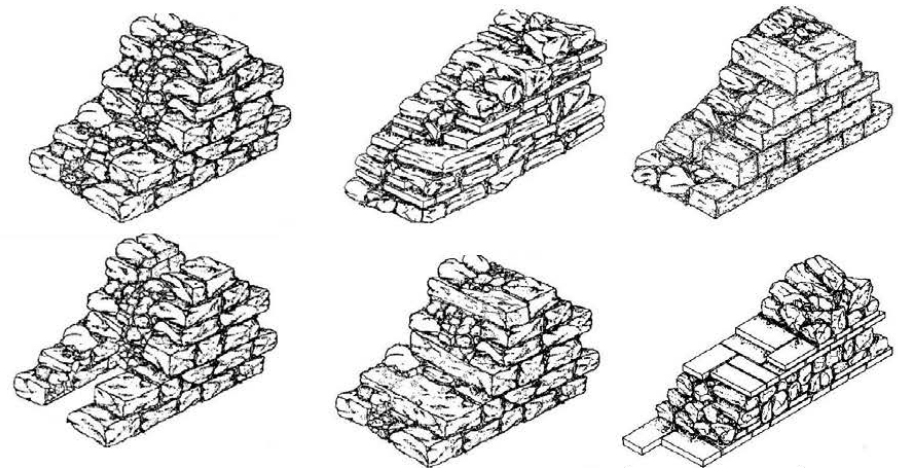

Figure 2-1 Examples of double leaf masonry wall construction systems (typologies A and B) presented in: Rilevamento della vulnerabilita' sismica degli edifici in muratura, Ferrini et al. ([71] p.20, 21).

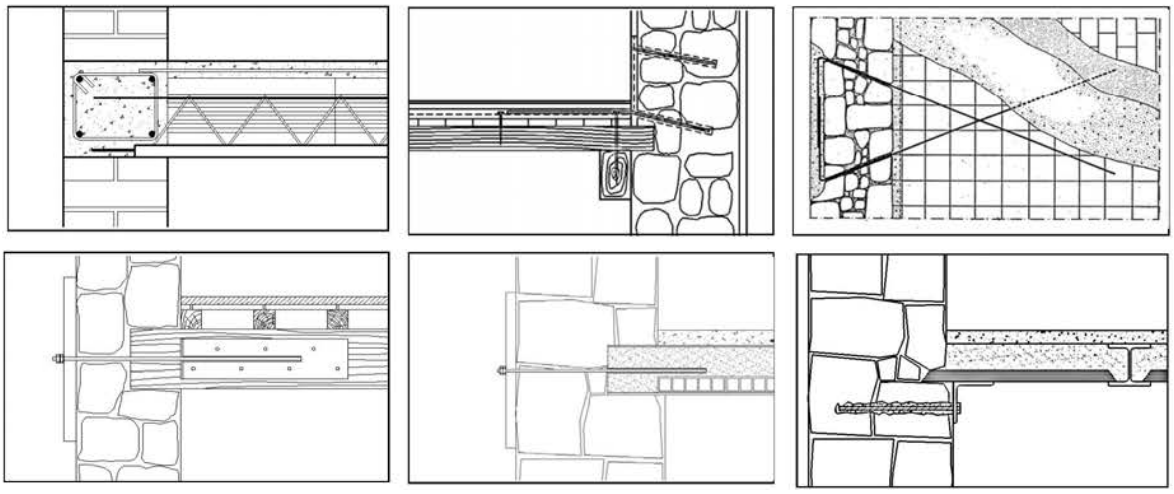

Figure 2-2 Examples of slab-wall junction details presented in: Rilevamento della vulnerabilita' sismica degli edifici in muratura, Ferrini et al. ([71] p. 54, 55).

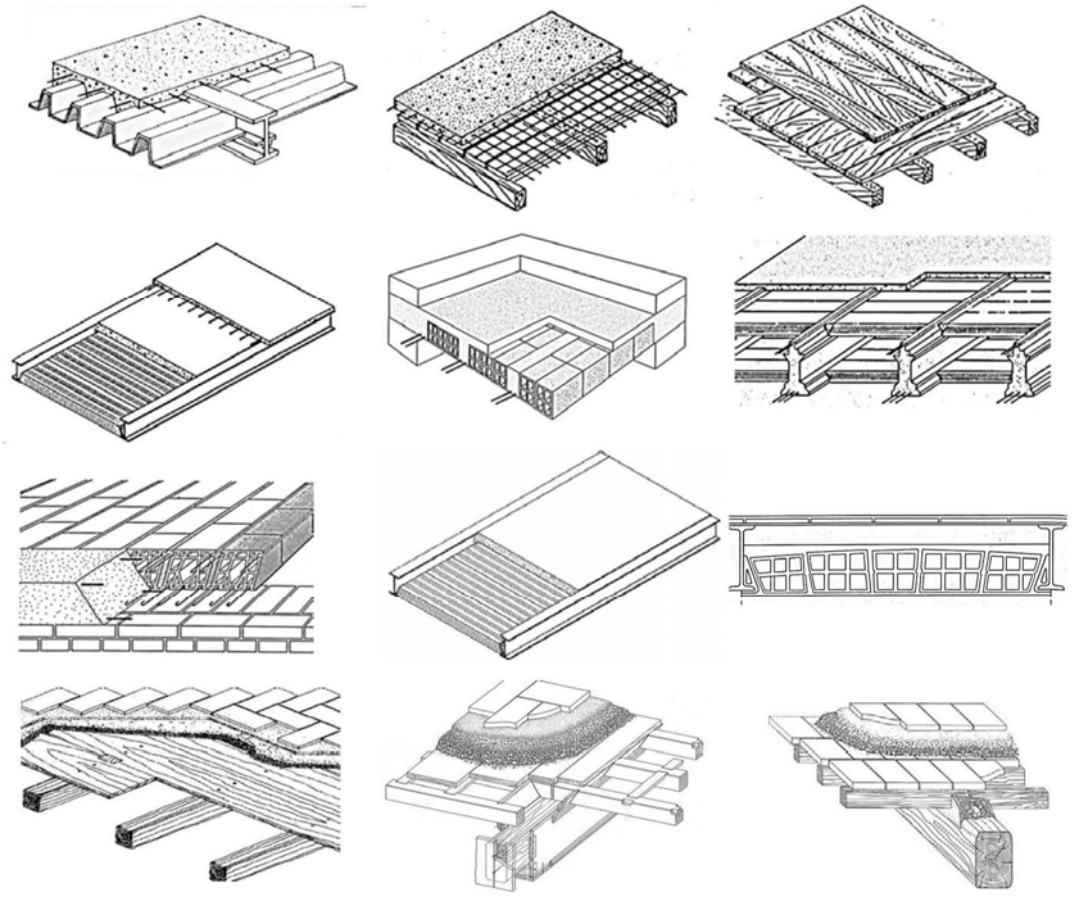

Figure 2-3 Examples of rigid, semi-rigid and deformable slab construction system details presented in: Rilevamento della vulnerabilita' sismica degli edifici in muratura, Ferrini et al. ([71] p.49-52).

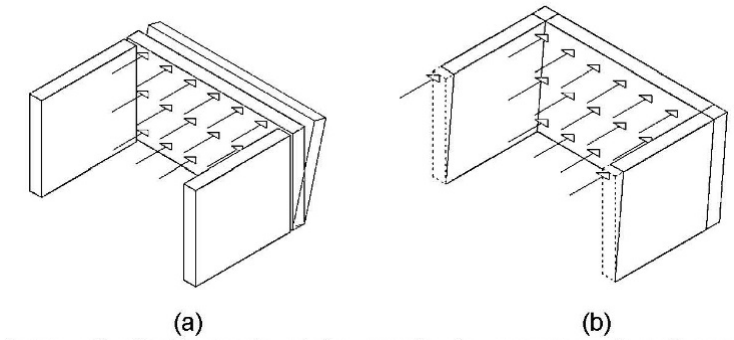

Figure 2-4 Out-of-plane forces acting on masonry walls in cases where an adequate connection between perpendicular walls is (a) not present (b) present. Regione Toscana Giunta Regionale ([74] p.6).

The GNDT level 2 seismic vulnerability assessment method gives significant bearing to the resistance of the wall construction, and the 'box-like' effect resulting from the presence of adequate and effective ties between perpendicular walls and between the walls and the overlying slabs, in addition to the presence of reinforced tie beams above all perimeter and primary internal walls. These beams have to cover the whole thickness of the wall cross-section. The very low tensile capacity of isolated unreinforced masonry walls results in the very low resistance of these walls to forces which act

perpendicular to their plane. Hence, as explained in Figure 2-4, the presence of shear walls, which are effectively bonded to each other and to the overlying slabs at every level, in the two principal directions of a building, reduces the incidence of out-of-plane failure mechanisms, since such out-of-plane forces would be resisted by the perpendicular shear walls through their flexural and shear capacity (depending on their slenderness). Furthermore, the diaphragm action of the slabs is essential for the adequate transmission of seismic forces to the masonry walls [74].

However, while the GNDT level 2 method takes into consideration the possible presence of an abrupt reduction in lateral storey stiffness (such as, in the case of a soft storey) through Parameter 7 and, indirectly through Parameters 3 and 8, this method fails to identify a number of shortcomings in the regularity of structures on plan and throughout their height, when compared to the guidelines provided by Eurocode 8: Part 1 [4]. Some examples are: the asymmetrical layout of shear walls; the presence of differing cross-sectional areas of shear walls in the two principal plan orientations; the variation in size and position of wall openings in overlying storeys (which can give rise to stress concentrations and/or result in very slender wall sections between openings); the presence of misaligned floors on opposite sides of a party wall or a main lateral force-resisting wall in the same building (which can cause a 'hammering' effect on the common wall); and the construction of additional floors over the existing masonry construction, which, if not effectively tied to the original construction, can lead to discontinuities in the load path. Furthermore, the use of different materials in the construction of additional storeys, would result in differences in the lateral storey stiffness of the new floors when compared to the rest of the building [74].

2.3.2 Regione Toscana / Servizio Sismico Regionale (SSR) Form for the assessment of deficiencies in masonry buildings *(Scheda delle carenze per edifici in muratura)*

Most of the omissions of the GNDT second order assessment method [26], particularly with respect to the possible causes of plan irregularity (which go beyond the overall plan shape of the building, and the building characteristics which can give rise to irregularities throughout the height of the building) are addressed in the Regione Toscana / SSR Form for the assessment of deficiencies in masonry buildings [75]. Through this form, the assessor is guided through a list of twenty-two possible deficiencies, which have a bearing on the seismic resistance of a masonry structure. Every deficiency is rated in Classes A to D, in accordance with the scenarios presented in the manual to the form, where Class D corresponds to a severe case of deficiency. The form specifies a weighting (p_{1k}) corresponding to every deficiency, and a score (c_k) corresponding to every deficiency class. The deficiencies considered by this method fall under five main categories, with a weighting (p_{2j}) assigned to every respective (j^{th}) category. The deficiency index (i_c) is, hence, obtained from:

$$i_c = \sum_{k=1}^{22} c_k p_{ik} p_{2j}$$

Equation 2-2

The deficiency index is converted to a percentage of the overall maximum deficiency index based on the maximum scores and weightings for all the twenty-two deficiencies. The resulting 'Low', 'Medium'

or ‘High’ deficiency rating is obtained through the comparison of the percentage deficiency index to the ranges specified in the manual for the respective ratings.

The five categories of seismic resistance deficiencies consist of shortcomings in:

i. the wall construction typology;
ii. the connection between structural elements and the presence of flexible intermediate slab and roofing systems;
iii. the presence of irregularities (on plan and throughout the building height);
iv. the presence of structural members, which exert side thrusts, which are not resisted or cancelled;
v. foundation systems.

The wall construction systems considered in the manual are the same as those reported in the Regione Toscana modified version of the GNDT level 2 method [71]. Categories (i), (ii) and (iv) take into consideration most of the scenarios assessed in Parameters 1, 2, 5 and 9 of the GNDT second level assessment form. However, Category (i), in the assessment Form for deficiencies, includes an additional verification, which consists of the assessment of whether, at any particular storey level, and in any one of the two principal plan orientations, the wall area resisting seismic actions is insufficient. This is done through a comparison of the minimum percentage wall area to reference values given in the manual. The values vary depending on the floor number and the type of masonry wall construction.

The irregularities considered under Category (iii), which are not included in the GNDT level 2 assessment method mainly consist of:

a) a plan irregularity resulting from a significant difference between the wall areas resisting seismic actions in the two principal plan orientations;
b) a significant eccentricity between the centre of mass of the main lateral force resisting elements and the centre of gravity of the plan layout, hence, resulting in the development of torsional forces;
c) the irregular distribution of walls throughout the different storey levels, where the significantly higher resistance to lateral forces of a higher floor level, when compared to its underlying floor, (resulting from a change in the type of wall construction material or an increase in wall thickness) is also considered;
d) the presence of loadbearing walls which do not reach down to foundation level, but stop at a higher slab level;
e) the presence of misaligned floors;
f) the presence of slab systems which have different characteristics (with particular reference to the in-plane stiffness) at the same storey level, hence leading to an increase in the eccentricity between the centre of gravity and the centre of resistance at this storey level;
g) the presence of apertures on different storeys, which are not vertically-aligned to each other, hence resulting in more complex load paths, and possible stress concentrations.

Furthermore, Deficiency Category (v) takes into account the reduction in seismic resistance, which would arise in the presence of significant differential settlements of foundations and walls, which are out of plumb. It must be noted that, in Parameter 4 of the GNDT level 2 assessment method [26], the distinction, between the ground consisting of rock or of a less stiff material, is intended to take into consideration the possibility of differential settlement in the event of an earthquake. On the other hand, Parameter 11 of the same method does not include any consideration of differential settlement in any of the Classes A-D. Hence, the reduced resistance to seismic excitations of a building, with this type of damage, would not be identified by the GNDT level 2 assessment method [26]. On the other hand, it could be concluded that such settlements would give rise to the formation of cracks, which would still be identified under Parameter 11 of the GNDT second level assessment method [26].

Of major concern in the construction scenario of the Maltese Islands is the inadequacy, of masonry hollow blocks with large voids for the resistance of seismic actions, a limitation which was expressed in both the Regione Toscana modified version of the manual to the GNDT level 2 method [71] and the manual to the Form for deficiencies in masonry buildings [75]. While the Parameter 2 of the Regione Toscana GNDT level 2 method attributes a Class D to masonry walls constructed in hollow blocks which have a void area larger than 45% of the wall area, in the manual to the Form for deficiencies in masonry buildings, limits are based on the area of walls constructed in hollow blocks when compared to the overall floor area, with a serious deficiency resulting, when the area of such walls exceeds 10% of the floor area. As included in Table 2-3, the study carried out by Borg [20] confirmed the reduction in the seismic resistance of contemporary loadbearing unreinforced masonry structures constructed in hollow concrete blockwork when compared to softsone, while Bonello [21] showed that this reduced level of seismic resistance is exhibited even in the case of structures constructed in hollow concrete blockwork, which are located within a building aggregate.

Furthermore, the maximum number of floors considered in the manual to the Form for deficiencies is five floors. In addition, the authors clearly state that the building typology considered in the manual, with respect to the existing buildings, has wooden floors, which are flexible in their plane of loading and are, hence ineffective in providing adequate ties to the top of the walls, particularly in the case of thick walls. Such flexible floor constructions would also be incapable of ensuring an even transmission of seismic forces to the underlying walls, in view of their reduced stiffness in the plane of loading. This effect, together with the wall typologies indicated in the manual, suggests that even this assessment form is mostly intended for the assessment of a traditional masonry construction typology.

2.3.3 MEDEA - Manual for the assessment of damages and safety for use of ordinary buildings (*Manuale di Esercitazioni sul Danno Ed Agibilità per edifici ordinari*)

The primary purpose of the MEDEA method, developed by Zuccaro and Papa in 2001, is the assessment of the seismic damage in masonry and reinforced concrete structures, in a post-earthquake scenario, through the identification of the visible damage from a predefined set of damage typologies (for vertical structures, horizontal structures, stairs and non-structural elements respectively), which are, in turn, correlated with corresponding failure mechanisms, as reproduced in Figure 2-5 in the case of masonry structures. This damage assessment, therefore, enables the assessor to evaluate the safety

for use of the buildings, and to propose emergency strengthening measures. Furthermore, the MEDEA method can also be applied in the pre-event evaluation of the construction characteristics of a structure, with respect to the identification of the failure mechanisms, which are most likely to be activated in a seismic occurrence, hence resulting as a seismic vulnerability assessment tool. While the author of this thesis was unable to obtain access to the original version of the MEDEA manual, information on the manual was obtained from a number of other sources [73] [76] [77] [78].

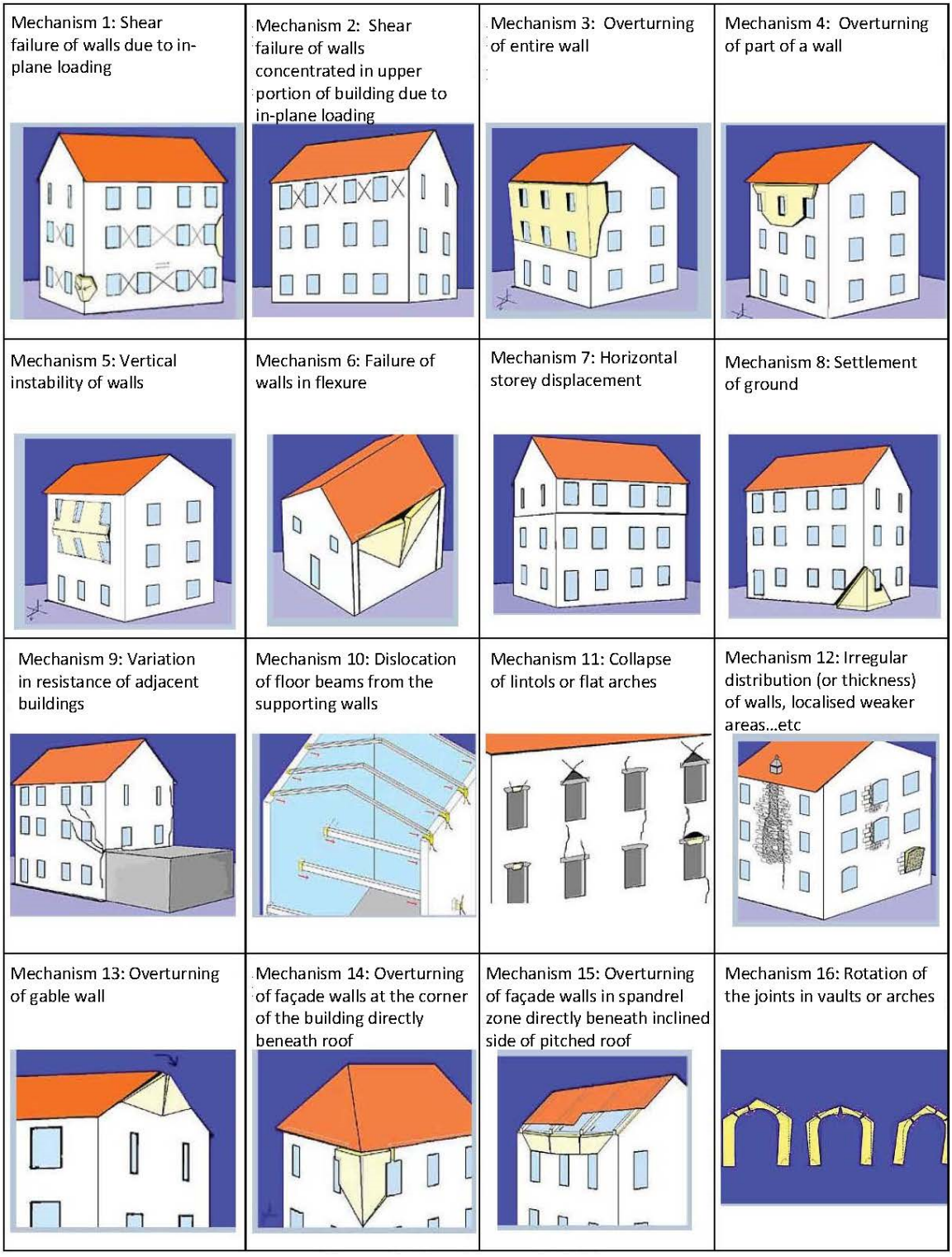

Figure 2-5 Failure mechanisms considered for masonry structures in MEDEA. Lemme et al. ([73] p.III-10)

A number of structural deficiencies identified by the GNDT level 2 method [26] and the Form for the assessment of deficiencies in masonry buildings [75] form the basis of the main failure mechanisms considered in the MEDEA manual. These include primarily:

a) the low tensile capacity of walls, which is further aggravated when low quality materials are used in the wall construction (Mechanism 1);
b) the presence of double leaf walls, where the two leaves are not adequately bonded to each other, and where, if the gap between the two walls is filled with infill material, this material exerts a pressure on the outer leaf of the wall, causing its collapse (Mechanism 5);
c) the presence of tie beams cast in recesses in double leaf walls, and hence, not covering the whole wall thickness (Mechanism 5);
d) the absence or inadequate connection between orthogonal walls and/or between walls and intermediate slabs or roofing structures (Mechanisms 3, 4, 5, 6, 10, 14, 15);
e) the variation in thickness of wall sections throughout the height of the building (Mechanism 2);
f) the presence of side thrusts from roofing structures, which are not resisted (Mechanisms 2, 3, 4, 14);
g) the variation in stiffness throughout the height of a building, or between adjacent buildings (Mechanism 9);
h) irregularity in the material of the façade, the presence of local reductions in façade thickness resulting in a reduced resistance, such as, in closing up of wall openings (Mechanism 12);
i) the presence of a ground geology, which is susceptible to differential settlement under seismic actions (Mechanism 8);
j) the presence of misaligned floors and roofs (Mechanisms 9, 13);
k) the presence of vaults or arches which are not kept in compression through steel ties or other devices (Mechanisms 11, 16).

While the MEDEA assessment method can be applied to other countries, which have similar construction typologies as considered in this method for the Italian context, the use of MEDEA in the Maltese Islands, for the assessment of contemporary loadbearing URM buildings, would require the prior modification of the damage typologies and collapse mechanisms, to reflect the local construction practices, particularly with respect to the construction of roofs, intermediate slabs and walls. Hence, all mechanisms related to the exertion of side thrusts from pitched roofs, arches or vaults would not be applicable in the case of this building typology, whereas additional mechanisms related to the specific building characteristics, which are predominant in this local typology, would have to be included. Two such examples are the weak storey and ground settlement collapse mechanisms, which are included with the global collapse mechanisms for reinforced concrete structures in MEDEA, but which are very relevant in the scenario of the contemporary loadbearing URM building typology of the Maltese Islands, in view of the prevalence of open plan layouts without intermediate walls at the lowermost level, and the ground geology present locally.

While a seismic vulnerability rating cannot be obtained from the use of this method, the understanding, of the influence on the seismic response of particular structural and construction characteristics, which tend to weaken the resistance of a structure to seismic actions, is of fundamental importance in the investigation of the seismic vulnerability of a building typology.

2.3.4 Italian pre- and post-earthquake survey methods: CLE; AeDES; and the Form for the assessment of seismic vulnerability arising from geological factors

While the seismic vulnerability rating of a structure cannot be concluded from the pre-event method intended for use in the planning of emergency activities (such as CLE [79]), and the post-earthquake rapid screening procedures for the assessment of the safety for use of buildings stipulated in the Italian laws (such as AeDES [80]), the building parameters considered in these methods can be considered to be indicators of the seismic resistance of the evaluated structure.

The CLE, 'Condizione Limite per l'Emergenza dell'insediamento urbano' [79], is a pre-earthquake procedure intended mainly for use in the planning of emergency operations by the entities, which are responsible for such operations in a seismic event. In the pre-event planning stage, such entities would need to identify strategic buildings (from where emergency operations would be coordinated), and large emergency areas (where tents can be erected to house people who would have vacated their homes and for the storage of equipment required in the emergency operations), in addition to the identification of the main emergency routes to these strategic buildings/areas, such that accessibility to and between these locations, and to nearby towns, is ensured at all times. Consequently, the five forms, which constitute the CLE procedure, review the main seismic vulnerability indicators of these locations, the main infrastructural routes, and the buildings (considered both in isolation and in the aggregates), in order to identify possible critical elements or junctions which, through failure, could interfere with the smooth running of emergency operations. The five forms comprise: i) strategic building (ES), ii) emergency area (AE), iii) infrastructure for accessibility and connection (AC), iv) structural aggregate (AS) and v) single structural unit (US).

The characteristics identified in the forms for the strategic building (ES), the single structural unit (US) and the structural aggregate (AS) can be considered as indicators of the seismic vulnerability of buildings in an urban context. The parameters recorded in the first and second sections of the strategic building (ES) form and the single structural unit (US) form are in essence the same. The main building characteristics considered in these forms include:

- the position of the building in the aggregate;
- whether the building has a façade on a main infrastructural route;
- whether the building has a specialised structural system (such as, in the case of churches, theatres, towers,…etc.);
- the total number of floors and the number of floors below street level;
- the floor-to-ceiling height, the average surface area per floor and the presence of a double height space directly facing a main infrastructural route;
- the type of vertical structural system and the quality of the masonry wall construction;

- the presence of isolated columns or piers, or alternatively, open storeys constructed over columns with no loadbearing walls ('piano pilotis' in Italian);
- the construction of additional storeys over the original building;
- the presence of visible damages to structural elements;
- the state of maintenance of the building;
- the ground morphology and the position of the building with respect to a steep slope;
- the microseismic rating of the site and, if unstable, the type of instability; and
- whether the building is at possible risk from a landslide or flooding.

While the parameters considered in the third section of both forms are mostly related to the assessment of exposure, parameters considered in the strategic building (ES) form, such as the year of construction, the date of an event which caused damage to the building, and the type of structural interventions carried out (in particular, any extensions to the original building or changes in use which caused an increase in storey loads of over 20% and any strengthening measures carried out), can be of significant bearing in the assessment of the seismic vulnerability of a structure.

The main limiting parameter with respect to the possible interference of the building aggregate, or the individual / strategic buildings, with respect to the infrastructural route, seems to be attributed to the height of the buildings, when the building height is greater than the width of the road or the closest point in the perimeter of the emergency area. Additional building characteristics, which could influence the seismic resistance of buildings within an aggregate identified by the form for structural aggregates (AS) include: the presence of vaults or arches; the joining of originally-separate buildings and the construction of areas, which were previously intended as voids or courtyards in an aggregate; the misalignment of the topmost roof, intermediate floors, façade walls or internal spaces; the presence of a narrow and long building (where the ratio of length-to-width exceeds 4) at the corner of an aggregate; the presence of structural or non-structural elements, which are attached or inadequately tied to facades; the irregular distribution of openings on facades, and the presence of damaged or degraded individual structural units within the aggregate.

The AeDES (Agibilia' e Danno nell' Emergenza Sismica) level I survey [80] [81][1] for the assessment of damage in ordinary masonry, concrete, or reinforced concrete or steel frame structures, the safety for use, and the suggestion of the emergency measures required, is intended as a fast post-event method to be applied on an urban scale as part of the immediate response to an earthquake. It guides the assessors to carry out a visual survey through the completion of nine sections, which consist of:

[1] A second edition of the AeDES manual and the corresponding form [81] was issued in 2014. The work reported in this thesis which is related to the AeDES manual had already been completed by the time the second edition was made available. Hence, any reference to the AeDES form and its manual in this thesis refers to the reprint of the first edition of the AeDES manual and the corresponding form published in June 2009 [80]. It must be noted, however, that the differences between the two versions of the form are not of a significant nature.

a) Section 1: identification of the building under assessment;
b) Section 2: description of the building with respect to number of floors, floor-to-ceiling height, age, floor area, uses and its occupancy;
c) Section 3: building typology, considering the main vertical and horizontal structural systems;
d) Section 4: damages to vertical structural elements, slabs, stairs and infill walls, damages which were present prior to the seismic event and emergency measures already in place at the time of the assessment;
e) Section 5: damages to non-structural elements and emergency measures carried out;
f) Section 6: risk of damage from other constructions and emergency measures effected;
g) Section 7: geotechnics and foundations, considering the morphology of the site, the presence or risk of foundation or ground settlement and the presence of the building directly beneath a steep drop in topography;
h) Section 8: assessment of the overall risk rating of the structure (which can vary between: 'low', 'low with additional measures' or 'high') and its safety for use through a consideration of the risk levels resulting from Sections 3 to 7 of the Form. The accuracy of the information upon which the assessment is based and any (additional) emergency measures proposed by the assessor are also recorded;
i) Section 9: other observations which could have influenced the risk rating determined in Section 8 are recorded by the assessor.

Even though the evaluation of the risk level concluded by the assessor retains a level of subjectivity, the guidelines provided in the manual to the form attempt at reducing the variability between the basis of judgement of different assessors. While the building characteristics identified through the AeDES form, and the resulting risk rating, can be indicative of a level of seismic vulnerability, the qualitative nature of the assessment, and the intrinsic subjectivity of the rating, make the form inappropriate for the assessment of the seismic vulnerability of structures, unless it is revised to include a calibration of the data collected from the respective sections, or accompanied by detailed structural calculations.

Another Form [82], originally developed by the GNDT and the Structural Engineering Department of the Politecnico di Milano, guides the assessor to evaluate the main characteristics of the site where the building is located, which characteristics could have a direct bearing on the building's seismic response, and hence its seismic vulnerability. The information recorded includes mainly the site morphology, the surface geology and the ground formation layers present at a distance greater than 2 m from the surface, the hydrology of the site (the presence of water courses, streams or wells), and the risk of landslides and/or erosion. No seismic vulnerability rating can be obtained directly from the Form. Hence, its use during a broader seismic vulnerability assessment would be limited to provide a standard checklist for the collection of information describing the characteristics of the site, and to facilitate the correlation of the characteristics of different sites, and the different degrees of damage recorded in the overlying buildings.

A more detailed version of this Form was developed subsequently by Di Capua et al. [83] as part of the Relius Project which, apart from the morphological characteristics, also allows for the geotechnical and geophysical characterisation of the site, and the preliminary estimation of the amplification effect of the site through the definition of the 'amplification factor', in line with the Italian national and regional regulations. While a complete assessment would require a number of on-site tests, laboratory investigations and an H/V spectral ratio assessment of ambient noise, in the context, and within the area of expertise of the present study, the main additional ground characteristics recorded in the detailed form, which are of particular relevance, are the thickness, and the angle of inclination of the ground strata. As explained by the authors, the variation in the properties of the ground formation layers overlying the bedrock, and in the topography of the site, can result in the alteration of the frequency and amplitude characteristics of a seismic excitation, and can, hence, have a determining effect on the different seismic response exhibited by buildings of the same typology during the same seismic event. This Form finds its scope in both pre- and post-event scenarios. Possible uses range from the evaluation of the seismic risk of an area to the post-earthquake safety for use and damage assessments, where the degree of damage can be correlated with the characteristics of the respective sites.

2.4 Seismic Vulnerability Assessment Methods in Use in the United States

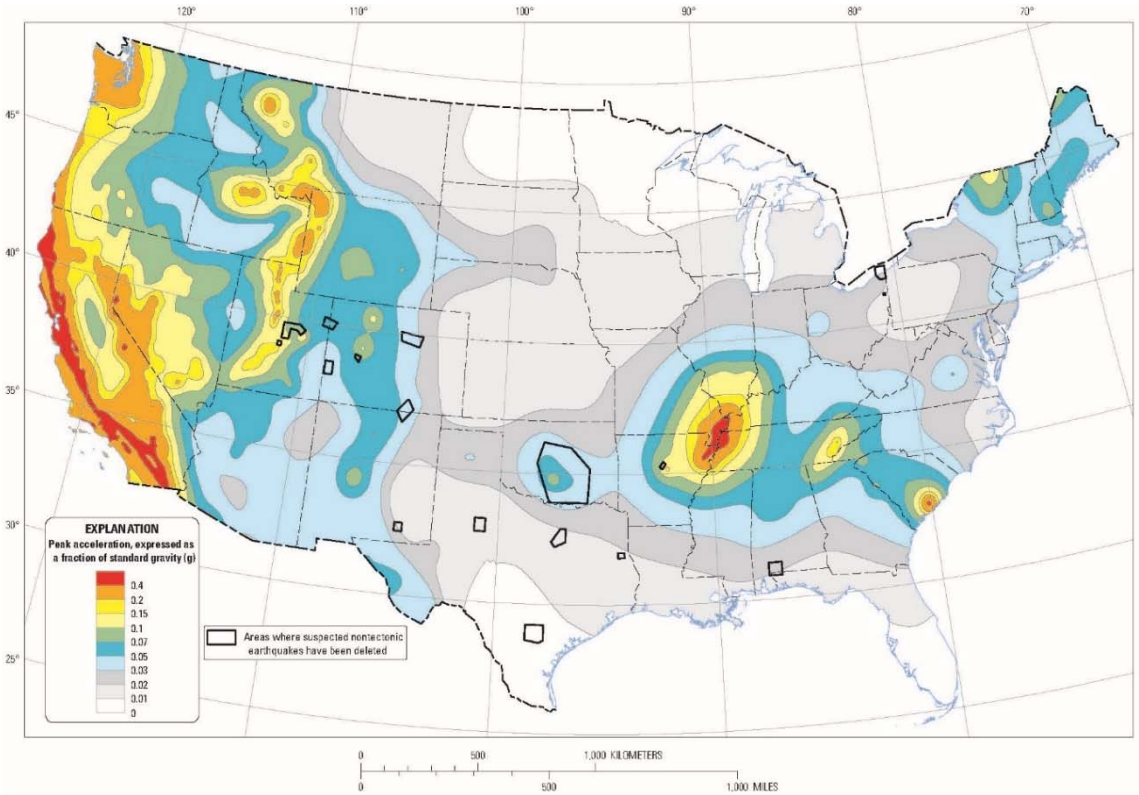

Figure 2-6 U.S. Geological Survey (USGS) 2014 National seismic hazard map of the United States for a 10% probability of exceedance in 50 years (ftp://hazards.cr.usgs.gov/web/nshm/conterminous/2014/2014pga10pct.pdf).

The varying degree of seismicity of the United States is evidenced by the 2014 U.S. Geological Survey (USGS) National seismic hazard map of the United States [84], which is reproduced in Figure 2-6. The occurrence of a number of major earthquakes hitting various regions from California (Fort Tejon M7.9,

1857; San Francisco M7.9, 1906; Loma Prieta M6.9, 1989; Northridge M6.7, 1994 [85]; South Napa M6.0, 2014) and Hayward Fault (M6.8, 1868) to New Madrid (1811-1812) and Virginia (M5.8, 2011) [86], explains the continuous research efforts and funds devoted to the development and updating of seismic vulnerability assessment methods in the United States. Apart from the Earthquake Model of the HAZUS®-MH (HAZards U.S. MultiHazard) software [87] released by FEMA under a contract with NIBS (National Institute of Building Sciences) for the estimation of potential losses resulting from earthquakes, FEMA 450/451 [88] [89] and FEMA 454 [57] recommendations for the seismic design of new buildings, and the FEMA P-58-1, 2 [90] [91] performance-based assessment methodology for new and existing buildings, FEMA 154 [27] [92] and ASCE/SEI 41-13 [93] (and its forerunner, ASCE /SEI 31-03 [61]) provide a rapid and a more detailed assessment method of the seismic vulnerability of existing buildings, respectively.

The Earthquake Model of HAZUS®–MH software [87] estimates the potential '*damage to'* the built environment: *'buildings, essential facilities, transportation, utility lifelines*', the direct and indirect *'economic loss and social impact*' (such as, the number of expected casualties and the required provision for alternative accommodation for displaced households) and the induced losses (such as, damage due to fire, inundation, hazardous material release and debris) '*from* (the) *earthquake…hazard'* ([94] p.2). The considered earthquake hazard is obtained either from a single earthquake scenario or through a statistical analysis of past seismic occurrences in the region under study, hence finding its main scope in the pre-earthquake planning phase of emergency response operations, in economic loss estimates and in the evaluation and reduction of seismic risk. While reference to FEMA 450/451 [88] [89], FEMA 454 [57] and FEMA P-58-1, 2 [90] [91] can be found in other sections of this thesis, the rapid assessment method presented in FEMA 154 [27] [92] was considered to be more relevant to the present study, and hence, a brief overview of this document will ensue in Section 2.4.1.

2.4.1 FEMA 154: Rapid visual screening of buildings for potential seismic hazards

The FEMA 154 (second edition) [27] procedure is intended to provide users with a quick seismic vulnerability assessment method which, through an external visual survey, allows for the categorisation of buildings into those which are acceptable 'with respect to the risk to life safety' [27] and, if a final score of 2 (or alternative cut-off score determined by the investigating authority) or less is obtained, those which could be potentially-hazardous during a seismic event, hence requiring a more detailed seismic assessment. Three different forms are available for the 'Low', 'Medium' and 'High' seismicity regions of the United States as reproduced from FEMA 310[2]. The method consists of a score assessment procedure, where a 'Basic Structural Hazard Score' is assigned based on the construction

[2] FEMA 310 was replaced by ASCE/SEI 31-03 in 2003, which was, in turn, subsequently replaced by ASCE/SEI 41-13 in 2014.

typology, the lateral force–resisting system and construction methods and materials applicable to every seismicity region, assuming a low-rise building constructed on soil type B (rock) [95]. This basic score is modified through the addition (or deduction) of 'Score Modifiers' attributed to the following four building characteristics, which characteristics, when present, are expected to influence the seismic response of the building typologies expressed by the 'Basic Structural Hazard Scores':

a) Number of storeys: Two separate score modifiers are specified for mid-rise buildings having a height of four to seven storeys, and for high-rise buildings which are higher than seven storeys. While a score modifier of -0.6 is specified for mid-rise unreinforced masonry buildings, in 'low' seismicity regions similar to the Maltese Islands, no score modifier for high-rise buildings is specified for this typology, on the assumption that unreinforced masonry buildings do not exceed a height of seven storeys. The presence of unreinforced masonry loadbearing buildings with an overall height of more than seven storeys cannot be excluded in the Maltese Islands.
b) Vertical irregularity: This parameter mainly accounts for the deleterious effect, on the seismic resistance of structures, of variations in lateral storey stiffness throughout its height. The vertical irregularities considered in FEMA 154 (second edition) [27] include the presence of setbacks, soft storeys, and hillside buildings (which could lead to a differential stiffness in the lower levels due to varying column/wall heights along the sloping terrain, or a different degree of restraint to horizontal displacement throughout the floor levels which are partially below ground). A 'Score Modifier' of -1.5 is attributed to the presence of one or more of these vertical irregularities in the case of unreinforced masonry buildings in 'low' seismicity zones.
c) Plan irregularity: The irregularities considered by the 'Score Modifiers' include plan shapes with re-entrant corners, which could give rise to stress concentrations, and building layouts which provide a different resistance to seismic forces, or a significantly-different stiffness of the main resisting members in the two main orthogonal directions. Examples of such irregularities are wedge-shaped buildings, or corner buildings where two of the facades include openings, while the other two facades are solid. It is not clear whether other plan irregularities which result in eccentricities between the centre of resistance and the centre of stiffness, apart from the examples given in the handbook to the FEMA 154 method (second edition) [27], such as the presence of a narrow and long plan layout, are considered in the estimation of the 'Score Modifier' for this parameter. However, the inclusion of a significantly longer list of possible plan irregularities in the subsequent edition of the manual, FEMA P-154 (third edition) [92], suggests that plan irregularities arising from narrow and long plan configurations are ignored in the second edition of this assessment method. A 'Score Modifier' of -0.8 is assigned if one or more of the plan irregularities considered by the FEMA 154 (second edition) [27] procedure is present in the surveyed building.
d) Soil types C (soft rock, very dense soil), D (stiff soil) and E (soft soil): The 'Score Modifiers' corresponding to these soil types take into account the modification in the seismic ground motion accelerations, and the consequent expected increase in damage, resulting from soil types, which are less stiff by varying degrees than soil type B. Increasingly negative 'Score Modifiers' are assigned to soil types C, D and E (-0.4, -0.8 and -1.4 respectively for unreinforced

masonry buildings in 'low' seismicity regions), thus reflecting the increase in amplification of the seismic vibrations with reduction in soil stiffness. However, this method takes into consideration only a single soil layer and, hence, ignores the additional effects caused when overlying layers with different material properties are present.

In addition to the above, two 'Score Modifiers' are specified for 'Pre-code' and 'Post-benchmark'. These are related to whether the building under assessment was designed and constructed before or after the seismic codes, corresponding to the building typology being surveyed, were in force, and had been updated. Since the 'Basic Structural Hazard Score' for 'low' seismicity regions is based on buildings constructed before the introduction of seismic codes, the 'Pre-code' modifier is not applicable in the case of buildings located in 'low' seismicity zones.

The 'Basic Structural Hazard Scores' and 'Score Modifiers' were generally obtained from the HAZUS (1999 SR2 edition) fragility curves of the structural typologies considered in the FEMA 154 assessment method (second edition) [27] and, together with the Final Score, are associated with the probability of building collapse in the event that the maximum seismic action occurs at the site. However, FEMA 155 (second edition) [95] explains that the wide range of possible building forms and characteristics, which could lead to a vertical irregularity, conditioned the estimation of 'Score Modifiers' for this building deficiency to be based on expert knowledge. In the case of 'High' and 'Moderate' seismicity regions, the 'Score Modifier' assigned to this building attribute alone leads to a final score below the cut-off score of 2, hence leading to the requirement of a detailed assessment. Furthermore, in the estimation of the 'Score Modifier' associated with the presence of plan irregularities, a seismic action of a higher magnitude was adopted in order to achieve a similar increase in seismic vulnerability as would result from eccentricities between the centre of resistance and the centre of mass.

FEMA 154 (second edition) [27] considers a seismic action with a 2% probability of exceedance in 50 years (equivalent to a 2,475 year average return period), multiplied by a factor of 2/3, in order to obtain the 'Maximum Considered Earthquake' (MCE) ground motions in accordance with FEMA 310. This seismic action is, therefore, likely to be more severe than that complying with the recommended design seismic action for the No Collapse Requirement, to be used in the absence of a National Annex in accordance with Clause 2.2(1)P of Eurocode 8: Part 1 [4], where a 10% probability of exceedance in 50 years (equivalent to a 475 year reference return period) is specified.

The URM building typologies considered in FEMA 154 (second edition) [27] have the following general characteristics:

i. a height of one to six storeys;
ii. timber floor and roof diaphragms;
iii. wall thicknesses in residential buildings of 228 mm in the upper storeys and 457 mm in the lower floors;
iv. weak mortar used in the construction of walls, including very little cement.

These characteristics suggest that the direct application of the FEMA 154 (second edition) [27] rapid assessment method without prior modification of the 'Basic Structural Hazard Scores' and 'Score

Modifiers' to URM buildings with different construction characteristics, can lead to inconclusive results. Furthermore, in the case of the vertical and plan irregularity 'Score Modifiers', while the number of possible building characteristics considered in FEMA 154 (second edition) [27] which could give rise to these irregularities is not very exhaustive, this seismic vulnerability assessment method does not take into account the increase in severity of the resulting vulnerability level when more than one type of vertical or plan irregularity is present.

The 2015 revised version of the FEMA P-154 procedure (third edition) [92][3] attempts to address the shortcomings of the second edition. While keeping the rapid screening format of the second edition, the revised form considers five seismicity regions, instead of the three regions considered in the previous version, and allows for a first level assessment, and an additional, optional, second level check.

FEMA P-154 (third edition) [92] considers a seismic action equivalent to the 'risk-targeted Maximum Considered Earthquake ground motions' (MCE_R), which take into consideration the probability of damage which could pose a risk to life during a particular time span, as opposed to the single magnitude of seismic action considered in MCE ground motions in FEMA 154 (second edition) [27] [96]. In the first level assessment, the presence of a geological hazard (the risk of liquefaction, landslide or surface fault rupture, or the presence of soil type F, poor soil), inadequate separation gaps between adjacent buildings (hence, leading to the risk of damage due to pounding), the risk of a falling hazard from a nearby building, or a significantly-damaged state of the surveyed building, would automatically require a detailed structural evaluation. Furthermore, while the 'Basic Score' (a revised version of the 'Basic Structural Hazard Score' of the second edition) was based on a soil type CD, which is an average between soil types C and D, 'Score Modifiers', corresponding to a more comprehensive list of seven vertical irregularities (which are further subdivided into 'severe' and 'moderate' irregularities), five plan irregularities and the influence of soil types A / B or E, are specified. The vertical irregularities considered in the handbook are: (i) the presence of a sloping site, (ii) a weak or soft storey, (iii) cripple walls, reduced wall areas due to the presence of large openings, (iv) out-of-plane setbacks, (v) in-plane setbacks, (vi) short column or pier due to infill walls and/or the presence of windows or door openings, and (vii) misaligned slab levels in adjacent buildings. The five plan irregularities considered include: (i) layouts which result in the formation of torsional forces, such as significantly different stiffness or lateral load resistance in the two main orthogonal directions, (ii) buildings with plan configurations, where the facades do not meet at 90° , hence leading to torsional forces, (iii) plan shapes with re-

[3] The work reported in this thesis, which is related to the FEMA 154 seismic vulnerability check, had already been completed by January 2015, when the third edition of the handbook [92] was issued. Hence, unless otherwise stated, any reference to the FEMA 154 rapid assessment method in Chapters 3 and 4 of this thesis refers to the second edition published in March 2002 [27]. Information on the third edition included in this Section was limited to a review of the main differences between the two versions of the methodology, and the additional factors considered in the latest edition, considered of particular relevance to the current Section.

entrant corners, (iv) the presence of openings in the floor and roof slabs, and (v) beams which are not centred on the supporting columns. 'Pre-code' and 'Post-benchmark' scores were retained from the previous version, though their values were updated. The separate 'Score Modifiers' linked to the number of storeys of the second edition are no longer present, and are instead replaced by two 'Score Modifiers' for soil type E, for buildings which have a height of one to three storeys, or higher than three storeys, respectively. Unlike its forerunner, the FEMA P-154 (third edition) [92] first level assessment includes a minimum score, which considers the worst combination of parameters for every structural typology in the context of the United States.

The second level assessment is based on the final score obtained through the first level assessment. However, it requires the subtraction of the level one 'Score Modifiers' for vertical and plan irregularities, thereby resulting in an 'adjusted baseline score'. The distinct 'Score Modifiers' assigned in the second level check, to the different types of vertical and plan irregularities, the presence of redundancies in the lateral-force resisting elements, the risk of pounding and, in the case of unreinforced masonry buildings, the presence of gable walls and seismic strengthening measures, are added (or subtracted) from this baseline score to obtain the second level final score. While the same vertical and plan irregularities are considered in the first and second level assessments, in the second level check, it is possible to take into account the added vulnerability associated with the presence of more than one irregularity from the same category. Furthermore, an additional 'Score Modifier', corresponding to any 'other irregularity', is present in both vertical and plan irregularity categories. This automatically covers all possible irregularities, which could be present in the surveyed building. On the other hand, in order not to overestimate the cumulative effect of the different types of irregularities, 'Score Modifiers' for plan and vertical irregularities in the level 2 check are subjected to a maximum 'capping' value. This maximum score can, however, also be considered to limit the proper representation of the different ranges of seismic vulnerability, in the case of a building typology, which could include two or more vertical or plan irregularities. A recommended cut-off score of 2 is applicable to both the first and second level assessment methods.

Furthermore, it should be noted, that the Eurocode 8: Part 1 [4] No Collapse Requirement defined in Clause 2.1(1)P for the design of new structures is centred on assuring that the seismic response of a structure does not result in 'local or global collapse', hence 'retaining its structural integrity and a residual load bearing capacity after the seismic events' [4]. The corresponding Limit State for Significant Damage as defined in Eurocode 8: Part 3 [97] Clause 2.1(1)P and based on the same recommended return period of 475 years (equivalent to a 10% level of exceedance in 50 years), refers to a significantly-damaged structure which, however still retains some residual capacity. FEMA P-154 (third edition) [92] is centred on the evaluation of the risk to collapse, which could be partial or complete and is the direct result of dynamic instability arising from significant displacement.

2.5 Other Methods

The damage probability index method involves the estimation of the probability of a structural typology achieving a particular level of damage when subjected to a seismic event of fixed intensity

through Damage Probability Matrices (DPM). While damage probability matrices are usually based on a vast database of damage data from past earthquakes, which are not available in the case of the Maltese Islands, Camilleri [7] proposed a mean damage ratio corresponding to MSK intensities V to XI for seven different building typologies present in Malta and Gozo. Following the consideration of the irregularities in stiffness and layout which are typically present in local constructions, the author applied a number of 'enhanced factors 'F_{ri}', corresponding to the increase in expected damage ratio for every type of irregularity, which factors were obtained from a Swiss Re Zurich handbook on risk assessment with respect to the risk from earthquakes and volcanic eruptions [98]. Based on the assumption of a low variation in the degree of irregularity and asymmetry in Maltese constructions, the author proposed a damage probability matrix for the Maltese Islands, which is hereby reproduced as Table 2-9. The significant influence which the construction materials and construction details, corresponding to a particular building typology, have on its resistance and behaviour under seismic actions, raise concerns regarding the direct use of generalised factors without prior calibration with respect to the particular typology under study. In this regard, the author of this thesis is not aware of any numerical verifications carried out to date on the values reported in this table.

Table 2-9 Damage probability matrix for buildings in the Maltese Islands proposed by Camilleri ([7] p.28).

Damage class % of value			Mean damage ratio (MDR) (%)									
			1.5	3	5	10	25	37.5	50	60	70	85
0	-1.5	(A)	83	73	60	36	9	2				
1.5	-3	(B)	17	25	26	23	9	3				
3	-6	(C)		2	10	18	11	5	2			
6	-12.5	(D)			3	12	18	12	6	2	1	
12.5	-25	(E)			1	8	24	24	15	7	3	
25	-50	(F)				3	19	28	29	23	18	10
50	-100	(G)				1	10	29	48	68	78	90

As an alternative method for the estimation of the probability of damage, which overcomes the limitations of the damage probability matrices, Giovinazzi and Lagomarsino [99] proposed a correlation between the damage probability matrix method and the vulnerability index method, through the construction of damage probability matrices corresponding to the EMS-98 [100] vulnerability classes, and corresponding vulnerability curves for every class and construction typology. The authors, hence, developed an analytical equation, which expresses the degree of damage as a function of the vulnerability index and the macroseismic intensity, hereby reproduced as Equation 2-3,

$$\mu_D = 2.5\left[1 + tanh\left(\frac{I + 6.25V - 13.1}{2.3}\right)\right]$$

Equation 2-3

where, μ_D is the mean damage grade, I is the macroseismic intensity in accordance with EMS-98 [100] and V is the vulnerability index.

On the other hand, the FaMIVE (Failure Mechanism Identification and Failure Evaluation) automated procedure, developed by D'Ayala [65] and D'Ayala and Speranza [101], consists of a 'limit state lower

bound analysis of the external' [101] loadbearing envelope of masonry buildings, through the identification of the most likely failure mechanisms from the program's database (based on the wall restraints and the materials used in the wall construction), and the estimation of the corresponding ultimate failure load factor (the 'equivalent shear capacity', worked out as a percentage of the gravitational force) for the horizontal seismic forces acting at slab levels throughout the building height. Hence, based on the comparison of the location's expected earthquake intensity, (in terms of the design peak ground acceleration expressed as a percentage of the acceleration due to gravity), to the lowest ultimate failure load factor resulting from the considered failure mechanisms, an estimate of the seismic vulnerability of the structure under assessment can be obtained.

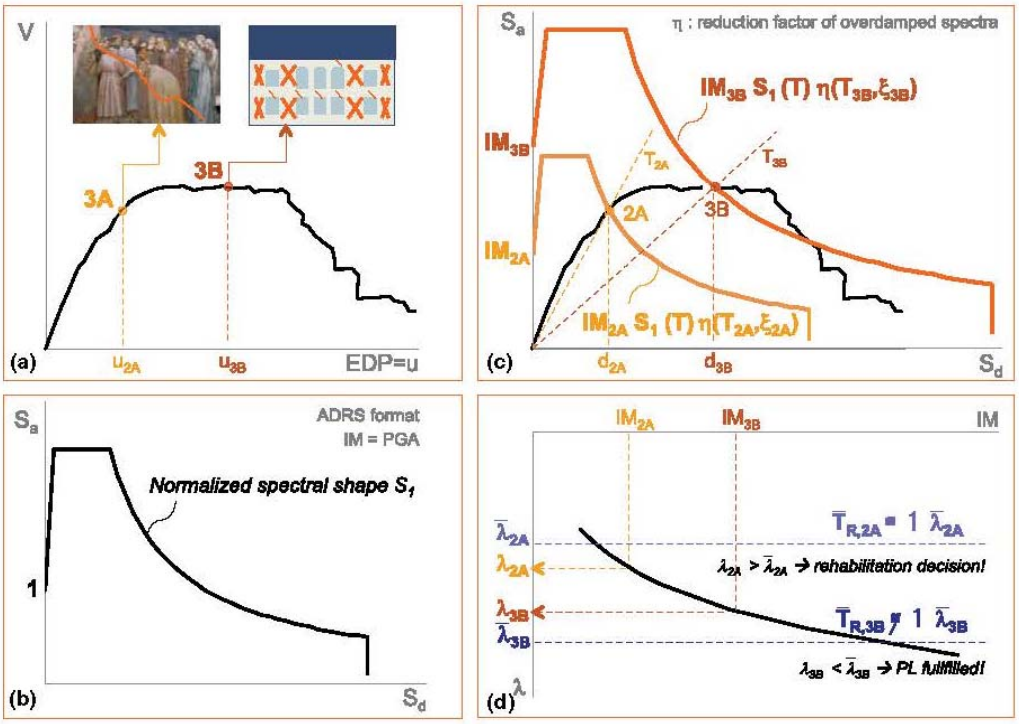

Figure 2-7 Outline of the main stages of the performance-based assessment of architectural and artistic assets proposed in the PERPETUATE Project by Lagomarsino and Cattari ([102] p.17).

Furthermore, a displacement-capacity approach, within the context of a performance-based assessment of the seismic vulnerability of historic buildings, was proposed in the PERPETUATE European research project [102], where the displacement at a particular position of the structure, considered as the 'Engineering Demand Parameter' (EDP), (corresponding to target Performance Levels), is identified on the pushover curve, in the case of non-linear static analysis, or on the incremental dynamic analysis curve (IDA), if a non-linear dynamic analysis is performed. Seismic demand is defined through the acceleration-displacement response spectrum of the site in the case of non-linear static analysis, or through the use of multiple ground motion records for non-linear dynamic analysis. Following the definition of the seismic demand as a function of the intensity measure (such as, peak ground acceleration) of the location of the building under assessment, the maximum intensity measure corresponding to every target performance level (IM_{PL}) is evaluated and this is cross-checked

with the hazard curve to obtain the yearly probability of exceedance of the corresponding earthquake intensity for the site. The main stages of the PERPETUATE procedure are summarised in Figure 2-7.

2.6 Aggregate Effect

The manual to the GNDT first level assessment [69] explains that an 'aggregate', as defined by the Italian Department of Civil Protection, is a group of individual structures consisting of different layouts and building characteristics, which can, however, exhibit a combined response to a static or dynamic action. This combined response is achieved through an effective connection between the individual structures. A separation gap between the structures, which complies with the dimensions specified in the appropriate regulations for the design of buildings under static and seismic loading, indicates the presence of two separate distinct aggregates. The 'aggregate effect' is, hence, the altered structural response to seismic actions resulting from the position and the interaction of a structure with the other buildings in the aggregate.

Benedetti and Petrini [70] acknowledge that the presence of a building within an aggregate could alter its seismic vulnerability. However, the authors explain that the behaviour of the resulting complex structure is influenced by a variety of factors, which go beyond the characteristics of the single building unit. The complexity of the behaviour, and the broad range of possible scenarios, make it very hard to establish the influence of the aggregate effect on the seismic vulnerability of the single building unit. The authors, therefore, suggest that scores can only be attempted on a case-by-case basis, following the completion of the Form for all the single units, which make up the aggregate. Benedetti and Petrini [70] also suggest that the cases when party walls are shared must be distinguished from those where separate party walls are present for each building, even though these walls might not be separated by an adequate joint.

While the GNDT second level assessment [26] does not include any consideration of this effect, the Regione Toscana Form for the assessment of deficiencies in masonry buildings [75] partially takes into account the influence of adjacent buildings through Deficiency Category (i) where, in the assessment of the adequacy of the wall area resisting seismic actions at every floor level, when the building under examination shares its party wall with an adjacent structure which, in turn, has slabs spanning on this common wall, then half the span of these slabs in the adjacent building must be added to the floor area of the storey level under assessment of the test building. Furthermore, Deficiency Category (iii) considers also the intermediate and roof slabs of the adjacent construction in the assessment of the seismic resistance deficiency, related to the presence of misaligned floors on opposite sides of a common wall. Such a misalignment of slab levels could give rise to a 'hammering effect' on the common wall and, depending on the magnitude of the shift between the respective slab positions on the opposite sides of the wall, to either flexural or shear failure of the common wall.

In the context of the Maltese Islands, Bonello [21], Zammit [22] and Azzopardi [23] studied the seismic resistance of two-, three- and four-building aggregates considering contemporary loadbearing unreinforced masonry buildings constructed in globigerina limestone or hollow concrete blockwork masonry, with plan length-to-width ratios of 2:1, 4:1 and 6:1 and mortar grades of 2 N/mm^2, 3.5 N/mm^2

and 5 N/mm^2 through an adaptation of the Equivalent Frame Method proposed by Bhowmik and Mohanty [103] for the consideration of a whole building aggregate. The results obtained by Bonello [21] show that masonry buildings constructed in globigerina limestone exhibit a significantly higher increase in seismic resistance (of around 150%) when located within an aggregate when compared to the individual building case than equivalent structures constructed in hollow concrete blockwork masonry. On the other hand, in the presence of lower mortar strengths and weaker subsoils (such as in the case of clay), the exhibited increase in seismic resistance due to the presence of the structure within an aggregate is negligible, resulting in no increase in the maximum allowable building height. Furthermore, Zammit [22] showed that building characteristics which alter the lateral storey stiffness throughout the building height of the masonry structures (in particular, the presence of setbacks at the topmost storey and a double height space between the ground floor and the first floor of the structure) result in a reduction of one to five storeys in the maximum allowable building height for collapse resistance when present in a two-, three- or four-building aggregate when compared to the cases investigated by Bonello [21], which exhibited a regular lateral storey stiffness throughout their height. In both studies [21] [22], the two-building aggregate configuration results in the highest rate of strength increase whereas, for larger aggregates, the beneficial effect on the seismic resistance resulting from the increase in building aggregate sway stiffness is counteracted by the increase in building aggregate mass which, therefore, leads to higher lateral shear forces which, in addition to the higher torsional forces, does not allow an appreciable higher seismic resistance to be achieved. Bonello [21] also showed that the structures positioned at the outer edges of the building aggregate resist most of the torsional moments, hence, resulting in a lower overall maximum allowable building height than the central structures. This was also confirmed by Azzopardi [23] in terms of maximum heights for resistance of collapse. In addition, Azzopardi [23] concluded that the misalignment of transverse walls in adjacent masonry buildings located within a building aggregate generally results in an increased seismic resistance, which is exhibited either only in terms of a lower interaction ratio in the main piers of the structures, or in a higher maximum number of floors for collapse resistance in conjunction with a lower interaction ratio in the main piers. However, the results obtained by Azzopardi [23] also suggest that masonry aggregates with misaligned transverse walls in adjacent buildings, constructed using hollow concrete blockwork masony and a mortar grade of 2 N/mm^2, on a clay subsoil, would not exhibit any increase in seismic resistance when compared to the corresponding aggregates investigated by Bonello [21] with aligned transverse walls.

In addition, an investigation was carried out by Said [24] on the seismic resistance of contemporary URM structures with plan length-to-width ratios of 1:1, including a soft storey at the lowest level when located in a two-building aggregate. The results from this study suggest that, while an increase in seismic resistance is exhibited when the structure is considered as acting in combination with another structure (with an identical plan configurations and overall height), when compared to the resistance of an isolated building on a rock subsoil, the increase in resistance is not enough for the structure to sustain an additional storey prior to failure, in comparison to the single building case.

Table 2-10 Studies investigating the seismic response of buildings in aggregates through numerical modelling (Part 1).

Publication year	Study	Numerical modelling method	Analysis technique	Software program	Study details
2010, 2011, 2015	Formisano et al. [28] [29] [30] [31]	Frame by macro-elements (FME)	Non-linear static (pushover) analysis	3Muri®	Determination of the parameter weightings through the comparison of the resulting ratio of maximum displacement (demand) to ultimate displacement (capacity) for isolated building vs. building response in an aggregate. 5 Parameters which can influence the seismic response of buildings in an aggregate investigated.
2015	Maio et al. [104]	Frame by macro-elements (FME)	Non-linear static (pushover) analysis	3Muri®	Analysis of model representing whole aggregate and comparison to seismic vulnerability index resulting from methods proposed by Vicente et al. [105] and Formisano et al. [28]. Good correlation between results. The method proposed by Formisano et al. [28] results in a lower probability of damage associated with EMS-98 intensities VII, VIII and IX.
2014	Maio et al. [106]	Frame by macro-elements (FME)	Non-linear static (pushover) analysis	3Muri®	Investigation of the seismic response of an aggregate consisting of row development of 6 historic masonry buildings in San Pio delle Camere. Comparison to seismic vulnerability index resulting from methods proposed by Vicente et al. [105] and Formisano et al. [28]. The method proposed by Vicente et al. [105] results in a marginally higher seismic vulnerability index.
2012	Marques et al. [107]	Frame by macro-elements (FME)	Non-linear static (pushover) analysis	TREMURI (research version)	Study of three scenarios for a contemporary masonry structure: independent buildings, a 3-building aggregate consisting of buildings of the same height with all buildings aligned and a 3-building aggregate including buildings of the same height, which are misaligned with respect to each other. No increase in resistance is exhibited by the structures when modelled in the aggregate and no decrease in base shear results, but a 20-40% decrease in displacement capacity is noted.

Table 2-11 Studies investigating the seismic response of buildings in aggregates through numerical modelling (Part 2).

Publication year	Study	Numerical modelling method	Analysis technique	Software program	Study details
2010	Senaldi et al. [108]	Frame by macro-elements (FME)	Non-linear (incremental) dynamic analysis, 7 real accelero-grams scaled to the p.g.a. of response spectrum	TREMURI (research version)	Investigation of response of single room and two-room units in row developments of 3, 5 and 9 units when compared to the corresponding isolated building cases. The influence of flexible horizontal structural systems was also investigated.
2007	Rush [109]	Frame by macro-elements (FME)	Non-linear static (pushover) analysis	TREMURI (research version)	Investigation of the influence of 5 parameters on the seismic vulnerability of buildings within an aggregate, namely: a) wall stiffness; b) building height; c) weight of building and stiffness of the horizontal structural systems; d) connection between adjacent buildings; and e) position of building in aggregate. Results suggest that (b) and (d) have the highest bearing on the seismic response.
2004	Ramos and Lourenço [110]	Finite Element Analysis	Non-linear static analysis	DIANA®	Study of aggregate consisting of 18th century masonry 'Pombaline' buildings. Internal walls and intermediate timber roof/floor structures were not included in the numerical model. Results suggest that the buildings, which do not include rigid horizontal structural systems, are more vulnerable. Buildings modelled within an aggregate are less flexible and have a higher safety factor than when modelled as isolated.

The results from studies involving the numerical modelling of aggregates under seismic actions, summarised in Tables 2-10 and 2-11, show that the location of the building in the aggregate (whether in the middle or at the end), together with the characteristics of the buildings, which are directly adjacent to the building under evaluation (particularly with respect to the variation in stiffness, height, the risk of pounding and the rigidity and misalignment of the horizontal diaphragms), can either provide additional restraint to the displacement of the assessed building - hence resulting in an improved seismic resistance - or lead to a premature failure, as in the case when local failure due to pounding occurs. Apart from the factor related to the geographical location of most of the quoted studies in Tables 2-10 and 2-11, the main reason behind the selection of the macroelement modelling and the non-linear static (pushover) analysis, in most of the reviewed studies, is the lower

computational effort required to carry out such analyses for large scale models. The non-linear time-history analysis of more refined spatial models of aggregates, though possible, would require higher processing power and longer analysis durations.

Table 2-12 Parameters proposed by Formisano et al. [28] [29] [30] [31] as an extension to the Benedetti et al. [70] seismic vulnerability assessment method for the consideration of the aggregate effect in the seismic vulnerability evaluation of buildings ([30] p. 12).

Parameter number	Parameter description	Class scores				Weightings
		A	B	C	D	
1	Presence of adjacent buildings with different height	-20	0	15	45	1
2	Position of the building in the aggregate	-45	-25	-15	0	1.5
3	Number of staggered floors	0	15	25	45	0.5
4	Structural heterogeneity among adjacent structural units	-15	-10	0	45	1.2
5	Percentage difference of opening areas among adjacent facades	-20	0	25	45	1

Formisano et al. [28] [29] [30] [31] also used a numerical modelling method, which is based on a frame-by-macroelement representation of masonry structures, for the calibration of the construction scenario class scores, and parameter weightings corresponding to their proposed five additional parameters, which were intended as an extension of the Benedetti and Petrini assessment method [70]. The five proposed parameters, which are reproduced in Table 2-12, together with the class scores and parameter weightings, result in the refinement of the seismic vulnerability index with respect to the influence of the aggregate effect in the seismic vulnerability evaluation of buildings located in aggregates. Through the assignment of negative and positive scores, corresponding to the different construction scenarios, this method captures the variability of the influence which characteristics, such as the height and stiffness of adjacent structures and their facades, and the position of the building in the aggregate, can have on its seismic response. Even this proposed method considers masonry typologies present in historic centres, therefore, resulting in class scores and parameter weightings, which cannot be applied directly to newer constructions without prior recalibration. The seismic resistance of the structures was assessed by the authors through the numerical analysis of the different scenarios for the investigation of the seismic vulnerability variation in the presence of the five proposed additional building attributes. The response parameters (the maximum horizontal displacement, representing the earthquake demand, and the ultimate building displacement, representing the building capacity) extracted from the numerical models were then used for the determination of the corresponding weightings and class scores of the five proposed additional parameters. Hence, while class scores and parameter weightings would have to be recalibrated if the method is applied to a different masonry building typology, the overall enhancement or deterioration of the seismic resistance resulting from the presence of particular building characteristics, remain applicable.

Table 2-13 Parameters, class scores and parameter weightings of the vulnerability index method proposed by Vicente et al. [105] for the seismic vulnerability assessment of masonry buildings in aggregates for the historical city centre of Coimbra, Portugal.

Parameter number	Parameter description	Vulnerability class C_{vi}				Weightings
		A	B	C	D	p_i
P1	Type of resisting system	0	5	20	50	0.75
P2	Quality of resisting system	0	5	20	50	1
P3	Conventional strength	0	5	20	50	1.5
P4	Maximum distance between walls	0	5	20	50	0.5
P5	Number of floors	0	5	20	50	1.5
P6	Location and soil condition	0	5	20	50	0.75
P7	Aggregate position and interaction	0	5	20	50	1.5
P8	Plan configuration	0	5	20	50	0.75
P9	Regularity in height	0	5	20	50	0.75
P10	Wall openings in alignment	0	5	20	50	0.5
P11	Horizontal diaphragms	0	5	20	50	1
P12	Roof system	0	5	20	50	1
P13	Fragilities and conservation state	0	5	20	50	1
P14	Non-structural elements	0	5	20	50	0.5

Vicente et al. [105] proposed another method which is based on the GNDT second level assessment vulnerability index methodology [26], but which includes a re-arrangement of the sequence of evaluated parameters and an alteration of most of the parameter weightings and the class scores corresponding mainly to construction scenario Classes C and D, when compared to the GNDT level 2 assessment method. Moreover, the method proposed by Vicente et al. [105] takes into consideration three additional parameters aimed at assessing the alteration in seismic vulnerability, resulting from the aggregate effect. The assessment of seismic vulnerability is thus based on a total of 14 parameters as reproduced in Table 2-13. The additional parameters considered by this method include the number of floors, the position of the building in the aggregate, and the presence and alignment of wall openings. While, as in the method proposed by Benedetti and Petrini [70], the weightings for the 14 parameters seem to be based on the relative degree of importance of the different parameters, the referenced study, however, does not mention any numerical analyses carried out for the verification of these weightings, and does not include details of the criteria corresponding to the different construction scenario classes for every parameter, hence making the re-calibration and use of an adapted form of this method for the seismic vulnerability assessment of a different masonry building typology highly unlikely.

Moreover, another vulnerability index method proposed by Ferreira et al. [66], which considers only five parameters (reported in Figure 2-14), attempts to evaluate the seismic vulnerability of the aggregate as a whole, and not that of a building within an aggregate. This method is based on the assumption that buildings within an aggregate are constructed in similar materials, and using similar construction details. In the case of the first three parameters, it associates an increase or decrease in

seismic vulnerability (corresponding to a progression from Class A to D) with the percentage number of buildings within the aggregate, which include, or do not include, the undesired, or desired, particular building characteristics, respectively. While all details pertaining to the construction scenario classes are given by the authors, the referenced study does not explain how the class scores and parameter weightings were derived, and does not propose ranges for the different grades of seismic vulnerability (such as for 'Low', 'Medium' and 'High' ratings) corresponding to this method.

Table 2-14 Parameters, class scores and parameter weightings of the vulnerability index method proposed by Ferreira et al. [66] for the seismic vulnerability assessment of aggregates of masonry buildings.

Parameter number	Parameter description	Vulnerability class C_{vi}				Weightings
		A	B	C	D	p_i
P1	Quality of masonry fabric	0	5	20	50	1.5
P2	Misalignment of openings	0	5	20	50	0.5
P3	Irregularities in height	0	5	20	50	0.75
P4	Plan geometry	0	5	20	50	0.75
P5	Location and soil quality	0	5	20	50	0.75

Furthermore, the University of Padova, developed 'VULNUS', an automated procedure for the assessment of the global seismic vulnerability of regular (in plan and in elevation) low-rise masonry buildings, both when isolated or within an aggregate. The VULNUS procedure is based on the definition of two indices, namely, the I1 index, which consists of the ratio of 'the critical value of the mean seismic acceleration response corresponding to the in-plane resistance of wall systems'… to 'the acceleration of gravity 'g'' [111], and the I2 index, which corresponds to the ratio of the corresponding mean seismic acceleration response to out-of- plane loading, to the acceleration due to gravity 'g'. The method requires the input of information obtained from a detailed survey of the structure/s, through which critical parts of the structure (macroelements), which are likely to fail from in-plane or out-of-plane mechanisms, are identified. Based on this information, the I1 index and the I2 index are evaluated, and the accelerations at the floor levels throughout the height of the building are derived. Furthermore, the combination of indices I1 and I2 with another index I3, which is based on the information gathered for the compilation of the GNDT second level assessment form, results in the determination of the 'probability of heavy damage' for the building or aggregate under evaluation. Munari et al. [111] [112] published a number of studies on the seismic vulnerability assessments of aggregates in historical Italian villages using this methodology. Higher I1 indices than I2 indices, resulting from these studies, suggest a lower resistance of masonry walls to out-of-plane loading. Higher indices were also obtained for buildings which had undergone strengthening measures, and for buildings positioned in an aggregate (though not at the end position), when compared to unstrengthened or isolated buildings, respectively.

Furthermore, studies by Valluzzi et al. [113], Munari et al. [114] and da Porto et al. [115], amongst others, used VULNUS in combination with C-Sisma for the study of masonry building aggregates. C-Sisma is an automated procedure for the identification of the local failure mechanisms of the macroelements, which includes a database with a total of 33 failure mechanisms, typical of wall

constructions. Hence, based on the post-earthquake surveyed damages, the corresponding local failure mechanisms can be identified.

2.7 Numerical Modelling Techniques: FEM, EFM, DEM, AEM

The accurate representation of the stiffness of a structure, its load-resisting system, the connection between different structural members and its load – displacement response, up to a state of progressive collapse, is of utmost importance for the validity of the results of a numerical analysis. The numerical modelling of structures consisting of distinct elements, with virtually no tying action apart from the frictional forces acting between the respective elements, as in the case of unreinforced masonry constructions, poses even greater challenges and, in a context where there is insufficient, or the complete absence of post-earthquake damage data which can be used for the verification of the structural behaviour represented by the numerical model, the identification of the modelling technique, which best reproduces the structural response of a particular building typology, becomes imperative. A review of the four main numerical modelling techniques considered in this study is presented below.

The traditional method used by researchers for the investigation of the behaviour of structures is based on a Finite Element Method (FEM) simulation, where every member in a structure is subdivided into smaller elements (determined through the specified mesh density). Elements are joined to each other at nodes, which can displace, but which, therefore, do not allow the complete detachment of one element with respect to an adjacent element [116], hence leading to limitations in the adequate representation of the formation and propagation of cracks, and in progressive collapse scenarios, when a medium, which is subject to cracking, such as concrete or masonry construction, is modelled. While alternative modelling techniques, such as the use of multiple node IDs at expected crack positions, were proposed, the resulting inaccurate estimation of stresses at the crack position (at the separation of the two nodes), leads to inaccuracies in the rest of the modelled structure. Furthermore, whereas the anticipation of the correct crack pattern, and direction of propagation is not always possible [38], the formation of cracks within a structure leads to a change in the structure's overall stiffness. The 'smeared crack' technique, adopted in FEM models to simulate this variation in stiffness, is reported to result in the accurate estimation of displacements and forces at failure. However, this technique requires very complex models and cannot be applied to simulate the separation between abutting structural members [117]. On the other hand, the 'discrete cracks' technique, where cracks are modelled as separate 'elements', is reported to be more indicated for models, which include a limited number of cracks [41].

Furthermore, the advancement in the techniques used for the representation of the effects of contact between separate surfaces or nodes through different types of contact elements using Finite Element Modelling has led to the accurate simulation of scenarios involving small and large magnitudes of relative sliding and displacement. Nevertheless, this requires a considerable computational effort in order to be applied to the numerical representation of an entire masonry structure with every masonry block represented by 8-node hexahedron elements and the contact between respective blocks being

controlled through specialised discretisations such as the B-Spline surface proposed by Santos and Bandeira [118], or the definition of the applicable contact element case available in commercial software applications, such as ANSYS® [119]. Finite element models tend to be very computationally demanding, particularly when adopted for the representation of masonry structures, in view of the structural and construction details corresponding to such structures, together with the non-linear 'hereditary' [120] (with respect to load and damage history) material behaviour, especially with respect to the deterioration of the structural stiffness and strength under cyclic loading [121]. The complexity of these models is reported to increase in cases of non-linear response and when large displacements are present. This complexity is further aggravated by the distinct nature of the blocks making up every wall panel, with a mortar thickness at the blocks' interfaces, therefore, making the modelling of individual blocks unfeasible in large spatial models.

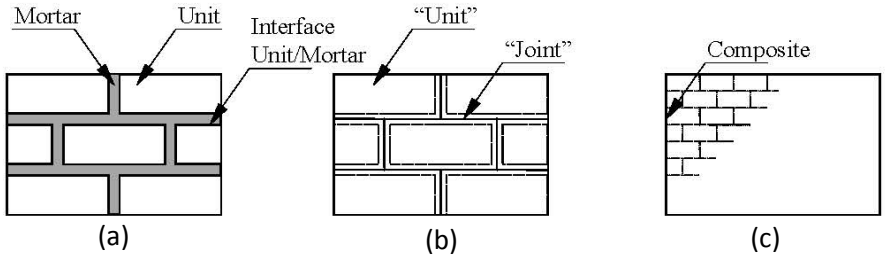

Figure 2-8 Modelling techniques for masonry walls (a) detailed micromodelling (b) simplified micromodelling (c) macromodelling (homogenised continuum) [122].

Hence, in cases where the global model response of a masonry structure is investigated, masonry wall panels are represented through a homogenised continuum, considering an averaged constituent material behaviour for the masonry blocks and the mortar joints. This continuum, though subdivided into finite elements through the definition of the mesh, does not reflect the actual organisation of the masonry blocks in the wall, nor take into consideration the type of wall bond pattern. Modelling of the individual blocks and mortar joints (Finite Element Modelling with Discontinuous Elements, FEMDE), with the consideration of different constitutive models for the behaviour of these two materials, is generally limited to the study of particular building elements [121]. In the case of 'micromodelling' of masonry walls, Lourenço [122] further distinguishes between two modelling techniques, namely 'detailed' and 'simplified' micromodelling, where the difference mainly lies in the representation of the mortar joints, as reported in Figure 2-8 . DIANA, developed by TNO DIANA BV, and ANSYS Structural, developed by ANSYS, Inc., are structural simulation software packages based on the Finite Element Method.

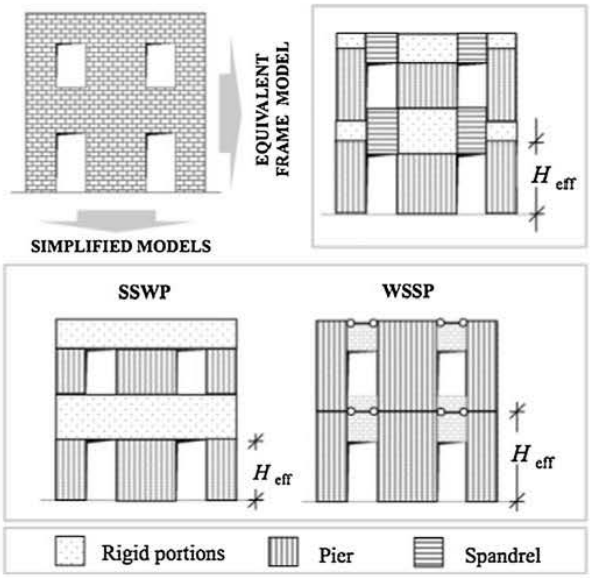

Figure 2-9 URM wall idealization according to simplified (strong spandrels-weak piers 'SSWP' and weak spandrels-strong piers 'WSSP') and equivalent frame models. Lagomarsino et al. ([123] p. 1788).

The Equivalent Frame Method (EFM) involves the simulation of masonry wall panels with a regular distribution of openings, as frames consisting of one-dimensional line elements which represent equivalent spandrel beams and piers with shear deformation, and with rigid nodes at their intersections, while in the case of masonry walls with no openings the rigidity is computed as the sum of the flexural and the shear sway stiffnesses. The pier elements are considered to exhibit an elastoplastic behaviour under dynamic loads. Piers are considered as the main vertical and horizontal load resisting elements, while the spandrels join adjacent piers and make them act in combination in the resistance of horizontal loads [123]. As outlined by Magenes [124], the possible failure mechanisms in pier elements are a) flexural or 'rocking' failure (when the maximum moment in the pier reaches the ultimate moment capacity of the section), b) diagonal shear cracking (when the lower value between the strength of the mortar or the masonry block element is attained), and c) shear sliding (which depends on the shear strength of the mortar joints and the degree of flexural cracking present). The failure mechanisms for spandrel elements are flexure and shear. This type of approach is aimed at a global analysis of structures, and considers only the in-plane response of the wall panels, while out-of-plane collapse mechanisms are disregarded, hence assuming that the structure behaves like a rigid box through the provision of ties or ring beams at slab levels and the rigid connection between intersecting walls. The slabs, on the other hand, are considered as pure diaphragms for the transfer of the lateral forces to the vertical load bearing elements, without any out-of plane stiffness. The frame-by-macro element (FME) modelling idealisation of masonry walls, used in the 3Muri® numerical software package (developed by S.T.A.DATA srl), is based on the equivalent frame method [123] (Figure 2-9).

3Muri® is a commercial numerical software package, which originated from the research version TREMURI, which was developed by Professor Sergio Lagomarsino and his collegues at the University of Genoa, in Italy, specifically for the seismic assessment of masonry structures, while also allowing the modelling of reinforced concrete and steel structural elements. Full details of the macro-element

model for the representation of a masonry panel proposed by Gambrotta and Lagomarsino, where every macro-element is considered to be subdivided into three parts, a superior and an inferior section where bending and axial deformations take place, and a central part where deformation due to shear is considered (reproduced in Figure 2-10), are given in Galasco et al. [125].

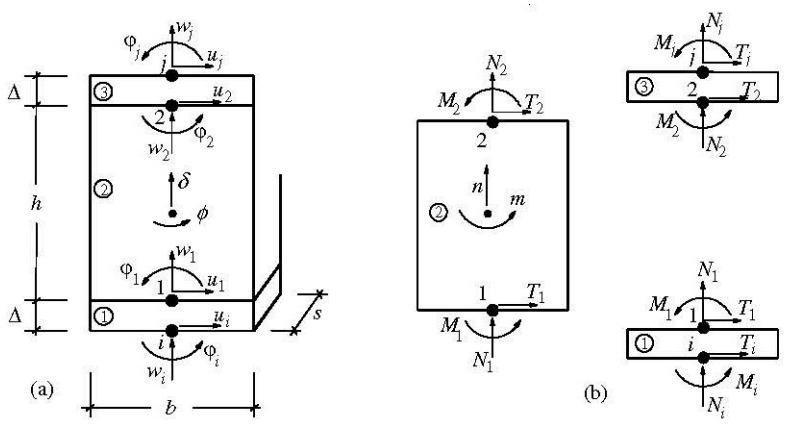

Figure 2-10 Kinematic model for the macro-element representing a masonry panel proposed by Gambrotta and Lagomarsino. Source: Galasco et al. [125].

1) initial stiffness given by elastic (cracked) properties;
2) bilinear behaviour with maximum values of shear and bending moment as calculated in ultimate limit states;
3) redistribution of the internal forces according to the element equilibrium;
4) detection of damage limit states considering global and local damage parameters;
5) stiffness degradation in plastic range;
6) secant stiffness unloading;
7) ductility control by definition of maximum drift (δu) based on the failure mechanism, according to the Italian seismic code:

$$\delta_u = \frac{(u_j - u_i)}{h} + \frac{(\varphi_j + \varphi_i)}{2} = \begin{cases} 0.4\% & \text{shear} \\ 0.6\% & \text{bending} \end{cases}$$

8) element expiration at ultimate drift without interruption of global analysis.

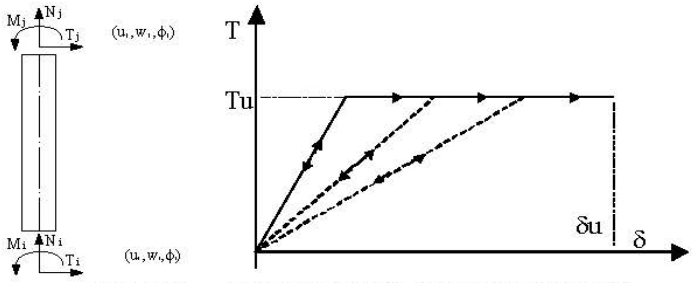

Figure 2-11 Non-linear beam element model implemented in TREMURI research version and adopted in 3Muri commercial version of the software program. Source: Galasco et al. ([126] p.3).

The main masonry and reinforced concrete structural elements are based on a 'non-linear beam model with lumped inelasticity idealization' [123], a full description of which is given by Galasco et al. [126] and is hereby reproduced in Figure 2-11. The computational effort required for the development of the numerical models and the computational demand for their analysis is significantly reduced through:

a) a simplification of the level of detail of the numerical models (such as the inability of specifying a damp proof course at a particular position in a wall, reinforced concrete lintels over wall openings, or the presence of pre-existant cracks);
b) the standardisation of the stiffness of the masonry and concrete elements to a single value defined by the user and applicable throughout the analysis, and of the restraints at the intersection between different structural elements (by assuming, by default, a full coupling between intersecting or adjacent walls and a rigid restraint at all slab boundaries) and at the base of the modelled structure;
c) the smearing of material properties over every defined wall panel; and
d) the restriction of the number of degrees of freedom of the numerical model.

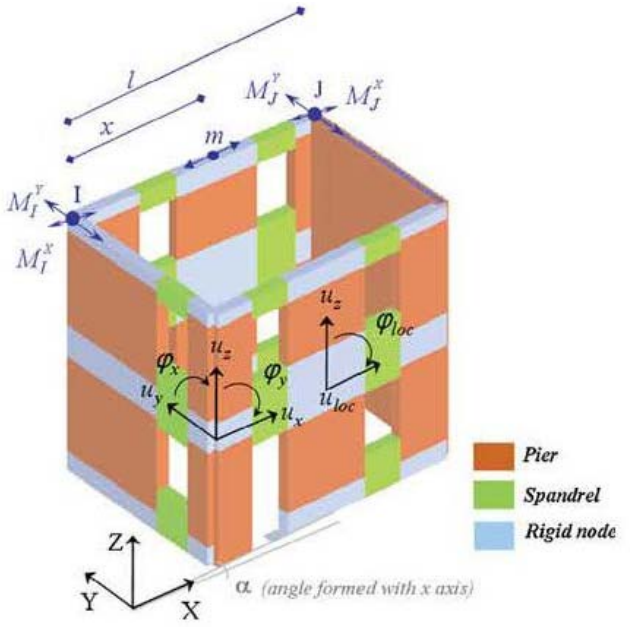

Figure 2-12 Degrees of freedom in 3-dimensional numerical model in TREMURI (research version) and adopted in 3Muri® (commercial version) numerical software. Source: Lagomarsino et al. ([123] p. 1794).

In 3Muri®, walls are represented by two-dimensional plane frames with three degrees of freedom within their plane in the local coordinate system (in-plane translations in the two orthogonal directions, u_x (or u_y), and u_z, and an in-plane rotation, φ). The assemblage of the two dimensional plane frames results in three-dimensional numerical models where, at the intersection of perpendicular walls, five degrees of freedom in the global coordinate system result (translations in the x- and y-plan directions and in the vertical z-direction, u_x, u_y and u_z respectively, and rotations about the x- and y-plan orientations, φ_x and φ_y, respectively), as represented in Figure 2-12. Since out-of-plane actions on walls are disregarded, any out-of-plane forces acting on a two-dimensional wall panel are transferred through the closest three-dimensional nodes to the intersecting perpendicular walls. Furthermore, the slabs are represented as orthotropic horizontal membranes with two translational degrees of freedom within their plane with respect to the two orthogonal plan directions (u_x and u_y) [123].

The 3Muri® non-linear static pushover analysis involves the application of a monotonically increasing lateral load distribution in addition to the gravity loads until the capacity criterion for the limit state

under consideration is reached in accordance with Clause C.3.3(2) and Section C.4 of Eurocode 8: Part 3 [97]. Every 3Muri® pushover analysis considers 24 different load distributions (for static and modal load distributions in the positive and negative x- and y-plan orientatons and the presence of an accidental eccentricity in both main plan orientations in accordance with the recommendation of Clause 4.3.3.4.2.2 of Eurocode 8: Part 1 [4]). The resulting base shear – displacement curves (also referred to as 'pushover curves') describe the inelastic response of the multi-degree-of-freedom system to the applied lateral loading for every different load distribution considererd. The seismic assessment is based on the comparison of the maximum displacement of the structure for a particular limit state (resulting following the attainment of the limiting capacity criterion during the pushover analysis), to the target displacement obtained from the elastic acceleration response spectrum for an equivalent single degree of freedom system in accordance with Clause C.3.3(3) of Eurocode 8: Part 3 [97]. Hence, for this comparison to be carried out, the pushover curve describing the multi-degree-of-freedom system is converted to a capacity curve for an equivalent single degree-of-freedom system through the transformation of the maximum displacement, mass, force and period of the multi-degree-of-freedom system to the corresponding values with respect to the equivalent single degree-of-freedom system using the N2 method [127], which method is also implemented in Annex B of Eurocode 8: Part 1 [4].

The presence of construction details, which ensure a rigid connection between intersecting walls and between walls and slabs which are essential for a structure to behave as a rigid box, cannot be assumed in all structures, and certainly not in the case of the contemporary loadbearing unreinforced masonry building typology present in the Maltese Islands, where the typical construction details, plan layouts and wall thicknesses impede such a structural behaviour. De Sutter [128] showed that the natural frequency of a masonry wall depends on its dimensions, density, Young's Modulus of Elasticity and boundary conditions. Hence, by extension, these physical properties have an effect upon the natural frequency of the whole modelled structure. Furthermore, Morandi [129] also concluded that the degree of connection between intersecting walls influences the extent of redistribution of forces, which can take place within a structure and, hence, the extent of the inelastic behaviour, which can be exhibited by the structure (the additional seismic forces which can be sustained by the structure following the attainment of the elastic limit of the main lateral force resisting elements). Therefore, the correct representation of the degree of restraint present in the structure between the main structural elements is essential for the accurate assessment of its seismic resistance.

Lagomarsino and Cattari [130] highlighted the importance of the selection of the lateral load distributions, the control node and the displacement, which will be represented by the pushover curve, for the validity of a non-linear static assessment. Two lateral force distributions are generally required by seismic codes due to the variation in the distribution of inertial actions with the progression of damage in a structure during a seismic event. Clause 4.3.3.4.2.2 of Eurocode 8: Part 1 [4] recommends the consideration of a 'uniform' (or 'static', as defined in 3Muri®) load distribution which is proportional to the mass of the different storeys in the structure, and a 'modal' load distribution, proportional to the first mode of vibration or taking into consideration all the modes of vibration,

which have a significant effect upon the seismic response, in accordance with Clauses 4.3.3.3.1(2)P and (3) in Eurocode 8: Part 1 [4]. Endo et al. [131] note that advanced pushover methods, which take into consideration higher modes of vibration, such as multi-modal pushover analysis, as proposed by Chopra and Goel [132], are mainly intended for frame structures and involve the application of modal combination rules, such as the SRSS (square root of the sum of the squares method) or the CQC (complete quadratic combination method), which seem too approximate in the context of a non-linear analysis. Furthermore, Kreslin and Fajfar [133] proposed an extension of the N2 method to take into consideration the effects of higher modes of vibration in plan and elevation by considering that the structure does not enter the inelastic range when higher modes of vibration are activated. This assumption enables the estimation of higher mode effects through elastic modal analysis and the use of combination methods for the determination of the overall response, which is then applied to the results of the basic N2 method through the use of correction factors. On the other hand, several adaptive pushover analysis procedures were developed which involve the updating of the lateral force distribution at every step of the analysis, by considering the real-time change in resistance of the structure due to propagation of damage. Galasco et al. [126] developed a type of 'seismic adaptive pushover' (SDAP) method, which was implemented in TREMURI (research version), where the force distribution at every analysis step is based on the deformed shape of the structure resulting from the previous analysis step, and where, the lateral force distribution at any analysis step cannot exceed the lateral force distributions resulting from the 'uniform' and 'modal' (for the fundamental mode of vibration) force distributions. It is not clear whether this method has been implemented also in the 3Muri® software package.

While Finite Element Models were reported to result in a more accurate representation of the in-plane and out-of-plane behaviour of masonry wall constructions during seismic excitations, together with the more accurate prediction of the locations of the resulting damages in the modelled structures, Equivalent Frame Models might be more computationally feasible, while still maintaining a discrete level of accuracy [134]. The latter, on the other hand, might ignore relevant failure modes in the case of structures with flexible diaphragms, or with inadequate tying action between the diaphragms and the vertical structural elements. Furthermore, since classical non-linear static (pushover) analysis considers only the fundamental mode of vibration of a structure, hence assuming a linear distribution of drift throughout the height of the building, the widespread use of the Equivalent Frame Method, in combination with a classical non-linear static analysis method could omit collapse mechanisms resulting from higher failure modes, particularly when building characteristics, which introduce a sudden change in the lateral storey stiffness of the structure, as in the case of a soft storey, are present. On the other hand, Chidiac et al. [135] reported that the natural frequencies up to the fifth mode of vibration, obtained through ambient noise measurements on an unreinforced masonry tower were overall in agreement with the corresponding fundamental frequencies obtained from a finite element model of the tower.

The higher accuracy associated with micromodelling, particularly in the case of the representation of masonry structures, is achieved in the Distinct Element Method (DEM), which was originally developed

by P.A. Cundall for the study of fractured rock [136]. Structures are modelled as a collection of individual, rigid or flexible elements, which interact at contact points along their external faces, and which can displace, rotate and move apart, or form new contacts, as a result of the displacements, hence, enabling the simulation of collapse mechanisms resulting from 'sliding, rotation or impact' forces [121]. Contact points are represented by normal and shear stresses through elasto-plastic contact elements which follow a Coulomb slip criterion [121]. Large displacements can be achieved, therefore, making the method suitable for simulation of the behaviour of masonry structures in progressive collapse scenarios. Even though the Distinct Element Method was used in studies involving a variety of structural systems, ranging from stone bridges to masonry tunnel support structures [137], column-architrave models [138] and historical minarets [139], amongst others, Roca et al. [140] report that this modelling method is ideally suited for the simulation of structures consisting of individual rectangular blocks. The degree of accuracy for the estimation of stresses between discrete blocks depends on the size of the blocks, and the number of contact elements specified. Hence, while in the case of large structures, the computational requirements of this modelling method can lead to the representation of a larger wall area through a single discrete element, this results in the reduction of the model's accuracy, and prevention of the identification of local damage effects. Furthermore, the Distinct Element Method requires the gradual application of the modelled structure's self-weight over a number of time steps during static analysis [41], which time steps are a function of element size, material and mass [41]. UDEC and its three-dimensional version, 3DEC by Itasca Consulting Inc., are commercially available software packages based on this modelling method.

The Applied Element Method (AEM), developed by Kimiro Meguro and Hatem Tagel-Din at the University of Tokyo, is based on the representation of a structural member as a collection of 'virtual elements connected through (shear and normal) springs (which are distributed around the external faces of the elements),'…'where each spring represents the stresses, strains, deformation and failure of the structure' [38]. As presented in Figure 2-13, the springs are considered to act between the centrelines of adjacent members and their properties are based on the material properties specified for the member, in the case of elements within the same structural member, or the interface material, in the case of interface springs between distinct structural members or materials. While deformations are not allowed at element level, the connection of the individual elements through springs ensures that large deformations within a structural member are possible. Hence, this numerical modelling method allows the effective simulation of damage and collapse behaviours through allowing (a) partial connectivity between elements, which could result because of the failure of a number of springs, while other springs are still effective, as occurs during the process of crack formation and progression or during differential displacement, and (b) the complete detachment of one element with respect to the adjacent element/elements, as would occur in the process of collapse. Therefore, as shown in Figure 2-14, a number of failure modes, which are particularly applicable to masonry structures, can be represented with significant accuracy.

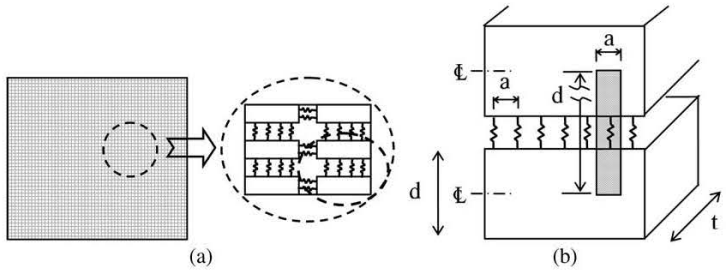

$$K_n = \frac{E \cdot a \cdot t}{d}, \qquad K_s = \frac{G \cdot a \cdot t}{d}$$

Where,

K_n is the stiffness of the normal spring;

K_s is the stiffness of the shear spring;

E is the Young's Modulus of the material;

G is the Shear Modulus of the material;

a is the distance between the springs;

d is the length of the represented area of every spring (between element centres);

t is the thickness of the element.

Figure 2-13 Modelling a wall with AEM (a) element generation and spring distribution (b) area of influence of each spring. General equations governing the stiffness of normal and shear springs are also included ([40] p. 404).

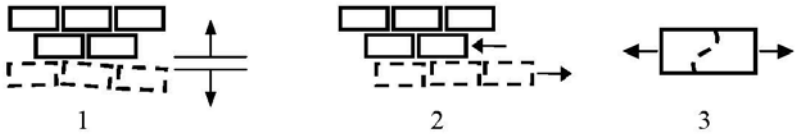

Figure 2-14 Dominant failure modes in masonry units: (1) joint de-bonding, (2) units sliding along bed or head joints and units cracking under direct tension ([41] p. 123).

ELS® by Applied Sciences International Inc. was the only commercially-available numerical software package based on the Applied Element Method at the start of the study presented herein. It is equipped with an advanced user graphic interface and computer aided design tools in order to ease the computational effort required for the development of the numerical models, which can be carried out without code writing. Automatic wall generation tools allow the representation of masonry walls in two ways, namely a) as a homogenised wall panel, where the averaged material properties of the masonry blocks and the mortar joints are considered, and where the mesh, defined by the user, would not follow the wall bond pattern and would, very likely, not result in element sizes which correspond to the actual masonry block dimensions, or (b) as individual masonry blocks with mortar joints, through a realistic simulation of the staggered pattern of the wall. Furthermore, if the actual distribution of blocks in a wall is required, walls can be defined through the specification of individual three-dimensional units representing the blocks, and a mortar interface material can be specified in the region of the horizontal and vertical mortar joints. In the case of masonry walls modelled as a homogeneous material, alternative equivalent stiffnesses reflecting the averaged material properties, become applicable for brick-mortar-brick normal and shear springs. These are presented in Figure 2-15.

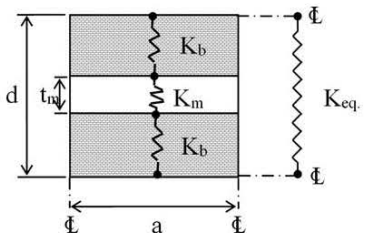

$$\frac{1}{Kn_{eq.}} = \frac{d - t_m}{E_b \times a \times t} + \frac{t_m}{E_m \times a \times t},$$

$$\frac{1}{Ks_{eq.}} = \frac{d - t_m}{G_b \times a \times t} + \frac{t_m}{G_m \times a \times t}$$

Where,

K_{neq} is the equivalent stiffness of the brick-mortar-brick normal spring;

K_{seq} is the equivalent stiffness of the brick-mortar-brick shear spring;

E_b and E_m are the Young's Moduli for the brick and mortar, respectively;

G_b and G_m are the Shear Moduli for the brick and mortar, respectively;

a is the distance between the springs;

d is the length of the represented area of every spring (between element centres);

t and t_m are the thickness of the element and the mortar joint, respectively.

Figure 2-15 Modelling of masonry construction with mortar joints, including equivalent stiffness of normal and shear springs at the brick-mortar interface ([40] p. 405).

While Meguro and Tagel-Din [117] proposed two methods for the accurate simulation of Poisson's ratio effects, namely a) the addition of another two degrees of freedom to the elements' stiffness matrix and b) the linking of the element's stiffness matrix to that of adjacent elements (through the summation of the stiffness matrices corresponding to the interface springs) in order to ensure the deformability of the assemblage of elements constituting the structural member, the version of ELS® available at the start of this study (version 3.1) considers a Poisson's ratio of zero.

Element size influences the accuracy of the calculated displacements, since the subdivision of a structure into larger, as opposed to smaller elements, would result in a higher stiffness. This leads to smaller displacements of the structure, and an inaccurate, higher structural resistance to the applied actions. Similarly, increasing the number of connecting springs between element interfaces increases the accuracy of the estimated displacements, which becomes more important in non-linear analyses, particularly for the accurate simulation of crack formation and propagation. However, both the subdivision of structural members into a higher number of elements, and the increase in the number of connecting springs, result in considerable increases in the processing time. Meguro and Tagel-Din [141] [117] report that, in the case of elastic analysis, increasing the number of elements would have a higher influence on the accuracy of the model than increasing the number of connecting springs between elements.

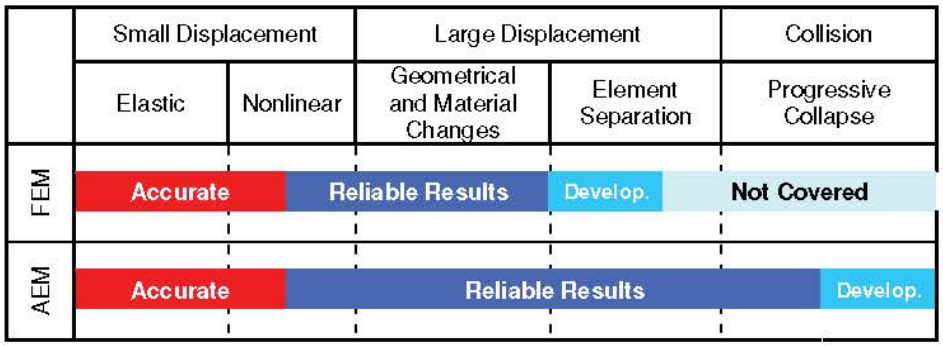

Figure 2-16 Analysis domains of Applied Element Method ([142] as reported in ([38] p. ST-401-4)).

The Applied Element Method is considered to combine the desirable features of Finite Element and Distinct Element modelling techniques, while overcoming the main shortcomings of these modelling methods. The capabilities of Finite Element methods to portray a structure's response to a particular action, before an advanced stage of failure is reached, are indisputable. As discussed earlier, while alternative methods were developed for the representation of cracks and their propagation in Finite Element Modelling, these methods still have a number of limitations. Meguro and Tagel-Din [117] explain that, while the node connectivity at contact points between adjacent elements in Finite Element Models presents the main restriction on their use for the simulation of collapse scenarios, Distinct Element methods can simulate structural behaviour throughout all stages of loading up to collapse, falling behind when compared to Finite Element Methods, only with respect to the accuracy of the magnitude of displacements in the initial stages of failure, and the longer required processing durations. On the other hand, as indicated in Figure 2-16, the spring connectivity between adjacent elements in the Applied Element Method ensures that the structure's response, from the initial loading stages up to progressive collapse, can be accurately modelled, without the need of the pre-determination of crack positions, while still achieving FEM's accuracy in the structural response parameters.

Based on the above, in a scenario as that of the Maltese Islands, where no damaging earthquake has occurred since the emergence of the contemporary loadbearing URM building typology under study, the Applied Element Method was considered as the most adequate numerical modelling method for the study of the seismic response of this construction typology. This numerical modelling method was, hence, selected for the investigation of the influence of the presence of particular construction characteristics, ground formation scenarios and subsoil modelling methods on the seismic response of the URM building typology under study.

On the other hand, the limitations imposed by the frame by macro-element (FME) modelling idealisation, particularly in the case of the numerical simulation of the seismic resistance of the contemporary loadbearing unreinforced masonry construction typology under study (whose general construction characteristics were outlined in Section 1.1 of this thesis) especially with respect to the assumed behaviour of the analysed structures as a rigid box (and, hence, the inability of this modelling method to consider out-of-plane collapse mechanisms) is fully acknowledged. However, in view of the

long modelling and analysis times, and the examination of the detailed output required by the Applied Element Method, a comparison of the seismic resistance resulting from numerical models analysed through a full non-linear dynamic analysis and that obtained through a simpler non-linear static pushover analysis using the Equivalent Frame Method, was carried out in this research study in order to establish whether a reliable estimate of the behaviour of the masonry building typology under study can be obtained through a less computationally-demanding method of analysis.

2.8 Other Considerations in Numerical Modelling

As acknowledged by Rota et al. [143], the possible sources of uncertainty, and their influence on the structural response, should be taken into consideration in the evaluation of the results of a seismic vulnerability assessment of an existing structure carried out through numerical modelling. However a level of uncertainty can also be associated with the numerical models of new structures in view of modelling-related assumptions. Such sources of uncertainty can have a significant bearing on the stiffness of the model and, hence, on the simulated displacements and overall response to the applied actions. Possible examples can be the selection of the correct constitutive models for the definition of the materials of the main structural members and their interface materials, particularly with respect to their response to dynamic actions; the definition of the correct member restraints and model boundary conditions, the proportions of structural members (such as slab and wall thicknesses in a masonry structure); the assumed details at junctions between separate members and the way these details are represented in the numerical model; together with the duration, frequency and intensity of the applied earthquake ground motions [124]. The numerical modelling method (as discussed in Section 2.7), the complexity of the numerical model (planar or spatial), and the type of analysis (non-linear static, non-linear dynamic, linear-elastic), can all have a bearing on the accuracy of the resulting structural behaviour and the model response parameters. Eurocode 8: Part 3 [97] partially takes into account this uncertainty with respect to the seismic evaluation of existing structures, through the definition of different 'Knowledge Levels', corresponding to which, the acceptable method of analysis and the values to be adopted with respect to confidence factors, can be established.

2.9 Conclusion

The reviewed literature highlights the features of the contemporary loadbearing URM structures under study, which could be potentially hazardous in an earthquake scenario. These building characteristics are not limited to the intrinsic vulnerability associated with the masonry wall fabric and the quality and grade of materials used, but include the construction details commonly in use (such as the seating details of the cast in-situ and precast prestressed concrete slab planks, with no positive connection to the underlying walls, the absence of peripheral ties or ring beams and the general practice of constructing masonry walls with no mortar in the vertical joints between the masonry blocks), and particular building characteristics (such as the sudden reduction of lateral storey stiffness resulting from the presence of soft storeys), which can cause a localised amplification of displacements and an earlier onset of collapse. A number of existing seismic vulnerability assessment methods and possible numerical analysis methods were also reviewed.

Chapter 3 METHODOLOGY AND ITS APPLICATION

3.1 Introduction

The absence of earthquake damage data for the contemporary loadbearing URM building typology under investigation conditioned the study of the seismic vulnerability of this building typology to be carried out through a 'hybrid' approach, as defined by Calvi et al. [34]. The following sections give a concise overview of the three-staged process through which the seismic response of the contemporary loadbearing URM building typology and, hence, its vulnerability under seismic actions, was investigated in this study. This process consists of:

1. the development of a preliminary version of a rapid assessment form for the seismic vulnerability evaluation of this building typology, (hereafter referred to as the 'New Form'), together with its corresponding rating system, and the use of the New Form for the evaluation of a total of 183 buildings in the Test Sites of Xemxija (Malta) and Nadur (Gozo),
2. the verification checks carried out on the developed rating system, (which range from comparisons of the scores resulting from the use of the New Form to those obtained through a GNDT second level assessment [26] [71], a FEMA 154 (second edition) assessment [27] and an aggregate check based on the method proposed by Formisano et al. [28] [29] [30] [31]); and a statistical analysis of the results obtained in the Test Sites for the identification of the main predictors of the final seismic vulnerability rating, and
3. the numerical analysis of the seismic response of this building typology, first, through a full non-linear time-history dynamic analysis for the investigation of the influence which particular building characteristics and ground formation layers and ground modelling techniques have on the structural behaviour under seismic actions, and secondly, through the investigation into whether a non-linear static (pushover) analysis, which assumes a box-like structural behaviour, can adequately predict the response of the URM building typology under study, including the study of the seismic response in the presence of additional building characteristics; the modelling assumptions made, and their verification in both cases.

The work pertaining to the first and second stages of this study was carried out by the author in her capacity as a Research Support Officer I with the Faculty for the Built Environment of the University of Malta, as part of the deliverables of the University of Malta for the SIMIT Project (Project Code: B1-2.19/11), which was part-financed by the European Union under the European Regional Development Fund (ERDF 2007-2013). While the analysis of all results was carried out by the author, the contribution

of the rest of the research team working on the SIMIT Project, with respect to the retrieval of the development permit drawings from the Malta Planning Authority of part of the buildings in the Test Sites, the completion of the corresponding seismic vulnerability assessments, together with the completion of the GNDT second level [26] and FEMA 154 (second edition) [27] assessments, is hereby being acknowledged.

3.2 Development of a New Seismic Vulnerability Assessment Form (New Form)

The extensive review of the building characteristics, which are typical of the contemporary loadbearing URM building typology, and which could be of detriment to its seismic resistance, together with the in-depth study of a number of seismic vulnerability assessment methods, which are in use in other countries, suggested the need of the development of a new seismic vulnerability assessment form for the building typology under study. This was mainly due to:

a) the intrinsic differences in the wall and slab construction systems of the contemporary loadbearing URM typology and those considered in these methods, where, in the case of the Italian methods reviewed, a building typology normally associated with older town centres, and closer to the local traditional building typology, is generally applicable;
b) the different details and materials used in the construction of masonry buildings in other countries, in addition to the different mechanical properties of these materials when compared to the investigated URM building typology in the Maltese Islands (such as: the weak mortar, and the general practice of the simple placement of precast prestressed concrete slabs, typically used to roof over the soft storey at the lowermost level, directly over a reinforced concrete spreader beam, without any connection between these precast units and the underlying walls [7]; the absence of peripheral ties or ring beams at floor levels, and of a connection between the slabs and the lateral load resisting elements, even when the roofing system consists of cast in-situ concrete slabs; the frequent use of (unreinforced and un-infilled) hollow concrete blockwork for the construction of loadbearing walls; the bearing of slabs only on the inner leaf of double leaf walls; and the common practice of using thick-gauge polyethylene sheeting within the first horizontal course above road level as a damp proof course);
c) the added seismic vulnerability, which can be associated with the presence of one or more seismic vulnerability characteristics on more than one level, or in more than one form, as opposed to the sole consideration of a 'test floor' which represents the worst case scenario, as in the case of the GNDT second level assessment method [26];
d) the additional building characteristics, typical of the contemporary loadbearing URM building typology, which are not considered in the existing methods (such as: the presence of, at least, one soft storey at the lowermost level, open plan spaces in the residential levels, and long corridors directly abutting party walls, which are a direct consequence of the very rectangular building site proportions; the use of single leaf party walls, whether the party walls are shared or not, and the absence of an adequate separation gap between party walls when these are

not shared by adjacent buildings; and the presence of double height spaces, setbacks and projecting rooms / balconies in the apartment levels);

e) the predominantly rectangular plan and elevation proportions;

f) the fact that local building regulations do not restrict the presence of storeys with no internal walls at the lower levels.

The background to the identification of the building characteristics, to be included in the new seismic vulnerability assessment form for the Maltese Islands, was provided by:

i. the building attributes, which are associated with an adequate resistance to seismic actions, and the structural regularity criteria recommended in Section 4.2 of Eurocode 8: Part 1 [4];

ii. the parameters considered in a number of existing seismic vulnerability assessment methods [26] [27] [69] [70] [71] [73] [75] [79] [80] [82] [92] [95] [96], the background principles governing the effects of such parameters on the seismic behaviour of unreinforced masonry structures, and the relative weightings assigned (where present); and

iii. the results of past local research studies on the critical form of the building typology under investigation [16] [17] (i.e. in the case of buildings which include, at least, one soft storey at the lowermost level),

which documents, were reviewed in Chapter 2[4]. These documents, together with the results published in international research studies on the influence which particular building characteristics have on the seismic response of loadbearing URM buildings, led to the development of the rating system for the New Form, through the identification of thirteen building characteristics, which were considered to have a major bearing on the seismic vulnerability rating of this building typology, and the relative weightings attributed to every category of characteristics evaluated in the six sections of the New Form (Sections 2, 3, 4, 5, 6 and 8) upon which the final seismic vulnerability rating is based. The New Form, a copy of which is included in Figures 1 to 11 of Appendix A, includes a total of 147 entries in the preliminary format, which is presented in this study. Tables 1 to 10 in Appendix A indicate the direct correspondence between the individual entries of the New Form and the parameters considered in the main existing Italian seismic vulnerability assessment methods reviewed.

[4] The development of the preliminary version of the new seismic vulnerability assessment form and the corresponding rating system, the verification of the resulting seismic vulnerability outcomes through a comparison with the outcomes resulting from other seismic vulnerability assessment methods in use in other countries of the 183 buildings in the Test Sites and the statistical analysis of the results for the identification of the main seismic vulnerability predictors of the URM building typology under study presented in the ensuing Sections of this Chapter were completed before the work carried out by Marmara' [18], Tong [19], Borg [20], Bonello [21], Zammit [22], Azzopardi [23] and Said [24] were undertaken. Hence, the results of these latter studies could not be taken into account in the development of the rating system for the New Form and in the subsequent stages of the present study with respect to the verification of these seismic vulnerability ratings.

The New Form was first tested on a small building aggregate in Msida in Malta, after which, it was first improved, and then used for the evaluation of the seismic vulnerability of a total of 183 contemporary loadbearing URM buildings located in the Test Sites of Xemxija, in Malta, and Nadur, in Gozo. Since internal inspections of the buildings were not possible, information regarding internal layouts was obtained from the development permit drawings of the buildings under evaluation which, when available, were obtained from the Malta Planning Authority. In a significant number of cases, either no development permit drawings were traced, or the sourced drawings related to only part of the building. Hence, entries, such as the masonry construction material of the walls, were assumed on the basis of the approximate age of the building, whereas other entries relating to the presence of specific characteristics could not be verified.

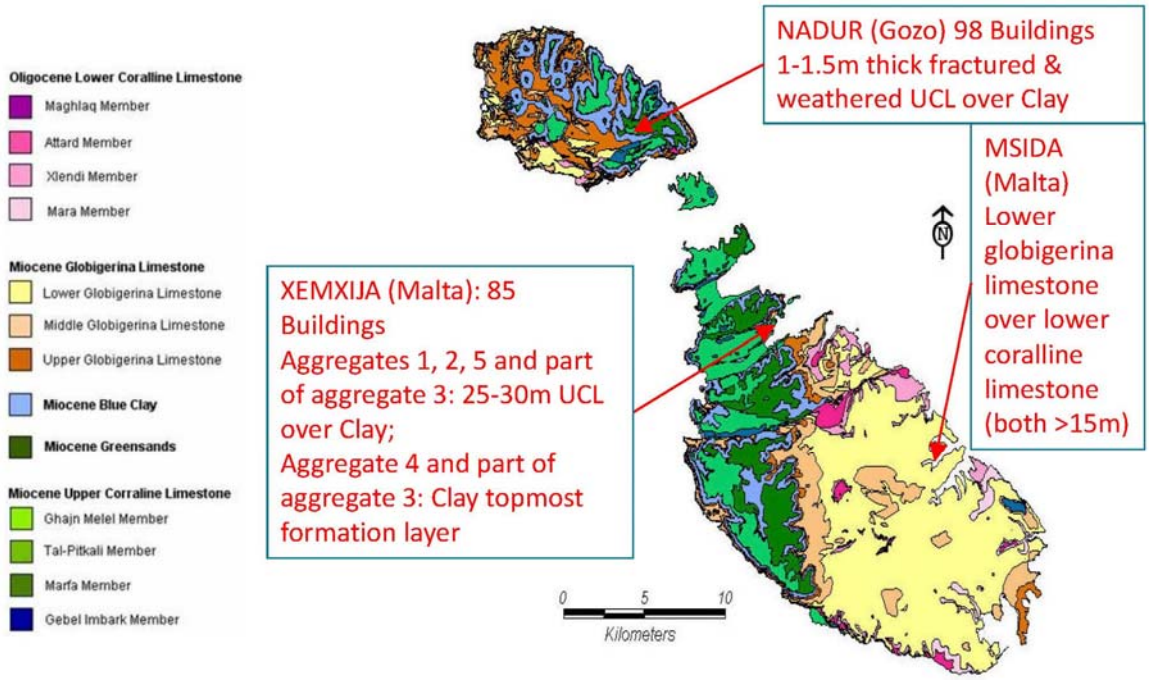

Figure 3-1 Geological map of the Maltese Islands (http://www.electricyouniverse.com/eye/images/geulogy/malta/malta-geological-map-limestone-clay-greensand.jpg).

The locations of the Test Sites were chosen in view of the geological characteristics of these sites, and the increased seismic vulnerability of the critical form of the building typology under study, associated with the presence of a clay subsoil as reported in local studies by by Galdes [17], Marmara' [18] and Tong [19]. Figures 3-2 and 3-3 indicate the position and the geology of the five blocks of building aggregates[5] considered in this study for the Xemxija Test Site, while Figure 12 in Appendix A includes

[5] The term 'blocks of aggregates' hereby refers to the conglomeration of buildings, which is demarcated by the streets which provide access to the individual buildings constituting these blocks and, hence, consists of a number of aggregates. Building aggregates and individual buildings were identified in accordance with the definitions given in the GNDT first level assessment manual [69]. Party walls were assumed as either shared or unshared throughout the height of the building/s.

the building reference numbers corresponding to the seismic vulnerability assessments carried out. Figures 3-4 and 3-5 together with Figure 13 in Appendix A report the equivalent information for the five blocks of building aggregates considered in the Nadur Test Site. The Geological Maps for the Maltese Islands (a simplified version is reported in Figure 3-1) indicate that almost all the buildings in the Test Sites are located on a subsoil, which consists of an upper coralline limestone layer overlying a clay layer. The only exceptions are the lower part of 'Aggregate 3' and 'Aggregate 4' in Xemxija, where the upper coralline limestone layer is most likely absent in view of the sloping terrain, hence resulting in the buildings being constructed either directly on the clay layer, or on large upper coralline limestone boulders which got detached from the upper coralline limestone layer present further up the Xemxija slope.

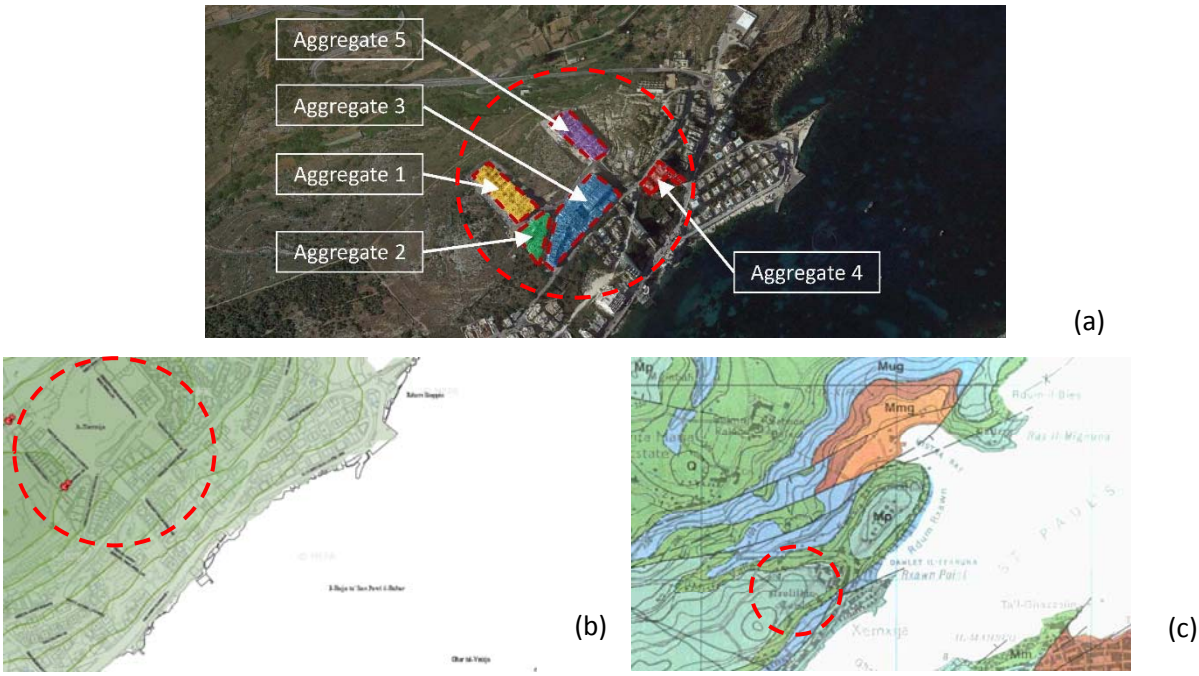

Figure 3-2 Position of Aggregates 1-5 in Xemxija Test Site on (a) Google earth image, (b) Malta Planning Authority Mapserver (accessed 24.09.2015), (c) Geological Map of the Maltese Islands -Sheet 1 [144].

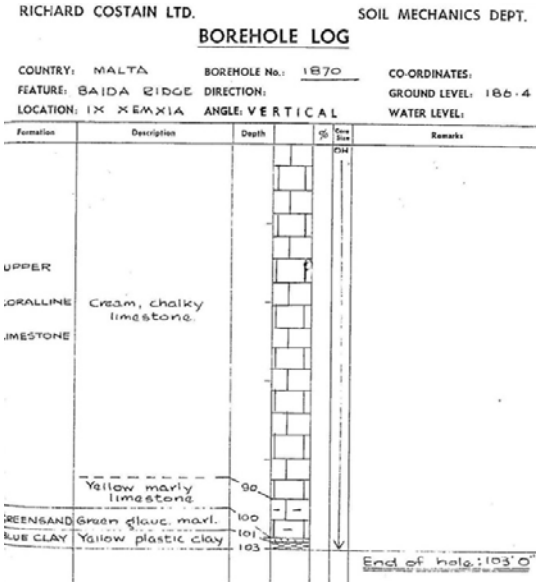

Figure 3-3 Borehole report for Xemxija in the vicinity of Aggregate 1 (Engineers Binnie, Deacon and Gourley, 1958) [145].

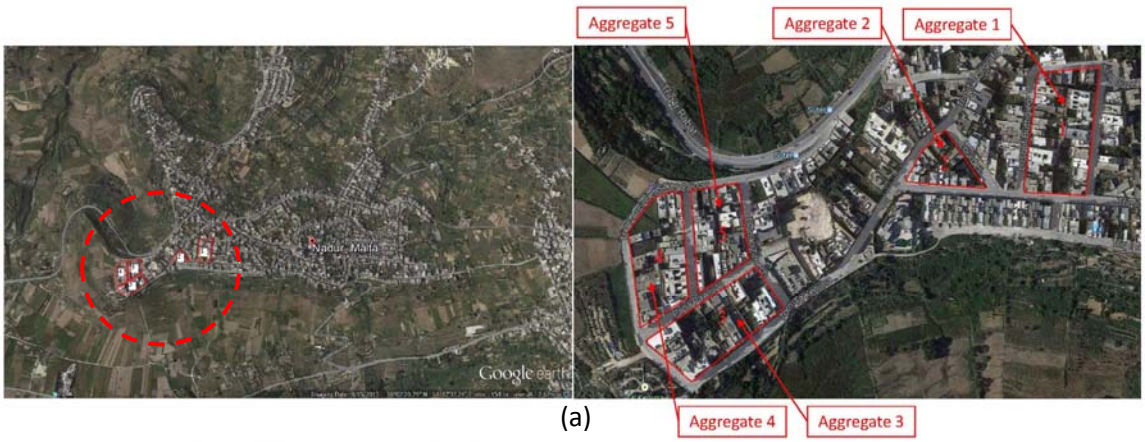

(a)

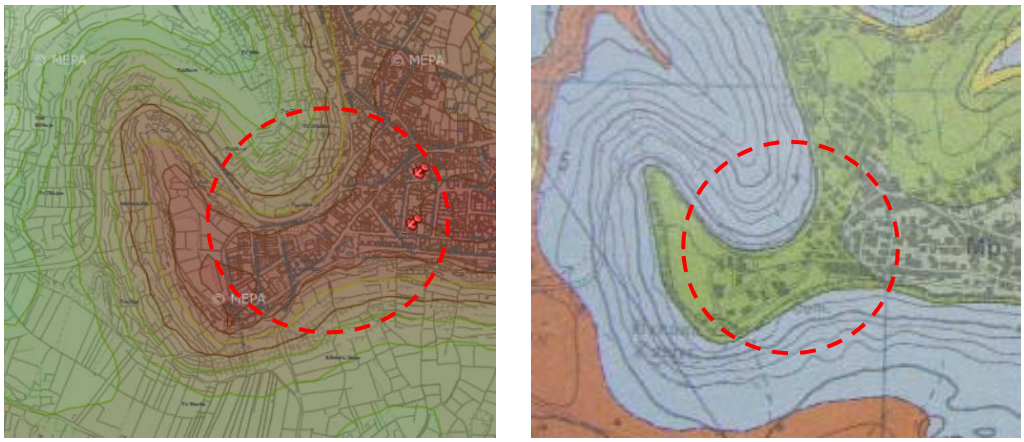

(b) (c)

Figure 3-4 Position of Aggregates 1-5 in Nadur Test Site on (a) Google earth image, (b) Malta Planning Authority Mapserver (accessed 24.09.2015), (c) Geological Map of the Maltese Islands -Sheet 2 [146].

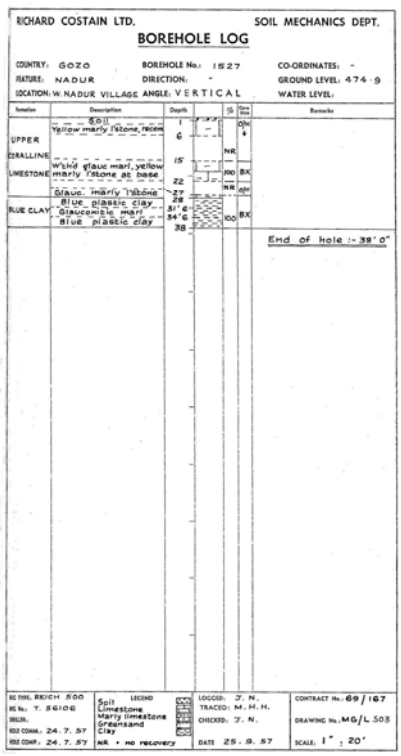

RICHARD COSTAIN LTD. SOIL MECHANICS DEPT.

BOREHOLE LOG

COUNTRY: GOZO BOREHOLE No.: 1527 CO-ORDINATES: -
FEATURE: NADUR DIRECTION: - GROUND LEVEL: 474·9
LOCATION: W. NADUR VILLAGE ANGLE: VERTICAL WATER LEVEL:

Formation	Description	Depth	%	Core Size	Remarks
	Soil	1		O/H	
UPPER CORALLINE LIMESTONE	Yellow marly ?stone, recem	6		+	
	W/ind glauc mart, yellow marly ?stone at base	15		NR	
		22		100	BX
	Glauc. marly ?stone	27		NR	
BLUE CLAY	Blue plastic clay	28			
	Glauconitic mart	31'6			
	Blue plastic clay	34'6		100	BX
		38			

End of hole :- 38'0"

RIG TYP. REICH 500 RIG No. T. 56106 DRILLER: HOLE COMM.: 24.7.57 HOLE COMP.: 24.7.57

LEGEND: Spit Limestone, Marly limestone, Greensand, Clay, NR = no recovery

LOGGED: J. N. TRACED: M. H. H. CHECKED: J. N. DATE 25·9·57

CONTRACT No. 69/167 DRAWING No. MG/L 503 SCALE 1" : 20'

(a)

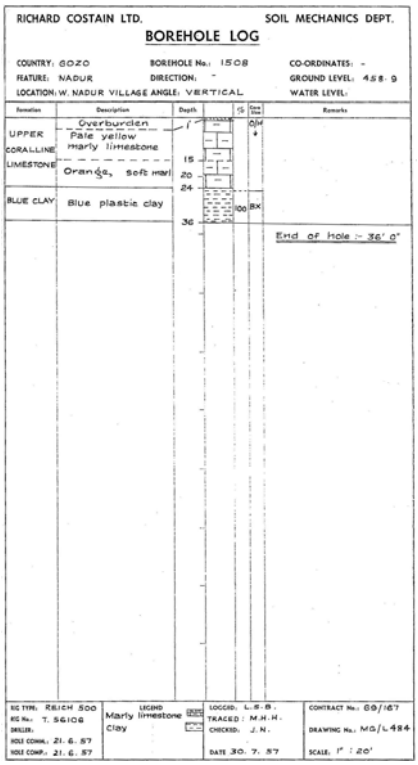

RICHARD COSTAIN LTD. SOIL MECHANICS DEPT.

BOREHOLE LOG

COUNTRY: GOZO BOREHOLE No.: 1508 CO-ORDINATES: -
FEATURE: NADUR DIRECTION: - GROUND LEVEL: 458·9
LOCATION: W. NADUR VILLAGE ANGLE: VERTICAL WATER LEVEL:

Formation	Description	Depth	%	Core Size	Remarks
	Overburden	1'		O/H	
UPPER CORALLINE LIMESTONE	Pale yellow marly limestone	15		+	
	Orange, soft marl	20			
		24			
BLUE CLAY	Blue plastic clay	36		100	BX

End of hole :- 36'0"

RIG TYP. REICH 500 RIG No. T. 56106 DRILLER: HOLE COMM.: 21.6.57 HOLE COMP.: 21.6.57

LEGEND: Marly limestone, Clay

LOGGED: L.E.B. TRACED: M.H.H. CHECKED: J.N. DATE 30.7.57

CONTRACT No.: 69/167 DRAWING No.: MG/L 484 SCALE 1" : 20'

(b)

Figure 3-5 Borehole reports for Nadur (a) between Aggregates 3 and 5, and (b) in the vicinity of Aggregate 1 (Engineers Binnie, Deacon and Gourley, 1958) [147].

The respective thicknesses of the upper coralline limestone and clay layers were obtained with reference to the results of borehole investigations were carried out during the British period [145] [147], and the Geological Maps of the Maltese Islands (Sheets 1 and 2) [144] [146], which information was verified through the contour levels indicated on the Malta Planning Authority Mapserver. In the case of the Xemxija Test Site, the thicknesses of the underlying ground formation layers in the vicinity of 'Aggregate 1' (located at the highest position on the Xemxija slope) were based on the assumption that the bottom of the clay layer coincides approximately with the mean sea level, as in the case of nearby Wardija. Hence, as evidenced from Figures 3-2 and 3-3, the overall depth of around 60.96 m, obtained from the contour levels in the region of 'Aggregate 1' up to Xemxija Bay indicated on the Geological Map of the Maltese Islands (Sheet 1) [144], together with the depth of upper coralline limestone reported in borehole investigations carried out by Engineers Binnie, Deacon and Gourley in 1958 [145], suggest that the geology in the vicinity of 'Aggregate 1' consists of a top layer of upper coralline limestone with a thickness of around 30 m, and an underlying (approximately) 30.96 m thick clay layer. While 'Aggregate 5' is likely to have a similar underlying geology to 'Aggregate 1', the thickness of the upper coralline limestone in 'Aggregates 2 and 3' varies in view of the sloping terrain. As explained earlier, 'Aggregate 4' is likely to be constructed directly over the 30 m thick clay layer. The microseismic rating of the buildings considered in this study in the Xemxija Test Site was, therefore:

- Aggregates 1, 2, 5 and the upper part of Aggregate 3: stable with amplifications (in view of the presence of the clay layer, and the relatively thick overlying upper coralline limestone layer);
- Aggregate 4 and the lower part of Aggregate 3: unstable with differential settlement (in view of the surface clay layer).

In the case of Nadur, the report of the geological investigations carried out by Engineers Binnie, Deacon and Gourley in 1958 [147] indicates a thickness of upper coralline limestone of around 8.534 m between 'Aggregates 3 and 5', and 7.315 m in the vicinity of 'Aggregate 1', as evidenced in the borehole records reproduced in Figure 3-5. Nevertheless, experience from past projects, in the area close to the ridge, suggests that upper coralline limestone thicknesses of between 1.0 m to 1.5 m could be present, with this layer exhibiting extensive weathering and fractures. Hence, a worst case scenario of an upper coralline limestone thickness of 1.5 m for all the aggregates evaluated in Nadur was considered in this study. The thickness of clay in Nadur was calculated based on the assumption that the bottom of the clay layer coincides approximately with the top of the closest globigerina limestone outcrop, which is located in the area indicated as 'Ta' Bordin' on the Geological Map. Figure 3-4(c) indicates that the contour levels of the Geological Map for the Maltese Islands (Sheet 2) [146], for the study area in Nadur, suggest that, at the highest point, the top of the upper coralline limestone layer is located at around 144.78 m above mean sea level, whereas the top of the closest globigerina limestone outcrop is positioned at around 83.82 m above the same datum. Hence, the geology in the area of the Test Site of Nadur, considered in this study, consists of an upper coralline layer of around 1.5 m thickness, and an underlying clay layer of around 59.46 m thickness. The microseismic rating for all the five Nadur aggregates was considered as 'unstable with differential settlement', in view of the very thin and fractured upper coralline limestone layer.

The validity of the developed rating system for the New Form was investigated through three main verification checks, namely:

i. the comparison of the final seismic vulnerability rating obtained through the use of the New Form on the seismic vulnerability evaluation of the 183 buildings in the Test Sites of Xemxija and Nadur, to the ratings obtained following a GNDT second level assessment [26] and a FEMA 154 (second edition) assessment [27] of the same buildings (where, in the case where a range of weightings was available in the GNDT level 2 assessment, the more conservative option was always selected, and a 'Low Seismicity' form was used in the case of the FEMA 154 verification);

ii. the comparison of the seismic vulnerability rating of the buildings in the Test Sites, resulting from Sections 2, 3, 4, 5 and 6 of the New Form, considered one at a time, to the score obtained from the corresponding parameters in the GNDT level 2 assessment method [26], with respect to which, the degree of correspondence between the building attributes considered in these five sections of the New Form and the corresponding GNDT level 2 parameters is summarised in Figures 3-6 to 3-10;

iii. the comparison of the final seismic vulnerability rating, obtained for the assessed buildings using the New Form, to the outcome of the GNDT second level assessment method [26] and the score resulting from the method proposed by Formisano et al. [28] [29] [30] [31], which is aimed at evaluating the seismic vulnerability of buildings located within an aggregate, and which was applied to the GNDT second level assessment method [26] in the present study.

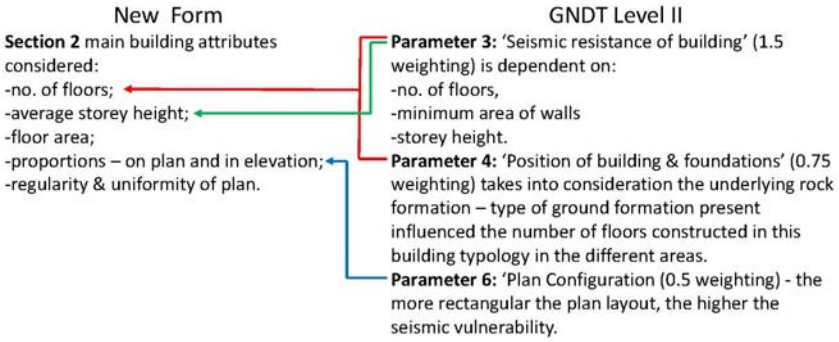

Figure 3-6 Comparison of the building characteristics considered in Section 2 of the New Form to those considered in the corresponding Parameters 3, 4 and 6 of the GNDT second level assessment method.

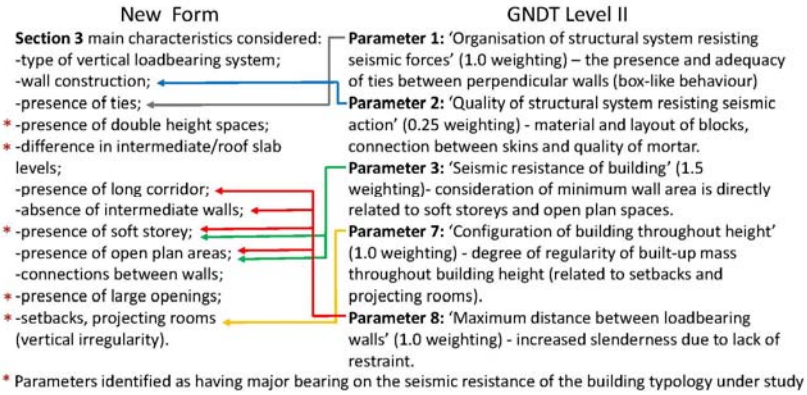

Figure 3-7 Comparison of the building characteristics considered in Section 3 of the New Form to those considered in the corresponding Parameters 1 to 3, 7 and 8 of the GNDT second level assessment method.

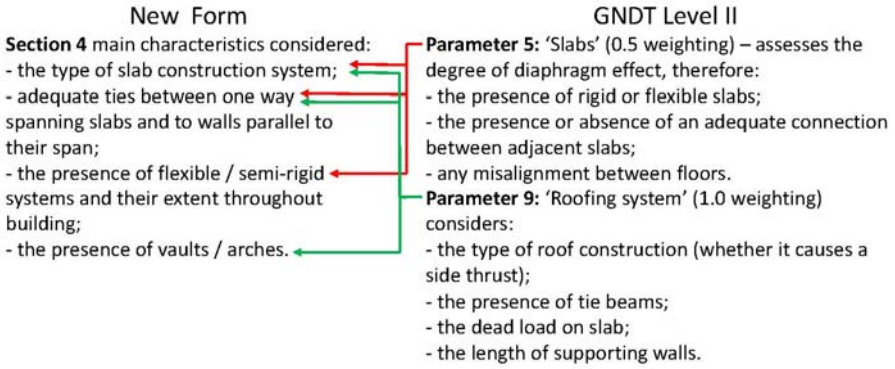

Figure 3-8 Comparison of the building characteristics considered in Section 4 of the New Form to those considered in the corresponding Parameters 5 and 9 of the GNDT second level assessment method.

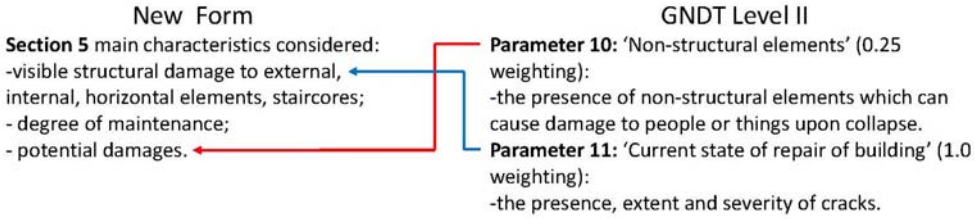

Figure 3-9 Comparison of the building characteristics considered in Section 5 of the New Form to those considered in the corresponding Parameters 10 and 11 of the GNDT second level assessment method.

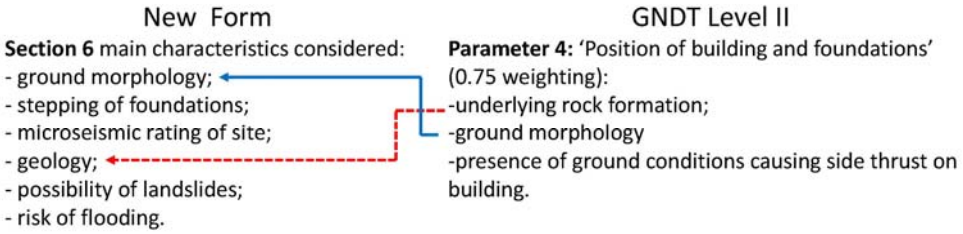

Figure 3-10 Comparison of the site characteristics considered in Section 6 of the New Form to those considered in the corresponding Parameter 4 of the GNDT second level assessment method.

The work carried out in this study with respect to the development of the New Form and the corresponding rating system, together with the first two verification checks (i and ii) was published by Torpiano et al. [5] [6] [25]. The work reported in these publications forms an integral part of the study presented in this thesis and provides an important background to the subsequent stages of this study. Nevertheless, in order to avoid repetition, the work presented in these publications was not included in this Chapter, and these publications were instead reproduced as Documents (i), (ii) and (iii) in Appendix B, where, out of the three documents, Document (i) gives the most detailed description of the work carried out and analysis of the results obtained.

3.2.1 'Aggregate effect' verification

The method proposed by Formisano et al. [28] [29] [30] [31], as an extended version of the Benedetti and Petrini seismic vulnerability index method [68] for the evaluation of the seismic vulnerability of buildings located within an aggregate, discussed in Section 2.6 of this thesis, was chosen for the evaluation of the aggregate effect of the buildings in the Test Sites, when compared to similar vulnerability index methods proposed by Vicente et al. [105] and Ferreira et al. [66], since, in the latter two methods, no detail regarding the derivation of the new or altered parameter weightings was made available. Furthermore, these publications [105] [66] do not include the vulnerability index ranges, which correspond to the different final seismic vulnerability ratings. The method presented by Benedetti and Petrini [70] is considered to be the forerunner of the GNDT second level assessment method [26], which was applied in the present study for the assessment of the 183 buildings in Xemxija and Nadur as explained in Section 3.2 and Documents (i), (ii) and (iii) of Appendix B [5] [25] [6], in order to obtain some insight into the validity of the developed rating system for the New Form. Hence, in the present study, the analysis of the influence of the 'aggregate effect' on the seismic vulnerability of masonry buildings, and the verification with respect to whether the proposed New Form and corresponding rating system adequately identify this alteration in seismic resistance, were investigated through the comparison of the seismic vulnerability ratings resulting from the application of the method proposed by Formisano et al. [28] [29] [30] [31] to the GNDT level 2 method [26] (hereafter referred to also as 'the extended GNDT second level assessment method', or the 'extended GNDT level 2 method') to those obtained from the (original) GNDT second level assessments [26] and the evaluations carried out using the New Form for the 183 assessed buildings. The comparison of these ratings is summarised in Figures 3-11 to 3-14 and in Figures 14 and 15 of Appendix A. Tables 11 to 23 in Appendix A present the results of the comparison in tabular format. These tables report the normalised seismic vulnerability indexes which resulted from the assessments of the 183 buildings in the Test Sites, using the original and extended versions of the GNDT second level assessment method, and include observations on the ratings.

The additional parameters proposed by Formisano et al. [28] [29] [30] [31] do not seem to consider the possibility of adjacent (abutting) constructions, which form part of the same urban block but which do not share a common party wall. This is most likely due to the specific focus of this method with respect to the older masonry buildings present in historical towns in Italy, where the diachronic evolution of these urban centres most often led to the addition of floors over existing buildings, and the construction of additional rooms or separate units on plan, sharing the (previously external) common walls between the two constructions [31]. Hence, this method considers a context, where the construction of independent party walls, which are, however, abutting, is not generally present, unless an older building within the aggregate was demolished and replaced by a newer construction in recent years (which case does not seem to be taken into account). Since the masonry building typology under investigation in the present study is related to more recent constructions present in newer urban areas of the Maltese Islands, where unshared party walls and vacant sites can be commonly found, a number of approximations were made by the author of this thesis, in the identification of the construction scenario classes of the additional parameters proposed by Formisano

et al. [28] [29] [30] [31] during the assessment of the buildings in the Test Sites using this extended GNDT second level assessment method, with respect to the different cases, where these two characteristics were present. These approximations are mainly related to the first four additional parameters proposed by Formisano et al. [28] [29] [30] [31], and consist of the following:

a) the presence of a vacant site was considered as the presence of a building of lower overall height in the first additional parameter ('Presence of adjacent buildings with different height');
b) the buildings, whose party walls are not shared on one side only, were considered as having a lower building on the side of the unshared party wall in the first additional parameter ('Presence of adjacent buildings with different height'), and as being located at the 'edge' position of the aggregate in the second additional parameter ('Position of building in aggregate'), while in the case of the fourth and fifth additional parameters ('Presence of staggered floors' and 'Structural heterogeneity among adjacent structural units', respectively), the entries were based on the differences between the type of structural system and the presence of staggered buildings on the side where the party wall is shared ;
c) the entries corresponding to a score of 0, in all the five additional parameters, were selected in the case of buildings, which have a vacant site on both sides, since no 'aggregate effect' can be present in such cases;
d) the entries corresponding to a score of 0 were selected for the first four additional parameters, in the case of buildings, which are positioned in an urban block, but which have unshared party walls on both sides. The fifth additional parameter ('Percentage difference of opening areas among adjacent facades') was evaluated based on the characteristics of the elevations of the building under assessment and the adjacent constructions.

The combined response to seismic actions is a fundamental requirement of the buildings forming an aggregate, as defined in the GNDT first level assessment method [69]. Therefore, it is hereby being acknowledged that the presence of independent party walls, which are constructed directly abutting each other, as is common in local construction practice, could not always be indicative of a separate structural response to seismic actions, since, during low frequency vibrations, the in-phase vibration of the respective buildings could occur, hence resulting in the buildings acting in combination. Nevertheless, the out-of-phase vibration, which could be triggered by the different dynamic properties of the abutting buildings, and the differences between their respective lateral storey stiffnesses, would present a risk of damage due to pounding, which is not being taken into account in this study neither in the additional parameters proposed by Formisano et al. [28] [29] [30] [31] nor in the decision of the current author to consider the presence of independent abutting party walls as indicative of separate aggregates during the identification of the aggregates in the Test Sites. However, this decision was based on the recognition that the identification of the occurrence, or otherwise, of a combined response to seismic excitations or pounding, can only be carried out following a detailed investigation of the seismic response of adjacent abutting constructions, in the presence of different building characteristics, misaligned roof and intermediate slab levels, and different building proportions of the

respective buildings. This investigation could not be carried out as part of this thesis due to time limitations.

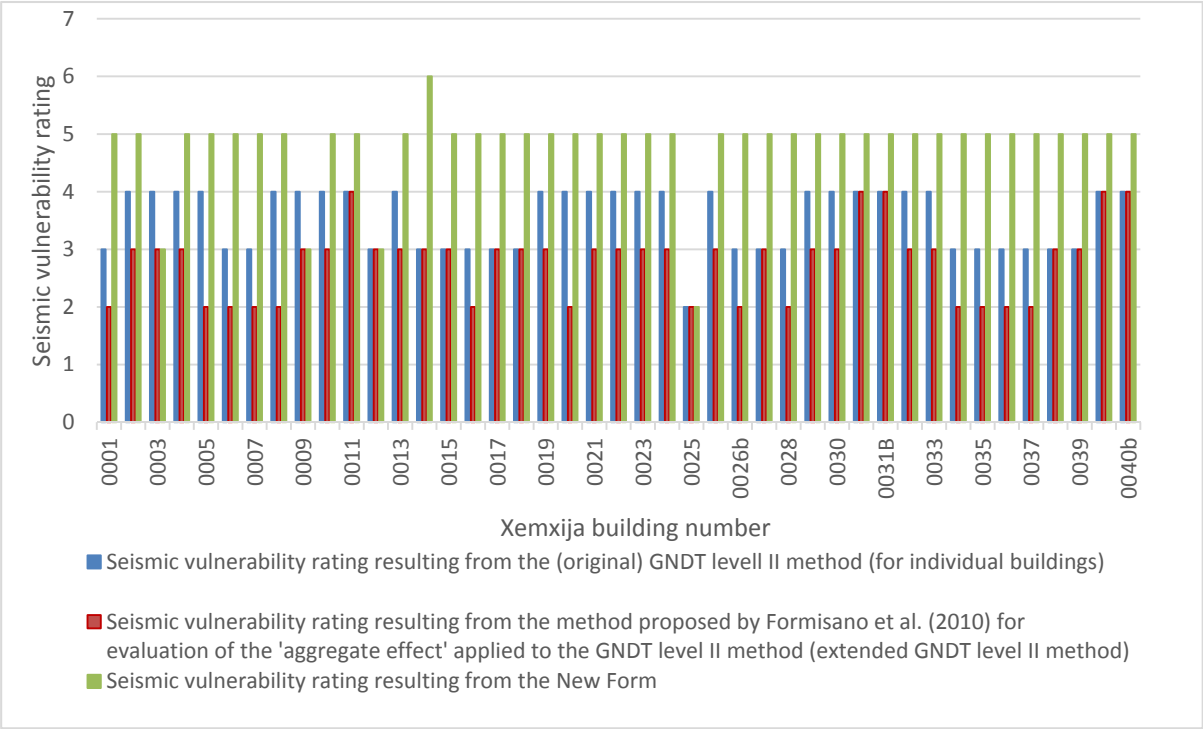

Figure 3-11 Comparison of the seismic vulnerability ratings resulting from the original GNDT level 2 method, the extended GNDT level 2 method (including the parameters proposed by Formisano et al.[28]) and the New Form for buildings 0001 to 0040b in Xemxija.

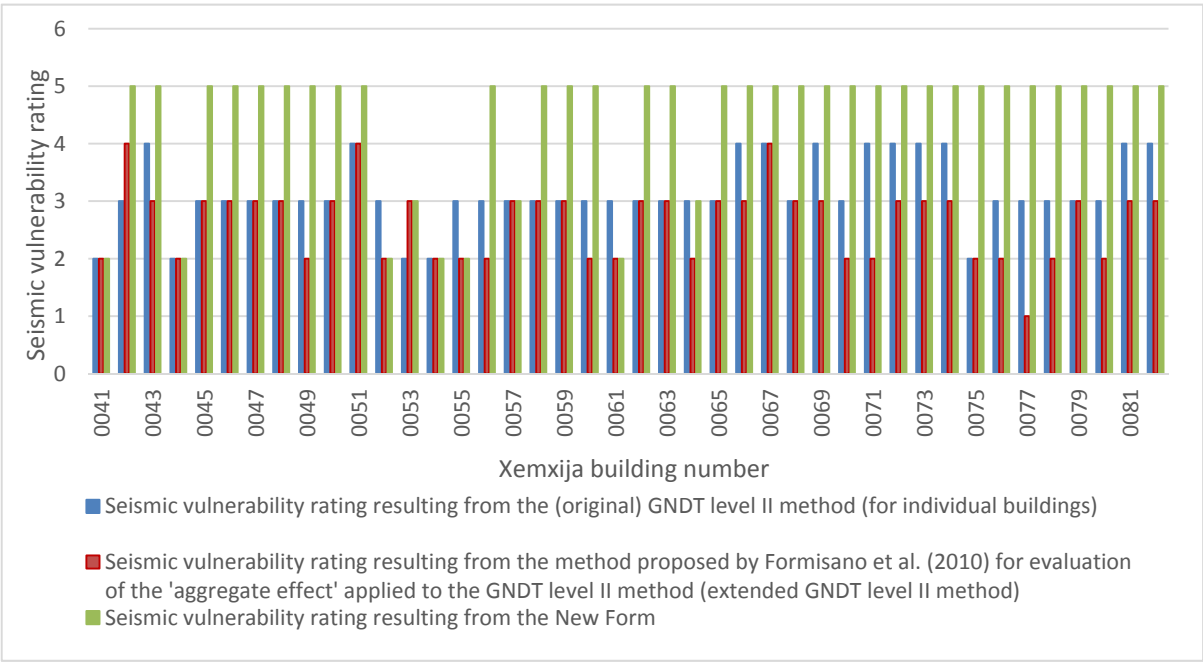

Figure 3-12 Comparison of the seismic vulnerability ratings resulting from the original GNDT level 2 method, the extended GNDT level 2 method (including the parameters proposed by Formisano et al.[28]) and the New Form for buildings 0041 to 0082 in Xemxija.

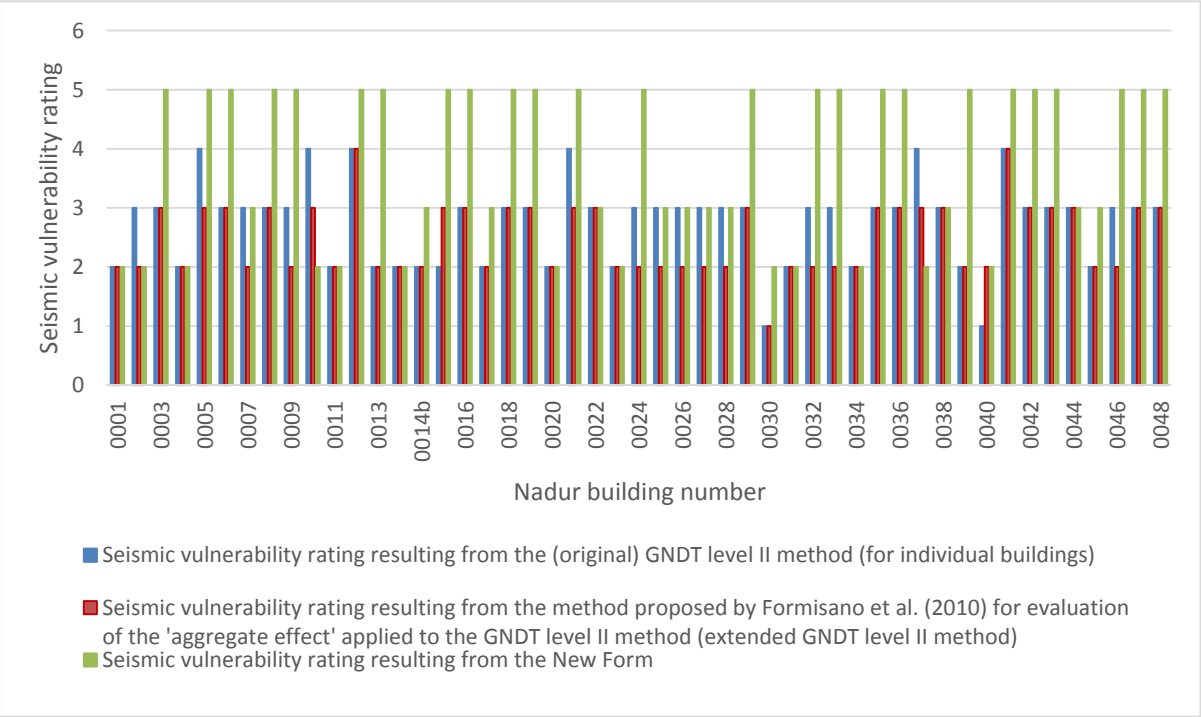

Figure 3-13 Comparison of the seismic vulnerability ratings resulting from the original GNDT level 2 method, the extended GNDT level 2 method (including the parameters proposed by Formisano et al.[28]) and the New Form for buildings 0001 to 0048 in Nadur.

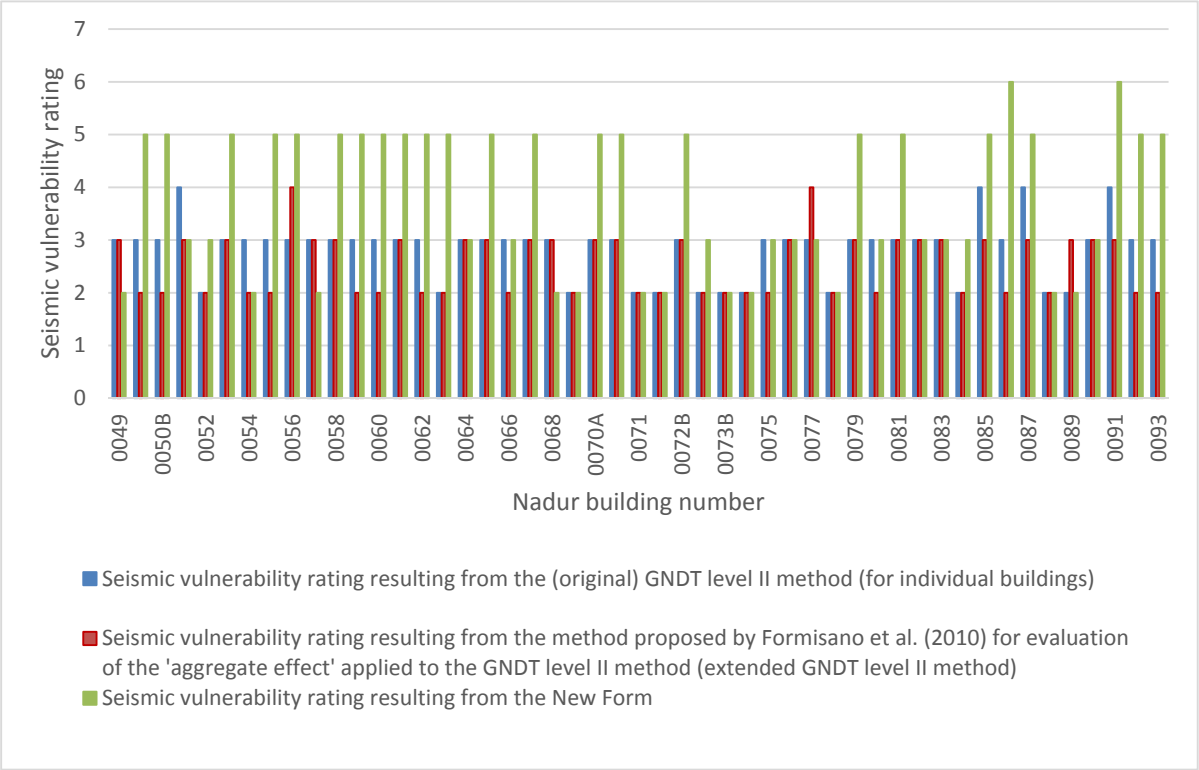

Figure 3-14 Comparison of the seismic vulnerability ratings resulting from the original GNDT level 2 method, the extended GNDT level 2 method (including the parameters proposed by Formisano et al.[28]) and the New Form for buildings 0049 to 0093 in Nadur.

The seismic vulnerability ratings obtained from the extended GNDT level 2 assessment were interpreted on the basis of the same ranges of seismic vulnerability outcomes for 'Adequate', 'Low', 'Medium-low', 'Medium', 'Medium-high' and 'High', which were applied in the case of the assessments carried out using the original GNDT second level method [26] on the same buildings in the Test Sites. These ranges of ratings were altered in the present study, as reported in Table 1 of Torpiano et al. [5], which is reproduced as Document (i) in Appendix B. Moreover, the graphical representation of the comparison between the seismic vulnerability ratings of the assessed buildings, obtained using the original and extended forms of the GNDT second level assessment method, and the New Form presented in Figures 3-11 to 3-14, is based on the system of weightings assigned to the seismic vulnerability outcomes indicated in Table 2 of the same document [5].

Figures 3-11 to 3-14 together with Figures 14 and 15, in addition to Tables 11 to 23 in Appendix A indicate that the seismic vulnerability ratings, resulting from the use of the extended GNDT level 2 method on the buildings in the Test Sites, exhibit an increase in rating by 1 grade in 3.83% of the assessments and a decrease of 1 to 2 grades in 43.17% of the evaluated buildings, when compared to the seismic vulnerability scores obtained for the same buildings using the original GNDT second level method [26], consequently presenting an even larger divergence from the ratings obtained from the use of the New Form. Furthermore, a 57.65% decrease in seismic vulnerability rating of 1 to 2 grades was observed, when the extended GNDT level 2 assessment was applied to the Xemxija buildings when compared to the original GNDT level 2 evaluations, while in the Nadur Test Site this decrease resulted in 30.61% of the buildings. This variation in the 'sensitivity' of the buildings, in the two locations, to the alteration in seismic vulnerability rating, when the parameters which take into account the variation in resistance of buildings located within an aggregate are considered, could be due to a number of factors related to the differences in the urban fabric of the two towns, namely:

a) the presence of smaller aggregates in Nadur, resulting from more frequent cases of unshared party walls and a higher number of vacant sites, led to the evaluation of a higher number of buildings as 'isolated' constructions, where no 'aggregate effect' would be present;
b) a higher difference in the percentage area of openings of adjacent buildings in Nadur;
c) a higher difference in the overall building heights of adjacent buildings in Nadur.

The normalised seismic vulnerability index resulting from the extended GNDT second level assessment (which consists of the original GNDT second level parameters [26] and the additional five parameters, which assess the 'aggregate effect' on the seismic vulnerability of masonry buildings, as proposed by Formisano et al. [28] [29] [30] [31]) was calculated on the basis of the revised (higher) maximum score resulting from the consideration of the additional parameters. A close examination of the building characteristics identified by the additional parameters proposed by Formisano et al. [28] [29] [30] [31] in the buildings of the Test Sites, together with the corresponding seismic vulnerability indices and the final ratings obtained from the extended and the original GNDT level 2 assessments in Tables 11 to 23 of Appendix A, suggests that the revision of the maximum score in the extended method, though necessary, resulted in cases where, even though a number of characteristics, which are expected to increase the seismic vulnerability of the building, were identified, the normalised seismic vulnerability

index obtained had a lower magnitude than that of the corresponding original GNDT second level assessment. It is not clear to the author of this thesis, whether this aspect was investigated by the authors of the extended method, and whether the lower seismic vulnerability rating resulting in such cases is, in fact, intentional and expresses the decrease in seismic vulnerability resulting from the location of the building in the aggregate, even if particular characteristics, which are associated with a decrease in building resistance, are present. Furthermore, the results in Tables 11 to 23 of Appendix A also indicate that, in view of the wide ranges of values corresponding to the different rating classes, small changes in the normalised seismic vulnerability index do not translate as an observed difference in the seismic vulnerability rating.

Hence, caution must be exercised in the interpretation of the variation in the seismic vulnerability ratings obtained from the three methods under comparison. On the other hand, these comparisons suggest that, while the New Form includes a number of entries[6] which identify the possible interaction of the building under assessment within the context of an aggregate, the developed rating system for the New Form considers the difference in the overall heights of adjacent buildings as the only 'aggregate effect' parameter, which has a major bearing on the final seismic vulnerability rating, where a minimum misalignment of one floor is considered to impair the seismic resistance of the structure under evaluation. This rating system could lead to a more realistic assessment if the contribution of factors, such as, the position of the building in the aggregate, the misalignment of intermediate floors and the sharing or unsharing of party walls in adjacent constructions (and consequently, the risk of pounding) to the seismic response of buildings, are also taken into account.

3.3 Statistical Analysis

As explained in the work published by Torpiano et al. [5] [6], with respect to the development of the New Form, and the corresponding rating system, which is reproduced as Documents (i) and (iii) of Appendix B, the identification of the thirteen building attributes out of the 147 entries of the preliminary version of the New Form, which were considered to be principal indicators of the seismic

[6] Such entries include:

i. entry 23: Position in block/aggregate;
ii. entry 56: Difference in level of floor slab at Level 2 in adjacent building along left / right hand side party wall;
iii. entries 57 and 58: Difference in plane of front / rear façade walls of adjacent buildings on the right / left of building being assessed;
iv. entry 61: Vacant site directly adjacent to building;
v. entry 62: Evidence of a shared party wall;
vi. entry 64: Misalignment of the internal spaces of abutting properties;
vii. entry 87: Evidence of post-construction joining of originally separate individual buildings or post-construction additions in areas, which were originally left as voids in building aggregate.

vulnerability rating of the contemporary loadbearing URM building typology in the Maltese Islands, was based on:

a) the parameters considered in the pre- and post-event seismic vulnerability assessment methods, their relative weightings and their influence on the seismic response of structures;
b) the structural behaviour under seismic actions reported in international studies, when specific building characteristics are present, particularly in the case of the presence of a soft storey;
c) results from past local studies on the critical contemporary loadbearing URM building typology.

Hence, a further verification of the developed rating system for the New Form was carried out through a three-stage statistical analysis of the correspondence between 143 entries of the New Form, and the seismic vulnerability ratings, with the objective of identifying which building characteristics are significant indicators of the seismic vulnerability rating. IBM SPSS Statistics Version 23 was used for these statistical analyses, which are summarised below.

i. A univariate analysis of the characteristics recorded in the individual sections of the New Form was carried out with respect to the respective seismic vulnerability ratings resulting from their respective Section. The ordinal categorical nature of the seismic vulnerability ratings ('Low', 'Medium', 'High' in the case of Sections 2, 4, 5, 6 and 8, and the same rating categories in addition to 'Medium-low' and 'Medium-high' in the case of Section 3), which was considered as the dependent variable in all analyses, led to the use of non-parametric univariate tests. The Kruskal Wallis test, which is a non-parametric alternative of the One-Way ANOVA test, was used to compare mean seismic vulnerability ratings across the levels of a categorical seismic vulnerability parameter. On the other hand, the Spearman correlation test, which is a non-parametric alternative to the Pearson correlation test, was used to measure and assess the strength of the relationship between seismic vulnerability ratings and a continuous seismic vulnerability parameter. A 0.05 level of significance was adopted for both tests, where statistical significance is obtained when the p-value is less than the 0.05 criterion.
ii. The major limitation of the Spearman correlation and Kruskal Wallis tests is that they relate seismic vulnerability ratings to one seismic vulnerability parameter only. However, the goal of a research study is to analyze these seismic vulnerability parameters collectively. To overcome this limitation, the building characteristics of every individual section of the New Form, which resulted as significant predictors through the Univariate analysis tests, were analysed in combination, one section at a time, through a multivariate Ordinal Logistic Regression Analysis, with respect to the seismic vulnerability rating of their respective section.
iii. The building characteristics, which resulted as significant predictors of the seismic vulnerability outcomes of the individual sections, were analysed in combination with respect to the overall final seismic vulnerability rating, resulting from Section 10 of the New Form, through an Ordinal Logistic Regression Analysis.

The backward elimination process carried out in the third stage multivariate analysis resulted in the definition of a parsimonious model, which included eleven significant predictors of the final seismic

vulnerability rating, which characteristics were ranked in order of significance through their respective p-values. These resulting eleven significant predictors are as follows (in order of decreasing significance):

i. total number of floors (New Form entry 26);
ii. presence of large openings on main façade 4 (New Form entry 76);
iii. presence of slabs spanning in one direction and not tied to each other / to walls parallel to their span (New Form entry 92);
iv. absence of intermediate walls in loadbearing masonry building in one or more storeys (New Form entry 65);
v. presence of double height spaces facing infrastructure for accessibility / connection (New Form entry 54);
vi. presence of long corridor / garage / other open plan space directly adjacent to party wall (New Form entry 63);
vii. evidence of shared party wall (New Form entry 62);
viii. presence of setbacks along main façade 3 at level 1 (New Form entry 80b);
ix. presence of projecting rooms / balconies at two or three levels (New Form entry 82c);
x. proportions of building on plan at typical plan level (width : length) (New Form entry 33);
xi. vacant site directly adjacent to building (New Form entry 61).

The work carried out by the author of this thesis, on the statistical analysis of the data recorded in the 183 buildings evaluated using the New Form, was reported and discussed in Sapiano et al. (to be submitted for publication) [148] and is being reproduced in this thesis as Document (iv) in Appendix B, instead of being inserted in the main text in order to avoid repetition.

3.4 Numerical Analysis using ELS®

In the study presented herein, the software package ELS (Extreme Loading® for Structures by ASI) Version 3.1 was used for the investigation of the influence on the response of the contemporary loadbearing URM building typology to seismic excitations resulting from the presence of six of the main building characteristics, which were identified in the developed rating system for the New Form as principal indicators of the seismic vulnerability rating of this building typology. This investigation was carried out through a number of full non-linear dynamic analyses, which considered a range of different construction scenarios (presented in Section 3.4.8), and the examination of the change in dynamic properties of the analysed models under static and dynamic loads following the analysis for two eigen modes of the building numerical models. This software package was the only commercially-available numerical modelling software package based on the Applied Element Method (AEM) at the start of this research study, and was selected in view of the added capabilities (when compared to other modelling methods, such as the Finite Element Method (FEM) and the Distinct Element Method (DEM)) associated with this numerical modelling method, to adequately represent the element displacements and separations resulting from the formation and propagation of cracks up to a state of

progressive collapse, particularly in structures consisting of discrete elements connected by a weaker interface material, as in the case of the loadbearing URM structures under study.

3.4.1 Trial models and modelling of wall-to-wall junctions

In view of the limited information provided in published international studies, and the manuals of the chosen software program regarding the modelling techniques employed for the modelling of masonry structures using ELS®, and their analysis under seismic loads, the present study in this thesis started with the construction of a number of trial models consisting of a single room (with an overall height of 1 storey), a double height room, and trial models of an existing six-storey building in the Test Site of Xemxija (Building Number 0011), where, in the latter case, the modelling of ground formation layers and their restraints, amongst other factors, were investigated.

The single-room models were used mainly to master the basic modelling techniques of ELS®, such as the definition of walls, wall openings (as indicated in Figure 3-15) and reinforced concrete slabs, in addition to the modelling of bondstones in double leaf walls, reinforced concrete lintels over wall openings, including their bearing on the supporting wall areas, and the definition of a concrete interface material between concrete lintels or slabs, and the supporting walls at the bearing position through the specification of different material springs in these regions. In view of the contained size of these numerical models when compared to the full scale six-storey final building numerical models, the formation of cracks and the stress variations under dynamic loads could be visualised effectively.

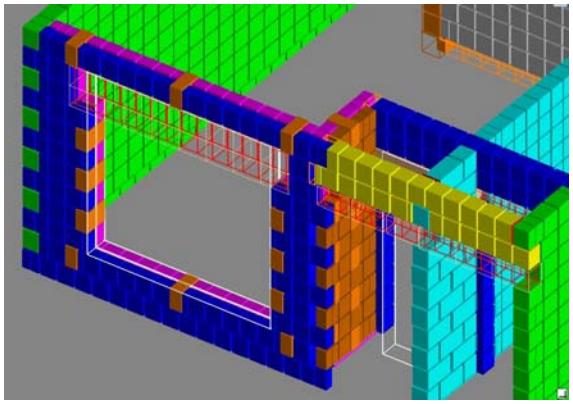

Figure 3-15 Image indicating bearing of reinforced concrete lintels on supporting wall and the modelling of bonded double leaf walls in jambs of openings.

All wall panels in the trial numerical models and the final full scale numerical models were defined using the software's automatic wall generation function for the realistic representation of masonry walls with staggered joints (as individual masonry blocks with mortar joints). The study of the modelling of the wall-to-wall junctions was given particular attention through the single room numerical models. Three modelling options were investigated, namely:

a) interlocked: the interlocking of courses at the junction between intersecting walls, in accordance with normal construction practice;
b) abutting: the modelling of junctions between intersecting walls as 'abutting', where one wall stops in line with the face of the intersecting wall, and, hence, no interlock is provided, and mortar is specified as the interface material between the two walls throughout their height;

c) fused: the modelling of junctions between intersecting walls as 'fused', where the interface material throughout the height of the junction between the two walls is specified as the material of the walls, or the weaker material of the two walls, if the two intersecting walls have different material properties, therefore, creating T-shaped or L-shaped masonry blocks at every course.

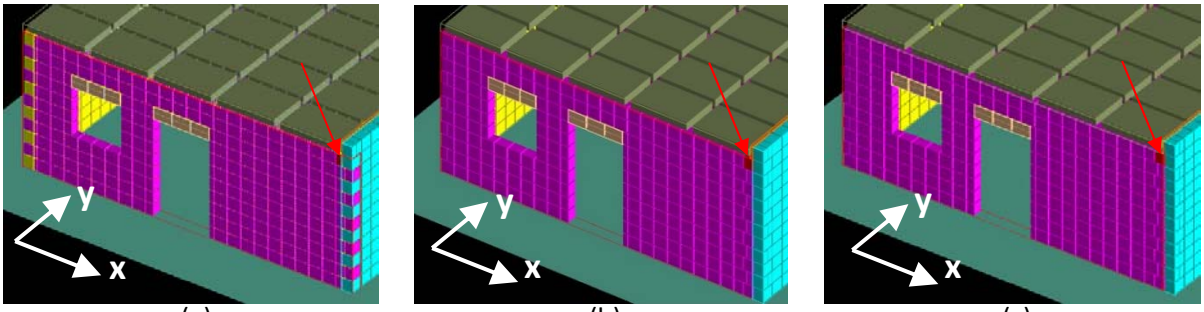

(a) (b) (c)

Figure 3-16 Position of the element at the top right corner of the three analysed single room numerical models for the comparison of displacements in the a) interlocking, b) fused and c) abutting options of the modelling of wall-to-wall junctions.

Table 3-1 Maximum x- and y-displacements of the corresponding element at the top right corner of the three analysed single room numerical models for the a) interlocking, b) fused and c) abutting options of the modelling of wall-to-wall junctions.

Modelling of wall-to-wall junction	Maximum displacement in x-direction	Maximum displacement in y-direction
Interlocking	$+8.69 \times 10^{-6}$mm	-6.33×10^{-5}mm
Fused	$+2.44 \times 10^{-7}$mm	-4.44×10^{-5}mm
Abutting	$+7.35 \times 10^{-6}$mm	-1.44×10^{-4}mm

Table 3-2 Comparison of the maximum x- and y-displacements of the corresponding element at the top right corner of the three analysed single room numerical models for the a) interlocking, b) fused and c) abutting options of the modelling of wall-to-wall junctions.

Interlocking vs. Fused			Interlocking vs. Abutting	
Maximum x-displacement	35.61 times larger in case of interlocking		Maximum x-displacement	1.18 times larger in case of interlocking
Maximum y-displacement	1.43 times larger in case of interlocking		Maximum y-displacement	2.27 times larger in case of abutting

The comparison of the maximum x- and y-displacements, recorded for the same element in the top right corner of the corresponding façade, in three identical single room numerical models (in Figure 3-16), which differ only with respect to the modelling of the wall-to-wall junctions, and which were analysed under the same ground motion record applied along the weaker y-y orientation of all numerical models (summarised in Tables 3-1 and 3-2) suggested that the fused option resulted in lower displacements than both the interlocking and the abutting options in both x- and y- orientations. This indicates that the definition of the material of the springs at the wall-to-wall junction, as equivalent to the material or the walls (or to the weaker of the two walls, if the walls consist of different materials), results in a much stiffer connection between the two walls (hence, providing a higher restraint to

rotation at this junction) than that resulting when the material at the junction is defined as mortar (as in the 'abutting' option) or when the junction is modelled as interlocking, where, in the latter case, a degree of rotation between the blocks of the two walls at the intersection is still possible. Furthermore, the weaker interface material (specified as mortar) in the abutting option resulted in a larger displacement in the y-direction than that obtained in the case of the interlocking option.

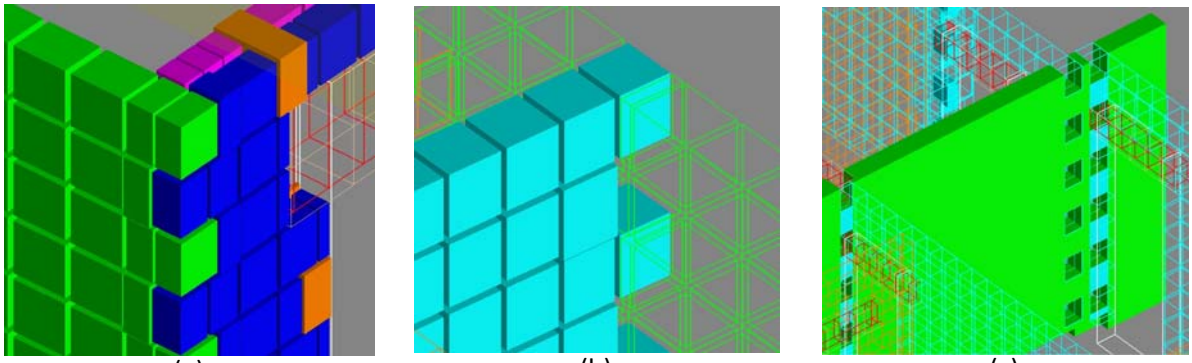

Figure 3-17 Images of interlocked wall junctions a) between the front facade and a party wall, b) between an internal wall and a party wall, c) between the internal walls framing into the common party wall in a two- or three-building control numerical model.

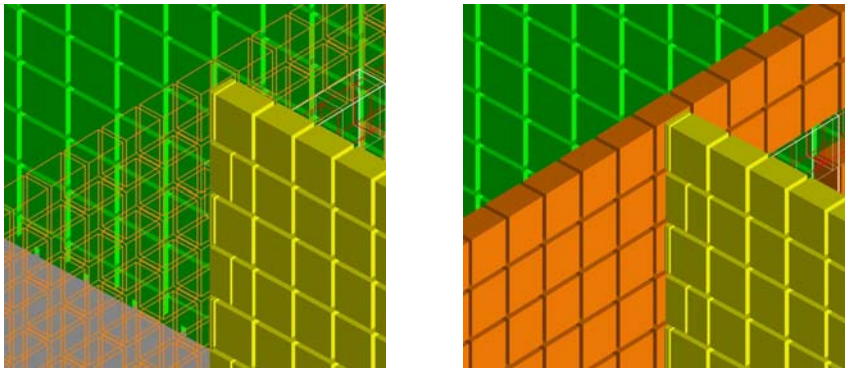

Figure 3-18 A 'fused' junction at the intersection of two internal walls.

Local masonry construction practice involves the interlocking of alternate courses at all wall intersections. However, in view of the extended modelling time required for the modelling of all wall-to-wall junctions of the final full scale numerical models with interlocking courses, the risk of errors occurring in the modeller file when elements are extracted from the walls in order to form the interlocked courses and the limitations with respect to the consequent increase in the overall number of elements of the models resulting from the modelling of interlocked courses, a simplification in the modelling of the junction between intersecting walls was adopted. This simplification consisted in:

i. the modelling of all junctions between external walls or between internal walls and external walls as 'interlocked' (as presented in the images of Figure 3-17), thus ensuring that the stiffness of the connections forming the external envelope of the modelled structures is accurate;
ii. the modelling of all junctions between all other internal walls as 'fused' (as indicated in Figure 3-18) through the definition of the interface material at the junction between the two walls as

the material of these walls, or as the weaker of the two walls, if the walls have different material properties.

While the simplification with respect to the modelling of internal wall-to-wall junctions as 'fused' might have resulted in a higher lateral storey stiffness in the storeys above the semi-basement level in the final full scale numerical models, and hence, a larger stiffness gradient at slab over semi-basement level in the cases when a soft storey is present, this option was selected as opposed to the 'abutting' option since, in view of the weak quality of the local mortar, which is also reflected in the material properties of the mortar specified in the numerical models, the latter option was considered to provide a more unrealistic end-restraint condition, particularly in the case of out-of-plane loaded walls.

3.4.2 Additional modelling techniques adopted: cast in-situ slabs, precast prestressed slabs, double leaf walls, hollow concrete blockwork walls and damp proof course

Reinforced cast in-situ slabs were specified at all levels in the numerical models of the existing Xemxija building (Building Number 0011), and throughout the final set of numerical models analysed under dynamic loading, with the exception of the slab over semi-basement level in the models, which include a soft storey at the lowermost level. In this case, precast prestressed concrete slabs with a reinforced cast in-situ topping were defined. Reinforced cast in-situ concrete slabs were generally modelled with a bearing on half the thickness of the supporting walls, except in case of slab edges at shaft positions, where the slabs were modelled to bear on the whole wall thickness. Slab thicknesses and reinforcement quantities were based on the length of their effective spans and their loading, considering typical floor build-up details, and the uses of the spaces specified in the development permit drawings. No peripheral ties or ring beams were defined in slabs, in accordance with typical local construction practice for the scale of the buildings under investigation; however the slab reinforcement of every slab was anchored / lapped on adjacent slabs in accordance with code requirements.

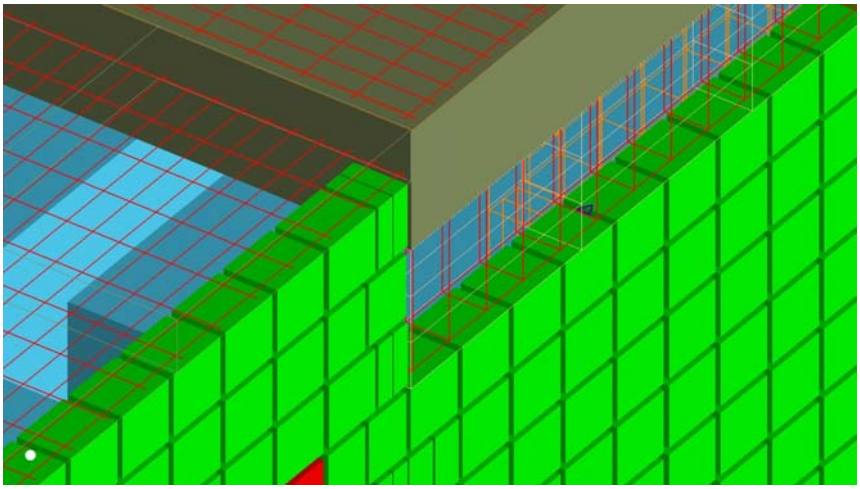

Figure 3-19 Precast prestressed concrete slabs (in grey) with a reinforced cast in-situ concrete topping and bearing over a reinforced concrete spreader beam at the wall supports, with no reinforced connection between the spreader beam and the precast slabs.

460 mm thick precast prestressed concrete slabs were specified at slab over semi-basement level in all models, which include a soft storey at semi-basement level, with reference to the 'Precast Prestressed Concrete Panels - Safe Load Tables' of Ballut Blocks Services Ltd., Malta (http://www.ballutblocks.com, downloaded on the 2nd March 2015) [149], and following the calculation of the worst shear loading case acting on these slabs. The precast prestressed concrete slabs were defined in the numerical models as individual solid slabs with a maximum width of 1200 mm, a minimum width of 600 mm, and with a corrected density in order to take into account of the presence of the voids within their cross-section. It is hereby noted that the slabs were modelled as solid members since the modelling of the voids would have caused an increase in the number of elements in the models, which had to be kept to a minimum in order to limit analysis run times. Mortar was intentionally specified as the interface material between the individual precast units, in order to ensure that the these units were interpreted by the software program as separate structural members connected only through the overlying 50 mm thick reinforced concrete topping. The definition of a concrete interface material between the units would have led the software program to consider the slab over semi-basement level as consisting of one single continuous (jointless) concrete section. The precast prestressed concrete slabs were defined as spanning between the party walls, and positioned in simple bearing over 228 mm wide by 530 mm deep reinforced concrete spreader beams, which are cast directly over the supporting party walls, with no reinforced connection between these spreader beams and the underlying walls, or the spreader beams and the precast units or their cast in-situ concrete topping, as indicated in Figure 3-19. The concrete spreader beams were reinforced with the minimum reinforcement required by the design codes for their cross-sectional dimensions, and were defined only along the party walls (not along the façade walls) hence not providing any ring-beam action at this slab level. While the author acknowledges the shortcomings of the resulting construction detail at the bearing of the precast prestressed concrete slabs, this detail was specified in the numerical models, since it is in accordance with the typical construction practice in the Maltese Islands.

All reinforced concrete beams and reinforced concrete lintels were dimensioned and reinforced in proportion to their span and superimposed loading. A 190 mm bearing length on the supporting walls was specified for all concrete beams and lintels.

While ELS® allows for the subdivision of members into a number of elements, hence resulting in a higher accuracy in the estimation of the stresses and strains acting on the members when a finer mesh is specified, since failure in concrete slab members under dynamic actions was not considered to be of particular importance, when compared to the failure of masonry walls, all slabs were subdivided into elements with approximate dimensions of 1 m length by 1 m width. Similarly, spreader beams, reinforced concrete structural beams and reinforced concrete lintels were subdivided in approximately 1 m long sections throughout their length. On the other hand, since the masonry walls provide the primary lateral load resistance under seismic excitation, all masonry blocks in the walls defined in the analysed models were split into two elements along their length. Five springs were specified at all element interfaces.

Table 3-3 Altered material properties of walls in the analysed numerical models.

	Ratio of net to gross surface area of hollow concrete blocks	Original compressive strength (N/mm^2)	Revised compressive strength for walls constructed in hollow blocks but modelled as solid blocks (N/mm^2)	Original friction coefficient	Revised friction coefficient in hollow concrete blockwork walls	Original density of mortar (kg/m^3)	Revised density of mortar in hollow concrete blockwork walls (kg/m^3)
228 mm thick double density hollow concrete blockwork walls	0.718	7.50	5.385	0.40	0.287	n/a	n/a
Mortar for 228 mm thick double density hollow concrete blockwork walls	n/a	2.00	1.436	0.40	0.287	1760	1263.7
Mortar for 228 mm thick double density hollow concrete blockwork walls at damp proof course	n/a	2.00	1.436	0.40	0.211	1760	1263.7
153 mm thick hollow concrete blockwork walls	0.645	7.50	4.838	0.40	0.258	n/a	n/a
Mortar for 153 mm thick hollow concrete blockwork walls	n/a	2.00	1.290	0.40	0.258	1760	1135.2
Mortar for 153 mm thick hollow concrete blockwork walls at damp proof course	n/a	2.00	1.290	0.40	0.190	1760	1135.2
Mortar for 228 mm thick globigerina limestone (softstone) walls at damp proof course	n/a	2.00	n/a	0.40	0.294	1760	1760

Wall materials and thicknesses specified in the numerical models consist of:

a) 228 mm thick local globigerina limestone (softstone) walls constructed from solid blocks of the same material, with overall dimensions of 558.8 mm length by 228 mm breadth and 265 mm height, defined mainly in the party walls;
b) 228 mm thick hollow double density and 153 mm thick hollow concrete blockwork walls constructed from hollow blockwork units (also referred to herein as HCB), with overall dimensions of 457 mm length by 228 mm breadth and 265 mm height, and 457 mm length by 153 mm breadth and 265 mm height, respectively. Void areas and self-weights corresponding to these concrete blocks were obtained with reference to the data sheet for the concrete blocks produced by Ballut Blocks Services Ltd., Malta (http://www.ballutblocks.com, downloaded on the 25th February 2015) [150]. These walls were defined mainly in the front and rear façades and in the internal walls. Wall thicknesses defined in the analysed numerical models of Xemxija Building Number 0011 were based on the wall thicknesses indicated in the development permit drawings of this building. Similarly, the wall thicknesses defined in the final set of analysed numerical models were based on the wall thicknesses indicated on the typical floor level of the development permit drawings of the same Xemxija building.

All party walls were considered to be continuous in the same vertical plane throughout their height while, in the two- and three-building control numerical models, common party walls were modelled as shared throughout the height of the buildings. Double walls in the front façade of the numerical models of Building Number 0011 in Xemxija, and in the final set of analysed numerical models, were modelled with a hollow cavity between the two leaves and with bondstones tying the two leaves together in accordance with the construction practice in the Maltese Islands. Moreover, since the modelling of hollow concrete blockwork walls with voids, while possible, would result in an increase of the total number of elements in the analysed models, and hence, in the processing time of every model, these walls were instead modelled as composed of solid blocks with adjusted values of compressive strength and frictional coefficient to reflect the actual contact area present between any two overlying blocks (based on the ratio of the net surface area to the gross surface area of the blocks). While the tensile strength of mortar was specified as 0 N/mm^2, in view of the weak quality of the local mortar, in the case of the mortar joints in hollow concrete blockwork walls, an alternative mortar with a lower compressive strength and a revised density, based on the actual contact area of the blocks, was defined for each HCB wall type.

The altered material properties of hollow blockwork walls and the corresponding mortar types specified for their joints are summarised in Table 3-3. In addition, the properties of all the materials specified in the full scale numerical models are summarised in Table 24 in Appendix C, while the sources from where particular material properties were obtained, or the way they were derived, is summarised in Table 25 of Appendix C. Whenever possible, material properties were based on manufacturers' data sheets or past local studies [150] [151] [152] [153] [154] [155]. However, in the cases where these studies were not available, reference was made to international publications and codes of practice [156] [157] [158] [159] [160].

Furthermore, the damp proof course (also referred to herein as DPC), which, as indicated in Figure 3-20, was specified in the analysed models of Xemxija Building Number 0011, and in the final set of analysed numerical models at the first mortar joint above the slab over semi-basement level, was modelled through the variation of the friction coefficient of the mortar at this joint (as reported in Table 3-3).

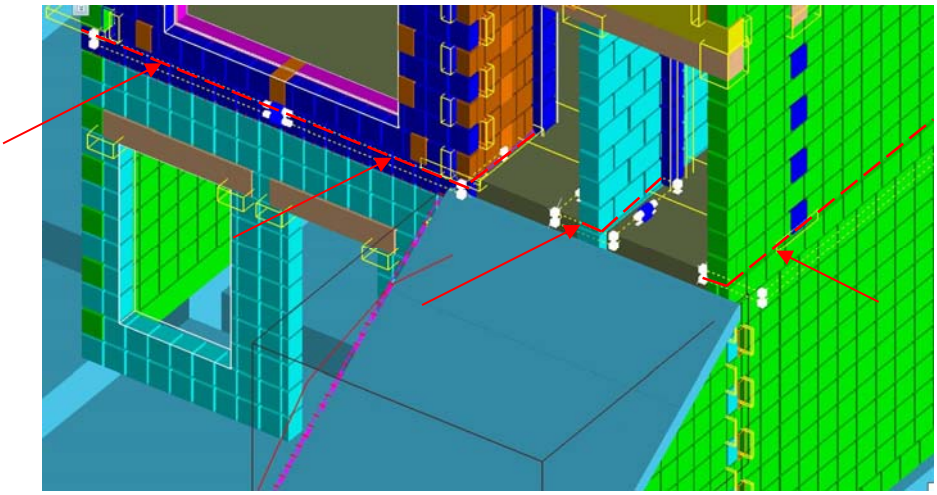

Figure 3-20 Position of damp proof course in full scale analysed numerical models.

The reduction in friction coefficient of the mortar at the position of the damp proof course was based on the results published by Saliba [161] for the maximum shear attained by masonry triplets, with three different types of damp proof courses, and considering three levels of pre-compression loads, which are reported in Table 26 of Appendix C. In the case of the full scale structures modelled in the present study, if slabs are considered to span between the party walls, the maximum precompressive stress per storey per metre length of party wall is around 0.125 N/mm^2, which would, hence, be equivalent to 0.25 N/mm^2 in the case of two floors above the damp proof course. With reference to the results reported by Saliba [161] and the comparison of the average maximum shear force attained in the presence of the three types of damp proof course materials considered by the author to the average maximum shear force resulting from equivalent triplets which do not contain a damp proof course, as summarised in Table 27 of Appendix C, a reduction factor of 0.573 should be applicable if a damp proof course consisting of polyethylene sheets (Low Density Polyethylene, L.D.P.E.) is considered under a pre-compressive stress of 0.25 N/mm^2. For buildings with more than two floors above the damp proof course, a proportional increase in pre-compressive stress would be present in the party walls. Furthermore, if not all slabs span directly on to the party walls, the pre-compressive stress at the level of the damp proof course would be lower than 0.125 N/mm^2 in the party walls, and higher in the internal walls. Hence, in view of:

a) the sequence of analyses planned for the present study, which consisted of the analysis of structures with a maximum height of six floors and the subsequent gradual reduction in number of floors until resistance to collapse is achieved, in addition to
b) the different stress levels present along the party walls arising from the variation in the spans of slabs loading these walls, and

c) the different types of damp proof course materials, which could typically be present in a contemporary loadbearing URM building typology depending on the age of the structures[7],

it was not considered practical to specify mortars with different friction coefficients at different positions along the length of the party walls, depending on the particular stress level present, and to alter these values at every reduction in the total number of floors. Therefore, with reference to Table 27 in Appendix C, a mortar with a friction coefficient equivalent to 0.737 times that of a normal local mortar was specified at the mortar joint at the position of the damp proof course in the full scale numerical models analysed using ELS®. According to the results reported by Saliba [161], this reduction factor is equivalent to the worst case scenario out of the three types of damp proof course materials considered in the study, for a pre-compressive stress of 0.50 N/mm^2 (hence, equivalent to around four floors with slabs spanning between party walls). In the cases where the damp proof course was specified in hollow concrete blockwork walls, this friction coefficient was reduced further to take into account of the actual contact area of the blocks as described earlier.

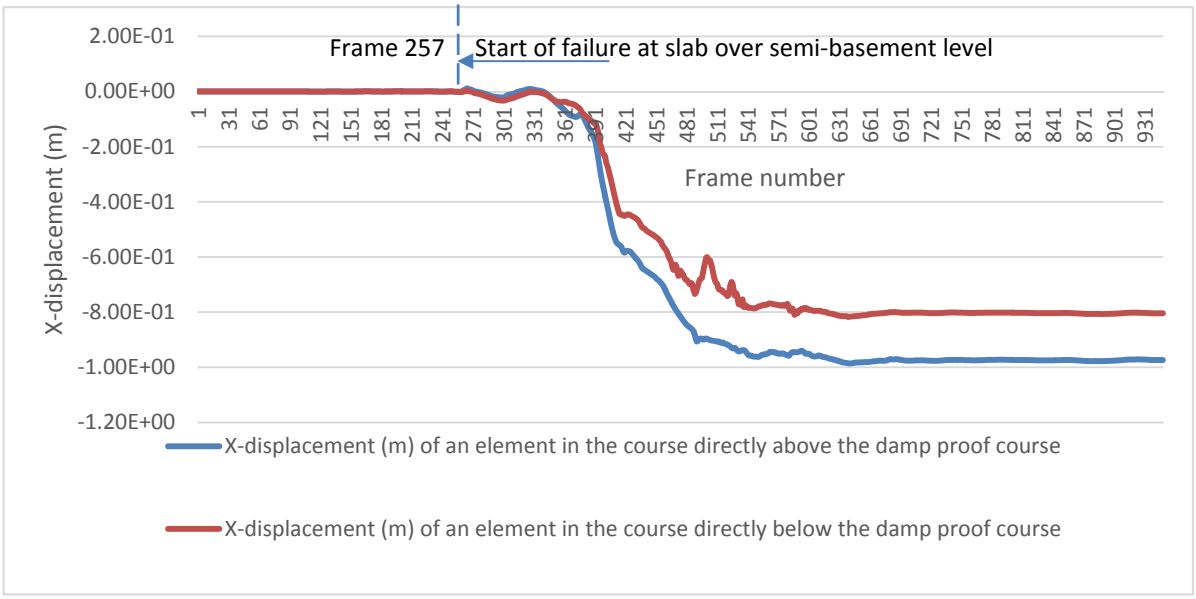

Figure 3-21 Comparison of x-displacement variation throughout the dynamic analysis of two overlying elements in the left hand side party wall of Model 42v2 positioned directly above and below the damp proof course respectively.

[7] Even though the use of polyethylene damp proof courses should be avoided in seismic zones, their widespread use in the contemporary loadbearing URM masonry building typology in the more recent structures throughout the Maltese Islands is indicative of the general disregard of seismic requirements during construction.

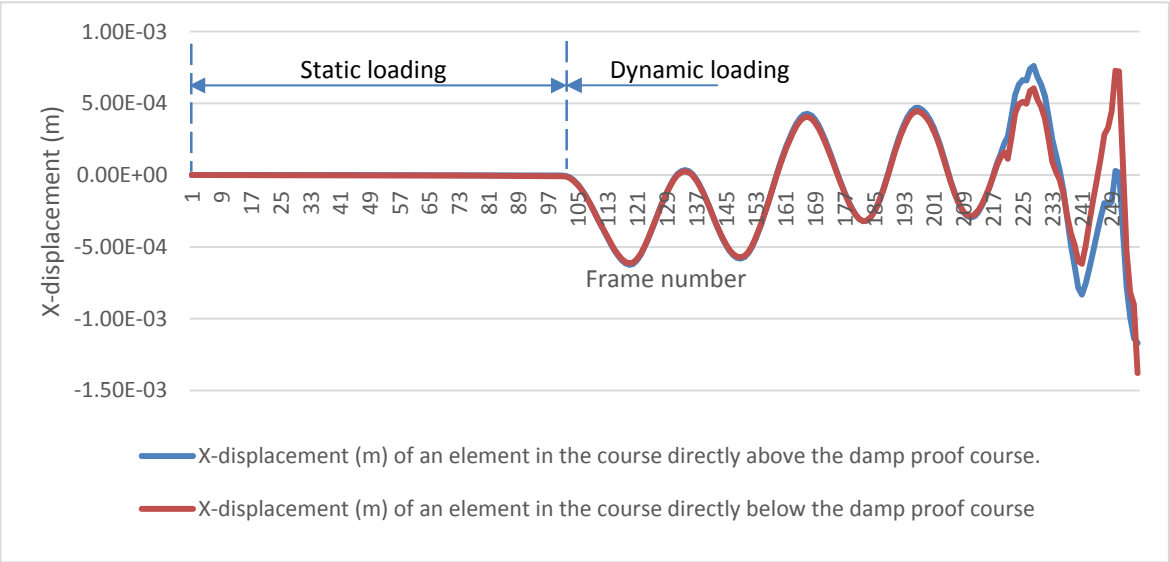

Figure 3-22 Comparison of x-displacement variation prior to the start of failure (frames 1-256) during the dynamic analysis of Model 42v2 of two overlying elements in the left hand side party wall positioned directly above and below the damp proof course respectively.

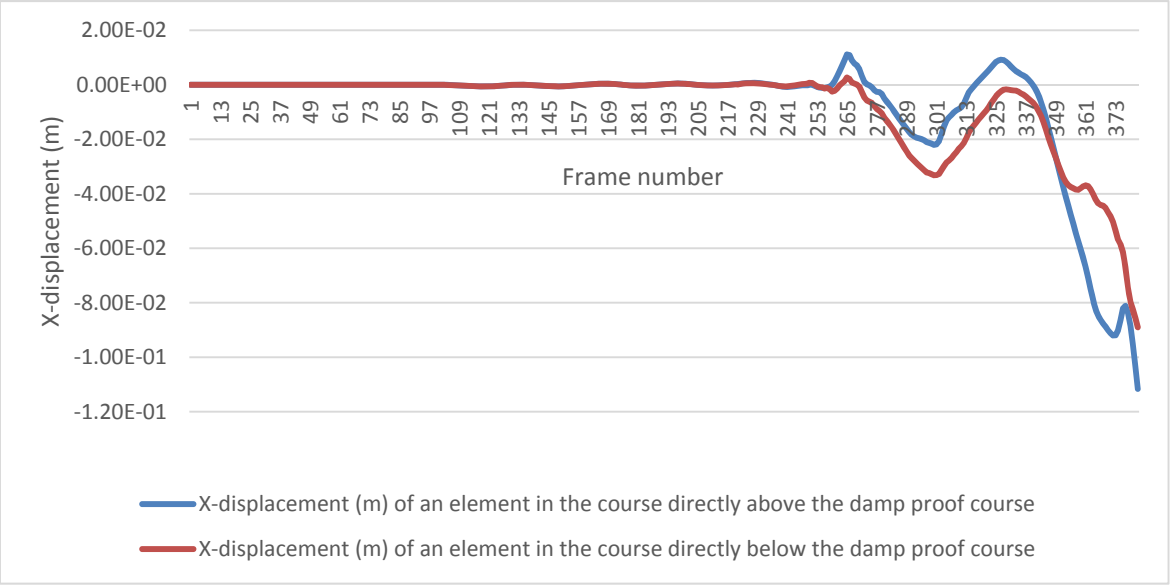

Figure 3-23 Comparison of x-displacement variation during the dynamic analysis up to the end of collapse (frames 1-382) of Model 42v2 of two overlying elements in the left hand side party wall positioned directly above and below the damp proof course respectively.

The verification of the validity of the method adopted for the modelling of the damp proof course was carried out through the comparison of the x-displacements of two overlying elements in the left hand side party wall of Model 42v2 (six-storey control numerical model analysed on a 30 m thick upper coralline limestone layer modelled as a three-dimensional block), through a non-linear dynamic analysis using ELS® under the action of the input simulated ground motion record presented further on in Figure 3-29 (Section 3.4.5). This ground motion record was subsequently used as the input seismic acceleration in all the final numerical models analysed using ELS® in the present research study. The two overlying elements in the left hand side party wall whose x-displacements were compared,

are respectively positioned directly above and directly below the damp proof course and are, hence, separated only by the mortar joint where the damp proof course is located. The start of failure at slab over semi-basement level in Model 42v2 was identified at frame number 257, whereas the analysis time at complete collapse was identified as frame 382. Figures 3-21, 3-22 and 3-23 indicate that, whereas the x-displacement throughout the static loading stage, and in the initial 100 frames of the dynamic loading stage, of the two elements under examination is approximately equal, a visible shift in the displacements of the two overlying elements occurs at around frame 220. This discrepancy in x-displacement values of the two overlying masonry blocks can be attributed to sliding of the upper element with respect to the lower block in view of the reduced friction coefficient of the mortar at the damp proof course, hence, suggesting that the modelling of the damp proof course can be considered as adequate.

3.4.3 Modelling of ground, material properties and restraints

Ground can be modelled in two main ways in ELS®, namely, as a material specified at the numerical model's Minimum Z position, or as a system of three-dimensional blocks, which represent the thickness and material properties of the ground layers present over the bedrock, which is, in turn, defined as a material at the model's Minimum Z position. The present study sought to investigate the influence which different ground formation layers, and different modelling methods, have on the seismic resistance of the contemporary loadbearing masonry building typology.

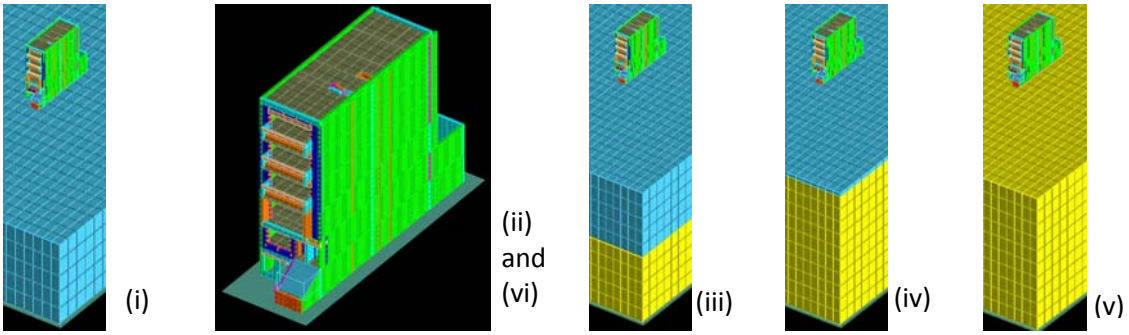

Figure 3-24 Ground formation scenarios investigated.

In view of the variety of ground formation scenarios which could be present in the Maltese Islands, and taking into consideration the additional seismic vulnerability associated with buildings located in areas with a clay subsoil, six alternative scenarios were investigated (as indicated in Figure 3-24), namely:

i. a single 30 m thick upper coralline limestone layer modelled as a three-dimensional block;
ii. upper coralline limestone specified as the material of the ground at the model's Minimum Z position;
iii. a 30 m thick upper coralline limestone layer overlying a 30 m thick clay layer (similar to the geology at the top of the Xemxija hill), where both layers are modelled as three-dimensional blocks;
iv. a 1.5 m thick upper coralline limestone layer overlying a 60 m thick clay layer (similar to the geology of the Nadur Test Site), where both layers are modelled as three-dimensional blocks;

v. a single 60 m thick clay layer modelled as a three-dimensional block;

vi. clay specified as the ground material at the model's Minimum Z position.

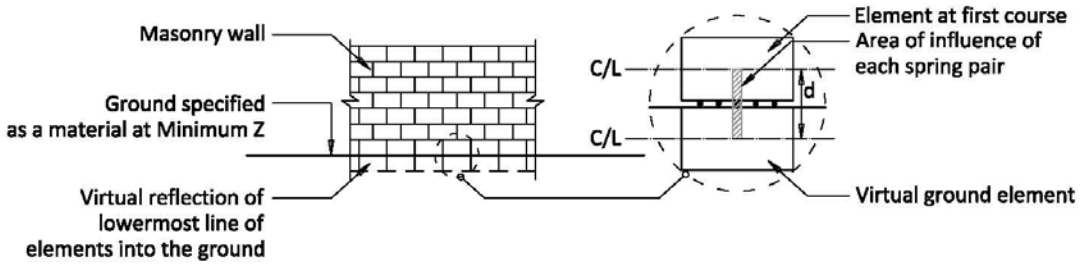

Figure 3-25 Representation of ground modelled as a material at the model's Minimum Z position using ELS® (blow-up detail reproduced in-part from Karbassi and Nollet ([39] p. 1355)).

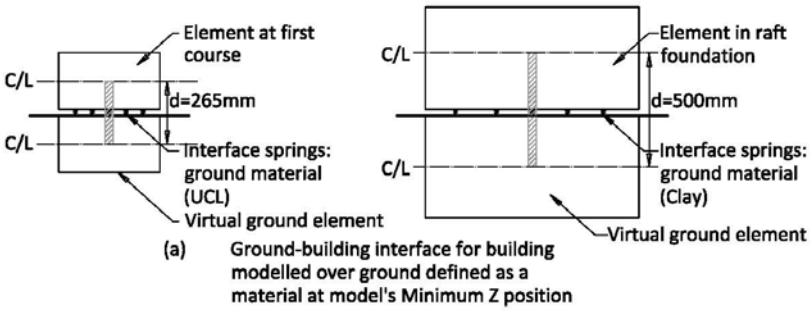

(a) Ground-building interface for building modelled over ground defined as a material at model's Minimum Z position

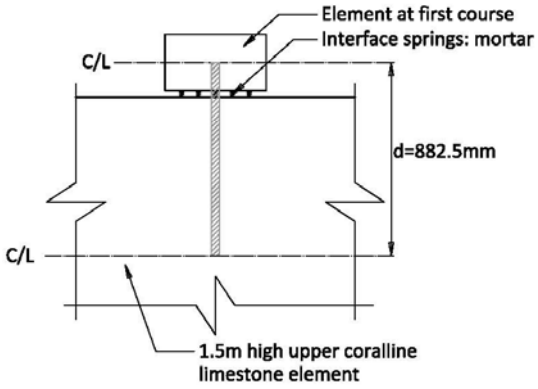

(b) Ground-building interface when building overlies a 1.5m thick upper coralline limestone layer

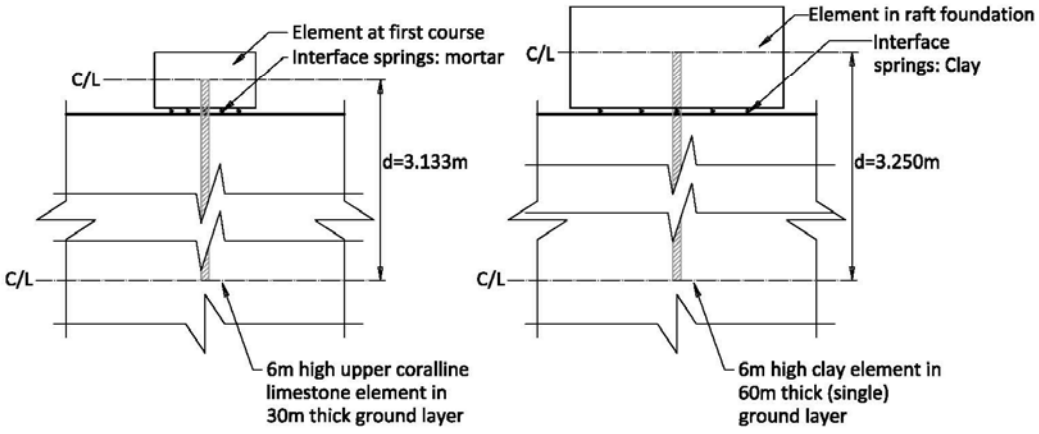

(c) Ground-building interface when building overlies a 30m thick upper coralline limestone layer or a 60m thick clay layer

Figure 3-26 Ground-building interface for the different ground scenarios investigated.

In all ELS® structural models the material of the ground at the model's Minimum Z position must be specified by the user. This defined material can either represent the bedrock, in the case where the upper ground formation layers are modelled as three-dimensional blocks, or alternatively, it can be used as a modelling simplification of the geological conditions of the site, in which case the base of the modelled structure starts at the Minimum Z position of the model.

ELS® interprets ground or bedrock, defined as a material at the Minimum Z position of the numerical model, as a virtual reflection of the first line of elements above Minimum Z into the ground, as presented in Figure 3-25. The mirrored 'virtual elements' representing the ground are assigned the material properties corresponding to the specified ground material, and are restrained against all translations and rotations. Figure 3-26 shows how the distance between the centre of resistance of an element in the first course of the analysed masonry buildings, and the first underlying line of elements in the ground varies depending on the type of modelling of the ground layers, and the size of the elements defined in the modelling of the subsoil, hence, resulting in a significantly different stiffness of restraint at the base of the modelled building. Furthermore, the interface material between the first course and the underlying subsoil determines the stiffness of the springs at this junction, hence, also influencing the restraint provided at the base of the modelled structures. Whereas the interface material, which can be specified between ground modelled at Minimum Z and any overlying element, can only be defined as either the material of the ground or the material of the structure, when ground is modelled as three-dimensional blocks, the interface material between the ground and the building would be mortar by default. However this interface material can also be altered by the user. In the full scale numerical models analysed in this study, the interface materials defined at the base of the modelled structure and in the ground layers were as follows:

a) in the case of structures modelled directly over ground defined as a material at the model's Minimum Z position, the interface material, between ground modelled at Minimum Z and the overlying structure, was specified as the ground material, hence, upper coralline limestone or clay;
b) in the case of the models where the ground layers were represented as three-dimensional blocks, the interface material, between bedrock (defined as upper coralline limestone) at Minimum Z and a ground layer modelled as a three-dimensional block, was specified as the bedrock material, hence, upper coralline limestone;
c) in the case of all structures analysed on upper coralline limestone modelled as a three-dimensional element, the building was modelled as erected directly on levelled rock with no concrete foundations, but with mortar as interface material between the lowermost course of the structure and the topmost line of elements of the upper coralline limestone three-dimensional block;
d) in the case of all structures analysed over a single 60 m thick clay layer, or clay defined as a material at the model's Minimum Z position, a 500 mm thick reinforced concrete raft foundation was defined directly beneath the whole area of the building at semi-basement level, with the interface material between the lowermost course of the structure and the

foundation defined as mortar, and that between the foundation and the clay layer defined as clay;

e) in the analysed numerical models, which include two overlying ground layers, both defined as three-dimensional blocks, the interface material between the clay and the upper coralline limestone layers was defined as clay.

As far as the author is aware, only translational and rotational restraints can be defined in ELS®, whereas spring supports, with a spring stiffness which can be altered, cannot be defined. Hence, in order to represent the infinite nature of the ground layers, and to reduce the influence on the seismic behaviour of the investigated structures arising from possible reflections of seismic vibrations along the external faces of the ground formation layers modelled as three-dimensional blocks, these ground layers were modelled in this study with overall plan dimensions of 100 m length and 137 m breadth (corresponding to 15 times the width and 6 times the length of the single building models at semi-basement level). In all analysed numerical models, the modelled structures were positioned centred on these three-dimensional ground blocks. Due to time limitations, the investigation of the influence of the further enlargement or reduction of these three-dimensional blocks, representing the ground layers on the seismic response of the modelled structures, could not be carried out as part of the study presented herein. Moreover, the software licence limitation on the maximum number of elements, the particular concern of keeping the number of elements in the analysed numerical models to a minimum in view of the long processing run times, and the requirement of not having a large discrepancy between the element sizes of ground layers, when compared to those constituting the overlying structures [162] (Dr. Huda Helmy, Consultation Department, Applied Science International, LLC, personal communication by email, huda@appliedscienceint.com, 9th September 2015) imposed a restriction on the overall size of the three-dimensional blocks representing the ground layers and, consequently, on the number and size of the elements in which these ground layers were subdivided.

The three-dimensional blocks representing upper coralline limestone and clay were respectively subdivided into equally sized elements (of 3.33 m length, 4.57 m breadth and 6 m height) in both the 30 m thick and the 60 m thick cases, in all the single and two-building models. In view of the limit on the maximum number of elements allowed by the software licence, in the three building control models the 60 m thick clay layer was subdivided into a smaller number of elements, keeping the same plan dimensions of the individual elements as that of the three-dimensional ground elements defined in the other models, but with a height of 8.57 m. On the other hand, the 1.5 m thick upper coralline limestone layer was subdivided in elements with overall dimensions: 3.33 m length, 4.57 m breadth and 1.5 m height, in all the analysed full scale numerical models. It is, however, acknowledged that the alteration of the height of the elements constituting the clay layer in the three-building control models could have influenced the transfer of seismic vibrations between the clay and the upper coralline limestone layers in view of the increased eccentricity between the elements at the interface between the two materials and, hence, the degree of restraint at the base of the overlying structures.

The restraints to the ground layers, the material properties of these layers, and the materials defined at their interfaces (between the bottom face of the lower ground formation layer and the bedrock;

between the top face of the upper ground formation layer and the overlying structure; and between the two ground formation layers in two-layer subsoil systems investigated) were fine-tuned through the examination of the variation in transverse x-accelerations and displacements of vertically aligned elements in the ground layers, and at first course (in the left party wall) in a number of trial models of Xemxija Building Number 0011, which results are reproduced in Figures 16 and 17 in Appendix C.

Table 3-4 summarises the main revisions to the material properties resulting from this investigation, which properties were subsequently applied to the final set of full scale numerical models analysed in this study. Moreover, Table 3-5 reports the characteristics of the main trial models, which were used in the identification of the modelling parameters, which required modification. While the original clay properties specified in the trial numerical models were based on the results for stiff clay from international sources, Table 3-5 indicates that the compressive strength of clay was increased by around four times in view of stability errors experienced during the static loading stage in earlier trial models. This increase was not envisaged to alter the model behaviour, since failure of the ground in compression is, in practice, very unlikely.

Table 3-4 Original and revised material properties used in the numerical modelling of the subsoil scenarios investigated in this study.

	Clay layer modelled as a a three-dimensional block	Clay as interface material between clay and upper coralline limestone layers modelled as three-dimensional blocks	Upper coralline limestone as interface material between upper coralline limestone ground at model's Minimum Z and overlying ground layer modelled as a three-dimensional block
Original density (kg/m^3)	1800	1800	2059
Revised density (kg/m^3)	0	0	n/a
Original compressive strength (N/mm^2)	1.2	1.2	30
Revised compressive strength (N/mm^2)	4.903	4.903	n/a
Original Young's Modulus (N/mm^2)	50	50	55000
Revised Young's Modulus (N/mm^2)	204.3	204.3	n/a
Original Shear Modulus (N/mm^2)	16.7	16.7	22000
Revised Shear Modulus (N/mm^2)	68.1	68.1	n/a
Original friction coefficient	0.85	0.85	0.40
Revised friction coefficient	n/a	1.00	1.00

Table 3-5 Characteristics of main trial models analysed for the investigation of the ground modelling parameters to be adopted in the final set of full scale models.

Trial model number	Modelled structure based on Xemxija 0011	Number of storeys	Subsoil scenario investigated	Restraints to ground layers	Friction coefficient of interface materials	Other alterations
10	Yes	6	30 m UCL over 30 m clay	Both layers: elements on external faces restrained as per Figure 3-27	0.4 UCL; 0.85 clay	Increased compressive strength of clay: 4.903 N/mm^2
11	Yes	6	1.5 m UCL over 60 m clay	Both layers as (10)	as (10)	n/a
22	Yes	6	30 m UCL over 30 m clay	Both layers as (10)	1.0 UCL; 1.0 clay	n/a
16	Yes	5	1.5 m UCL over 60 m clay	Both layers as (10)	as (10)	n/a
30	Yes	5	1.5 m UCL over 60 m clay	Only clay layer restrained as (10); UCL unrestrained	1.0 UCL; 1.0 clay	Increased Young's modulus and Shear modulus of clay; revised density of clay to 0 kg/m^3.

The trial numerical models listed in Table 3-5 were all analysed using the same Magnitude 7.6 simulated ground motion record, with a hypocentral distance of 170.30 km, an epicentral distance of 139.91 km, and with a scaled peak ground acceleration of 0.10g, a time-step of 0.08s and an overall (shortened) duration of 8.48 s, which was applied to the final set of full scale models analysed in this study. Details of this simulated ground motion record are discussed in Section 3.4.5 of this thesis.

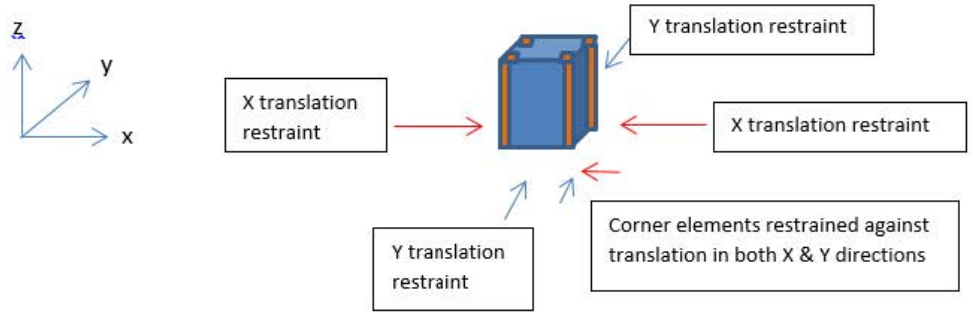

Figure 3-27 Translational restraints to ground formation layers as defined in the analysed numerical models.

In trial numerical models 10, 11, 22 and 16, two-layer subsoil scenarios were analysed with the following restraint conditions for both overlying ground layers, as indicated in Figure 3-27:

a) the elements positioned on the two external faces perpendicular to the x-direction of the model were restrained against translation in the x- direction;
b) the elements located on the other two external faces which are perpendicular to the y-direction of the model were restrained against translation in the y-direction;

c) corner elements throughout the height of both ground layers were restrained against translations in both x- and y-directions.

Table 3-4 shows that friction coefficients of 0.4 and 0.8 were originally defined for the upper coralline limestone interface material between the bedrock at the model's Minimum Z position and the lowermost ground layer, and for the clay interface material between the clay layer and the overlying upper coralline limestone layer, respectively. The comparison of x-accelerations and x-displacements recorded in the elements at the bottom and top faces of the overlying ground layers and at first course reported in Figures 16 and 17 of Appendix C, suggested that, whereas in Models 10, 11 and 16 there was an evident amplification of x-accelerations and displacements between the bottom and top faces of the clay layer, the corresponding values along the bottom and top faces of the upper coralline limestone layer, and at the first course of the semi-basement level of the building, were significantly lower, similar in magnitude to those recorded along the bottom face of the clay layer. This suggested that the amplification of seismic vibrations occurring in the clay layer were not being transferred to the overlying layer and, hence, to the modelled structure. Hence, in order to verify whether this failure in the transmission of seismic vibrations could be due to the slipping of the upper coralline limestone layer over the clay layer, Model 22 was analysed with revised friction coefficient value of 1.0 for the clay interface material, defined between the clay and the upper coralline limestone layers. Furthermore, the significantly lower values of maximum x-acceleration recorded in the element at the bottom of clay layer in Models 10 and 11 (0.40 m/s^2 and 0.11 m/s^2, respectively), when compared to the maximum peak ground acceleration of the input simulated ground motion record (0.98 m/s^2), suggested that the clay layer might also be slipping with respect to the bedrock. Hence, a friction coefficient of 1.0 was also specified for the upper coralline limestone interface material between the bedrock at Minimum Z and the clay layer. However, Figures 16(c) and 17(c) in Appendix C indicate that, apart from some variation in the degree of amplification of the x-accelerations occurring through the clay layer, the change in the friction coefficient of the materials specified at the interface between the bedrock and the lower ground formation layer and between the two subsoil layers, did not result in an improved transfer of seismic vibrations to and through the upper coralline limestone layer, to the modelled structure.

The comparison of the x-displacements recorded in the vertically aligned elements in the clay and upper coralline limestone layers reported in Figure 17 (a to d) of Appendix C suggests that, when the external faces of both ground layers are restrained against translations in the x- or y-direction, whereas the clay, due to its lower stiffness, is capable of undergoing horizontal deformation within the extents of the 100 m x 137 m three-dimensional block, the higher stiffness of the upper coralline limestone layer does not allow such deformations to occur in this layer when it is restrained. This prevents the transfer of the amplified vibrations resulting from the surface of the clay layer to the masonry structure modelled above the upper coralline limestone layer. Therefore, while the restraints of the clay layer were retained, the restraints to the upper coralline limestone layer were removed in Model 30.

Furthermore, changes in the material properties of clay were also carried out in Model 30. While only the results pertaining to the main trial numerical models are being reported herein, whereas no further

stability errors were experienced in the numerical models, which considered a 1.5 m thick upper coralline limestone layer over a 60 m thick clay layer, or a 30 m thick upper coralline limestone layer over a 30 m thick clay layer, following the increase in compressive strength of clay, recurrent stability errors during the static loading stage of the numerical analyses, in models analysed on a single 60 m thick clay ground formation layer modelled as a three-dimensional element, were still observed. Such stability errors were confirmed by the ELS® Consultation Department to be likely due to a loss in z-restraint of an element or object [163] (Dr. Huda Helmy, Consultation Department, Applied Science International, LLC, personal communication by email, huda@appliedscienceint.com, 13th October 2015). Hence, since all the final set of full scale models were intended to have the same material properties, in order to define clay as pre-consolidated under the effect of its own self-weight from the very start of the numerical analysis, the density of clay was reduced from 1800 kg/m^3 to 0 kg/m^3 in Model 30. In addition, in the same model, the Young's modulus and the Shear modulus of clay were increased by the same proportion as the earlier increase in compressive strength of the same material. The latter measure was aimed at reducing the deformability (hence, the compressibility) of the clay layer to the superimposed static loads, apart from reducing the differential stiffness gradient between the two soil layers, therefore enhancing the transfer of seismic vibrations between these ground layers. Moreover, the friction coefficients of the upper coralline limestone and clay interface materials in the ground layers were both retained at a value of 1.0 in this trial model. Figures 16(e) and 17(e) in Appendix C indicate that the x-accelerations and displacements recorded in elements positioned along the bottom and top faces of the upper coralline limestone layer, and at first course in Model 30, are only marginally lower than the corresponding values recorded in the element along the top face of the clay layer, hence suggesting that an adequate transfer of seismic vibrations (including that of any amplification of these vibrations by the soil layers) from the bedrock to the modelled masonry structures was achieved. In view of the results obtained for Model 30, the removal of the restraints to the upper coralline limestone layer in the two-layer systems investigated, the alterations to the friction coefficients of the interface materials of the ground layers, and the revised material properties of clay, were reflected even in the final set of full scale numerical models. On the other hand, the restraints to the lower ground layer in the two-layer systems, and to the single layer in the numerical models analysed on a single ground layer defined as a three-dimensional block, were retained.

3.4.4 Gravity loads

The combination of gravity loads acting on the modelled structures, which, under seismic excitations, constitute the inertia of these structures, to the resulting displacement and deformation triggered by the seismic actions, were calculated in accordance with the load combination indicated in Clause 3.2.4(2)P of Eurocode 8: Part 1 [4], reported hereunder as Equation 3-1. With reference to Clause 4.2.4(2)P of Eurocode 8: Part 1 [4], in addition with Table A1.1 of Appendix A1 in EN1990:2002 [164], and, in the absence of a National Annex to Eurocode 8 for the Maltese Islands, Table 4.2 of Eurocode 8: Part 1 [4], the combinations of gravity loads acting on the structure at every storey were evaluated through Equations 3-3 or 3-4 for masses at roof level or in 'independently occupied storeys' [4], respectively. These combinations of gravity loads were applied to the analysed models as 'Stage 1'

(gravitiational, static) loads, through an alteration of the densities of the respective slabs, as summarised in Figure 18 of Appendix C, in order to ensure that they are considered as part of the inertia of the structure by the ELS® Solver. Service loads at the level of the roof over the penthouse were limited to a small area in every analysed model.

$$\sum G_{kj}" + "\sum \psi_{E,i} \,.\, Q_{ki}$$

Equation 3-1

Where, as defined in Eurocode 8: Part 1 [4],

G_{kj} consists of the characteristic permanent loads arising from the self-weight of the horizontal structural members, the floor build-up and services,

Q_{ki} consists of the characteristic value of variable loads acting on every slab,

$\psi_{E,I}$ is the combination coefficient for the variable actions obtained from Clause 4.2.4(2)P in Eurocode 8: Part 1 [4], reported hereunder as Equation 3-2

$$\psi_{E,i} = \phi\psi_{2i}$$

Equation 3-2

where,

ψ_{2i} is the 'combination coefficient for the quasi-permanent value of variable action Q_i' [4], specified as 0.3 for category A (residential buildings) in Table A1.1 of Appendix A1 in EN1990:2002 [164],

ϕ is specified as 1.0 for roofs and 0.5 for 'independently occupied storeys' in Table 4.2 of Eurocode 8: Part 1 [4].

$$\sum G_{kj}" + "\sum (1.0) \,.\, (0.3) \,.\, Q_{ki}$$

Equation 3-3

$$\sum G_{kj}" + "\sum (0.5) \,.\, (0.3) \,.\, Q_{ki}$$

Equation 3-4

3.4.5 Ground motion record

A simulated ground motion record for Malta, obtained from the database of the Seismic Monitoring and Research Unit (SMRU) of the University of Malta, was used as the input seismic acceleration in all the analysed models. The synthetic seismogram was generated by the SMRU using the stochastic, finite-source simulation program EXSIM [165], in which the 1693 earthquake source was modelled as a plane fault, whose dimensions are derived from its moment magnitude. Trials with two simulated records having the same magnitude, the same peak ground acceleration, but with a different duration, and a different intensity of 'peaks' which are close to the maximum peak ground acceleration value, resulted in a different behaviour of the numerical model, with identical models resulting in collapse in one case, and resisting collapse in the other case. The shortened ground motion records, scaled to a

maximum peak ground acceleration of 0.10g corresponding to these two simulated earthquakes, are reproduced in Figures 3-29 and 3-31 respectively, whereas the respective original ground motion records from which these shortened acceleration-time series were obtained, with a revised time step and scaled to a maximum p.g.a. of 0.1g are presented in Figures 3-28 and 3-30.

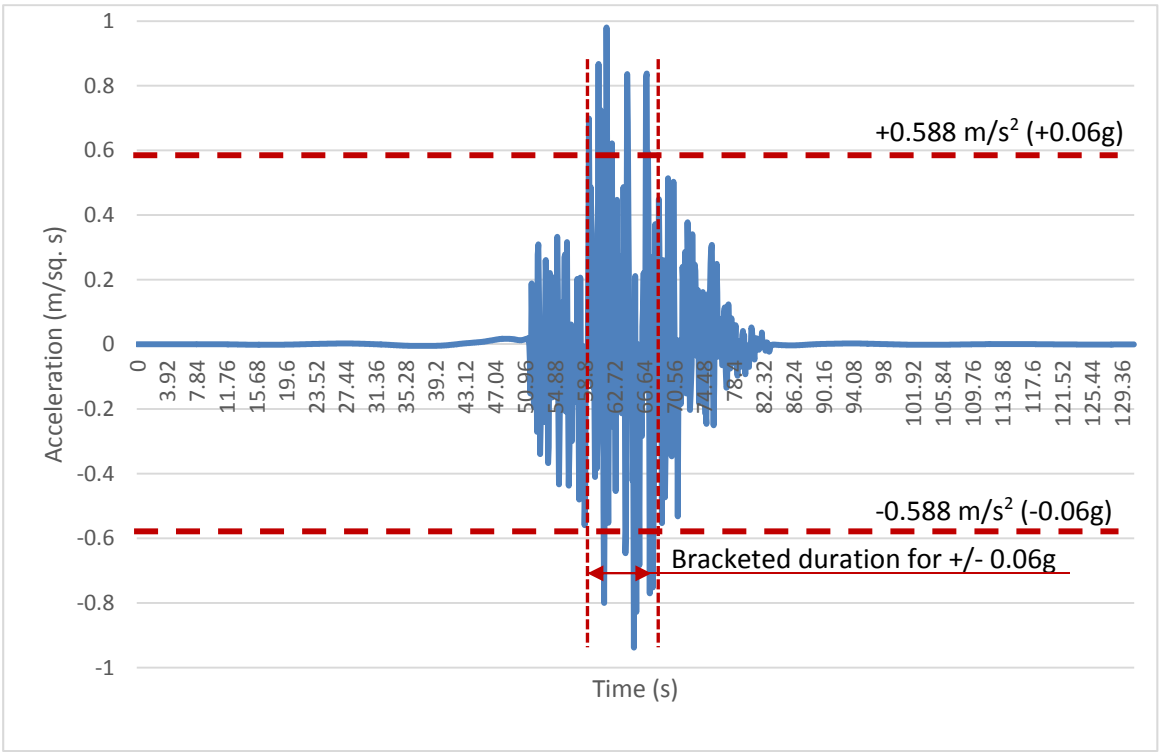

Figure 3-28 Magnitude 7.6 simulated ground motion record with a hypocentral distance of 170.30 km and an epicentre at 139.91 km to the North-East of Malta, an amended time step of 0.08s and scaled to a maximum p.g.a of 0.1g (and original duration), indicating portion corresponding to a bracketed duration of +/-0.06g reproduced in Figure 3-29.

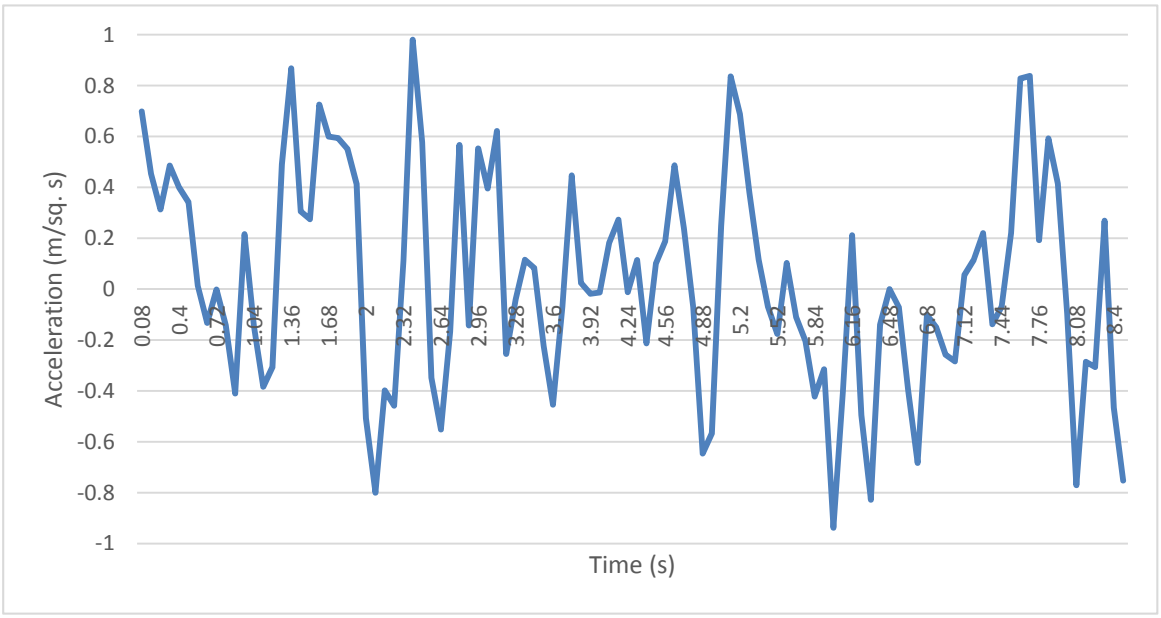

Figure 3-29 Simulated ground motion record of a magnitude 7.6 earthquake with a hypocentral distance of 170.30 km and an epicentre at 139.91 km to the North-East of Malta, an amended time step of 0.08 s, scaled to a peak ground acceleration of 0.10g and shortened for a bracketed duration of +/-0.06g.

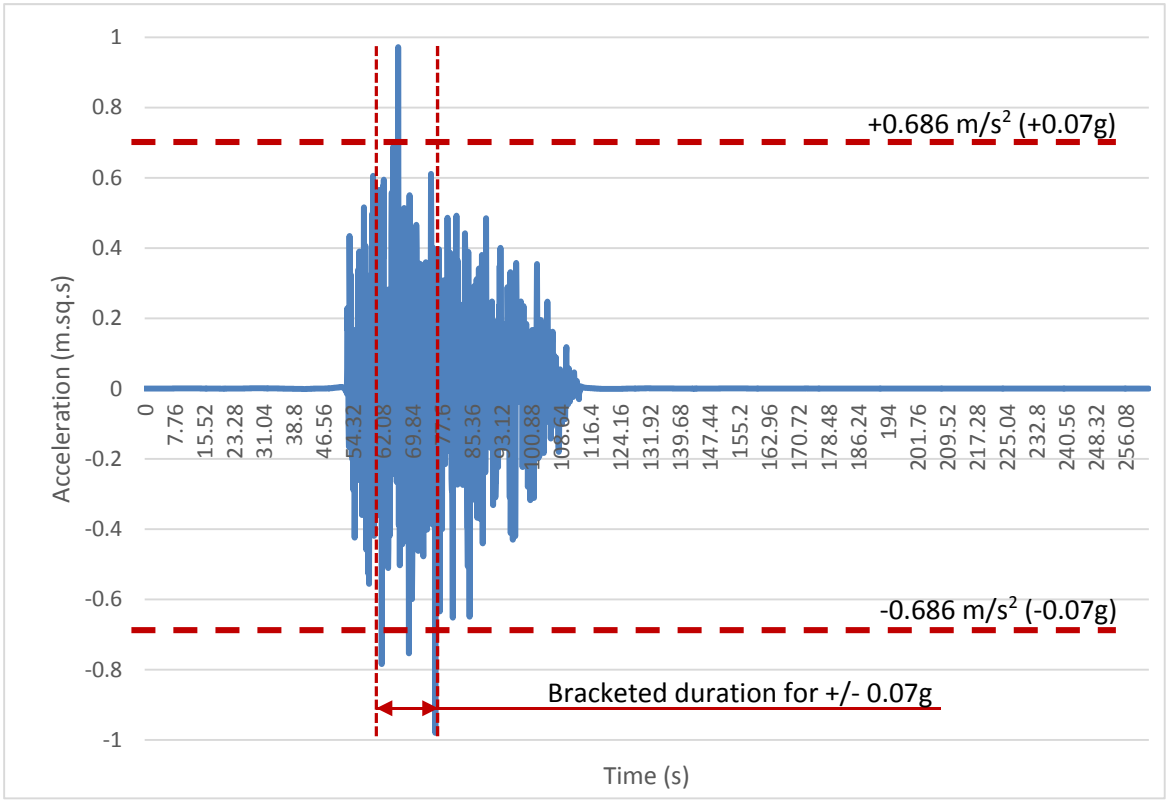

Figure 3-30 Magnitude 7.6 simulated ground motion record with a hypocentral distance of 140.12 km and an epicentre at 135.95 km to the North-East of Malta, an amended time step of 0.08s and scaled to a maximum p.g.a of 0.1g (and original duration) indicating portion corresponding to a bracketed duration of +/- 0.07g reproduced in Figure 3-31.

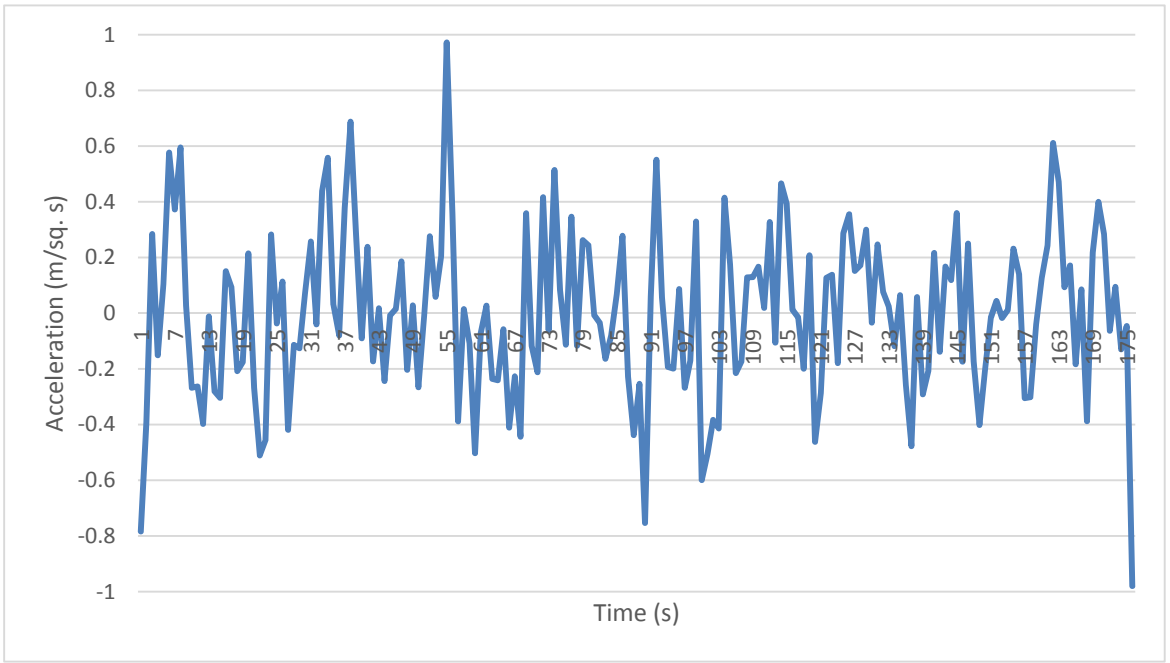

Figure 3-31 Simulated ground motion record of a magnitude 7.6 earthquake with a hypocentral distance of 140.12 km and an epicentre at 135.95 km to the North-East of Malta, an amended time step of 0.08 s, scaled to a peak ground acceleration of 0.10g and shortened for a bracketed duration of +/-0.07g.

For structures located in areas with a design peak ground acceleration on rock lower than 0.25g, Clauses 4.3.3.5.1(7)P and 4.3.3.4.3(3) of Eurocode 8: Part 1 [4] specify that three-dimensional numerical models of these structures should be analysed under seismic accelerations acting simultaneously in the x- and y-plan directions, and that a minimum of seven different ground motion records should be used for determination of the resistance of these structures to dynamic loading in the form of seismic excitations, through the use of the resulting mean design values of 'action effects' on the structures. Nevertheless, in view of the particular concern regarding the limitation of analysis times, and the size of the output files generated by every analysis, in addition to the consideration that the aim of the numerical analyses in the study presented herein was to examine the influence of particular building characteristics on the seismic vulnerability of the loadbearing URM typology under study and their relative importance, the same ground motion record was used in all final analyses, and it was applied only in the weaker transverse x-direction of every analysed structure.

In the absence of a National Annex to Eurocode 8 for the Maltese Islands, the use of a simulated ground motion record for Malta, which was based on an approximation of the worst past seismic event in the recorded history of the Maltese Islands, was considered adequate for the objectives of the study presented herein. Infact, the chosen simulated record was intended to be similar to that of the earthquake which hit the Maltese Islands on the 11th January 1693 in order to obtain an indication of the behaviour of such buildings in the event that such an earthquake had to repeat itself. The simulated record represented a magnitude 7.6 earthquake with a hypocentral distance of 170.30 km and an epicentral distance of 139.91 km to the North-East of Malta. The original time step was 0.002 s, the original length of the record was of 131.07 s, and the maximum peak ground acceleration was 0.637 m/s^2. In order to limit the analysis time, the length of the ground motion record was reduced to 8.48s by increasing the time step to 0.08 s, and using a bracketed duration (as defined by Corchete ([166] p. 32): '*the bracketed duration is the time duration of the ground shaking, defined as the elapsed time between the first and last acceleration excursions greater than some reference value*') of +/- 0.06g. Eight step divisions were specified for every time step in the numerical models, hence, meaning that the ELS® Solver produced an output every 0.01s. The number of step divisions specified were based on a compromise between the duration of the analysis run times, and the level of accuracy of structural response required in the analysed structures.

In the absence of a National Annex for Malta to Eurocode 8 [4], advice with respect to the maximum peak ground acceleration to be used in non-linear numerical analyses of buildings under seismic loads was sought from Prof. Pauline Galea (Head of the Department of Geosciences of the University of Malta, personal communication, 29th February 2016), who confirmed that the seismic hazard for Malta on rock (equivalent to ground type A in accordance with Table 3.1 of Eurocode 8: Part 1 [4]) for a 475 year return period was estimated at a mean maximum peak ground acceleration of 0.08g based on a 50% fractile. A 95% fractile is required for use in numerical analysis of structures, and its equivalent value for the Maltese Islands would be of around 0.12g. Reference was also made to the hazard map for the Maltese Islands based on the SHARE 2013 European Seismic Hazard Model of the European Facilities for Earthquake Hazard and Risk (EFEHR) [167], which indicates a maximum peak ground

acceleration for Maltese Islands of between 0.100-0.125g for rock and for a 95% fractile as reported in Figures 3-32 and 3-33.

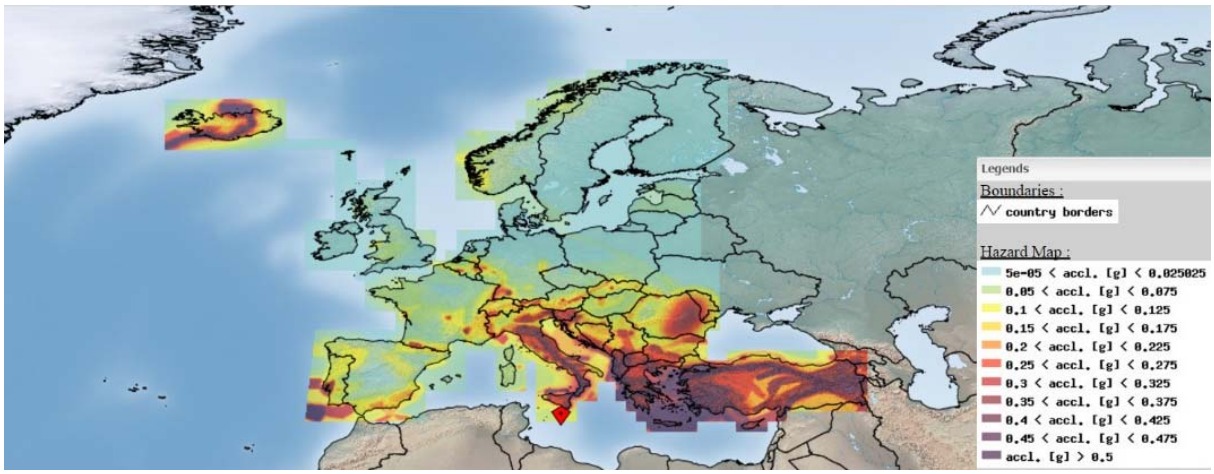

Figure 3-32 EFEHR SHARE 2013 European Hazard Model for a probability of exceedance of 10% in 50 years and a 95% fractile (http://www.efehr.org:8080/jetspeed/portal/HazardMaps.psml, downloaded on 5-06-2017).

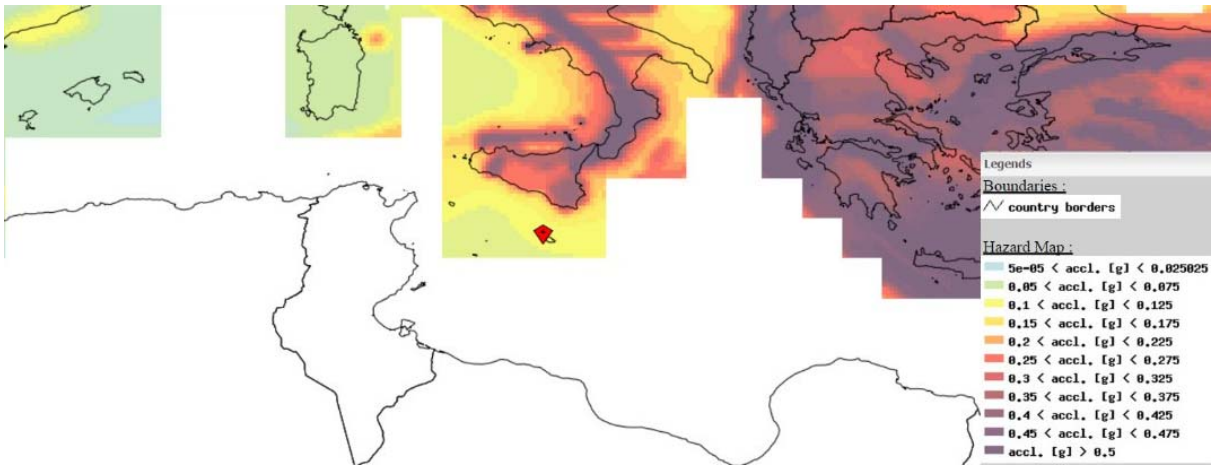

Figure 3-33 EFEHR SHARE 2013 European Hazard Model for a probability of exceedance of 10% in 50 years and a 95% fractile: zoomed on the Maltese Islands (http://www.efehr.org:8080/jetspeed/portal/HazardMaps.psml, downloaded on 5-06-2017).

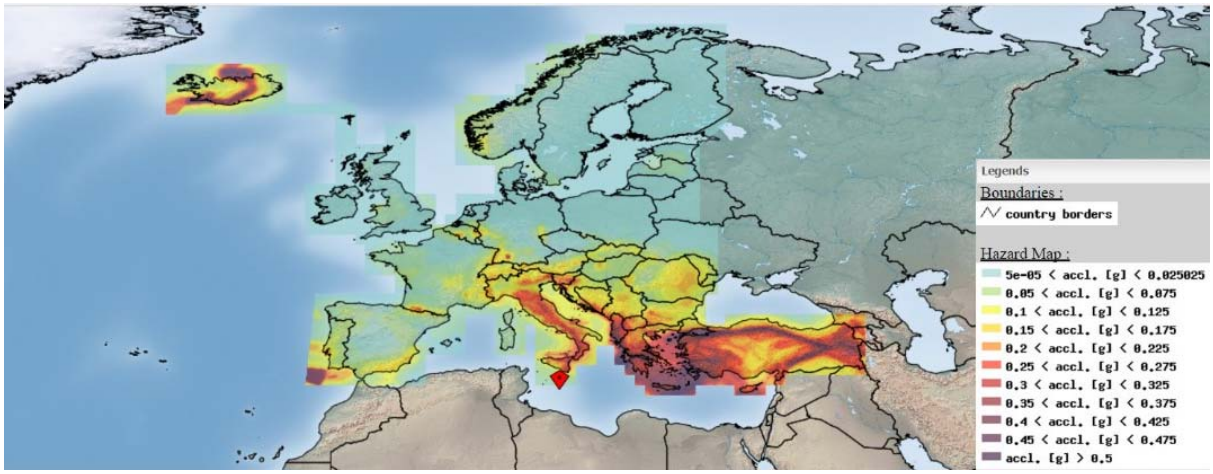

Figure 3-34 EFEHR SHARE 2013 European Hazard Model for a probability of exceedance of 10% in 50 years and a 50% fractile (http://www.efehr.org:8080/jetspeed/portal/HazardMaps.psml, downloaded on 5-06-2017).

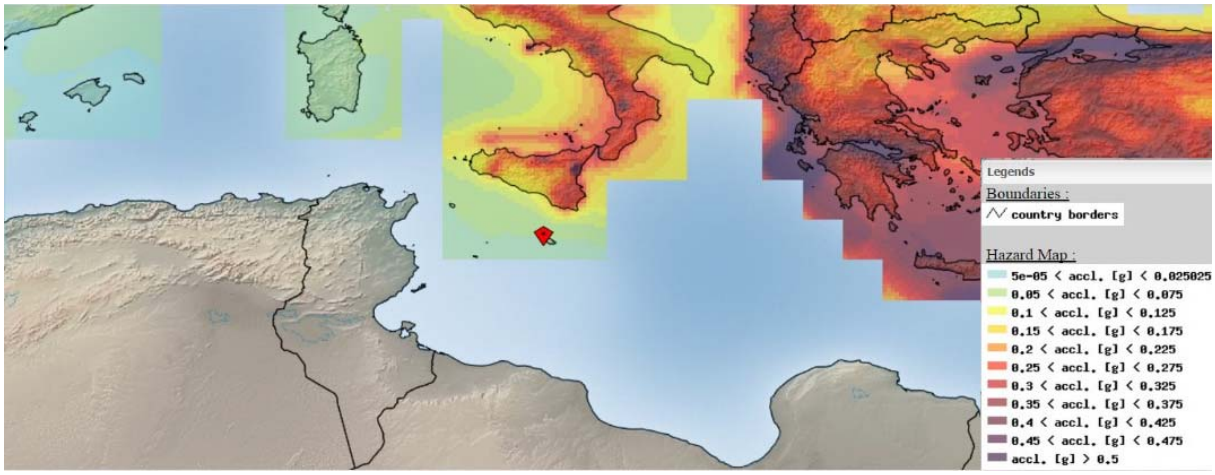

Figure 3-35 EFEHR SHARE 2013 European Hazard Model for a probability of exceedance of 10% in 50 years and a 50% fractile: zoomed on the Maltese Islands (http://www.efehr.org:8080/jetspeed/portal/HazardMaps.psml, downloaded on 5-06-2017).

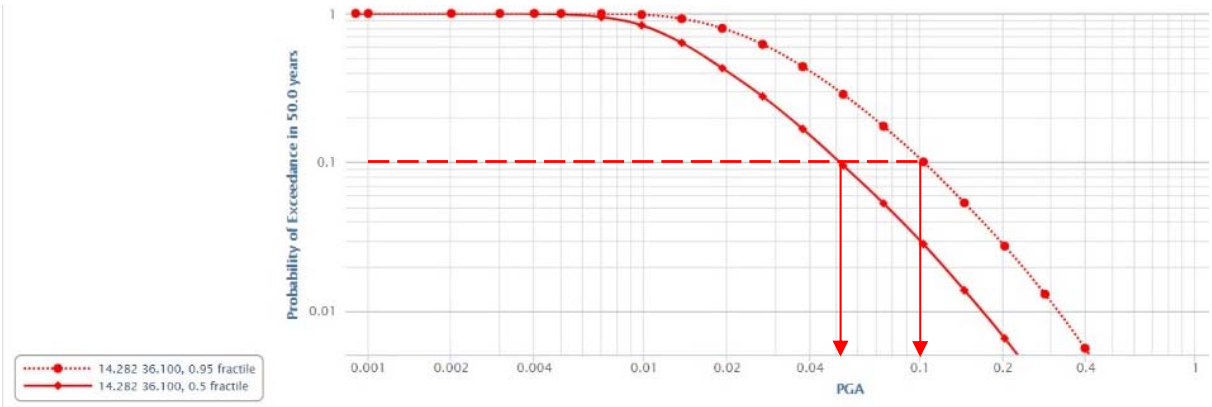

Figure 3-36 EFEHR hazard curves for the Maltese Islands for a probability of exceedance of 10% in 50 years and a 95% or a 50% fractile (http://www.efehr.org:8080/jetspeed/portal/HazardCurves2.psml, downloaded on 5-06-2017).

On the other hand, the EFEHR mean value of peak ground acceleration based on a 50% fractile [168] is indicated as 0.050-0.075g as reported in Figures 3-34 and 3-35. Furthermore, Figure 3-36 shows that the EFEHR hazard curve for the Maltese Islands [169] with a 95% fractile indicates a maximum peak ground acceleration of around 0.10g, whereas for a 50% fractile the mean maximum peak ground acceleration is around 0.054g, hence lower than that resulting from local studies. In the absence of design data and of further studies by seismologists, the EFEHR value for 95% fractile (0.10g) was used in this study. The simulated ground motion record was, hence, scaled to a maximum peak ground acceleration of 0.10g.

Clause 3.2.3.1.3(1)P in Eurocode 8: Part 1 [4] allows the use of simulated accelerograms, which take into consideration the realistic properties of the source and the site and the scaling of these accelerograms to the value of the site's design peak ground acceleration (which is equivalent to the design ground acceleration on ground type A multiplied by the soil factor). Furthermore, Senaldi [170] refers to the conclusions drawn by Bommer et al. [171] confirming the acceptability of the 'linear scaling of the amplitude of records'… 'in particular, for those records of earthquakes with similar magnitude to that of the earthquake scenario, since the shape of the response spectrum is not highly sensitive to distance' [170]. Amongst others, the studies carried out by Senaldi [170] and Valente and Milani [35] include similar scaling of ground motion records as performed in the study presented herein. On the other hand, since in the present study different subsoil scenarios were investigated through the specific modelling of the ground layers as three-dimensional blocks, or as a material defined at the model's Minimum Z position, a simulated ground motion record for ground type A (as defined in Table 3.1 of Eurocode 8: Part 1 [4]) was applied as input seismic acceleration at the Minimum Z position of all the analysed numerical models, without further modification with respect to the different subsoil cases investigated.

The original simulated ground motion record obtained from the Seismic Monitoring and Research Unit (SMRU) database, the resulting accelerograms following the alteration of the time step, and, subsequently, following the scaling of the accelerations to a peak ground acceleration of 0.10g, are summarised in Figure 19 in Appendix C. The shortened, scaled version of this simulated ground acceleration time-history which was used in all the full scale numerical models analysed in ELS® as input seismic action, is also presented in Figure 3-29.

Moreover, Clause 3.2.3.1.2(1)P of Eurocode 8: Part 1 [4] states that artificial accelerograms used as input ground accelerations in the dynamic analysis of numerical models must be consistent with the elastic response spectrum defined in Clause 3.2.2.2 of the same code, for which the period values (T_B, T_C, T_D) and the soil factor (S) should be defined in the National Annex. In the absence of a National Annex for Malta to Eurocode 8 [4] and, since the simulated ground motion record selected for use as input seismic action in all final ELS® numerical analyses represented a magnitude 7.6 earthquake with a hypocentral distance of 170.30 km and its epicentre at 139.91 km to the North-East of Malta, the original acceleration response spectrum corresponding to the ground motion record normalised with respect to the maximum p.g.a of 0.10g (reproduced in Figure 3-37) was converted to the corresponding

idealised acceleration response spectrum[8] [172] and superimposed on the Eurocode 8 Part 1 Type 1 elastic response spectrum for Type A ground (defined in Clause 3.2.2.1 and Table 3.2 in Eurocode 8 Part 1 [4]), reported in Figure 3-38. Both acceleration response spectra presented in Figures 3-37 and 3-38 were derived from the shortened scaled version of the input simulated ground motion record by the SMRU of the University of Malta.

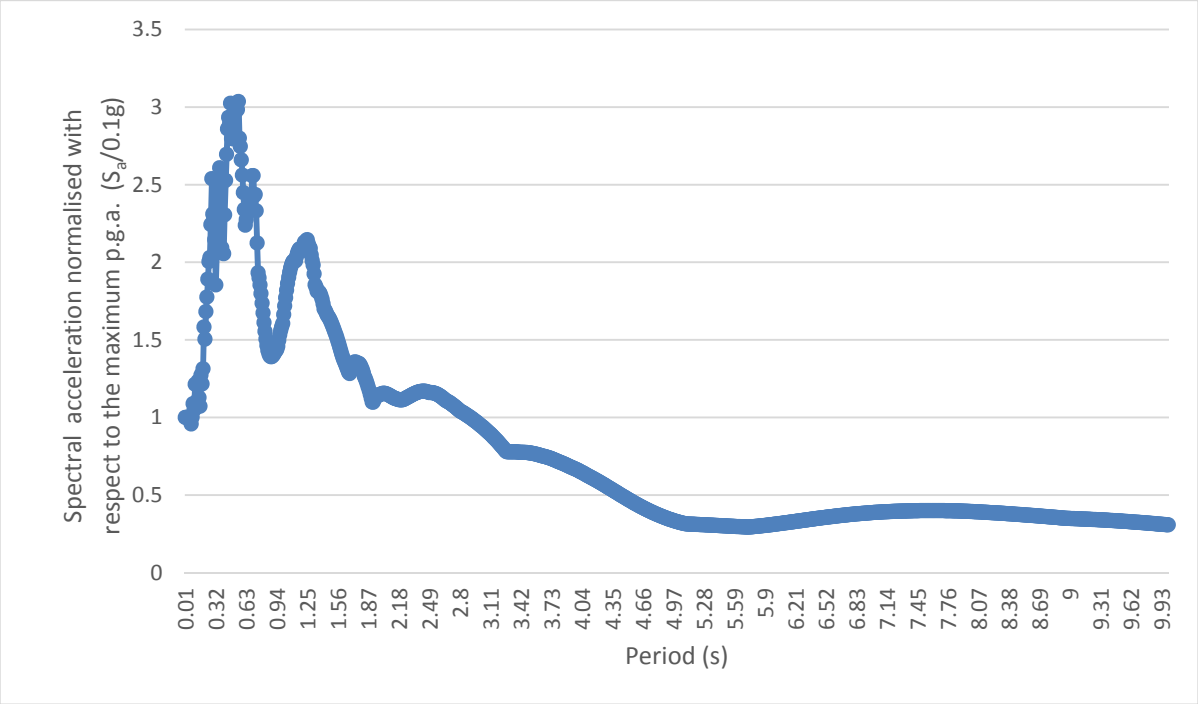

Figure 3-37 Original acceleration response spectrum of the shortened and scaled version of the simulated ground motion record used as input ground acceleration in all ELS® numerical analyses, divided by 0.1g (the maximum p.g.a for the Maltese Islands).

[8] The 'idealised acceleration response spectrum' is referred to by seismologists as the 'design response spectrum', in which context, 'design' does not imply the reduction of the original response spectrum for the indirect consideration of the inelastic response of structures, as recommended in Clause 3.2.2.5 of Eurocode 8 Part 1 [4], but instead, the equivalent 'average' acceleration response spectrum derived from the peak response which different structures would exhibit under the actions of the input simulated ground motion record in accordance with the method recommended in the Guidelines for seismic microzonation [172] .

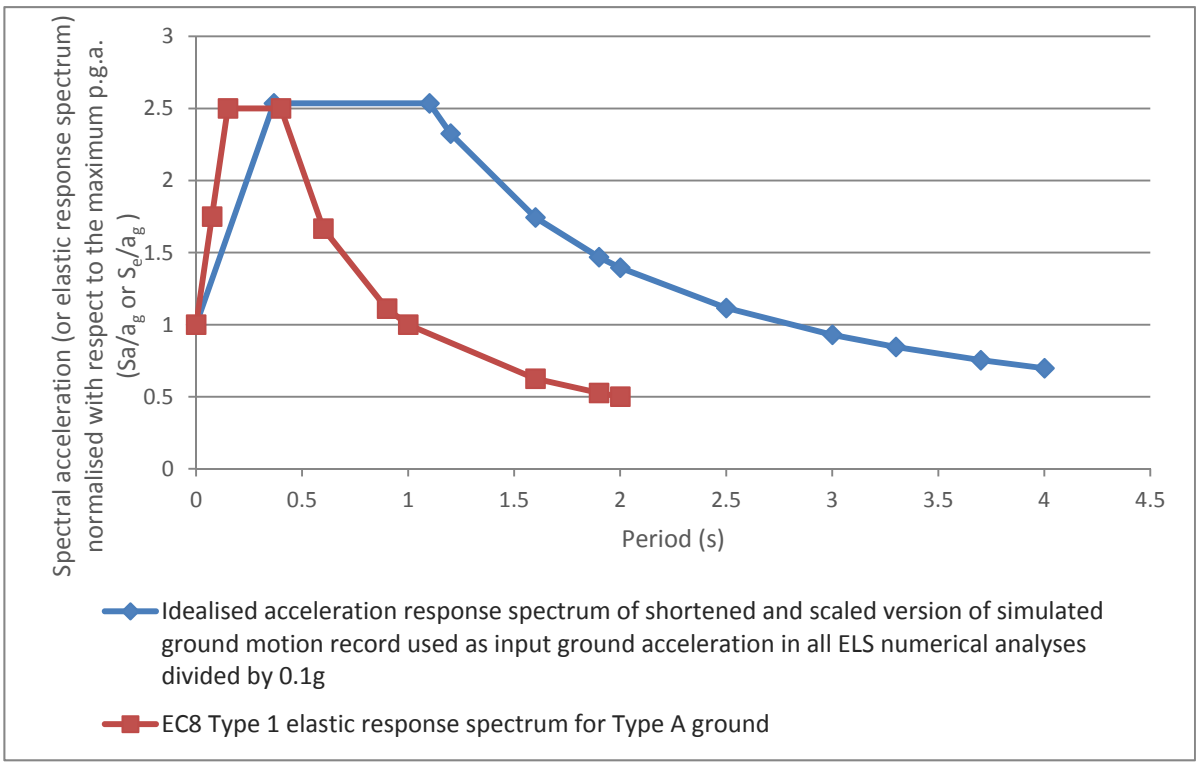

Figure 3-38 Superimposition of the idealised acceleration response spectrum derived from the input simulated ground motion record on the Eurocode 8 Part 1 Type 1 elastic response spectrum for Type A ground.

The comparison of the idealised acceleration response spectrum of the input simulated ground motion record to the Eurocode 8 Part 1 Type 1 elastic response spectrum for Type A ground [4] in Figure 3-38 shows that both response spectra have similar maximum accelerations of circa 2.5 times the design ground acceleration on ground Type A. Furthermore, with reference to the natural frequency results of the final set of numerical models analysed using ELS® summarised in Table 31 of Appendix D and discussed in Section 4.2.1 of this thesis, for the range of first (fundamental) mode frequencies in the transverse x-direction of the typical unreinforced loadbearing masonry buildings for the cases considered in this research study (circa 2.50 Hz to 7 Hz in the six- to three-storey analysed numerical models which include a soft storey and in the six- to four-storey investigated cases which do not include a soft storey at semi-basement level) the difference in the accelerations of both response spectra varies between a maximum of 34% at a frequency of 7.00 Hz (equivalent to a period of 0.14 s) and a minimum of almost 0% at a frequency of 2.50 Hz (equivalent to a period of 0.40 s).

A ground motion record is not defined only by its maximum peak ground acceleration, but also by the range of ground motion frequencies emitted by the source. The comparison presented in Figure 3-38 suggests that the numerical models analysed using ELS® have been subjected to maximum accelerations which are consistent with the Eurocode 8 Type 1 elastic response spectrum on Type A ground [4]. However, as discussed above, through the selected input simulation ground motion record, in the present research study, these numerical models have, in most cases, been subjected to a range of lower magnitude ground accelerations (hence, a lower seismic load) than would be described by a seismic event which would correspond completely to a Eurocode 8 Type 1 elastic response spectrum for Type A ground [4]. Furthermore, for complete correspondence, the frequency

range of the simulated ground motion record over which the maximum accelerations occur, should coincide with the corresponding frequency range of the Eurocode 8 Part 1 Type 1 elastic response spectrum on Type A ground [4]. This requirement is not completely satisfied by the selected ground motion record for use in this research study. Hence, in view of the reservations discussed above, it is acknowledged that the simulated ground motion record (used as input seismic action in all the final numerical analyses carried out using ELS® in the present research study) exhibits only a partial correspondence with the Eurocode 8 Part 1 Type 1 elastic response spectrum for type A ground [4]. Nevertheless, in the context of the objectives of the present research study, the consistent use of the same simulated ground motion record as input seismic action in all the numerical analyses, ensures that the observed relative influence, of the investigated characteristics on the seismic response of the contemporary loabearing unreinforced masonry building typology, is still valid.

3.4.6 Constitutive material models

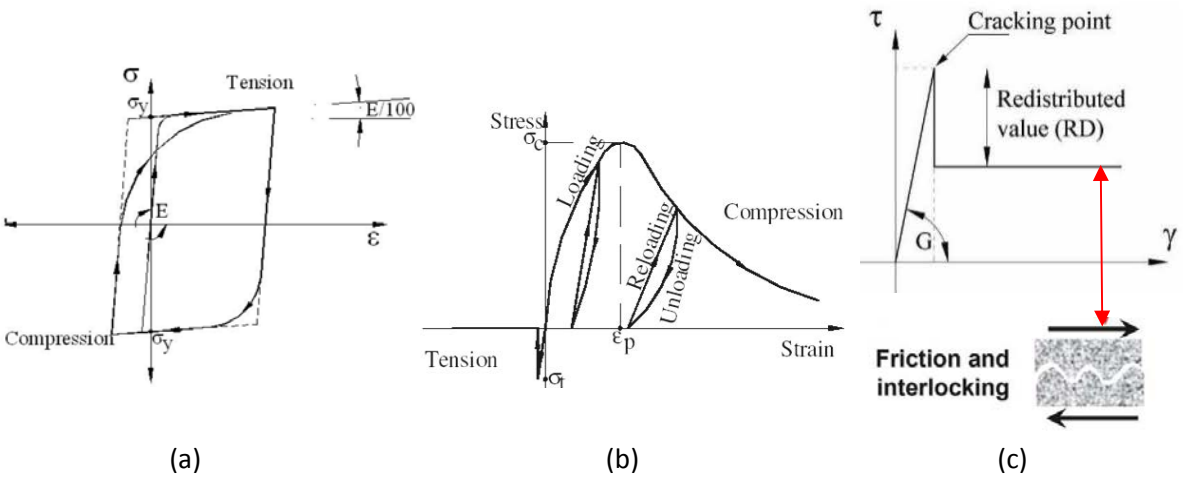

(a) (b) (c)

Figure 3-39 Constitutive models in ELS® for (a) steel, (b) concrete under axial stresses, (c) concrete under shear stresses ([173] p. 48).

The default materials available in ELS® consist of a) the 'elastic model', described in the ELS® Theoretical Manual [173], as corresponding to materials which have a continuously constant stress-strain ratio; b) the 'concrete models', where separate models are available for high strength and normal strength concrete; c) the 'steel model'; d) the 'bricks model'; e) the 'mortar model'; f) the 'glass model'; g) the 'aluminium model'; and h) the 'tension model'. However, the constitutive models considered in ELS® are limited to the 'elastic model', the 'steel model' and the 'concrete model', while the behaviour of other materials defined in the numerical models is considered to follow one of these three constitutive models.

The 'elastic model' assumes an indefinitely constant stress-strain relationship. Glass is described by the ELS® Theoretical Manual [173] as deemed to follow this model, in view of 'its linear elastic behaviour up to tension failure' [173]. The 'steel model', which is defined in the same Manual [173] as representing the behaviour of both steel reinforcement within reinforced concrete sections, and structural steel sections, is based on the stress-strain behaviour presented by Ristic et al. [174], reproduced herein as Figure 3-39(a). The ELS® Theoretical Manual [173] explains that the steel tangent stiffness is based on the strain of the steel material spring in the model, the current loading or

unloading stage, and the stress-strain history of the spring, where in stress–reversal situations, such as seismic loading, plastic deformation can start at lower stress values for every cycle (Bauschinger Effect).

Bricks, mortar and concrete are considered to follow the 'concrete model' by the ELS® software package. This model defines concrete under compression loading during static analysis as following the Maekawa compression model (reproduced in Figure 3-39(b)) for a minimum value of allowed stiffness equivalent to 1% of the initial stiffness value, hence taking into consideration the loss in strength due to cracking, but excluding the possibility of compression crushing, in which case the structure or member would lose its z-restraint, causing a stability error. Tagel-Din and Meguro [175] explain that, during no-linear dynamic analysis, a zero minimum value of stiffness is allowed, until the crack closes because of reversal of loads. The stiffness of concrete springs under tensile forces is equivalent to the initial stiffness up to failure (cracking), when the stiffness is reduced to zero. Failure in the 'concrete model' is considered to occur when the major principal stress is equivalent to the tensile strength specified for the material. Figure 3-39(c) indicates that a linear relationship between shear stress and shear strain is assumed in concrete until failure, which causes a sudden reduction in shear stress, the magnitude of which is governed by the friction and aggregate interlock throughout the crack.

In the present study, while both stone and hollow concrete blocks were defined as alterations of the 'bricks' material properties, therefore, resulting in their assumed behaviour following the 'concrete constitutive model' during the numerical analyses, in the absence of the availability of material models which describe the behaviour of ground materials, upper coralline limestone and clay were also defined through the alteration of material properties of concrete, hence, assuming a similar stress-strain and shear stress-shear strain behaviour under dynamic loading, as considered by the software for concrete. While this assumed behaviour can be considered to adequately represent the response of stone blocks, hollow concrete blocks and upper coralline limestone to dynamic loading, major discrepancies are present between the constitutive models adopted by the ELS® software program for the 'concrete model', and the real behaviour of the blue clay present in the Maltese Islands.

While concrete and steel exhibit an approximately linear stress-strain behaviour, hence, a constant Young's Modulus for the first part of the stress-strain curve, clay usually displays an S-shaped relationship, which suggests that the Young's Modulus of this material is in constant variation with changes in strain level. Whereas under monotonic static loading, in the initial loading stages, clay exhibits a relatively high stiffness at low values of strain, plastic deformation within this material tends to occur around foundations, even though the applied stress would be significantly lower than the allowable bearing pressure, hence leading to the decrease in the Young's Modulus and the redistribution of stress to the areas, which are still partially elastic, making different values of Young's Modulus applicable to different locations of the clay layer in the same numerical model. During cyclic loading, the accumulation of strain with every cycle and, hence, the loading history and the degree of consolidation or over-consolidation, influence the behaviour of clay. Furthermore, the rapidly-changing forces and load reversal, which characterise seismic excitations, suggest that the behaviour

of clay should be best represented in a numerical model in its undrained state, through its undrained modulus, which is also dependent on the varying levels of strain at the different positions throughout the modelled clay mass. The blue clay present in the Maltese Islands can be considered as an over-consolidated clay, whose stress history has a bearing on its loading behaviour, because of the high level of loading to which it was subjected over time [176] (Perit Adrian Mifsud, Assistant Lecturer in Civil and Structural Engineering at the Faculty for the Built Environment of the University of Malta, personal communication by email, adrian.mifsud@um.edu.mt, 8th June 2017).

Hence, while the definition of an alternative constitutive material model for clay could not be carried out by the author, within the limits of the available software, the author hereby acknowledges that the possibly inaccurate modelling of the variation of Young's modulus of clay, throughout the dynamic analysis, is likely to have had a bearing on the ability of this ground layer to deform, and consequently, on its ability to amplify and transfer the seismic excitations to the overlying upper coralline limestone layer and to the modelled structures. Furthermore, it is likely that the alteration of the density of this clay material to 0 kg/m^3, and of its Young's and Shear Moduli in order to solve stability problems in the static loading stage, further exacerbated the inaccurate modelling of the behaviour of this ground layer in the present study.

3.4.7 Ambient noise verification of modelling assumptions

The overall accuracy of the modelling techniques used in the numerical models was verified through the comparison of the natural frequency under static loads, resulting from the analysis of a numerical model of Xemxija Building Number 0011 for two eigen modes, to that obtained from ambient noise measurements carried out on site on the same building by the Seismic Monitoring and Research Unit (SMRU) of the University of Malta. Roca et al. [140] consider such a comparison to be an adequate method of validation, particularly with respect to the modelling of the connections between different elements in a structure.

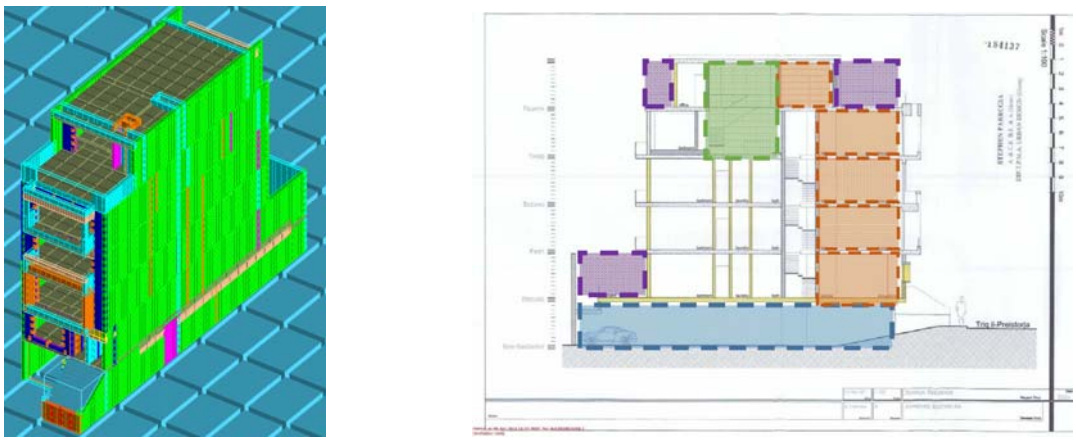

Figure 3-40 Xemxija Building Number 0011: 3-dimensional view of ELS® numerical model and longitudinal section.

Figure 3-41 Development Permit Drawing of Xemxija Building Number 0011 including the identification of building characteristics, which could influence its structural response (Malta Environment and Planning Authority Mapserver https://www.mepa.org.mt/mepa-mapserver).

The ELS® model of Xemxija building 0011 (Model 129) was based on the Development Permit Drawings retrieved from the Malta Planning Authority for this building, which are reproduced in Figures 3-40 and 3-41. Furthermore, the geology of the area, where the building is located, was confirmed to consist of an (approximately) 30 m thick layer of upper coralline limestone over a clay layer of around the same thickness as explained in Section 3.2 of this thesis. Hence, in view of the thick surface upper coralline limestone layer, the ELS® modal analysis of this building was analysed on ground defined as upper coralline limestone at the model's Minimum Z position.

Figure 3-42 A Tromino ™ tromograph used for the ambient noise recordings carried out in Xemxja Building Number 0011 by the Seismic Monitoring and Research Unit (SMRU) of the University of Malta.

The instruments used for the ambient noise measurements were Tromino ™ tromographs, each recording three orthogonal components of ground velocity. Figure 3-42 shows one of the tromographs used for this study. Measurements were taken at roof level, first floor level and at ground floor level. Noise recordings were carried out at a sampling frequency of 128 Hz, and for a duration of 20 minutes. All instruments were aligned with the N-S direction along the long side of the building (longitudinal), the E-W direction corresponding to the short dimension (transversal). All data processing was carried out using the dedicated software Grilla ™ (www.micromed.eu).

For evaluation of the spectral ratios, the time series were divided into 20 s non-overlapping time windows. For each time window, the Fourier amplitude spectra for each ground component were computed, and 10% smoothing was applied, using a triangular window. For the calculation of the HVSR (Horizontal-to-Vertical Spectral Ratio) at a given point, the geometric mean of the two horizontal spectra is computed and divided by the vertical spectrum. Alternatively, the Floor Spectral Ratio is computed by dividing the horizontal spectrum of a given component at a higher floor by that at the ground floor, which is used as a reference level. The final curve is the mean of the curves from all the time windows, after having removed any time windows containing spurious noise.

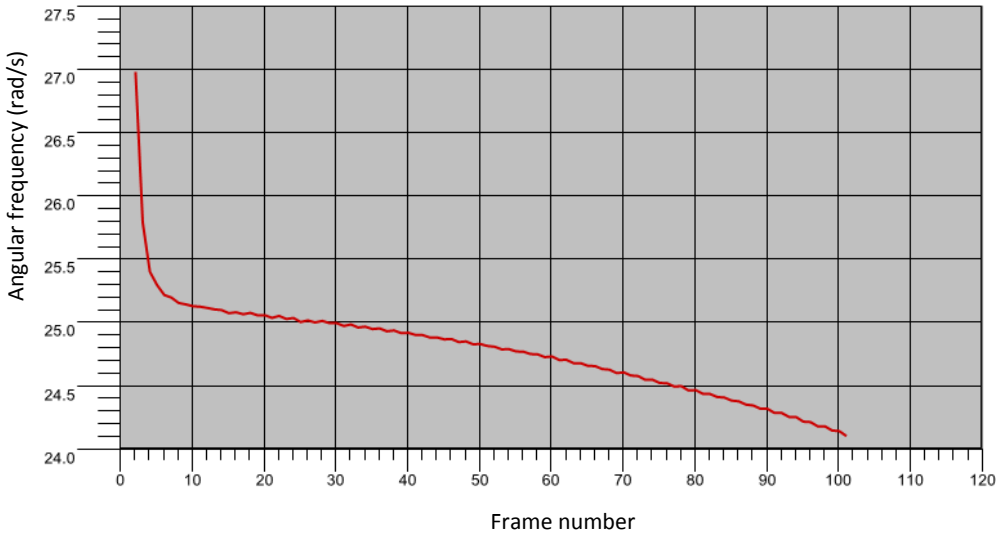

Figure 3-43 Variation in angular frequency throughout the static loading stage for the transverse direction of Xemxija Building Number 0011 resulting from the numerical analysis of a model of this building.

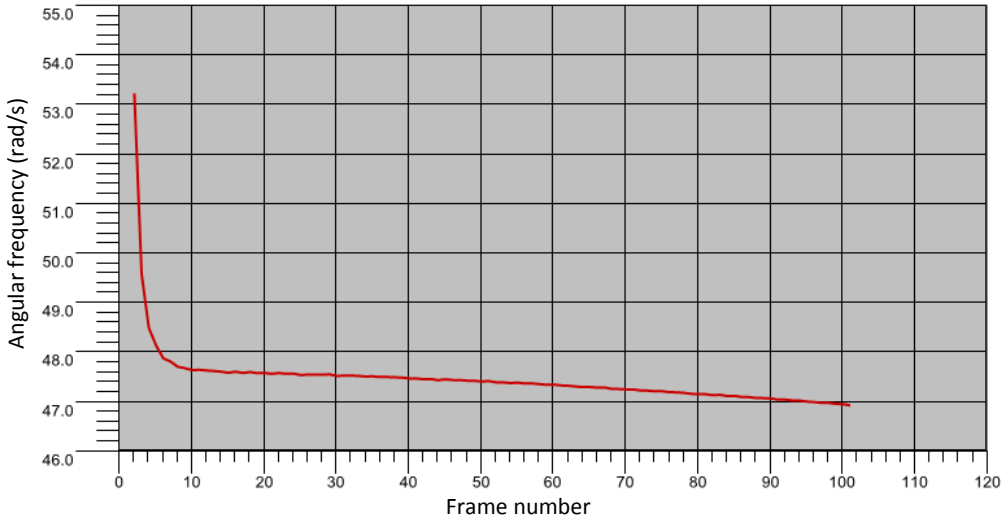

Figure 3-44 Variation in angular frequency throughout the static loading stage for the longitudinal direction of Xemxija Building Number 0011 resulting from the numerical analysis of a model of this building

.

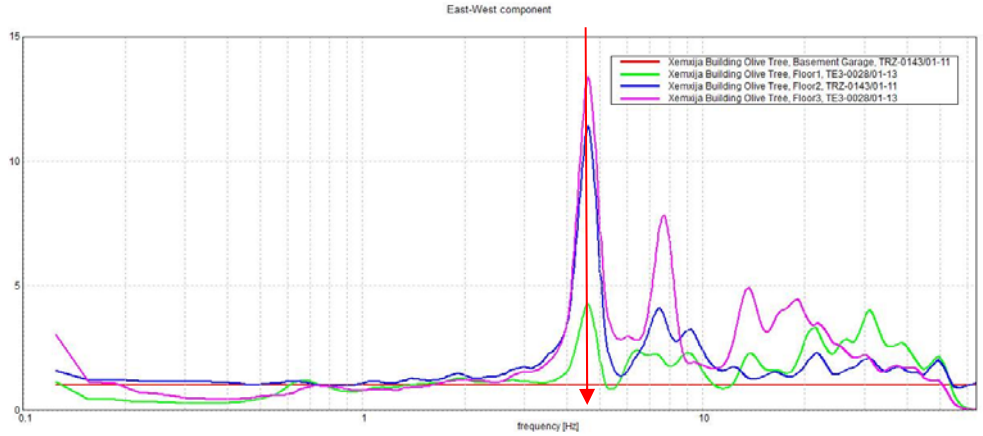

Figure 3-45 Floor Spectral Ratios for the transverse direction of the six-storey Xemxija Building Number 0011 resulting from ambient noise measurements.

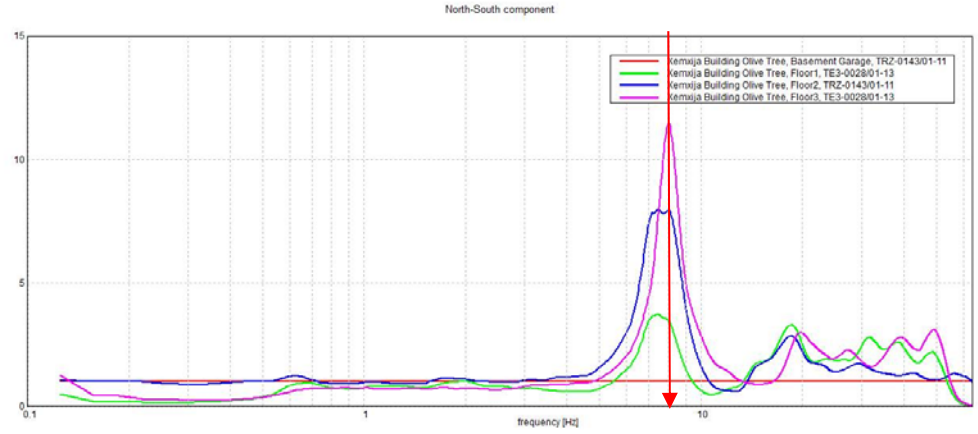

Figure 3-46 Floor Spectral Ratios for the longitudinal direction of the six-storey Xemxija Building Number 0011 resulting from ambient noise measurements.

Figures 3-43 and 3-44 show that the first fundamental modes of vibration in the transverse and the longitudinal directions, resulting at the end of the static loading stage in the numerical model of Xemxija Building Number 0011 analysed for two eigen modes, are 24.108 rad/s and 46.931 rad/s respectively (equivalent to 3.804 Hz and 7.413 Hz respectively). Figures 3-45 and 3-46 indicate that the corresponding natural frequencies in the transverse and longitudinal directions of the same building, resulting from ambient noise recordings carried out on site, are around 4.8 Hz and 8 Hz respectively. The 1 Hz maximum discrepancy between the results obtained in the transverse direction could be due to a number of factors, which are not related to the numerical modelling techniques applied in the construction of the numerical models. These include:

i. the location of the existing building within the building aggregate, whereas it was numerically modelled in isolation;
ii. the possibility of variations in the stiffness of the structure between the existing building and its numerical model, since the wall thicknesses indicated in the Development Permit Drawings

could have been altered during construction, and the slab thicknesses could have been different from those assumed in the numerical model;

iii. the consideration that the ambient noise measurements were carried out in winter, when most of the building was vacant, whereas in the numerical model the densities of the slabs at every level were altered to include the variable load in accordance with the recommendations of Eurocode 8: Part 1 [4], as explained in Section 3.4.4 of this thesis.

Hence, in view of the above, this degree of discrepancy between the natural frequency results, obtained by the ambient noise measurements and by numerical modelling, was considered acceptable, and an indication of the adequate numerical modelling of the analysed structure.

3.4.8 Final set of analysed numerical models in ELS®

The final analysis stage started with the analysis of a six-storey 'control' numerical model (which consisted of the typical plan layout at every level) for the six different ground formation cases listed in Section 3.4.3 of this thesis. The plan layout at Level 1 indicated in the Development Permit Drawings of Xemxija Building Number 0011 was adopted as the 'typical plan layout' in these models.

For every ground formation type, the corresponding control numerical model was re-analysed following the reduction of one floor at a time, until the resulting numerical model resisted collapse. Subsequently, the control numerical model was amended to include a soft storey at semi-basement level, setbacks at penthouse level, and a double height space between Levels 0 and 1. These characteristics were first introduced one at a time in the six-storey single building control numerical model. Since, as identified in separate studies by Farrugia [16], Galdes [17], Marmara' [18] and Tong [19] the presence of a soft storey is considered to constitute the critical case of the contemporary loadbearing URM building typology, the presence of setbacks at penthouse level and that of a double height space between Levels 0 and 1 were next analysed, separately, in conjunction with the presence of a soft storey and, subsequently, all three characteristics where introduced together in the control numerical model. Finally, a two-building aggregate case, and a three-building aggregate case, with shared common party walls throughout their height, were also analysed, starting from an overall height of six floors. The buildings forming the aggregates were control buildings in all cases, that is, they consisted of the same typical plan layout adopted in the single control building cases at all levels. The analysis of every investigated case was repeated with reduction in number of floors until collapse was resisted in the respective investigated construction scenarios. The plan layouts corresponding to the investigated cases are reported in Figures 20 to 32 in Appendix C.

While the amplification of seismic accelerations was expected to occur whenever a clay layer was present, the transfer of this effect to the modelled structures was considered to be more significant when a thinner (such as the 1.5 m thickness scenario) upper coralline limestone layer was present, when compared to the alternative investigated scenario, with a thicker (as in the 30 m thickness scenario) upper coralline limestone layer, in view of the relatively low maximum peak ground acceleration considered for the Maltese Islands, and the smaller mass which had to be mobilised in the former case. The resistance to collapse under seismic excitations of the analysed control numerical

models in the case of the 30 m thick upper coralline limestone over 30 m thick clay scenario at five storeys, when compared to the resistance of the corresponding control numerical models analysed on 1.5 m thick upper coralline limestone over 60 m thick clay at three storeys, confirmed the validity of this assumption. Hence, whereas the control numerical models were analysed on six different ground formation scenarios, the numerical models which were used to investigate the change in seismic response of the contemporary loadbearing masonry building typology, in the presence of the three additional building characteristics, and the two- and three-building control cases, were all analysed on ground defined as 1.5 m thick upper coralline limestone on 60 m thick clay, where both layers were modelled as three-dimensional blocks. Upper coralline limestone, with a friction coefficient of 1.0, was specified as interface material between bedrock and the (lower) clay layer, while clay with a friction coefficient of 1.0 was defined as interface material between the clay and the upper coralline limestone ground layers as discussed in Section 3.4.3. This ground formation typology was selected as it represented a worst case scenario, when compared to the thick upper coralline limestone cases. The scaled and shortened simulated ground motion record presented in Figure 3-29 of Section 3.4.5 was applied at the models' Minimum Z position in the transverse x-direction of every numerical model.

The effect of the variation in the overall building height, on the resistance of the buildings to seismic actions, was studied in all the investigated cases through the examination of the variation in the building response parameters, with reduction in the number of floors. Moreover, the single building control models were analysed on the six different subsoil and ground modelling scenarios, in order to examine the influence, which the presence of different ground formations and ground modelling techniques have on the seismic response of the building typology under study. The variation in building response, in the presence of the three additional building characteristics and the two- and three-building control models, was furthermore investigated through the comparison of the building response parameters resulting from the non-linear dynamic analyses of these numerical models to the corresponding single building control numerical models analysed on the same subsoil case.

The variation in the building response of the analysed numerical models, in the presence of the investigated subsoil scenarios and the three additional building characteristics, was studied through the comparison of the analysis run times at which the start and end of collapse were identified, the duration of collapse, and the displacement profile at the time of maximum x-displacement at the corresponding position in the analysed numerical models, prior to the start of collapse. In addition, to the different x- accelerations recorded through the ground layers and at the first course level in the semi-basement level and the variation in relative x-displacements at specific times during the numerical analyses were analysed in detail. Furthermore, the comparison of the variation in the dynamic properties, of the analysed numerical models at the end of the static and dynamic loading stages, was used to obtain insight into the potential seismic vulnerability, which could be associated with the investigated cases, and the extent of the damage resulting in the analysed structures, following exposure to the same simulated seismic excitations. The comparison of the predominant frequencies in the acceleration spectrum, principally with respect to the ground layers, to the predominant frequencies in the input simulated ground motion record, was carried out in order to

ascertain whether particular building responses could be attributed to the occurrence of resonance, or resonance effects, within the subsoil layers.

3.5 Numerical Analysis using 3Muri®

In view of the significant computational demand of the non-linear dynamic analyses carried out with ELS®, the final stage of the study presented herein involved the numerical modelling of the control numerical models and the control numerical models including either a soft storey at the lowest level, setbacks at penthouse level or a double height space between Levels 0 and 1, on upper coralline limestone and clay subsoils, respectively, through the software 3Muri® version 11.5.0.6 by S.T.A. DATA srl. A non-linear static (pushover) analysis was carried out on equivalent control and single-parameter cases, as had been analysed using ELS®, and the comparison of the main response parameters, extracted from the corresponding numerical models, used in order to verify whether a non-linear static analysis can give an accurate representation of the seismic resistance of the contemporary loadbearing URM building typology under study. The main response parameters compared were the maximum URM building height at which an adequate seismic resistance was exhibited by the corresponding numerical models with respect to the equivalent limit state, the natural frequencies in the x- and y-plan directions for the first mode of vibration and the maximum displacement at the level of the control node resulting from load distributions applied in the numerical models' x-x plan (transverse) orientation.

The main concerns about the use of pushover analysis for the seismic assessment of the masonry building typology under study were mainly related to the prevailing assumptions in non-linear static analysis methods of a box-like behaviour in the analysed structures and the consideration of load distributions with respect to the first mode of vibration, but which, therefore, would ignore higher modes of vibration. A box-like behaviour ensures that no out-of-plane failure mechanisms can be activated through the provision of a rigid connection between slabs and walls throughout slab boundaries and the rigid connection between intersecting walls. The material properties (such as the low grade of mortar used in the local wall construction) and the construction (such as the relatively thin single wall sections, the absence of mortar in the vertical joints in the walls and the absence of ring beams or peripheral ties at floor level) and spatial characteristics (such as the long corridors and large open plan areas which result in long unrestrained lengths of walls and the large openings on façades) of the building typology under study make it very unlikely that a box-like behaviour can be exhibited by such URM buildings. Furthermore, the typical presence of a soft storey at the lowermost level, and of other characteristics which can have a bearing on the lateral storey sway stiffness, is likely to lead to higher modes of vibration having a significant influence on the seismic response. 3Muri® was selected for this research investigation, since (i) it is a commercial software package, which can perform a non-linear static analysis, particularly conceived for the seismic assessment of loadbearing masonry structures, which can be carried out with respect to the requirements of the Eurocodes and, (ii) preliminary trial models suggested that all modes of vibration, selected by the user following a modal analysis of the modelled structures, were taken in consideration in the non-linear static analysis when a 'uniform' and 'modal' pushover verification was selected, in addition to load distributions

taking into account accidental eccentricities, in accordance with the requirements of Clause 4.3.3.4.2.2 of Eurocode 8: Part 1 [4].

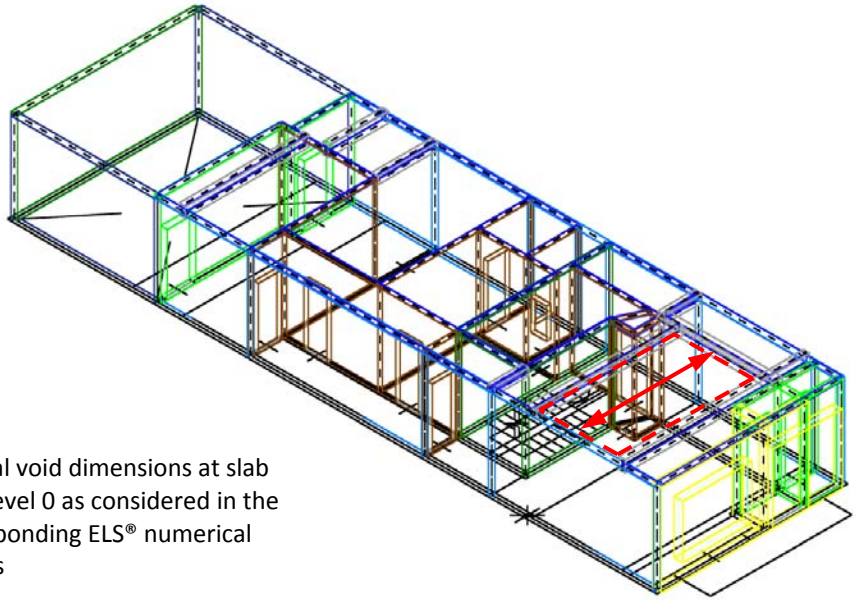

(a) Original void dimensions at slab over Level 0 as considered in the corresponding ELS® numerical models

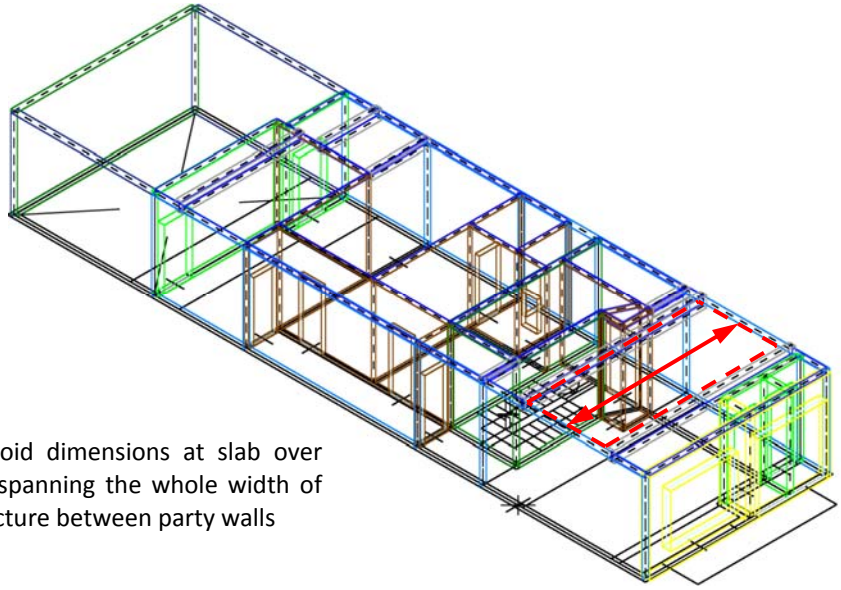

(b) Wider void dimensions at slab over Level 0 spanning the whole width of the structure between party walls

Figure 3-47 Additional case investigated using 3Muri® of control numerical model with a wider double height space between Levels 0 and 1, which spans the whole width of the structure between party walls. This case was investigated for the URM building situated on an upper coralline subsoil only.

Furthermore, the detailed evaluation of the response parameters extracted from the numerical models analysed in ELS® suggested the importance of investigating the seismic response of numerical models, which include a double height space between Levels 0 and 1, where the void in the slab at Level 1 had the same length as the previously investigated case, but it was wider, thereby extending over the whole width of the structure between party walls, as indicated in Figure 3.47. Moreover, the study of the seismic response of similar control numerical models and numerical models which include

either a soft storey or a double height space between Levels 0 and 1 (albeit with the plan layouts having extended length-to-width ratios of 4:1, as compared to the 2.75:1 plan ratios originally investigated in ELS®) was considered important, since a plan ratio of 4:1 is very common in the local building typology under study and it corresponds to the limiting plan slenderness ratio considered in Clause 4.2.3.2(5) of Eurocode 8: Part 1 [4] for plan regularity. The extension in plan layout resulted in an additional room with an overall length of around 3 m within the length of the corridor, thereby causing a lengthening of the unrestrestrained length of the longitudinal party wall in the area of the corridor, and a 5 m extension to the open plan area on the front of the URM building, as reproduced in Figure 3.48. In view of the time limitations related to the available duration of the software licence, these seismic analysis cases could not be investigated using ELS® and were, hence, studied only using 3Muri®.

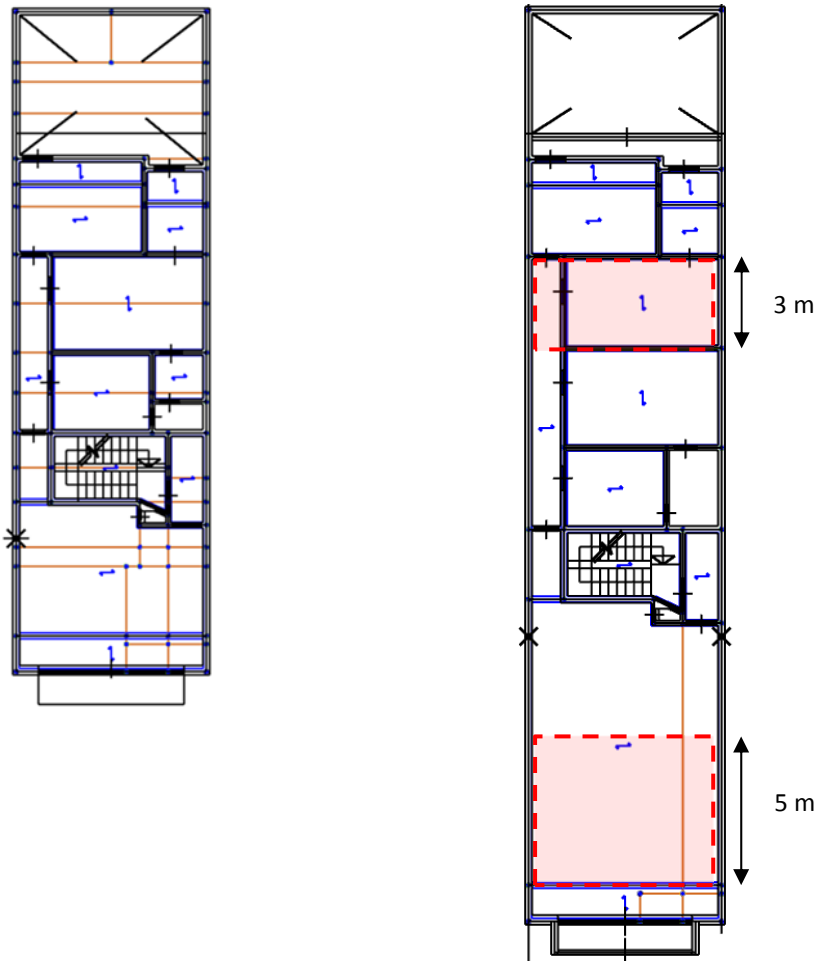

(a) Original plan length-to-width proportions of 2.75:1

(b) Extended plan length-to-width proportions of 4:1 including positons on plan affected by extension in layout

Figure 3-48 Additional case investigated using 3Muri® for an extended plan layout with a length-to-width proportion of 4:1. This case was investigated for the URM building situated on upper coralline limestone and clay subsoils, respectively.

Moreover, the presence of shear failure in the longitudinal walls and the main transverse walls with respect to the limit state of Significant Damage, in addition to the maximum URM building height at

which the resulting average value of the reduction factor 'q_u' with respect to the limit state of Near Collapse (obtained from the pushover analyses) was lower than the equivalent maximum allowable limit on 'q_u' estimated in this research study (from the behaviour factor 'q' for irregular masonry structures designed in accordance with Eurocode 6) were also examined for all the analysed numerical models. These additional verifications were carried out in order to assess whether these parameters could constitute valid alternative or additional capacity criteria for a more accurate assessment of seismic resistance.

3.5.1 Trial models and modelling considerations in 3Muri®

A number of full scale numerical models of the control numerical models and the control numerical models including either a soft storey at the lowest level, setbacks at penthouse level or a double height space between Levels 0 and 1 were developed in 3Muri® in order to investigate the most adequate way to model the particular characteristics present in the contemporary loadbearing URM typology under study with the functions available in this numerical software package. It was ensured at all times that variations with respect to the corresponding numerical models analysed in ELS® were restricted only to the cases, which were dictated by the requirements or the limitations of the 3Muri® software package.

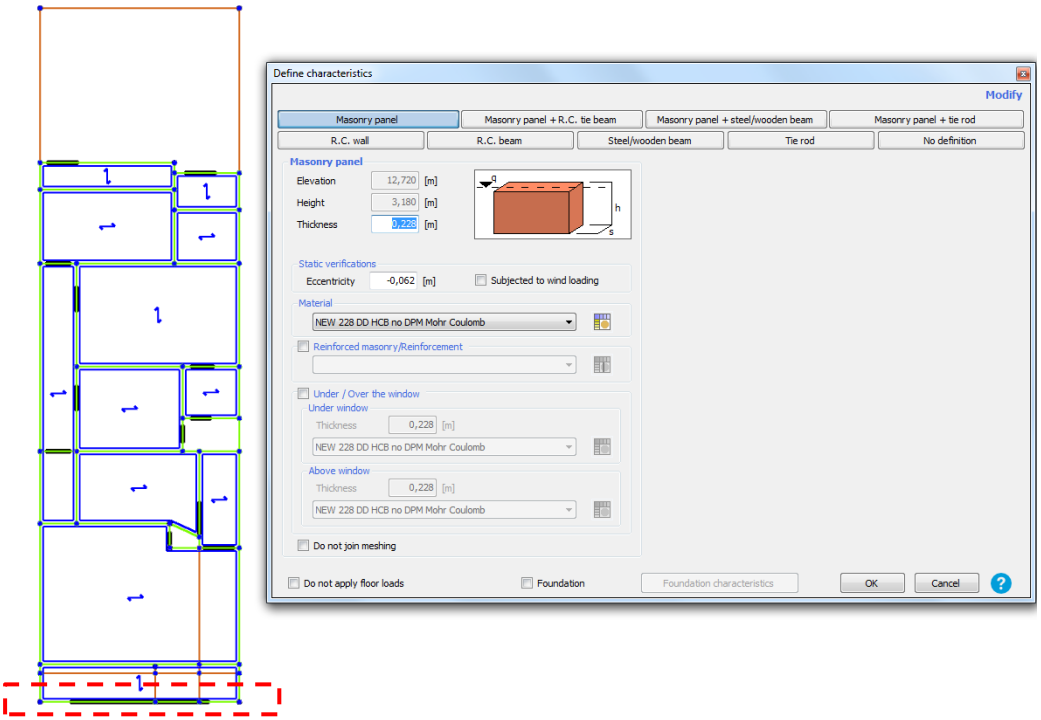

Figure 3-49 Front facade modelled as a single 228 mm thick hollow concrete blockwork wall positioned along the centreline of the external leaf of the double leaf wall and loading from slab defined at an eccentricity: typical floor plan and masonry wall settings in 3Muri®.

In 3Muri®, walls are defined as single panels with the specified material properties smeared throughout the whole panel and not as individual masonry blocks with mortar at the joints as in ELS®. Hence, the degree of fixity of wall-to-wall junctions and between walls and slabs around slab boundaries cannot be controlled by the user, while, by default, a full coupling is assumed in 3Muri® between all intersecting walls and similarly a rigid connection is assumed in 3Muri® at all slab

boundaries. This ensures the satisfaction of the pre-determined default assumption in 3Muri® that all analysed structures exhibit a box-like behaviour, and therefore, the disregard of out-of-plane actions and associated failure mechanisms.

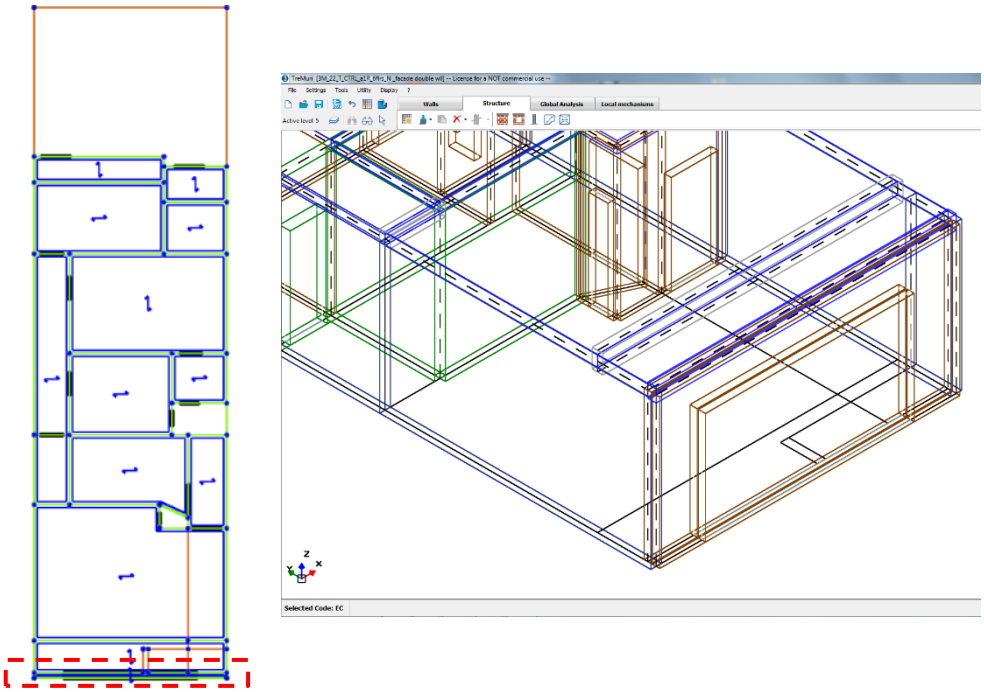

Figure 3-50 Front facade modelled as two 153 mm thick hollow concrete blockwork walls defined 25 mm apart and slabbed over, at every slab level, by a 300 mm thick reinforced concrete slab: Typical floor plan and 3-dimensional view of 3Muri® numerical model in area of front facade.

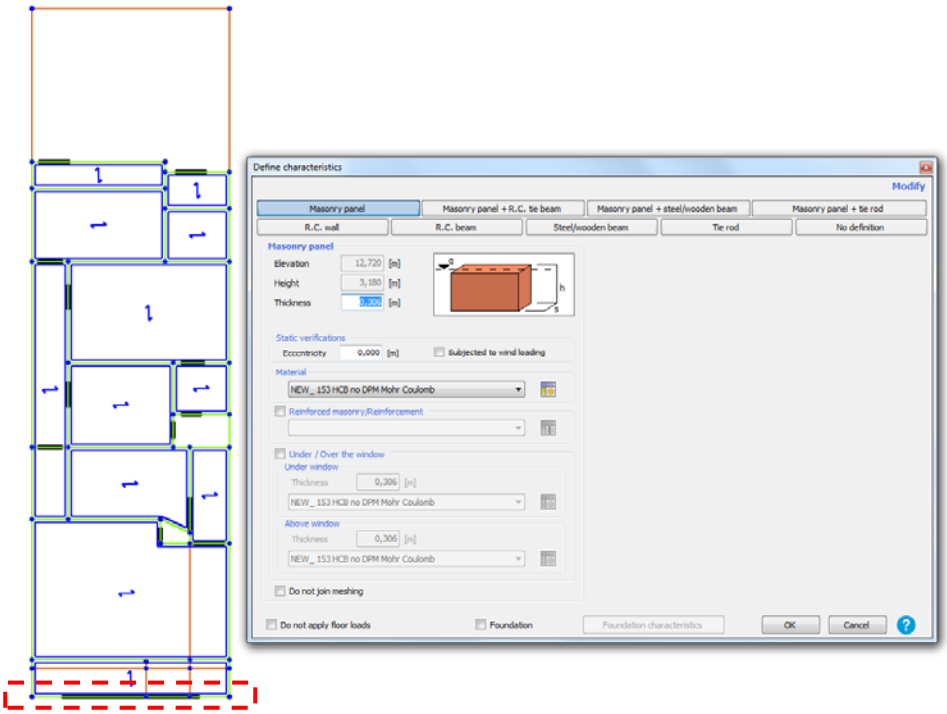

Figure 3-51 Front facade modelled as a single wall with an equivalent thickness of 306 mm defined along the equivalent centreline of the double leaf wall and with the material properties of a 153 mm thick hollow concrete blockwork wall: typical floor plan and masonry wall settings in 3Muri®.

In this context, three different representations were considered for the numerical modelling of the double leaf front façade (modelled in the numerical models analysed in ELS® as two 153 mm thick

hollow concretre blockwork walls with a 25 mm gap and bonded through bondstones) as reported in Figures 3-49, 3-50 and 3-51, namely:

a) a single 228 mm thick hollow concrete blockwork wall assumed to be positioned along the centreline of the external leaf of the double leaf wall and with the load from the slab defined at the equivalent eccentricity, which would result if the slab had to load the centreline of the double leaf wall when both leaves are considered;
b) two 153 mm thick hollow concrete blockwork walls defined 25 mm apart and slabbed over, at every slab level, by a 300 mm thick reinforced concrete slab (since bondstones cannot be defined in 3Muri®), while only the inner leaf was loaded by the main slab of the room;
c) a single wall with an equivalent thickness of 306 mm defined along the equivalent centreline of the double leaf wall and with the material properties of the 153 mm thick hollow concrete blockwork wall.

The single 228 mm thick single hollow concrete blockwork option was considered to be the most inaccurate representation, since it did not correspond to the required double wall in mass, stiffness or capacity. On the other hand, the second representation, which included the two 153 mm thick hollow concrete walls, while more accurate than the first option, was still likely to introduce errors in the stiffness of the wall when compared to the case when the two leaves are connected through bondstones. In addition, the nodes at the junction between the walls representing the front façade and the longitudinal party walls are likely to be more rigidly restrained than in the real life scenario, in view of the thick concrete slab defined at every general slab level, thereby, possibly influencing the accuracy of the displaced plan shapes. The third option, while ignoring the possible failure due to 'punching' at bonstone positions (which cannot be taken into account in 3Muri®, since it consititutes an action out of the plane of the wall, in which orientation the wall is assumed as having no stiffness), represents correctly the in-plane stiffness of the wall and ensures that all actions are resisted by the whole equivalent wall thickness. The latter was, hence, considered to be the most accurate representation of the double wall on the front façade out of the three options, and this modelling representation was used in the final set of numerical models analysed using 3Muri® in the present research study.

Furthermore, while in the numerical models analysed using ELS®, the presence of the damp proof course was represented through the alteration of the friction coefficient of the first horizontal mortar joint above slab Level 0 in all external walls (including the party walls), in 3Muri® the properties of a particular mortar joint cannot be altered, since the material properties assigned to the particular wall type are attributed to the whole wall panel. Moreover, attempts to define a storey with an overall height of one course, where the material properties of that course would be altered to reflect the reduced shear resistance of the wall due to the presence of the damp proof course, and where no slab would be defined above this single-course high storey, were not allowed by 3Muri®.

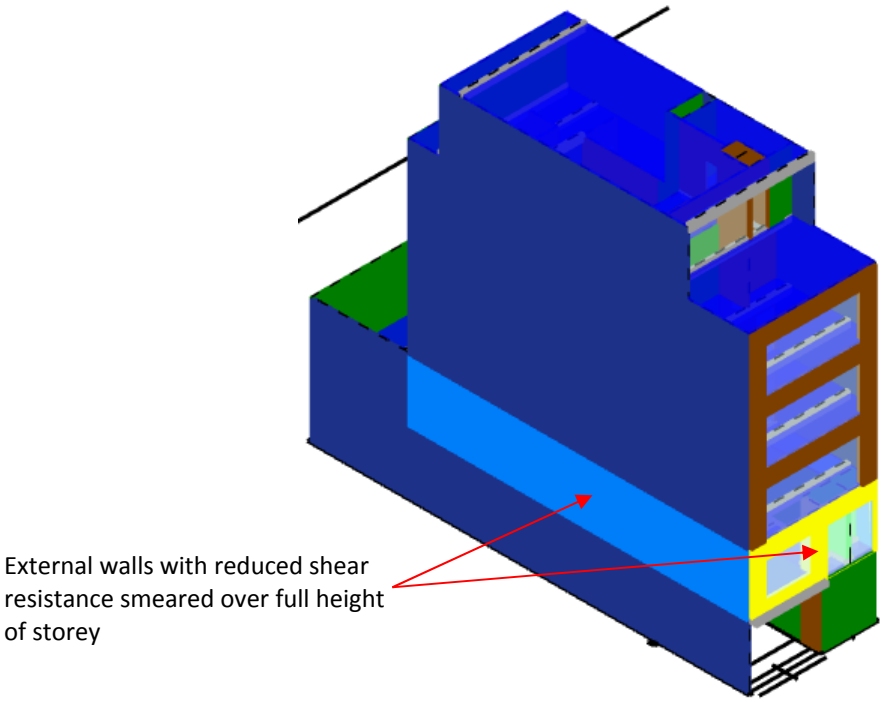

Figure 3-52 Presence of damp proof course represented by a reduction in shear capacity of all external walls at Level 0.

The presence of the damp proof course was, therefore, represented by the reduction of the shear capacity of the external walls at Level 0 by a factor of 0.737, as indicated in Figure 3-52. This reduction factor was derived from the results corresponding to the highest reduction in shear resistance out of the three damp proof course materials investigated by Saliba [161] for a pre-compressive stress of 0.5 N/mm^2, which is approximately equivalent to the stress at the base of a 228 mm thick solid wall from an overlying structure with an overall height of around four storeys and with slabs spanning onto party walls, as discussed in detail in Section 3.4.2.

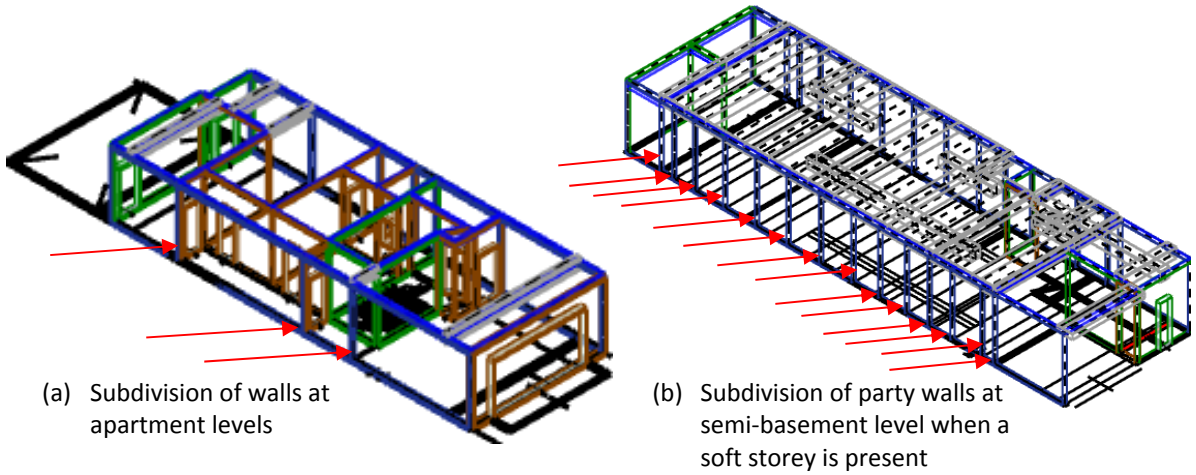

(a) Subdivision of walls at apartment levels

(b) Subdivision of party walls at semi-basement level when a soft storey is present

Figure 3-53 Subdivision of walls into separate sections where meshing is not joined with that of adjacent levels at a) apartment levels, and b) semi-basement level in the case of a soft storey.

Moreover, in 3Muri®, no 45 degree distribution of reactions at beam supports is considered through walls, hence, implying that the whole length of every wall panel that is not subdivided and whose meshing is not joined with that of adjacent panels, is considered effective in supporting the load from

the overlying structure. Therefore, as indicated in Figure 3-53, at all levels in numerical control models and in the control numerical models which include setbacks or a double height space, and in the apartment levels in the numerical models, which include a soft storey at semi-basement level, the transverse walls were not subdivided into separate sections except at changes in material or wall thickness, in view of their relatively short length, while the longitudinal party walls were split at all junctions with perpendicular (transverse) walls and the meshing between the separate wall sections was not joined. On the other hand, at semi- basement level, in the case of control numerical models with a soft storey at this level, the party walls were split at the junction with every beam defined at slab over semi-basement level and the meshing between the different wall sections was similarly not joined, therefore, ensuring that the reactions from the beams are considered as supported by a length of wall, which is significantly longer than the length resulting from a 45 degree dispersion.

In addition, since slabs in 3Muri® are represented as orthotropic horizontal membranes which transfer the horizontal forces to the vertical loadbearing walls, but which do not have any bending stiffness out of their plane, beams have to be inserted to support loads from the overlying structure at every shift in wall position and, in the case of a soft storey, at all overlying wall positions at slab over semi-basement level. Failure to provide such beams, or if the specified beams do not have the required capacity to sustain the overlying loads, results in the loss of vertical restraint to the overlying walls, which, in turn, generates an error in the non-linear pushover analysis, which therefore, cannot be completed. Hence, as shown in the example of the control numerical model with setbacks at penthouse level in Figure 3-54(a), beams were specified directly beneath all affected walls at changes in plan layouts in overlying floors.

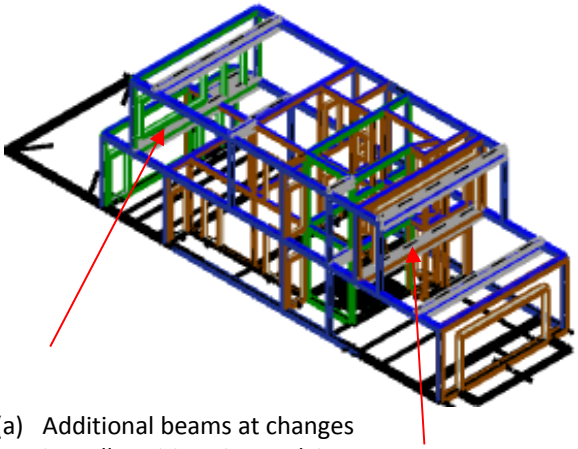

(a) Additional beams at changes in wall positions in overlying floor of control numerical model with setbacks at penthouse level

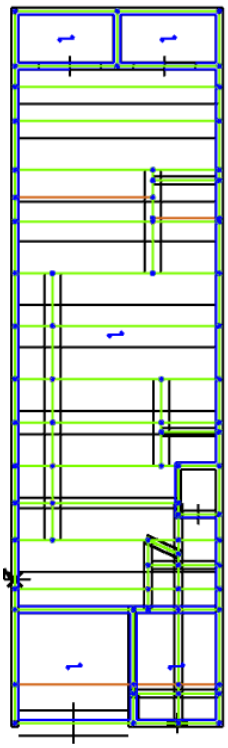

(b) Beam layout at slab over semi-basement level in control numerical models which include a soft storey at semi-basement level

Figure 3-54 Additional beams inserted in apartment levels at changes in wall positions and at slab over semi-basement level in control numerical models, which include a soft storey at the lowest level.

Furthermore, in the case of the control numerical models with a soft storey at semi-basement level, as indicated in Figures 3-53(b) and 3-54(b) at slab over semi-basement level, 1.999 m wide by 0.460 m deep reinforced concrete beams were specified directly beneath all transverse walls, while beams of different widths and 0.460 m depth were specified in the gaps resulting between the 1.999 m wide beams. Additional transverse and longitudinal reinforced concrete beams were inserted to coincide with the centreline of all remaining walls, which were otherwise not located directly above the centreline of a transverse beam. These additional beams were specified at the minimum approximate size, which was required in view of their span and loading since they overlapped in position with the main transverse beams and, hence, they introduced a margin of error in the mass of the floor. The 0.460 m depth of the main beams at slab over semi-basement level was specified in order to ensure that the 3Muri® numerical models including a soft storey would result in the same stiffness at slab over semi-basement level as the corresponding numerical models analysed using ELS®, where hollow core precast prestresssed concrete slabs of 0.460 m depth were defined. Moreover, all beams at slab over semi-basement level were assigned the same density as was specified for the hollow core prestressed precast concrete slabs in ELS®. The 1.999 m width of the main concrete beams positioned directly beneath the main transverse walls resulted from the maximum limit on the width of concrete beams allowed in 3Muri®, which must be less than 2 m. In addition, since a horizontal diaphragm must be specified for all storeys, the reinforced cast in-situ concrete topping specified as 0.05 m thick in the corresponding ELS® numerical models above the precast prestressed hollow core slabs, was hence specified in the 3Muri® numerical models as a 0.2 m concrete slab with 0.25 times the density of the normal concrete slabs, hence, ensuring that the mass of the topping is still equivalent to that in ELS®. The concrete spreader beams, which were specified in ELS® over the party walls to provide a level bearing surface for the precast prestressed hollow core concrete slabs and to distribute the loads from these slabs evenly onto the party walls, could not be represented in 3Muri®. However, all beams defined in 3Muri®, including the beams specified at slab over semi-basement level in numerical models, which include a soft storey, were specified in simple bearing on the supporting walls (or beams) by introducing a discontinuity at the extents of the beams, hence, resulting only in a vertical reaction at the supported end.

Furthermore, the presence of a balcony or a room projecting from the façade are common construction characteristics of the contemporary loadbearing masonry building typology in the Maltese Islands. While balconies are typically constructed as cantilevered cast in-situ reinforced concrete slabs, continuous with the reinforced concrete slab of the first (outer) room, rooms projecting from the façades are generally enclosed by masonry walls and their slabs are constructed in a similar way as described for balconies. Hence, in practice these structures result in a main vertical reaction imposed on the façade wall, a moment induced in the slab of the first room and a smaller reaction imposed on the walls of the first room, depending on the direction of span of the slab. On the other hand, the 3Muri® 'balcony' definition function represents a balcony which is attached to the façade, therefore, resulting in a vertical reaction and a moment imposed on the façade wall (where the effect of the latter is ignored in 3Muri®, since it constitutes an out-of-plane action on the wall) and, hence, it does not completely represent the actions resulting from a balcony in the case of the typical

construction of the building typology under study. Since cantilevered concrete slabs cannot be defined in 3Muri®, trial models were used to investigate the most accurate way to represent the influence of balconies and rooms projecting from the façade, which are typical of the URM building typology under study, on the stiffness, mass and the possible eccentricity between the centre of mass and the centre of resistance of the numerical models.

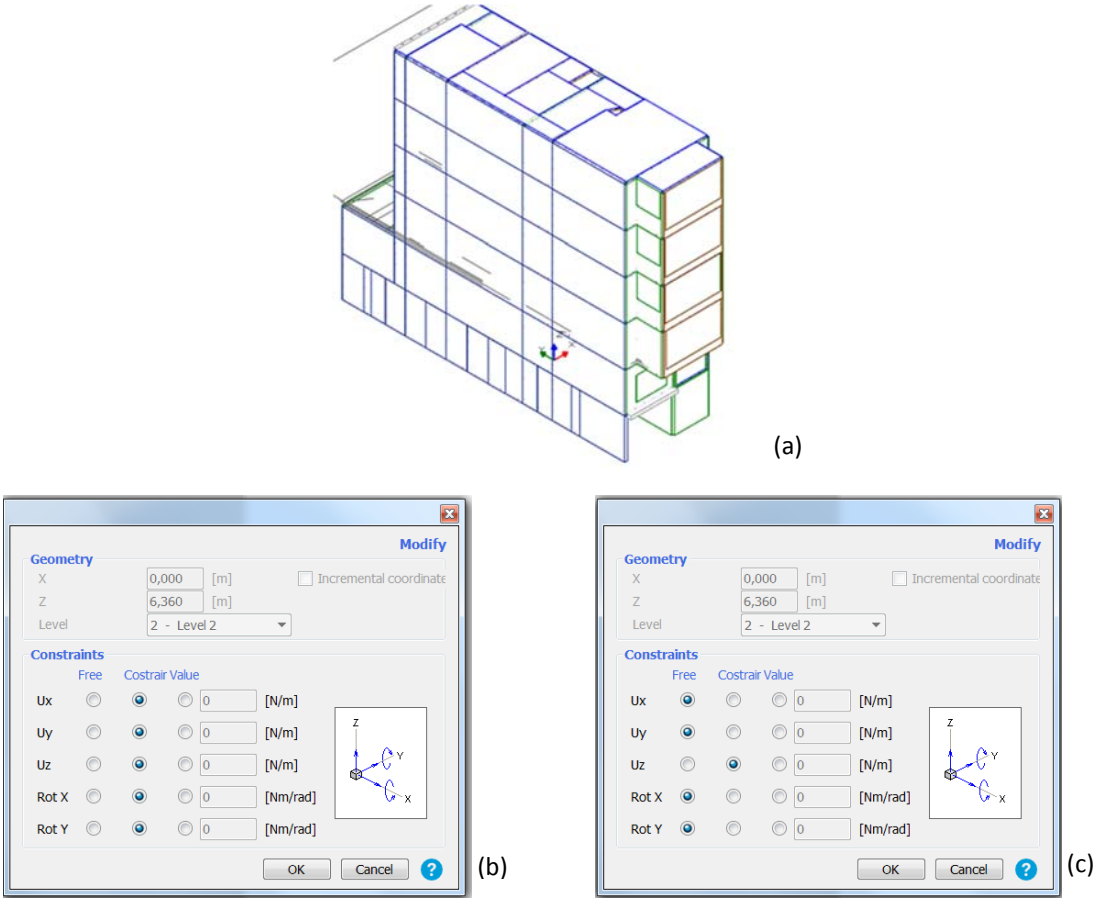

Figure 3-55 Investigated option of modelling the balconies and room projecting on the facade as having double the span and supported on walls with altered support restraints: (a) 3-dimensional view of 3Muri® model; (b) default wall restraints; (c) altered wall restraints.

While beams whose end restraints are not defined as 'discontinuous' in 3Muri®, should theoretically imply that their edges are embedded in the supporting member, the modelling of the balcony and projecting room slabs as having double the intended span and spanning between the front façade and a reinforced concrete beam which was, in turn, supported on two reinforced concrete beams at its ends cantilevering from the facade, caused errors in the analysis. Hence, instead, an attempt was made to model the balcony slab at level 1 through the 3Muri® 'balcony' function and to define walls to support the rooms projecting from the façade and the balcony slabs from Level 1 upwards, which were, in turn, defined as simply supported reinforced concrete slabs spanning between the façade and the outer wall, and with double the intended span of the cantilevered slabs. All walls defined in 3Muri® are assigned default x, y and z translation restraints and x, y rotation restraints at their base. However, these restraints can be altered by the user following the generation of the mesh. As indicated in Figure 3-55, the foundation restraints of the walls supporting the projecting structures were altered in order to result in only a vertical z-restraint. However, these foundation restraints resulted in the numerical

models not achieving the 20% decay in lateral resistance and, following an alteration in the program settings with respect to the non-linear static analysis, the numerical models did not reach convergence. The pushover analysis was only completed in the case where the default base restraints of the walls, defined supporting the rooms projecting from the façade and the balconies, were left unaltered. However, these restraints conditioned the displacement of the structure under lateral loading and were, therefore, not considered to be acceptable.

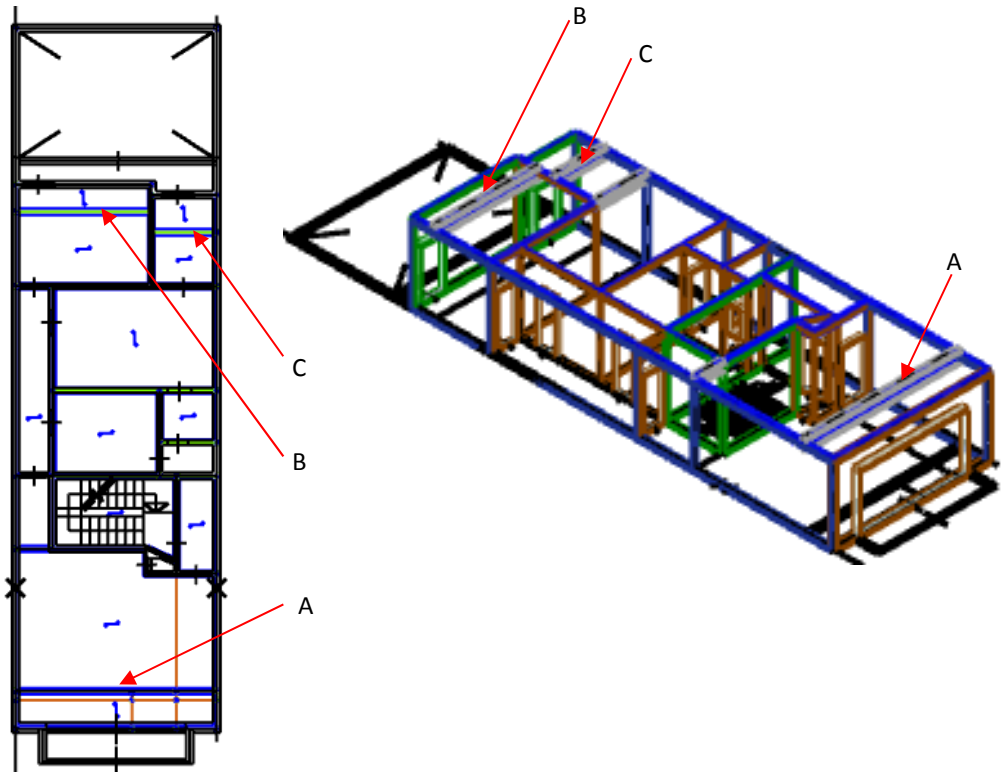

Figure 3-56 Plan and 3-dimensional view of typical floor level in 3Muri® control numerical model with additional beams (A, B and C) specified for support of area of slab with additional loads from balcony or room projecting on façade indicated.

Hence, the presence of balconies or rooms projecting from the façade was represented by distributing the total mass of these structures on an area of slab with equivalent depth as the projecting structure in the first outer room, in addition to the loads pertaining to the slab of that particular room, as shown in Figure 3-56. This slab was specified as spanning between the façade wall and a (new) reinforced concrete beam. This modelling representation ensured that the mass of the projecting structure is taken into consideration in the numerical model, while the resulting loading on the supporting walls was approximately correct. The main inaccuracy resulting from this modelling method is related to the position of the mass of the projecting structure, which could influence the extent of the eccentricity resulting between the centre of mass and the centre of resistance of the storey, and consequently, it could have a bearing on the magnitude of any resulting torsional moments. However, since the span of the considered façade projections was only around 1 m, the resulting inaccuracy was not considered to significantly affect the seismic response of the numerical models analysed using 3Muri®.

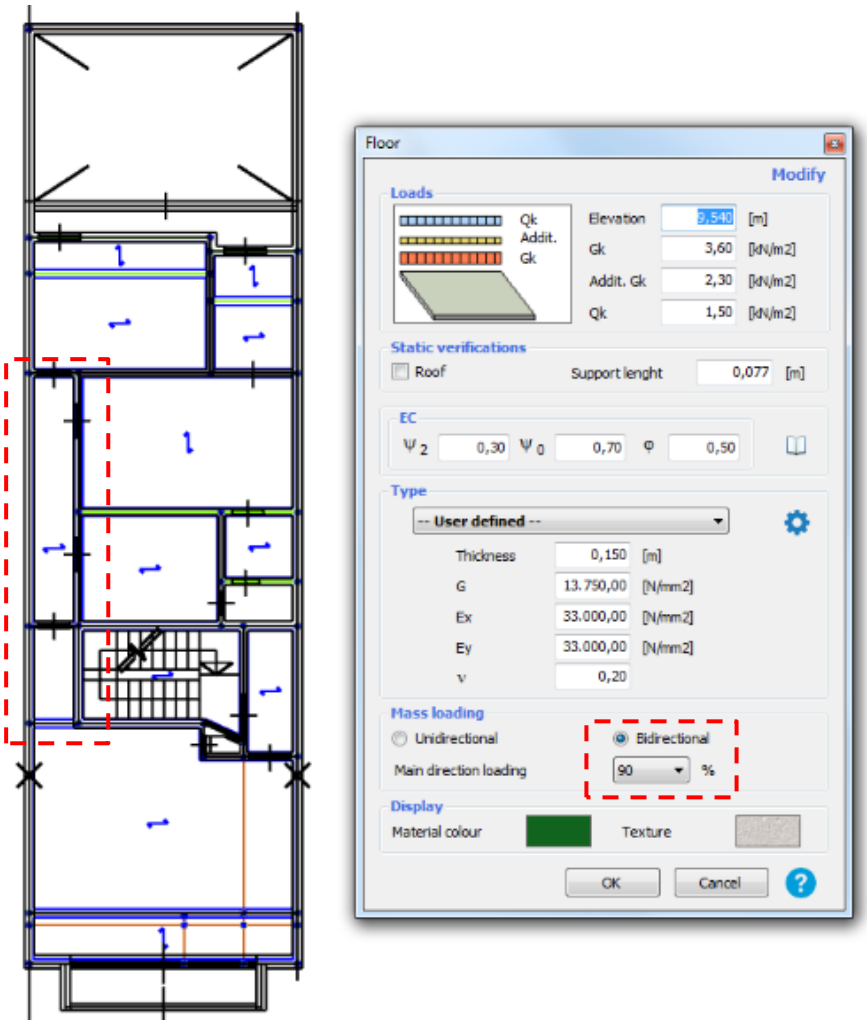

Figure 3-57 Example of bi-directional distribution of loading specified with respect to the slab over the corridor in a typical floor of the control numerical models analysed using 3Muri®.

Furthermore, the proportion of load supported by the walls, which are positioned in the x- and y-plan orthogonal directions, could influence the estimate of the natural frequency of the structure along these orientations. Since no reinforced concrete one-way spanning slab can be considered as loading solely the walls positioned perpendicular to its span, the reinforced concrete slabs defined in the numerical models analysed using 3Muri® were specified as bi-directional, with the main direction of warping parallel to the main direction of span of the slab and, with the percentage distribution of load on the supporting walls calculated on the basis of the proportion of their length with respect to the total slab perimeter as shown in the example of the slab over the corridor area in a typical floor reported in Figure 3-57. The same value of Young's Modulus of Elasticity in the x- and y-plan orientations was specified for all slabs.

3.5.2 Additional modelling considerations in 3Muri®: Modes of vibration, control node selection and plan layout rationalisation

In 3Muri®, the user can select the types of load distributions in the x- and y-plan orientations to be considered in the non-linear static analysis between 'uniform and static' and 'uniform and modal', where, both options satisfy the Italian seismic code requirements (Clause 7.3.4.1 in NTC18 [177]), while only the second option is in accordance with the requirements outlined in Clause 4.3.3.4.2.2(1) of Eurocode 8: Part 1 [4]. The selected load distributions are applied at the accidental eccentricities recommended in Clauses 4.3.3.4.2.2(2)P and 4.3.2(1)P of Eurocode 8: Part 1 [4]. The study presented herein considered the 'uniform and modal' pushover load distribution option in accordance with Eurocode 8 requirements. However, while Galasco et al. [126] proposed a 'seismic adaptive pushover (SDAP)' adaptation to the TREMURI (the research version of the 3Muri® software, from which the commercial version originated) analysis, where the force distributions considered in the modal load distributions at every pushover analysis step are based on the deformed shape of the structure in the previous analysis step, the implementation of this adaptation to the 3Muri® version used in this study, or any other form of adaptive or multi-modal pushover method cannot be assumed since no mention of it could be found in the 3Muri® technical manuals [178] [179] available to the author of this thesis. On the other hand, the technical manual for 3Muri® Version 11.4.0 [179] mentions the consideration of a displacement profile corresponding to the first mode of vibration.

Active in pushover		Mode	T [s]	mx [kg]	Mx [%]	my [kg]	My [%]	mz [kg]	Mz [%]
X dir.	Y dir.								
☑	☐	1	0,24131	726.550,33	67,63	971,68	0,09	42,61	0,00
☑	☐	2	0,17026	55.507,71	5,17	26.265,85	2,45	285,50	0,03
☐	☑	3	0,13171	156,64	0,01	769.495,19	71,63	3.809,98	0,35
☑	☐	4	0,07360	148.780,81	13,85	1.109,61	0,10	5,28	0,00
☐	☐	5	0,05720	40.102,35	3,73	12.551,68	1,17	2.470,85	0,23
☐	☑	6	0,05107	213,10	0,02	153.586,68	14,30	144.744,44	13,47
☐	☐	7	0,04256	26.366,33	2,45	363,48	0,03	598,89	0,06
☐	☐	8	0,04086	122,70	0,01	26.811,82	2,50	616.764,99	57,41
☐	☐	9	0,03866	223,77	0,02	387,89	0,04	63.520,87	5,91
☐	☐	10	0,03248	491,30	0,05	1.710,13	0,16	2.694,79	0,25
☐	☐	11	0,03164	24.226,69	2,26	1.329,00	0,12	6.780,64	0,63
☐	☐	12	0,03098	6.277,01	0,58	19.732,78	1,84	54.576,64	5,08
☐	☑	13	0,02760	3.749,08	0,35	1.392,91	0,13	506,77	0,05
☐	☐	14	0,02686	59,42	0,01	2.275,75	0,21	9.105,98	0,85
☐	☐	15	0,02605	7.709,55	0,72	837,80	0,08	120,22	0,01

Figure 3-58 Extract from 3Muri® modal analysis output for trial model where an additional mode of vibration with a percentage mass contribution of less than 5% was selected.

In the absence of further guidance from the S.T.A. DATA srl technical support, two trial models of the six-storey control numerical models on an upper coralline limestone subsoil were analysed where, in the first case only, the vibration modes with mass contributions of more than 5% were selected from the modal analysis results while, in the second case, an additional mode of vibration corresponding to a percentage mass contribution of 0.35% in the x-direction and 0.13% in the y-direction was also selected, as reproduced in Figure 3-58. The comparison of the number of unsatisfied verifications resulting from these two seismic analyses is presented in Table 3-6. As reported in Table 3-6 and Figure 3-59, a higher number of unsatisfied verifications, all corresponding to 'modal' load distributions, resulted in the trial model where the additional mode of vibration (Mode 13) was selected from the modal analysis, hence, suggesting that all modes of vibration selected by the user from the modal analysis results table are taken into consideration in the non-linear static analysis 'modal' load

distributions. However, pending clarification from the S.T.A.DATA srl technical support, the method used by the 3Muri® software for the consideration of the different modes of vibration could not be confirmed.

Table 3-6 Comparison of results of non-linear static analysis on corresponding trial models for verification of whether all selected modes of vibration are considered in 'modal' load distributions in the non-linear static analysis.

3Muri® model name	Modes of vibration in x-direction selected from modal analysis (% mass contribution)	Modes of vibration in y-direction selected from modal analysis (% mass contribution)	Near Collapse limit state: number of unsatisfied verifications (load distribution numbers)	Significant Damage limit state: number of unsatisfied verifications (load distribution numbers)	Damage Limitation limit state: number of unsatisfied verifications (load distribution numbers)
3M_18_T_CTRL_a1R_ 6flrs_ 3Muri v11_5_06	1 (67.63%); 2 (5.17%); 4 (13.85%)	3 (71.63%); 6 (14.30%)	0 (N/A)	0 (N/A)	12 (1-4; 9-16)
3M_18_T_CTRL_a1R_ 6flrs_ 3Muri 11_5_06_with mode 13	1 (67.63%); 2 (5.17%); 4 (13.85%)	3 (71.63%); 6 (14.30%); **13 (0.13%)**	2 (6; 19)	2 (6; 19)	17 (1-4; **6**; **8**-16; **19; 23-24**)
Note: 'Unsatisfied verifications' correspond to load distributions in the non-linear static analysis where the ratio of maximum displacement to target displacement is greater than 1 (i.e. failure of limit state)					

No.	Compute analysis	Earthquake direction	Seismic load	Eccentricity [m]
1	☑	+X	Uniform	0,000
2	☑	+X	Modal distribution	0,000
3	☑	-X	Uniform	0,000
4	☑	-X	Modal distribution	0,000
5	☑	+Y	Uniform	0,000
6	☑	+Y	Modal distribution	0,000
7	☑	-Y	Uniform	0,000
8	☑	-Y	Modal distribution	0,000
9	☑	+X	Uniform	1,119
10	☑	+X	Uniform	-1,119
11	☑	+X	Modal distribution	1,119
12	☑	+X	Modal distribution	-1,119
13	☑	-X	Uniform	1,119
14	☑	-X	Uniform	-1,119
15	☑	-X	Modal distribution	1,119
16	☑	-X	Modal distribution	-1,119
17	☑	+Y	Uniform	0,321
18	☑	+Y	Uniform	-0,321
19	☑	+Y	Modal distribution	0,321
20	☑	+Y	Modal distribution	-0,321
21	☑	-Y	Uniform	0,321
22	☑	-Y	Uniform	-0,321
23	☑	-Y	Modal distribution	0,321
24	☑	-Y	Modal distribution	-0,321

Figure 3-59 Extract from 3Muri® non-linear static analysis settings window indicating the additional load distributions, which resulted in unsatisfied verifications highlighted in a red box.

Moreover, Galasco et al. [126] discuss the importance of the adequate selection of a control node in a non-linear static analysis for the validity of the seismic assessment to be ensured. In the 3Muri® pushover analysis, the force distributions are increased such that the displacement resulting at every analysis substep in the control node (specified by the user) is equivalent to the maximum displacement defined by the user in the pushover analysis settings, divided by the number of substeps. In the study presented herein, the pushover curve describes the base shear variation of the structure throughout the non-linear static analysis with respect to the variation in displacement of a point, which approximately corresponds to the centroid of the storey where the control node was defined (and not the displacement of the control node itself). This is obtained through the consideration of the 'weighted average displacements' of the nodes in the storey of the control node as reproduced in Figure 3-60. This, therefore, explains why the control node must be chosen at the most flexible position of the structure, both with respect to height and plan layout of the structure, since, in order to ensure a conservative estimate of seismic resistance, the lowest force leading to failure (in terms of maximum displacement of the centroid of the storey at which the control node is selected) must be applied.

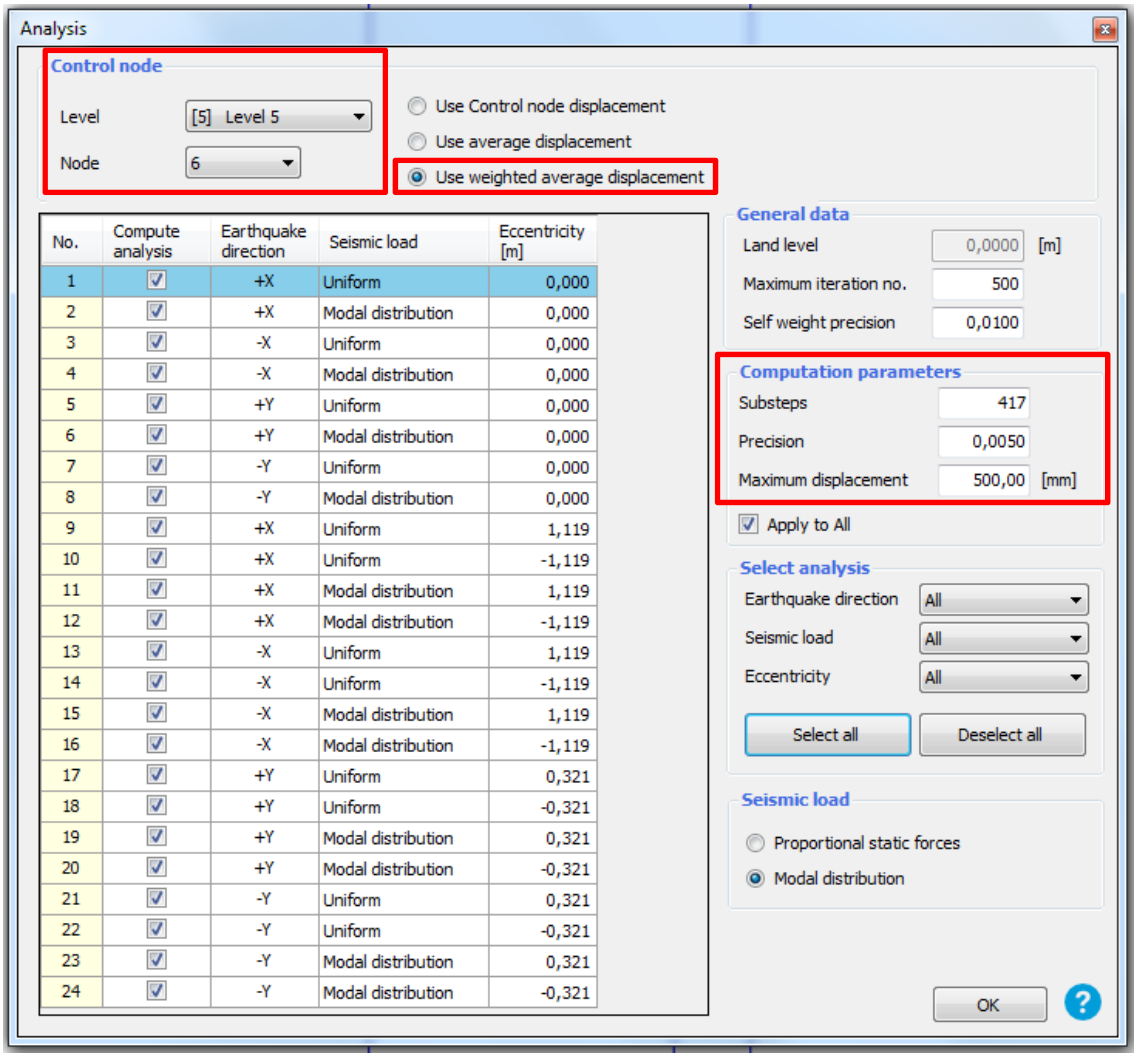

Figure 3-60 3Muri® non-linear static analysis settings window indicating the selection of the control node, the type of displacement described by the pushover curve and the pushover settings controlling the rate of load increment.

Hence, whereas the element in the left hand side party wall at slab over semi-basement level (whose response parameters were compared for the assessment of the influence of the presence of particular construction characteristics on the seismic response of the URM building typology under study in the ELS® numerical analyses) was used for the comparison of outputs from the numerical models, but did not have any bearing on the magnitude of the applied forces acting on these models, the control node in 3Muri® determines the force increment and the displacement magnitude at failure and is, therefore, an important input parameter of the non-linear static analysis. Furthermore, the definition of the control node at the position of the closest node present[9] in the left hand side party wall at slab over semi-basement level in the equivalent 3Muri® analyses, would have required a significantly higher force for the attainment of failure than a node positioned closer to the top of the structure, hence, resulting in an unconservative and unrealistic assessment of seismic resistance. This is clearly evidenced through the comparison of the displaced plan shapes (and the displacement at the position of the ELS® element indicated by a red 'X') corresponding to the fundamental mode of vibration in the x-direction for Levels -1 (semi-basement level), 3 and 4 (topmost storey) of the six-storey control numerical model analysed using 3Muri® on upper coralline limestone (Model 3M46) reported in Figure 3-61.

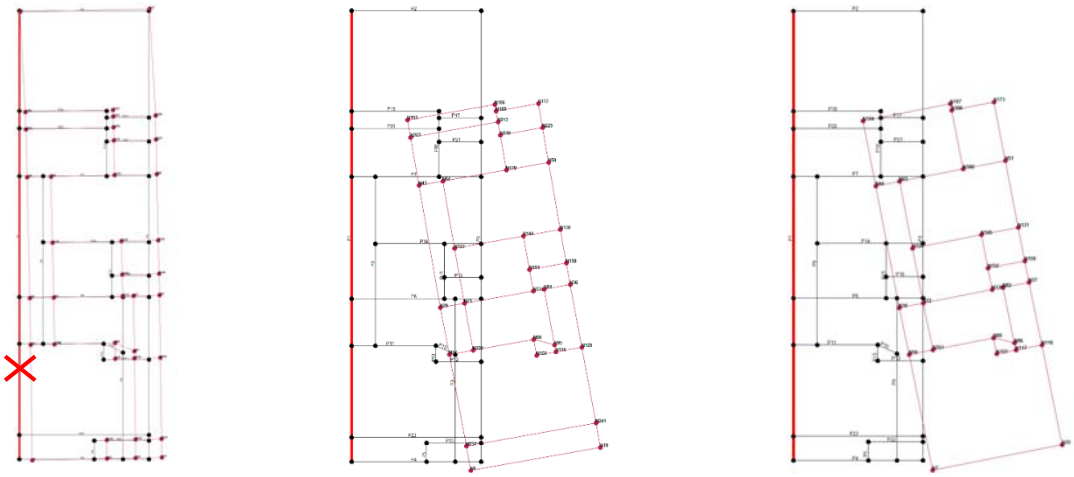

Level -1 Level 3 Level 4

Approximate position of element whose response parameters were compared in the numerical models analysed using ELS®

Figure 3-61 Comparison of displaced plan shapes at Levels -1, 3 and 4 corresponding to the fundamental mode of vibration in the x-direction in the six-storey control numerical model 3M46.

[9] The selection of a control node in the numerical models analysed using 3Muri® at the exact same position on plan as the element in the left hand side party wall whose response parameters were compared in the corresponding numerical models analysed using ELS®, was not possible since, in 3Muri®, nodes can only be defined at wall-to-wall, wall-to-beam or beam-to-beam intersections.

Table 3-7 Comparison of pushover analysis results when different control nodes are selected.

3Muri® model reference name	Level at which control node was selected in 10 storey model	Position of control node on plan	Justification for selection of control node	Near Collapse limit state: number of unsatisfied verifications (load distribution numbers)	Significant Damage limit state: number of unsatisfied verifications (load distribution numbers)	Damage Limitation limit state: number of unsatisfied verifications (load distribution numbers)
3M50	+7 (penultimate level)	Between front façade and left party wall	Maximum displacement at level +7 corresponding to the mode of vibration with the highest mass contribution in the x-direction (67.40%; first mode type of displacement)	7 (1-2; 4; 10;12;15-16)	0 (N/A)	12 (1-4; 9-16)
3M50b	+7 (penultimate level)	Between rear facade and right party wall	Maximum overall displacement at level +7 when all significant modes of vibration were considered. Corresponds to a torsional mode of vibration with 10.95% mass contribution in the y-direction.	0	0 (N/A)	12 (1-4; 9-16)
3M50c	+8 (topmost level)	Between front façade and left party wall	Maximum displacement at level +8 corresponding to the mode of vibration with the highest mass contribution in the x-direction (67.40%)	8 (1-2; 4; 9-10;12;15-16)	0 (N/A)	12 (1-4; 9-16)
3M50d	+7 (penultimate level)	Between rear façade and rear party wall	Maximum displacement at level +7 when the modes of vibration corresponding to the highest mass contribution in the x- and y-directions were considered. Corresponds to mode of vibration in the y-direction (56.92%; first mode type of displacement)	2 (10, 15)	0 (N/A)	12 (1-4; 9-16)

Moreover, it is important that the control node is selected at a storey whose plan layout (and, hence, lateral storey stiffness) is representative of the plan layout of most of the storeys in the structure, and at the same storey in all analysed models in order to guarantee comparability of results throughout the analysed numerical models. Therefore, in view of the above considerations and, since one of the characteristics investigated in the study presented herein was the presence of setbacks at penthouse level (in which case, the topmost storey was not representative of the underlying levels), the control node was selected in the slab over the penultimate storey in all numerical models analysed using 3Muri® in the present study. The influence on the seismic resistance exhibited by the analysed numerical models, of selecting a control node at the level of the floor of the highest storey (hence, in line with the slab over the underlying floor), when compared to the selection of a control node at the level of the roof of the highest storey was investigated through the ten-storey control trial models 3M50 and 3M50c, whose non-linear analysis results, are summarised in Table 3-7. In addition, Table 3-7 includes also the pushover analysis results for trial models 3M50b and 3M50d, where the difference in the non-linear static assessement resulted from the selection of control nodes at positions which exhibited a maximum plan displacement for modes of vibration with a significant mass contribution in the y-direction which were higher than the corresponding maximum plan displacement for the the mode of vibration with the highest mass contribution in the x-direction. In all cases, the control nodes were selected on the basis of the exhibited plan displacements at the relevant levels corresponding to the different modes of vibration and obtained using 3Muri® through the modal analysis of the structure.

The results summarised in Table 3-7 suggest that a lower seismic resistance is exhibited by the ten-storey control numerical model analysed on upper coralline limestone using 3Muri® when the control node is selected at the position which exhibits the maximum plan displacement corresponding to the mode of vibration with the highest mass contribution in the x-direction in the topmost storey (Trial Model 3M50c), when compared to the numerical model when the control node is selected in the underlying storey (Trial Model 3M50). However, the margin of error, resulting in the selection of the control node at the level of the slab over the penultimate storey when compared to when the control node is selected at the topmost storey, is considered to be acceptable. Moreover, the results presented in Table 3-7 also suggest that, for the rectangular plan confirgurations considered in this researched study, even if the maximum displacement exhibited in the mode of vibration with the highest mass contribution in the (weaker) transverse x-plan direction is lower than the overall maximum displacement exhibited in a mode of vibration with a significant mass contribution in the stronger longitudinal plan y-direction, the former, results in a worse case loading scenario since the transverse walls offer less resistance to lateral loading.

Hence, based on the above, in all numerical models analysed using 3Muri® in the present research study, the selection of the control node was carried out following a modal analysis through an inspection of the displaced plan shape at the penultimate level of the analysed structure, and corresponding to the node which exhibited the highest plan displacement in the mode of vibration with the highest mass contribution in the transverse x-direction. In all numerical models analysed

using 3Muri® in this research study, the control node was invariably located at the junction between the front façade and the left-hand side party walls. Moreover, in cases where the displacement exhibited by the node positioned at the junction between the front façade and the left-hand party wall was equivalent to that exhibited between the front façade and the right-hand party wall, the node on the side of the left-hand party wall was still specified as a control node for consistency throughout all numerical models and, since the collapse simulations obtained from the ELS® analyses indicated a clear tendency of the structures to shift to the left-hand side while collapsing. The presence of the control node at the junction between the front façade and the left-hand party wall, furthermore, justifies the adopted representation of the double wall along the front façade. This is because, the option with the alternative two leaves of masonry walls which are slabbed over by a 300 mm thick concrete slab, could have led to a higher restraint to the nodes at the junction between the front façade and the longitudinal party walls, thereby indirectly influencing the results of the non-linear static analysis.

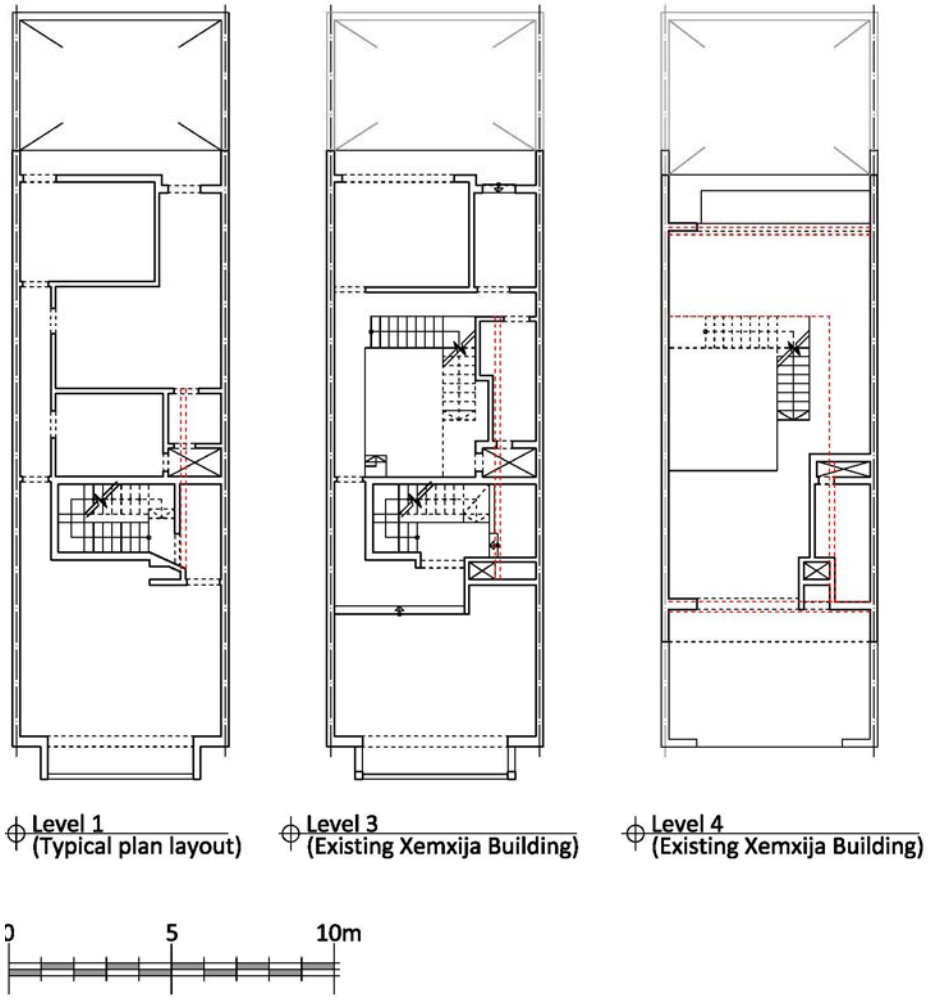

Figure 3-62 Minor rationalisation of plan layouts in 3Muri® (indicated through dashed red lines).

Furthermore, a minor rationalisation of the typical plan layouts and of the plan layouts of the topmost two storeys of the numerical model of the existing Xemxija building was carried out in order to remove marginal misalignments between parallel walls, which lead to narrow changes in direction in the walls and to members defined at a marginal offset from members, which are defined at a lower level (since the presence of very close nodes can cause errors in the seismic analysis). Figure 3-62 presents the

changes to the typical floor layout and the plan layouts of the topmost two storeys of the existing Xemxija building through dashed red lines superimposed on the original plan layouts.

3.5.3 Material properties and applied loading in 3Muri® non-linear static analysis

In all investigated cases, the direct correspondence and comparability between equivalent ELS® and 3Muri® analysed numerical models was ensured by keeping divergencies in plan layouts, wall and slab thicknesses, wall and slab material properties, slab span directions and loading to a minimum. Hence, the same wall material properties were specified in the 3Muri® numerical models, apart from additional material input parameters, which are requested by 3Muri®, based on the Eurocode 6 [157] verification of masonty constructions, namely the characteristic compressive strength of masonry (f_k), the shear strength limit (f_{vlim}) and the mean shear strength (f_{vmo}). All the input material properties specified in the 3Muri® numerical models are summarised in Tables 28 and 29 of Appendix C.

The characteristic compressive strength for masonry (f_k) was evaluated with reference to Equation 3.2 in Clause 3.6.1.2(2) of Eurocode 6 [157], reproduced hereunder as Equation 3-5:

$$f_k = K.f_b^{0.7}.f_m^{0.3}$$

Equation 3-5

where, f_k is the characteristic compressive strength of masonry in N/mm^2; f_m is the compressive strength of mortar in N/mm^2 (considered as 2 N/mm^2 throughout all numerical analyses carried out using ELS® and 3Muri® in the present research study; K is a constant corresponding to 0.45 for globigerina limestone masonry (Group 1 'dimensioned natural stone') and hollow concrete blockwork masonry (Group 2 'aggregate concrete units') as recommended in Table 3.3 of Eurocode 6 [157]; and f_b is the normalised mean compressive strength of units in the direction of the applied action effect determined from BS EN771-1 Annex A for 100 mm x 100 mm x 100 mm specimens, in N/mm^2. In the present study, the normalised compressive strength of units in the direction of the applied action effect was obtained by multiplying the mean compressive strength of masonry by a conversion factor to an equivalent air-dry conditioning regime and by the shape factor for normalised strength in accordance with the conversion tables prepared by Roberts [180].

Table 3-8 Conversion factors for calculation of normalised mean compressive strength of units in direction of applied action effect (f_b) derived from tables prepared by Roberts [180].

Wall material	Conversion factor to an equivalent air-dry conditioning regime	Shape factor for normalised strength
228 mm thick globigerina limestone masonry	0.800	1.194
153 mm thick hollow concrete blockwork masonry	1.000	1.344
228 mm thick hollow concrete blockwork masonry	1.000	1.194

The shear strength limit (f_{vlim}) in N/mm^2 was evaluated from the limit on the characteristic shear strength of masonry through Equation 3.6 in Clause 3.6.2(4) of Eurocode 6 [157], reproduced hereunder as Equation 3-6:

$$f_{vk} = 0.045\, f_b$$

Equation 3-6

where, f_{vk} is the characteristic shear strength of masonry in N/mm^2; and f_b is the normalised mean compressive strength of units in the direction of the applied action effect, as defined earlier.

Furthermore, in the specification of the material safety factor for globigerina limestone and hollow concrete blockwork masonry, reference was made to the table given in the Note to Clause 2.4.3(1)P of Eurocode 6 [157] for masonry made with units of Category II, any mortar and Class 5, hence, resulting in an initial partial safety factor of 3.0, and confirmed with reference to Clause N.A.2.1 in the National Annex to Eurocode 6 for the Maltese Islands [181]. A 'Category II' was considered applicable to both globigerina limestone and hollow concrete blockwork masonry in view of the variability of compressive strengths resulting from these masonry units even in the latter case where, even though manufactured in a controlled environment, large variations in the quality of hollow concrete blocks typically result between different manufacturers. The initial partial safety factor for materials of 3.0 was subsequently reduced to two-thirds of this value with reference to the Note to Clause 9.6(3) of Eurocode 8: Part 1 [4]. A final material safety factor of 2 was, therefore, specified with respect to all globigerina limestone and hollow concrete blockwork masonry in the numerical models analysed using 3Muri® in this research study.

Moreover, 3Muri® allows the user to specify the reduction factor to be applied to the stiffness of all masonry and concrete elements. In all numerical models analysed using 3Muri® for the study presented herein, a reduction factor of 2 (corresponding to half the elastic flexural and shear stiffness) was specified for all masonry and concrete elements in accordance with the recommended stiffness for cracked elements in numerical models given in Clause 4.3.1(7) of Eurocode 8: Part 1 [4].

In addition, 3Muri® allows the user to choose between two constitutive models for shear failure of masonry walls – the Mohr-Coulomb constitutive model and the Turnšek-Cacovic constitutive model where, the former considers a shear sliding failure while, the latter considers a shear failure governed by diagonal cracking, as represented in Figures 3-63 and 3-64.

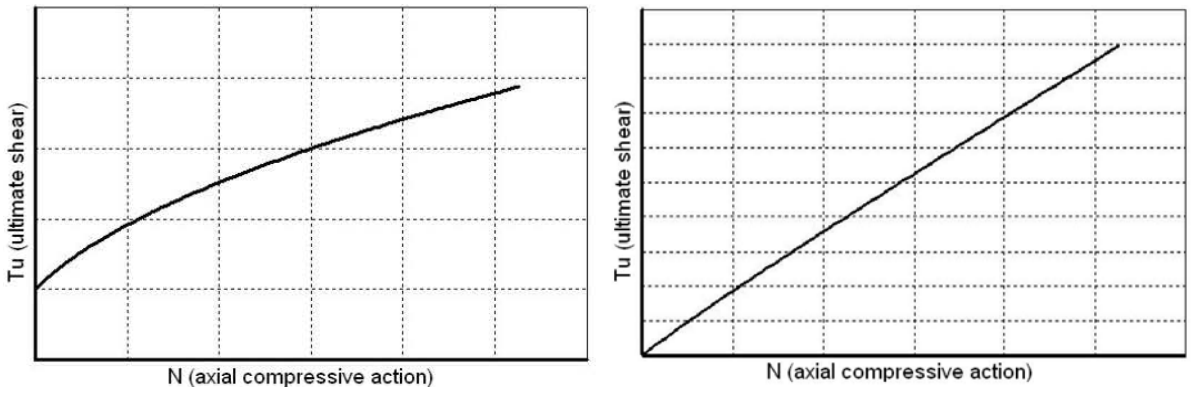

(a) Turnšek and Cacovic shear strength criterion (b) Mohr-Coulomb shear strength criterion

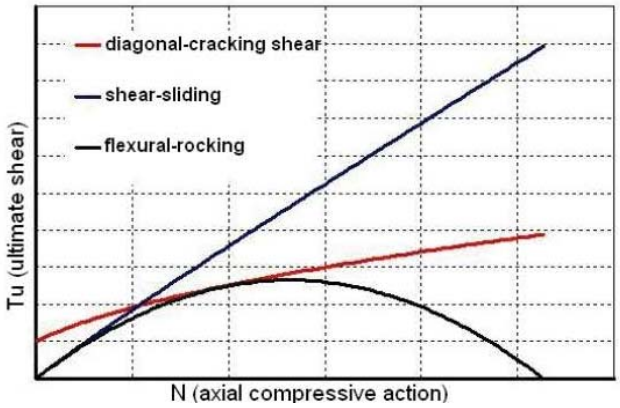

(c) Superimposition of strength criteria

Figure 3-63 Strength criteria considered in 3Muri®. Source: 3Muri® User Manual Release 11.4.0 ([179] p. 39, 40).

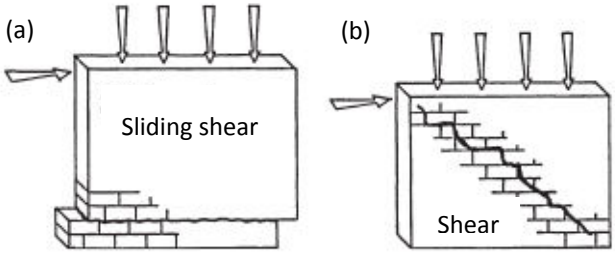

Figure 3-64 (a) Sliding shear failure and (b) diagonal shear failure in masonry walls. Source: Tomaževič [182].

Based on the comparison of experimental results and calculations, Tomaževič [182] concluded that the predominant shear failure mode in masonry structures is not sliding shear, as suggested in Clause 3.6.2 of Eurocode 6 [157], but diagonal shear failure. However, the investigations carried out by Tomaževič [182] considered a mortar grade of 5 N/mm^2 and 10 N/mm^2, while the same author commented on the occurrence of sliding shear in walls under seismic actions in cases when the walls are not heavily loaded and the mortar grade is low, adding that such a failure would typically occur in the upper portions of structures beneath rigid roofing systems, while diagonal shear failure was more likely to occur in the lower storeys. Hence, in the numerical models analysed using 3Muri® in the present study, since the consideration of both sliding and diagonal shear resistance, as suggested by Tomaževič [182]

for a conservative seismic assessment, could not be specified, in view of the presence of the thick gauge polyethylene sheeting at damp proof courses and the long distance between wall restraints (in corridors, open plan spaces and soft storeys), the Mohr-Coulomb shear failure criterion was, nonetheless, specified for all masonry walls.

In the case of the material properties of the steel reinforcement present in the reinforced concrete members, the characteristic yield strength of the steel reinforcement (f_{yk},) was considered to be 410 N/mm^2 in all numerical models analysed using 3Muri®, in accordance with the corresponding property used in all numerical models analysed using ELS®, in view of the date of construction of a large part of the building stock of the contemporary loadbearing URM building typology under study. Furthermore, the variation in shear strength of steel reinforcement was considered to be described by a normally distributed probability density function, where the value of the characteristic yield strength of steel reinforcement corresponds to a 5% fractile. Therefore, the characteristic yield strength of steel reinforcement can be evaluated from Equation 3-7 as follows:

$$f_{yk} \cong f_{ym} - 1.65\,\sigma_{fy}$$

Equation 3-7

where, f_{yk} is the characteristic yield strength of the steel reinforcement in N/mm^2; f_{ym} is the mean yield strength of steel reinforcement in N/mm^2; and σ_{fv} is the standard deviation of this normally distributed probability density function with respect to the variation in yield strength of steel reinforcement in N/mm^2.

Hence, a coefficient of variation (*C.O.V.*) of 0.06 (6%) was considered representative in the case of the probability density function describing the variation in yield strength of steel reinforcement, as indicated in Equation 3-8:

$$\frac{\sigma_{fy}}{f_{ym}} = c.o.v. \cong 0.06\ for\ steel\ reinforcement$$

Equation 3-8

where, *c.o.v.* is the coefficient of variation of the probability density function describing the variation in yield strength of steel reinforcement, while σ_{fy} and f_{ym} are as previously defined.

Therefore, the re-arrangement of Equation 3-8 and the substitution of the resulting term describing the standard deviation (σ_{fy}) in Equation 3-7, allowed the estimation of the mean yield strength of steel reinforcement through Equation 3-10.

$$f_{yk} \cong f_{ym} - 1.65(0.06\,f_{ym})$$

Equation 3-9

$$f_{yk} \cong 0.9\,f_{ym}$$

Equation 3-10

where, f_{yk} and f_{ym} are the characteristic yield strength of steel reinforcement and the mean yield strength of steel reinforcement, respectively, as previously defined.

Moreover, the same gravity loads were applied to the 3Muri® numerical models as discussed in Section 3.4.4 with respect to the numerical models analysed using ELS®.

3.5.4 Design seismic action and representation of geological conditions

In the non-linear static analysis carried out using 3Muri®, the numerical models are subjected first to the gravitational loads (static loading) and, subsequently, to a lateral load distribution where the magnitude of the applied lateral loads is increased at every substep by the same rate. Every pushover analysis in 3Muri® considers a total of 24 load distributions in accordance with the requirements of Clauses 4.3.3.4.2.2(1) and 4.3.3.4.2.2(2)P of Eurocode 8 [4]. The results of the non-linear static analysis are expressed in the form of a base shear versus displacement plot (called a pushover curve), which curve is a representation of the response of the structure to lateral loading based on the geometry of the structure and the material properties, irrespective of the magnitude of the design seismic action. The resistance of the structure in a particular earthquake scenario is assessed through the comparison of the maximum displacement exhibited by the structure during the non-linear static analysis corresponding to a particular limit state to the equivalent target displacement expected in the same structure under the design seismic action defined by the design peak ground acceleration (p.g.a.) on ground type A (Rock, in accordance with Table 3.1 of Eurocode 8: Part 1 [4]) and calculated through the horizontal elastic acceleration response spectrum. Similarly, the comparison of the maximum acceleration exhibited by the numerical model during the pushover analysis corresponding to a particular limit state with the equivalent maximum p.g.a. of the design seismic action for the same limit state, provides an indication of the adequacy of the resistance of the numerical model with respect to the applied seismic action. The 3Muri® Eurocode option allows the user to verfy the seismic resistance of the structure with respect to the three limt states considered in Eurocode 8: Part 3 [97] and defined in Clauses 2.1(1)P and 2.1(3)P of the same seismic code [97], namely, the limit states of Near Collapse, Significant Damage and Damage Limitation. The Note to Clause 2.1(1)P of Eurocode 8: Part 3 [97], while acknowledging some differences, states that the limit state of Significant Damage is approximately equivalent to the No Collapse Requirement defined in Clause 2.1(1)P of Eurocode 8: Part 1 [4] for new buildings. Hence, a maximum p.g.a. of 0.10g corresponding to the limit state of Significant Damage was considered in all numerical models analysed using 3Muri®, in accordance with the maximum p.g.a. derived for the Maltese Islands with respect to the No Collapse Requirement from SHARE 2013 European Seismic Hazard Model of the European Facilities for Earthquake Hazard and Risk (EFEHR) as described in Section 3.4.5 of this thesis. The maximum p.g.a. of the simulated ground motion record applied to all ELS® numerical models, was scaled to the same value.

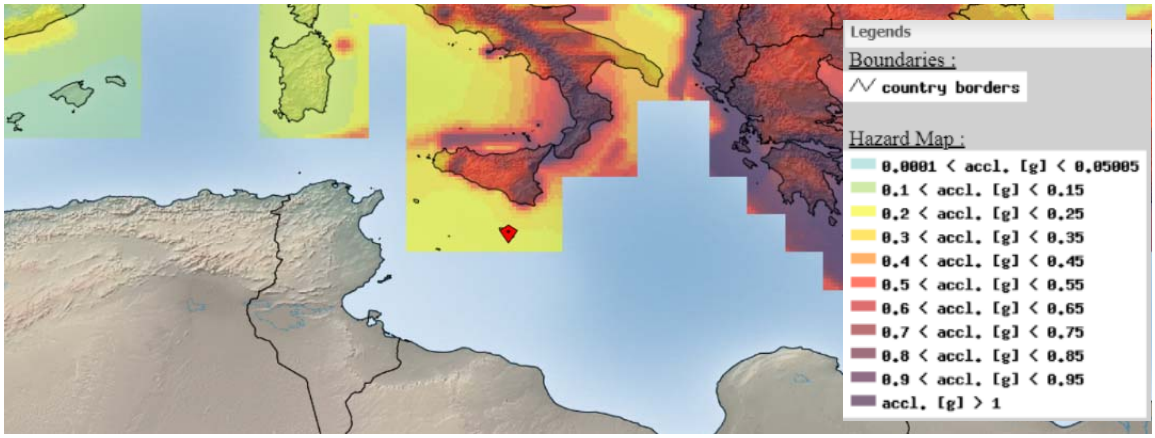

Figure 3-65 EFEHR SHARE 2013 European Hazard Model for a probability of exceedance of 2% in 50 years and a 95% fractile: zoomed on the Maltese Islands (http://www.efehr.org/en/hazard-data-access/hazard-maps/, downloaded on 18-06-2018).

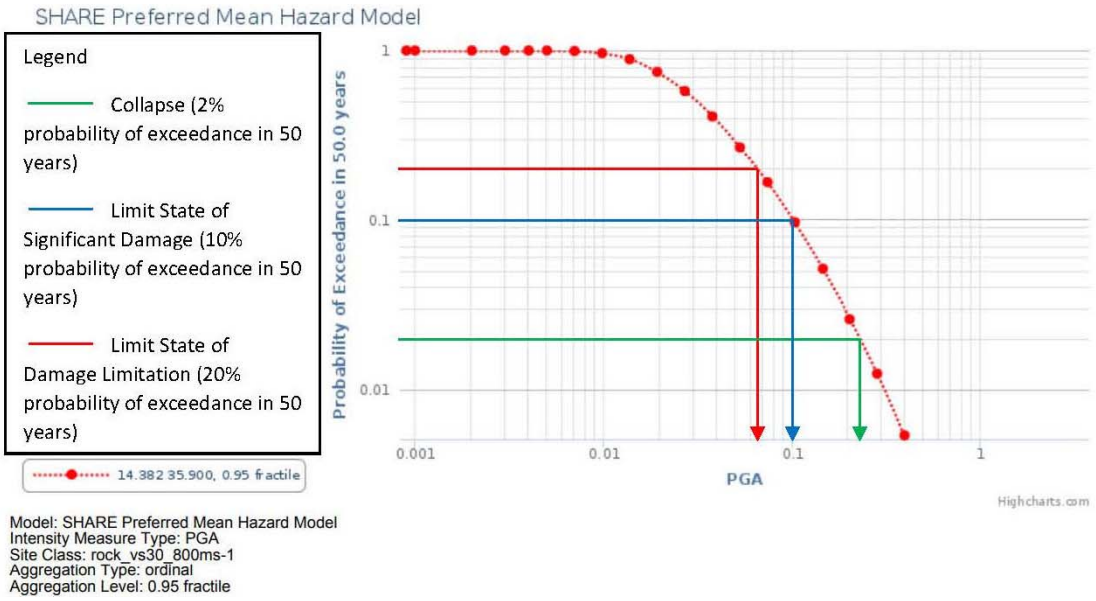

Figure 3-66 EFEHR hazard curve for the Maltese Islands for a 95% fractile indicating maximum p.g.a. corresponding to different limit states (http://www.efehr.org/en/hazard-data-access/hazard-curves/, downloaded on 18-06-2018).

The maximum p.g.a.'s for the Maltese Islands corresponding to the probability of exceedance of the limit state of Near Collapse and the limit state of Damage Limitation, for the definition of the design seismic action corresponding to these limit states in the numerical models analysed using 3Muri® were similarly derived with reference to the hazard map based on the SHARE 2013 European Seismic Hazard Model of the European Facilities for Earthquake Hazard and Risk (EFEHR) [183] and the EFEHR hazard curves for the Maltese Islands [184], reported in Figures 3-65 and 3-66, respectively. Therefore, with reference to the EFEHR hazard curve reproduced in Figure 3-66, for a 95% fractile, the maximum peak

ground accelerations on rock for the Maltese Islands associated with the three limit states and considered in all numerical models analysed using 3Muri® are as follows:

a) Limit state of Near Collapse: 0.24g;
b) Limit state of Significant damage: 0.1g;
c) Limit state of Damage Limitation: 0.067g.

Furthermore, the numerical models analysed using 3Muri® in this research study considered two main subsoil scenarios, namely ground formations consisting of upper coralline limestone or clay. While the material properties specified with respect to these two ground materials were the same as in the case of the corresponding materials specified in all the final numerical models analysed using ELS®, the influence of the ground material is only taken into consideration in 3Muri® through the specification of the periods T_B, T_C and T_D and the soil factor, S, corresponding to the elastic response spectrum, and in the calculation of the K-Winkler coefficient of subgrade reaction.

The simulated ground motion record applied as a design seismic action in all numerical models analysed using ELS® had a magnitude of 7.6, a hypocentral distance of 170.30 km and an epicentral distance of 139.91 km to the North-East of Malta. In all numerical analyses carried out using 3Muri®, a Type 1 elastic response spectrum was considered and the corresponding values of periods T_B, T_C and T_D and the soil factor, S, recommended in Table 3.2 of Eurocode 8: Part 1 [4] for ground types A (rock) and B (clay) were applied in the respective numerical models analysed using 3Muri®.

On the other hand, the K-Winkler coefficient of subgrade reaction (k_s) was estimated through the relationship proposed by Vesic (reproduced in this study in Equation 3-11), in view of the adequacy of this relationship to estimate contact pressure and soil settlement, as reported by Sadrekarimi and Akbarzad [185].

$$k_s = \frac{0.65.E_s}{B(1-\nu_s^2)} \sqrt[12]{\frac{E_s B^4}{EI}}$$

Equation 3-11

where, E_s is the Young's Modulus of the subsoil material in N/mm^2; ν_s is the Poisson's ratio of the subsoil material; B is the width of the foundation in mm; E is the Young's Modulus of the foundation in N/mm^2; and I is the moment of inertia of the foundation in mm^4. The foundation types and sizes on upper coralline limestone and clay subsoils considered in the numerical models analysed using 3Muri® in the present study correspond to the equivalent cases considered in the numerical models analysed using ELS®.

Table 3-9 Summary of K-Winkler coefficient for subgrade reaction corresponding to the wall types present in the numerical models analysed using 3Muri® in this research study.

Party walls (228 mm globigerina limestone)	On upper coralline limestone: no foundation (1 additional course of wall material)	K-Winkler coefficient of subgrade reaction for UCL = 18,982.9 daN/cm^3		
	On clay: 500 mm thick raft foundation		Foundation projects on one side of wall only	K-Winkler coefficient of subgrade reaction for clay = 20.951 daN/cm^3
			Foundation projects on both sides of wall	K-Winkler coefficient of subgrade reaction for clay = 14.785 daN/cm^3
228 mm HCB walls	On upper coralline limestone: no foundation (1 additional course of wall material)	K-Winkler coefficient of subgrade reaction for UCL = 18,791.1 daN/cm^3		
	On clay: 500 mm thick raft foundation		Foundation projects on one side of wall only	K-Winkler coefficient of subgrade reaction for clay = 21.537 daN/cm^3
			Foundation projects on both sides of wall	K-Winkler coefficient of subgrade reaction for clay = 15.264 daN/cm^3
153 mm HCB walls	On upper coralline limestone: no foundation (1 additional course of wall material)	K-Winkler coefficient of subgrade reaction for UCL = 24,735.9 daN/cm^3		
	On clay: 500 mm thick raft foundation		Foundation projects on both sides of wall.	K-Winkler coefficient of subgrade reaction for clay = 15.994 daN/cm^3
Front façade double wall modelled as equivalent 306mm thick HCB wall	On upper coralline limestone: no foundation (1 additional course of wall material)	K-Winkler coefficient of subgrade reaction for UCL = 15,582.8 daN/cm^3		
	On clay: 500 mm thick raft foundation		Foundation projects on one side of wall only	K-Winkler coefficient of subgrade reaction for clay = 20.305 daN/cm^3
			Foundation projects on both sides of wall	K-Winkler coefficient of subgrade reaction for clay = 14.719 daN/cm^3

The K-Winkler coefficients for subgrade reaction calculated through the relationship proposed by Vesic for the wall types considered in the numerical models analysed using 3Muri® are summarised in Table 3-9. In the case of numerical models analysed on upper coralline limestone, the considered foundation consisted only of an additional course of the respective wall material. On the other hand, numerical

models analysed on clay were considered to have a 500 mm thick concrete raft foundation over the whole area of the masonry building, which did not project outwards from the footprint of the structure. The width of the foundation beneath the respective walls considered for the evaluation of the moment of inertia of the foundation in the case of a raft foundation on clay, was considered as the width resulting from the wall thickness and a 45 degree dispersion through the foundation. Furthermore, the length of the foundation was considered as 1,000 mm in the case of globigerina limestone (solid) masonry walls, whereas, in the case of the hollow concrete blockwork walls the equivalent length of foundation corresponding to a 1,000 mm length of wall, with the same overall thickness, was calculated in order to take into account the presence of voids.

3.5.5 Final set of numerical models analysed using 3Muri®

The final set of numerical models analysed using 3Muri® in this research study included the control numerical models, and the control numerical models with either a soft storey at semi-basement level, setbacks at penthouse level or a double height space between Levels 0 and 1 on an upper coralline limestone and a clay subsoil, respectively, for plan layouts, which included only minor variations when compared to the corresponding numerical models analysed using ELS®. These numerical models were analysed starting from a height of six storeys, and for the addition and/or reduction of one storey at a time until an adequate seismic resistance was achieved with respect to the limit states of Near Collapse and Significant Damage. The minimum and maximum resulting building heights of the analysed structures were one and fifteen storeys, respectively, including the basement level. Furthermore, the six-storey existing Xemxija Building Number 0011 was also modelled using 3Muri® on upper coralline limestone and clay, respectively.

Moreover, four additional cases were investigated using 3Muri®, which were not modelled using ELS®. The first additional case consists of the control numerical model with a double height space between Levels 0 and 1 and with a wider void at slab Level 1, which spans over the entire width of the structure between the longitudinal party walls. This case was investigated on an upper coralline subsoil only. The seismic response of numerical models with extended plan length-to-width proportions of 4:1 were also investigated in the case of the control numerical models and numerical models including a soft storey at the lowest level or a double height space (with the original size of void) between Levels 0 and 1, on an upper coralline limestone and a clay subsoil, respectively.

3.6 Conclusion

The work carried out in this study, presented in the foregoing sections, includes a progressive sequence of investigations with the aim of evaluating the seismic vulnerability of the contemporary loadbearing URM building typology in the Maltese Islands, and the variation of this vulnerability to seismic excitations with changes in the overall building height, the presence of different ground formation scenarios and ground modelling techniques, and in the presence of a number of construction characteristics, commonly present in this building typology. The adequacy of the non-linear static analysis carried out using the software program 3Muri® for the seismic assessment of the URM building typology under study was also investigated.

The study started off with an extensive review of the building characteristics, which are typically found in the local masonry construction typology under investigation, and which could alter its seismic response, the review of existing seismic vulnerability assessment methods for masonry structures and the development of a preliminary assessment form for the seismic vulnerability evaluation of this typology and its corresponding rating system, based on results of previous local studies, and the relative weightings attributed to particular characteristics in existing assessment methods. The comparisons of the final seismic vulnerability outcomes, and the seismic vulnerability ratings resulting from the main sections of the New Form (when it was applied for the evaluation of 183 buildings located in the Test Sites of Xemxija in Malta, and Nadur in Gozo) to the ratings obtained through a GNDT second level assessment [26], and a FEMA 154 (second edition) [27] evaluation of the same buildings, gave a satisfactory degree of confidence in the validity of the developed rating system for the New Form. On the other hand, the comparison of the seismic vulnerability ratings resulting from the use of the New Form to those obtained from a GNDT second level assessment [26], and an extended GNDT second level assessment (which includes five additional parameters proposed by Formisano et al. [28] [29] [30] [31], which attempt to take into account the influence of the 'aggregate effect' in the evaluation of the seismic vulnerability rating), suggested that the proposed rating system for the New Form was more conservative and it might not reflect enough the potential alteration in building resistance resulting from its location within an aggregate. The statistical analysis of the 183 building surveys allowed the identification of the eleven most significant predictors of the final seismic vulnerability rating out of a total of 143 parameters from the New Form. If the limitations posed by the building characteristics present in the considered sample are taken into account, the eleven significant predictors appear to be in overall agreement with the characteristics identified as having a major bearing on the final rating, in the developed rating system for the New Form.

The results of these studies provided the background for the identification of the six characteristics, which were investigated through the non-linear time-history dynamic analysis of numerical models, for the study of the influence, which these characteristics have on the seismic response and the variation in the dynamic properties of the building typology under study. While a number of assumptions were made, and simplified modelling techniques were devised and applied in the numerical analyses carried out, the validation studies carried out suggest that the analysed numerical models represent moderately well real-life construction scenarios. Furthermore, while the results obtained cannot be generalised because of the alteration of a number of properties, and the consideration of a single simulated seismic event, nonetheless these results, which are evaluated in detail in Chapter 4 of this study, provide significant indications on the relative influence of the investigated characteristics upon the seismic response of the building typology under study and, hence, on its corresponding seismic vulnerability.

Furthermore, the comparison of the response parameters resulting from the non-linear static analyses carried out using 3Muri® to those of the corresponding non-linear dynamic analyses carried out using ELS® (discussed in Chapter 5), gives some insight into the adequacy of a pushover analysis, which assumes (by default) a box-like behaviour of the analysed structures, in the case of the URM building

typology under study, where the actual spatial and construction characteristics typically present do not guarantee such box-like behaviour. In addition, the non-linear static analysis results obtained from the numerical models analysed using 3Muri®, give further information about the variation in structural ductility demand of the numerical models in the presence of the investigated building characteristics.

The above provide an important background to future studies in this research area.

Chapter 4 ELS® NUMERICAL ANALYSIS: EXAMINATION OF RESULTS AND DISCUSSION

4.1 Background and Scope

The actual influence, which the main characteristics considered in the developed rating system for the New Form have on the seismic performance on the building typology under investigation, could not be confirmed through on site assessments of the building stock or databases of damages resulting from past earthquakes, as was done in a number of international studies, such as the study by Benedetti and Petrini [70], which formed the basis of the GNDT second level assessment method [26]. Hence, in the present study, the relative influence, which the main building parameters identified in the developed rating system for the New Form have on the structural response of the contemporary loadbearing masonry building typology, was investigated through the non-linear dynamic analysis of numerical models using the software package ELS®, which is based on the Applied Element Method and is, hence, capable of predicting the structural response throughout a seismic event up to a state of progressive collapse. The main parameters investigated were:

i. the influence of the type of ground formations present and the different modelling techniques for the modelling of the ground ;
ii. the presence of a soft storey at semi-basement level;
iii. the presence of setbacks at penthouse level (having dimensions as stipulated by the planning regulations which were in force in the Maltese Islands until November 2015);
iv. the presence of a double height space between Levels 0 and 1;
v. the presence of two or three identical buildings acting in combination through the sharing of their party walls;
vi. the variation in the building response in the presence of parameters i-v above with a reduction in number of storeys, starting from a height of six floors until a height was reached were the respective models resisted collapse.

Plan layouts corresponding to the cases investigated through numerical modelling in this study are presented in Figures 20 to 32 of Appendix C.

The results reported and discussed in the ensuing Sections with respect to the influence of 6 different ground formations and the different modelling techniques for the representation of the ground were

presented by the author during the 36th General Assembly of the European Seismological Commission in Malta in September 2018. The submitted abstract is included as Document (v) in Appendix B [186].

4.2 Outline of Data Extracted from the Analysed Models and Background to the Discussion of the Results

A total of 50 numerical models[10]were analysed using ELS® under the effect of the simulated ground motion record of a Magnitude 7.6 earthquake with a hypocentral distance of 170.3 km and with an epicentral distance at 139.91 km to the North-East of Malta, which was obtained from the database of the Seismic Monitoring and Research Unit of the University of Malta. The main output from these 50 models includes:

a) accelerations in the x-, y- and z-directions at a minimum of four positions[11] throughout all the numerical models (namely, the middle of the lower ground formation layer, the middle of the upper ground formation layer, or the full thickness of the 1.5 m thick upper coralline limestone layer (UCL), whenever this was the upper formation layer in the numerical model, at first course and at slab over semi-basement level);

b) displacements in the x-, y-, and z-directions under static and dynamic loads at a minimum of eight positions[12] (namely, at the four positions mentioned in (a) above in addition to slab over Level 0, slab over Level 1, penthouse floor and slab over penthouse level as indicated in Figures 4-1 and 4-2) throughout the 50 models;

c) the predominant frequencies in the acceleration spectrum at the four positions mentioned in (a) above for all the numerical models, in order to obtain an indication with respect to the occurrence of resonance effects;

d) the fundamental frequencies in the x-x and y-y plan orientations of the analysed numerical models after the application of the gravity loads and at the end of the dynamic loading.

[10] Table 30 in Appendix D includes the list of numerical models and the description of the seismic vulnerability characteristics, the number of storeys and the ground formation layers considered in every case.

[11] In the six-storey control numerical models, accelerations in the x-, y- and z-directions were also extracted for the bottom-most and the top-most elements of every ground formation layer present in addition to the positions mentioned in the text.

[12] In the six-storey control numerical models, displacements in the x-, y- and z-directions were also recorded for the bottom-most and the top-most elements of every ground formation layer present. In the case of the six-storey control numerical model analysed on 30 m thick rock (Model 42v2), displacements in the course positioned directly below and directly above the damp proof membrane were also documented.

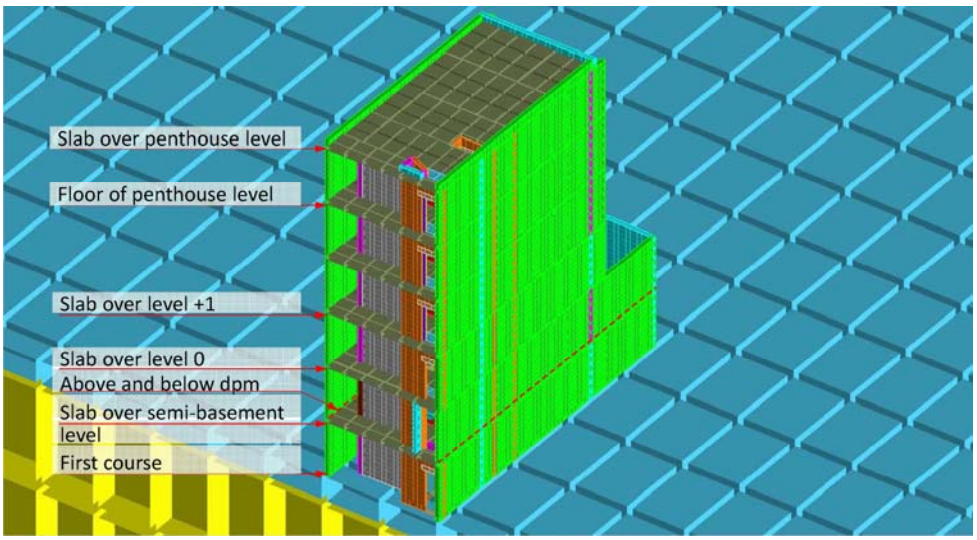

Figure 4-1 Positions throughout building height at which data was extracted from the numerical models.

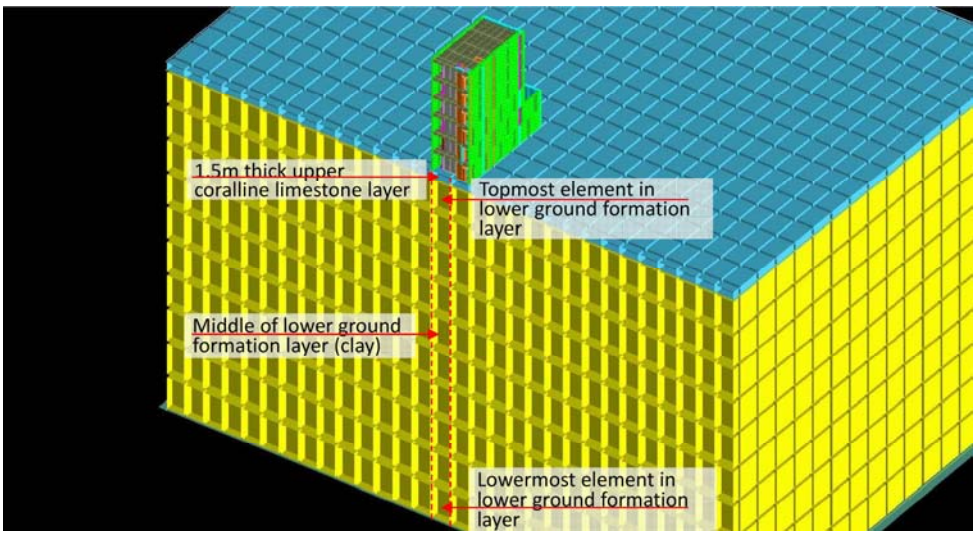

Figure 4-2 Positions throughout the thickness of the ground formation layers at which data was extracted from the numerical models.

Data was extracted from all numerical models from corresponding elements in the left hand side party wall along, a transverse section through the model located at 7.5 m from the foremost point in the model (the outer face of the outer wall positioned in the x-x orientation and supporting the entrance steps to Level 0). The position of this transverse section in the apartment levels is located in the front room, at around 1.13 m from the outer face of the central stairwell wall and is indicated as Section AA in Figures 20 to 32 in Appendix C, which consist of the plan layouts corresponding to the investigated cases. The positions at which data was extracted from the numerical models were described as 'slab levels' in this thesis. However, this description was used in order to simplify the reference, since an accurate description would have been too long to be used repeatedly in the text. The exact position of the elements considered was the first course directly beneath the respective slab levels quoted. The main reason for the extraction of data at these positions, and not exactly at the slab levels, was to ensure that data was recorded in the exact equivalent elements at all levels in the corresponding models, in view of the following limitations if the elements in the party wall, directly abutting the slab edges had been used instead:

i. in general, the extents of slabs adjacent to party walls were modelled to bear on half the thickness of the party walls, therefore, allowing space for a masonry block having a width of half the wall thickness to be placed in the party wall directly abutting the edge of the slabs in the case of single building models. However, in the cases where a soft storey was included at slab over semi-basement level, the slab at this level, which was modelled as a precast prestressed hollow core concrete slab with a reinforced cast in-situ concrete topping, was extended over the whole thickness of the party wall, therefore, leaving no space for the masonry 'half-block' to fit;
ii. the masonry 'half-blocks' would not be present in the party walls at the levels of the slabs in the case of a shared party wall in the two-building and the three-building models investigated.

Since the seismic accelerations were applied in the transverse direction (positive x-direction), which is the weaker direction of all the numerical modelled buildings, only the displacements and accelerations extracted for this orientation were considered in this study, when investigating the behaviour of the models prior to and at the start of failure. The occurrence of complete collapse, on the other hand, was identified through the displacements in the z-direction. Blocks can continue rolling on the ground, or on the debris, even after collapse would have occurred. Hence, the time of collapse was not clearly identifiable from the x-displacement – time plots. On the other hand, in the case of displacement in the z-direction, even though blocks could bounce, or roll lower down a debris pile following the initial impact, the time of the initial impact is generally clearly identifiable from the z-displacement – time plots, therefore, allowing a more accurate estimate of collapse duration to be obtained. The extracted displacements and accelerations were processed to yield the following information:

i. the analysis run time (and frame number) at which the onset of failure was identified at slab over semi-basement level;
ii. the collapse duration;
iii. the maximum acceleration in the x-direction at a minimum of four positions in the numerical model (as listed in (a) above) prior to the start of failure at slab over semi-basement level, the analysis run time (and frame number) when this maximum acceleration occurred, and the ratio of this maximum acceleration to the maximum input peak ground acceleration for the same analysis interval;
iv. the comparison of the magnitude of the relative displacement in the x-direction, at the start of failure, in every numerical model with additional seismic vulnerability characteristics, to

every corresponding[13] numerical model which includes additional seismic vulnerability characteristics, and to the corresponding control numerical models, readings taken at slab over semi-basement level;

v. the comparison of the magnitude of the relative x-displacement at slab over semi-basement level, in every numerical model with additional seismic vulnerability characteristics, to the corresponding control model, readings taken at the analysis run time of the start of failure at slab over semi-basement level of the corresponding control numerical model;

vi. the x-displacement at the onset of failure, at the six positions throughout the height of the numerical models indicated in Figure 4-1, together with the corresponding analysis run time and frame number at which the start of failure is identified for every respective position;

vii. the x-displacement in the middle of the lower ground formation layer and the middle of the upper ground formation layer (or the whole thickness of the 1.5 m thick upper coralline limestone layer in the thin rock on clay ground cases), at the time of the start of failure at slab over semi-basement level of the same numerical model;

viii. the maximum x-displacement at the six positions throughout the height of the numerical models indicated in Figure 4-1, during the dynamic loading stage, prior to the onset of failure at every respective position;

ix. the relative x-displacement at the six positions throughout the height of the numerical models indicated in Figure 4-1, at the time of maximum x-displacement at slab over semi-basement level, during the dynamic stage before the start of collapse at this position;

x. the identification of differences in the collapse modes of the numerical models from a study of the displacement–time behaviour of the modelled buildings during the static and dynamic loading stages prior to start of collapse, together with the deflected shape of the buildings at the time of maximum x-displacement at semi-basement level before the onset of failure.

All investigated cases in this study started with the analysis of a six-storey numerical model, which was re-analysed with a reduction in height of one storey at a time, until the numerical model resisted collapse. This resulted in a maximum height of six storeys and a minimum height of three storeys in the analysed numerical models. Therefore, the relative positions above first course of the slab over the penthouse level, the floor of the penthouse and slab Level 1, vary in numerical models of different heights; whereas the slab over Level 0 varies between being an intermediate floor slab or the

[13] The term 'corresponding' numerical model is hereby being used to mean a numerical model with the same number of storeys and modelled on the same ground formation layers. Therefore, a comparison of the relative x-displacements at the onset of failure at slab over semi-basement level between numerical models, which include different seismic vulnerability characteristics but have the same total number of storeys and are modelled on the same ground formation layers, was carried out. These relative x-displacements are also compared to the relative x-displacement at slab over semi-basement level at the start of failure in the corresponding control numerical model.

penthouse roof slab in the three-storey cases, hence, resulting in different loading conditions and slab thicknesses. On the other hand, the position above first course of the slab over semi-basement level is constant in all the analysed numerical models. In addition, the slab over semi-basement level is always an intermediate slab and is positioned directly above the soft storey and directly below the double height space. Therefore, the displacements at this position are directly affected by the presence of such characteristics, when present. Hence, in this thesis, except in cases (vi) and (viii) above, where the displacement was recorded at the start of failure or prior to the start of failure, respectively, at the six positions in the numerical model, comparisons at the time of the start of failure between different numerical models always refer to the start of failure at slab over semi-basement level. This was done in order to ensure that the start of failure at exactly the same position in the numerical models was considered in all comparisons.

A further 91 numerical models were analysed in order to investigate the effect which the number of storeys, the type of ground formation, and the additional seismic characteristics studied, have on the variation of the natural frequency of the building throughout the static and dynamic loading stages, and in order to obtain an indication of the degree of damage suffered by the buildings, which resisted collapse. The natural frequency, in the transverse and the longitudinal direction of the analysed numerical models which resisted collapse, was determined at the end of the static (corresponding to the application of the gravitational loads) and dynamic (corresponding to the application of the simulated ground motion record) stages for two ground formation cases, namely for ground modelled as upper coralline limestone at Minimum Z, and for ground modelled as clay at Minimum Z. On the other hand, only the natural frequency in the transverse and the longitudinal directions of the numerical models at the end of the static loading stage for the two cases of ground formations, was considered in the analysed numerical models which resulted in collapse.

The discussion of results which ensues reviews the variation in the results obtained, and attempts to suggest possible reasons for such variations based on observations by the author of this thesis as well as published literature. The results obtained for the natural frequencies of the analysed numerical models, and the predominant frequencies in the acceleration spectrum, at the four positions described in (a) and (c) above, are discussed first, since these results are then referred to in the interpretation of the variation in the acceleration and displacement results. In every case, when applicable, the variation in the behaviour of the control numerical models was first evaluated, in order to assess the effect, which the different ground formations and modelling methods have on the seismic resistance of the building; following which, the behaviours of the numerical models, which include the additional seismic vulnerability characteristics, were compared to each other and to the corresponding control numerical model. Excerpts of the results were reproduced in the relevant sections of this text where they were discussed, however the main results can be found in Appendix D. In cases where results of the variation in structural response parameters with reduction in number of storeys were included in the form of plots in the following sections, the sequence of the number of storeys reproduced in the abscissa of these plots follows that of the analysed numerical models (in descending order of number

of floors: six storeys – five storeys – four storeys – three storeys) in order to facilitate the interpretation of results between the discussion presented in the text and the corresponding plots.

4.2.1 Natural frequency estimates

The main dynamic properties of structures, which influence behaviour under seismic loads, are the stiffness, the mass and the damping. The natural frequency of a structure is the frequency at which it will vibrate if set into motion, and can be estimated for a single degree of freedom system from the relationship [187] presented in Equation 4-1, which indicates that the natural frequency of a structure is directly proportional to its stiffness.

$$f_n = \frac{1}{2\pi}\sqrt{\frac{k}{m}}$$

Equation 4-1

where f_n is the frequency of the system in the nth mode of vibration in Hertz (Hz), k is its sway stiffness in N/m and m its mass in kg.

As explained by Trifunac et al. [188], the 'pure' natural frequency of a structure should be obtained by modelling the structure on an infinitely stiff ground, where movements at the building's supports are restrained in all directions. This would result in a significantly higher natural frequency than the fundamental frequency of the same structure erected on a ground which is less stiff and would, hence, exhibit some additional degree of flexibility in the restraint provided at the base of the structure. The building would act as one 'system', together with its foundations and the underlying ground. However, in this study, the natural frequency was estimated in order to obtain an insight into the behaviour of the analysed numerical models on different ground formations, with variations in the number of storeys, and in the presence of particular seismic vulnerability characteristics. Since none of the six ground formation cases modelled could be classified as having an infinite stiffness, natural frequency estimates, for use in the interpretation of the acceleration and displacement results extracted from the analysed numerical models, had to represent the particular ground types which were present in the modelled cases.

The behaviour of the control numerical models under dynamic excitation in terms of the number of storeys for collapse resistance, the time of start of failure at slab over semi-basement level and the collapse duration, for the six different geologies representing the ground formation layers investigated, which will be discussed in the subsequent sections of this chapter, suggested that the modelling of the ground formations considered in this study could be broadly classified into 'rock'

cases[14] and 'clay' cases[15]. Hence, in the analysis of numerical models for the estimation of natural frequency in the first two eigen modes (the fundamental frequencies in the transverse and longitudinal directions of every model), the ground was specified as either upper coralline limestone or clay set at the respective numerical model's Minimum Z position. This choice of modelling, as opposed to the modelling of ground formation layers as three-dimensional blocks, ensured that the resulting values of natural frequency corresponded to the modelled building (from first course upwards), and were not altered by the arbitrary proportions of the three-dimensional blocks adopted for the modelling of the ground formation layers, while still exhibiting the effects of the different ground types on the natural frequency of the modelled buildings.

Since this study involved ground types, which differed significantly in stiffness and mass, the transmission of earthquake vibrations from these ground types to the overlying structures would inevitably be different. Hence, all analysed models were investigated under both generalised cases of ground formations considered in order to study the effect which different ground formations have on the dynamic properties of such buildings. However, whenever reference was made in this thesis to the natural frequency results, as an indication of the relative stiffness of the models, and/ or in order to get an indication of the possibility of occurrence of resonance, only the results corresponding to the equivalent ground case of the model under assessment were quoted.

It is acknowledged that the approximation of the different ground formation cases to 'upper coralline limestone' or 'clay at Minimum Z', where the properties of upper coralline limestone and clay are left constant for all the cases, may have introduced a marginal degree of inaccuracy in the values of natural frequency quoted for numerical models analysed under dynamic loads, where more than one ground formation layer was present. The full extent of the effect, which soil-structure interaction has on the natural frequency of a building, might not have been accurately represented, in particular, in the case of numerical models, where the ground consisted of 30 m thick upper coralline limestone on 30 m thick clay (approximated as upper coralline limestone at Minimum Z for natural frequency analyses) and, to a lesser degree, in view of the considerably lower thickness of the upper ground layer when compared to the lower ground layer, in the cases where the ground formation consisted of 1.5 m thick upper coralline limestone on 60 m thick clay (analysed as clay at Minimum Z for natural frequency analyses). The actual values of natural frequencies of such cases would likely lie between the values

[14] The 'rock' cases include: a single 30 m thick upper coralline limestone layer, modelled as a three-dimensional element; upper coralline limestone specified at the numerical model's Minimum Z position; and a 30 m thick upper coralline limestone layer overlying a 30 m thick clay layer, both layers modelled as three-dimensional blocks.

[15] The 'clay' cases include: 1.5 m thick upper coralline limestone on 60 m thick clay, both modelled as three-dimensional blocks; a single 60 m thick clay layer modelled as a three-dimensional block; and clay specified at the numerical model's Minimum Z position.

obtained from the rock at Minimum Z and the clay at Minimum Z analyses, with the values being closer to one of the two cases depending on the most predominant material in the modelled ground geology. This is suggested also from a study of the maximum accelerations at the first course in the semi-basement level prior to the start of failure at slab over semi-basement level, which are summarized in Table 39 of Appendix D. Model 44v2 (6-storey control numerical model on 30 m thick upper coralline limestone over 30 m thick clay) resulted in the highest maximum x-acceleration at the first course in the semi-basement level, when compared to the other five 6-storey control numerical models investigated. Even though Model 44v2 is being considered as a 'rock case' in this study, in view of the high thickness of the rock layer, and since its resistance to collapse at five floors corresponds to the resistance of the other rock cases, a more exact natural frequency value for this model (under static loads only) in the transverse direction is likely to lie between that of the equivalent numerical model analysed on upper coralline limestone at Minimum Z (3.882 Hz) and that of the corresponding case analysed on clay at Minimum Z (2.623 Hz). In the latter case, the close proximity of the natural frequency of the numerical model to the predominant frequency range of the input ground accelerations[16] (as reported in Table 34 of Appendix D) suggests that the high maximum x-acceleration at the first course in the semi-basement level could be partly attributed to resonance effects. The complex interaction between ground and building vibrations, however, cannot rule out that such amplification of accelerations might be the result of a complex process of re-transmission of vibrations between the building, the upper and the lower ground formation layers present, or the higher inertia of the building and the upper coralline layer over the clay layer. In view of time limitations, an investigation of the effect of the variation in the material properties of upper coralline limestone and clay, when specified as materials at Minimum Z, to represent better the effect of multiple ground formation layers, was not possible. Furthermore, the resistance to collapse of all single building control 'rock case' numerical models at five floors, and the single building control numerical model cases on 1.5 m thick upper coralline limestone on 60 m thick clay, and the single 60 m thick clay layer, at three floors, suggested that the approximation of using the same upper coralline limestone and clay properties for all respective cases, in the numerical analyses carried out for the determination of natural frequency, was acceptable.

4.2.1.1 Natural frequency comparisons under static and dynamic loading

In all the numerical models developed for this study, 100 load increments were specified for all the static loads. Therefore, the static loading stage resulted in analysis frames 1 to 101. Eight step divisions were specified in the case of the input ground motion accelerations which had a time step of 0.08 s, and were applied in the x-(transverse) orientation of the analysed structures. The dynamic loading

[16] Energy content of input ground motion lies mainly between frequencies of 0.8 Hz and 2.95 Hz in the acceleration spectrum, with an additional predominant frequency in the vicinity of 6 Hz.

stage, hence, includes analysis frames 102 to 949. Plots of angular frequency versus frame number were extracted following the analysis of the models for two eigen modes, from which the natural frequency was obtained for both modes from the following relationship:

$$\omega = 2\pi f$$

Equation 4-2

where, ω is the angular frequency in radians per second (rad/s) and f is the frequency in Hertz (Hz). The shape of the angular frequency versus frame number plot, for the static loading stage, typically consisted of a sharp drop between frame numbers 1 to 8, followed by a straight line or a shallow curve with an overall negative gradient as seen in Figure 4-3. In the majority of the numerical models analysed on upper coralline limestone on Minimum Z, and in a number of models analysed on clay at Minimum Z, a marginal degree of oscillation was noted in the plots between frames 8 and 101, whereas a more pronounced oscillation over the same analysis time was observed in the models which resisted collapse, when ground was specified as clay at Minimum Z as shown in Figure 4-4. This oscillatory pattern during the static loading stage could be due to issues related to numerical convergence.

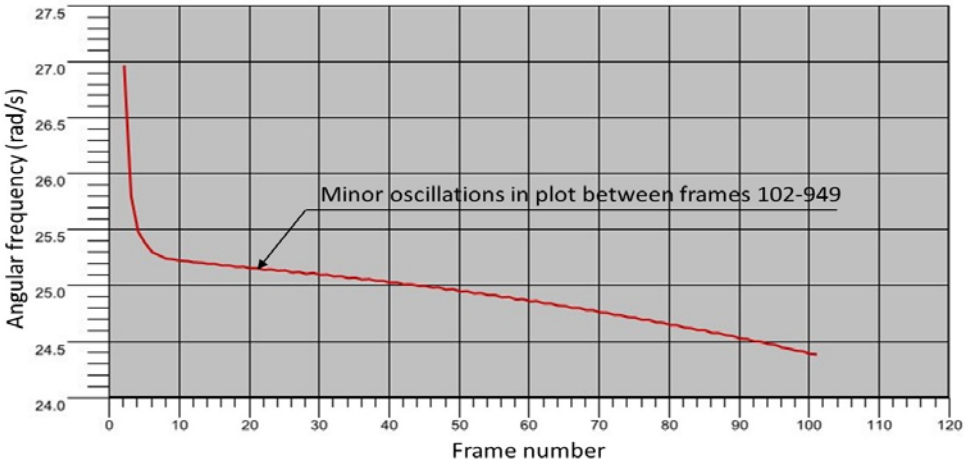

Figure 4-3 Plot of angular frequency versus frame number in the transverse direction of the 6-storey single building control numerical model analysed on upper coralline limestone at Minimum Z for the static loading stage only.

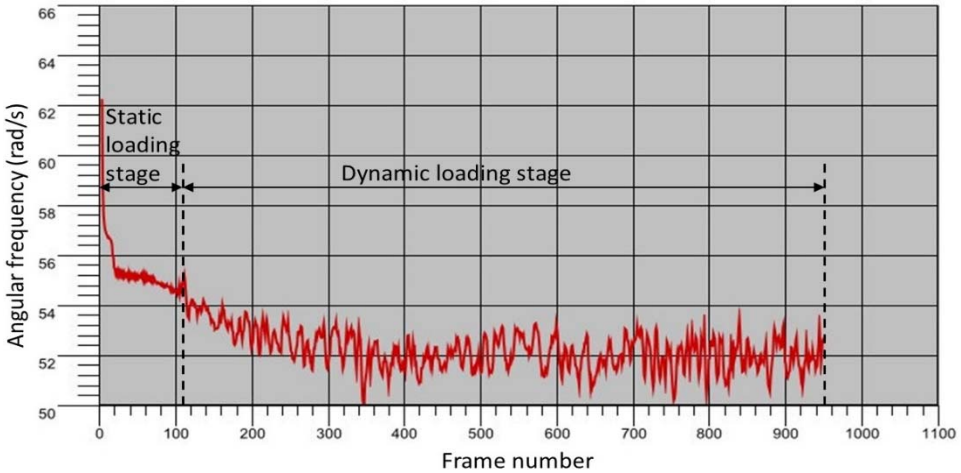

Figure 4-4 Plot of angular frequency versus frame number in the longitudinal direction of the 3-storey single building control numerical model analysed on clay at Minimum Z for both static and dynamic loading stages.

A marked zigzag pattern, as seen in Figure 4-4, was obtained during the dynamic loading stage (frames 102-949) in all numerical models which resisted collapse, irrespective of the ground material specified at Minimum Z. The natural frequency of the building under static loading was obtained at the end of the application of the static load (frame 101), whereas, in view of the oscillatory nature of the angular frequency versus frame number plot, during the dynamic loading stage, the natural frequency at the end of this stage was based on the average between the values of angular frequency given in the plot for the last peak and the last trough.

The pronounced zigzag pattern of the angular frequency versus the frame number plots, for the numerical models which resisted collapse, tends to indicate that, under the effect of seismic actions, the modelled structure is oscillating about a mean frequency which is gradually decreasing. In view of the oscillatory nature of seismic excitations, the modelled building is first caused to displace in one direction, hence, forming tensile cracks due its displaced profile, then, immediately afterwards, the building is displaced in the opposite direction. The joints, which would have been stressed, but which would have not yet failed, therefore close again, whereas new joints become highly stressed, some of which, fail in tension. This behaviour continues throughout the duration of the seismic ground motion and leads to a progressive degradation of the stiffness of the building through the formation of cracks. Therefore, even though the structure would have resisted collapse, the decrease in natural frequency indicates a decrease in stiffness, which probably results from the formation of cracks. Furthermore, during the oscillation of the structure under seismic actions, the deflected shape of the building results in a temporary increase in the building stiffness, which could explain the peaks in natural frequency in this part of the analysis.

In ELS®, cracks form when the separation strain of the normal and shear springs, which were present at the element-element interface, is exceeded, therefore, leading to the failure of these springs. If the elements come in contact again, these springs do not re-form, but, in the case of the dynamic stage only, contact springs form, meaning that the two elements are then just in contact, and friction is present between their respective surfaces. In ELS®, whenever elements are forced to move away from each other, therefore, causing the springs at their interface to be in tension, the colour of the springs changes to yellow. Once the springs crack, they are no longer present and, hence, do not remain visible. In view of the large scale of the analysed numerical models and the relatively small scale of the masonry blocks forming the walls, the colour change at the stressed springs is only marginally visible in the closer areas of the numerical model, and with some difficulty. Hence, the difference between the natural frequency at the end of the static loading stage, and that resulting following the dynamic loading stage, in the numerical models which resisted collapse, was studied in order to gain insight into the degree of damage sustained by the different modelled cases under investigation.

A similar reduction in natural frequency was identified in the Millikan Library building at the California Institute of Technology during the February 9, 1971, Magnitude 6.4 San Fernando earthquake [43]. When compared to natural period results obtained for the building, from induced vibration tests carried out prior to the earthquake, the natural period in the north-south orientation of the building

during the 1971 earthquake exhibited an increase from 0.51 to 0.62 seconds, and in the east-west direction from 0.66 to 0.98 seconds. Damping ratios also increased from between 1.2% and 1.8% to 6.4% in the north-south orientation and from between 0.4% and 1.5% to 7% in the east-west orientation. Even though no damage to the structure was reported after the earthquake, except for some minor damage to the plastering, Chopra [43] attributes the increase in natural period, and in damping, to structural deterioration and hence, the consequent loss of stiffness.

Calvi et al. [44] reviewed a number of studies which investigated the change in natural frequency and fundamental period of reinforced concrete structures before and after the occurrence of an earthquake through either recordings of the buildings' response, or through experimental and/ or analytical studies. In all cases, an increase in fundamental period, and hence, a reduction in natural frequency were noted, which effects were attributed to the degree of damage suffered by the investigated structures. A similar frequency shift was also obtained by Mucciarelli et al. [45], which study was also mentioned by Calvi et al. [44]. Mucciarelli et al. [45] investigated the reduction in frequency of a four-storey reinforced concrete building during the Magnitude 5.3 earthquake which hit the Italian town of Bonefro in the Molise region on the 1st November 2002, and which followed one day after another seismic occurrence of a similar magnitude. Ambient vibration readings of the already damaged building, which were in progress when the second earthquake struck, indicated a reduction in natural frequency (obtained using four different methods, namely, short-time Fourier transform (STFT), wavelet transform (WT), horizontal-to-vertical moving window ratio (HVMWR), and horizontal-to-vertical spectral ratio (HVSR)) of between 28% and 48% in the north-south direction, and between 35% and 50% in the east-west direction. Mucciarelli et al. [45] attribute this reduction in natural frequency to the decrease in the stiffness of the damaged structure.

Trifunac et al. [188], however add that, following a seismic event, the lengthening of the fundamental period of a building (corresponding to a consequent decrease in its natural frequency), which is not constructed on an infinitely rigid ground, is not solely due to the formation of cracks in the damaged structure, but is also in part due to the reduction in stiffness arising from the damage suffered by the ground during the seismic event. Hence, according to the authors, attributing the increase in natural frequency exclusively to the propagation of damage in the structure would result in an over-estimation of the ductility capacity of the structural system. However, in the present study, while it is acknowledged that the stiffness of the material specified for the ground affects the stiffness of the structural model as a whole, since the ground was specified as a material at the structural model's Minimum Z position, instead of being modelled as a three-dimensional mass, damage propagation through the ground cannot occur in the numerical models which were analysed for natural frequency. Hence, the reduction in natural frequency is being proposed as resulting wholly from the stiffness degradation of the modelled building and not from that of the ground.

Clause 4.3.1(7) of Eurocode 8: Part 1 [4] and, more specifically in the case of masonry structures, Rule (3) in Clause 9.4 of Eurocode 8: Part 1 [4], state that the stiffness of a cracked structure may be estimated as half that of the uncracked structure. Hence, with reference to Equation 4-1, in the case

of a single degree of freedom system, since the mass of the cracked structure would be equivalent to that of the same undamaged structure, these provisions in Eurocode 8: Part 1 [4] signify that the natural frequency of a cracked structure can be estimated to decrease by 30% from that of the undamaged building. The natural frequency results of the analysed numerical models, which are summarised in Table 31 in Appendix D, indicate that the reduction in natural frequency, and hence in the stiffness, of the analysed numerical models, which resisted collapse after being subjected to a seismic excitation, did not exceed 7% in the models which did not include a soft storey at semi-basement level. This reduction did not appear to vary significantly between the two cases of ground formations modelled. On the other hand, as summarized in Table 4-1, in the analysed models which include the presence of a soft storey at semi-basement level, the observed reduction in natural frequency was between 22% and 30.1% for the models analysed on clay at Minimum Z, and between 10.7% and 17.6% for the models analysed on upper coralline limestone at Minimum Z. This suggests that, when subjected to the same seismic excitation, the degree of damage suffered by the analysed buildings was around twice as much when buildings are constructed on clay than when constructed on a stiffer rock, as in the case of upper coralline limestone[17]. The pronounced reduction in natural frequency after exposure to seismic excitation in the cases when a soft storey was present also demonstrates that the presence of a soft storey reduces significantly the seismic resistance of the masonry buildings and, even if collapse is resisted, the resulting degree of damage would be appreciably higher.

Table 4-1 Percentage decrease in natural frequency at the end of the dynamic loading stage in numerical models which resisted collapse.

Material specified for ground at Minimum Z	Percentage decrease in natural frequency at the end of the dynamic loading stage according to orientation			
	Without a soft storey at semi-basement level		With a soft storey at semi-basement level	
	Transverse direction	Longitudinal direction	Transverse direction	Longitudinal direction
Clay	3.2-5.3%	2.5-7%	22.8-30.1%	22-26.2%
Upper coralline limestone	0.2-6.8%	1.7-4.8%	16-17.6%	10.7-13.4%

As explained in Chapter 3 of this thesis, the compressive strength, the Young's Modulus of Elasticity and the Shear Modulus of Elasticity specified in the numerical models for clay were increased by around four times, and the density was reduced to 0 kg/m^3, in view of persistent stability errors experienced during the static loading stage of the analysis when values, which described more accurately the properties of the local clay, were used. Furthermore, in the case of upper coralline

[17] As indicated in Table 24 in Appendix C, the Young's Modulus of Elasticity of upper coralline limestone was specified as 807.6 times higher than that of clay and its Shear Modulus of Elasticity was specified as 107.7 times higher than that of clay in all numerical models analysed for this study.

limestone material properties, the average density value resulting from studies carried out by Bartolo [155] was used, whereas the Elastic Modulus of Elasticity at the top of the range indicated for limestones [159] and, hence, applicable to the stiffer limestones, was adopted. The Shear Modulus of Elasticity for upper coralline limestone was derived from the following relationship [189] using a Poisson's ratio of 0.25:

$$G = \frac{E}{2(1+\nu)}$$

Equation 4-3

where, G is the Shear Modulus of Elasticity in N/mm^2, E is the Elastic Modulus of Elasticity in N/mm^2 and ν is the Poisson's ratio. Using these material properties, the shear wave velocity for upper coralline limestone[18] computed using the following relationship [190]:

$$V_s = \sqrt{\frac{G_{max}}{\rho}}$$

Equation 4-4

resulted as 3,268.76 m/s, where V_s is the shear wave velocity in m/s and ρ is the density in kg/m^3. When compared to the shear wave velocities obtained by Farrugia et al. [191], through in-situ passive seismic wave techniques at seven different localities in the Maltese Islands, this value of shear wave velocity for upper coralline limestone results in almost three times the highest value obtained. Such a high value of shear wave velocity would very likely be present in the case of very stiff rock with no fractures. The relative stiffnesses of the upper coralline limestone and clay layers affect the transmission of seismic waves through and between these layers, as well as to and from the overlying structures, hence resulting in a different behaviour of the structures in the presence of seismic forces. Therefore, in view of the fact that the material properties specified for upper coralline limestone and clay in the numerical models were different from the properties of these materials present locally, the damage sustained by the analysed numerical models cannot be considered as representative of the degree of damage which would be sustained by contemporary loadbearing URM structures in areas of the Maltese Islands. On the other hand, however, the consistency of the material properties specified for these ground formation layers, throughout all the analysed numerical models, ensured that the validity of the results obtained in the context of the assessment of the variation in seismic vulnerability of contemporary loadbearing URM structures, when particular seismic vulnerability characteristics are present, was retained. Furthermore, as seen in Figures 4-5, 4-6, 4-7 and 4-8, the significant reduction in natural frequency, in the numerical models which were analysed on clay specified at Minimum Z,

[18] The shear wave velocity for clay with the material properties specified in the numerical model could not be calculated using the same relationship since a density of 0 kg/m^3 was specified for this material in order to set it at a pre-compressed state under its self-weight from the very start of the analysis.

could be considered as indicative of the behaviour of the construction typology under investigation, if constructed on ground which is even less stiff than the one specified in the models. This, in addition to the consideration that all the cases investigated were analysed under the same input seismic ground accelerations, and that a limited number of seismic vulnerability characteristics were studied, indicates that further studies of the behaviour of the contemporary loadbearing URM building typology, using more accurate definitions of the properties of geological materials, a wider range of seismic vulnerability characteristics, and subjected to different ground motion records, are required before any definitive comparisons to the percentage reduction in the natural frequency of the building typology under study, to that suggested in Eurocode 8: Part 1 [4], can be drawn.

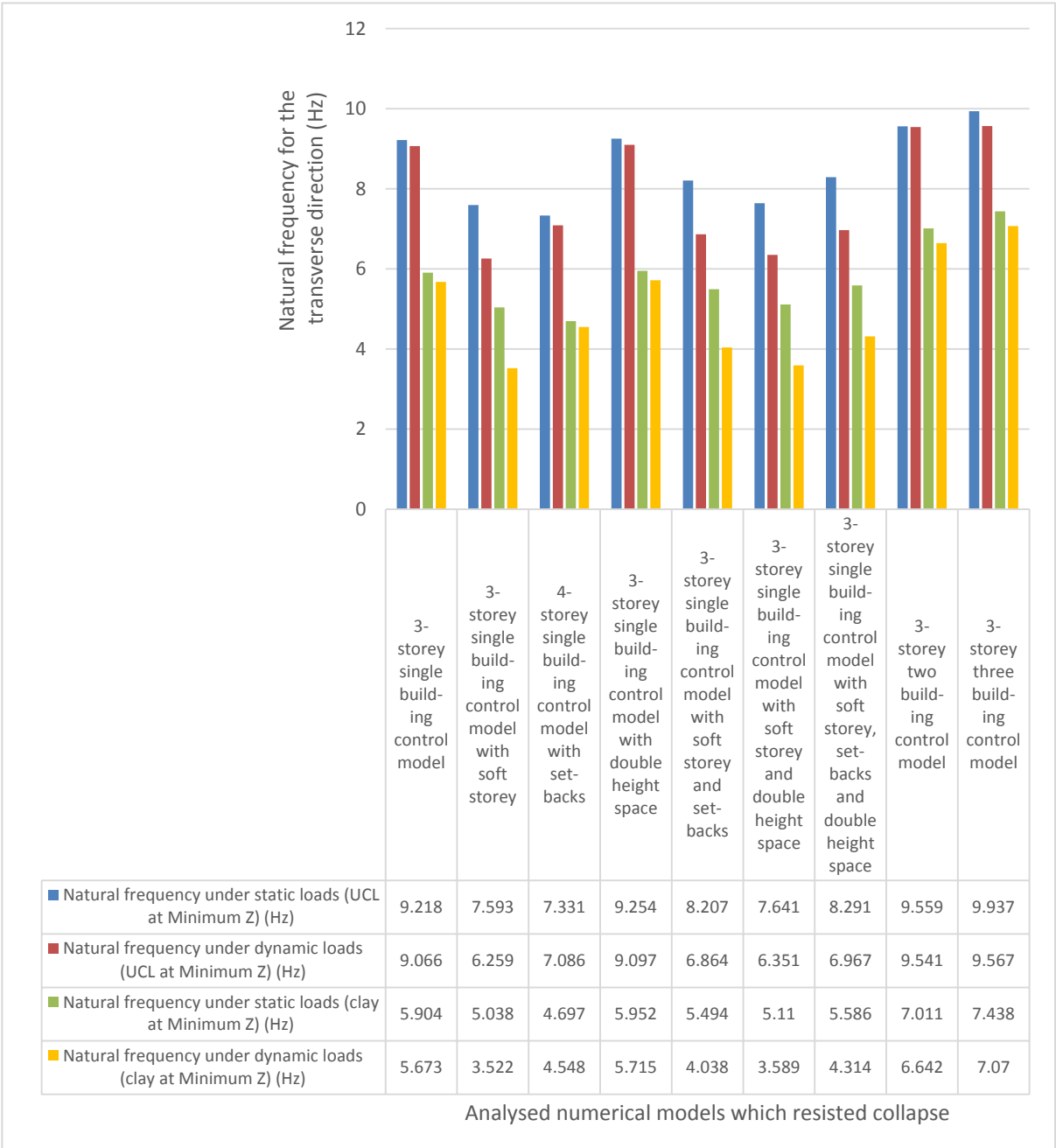

Figure 4-5 Variation in natural frequency following static and dynamic loading in the analysed numerical models which resisted collapse.

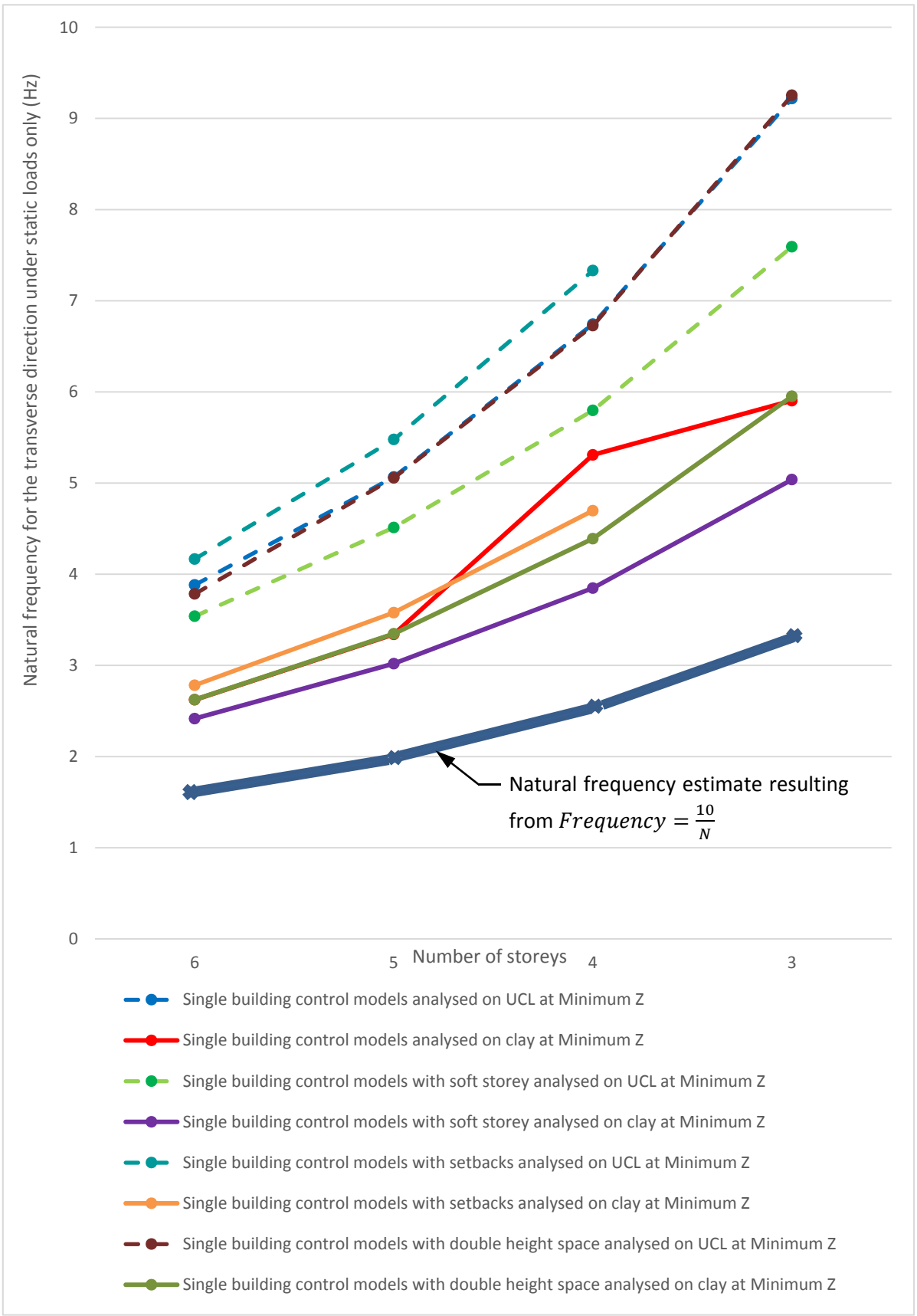

Figure 4-6 Variation in natural frequency for the transverse direction of single building control numerical models and numerical models which include one additional seismic vulnerability characteristic with number of floors and subsoil material.

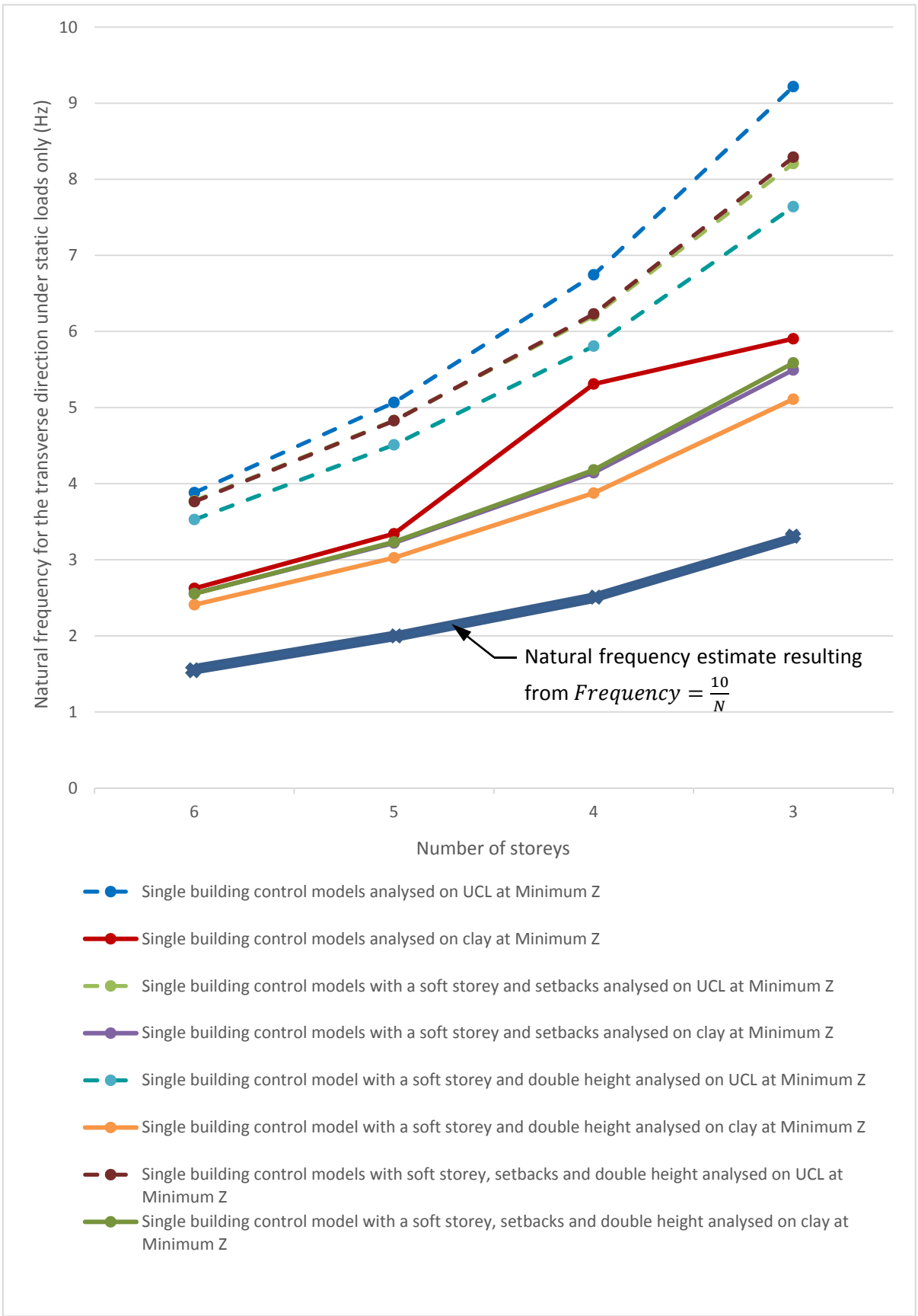

Figure 4-7 Variation in natural frequency for the transverse direction of single building control numerical models and numerical models which include two/three additional seismic vulnerability characteristics with number of floors and subsoil material.

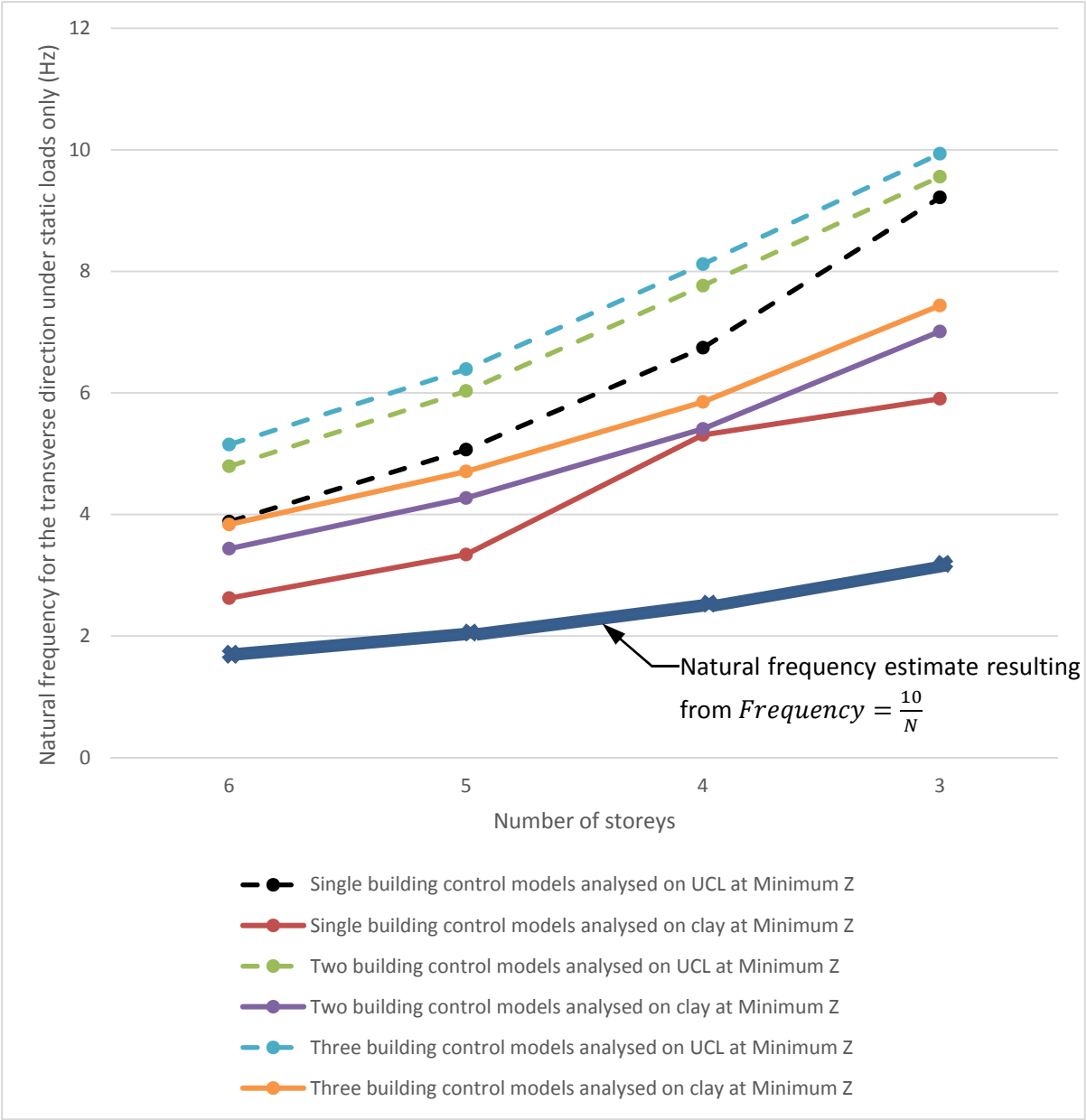

Figure 4-8 Variation in natural frequency for the transverse direction of single, two- and three-building control numerical models with number of floors and subsoil material.

Figures 4-6, 4-7 and 4-8 show how the basic equation for the estimation of natural frequency used by seismologists (Frequency = 10/N, where N is the number of floors of the building above the ground) provides a lower-bound estimate of the natural frequency in the transverse x-direction of the investigated cases considered in the present research study. Furthermore, the natural frequency results summarised in Figures 4-5, 4-6, 4-7 and 4-8 and in Table 31 in Appendix D indicate higher values of natural frequency at the end of both static and dynamic loading stages, when numerical models were analysed on ground specified as upper coralline limestone at Minimum Z, when compared to the equivalent numerical models analysed on clay at Minimum Z. It is likely that this occurs in view of the contribution of the stiffness of the material specified for the ground to the overall stiffness of the model and the way ELS® interprets ground specified as a material at Minimum Z, as explained in Section 3.4.3 of this thesis. In ELS®, ground specified as a material at the Minimum Z position of the numerical

model is represented as the virtual reflection of the first line of elements of the model into the ground. These virtual elements are assigned the specified material properties for the ground, and are restrained in all directions. Therefore, when calculating the stiffness and, hence, the natural frequency, of a numerical model which includes a structure specified on ground set at Minimum Z, ELS® takes into consideration the stiffness of the material specified for the ground in conjunction with that of the structure, in order to work out the stiffness of the whole numerical model. Structures modelled on clay at Minimum Z, therefore, resulted in a lower value of natural frequency than the corresponding models set on upper coralline limestone at Minimum Z in view of the lower stiffness of the former ground material. The less stiff material would also constitute a different oscillator in the transmission of earthquake vibrations to the overlying structure. Table 31 in Appendix D indicates how the value of natural frequency obtained in the transverse direction, at the end of the static loading stage, for numerical models specified on clay at Minimum Z, worked out as a percentage of the value of natural frequency of the corresponding models defined over upper coralline limestone specified at Minimum Z, was fairly consistent throughout all analysed models and varied between:

a) 64.0% and 67.6% in the case of the six-, five- and three-storey control numerical models[19] and 78.7% in the case of the four-storey control numerical model;
b) 64.1% and 69.3% in the case of the numerical models which include one to three additional seismic vulnerability characteristics, and the two- and three-building cases (which range is applicable throughout the six-, five-, four- and three-storey cases investigated).

In the longitudinal direction, the percentage of the natural frequency estimates, at the end of the static loading stage of corresponding models analysed on clay at Minimum Z to those obtained when the ground was specified as upper coralline limestone at Minimum Z, resulted as follows:

a) between 81.8% and 88.1% in the case of the six-, five- and four-storey control numerical models and 94.5% in the case of the three-storey control numerical model;
b) between 72.5% and 91.5% in the case of the numerical models which include additional seismic vulnerability characteristics, and the two- and three-building cases (which range is applicable throughout the six- to three-storey cases).

Furthermore, the natural frequency value, obtained at the end of the dynamic loading stage in the numerical models analysed on clay at Minimum Z, worked out as a percentage of the natural frequency value, resulting after exposure to the same dynamic loading from the corresponding numerical models analysed on upper coralline limestone at Minimum Z, for the cases which resisted collapse, varied between:

[19] The term 'control' numerical models is hereby being used to mean models with the same typical floor layout at every floor level.

a) in the transverse direction: 56.3%-64.2% for single building numerical models which include one to three additional building characteristics (which range is reduced to 56.3%-61.9% if only the numerical models which include a soft storey at semi-basement level, are considered), and 69.6% and 73.9% for the two- and three-building control numerical models respectively;
b) in the longitudinal direction: 65.3%-91.3%. This variation reduces to 65.3%-71.6% when only the numerical models which include a soft storey at semi-basement level, are considered, hence, the upper part of the range resulted from numerical models which include setbacks at penthouse level, or the presence of a double height space alone, or alternatively, consist of two- or three-building control numerical models.

The above results indicate that there was a relatively consistent decrease in natural frequency at the end of the static loading stage, in the transverse direction of the building, of 30%-36% for numerical models analysed on clay, when compared to the stiffer upper coralline limestone, and that this decrease was amplified further to around 38%-44% after dynamic loading, in particular, in the single building numerical models. It was also noted that a lower decrease in natural frequency after static loading resulted in the longitudinal direction of the numerical models, which direction, however, still exhibited a 28.4%-34.7% decrease in the numerical models, which include a soft storey following dynamic loading. Hence, whereas in the case of natural frequency estimates obtained after static loading, the lower natural frequency obtained from the numerical models analysed on clay at Minimum Z could be attributed to the lower stiffness of the ground material, following dynamic loading, other factors such as the amplification of seismic accelerations, through the less stiff geological formations, the occurrence of soil-structure interaction and, possibly, resonance effects, could also be contributing towards the higher decrease registered in natural frequency and, hence, the higher degree of damage sustained. This decrease seems to have affected less the longitudinal direction than the transverse direction of the building models. This might have been due to the narrow and long plan configuration of the analysed structures, which lead to a higher stiffness and, hence, a higher seismic resistance, of the building numerical models in this orientation.

4.2.1.2 Variation in natural frequency with reduction in number of storeys

Table 31 in Appendix D indicates that, in all the investigated cases, an increase in natural frequency and, hence, stiffness, was obtained with every reduction in the total number of storeys, irrespective of the ground type and orientation with respect to the modelled structures. Generally, the percentage increase at every reduction in number of floors also increases at every step, with a few exceptions. An example is the high increase (58.905%) in the natural frequency in the transverse direction of the four-storey control numerical model, when compared to the corresponding five-storey numerical model, with ground specified as clay at Minimum Z. Another example is provided by the significantly lower values of percentage increase in natural frequency, obtained in the longitudinal direction for the five-storey control numerical model (1.015%), the five-storey numerical model including a double height space between Levels 0 and +1 (1.504%) and the five-storey two- and three-building control numerical models (10.066% and 6.842% respectively), when compared to their corresponding six-storey cases, with ground specified as upper coralline limestone at Minimum Z. Since these cases cause shifts in

the average values, the average percentage increase in natural frequency with reduction in number of storeys presented in Tables 32 and 33 of Appendix D, was subdivided in order to give a more accurate representation of the actual variations. The results in these tables suggest that the increase in natural frequency, with every single storey decrement, is marginally higher in the transverse direction than in the longitudinal direction of the modelled buildings. Furthermore, if only the numerical models, which include a soft storey at semi-basement level were considered, the percentage increase in natural frequency, in the transverse direction, increases from 27.917% (from six to five storeys) to 31.961% (from four to three storeys), in numerical models analysed on upper coralline limestone at Minimum Z, and from 25.816% (from six to five storeys) to 32.244% (from four storeys to three storeys), when the ground was specified as clay at Minimum Z. Therefore the rate of increase in natural frequency does not seem to be affected by the different ground geology.

A comparison of the natural frequency results obtained for the cases when setbacks, a soft storey or a double height space are present as the only additional seismic vulnerability characteristic and their corresponding control numerical model, suggests that, irrespective of the ground geology, the addition of setbacks to the control numerical model results in an increase in natural frequency in both the longitudinal and the transverse directions. The results also indicate that the presence of a soft storey at semi-basement level causes a reduction in natural frequency in the six-, five-, four- and three-storey numerical models analysed, when compared to the corresponding control numerical models, for both ground formation cases considered, and in both building orientations. On the other hand, the presence of a double height space results in a marginal reduction in natural frequency when compared to the corresponding control numerical models at six, five and four storeys, in both the transverse and the longitudinal directions, when modelled on upper coralline limestone. When modelled on clay, this decrease is only evident in the longitudinal direction for the five- and the three-storey cases, and in both longitudinal and transverse directions in the four-storey case. In the rest of the cases modelled on clay at Minimum Z, the presence of a double height space results in a marginally higher natural frequency than the corresponding control model.

Moreover, particularly in the transverse direction, higher increases in natural frequency with reduction in number of storeys were observed in the case of single building control numerical models, and numerical models which include a setback or a double height space as the only additional seismic vulnerability characteristic, than in cases where a soft storey was present, either in isolation or in conjunction with other variations to the control numerical model. This higher rate of increase in stiffness for every reduction in number of floors seems to suggest that the presence of setbacks at penthouse levels (in the proportions which were allowed by local planning regulations until the issue of the 'Development Control Design Policy, Guidance and Standards 2015' [192]) or a double height space between levels 0 and 1 (as modelled in the investigated cases) is not as deleterious to the seismic resistance of the contemporary loadbearing URM building typology under study, as much as the presence of a soft storey.

The control models analysed in this study have the identical plan layout repeated at every floor. Hence, while the seismic resistance of such structures is still affected by particular planning characteristics, such as the presence of a large open plan on the front end of the building, the long corridor adjacent to the left hand side party wall, and the unsymmetrical plan layout, the stiffness is constant throughout the building height. The behaviour of a cantilevered beam, with regular cross-section, could be considered as a simplified example of the behaviour of the control models. The fundamental frequency of such a beam, under undamped free vibrations, in the case when one of the ends of the beam is restrained against rotations and translations, and the other end is free, is as follows [193]:

$$f = 3.516\sqrt{\frac{EI}{mL^4}}$$

Equation 4-5

where *f* is the natural frequency in Hertz (Hz), *E* is the Young's Modulus of Elasticity in N/mm^2, *I* is the second moment of area in mm^4, and *m* is the mass in kg. Equation 4-5 indicates that, in view of the uniform properties present throughout the length of the cantilever, the length and the mass become the most governing factors with respect to the natural frequency, where a reduction in length and, hence, in mass, results in an increase in natural frequency. Furthermore, the exponent applied to the 'length' variable in the same equation leads to an increase in the percentage increment of natural frequency with every storey reduction in the modelled control buildings.

In the case of the control numerical models, to which setbacks were added at penthouse level, if the same cantilevered beam simplification is applied as in the case of the control numerical model, which does not include any additional seismic vulnerability characteristics, the irregularity in the simplified beam case would consist of a reduction in cross-section close to the free end of the beam, whereas the rest of the beam would be uniform. Therefore, when compared to the case of the control model where all the floors were kept identical, the main effects of the irregularity would most likely consist of a reduction of the structure's stiffness at the topmost storey[20], as investigated by Al-Ansari [58] [59] and, in view of the reduction in floor area at the top floor, a lower structural mass for the same overall height of building. Equation 4-5 indicates that natural frequency is directly proportional to the square root of the moment of inertia of the structure, but inversely proportional to the square root of its mass. Hence, the comparison of the increase in natural frequency of the control numerical models, which include a setback at penthouse level, to that resulting from the six-, five-, and four-storey corresponding control numerical models, which do not include additional characteristics, suggests that the effect of the decrease in mass was higher than that caused by the decrease in moment of inertia,

[20] This modification to the structure's stiffness would be expected to be lower in the cases with the higher number of floors in view of the lower overall proportion of the presence of the irregularity when compared to the overall height of the building.

in such cases. With reference to the recommendations given by Parisi [60], in the case of buildings with setbacks of limited proportions distributed throughout their height, the lower position of the centre of mass results in a lower overturning moment, and hence, an increased stability. In the case of the analysed numerical models which include setbacks, the shift in centre of mass when compared to the corresponding control models is marginal, when considering the limited proportions of the setback areas. Hence, while the lowering of the centre of gravity could have had a bearing on the increased resistance exhibited by these numerical models, it is likely that the decrease in building mass provided a larger contribution to the improved seismic response of these numerical models.

This interpretation of the effect of setbacks is, however, only being limited to the context of the local planning regulations governing setbacks at penthouse levels, which were in force in the Maltese Islands until the November 2015, and is not intended to be extrapolated with respect to the effect which setbacks of different proportions and/ or at various levels throughout the building height would have on the moment of inertia, the mass and, hence, the natural frequency and the seismic response of this building type. The overall dimensions[21] of the modelled structures were based on the dimensions of the Xemxija Building Number 0011, whose natural frequency resulting from the numerical model was compared to the one obtained through ambient noise measurements, in order to verify the accuracy of the modelling assumptions. While the latter is an existing building, the contemporary loadbearing URM building typology under study typically consists of very rectangular plan dimensions with high length-to-width ratios, with the typical narrow and long plot proportions present in the Maltese Islands in areas zoned for terraced (row) developments. The typical width of plots for this building typology could generally vary between 6.40 m and 7.32 m, whereas the length would range between 25.90 m and 30.50 m. Hence, with reference to Clause 4.2.3.3(5c) of Eurocode 8: Part 1 [4], all modelled cases would classify as 'non-regular' in elevation, since the sum of the setbacks in the penthouse level of the analysed models results as 32.6% that of the longitudinal dimension of the underlying floor (therefore, exceeding the Eurocode 8 recommendation by 22.6%), and 47.5% of the longitudinal dimension of the storey at semi-basement level (therefore, exceeding the Eurocode 8 recommendation by 17.5%). These values, however, can very likely be considered to be close to the maximum percentages for this building typology since, generally, in the case of longer plots, a larger plot area is constructed, with the same minimum setbacks and back yard sizes stipulated by the planning/ sanitary regulations, therefore, resulting in an overall lower percentage of setback floor area when compared to the underlying floor, and to the area of the floor at the lowest level.

[21] The overall plot dimensions of all the analysed models consisted of a width of 6.40 m and a length of 25.48 m. This resulted in a 22.61 m length of building at semi-basement level and a 17.62 m length of building at all levels positioned between the semi-basement and the floor of the penthouse. A front setback of 4.25 m and a rear setback of 1.5 m were specified at penthouse level.

The effect, of the introduction of a double height space between Levels 0 and 1 in the front room of the modelled structures, on the natural frequency, when compared to the natural frequency of the corresponding control numerical models, was expected to result in a consistent, more than marginal, reduction in natural frequency in both building orientations, and for both ground types considered, in view of:

a) the introduction of an irregularity in the path along which seismic accelerations had to be transferred to the vertical structural elements, therefore, leading to stress concentrations, and secondary moments in the portions of the slabs which are next to the slab void as explained in ASCE 31-03 [61];
b) the consequent reduced degree of restraint of the section of the party wall which is directly abutting the void, leading to a more slender wall element at just one floor above the base of the building, where most of the structural mass would be present. Such wall sections would be more prone to an increase in the curvature of their deformed profile (due to their increased slenderness) and increased deflection, hence, the induced moments would tend to lead to an earlier failure;
c) the local reduction in the stiffness of the building, in the area where the double height space was specified, therefore, resulting in a non-uniform stiffness throughout the building height.

Clause 4.2.1.5(2) of Eurocode 8: Part 1 [4] states that the presence of large voids in slabs, especially when positioned very close to loadbearing walls, can interrupt the connection and, hence, the transfer of forces to these walls. Furthermore, Öztürk [62] points out that the Turkish Earthquake Code does not recommend the presence of voids in slabs having an area greater than one third that of the floor area, since it would constitute a plan irregularity. In such cases, continuity of slabs, and the uniform transmission of forces to the vertical walls, cannot be assumed, and the slabs would not be considered as acting as rigid slab construction systems. In Öztürk's study [62], the introduction of large voids in reinforced concrete frame structures, without the frame continuity through the voids, resulted in larger displacements, and, in particular, in the case where the void was positioned at one end of the building, the slabs no longer displaced as rigid diaphragms.

The discrepancy between the natural frequency results obtained in this thesis, in the case of the numerical models in which a double height space was included between Levels 0 and 1, when compared to the corresponding control numerical models and the expected results, might have been due to a number of factors:

i. the size of the void, 5.00 m in width by 3.15 m in length, when compared to the overall area of the storey (equivalent to 14% of the floor area), might not have been large enough to trigger the effects listed in (a) to (c) above;
ii. the limited length of the party wall (3.15 m), whose effective height is double that of the adjacent walls, in view of the location of the void, ensures that some form of partial restraint is still provided by the adjacent wall sections, hence, resulting in a only a reduced effective change in stiffness for this wall section;

iii. the modelling of the bounding of the void on three of its sides by 250 mm thick reinforced concrete slabs at the level of the slab over Level 0, which slabs were sized based on the largest of the three spans, might have resulted in the slabs having enough capacity to cater for the additional stresses induced and, in view of their thickness, providing additional stiffness to the front part of the building around the void.

Therefore, the results obtained in this thesis with respect to the consequence of a double height space as the only additional seismic vulnerability characteristic present, or in combination with other seismic vulnerability characteristics on the seismic resistance of the contemporary loadbearing building typology, must be interpreted with caution. Additional analyses, excluding the three thick slabs around the double height void at slab over Level 0, hence, also resulting in a larger void, which would also ideally incorporate the full width of the buildings between both party walls, would be required before any generalisations can be drawn. These additional analyses could not be carried out as part of this study due to time constraints with respect to the availability of the ELS® software licence. However, this case was investigated using 3Muri® and the results obtained are discussed in Chapter 5 of this thesis.

On the other hand, the lower natural frequency obtained from the modelled structures which included the presence of a soft storey at semi-basement level, when compared to the corresponding control numerical models and the higher degree of damage (estimated through the percentage reduction in natural frequency at the end of the dynamic loading stage) sustained by the models which included a soft storey and resisted collapse, when compared to the corresponding numerical models where no soft storey is present, is in line with the behaviour of buildings incorporating soft storeys, as reported in literature. Whereas the control numerical model exhibits a regular stiffness throughout the building height, in the models which include a soft storey at semi-basement level, the lower stiffness of the lowermost storey reduces the overall stiffness of the building and, hence, its natural frequency.

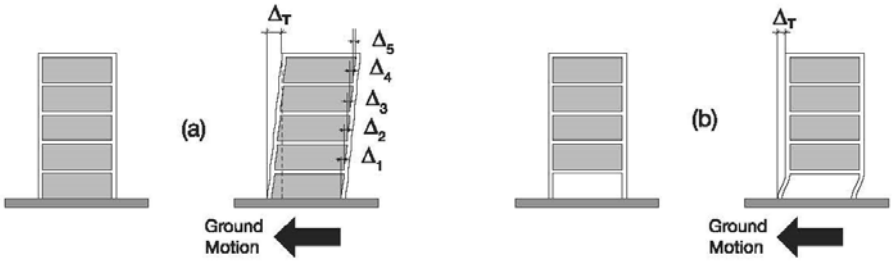

Figure 4-9 Distribution of total displacement generated by an earthquake in (a) a regular building (as in the case of the analysed control numerical models) and, (b) a building with a soft storey irregularity [56].

As explained by Arnold and Reitherman [55], in the context of the termination of shear walls above the first floor level in reinforced concrete structures, the stiffness gradient, and the discontinuity in the load paths, gives rise to stress concentrations at the transition, which can result in overstressing. Furthermore, Guevara-Perez [56] explains that, whereas in a building which has a uniform stiffness at all levels, the relative displacements caused by the seismic excitations would be gradually distributed throughout all the floors, in the presence of a soft storey at the lowermost level of the building, the reduced stiffness and, hence, the increased flexibility of this level when compared to the more rigid

overlying levels, would attract a major proportion of the earthquake induced forces. This, results in higher displacements in the walls present at this level which could lead to collapse. Figure 4-9(b) indicates how the high stiffness gradient, between a soft storey at the lowermost position and the levels above it, in addition to the high structural vertical loads acting at this position, would give rise to large moments in the party walls (P-delta effects), as a consequence of the large induced displacements.

4.2.2 Predominant frequencies in the acceleration spectrum and resonance effects

Earthquake excitations cause buildings to vibrate. However, when the seismic impulses transferred from the ground to the building coincide with the natural period of the structure, the latter would experience major amplification of vibrations and accelerations caused by resonance [57]. Murty et al. [54] point out that, for resonance to occur, the earthquake ground motion must sustain the same frequency of vibration for a prolonged duration and, hence, in view of the randomly varying nature of earthquake excitations, such a phenomenon is very unlikely to occur in its 'pure' form. Murty et al. [54] explain that, however, in the cases where the seismic ground motions have a frequency which is close to the natural frequency of the building, but which is not sustained for a considerable duration, 'an increased response but not resonance' [54] occurs. This 'increased response' is being referred to as 'resonant behaviour' or 'resonance effects' in this thesis.

Amplification of structural response, however, cannot be solely attributed to the occurrence of resonance effects, especially in cases when the underlying ground formation is not infinitely stiff. Various authors (including, Gueguen et al. [46], Lou et al. [47], Farghaly et al. [48], Reza Tabatabaiefar et al. [49], Xiong et al. [51]) explain that free-field ground motions are not affected by the presence of buildings only in the ideal scenario when the ground is infinitely rigid. When buildings are constructed over more flexible ground, apart from the elongation of the natural period of the buildings in proportion to the relative stiffness of the ground and the structures as mentioned in Section 4.2.1, a complex interchange, between the vibrations of the ground and the energy dissipated back into the ground by the vibrating overlying buildings, is triggered. This behaviour is even more pronounced if the structure is very stiff and has a high mass [50]. In the case of very soft ground, this soil-structure interaction leads to the alteration of the free-field ground motion even a considerable distance away, therefore affecting and, at the same time, being modified by, the response of other buildings.

Reza Tabatabaiefar et al. [49] explain that, particularly in the case of moment-resisting frames, soil-structure interaction effects are pronounced when the shear wave velocity of the underlying ground is less than 600 m/s. In the local scenario, from the results obtained by Farrugia et al. [191], shear wave velocities, specific to the different ground layers, indicate that, in the case of thicknesses between around 8 m and 20 m, unfractured upper coralline limestone top layers have a shear wave velocity of between 700 m/s (Mdina) to 1,070 m/s (Mgarr), whereas, in the case of fractured upper coralline limestone, the shear wave velocity drops to between 300 m/s (uppermost portion of layer in Mdina) and 550 m/s (Xemxija and uppermost section in Selmun). The thickness of the clay layers varies between 30 m in Mdina and 47 m to 55 m in the other investigated localities. However, the

corresponding shear wave velocities vary between 400 m/s in Mdina and Xemxija and 475 m/s to 500 m/s in the other areas. Farrugia et al. [191] attribute the higher values to cases where the clay has undergone a higher degree of compaction due to a heavier and denser overlying mass of rock. These values indicate that the shear wave velocities of thinner fractured layers of upper coralline limestone could be very similar to those of the clay layer, and, in both cases, result as lower than the 600 m/s threshold suggested by Resa Tabatabaiefar et al. [49]. Hence, out of the seven localities investigated by Farrugia et al. [191], shear wave velocities of the upper 30 m of ground of between 840 m/s and 890 m/s only result in areas where the upper coralline limestone is around 50 m – 55 m thick and is free from fractures. In areas where the thickness of the upper coralline limestone layer is between 10.0 m and 22.5 m, out of which 12.5 m - 22.5 m are unfractured, the shear wave velocity in the upper 30 m varies between 600 m/s – 670 m/s, whereas in Mdina and Xemxija, where upper coralline limestone thicknesses are between 8 m and 15 m (and this layer is either highly fractured in part of its depth (Mdina) or has fractures which extend throughout its depth (Xemxija)) the shear wave velocity of the ground for the upper 30 m drops to 454 m/s and 471 m/s respectively. Based on the conclusions drawn by Reza Tabatabaiefar et al. [49], this implies that in the Maltese Islands, even in areas where the upper coralline limestone layer is of medium thickness and relatively unfractured, the effects of soil-structure interaction can have a significant bearing on the buildings' behaviour under seismic forces.

It must be noted that the thicknesses of the ground formation layers resulting from the investigations carried out by Farrugia et al. [191], do not agree with the upper coralline limestone and clay thicknesses considered in the present study, neither in the case of the 1.5 m thick upper coralline limestone layer on the 60 m thick clay layer case (considered in this study as a worst case scenario for Nadur), nor for the 30 m thick upper coralline limestone layer on the 30 m thick clay layer case (considered in this study for Xemxija). Whereas in the case of Nadur, this study considered the geology at the edge of the urban development to the West of the village just before the ridge, the investigation carried out by Farrugia et al. [191] included the area to the Eastern extremity of the locality, in the vicinity of Sopu Tower [194] (D. Farrugia, Ph.D. graduate, Department of Geosciences, Faculty of Science, University of Malta, personal communication by email, dfarrugia28@gmail.com, 29th September 2016). The thickness of upper coralline limestone specified for the Nadur case, in the present study, was based on experience of past construction projects in the vicinity of the area under consideration, whereas the thickness of the same rock formation in Xemxija was based on records of borehole investigations carried out during the British Period in the Maltese Islands [145]. The thickness of the clay layer was, in both cases, obtained through a cross- examination of the geological map, and the number of contour lines present on the Mapserver of the Malta Planning Authority. In the case of Xemxija, the inclination of the ground formation layers can most likely explain the difference between upper coralline limestone thicknesses.

In order to obtain an insight with respect to the possibility of whether the occurrence of resonance could be the main contributor towards the amplification of accelerations, and / or relative displacements identified prior to the onset of collapse in a number of analysed numerical models

(which will be discussed in detail in the subsequent sections of this Chapter), predominant frequencies in the acceleration spectrum were derived from the acceleration versus time plots at a minimum of four positions in every numerical model analysed in this study. The four positions considered consisted of: the middle element in the lower ground formation layer, the middle element in the upper ground formation layer (or, an element corresponding to the whole thickness of the layer, in the cases where the layer consisted of 1.5 m thick upper coralline limestone whose thickness was not subdivided further in the numerical models), an element at the level of the first course at the semi-basement level, and an element at slab over semi-basement level. All elements considered were positioned in the left hand side party wall or, in the case of elements in the ground layers, directly aligned with it and along the same transverse section through the building along which the corresponding accelerations and displacements were extracted from various positions in the numerical models. Hand-drawn trendlines were drawn through the mean values of the resulting power spectral density (g2/Hz) versus frequency (Hz) plots, from which approximate values of frequency at peaks were identified. The exact values of these predominant (peak) frequencies were located through a close inspection of the raw data, from which, the power spectral density versus frequency plots had been obtained. The predominant frequencies identified at each of the four positions in the models were then compared to the main frequency components of the simulated ground motion record, which was used as input seismic acceleration in the transverse (x) direction of all analysed numerical models.

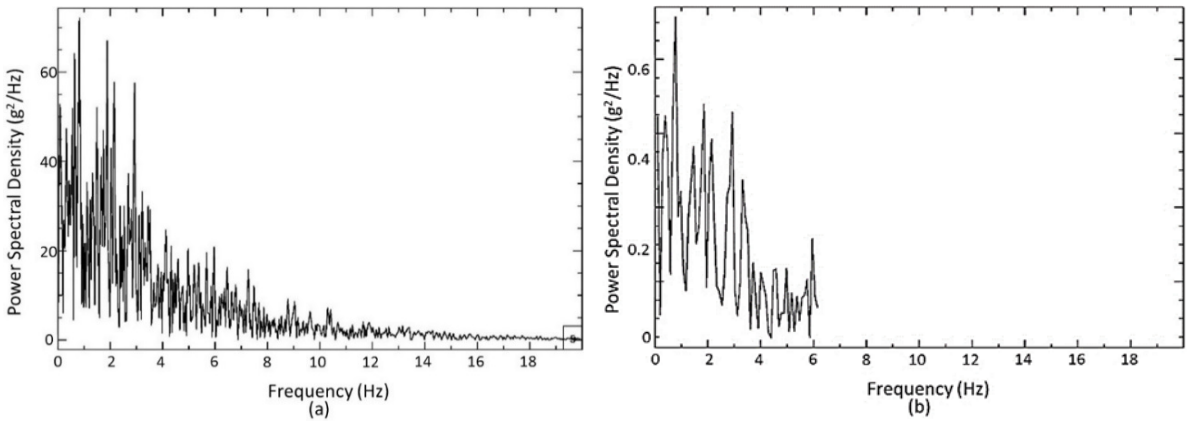

Figure 4-10 Frequency spectra of the simulated ground motion record derived from the acceleration - time plot by SMRU (UOM) for (a) original length of record (b) shortened record with a bracketed duration of +/-0.6g used in the analyses.

The resulting frequency spectra, which are included in Figures 4-10 (a) and (b) for the original ground motion record and the shortened record[22] respectively, were derived from the simulated input acceleration time series through a Fast Fourier Transform analysis by the Seismic Monitoring and Research Unit (SMRU) of the University of Malta (UOM). These frequency spectra indicate that the

[22] The original simulated ground motion record was shortened to 8.48 s by increasing the time step to 0.08 s and using a bracketed duration of +/-0.06g as explained in Section 3.4.5 of this thesis.

energy content of the input ground motion record lies mainly between frequencies of 0.800 Hz and 2.950 Hz in the acceleration spectrum, with the main peak frequency occurring at 0.800 Hz while lower peaks peaks are observed at around 1.875 Hz and 2.950 Hz. An additional notably lower peak frequency is evident in both the original and the shortened records at around 6.00 Hz.

The comparison of the predominant frequencies of the simulated input ground motion record to the natural frequencies of the analysed models on upper coralline limestone or clay at Minimum Z summarised in Table 31 in Appendix D and discussed in Section 4.2.1 of this thesis, suggests that it is very unlikely that resonance occurred in the analysed structures, since the resulting natural frequencies do not coincide with the peak predominant frequency of 0.800 Hz of the input acceleration – time series. Resonance effects due to higher frequencies, as distinguished from the occurrence of 'pure' resonance, on the other hand, cannot be excluded in the six-storey single building numerical models analysed on clay at Minimum Z, whose natural frequency in the transverse direction under static loading resulted between 2.408 Hz to 2.782 Hz, hence, within the main frequency range of the input ground motion record. Moreover, similar effects could have occurred in the five-storey two-building control numerical model analysed on upper coralline limestone at Minimum Z (whose natural frequency in the transverse direction under static loads resulted as 6.033 Hz), as well as in the three-storey single building control numerical model, and the corresponding control numerical model which included the presence of a double height space when analysed on clay at Minimum Z (where natural frequencies in the transverse direction under static loading of 5.904 Hz and 5.952 Hz, respectively, were obtained) because of the proximity to the 6.000 Hz peak frequency in the input ground motion record. Furthermore, resonance effects after initial structural degradation could have occurred in the four-storey single building control numerical models, which included either only the presence of a soft storey at semi-basement level and setbacks at penthouse level, or also a double height space in addition to these seismic vulnerability characteristics, when analysed on upper coralline limestone at Minimum Z. The natural frequency in the transverse direction of these numerical models under static loads resulted in 6.206 Hz and 6.230 Hz respectively, hence only 3.43% and 3.83% higher than the 6.000 Hz peak frequency of the input simulated ground acceleration.

As explained earlier, in the case of the ground formation layers, and their resulting response to the applied seismic excitations, as well as the effect of their vibrations on the overlying structures, the outcome of this study cannot be generalised to the local scenario, in view of the altered material properties of the ground layers. In addition, from a local point of view, Farrugia et al. [191] reported peak frequencies of between 1 to 2 Hz in all the seven localities investigated throughout the Maltese Islands, whereas, an earlier study by Vella et al. [195], covering 202 locations in Malta and 67 in Gozo, showed peak frequencies ranging between 2-10 Hz in places where a clay outcrop was present, and between 1-2 Hz in the case of upper coralline limestone outcrops. This suggests that the occurrence of a seismic excitation equivalent to the input ground motion record adopted in the present study would have most likely caused resonance effects in the subsoil at these sites. Furthermore, the comparison of the peak frequencies in the subsoil layers with the natural frequencies resulting from the analysis of the modelled structures for two eigen modes on upper coralline limestone and clay at

Minimum Z, summarized in Table 31 of Appendix D, also indicate the likelihood of resonant behaviour throughout the building typologies investigated in the present study on similar ground formations.

Nevertheless, as discussed in Section 3.4.5 of this thesis, the energy content of the simulated ground motion record used as input seismic action in all final numerical models analysed using ELS® lies in a lower range of frequencies (between 0.80 Hz and 2.95 Hz) than the Eurocode 8 Part 1 Type 1 elastic response spectrum on Type A ground [4] (whose energy content lies between 2.50 Hz and 6.67 Hz). This, in addition to the peak frequencies reported throughout the Maltese Islands by Vella et al. [195] and Farrugia et al. [191], implies that in a real life scenario, an earthquake ground motion corresponding completely with the characteristics of the Eurocode 8 Part 1 Type 1 elastic response spectrum for Type A ground [4] would likely lead to resonance effects in the ground layers only in areas where a clay outcrop is present. Resonance effects would be highly unlikely in areas where an upper coralline limestone outcrop is present.

Notwithstanding, since all numerical models have been analysed with the same input ground motion record, their behaviour can still provide valid insight into the response of the modelled structures within the limits of this study. Therefore, the identification of predominant frequencies in the ground layers of the numerical models which coincide with the predominant frequencies of the input simulated ground motion record, and which, could explain increased responses exhibited by the analysed numerical models, remains an important consideration in the interpretation of the response parameters extracted from the numerical models analysed using ELS® in this research study.

Figures 4-11 and 4-12 show the frequency spectra for the Models 45v2[23] and 63[24] represented through power spectral density against frequency plots, and including the hand drawn trendlines. A detailed review of the power spectral density against frequency plots for the analysed numerical models resulted in the information summarised in Table 34 of Appendix D. This table presents the main predominant frequency (corresponding to the highest value of power spectral density which is equivalent to the first mode natural frequency) in the acceleration spectrum of the elements investigated at the four positions in the analysed numerical models, in addition to the presence of any secondary frequencies (corresponding to lower power spectral densities and resulting from higher

[23] As summarised in Table 30 in Appendix D, Model 45v2 consists of the six-storey single building control numerical model analysed on a 1.5 m thick upper coralline limestone layer overlying a 60 m thick clay layer, with both ground formation layers modelled as three-dimensional blocks. This model collapsed when analysed under the simulated input ground motion record.

[24] As summarised in Table 30 in Appendix D, Model 63 consists of the three-storey single building control numerical model analysed on a 1.5 m thick upper coralline limestone layer overlying a 60 m thick clay layer, with both ground formation layers modelled as three-dimensional blocks. This model resisted collapse when analysed under the applied seismic load.

vibration modes), which fall within the main energy range of the input ground motion record, and the energy distribution of the frequency spectrum in the x-direction at the four positions.

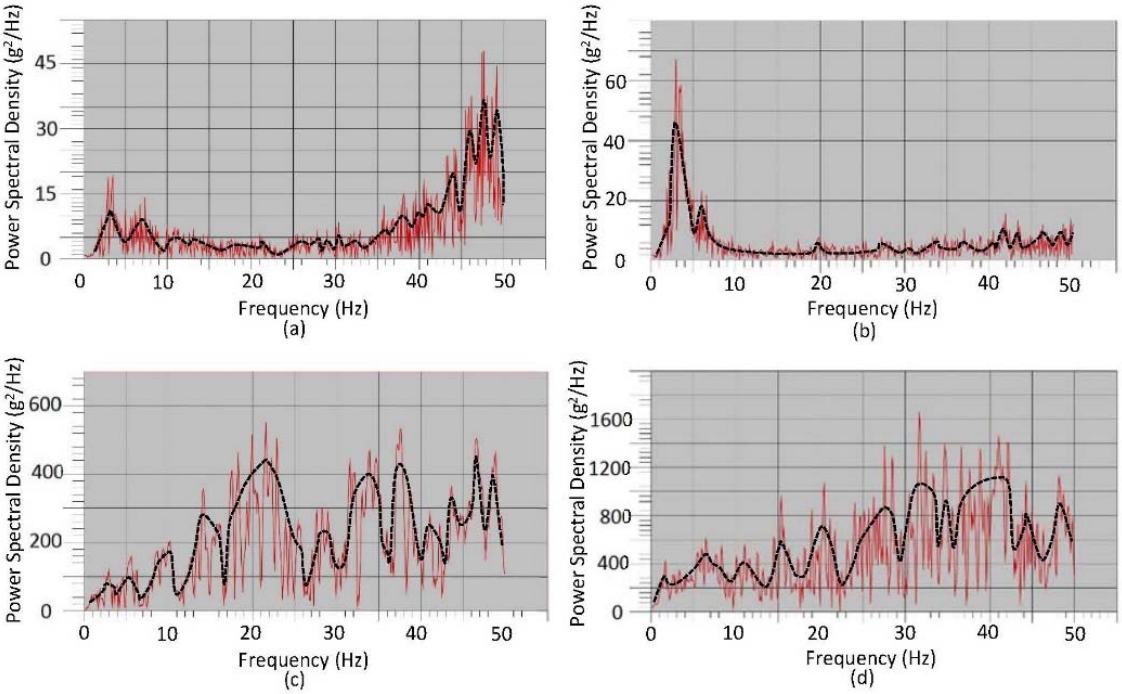

Figure 4-11 Plots of Power Spectral Density(g^2/Hz) against Frequency (Hz) derived from the x-acceleration spectrum of Model 45v2 at:(a)mid-depth of clay,(b)1.5 m thick upper coralline limestone,(c)first course,(d)slab over semi-basement level, including trendlines.

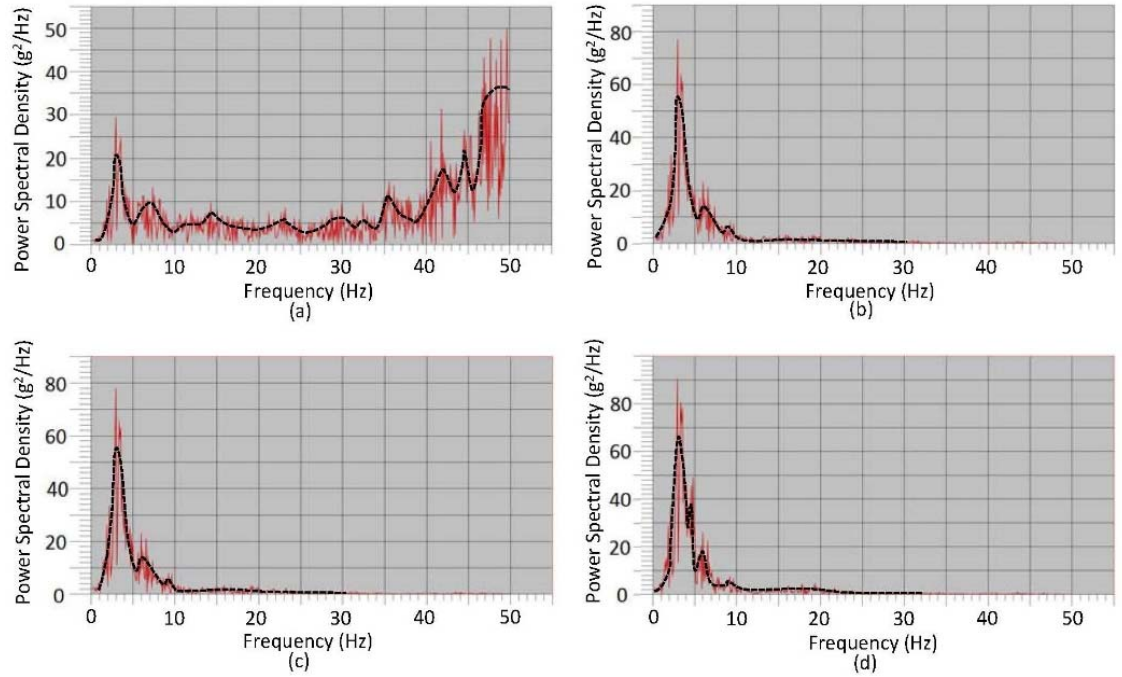

Figure 4-12 Plots of Power Spectral Density(g^2/Hz) against Frequency (Hz) derived from the x- acceleration spectrum of Model 63 at:(a)mid-depth of clay,(b)1.5 m thick upper coralline limestone,(c)first course,(d)slab over semi-basement level, including trendlines.

In simple terms, and in the context of the present study, the power spectral density represents the degree of contribution which every frequency has in the acceleration – time plot of the element under study. Therefore, in order to assess whether resonance effects could have played a role in the

response of a particular model, the distribution of energy content of the frequency spectrum, and the magnitude of the power spectral density peaks within the main energy range of the frequency spectrum of the input ground motion, were considered.

The difference in energy distribution, and in the frequencies associated with peak power spectral density values at corresponding positions in Models 45v2 and 63, are immediately apparent from Figures 4-11 and 4-12. A study of the power spectral density against frequency plots for the models analysed on 1.5 m thick upper coralline limestone on 60 m thick clay, indicates that the energy distribution exhibited in the plots of the corresponding six-storey control numerical model (Model 45v2) is very similar to that resulting at these positions from the analysed numerical models which did not include a soft storey, and which resulted in collapse when analysed on the same ground formations. In these cases, the predominant peak frequency values obtained at the first course of the semi-basement level and the slab over semi-basement level were located in the upper half of the frequency range, and the energy content was either almost even throughout most of the frequency range, or increased gradually in the higher end of the frequency range. On the other hand, the lower peak frequencies obtained at the first course of the semi-basement level and at the slab over semi-basement level in Model 63, were similar to those resulting at the same positions from the corresponding numerical models, which resisted collapse, irrespective of the type or thickness of ground formation layers modelled. The energy content in these cases is generally concentrated around a very short range of frequencies towards the lower end of the frequency range. In the numerical models which included a soft storey, the magnitude of the peak frequencies at the first course at semi-basement level was similar to that resulting from Model 45v2, in the cases which resulted in collapse, and similar to that obtained from Model 63 for the three-storey cases which resisted collapse. On the other hand, at slab over semi-basement level, the peak frequencies obtained at the level of the concrete spreader, in the numerical models which included the presence of a soft storey, were generally within the high end of the range in most of the six- and five-storey cases, whereas, in the case of the four- and three-storey numerical models analysed, the energy content was generally concentrated within the lower frequency range. The exceptions to the latter include Model 89 (six-storey control model including a soft storey at semi-basement level and setbacks at penthouse level), Model 91 (five-storey control model including a soft storey at semi-basement level and setbacks at penthouse level) and Model 71 (five-storey control model including a soft storey at semi-basement level), whereas low peak frequencies resulted for the rest of the cases, irrespective of whether or not they resisted collapse.

Furthermore, it should be noted that the elevated peak frequency values obtained at the first course at semi-basement level and at the slab over semi-basement level from the higher buildings which resulted in collapse and the corresponding lower frequency values obtained from the lower buildings which resisted collapse, as reported above, might seem to be in contradiction with the natural frequencies obtained for the corresponding models when analysed for two eigen modes on upper coralline limestone or clay at Minimum Z as well as the discussion in Section 4.2.1.2 of this thesis with regards to the expected increase in natural frequency with reduction in number of floors resulting from

an increase in stiffness of the structure. However, this apparent discrepancy between these two sets of results is addressed below.

Whereas the values of natural frequency discussed in Section 4.2.1.2 refer to the complete structures analysed for the two main ground types, the peak frequencies at the first course at semi-basement level and at the slab over semi-basement level summarised in Table 34 of Appendix D and discussed above, refer to the predominant frequencies in the acceleration spectrum of an element in the first course and an element positioned immediately beneath the slab over semi-basement level in the analysed numerical models. As explained in Section 3.4.2, in the modelling in ELS®, every masonry block was defined as split in the direction of its length into two elements, such that any shear failure of the blocks could be identified. Therefore, the elements in the left hand side party wall, for which peak frequencies were obtained at the first course of the semi-basement level and at the slab over semi-basement level, consist of masonry blocks of standard height (265 mm) and breadth (228 mm) but with half the standard length (279 mm). The springs between the two abutting halves of every masonry block in the models were defined as having the same material properties as the masonry blocks, whereas those between any two adjacent masonry blocks were defined as having the material properties of local mortar. In the cases which included a soft storey, in view of the presence of the reinforced concrete spreader defined directly beneath the hollow core precast prestressed concrete slabs at slab over semi-basement level, the element for which the peak frequencies were extracted consisted of an approximate length of 1,000 mm from a longer continuous reinforced concrete spreader beam with basic cross-sectional dimensions of 228 mm width and 530 mm height. Concrete springs were defined at the interface between the different elements of the spreader beam. In the latter cases, data was extracted for the element in the spreader beam and not for the first masonry element in the wall beneath the level of the beam in order to ensure that data was extracted from the same positions for every analysed model.

The peak frequency obtained from the acceleration spectrum of an element, which corresponds to half a masonry block or to a 1,000 mm length of spreader beam, cannot coincide with the natural frequency of the structure as a whole, but it is a result of the variation of the acceleration of the element under consideration for the duration of the analysis. Hence, the peak frequency obtained for an element in a wall at the lowest storey of a relatively high building would most likely result in an elevated value because the high overburden provided by the overlying floors would hold the block rigidly in place, therefore containing its movement. On the other hand, a block at the same position in the structure, but with a significantly lower number of storeys above it would be held less rigidly and, hence, its movement would result in a lower peak frequency of oscillation.

The above also suggests that no information with respect to the occurrence of resonance effects can be drawn from the peak frequencies resulting from the acceleration spectrum of elements at the first course of the semibasement level and at the slab over semi-basement level. Insight into the occurrence of such effects in the structures as a whole can only be obtained through a comparison of the natural frequency of the structures when modelled on the corresponding ground type defined at

Minimum Z with the predominant frequencies identified in the acceleration spectrum of the input ground motion record, as discussed in the first part of this Section.

On the other hand, the elements in the ground formation layers, for which predominant frequencies resulting from the acceleration spectrum were extracted, were either located at approximately mid-depth through the respective layers, or, in the case of the 1.5 m thick upper coralline limestone layer, consisted of the full depth of the layer, and in all cases, were connected to the immediately contiguous elements of the same ground formation layer through springs which exhibit the same material properties as the rest of the respective ground layer. Furthermore, the degree of restraint of the elements under consideration would remain constant for the respective subsoil layers in the different cases investigated, and would not be affected in terms of magnitude of overburden by variations in the height of the overlying structures. Hence, the comparison of the predominant frequencies resulting from the acceleration spectrum of the elements in the middle of a ground layer (or consisting of the full depth of a thin ground layer) with the energy content of the frequency spectrum of the input ground motion record, could possibly be used to deduce whether resonance or resonance effects could have occurred in the subsoil layers during the dynamic analysis.

The peak and secondary frequencies, resulting from the elements in the ground formation layers of the analysed numerical models, which fell within the main energy range of the frequency spectrum of the input ground motion record, are highlighted in grey in Table 34 of Appendix D; and, the likelihood of resonance effects in the respective subsoil layer/s is shown in the last two columns of the same table. The information summarised in this table indicates that high peak frequencies resulting from the first mode of vibration ranging between 44.73 Hz – 50.00 Hz were obtained in all analysed numerical models in the case of the clay layers, whereas lower secondary frequencies of 1.86 Hz, 2.93 Hz, 3.03 Hz and 5.96 Hz, which fall within the main energy content of the input ground motion, and almost coincide with the secondary predominant frequencies of this acceleration time series, are also present in the clay layer in 58% of the analysed numerical models. In such cases, it is likely that resonance effects might have occurred in this layer during the dynamic analysis. The likelihood of the occurrence of 'pure' resonance is not being considered in these cases, because these secondary frequencies obtained for an element half way through the depth of the clay layer correspond to significantly lower values of power spectral density and would, hence, in accordance with the suggestions made by Murty et al. [54], probably not have been sustained long enough for 'pure' resonance to occur. It must be stressed again that, in view of the increase in the compressive strength, the Young's Modulus and the Shear Modulus of clay used in the numerical models (from the actual properties of this type of subsoil present in the Maltese Islands), in addition to the reduction of the density of clay to 0 kg/m3, the results obtained for this layer might not reflect actual behaviour and the peak frequencies obtained are not necessarily indicative of the local scenario. The high discrepancy between the peak frequencies resulting for this ground formation layer, and those reported by Vella et al. [195], might be due to these variations in the material properties specified in the numerical models. Hence, the discussion of the results obtained in the present study is being made solely in the context of the behaviour of the analysed numerical models.

The peak frequency for upper coralline limestone in the numerical models which were analysed on a 30 m thickness of this material resulted as 27.93 Hz in both the six- and the five-storey models. A secondary frequency of 2.93 Hz, hence, coinciding with the main frequency range of the input ground motion record and with one of its secondary predominant frequencies, was also obtained in both cases, therefore, suggesting the occurrence of resonance effects in this subsoil layer. In the three numerical models analysed over a 30 m thick upper coralline limestone layer overlying a 30 m thick clay layer (namely, Models 44v2 and 50, which consist of the six- and five-storey control models, respectively, and Model 129 which consists of the six-storey existing Xemxija Building Number 0011) a peak frequency corresponding to the first vibration mode of 1.86 Hz, and a secondary frequency at 5.96 Hz were obtained in all three cases. Both these frequencies fall within the main energy content of the input ground motion and coincide with secondary predominant frequencies of this acceleration time series, therefore, suggesting the likelihood that resonance effects could have influenced the behaviour of this subsoil layer in these models. While in all the models analysed on 1.5 m thick upper coralline limestone over 60 m thick clay, the upper coralline limestone layer exhibited a predominant frequency and, at least, one secondary frequency, which fell within the main energy range of the input ground motion record, not all of these frequencies coincided with, or were sufficiently close to, a predominant frequency in the main energy range of the input seismic accelerations. A peak frequency in the upper coralline limestone layer of 2.93 Hz resulted in 88.0% of the numerical models analysed on 1.5 m thick upper coralline limestone over 60 m thick clay, whereas 82.4% of the numerical models analysed on this ground type resulted in a secondary frequency at 5.96 Hz. Resonant effects cannot be excluded in the upper coralline limestone layer of these numerical models since these frequencies coincide with the predominant frequencies in the main energy range of the input ground motion.

Even in the case of upper coralline limestone, however, the discrepancy between the peak frequencies obtained from the numerical models and those reported by Farrugia et al. [191] and Vella at al. [195], is immediately apparent. This discrepancy, though of a significantly lower degree than in the case of the clay layer, might be due to the high values of density and shear modulus assigned to upper coralline limestone in the numerical models. This apparent over-estimation in the material properties specified for upper coralline limestone becomes evident, when the corresponding value of shear wave velocity derived from these material properties is compared to the in-situ values obtained by Farrugia et al. [191] for this subsoil layer as explained in Section 4.2.1.1 of this thesis. This comparison suggests that a discrepancy of, at least, the order of 3 times was evidenced in the shear wave velocity values of upper coralline limestone. This, therefore, indicates that the specified material properties for this ground layer represented a significantly stiffer unfractured material than is present in parts of the Maltese Islands, as reported by these authors. Furthermore, this excessive stiffness attributed to the upper coralline limestone layer in the numerical models, through the specified material properties, in combination with the 0 kg/m3 value of density specified for clay, might have resulted in an excessively

high impedance contrast[25] between the two subsoil layers. While most international studies consider the transmission of vibrations from the bedrock through a softer overlying ground layer, in the two-layer systems overlying the bedrock which were investigated in the present study, the resulting reduced transmission of vibrations from the clay layer through the upper coralline limestone layer might explain the relatively consistent energy distribution in the frequency spectra of the elements in the upper coralline limestone and clay layers, as well as, the little or no variation in magnitude of the peak frequencies in these layers, in all the numerical models which were analysed on a two-layer ground formation system. While, as mentioned at the start of this Section, soil-structure interaction effects are triggered when buildings are constructed on a flexible subsoil [46] [47] [48] [49] [51], the presence of an extremely stiff rock layer over the more flexible clay layer might have severely reduced the transmission of vibrations from the clay layer to the overlying structure, and vice versa, in the numerical models. However, this effect would not occur in the real scenario on the Maltese Islands, where soil-structure interaction would most likely occur in most areas where a fractured upper coralline limestone layer is present, as suggested by the shear wave velocity values reported by Farrugia et al. [191], and the limits on shear wave velocities suggested by Reza Tabatabaiefar et al. [49] for the occurrence of the transmission of vibrations to and from the building. This observation, however, would have to be confirmed through further numerical modelling, by investigating the change in the maximum accelerations and peak frequencies in the ground layers and in the building following variations in the stiffness of the ground layers.

In addition to the considerations discussed above, failure on the side of ELS® to accurately model the transfer of vibrations between the two subsoil layers in view of the 0 kg/m3 value of density specified for clay cannot be excluded. It must be pointed out that ELS®, the numerical modelling software program used in this study, is mainly intended for the analysis of structures under static, dynamic, blast and impact loads, and is not specifically designed for the modelling and analysis of site response under different geological ground conditions. The results obtained in the present study, with respect to the accelerations and displacements extracted from elements in the ground layers (when modelled as three-dimensional elements), and at a number of positions throughout the height of the modelled buildings and the variation in the distribution of stress contours on the outer surfaces of these three-dimensional blocks representing the subsoil layers throughout the analysis (as demonstrated in Figures 4-13, 4-14 and 4-15 for Model 50) seem to suggest that an acceptable transfer of seismic excitations from the bedrock through the soil layers to the overlying structure occurs during the analysis. Furthermore, an amplification or reduction of the signal, as expected in accordance with the subsoil characteristics, is observed.

[25] Impedance is the product of the density of the soil and its shear wave velocity, while the impedance ratio (or contrast) is the ratio of the impedance of the lower ground layer to that of the overlying ground layer [53].

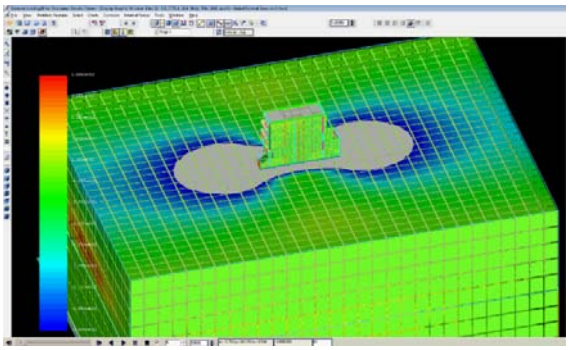

(a) Analysis frame 61 (static loading stage)

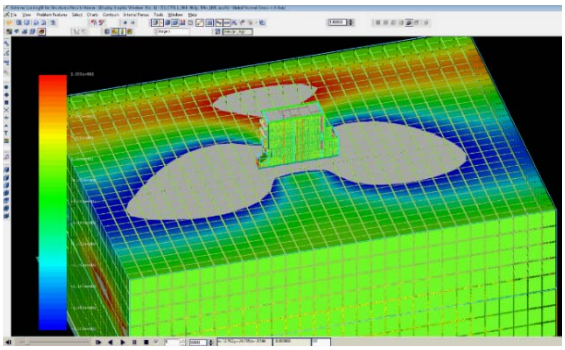

(b) Analysis frame 101 (end of static loading stage)

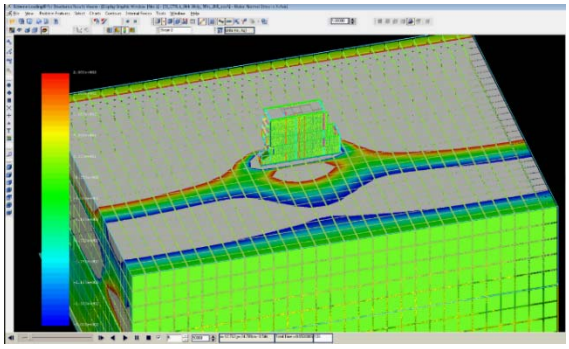

(c) Analysis frame 106 (dynamic loading stage)

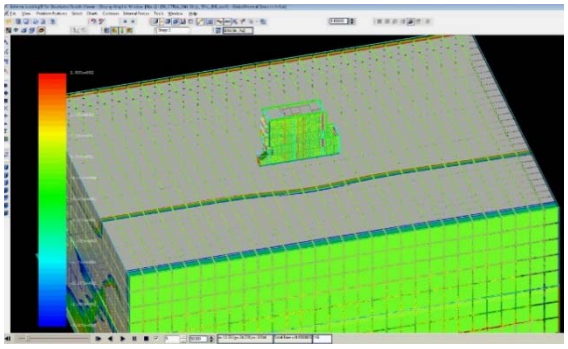

(d) Analysis frame 116 (dynamic loading stage)

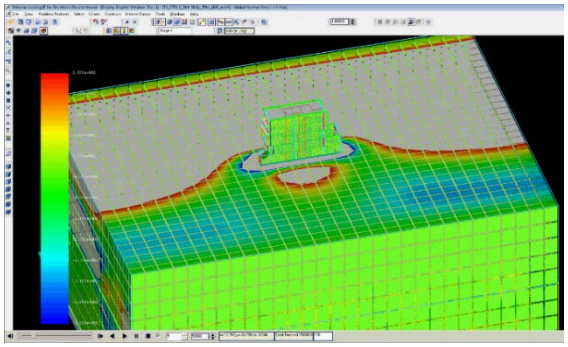

(e) Analysis frame 176 (dynamic loading stage)

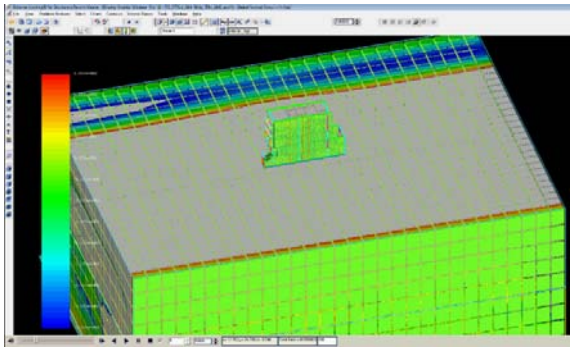

(f) Analysis frame 186 (dynamic loading stage)

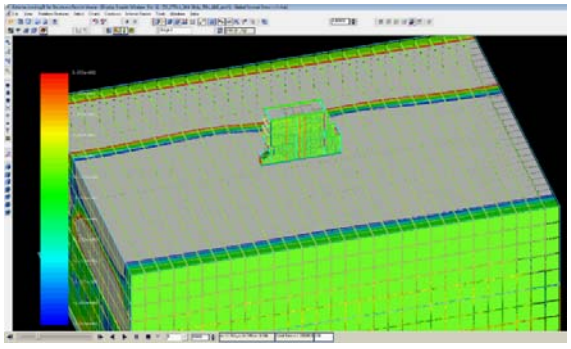

(g) Analysis frame 236 (dynamic loading stage)

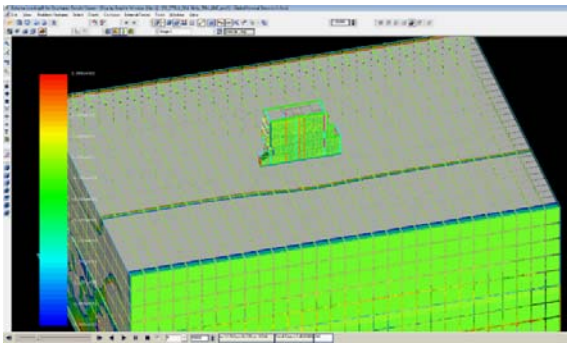

(h) Analysis frame 246 (dynamic loading stage)

Figure 4-13 Stress contours in subsoil layers of Model 50 (30 m thick upper coralline limestone layer over 30 m thick clay layer) during the static loading stage and during the dynamic loading stage, up to analysis frame number 246.

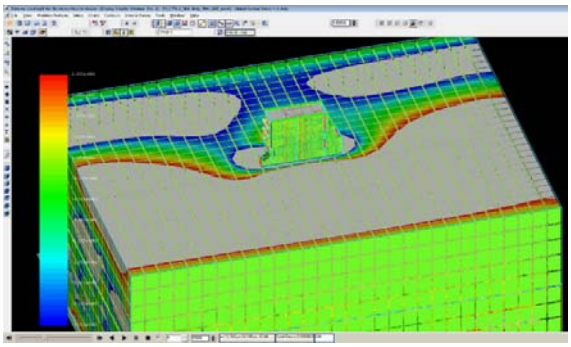

(a) Analysis frame 346 (dynamic loading stage)

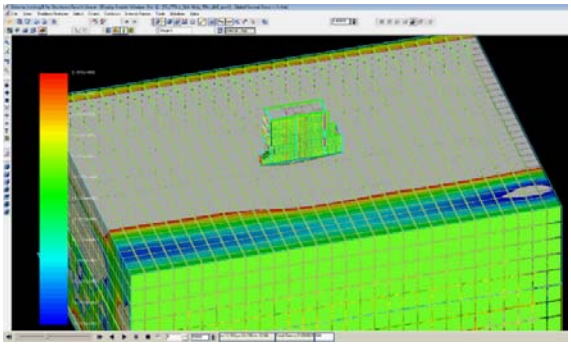

(b) Analysis frame 366 (dynamic loading stage)

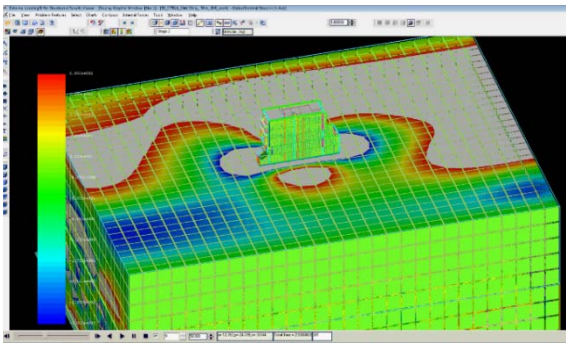

(c) Analysis frame 381 (dynamic loading stage)

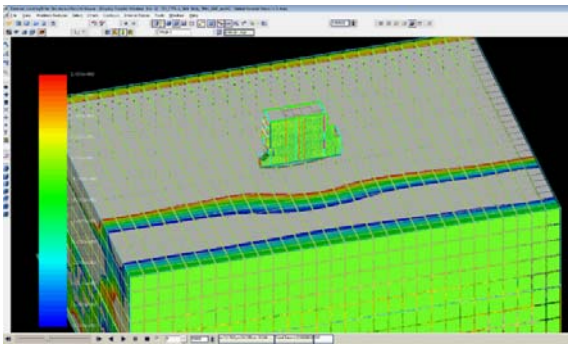

(d) Analysis frame 391 (dynamic loading stage)

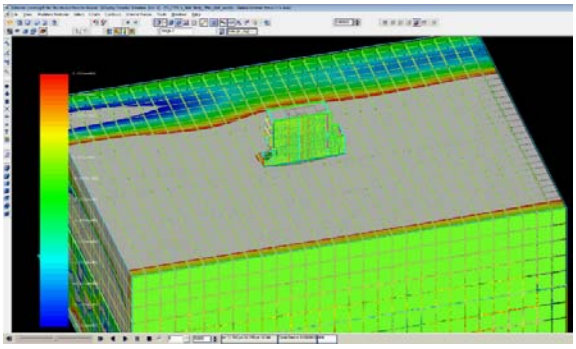

(e) Analysis frame 486 (dynamic loading stage)

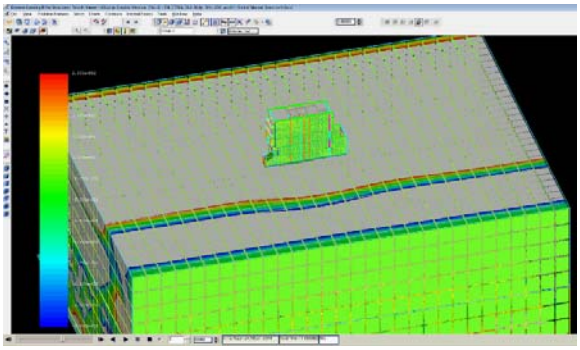

(f) Analysis frame 586 (dynamic loading stage)

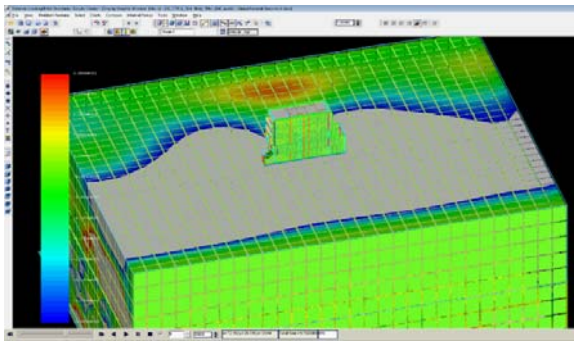

(g) Analysis frame 616 (dynamic loading stage)

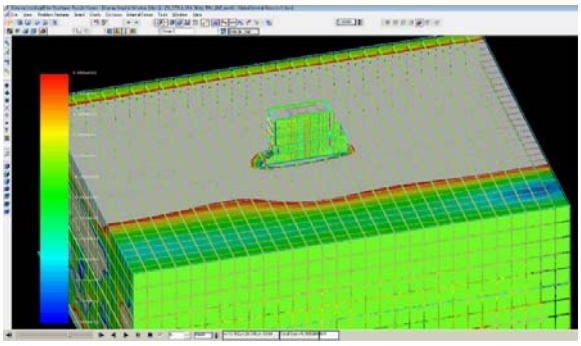

(h) Analysis frame 671 (dynamic loading stage)

Figure 4-14 Stress contours in subsoil layers of Model 50 (30 m thick upper coralline limestone layer over 30 m thick clay layer) during the dynamic loading stage between analysis frames 346-671.

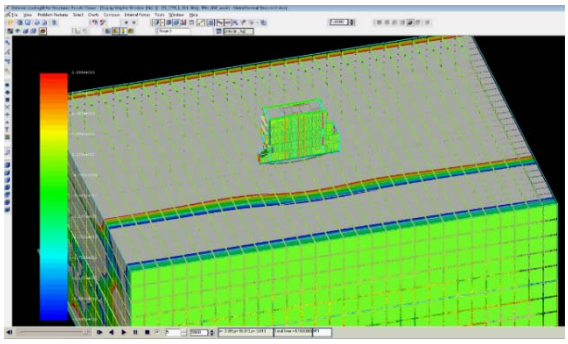

(a) Analysis frame 911 (dynamic loading stage)

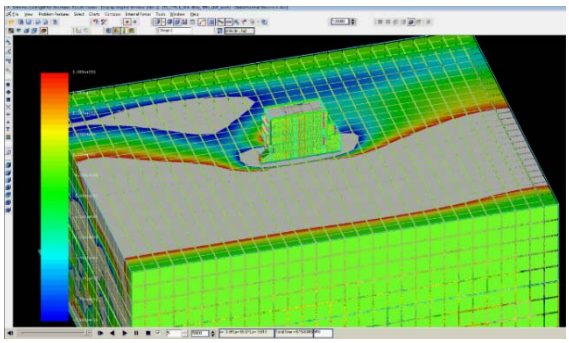

(b) Analysis frame 916 (dynamic loading stage)

Figure 4-15 Stress contours in subsoil layers of Model 50 (30 m thick upper coralline limestone layer over 30 m thick clay layer) during the dynamic loading stage between analysis frames 911-916.

However, even though the software is marketed as being capable of representing accurately soil-structure interactions, since documentation regarding a specific validation exercise of the software program with respect to soil-structure interaction effects has not been traced by the author, and since no information regarding modelling of ground layers or the assumed constitutive models for the ground layers is present in the software's user manuals, the consideration that peak frequency, acceleration and displacement results in the ground layers, and throughout the modelled structures, could have been affected by software or modelling limitations, or by limitations imposed by the specified input parameters, which had to be varied in order to eliminate recurrent stability errors, cannot be excluded. Moreover, since spring supports could not be specified along the external faces of the three-dimensional elements representing the ground layers in ELS®, and in order to avoid as much as possible that the reflection of vibrations at the outer faces of the three-dimensional ground elements influenced the behaviour of the analysed structures, the representation of the infinite nature of the ground layers was attempted by modelling the three-dimensional blocks representing the ground layers with overall plan dimensions of 100 m width and 137 m breadth, which dimensions correspond to fifteen times the width and around six times the length at semi-basement level of the analysed structures respectively in the case of the single building numerical models. It is acknowledged that these dimensions were selected arbitrarily, and that, in view of time limitations and limitations on analysis time and the maximum number of elements which could be handled by the software, the variation of the structural response to changes in the size of these three-dimensional blocks or the number of elements in which they were subdivided, was not investigated in the present study. The dimensions of the three-dimensional blocks representing the ground layers were kept constant throughout all the analysed numerical models, while the number of elements in which these blocks were subdivided were altered only in the case of the three-building control numerical models, in view of the licence limit on the total number of elements supported by the software.

4.2.3 Comparison of variation in structural response parameters recorded at slab over semi-basement level

In his 2007 review of the available methods for the assessment of the collapse resistance of structures in the presence of earthquake forces, Villaverde [196] concludes that an accurate estimate of structural resistance to collapse can be obtained through a finite element analysis which accurately predicts the deformed shape of the structure under seismic loads, and updates this deformed shape at every analysis time step. The close examination of the variation of a particular structural response parameter throughout the analysis, such as the lateral displacement at a particular position in the model, allows the identification of the start of failure at the point at which an abrupt increase in the magnitude of the response parameter is recorded during the numerical analysis. The 'start of failure' of the numerical models analysed in the present study was identified as the point, during the dynamic analysis, where irreversible displacement in the x- (transverse) direction started at slab over semi-basement level. The reasons governing the choice of displacement direction, and the selected position in the building models for assessing this response parameter, were already discussed in Section 4.2 of this thesis. The main interpretation of the variation in accelerations and displacements in the analysed numerical models, which follows in the subsequent sections of this thesis, was based on the results obtained at the corresponding times at which the onset of collapse was identified in every analysed case. The approximate time of start of collapse was identified through the x-displacement–time plots, extracted for every analysed numerical model, after which, a more accurate identification of the analysis time was obtained through the examination of the raw displacement data in the region of the time identified from the plots.

4.2.3.1 Displacement behaviour

The determination of the start of collapse led to the identification of three main displacement behaviours of the analysed buildings, under static and dynamic loads, prior to the onset of collapse. These include:

a) Type A:

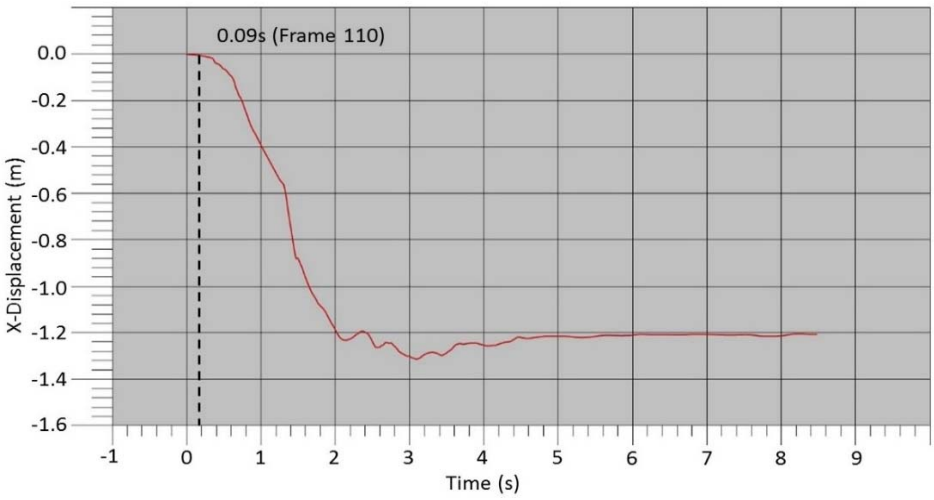

Figure 4-16 X-displacement - time plot for element at slab over semi-basement level for Model 46, 6-storey control numerical model analysed on a 60 m thick clay layer modelled as a 3-dimensional block.

A marginal (varying) negative x-displacement is present during the static loading stage and the first part of the dynamic loading stage which is followed by a sudden increase in negative displacement. The time of start of failure, defined by the start of irreversible x-displacement, was determined at the point when the gradient of the displacement – time plot increased. Figure 4-16 indicates a Type A x-displacement–time behaviour in Model 46.

b) Type B:

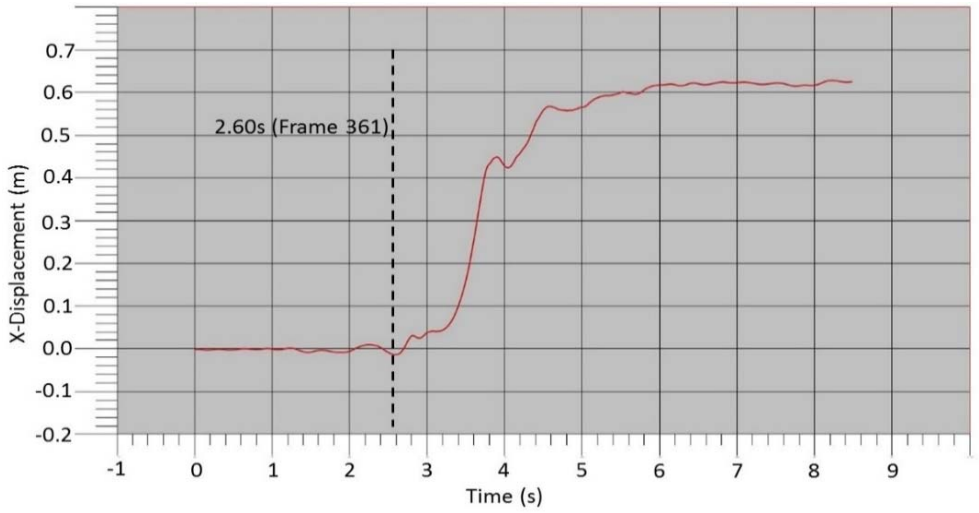

Figure 4-17 X-displacement - time plot for element at slab over semi-basement level for Model 73, 4-storey control numerical model with soft storey at semi-basement level analysed on a 1.5 m thick upper coralline limestone layer over a 60 m thick clay layer modelled as 3-dimensional blocks.

A marginal varying positive /negative x-displacement is present during the static loading stage and the first part of the dynamic loading stage, which, following a dip (maximum negative displacement) or a peak (maximum positive displacement) displaces irreversibly in the positive or negative x-direction respectively. The time of start of failure was determined at the time of the first analysis frame after the dip or peak in x-displacement. Figure 4-17 indicates a Type B x-displacement–time behaviour in Model 73.

c) Type C:

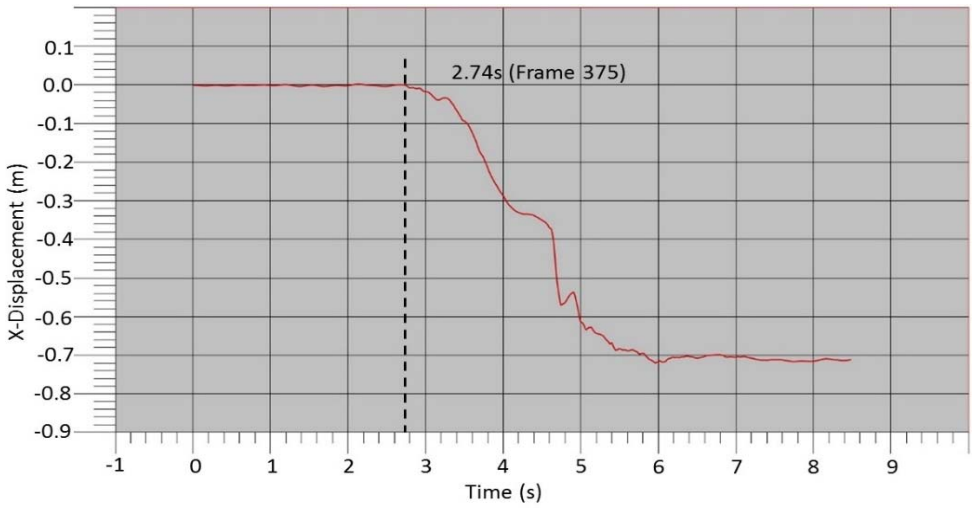

Figure 4-18 X-displacement - time plot for element at slab over semi-basement level for Model 57, 5-storey control numerical model analysed on clay specified at Minimum Z.

A marginal (varying) negative x-displacement during the static loading stage and, in most cases, the first part of the dynamic loading stage is present, which is followed by a marginal variation between negative and positive displacement values for part of the dynamic loading stage, until the displacement increases irreversibly in the negative x –direction. The time of start of failure was determined at the start of the increase in gradient of the x-displacement–time plot. Figure 4-18 indicates a Type C x-displacement–time behaviour in Model 57.

As previously explained, only the behaviour of the structures in the x-direction was investigated in this study. While a vertical negative displacement, during the static loading stage, could be attributed to the compression of the mortar under the increasing static loads, Casolo et al. [197] suggest that the recorded marginal x-displacements under static loading could be due to the presence of irregularities either in the geometry of the analysed structures, or in the generation of the mesh in the numerical models (such as, at sudden changes in cross-section or at the junction between different elements). The latter is not likely to occur in models analysed with ELS®, since partial connectivity is possible when a member, which is split into a finer mesh, is physically touching another member (or an abutting area of the same member which is modelled separately), which is subdivided into smaller elements [173] as long as: i) drastic differences in the element sizes resulting after meshing are avoided (as was done in the numerical models analysed for this study), and ii) the aspect ratio of the element sizes resulting from the meshing does not exceed 3 [162] [198] (Dr. Huda Helmy, Consultation Department, Applied Science International, LLC, personal communications by email, huda@appliedscienceint.com, 9th September 2015 and 13th April 2016, respectively). Even though the differences between the three types of displacement behaviour (Types A-C), prior to the start of collapse, might seem only marginal, the consistency in the displacement behaviour types, corresponding to the presence of particular characteristics, as evidenced from the results summarised in Tables 35 to 38 of Appendix D, suggests that the respective behaviours might be a consequence of the diverse stiffnesses of the analysed structures, and the variation in the stiffness of the numerical models throughout their height, and throughout the duration of the analysis. Tables 35 and 36 of Appendix D indicate that all the single building control numerical models and the models which include one additional seismic vulnerability characteristic in addition to the control model layout (with the exception of Models 69, 71 and 73, which include a soft storey at semi-basement level) exhibit a Type C behaviour, at an overall height of one storey higher than that of the corresponding numerical model which resisted collapse. On the other hand, a Type A displacement behaviour was identified in the equivalent models with a higher number of storeys. As explained in Section 4.2.1, the numerical models which include either a double height space between Levels 0 and 1 (Models 99, 101 and 103), or setbacks at penthouse level (Models 79 and 81), as the only additional seismic vulnerability characteristic to the control model, resulted in only a marginal decrease in natural frequency in the transverse direction when compared to the control model in the case of the former characteristic, and an increase in natural frequency in the six- and five-storey models in the case of the latter characteristic. Hence, the very close or higher natural frequency of these numerical models, when compared to the control model, suggests a similar or higher overall model stiffness when compared to the corresponding control model, which would justify

a similar displacement behaviour. On the other hand, the models, which included a soft storey at semi-basement level (Models 69, 71 and 73), resulted in a decrease in natural frequency in the transverse direction of between 8% to 28% when compared to the control model. The six-, five- and four-storey models, which included a soft storey as the only seismic vulnerability characteristic in addition to the control model layout, all exhibited a Type B displacement behaviour, before the start of failure at slab over semi-basement level. The same displacement behaviour was identified in the numerical models which include a soft storey at semi-basement level and a double height space between Levels 0 and 1 (Models 109, 110 and 113). This further suggests that the 250 mm thick slab bounding the void of the double height space on three sides, and the relatively small proportions of the void in the slab, which were specified in the models which included a double height space in this study, partially diminished the expected structural response linked to the formation of collapse mechanisms, resulting from a localised reduction in floor stiffness, and the reduced restraint of the party wall directly abutting the void. This led to the displacement behaviour, prior to the onset of failure of the control models which include both a soft storey and a double height space, to be very similar to that of the models which include only a soft storey.

The numerical models which include a soft storey at semi-basement level and setbacks at penthouse level (Models 89, 91 and 93), exhibited a Type C behaviour at six storeys, and a Type B behaviour at five and four storeys, whereas the numerical models which include all three additional seismic vulnerability characteristics (soft storey at semi-basement level, setbacks at penthouse level and double height space between Levels 0 and 1, namely Models 119, 121 and 123), resulted in a Type B displacement behaviour at six floors, and a Type C displacement behaviour at five and four floors. Type B displacement behaviour was also identified in the two six-storey numerical models of the existing Xemxija Building Number 0011 (Models 128 and 129). This building includes a large open plan without intermediate walls at semi-basement level, the termination of main loadbearing walls at slab over semi-basement level, a double height space between the floor directly beneath the penthouse and the penthouse level, and setbacks at penthouse level. Hence, it includes a significant reduction in stiffness at the very bottom and at the very top of the building. On the other hand, the two-building and three-building control models resulted in a Type B behaviour at six and five storeys and a Type C behaviour at a height of four storeys.

It was noted that, in most analysed cases which resulted in collapse, the main transverse direction of collapse was the negative x- direction. This was probably due to the reduced restraint of the left hand side party wall, in view of the limited number of cross walls framing into it. This reduced restraint is present in every 'typical' floor plan level and is, therefore, consistent throughout the height of the control numerical models, in models which include setbacks at penthouse level or a double height space, and from Level 0 upwards in the models which include a soft storey at semi-basement level.

It appears that, few international studies have investigated the displacement behaviour of masonry structures under seismic loads (such as the studies by Uva et al. [199] and Casolo et al. [197]), and even fewer studies have considered structures, which result in partial or total collapse (such as the study

carried out by Valente et al. [35]). Moreover, the author has been unable to trace similar studies, which investigate in comparable detail, the variation in displacement behaviour of masonry structures, which include different building characteristics, with the aim of gaining insight into the influence, which the presence of particular characteristics have on the seismic vulnerability of these structures. The examination of the above results, however, seem to suggest that a Type A displacement behaviour prior to the onset of collapse at slab over semi-basement level is exhibited by structures which have a higher stiffness, and a relatively constant rigidity distribution throughout their height, hence, resulting in building oscillations, which are not large enough to cause the building to displace bodily from the negative x-displacement range to the positive x-displacement range.

On the other hand, a Type B displacement behaviour seems to be associated with more flexible models which have a reduced stiffness at particular floors, as in the case of the numerical models of the six-storey existing Xemxija building (Models 128 and 129), the control numerical models which include a soft storey (Models 69, 71 and 73) , the six-storey numerical model which includes the combination of a soft storey with a double height space (Model 109), and the five- and four-storey numerical models (Models 91 and 93) which include a soft storey and setbacks. The localised reduction in stiffness of these models and, hence, their localised increased flexibility, is most likely to cause the structures to go through larger displacements ranging between positive and negative displacement values, as they oscillate under the effect of seismic excitations in view of the higher proportion of seismic forces acting at the lowermost level . This observation is in accordance with the explanation of the consequences of the localised increased flexibility of structures, which include a soft storey given by Guevara-Perez [56] and FEMA 454 [57], where the higher displacements in the walls of the soft storey are attributed to the higher concentration of seismic forces acting at this level, because of its reduced stiffness when compared to the overlying levels.

The exceptions to this trend are the six- and five-storey two-building and three-building control numerical models, which consist of the same typical floor layout at every floor, however, which include two or three buildings with shared party walls respectively. While, the single-building numerical models analysed in this study have a length-to-width ratio on plan of around 2.75 at all storey levels between Level 0 and the floor of the penthouse, the consideration of the combined action of two- or three-building control numerical models would result in a decreased length-to-width ratio to around 1.37 and 0.92, respectively. Therefore, a displacement mode associated with a stiffer structure would have been expected in such models in view of the less rectangular plan proportions, and the additional degree of restraint which buildings in an aggregate were observed to give each other, in international studies carried out by Formisano et al. [28] [30], Ferreira et al. [66] and Ulrich et al. [200], in particular, in the case when the aggregate is composed of similar structures and when all the buildings in the aggregate have the same overall height. However, a close study of the failure mode of these structures through the exported simulations suggests that collapse is initially triggered off by the buckling failure of the shared party walls located at the front end of the structures at semi-basement level. Failure quickly progresses to the external party walls at the same level, therefore, causing the structures to dip forward, leading to the almost simultaneous failure of the overlying walls at Level 0. Figures 4-19

to 4-30 include snapshots taken from the simulations of the six-storey two-building (Model 130) and three-building (Model 138) control numerical models at the end of the static loading stage (frame 101), and at various times throughout the dynamic loading stage.

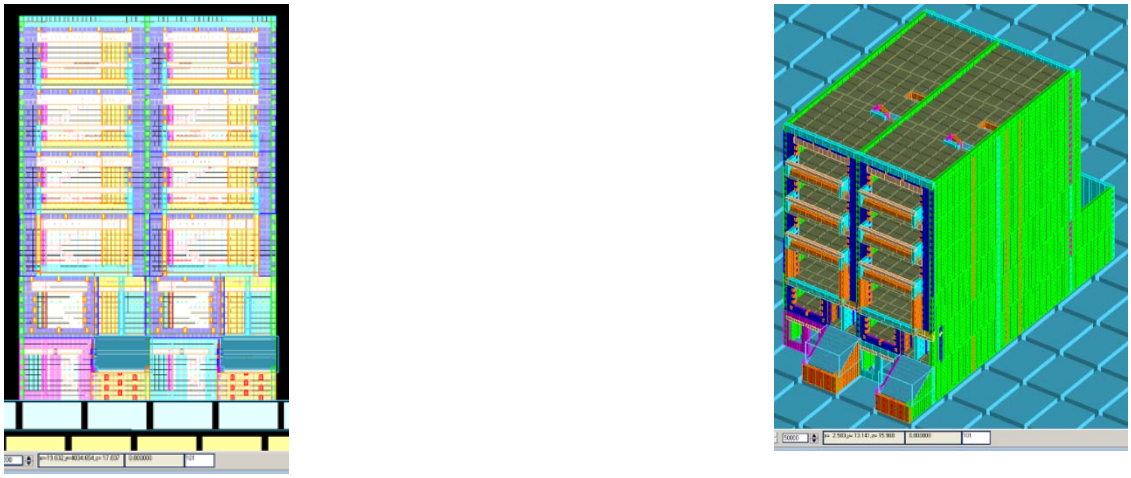

Figure 4-19 Front and isometric view of two-building control model (Model 130) at frame 101 (end of static loading stage).

Figure 4-20 Front and isometric view of two-building control model (Model 130) at frame 141 (dynamic loading stage).

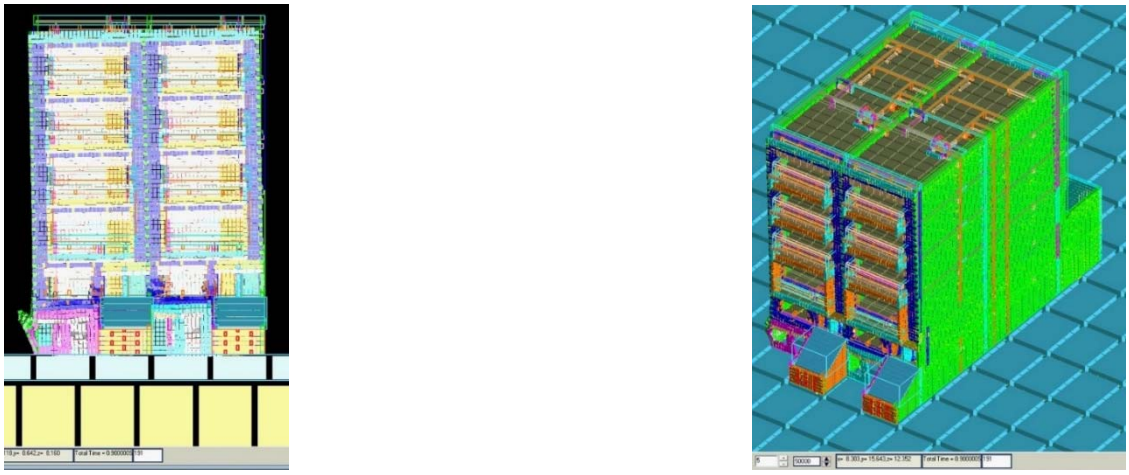

Figure 4-21 Front and isometric view of two-building control model (Model 130) at frame 191 (dynamic loading stage).

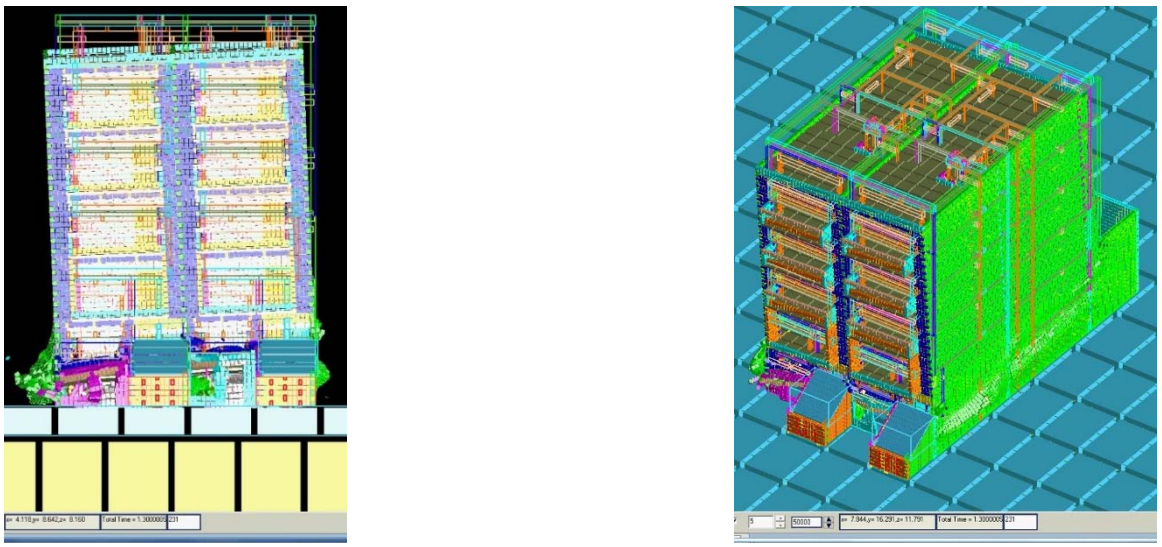

Figure 4-22 Front and isometric view of two-building control model (Model 130) at frame 231 (dynamic loading stage).

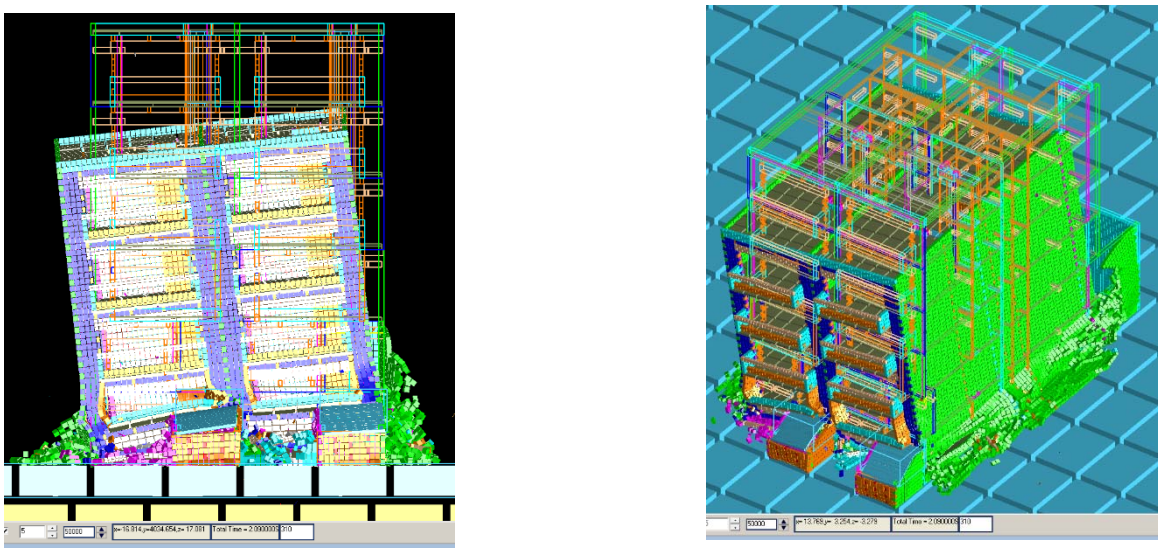

Figure 4-23 Front and isometric view of two-building control model (Model 130) at frame 310 (dynamic loading stage).

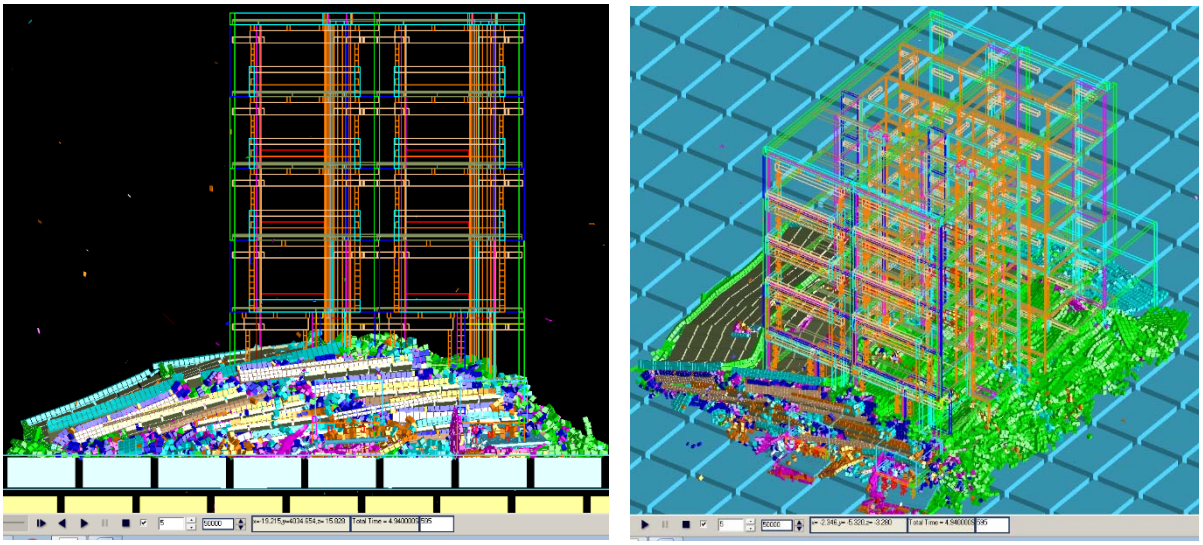

Figure 4-24 Front and isometric view of two-building control model (Model 130) at frame 595 (dynamic loading stage).

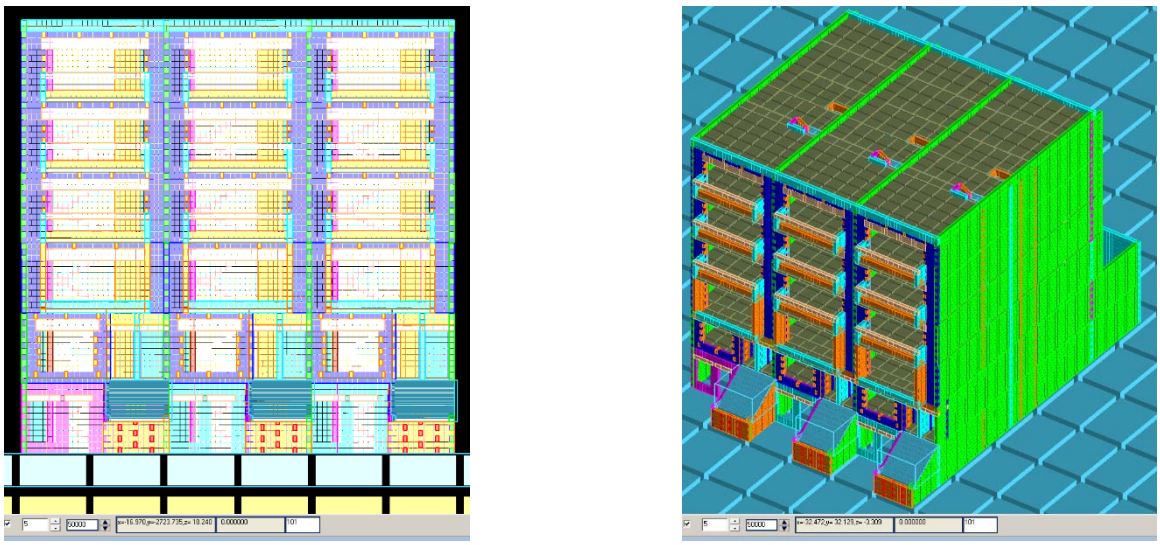

Figure 4-25 Front and isometric view of three-building control model (Model 138) at frame 101 (end of static loading stage).

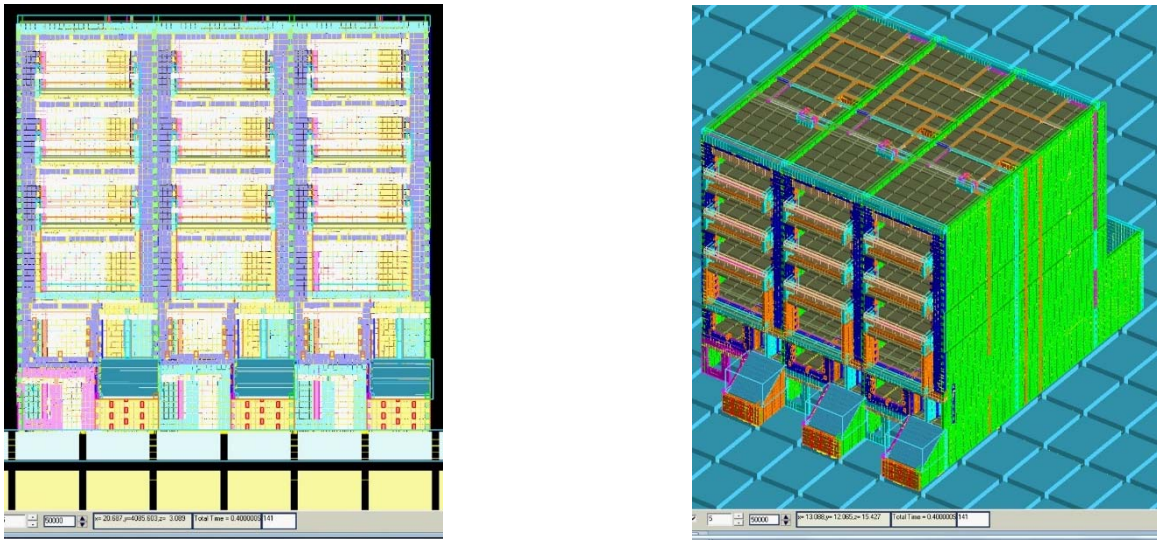

Figure 4-26 Front and isometric view of three-building control model (Model 138) at frame 141 (dynamic loading stage).

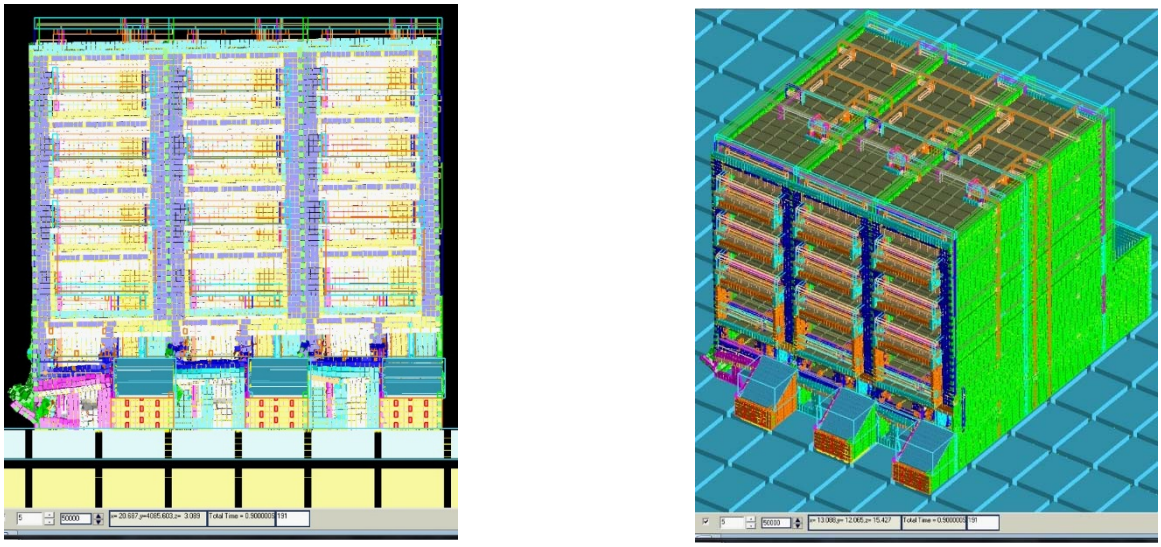

Figure 4-27 Front and isometric view of three-building control model (Model 138) at frame 191 (dynamic loading stage).

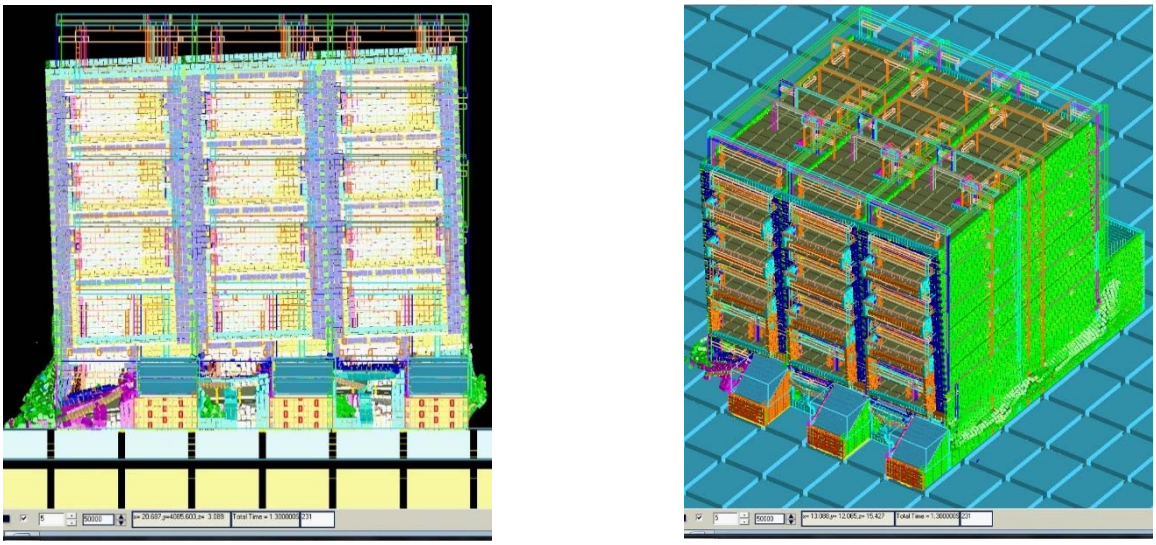

Figure 4-28 Front and isometric view of three-building control model (Model 138) at frame 231 (dynamic loading stage).

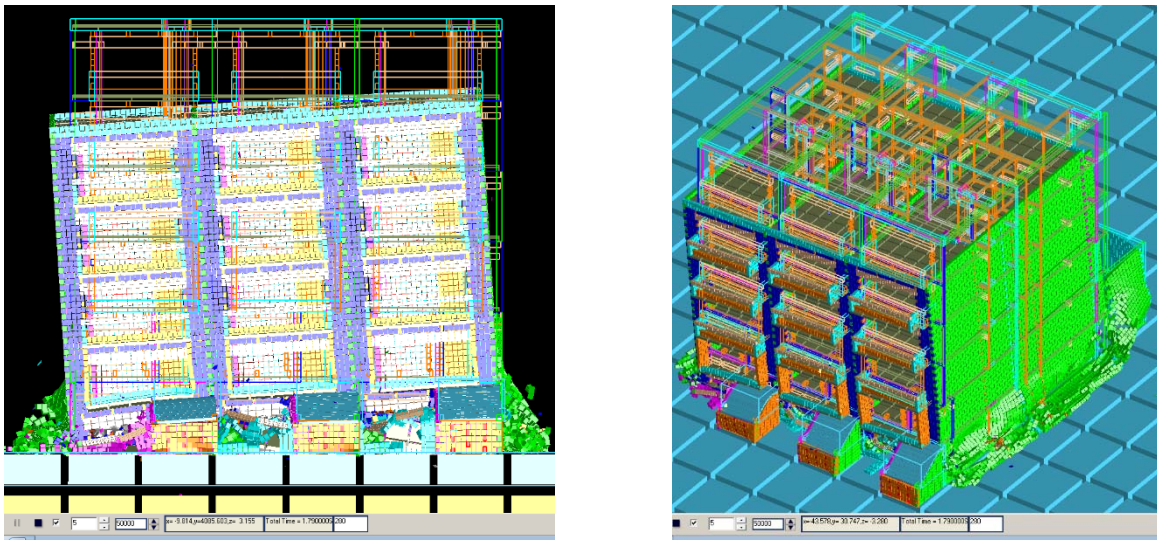

Figure 4-29 Front and isometric view of three-building control model (Model 138) at frame 280 (dynamic loading stage).

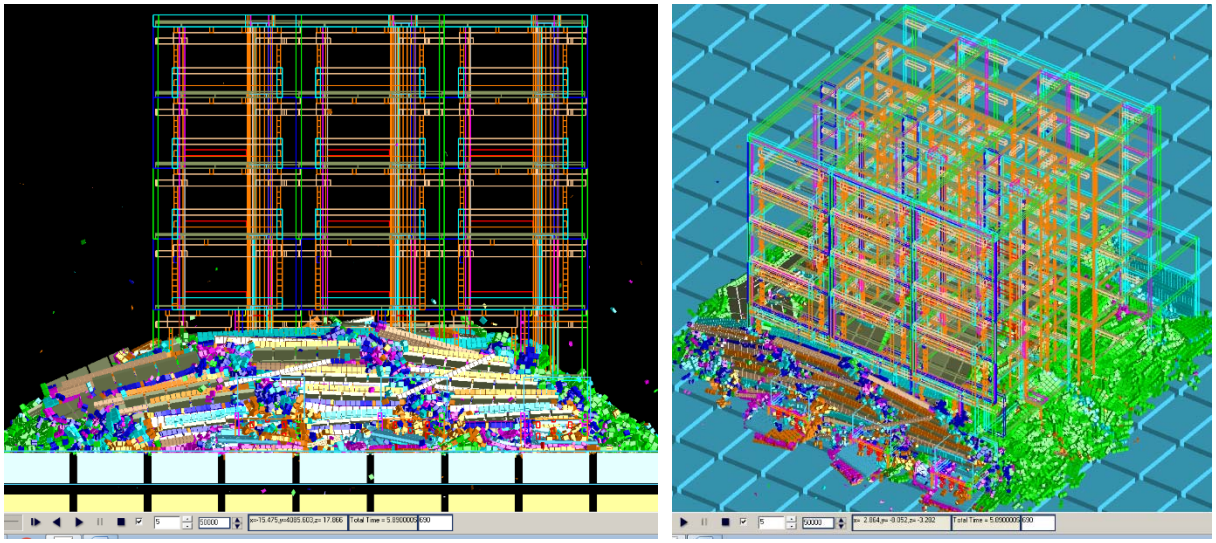

Figure 4-30 Front and isometric view of three-building control model (Model 138) at frame 690 (dynamic loading stage).

Bernal [201] explains that unless the gravitational loads acting on a structure are not too close to its loadbearing capacity to ensure stability under static loading conditions, these permanent loads do not typically have a significant bearing on the inelastic seismic response of the structure. However, the total characteristic (unfactored) gravity load at the top of the shared party wall, in line with the front room at semi-basement level, resulting from the overlying storeys in the two-building and the three-building control numerical models calculated in accordance with Clause 3.2.4(2)P of Eurocode 8: Part 1 [4] (which is equivalent to the sum of the characteristic permanent and imposed loading specified as gravity loads in the analysed numerical models) amounts to around 356 kN/m in the six-storey models and 288 kN/m in the five-storey cases. This load would be very close to exceeding the masonry wall's bearing capacity, especially considering the large unrestrained length of the party wall present between the front façade and the first intersecting wall (towards the rear end of the building) in the typical floor layout. Hence, under the effect of seismic excitations, even minor displacements in the overlying structure are likely to give rise to the formation of large moments in the semi-basement party walls due to P-delta effects, which might lead to their failure.

The close analysis times at which the onset of collapse was identified at slab over semi-basement level in the corresponding six-, five- and four-storey two-building and three-building control numerical models[26] could be interpreted as indicating only a marginal improvement in seismic resistance between the two- and the three-building cases investigated. A low increase in natural frequency between the corresponding two- and three-building cases is also reported in Table 31 of Appendix D (namely, 4% to 7% when analysed on upper coralline limestone at Minimum Z, and 6% to 12% when analysed on clay at Minimum Z). On the other hand, the marginal difference between the analysis times at the onset of failure in the corresponding six- and five-storey models, together with the significant delay in the start of collapse resulting in the four-storey cases when compared to the higher counterparts, might be also be considered to confirm this proposed failure mechanism for the six- and five-storey two- and three-building control numerical models. Hence, the oscillations, which result in varying displacements throughout the positive and the negative displacement range exhibited by the six- and five-storey two- and three-building control numerical models before the start of failure, are most likely the result of the loss in stiffness of the walls at semi-basement level, due to failure arising from P-delta effects in view of the high loads from the overlying storeys and the building displacements

[26] Table 38 in Appendix D indicates that the start of collapse at slab over semi-basement level was located at frame 190 (equivalent to 0.89 s of dynamic analysis) in the six-storey two-building control numerical model (Model 130), at frame 194 (equivalent to 0.93 s of dynamic analysis) in the equivalent five-storey numerical model (Model 132) and at frame 580 (equivalent to 4.79 s of dynamic analysis) in the four-storey case (Model 134). In the three-building control numerical models, start of failure at slab over semi-basement level was identified at frame 185 (equivalent to 0.84 s of dynamic analysis) in the six-storey model (Model 138), at frame 214 (equivalent to 1.13 s of dynamic analysis time) in the five-storey case (Model 140) and at frame 582 (equivalent to 4.81 s of dynamic analysis) in the corresponding four-storey numerical model (Model 142).

triggered off by the seismic excitations. Alternatively, the x-displacement behaviour resulting from the two- and three-building control models could suggest that, while the less rectangular proportions of the two- and three-building models result in an increase in stiffness, which is expected to lead to an increased seismic resistance, the consequent increase in seismic mass, particularly at increased overall building heights and, hence, the higher inertia of the analysed structures, consisting of more than one building, causes a higher base shear which exceeds the capacity of the transverse walls at the lowest storey level.

In most investigated cases, a Type C displacement behaviour, before the identification of the start of failure at slab over semi-basement level, is associated with a later analysis time for the onset of collapse, and is exhibited by the numerical models which are one storey higher than the corresponding model which resists collapse for the same case (or two storeys, in the case of the five- and four-storey control models with a double height space, and the corresponding models which include a soft storey, setbacks and a double height space in combination). Therefore, this behaviour, appears in models which have a higher resistance to the seismic excitations, but which still fall short of the demand imposed by the input simulated ground motion record. The varying displacement, within the positive and negative displacement range, suggests that the structure is caused to oscillate through a larger displacement range as it approaches the point in the analysis when the start of collapse was identified. These large oscillations could be the result of the reduced structural stiffness arising from the formation of cracks, as the structure approached collapse.

4.2.3.2 Comparison of the analysis time at onset of failure and the relative displacements at slab over semi-basement level in the single building control models

As explained in Section 4.2.3.1, a thorough review of studies investigating the seismic vulnerability of masonry structures through numerical modelling techniques, carried out by the author, suggests that past studies were generally directed towards the comparison of the seismic behaviour, exhibited by structures through different modelling techniques and analysis methods [202], with scaled laboratory models [203], or with actual buildings damaged after seismic events [121]; the development of fragility [40] or capacity curves [204] [205] [126] and the use of these methods for the seismic assessment of an urban area [65]; and the study of collapse mechanisms [206]. Apart from a few exceptions, such as the work presented by Formisano et al. [28] [29] [30] [31] and Senaldi et al. [108], on the parameters affecting the seismic vulnerability of masonry buildings located in aggregates and the studies performed by Casolo et al. [207] [208] [197] and Valente et al. [35] on historical masonry towers, (where, however, the building typology investigated is completely different from the one considered in the present study), past studies involving numerical analysis of masonry structures under seismic loads do not generally investigate the seismic vulnerability associated with specific building characteristics, particularly from the point of view of the variation in the time of start of failure, the relative displacements at the start of failure, and the maximum displacement and maximum acceleration prior to failure, as was attempted in this study. Furthermore, when maximum displacements were investigated in published studies, the maximum displacement of the centroid of a particular floor level (in most cases, the topmost roof) was considered, and not the displacement of a

particular masonry block in the party wall at a lower floor level, as in the present study[27]. Hence, direct comparison of the results obtained in the present work to those obtained in previous studies could not be carried out, and the interpretation of the behaviour of the analysed structures was based, where possible, on literature which focused on the effect which the presence of such building characteristics would have on the seismic resistance of structures.

If the definition of the start of failure is assumed to be correct, or at least, if the criteria for its identification are kept unchanged in all numerical models under comparison, a delay in the start of failure can be considered as indicative of a higher seismic resistance when the same ground motion record is applied, and only one variable is altered at a time in the numerical models. In the case of the single building control models analysed in this study, the modelled structures were unaltered, and the effect on the building response to the simulated input ground motion record, for different ground formations and different modelling techniques for the representation of the underlying subsoils, was investigated.

Back in 1957, Gutenberg [52] reported an increased amplitude of vibrations resulting from microseisms at sites, which were located on alluvium depths of more than 500 feet when compared to a site located on a rock outcrop within 30 miles away at Pasadena, California. Eurocode 8: Part 1 [4] confirms this observation by defining not only two different categories of elastic response spectra, depending on the level of seismicity of the site (high seismicity: M_s>5.5, moderate seismicity M_s≤5.5), but also by defining five different sets of response spectra (corresponding to ground types A to E), for each category depending on the average shear wave velocity in the upper thirty metres of ground. Moreover, Lang [53] explains that the amplification of seismic vibrations transferred from the bedrock, through an overlying system of sedimentary ground layers occurs due to the impedance contrast between overlying ground formation layers. A high impedance contrast, resulting from the presence of a softer ground layer over a stiffer ground layer or bedrock, gives rise to amplifications of the earthquake vibrations. While, generally, published studies seem to focus more on situations where softer ground layers overlie dense bedrock, by inference, in cases where a hard top rock layer, such as upper coralline limestone, overlies a softer ground layer, such as clay, which, in turn, rests on the bedrock, as in the two-layer cases investigated in this study, an amplification of the seismic signal in the clay layer and a de-amplification of the signal in the upper rock layer would be expected. Table 39 in Appendix D indicates that, in most of the models analysed in this study on a two-layer ground system and resulting in collapse, the maximum acceleration recorded in the clay layer, prior to the onset of collapse, was higher than the peak value of ground acceleration of the simulated earthquake record, within the same analysis interval, while a decrease in acceleration was recorded in the overlying upper

[27] The reasons behind the selection of this position for the extraction of data from the analysed models were explained in Section 4.2 of this thesis.

coralline limestone layer. Exceptions to this trend resulted in Models 45v2, 89, 109, 128, 138 and 140, where the maximum acceleration recorded in the clay layer was lower than the maximum ground acceleration of the seismic excitation, even though the material properties specified for the clay and the upper coralline limestone ground layers were kept constant throughout all the analyses carried out in this study. Furthermore, it should be noted that Models 89, 138 and 140 exhibited an increase in maximum acceleration in the upper coralline limestone layer, when compared to the maximum acceleration recorded in the underlying clay layer, prior to the start of failure at slab over semi-basement level. Moreover, out of the numerical models analysed on a single layer of clay, in Models 46 and 58, a lower maximum acceleration than the peak acceleration in the seismic signal before the start of failure was recorded. These anomalous results cannot be explained without further investigations. It should be noted, however, that the resulting interaction between the trapped seismic vibrations within the ground (which, as explained by Lang [53], can lead to 'resonance patterns') might not allow for the straightforward identification of the amplification or de-amplification effects within the ground layers, simply through the interpretation of maximum acceleration values within the specific ground layers especially when a software package, which is aimed at modelling the behaviour of structures, and not of ground layers, is used, as in the present study. Furthermore, due to the reservations discussed in Section 4.2.2 of this thesis, regarding the material properties specified for the clay and the upper coralline limestone, it is not possible to comment further on the degree of amplification or de-amplification of the seismic signal occurring specifically within the modelled layers, as suggested by the extracted values of maximum acceleration in these ground layers prior to the onset of collapse. Hence, this study focuses on the effect, which the different ground layers seem to have had on the seismic behaviour of the modelled structures.

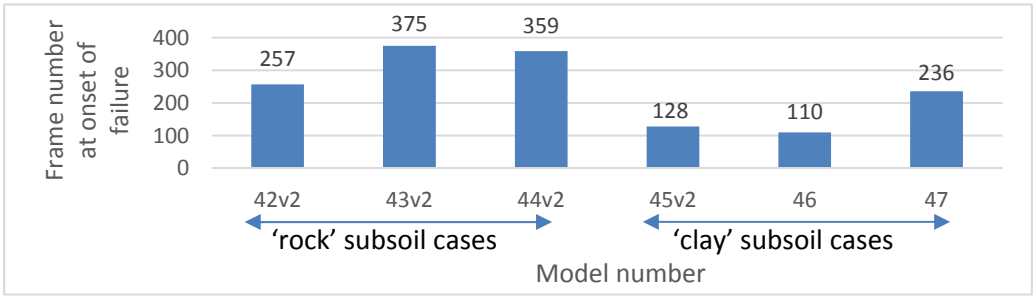

Figure 4-31 Variation in time of onset of failure at slab over semi-basement level in the six-storey single building control numerical models.

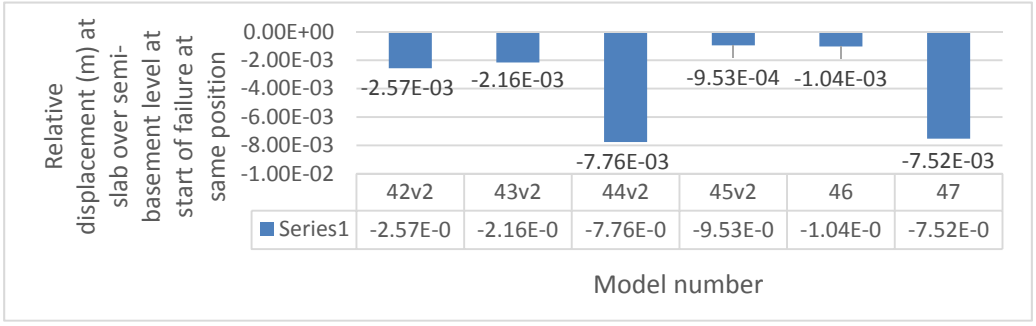

Figure 4-32 Variation in relative x-displacement at start of failure at slab over semi-basement level in the six-storey single building control numerical models.

The comparison of the analysis times, and the corresponding x-relative displacements at the onset of collapse at slab over semi-basement level, in the six-storey single building control models from Table 35 in Appendix D, suggests that, as reported in published studies mentioned in the foregoing discussion, the type of subsoil on which the structure is erected, and the way the subsoil is modelled in the numerical analysis, could affect the magnitude of its oscillations, both due to varying degrees of amplification of accelerations, and due to variations in the degree of restraint at the base of the structure.

Table 35 in Appendix D together with Figures 4-31 and 4-32 indicate that Model 44v2[28] exhibited the highest relative displacement, whereas Model 43v2[29] resulted in the latest start of failure out of the analysed six-storey control numerical models. The latter also exhibited a smaller relative displacement at start of failure than the corresponding control model, analysed on a 30 m thick upper coralline limestone layer (Model 42v2). A comparison of the six-storey single building control numerical models on 'clay subsoil cases' indicates that the lowest relative displacement, at start of failure, was obtained in Model 45v2[30], which displacement was only marginally lower than that obtained in the corresponding control model analysed on 60 m thick clay only (Model 46), which recorded the earliest onset of collapse out of all analysed six-storey control cases. The largest relative displacement, which also corresponds to the latest time of start of failure for the 'clay subsoil cases', was obtained in Model 47 (analysed on clay specified at Minimum Z).

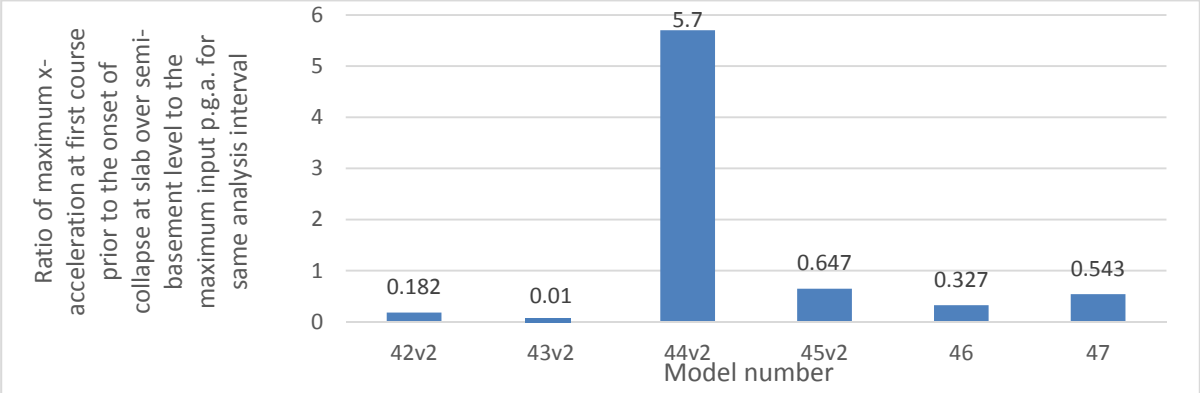

Figure 4-33 Ratio of maximum x-acceleration at first course prior to the onset of collapse at slab over semi-basement level to the maximum input peak ground acceleration for the same analysis interval in the six-storey single building control numerical models.

[28] Model 44v2 corresponds to the six-storey single building control numerical model analysed on a 30 m thick upper coralline limestone layer overlying a 30 m clay layer, where both ground layers were modelled as three-dimensional blocks.

[29] Model 43v2 corresponds to the six-storey single building control numerical model analysed on ground specified as upper coralline limestone at Minimum Z.

[30] Model 45v2 corresponds to the six-storey single building control numerical model analysed on a 1.5 m thick upper coralline limestone layer overlying a 60 m thick clay layer.

These trends in relative displacement at slab over semi-basement level, at start of failure, between the six-storey control numerical models, are also reflected in the ratio of the maximum x-acceleration at the first course of the semi-basement level of every respective numerical model, before the onset of collapse to the maximum input peak ground acceleration, for the same time interval as reported in Table 39 of Appendix D. The higher relative displacement, which also corresponds to a higher amplification of accelerations in Model 44v2 than in the other 'rock' subsoil cases, could be due to the amplification of the seismic excitations through the softer clay layer. On the other hand, the significantly higher amplification of accelerations obtained at the first course in this model, when compared to the other 'clay' subsoil cases, which all include a thicker clay layer, evidenced from Figure 4-33, suggests that resonance effects might have been triggered off in this case.

As explained in Section 4.2.1, since Model 44v2 was analysed on a 30 m thick upper coralline limestone layer overlying a 30m thick clay layer (both modelled as three-dimensional blocks) it is likely that the exact natural frequency of the model lies between the value obtained when the structure was analysed for two eigen modes on upper coralline limestone at Minimum Z (3.882 Hz), and that obtained on clay at Minimum Z (2.623 Hz), therefore, close to the secondary peak frequency of 2.950 Hz of the simulated ground motion record. Furthermore, Table 34 in Appendix D indicates that, out of the six-storey single building control models, Model 44v2 is the only model which resulted in predominant secondary frequencies, in both the clay and the upper coralline limestone layers, which coincide with the predominant frequencies in the main energy content of the input ground motion record. This, therefore, suggests that resonant behaviour due to subsoil resonance could occur, thereby explaining the higher amplification of accelerations and the higher relative displacements recorded for Model 44v2.

Furthermore, the delay in the start of failure of Models 43v2 and 47[31], when compared to the other 'rock' and 'clay' subsoil cases respectively, as seen in Figure 4-31, is most likely due to the additional degree of restraint resulting at the base of the structure, through the definition of the ground as a material at the structural model's Minimum Z value as explained in Sections 3.4.3 and 4.2.1 of this thesis. ELS®, idealises a ground specified as a material at Minimum Z as the reflection of the first line of elements into the ground, where the resulting virtual line of elements representing the ground are given the material properties specified for the ground, and are fixed in all directions against translations and rotations. In the case of the models analysed in this study, the first line of elements consists of masonry blocks. This implies that, in view of the relatively small size of the virtual ground elements and, consequently, the small distance between the centroids of these elements and the elements at first course, models which are analysed on this type of ground representation have a

[31] Model 47 corresponds to the six-storey single building control model analysed on ground specified as clay at Minimum Z.

higher restraint at their base than those modelled on ground layers specified as three-dimensional blocks. This additional degree of restraint might be the main contributing factor to the later start of failure of Models 43v2 and 47, when compared to the other corresponding 'rock' and 'clay' subsoil cases.

Furthermore, in ELS®, the springs between the ground material specified at Minimum Z and the first course of the building can only be defined as corresponding to either the material of the ground or the material of the structure, which, in models analysed on ground specified at Minimum Z, would correspond to the material of the first course of the semi-basement level. In this study, in the models analysed on ground at Minimum Z, these interface springs were defined as corresponding to the material of the ground. On the other hand, whenever the ground layers were modelled as three-dimensional blocks, the material of the interface springs, between the bedrock at Minimum Z (specified as upper coralline limestone with a friction coefficient of 1.0 for all the analysed cases) and the lower face of the lower subsoil layer, was specified as the ground (bedrock) material; while the material of the interface springs, between the upper face of the upper subsoil layer and the first course of the semi-basement level, in the two-layer subsoil systems investigated, was defined as mortar. In the models analysed over a single 60 m thick clay layer, the material of the interface springs between the raft foundation and the clay layer, were defined as clay. Furthermore, the Young's Modulus defined for mortar in this study was around 39 times higher than that of clay and around 0.15 times that of upper coralline limestone. The stiffness of the material of the interface springs, between the first course of the semi-basement level and the underlying ground (modelled as three-dimensional blocks or as a material at Minimum Z), could, therefore, explain the different relative displacements obtained at slab over semi-basement level, in the six-storey single building control models. The higher restraint provided to the base of the modelled structure in Model 43v2, resulting from the presence of the stiffer upper coralline limestone interface springs between the first course of the semi-basement level and the ground level, could explain the lower relative displacement recorded at slab over semi-basement level in this model, when compared to that recorded in the other corresponding 'rock' subsoil cases (Models 42v2, and 44v2). Similarly, the more flexible interface springs, defined as clay in Model 47, could explain the larger relative displacements obtained at slab over semi-basement level in this model, when compared to the relative displacements obtained at the same position in Model 45v2 where the material of the interface springs was defined as mortar. Moreover, the discrepancy between the relative displacements at slab over semi-basement level resulting from Models 46 and 47, which are both analysed on clay, but where, in the former case, clay is modelled as a three-dimensional block, whereas, in the latter clay is defined as a material at the Minimum Z position of the model, are most likely due to the difference in the stiffness of the materials at the interface between the ground / bedrock and the overlying modelled structures which were defined as upper coralline limestone and clay respectively.

While all single building control models analysed on the three investigated 'rock' subsoil cases resisted collapse at five floors, the 'clay' subsoil cases resisted collapse at four floors (in Model 59 where ground was modelled as clay at Minimum Z), and three floors (in Model 63, analysed on 1.5 m thick upper

coralline limestone on 60 m thick clay, and in Model 64, analysed on 60 m thick clay), depending on the modelling of the ground layers. This suggests that the single building control models analysed on the 'clay' subsoil cases, in the present study, experienced a higher degree of damage and, hence, exhibited a reduced seismic resistance, for the same overall height and under the same seismic excitation, than the corresponding models analysed on the 'rock' subsoil cases, in accordance with the behaviour reported in published studies. The higher restraint provided to the base of the structure in the cases modelled on clay at Minimum Z, as discussed above, is very likely to be the main cause of the delayed onset of failure recorded in these numerical models, when compared to the other 'clay' subsoil cases and the resistance to collapse at one storey higher than in the other corresponding cases.

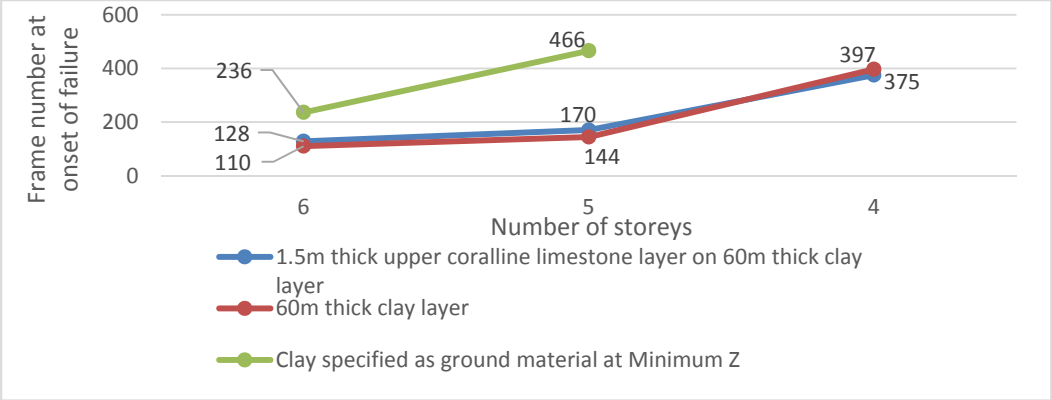

Figure 4-34 Variation in time of onset of failure at slab over semi-basement level in the single building control numerical models analysed on 'clay' subsoil cases with reduction in number of storeys.

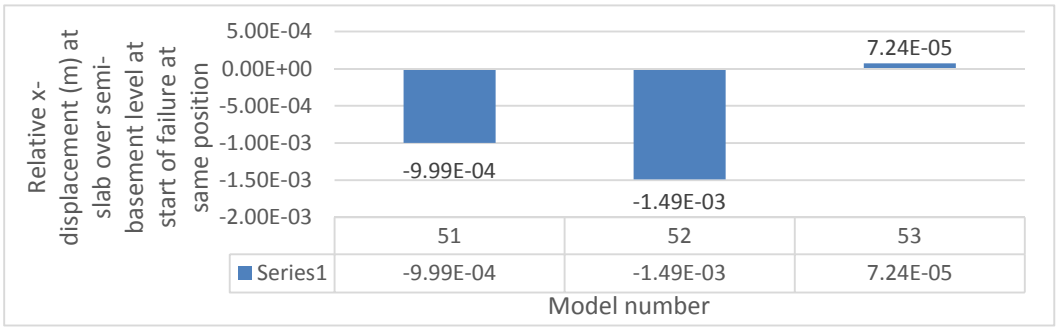

Figure 4-35 Variation in relative x-displacement at slab over semi-basement level at onset of failure at the same position in the five-storey single building control numerical models analysed on 'clay' subsoil cases.

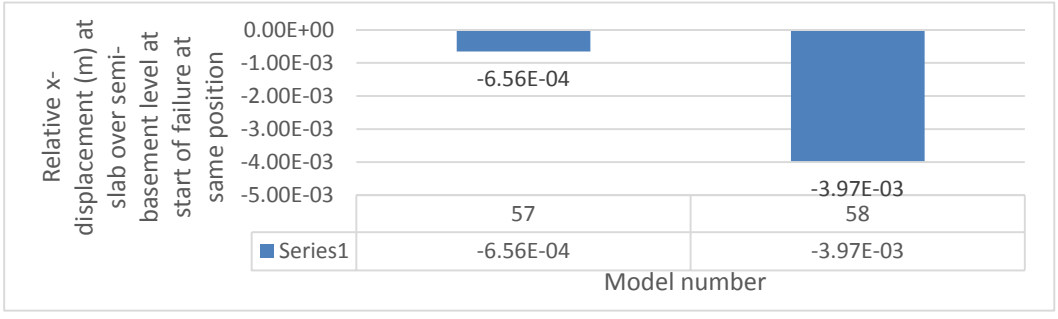

Figure 4-36 Variation in relative x-displacement at start of failure at slab over semi-basement level in the four-storey single building control numerical models analysed on 'clay' subsoil cases.

In every control case investigated, the start of failure is delayed further with every decrease in number of storeys. Figures 4-34, 4-35 and 4-36 indicate that, while the trends in the variation of time of start of failure and the relative displacement at this time at slab over semi-basement level, discussed above

for the six-storey single building control models modelled on 'clay' subsoil cases, are present also in the corresponding four-storey buildings, the equivalent five-storey models only exhibit similar trends with respect to the time of onset of failure. In these five-storey cases, the relative displacement at slab over semi-basement level is lowest in Model 53 (analysed on clay at Minimum Z) and highest in Model 52 (analysed on 60 m thick clay). Taking into consideration the resistance to collapse of the control numerical model analysed on clay at Minimum Z at four floors, when compared to the resistance of the other two corresponding 'clay' subsoil cases for three floors, the lower relative displacement recorded in Model 53 could have been caused by the combined effect of the increased stiffness of the model resulting from the reduction in height, and the additional restraint provided by the modelling of the ground as clay at Minimum Z in ELS® as discussed above.

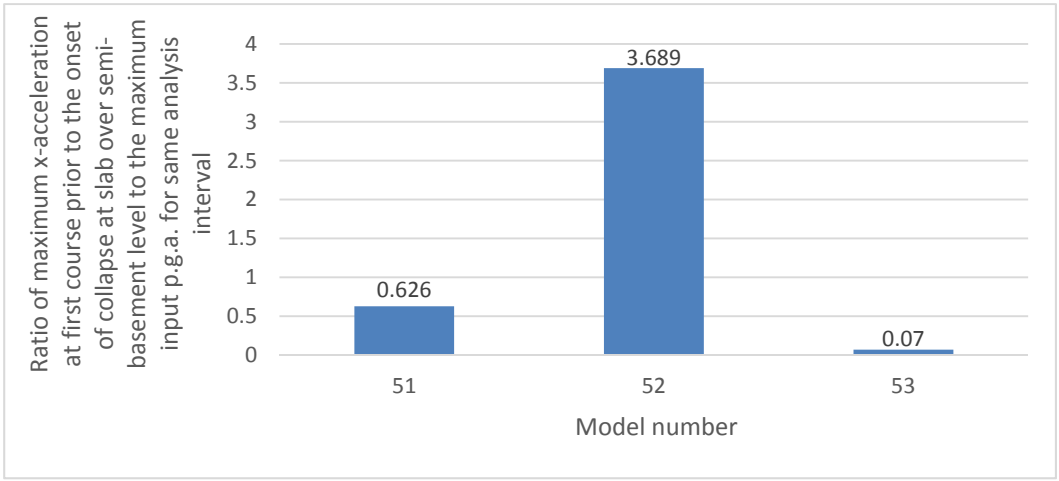

Figure 4-37 Ratio of maximum x-acceleration at first course of semi-basement prior to the onset of failure to the maximum input peak ground acceleration for the same analysis interval in the five-storey single building control numerical models analysed on 'clay' subsoil cases.

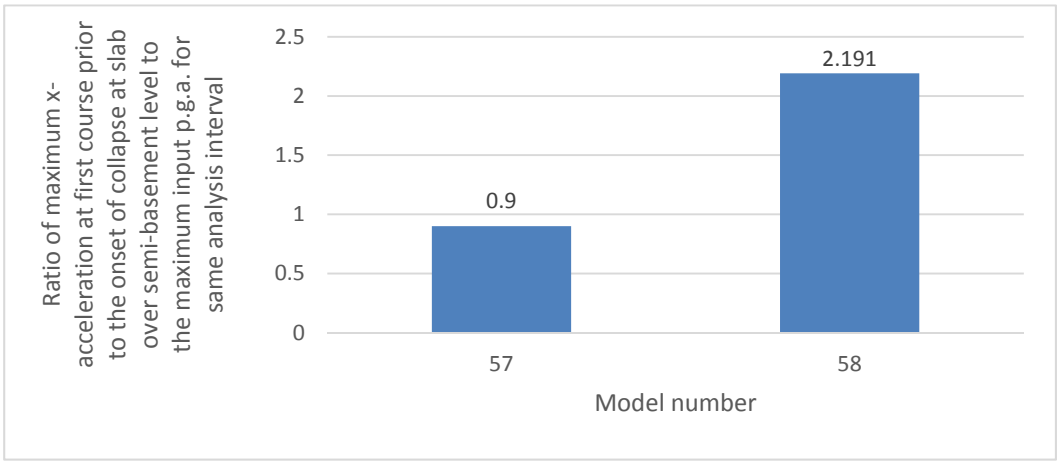

Figure 4-38 Ratio of maximum x-acceleration at first course of semi-basement prior to the onset of failure to the maximum input peak ground acceleration for the same analysis interval in the four-storey single building control numerical models analysed on 'clay' subsoil cases.

While Figures 4-35 and 4-37 and Table 39 in Appendix D indicate that the high relative displacement obtained in Model 52 corresponds to the highest amplification of accelerations at first course of the semi-basement level, when compared to the other two five-storey single building control numerical models analysed on the corresponding 'clay' subsoil cases, Table 34 in Appendix D suggests that this

amplification is not likely to be caused by resonance effects in the ground layer, since no predominant frequencies coinciding with the main frequencies of the input ground motion record were present in this case. Furthermore, Figures 4-36 and 4-38 indicate that, in the equivalent four-storey cases, a similar higher displacement was obtained in Model 58 (analysed on 60 m thick clay), which also corresponds to a higher amplification of accelerations at first course of the semi-basement level, which is not probably due to resonance effects for the same reasons as discussed for the five-storey case.

In addition, it should be noted that, the-single building control numerical models analysed on a 1.5 m layer of upper coralline limestone over a 60 m thick clay layer which ended in collapse (Models 45v2, 51 and 57), show a marginal increase in the relative displacement at the onset of collapse at slab over semi-basement level with reduction in number of floors from a height of six storeys to five storeys, and a 34.3% decrease in relative displacement from five storeys to four storeys. A similar decrease in relative displacement, though of a higher magnitude (99%), was observed between the six- and five-storey single building control models analysed on clay at Minimum Z (Models 47 and 53 respectively). This decrease in relative displacement, with reduction in number of storeys, could likely be attributed to the increased stiffness of the structures which have a lower overall height. On the other hand, the corresponding single building control numerical models, analysed on a 60 m thick clay layer (Models 46, 52 and 58), exhibit an increase in relative displacement at slab over semi-basement level with reduction in number of floors (43.3% increase from six to five storeys and 166% increase from five to four storeys).

As discussed in Section 4.2.2, when a very stiff building is constructed on flexible ground, a significant alteration of the free-field ground motion occurs, arising from the interchange of vibrations between the ground and the structure [50]. The higher relative x-displacement at slab over semi-basement level, and its increase with reduction in height of the analysed models, in addition to the higher amplification of accelerations at first course of the semi-basement level, reported in Figures 4-35 to 4-38 for the stiffer five- and four-storey single control buildings modelled on 60 m thick clay (Models 52 and 58, respectively), and the absence of such a behaviour in the corresponding less stiff (in view of its height) six-storey case (Model 46), suggest that the transfer of seismic vibrations between the flexible clay layer and the significantly stiffer overlying structure, resulting from soil-structure interaction, might have caused the increased accelerations. This, in turn could have induced the high relative displacements. Furthermore, the higher amplification of seismic effects, resulting in these five- and four-storey control models analysed on a 60 m thick clay layer overlying the bedrock, in particular, when compared to the corresponding cases analysed on a 1.5 m thick upper coralline limestone layer overlying a 60 m thick clay layer (Models 51 and 57), could be due to the absence of the upper coralline limestone layer. As discussed above and in detail in Sections 4.2.1.1 and 4.2.2, in the case when a 1.5 m thick upper coralline limestone layer is present, a high impedance contrast is very likely to have resulted between this layer and the underlying clay layer, in view of the high stiffness attributed to the upper coralline limestone layer (through the specified properties of this material in the numerical models), thereby limiting the transfer of seismic vibrations to the building, and resulting in a de-

amplification of the earthquake excitations reaching the modelled structures, which in turn exhibited lower relative displacements than their counterparts modelled on a single clay layer.

The results discussed above, therefore, stress the influence which the material of the ground, and its modelling in numerical analyses packages, has on the seismic response of a typical contemporary loadbearing masonry structure. While confirming, within the limits of this study, the added seismic vulnerability which can be associated with ground types, where softer materials such as clay, are present, the precise magnitude of the relative level of seismic vulnerability linked to every ground type, investigated in the context of the geology of Maltese Islands, requires further investigation in view of the concerns regarding the material properties specified for the modelled ground layers when compared to published results [191] [195] as explained in Section 4.2.2 and the consequent possible exacerbation of their effects on the building response when compared to the results of this study. The importance of the correct choice of modelling, depending on the objectives of the study, is also evidenced.

4.2.3.3 Comparison of the analysis time at onset of failure and the relative displacements at slab over semi-basement level in multiple building control models

The following section examines the seismic response of a typical contemporary loadbearing URM building to seismic excitations, when acting in combination with adjacent buildings of identical height and configuration, through the sharing of the intermediate party walls and considering only one ground formation typology, namely a 1.5 m thick upper coralline limestone layer over a 60 m thick clay layer, where both layers are modelled as three-dimensional blocks.

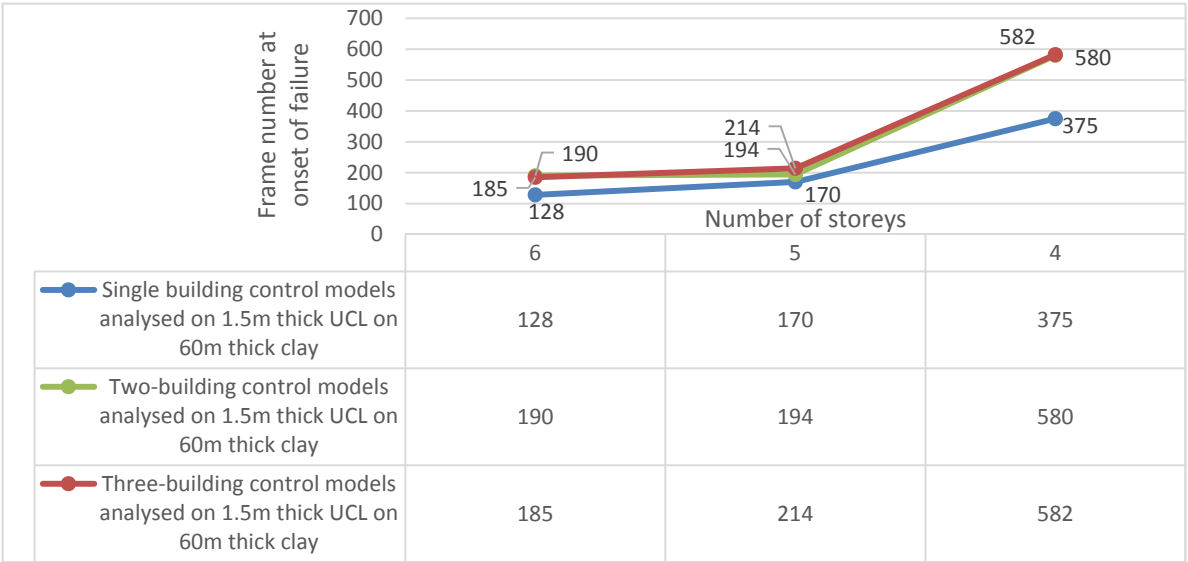

Figure 4-39 Variation in time of onset of failure at slab over semi-basement level in the single, two- and three-building control numerical models analysed on 1.5 m thick UCL on 60 m thick clay with reduction in number of storeys.

A comparison of the analysis times at the onset of failure, resulting from the two- and three-building control numerical models to the corresponding single building control numerical model, as presented in Figure 4-39 and in Table 38 of Appendix D, shows that, even though all the two- and three-building control cases investigated result in a delay in the start of failure, when compared to the equivalent

single building control models, only a marginal variation is observed between the analysis times at start of collapse (of between 2 and 10 frames, equivalent to 0.02 s to 0.10 s of analysis time) of the corresponding two- and three-building control cases investigated respectively. Hence, while, as reported in literature [28] [30] [66] [200], the increased regularity in the plan proportions and the higher overall stiffness resulting from the combination of two or three identical buildings sharing party walls (which is also evidenced by the increase in natural frequency of the combined models reported in Table 31 of Appendix D) translates into a higher seismic resistance than the corresponding single building control model, the cases analysed in this study seem to suggest that the increase in seismic resistance between the two- and three-building configurations is not significant.

Furthermore, the significantly smaller delay in the start of failure, exhibited by the six- and five-storey two- and three-building control models, when compared to the corresponding single building control models (amounting to an average of 60 and 34 frames for the six-storey and the five-storey cases respectively, when compared to the delay of 206 frames resulting in the four-storey cases) suggests that, since the materials of the structure and building characteristics remain unchanged, the main structural response parameter causing failure in the combined models is not related to a property of the structure, which varies appreciably with the change in building proportions, such as the building stiffness. As discussed in Section 4.2.3.1, the main cause of failure in these multiple-building cases is likely to be either due to the failure of the party walls at slab over semi-basement level resulting from the large moments induced by the oscillations of the structure and the high overlying structural mass, or, alternatively the resulting increase in seismic mass, which leads to an increase in base shear.

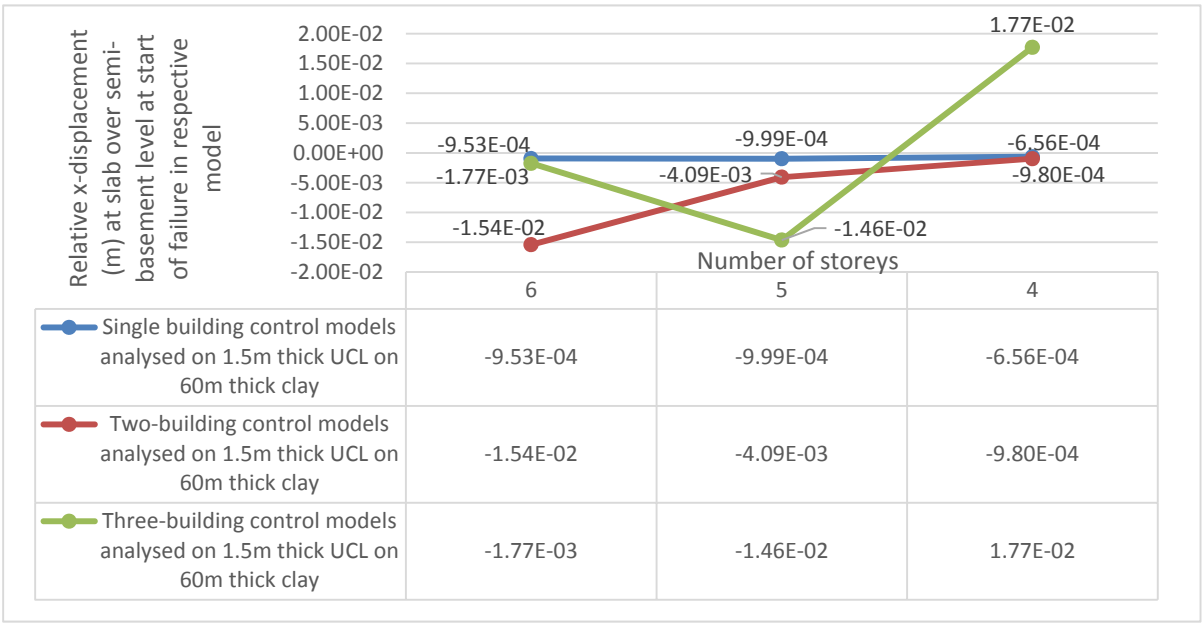

Figure 4-40 Variation in relative x-displacement at start of failure at slab over semi-basement level in the single, two- and three-building control numerical models analysed on 1.5 m thick UCL on 60 m thick clay with reduction in number of storeys.

Moreover, Figure 4-40 shows that a marginal relative x- displacement at slab over semi-basement level at the start of failure is exhibited by the six-, five- and four-storey single building control models analysed on 1.5 m thick upper coralline limestone over 60 m thick clay (Models 45v2, 51 and 57). On

the other hand, while the increase in stiffness of the combined models discussed earlier could be expected to result in a reduction in the relative displacement, with increase in number of structural units, higher (magnitude) values of relative x-displacement at the equivalent positions are recorded in the corresponding two- and three-building control models.

Equation 4.5 in Clause 4.3.3.2.2(1)P of Eurocode 8: Part 1 [4] defines the base shear force in the lateral force simplification as:

$$F_b = S_d(T_1).m.\lambda$$

Equation 4-6

where, as defined in the same Clause, F_b is the seismic base shear in N, $S_d(T_1)$ is the design acceleration spectrum value at the structure's natural period T_1 (in the first mode of vibration) in the direction under consideration in m/s^2, m is the mass of the structure above the foundation or a rigid basement in kg and λ is the correction factor. Furthermore, the horizontal seismic action acting at the ith floor, defined in Clause 4.3.3.2.3(2)P of Eurocode 8: Part 1 [4] for the same lateral force method of analysis, is defined as:

$$F_i = F_b.\frac{s_i m_i}{\sum s_j m_j}$$

Equation 4-7

where F_i is the horizontal seismic force acting at the ith floor in N, F_b is the base shear force due to seismic excitation as defined by Equation 4-6 in N, s_i and s_j are the displacements (in m) of the corresponding storey masses m_i and m_j (in kg) in the deformed shape of the structure arising from its first mode of vibration. Therefore, since the fundamental period of a structure is the inverse of its natural frequency [43], with reference to Equations 4-1 and 4-5 in Sections 4.2.1 and 4.2.1.2 of this thesis for the natural frequency of a single degree of freedom system and that of a cantilevered beam with regular cross-section respectively, and considering that no additional seismic vulnerability characteristic which could affect the deformability of the models was introduced in the combined cases, the higher relative x-displacements resulting from the three- and, to a lesser extent, the two-building control models when compared to the corresponding single building control models, suggest that the higher base shear resulting from higher inertial mass present in the combined cases, had a higher bearing on the displacement of these models than the increase in stiffness.

Figure 4-40 also indicates that the highest relative x- displacement at slab over semi-basement level at the start of failure in the six-storey numerical models is exhibited by the two-building control case, which relative displacement is 16.18 times higher than the corresponding displacement in the single building control numerical model. On the other hand, the highest relative x-displacements at slab over semi-basement level at the onset of collapse in the five- and four-storey cases are obtained from the three-building control numerical models (which result in equivalent relative x-displacements of 14.66 and 27.01 times higher respectively than the corresponding relative x-displacements recorded for the single building control model). A similar trend in the numerical models exhibiting the highest relative x-displacement is observed also in the comparison of the magnitude of the relative x-displacements at slab over semi-basement level at the time, which corresponds to the occurrence of the maximum x-

displacement prior to the onset of collapse at the same position during the dynamic analysis. These results are summarised in Figure 4-41.

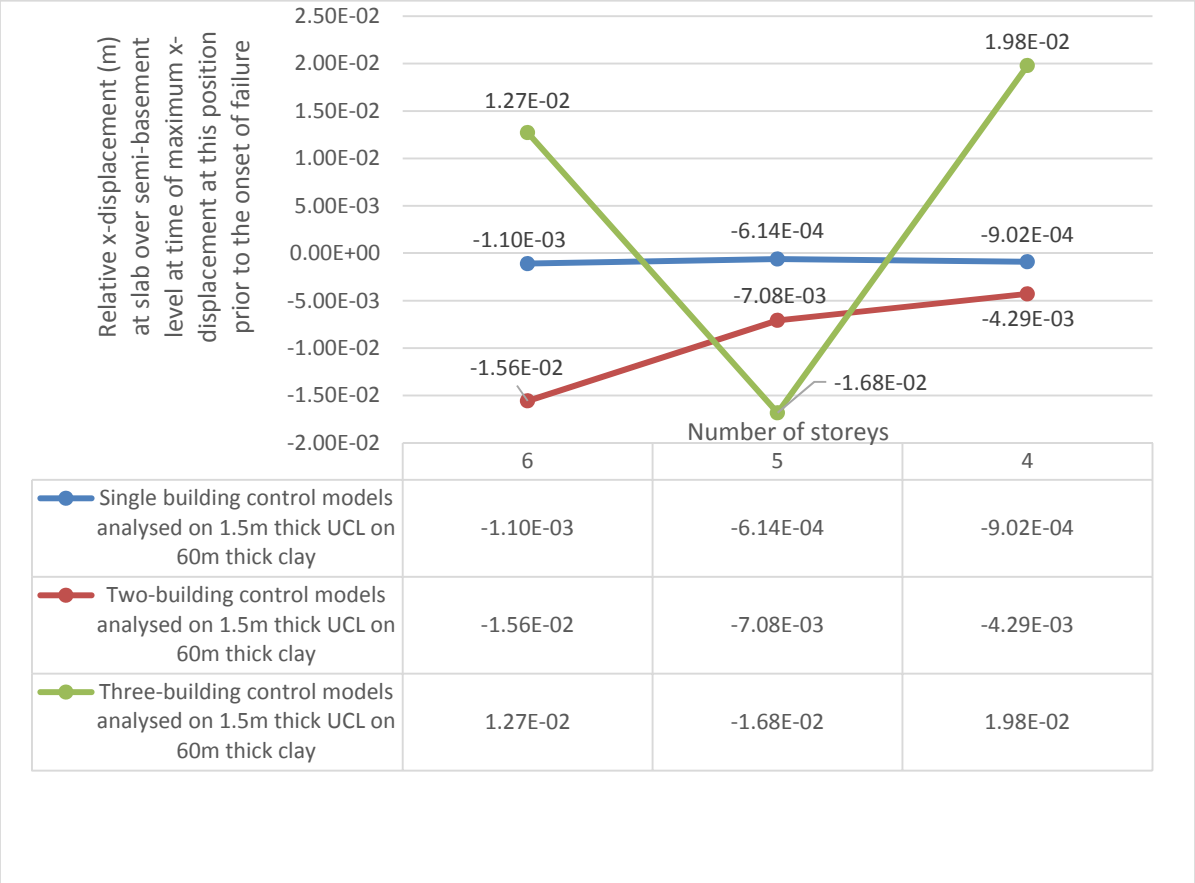

Figure 4-41 Variation of relative x-displacement at slab over semi-basement level at time of maximum x-displacement at this position prior to the onset of collapse with number of storeys in single, two- and three-building control numerical models.

Furthermore, Figure 4-40 also shows that, the two-building control numerical models exhibit a consistent decrease in relative displacement at slab over semi-basement level at start of failure with reduction in number of storeys (73.4% decrease between the six- and the five-storey models and a 76.0% decrease between the five- and the four-storey cases) whereas the corresponding three-building control numerical models resulted in a significant increase in relative displacement at the same position with every floor reduction (725.0% increase between the six- and the five-storey numerical models and 21.2% increase between the five-and the four-storey numerical models). As discussed earlier, the single building control numerical models analysed on a 1.5 m thick upper coralline limestone layer overlying a 60 m thick clay layer exhibited a marginal increase (4.8%) in relative x-displacement at slab over semi-basement level at the start of failure with the reduction in height from six to five storeys and a decrease in relative x-displacement of 34.3% between the five- and the four-storey numerical models. As discussed in the case of the single building control numerical models analysed on the 'clay' subsoil cases, a decrease in relative x-displacement with decrease in the overall building height could be attributed to an increase in stiffness and, hence, a higher resistance to deformation. On the other hand, Table 34 in Appendix D suggests that the increase in displacement

exhibited by the three-building control numerical models, which resulted in collapse, could be due to resonance effects within the ground layers coupled with the higher inertial mass, since in the six-, five- and four-storey three-buildings control numerical models, the peak frequency of the upper coralline limestone layer and a secondary frequency of the clay layer fall within the main energy range of the simulated ground motion record. This is also suggested from the maximum x-accelerations recorded in the ground layers prior to the onset of collapse at slab over semi-basement level reported in Table 39 of Appendix D. The six- and five-storey three-building control numerical models are among the few cases where the amplification of maximum x-accelerations in the upper coralline limestone layer before the start of failure when compared to the maximum input peak ground acceleration for the same analysis interval are higher than in the clay layer.

Moreover, the higher amplification of maximum x-accelerations recorded at first course of the semi-basement level prior to the onset of collapse exhibited by all the three-building control numerical models which resulted in collapse, followed by the corresponding two-building control numerical models as reported in Figure 4-42, could also be the direct consequence of resonance effects in the ground layers.

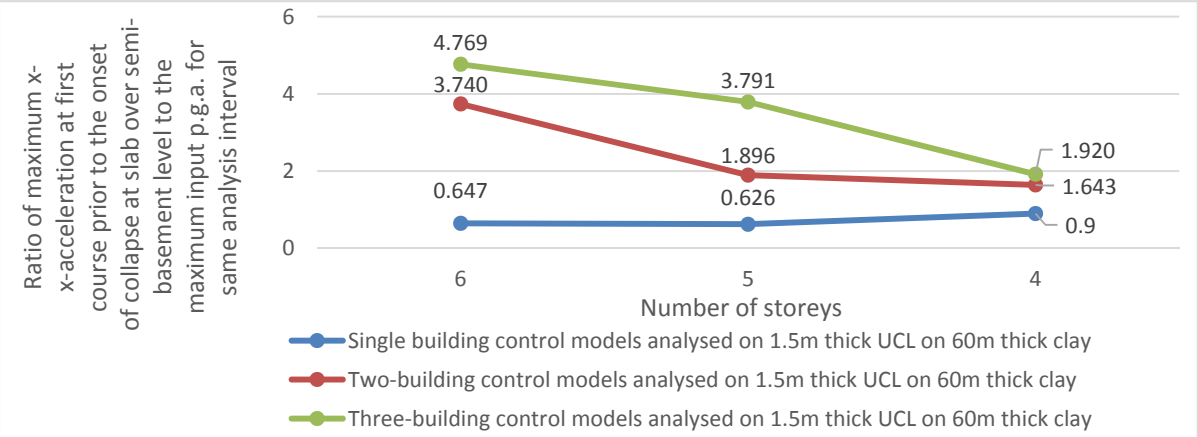

Figure 4-42 Variation in ratio of maximum x-acceleration at first course prior to the onset of collapse in every model to the maximum input p.g.a. for the same time interval in the single, two- and three-building control numerical models with reduction in number of floors.

Additional analyses of two- and three-building control numerical models including the effect of variations in the height of the adjacent structures and the presence of seismic vulnerability characteristics in one or more buildings could not be carried out as part of the present study in view of time constraints. Further studies are, however, required before any generalisations on the enhancement of the seismic resistance of the investigated masonry typology when located within an aggregate, and with shared party walls, can be made.

4.2.3.4 Comparison of the analysis time at onset of failure and the relative displacements at slab over semi-basement level in control models including one or more additional seismic vulnerability characteristics

Following the investigation of the variation in the seismic response of the control models under different ground formations and different representations of the ground in the numerical models, in addition to the variation in response when more than one control model act in combination, the present study proceeded to examine the seismic response of the altered single building control models when specific building characteristics were introduced, first one at a time, then in combination, keeping the ground formation layers unchanged.

It could be argued that, if the ground motion record and the type of ground formation upon which a structure is analysed are unchanged, then the time it takes a number of structures, which include some variations, to start showing signs of failure and the magnitude of their displacement at the onset of failure could be indicative of their structural ductility capacity. Park [209] defines 'ductility' in earthquake engineering as: "the ability of a structure to undergo large amplitude deformations in the inelastic range without substantial reduction in strength", adding that, the dissipation of energy is a primary attribute for the ductility capacity of structures. On the other hand, Priestley et al. [210] and FEMA 454 [57] explain that, while a structure must have sufficient 'strength' to support the loads acting on it within acceptable stress limits and limit displacements, the 'stiffness' of the structure is related to its degree of deformability under loading and, hence, can be directly linked to the structure's vulnerability to damage. While both stiffness and ductility influence the seismic response of structures, the first by limiting deformation demands, and the second by allowing the dissipation of energy such that higher deformations of the structure can be accommodated without failure, these two properties are antagonistic in their effect on the seismic resistance of structures when considered in their 'pure' form, hence, leading to stiffer (brittle) structures failing at lower values of lateral displacements, as evidenced by the results of the analysed control numerical models when compared to the numerical models which included additional building characteristics, which are presented in this section. However, while ductility capacity might be a desirable attribute in the seismic response of a structure, it must be carefully distinguished from an increased flexibility caused by a localised reduction in the stiffness of the structure, which can give rise to larger displacements (ductility demand), and which can then lead to the formation of collapse mechanisms. The assessment of a structure's seismic resistance, therefore, cannot be based solely on its maximum displacement, when building characteristics, which intrinsically cause larger displacements are present.

Priestley [211] showed that, whereas the concept of ductility might seem completely detached from unreinforced masonry structures as it is generally associated with inelastic straining of steel reinforcement or structural steel members, it should include, to some degree, even masonry structures, since the failure load under seismic excitations of an out-of-plane loaded wall exceeds the ultimate load predicted through elastic analysis. Priestley [211] gave an outline of the seismic load path in an unreinforced masonry building, in particular, highlighting the way the earthquake forces are transferred from the ground to the walls, which are perpendicular to the main earthquake excitation

direction and are, hence, subjected to out-of-plane inertia loads as the building displaces under the effect of seismic motion. Figure 4-43 summarises the energy transfer from the in-plane shear walls, which respond to the seismic excitations in proportion to their stiffness, height and their loading from the overlying floor and perpendicular walls, and the transfer of these excitations in the form of accelerations and displacements to the diaphragms, which, if rigid, would have the same accelerations and displacements throughout their area as those at the end of the in-plane shear walls, hence, transferring these accelerations and displacements to the out-of-plane loaded walls.

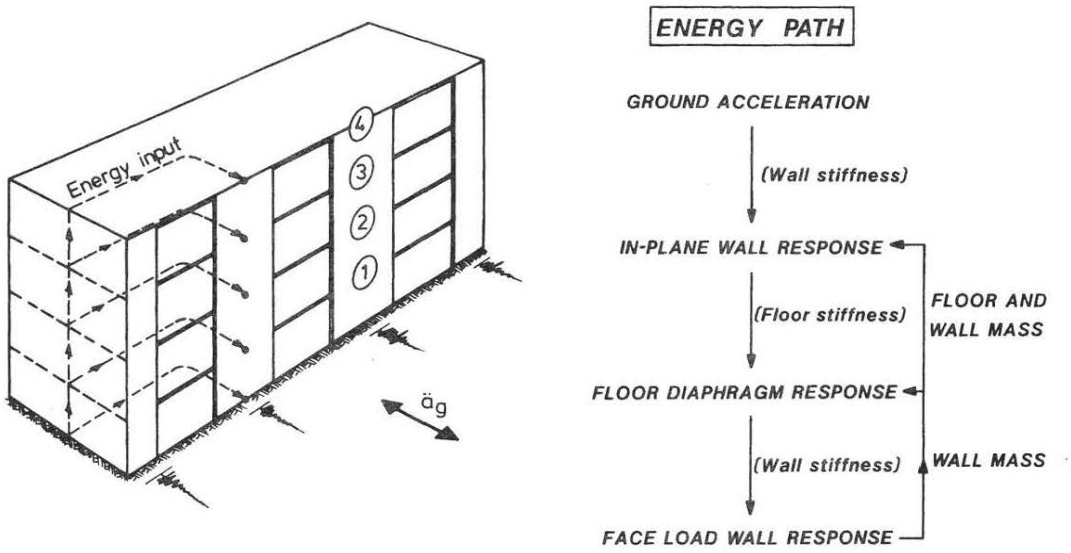

Figure 4-43 Seismic load path in an unreinforced masonry building ([211] p. 194).

However, Priestley's [211] seismic load path is based on the assumption of a regular building with no particular changes in stiffness present. Considering, for simplicity, the walls at ground floor of the structure described by Priestley [211], studies [55] [56] indicate that the magnitude of the earthquake actions transferred to the same walls at ground floor would be significantly increased if a soft storey were present at this level, thereby reducing the lateral storey stiffness of the building at the same level. The consequent larger lateral displacements to which these walls would be subjected under the same seismic ground motion, coupled with the higher proportion of gravity loads from the overlying floors acting on the same walls, in view of the reduced wall area at this level, leads to a higher risk of failure due to P-delta effects. Therefore, while a higher maximum displacement would be expected to be reached by such a structure prior to the onset of failure, these higher displacements cannot technically be attributed to an increased ductility capacity but, to a change in the mode of failure as a consequence of a localised reduction in the stiffness of the structure, even more so if there are no significant delays in onset of failure. Hence, the interpretation of displacement values for the estimation of the relative seismic vulnerability rating to be associated with particular building characteristics must be carried out with caution and requires the consideration of other structural response parameters in combination.

The direct comparison of the analysis times at which the start of failure was identified at slab over semi-basement level in all the analysed numerical models for the determination of a relative degree of seismic vulnerability to be associated with the investigated characteristics cannot be carried out

because every building alteration would generate a different structural response and a different displacement mode under seismic forces. Hence, in the following section, the analysed models which include one, two or three additional building characteristics were compared separately to the corresponding control models in order to obtain some insight with respect to the influence of the respective investigated characteristics on the structural seismic response.

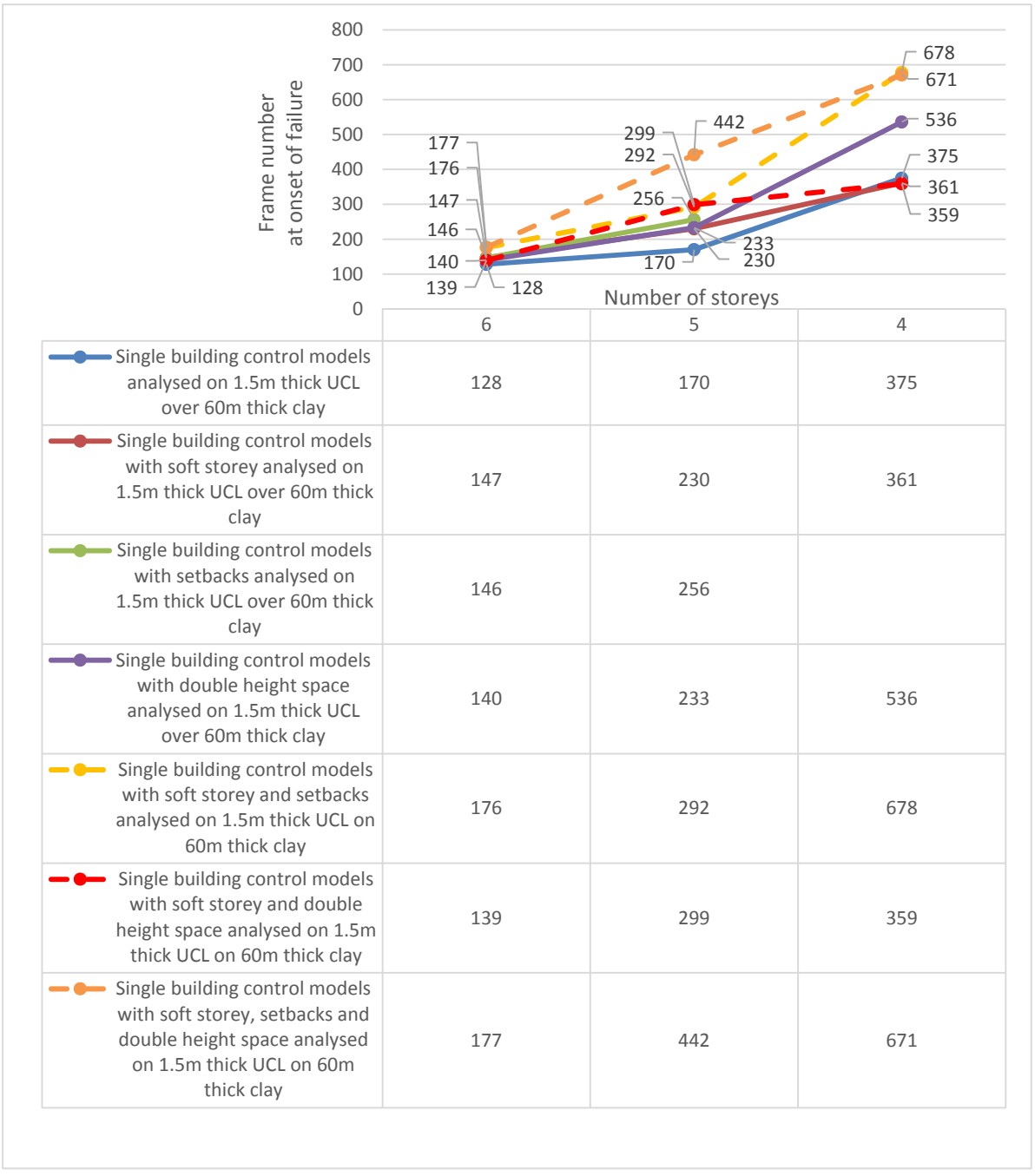

	6	5	4
Single building control models analysed on 1.5m thick UCL over 60m thick clay	128	170	375
Single building control models with soft storey analysed on 1.5m thick UCL over 60m thick clay	147	230	361
Single building control models with setbacks analysed on 1.5m thick UCL over 60m thick clay	146	256	
Single building control models with double height space analysed on 1.5m thick UCL over 60m thick clay	140	233	536
Single building control models with soft storey and setbacks analysed on 1.5m thick UCL on 60m thick clay	176	292	678
Single building control models with soft storey and double height space analysed on 1.5m thick UCL on 60m thick clay	139	299	359
Single building control models with soft storey, setbacks and double height space analysed on 1.5m thick UCL on 60m thick clay	177	442	671

Figure 4-44 Variation in the analysis stage at onset of failure at slab over semi-basement level with reduction in number of storeys of all single building control numerical models which include one to three additional seismic vulnerability characteristics.

Tables 36 and 37 in Appendix D and Figure 4-44 present the variation in the analysis time at which the onset of failure at slab over semi-basement level was identified for the single building numerical

models, which include one to three additional seismic vulnerability characteristics with the reduction in number of storeys when compared to the corresponding single building control numerical models. A delay in the start of failure when compared to the corresponding single building control numerical models was observed in almost all six- and five-storey cases and in four out of the six four-storey cases analysed, which delay was generally higher in the models which include two or more additional building characteristics than in the cases, which include only one building parameter in addition to the control model.

Furthermore, the effect of the presence of a building characteristic on the seismic resistance of a structure can vary depending on its location in the structure and the overall number of storeys present. This study focused mainly on the influence of the latter, while considering only briefly in Section 4.2.3.5 of this thesis the effect of the variation in the position of a sudden reduction in storey stiffness on the seismic response of the masonry building typology under investigation. While a delay in the onset of failure at slab over semi-basement level was recorded in all the six- and five-storey single-characteristic numerical models analysed in this study, when compared to the corresponding control models, the analysis times at which the start of failure was identified in these cases varies only marginally when considering numerical models of the same overall height (1 to 7 frames in the six-storey models, equivalent to 0.01 s - 0.07 s, and 3 to 30 frames in the five-storey models equivalent to 0.03 s - 0.30 s, where a variation of 3 frames resulted in two out of the three five-storey single-characteristic cases). The drawing of direct comparisons between the analysis times at onset of failure and the relative seismic vulnerability which is to be associated with every building characteristic considered in this study cannot be made for these building heights in the single parameter cases as the identification of the time of start of collapse, though consistent throughout all the fifty numerical models analysed, could be prone to errors within such a tight range of variation. On the other hand, at four storeys, where the presence of the modelled irregularities form a larger proportion of the overall height of the structure, while the numerical model which includes setbacks at penthouse level resists collapse (Model 83), a significant delay in the onset of failure of 161 frames (1.60 s) when compared to the corresponding control numerical model was exhibited by the numerical model which includes a double height space between Levels 0 and 1 (Model 103). Furthermore, the four-storey numerical model which includes a soft storey at semi-basement level (Model 73) resulted in a marginally earlier start of failure (14 frames, 0.13 s) than the four-storey single building control numerical model analysed on the same ground formation (Model 57). These results tend to suggest that, based on the indications obtained from the time of start of failure at slab over semi-basement level, and within the limits of the structures modelled under this study (with respect to the proportions of the setbacks and the size, detailing and position of the void modelled in the case of the double height space, as discussed in Section 4.2.1.2 of this thesis) the presence of setbacks at penthouse level seem to have the least impact on the seismic resistance of the modelled structures, while a more deleterious effect may be attributed to the presence of a soft storey, and, to a significantly lesser extent, to the presence of a double height space. The pronounced debilitating effect which the presence of a soft storey has on the seismic resistance of a structure, as evidenced from these results, is in line with the explanation of the seismic

response of structures, which include a soft storey, given by Arnold and Reitherman [55], Guevara-Perez [56] (as discussed in Section 4.2.1.2) and FEMA 454 [57]. In addition, studies carried out by Sucouglu et al. [212] involving the statistical correlation of eight seismic vulnerability characteristics in a number of buildings, which were damaged after the 1999 Düzce earthquake, identified the presence of a soft storey in the highest seismic vulnerability category, with an associated seismic vulnerability, which increased with an increase in number of storeys.

A study of the analysis times at which the onset of failure was identified at slab over semi-basement level in the numerical models which include the presence of a soft storey or a double height space as the only additional building characteristic when compared to the corresponding control numerical model, together with the expected structural behaviour of the buildings, which include these building characteristics, suggests that the observed delay in the onset of failure in such cases is very likely a consequence of the reduced stiffness of these models when compared to the control model, hence resulting in a less abrupt loss of integrity. In the case of the models, which include setbacks at penthouse level, the reduced gravity load from the topmost storey and the improved stability resulting from the lowering of the centre of mass, as observed by Parisi [60], together with the reduced seismic mass, are likely to be the main contributors to the delay in the start of failure. The reduction in stiffness could also be considered as the main factor causing the delays in the start of failure recorded in the analysed numerical models, which include two to three additional seismic vulnerability characteristics. However, in such cases, the structural response would very likely be influenced by the combination of the additional characteristics investigated, therefore, giving rise to more complex behaviours which cannot be simply identified with reference to the time of start of failure.

As in the case of the single characteristic numerical models, the interpretation of the relative degree of seismic vulnerability from the analysis time at the onset of failure at slab over semi-basement level in the analysed models, which include the presence of two of more additional seismic vulnerability characteristics, is not possible in the cases where the identified analysis times are very close in view of the possible margin of error resulting from the identification of the start of collapse and the complex behaviour triggered off by the presence of more than one additional characteristic acting in combination. With reference to Figure 4-44, such cases include:

a) for six storeys, the numerical model analysed with a soft storey at semi-basement level and setbacks at penthouse level (Model 89) and the numerical model which includes all the three additional seismic vulnerability characteristics investigated in combination (Model 119), whose analysis times at the onset of failure vary by only 1 frame (0.01 s);
b) for five storeys, the numerical model analysed with a soft storey at semi-basement level and setbacks at penthouse level (Model 91) and the numerical model analysed with a soft storey at semi-basement level and a double height space between levels 0 and 1 (Model 111), where identification of the start of failure varies by only 7 frames (0.07 s); and

c) for four storeys, the corresponding four-storey numerical models of the cases listed in (a) above (Models 93 and 123 respectively), whose analysis times at the onset of failure, vary by 7 frames (0.07 s).

On the other hand, the significantly earlier analysis times at which the start of collapse at slab over semi-basement level was identified in the six- and four-storey numerical models which include a soft storey at semi-basement level and a double height space between Levels 0 and 1 (Models 109 and 113), particularly, when compared to the corresponding numerical models which include a soft storey at the same position and setbacks at penthouse level (Models 89 and 93), suggest that the former combination of seismic vulnerability characteristics presents a worse threat to the seismic resistance of structures. As explained above, this behaviour might be partially due to the severely reduced stiffness at the lowermost floors of these structure in view of the presence of the soft storey and the double height space. Furthermore, a significant delay in the start of failure at slab over semi-basement level is exhibited by the four-storey numerical model, which includes a soft storey at semi-basement level and setbacks at penthouse level (Model 93), and the corresponding numerical model, which includes all three additional seismic vulnerability characteristics in combination (Model 123), when compared to the corresponding control numerical model (Model 57), and the four-storey numerical model, which includes a soft storey as the only seismic vulnerability characteristic (Model 73). This delay could be attributed to the presence of setbacks at penthouse level which, as discussed above, results in a lower gravity load from the penthouse level and a downward shift of the centre of mass of the structures, hence, leading to a higher stability, as suggested by Parisi [60].

Nevertheless, as discussed above, the complex structural behaviour activated by the presence of two or more seismic vulnerability characteristics acting in combination cannot be overlooked and a detailed study of the deformation of the analysed structures, the variation in stress levels and the identification of the collapse modes is required before any inference on the relative degree of seismic vulnerability which can be linked to the presence of more than one building characteristic, can be made. In addition, in view of the limitations identified in Section 4.2.1.2 (with respect to the proportions of setbacks and the size, position and detailing of the double height space), which are suspected to have had a bearing on the results obtained in the present study, for any such conclusions to be reached, additional investigations including the variation in the size of the void forming the double height space and the size of the setbacks in both the single characteristic and the combined characteristics cases would be required. These investigations could not be carried out as part of the present study in view of time limitations. This study, on the other hand, attempted to obtain further insight into the relative seismic vulnerability, which can be attributed to the presence of a soft storey at semi-basement level, setbacks at penthouse level and a double height space between Levels 0 and 1, by examining the variation of the relative x-displacement at slab over semi-basement level at different analysis times in the analysed numerical models, which include one to three of these characteristics in combination with the reduction in number of storeys, as reported in Tables 40, 41 and 42 of Appendix D and in Figures 4-45, 4-46 and 4-47.

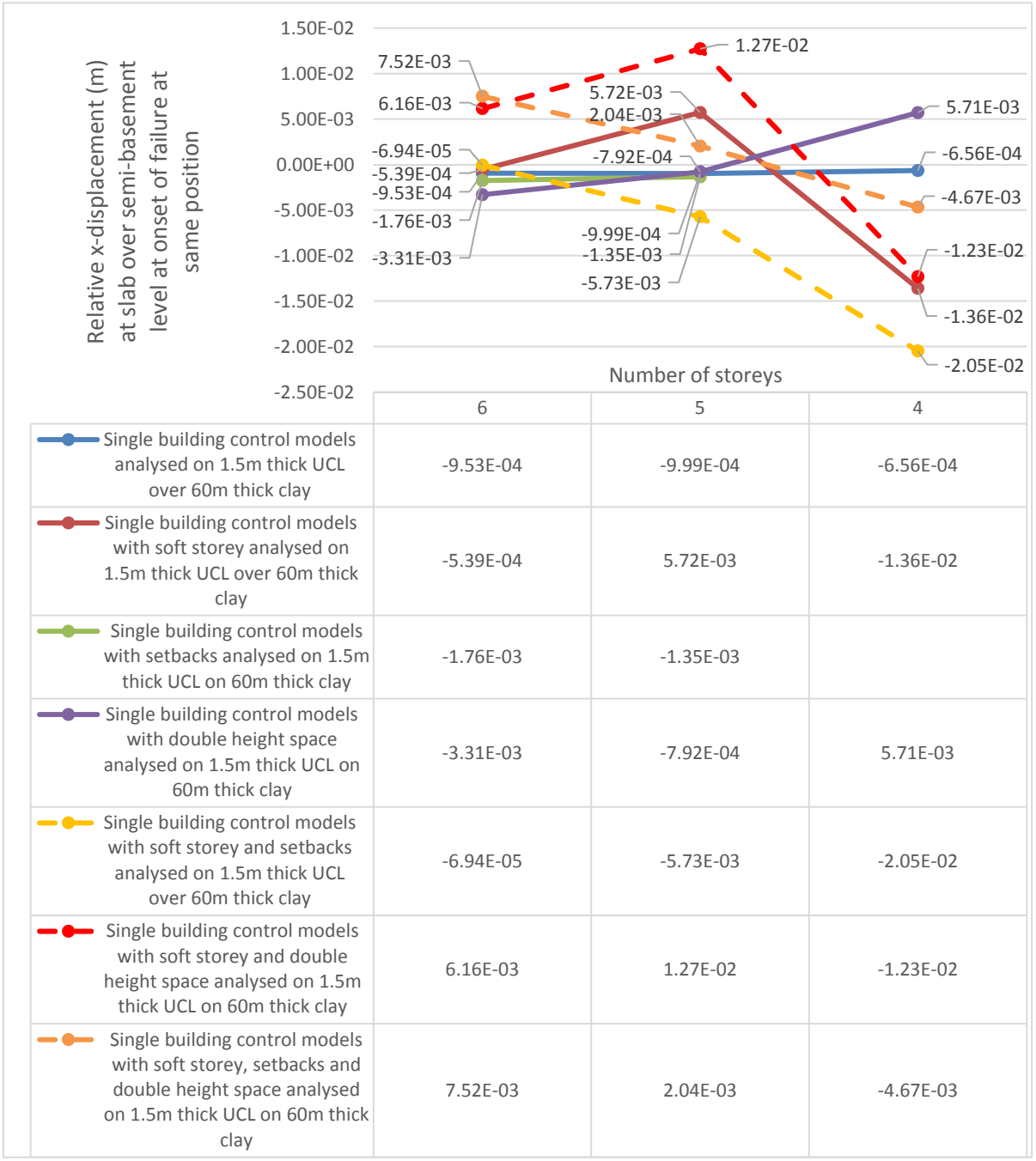

	6	5	4
Single building control models analysed on 1.5m thick UCL over 60m thick clay	-9.53E-04	-9.99E-04	-6.56E-04
Single building control models with soft storey analysed on 1.5m thick UCL over 60m thick clay	-5.39E-04	5.72E-03	-1.36E-02
Single building control models with setbacks analysed on 1.5m thick UCL on 60m thick clay	-1.76E-03	-1.35E-03	
Single building control models with double height space analysed on 1.5m thick UCL on 60m thick clay	-3.31E-03	-7.92E-04	5.71E-03
Single building control models with soft storey and setbacks analysed on 1.5m thick UCL over 60m thick clay	-6.94E-05	-5.73E-03	-2.05E-02
Single building control models with soft storey and double height space analysed on 1.5m thick UCL on 60m thick clay	6.16E-03	1.27E-02	-1.23E-02
Single building control models with soft storey, setbacks and double height space analysed on 1.5m thick UCL on 60m thick clay	7.52E-03	2.04E-03	-4.67E-03

Figure 4-45 Variation in relative x-displacement at start of failure at slab over semi-basement level in the single building control numerical models including one to three additional seismic vulnerability characteristics with reduction in number of storeys.

With reference to Figure 4-45, almost all analysed cases, including one to three additional seismic vulnerability characteristics resulted in a higher magnitude of relative x-displacement at slab over semi-basement level at the onset of failure, when compared to the corresponding control numerical model. The only exceptions to this trend are the six-storey numerical model including a soft storey at semi-basement level (Model 69), the six-storey numerical model with a soft storey at semi-basement level and setbacks at penthouse level (Model 89) and the five-storey numerical model with a double height space between Levels 0 and 1 (Model 101). Furthermore, the results show that there is an overall increase in magnitude of the relative x-displacement at slab over semi-basement level of the

four-storey cases when compared to the corresponding six-storey numerical models which include one to three additional seismic vulnerability characteristics. This increase could be attributed to the higher proportion of the irregularity to the overall size of the structure, thereby giving rise to higher displacements in the four-storey cases.

On the other hand, a reduction in the magnitude of relative x-displacement is observed in the five-storey single building numerical models when compared to their six-storey counterparts in the cases which include either setbacks (Model 81) or the presence of a double height space (Model 101) as the only additional seismic vulnerability characteristics, or the three investigated characteristics acting in combination (Model 121). The resistance to collapse of the four-storey numerical model, which includes the presence of setbacks (Model 83), and the higher stability, which can be attributed to the corresponding five-storey case (Model 81), in view of the lowering of the centre of mass resulting from the presence of the setbacks at the topmost storey as explained by Parisi [60], suggests that the reduced x-displacements in the five-storey numerical model, which includes setbacks, might be the consequence of this increased stability together with the lower base shear resulting from the reduction in building mass at penthouse level, when compared to the corresponding six-storey case. Whereas other complex interactions between the effects of the various building characteristics on the seismic response of the five-storey numerical model, which includes all three additional seismic vulnerability characteristics investigated, cannot be excluded, the increased stability due to the lowering of the centre of mass in addition to the reduction in base shear resulting from the decrease in building mass, could also have a bearing on the reduced x-displacement exhibited by this model while the overall height of the building might be still too large for the effect of the other irregularities to predominate (in the form of increased displacements).

In the case of the numerical models in this study investigating the presence of the double height space, a number of factors, which are related to the position, proportions and detailing of the area around the double height void, could have a bearing on the seismic response and on the analysis results extracted from these models for comparison with the other investigated cases. These factors include the restriction of the void to (part of) the area of the front room, the limited overall dimensions of the void and the 250 mm thick reinforced concrete slab present on three of its sides, the position of the double height space between Levels 0 and 1 and, hence, not at the lowermost possible level, and the partial stabilising effect of the presence of the stairwell, located just 1.45 m away and running throughout all the floors of the analysed numerical models, which include a double height space as the only seismic vulnerability characteristic. Furthermore, while the reasons behind the selection of the slab over semi-basement level for the extraction of data from all the analysed numerical models were explained in Section 4.2, the relative x-displacements extracted at this position in the case of the models which include the presence of a double height space might not give enough insight into the structural behaviour of these models. The deformed profiles under seismic loads of the models which include a double height space between Levels 0 and 1 as the only additional seismic vulnerability characteristic, are expected to result in a linear variation in x-displacement in the lowermost storey, starting from the first course of the semi-basement level and reaching a low magnitude x-displacement

at slab over semi-basement level, whereas the main increase in x-displacement would be expected to occur at the levels where the double height space is located. Hence, the variation in the magnitude of the relative x-displacements resulting at slab Levels 1 and 2 with the reduction in number of storeys might not be entirely reflected in the observed relative x-displacements at slab over semi-basement level[32]. Therefore, while, in general, the reduced stiffness of the area of the building incorporating a double height space would be expected to exhibit increased x-displacements at all building heights when compared to the corresponding control models, it is likely that the reduced magnitude of the relative x-displacement at slab over semi-basement level at the start of failure resulting for the five-storey single building model, which includes a double height space, when compared to the equivalent six-storey case, and also the reduced x-displacement exhibited by the five-storey case when compared to the corresponding control numerical model, might be the result of a combination of the factors discussed above.

The comparison of the single characteristic cases reveals that, in the six-storey cases, the highest increase in relative x-displacement at slab over semi-basement level at the time of start of collapse, when compared to the corresponding control numerical model, is exhibited by Model 99 (which includes a double height space), followed by Model 79 (which includes setbacks at penthouse level). On the other hand, in the five- and the four-storey cases, the highest increase in relative x-displacement was recorded in the corresponding numerical models, which include a soft storey at semi-basement level (Models 71 and 73 respectively), which, in the case of the five-storey models, is followed by Model 81 (which includes setbacks at penthouse level). The relative variation in the x-displacements exhibited by the four-storey, and, to some extent, the five-storey single characteristic cases investigated could have been anticipated to some degree, considering the explanation given by various authors [55] [56] [57] of the increased displacement caused by the higher concentration of seismic forces acting at a position in a structure where a localised reduction in stiffness is present, particularly, if this reduced stiffness occurs at the lowermost portion of a building, and the considerations discussed in Section 4.2.1.2 and the recommendations given by Parisi [60] in the case of the presence of setbacks, as mentioned earlier. On the other hand, the results obtained for the six-storey cases are in contradiction with these findings, particularly in the case of Model 69 (the six-storey numerical model which includes a soft storey at semi-basement level), which resulted in the lowest relative x-displacement.

[32] This issue is not likely to affect the numerical models which include the presence of setbacks since, in such models, the only variation in plan layout occurs at the topmost level. A gradual linear variation in x-displacement throughout the floors is, therefore, expected in numerical models which include setbacks at penthouse level, allowing the identification of the variation in response when compared to the corresponding control numerical model and to the numerical models, which include the presence of a soft storey, through the relative x-displacement values read at slab over semi-basement level.

In view of the close analysis times at which the start of failure was identified in the single and the combined characteristics cases, as discussed earlier and reported in Figure 4-44, the comparison of the relative x-displacements at slab over semi-basement level of the analysed numerical models, which include one to three additional seismic vulnerability characteristics, at the time when the onset of collapse was identified in the corresponding control numerical model, was carried out in order to examine the variation in the degree of deformation of all corresponding models at the same position and at the same analysis time. This information is summarised in Figure 4-46.

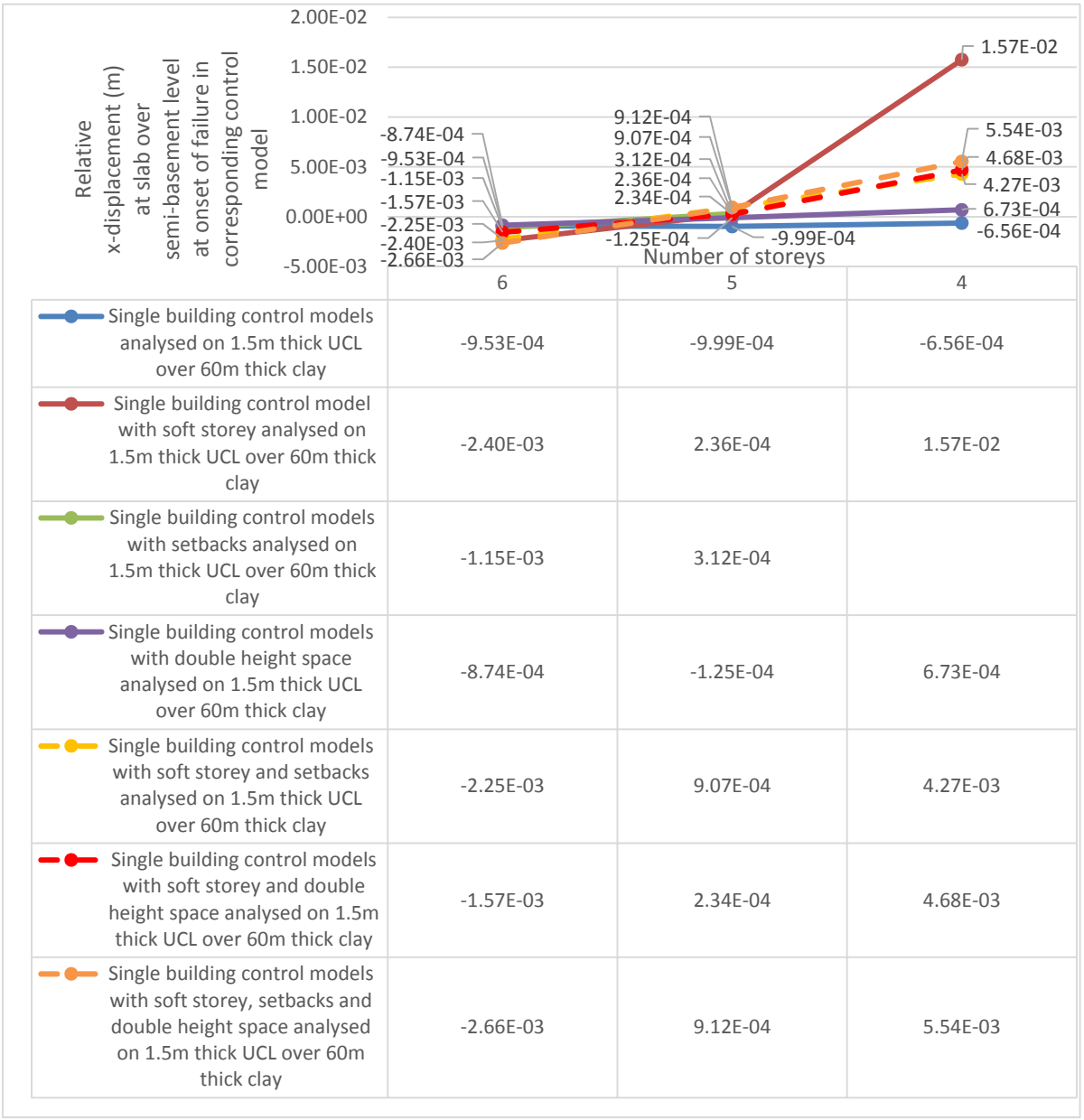

	6	5	4
Single building control models analysed on 1.5m thick UCL over 60m thick clay	-9.53E-04	-9.99E-04	-6.56E-04
Single building control model with soft storey analysed on 1.5m thick UCL over 60m thick clay	-2.40E-03	2.36E-04	1.57E-02
Single building control models with setbacks analysed on 1.5m thick UCL over 60m thick clay	-1.15E-03	3.12E-04	
Single building control models with double height space analysed on 1.5m thick UCL over 60m thick clay	-8.74E-04	-1.25E-04	6.73E-04
Single building control models with soft storey and setbacks analysed on 1.5m thick UCL over 60m thick clay	-2.25E-03	9.07E-04	4.27E-03
Single building control models with soft storey and double height space analysed on 1.5m thick UCL over 60m thick clay	-1.57E-03	2.34E-04	4.68E-03
Single building control models with soft storey, setbacks and double height space analysed on 1.5m thick UCL over 60m thick clay	-2.66E-03	9.12E-04	5.54E-03

Figure 4-46 Variation in relative x-displacement at slab over semi-basement level (at time of start of failure at same position in corresponding control models) of single building numerical models including one to three additional seismic vulnerability characteristics.

Figure 4-46 indicates that, with the exception of the six-storey numerical model which includes a double height space as the only additional seismic vulnerability characteristic (Model 99), the other five six-storey cases and all the four-storey numerical models, which include one to three additional building characteristics, exhibit a higher (in magnitude) relative x-displacement at slab over semi-

basement level at the analysis time corresponding to the time of the start of failure at this position in the corresponding control models. On the other hand, a lower value (in magnitude) of relative x-displacement was recorded in all the analysed five-storey numerical models, which include one to three additional building characteristics. Furthermore, while a reduction in relative x-displacement is observed in all the five-storey numerical models when compared to their six-storey counterparts, an overall increase in magnitude of relative x-displacement is evident in the four-storey numerical models, when compared to the six-storey equivalents. The only exception to this trend was exhibited by the four-storey single building numerical model which includes a double height space between Levels 0 and 1 (Model 103, which results in a lower relative x-displacement than the corresponding six-storey case (Model 99).

The relative x-displacements at slab over semi-basement level at the analysis times corresponding to the start of failure at the same position in the corresponding control numerical models reported in Figure 4-46, are not associated with the mobilisation of failure mechanisms in the cases where these analysis times occur before the onset of collapse of the respective models. Therefore, it may be argued that the comparison of these relative x-displacements at a time, during the dynamic analysis of the respective models, which corresponds to the start of failure of the corresponding control model, in conjunction with a consideration of the analysis time at which the start of failure was identified for the numerical models under comparison, can provide an indication of the relative deformation ability of the models when compared to the corresponding control models and, hence, to a certain extent, an indication of the relative ductility capacity of these structural systems. In this light, while, as discussed earlier, the effect of a particular seismic characteristic on the response of a structure to earthquake excitations can vary depending on the overall height of the structure and the position of the irregularity, the magnitude of the relative x-displacement results obtained from analysed models reported in Figure 4-46 considered in combination with the corresponding comparison of the analysis times at the start of failure of the respective models recorded in Figure 4-44 indicate that:

i. for the analysed six-storey cases, which include one additional building characteristic, the lowest relative x-displacement and the earliest start of collapse occur in the numerical model, which includes a double height space (Model 99). On the other hand, the numerical model with a soft storey at semi-basement level (Model 69) results in the highest relative x-displacement and the latest start of failure, followed by the numerical model which includes setbacks at penthouse level (Model 79).
ii. while the four-storey numerical model, which includes setbacks at penthouse level (Model 83), resists collapse, its five-storey equivalent (Model 81) results in the latest start of failure and the highest relative x-displacement when compared to the other single characteristic five-storey numerical models. However, its relative x- displacement is lower than that of the corresponding control numerical model.
iii. At a height of four storeys, the numerical model which includes a soft storey at semi-basement level (Model 73) exhibits the highest relative x-displacement. However, this also corresponds to an earlier start of failure than the equivalent four-storey control numerical model.

Furthermore, the four-storey numerical model which includes a double height space (Model 103), results in the second highest relative x-displacement and the highest delay in the onset of collapse. These results suggest that, whereas in higher structures the height can also have a significant bearing on the seismic response (hence, indicating that, when additional seismic characteristics are also present, the exhibited response is the result of the combined effects of the height and the presence of the irregularity). At a height of four storeys, the proportion of an irregularity, which is located at (only) one particular level in the structure when compared to the building volume, is very high. Therefore, the overall debilitating or enhancing effect of the characteristic is more evidently exposed by the structural behaviour. Thus, in the four-storey analysed models, the earlier start of collapse exhibited by Model 73 when compared to the corresponding control model does not allow the interpretation of the higher relative x-displacement resulting from the former as an increased ductility capacity (since this higher displacement occurs after the start of collapse in this model), but rather it associates this characteristic with a higher ductility demand, and a higher relative seismic vulnerability rating. On the other hand, the significant delay in the start of failure (161 frames, 1.61 s) and the higher relative x-displacement resulting from Model 103, even though second highest in magnitude to Model 73, is likely to indicate a higher ductility capacity than the corresponding control model. Furthermore, the resistance to collapse of the numerical model which includes setbacks at penthouse level at a height of four storeys (Model 83), when compared to the collapse resistance of the control model at three storeys, tends to indicate that this characteristic, at the position and in the proportions considered in the present study, results in a higher resistance to seismic excitations. As explained previously, the reduction in the inertial mass and the lowering of the centre of gravity as suggested by Parisi [60] are likely to be the main reasons behind this increased resistance.

iv. In the six-, five- and four-storey numerical models which include two to three seismic vulnerability characteristics, the numerical models which include all three investigated characteristics in combination (Models 119, 121 and 123) always result in the highest relative x-displacement when compared to the other 2 two-characteristics cases, which relative x-displacements are higher than those resulting from the corresponding control numerical models at heights of six and four storeys. These models also result in the highest delay in the onset of failure when compared to the corresponding control numerical model, with the exception of the four-storey case, which shows a marginally lower delay (7 frames, 0.07s) in the start of failure than the numerical model which includes a soft storey and setbacks in combination. The higher tendency of these models to deform is in line with the increase in storey displacements at the positions which exhibit a sudden reduction in the stiffness of a structure as reported in literature [54] [55] [56] [57]. On the other hand, a lower relative x-displacement results from all the five-storey two- and three-characteristics models (Models 91, 111 and 121) when compared to the corresponding control numerical model.

As discussed earlier, in the case of the presence of a double height space, the observed reduced impact on the stiffness of the structures is suspected to be affected by the position and proportions of the void in the slab at Level 1 and the detailing of the slabs around the void as modelled in this study. However, the increased x-displacements recorded from the numerical models, which include the investigated characteristics, particularly in the case of soft storeys and, to a lesser extent, when a double height space is present, is likely to be mainly a consequence of the variation in stiffness of the respective structures when compared to the control numerical model. As discussed previously and as reported in literature, this localised reduction in stiffness results in the concentration of a higher proportion of earthquake forces in the floor where the irregularity is present, thereby giving rise to higher displacements, which can lead to collapse due to P-delta effects. Hence, based on the above results, in the cases where a structure which includes a particular building characteristic, resists collapse at a higher number of storeys (as in the numerical models which include setbacks at penthouse level analysed in this study) or at a significantly later stage in the dynamic analysis for the same overall height when compared to the corresponding control model, this ductility capacity can be considered as beneficial to the structural seismic resistance. However, when the increased flexibility causes displacements which, combined with the gravity load of the structure, results in the formation of failure mechanisms at an earlier stage than the onset of failure in the corresponding control model, then this increased flexibility becomes undesirable and the building characteristics which cause it can be considered to increase the structure's seismic vulnerability.

Moreover, at heights of six and five storeys, a delay in the start of failure was observed in the numerical models which include a soft storey or a double height space when compared to the start of failure in the corresponding control numerical model. However, the relatively small delay (on average, 0.16 s in the six-storey and 0.62 s in the five-storey single characteristic cases analysed in this study) does not allow the drawing of conclusions regarding the relative severity which can be associated with the different seismic vulnerability characteristics investigated.

Furthermore, since the relative x-displacements at slab over semi-basement level at the onset of failure of the respective numerical models did not correspond to the maximum x-displacements undergone by the respective models at this position, a comparison of the relative x-displacements at the time corresponding to the maximum x-displacement at slab over semi-basement level prior to the start of failure was carried out, as reported in Table 41 in Appendix D and summarised in Figure 4-47. While the six-storey numerical model which includes setbacks at penthouse level, results as the only case which exhibits a lower (maximum) relative x-displacement when compared to the corresponding control numerical model, all the other investigated cases result in higher magnitude maximum relative x-displacements. Similarly to the observed ranking of the relative x-displacements at the time of start of failure at slab over semi-basement level in the corresponding control model discussed above, the six- and four-storey numerical models which include a soft storey as the only additional building characteristic (Models 69 and 73) result in the highest (in magnitude) relative x-displacements at this analysis time, followed by the numerical model which includes setbacks (Model 79) at six storeys and the numerical model which includes a double height space (Model 103) at four storeys. Hence, the

interpretation of the relative ductility capacity or ductility demand imposed by the respective characteristics and the relative seismic vulnerability inferred by the results summarised in Figure 4-46 applies even in this case.

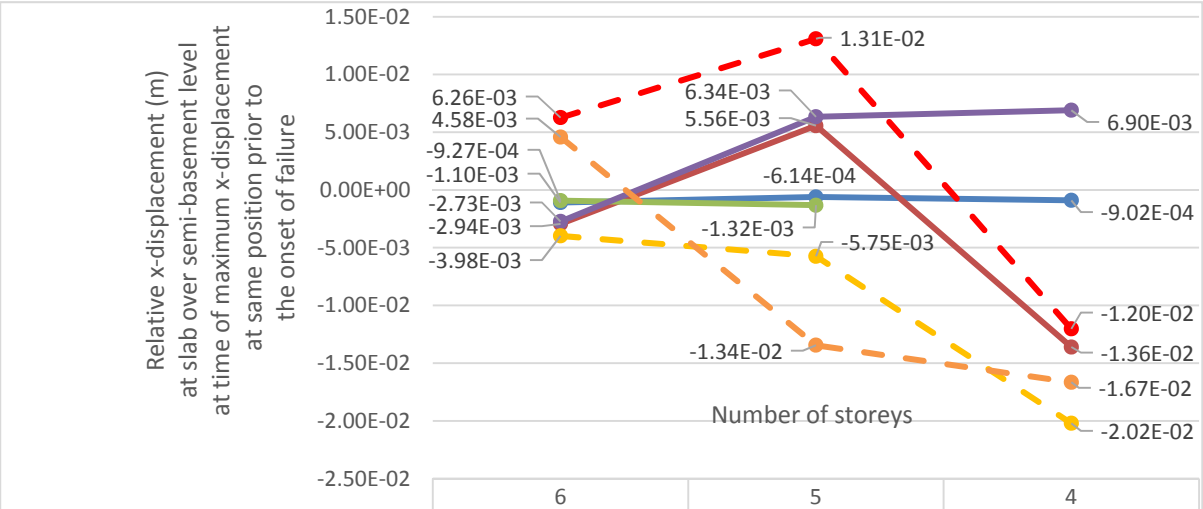

	6	5	4
Single building control model analysed on 1.5m thick UCL over 60m thick clay	-1.10E-03	-6.14E-04	-9.02E-04
Single building control model with soft storey analysed on 1.5m thick UCL over 60m thick clay	-2.94E-03	5.56E-03	-1.36E-02
Single building control model with setbacks analysed on 1.5m thick UCL over 60m thick clay	-9.27E-04	-1.32E-03	
Single building control model with double height space analysed on 1.5m thick UCL over 60m thick clay	-2.73E-03	6.34E-03	6.90E-03
Single building control model with soft storey and setbacks analysed on 1.5m thick UCL over 60m thick clay	-3.98E-03	-5.75E-03	-2.02E-02
Single building control model with soft storey and double height space analysed on 1.5m thick UCL over 60m thick clay	6.26E-03	1.31E-02	-1.20E-02
Single building control model with soft storey, setbacks and double height space analysed on 1.5m thick UCL over 60m thick clay	4.58E-03	-1.34E-02	-1.67E-02

Figure 4-47 Variation in relative x-displacement at slab over semi-basement level at time of maximum x-displacement prior to start of failure at same position in numerical models including one to three additional seismic vulnerability characteristics.

On the other hand, at a height of five storeys, while the numerical model which includes a soft storey (Model 71) retains the second highest relative x-displacement, the highest (in magnitude) maximum relative x-displacement is exhibited by the numerical model which includes a double height space (Model 101). Moreover, in the case of the two and three characteristics cases investigated, the numerical model, which includes the three building characteristics examined in this study acting in

combination, results in the highest (in magnitude) relative x-displacement at slab over semi-basement level at the time corresponding to the maximum relative x-displacement at the same position only for a height of five storeys (Model 121). This combination exhibits the second highest relative x-displacements out of the combined characteristics cases in the six- and four-storey numerical models (Models 119 and 123), whereas the corresponding highest relative x-displacements in the six- and four-storey combined characteristics numerical models were exhibited by the numerical model which includes a soft storey and a double height space (Model 109) and the numerical model which includes a soft storey and setbacks (Model 93), respectively.

Based on Park's [209] definition of 'ductility', which was quoted at the start of this section, the comparison of the relative x-displacements at a particular position in the analysed numerical models at the time during the dynamic analysis when the corresponding control numerical model started to exhibit signs of failure, as discussed above, with reference to the relative x-displacements reported in Figure 4-46, can give an indication of the relative ductility capacity which can be associated with the presence of different characteristics. However, as explained by Chopra [43], the variation in deformation of a structure throughout the duration of a seismic excitation depends on the variation of its flexural rigidity (EI) and its mass throughout its height and, hence, on the triggered natural modes of vibration. Therefore, considering that the main cause of failure in, at least, two of the investigated cases (the presence of a soft storey and, to a lesser extent, the presence of a double height space) is most likely a consequence of a failure mechanism triggered off by the large displacements, it may be concluded that, where discrepancies between the two outcomes exist, then the relative x-displacements at slab over semi-basement level at the analysis time corresponding to the maximum x-displacement identified at this position prior to the onset of collapse is likely to give a better representation of the relative seismic vulnerability ranking, which is to be attributed to the investigated parameters.

In the single characteristic cases, the relative x-displacement values at the analysis time corresponding to the start of failure at slab over semi-basement level and those at the time of the maximum x-displacement recorded at the same position in the respective numerical models both indicate that the highest relative x-displacement at a height of six and four floors is exhibited by the numerical models which include a soft storey at slab over semi-basement level (Models 69 and 73) and, an identical order of ranking in the magnitude of the relative x-displacement results at an overall height of four floors is evident in both cases. A higher seismic vulnerability associated with the presence of a soft storey at slab over semi-basement level is, therefore, implied by these results. Two main discrepancies, however, result between the relative x-displacement values at these two analysis times:

i. A lower relative x-displacement and, hence, a lower associated seismic vulnerability in the case of the presence of setbacks at penthouse level when compared to the presence of a double height space at an overall height of six storeys;

ii. A higher relative x-displacement resulting from the five-storey model which includes a double height space when compared to the other corresponding single characteristic models investigated.

In the five-storey single characteristic models, the 14% higher relative x-displacement resulting from the presence of a double height space (which is restricted to a limited area of the front room and is located at a higher storey than the position, where the displacement readings are taken in all the numerical models) when compared to that of a soft storey (which extends throughout the lowermost level of the structure, which level coincides with the position where the displacement values are recorded) still seems to contradict the expected structural response based on published literature as discussed previously. However, if the presence of the soft storey is temporarily excluded from the comparison of the five-storey relative x-displacement values, since it emerges as the characteristic which can be associated with the highest degree of seismic vulnerability from the six- and the four-storey numerical models, then the relative x-displacement results at the analysis time corresponding to the maximum x-displacement at a height of five floors would confirm the relative seismic vulnerability ranking observed from the six- and four-storey analysed numerical models and that proposed by the author based on the comparison of the analysis times at start of failure of the respective cases. The presence of a double height space between Levels 0 and 1 would then be attributed a higher seismic vulnerability rating than the presence of setbacks. The lower (in magnitude) maximum relative x-displacement exhibited by the six-storey numerical model which includes setbacks, when compared to the corresponding control numerical model, the least relative x-displacement at start of failure resulting in the five-storey equivalent model when compared to the magnitude of the relative x-displacements recorded in the corresponding five-storey numerical model including a soft storey, and the resistance to collapse of the four-storey numerical model with setbacks is likely to confirm the lower level of seismic vulnerability, which would be linked to the presence of setbacks at penthouse level when compared to the other seismic vulnerability characteristics.

The ranking of the ratio of maximum x-acceleration at first course of the semi-basement level prior to the onset of failure at slab over semi-basement level to the maximum input peak ground acceleration for the same analysis interval recorded in Table 38 of Appendix D and summarised in Figure 4-48 in the case of the six- and five-storey single characteristic models, is in agreement with the ranking of the relative x-displacements at slab over semi-basement level at the analysis time corresponding to the maximum x-displacement at the same position prior to the start of failure. On the other hand, at a height of four storeys, the highest amplification of x-accelerations at first course of the semi-basement level was exhibited by the numerical model, which includes a double height space (Model 103), therefore, not resulting in agreement with the ranking suggested by the relative x-displacements and the time at start of failure.

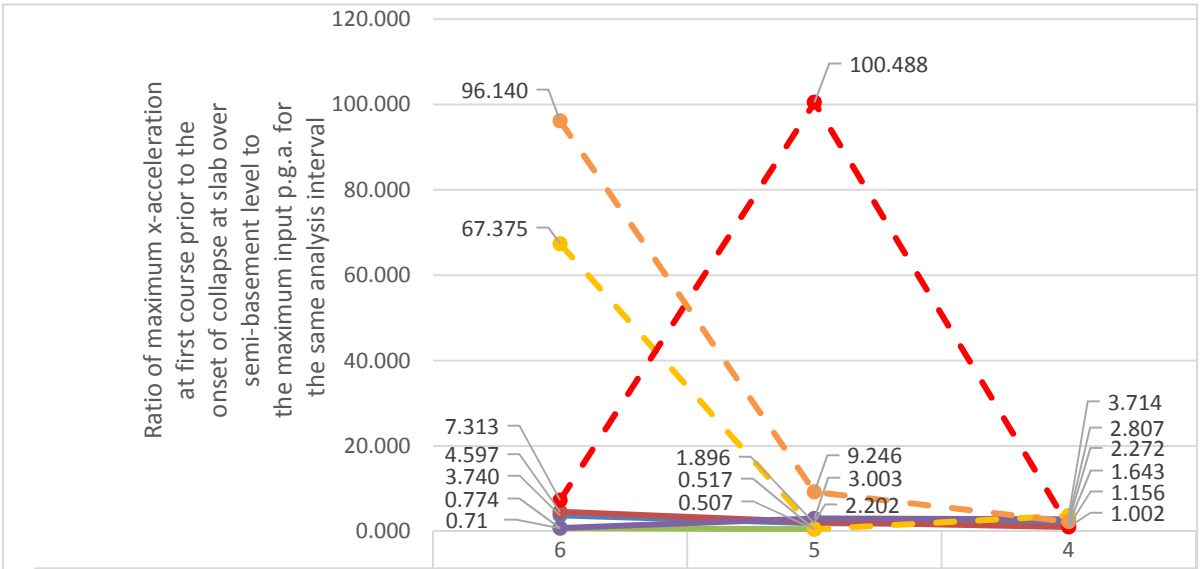

Single building control models analysed on 1.5m thick UCL over 60m thick clay	3.740	1.896	1.643
Single building control models with soft storey analysed on 1.5m thick UCL over 60m thick clay	4.597	2.202	1.002
Single building control models with setbacks analysed on 1.5m thick UCL over 60m thick clay	0.71	0.517	
Single building control models with double height space analysed on 1.5m thick UCL over 60m thick clay	0.774	3.003	2.807
Single building control models with soft storey and setbacks analysed on 1.5m thick UCL over 60m thick clay	67.375	0.507	3.714
Single building control models with soft storey and double height space analysed on 1.5m thick UCL over 60m thick clay	7.313	100.488	1.156
Single building control models with soft storey, setbacks and double height space analysed on 1.5m thick UCL over 60m thick clay	96.140	9.246	2.272

Figure 4-48 Comparison of ratio of maximum x-acceleration at first course of semi-basement level prior to the onset of failure at slab over semi-basement level to the maximum input peak ground acceleration for the same time interval during the dynamic analysis.

With reference to Table 31 in Appendix D, the occurrence of resonance in the analysed six-, five- and four-storey models, which include one to three additional building characteristics, is not likely if the structures are considered in an undamaged state, since the natural frequencies of these structures, when analysed on clay at Minimum Z, resulted as higher than the main peak frequency and either lower (in the case of the six-storey numerical models) or higher than the highest secondary peak frequency of the input simulated ground motion record. On the other hand, resonance effects

following the initial degradation of the structures cannot be excluded in the five-storey cases, which include either a soft storey, setbacks or a double height space as the only additional building characteristic, since the natural frequency of these numerical models, in the transverse direction, when analysed on clay at Minimum Z, are 2.3%, 21.3% and 13.44%, respectively, higher than the highest secondary peak frequency in the main energy range of the input simulated ground motion record.

Therefore, while resonance effects after initial degradation of the structure could contribute to the high relative x-displacement recorded in the five-storey numerical model, which includes a double height space (Model 101), they are still more likely to occur in the equivalent numerical model which includes a soft storey (Model 71), since the difference between its natural frequency in the undamaged state and the secondary peak frequency of the simulated ground motion record is smaller (2.3%). Furthermore, as suggested by the frequency values summarised in Table 34 of Appendix D, resonance effects in the ground layers cannot be excluded in most of the six-, five- and four-storey single characteristic cases, with the exception of Models 79 and 103, in view of the presence of a secondary frequency in the clay layer and the peak frequency together with a secondary frequency in the upper coralline limestone layer, which fall within the main energy range of the input simulated ground motion record. Hence, since this correspondence in frequencies is not limited to specific numerical models, which exhibit an unexpected seismic response, the occurrence of resonance effects in the ground layers is not likely to justify any particular high relative x-displacement resulting from one numerical model over another.

Similarly, the occurrence of resonance in the two to three characteristic six-, five- and four-storey numerical models when considering the structures in their undamaged state, is highly unlikely since, as recorded in Table 31 of Appendix D, the natural frequencies in the transverse direction of these structures when analysed on clay at Minimum Z are higher than the main peak frequency and, either lower (in the six-storey numerical models), or higher, than the highest secondary peak frequency in the main energy range of the input simulated ground motion record. Furthermore, as observed in the single parameter cases, resonance effects following initial degradation cannot be excluded in the five-storey combined characteristics cases since their natural frequencies in the undamaged state are 2.6% to 9.6% higher than the highest secondary peak frequency in the main energy range of the input simulated ground motion record, with the lowest value corresponding to the numerical model which includes a soft storey and a double height space in combination (Model 111). Moreover, with the exception of the clay layer in Models 91, 109 and 123, the information reported in Table 34 of Appendix D suggests that resonance effects in the ground layers cannot be excluded in any of the combined cases. In view of the above, it is highly unlikely that specific unexplained magnitudes of relative x-displacements resulting from any of the combined six-, five- or four-storey numerical models can be attributed to the occurrence of resonance or resonance effects in the respective numerical models or in the ground layers.

It is worth noting that a limited number of cases resulting from the comparisons of the response parameters extracted from the numerical models analysed in this study could not be interpreted by the author based on the structural behaviour under seismic excitation associated in literature with the presence of the investigated building characteristics. Nevertheless, the results discussed in the foregoing section provide strong indications with respect to the relative ductility capacity or ductility demand and seismic vulnerability which can be linked with the building characteristics under study. The significant delay (1.16 s) in the start of failure of the four-storey numerical model which includes a double height space (Model 103) when compared to the corresponding control numerical model, together with the marginally higher relative x-displacement recorded at slab over semi-basement at the start of failure can be indicative of a higher ductility capacity. The resistance to collapse of the four-storey numerical model which includes the presence of setbacks, when compared to the resistance at three storeys of the corresponding control numerical model and the other single characteristic cases, suggests that the lowest seismic vulnerability rating can be attributed to this characteristic when compared to the other investigated parameters. On the other hand, while, as observed in the previous Sections of this thesis, the influence of the overall building height and the underlying ground cannot be ignored, the examination of the variation in the relative displacements at various analysis times on the same ground type, the time at which the start of failure was identified in the analysed numerical models and the significantly higher reduction in the natural frequency of the analysed structures after the dynamic loading stage when compared to the natural frequency at the end of the static loading stage all suggest that the presence of a soft storey at semi-basement level can likely be associated with the highest relative degree of seismic vulnerability when compared to the other two investigated building characteristics, followed by the presence of a double height space.

4.2.3.5 Comparison of the seismic response of the analysed six-storey numerical models including three additional seismic vulnerability characteristics: effect of the variation in the ground formation layers and position of double height space

In the foregoing section, the variation in the seismic response of contemporary loadbearing URM buildings in the presence of one to three additional building characteristics was studied for different overall building heights, considering the respective additional characteristics at the same plan position and in the same storey level whenever these were present. Furthermore, all the single and combined characteristics cases investigated consist of an alteration of the corresponding control numerical model to include the respective building characteristics. Therefore in all cases, the same typical floor layout, which is present at every storey of the corresponding control numerical model is, hence, retained at the floor levels which do not include one of the additional characteristics.

As explained in Section 3.4.8 and with reference to the plan layouts of the analysed cases presented in Figures 20 to 32 in Appendix C, the control numerical models were based on the typical floor layout of an existing six-storey contemporary loadbearing URM building located in Xemxija, in Malta, which building was modelled in ELS® and its natural frequency was compared to the natural frequency of the existing building as a verification of the accuracy of the adopted modelling techniques. Therefore, the analysed models consist of the same overall plan dimensions, storey heights and wall thicknesses of

Xemxija Building Number 0011 and incorporate the typical floor plan layout and the corresponding storey façade of this structure at every level, which does not include an additional building characteristic. At the positions where the setbacks or a double height space was introduced in the numerical models, the alterations to the plan layout were restricted to the areas affected by the introduction of the particular building characteristic under study. Furthermore, while the introduction of the soft storey in the analysed numerical models involved the removal of all the internal walls at semi-basement level from the original control numerical model, the size and position of the setbacks were in accordance with the planning regulations, which were in force in the Maltese Islands up to November 2015, therefore, coinciding with the dimensions of the setbacks in the Xemxija building. The double height space in the analysed models was created through the formation of a 3.15 m wide by 5.00 m long void in the slab of the front room over Level 0, which void directly abuts the left hand side party wall. Moreover, in the control numerical models and in the numerical models which include the presence of a double height space or setbacks, the main staircore extends throughout all the floor levels, whereas it is absent at semi-basement level in the numerical models, which include a soft storey at this position.

Models 128 and 129 consist of the structure of the existing Xemxija Building Number 0011 analysed in isolation (i.e. as a single building numerical model in both cases) on 1.5 m thick upper coralline limestone over 60 m thick clay, and 30 m thick upper coralline limestone over 30 m thick clay respectively, where the latter ground formation case corresponds to the real subsoil scenario of the existing building at the top of the Xemxija hill. As indicated in the Development Permit Plans of Xemxija Building Number 0011, which are reproduced in Figure 20 of Appendix C, this building consists of an open plan area in the front half of the building at semi-basement level, a typical floor layout at Levels 0, 1 and 2 (with the exception of an additional wall running parallel to the right hand side party wall in the front room at Level 0), an altered layout in the rear half of the plan at Level 3, a double height space created through the formation of a 4.76 m wide and 4.33 m long void between Levels 3 and 4, and an open plan at penthouse level (Level 4), where setbacks are also present. The main staircore extends between Levels 0 and 3 and is, therefore, absent at semi-basement level and at penthouse level.

Therefore, the main differences between Model 128 and the six-storey single building numerical model which includes the three investigated building characteristics in combination (Model 119) include:

a) the extent of the soft storey / open plan at slab over semi-basement level;
b) the plan layouts at Levels 3 and 4;
c) the size and position on plan of the double height space and the storey level at which it is located;
d) the extent of the main stairwell, which stops at Level 3 in Model 128 and at Level 4 in Model 119.

All the above-listed differences are most likely to have a bearing on the seismic response of the respective structures. However, while the reduction of the open plan area at slab over semi-basement level is expected to increase the stiffness of the Models 128 and 129 when compared to that of Model 119, the positioning of the double height space between the penthouse level and the floor below it, together with the open plan layout at Level 4 and the absence of the staircore at this level in Models 128 and 129 suggests a significant reduction in stiffness at Levels 3 and 4 when compared to the corresponding levels in Model 119.

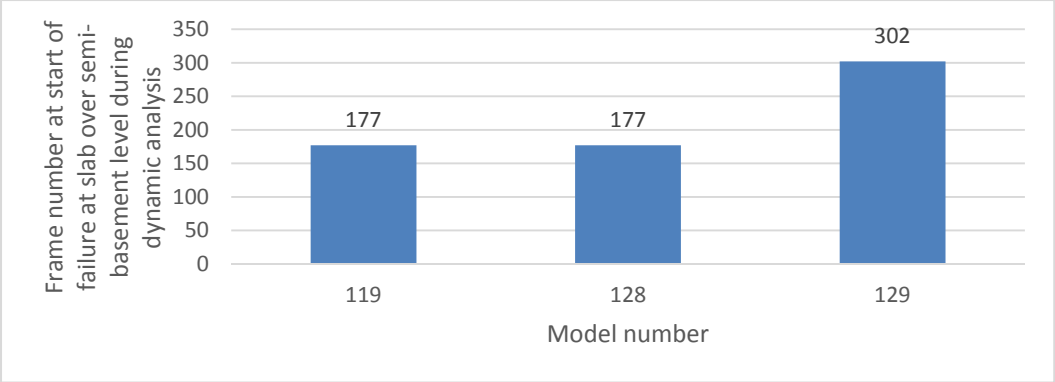

Figure 4-49 Comparison of the analysis time corresponding to the start of failure at slab over semi-basement level in Models 119, 128 and 129.

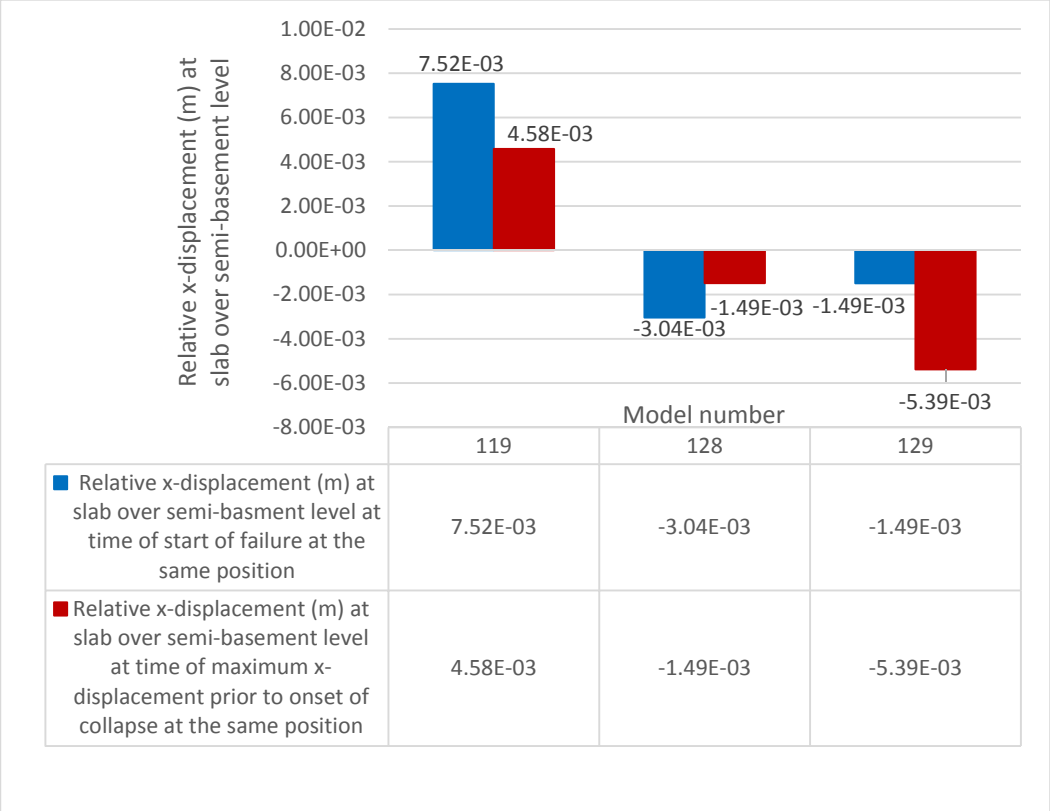

	119	128	129
Relative x-displacement (m) at slab over semi-basment level at time of start of failure at the same position	7.52E-03	-3.04E-03	-1.49E-03
Relative x-displacement (m) at slab over semi-basement level at time of maximum x-displacement prior to onset of collapse at the same position	4.58E-03	-1.49E-03	-5.39E-03

Figure 4-50 Comparison of the relative x-displacement at slab over semi-basement level at different analysis times for Models 119, 128 and 129.

Hence, with reference to Figure 4-49 and Tables 36 and 37 in Appendix D, while the start of failure at slab over semi-basement level in Models 119 and 128 was identified at the same analysis time, Figure 4-50 shows that the magnitude of the relative x-displacement at the start of failure at slab over semi-basement level and the magnitude of the relative x-displacement at slab over semi-basement level at the analysis time corresponding to the maximum x-displacement prior to the onset of collapse at the same position in the models, are 147.4% and 207.4% respectively higher in Model 119 than Model 128. Furthermore, as reported in Figure 4-51, the relative x-displacement at slab over penthouse level at the analysis time, which corresponds to the maximum x-displacement at slab over semi-basement level prior to the start of failure at the same position, is higher in Model 119 than in Model 128. On the other hand, a lower relative x-displacement is exhibited at the slab over the penthouse level by Model 119 at the time which corresponds to the maximum x-displacement prior to the start of collapse at the penthouse slab level.

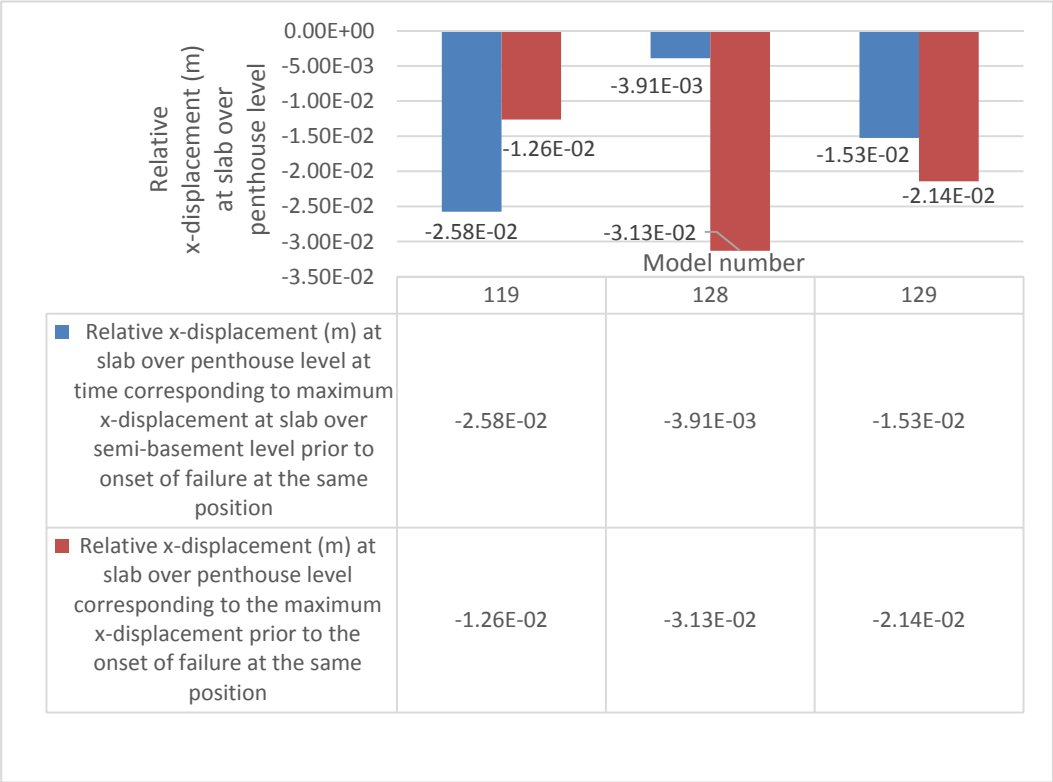

Figure 4-51 Comparison of the relative x-displacement at slab over penthouse level at different analysis times for Models 119, 128 and 129.

These variations in the displacements of the two models can be explained by considering the positions where the main building characteristics, which cause increased displacements in structures under the effect of seismic excitation, are located in the respective models. The higher relative x-displacements corresponding to the analysis time at which the onset of collapse was identified at slab over semi-basement level exhibited by Model 119 when compared to Model 128, are most likely caused by the presence of the soft storey and the double height space in the vicinity of this position. On the other hand, in Model 128, while the open plan area at semi-basement level is expected to result in a smaller

reduction in the stiffness of the lowermost storey when compared to the soft storey present in Model 119, the resulting decrease in storey stiffness caused by the presence of the double height space between Levels 3 and 4 and the open plan at Level 4 could explain the higher relative x-displacements recorded at slab over penthouse level at the analysis time corresponding to the maximum x-displacement at this position.

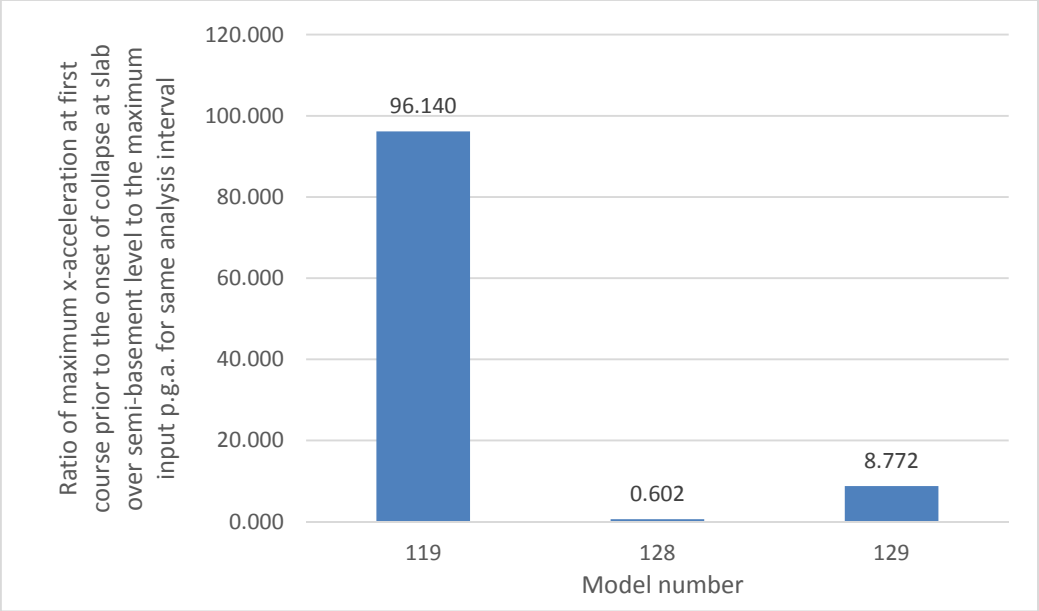

Figure 4-52 Comparison of the ratio of maximum x-acceleration at first course of semi-basement prior to the onset of failure at slab over semi-basement level to the maximum input p.g.a. in the input simulated ground motion record for the same analysis interval in Models 119, 128 and 129.

The higher amplification of seismic accelerations at first course of the semi-basement level prior to the onset of collapse at slab over semi-basement level exhibited by Model 119 when compared to Model 128, as reported in Table 39 of Appendix D and summarised in Figure 4-52, could also lead to the higher relative x-displacements exhibited by the former model at this analysis time. Furthermore, as recorded in Table 34 in Appendix D, the secondary peak frequency identified in the clay layer and the main and secondary peak frequencies in the upper coralline limestone layers, coinciding with secondary frequencies in the main energy range of the input simulated ground motion record, suggest that resonant effects in the ground layers could explain the amplification of accelerations at first course of the semi-basement level and, hence, the increased displacements resulting from Model 119.

The above results, therefore, seem to indicate that the position throughout the height of a six-storey masonry structure of a storey, which has a reduced stiffness when compared to the other floors, would have no significant bearing on its time of start of failure, but would generate increased displacements in the region of the irregularity at the onset of failure of the level where the irregularity is present. Nevertheless, the basic differences discussed at the start of this Section between Models 119 and 128, the difference in the type and extent of the compared irregularities present in the two models and the limitation of the comparison to the six-storey case should be noted. These differences do not allow any generalisations to be made on the effect of the position of a storey with a reduced stiffness on the seismic response of a structure, based on the results of this comparison. However, they highlight the

importance of further investigations to be carried out through the comparison of the seismic response of different structures with reduction in number of storeys, which structures would have a typical floor layout at all levels, except for the position of the less stiff storey, whose layout would also be kept identical in both cases.

On the other hand, the comparison of the seismic response exhibited by Models 128 and 129, could confirm, or otherwise, the influence of the variation in the ground formation layers suggested by the results reported in this study for control Models 45v2 and 44v2. The comparison of the analysis stage at which the start of failure was identified at slab over semi-basement level in Models 128 and 129, as reported in Figure 4-49, indicates that Model 129 exhibits a significant delay in the onset of collapse, when compared to Model 128. This structural response is in agreement with the responses of the corresponding six-storey control models analysed on the equivalent ground formations (Models 44v2 and 45v2 respectively) and is likely to be caused by the different degree of amplification of seismic accelerations in the clay layers of different thickness and the impedance contrast of the two ground layers as discussed in Sections 4.2.2 and 4.2.3.2. On the other hand, the comparison of the relative x-displacements recorded at slab over semi-basement level at the onset of collapse in the same models based on the information recorded in Figure 4-50 indicates that Model 129 exhibits a reduced relative x-displacement at the same analysis time when compared to Model 128. This is in contrast with the response of control Model 44v2 when compared to that of Model 45v2. However, it should be noted that a higher overall absolute x-displacement was recorded at this position in Model 129, therefore, suggesting that a higher displacement resulted in the ground formation layers. Furthermore, a higher relative x-displacement at slab over semi-basement level, at the analysis time which corresponds to the maximum x-displacement at the same position in the numerical model prior to the start of failure, was observed for Model 129 when compared to Model 128. The predominant frequencies recorded in the ground layers of the analysed numerical models and summarised in Table 34 in Appendix D suggest that these results may be justified by the possible occurrence of resonance effects in both ground layers of Model 129, since two secondary peak frequencies in the clay layer and the main peak frequency together with a secondary frequency in the upper coralline limestone layer coincide with secondary peak frequencies within the main energy range of the input simulated ground motion record. This could also explain the higher ratio of maximum x-acceleration recorded at the first course of the semi-basement level of the same model before the start of failure to the maximum peak ground acceleration in the input simulated ground motion record for the same time interval as reported in Table 39 of Appendix D and in Figure 4-52.

Furthermore, the information reported in Figure 4-51 shows that, while Model 129 exhibits a higher relative x-displacement at slab over penthouse level at the analysis time when the maximum x-displacement was recorded at slab over semi-basement level, Model 128 results in a higher relative x-displacement at slab over penthouse level at the analysis time corresponding to the maximum x-displacement at this position. Moreover, with reference to Tables 40 and 41 in Appendix D, it is evident that Model 129 exhibits a delay in the onset of failure and in the analysis time corresponding to the

maximum x-displacement at almost every level where the structural responses were recorded (with the only exception resulting at slab over Level 0 in both cases), when compared to Model 128.

These results, therefore, suggest that, while a higher overall seismic resistance seems to be exhibited by Model 129 when compared to Model 128, in view of the delays in the start of failure recorded in the former case, even though the two structures are identical, the different vibration modes induced in the two models lead to different displacement behaviours throughout the dynamic analysis. Since the same simulated ground motion record was applied in both cases, the variation in the displacement behaviour can most likely be associated with the influence of the different ground formations present, therefore, suggesting that a subsoil consisting of 1.5 m thick upper coralline limestone over 60 m thick clay presents a more deleterious scenario in the presence of seismic excitations than a 30 m thick upper coralline limestone layer overlying a 30 m thick clay layer. This conclusion is in agreement with the interpretation of the seismic response of the control models analysed on different ground formation layers discussed in Section 4.2.3.2. These results also suggest that, for any comparisons of relative ductility capacity to be carried out on different structures, the ground formation layers must be kept unchanged.

4.2.4 Deformed shapes

The findings of the foregoing sections suggest that different ground formations and the presence of different building characteristics, or building proportions, can have a direct bearing on the natural periods of a structure and, hence, on its corresponding modes of oscillation under seismic forces and the variations in relative displacement of its respective storeys. Murty et al. [54] discuss in detail the various aspects, which can have a bearing on the modes of oscillation of a structure, with the main factors considered by the authors being: the geometric and material properties of the load-resisting elements and the properties of the junctions between these elements, the flexural stiffness of the structure's main horizontal and vertical elements, the axial stiffness of the walls, the support conditions of the walls at the base of the structure, the building height and the variation in lateral storey stiffness throughout the height of the structure.

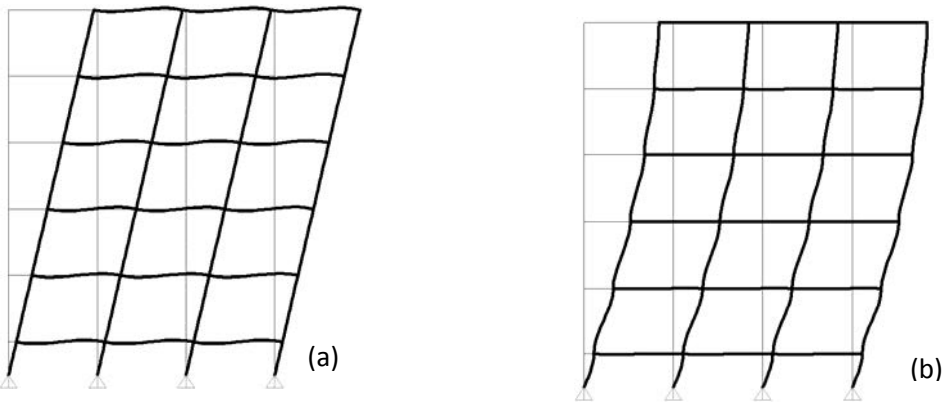

Figure 4-53 (a) Shear-type, and (b) flexural-type deformation behaviour in fundamental mode of vibration of a structure ([54] p. 32).

Of particular interest to the present study is the influence of the relative flexural stiffness of the horizontal and vertical structural elements on the resulting shear-type or flexural-type deformation behaviour in the fundamental mode of vibration as represented schematically in Figure 4-53. The walls of a contemporary loadbearing URM building in the Maltese Islands are intrinsically brittle, since they are composed of an assemblage of discrete masonry blocks with a thin layer of very weak mortar at their junctions, therefore, suggesting that the (undesired) flexural-type deformation, which would result especially in storeys with large open areas or complete absence of internal walls (soft storeys), can cause failure of these walls. The reinforced concrete slabs, on the other hand, provide a rigid diaphragm and should, therefore, distribute the earthquake forces evenly to the supporting walls in a regular building. However, even in such a case, the normal practice of not including tying reinforcement at the perimeter of floors, the reduced bearing of the slabs on the supporting walls and the failure to provide a ring beam around the whole perimeter when precast prestressed concrete slabs are used, reduces the potential rigid 'box-like' behaviour of this construction typology. Moreover, the failure to effectively tie the walls to the slabs at the perimeter of the building creates only a partial restraint at the top of every storey and, hence, a higher rotation at the wall – slab junction. This leads to a flexural-type deformation behaviour.

Furthermore, Murty et al. [54] explain how, when a flexible ground is present, vertical structural members resting on individual foundations would experience rotational flexibility at their base, therefore, giving rise to increased displacements in the lower floors of the structure. This situation is very common in the earlier contemporary loadbearing URM buildings present in the Maltese Islands in areas where a clay subsoil is present, and, is aggravated further, in cases where additional storeys were constructed over these structures in view of increased height limitations allowed by local planning regulations. Moreover, while, as explained by Murty et al. [54], a shear-type deformation generally corresponds to the first mode of vibration of a low-height structure, the increased flexibility resulting from an increase in the height of the structure would give rise to an increased period and a flexural-type behaviour in the vertical members of the lower storeys.

In addition, Murty et al. [54] confirm that the variation in lateral stiffness of the floors throughout the height of a building also affects the deformed shape of the oscillation mode. Hence, any building characteristic, which alters significantly the lateral storey stiffness of a floor from that of the floor above or below it, would significantly alter the mode shape of the structure, when compared to a case where all the floors have the same lateral stiffness.

The comparison of the deformation modes of the analysed numerical models at the analysis time corresponding to the maximum x-displacement at slab over semi-basement level prior to the onset of collapse at this position in every respective model was included in Figures 37 to 45 in Appendix D, while the comparison of the deformed shapes of the six-storey single building control models was included in Figure 4-54, as an example. While deformation shapes at other analysis times corresponding to the failure of different levels in the structure could have presented some variations when compared to those resulting at the time of maximum displacement at slab over semi-basement level, this analysis

time was selected since the main comparisons carried out in this study have focused on structural response parameters recorded at this loading stage corresponding to this position in the numerical models.

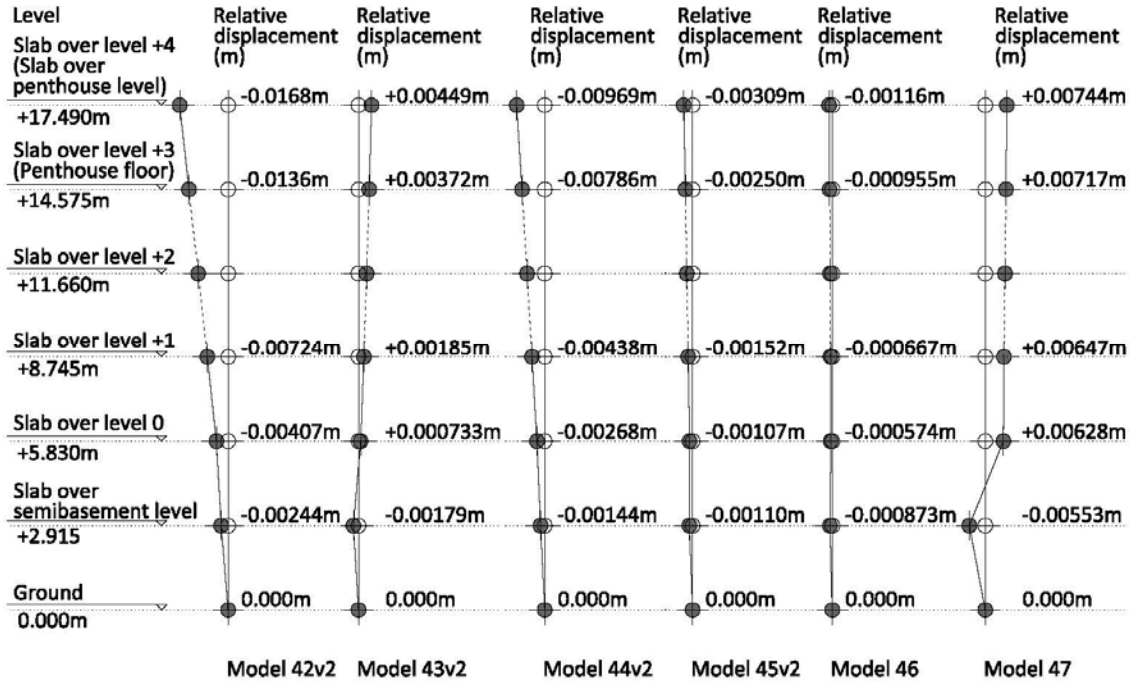

Figure 4-54 Comparison of the x-displacement mode throughout the 6-storey single building control numerical models at the analysis times corresponding to the maximum x-displacement at slab over semi-basement level before the start of failure in the same position.

The variations in the relative x-displacements at every floor resulting from the analysed cases together with the position and the magnitude where the maximum values of relative x-displacement occur in the respective numerical models as illustrated in Figures 37 to 45 of Appendix D, give further insight into the discussions presented in the previous sections of this thesis regarding the influence of particular building characteristics on the seismic response of the structures under investigation. The influence of the subsoil material and modelling on the deformed profile of the corresponding structures together with the variation in this influence with the reduction in number of storeys is evident in Figures 37 to 39 of Appendix D. While a deformation profile corresponding to the first fundamental mode of oscillation results in most cases, a second mode of vibration is exhibited by the six-storey single building control numerical models analysed on upper coralline limestone and clay at Minimum Z (Models 43v2 and 47 respectively) and a third mode of vibration results from the four-storey single building control numerical model analysed on 60 m thick clay (Model 58). In addition, the highest relative x-displacement at the slab over the penthouse level at the selected analysis time was exhibited by the single building control numerical model analysed on 30 m thick upper coralline limestone (Model 42v2, 16.8 mm), whereas at slab over semi-basement level the highest relative x-displacement was recorded in the four-storey numerical model analysed on 60 m thick clay (Model 58, 12.6 mm).

Moreover, the higher magnitude of relative x-displacements resulting at every storey of the two- and three-building numerical models when compared to the corresponding single building control numerical model was evidenced in Figures 40 to 42 of Appendix D. The change in gradient in the displacement variation above the slab over semi-basement level in the corresponding six- and four-storey cases was not anticipated since no change in the internal layout from that of the control numerical model was present in the single buildings from which these combined numerical models were composed. A state of ongoing failure at the respective analysis times at which the onset of collapse was identified in these cases could possibly explain these high displacements. In addition, it is noted that a displacement profile corresponding to the second vibration mode was exhibited by the six- and four-storey three-building control numerical models.

Furthermore, when considering the variation in the x-displacement profile of the models which include one additional building characteristic presented in Figures 43 to 45 of Appendix D, the higher displacement gradient resulting at the semi-basement level and the lower, almost linear variation in the x-displacement of the upper levels exhibited, in particular, by the six- and four-storey single building numerical models (Models 69 and 73), which include a soft storey at slab over semi-basement level, is in accordance with the displacement behaviour predicted in research literature [56] in the case of soft storeys as discussed in previous Sections of this Chapter. This also applies to the linear variation in x-displacement resulting from the six- and five-storey numerical models which include setbacks at penthouse level (Models 79 and 81). In the case of the numerical models which include a double height space between Levels 0 and 1, the sudden change in gradient at slab Level 0 of the x-displacement profile evidenced by the six-storey case (Model 99) indicates that, notwithstanding the modelling limitations of the double height space discussed in Sections 4.2.1.2 and 4.2.3.2, the variation in stiffness caused by the presence of the double height space, when compared to the floors above and below it, was significant enough to lead to a variation in the deformation profile at this position. Moreover, an x-displacement profile, which corresponds to the second mode of vibration, was exhibited by the corresponding five- and four-storey numerical models (Models 101 and 103), where the latter resulted in a significant increase in x-displacement at slab over penthouse level (280.9 mm), when compared to the other single characteristic case (Model 73) and the equivalent single building control numerical model (Model 57).

In the numerical models which include two additional characteristics in combination, at a height of six and five storeys, the numerical models which include a soft storey and setbacks (Models 89 and 91) exhibited a high change in gradient at slab over semi-basement level, similar to the cases where only a soft storey is present. An almost linear variation in displacement throughout the floors and high displacement at penthouse level (105.8 mm) resulted in the corresponding four-storey case. The reduced stiffness of the topmost level could have been the main cause of this large displacement. On the other hand, while the four-storey numerical model, which includes a soft storey and a double height space (Model 113), resulted in a deformation profile with a higher gradient in the lowermost storey and a linear variation (lower) in displacement in the floors above semi-basement level, similar to those obtained in the cases which include only a soft storey, the six-storey (Model 109) and five-

storey (Model 111) corresponding cases resulted in a second mode displacement, with the latter exhibiting a significant relative x-displacement (253.9 mm) at slab over penthouse level. Furthermore, it should be noted that, with the exception of the four-storey numerical model which includes a soft storey and a double height space (Model 113), all the other six-, five- and four-storey two-characteristic cases exhibited a higher relative x-displacement at slab over semi-basement level and at slab over penthouse level than the corresponding single characteristic cases.

The five- and four-storey numerical models (Models 121 and 123 respectively), which investigated the influence of the combination of the three investigated building characteristics, exhibited a sudden change in displacement gradient at slab over semi-basement level and a linear variation in x-displacement, similar to that obtained in the soft storey cases. The six-storey combined numerical model (Model 119) resulted in an x-displacement profile that corresponds to a second mode of vibration. Furthermore, this model exhibited a higher relative x-displacement at slab over semi-basement level than the models which represent the existing Xemxija Building Number 0011 (Models 128 and 129). This increased displacement was not anticipated since, even though Models 128 and 129 do not include a full soft storey at semi-basement level, they have a double height space located between the uppermost two levels of the structure, hence suggesting the formation of higher displacements in the higher floors. However, the shifted location of the double height space towards the centre of the storey (in the longitudinal plan direction) is likely to have contributed to limit the magnitude of the resulting displacements.

It should be noted that the detailed examination of the particular displacement magnitudes resulting from the displacement response of the different analysed cases with reduction in number of storeys was not the main intention behind this Section, since most variations at slab over semi-basement level were already discussed in the preceding Sections. Furthermore, a more detailed examination would require the comparison of the displacement modes even at the analysis time corresponding to the maximum displacement at slab over penthouse level before the start of failure at this position, where most of the high magnitude displacements were located. This further comparison could not be carried out in this study due to time limitations.

As explained by Murty et al. [54], while the seismic response of a structure is the result of the responses corresponding to all its vibration modes, the relative bearing of the various modes of oscillation on the final response would be different and a reduced number of modes would generally govern most of the response parameters. Moreover, according to Bernal [201], the risk of structural collapse is highly dependent on the deformed shape of the structure just before the onset of failure. Therefore, the results presented in this Section, especially in the single characteristic cases, confirm the influence, which the investigated characteristics have on the lateral storey stiffness and, hence, on the deformation response. Furthermore, the resulting x-displacement modes also indicate that, in a number of numerical models, the x-deformation profile corresponding to the maximum x-displacement prior to the onset of failure at slab over semi-basement level, resulted from a higher mode of vibration. The identification of deformations corresponding to higher displacement modes at

this selected analysis time suggests that higher vibration modes are responsible for the occurrence of failure at slab over semi-basement level and, hence, highlights the relevance of the non-linear dynamic analysis carried out in this study, when compared to a classic non-linear static (Pushover) alternative approach which would not have captured such deformation behaviours [207] [208] [197].

4.2.5 Collapse duration

Clause 2.2(1)P in Eurocode 8: Part 1 [4] defines the No Collapse Requirement as ([4] p. 29):

> 'The structure shall be designed and constructed to withstand the design seismic action…without local or global collapse thus retaining its structural integrity and a residual loadbearing capacity after the seismic events.'

Therefore, while as discussed in Sections 4.2.3.2 to 4.2.3.5, the analysis time at which the start of failure is identified in a structure subjected to seismic excitations is likely to give indications regarding its collapse resistance under seismic loading, once failure starts, the building is already unrecoverable, and so, collapse duration is less of interest from a structural point of view. Hence, for the sake of completeness, this Section will only include a brief overview of the collapse durations which resulted from the analysed numerical models which ended in complete collapse. The respective collapse durations are summarised in Figures 4-56, 4-57 and 4-58 for the six-, five- and four-storey cases, while Figure 4-55 includes a legend for the highlighted results in these three figures.

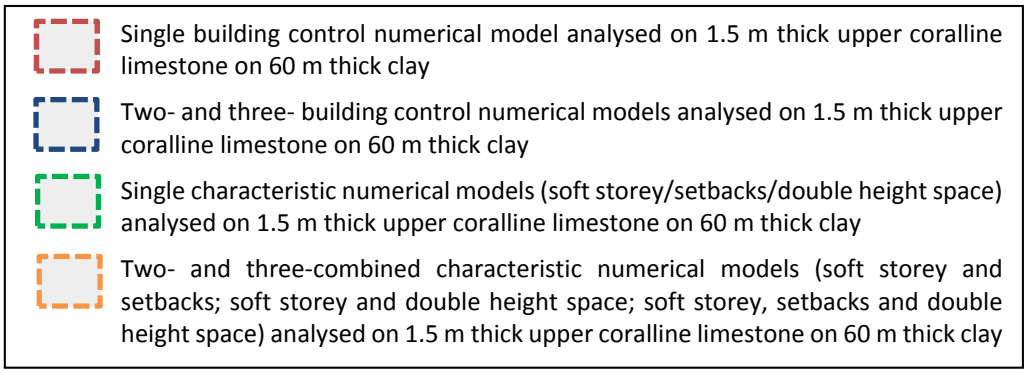

Figure 4-55 Legend for the results highlighted in Figures 4-56, 4-57 and 4-58.

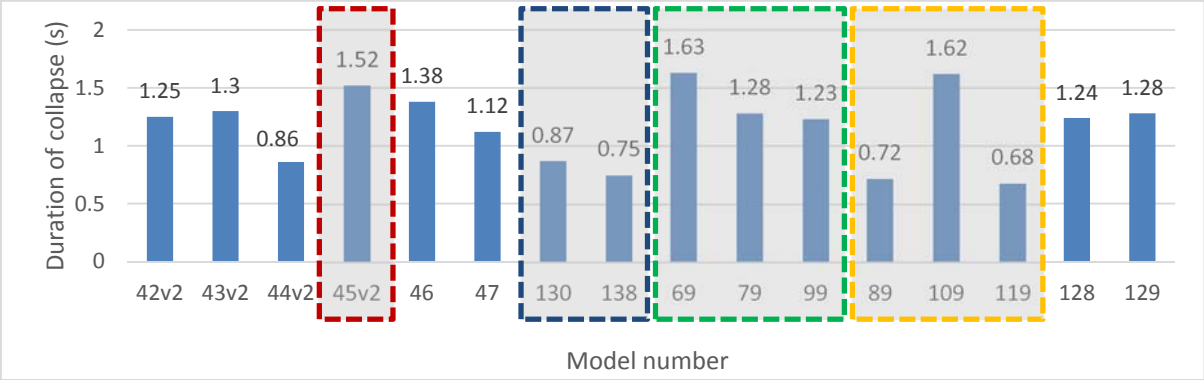

Figure 4-56 Duration of collapse (s) resulting from the six-storey analysed numerical models which ended in collapse.

Figure 4-56 indicates that the six-storey single building control numerical model analysed on 1.5 m thick upper coralline limestone over 60 m thick clay (Model 45v2) resulted in the longest collapse duration (1.52 s) out of the six-storey single building control cases, while the corresponding six-storey single building control numerical model analysed overlying 30 m thick upper coralline limestone on 30 m thick clay (Model 44v2), resulted in the shortest duration (0.86 s). Model 43v2, the corresponding six-storey single building control numerical model, analysed on upper coralline limestone at Minimum Z, resulted in the longest collapse duration out of the 'rock' subsoil cases (1.30 s), followed closely by the equivalent numerical model analysed on a single layer of 30 m thick upper coralline limestone (Model 42v2, 1.25 s). Similarly, the shortest collapse duration in the 'clay' subsoil cases was recorded in the six-storey numerical model analysed on clay at Minimum Z (Model 47, 1.12s). It is noted that the six-storey numerical models, which exhibit the longest collapse durations for the 'rock' and 'clay' subsoil cases (Models 43v2 and 45v2 respectively), also result in the lowest relative displacements at slab over semi-basement level prior to the onset of collapse at this position for the two groups of ground cases considered, while Model 43v2 also results in the latest start of failure at slab over semi-basement level out of the 'rock' subsoil cases. This suggests that the variation in degree of restraint at the base of the building resulting from the modelling of the ground and the material specified for the interface springs located between the first course of the semi-basement level and the ground, as discussed in Section 4.2.3.2, is likely to have a bearing, not only on the displacement of the numerical model, but also on its collapse duration. The higher stiffness of the upper coralline limestone springs present at this junction in Model 43v2 (analysed on upper coralline limestone at Minimum Z) when compared to the weaker mortar springs present in Models 42v2 and 44v2, in conjunction with the stiffer restraint provided when ground is modelled as a material at Minimum Z in ELS®, as explained in Section 4.2.3.2, are likely to be responsible for the lower displacements and the longer collapse durations exhibited by Model 43v2. Similarly, in the 'clay' subsoil cases, the mortar springs, present between the first course of the semi-basement level and the upper ground layer in Model 45v2, provide a higher restraint than the clay springs specified in Model 47. Furthermore, in Model 45v2, the mortar springs are connected to upper coralline limestone springs (at the surface of the upper ground layer), which result in a higher restraint than the clay springs located at the boundary of the uppermost clay element forming the clay layer in Model 46, in view of their higher stiffness (the Young's Modulus of mortar, as defined in the numerical models, is 39 times higher than that defined for clay). The results obtained for the six-storey single building control numerical models, therefore, suggest that this higher restraint allows smaller displacements to take place in the analysed numerical models and leads to longer collapse durations.

It should be noted, however, that the collapse durations of the existing Xemxija Building Number 0011 analysed on 1.5 m thick upper coralline limestone overlying 60 m thick clay and, 30 m thick upper coralline limestone overlying 30 m thick clay (Models 128 and 129), varied only marginally (1.24 s and 1.28 s respectively), hence, putting in question the influence which the ground materials and the numerical modelling of the ground might have on the duration of collapse of a structure, as discussed above. This discrepancy in these results, when compared to those obtained from the corresponding

single building control numerical models (Models 45v2 and 44v2) cannot be attributed to the occurrence of resonance effects in the ground layers since Table 34 in Appendix D shows that both Models 129 and 44v2 exhibit a secondary peak frequency in the clay layer, and a main and secondary peak frequency in the upper coralline limestone layer, which coincide with secondary frequencies in the main energy range of the simulated input ground motion record, hence, not explaining the difference in behaviour between the two models. On the other hand, whereas Models 45v2 and 44v2 are relatively regular numerical models (not in their typical plan layout, but since the same layout is present at all the six storeys), Models 128 and 129 include a number of variations to the typical plan at semi-basement level and at Levels 3 and 4, which variations all influence in a complex manner the resulting seismic response and, hence, the variation in lateral storey stiffness throughout their height, their deformation mode and their failure mode, making their collapse durations not directly comparable to those resulting from the corresponding single building control models.

Figure 4-56 also indicates that the six-storey three-building control numerical model (Model 138) resulted in a reduction of the duration of collapse of almost 50% (0.75 s), when compared to the corresponding single building control numerical model. The six-storey two-building case (Model 130) exhibited only a marginal increase (0.87 s) in duration of collapse when compared to the three-building counterpart. The close collapse durations obtained from Model 130 and 138 in addition to the close analysis times at which the start of collapse was identified in these two numerical models suggest that the failure mechanism triggered in both numerical models is similar and that they do not exhibit a significant improvement in seismic resistance when compared to each other.

Generally, a stiffer building would be expected to lose its integrity more abruptly than a more flexible structure. This is confirmed from the results of the collapse durations of the six-storey numerical models which include one additional building characteristic summarised in Figure 4-56. The durations of collapse of these six-storey structures varies between 1.63 s and 1.23 s, with the numerical model which includes a soft storey at semi-basement level (Model 69) exhibiting the longest duration, while the collapse duration in the corresponding numerical models, which include either setbacks at penthouse level (Model 79) or a double height space (Model 99), varies only marginally (1.28 s and 1.23 s respectively). As discussed in Section 4.2.3.4, Model 69 exhibited the highest delay in the start of failure and the highest relative x-displacement at the analysis time corresponding to the onset of failure at slab over semi-basement level in Model 45v2, while the earliest onset of failure among the single characteristic numerical models was exhibited by Model 99, where the lowest relative displacement at the same analysis time was recorded. Hence, the numerical model ranking resulting from the comparison of the collapse durations corresponds with the order of ranking obtained from the comparison of the analysis times at the start of failure and the relative x-displacement at slab over semi-basement level at the time of the start of collapse at this same position of the corresponding single building control numerical model.

On the other hand, in the case of the numerical models which include two or three additional building characteristics, the ranking resulting from the collapse duration of the respective models is not in

agreement with that derived from the analysis times when the start of collapse was identified at slab over semi-basement level from the respective numerical models. The variation in the relative displacements at the different analysis times discussed in Section 4.2.3.4 is not considered in this comparison in view of the variation in lateral storey stiffness caused by the presence of the additional building characteristics positioned at different levels throughout the height of the analysed models, hence triggering deformation modes associated with the failure mechanisms, which cannot be predicted and resulting in a complex overall structural behaviour. Therefore, while the earlier start of failure exhibited by the six-storey numerical model which includes a soft storey and a double height space (Model 109) suggests a higher seismic vulnerability associated with this combination of building characteristics, the longer collapse duration resulting from this numerical model is likely to be indicative of a more ductile failure than the other 2 six-storey combined characteristic models (as opposed to a higher ductility capacity which would have been evidenced if Model 119 would have exhibited a significant delay in the start of failure when compared to the other 2 two-characteristics cases). Furthermore, the corresponding six-storey numerical models which include a soft storey at semi-basement level and setbacks at penthouse level (Model 89) and the numerical model which includes all three investigated building characteristics in combination (Model 119) show only marginal variations in the collapse durations and in the time of start of failure at slab over semi-basement level.

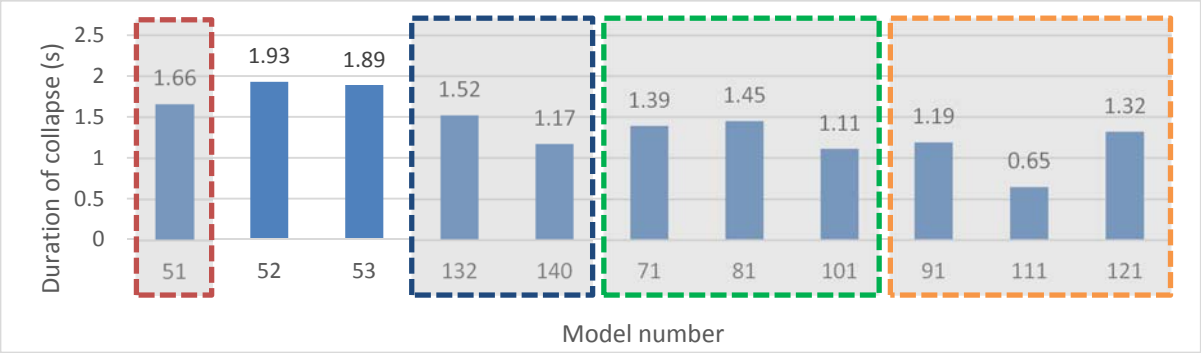

Figure 4-57 Duration of collapse (s) resulting from the five-storey analysed numerical models which ended in collapse.

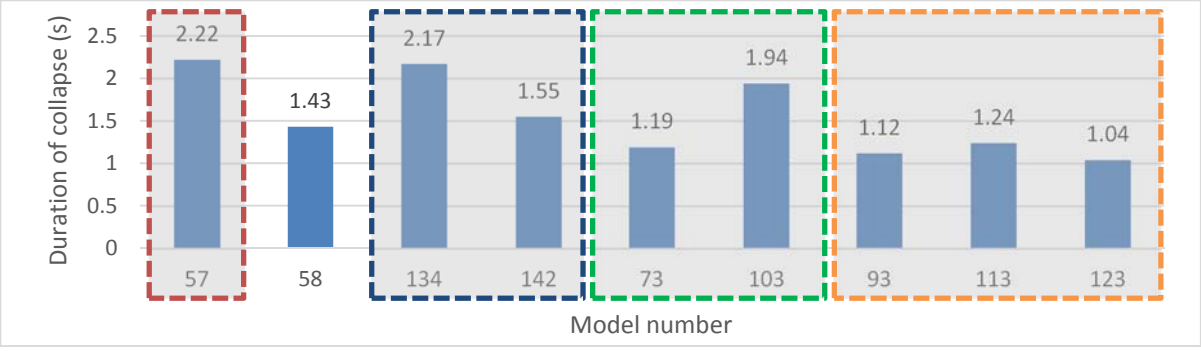

Figure 4-58 Duration of collapse (s) resulting from the four-storey analysed numerical models which ended in collapse.

Figure 4-57 indicates that, in contrast to the six-storey case, the five-storey single building control numerical model analysed on 1.5 m upper coralline limestone overlying 60 m thick clay (Model 51) resulted in the shortest collapse duration (1.66 s) out of the 'clay' subsoil cases, whereas the five-storey single building control numerical model analysed on a single layer of 60 m thick clay (Model 52) exhibited the longest collapse duration (1.93 s), followed closely by the corresponding numerical model analysed on clay at Minimum Z (Model 53, 1.89 s). In the comparison of the collapse duration of the four-storey analysed numerical models reported in Figure 4-58, a longer duration of collapse is exhibited by the four-storey single building control numerical model analysed on 1.5 m thick upper coralline limestone overlying 60 m thick clay when compared to the corresponding numerical model analysed on a single 60 m thick clay layer. These trends are not in agreement with the ranking resulting from the comparison of the analysis times at the start of failure since, the earliest start of failure is exhibited by the five- and four-storey numerical models which evidenced the longest collapse durations. Furthermore, the five- and four-storey two-building control numerical models (Models 132 and 134) resulted in only a marginally shorter collapse duration (1.52 s and 2.17 s respectively), when compared to the corresponding single building control numerical models, which, however were 1.28 and 1.40 times, respectively, longer than the duration of collapse of the equivalent three-building control cases (Models 140 and 142). The five- and four-storey two- and three-building control cases exhibited only a marginal variation in the start of failure at slab over semi-basement level. However, in both cases, failure started earlier in the two-building case. The variation in the duration of collapse of the single building control numerical models analysed on the different ground types and the two- and three-building control numerical models is likely to be due to the variation in the failure mode of the respective model, which might be influenced by the varying degree of restraint at the base of the different models, the model stiffness and failure mechanism.

In the five- and four-storey cases which include a single additional building characteristic, the longest collapse duration was recorded in the numerical model which includes setbacks at penthouse level (Model 81, 1.45 s) and in the numerical model which includes a double height space between Levels 0 and 1 (Model 103, 1.94 s) respectively. These results coincide with the latest start of collapse in both cases. As discussed in Section 4.2.3.4, considering that the four-storey numerical model which includes setbacks at penthouse level resists collapse, the higher resistance to collapse of the equivalent five-storey case when compared to the corresponding numerical models, which include a soft storey or a double height space and which resisted collapse at three storeys, could have been anticipated. Furthermore, the increased delay in the onset of failure exhibited by the four-storey model which includes a double height space, when compared to the corresponding control numerical model, is indicative of a higher resistance to failure, whereas, the longer collapse duration, suggests a more ductile failure mode.

Figures 4-57 indicates that the five-storey numerical model which includes the three investigated building characteristics in combination (Model 121) results in the longest collapse duration (1.32 s) for the five-storey two- and three-characteristic cases. This numerical model also exhibited the highest delay in the start of failure, when compared to the corresponding five-storey single building control

numerical model, and the highest relative displacement at slab over semi-basement level at the analysis time corresponding to the start of failure at the same position in the corresponding control numerical model. These results suggest that a higher level of ductility capacity can be attributed to Model 121 when compared to the other five-storey two-characteristic cases considered in this study. On the other hand, at a height of four storeys, the longest collapse duration was exhibited by the model which includes a soft storey and a double height space (Model 113, 1.24 s), which model, however, resulted in an earlier start of collapse than the corresponding four-storey single building control numerical model. Hence, while the latter suggests that a higher degree of seismic vulnerability can be associated with this combination of building characteristics, the longer collapse duration suggests a marginally more ductile failure.

The results discussed above suggest that, the collapse duration of a structure could be influenced, in part, by the stiffness of the base restraint, the stiffness of the structure and its variation throughout the building height and, consequently, the mode of collapse. Nevertheless, a structure with a longer duration of collapse cannot be necessarily classified as having a higher resistance to seismic loads, since once collapse starts, the resistance of the structure degrades rapidly. However, the collapse duration can be indicative of a ductile or a more abrupt failure mode, when the seismic behaviour of buildings of the same height and the same typology are compared.

4.3 Comparison of Seismic Vulnerability Ratings: New Form, GNDT Second Level Assessment, FEMA 154 and Numerical Analysis Results

The seismic vulnerability ratings resulting from the New Form, the GNDT second level assessment [26] and the FEMA 154 (second edition) [27] assessments were compared to the results of the numerical simulations carried out on the contemporary loadbearing typology under study under a simulated seismic action for Malta with a maximum peak ground acceleration of 0.10g, a Magnitude of 7.6, a hypocentral distance of 170.30 km and an epicentral distance of 139.91 km, through the comparison of the assessment ratings resulting from these three seismic vulnerability methods for Xemxija Building Number 0011 and the seismic resistance exhibited by the corresponding numerical model analysed on the same ground formations (Model 129). The final score of FEMA 154 (second edition) [27] for this building resulted as 2.5, therefore, suggesting that no detailed seismic assessment is required. On the other hand, the GNDT level 2 assessment [26] and the assessment carried out using the New Form on Xemxija Building Number 0011 resulted in 'Medium' and 'Medium-high' seismic vulnerability ratings, respectively. Based on the seismic vulnerability ranges proposed in Table 2 of Torpiano et al. [5], which is reproduced as Document (i) in Appendix B, these seismic vulnerability ratings both suggest that a detailed seismic assessment of the building is required. The ratings obtained from the latter two methods were confirmed through the full dynamic analysis of Model 129 which resulted in collapse, hence, suggesting that the additional conservativism of the resulting ratings when compared to the FEMA 154 (second edition) [27] assessment, is likely to result, not from an over-estimation of the seismic vulnerability of the assessed structures, but from a more accurate evaluation of the factors which influence the structure's seismic resistance.

4.4 Summary and Conclusions

The foregoing sections attempt to identify the relative seismic vulnerability, which can be attributed to the investigated characteristics listed in Section 4.1 in the context of the contemporary loadbearing URM building typology. The study looked into the variation of the dynamic properties of the numerical models (through the analysis of the variation in natural frequency in the transverse and longitudinal directions of every analysed model at the end of both static and dynamic loading cases for two main geological scenarios (upper coralline limestone or clay at Minimum Z), the predominant frequencies in the acceleration spectrum, particularly, in the case of the subsoil layers, and the variation of a number of structural response parameters (namely: the x-displacement behaviour prior to the identification of the start of collapse at slab over semi-basement level, the analysis time at the start of failure, the relative x-displacement at slab over semi-basement level at a number of different instances during the dynamic analysis, the ratio of the maximum x-acceleration recorded at first course of the semi-basement level prior to the start of failure at slab over semi-basement level to the maximum peak ground acceleration in the input simulated ground motion record for the same time interval, the deformed shapes of every numerical model which resulted in collapse at the analysis time corresponding to the maximum x-displacement at slab over semi-basement level prior to the start of failure, and the collapse duration).

The results obtained from this study suggest that the material properties and the thickness of the ground formation in addition to the modelling techniques used to model the ground have a direct bearing on the seismic response of structures. This was evidenced by the higher natural frequencies obtained for the same numerical models when analysed on upper coralline limestone than on clay and by the higher decrease in natural frequency reported between the values resulting at the end of the dynamic loading stage, when compared to those obtained at the end of the static loading stage, when the numerical models, which include a soft storey, were analysed on clay at Minimum Z, when compared to the results obtained for the corresponding numerical models analysed on upper coralline limestone at Minimum Z. Furthermore, the overall heights at which the corresponding single building control numerical models analysed on the six different ground formation scenarios resisted collapse, strongly suggest that structures erected on subsoils, which are predominantly of a lower stiffness, have a higher associated seismic vulnerability. All the numerical models analysed on the 'rock' subsoil cases (that is, 30 m thick upper coralline limestone layer modelled as a three-dimensional block; 30 m thick upper coralline limestone layer overlying a 30 m thick clay layer, both modelled as three-dimensional blocks; and upper coralline limestone defined as the ground material at Minimum Z) resisted collapse at a height of five storeys. The numerical models analysed on the 'clay' subsoil cases resisted collapse at a height of four floors when modelled on clay specified as the ground material at Minimum Z, and when modelled on a 1.5 m thick upper coralline limestone layer overlying a 60 m thick clay layer (both modelled as three-dimensional blocks), only in the case of the numerical model which included the setbacks at penthouse level. All other numerical models analysed on a 1.5 m thick upper coralline limestone layer overlying a 60 m clay layer, and those analysed on a single 60 m thick layer of clay (modelled as three-dimensional blocks), resisted collapse at three floors. While this outcome might

seem to contradict the results reported by Farrugia [16], Galdes [17], Marmara' [18] and Tong [19] the apparently excessive shear wave velocity corresponding to the material properties specified for upper coralline limestone in the numerical models, when compared to the results reported from site investigations carried out locally [191], and the altered compressive strength, Young's Modulus, Shear Modulus and the 0 kg/m^3 density specified for clay in order to solve persistent stability errors in the static loading stage, might have caused delays in the failure of the analysed structures due to reduced amplifications of accelerations and reduced transfer of vibrations to and from the modelled buildings when compared to a real life scenario in the Maltese Islands. In addition to the latter observation, since all numerical analyses have been carried out using the same seismic ground acceleration, while the comparison of the results obtained for the different model variations investigated provides valid information regarding the influence of the studied seismic vulnerability characteristics on the seismic response of the contemporary loadbearing URM building typology, the actual values of start of collapse, collapse duration or number of storeys resisting collapse resulting from this study cannot be generalised for the contemporary loadbearing URM typology present in the Maltese Islands under the effect of a Magnitude 7.6 earthquake.

In the numerical analyses, the increase in seismic vulnerability with increase in building height was evidenced by both earlier start of failure and the shorter failure times. Furthermore, while the relative degree of seismic vulnerability corresponding to the presence of a combination of two or three building characteristics is not always clear from the results obtained in view of the complex interactions which these characteristics have on the seismic response of a structure, the relative influence of the investigated characteristics is more evident through the comparison of the seismic response of the numerical models, which include one additional building characteristic at a time. The resistance to collapse at four storeys of the analysed numerical model which includes setbacks at penthouse level, when compared to a collapse resistance at three floors in the corresponding control numerical models and in the numerical models which include either a soft storey or a double height space, is likely to indicate a lower relative seismic vulnerability rating linked to this characteristic. On the other hand, a higher seismic vulnerability rating associated with the presence of a soft storey at semi-basement level when compared to that of setbacks at penthouse level or a double height space (of limited proportions) between Levels 0 and 1 was suggested due to:

a) the higher reduction in natural frequency between the end of the static loading stage and the dynamic loading stage exhibited by the numerical models which resisted collapse and included a soft storey, hence, suggesting a higher degree of resulting damage in the structures;
b) the comparison of the analysis times at which the start of collapse was identified in the single characteristic numerical models, in particular, at a height of four storeys;
c) the higher relative x-displacement at slab over semi-basement level, resulting at the time of the maximum x-displacement prior to the start of failure at the same position in the numerical model, particularly, in the six- and four-storey numerical models which include this building characteristic, when compared to the corresponding numerical models which include setbacks or a double height space.

Moreover, the modelling of the double height space in this study (the dimensions and position of the void forming the double height space, in addition to the detailing of a thick slab on three of its sides) is likely to have influenced the seismic response of the respective numerical models and, hence, the relative seismic vulnerability rating, which should be associated with this building characteristic might have not been appropriately evidenced by the results obtained from the analysed numerical models. On the other hand, the comparison of the relative x-displacements at slab over semi-basement level at the time of the start of failure at the same position of the control numerical model, seems to associate a higher relative ductility capacity with the presence of a double height space, particularly at a height of four storeys. Furthermore, the close analysis times at the start of failure at slab over semi-basement level in the two- and three-building numerical models seem to suggest that only a marginal variation in response is evidenced between these two cases. However, these analysis times, in addition to the collapse behaviour prior to the start of failure, could even be an indication of a collapse mechanism related to P-delta effects resulting from the seismic displacements in view of the high gravity loads acting on the walls at semi-basement level. Alternatively, the results obtained could suggest that the increase in inertia of the multiple-building numerical models arising from the larger building mass, particularly, at elevated overall building heights, leads to an increase in base shear which exceeds the resistance of the lateral-load resisting structural members at the lowermost storey level.

The deformed shapes of the structures at failure highlight the influence of the variation in the lateral storey stiffness of the analysed structures in the presence of the studied building characteristics on the failure mode of the analysed numerical models. The higher modes of vibration associated with the displacement profiles exhibited by a number of analysed numerical models, at the analysis time corresponding to the maximum x-displacement prior to the start of collapse, also justify the choice of the type of numerical analysis carried out in this study.

Furthermore, while the significantly high displacements recorded in a number of numerical models at the slab over the penthouse level raise concerns with respect to the accuracy of the identification of the onset of failure as proposed in this study, the consistent assessment of the start of collapse throughout all numerical models ensures that the same level of error (if present) can be associated with every model, hence preserving the validity of the extracted results and the corresponding conclusions.

Chapter 5 3MURI® NUMERICAL ANALYSIS: EXAMINATION OF RESULTS AND DISCUSSION

5.1 Introduction

The structural response parameters discussed in the foregoing chapter enabled the identification of areas where the ELS® analysis could be improved further to enable a more accurate simulation of the seismic response of the unreinforced loadbearing masonry building typology under study, such as in the representation of the ground layers and their material constitutive models. Nevertheless, the control of the user on the material properties and the restraints of every element and at every interface in the model, in addition to the capability of the Applied Element Method in the simulation of crack propagation up to a state of progressive collapse highlight the significant potential of this numerical modelling method with respect to the accurate representation of the seismic response of a masonry structure. On the other hand, the computational demand of a full non-linear time-history analysis using ELS® are significant when considering the time required to develop a numerical model of a structure, the processing power required, the processing time and the time required by the user to analyse the output. Furthermore, when masonry buildings of substantial size are modelled, as in the case of this research study, using the realistic masonry wall representation option, where every block in the wall is modelled as a separate element, identifying the type of failures and the wall areas which experience damage proves to be difficult and time-consuming in view of the scale of the models when compared to the size of the joints between the separate elements (e.g. mortar-block or block-block interfaces).

This research study is the first attempt to investigate the seismic response of the contemporary unreinforced loadbearing masonry building typology present in the Maltese Islands through numerical modelling. It is therefore incumbent to prepare the way for further studies, which could use this research work as their starting point. Therefore, an investigation into whether a simplified and less computationally-demanding procedure could reliably predict the seismic resistance of this URM building typology was carried out as the final stage of this research study. Non-linear static (pushover) analyses using the commercial software 3Muri® by S.T.A. DATA srl, which is based on the Frame by Macro-Element Method and uses an equivalent frame modelling approach, were carried out on the control case and the single parameter cases considered in the ELS® seismic analyses (which include: the presence of a soft storey at the lowermost storey; a double height space between Levels 0 and 1; and setbacks at the topmost storey; for plan layouts with length-to-width proportions of 2.75:1,

hereinafter referred to as the 'original plan proportions') for two subsoil cases: upper coralline limestone and clay, respectively. The plan layouts, plan proportions, wall thicknesses, wall materials, slab thicknesses, slab spanning direction and superimposed loading, and the subsoil material properties considered were consistent with the corresponding ELS® numerical models with the exception of a minor rationalisation of the plan layouts with respect to the alignment of walls (as indicated in Figure 3-58), which were only marginally shifted with respect to each other, which misalignment could have otherwise caused problems during the generation of the mesh of the 3Muri® numerical models. These changes were not deemed to have a significant influence on the overall seismic behaviour of the numerical models.

Moreover, the examination of the response parameters resulting from the non-linear dynamic analyses carried out using ELS® exposed how specific building characteristics very likely had a bearing on the observed results. As discussed in Section 4.2.1.2 of this thesis, the analysed numerical models had a length-to-width plan ratio of 2.75:1 at the typical floor level. However, a length-to-width plan ratio of 4:1, which corresponds to the limit on plan slenderness recommended in Clause 4.2.3.2(5) of Eurocode 8: Part 1 [4], would be easily found in the Maltese Islands for the building typology under study. In addition, Section 4.2.1.2 of this thesis also discusses how the limited size of the void in the slab over Level 0 and the additional restraint provided by the 250 mm thick slabs bounding the slab void on three sides in the numerical models, which include a double height space, could have influenced the seismic response of this particular case. Hence, in order to examine the effect of these building characteristics on the seismic behaviour of the contemporary URM buildings under study, the following additional cases were investigated through a non-linear static analysis;

a) the control case, similar in plan layout to the control numerical models analysed using ELS®, however, with a length-to-width ratio of 4:1, analysed for both subsoil scenarios: upper coralline limestone and clay, respectively;
b) the presence of a double height space between Levels 0 and 1, with the same size and position of void with respect to the front façade as in the original investigated cases, however, with a revised plan length-to-width ratio of 4:1, and analysed on both upper coralline limestone and clay, respectively;
c) the presence of a soft storey at semi-basement level, with a revised plan length-to-width ratio of 4:1 and analysed on both upper coralline limestone and clay, respectively;
d) the presence of a double height space between Levels 0 and 1, with the void spanning the entire width between the longitudinal party walls, with the original plan length-to-width ratio of 2.75:1 and analysed on upper coralline limestone only.

Cases (a) to (c) listed above with length-to-width plan proportions of 4:1 will hereinafter be referred to as the 'extended' cases or the 'extended' plan layouts. The existing Xemxija building, which was used for the verification of the modelling techniques adopted in the ELS® numerical models, was re-modelled using 3Muri® and analysed for the two subsoil cases of upper coralline limestone and clay, respectively.

Plan layouts for the existing Xemxija building, the control model, the control model with a soft storey at semi-basement level, the control model with setbacks at the topmost storey and the control model with a double height space between Levels 0 and 1 presented in Figures 20 to 24 of Appendix C remain applicable for the corresponding 3Muri® numerical models with the original plan proportions. Plan layouts corresponding to the additional cases listed in (a) to (d) above investigated using 3Muri® are presented in Figures 33 to 36 of Appendix C.

As a non-linear static analysis method, 3Muri® considers only the global response of structures, therefore, taking into account only the in-plane resistance of walls and the ability of the horizontal diaphragm to transfer the horizontal applied loads. This method assumes the presence of construction details which ensure a box-like behaviour of the analysed structure, hence, preventing the activation of out-of-plane failure mechanisms in walls and the full coupling between intersecting walls [123]. Several authors [124] [213] raised concerns over the use of the pushover analysis method for the assessment of structures where the construction detailing does not guarantee a box-like behaviour. It is acknowledged, that in the context of the URM building typology under study, while the cast in-situ concrete slabs can be considered to provide a relatively rigid diaphragm for the transfer of seismic loads to the vertical loadbearing members, the absence of reinforced peripheral ties at slab levels, the absence of a reinforced connection between slabs and walls, the use of thick gauge polyethylene sheets as a damp proof course material at Level 0 and the presence of long unrestrained lengths of walls with no cross walls in open plan areas, corridors and soft storeys could result in a seismic response which differs significantly from that resulting from the assumptions forming the basis of the pushover analysis method. Moreover, in the context of the contemporary unreinforced loadbearing masonry buildings present in the Maltese Islands, while laboratory investigations on the degree of coupling between intersecting walls were not performed to date, the relatively slender single wall thicknesses typically used for the construction of party walls, internal walls and rear facades, the low mortar quality, the typical absence of mortar in the vertical joints between blocks during the construction of walls and the frequent use of hollow concrete blockwork for the construction of walls, therefore, resulting in a reduced contact area between overlying blocks, in addition to the presence of long unrestrained lengths of walls, as mentioned previously, makes the achievement of full coupling between intersecting walls very unlikely.

Furthermore, the displaced building profiles resulting from the non-linear dynamic analyses using a single simulated ground motion record carried out through ELS®, suggest that higher modes of vibration than the fundamental mode are relevant in the seismic response of the building typology under study. While classic pushover methods take into consideration only the fundamental mode of vibration of the analysed structures, in the 3Muri® version used in the present study, uniform and modal load distributions are considered. The modes of vibration in the x- and y-directions, which result in a percentage mass contribution in the respective direction of 5% or more were selected by the author following a modal analysis in accordance with the requirements outlined in Clause 4.3.3.3.1(3) of Eurocode 8: Part 1 [4]. Unfortunately, requests for clarification from the 3Muri® technical support on whether the modal load distributions considered in the pushover analysis take into account all the

modes of vibration selected by the user following the modal analysis were not forthcoming at the time of writing. However, the comparison of results obtained from two identical trial models, where the selection of an additional mode of vibration resulted in a higher number of unsatisfied verifications, suggests that all the vibration modes selected by the user following the modal analysis are taken into consideration during the calculation of the 'modal' load distribution cases during the non-linear static analysis.

In Chapter 4 of this thesis, the engineering principles and findings published in literature were applied for the interpretation of the variation in the response parameters extracted from the ELS® models with respect to the influence, which the investigated characteristics have on the seismic response of the contemporary loadbearing unreinforced masonry buildings present in the Maltese Islands. On the other hand, throughout the following sections, when applicable, the response parameters and the overall seismic response exhibited by corresponding ELS® and 3Muri® numerical models are directly compared in order to gain insight into the degree of reliability of the non-linear static pushover analysis for the simulation of the seismic resistance of the URM building typology under study.

5.2 Outline of Data Extracted from the Analysed 3Muri® Numerical Models and Background to the Discussion of the Results

A non-linear static (pushover) analysis was carried out on a total of 116 numerical models[33] [34]. The main response parameters, which are reviewed in the ensuing sections include:

a) the height at which the analysed cases exhibited an adequate seismic resistance with respect to a seismic event with an intensity corresponding to the maximum p.g.a. specified for the Maltese Islands for limit states of Significant Damage and Near Collapse as defined in Clause 2.1(1)P of Eurocode 8: Part 3 [97];
b) the natural frequency in the x- and y-directions and the different modes of vibration of the analysed numerical models;
c) the maximum displacement exhibited by the analysed numerical models mainly with respect to load distributions applied in the numerical models' transverse x-x orientation, for the limit states of Significant Damage and Near Collapse;
d) the presence of shear failure in the walls of the control models and the control models with a soft storey at semi-basement level with respect to the limit state of Significant Damage;

[33] Table 43 in Appendix E includes the list of numerical models analysed with 3Muri®, the description of the seismic vulnerability characteristics, the number of storeys, the plan proportions, the ground material considered and a summary of the results of the non-linear static pushover analysis.

[34] In order to distinguish between the numerical models analysed using ELS® and 3Muri®, the 3Muri® numerical model numbers are referenced in this document using the prefix '3M', e.g. 3M46 is the six-storey control numerical model analysed on upper coralline limestone using 3Muri®.

e) the variation in the average values of the reduction factor 'q_u' resulting from load distributions applied in the x- and y-orientations throughout the analysed models for the limit state of Near Collapse, as estimated from the results of the pushover analysis.

Every 3Muri® non-linear static pushover analysis consists of 24 pushover analyses performed on the same structure, which include the uniform and modal load distributions in the positive and negative x- and y-directions, together with the consideration of 3 different accidental eccentricities as recommended in Clauses 4.3.3.4.2.2(1) and 4.3.3.4.2.2 (2)P of Eurocode 8: Part 1 [4]. In the 3Muri® non-linear static pushover analysis, the analysed structure is subjected to vertical gravitational loads in addition to a monotonically increasing lateral load until the limit state failure criterion is reached. The default Eurocode 8 option of the 3Muri® pushover analysis assesses the adequacy of the seismic resistance of the new or existing modelled structures based on the comparison of the maximum displacement reached by the structure (representing the displacement capacity of the structure in accordance with the capacity criteria given in Eurocode 8: Part 3 Clauses C.3.3 to C.4.1.3 [97] for the limit states of Near Collapse, Significant Damage and Damage Limitation), to the target displacement (which represents the seismic displacement demand of the earthquake on the structure) for each of the 24 load distributions considered. In the default displacement capacity criterion, an adequate seismic resistance of the analysed structure with respect to the particular limit state being assessed is obtained if the ratio between these two displacement values is greater than 1 for all load distributions. Similarly, an alpha ratio (equivalent to the ratio between the maximum acceleration resulting in the numerical model for the particular load distribution during the pushover analysis and the maximum peak ground acceleration for the limit state under consideration) greater than 1 for all the 24 load distributions considered by the program also suggests that the analysed structure has an adequate seismic capacity to sustain an earthquake of the specified intensity for the particular limit state.

A maximum displacement to target displacement ratio greater than one for a particular limit state (which would consequently also result in an alpha ratio greater than one for the same limit state) for a specific load distribution is termed by 3Muri® as a 'satisfied verification'. In ELS®, the most basic indicator of the seismic resistance of the analysed structure is the resistance of the structure to collapse. However, since, by definition, all pushover analyses end in collapse, in 3Muri®, the adequacy of the structure to resist an earthquake of a particular intensity with respect to a specific limit state is assessed through the positive verification of the comparison between the maximum and target displacements (or the alpha ratios) for all the 24 load distributions for that limit state, as explained above. The results obtained in this research study and discussed in the ensuing sections raise concerns on whether this criterion of assessment classifies adequately the seismic resistance of the contemporary loadbearing masonry building typology present in the Maltese Islands, hence giving rise to the question of whether alternative or additional failure criteria would result in a more reliable estimate of the building height at which an adequate seismic resistance is exhibited for the investigated cases when a non-linear static pushover analysis is carried out.

The results reported in Table 43 of Appendix E indicate that the number of unsatisfied verifications resulting for a particular case with respect to the same limit state do not necessarily increase with

increase in number of floors. This apparent inconsistency in the results could be due to the pushover analysis settings in view of the magnitude of the increase in displacement which is applied to the numerical model at every analysis substep and the corresponding identification of failures in numerical models, which have a different seismic capacity by virtue of their different building heights. Therefore, particularly when comparing the seismic response of numerical models which include different seismic vulnerability characteristics, or when considering the same analysis case but different heights, the ensuing discussion does not evaluate the exhibited structural response of the analysed cases based on the number of unsatisfied verifications corresponding to every limit state, but rather, with respect to the maximum building height at which no unsatisfied verifications were obtained with respect to the considered limit states.

In the following cases with the original plan proportions, namely, the control numerical models, the control numerical models with a double height space between Levels 0 and 1 and the control numerical models with a soft storey at semi-basement level, in addition to the control numerical models with a soft storey at semi-basement level with an extended plan layout, the 3Muri® analyses were carried out starting from a height of six floors and increasing or decreasing the number of storeys one at a time until the maximum building heights at which no unsatisfied verifications for the Near Collapse and Significant Damage limit states resulted, were identified. This resulted in a maximum building height of analysed numerical model of fifteen floors and a minimum height of one floor. In the cases where a particular building height resulted in no unsatisfied verifications, whereas, after a further decrease in number of floors, unsatisfied verifications resulted, such cases were checked again for a reduced number of floors and the building height quoted in this study refers to the lower height for which no unsatisfied verifications resulted for the limit states under consideration. Since no investigated case resisted in collapse at a height of more than five floors among the cases analysed using ELS®, the 3Muri® numerical models investigating the response of the control model with setbacks at penthouse level were analysed up to a maximum height of six floors, the control case with a double height space between Levels 0 and 1 where the slab void spanned the whole width of the structure between the longitudinal party walls was analysed up to a maximum building height of ten floors, while the cases with the extended plan layouts which consisted of the control model and the control model with a double height space, were analysed up to a maximum building height of seven and eight floors, respectively.

As explained in Section 4.2, in the numerical analyses carried out using ELS®, the simulated ground motion record was applied to all numerical models in the transverse x-direction, which was the weaker orientation of all analysed cases in view of their plan proportions. Hence, the accelerations and displacements discussed in Chapter 4 were always related to the transverse x-direction of the analysed numerical models. In order to ensure comparability of results between the ELS® and the 3Muri® seismic analyses, the maximum displacement values reported in this study in the following sections with respect to the 3Muri® analyses refer to the maximum displacement obtained for every analysed numerical model when considering only the 12 load distributions where the load is applied in the transverse x- direction of the numerical models.

5.2.1 Building height for adequate seismic resistance: Comparison of seismic resistance exhibited by corresponding cases analysed using 3Muri® and ELS®

The different levels of detail which characterise the ELS® and the 3Muri® models, in addition to the different methods of load application and, hence, the different output extracted from the non-linear dynamic and the non-linear static methods, respectively, suggest that the strongest basis of comparison of the results obtained from these two different seismic analysis methods is the maximum building height at which the analysed cases exhibited an adequate seismic resistance, i.e. collapse resistance, in the case of ELS®, and no unsatisfied verifications, in the case of 3Muri®. However, for the comparison to be valid, it has to take into consideration the building response at the same limit state.

As explained in Section 3.4.5 of this thesis, the simulated input ground motion record used in ELS® was scaled to a maximum p.g.a. of 0.10g based on the seismicity of the Maltese Islands as indicated by the EFEHR SHARE 2013 Hazard model for a probability of exceedance of 10% in 50 years and a 95% fractile. In the absence of a National Annex for the Maltese Islands to Eurocode 8, this probability of exceedance is in accordance with the recommendations of Note 1 to Clause 2.1(1)P of Eurocode 8: Part 1 [4] for the design seismic action in accordance with the No Collapse Requirement defined in the same Clause. Therefore, from the point of view of choice of simulated accelerogram (equivalent to the 'design seismic action' in a non-linear dynamic analysis) all the ELS® numerical analyses were carried out with respect to the No Collapse Requirement and, hence, the resulting building height at collapse resistance for every analysed case is with respect to this limit state. Furthermore, it must be noted that the absence of 'local or global collapse' [4] and the resultant degree of 'structural integrity' [4] of the ELS® numerical models following the application of the simulated ground motion record, was not only verified through the simulations, but also through the comparison of the natural frequency of the analysed numerical models at the end of the dynamic loading stage to the corresponding natural frequency at the end of the static loading stage. This ratio is directly indicative of the residual stiffness of the analysed numerical model and, hence, the residual structural integrity after the simulated seismic event. This comparison is reported in Table 31 of Appendix D, with the percentage natural frequency in the transverse x-orientation of the numerical models at the end of the dynamic loading stage when compared to the natural frequency in the same orientation at the end of the static loading stage varying between 82.4% to 99.8% on upper coralline limestone and 69.9% to 96.8% on clay, and where percentages lower than 95% only resulted in cases, which included a soft storey in both subsoil cases. These values, therefore, suggest that all structures resulting as resisting collapse from the ELS® analyses, retained most of their stiffness and, hence, their structural resistance.

On the other hand, the 3Muri® Eurocode module carries out the seismic assessment of all new and existing structures in accordance with the recommendations of Eurocode 8: Part 3 [97], by checking every analysed structure with respect to the limit states of Near Collapse, Significant Damage and Damage Limitation. The Note to Clause 2.1(1)P of Eurocode 8: Part 3 [97], while acknowledging a degree of discrepancy in the associated level of damage, states that the No Collapse Requirement

defined in Clause 2.1(1)P of Eurocode 8: Part 1 [4] corresponds approximately to the limit state of Significant Damage defined in Clause 2.1(1)P of Eurocode 8: Part 3 [97].

Hence, in principle, the maximum building heights at which an adequate seismic resistance was exhibited by the 3Muri® numerical models when considering the specified maximum p.g.a. for the limit state of Significant Damage should be comparable to the building heights at which collapse was resisted in the corresponding numerical models which were analysed using ELS®. Figures 5-1 to 5-4 and Table 44 in Appendix E summarise the comparison of the building heights at which the control numerical models and the single parameter cases (with an original plan length-to-width ratio of 2.75) exhibited an adequate seismic resistance when analysed using 3Muri® and ELS® on an upper coralline limestone and/or a clay subsoil.

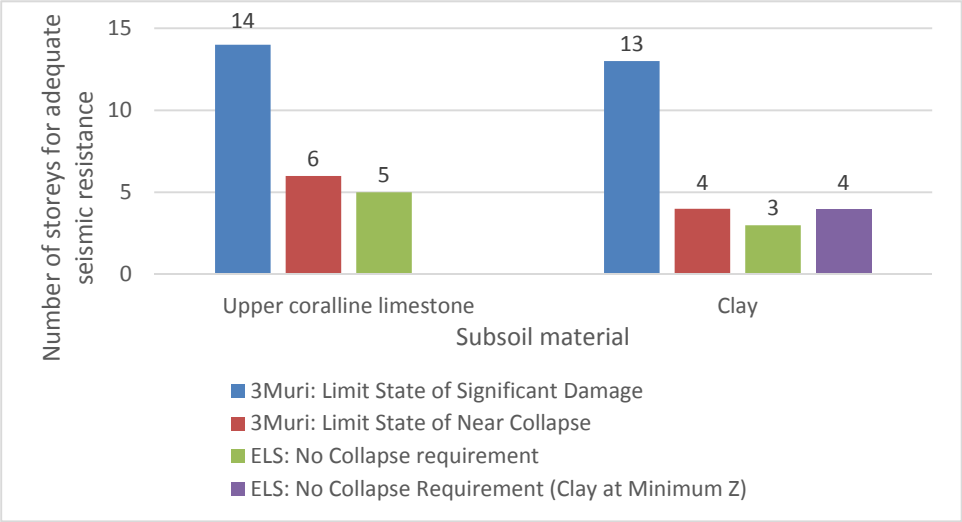

Figure 5-1 Comparison of the number of storeys at which an adequate seismic resistance was exhibited by the control numerical models using 3Muri® and ELS®.

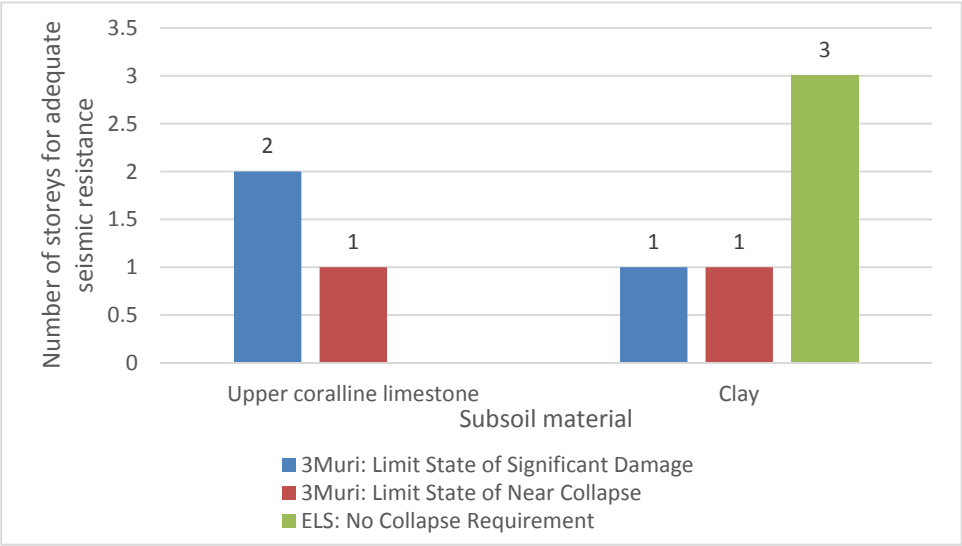

Figure 5-2 Comparison of the number of storeys at which an adequate seismic resistance was exhibited by the control numerical models with a soft storey at semi-basement level using 3Muri® and ELS®.

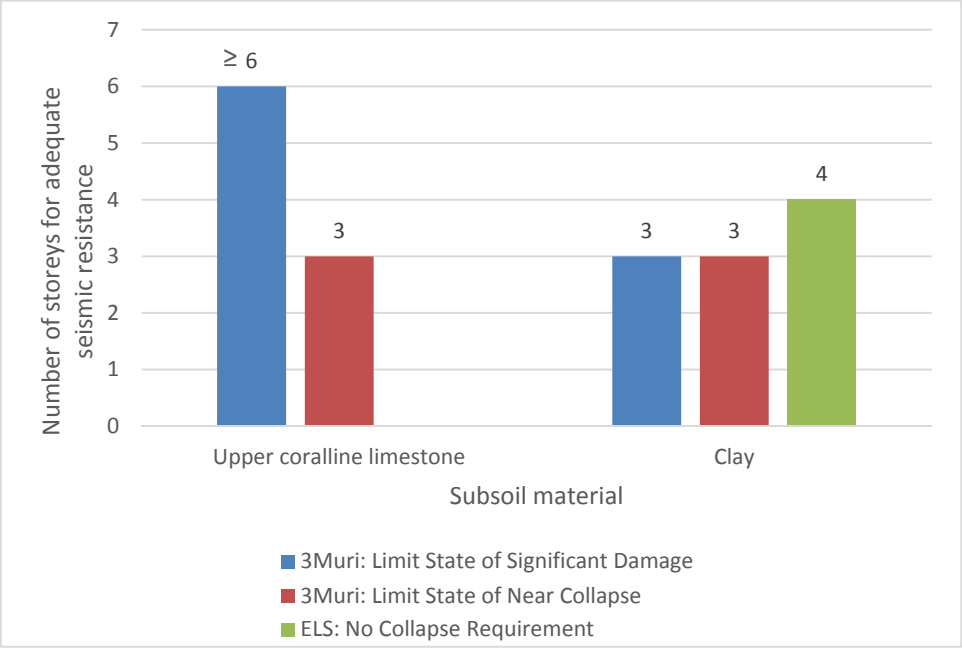

Figure 5-3 Comparison of the number of storeys at which an adequate seismic resistance was exhibited by the control numerical models with setbacks at penthouse level using 3Muri® and ELS®.

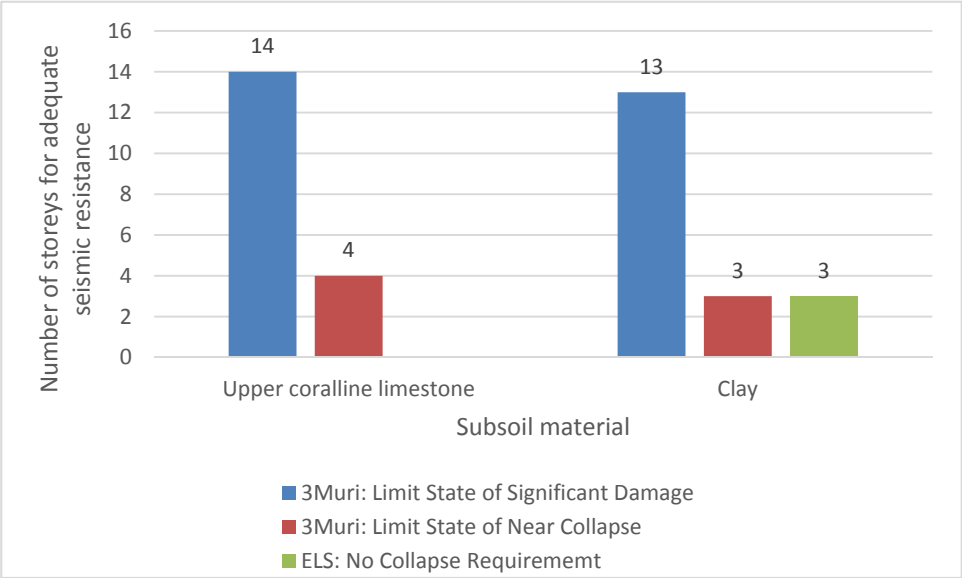

Figure 5-4 Comparison of the number of storeys at which an adequate seismic resistance was exhibited by the control numerical models with a double height space between Levels 0 and 1 using 3Muri® and ELS®.

Figures 5-1 to 5-4 indicate that, the results of the numerical models analysed using 3Muri® generally reflect the expected reduction in resistance between cases analysed on upper coralline limestone and clay and between cases analysed with respect to the limit state of Significant Damage and Near Collapse. However, the pronounced extent of the latter building height discrepancy is questionable in the case of the control numerical models and the control numerical models, which include a double height space between Levels 0 and 1. On the other hand, this expected reduction in seismic resistance,

is exhibited to a lesser extent in the numerical models with a soft storey at semi-basement analysed on upper coralline limestone and clay and the control numerical models with setbacks at penthouse level analysed on clay. Furthermore, Figures 5-1 and 5-4 suggest that the building heights at which an adequate seismic resistance is exhibited in 3Muri® with respect to the Limit State of Significant Damage differ significantly from the height at collapse resistance exhibited by the corresponding numerical models analysed using ELS® in the following cases:

a) control numerical models[35] analysed on upper coralline limestone and clay, respectively;
b) the control numerical models with a double height space between Levels 0 and 1 analysed on clay.

Nevertheless, the building heights which resulted in an adequate seismic resistance in 3Muri® for these cases with respect to the limit state of Near Collapse were considerably in better agreement with the heights at which the corresponding numerical models resisted collapse in ELS®. While indicating a level of agreement between the results obtained from these two analysis methods, the validity of this outcome is debatable since, as explained above, the probability of exceedance and the associated level of damage and residual structural resistance of the No Collapse Requirement considered in the ELS® analyses refer to a less severe design seismic action and a lower level of structural damage than that defined for the limit state of Near Collapse. The building heights obtained from the ELS® analyses resulted as more conservative by one storey when compared to those obtained with respect to the limit state of Near Collapse in the corresponding 3Muri® analyses for both subsoil cases considered for the control numerical models. On the other hand, in the case of the control numerical models with a double height space between Levels 0 and 1, analysed on a clay subsoil, the building height for adequate seismic resistance resulted as three floors for both the ELS® analysis and for the 3Muri® analysis with respect to the limit state of Near collapse.

Moreover, the results reported in Figures 5.2 and 5.3 suggest that, in the case of the control numerical models with a soft storey at semi-basement level and the control numerical models with setbacks at penthouse level, the building heights at which an adequate seismic resistance was exhibited in the

[35] Model 3M170 (one-storey control numerical model analysed on upper coralline limestone) resulted in 2 unsatisfied verifications for the limit state of Near Collapse, while Models 3M169, 3M168, 3M55, 3M54 and 3M46 (corresponding to the two-, three-, four-, five- and six-storey control numerical models analysed on upper coralline limestone) resulted in no unsatisfied verification for the same limit state. On the other hand, 3 unsatisfied verifications resulted in Model 3M47v2, the seven-storey control numerical model analysed on upper coralline limestone. In view of the five storey 'gap' where no unsatisfied verifications for the limit state of Near Collapse resulted (i.e. from the two-storey to the six-storey models) and after taking into account that the corresponding one-storey control numerical model with a soft storey at semi-basement level (Model 3M75) resulted in no unsatisfied verifications for the limit state of Near Collapse, the result obtained from Model 3M170 was considered anomalous and the lowest height at which the control numerical model exhibited an adequate resistance with respect to the limit state of Near Collapse on an upper coralline limestone subsoil was considered to be six floors.

3Muri® numerical models analysed on clay with respect to the limit state of Significant Damage were fairly close to the building heights resisting collapse obtained in the corresponding ELS® analyses.

The case of the control numerical model with setbacks at penthouse level analysed in 3Muri® was investigated for building heights between three to six storeys. This case will be temporarily excluded from the discussion on the comparison of the seismic capacity resulting from the 3Muri® and the ELS® numerical models based on the building height at which an adequate seismic resistance is exhibited in view of a number of factors, amongst which, is the high discrepancy between the building height at which an adequate seismic resistance was exhibited with respect to the limit state of Significant Damage when analysed on upper coralline limestone and on clay, respectively. Furthermore, the maximum building height at which no unsatisfied verifications were obtained for the limit state of Significant Damage when analysed on clay was reported at three floors, since at four floors (Model 3M165), 2 unsatisfied verifications resulted for the limit state of Significant Damage. However, no unsatisfied verifications resulted for the same limit state in the corresponding five- and six-storey numerical models. Similarly, the building height at which an adequate seismic resistance was exhibited with respect to the limit state of Near Collapse for the corresponding cases analysed on upper coralline limestone and on clay was three storeys in both cases. However, whereas the control numerical models with setbacks with a height of four or more storeys all resulted in unsatisfied verifications with respect to the limit state of Near Collapse when analysed on clay, in the case of the corresponding numerical models analysed on upper coralline limestone, 2 unsatisfied verifications with respect to the limit state of Near Collapse resulted in the four-storey case (Model 3M162), while no unsatisfied verifications with respect to the same limit state resulted in the corresponding five- and six-storey numerical models. Therefore, since the resistance of control numerical models with setbacks at penthouse level could not be verified through non-linear static pushover analysis for building heights higher than six storeys (due to time limitations), it could not be ascertained whether the 3Muri® results exhibited by this particular case should be considered anomalous, confirmation of which would effectively mean that a higher number of storeys corresponding to the maximum building height for adequate seismic resistance would become applicable. However, this latter observation is highly unlikely when one considers the trend in the results obtained in the ELS® analyses.

In addition, the validity of results suggesting that the control case and the case of the control numerical model with a double height space between Levels 0 and 1 for the contemporary loadbearing URM building typology under study exhibit an adequate seismic resistance with respect to an earthquake with a maximum p.g.a. of 0.10g (for the limit state of Significant damage) at maximum heights of fourteen and thirteen floors, respectively, must be considered with caution. This caution is particularly due in view of the relatively thin single leaf walls and the low mortar grade, which generally characterise the main vertical loadbearing elements of this URM building typology, where the vertical forces acting under static loads only would be very likely close to the limit of compressive resistance of these masonry walls at such building heights, especially in the wall areas supporting the larger slab spans.

Furthermore, the aim behind the numerical analyses carried out using ELS® in this research study was to compare the influence and the relative importance, which the investigated building characteristics have on the seismic resistance of the building typology under study. Therefore, while the analysis of all the investigated cases using only one simulated ground motion record, applied only in the weaker transverse x-direction of the analysed numerical models, was considered acceptable with respect to this aim, it is acknowledged that the results obtained using ELS® can only be considered to be indicative of the seismic resistance of the analysed cases since the verification did not constitute a complete non-linear dynamic assessment in accordance with the recommendations of Clauses 3.2.3.1.1(2)P, 3.2.3.1.2(4) and 4.3.3.4.3(3) of Eurocode 8: Part 1 [4]. Notwithstanding, the extent of the pronounced discrepancy between the seismic resistance of the control numerical models and the control numerical models with a double height space between Levels 0 and 1 analysed using 3Muri® in terms of the building height at which an adequate seismic resistance was exhibited by these investigated cases for the limit state of Significant Damage when compared to the seismic resistance of the corresponding models analysed using ELS® in terms of the building height at collapse resistance analysed with respect to the No Collapse Requirement, cannot be justified by the limited loading scenario considered in the numerical analyses carried out using ELS®. On the other hand, with reference to Figure 5-2, the closer estimate obtained from the 3Muri® control numerical models, which include a soft storey at semi-basement level for the limit state of Significant Damage when compared to the building height at collapse resistance of the corresponding numerical models analysed using ELS®, where the 3Muri® building height for adequate seismic resistance results as more conservative than the corresponding ELS® building height by two floors, suggests that the reason behind this different predicted behaviour could be due to the assumptions at the basis of this non-linear static pushover analysis method.

The global analysis of the analysed structures carried out using 3Muri® assumes that the masonry walls have a high resistance to in-plane actions and that the resistance of the walls to out-of-plane actions can be ignored. For this global resistance to be achieved, the structure has to behave like a rigid box through the full coupling between intersecting walls and rigid restraints at slab boundaries, hence, resulting in a higher global resistance of the structure than the resistance of the individual walls [178]. Peripheral ties or ring beams at slab levels are generally absent in the loadbearing URM building typology under study and no reinforced connection is typically present between slabs and loadbearing walls. However, though not fully connected, a degree of load transfer can be expected to be present between the slabs and the loadbearing walls particularly when the vertical structural system consists of softstone masonry walls and when the slabs are constructed in reinforced cast in-situ concrete and are not the result of subsequent alterations to the structure, in view of the rigidity of the cast in-situ slabs, the continuity of their reinforcement, the general practice of bearing the slabs over the full

thickness of the supporting walls and the high self-weight of the walls[36]. On the other hand, as discussed in Section 5.1, the presence of full coupling between intersecting walls and between walls and slabs is very unlikely in the contemporary loadbearing masonry building typology present in the Maltese Islands. The results reported in Figures 5-1 to 5-4 suggest that this 'incorrect'[37]representation of the wall-to-wall and wall-to-slab junctions in the 3Muri® models influences more the simulated response of the control numerical models and the control numerical models, which include a double height space between Levels 0 and 1, when compared to the control numerical models with a soft storey at semi-basement level. This difference in seismic resistance prediction is likely to be due to the large displacements resulting at the level of the soft storey, which counteract the effect of the additional stiffness resulting from the assumed coupling, which is only present from Level 0 upwards in the latter case. Furthermore, the reduced area of masonry walls present at the level of the soft storey limits the artificial beneficial box-like behaviour effect on the resistance of the structure at this level to the few wall junctions present. Hence, the artificial beneficial effect of the assumed full coupling results in a higher stiffness to displacements and an apparent increase in seismic resistance in the case of the control numerical models and the control numerical models with a double height space between Levels 0 and 1, where the drift between floors is comparable throughout the entire height of the structure. This tends to lead to the over-estimation of the maximum building height at which an adequate seismic resistance is exhibited by these cases such that a more realistic estimate of seismic resistance is obtained only if a more severe ultimate limit state (Near Collapse) than the one upon which the assessment is actually being based (Significant Damage), is considered.

In the ensuing sections an attempt is made towards the identification of an alternative or an additional failure criterion, which would result in a more reliable estimate of the building height at adequate seismic resistance of a contemporary loadbearing unreinforced masonry structure with respect to the limit state of Significant Damage using the 3Muri® non-linear static pushover analysis. Until more reliable failure criteria are identified for use in the assessment of the seismic response of the URM building typology under study, based on the above discussion, it is suggested that only structures which include a significant variation in the lateral storey stiffness between overlying floors are assessed with respect the limit state of Significant Damage, while structures which exhibit a more constant lateral

[36] The adequacy of the connection between walls and slabs can be expected to be significantly reduced in cases when the vertical loadbearing system consists of hollow concrete blockwork walls, when precast concrete slab construction systems without a reinforced concrete topping and a ring beam are present and when the slabs are the result of subsequent building alterations, hence, having a reduced width of bearing on the supporting walls. The use of hollow concrete blockwork walls for most of the vertical loadbearing elements became prevalent in recent years, particularly in Malta, and to a significantly lower extent, in Gozo.

[37] Where 'incorrect' is herein solely referring to the representation of the construction details typically present in the contemporary loadbearing unreinforced masonry building typology present in the Maltese Islands.

storey stiffness throughout the building height are assessed with the more severe limit state of Near Collapse.

5.2.2 Building height for adequate seismic resistance: Comparison of seismic resistance exhibited by additional cases analysed using 3Muri®

In this section, the influence on the seismic capacity of the URM building typology under study of the presence of a double height void which spans the entire width of the structure between longitudinal party walls at slab Level 1 (keeping the original plan length-to-width ratio of 2.75), and the influence of extending the plan length-to-width ratio to 4:1 in the control numerical models, the control numerical models with a soft storey and the control numerical models with a double height space between Levels 0 and 1, is examined with respect to the building height at which an adequate seismic resistance corresponding to the limit states of Significant Damage and Near Collapse is achieved according to the 3Muri® failure criterion for satisfied verifications (i.e. where the ratio between the maximum displacement and the target displacement is greater than 1, or similarly, the alpha ratio is greater than 1). In all the investigated cases, the resulting building heights for adequate seismic resistance are compared to the outcome exhibited by the corresponding original cases analysed using 3Muri® for the same limit states and discussed in Section 5.2.1.

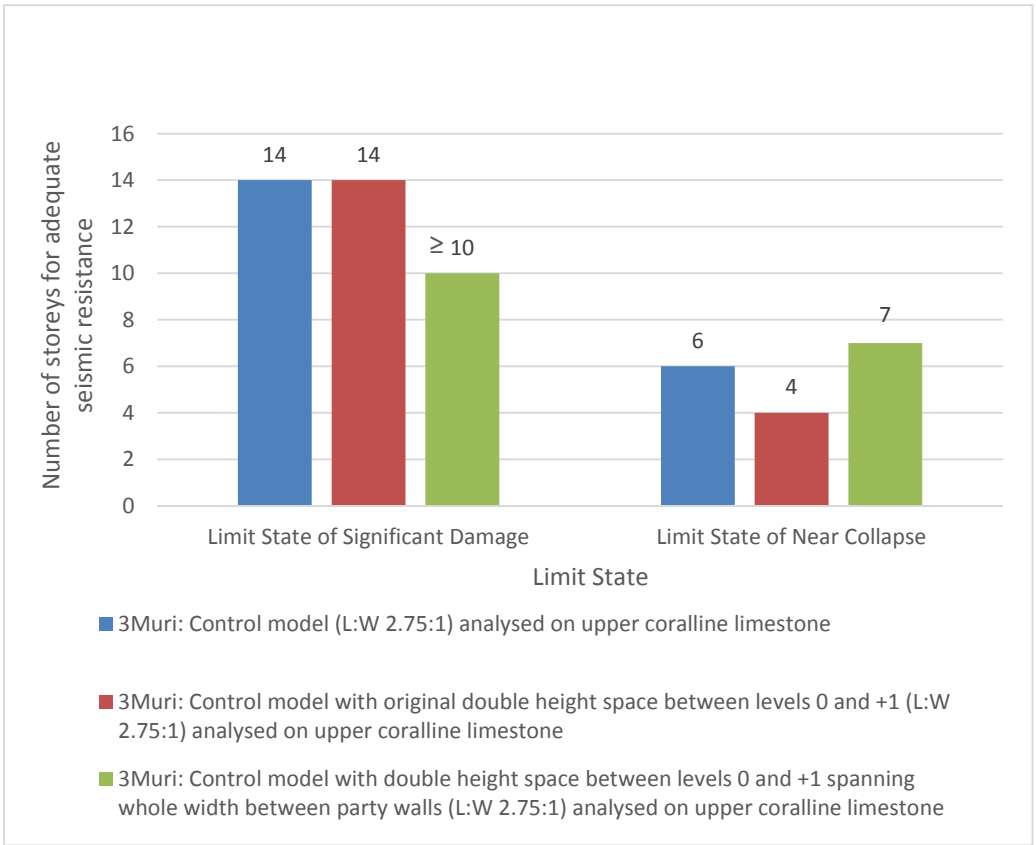

Figure 5-5 Comparison of the maximum number of storeys for adequate seismic resistance by the control numerical models with a double height void spanning the whole width of the structure between party walls vs.the original width of void and vs. the control case.

The investigated case of the control numerical model with the original plan proportions and with a double height space between Levels 0 and 1 which spans the whole width of the structure between the longitudinal party walls, was analysed using 3Muri® for overall building heights of between four and ten storeys on upper coralline limestone only. Figure 5.5 reports the comparison of the resulting building height for adequate seismic resistance in accordance with the limit states of Near Collapse and Significant Damage of this case to the corresponding building heights resulting from the control numerical model and from the control numerical model with a double height space between Levels 0 and 1 with the original void proportions. The building height for adequate seismic resistance resulting from the numerical control models with a wider double height void could not be identified with respect to the limit state of Significant Damage since no unsatisfied verifications resulted with respect to this limit state up to a height of ten storeys. Hence, a comparison of the exhibited behaviour with respect to this limit state cannot be made. The widening of the void was expected to result in a reduced seismic resistance when compared to the corresponding case with the original void proportions in view of:

a) the elimination of the 250 mm thick slab spanning parallel to the right hand side party wall, with the resulting loss of the stiffening effect and the redistribution of horizontal seismic actions around the void provided previously by this slab;
b) the reduced restraint of the party walls on both sides of the void and the consequent increase in slenderness due to the absence of the slab at Level 1 within the area of the void.

Notwithstanding, the maximum height at which no unsatisfied verifications resulted with respect to the limit state of Near Collapse was at seven floors. This result implies that the control numerical model with the wider double height void exhibited an increased resistance by one storey when compared to the corresponding control case, and a higher resistance by three storeys when compared to the control numerical model including a double height void with the original (narrower) proportions and positioned directly abutting the left party wall. This increased seismic resistance suggests that, since the out-of-plane resistance of walls is ignored in 3Muri®, the reduction in the resistance of the party walls in the area of the void resulting from the increased slenderness was overlooked by this method of assessment. On the other hand, the effect of the more symmetrical mass distribution resulting from the widening of the void to the entire width of the structure and the reduction in the building mass positioned further away from the centroid of the storey might have resulted in a reduction of the eccentricity of the centre of mass and, hence, a reduction of the torsional moments when compared to the control case and the control case with the narrower double height void. Consequently, this would lead to an overall increase in the exhibited seismic resistance of the building, which is likely to be over-estimated by 3Muri® for the Near Collapse limit state.

Figures 5-6 and 5-7 report the comparison of the maximum height at which an adequate seismic resistance was exhibited by the control numerical model and the control numerical model with a soft storey at semi-basement level with overall plan length-to-width proportions at the typical storey level of 4:1 and 2.75:1, with respect to the limit states of Significant Damage and Near Collapse, and analysed on upper coralline limestone and clay. It is noted that, as indicated in Figure 5-7, the control numerical model including a soft storey at semi-basement level and with an extended plan layout does

not exhibit an adequate seismic resistance with respect to the limit state of Near Collapse at a height of one storey, neither when analysed on an upper coralline limestone subsoil, nor when a clay subsoil is considered.

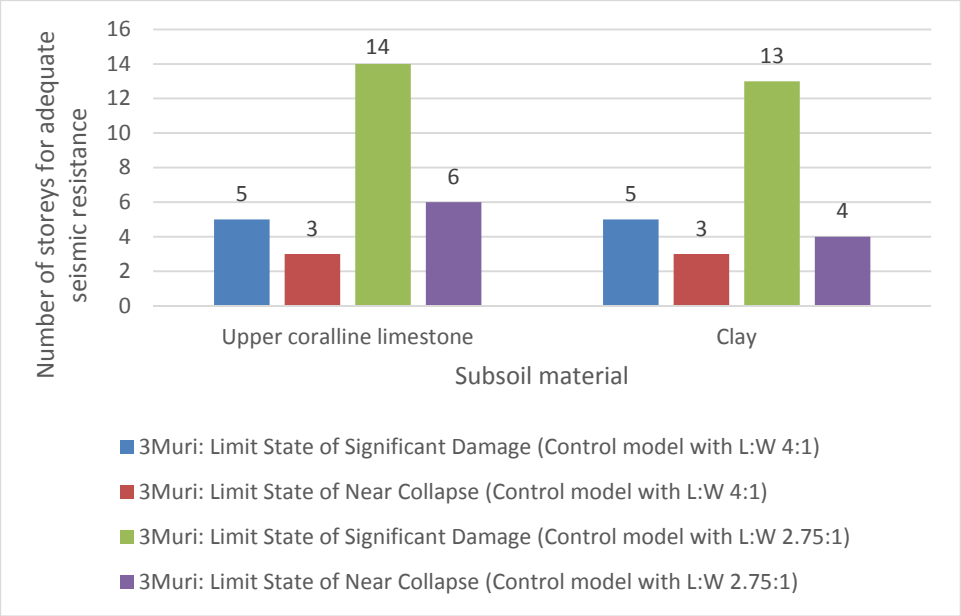

Figure 5-6 Comparison of the maximum number of storeys for adequate seismic resistance of the control numerical model with plan length-to-width ratio of 4:1 with the resistance of the corresponding control numerical model with a plan ratio of 2.75:1.

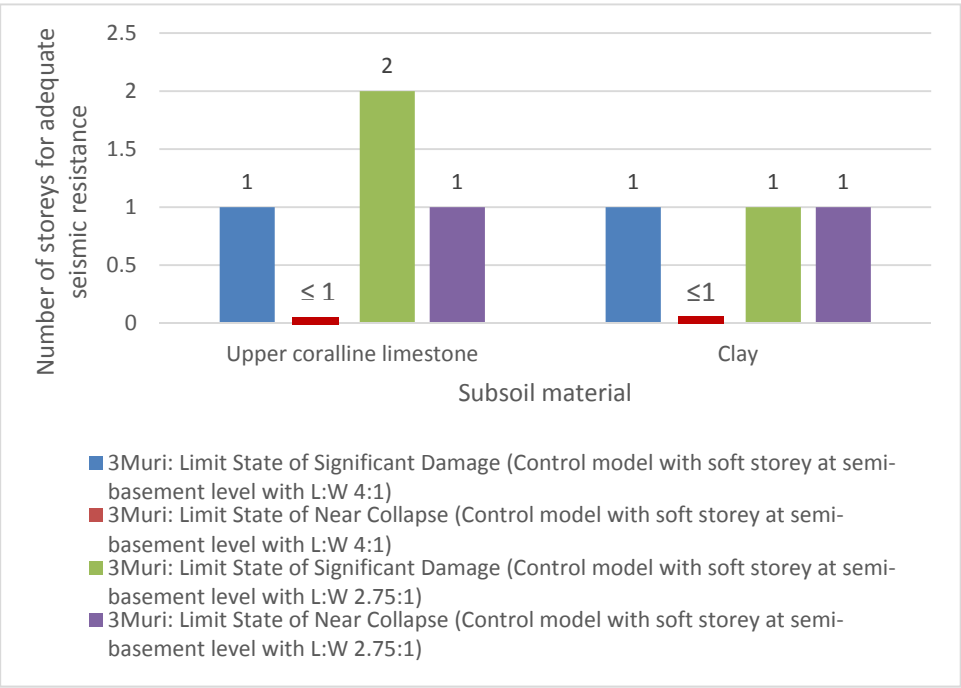

Figure 5-7 Comparison of the maximum number of storeys for adequate seismic resistance of the control numerical model including a soft storey (plan length-to-width ratio of 4:1) with the resistance of the corresponding numerical model (plan ratio of 2.75:1).

The results presented in Figures 5-6 and 5.7 with respect to the control numerical models and the control numerical models with a soft storey at semi-basement level with extended plan layouts reflect the expected decrease in seismic resistance, which is consequent to the elongation of the plan proportions and, in particular, the extension of the front room by around 5 m, while most of the walls are positioned between the stairwell and the rear elevation. This leads to the increase in torsional forces due to an increased eccentricity between the centre of mass and the centre of resistance of the building.

Figure 5-6 indicates that the height at which the control numerical model with extended plan proportions exhibits an adequate seismic resistance with respect to the limit state of Significant Damage when compared to response exhibited by the corresponding control numerical models with a plan length-to-width ratio of 2.75:1 reduces from a height of fourteen to a height of five floors when analysed on upper coralline limestone, and from a height to thirteen floors to a height of five floors when analysed on clay. The verification of this result by direct comparison to a corresponding ELS® case cannot be carried out since the cases with extended plan proportions were not modelled using ELS®. However, the comparison of this exhibited seismic resistance to the building height at collapse resistance resulting from the control numerical models with the original plan proportions analysed using ELS®[38] suggests that, while the extent of over-estimation of the seismic resistance of the extended control numerical model seems to be significantly reduced when compared to the seismic resistance of the control numerical model with the original plan proportions analysed using 3Muri®, a degree of over-estimation still remains in the numerical models analysed using 3Muri®.

With reference to the plan layout of the control numerical models with the extended plan proportions when compared to the plan layout of the control numerical models with the original proportions reproduced in Figures 33 and 21 of Appendix C respectively, the extended layout was obtained through the insertion of an additional room directly behind the room abutting the rear façade and the extension of the front room. Hence, the control numerical models with an extended plan layout include only one additional transverse wall. However, the elongation of the plan results in the lengthening of the unrestrained wall in the corridor by around 3 m and the lengthening of the front open plan room by 5 m. The extended plan layouts, therefore, result in only a marginal increase in the estimated seismic resistance in the transverse direction arising from the assumed full connection between intersecting walls. Thus, with reference to the discussion in Section 5.2.1 on the possible

[38] The control numerical models with the original plan proportions analysed using ELS® resisted collapse at a building height of five floors in all 'rock' subsoil cases, at three floors when analysed on a 1.5 m thick upper coralline limestone layer overlying a 60 m thick clay layer, and when analysed on a single 60 m thick clay layer, while this case resisted collapse at a building height of four floors when analysed on clay defined at the model's Minimum Z position. The control numerical models with the extended plan proportions analysed using 3Muri® exhibited an adequate seismic resistance with respect to the limit state of Significant Damage at a maximum height of five floors when analysed on both upper coralline limestone and clay subsoils, respectively.

cause of the over-estimation in seismic resistance resulting in the control numerical models with the original plan proportions, when compared to the resulting seismic resistance exhibited by the control numerical models with a soft storey and with the original plan proportions analysed using 3Muri®, it is likely that the reduction in seismic resistance resulting from the elongation of the plan (which leads to a higher eccentricity between the centre of mass and the centre of stiffness of the floor and, hence, an increase in the torsional moments) is of significant magnitude, partially cancelling out the artificial increase in resistance due to the assumed box-like structural behaviour (and, consequently, the full coupling at wall-to-wall and wall-to-slab junctions). These results further suggest that, in a real life scenario where the full coupling between intersecting walls and between walls and slabs would not be present, the building height for adequate seismic resistance with respect to the limit state of Significant Damage would still likely be lower than the building height estimated by 3Muri® for the same limit state.

Moreover, it is noted that the maximum building heights for adequate seismic resistance exhibited with respect to the limit states of Significant Damage and Near Collapse resulting from the numerical analysis on an upper coralline limestone or clay subsoil, remain unchanged. Nevertheless, the results of the non-linear static analyses summarised in Table 43 of Appendix E indicate that an increase in the number of unsatisfied verifications for the limit state of Significant Damage is exhibited by the six-storey control numerical model[39] with the extended plan proportions when analysed on a clay subsoil when compared to the corresponding six-storey extended control numerical model analysed on an upper coralline limestone subsoil, while the same number of unsatisfied verifications resulted in the corresponding four-storey models[40] for the two subsoil cases when analysed with respect to the limit state of Near Collapse. Conversely, the control numerical model with a soft storey and with extended plan proportions results in the same number of unsatisfied verifications at a height of two floors[41] with respect to the limit state of Significant Damage and in an increase in the number of unsatisfied verifications at a height of one floor[42] with respect to the limit state of Near Collapse, when analysed

[39] The six-storey control numerical models with extended plan proportions correspond to the lowest building height for which unsatisfied verifications with respect to the limit state of Significant Damage resulted when this case was analysed on both an upper coralline limestone and a clay subsoil, respectively.

[40] The four-storey control numerical models with extended plan proportions correspond to the lowest building height for which unsatisfied verifications with respect to the limit state of Near Collapse resulted when this case was analysed on both an upper coralline limestone and a clay subsoil, respectively.

[41] The two-storey control numerical models with a soft storey at semi-basement level and with extended plan proportions correspond to the lowest building height for which unsatisfied verifications with respect to the limit state of Significant Damage resulted when this case was analysed on both an upper coralline limestone and a clay subsoil, respectively.

[42] The one-storey control numerical models with a soft storey at semi-basement level and with extended plan proportions resulted in 2 unsatisfied verifications when analysed on an upper coralline limestone subsoil with respect to the limit state of Near Collapse and in 7 unsatisfied verifications when analysed on a clay subsoil with respect to the same limit state.

on clay as compared to the results obtained on an upper coralline limestone subsoil. In such cases, the increase in number of unsatisfied verifications resulting when the same structure is analysed on different subsoils, can be considered indicative of a lower resistance to the seismic action specified with respect to the particular limit state. Nevertheless, the only marginal reduction in seismic resistance exhibited by the analysed extended control numerical models with or without a soft storey at semi-basement level when analysed on clay as compared to the exhibited seismic resistance when the same cases are analysed on upper coralline limestone, solely evidenced by a small difference in the number of unsatisfied verifications with respect to one of the two limit states considered (i.e. the Significant Damage limit state), remains somewhat anomalous.

Figure 5-8 reports the comparison of the seismic resistance of the control numerical models with a double height space between Levels 0 and 1 and with a plan length-to-width ratio of 4:1 to the seismic resistance exhibited by the corresponding control numerical models with a double height space and with the original plan proportions, in terms of the building height at adequate seismic resistance with respect to the limit states of Significant Damage and Near collapse, for an upper coralline limestone or clay subsoil, respectively.

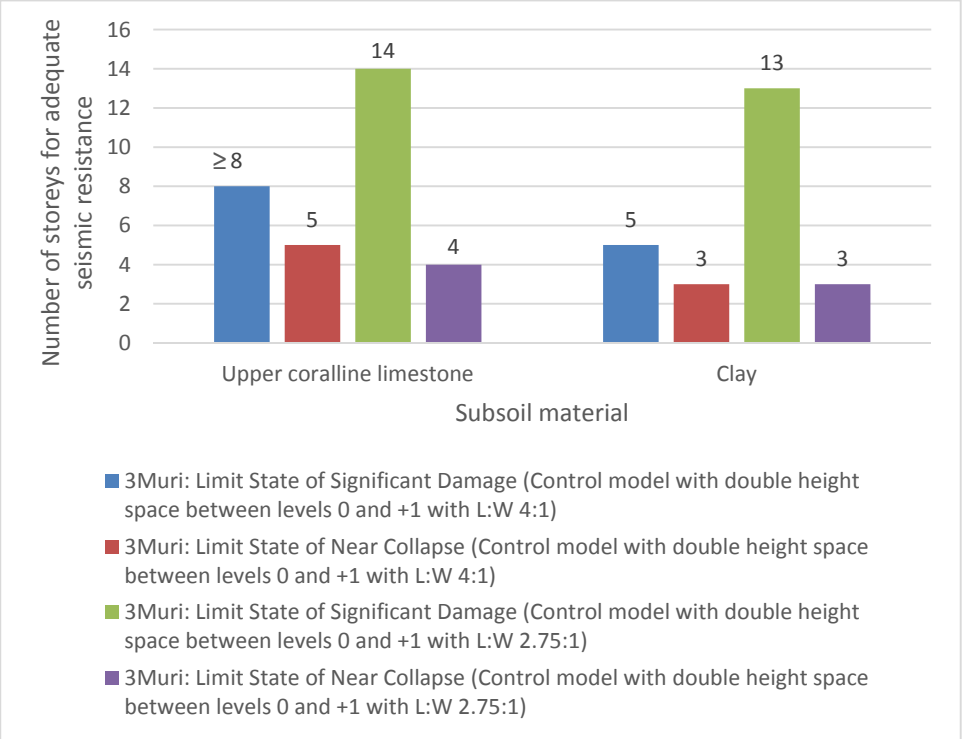

Figure 5-8 Comparison of the maximum number of storeys for adequate seismic resistance of the control numerical model including a double height space (plan length-to-width ratio of 4:1) with the resistance of the corresponding numerical model (plan ratio of 2.75:1).

When considering the limit state of Near Collapse, the control numerical models including a double height space between Levels 0 and 1 and with the extended plan proportions exhibit an adequate seismic resistance at a maximum height of one storey more than the corresponding control numerical model with a double height space and the original plan proportions when analysed on upper coralline limestone. Furthermore, the same maximum building height for adequate seismic resistance of 3

storeys resulted for the extended and original cases with respect to the limit state of Near Collapse when clay was considered as the subsoil material.

With reference to the results of the non-linear static analysis presented in Table 43 of Appendix E, the four storey control numerical model with a double height space between Levels 0 and 1 and with an extended plan layout, resulted in a lower number of unsatisfied verifications when analysed on clay with respect to the limit state of Near Collapse when compared to the corresponding four-storey control numerical model including a double height space between Levels 0 and 1 and with the original plan proportions. This result suggests a higher resistance to the seismic actions with respect to the limit state of Near Collapse even when a clay subsoil is considered. This higher seismic resistance could be the result of the position of the void at the farthest end of the extended storey, hence causing a backwards shift in the centre of mass which is likely to have led to a reduction in the eccentricity between the centre of mass and the centre of resistance, thereby reducing the torsional moments acting on the storey.

On the other hand, the control numerical models with a double height space between Levels 0 and 1 and with extended plan proportions were analysed using 3Muri®, for building heights of three to eight storeys. Therefore, the effect of the elongation of the plan layout on the seismic resistance in the case of an upper coralline limestone subsoil could not be verified with respect to the limit state of Significant Damage, since no unsatisfied verifications resulted with respect to this limit state up to a height of eight storeys. However, the extended control numerical models with a double height space between Levels 0 and 1 analysed on clay with respect to the limit state of Significant Damage exhibit a reduction in seismic resistance from thirteen storeys to five storeys when compared to the corresponding numerical models with a double height space at the same level and position, however, with the original plan proportions. Nevertheless, whereas the six-storey numerical control model including a double height space between Levels 0 and 1 and with extended plan proportions analysed on clay, results in 1 unsatisfied verification with respect to the limit state of Significant Damage, the corresponding seven and eight-storey models do not result in any unsatisfied verifications with respect to the same limit state.

The limit state of Significant Damage refers to a seismic action with a higher probability of exceedance in 50 years and, hence, a less severe state of damage in the structure when compared to the Near Collapse limit state. It does not correspond to a change in the plan layout or the structural members. Therefore, if the extension of the plan layout with a double height void almost abutting the front façade results in an increased resistance with respect to the limit state of Near Collapse, it is expected to exhibit a similar increase in resistance when assessed with respect to the limit state of Significant Damage. Hence, it is anomalous that this discrepancy in the seismic resistance exhibited by the extended plan layout, which includes a double height space, when compared to the seismic resistance of the corresponding case including a double height space of the same size and position with respect to the front façade, however, with the original plan proportions, depends on the limit state to which the assessment is carried out.

Thus, in the case of the extended plan layout control numerical model with a double height space between Levels 0 and 1, while the improved seismic resistance exhibited by the numerical models analysed using 3Muri® with respect to the limit state of Near Collapse can be explained in terms of the reduction of torsional actions, the reduction in seismic resistance exhibited by the same case with respect to the limit state of Significant Damage when analysed on a clay subsoil cannot be justified.

5.2.2.1 Comparison of seismic capacity to results obtained by Borg [20] for the control numerical models

Table 5-1 Maximum number of floors for collapse resistance of a contemporary loadbearing URM structure without additional seismic vulnerability characteristics for mortar grade M2, 2 masonry wall materials and 3 subsoil alternatives. Extract from Borg [20].

Wall material	Maximum number of floors for collapse resistance for different subsoil types and plan proportions: 2:1			Maximum number of floors for collapse resistance for different subsoil types and plan proportions: 3:1			Maximum number of floors for collapse resistance for different subsoil types and plan proportions: 4:1		
	Rock Type A	Clay Type B	Clay Type C	Rock Type A	Clay Type B	Clay Type C	Rock Type A	Clay Type B	Clay Type C
Softstone	4	3	3	5*	3*	<3	5	4	3
HCB	<3	<3	<3	<3	<3	<3	<3	<3	<3
Note: * indicates that the structure resists collapse, but is very close to failure at this height									

Table 5-2 Maximum number of floors for adequate seismic resistance exhibited by the control numerical models with original or extended plan proportions resulting from a full non-linear dynamic analysis (ELS®) and a non-linear static pushover analysis (3Muri®).

Software used - Analysis method	Maximum number of floors for adequate seismic resistance with plan proportions: 2.75:1			Maximum number of floors for adequate seismic resistance with plan proportions: 4:1	
	Rock subsoil	Clay subsoil		Rock subsoil	Clay subsoil
ELS® - Full non-linear dynamic analysis	5	3 (on 1.5 m UCL over 60 m clay; and 60 m clay only)	4 (on clay defined at model's Minimum Z position)	N/A	N/A
3Muri®: Non-linear static pushover analysis	SD: 14	SD: 13		SD: 5	SD: 5
	NC: 6	NC: 4		NC: 3	NC: 3
Note: SD and NC refer to the limit states of Significant Damage and Near Collapse, respectively.					

Table 5-1 reproduces an extract of the results reported by Borg [20] with respect to the maximum building heights at collapse resistance of a typical contemporary loadbearing unreinforced masonry building with no additional seismic vulnerability characteristic, with mortar grade M2 (equivalent to a compressive strength of 2 N/mm^2), plan length-to-width proportions of 2:1, 3:1 and 4:1, on 3 subsoil types, namely, Rock Type A, Clay Type B and Clay Type C, as defined in Table 3.1 of Eurocode 8: Part 1 [4]. The reported results consider structures whose main vertical loadbearing system consists entirely

of softstone masonry or hollow concrete blockwork masonry walls, respectively. The building heights for collapse resistance were determined by Borg [20] using a modified version of the 'Equivalent Frame Method' proposed by Bhowmick and Mohanty [103]. The study carried out by Borg [20] considered a building typology, which is equivalent to that of the control numerical models investigated in this research study. The maximum building heights for collapse resistance reported in Table 5-1 were based on a maximum p.g.a. of 0.10g, which is also in accordance with the maximum p.g.a. of the simulated ground motion record used in the non-linear dynamic analysis carried out using ELS® and the non-linear static pushover analysis carried out using 3Muri® with respect to the limit state of Significant Damage by the author of this thesis. However, the assessment carried out by Borg [20] considered a Type 2 spectrum, as defined in Clause 3.2.2.2(2)P and Table 3.3 of Eurocode 8: Part 1 [4], hence taking into account a seismic event with a surface wave magnitude not exceeding 5.5. The simulated ground motion record used for the non-linear dynamic analyses carried out using ELS® has a magnitude of 7.6, a hypocentral distance of 170.30 km and an epicentral distance of 139.91 km, while the non-linear static analysis carried out in 3Muri® considered a Type 1 spectrum as defined by Table 3.2 of Eurocode 8: Part 1 [4]. Hence, in both cases, a more severe earthquake magnitude than that assumed by Borg [20] was considered.

Furthermore, while Borg [20] considered URM buildings where the vertical construction system consisted entirely of either softstone or hollow concrete blockwork walls, the numerical control models considered in the present study include softstone masonry party walls and hollow concrete blockwork internal walls and facades. The shear walls positioned in the weaker transverse x-x orientation of the control numerical models all consist of hollow concrete blockwork walls, hence suggesting that the resistance to seismic actions of these control models should be considered more comparable to the hollow concrete blockwork structures evaluated by Borg [20].

Table 5-2 presents the maximum heights at which the control numerical models with the original length-to-width plan proportions of 2.75:1, and the extended plan proportions of 4:1, resisted collapse when analysed through a non-linear dynamic analysis using ELS®, and resulted in an adequate seismic resistance with respect to the limit states of Significant Damage and Near Collapse when analysed through a non-linear static pushover analysis using 3Muri®, on a subsoil consisting of upper coralline limestone or clay, respectively. Notwithstanding the acknowledged differences in the earthquake magnitude and the material of the vertical loadbearing masonry walls, a comparison of the building heights at which an adequate seismic resistance was obtained in the control numerical models analysed in the present study to the results obtained by Borg [20] for contemporary loadbearing URM buildings with corresponding plan proportions and subsoil materials, was carried out in order to gain some insight into the degree of agreement between the two sets of results, taking into consideration these discrepancies.

Tables 5-1 and 5-2 indicate that the numerical control models with a 2.75:1 length-to-width ratio at the typical floor level analysed using ELS® on all considered 'rock' subsoil cases (equivalent to ground Type A, as defined in Table 3.1 of Eurocode 8: Part 1 [4]) and on 2 out of the 3 considered 'clay subsoil' cases (equivalent to ground Type B, as defined in Table 3.1 of Eurocode 8: Part 1 [4]) exhibited a

resistance to collapse at the same maximum height as the corresponding cases evaluated by Borg [20] for a building with length-to-width plan proportions of 3:1, with softstone masonry loadbearing walls, on rock Type A and clay Type B, respectively. Consequently, these control numerical models exhibited a higher seismic resistance than the corresponding cases evaluated by Borg [20], which consider the vertical loadbearing structure as consisting entirely of hollow concrete blockwork walls and a design seismic action corresponding to an earthquake of lower magnitude.

The plan configuration used by Borg [20] is only marginally more elongated (3:1 vs. 2.75:1) than the corresponding plan layout adopted in the present study for the control numerical models and considered in the above comparison, and so this should not have a significant influence on the results obtained. However, the agreement between the building heights at collapse resistance resulting from the investigation carried out by Borg [20] and the study presented herein, was obtained for the case, considered by Borg [20], of a structure with softstone masonry loadbearing walls throughout. This vertical loadbearing system is associated with a higher resistance to seismic actions than a corresponding structure where most of the walls are constructed in hollow concrete blockwork (particularly, in view of the reduced contact area present between overlying hollow concrete blockwork courses), as in the case of the analysed control numerical models. Furthermore, as explained previously, a seismic event with a less severe magnitude was taken in consideration by Borg [20]. On the other hand, though the softstone masonry structures assessed by Borg [20] resisted collapse at the same heights as the corresponding cases evaluated using ELS®, these structures were described as being very close to failure, whereas the ELS® numerical models retained most of their structural integrity, as confirmed from the natural frequency of these models at the end of the dynamic loading stage when compared to the natural frequency at the end of the static loading stage[43]. The combination of all these considerations, therefore, suggests that the method used by Borg [20] results in a more conservative estimate than the non-linear dynamic assessment carried out using ELS®.

Moreover, similarly to the comparison between the building heights at adequate seismic resistance resulting from the control numerical models with a plan length-to-width ratio of 2.75:1 analysed through a non-linear static pushover analysis using 3Muri® to the corresponding ELS® outcomes discussed in Section 5.2.1, the 3Muri® control numerical models exhibit an excessively high resistance when compared to the building heights at collapse resistance reported by Borg [20] for both rock and clay subsoils, when the limit state of Significant Damage is considered. The comparison of the building heights for adequate seismic resistance with respect to the limit state of Significant Damage when a rock subsoil is considered for the control numerical models with a plan length-to-width ratio of 4:1

[43] The natural frequency of the numerical control models at the end of the dynamic loading stage worked out as a percentage of the natural frequency of the same numerical models at the end of the static loading stage is around 96% in the transverse x-x orientation and around 94% in the longitudinal y-y orientation of the analysed control model. The percentages quoted are average values obtained in the respective plan direction for rock and clay subsoils.

reported in Tables 5-1 and 5-2, indicates a complete agreement with the case, considered by Borg [20], of structures with a loadbearing system consisting entirely of softstone masonry walls. However, the corresponding comparison of the resulting maximum safe building heights obtained with respect to the limit state of Significant Damage (in 3Muri®), a softstone masonry vertical loadbearing system (in Borg [20]), and when a clay subsoil is considered, suggests that the extent of this discrepancy is significantly lower (one storey higher maximum safe buiding height obtained from the 3Muri® analyses) in this case, when compared to the maximum safe building height resulting from these two methods for control numerical models with a plan length-to-width ratio of 2.75:1.

On the other hand, the maximum building heights at which an adequate resistance was exhibited in the control numerical models analysed using 3Muri® with respect to the limit state of Near Collapse when compared to the corresponding maximum building heights at collapse resistance reported by Borg [20] for softstone masonry structures, result lower by two storeys in the case of the control numerical models with extended plan layout proportions analysed on a rock subsoil. In the corresponding case analysed on a clay subsoil, the height at collapse resistance estimated by Borg [20] is higher than the 3Muri® height at adequate seismic resistance by one storey. On the other hand, in the case of the numerical control models with a length-to-width plan ratio of 2.75:1, the 3Muri® heights at adequate seismic resistance with respect to the limit state of Near Collapse, are one storey higher than the corresponding heights at collapse resistance reported by Borg [20] for both rock and clay subsoil cases. Thus, the differing limit states and the seismic resistance associated with the type of masonry walls with respect to which the closer estimates of seismic capacity are obtained using 3Muri® and in the results reported by Borg [20] for a building typology equivalent to the numerical control models, suggest that the method of seismic assessment used by Borg [20] leads to a more conservative assessment than 3Muri®, while also confirming that the 3Muri® non-linear static pushover analysis with respect to the limit state of Significant Damage is likely to result in an over-estimation of the seismic resistance of the control numerical models.

Therefore, the comparison of the maximum safe building heights resulting from this research study with respect to the numerical control models with the original plan proportions analysed using ELS® to the corresponding maximum building heights obtained by Borg [20], shows that the results obtained by Borg [20] are in agreement with the outcomes obtained from the ELS® analyses, hence, suggesting a more conservative result by Borg [20]. On the other hand, the comparison of the maximum building heights for adequate seismic resistance exhibited by the control numerical models with the original plan layout proportions analysed using 3Muri® to the corresponding results obtained by Borg [20] reconfirm that the seismic capacity exhibited by the 3Muri® numerical models with respect to the limit State of Near Collapse is closer to the seismic capacity evaluated by other methods for a less severe limit state. This reinforces the inference discussed in Section 5.2.1 with respect to the inapplicability of the assumptions at the basis of the non-linear static pushover method of analysis with regards to the analysis of the contemporary loadbearing URM building typology under study in the case when the lateral storey stiffness does not exhibit major changes throughout the building height.

5.2.3 Natural frequency estimates and modes of displacement for the dominant frequencies of vibration

The natural frequency for the main modes of vibration of the analysed numerical models was obtained using 3Muri® through a modal analysis for 15 modes of vibration, following which, only the modes of vibration with a percentage mass contribution higher than 5% were selected to be considered in the pushover analysis in accordance with Clause 4.3.3.3.1(3)P of Eurocode 8: Part 1 [4]. Table 45 in Appendix E reports the significant modes of vibration in the x-, y- and z-orientations for every numerical model analysed using 3Muri®. The ensuing discussion focuses on the comparison of the natural frequency estimates for the fundamental mode of vibration in the x- and y-orientations obtained through 3Muri®, when compared to the corresponding ELS® estimates, where available; the variation in natural frequency with reduction in number of floors exhibited by the 3Muri® numerical models; and the comparison of the influence on the natural frequencies resulting in corresponding models which include the alteration of the extent of a parameter, namely, the extended plan layouts when compared to the original plan layouts, and the wider void at slab Level 1 for the cases which include a double height space, when compared to the original size of void. The main modes of vibration exhibited by the analysed numerical models are also discussed.

The natural frequency estimates obtained through 3Muri® for the corresponding numerical models analysed on upper coralline limestone and on clay are identical, suggesting that 3Muri® considers the 'pure' natural frequency on an infinitely stiff subsoil as described by Trifunac et al. [188], hence, indicating that the influence of the subsoil on the seismic assessment carried out by this non-linear static pushover analysis method is through the parameters of the soil factor and the periods T_B, T_C and T_D describing the main points of the elastic response spectrum, which are specified by the user with reference to Tables 3.2 or 3.3 of Eurocode 8: Part 1 [4] depending on magnitude of the earthquakes considered at a particular site. Therefore, the results summarised in Table 45 of Appendix E and reported in the following discussion focus on the natural frequency on an upper coralline limestone subsoil only. Furthermore, since in the case of the natural frequency estimates obtained from 3Muri® with respect to the y-orientation of the analysed numerical models, the lowest significant mode of vibration does not always correspond to the mode of vibration with the highest percentage mass contribution (while the latter invariably corresponds with a 'first mode' type of displacement), the natural frequencies quoted in the ensuing discussion with respect to the 3Muri® estimates, always refer to the modes of vibration which correspond to the highest percentage mass contribution in the x- and y-orientations of the analysed numerical models. Similarly, the natural frequencies corresponding to the fundamental modes of vibration in the x- and y- direction are quoted in the case of the ELS® estimates.

5.2.3.1 Comparison of natural frequency estimates: Xemxija Building Number 0011

Table 5-3 Comparison of natural frequency estimates of Xemxija Building Number 0011.

Number of storeys	Natural frequency (Hz) estimate: 3Muri®		Natural frequency (Hz) estimate: ELS®		Natural frequency estimates: Percentage discrepancy 3Muri® vs. ELS® (%)			Natural frequency (Hz) from ambient noise measurements		Natural frequency estimates: Percentage discrepancy 3Muri® vs. Ambient noise (%)	
	X	Y	X	Y	X	Y		X	Y	X	Y
6	3.493	7.935	3.804	7.413	-8.2	7.0		4.8	8.0	-27.2	-0.8

As outlined in Section 3.4.7 of this thesis, the comparison of the ELS® estimate of the natural frequency resulting from the first mode of vibration in the x- and y-direction of the numerical model of Xemxija Building Number 0011 to the corresponding natural frequency values of the same building resulting from ambient noise measurements carried out on site in the building, were used as a verification of the adequacy of the modelling techniques and assumptions used in the ELS® numerical models. Table 5-3 extends this comparison also to the 3Muri® numerical model of this building. The comparison of the natural frequency estimates in the x- and y-orientations of this existing building to the corresponding ELS® estimates indicates that the 3Muri® estimates of the natural frequency in the x- and y-orientations are lower and higher, respectively, than the corresponding ELS® estimates by almost the same degree. While variations in the plan layouts, wall materials and thicknesses, beam and slab layouts, slab thicknesses and span directions, and the floor loading were kept to a minimum, marginal differences in the natural frequency could have been caused by a number of factors, namely:

a) in 3Muri® the slabs are modelled as orthotropic horizontal membranes (pure diaphragms), which transfer the seismic forces to the vertical loadbearing system, but which do not have an out-of-plane resistance to provide support to an overlying structure. Hence, a number of additional beams were inserted in the 3Muri® numerical model at positions where changes in the plan layout of overlying floors required the support of vertical loadbearing elements, which would have otherwise loaded a slab;
b) the additional structural mass arising from the partial overlap of longitudinal beams positioned at slab over semi-basement level to coincide with loadbearing walls present from Level 0 upwards, with the transverse beams defined at the same slab level (in order to approximate the self-weight and stiffness of the precast concrete hollow core slabs defined at this slab level in the corresponding numerical models analysed using ELS®). These additional longitudinal beams were required, even though the whole area of slab over Level -1 was defined as consisting of abutting beam sections, since, in 3Muri®, loadbearing elements are only capable of supporting the loads coming from structural elements, which are aligned with their centreline, whereas structural elements whose position coincides with the width of the supporting element (extending away from the centreline) are considered as unsupported and result in analysis errors if an additional beam is not specified at this position to support the overlying loads;

c) a possibly more accurate representation of the transfer of load from slabs in the two orthogonal directions by ELS®. In 3Muri®, slabs are defined through their self-weight, thickness, superimposed loading, the specification of the main span direction, the percentage bi-directionality of the slab in the main span direction, the Poisson's ratio, the Shear Modulus of Elasticity, and the Young's Modulus of Elasticity in the two main orthogonal directions. In the present study, the same Young's Modulus was defined in both slab directions and the percentage bi-directionality of the slabs was based on the ratio of the lengths of the sides of the slab in the two main directions. On the other hand, in ELS®, slabs are defined as reinforced concrete elements, that is, through a section thickness corresponding to the specified concrete density and concrete Young's Modulus of Elasticity; the definition of the reinforcement in the two orthogonal directions, including any overlap of reinforcement onto adjacent slabs; and the superimposed loading. Therefore, in ELS®, the proportion of load being transferred from the slabs to the loadbearing elements in the two main orthogonal directions, is not predetermined by the bi-directional ratio defined by the user, as in 3Muri®, but it is calculated based on the slenderness and deformed profile of the slab in the two orthogonal directions;

d) the length of the sections in which every wall defined in the 3Muri® models is subdivided influences the stiffness of the specific wall and, hence, the sway stiffness of the numerical model in the direction parallel to the plane of the wall. In 3Muri®, the verification of the capacity of a wall with respect to the applied actions considers every unsubdivided length of wall as a single section, hence, considering all applied loads as spread over the whole length of wall. However, a wall can only be subdivided at the position where it intersects with another structural element. Therefore, in order to ensure that the load distributions and, hence, the capacities and stiffnesses of the walls in the 3Muri® numerical models were as close as possible to a real life scenario, all the internal walls were modelled as a single length of element (due to their overall short lengths) except at changes in wall thickness. On the other hand, the longitudinal party walls were split at the intersections with the beams defined at slab over semi-basement level, when a soft storey was present, as in the case of the Xemxija building, and at the intersection with perpendicular walls, in the case of the apartment levels. Furthermore, the longitudinal wall located in the rear half of the floor plan at semi-basement level, was considered as non-loadbearing and, hence, it was defined as a single length of wall with no subdivisions. Hence, the way the walls were subdivided in the 3Muri® numerical models could have a direct bearing on the sway stiffness of the numerical models in the two orthogonal directions and, therefore, on their respective natural frequencies.

Furthermore, the natural frequency in the transverse x-direction for the fundamental mode of vibration estimated using 3Muri® resulted in an increased discrepancy with respect to the natural frequency of the existing building resulting from the ambient noise measurements, for the same direction, when compared to discrepancy resulting from the corresponding ELS® model of the same structure. However, only a marginal discrepancy resulted in the 3Muri® natural frequency estimate in the y-direction when compared to the corresponding ambient noise result. The factors discussed in

(a), (b) and (d) above could also have a bearing on this varying degree of discrepancy between estimated natural frequency values obtained using 3Muri® and the ambient noise measurements.

5.2.3.2 Natural frequency estimates: control numerical models and single parameter cases with original plan proportions

The comparison of the natural frequency estimates on an upper coralline limestone subsoil of the fundamental frequencies in the x- and y-orientations of the control numerical models and the control numerical models including a soft storey at semi-basement level, or setbacks at penthouse level or a double height space between Levels 0 and 1 resulting from the 3Muri® and ELS® numerical models is summarised in Figures 5-9 to 5-12 and in Table 5-4. Figures 5-9 to 5-12 indicate that the control numerical models and the single parameter cases (i.e. the control numerical models with only one additional building characteristic) analysed using 3Muri® exhibit the expected increase in natural frequency in the x- and y-directions with decreasing number of storeys, similarly to the behaviour exhibited by the corresponding numerical models analysed using ELS®.

Moreover, Table 5-4 shows that the natural frequency estimates obtained from the 3Muri® modal analyses are higher than the corresponding ELS® estimates for the control numerical models and the control numerical models including either setbacks at penthouse level or a double height space between Levels 0 and 1, with a maximum discrepancy of 11.3% in the x-direction and 71% in the y-direction. On the other hand, in the case of the control numerical models with a soft storey at semi-basement level, the 3Muri® natural frequency estimates result as lower than the corresponding ELS® estimates by a maximum of 31.1% in the x-direction. Nevertheless, in the y-direction, the 3Muri® natural frequency estimates of this case are marginally lower than the corresponding ELS® results only at a height of six storeys by 1.1%, whereas, marginally higher estimates result in the three- to five-storey control numerical models which include a soft storey at semi-basement level, reaching a maximum discrepancy for this case of 2.3% at a height of four storeys.

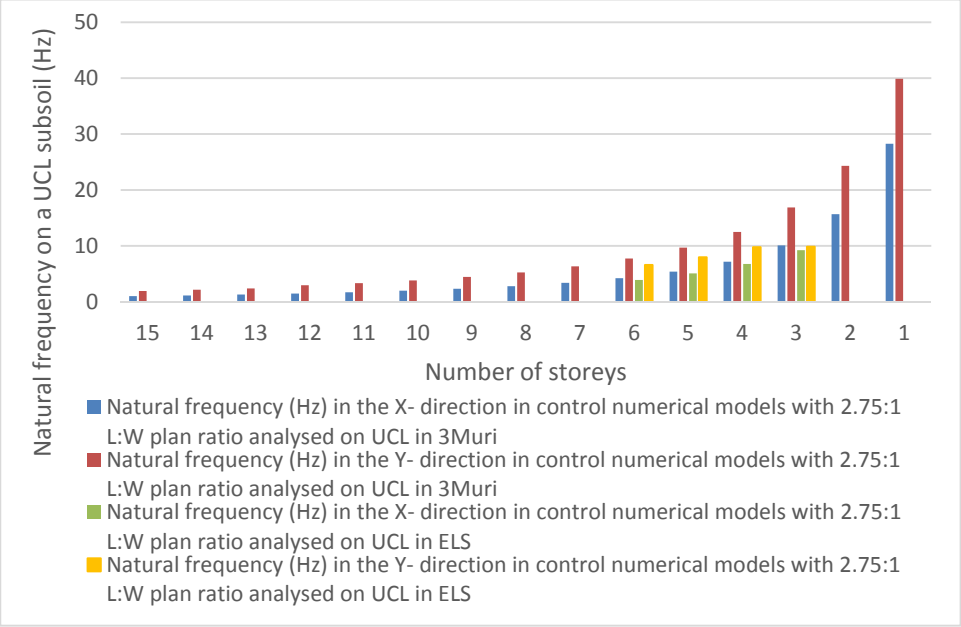

Figure 5-9 Comparison of natural frequency estimates in the x- and y-direction of numerical control models with 2.75:1 plan proportions analysed on a UCL subsoil using 3Muri® and ELS®.

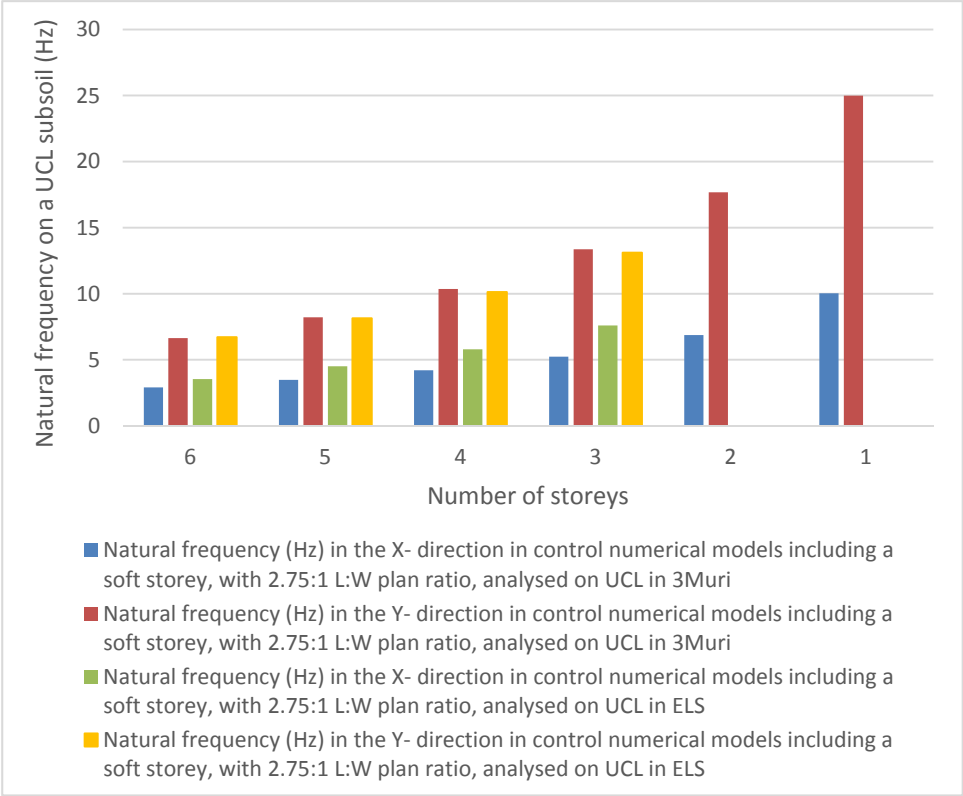

Figure 5-10 Comparison of natural frequency estimates in the x- and y-direction of numerical control models with a soft storey at semi-basement level and 2.75:1 plan proportions, analysed on a UCL subsoil using 3Muri® and ELS®.

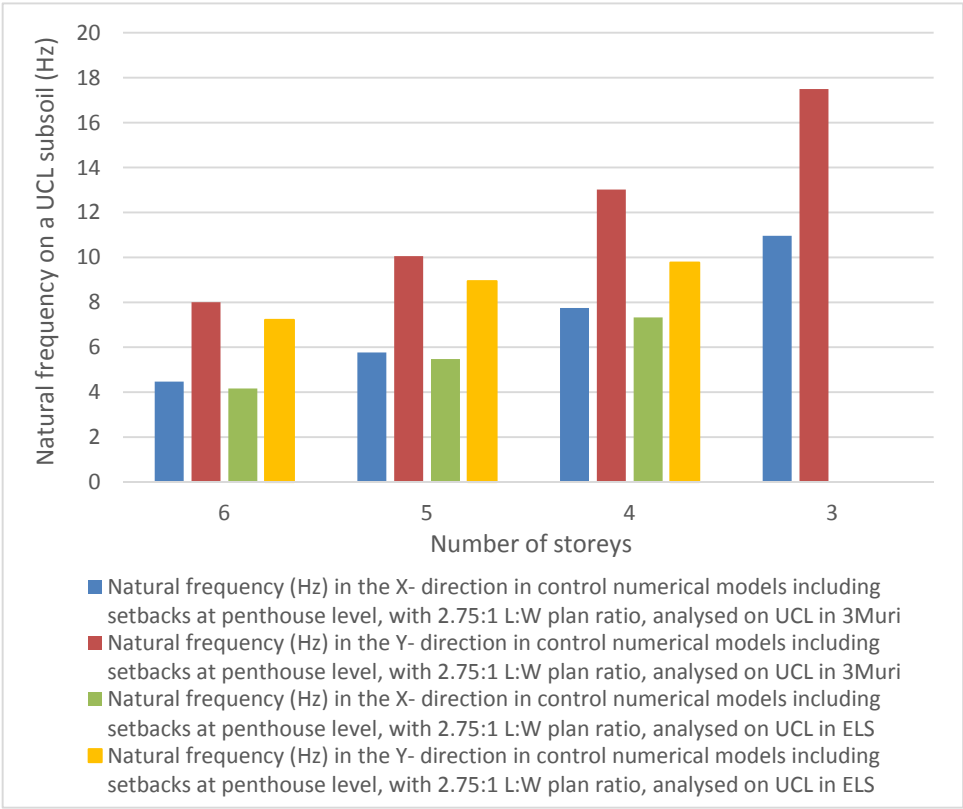

Figure 5-11 Comparison of natural frequency estimates in the x- and y-direction of numerical control models including setbacks at penthouse level and 2.75:1 plan proportions, analysed on a UCL subsoil using 3Muri® and ELS®.

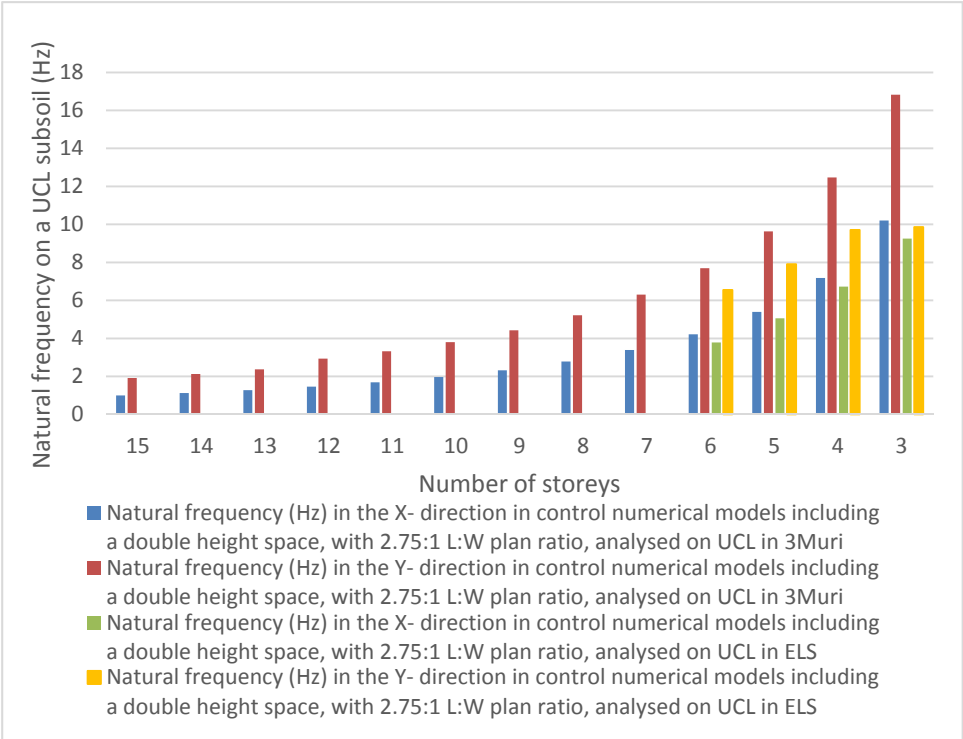

Figure 5-12 Comparison of natural frequency estimates in the x- and y-direction of numerical control models including a double height space between Levels 0 and 1, and 2.75:1 plan proportions, analysed on a UCL subsoil using 3Muri® and ELS®.

Table 5-4 Percentage discrepancy between corresponding natural frequency estimates resulting from the 3Muri® and ELS® analyses.

Natural frequency estimates: Percentage discrepancy 3Muri® vs. ELS® (%)								
Number of storeys	Control numerical models on a UCL subsoil		Control numerical models with a soft storey at semi-basement level on a UCL subsoil		Control numerical models with setbacks at penthouse level on a UCL subsoil		Control numerical models with a double height space between Levels 0 and 1 on a UCL subsoil	
	X	Y	X	Y	X	Y	X	Y
6	8.5	17.4	-17.6	-1.1	7.3	10.8	11.3	17.5
5	6.3	21.6	-23.0	0.8	5.3	12.4	6.6	21.8
4	6.1	28.0	-27.4	2.3	5.7	33.3	6.8	28.4
3	9.4	71.0	-31.1	1.9	N/A	N/A	10.2	70.7

The contrasting correspondence exhibited by the comparison of the natural frequency estimates resulting from the equivalent 3Muri® and ELS® analysed control numerical models and the control numerical models including either setbacks at penthouse level or a double height space between Levels 0 and 1, and with respect to control numerical models, which include a soft storey at semi-basement level suggests that the main factor influencing the natural frequency estimate obtained using 3Muri® is the different level of restraint assumed/specified between intersecting walls and at the junction between walls and slabs by 3Muri® compared to ELS®.

The influence of the wall dimensions, the density and Young's Modulus of Elasticity of the masonry wall material and the wall boundary conditions on the natural frequency of an unreinforced masonry wall was investigated by De Sutter [128] through a parametric analysis using the numerical modelling software Abaqus, which is based on the Finite Element Method (FEM). This parametric study resulted in the development of the following empirical formula for the approximate estimation of the natural frequency of an unreinforced masonry wall:

$$f = A.t.\sqrt{\left[\frac{E}{\rho}\right]}.L^B.H^C$$

Equation 5-1

where, *f* is the natural frequency of the wall in Hertz (Hz); *A*, *B*, and *C* are constants which depend on the boundary conditions of the wall; *t* is the thickness of the wall in cm; *E* is the Young's Modulus of Elasticity of the wall in GPa; *ρ* is the density of the wall in g/m^3 [44]; and, *L* and *H* are the length and the height of the wall in m, respectively. Figure 5-13 reproduces the 16 different cases of boundary conditions considered in the study by De Sutter [128]. The first 12 cases (A to L) correspond to the boundary conditions considered in Appendix E of Eurocode 6 [157], whereas, the last 4 cases are additional cases of alternative boundary conditions, which correspond with the cases considered by

[44] An example given by De Sutter [128] on the development of Equation 5-1 indicates the dimensional unit corresponding to the density of the wall as kg/m^3. However, the magnitude of the density used in the example suggests that the adopted value is more likely to correspond with the density of the wall in g/m^3. Since the reported example suggests that the natural frequency estimate obtained from the use of Equation 5-1 is calculated from parameters including the thickness of wall, length of wall, height of wall, Young's Modulus of Elasticity and wall density with dimensional units, which do not correspond to each other (as indicated above), the use of the dimensional unit for the density of the wall which is in accordance with the derivation of the approximate relationship reproduced in Equation 5-1 becomes even more important. While it is hereby acknowledged that the practice of using dimensional units, which do not correspond with each other results in a dimensional heterogeneity, which calls into question the validity of the frequency estimate resulting from the empirical relationship proposed by De Sutter [128], the reference to this relationship in this thesis is being made on the basis that the parametric method used for the derivation of this relationship, while not ensuring the validity of the estimated value of natural frequency, is likely to still represent adequately the relative difference between the natural frequencies resulting from walls with different boundary conditions. Requests for clarifications to the author and to the supervisor of the study [128] regarding the dimensional units corresponding to the parameters in Equation 5-1, unfortunately remained unanswered at the time of writing of this thesis.

Bogaert[45] in a Master's Degree dissertation presented to the University of Mons, a copy of which was not accessible for review by the author of this thesis. Furthermore, Table 5-5 reproduces the values for constants *A*, *B* and *C* derived by De Sutter through the parametric analysis [128].

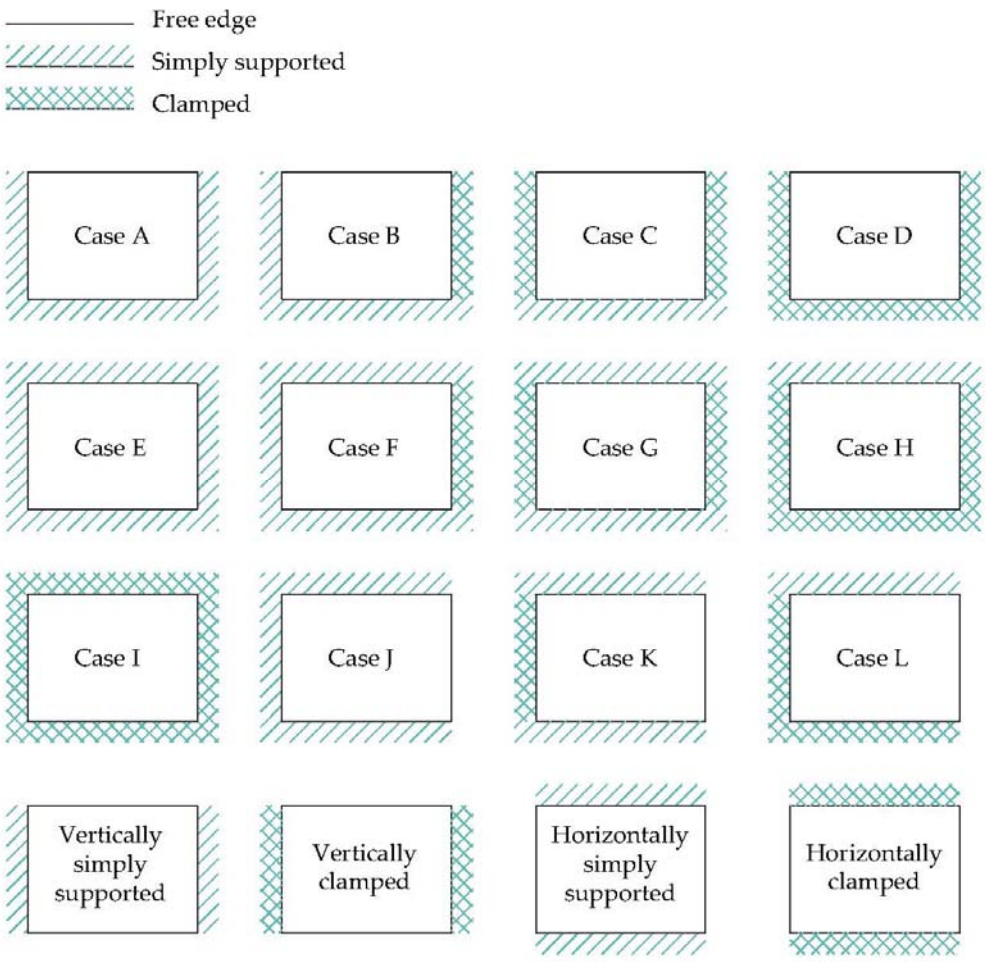

Figure 5-13 Wall boundary conditions considered by De Sutter. Reproduced from De Sutter ([128] p. 23).

[45] G. Bogaert. Calcul plastique de murs de maçonnerie sollicités hors du plan [Master's Degree Dissertation]. Mons: Université de Mons; 2016 (in French).

Table 5-5 Constants 'A', 'B' and 'C' proposed by De Sutter for the approximate estimation of the natural frequency of a masonry wall through Equation 5-1. Reproduced from De Sutter ([128] p. 27).

Boundary condition	A	B	C
Case A	140	-1.6	-0.2
Case B	210	-1.7	-0.13
Case C	305	-1.8	-0.1
Case D	280	-1.6	-0.2
Case E	160	-0.75	-0.75
Case F	217	-1.1	-0.5
Case G	266	-1.3	-0.3
Case H	262	-1	-0.5
Case I	266	-0.7	-0.7
Case J	139	-0.2	-1.6
Case K	123	-0.3	-1.3
Case L	166	-0.1	-1.5
Vertically simply supported	144	-2	0
Vertically clamped	323	-2	0
Horizontally simply supported	144	0	-2
Horizontally clamped	323	0	-2

Table 5-6 Comparison of percentage relative difference in the estimated natural frequency of a masonry wall when different boundary conditions are considered.

Wall boundary conditions considered in comparison	Percentage relative difference in natural frequency of masonry wall resulting from Equation 5-1 for different boundary conditions
Clamped on all sides (Case I) vs. Simply supported on all sides (Case E)	+85.550%
Clamped to adjacent walls but simply supported to overlying and underlying walls (Case G) vs. Simply supported on all sides (Case E)	+24.572%
Vertically clamped along sides and no connection to horizontal diaphragms along the top and bottom edges (second additional case) vs. Simply supported on all sides (Case E)	+16.500%

Table 5-6 presents the comparison of the percentage difference in the natural frequency of a 228 mm thick softstone masonry wall with a length of 3 m, a height of 3 m, a density of 17.26 kg/m^3 and Young's Modulus of Elasticity of 21,000 N/mm^2, obtained through Equation 5-1 when considering four different cases of wall boundary conditions, highlighted in grey in Table 5-5, namely, clamped on all sides (Case I), simply supported on all sides (Case E); clamped to walls but simply supported to slabs (Case G) and vertically clamped (second additional case considered by De Sutter [128]). The same percentage differences in natural frequency corresponding to the considered cases of boundary conditions were obtained for a 153 mm thick hollow concrete blockwork wall. The definition of the 'criss-cross' hatching in the legend to Figure 5-13 as 'clamped' and the use of the same hatching to describe the

boundary condition in Cases B, C, D, F, G, H, I, K and L, which, are confirmed by De Sutter [128] to correspond to the cases which have the same name in Annex E of Eurocode 6 [157], suggests that this end restraint corresponds to a 'fully restrained' edge or a 'continuous edge', as defined in the key to Figure E.1 of Annex E of Eurocode 6 [157] for the corresponding 'criss-cross' hatching. Hence, the natural frequency comparison presented in Table 5-6 suggests that, according to the empirical relationship proposed by De Sutter [128], the more restrained the boundary conditions of the wall, the higher is the resulting natural frequency of the wall panel and, consequently, of the building as a whole, when this affects all the walls in a loadbearing structure. Table 5-6 suggests that the percentage increase in natural frequency decreases from 85.550% to 24.527% when only vertical interfaces of the wall panel (hence, at the intersection with abutting walls) are considered as continuous, fully restrained junctions, whereas, the horizontal interfaces (with the foundations or the diaphragms) are considered as only restrained against translations (simply supported), when compared to the case where both the vertical and horizontal interfaces are simply supported. This highlights the influence which the degree of restraint defined at wall-to-wall and wall-to-slab junctions in a numerical model has on the resulting estimated natural frequency of the modelled structure.

As outlined in Section 3.4.1 of this thesis, in the numerical models analysed using ELS®, the junctions between any two intersecting external walls or between an external wall and an internal wall were modelled with interlocked courses, with mortar defined at the horizontal interfaces between the masonry blocks at these intersections. On the other hand, the junction between internal intersecting walls was modelled as 'fused' in the ELS® numerical models, therefore, considering a full coupling between these walls. It is acknowledged that the latter case results in an over-estimation of the lateral storey stiffness similar to the over-estimation resulting in 3Muri® in view of the blanket assumption of box-like structural behaviour (i.e. the full coupling at wall-to-wall intersections at the basis of the non-linear static pushover method of analysis used in 3Muri® and, with respect to which, the user has no control). However, the generally shorter length of internal walls determined by the size of rooms reduces the extent of this over-estimation at junctions between internal walls. On the other hand, the more accurate representation of the degree of connection between intersecting external walls and at the intersection between internal and external walls in the numerical models analysed using ELS® results in a more realistic simulation of the degree of restraint provided at these positions, hence, resulting in a more accurate estimate of the lateral storey stiffness and the verification of the capacity of these walls with respect to the out-of-plane mechanism, particularly, in the case of the longitudinal party walls along corridors, open plan spaces or in a soft storey, where the restraint from intersecting walls is significantly reduced. Furthermore, in the case of the wall-to-slab junctions modelled using ELS®, cast in-situ concrete slabs were defined as bearing on overlying walls, with concrete specified as the interface material between the underside of the slabs and the underlying wall, while mortar (with a compressive strength of 2 N/mm^2) was defined at the interface between the top face of the concrete slab and the underside of the overlying wall.

Therefore, the comparison of the percentage difference in natural frequency of masonry walls depending on the degree of restraint of their boundary conditions presented in Table 5-6, based on

the empirical formula for the estimation of the natural frequency of a masonry wall proposed by De Sutter [128], suggests that the consistently higher 3Muri® estimates of natural frequency in the case of the analysed cases, which do not exhibit major changes in lateral storey stiffness in overlying floors, is most likely due to the higher degree of coupling assumed between the intersecting walls and between walls and slabs in the 3Muri® numerical models when compared to the level of restraint specified by the author, particularly, at intersections with external walls, in the corresponding ELS® numerical models. On the other hand, the significantly lower estimates of natural frequency resulting from the 3Muri® numerical control models, which include a soft storey at semi-basement level when compared to the natural frequency estimates resulting from the corresponding ELS® models are likely to be due to the reduced number of wall-to-wall intersections present at the soft storey level and the compensating effect on the overall natural frequency of the structure, which results due to the severely reduced lateral storey stiffness at the level of the soft storey when compared to the over-estimated lateral storey stiffness of the underlying floors.

Table 5-7 Comparison of variation in natural frequency with reduction in the number of storeys of the numerical models with original plan proportions analysed using 3Muri®.

Storeys at which % discrepancy in natural frequency is calculated	% Discrepancy between 3Muri® natural frequency estimates between overlying storeys							
	Control (2.75:1 plan proportions)		Control with soft storey (2.75:1 plan proportions)		Control with setbacks (2.75:1 plan proportions)		Control with double height space (2.75:1 plan proportions)	
	X	Y	X	Y	X	Y	X	Y
15 to 14	12.8	11.4	N/A	N/A	N/A	N/A	12.8	11.3
14 to 13	13.6	11.6	N/A	N/A	N/A	N/A	13.5	11.5
13 to 12	14.4	23.2	N/A	N/A	N/A	N/A	14.5	23.7
12 to 11	15.5	13.1	N/A	N/A	N/A	N/A	15.5	13.0
11 to 10	16.7	14.8	N/A	N/A	N/A	N/A	16.6	14.7
10 to 9	18.0	16.3	N/A	N/A	N/A	N/A	18.1	16.3
9 to 8	19.7	18.0	N/A	N/A	N/A	N/A	19.7	18.0
8 to 7	21.3	20.8	N/A	N/A	N/A	N/A	21.8	20.7
7 to 6	24.9	22.2	N/A	N/A	N/A	N/A	24.4	22.2
6 to 5	27.8	25.1	19.2	23.7	29.0	25.6	28.0	25.1
5 to 4	32.9	29.2	21.1	26.2	34.3	29.5	33.3	29.4
4 to 3	40.9	34.9	24.3	28.9	41.4	34.4	42.0	34.9
3 to 2	55.3	44.2	31.2	32.3	N/A	N/A	N/A	N/A
2 to 1	80.6	64.1	46.1	41.4	N/A	N/A	N/A	N/A

Furthermore, when considering the variation in natural frequency with reduction in number of storeys of the numerical models with the original plan proportions analysed using 3Muri®, the rate of increase in natural frequency with reduction in the number of floors is higher with every storey decrement in all analysed cases. In addition, the comparison of the natural frequency estimates reported in Table 5-7 at changes in height of six to five floors, four to three floors and two to one floor (highlighted in

grey on Table 5-7) shows that, while the control numerical models and the control numerical models with setbacks at penthouse level or a double height space between Levels 0 and 1 exhibit a very similar rate of increase in natural frequency with reduction in number of floors, the rate of increase in natural frequency exhibited by the control numerical models, which include a soft storey at semi-basement level is significantly lower. This discrepancy increases with the reduction in number of floors.

The different rate of variation of the natural frequency exhibited by the latter two categories of investigated cases is likely to be due to the different degree of variation of the storey mass and lateral storey stiffness throughout the building height of the corresponding analysed models. While the analysed control numerical models have a constant mass and lateral storey stiffness throughout their building height, the control numerical models, which include a double height space, have only a very localised reduction in lateral storey stiffness and mass, which is partially compensated by the additional stiffness and mass resulting from the 250 mm thick slab, which bounds the double height void at Level 1 on three sides. This results in natural frequency estimates, which are very close for these two cases, as reported in Table 45 in Appendix E. Similarly, in the case of the control numerical models, which include setbacks at penthouse level, the variation in lateral storey stiffness and structural mass occurs only at the topmost storey, while these parameters are kept unchanged throughout the rest of the building height.

On the other hand, in the case of the control numerical models with a soft storey at semi-basement level, the significantly lower lateral storey stiffness at the lowermost storey when compared to the overlying floors results in a considerably lower natural frequency at all building heights, when compared to the cases, which exhibit a fairly regular distribution of lateral storey stiffness throughout their floors. Furthermore, Table 5-7 indicates that the degree of discrepancy between the rate of increase in natural frequency of the control numerical models and the corresponding control numerical models with a soft storey at semi-basement level increases with decrease in the number of floors due to the higher influence, which the soft storey has on the entire structure with every reduction in the number of floors, and hence, the increased effect of lower lateral storey stiffness at this level on the decrease of the overall sway stiffness and the natural frequency of the building as a whole.

5.2.3.3 Natural frequency estimates: additional cases analysed using 3Muri®

The present section examines the natural frequency estimates of the additional cases modelled using 3Muri®, namely the control numerical models with a double height space where the void in slab Level 1 was widened to the full width of the structure between the longitudinal party walls, keeping the original length-to-width plan proportions of 2.75: 1; and the cases with an extended length-to-width plan ratio of 4:1 with respect to the control numerical models and the control numerical models including either a soft storey at semi-basement level or a double height space between Levels 0 and 1.

Figure 5-14 reports the comparison between the natural frequency estimates in the x- and y-orientations of the control numerical models with the widened double height space between Levels 0 and 1 with respect to the corresponding control numerical models where the double height space was modelled with the original void proportions. This comparison indicates that there is merely a marginal discrepancy between the natural frequency estimates, hence, suggesting, with reference to Equation

4-5 reported in Section 4.2.1.2 of this thesis, that the effect of the reduction in lateral storey stiffness on the natural frequency of the structure was compensated by the opposing effect of the reduction in the mass of the slab in the area of the widened double height void. Furthermore, Figure 5-14 also indicates that, even in the case of the control numerical models with a wider void at slab Level 1, the natural frequency of the analysed numerical models increases with reduction in the number of storeys in both the numerical model's x- and y-orientations. The rate of increase at every storey decrement increases from 18% (between ten and nine storeys) to 33.6% (between five and four storeys) in the x-direction, and between 13% (between ten and nine storeys) to 29.4 % (between five and four storeys) in the y-direction.

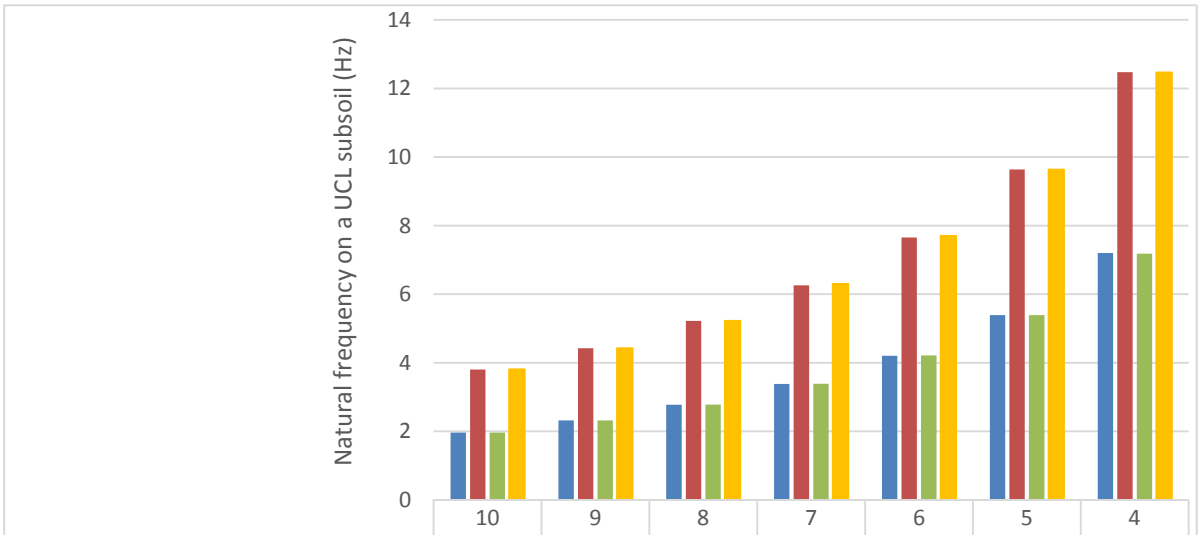

	10	9	8	7	6	5	4
Natural frequency (Hz) in the X-direction in control numerical models including a double height space over whole width of structure, with 2.75:1 L:W plan ratio, analysed on UCL in 3Muri	1.966	2.320	2.778	3.382	4.206	5.390	7.201
Natural frequency (Hz) in the Y-direction in control numerical models including a double height space over whole width of structure, with 2.75:1 L:W plan ratio, analysed on UCL in 3Muri	3.805	4.425	5.221	6.260	7.654	9.638	12.473
Natural frequency (Hz) in the X-direction in control numerical models including a double height space (original size), with 2.75:1 L:W plan ratio, analysed on UCL in 3Muri	1.966	2.321	2.779	3.386	4.213	5.391	7.184
Natural frequency (Hz) in the Y-direction in control numerical models including a double height space (original size), with 2.75:1 L:W plan ratio, analysed on UCL in 3Muri	3.806	4.426	5.221	6.302	7.698	9.631	12.466

Figure 5-14 Comparison of natural frequency estimates in the x- and y-directions of control numerical models including a double height space over the whole width of the structure with the corresponding case where the double height space retained the original width.

Figure 5-15 presents the comparison between the natural frequency estimates in the x- and y-directions of the cases with extended plan proportions investigated using 3Muri®, namely, the control numerical models and the control numerical models including either a soft storey at semi-basement level or a double height space between Levels 0 and 1. Figure 5-15 shows that, as was observed in Section 5.2.3.2 with respect to the analysed numerical models with original plan proportions, even in the extended plan layout cases, there is only a very minor difference between the natural frequency estimates in the x- and y-orientations of the control numerical models and the control numerical models with a double height space between Levels 0 and 1. On the other hand, a significantly higher discrepancy is observed between the natural frequency estimates of these cases and the numerical control models with a soft storey at semi-basement level and extended plan layout proportions.

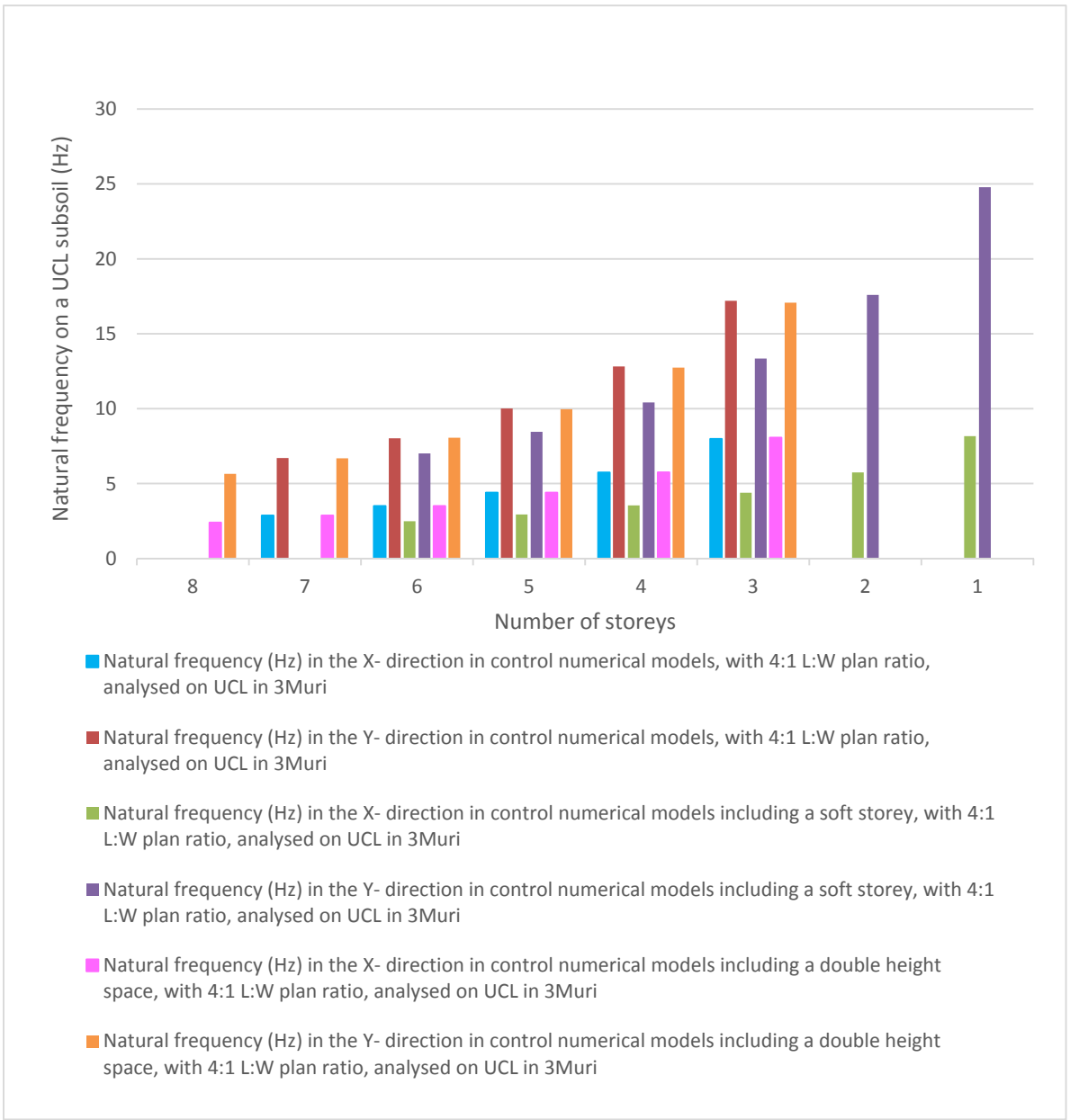

Figure 5-15 Comparison of natural frequency estimates in the x- and y-directions of control numerical models and control numerical models including either a soft storey or a double height space with extended length-to-width plan proportions of 4:1.

Moreover, similarly to the observed variation in natural frequency of the analysed models with the original plan proportions and reported in Table 5-7, Table 5-8 shows that, while an increase in natural frequency with reduction in number of floors is observed for every respective investigated case with extended plan layout proportions, this increase differs only marginally in the control numerical models and in the corresponding control numerical models which include a double height space between Levels 0 and 1, whereas a significantly lower increase in natural frequency is exhibited by the control numerical models, which include a soft storey at semi-basement level. The factors, which are likely to be influencing these natural frequency results were already discussed in Section 5.2.3.2 and remain applicable with respect to the investigated cases with extended plan layout proportions.

Table 5-8 Comparison of variation in natural frequency with reduction in number of storeys of the numerical models with extended plan layout proportions analysed using 3Muri®.

Storeys at which % discrepancy in natural frequency is calculated	% Discrepancy between 3Muri® natural frequency estimates between overlying storeys					
	Control (4:1 plan proportions)		Control with soft storey (4:1 plan proportions)		Control with double height space (4:1 plan proportions)	
	X	Y	X	Y	X	Y
8 to 7	N/A	N/A	N/A	N/A	19.6	18.3
7 to 6	22.0	19.6	N/A	N/A	22.0	20.6
6 to 5	25.4	24.9	18.2	20.5	25.4	23.7
5 to 4	30.6	28.0	20.4	23.3	30.9	27.8
4 to 3	39.0	34.2	23.8	28.1	40.2	34.0
3 to 2	N/A	N/A	30.9	31.8	N/A	N/A
2 to 1	N/A	N/A	42.2	40.9	N/A	N/A

Furthermore, the comparison of Tables 5-7 and 5-8 indicates that the analysed numerical models with the extended plan layout exhibit a lower increase in natural frequency at every storey decrement than the corresponding numerical models with original plan proportions. With reference to Equation 4-5 in Section 4.2.1.2 of this thesis, for a constant Young's Modulus of Elasticity and considering the same building heights, this lower rate of increase in natural frequency is likely due to the lower ratio between the moment of inertia of the structure (in the two respective plan directions) and its mass resulting at every reduction in the height of the building by one storey in the numerical models with the extended plan layout when compared to the numerical models with the original plan proportions.

In addition, Figures 5-16, 5-17 and 5-18 present the natural frequency estimates resulting from the 3Muri® modal analysis of the cases with plan length-to-width proportions of 4:1 compared to the natural frequencies resulting from the corresponding numerical models with plan length-to-width proportions of 2.75:1. As reported in Table 5-9, in all the three investigated cases (i.e. the control model, the control model with a soft storey and the control model with a double height space), the elongation of the plan layout resulted in the decrease of the natural frequency with respect to the transverse x-orientation of the modelled structures with an extended plan layout when compared to the corresponding structures with original plan proportions, with the rate of decrease in natural

frequency increasing marginally with every one storey decrement up to a maximum of 20.9%. On the other hand, a higher natural frequency corresponding to the longitudinal y-orientation of the numerical model was generally observed in the numerical models with the extended plan layout proportions when compared to the corresponding numerical models with the original plan proportions, with the rate of increase in natural frequency decreasing with every reduction in number of storeys. However, the one- to three-storey control numerical models including a soft storey at semi-basement level and extended plan layout proportions exhibited a marginally lower natural frequency in the y-direction than the corresponding analysed numerical models with the original plan dimensions, which reduction reached a maximum of 0.8% at a height of one storey. These results reflect the expected decrease in relative stiffness in the x-direction, which results due to the elongation of the plan layout in the y-direction, hence, leading to an increased plan slenderness in the transverse direction. Conversely, the extension of the plan in the y-direction leads to the generally higher stiffness of the numerical models in this orientation.

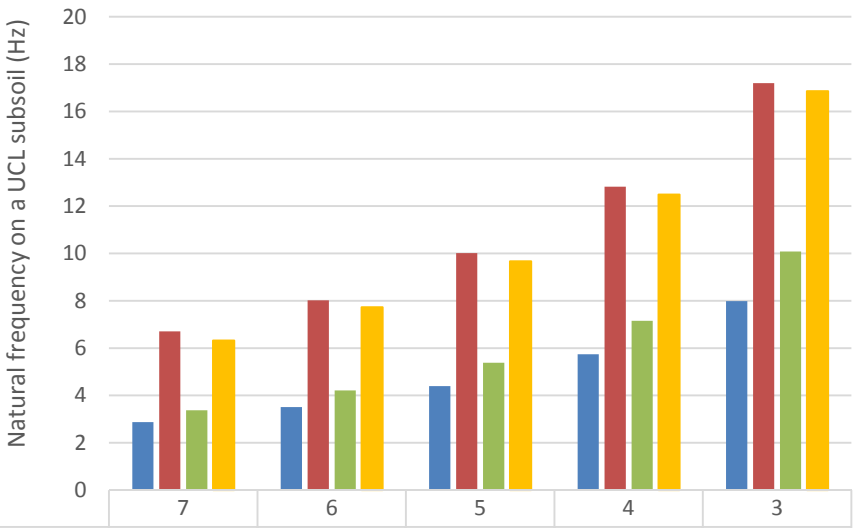

	7	6	5	4	3
Natural frequency (Hz) in the X-direction in control numerical models, with 4:1 L:W plan ratio, analysed on UCL in 3Muri	2.874	3.506	4.396	5.741	7.982
Natural frequency (Hz) in the Y-direction in control numerical models, with 4:1 L:W plan ratio, analysed on UCL in 3Muri	6.704	8.019	10.013	12.819	17.197
Natural frequency (Hz) in the X-direction in control numerical models, with 2.75:1 L:W plan ratio, analysed on UCL in 3Muri	3.372	4.212	5.384	7.155	10.080
Natural frequency (Hz) in the Y-direction in control numerical models, with 2.75:1 L:W plan ratio, analysed on UCL in 3Muri	6.322	7.726	9.668	12.492	16.855

Figure 5-16 Comparison of natural frequency estimates in the x- and y-directions of the control numerical models with extended plan layout proportions with the corresponding numerical models with original plan proportions.

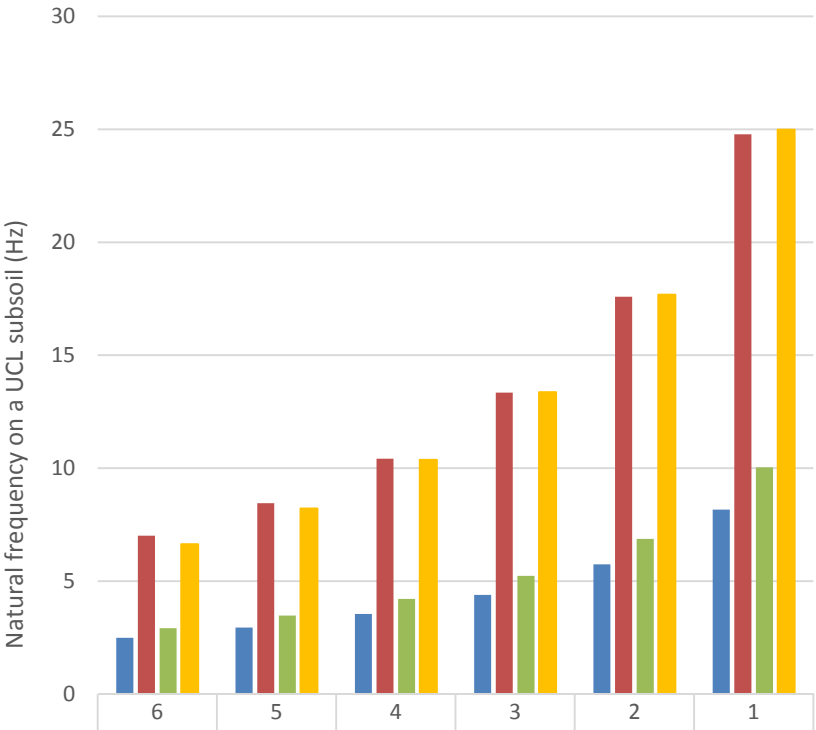

	6	5	4	3	2	1
Natural frequency (Hz) in the X-direction in control numerical models including a soft storey at semi-basement level, with 4:1 L:W plan ratio, analysed on UCL in 3Muri	2.489	2.941	3.541	4.385	5.739	8.163
Natural frequency (Hz) in the Y-direction in control numerical models including a soft storey at semi-basement level, with 4:1 L:W plan ratio, analysed on UCL in 3Muri	7.012	8.449	10.416	13.344	17.59	24.783
Natural frequency (Hz) in the X-direction in control numerical models including a soft storey at semi-basement level, with 2.75:1 L:W plan ratio, analysed on UCL in 3Muri	2.916	3.475	4.209	5.233	6.866	10.033
Natural frequency (Hz) in the Y-direction in control numerical models including a soft storey at semi-basement level, with 2.75:1 L:W plan ratio, analysed on UCL in 3Muri	6.637	8.213	10.365	13.362	17.677	24.988

Figure 5-17 Comparison of natural frequency estimates in the x- and y-directions of the control numerical models including a soft storey and extended plan layout proportions with the corresponding numerical models with original plan proportions.

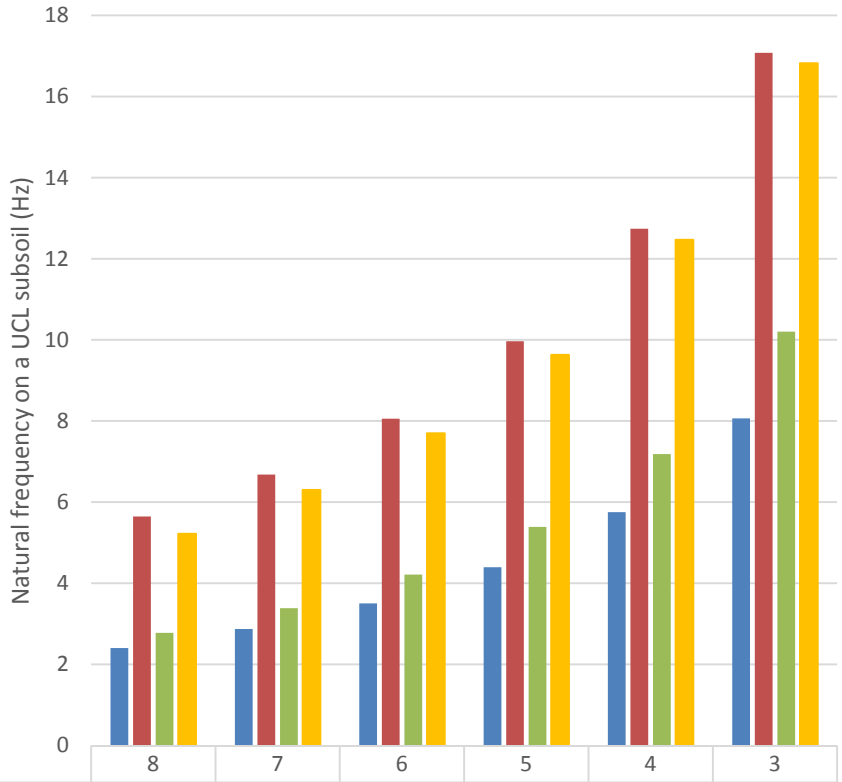

	8	7	6	5	4	3
Natural frequency (Hz) in the X-direction in control numerical models including a double height space, with 4:1 L:W plan ratio, analysed on UCL in 3Muri	2.402	2.872	3.504	4.395	5.752	8.065
Natural frequency (Hz) in the Y-direction in control numerical models including a double height space, with 4:1 L:W plan ratio, analysed on UCL in 3Muri	5.646	6.681	8.057	9.966	12.74	17.074
Natural frequency (Hz) in the X-direction in control numerical models including a double height space, with 2.75:1 L:W plan ratio, analysed on UCL in 3Muri	2.779	3.386	4.213	5.391	7.184	10.202
Natural frequency (Hz) in the Y-direction in control numerical models including a double height space, with 2.75:1 L:W plan ratio, analysed on UCL in 3Muri	5.221	6.302	7.698	9.631	12.466	16.821

Figure 5-18 Comparison of natural frequency estimates in the x- and y-directions of the control numerical models including a double height space and extended plan layout proportions with the corresponding numerical models with original plan proportions.

Table 5-9 Comparison of percentage discrepancy resulting between 3Muri® natural frequency estimates in the x- and y-directions of numerical models with extended plan layout proportions when compared to corresponding numerical models with original plan proportions.

Number of storeys	% Discrepancy between 3Muri® natural frequency estimates: Control (4:1 plan proportions) vs. Control (2.75:1 plan proportions)		% Discrepancy between 3Muri® natural frequency estimates: Control with soft storey (4:1 plan proportions) vs. Control with soft storey (2.75:1 plan proportions)		% Discrepancy between 3Muri® natural frequency estimates: Control with double height space (4:1 plan proportions) vs. Control with double height space (2.75:1 plan proportions)	
	X	Y	X	Y	X	Y
10	N/A	N/A	N/A	N/A	N/A	N/A
9	N/A	N/A	N/A	N/A	N/A	N/A
8	N/A	N/A	N/A	N/A	-13.6	8.1
7	-14.8	6.0	N/A	N/A	-15.2	6.0
6	-16.8	3.8	-14.6	5.7	-16.8	4.7
5	-18.4	3.6	-15.4	2.9	-18.5	3.5
4	-19.8	2.6	-15.9	0.5	-19.9	2.2
3	-20.8	2.0	-16.2	-0.1	-20.9	1.5
2	N/A	N/A	-16.4	-0.5	N/A	N/A
1	N/A	N/A	-18.6	-0.8	N/A	N/A

5.2.3.4 Modes of displacement corresponding to dominant frequencies of vibration

The overall displacement profiles in the transverse x-orientation of the numerical models analysed using ELS® discussed in Section 4.2.4 of this thesis were not obtained following a modal analysis but through a detailed review of the relative x- displacements occurring in an element in the left hand side party wall at all storeys of the analysed models at the analysis run time corresponding to the maximum x-displacement at slab over semi-basement level prior to the onset of collapse for every analysed numerical model. Nevertheless, all cases analysed using ELS®, with the exception of the two-building control numerical models, resulted in first and second vibration mode type of displacements between building heights of four to six storeys, while the four-storey control numerical model analysed on a 60 m thick clay modelled as a three dimensional block, exhibited a third vibration mode type of displacement. While the occurrence of more cases with displacement profiles corresponding with higher modes of vibration cannot be excluded, if the displacements of the numerical models had to be checked at a different analysis run time, the resulting profiles obtained in the current study suggest that the first and second modes of vibration (and, to a lesser extent, the third modes of vibration) are relevant modes of vibration with respect to the seismic response of the building typology under study. Furthermore, since in the study of the displaced profiles of the numerical models analysed using ELS®, the reviewed displacements were just of one element (corresponding to half a softstone masonry block) in a wall and not to the whole structure or to a storey (as in the case of 3Muri®), and since the corresponding y- and z-displacements were not taken into consideration, any distortions of the respective storeys, hence resulting in deviations from the ideal box-like behaviour, and any rotations of the storeys throughout the building height of the structure, could not be identified in ELS®.

Table 5-10 Summary of main modes of vibration exhibited by numerical models analysed using 3Muri®.

Description of investigated case	Main modes of vibration	Height of structure (number of storeys)	Height of structure (number of storeys)
		X-direction	Y-direction
Control (2.75:1 L:W plan ratio)	1, 2, 3, T	N/A	12, 14-15
	1, 2, T	2-3, 5	9-11
	1, T	1	8
	1, 2, 3	13	13
	1, 2	4, 6-12, 14-15	2-7
	1	N/A	1
Control with soft storey at semi-basement level (2.75:1 L:W plan ratio)	1, 2, T	3-4	N/A
	1, T	1-2	4
	1, 2	5-6	5-6
	1	N/A	1-3
Control with setbacks at penthouse level (2.75:1 L:W plan ratio)	1, 2	3-6	3-6
Control with double height space between Levels 0 and 1 (2.75:1 L:W plan ratio)	1, 2, 3, T	N/A	12-15
	1, 2, T	3-5	8-11
	1, 2, 3	13-15	N/A
	1, 2	6-12	4-7
	1	N/A	3
Control with double height space between Levels 0 and 1 with void over entire width of structure (2.75:1 L:W plan ratio)	1, 2, T	4-5	8-10
	1, 2(T)	N/A	5
	1, 2	6-10	4, 6-7
Control (4:1 L:W plan ratio)	1, 2, 3, T	6-7	N/A
	1, 2, 2/3, T	4-5	N/A
	1, 1/2, T	3	N/A
	1, 2	N/A	4-7
	1	N/A	3
Control with soft storey at semi-basement level (4:1 L:W plan ratio)	1, 2, T	6	N/A
	1, 2, 2(T)	N/A	6
	1, T	1-5	N/A
	1, 2	N/A	5
	1	N/A	1-4
Control with double height space between Levels 0 and 1 (4:1 L:W plan ratio)	1, 2, 3, T	6	N/A
	1, 2, 2/3(T), T	4-5	N/A
	1, 2, 2(T), T	7	6
	1, 2, T	3, 8	N/A
	1, 2	N/A	3-5, 7-8
XMX 0011	1,2	6	6

Table 5-11 Legend corresponding to Table 5-10.

Legend	
1, 2, 3	1st, 2nd and/or 3rd vibration mode type of displacement
T	Torsional displacement mode
A/B	Due to rotation of the storey about the vertical Z axis, part of the storey exhibits a A^{th} mode type of displacement, while another part exhibits a B^{th} mode type of displacement
C(T)	C^{th} vibration mode type of displacement with torsion
	Modes of vibration corresponding to structures with a maximum height of 6 floors

Since, as explained in Section 5.2.3, 3Muri® modal analysis results with respect to an upper coralline limestone or clay subsoil were identical, full correspondence resulted also between the displaced profiles and the percentage mass contributions for every vibration mode when numerical models were analysed on these two subsoils. Table 5-10 and Table 45 in Appendix E report the modes of displacement exhibited by the main frequencies of vibration in the x- and y-directions of every numerical model analysed using 3Muri®, which were obtained through the examination of the displacements of all the storeys in the analysed structures for the modes of vibration, which resulted in a percentage mass contribution of 5% or more.

The predominance of the first and second vibration mode type of displacements is in agreement with displacement modes resulting from the ELS® verification reported in Section 4.2.4 and Figures 37 to 45 of Appendix D. However, the comparison of the displacement modes resulting from the control numerical models and the control numerical models with one additional seismic vulnerability characteristic and with the original length-to-width plan proportions of 2.75:1 for a maximum height of six storeys[46] reported in Table 5-10, shows that the 3Muri® modal analyses do not result in any third mode type of displacements. Third vibration mode type of displacements only result in the control numerical models with extended length-to-width plan layout proportions of 4:1 and in the corresponding control numerical layout with a double height space between Levels 0 and 1 and with extended plan layout proportions.

On the other hand, Table 5-10 indicates the presence of torsional modes of vibration even at building heights of six storeys or less, which could not be detected from the ELS® output. An example of this situation is the torsional mode of vibration reported in Figure 5-19 for the three-storey numerical control model including a soft storey and original plan proportions (Model 3M79). Furthermore, as in the cases indicated in Figures 5-20, 5-21 and 5-22, the 3Muri® displaced plan shapes, for the different storeys of the analysed numerical models, show that most of the displaced profiles do not consist of 'purely' first, second or third vibration mode type of displacements, but a significant degree of rotation is also present. This rotation, is still likely to result due to the presence of torsional forces. The

[46] This maximum height was selected since the numerical models analysed using ELS® were verified between the heights of three to six storeys.

rectangularity of the plan layouts, the lack of symmetry in the wall distributions with respect to both the x- and y- directions, the difference in the room sizes and, hence, the slab thicknesses and slab span directions, in addition to the different variable loads associated with the differing uses of the internal spaces, make the presence of an eccentricity, between the centre of mass and the centre of resistance of the different storeys in the analysed numerical models, very likely.

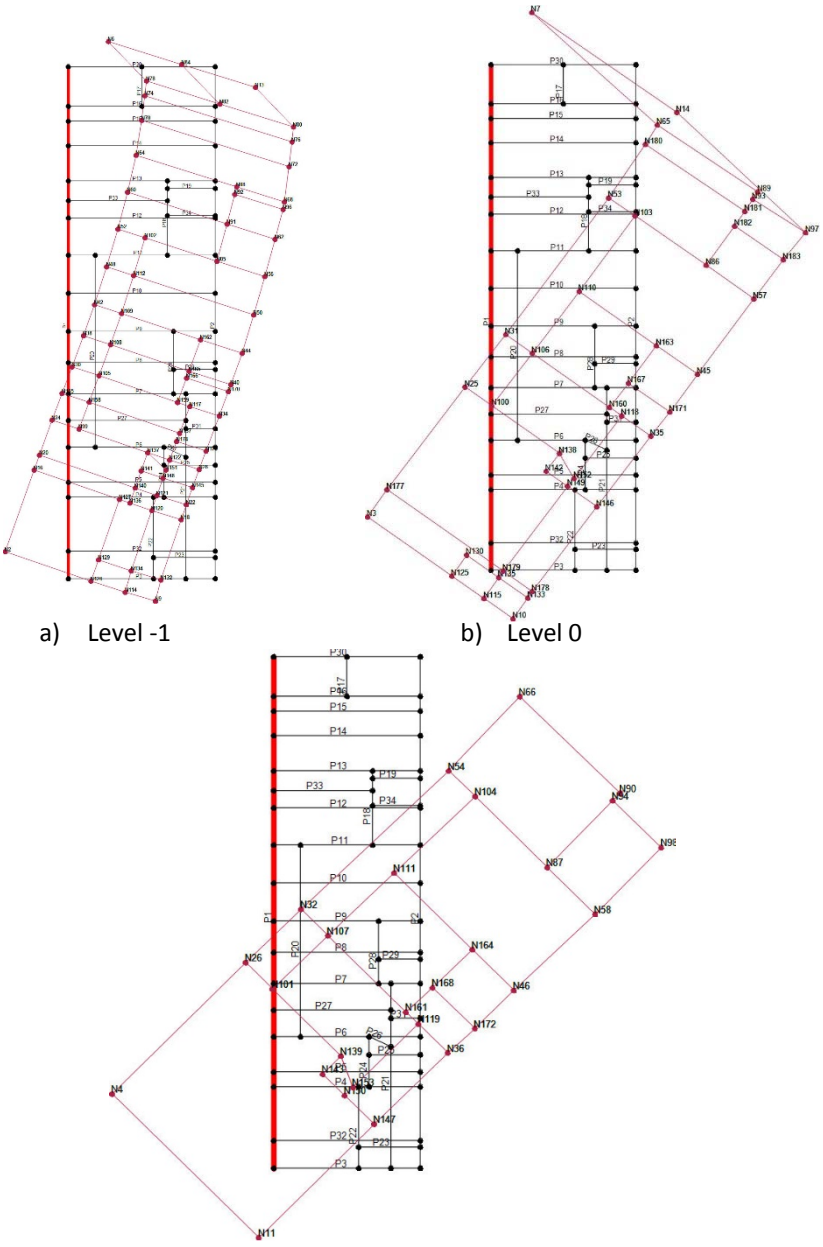

a) Level -1 b) Level 0

c) Level 1

Figure 5-19 Storey displacement profiles corresponding to a torsional vibration mode of the structure in the x-direction of the three-storey control numerical model including a soft storey and with 2.75:1 L:W plan proportions (Model 3M79).

Moreover, a comparison of the displacement modes and the building height of structure at which such modes of displacement are exhibited by the different analysed cases suggests that, even though there is only a marginal difference between the natural frequency estimates with respect to the fundamental mode of vibration corresponding to the control numerical models with the original length-to-width

plan ratio of 2.75:1 and the control numerical models with a double height space between Levels 0 and 1 with the same original plan proportions, as discussed in Section 5.2.3.2, the displacement modes corresponding to these two cases still differ. Similarly, the difference in displacement modes of the control numerical models with an extended plan layout and the corresponding control numerical models with a double height space between Levels 0 and 1 with an extended plan layout, was observed.

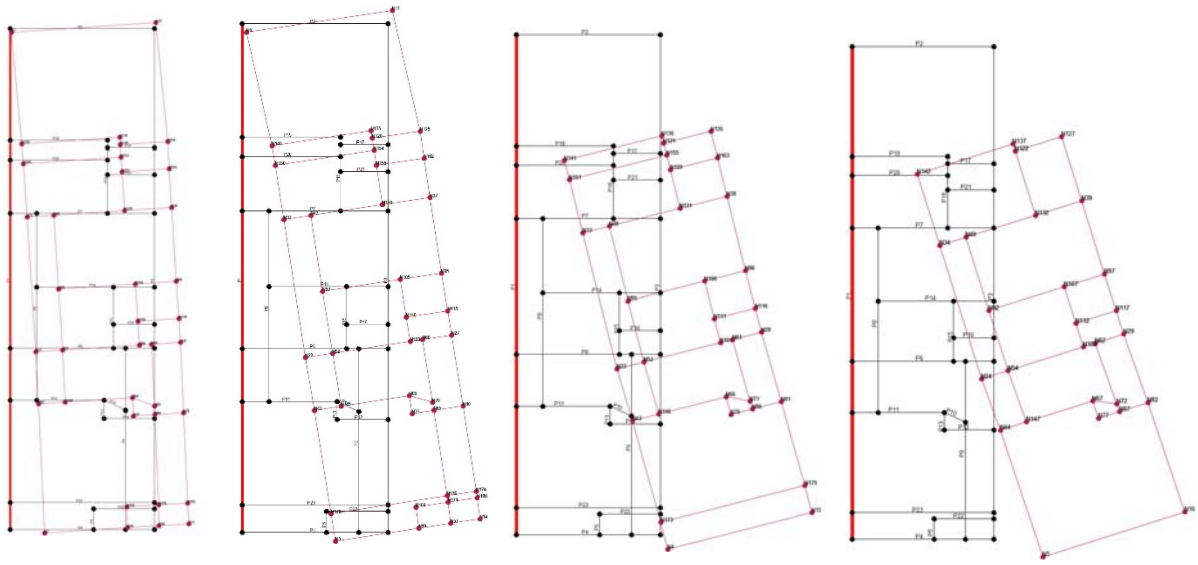

a) Level -1 b) Level 0 c) Level 1 d) Level 2

Figure 5-20 Storey displacement profiles corresponding to the mode of vibration with the highest percentage mass contribution in the x-direction of the four-storey control numerical model with 2.75:1 L:W plan proportions (Model 3M55).

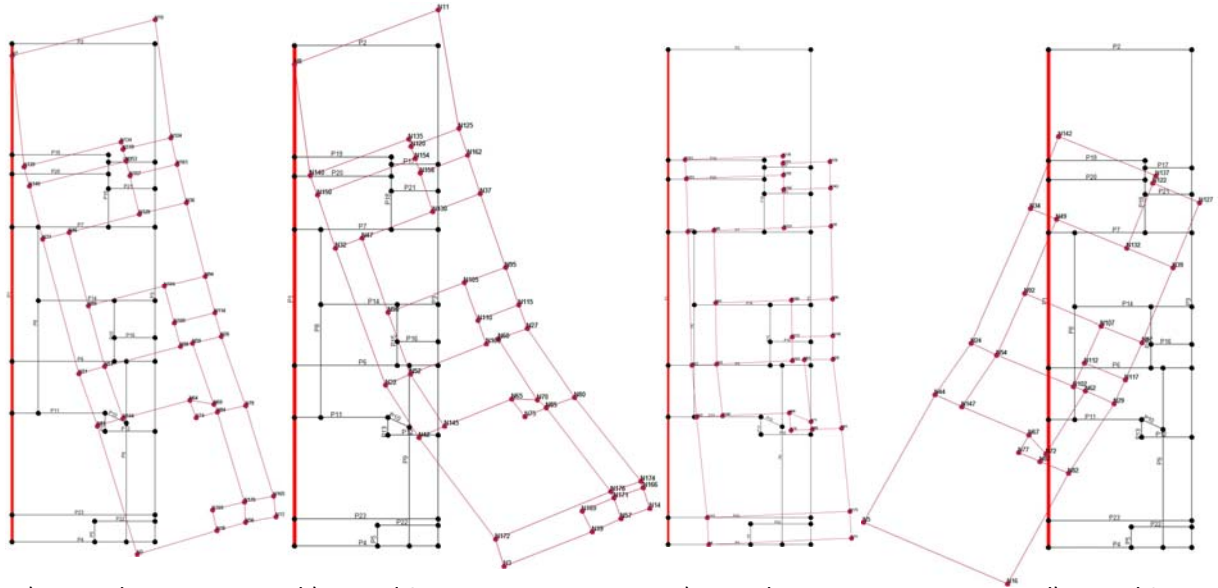

a) Level -1 b) Level 0 c) Level 1 d) Level 2

Figure 5-21 Storey displacement profiles corresponding to a second vibration mode overall displacement of the structure in the x-direction of the four-storey control numerical model with 2.75:1 L:W plan proportions (Model 3M55).

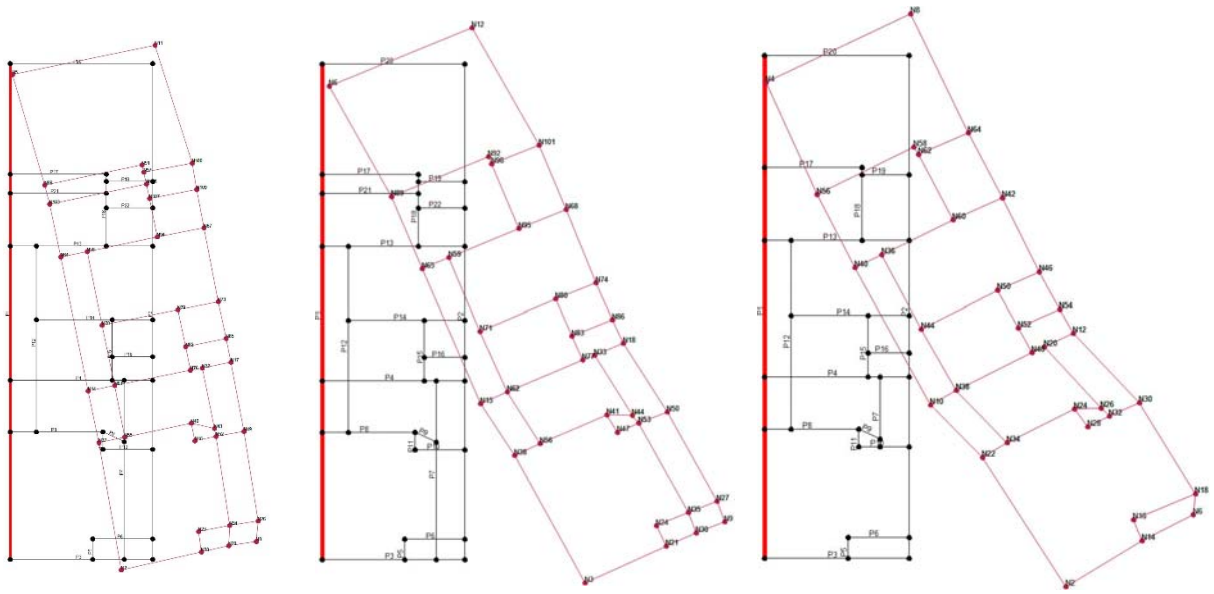

a) 3M169 Level -1 b) 3M169 Level 0 c) 3M170 Level -1

Figure 5-22 Storey displacement profiles corresponding to the mode of vibration with the highest percentage mass contribution in the x-direction of two- and one-storey control numerical models with 2.75:1 L:W plan proportions (Models 3M169 and 3M170, respectively).

Figures 5-19 to 5-22 show how the lower stiffness of the area of the courtyard at Levels -1 and 0, when compared to the rest of the floor plate, results in the distortion of the plan at these storeys at the junction between these two parts of the floor plate. Hence, the distortion resulting at this junction at Levels -1 and 0 was ignored in the assessment of the displaced plan shapes with respect to the ideal box-like behaviour. Nevertheless, all the analysed cases exhibit some degree of distortion at one or more storeys (excluding the area of the courtyard) and with respect to one or more main modes of vibration. While the degree of distortion present in different storeys of every analysed numerical model varies considerably from one case to another, this observation confirms that a 'box-like' behaviour cannot be assumed in the case of the building typology under study.

The comparison of the modal displacements corresponding to the main modes of vibration with respect to the x-direction exhibited at every storey of the analysed numerical models with a building height of six or less storeys shows that, particularly when a higher number of floors are present, the mode of vibration resulting in the maximum percentage mass distribution (and corresponding to a first vibration mode type of displacement) generally exhibits only a marginal degree of distortion at Level -1 only or at Levels -1 and 0, while the rest of the storeys exhibit a box-like behaviour. Modes of vibration corresponding to first mode type of displacements also result in plan distortions even at Level 1 at an overall height of three storeys, particularly, in the case of the control numerical models with setbacks at penthouse level, and the original 2.75:1 length-to-width plan proportions, the control numerical model with a double height space between Levels 0 and 1 and with the extended plan layout proportions of 4:1 and the control numerical model with the extended plan layout proportions only. On the other hand, higher modes of vibration result in significant plan distortions at various storey levels throughout the structures even at the higher building heights. Furthermore, as shown in Figures

5-21 and 5-22, the degree of plan distortion in the lower floors is observed to increase with reduction in number of storeys.

Furthermore, the natural period estimates of the main modes of vibration in the transverse x-direction of four cases analysed using 3Muri® on UCL and clay subsoils were compared to the corresponding Eurocode 8 Part 1 Type 1 elastic response spectra for Type A and B grounds [4], respectively. This comparison is presented in Figures 46 and 47 in Appendix E. The four cases considered consist of the following:

a) the five storey control numerical models with length-to-width plan proportions of 2.75:1 analysed using 3Muri® on UCL (model 3M54) and clay (model 3M59), respectively;
b) the five storey control numerical models including a soft storey at semi-basement level, with length-to-width plan proportions of 2.75:1, analysed using 3Muri® on UCL (model 3M71) and clay (model 3M77), respectively;
c) the six storey control numerical models with length-to-width plan proportions of 4:1 analysed using 3Muri® on UCL (model 3M116) and clay (model 3M123), respectively;
d) the five storey control numerical models including a soft storey at semi-basement level, with length-to-width plan proportions of 4:1, analysed using 3Muri® on UCL (model 3M140) and clay (model 3M146), respectively.

In view of the similarity of the results, only the cases corresponding with (a) and (c) analysed on UCL are reproduced in Figures 5-23 and 5-24.

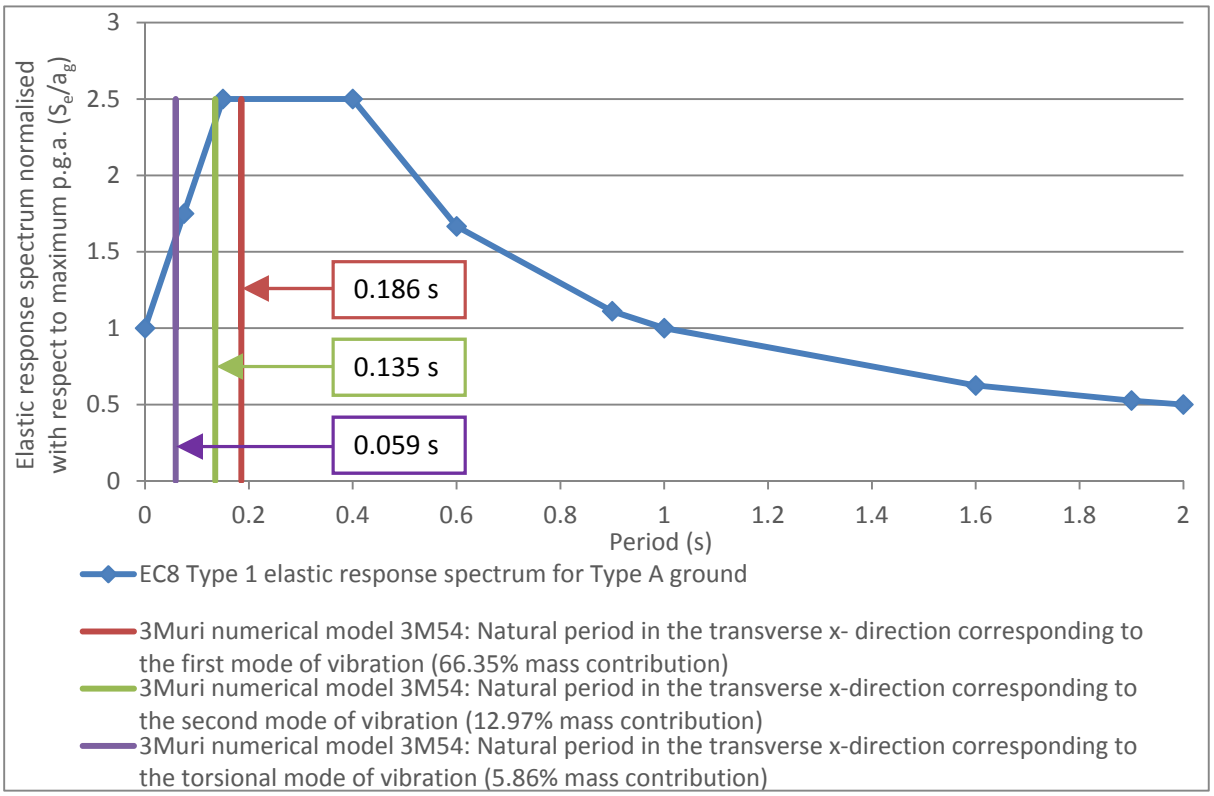

Figure 5-23 Comparison of natural period estimates for the main modes of vibration in the transverse x-direction of the five storey control numerical model with length-to-width plan ratio of 2.75:1 analysed on UCL using 3Muri® (3M54) to the Eurocode 8 Type 1 elastic response spectrum for Type A ground.

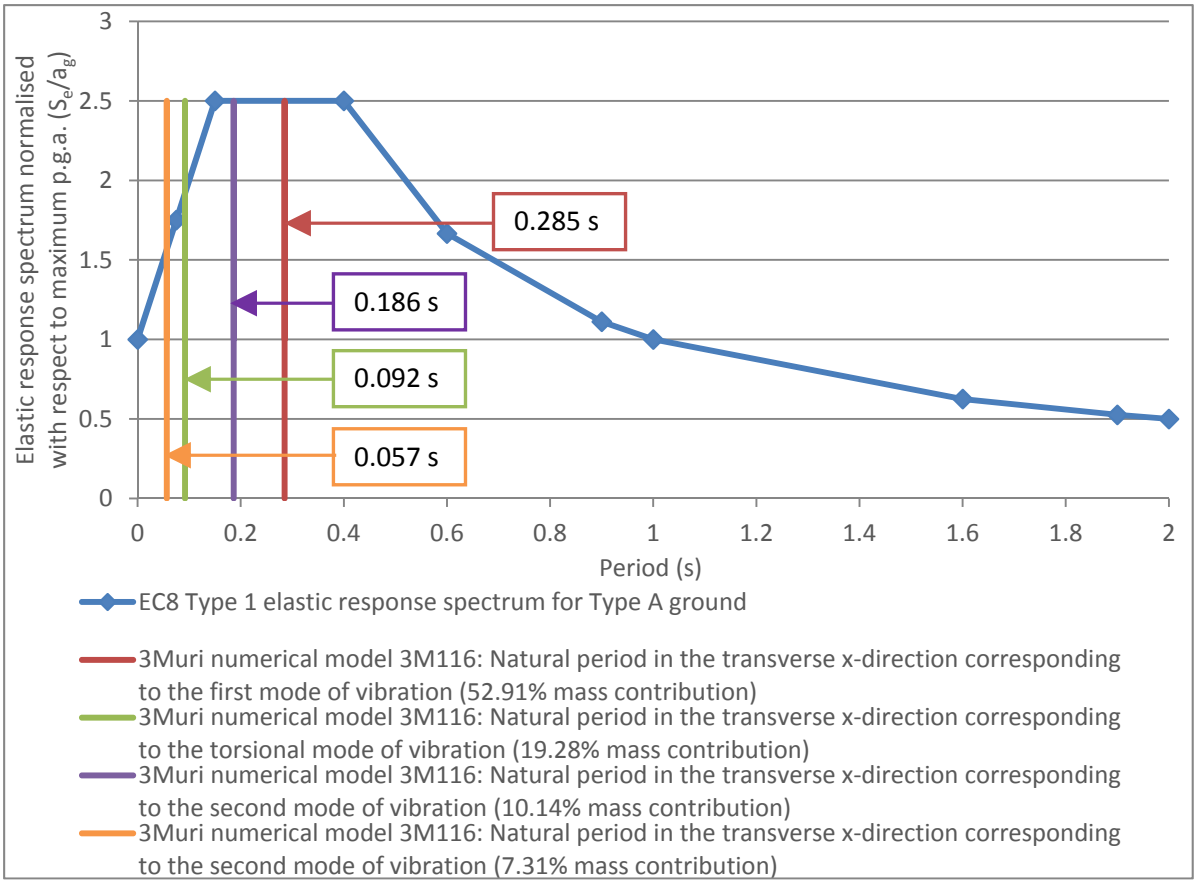

Figure 5-24 Comparison of natural period estimates for the main modes of vibration in the transverse x-direction of the six storey control numerical model with length-to-width plan ratio of 4:1 analysed on UCL using 3Muri® (3M116) to the Eurocode 8 Type 1 elastic response spectrum for Type A ground.

In general, the results presented in Figures 5-23 and 5-24 and in Figures 46 and 47 of Appendix D for the control numerical models and the control numerical models with a soft storey at semi-basement level with original and extended plan layout proportions, at heights of five and six storeys, respectively, and analysed on a UCL or clay subsoil, confirm that the mode of vibration corresponding to the highest natural period in the transverse x-direction, exhibits the first mode-type of displacement and results in the highest mass contribution in the transverse x-direction, which, in turn, corresponds to the highest spectral acceleration in the constant spectral acceleration range of the Eurocode 8 Type 1 elastic response spectrum [4] for the respective ground type in the numerical model. This, therefore, suggests that the first mode of vibration is, in most cases, the most significant mode of vibration for the building typology under study. Furthermore, Figures 46 (a) and 47 (a) in Appendix E, indicate that the mode of vibration in the transverse x-direction corresponding to a second mode-type of displacement in the five storey control numerical models with original plan proportions analysed using 3Muri® on a UCL or clay subsoil, respectively, results in the second highest percentage mass contribution, and only a marginally lower spectral acceleration on the Eurocode 8 Part 1 Type 1 elastic response spectrum [4] for the respective ground material than the first mode of vibration of the same numerical model. Hence, though less significant than the first mode of vibration, the second mode of vibration still provides a considerable contribution in the seismic response of the control numerical models investigated in this study, irrespective of the subsoil material.

Nevertheless, an exception to this trend is exhibited by model 3M140 (the six storey control numerical model including a soft storey at semi-basement level, with extended plan proportions, analysed on UCL using 3Muri®), as reported in Figure 46 (d) in Appendix E. In this case, even though the mode of vibration associated with the first mode-type of displacement corresponds to the highest percentage mass contribution (77.92%), this mode of vibration and the mode of vibration corresponding to the second mode-type of displacement (6.70% mass contribution), both result in a marginally lower spectral acceleration on the Eurocode 8 Part 1 Type 1 elastic response spectrum for Type A ground [4] than the torsional mode of vibration which, has a percentage mass contribution in the transverse x-direction of 9.57%. In model 3M 140, this torsional mode of vibration is the only mode of vibration which corresposnds to the highest spectral acceleration on the Eurocode 8 Part 1 Type 1 elastic response spectrum for Type A ground [4]. On the other hand, in the case of numerical model 3M146 (the control numerical model including a soft storey at semi-basement level, with extended plan proportions, analysed on clay using 3Muri®) the first and the torsional modes of vibration both correspond to the constant spectral acceleration part of the Eurocode 8 Part 1 Type 1 elastic response spectrum for Type B ground [4].

Figures 46 and 47 in Appendix E suggest that, while torsional modes of vibration with a percentage mass contribution of greater than 5% were not exhibited by the five storey control numerical models including a soft storey at semi-basement level, with original plan proportions analysed on UCL or clay subsoils, the equivalent five storey control numerical models with original plan proportions exhibit a torsional mode of vibration with a percentage mass contribution of 5.86% and corresponding to a considerably lower spectral acceleration on the the Eurocode 8 Part 1 Type 1 elastic response spectrum [4] for the respective ground type. This suggests that the significance of the torsional mode of vibration on the seismic response of the five storey control numerical models investigated in the present research study is considerably reduced, when compared to the modes of vibration exhibiting a first or second type of displacement.

On the other hand, Figures 5-24 and Figures 46 (c) and (d) and 47 (c) and (d) in Appendix E indicate that in the six storey control numerical models and control numerical models including a soft storey at semi-basement level with extended plan proportions analysed on both UCL and clay subsoils, torsional modes of vibration result in the second highest natural periods and the second highest percentage mass contribution after the first (fundamental periods), corresponding also to the highest spectral acceleration in the constant spectral acceleration range of the Eurocode 8 Type 1 elastic response spectrum [4] for the respective ground type in the numerical model. This, therefore, suggests that torsional modes of vibration provide a significant contribution in the seismic response of the building typology under study, particularly in cases when extended plan proportions are present.

5.2.4 Maximum displacement resulting from the analysed numerical models

In the 3Muri® non-linear static pushover analysis, a lateral load distribution is applied to the numerical model and increased monotonically such that the increase in displacement at every analysis substep is equal to the ratio between the maximum displacement and the number of substeps (both) specified

by the user in the pushover settings. This increase in lateral load distribution is sustained until the base shear drops to 80%, indicating the deterioration of the lateral load resisting system. The maximum displacement at which this 20% shear drop occurs corresponds to the maximum displacement of the structure with respect to the limit state of Near Collapse and is interpreted as a measure of the structure's seismic capacity with respect to the same limit state, as defined in Clause C.4.1.1(2) of Eurocode 8: Part 3 [97]. The maximum displacements extracted from 3Muri® with respect to the limit state of Significant Damage were verified to be equal to 0.75 times the maximum displacements resulting with respect to the limit state to Near Collapse for all analysed cases, in accordance with Clause C. 4.1.2(2) of Eurocode 8: Part 3 [97]. In every 3Muri® pushover analysis, this procedure is repeated for 24 times since the program considers the application of two load distributions, uniform and modal, in the positive and negative x- and y-directions, in accordance with Clause 4.3.3.4.2.2(1) of Eurocode 8: Part 1 [4], and with the accidental eccentricities recommended in Clause 4.3.2(1)P of Eurocode 8: Part 1 [4], which result in a total of 24 load distributions.

In all the numerical analyses carried out using ELS® in this research study, the simulated ground motion record was applied only in the weaker transverse x-x direction of the numerical models. Hence, the discussion of the resulting displacements presented in Chapter 4 of this thesis focused on the structural response in the x-x orientation of the analysed numerical models. As discussed in Section 3.4.5, the maximum p.g.a. of the simulated ground motion record applied in the ELS® analyses corresponds to the maximum p.g.a. for the Maltese Islands as indicated by the EFEHR SHARE 2013 Hazard model for a probability of exceedance of 10% in 50 years and a 95% fractile. This probability of exceedance corresponds to that recommended for the design seismic action in accordance with the No Collapse Requirement in Clause 2.1(1)P of Eurocode 8: Part 1 [4]. Hence, the ensuing discussion of the maximum displacements in the numerical models analysed using 3Muri® through a non-linear static pushover analysis where the control node was defined at the level of the floor of the topmost storey, is mainly focused on the 3Muri® displacement response resulting from load distributions applied to the analysed numerical models in the x-direction and with respect to the equivalent limit state of Significant Damage, as confirmed in the Note to Clause 2.1(1)P in Eurocode 8: Part 3 [97]. The maximum displacements were, on average, 1.297 to 1.489 times higher than the mean of the maximum displacements resulting from the twelve load distributions acting in the x-direction of every analysed numerical model, if the cases which include a soft storey are excluded. The control numerical models including a soft storey at semi-basement level with original and extended plan layout proportions resulted in maximum displacements, which were, on average, 1.733 and 2.212 times higher, respectively, than the mean maximumum displacement. These maximum displacements were compared to the maximum relative x-displacements recorded from an element in the left hand side party wall positioned at the level of the floor of the topmost storey prior to the start of collapse at the same position in the corresponding numerical models analysed using ELS® which resulted in collapse. This comparison is reported in Table 5-12.

Table 5-12 Comparison between maximum x-displacements resulting at slab over penultimate storey in corresponding numerical models analysed using 3Muri® and ELS®.

Number of storeys	3Muri®				ELS®		Comparison 3Muri® vs. ELS®	
	3Muri® model number	Description	Maximum displacement (m) from load distributions in the x- direction for the limit state of Near Collapse	Maximum displacement (m) from load distributions in the x- direction for the limit state of Significant Damage	ELS® model number	ELS® maximum relative x-displacement (m) prior to the start of collapse at level of floor of topmost storey	Percentage discrepancy: maximum x-displacements 3Muri® (NC) vs. ELS® (%)	Percentage discrepancy: maximum x-displacements 3Muri® (SD) vs. ELS® (%)
6	3M46	Control on UCL (L:W 2.75:1)	0.024	0.018	Mean: 42v2, 43v2, 44	0.006	296.4	197.3
6	3M58	Control on clay (L:W 2.75:1)	0.024	0.018	Mean: 45v2, 46, 47	0.007	234.6	151.0
5	3M59		0.021	0.016	Mean: 51, 52, 53	0.008	155.5	91.6
4	3M60		0.020	0.015	Mean: 57, 58	0.008	145.1	83.8
6	3M76	Control with soft storey at semi-basement level on clay (L:W 2.75:1)	0.060	0.045	69	0.002	3381.6	2511.2
5	3M77		0.106	0.080	71	0.004	2583.0	1912.2
4	3M78		0.365	0.273	73	0.011	3189.8	2367.3
6	3M167	Control with setbacks at penthouse level on clay (L:W 2.75:1)	0.029	0.022	79	0.010	198.8	124.1
5	3M166		0.026	0.020	81	0.016	64.7	23.5
6	3M94	Control with double height space between Levels 0 and 1 on clay (L:W 2.75:1)	0.024	0.018	99	0.009	175.5	106.6
5	3M95		0.023	0.017	101	0.006	255.5	166.6
4	3M96		0.021	0.016	103	0.007	197.0	122.8
NC: Limit state of Near Collapse; SD: Limit state of Significant Damage (as defined in Clause 2.1(1)P, EC8-1)								

Table 5-12 indicates that the maximum displacements resulting at the level of the control node from load distributions applied in the x-direction of the 3Muri® numerical models with respect to the limit state of Significant Damage are, on average, 655% higher than the maximum relative x-displacements recorded in an element in the left hand side party wall, at the same level of the 3Muri® control node, prior to the start of failure at the same position, in the corresponding ELS® models (if all the

corresponding cases analysed with the two software packages are considered). While the discrepancy is significant, the range over which the percentage discrepancy between the corresponding 3Muri® and ELS® values vary is also very wide, namely, between 23.5% and 2511.2%, with respect to the same limit state if the case of the control numerical models with a soft storey at semi-basement level is included, and between 23.5% and 197.3% if this case is excluded, which would lead to a reduction in the average percentage discrepancy to 118.6%. The extent of the discrepancy makes the comparability between these two sets of displacements seem dubious, particularly when considering the different nature of the applied seismic loading in the case of the non-linear static and non-linear dynamic analysis procedures.

However, Fajfar [127] explains that the displacement exhibited by a structure during a non-linear static pushover analysis, and represented through a pushover curve, should approximate the deformation of the same structure under dynamic analysis. Fajfar [127] also adds, that the maximum top displacement resulting in a structure during an earthquake of a specific intensity, derived from the elastic response spectrum (equivalent to the target displacement defined in Clause 4.3.3.4.2.3 of Eurocode 8: Part 1 [4] and calculated in accordance with Clauses B.5 and B.6 of Annex B to Eurocode 8: Part 1 [4] for a single or multiple degree-of-freedom systems, respectively), represents the average displacement, which should result from the applied seismic action, and that the dispersion of the values obtained for this response parameter can be considerably wide. As explained by Williams ([187] p. 56), the response spectrum is a representation of

> 'the peak response of an SDOF (single-degree-of freedom) structure to a particular earthquake, as a function of the natural period and damping ratio of the structure'.

It is derived from the peak response exhibited by different structures which have different characteristics and, consequently, different natural periods, under the same earthquake action. The elastic response spectrum, upon which the target displacement is calculated, is obtained following a statistical analysis of the response spectra of different earthquakes, which could affect a structure at a site.

The maximum displacement reported in Table 5-12 refers to the maximum displacement exhibited by the numerical models analysed using 3Muri® at the level of the control node just before the 20% drop in base shear resistance was achieved during the non-linear static pushover analysis, and it is not the target displacement. However, the reported maximum displacement for every analysed numerical model was obtained from the 12 load distributions corresponding to the application of load in the transverse x- direction, and the range of dispersion of the results quoted in the above comparison, with respect to the maximum relative x-displacement recorded in the corresponding ELS® models, represents investigated cases of the URM building typology under study, which include different seismic vulnerability characteristics and different building heights. Hence, by comparison to the dispersion of values of the maximum displacement exhibited by structures in a real life scenario when considering the target displacement acknowledged by Fajfar [127], a significant dispersion can be expected even between the maximum displacements estimated using 3Muri® for load distributions applied in the x-x orientation and the corresponding displacements obtained from a non-linear time-

history dynamic analysis. Nevertheless, Fajfar [127] does not give an indication of a realistic magnitude for such a dispersion, particularly in the case of unreinforced masonry structures, in which absence, the extent of the discrepancy obtained between the 3Muri® and the ELS® displacements remains debatable. This is being acknowledged particularly when considering the difference in the assumed /specified level of restraint at wall-to-wall connections and at slab boundaries for the two software packages, which likely resulted in the over-estimation of the height at adequate seismic resistance, as discussed in Section 5.2.1 of this research study.

Krawinkler and Seneviratna [214] note that the maximum roof displacement resulting from a pushover analysis is generally fairly accurate in structures, which do not exhibit major differences in strength or stiffness throughout their height. This could explain the significantly higher discrepancy resulting from control numerical models including a soft storey at semi-basement level. Furthermore, Azizi-Bondarabadi et al. [215] reported an overall good correlation between the in-plane wall displacements resulting from numerical models of two masonry structures analysed using TREMURI (the research version of 3Muri®) and the corresponding shake table test results of scaled models. However, Endo et al. [131] concluded that iterative pushover methods underestimate the structural displacement when compared to non-linear dynamic assessments.

The maximum relative x- displacements resulting from the ELS® numerical analyses and presented in Table 5-12 were obtained following a non-linear time-history dynamic analysis using one simulated ground motion record for the Maltese Islands, which was applied in the transverse x-x orientation of the analysed numerical models. The use of a single simulated ground motion record was acceptable with respect to the main aim behind the numerical analyses carried out using ELS®, namely the investigation of the effect which particular building characteristics have on the seismic response of the URM building typology under study as well as their relative influence on this seismic response. However, a more complete non-linear dynamic assessment of the numerical models analysed using ELS® through the use of a higher number of accelerograms could have resulted in a reduced discrepancy between the maximum displacements exhibited by the corresponding numerical models analysed using 3Muri® and ELS® in the present study.

Moreover, the maximum displacements resulting from the 3Muri® numerical models correspond approximately to the displacement of the centroid of the storey at the level of the control node. On the other hand, the maximum relative x-displacements prior to the onset of collapse in the corresponding ELS® numerical models and reported in Table 5-12 refer to the relative x-displacement of an element, which is equivalent to half a masonry block, at the level of the control node defined in 3Muri®, and positioned at 7.5 m from the outer face of the outer wall of the front façade of the modelled structures. The extraction of response parameters with respect to the centroid of a particular storey was not possible in the version of the ELS® software used in this research study. In addition, the comparison of response parameters obtained from elements at corresponding positions in numerical models, which included different building characteristics was considered desirable with respect to the investigation into the relative influence, which the modelled characteristics have on the seismic response of the structural typology under study. However, the displacement of a masonry

block, which forms part of a masonry wall, is influenced by a number of factors, amongst which, are the restraint provided at the interface with the surrounding blocks/ mortar and the degree of superimposed vertical loading. Furthermore, Figures 5-19 to 5-22 suggest that, depending on the main modes of vibration influencing the response of a structure under particular loading conditions, the relative x-displacement of the element in the left hand side party wall from which the ELS® response parameters were extracted, is likely to differ from the magnitude of the displacement of the centroid of the same storey at which the ELS® element is located. This, therefore, suggests that, except in the context of the overall trends in the variation of displacements for different heights of structures or in the presence of different seismic vulnerability characteristics, the magnitude of the maximum displacements resulting from load distributions applied in the x-direction of the 3Muri® numerical models is not directly comparable to the magnitude of the maximum relative x-displacements extracted from an element in the left hand side party wall in the corresponding numerical models analysed using ELS®.

Moreover, in the present study, the magnitude of the maximum displacement[47] obtained from the 12 load distributions applied in the x-direction of the corresponding numerical models analysed using 3Muri® on an upper coralline limestone or clay subsoil with respect to the same limit state, resulted as identical in the majority of cases[48]. On the other hand, the outcome of the 3Muri® seismic assessment for the two different subsoils differs since the magnitude of the target displacement, calculated with reference to the elastic response spectrum in Eurocode 8 [4], is dependent on the soil factor and elastic response spectrum periods T_B, T_C and T_D, which vary depending on the ground type. Therefore, while not having a direct implication on the validity of the seismic assessment outcome, the identical maximum displacements resulting from the corresponding non-linear static analyses on upper coralline limestone and clay subsoils puts into question the accuracy of the estimated maximum

[47] This maximum displacement is equivalent to the maximum displacement exhibited by the respective numerical models during the pushover analysis before the structural degradation (corresponding to a 20% decrease in base shear) is reached.

[48] Identical maximum displacements from load distributions applied in the x-direction resulted in all corresponding numerical models analysed using 3Muri® with respect to the same limit states on an upper coralline limestone subsoil and on a clay subsoil with the exception of Models 3M73 and 3M79 (the three-storey control numerical models with a soft storey at semi-basement level and with original proportions analysed on upper coralline limestone and clay, respectively), and Models 3M142 and 3M148 (the four-storey numerical models with a soft storey at semi-basement level and with extended plan proportions analysed on upper coralline limestone and clay, respectively). The maximum displacements resulting from the corresponding cases analysed on rock were 22.22% and 8.33% higher, respectively, than the equivalent cases analysed on clay. Similarly, Models 3M128 and 3M135 (the seven-storey control numerical models with a double height space between levels 0 and 1 and with extended plan layouts analysed on upper coralline limestone and clay, respectively) exhibited a marginal discrepancy of 0.04% in the magnitude of the maximum displacements resulting from the load distributions applied in the y-direction of the corresponding numerical models. The higher displacement was obtained in the case analysed on upper coralline limestone, which is clearly an anomaly.

displacements resulting from this method of analysis when compared to a real life scenario and, hence, the practical significance of the magnitude of such displacements.

Table 5-13 Cases resulting in anomalously high maximum displacements with respect to load distributions applied in the y-direction and comparison with magnitude of corresponding maximum displacements resulting from load distributions in the x-direction.

Number of storeys	3Muri® model number	Description	Anomalous maximum displacement (m) from load distributions in the y-direction for the limit state of Significant Damage	Maximum displacement (m) from load distributions in the x-direction for the limit state of Significant Damage
4	3M72	Control with soft storey at semi-basement level on UCL (L:W 2.75:1)	8.130	0.273
4	3M78	Control with soft storey at semi-basement level on clay (L:W 2.75:1)	8.130	0.273
7	3M128	Control with double height space between Levels 0 and 1 on UCL (L:W 4:1)	6.850	0.035
7	3M135	Control with double height space between Levels 0 and 1 on clay (L:W 4:1)	6.847	0.035
6	3M140	Control with soft storey at semi-basement level on UCL (L:W 4:1)	16.031	0.015
5	3M141		2.934	0.029
4	3M142		12.092	0.026
3	3M143		13.254	0.046
6	3M146	Control with soft storey at semi-basement level on clay (L:W 4:1)	16.031	0.015
5	3M147		2.934	0.029
4	3M148		12.092	0.024
3	3M149		13.254	0.046
5	3M157	Control with double height space between Levels 0 and 1 extending over whole width of structure on UCL (L:W 2.75:1)	4.212	0.018

Furthermore, Table 5-13 presents the cases where anomalously high maximum displacements resulted from the 12 load distributions applied in the y-direction of the analysed numerical models using 3Muri®. In all the cases exhibiting anomalously high displacements from load distributions in the y-direction presented in Table 5-13, the corresponding target displacement was lower in magnitude than the maximum displacement, therefore resulting in a satisfied verification. Clearly, an unreinforced loadbearing masonry structure cannot be expected to sustain displacements of such magnitudes. This

highlights the limitation of the restriction of the failure criterion in 3Muri® to the verification of the ratio between the maximum displacement at the centroid of the storey at which the control node is defined, to the target displacement, while disregarding the magnitude of the compared displacements and other considerations, which are discussed in the ensuing sections.

Table 5-14 Comparison of maximum displacements (m) resulting from load distributions applied in the x-direction of numerical models analysed on a UCL subsoil using 3Muri® with respect to the limit state of Significant Damage.

Number of storeys	Control on UCL (L:W 2.75:1)	Control with a soft storey at semi-basement level on UCL (L:W 2.75:1)	Control with setbacks at penthouse level on UCL (L:W 2.75:1)	Control with a double height space between Levels 0 and 1 on UCL (L:W 2.75:1)	Control with double height space between Levels 0 and 1 over entire width of structure on UCL (L:W 2.75:1)		Control on UCL (L:W 4:1)	Control with a soft storey at semi-basement level on UCL (L:W 4:1)	Control with a double height space between Levels 0 and 1 on UCL (L:W 4:1)
15	0.074			0.074					
14	0.068			0.067					
13	0.057			0.062					
12	0.063			0.064					
11	0.042			0.047					
10	0.036			0.044	0.039				
9	0.035			0.040	0.040				
8	0.035			0.033	0.036				0.052
7	0.022			0.022	0.025		0.036		0.035
6	0.018	0.045	0.022	0.018	0.023		0.031	0.015	0.031
5	0.016	0.080	0.020	0.017	0.018		0.027	0.029	0.029
4	0.015	0.273	0.014	0.016	0.015		0.025	0.026	0.026
3	0.011	0.011	0.016	0.011			0.020	0.046	0.022
2	0.019	0.020						0.022	
1	0.019	0.020						0.020	

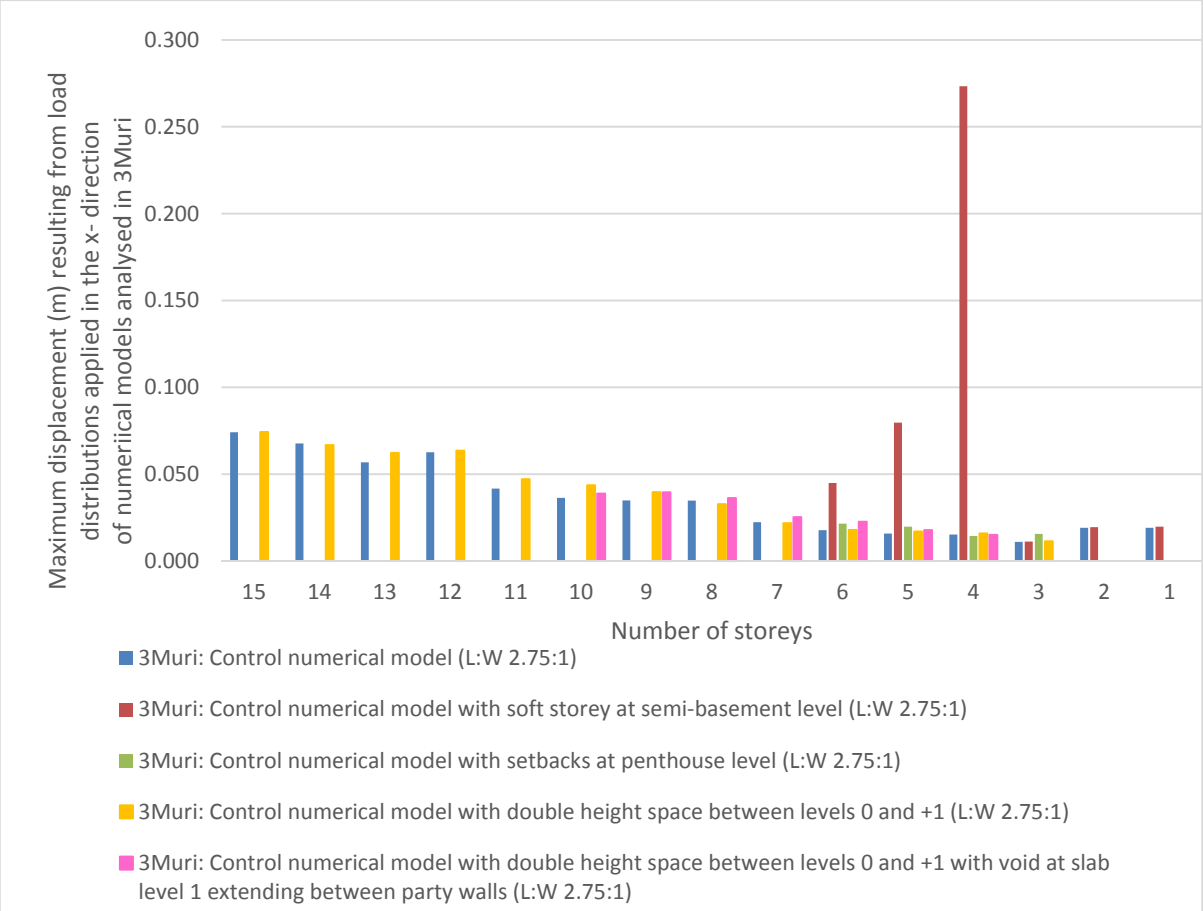

Figure 5-25 Comparison of maximum displacements (m) resulting from load distributions applied in the x-direction of numerical models with original plan proportions analysed on a UCL subsoil using 3Muri® with respect to the limit state of Significant Damage.

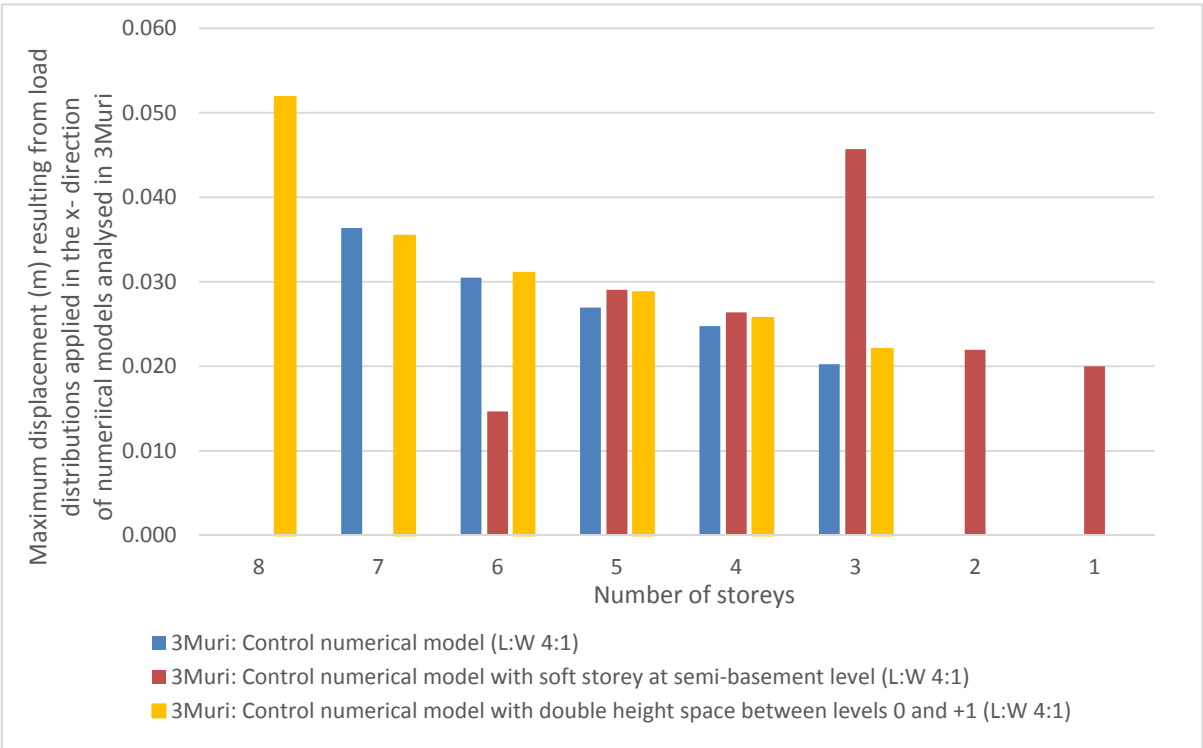

Figure 5-26 Comparison of maximum displacements (m) resulting from load distributions applied in the x-direction of numerical models with extended plan proportions analysed on a UCL subsoil using 3Muri® with respect to the limit state of Significant Damage.

Table 5-14 and Figures 5-25 and 5-26 report the comparison of the maximum displacement resulting from the load distributions applied in the x-direction in all the numerical models analysed on an upper coralline limestone subsoil using 3Muri® and verified with respect to the limit state of Significant Damage. While, generally, the magnitude of the maximum displacement decreases with reduction in number of floors in most investigated cases, the control numerical models with a soft storey at semi-basement level and with original plan proportions exhibit a significant increase in displacement with every storey decrement from six to five storeys and between five and four storeys, reaching a peak displacement of 0.273 m at a height of four storeys. Figure 4-45 in Chapter 4 of this thesis reports a similar increase in maximum relative x-displacement of the control numerical model including a soft storey analysed using ELS®. However, this increase occurs at a height of five storeys. The corresponding control numerical models including a soft storey and with extended plan proportions analysed using 3Muri® also exhibit a similar increase in maximum displacement at a height of three floors. The increase in maximum displacement for lower building heights is likely to occur due to the higher proportion of displacement associated with the soft storey irregularity out of the overall building displacement. The displaced shape of the structure during a seismic event could also lead to increased displacements due to P-delta effects, particularly in the case of a structure, which includes a soft storey at its lowermost level and a higher structural mass in the overlying floors.

Furthermore, Table 5-14 shows that there is only a marginal difference between the maximum displacements exhibited by the control numerical models and the control numerical models, which include a double height space for both cases with original or extended plan layout proportions. A similar close correlation between building responses for these two investigated cases was also identified with respect to the natural frequencies for the fundamental modes of vibration, and, to a lesser extent, the maximum building height at adequate seismic resistance, hence, suggesting that the limited size of the void at slab Level 1 and the stiffening effect of the 250 mm thick slabs which bound the void on three sides, might be reducing the potentially deleterious influence of a double height space and a void in a slab directly abutting a party wall. In addition, the closer correlation in response exhibited by these cases when modelled using 3Muri®, when compared to the corresponding ELS® models, could be due to the disregard, in the former case, of out-of-plane failure mechanisms, which would otherwise be triggered due to the loss of restraint of the party wall at the position of the void in the slab. Moreover, the control numerical models, which include setbacks at penthouse level, exhibit a minor increase in maximum displacement when compared to control numerical models with the same plan proportions.

In addition, the numerical models with extended plan layout proportions exhibit higher maximum displacements with respect to the load distributions applied in the x-direction than the corresponding numerical models with original plan proportions. This is likely due to the more slender proportions in the transverse x-x orientation of the extended plan layout cases and the higher seismic mass set in motion.

5.2.5 Shear failure in walls

As discussed in Section 5.2.1, a high discrepancy was observed between the maximum building height at collapse resistance in the numerical models, which did not include major changes in lateral storey stiffness throughout the height, analysed using ELS® with respect to the No Collapse Requirement, and the maximum building height at which adequate seismic resistance corresponding to the failure criterion (governed by the ratio of the maximum displacement to the target displacement) for the limit state of Significant Damage, resulted in the equivalent numerical models analysed using 3Muri®. On the other hand, closer correspondence with the ELS® safe building heights resulted in the case of the corresponding numerical models analysed using 3Muri® with respect to the Near Collapse limit state, which is, however, a more severe limit state than the No Collapse Requirement. Assumptions at the basis of the formulation of the 3Muri® numerical models, which cannot be controlled or altered by the user, were discussed in Section 5.2.1 as being the probable causes for this over-estimation in seismic resistance by 3Muri®.

Therefore, in an attempt to establish whether the maximum building height at which no shear failure is present in the walls of the numerical models analysed using 3Muri® with respect to the limit state of Significant Damage could result in a more realistic failure criterion with respect to this limit state, the presence of shear failure at displacement magnitudes, which are lower than the maximum displacement corresponding to the limit state of Significant Damage, was verified in all the walls, for all the 24 load distributions considered in every non-linear static analysis carried out for the study presented herein, with respect to the following two modelled cases using 3Muri®:

a) the control numerical models with original plan proportions analysed on an upper coralline limestone subsoil for overall building heights of one to fifteen storeys; and
b) the control numerical models including a soft storey at semi-basement level, with original plan proportions analysed on a clay subsoil for overall building heights of one to six storeys.

Figures 5-27 and 5-28 present examples of the presence of shear failure in a main longitudinal wall and in a main transverse wall, respectively. Furthermore, Tables 5-15 and 5-16 summarise the outcume of the shear failure verification with respect to the two considered cases, while indicating the maximum building heights at which the failure criterion with respect to the ratio of maximum displacement to target displacement is satisfied for the limit states of Near Collapse and Significant Damage in order to facilitate a comparison between the two sets of results. In all cases reported in Tables 5-15 and 5-16 'Y' (Yes) indicates that shear failure in the particular type of member (longitudinal wall / main transverse wall/ minor transverse wall / front facade) starts at a displacement which is lower than the maximum displacement corresponding to the limit state of Significant Damage for the load distribution under consideration, while ‘N’ (No) indicates that no shear failure is present in the walls up to the maximum displacement for this limit state.

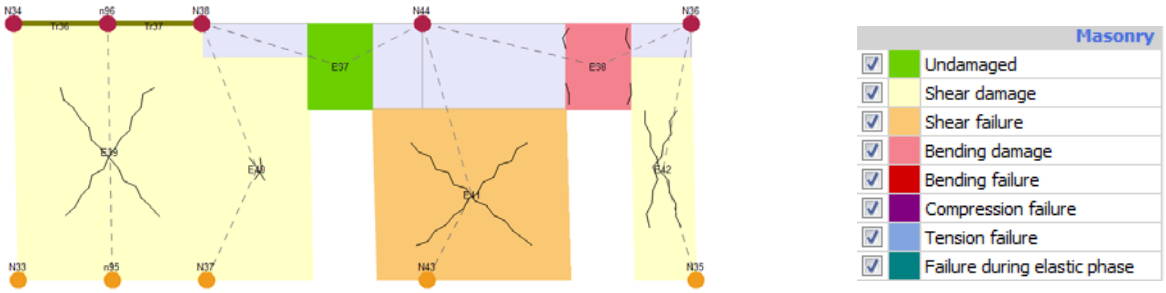

b) Wall elevation c) Legend

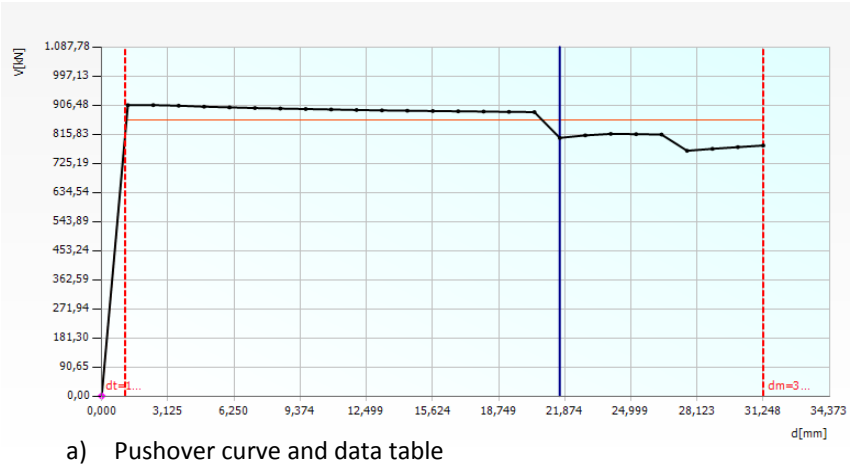

Step	Displacement [mm]	Shear [kN]
7	8,437	895,78
8	9,637	894,40
9	10,837	892,86
10	12,037	891,39
11	13,237	890,03
12	14,438	889,05
13	15,638	888,18
14	16,838	887,30
15	18,038	886,38
16	19,238	885,54
17	20,438	884,77
18	21,638	804,40
19	22,843	812,19
20	24,044	816,90
21	25,245	815,98
22	26,445	814,74
23	27,652	764,28
24	28,851	770,24
25	30,050	775,63
26	31,248	780,63

a) Pushover curve and data table

Figure 5-27 Shear failure (in orange) in central part of longitudinal corridor wall, in load distribution 7 of Model 3M170 at a displacement of 21.638 mm. The maximum displacement for the limit state of Significant Damage for the same load distribution is 23.436 mm.

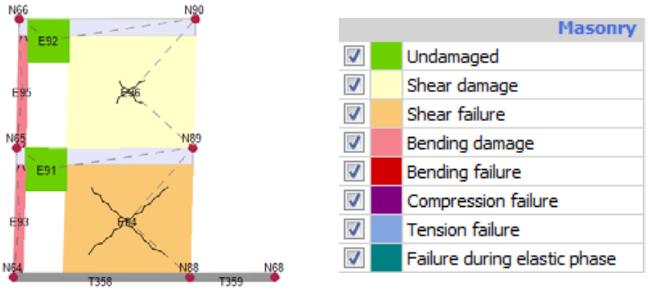

a) Wall elevation b) Legend

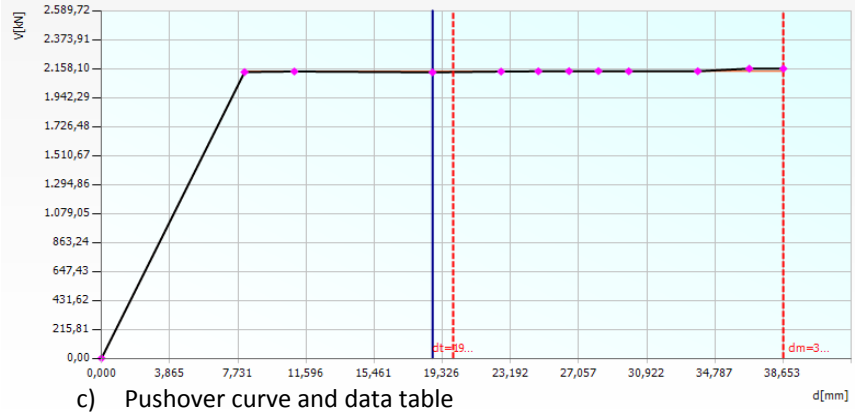

Step	Displacement [mm]	Shear [kN]
0	0,000	0,00
1	8,111	2.132,45
2	10,935	2.136,94
3	18,769	2.130,82
4	22,650	2.136,54
5	24,769	2.138,64
6	26,507	2.139,37
7	28,173	2.139,93
8	29,892	2.138,36
9	33,808	2.139,07
10	36,728	2.158,10
11	38,653	2.157,67

c) Pushover curve and data table

Figure 5-28 Shear failure (in orange) in rear facade (transverse wall), in load distribution 21 of Model 3M79 at a displacement of 18.769 mm. The maximum displacement for the limit state of Significant Damage for the same load distribution is 28.989 mm.

Table 5-15 Presence of shear failure with respect to limit state of Significant Damage in walls of control numerical models with original plan proportions analysed on upper coralline limestone using 3Muri® vs. building height at adequate seismic resistance for dm/dt criterion.

Control (L:W 2.75: 1) on upper coralline limestone subsoil							
Number of storeys	3Muri® Model number	Maximum height for adequate seismic resistance (displacement capacity criterion) with respect to limit state of Near Collapse (x)	Maximum height for adequate seismic resistance (displacement capacity criterion) with respect to limit state of Significant Damage (x)	Shear failure present in longitudinal walls with respect to limit state of Significant Damage: Yes (Y); No (N)	Shear failure present in main transverse walls with respect to limit state of Significant Damage: Yes (Y); No (N)	Shear failure present in minor transverse walls with respect to limit state of Significant Damage: Yes (Y); No (N)	Shear failure present in front façade with respect to limit state of Significant Damage: Yes (Y); No (N)
15	3M57			N	Y	N	Y
14	3M56		x	N	N	Y	Y
13	3M53			N	N	Y	Y
12	3M52			N	N	Y	Y
11	3M51			N	N	Y	Y
10	3M50			N	N	Y	Y
9	3M49			N	N	Y	Y
8	3M48			N	N	N	Y
7	3M47v2			N	N	N	Y
6	3M46	x		N	N	N	Y
5	3M54			Y	N	N	Y
4	3M55			Y	N	N	Y
3	3M168			Y	N	N	Y
2	3M169			Y	N	Y	Y
1	3M170	2 cases of (dm/dt)<1		Y	N	N	N

All the control numerical models analysed on 'rock' subsoil cases using ELS® resisted collapse at a maximum building height of five storeys, while the control numerical models with a soft storey at semi-basement level analysed on a predominantly-clay subsoil, resisted collapse at a height of three storeys. The 3Muri® control numerical models analysed on upper coralline limestone and the control numerical models with a soft storey at semi-basement level analysed on clay result in no unsatisfied verifications (hence, the positive verification of the maximum displacement to target displacement ratio for all the 24 load distributions) at building heights of fourteen storeys and one storey, respectively, with respect to the limit state of Significant Damage.

With reference to the information reported in Table 5-15, in the case of the control numerical models analysed using 3Muri® on an upper coralline limestone subsoil, the front facade did not result in shear failure at displacement magnitudes below the maximum displacement of the limit state of Significant

Damage only at a height of one storey. Similarly, with reference to Table 5-16, in the case of the control numerical model with a soft storey at semi-basement level analysed on a clay subsoil, shear failure resulted in the front facade at displacement magnitudes lower than the maximum displacement of the limit state of Significant Damage in all analysed cases, from one to six storeys in height. It was, therefore, concluded that the presence of slender piers was likely to lead to an early shear failure in the front façade. Furthermore, the consideration of the span direction of the reinforced concrete slab parallel to the front facade in the area of the front room suggests that failure of the front façade could lead to a collapse of part of the façade but it would not likely lead to major degradation of the strength of the whole structure. A similar consideration was made with respect to minor transverse walls, which consist of short lengths of wall with most of the wall area taken up by openings, such as in the case of the shorter part of the rear facade. Hence, the presence of shear failure in the front façade and in minor transverse walls was not considered a valid indicator of the seismic capacity of the analysed structures.

Table 5-16 Presence of shear failure with respect to limit state of Significant Damage in walls of control numerical models with soft storey and original plan proportions analysed on clay using 3Muri® vs. building height at adequate seismic resistance for dm/dt criterion.

Control with soft storey at semi-basement level (L:W 2.75: 1) on clay subsoil							
Number of storeys	3Muri® Model number	Maximum height for adequate seismic resistance (displacement capacity criterion) with respect to limit state of Near Collapse (x)	Maximum height for adequate seismic resistance (displacement capacity criterion) with respect to limit state of Significant Damage (x)	Shear failure present in longitudinal walls with respect to limit state of Significant Damage (Y/N)	Shear failure present in main transverse walls with respect to limit state of Significant Damage (Y/N)	Shear failure present in minor transverse walls with respect to limit state of Significant Damage (Y/N)	Shear failure present in front façade with respect to limit state of Significant Damage (Y/N)
6	3M76			Y	Y	Y	Y
5	3M77			Y	Y	Y	Y
4	3M78			Y	Y	Y	Y
3	3M79			Y	Y	Y	Y
2	3M80			Y	N	Y	Y
1	3M81	x	x	N	Y	N	Y

Nevertheless, Tables 5-15 and 5-16 indicate that the main transverse walls exhibit shear failure only at a height of fifteen storeys in the control numerical models analysed using 3Muri® on upper coralline limestone between heights of one to fifteen storeys, and at all building heights from one to six storeys (with the exception of the two-storey numerical model) in the case of the control numerical models, which include a soft storey at semi-basement level and were analysed on clay. On the other hand, the longitudinal walls exhibit shear failure in the control numerical models analysed on upper coralline limestone at building heights of one to five storeys. Moreover, no shear failure was exhibited along the longitudinal orientation at heights of six to fifteen storeys. Furthermore, the control numerical

models with a soft storey at semi-basement level analysed using 3Muri® on clay exhibit shear failure in longitudinal walls at heights of two to six storeys, while no shear failure in this orientation is exhibited at a height of one storey.

In the case of the control numerical models with a soft storey at semi-basement level analysed on clay, the absence of shear failure in the longitudinal and the main transverse walls occurs at building heights of one and two storeys, respectively, hence close to both the 3Muri® maximum building height for adequate seismic resistance with respect to the displacement capacity criterion for the limit state of Significant Damage and the maximum building height at which collapse was resisted in the corresponding ELS® numerical models. On the other hand, the absence of shear failure in the main transverse walls of the control numerical models analysed on rock at building heights, which are significantly higher than the maximum building height at which collapse was resisted in the corresponding ELS® numerical models, in addition to the presence of shear failure in longitudinal walls up to an overall building height of five storeys, while no shear failure is exhibited by the same walls at higher building heights, when it is known that the sway stiffness of shear walls decreases significantly with increase in height, cannot be justified, particularly in the context of the construction characteristics of contemporary loadbearing URM building typology in a real life scenario.

The presence of shear failure in 3 out of the 4 wall categories considered in this research study from building heights of two storeys upwards in the case of the control numerical models with a soft storey at semi-basement level analysed on clay when compared to the evidently lower occurrence of shear failure in the 4 wall categories in the case of the control numerical models analysed on rock, highlights the more severely damaged state of the control numerical models, which include a soft storey. Furthermore, it suggests that the reduced capacity of the latter case to redistribute forces following the exceedance of the shear resistance in several main structural elements since the majority of loadbearing walls do not go down to foundation level (thereby leading to a reduced wall area at the lowermost storey), leads to a significantly reduced seismc resistance.

As shown by Morandi [129] in a study on the overstrength factors applicable to masonry structures with and without flexural coupling between walls, while the redistribution of forces to other walls after the attainment of the maximum shear resistance of specific members could explain the occurrence of shear failure in longitudinal walls up to a height of five storeys in the control numerical models, while no shear failure is exhibited in longitudinal walls of corresponding numerical models at a higher number of storeys, this level of redistribution would only be possible in the presence of the full coupling between intersecting walls and the presence of ring beams at slab levels, both of which are assumed in 3Muri®. However, in the case of the contemporary loadbearing URM building typology under study, where the degree of coupling between intersecting walls might not be of the extent assumed in the 3Muri® numerical models and where the presence of a ring beam at storey perimeters is not typical, the absence of shear failure in longitudinal walls at building heights higher than five storeys, and in main transverse walls at heights below fifteen storeys in the control numerical models, is highly unlikely. It was therefore concluded that the shear failure in the main walls of the numerical models does not lead to reliable estimates of the seismc capacity of the building typology under study.

5.2.6 Variation of the reduction factor 'q_u' in the x- and y-directions resulting from the non-linear static pushover analyses

In the non-linear static pushover analysis carried out using 3Muri®, for every considered load distribution, the maximum displacement of the centroid of the storey at the level of the control node (indicative of the structure displacement capacity), resulting from the base shear – displacement curve corresponding to the particular load distribution considered for the analysed multi-degree-of-freedom system, must be compared to the seismic demand of the earthquake on the structure (i.e. the target displacement) as calculated from the elastic acceleration response spectrum for the equivalent single-degree-of-freedom system. Hence, the multi-degree-of-freedom system is converted to an equivalent single-degree-of-freedom system using the N2 method, which was developed by Fajfar [127] and which was also implemented in Annex B of Eurocode 8: Part 1 [4]. In structures which exhibit a non-linear response and whose fundamental period (T*) for the equivalent single-degree-of-freedom system is lower than the period at the end of the constant spectral acceleration section of the elastic response spectrum (T_c), the calculated target displacement for the equivalent single-degree-of freedom system (d^*_{et}), which is based on the assumption of infinite elastic response, must be adjusted to take into consideration this non-linear response of the structure through Equation B.10 in Annex B of Eurocode 8: Part 1 [4], which is hereunder reported as Equation 5-2:

$$d_t^* = \frac{d_{et}^*}{q_u}\left[1 + (q_u - 1)\frac{T_c}{T^*}\right] \geq d_{et}^*$$

Equation 5-2

where, d_t^* is the target displacement of the equivalent single-degree-of-freedom system with period T* and exhibiting a non-linear response in m; d_{et}^* is the target displacement of the equivalent single-degree-of-freedom system with period T* and unlimited elastic behaviour in m and q_u is the reduction factor, which is defined in Clause B.5 of Eurocode 8: Part 1 ([4] p. 217) as:

> 'the ratio between the acceleration in the structure with unlimited elastic behaviour $S_e(T^*)$ and in the structure with limited strength F_y^*/m^* '

and in Equation B.11 of Eurocode 8: Part 1 [4] as:

$$q_u = \frac{S_e(T^*)\, m^*}{Fy^*}$$

Equation 5-3

where, $Se(T^*)$ is the elastic acceleration response spectrum for a single-degree-of-freedom system with period T^* in m/s^2; m^* is the mass of the equivalent single-degree-of-freedom system in kg; and F_y^* is the yield force of the single-degree-of-freedom system in N.

On the other hand, the behaviour factor 'q', applied in the linear static analysis method as a reduction factor to the seismic actions derived from the elastic acceleration response spectrum such that the resulting design seismic action is lower than that derived assuming a linear elastic response, thereby, avoiding the need of an inelastic structural analysis, is defined in Clause 3.2.2.5(3)P of Eurocode 8: Part 1 ([4] p.41) as:

> 'an approximation of the ratio of the seismic forces that the structure would experience if its response was completely elastic with 5% viscous damping, to the seismic forces that can be used

in the design, with a conventional elastic model, still ensuring a satisfactory response of the structure'.

The behaviour factor 'q' takes into account the ability of the structure to dissipate energy, and the overstrength, which, represents the ability of the structure to redistribute the forces once elements reach their maximum flexural or shear strength, therefore, resulting in a higher ultimate resistance than the yield force used in design. Hence, by definition, the behaviour factor 'q' is equivalent to:

$$q = \frac{S_e(T^*)}{S_d(T^*)}$$

Equation 5-4

where, $S_e(T^*)$ is the elastic acceleration response spectrum for a single-degree-of-freedom system with period T^* in m/s^2; and $S_d(T^*)$ is the design acceleration response spectrum for a single-degree-of-freedom system with period T^* in m/s^2.

Fajfar [127] makes an explicit distinction between the reduction factor denoted by 'q_u' and the behaviour factor denoted by 'q'. This distinction is based on two main considerations. The first is the difference between the yield acceleration (Fy^*/m^*) and the design acceleration ($S_d(T^*)$), where the latter is typically a lower value since it includes a further reduction due to the overstrength. Eurocode 8: Part 1 [4] considers the additional reduction of seismic actions due to overstrength in the case of reinforced concrete and steel structures (in Tables 5.1 and 6.2 of Eurocode 8: Part 1 [4], respectively), however, not for masonry structures. In the case of masonry structures, the maximum values of behaviour factor 'q' are given in Table 9.1 of Eurocode 8: Part 1 [4], with the recommended value of 'q' for unreinforced masonry structures designed in accordance with Eurocode 6 [157], but where Eurocode 8 [4] considerations were omitted, defined as 1.5. In the absence of a National Annex to Eurocode 8 for the Maltese Islands, a behaviour factor 'q' of 1.5 is considered applicable to the URM building typology under study.

While Tomaževič et al. [216] confirmed the overall adequacy of the range of values for the behaviour factor 'q' recommended in Eurocode 8 with respect to the different masonry construction systems, Morandi [129] discussed the need for the consideration of overstrength factors even in the case of masonry structures. Based on the definition of the parameters indicated in Figure 5-29, Morandi [129] explains that the (overall) behaviour factor 'q' should be equivalent to the 'basic' behaviour factor 'q_o', which represents the ability of the structure to dissipate energy, multiplied by the overstrength factor (OSR) as follows:

$$q = \frac{F_{elmax}}{F_{el}} = \frac{F_{elmax}}{F_y} . \frac{F_y}{F_{el}} = q_o . \frac{F_y}{F_{el}} = q_o . OSR$$

Equation 5-5

where, F_{elmax} corresponds with the maximum capacity of the structure assuming an unlimited elastic behaviour in N; F_{el} represents the capacity of the structure when the first wall reached its maximum flexural or shear strength in N; and F_y is the base shear at yield in N. The overstrenght factor (OSR) is

defined as the ratio of the actual capacity of the structure to the capacity resulting from the application of seismic code methods.

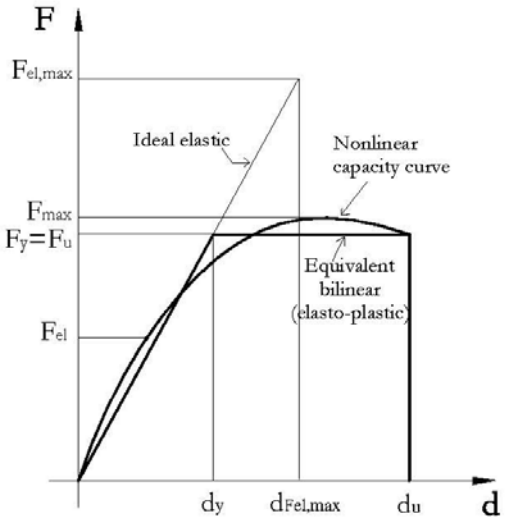

Figure 5-29 Parameters for the definition of the behaviour factor. Source: Morandi ([129] p. 76).

Furthermore, the results of the numerical analyses carried out by Morandi [129] suggest that structures, which do not have a full connection between intersecting or adjacent walls, result in a significantly lower base shear at yield and a lower displacement capacity when compared to corresponding structures, which exhibit full coupling between walls. Hence, a lower overstrength factor would be applicable to the former case with uncoupled walls. This reduction in overstrength factor is estimated by Morandi [129] to be around 6.67%, when considering buildings higher than two storeys, which satisify the criteria for 'simple masonry buildings' outlined in Clauses 9.2 and 9.5 of Eurocode 8: Part 1 [4] . Morandi [129] also quotes a shaking table study using scaled models by Benedetti [217] (that was not accessible to the author of this thesis) which concludes that an overstrength factor of 1.3 is generally adequate for regular unreinforced masonry buildings, which exhibit a box-like behaviour, and that, in the case of irregular masonry structures, this overstrength factor needs to be reduced by 30%. In the URM building typlology under study, some degree of irregularity is present even in the control numerical models, particularly with respect to the distribution of internal spaces, the room sizes, the wall thicknesses and the positions and sizes of wall openings, all of which could give rise to torsional effects. The extent of the structural irregularity is clearly increased further when double height spaces, setbacks and/or a soft storey are present or when the plan layout is elongated further. Therefore, if the additional influence, which the incorrect assumption of a box-like structural behaviour has on the behaviour factor of a contemporary loadbearing URM structure, had to be temporarily disregarded, since all the numerical models analysed using 3Muri® are based on this assumpion, the 30% reduction to the overstrength factor of 1.3 concluded by Benedetti [217], is likely to be applicable in the case of the building typlology under study, hence making the behaviour factor 'q' approximately equal to the 'basic' behaviour factor 'q_o'.

The second consideration with respect to the differentiation between the reduction factor 'q_u' and the ductility-dependant part of the behaviour factor 'q' (equivalent to 'q_o'), as highlighted by Fajfar [218], is based upon two main points, namely, that the values of the reduction factor 'q_u' and the behaviour

factor ‘q’ are based on different limit states; and that values given in seismic codes, such as the maximum behaviour factor values recommended for masonry buildings in Table 9.1 of Eurocode 8: Part 1 [4], include safety factors, and hence, they cannot be used in estimating limiting values with respect to a seismic demand parameter, as is the case with the target displacement.

The reduction factor ‘q_u’, as defined in Clause B.5 of Annex B to Eurocode 8: Part 1 [4], is used to determine the target displacement of the equivalent single-degree-of-freedom system and, hence, the seismic displacement demand of this equivalent single-degree-of-freedom system. The target displacement corresponds to the maximum displacement, which the earthquake under consideration, will impose on the structure at the level of the control node. Fajfar [218] defines 'failure' as the exceedance of the limit state of Near Collapse, which limit state is described in Clause 2.1(1) of Eurocode 8: Part 3 [97] as corresponding to a severely damaged structure, whose vertical loadbearing structural system still has enough capacity to carry the vertical loads, but whose lateral strength and stiffness are severely reduced and, hence, on the verge of failure. Consequently, if 'failure' is the exceedance of the limit state of Near Collapse, the maximum demand (in terms of target displacement) imposed by an earthquake on a structure, corresponds to the maximum displacement exhibited by the structure at the Near Collapse limit state. It can, therefore, be concluded, that the reduction factor ‘q_u’ as defined in Clause B.5 of Annex B in Eurocode 8: Part 1 [4] for the determination of the target displacement, is derived with respect to the limit state of Near Collapse. This also corresponds with the values of the reduction factor ‘q_u’ extracted from the numerical models analysed using 3Muri® in the present study, which are reported for the limit state of Near Collapse.

On the other hand, the recommendations for the design of structures in Eurocode 8: Part 1 [4] are in accordance with the No Collapse Requirement, since this is the ultimate limit state given in this seismic code. Thus, it follows, that the limiting values of the behaviour factor ‘q’ given in Table 9.1 of Eurocode 8: Part 1 [4], that are intended for use in the derivation of the design seismic action (reduced from the elastic response spectrum) and, consequently, of the base shear, the horizontal seismic forces and, hence, the corresponding maximum displacement of the structure (representing the displacement capacity of the structure), are in accordance with the No Collapse Requirement (or its equivalent, the limit state of Significant Damage).

In acknowledgement of the above discrepancies, Fajfar [218] makes reference to the (at the time, unpublished) findings of M. Dolšek, J. Žižmond and N. Lazar Sinković to derive the risk-targeted safety factor for the limit state seismic intensity (γ_{im}) as ‘the ratio between the spectral acceleration at failure S_{aNC} and the design spectral acceleration S_{aD}’ from the probability of exceeding the Near Collapse limit state (i.e. the probability of failure, P_{NC}), as follows:

$$P_{NC} = exp\left[0.5k^2\beta_{NC}^2\right]\frac{1}{T_{De}}\left(\frac{S_{aNC}}{S_{aD}}\right)^{-k}$$

Equation 5-6

where, T_{De} represents the return period of the design ground motion in years; k is a parameter related to the hazard curve (with respect to which, Fajfar [218] suggests that a value of 3 is applicable to high seismicity areas, and lower values are applicable in areas of lower seismicity); and β_{NC} represents the

dispersion arising from variations between ground motion records and modelling uncertainties (typically taken as 0.5).

The return period of a particular limit state is equivalent to the reciprocal of the probability of exceedance of that limit state. Hence,

$$\frac{S_{aNC}}{S_{aD}} = \left(\frac{T_{NC}}{T_{De}}\right)^{1/k} exp\left[0.5k\beta_{NC}^2\right] = \gamma_{im}$$

Equation 5-7

where, T_{NC} is the return period corresponding to the Near Collapse limit state in years [218].

In Equation 5-7, the first term [$(T_{NC}/ T_{De})^{1/k}$] represents the difference between probablility of failure (estimated with respect to the limit state of Near Collapse) and the probability of the design ground motion, while the second term [$exp(0.5k\beta_{NC}^2)$] represents the uncertainties related to the variations between different ground motion records and in the numerical modelling [218]. Therefore, applying Equation 5-7 in the context of the present study, for T_{NC} of 2,475 years, T_{De} of 475 years, k assigned a maximum value of 2 and β_{NC} assigned a value of 0.5, the risk-targeted safety factor for limit state intensity (γ_{im}) results as 2.931, that is, approximately equal to 3.

Fajfar [218], therefore, proposes that, the 'basic' behaviour factor 'q_o' is equivalent to the reduction factor with respect to the limit state of Near Collapse (q_u), divided by the risk-targeted safety factor for limit state intensity (γ_{im}), thereby, resulting in a redefinition of the behaviour factor 'q' as follows:

$$q = \frac{q_u . OSR}{\gamma_{im}}$$

Equation 5-8

Therefore, substituting in Equation 5-8 for an overstrength factor, OSR of 1.0, as concluded by Benedetti [217] in the case of irregular masonry structures, and a risk-targeted safety factor for limit state intensity of 3, as calculated with respect to the contemporary loadbearing URM building typology under study through Equation 5-7, the reduction factor 'q_u' results as equivalent to 3 times the behaviour factor 'q'. Consequently, the equivalent maximum recommended value for the reduction factor 'q_u' was obtained by multiplying the maximum value for behaviour factor 'q' given in Table 9.1 of Eurocode 8: Part 1 [4] with respect to unreinforced masonry structures, which were designed in accordance with Eurocode 6 [157] (without consideration of the requirements included in Eurocode 8 [4]), by a factor of 3. Hence, the equivalent maximum limit of 4.5 was considered applicable to the values of reduction factor 'q_u' resulting from the numerical models of the contemporary loadbearing URM building typology analysed in the present study using 3Muri®.

As discussed in Section 5.2.1, a high discrepancy resulted between the maximum building height at which collapse resistance was exhibited by the control numerical models and the control numerical models with a double height space between Levels 0 and 1 analysed using ELS® with respect to the No Collapse Requirement, and the maximum building height at which an adequate seismic resistance was exhibited in the corresponding numerical models with respect to the equivalent limit state of Significant Damage analysed using 3Muri®. On the other hand, a closer correlation was obtained in the case of the corresponding 3Muri® results with respect to the more severe limit state of Near

Collapse. As discussed earlier in Section 5.2.5, the consideration of the identification of shear failure in main walls did not lead to reliable indications of seismic capacity. Hence, in a further attempt to identify an alternative or an additional failure criterion which, when considered instead of or in conjunction with the failure criterion based on the maximum displacement to the target displacement ratio, would provide a more reliable estimate of the safe building heights of the URM building typology under study, the average value of the reduction factor 'q_u', resulting from the 24 load distributions in the numerical models' x- and y-directions for every non-linear static pushover analysis carried out using 3Muri®, was compared to the equivalent maximum value of 'q_u' of 4.5. This comparison is reported in Tables 5-17 and 5-18 and in Figures 5-30 to 5-33 in the case of the numerical models with original plan proportions, and in Tables 5-20 and 5-21 and Figures 5-34 and 5-35 with respect to the numerical models with extended plan layout proportions.

When applied within the limits recommended by a seismic code (Eurocode 8: Part 1 [4], in the case of the present study), the behaviour factor 'q' can be interpreted as representative of the acceptable level of ductility demand, which can be expected to be exhibited by particular structural systems. In this context, 'ductility' hereby refers to the ability of a structural system to displace, while still exhibiting an adequate vertical load carrying capacity without failing. In the linear elastic analysis procedure outlined in Eurocode 8: Part 1 [4], the maximum value of the behaviour factor 'q' corresponding to the structural system being designed or verified, is used to obtain the design seismic action (in the form of a design acceleration), which is, in turn, used in the evaluation of the base shear and the horizontal seismic forces which are applied at every storey. Hence, the method ensures that the expected ductility demand corresponding to the structural typology is not compromised. On the other hand, by definition, in a non-linear static (pushover) analysis procedure, as carried out using 3Muri®, where the failure criterion is defined as the ratio between the maximum displacement at the storey, where the control node is defined, and the target displacement, the horizontal loads are increased monotonically until the 20% drop in base shear is achieved in accordance with the capacity criterion defined in Clause C.3.3(2) of Eurocode 8: Part 3 [97] with respect to the limit state of Near Collapse. This means that the pushover analysis only stops once this criterion is reached, but it does not stop if the ductility demand of the numerical model, as represented by the reduction factor 'q_u', is higher than the recommended limits. This explains why higher values than the upper limit on the reduction factor 'q_u' derived from the value recommended for the behaviour factor 'q' in Table 9.1 of Eurocode 8 [4], resulted from the numerical models with original and extended plan layouts analysed using 3Muri®, as reported in Tables 5-17 to 5-22 and Figures 5-30 to 5-35. The red dashed line in Tables 5-17, 5-18, 5-20 and 5-21 and Figures 5-30, 5-32 and 5-34 represents the cut-off point between the numerical models, which result in average values for reduction factor 'q_u', which are less than or equal to the equivalent maximum value of 4.5, calculated with respect to the building typology under study, and the numerical models which result in higher average values of 'q_u'. In cases where the average magnitude of the reduction factor 'q_u' increases above 4.5 with an increase in number of floors, but reduces again to below the limit of 4.5 at a higher building height, the cut-off point, and hence, the corresponding building height at which the numerical models exhibit an acceptable level of ductility demand, was set at the lower maximum building height, which satisfied the limiting value of 'q_u' of 4.5.

Tables 5-17 to 5-22 indicate also the building heights at which an adequate seismic resistance was exhibited by the numerical models analysed using 3Muri® with respect to the limit states of Significant Damage and Near Collapse, hence, facilitating the comparison with the building heights at which the modelled structures exhibit an acceptable level of ductility demand. It must be noted, that, in all analysed cases, the y-direction resulted in an acceptable average magnitude of the reduction factor 'q_u'. However, since the weaker orientation of the analysed numerical models is always the x-x (transverse) orientation, the estimates of safe building heights for a level of ductility demand, which does not violate the Eurocode 8 [4] limits, reported in Tables 5-23 and 5-24 are indicated with respect to the results obtained for load distributions applied in the x-x orientation of the numerical models.

Table 5-17 Reduction factor (q_u) with respect to the limit state of Near Collapse resulting from numerical models with original plan proportions analysed on an upper coralline limestone subsoil using 3Muri®.

Number of storeys	Upper coralline limestone subsoil									
	Control (L:W 2.75:1)		Control with soft storey at semi-basement level (L:W 2.75:1)		Control with setbacks at penthouse level (L:W 2.75:1)		Control with double height space between Levels 0 and 1 (L:W 2.75:1)		Control with wider double height space between Levels 0 and 1 (L:W 2.75:1)	
	Mean q_u (NC): X	Mean q_u (NC): Y	Mean q_u (NC): X	Mean q_u (NC): Y	Mean q_u (NC): X	Mean q_u (NC): Y	Mean q_u (NC): X	Mean q_u (NC): Y	Mean q_u (NC): X	Mean q_u (NC): Y
15	4.773	2.422					4.800	2.454		
14	4.693	2.434					4.703	2.463		
13	4.568	2.425					4.618	2.445		
12	4.610	2.277					4.623	2.289		
11	4.758	2.273					4.803	2.322		
10	4.983	2.079					5.130	2.130	5.133	2.124
9	5.438	1.901					5.500	1.938	5.511	1.928
8	5.100	1.749					5.098	1.781	5.111	1.776
7	4.758	1.609					4.738	1.622	4.666	1.658
6	4.309	1.398	16.144	1.655	4.031	1.293	4.246	1.395	4.187	1.605
5	3.842	1.243	12.373	1.572	3.652	1.111	3.744	1.246	3.508	1.262
4	3.135	1.183	8.282	1.211	3.263	1.063	3.067	1.314	3.071	1.409
3	2.732	1.236	11.451	1.493	2.668	1.082	2.684	1.225		
2	2.447	1.148	7.737	1.453						
1	2.061	0.924	7.765	1.246						

Table 5-18 Reduction factor (q_u) with respect to the limit state of Near Collapse resulting from numerical models with original plan proportions analysed on a clay subsoil using 3Muri®.

Number of storeys	Clay subsoil							
	Control (L:W 2.75:1)		Control with soft storey at semi-basement level (L:W 2.75:1)		Control with setbacks at penthouse level (L:W 2.75:1)		Control with double height space between Levels 0 and 1 (L:W 2.75:1)	
	Mean q_u (NC): X	Mean q_u (NC): Y	Mean q_u (NC): X	Mean q_u (NC): Y	Mean q_u (NC): X	Mean q_u (NC): Y	Mean q_u (NC): X	Mean q_u (NC): Y
15	7.158	3.374					7.200	3.414
14	7.026	3.200					7.053	3.224
13	6.853	2.953					6.927	2.973
12	6.913	2.733					6.931	2.748
11	7.138	2.731					7.205	2.787
10	7.359	2.497					7.416	2.555
9	6.758	2.282					6.784	2.326
8	6.119	2.101					6.115	2.135
7	5.708	1.932					5.685	1.945
6	5.170	1.679	24.217	1.989	4.837	1.555	5.095	1.675
5	4.609	1.493	18.557	1.887	4.383	1.333	4.492	1.495
4	3.759	1.419	12.423	1.608	3.918	1.273	3.678	1.580
3			16.922	1.791	3.198	1.299	3.218	1.470
2			11.604	1.743				
1			9.319	1.493				

Table 5-19 Legend corresponding to colour coding in Tables 5-17 and 5-18.

Legend

Maximum height for adequate seismic resistance with respect to limit state of Near Collapse

Maximum height for adequate seismic resistance with respect to limit state of Significant Damage

Maximum height for adequate seismic resistance with respect to limit state of Significant Damage not identified up to height considered in investigations for this case

Maximum height for adequate seismic resistance with respect to limit states of Significant Damage and Near Collapse coincide

Numerical models with average $q_u \leq 4.5$ for specific direction of load distribution

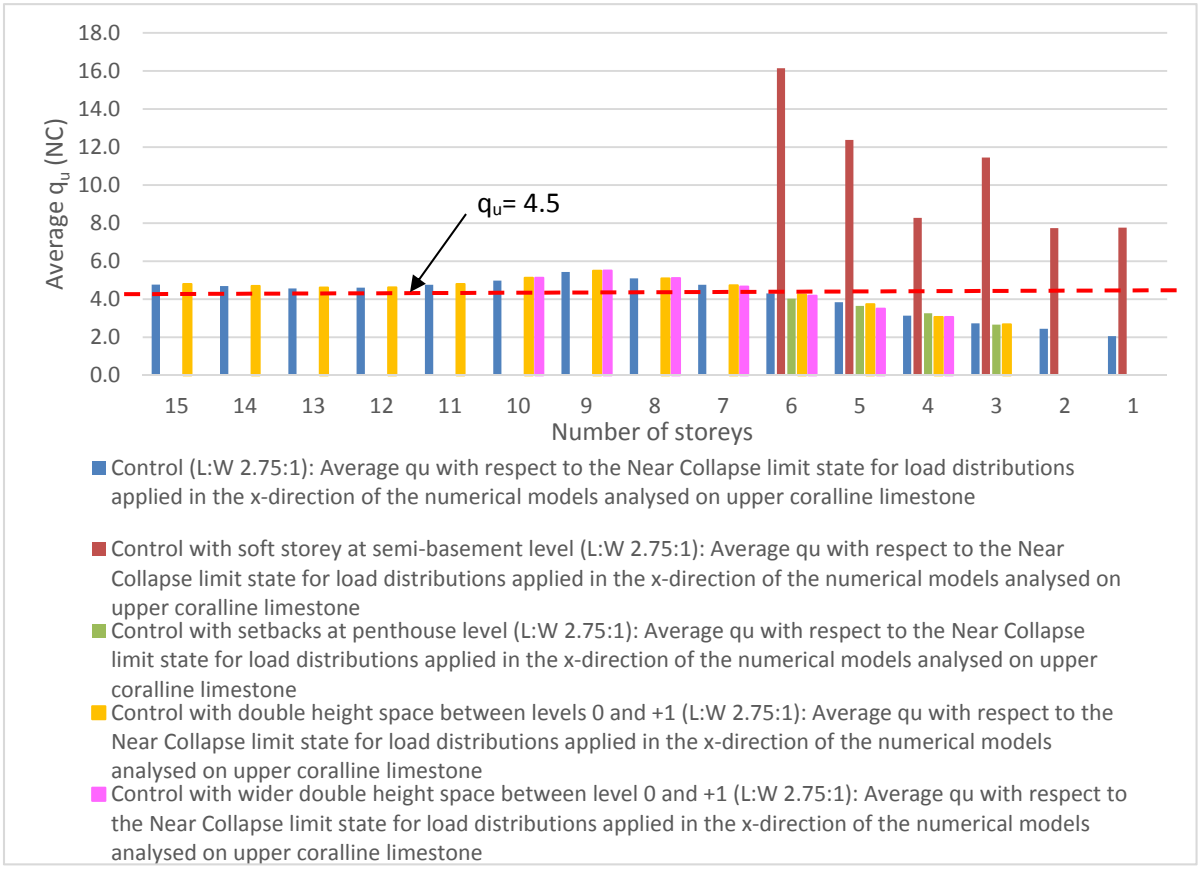

Figure 5-30 Average values of reduction factor 'q_u' resulting from load distributions applied in the x-direction of numerical models with original plan proportions analysed using 3Muri® on an upper coralline limestone subsoil.

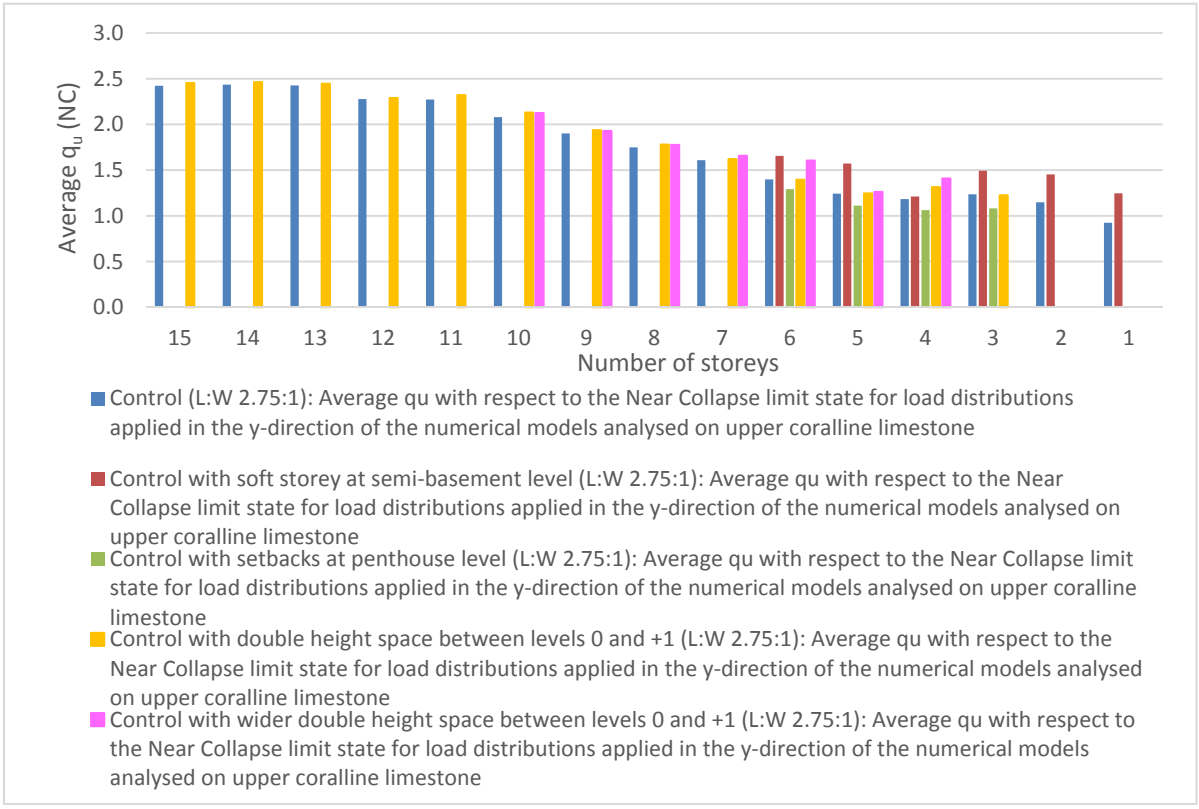

Figure 5-31 Average values of reduction factor 'q_u' resulting from load distributions applied in the y-direction of numerical models with original plan proportions analysed using 3Muri® on an upper coralline limestone subsoil.

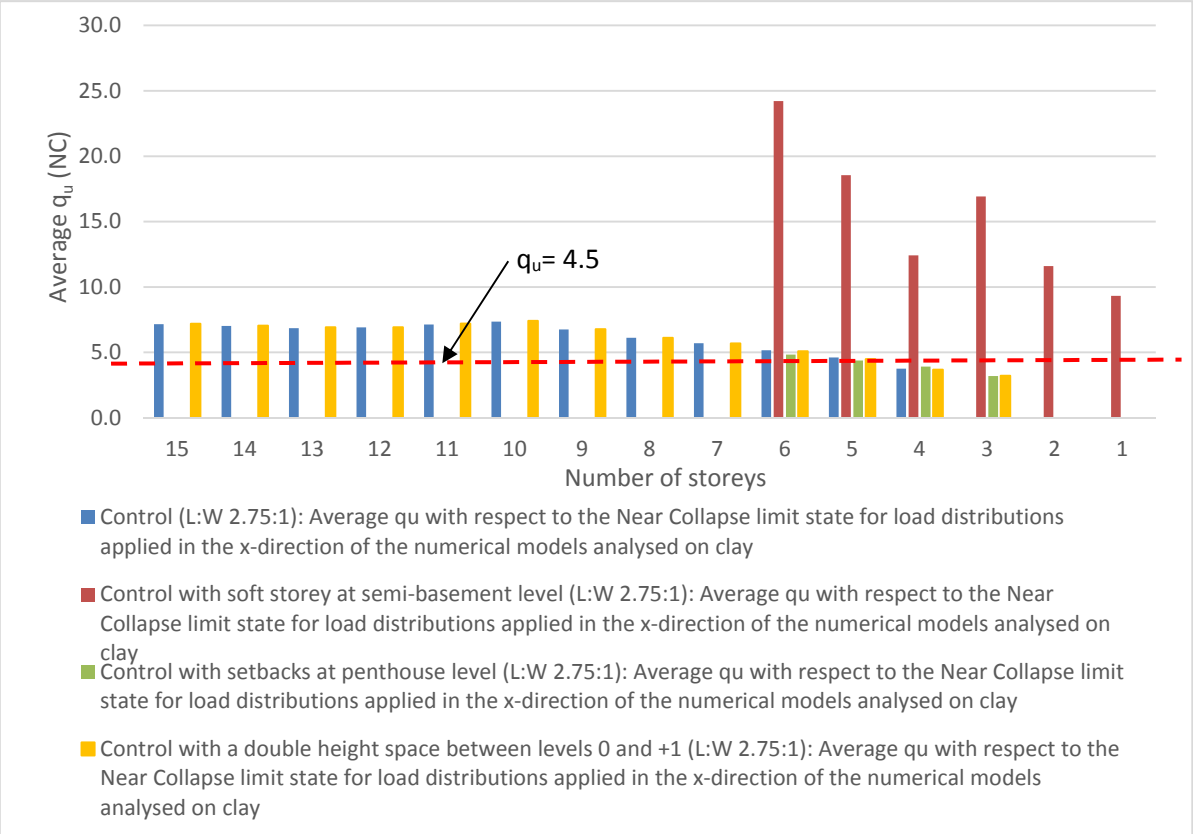

Figure 5-32 Average values of reduction factor 'q_u' resulting from load distributions applied in the x-direction of numerical models with original plan proportions analysed using 3Muri® on a clay subsoil.

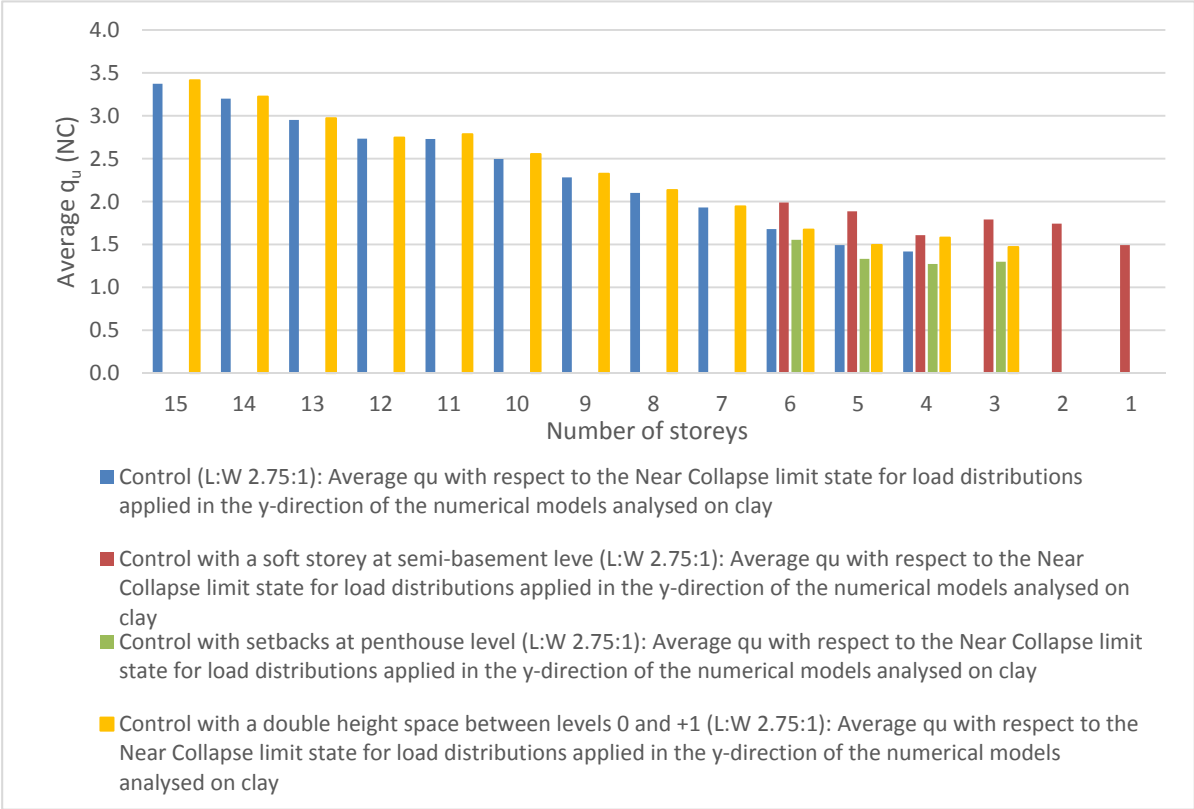

Figure 5-33 Average values of reduction factor 'q_u' resulting from load distributions applied in the y-direction of numerical models with original plan proportions analysed using 3Muri® on a clay subsoil.

Table 5-20 Reduction factor (q_u) with respect to the limit state of Near Collapse resulting from numerical models with extended plan layout proportions analysed on an upper coralline limestone subsoil using 3Muri®.

Number of storeys	Upper coralline limestone subsoil					
	Control (L:W 4:1)		Control with soft storey at semi-basement level (L:W 4:1)		Control with double height space between Levels 0 and 1 (L:W 4:1)	
	Mean q_u (NC): X	Mean q_u (NC): Y	Mean q_u (NC): X	Mean q_u (NC): Y	Mean q_u (NC): X	Mean q_u (NC): Y
8					5.774	1.456
7	5.603	1.319			5.168	1.272
6	4.903	1.097	40.552	1.259	4.714	1.099
5	4.283	0.890	25.589	1.378	4.086	0.909
4	3.583	0.817	13.652	1.793	3.488	0.821
3	2.820	0.823	13.687	1.458	3.163	0.867
2			8.204	1.315		
1			9.074	1.099		

Table 5-21 Reduction factor (q_u) with respect to the limit state of Near Collapse resulting from numerical models with extended plan layout proportions analysed on a clay subsoil using 3Muri®.

Number of storeys	Clay subsoil					
	Control (L:W 4:1)		Control with soft storey at semi-basement level (L:W 4:1)		Control with double height space between Levels 0 and 1 (L:W 4:1)	
	Mean q_u (NC): X	Mean q_u (NC): Y	Mean q_u (NC): X	Mean q_u (NC): Y	Mean q_u (NC): X	Mean q_u (NC): Y
8					6.969	1.748
7	6.722	1.579			6.202	1.592
6	5.885	1.314	60.827	1.657	5.657	1.318
5	5.143	1.068	38.387	1.862	4.904	1.091
4	4.300	0.981	20.588	2.489	4.167	0.982
3	3.385	0.988	20.529	1.989	3.795	1.041
2			12.304	1.581		
1			11.184	1.317		

Table 5-22 Legend corresponding to colour coding in Tables 5-20 and 5-21.

Legend	
	Maximum height for adequate seismic resistance with respect to limit state of Near Collapse
	Maximum height for adequate seismic resistance with respect to limit state of Significant Damage
	Maximum height for adequate seismic resistance with respect to limit state of Significant Damage not identified up to height considered in investigations for this case
	Limit state of Near Collapse results in 1 or more unsatisfied verifications even at a height of 1 storey
	Numerical models with average $q_u \leq 4.5$ for specific direction of load distribution

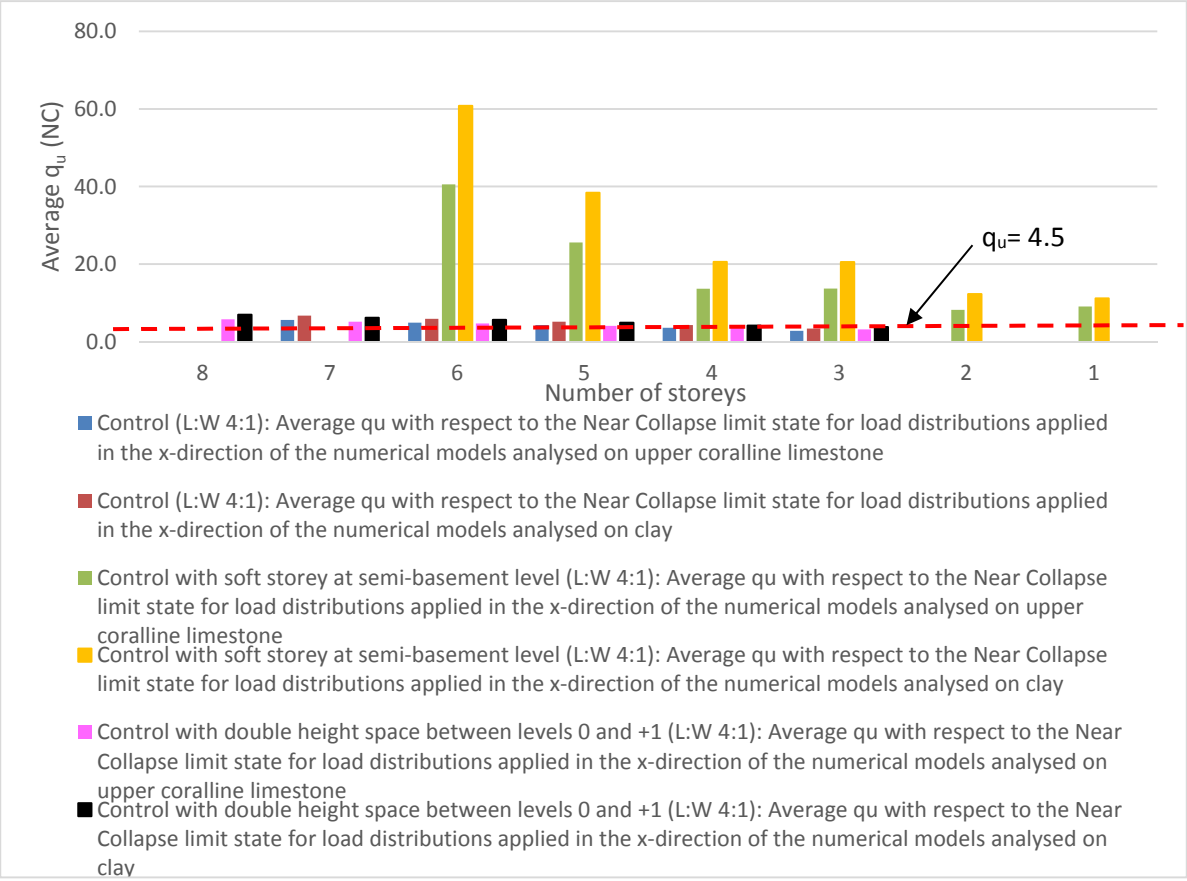

Figure 5-34 Average values of reduction factor 'q_u' resulting from load distributions applied in the x-direction of numerical models with extended plan layout proportions analysed using 3Muri® on upper coralline limestone or clay subsoils.

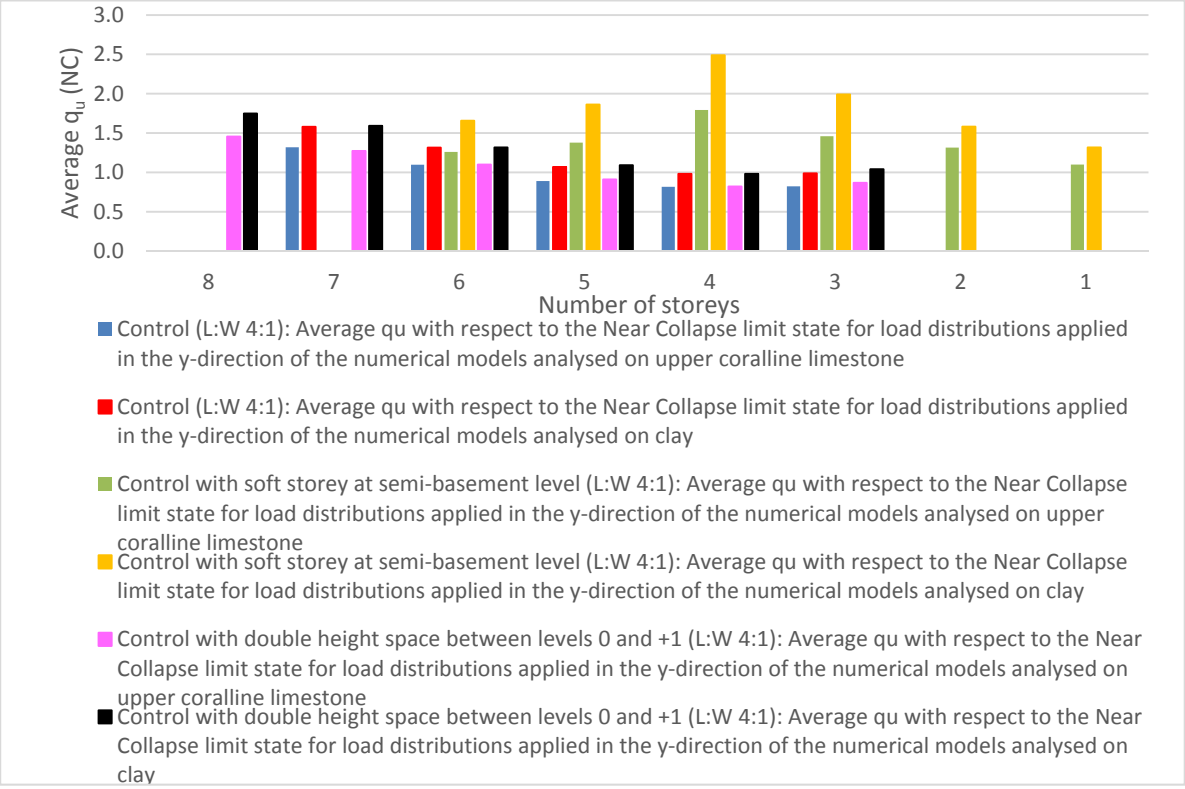

Figure 5-35 Average values of reduction factor 'q_u' resulting from load distributions applied in the y-direction of numerical models with extended plan layout proportions analysed using 3Muri® on upper coralline limestone or clay subsoils.

Table 5-23 Comparison of the maximum number of storeys at which adequate seismic resistance is obtained in numerical models with original plan proportions analysed using 3Muri® and ELS® when considering different failure criteria and limit states.

Case	Upper coralline limestone subsoil				Clay subsoil			
	3Muri® d_{max}/d_t (NC): X	3Muri® d_{max}/d_t (SD): X	3Muri® $q_u \leq 4.5$ (NC): X	ELS® (No Collapse Require-ment): X	3Muri® d_{max}/d_t (NC): X	3Muri® d_{max}/d_t (SD): X	3Muri® $q_u \leq 4.5$ (NC): X	ELS® (No Collapse Require-ment): X
Control (L:W 2.75:1)	6	14	6	5	4	13	4	3, 4
Control with soft storey at semi-basement level (L:W 2.75:1)	1	2	<1		1	1	<1	3
Control with setbacks at topmost storey (L:W 2.75:1)	3	≥6	≥6		3	3	5	4
Control with double height space between Levels 0 and 1 (L:W 2.75:1)	4	14	6		3	13	5	3
Control with double height space between Levels 0 and 1 over whole width of structure (L:W 2.75:1)	7	≥10	6					
	NC Safe building heights in structures which do not have major changes in lateral storey stiffness							

Table 5-24 Comparison of the maximum number of storeys at which adequate seismic resistance is obtained in numerical models with extended plan layout proportions analysed using 3Muri® when considering different failure criteria and limit states.

Case	Upper coralline limestone subsoil			Clay subsoil		
	3Muri® d_{max}/d_t (NC): X	3Muri® d_{max}/d_t (SD): X	3Muri® $q_u \leq 4.5$ (NC): X	3Muri® d_{max}/d_t (NC): X	3Muri® d_{max}/d_t (SD): X	3Muri® $q_u \leq 4.5$ (NC): X
Control (L:W 4:1)	3	5	5	3	5	4
Control with soft storey at semi-basement level (L:W 4:1)	<1	1	<1	<1	1	<1
Control with double height space between Levels 0 and 1 (L:W 4:1)	5	≥8	5	3	5	4
	NC Safe building heights in structures which do not have major changes in lateral storey stiffness					

The maximum and minumum values of reduction factor the 'q_u' resulting from the numerical models analysed using 3Muri® (with the exception of the numerical models with extended or original plan layout proportions, which include a soft storey at semi-basement level, Model 3M83 and Model 3M139, and which result in significantly higher variations in the values of reduction factor 'q_u')[49] are between 19.3% and 1.9% higher and between 18.1% and 2.2% lower than the average values for the value of 'q_u' corresponding to load distributions applied in the x-x orientation of the analysed models respectively (presented in Tables 5-17, 5-18, 5-20 and 5-21 and Figures 5-29, 5-32 and 5-34). In the case of numerical models, which include a soft storey analysed using 3Muri® in the present study, the maximum and minimum values of reduction factor 'q_u' are between 217.0% and 11.1% higher and

[49] Model 3M83 is the five-storey control numerical model with a double height space between Levels 0 and 1, with original plan proportions analysed on upper coralline limestone using 3Muri®, and Model 3M139 is the three storey control numerical model with a double height space between Levels 0 and 1, with extended plan proportions analysed on clay using 3Muri®.

between 95.8% and 10.0% lower than the average values shown in these Tables, respectively, for the x-x orientation of the load distribution.

Figures 5-30 to 5-35 indicate that there is an overall increase in the average magnitude of the reduction factor 'q_u' with increase in number of storeys and that the average 'q_u' values corresponding to the different analysed cases, where there is no major change in lateral storey stiffness throughout the building height, do not exhibit pronounced differences. On the other hand, significantly higher average 'q_u' values result in the case of the numerical models, which include a soft storey at semi-basement level, particularly, in the x-direction for the numerical models with original plan layout proportions and in both the x- and y-directions in the numerical models with extended plan layout proportions, to the extent that even the one-storey models analysed on upper coralline limestone or on clay, with original or extended plan layout proportions, result in average 'q_u' values in the x-direction which exceed the equivalent maximum limit of 4.5. This is most likely due to the higher displacements induced by the reduced lateral storey stiffness of the soft storey at the lowermost level of the analysed structures, in addition to the high mass of the overlying storeys, which aggravates further the displacements. Furthermore, by reference to Equation 5-3, the extent of the discrepancy in the average value of 'q_u', resulting from numerical models which include a soft storey when compared to the other investigated cases, suggests that the higher 'q_u' values could be indicative of the occurrence of 'first yield' at significantly lower magnitudes of base shear. This result confirms the unacceptability of soft storeys in structures, which are intended to resist seismic actions, as suggested in Clauses 4.2.3.3(2) and 4.2.3.3(3) of Eurocode 8: Part 1 [4]. Furthermore, this result stresses this unacceptability to a more significant extent than was observed from the numerical models analysed using ELS®, where, apart from the more pronounced seismic response (such as the higher displacements and the shorter analysis time for the identification of the start of collapse), the maximum building height at collapse resistance of numerical models, which include a soft storey, was equivalent to that of the control numerical model and the control numerical model with a double height space between Levels 0 and 1, for the same type of clay-predominant subsoil.

As indicated in Tables 5-17 to 5-24, in the control numerical model with original plan layout proportions, the maximum building height at which the average value of the reduction factor 'q_u' is within the equivalent acceptable limit of 4.5 corresponds with the building height at which an adequate seismic resistance is exhibited with respect to the failure criterion of the ratio of the maximum displacement to the target displacement for the Near Collapse limit state for both cases of upper coralline limestone and clay subsoils. However, this correspondence in response with respect to the limit state of Near Collapse is not reflected throughout all the investigated cases. For example, in the case of the numerical models with setbacks at penthouse level and original plan layout proportions, the maximum building height at which the resulting average 'q_u' value is lower than the maximum acceptable limit of 4.5, is higher than the maximum building height at which an adequate resistance is achieved with respect to the displacement criterion for both limit states of Near Collapse and Significant Damage and on both upper coralline limestone and clay subsoils. On the other hand, the corresponding case with a double height space between Levels 0 and 1 and original plan layout

proportions results in a maximum building height at which an acceptable average value of 'q_u' is exhibited (i.e. less than 4.5), which is higher than the maximum building height at adequate seismic resistance estimated from the displacement criterion with respect to the Near Collapse limit state and lower than the maximum height for adequate seismic resistance resulting from the displacement criterion with respect to the limit state of Significant Damage, on both upper coralline limestone and clay subsoils. Variations in the estimated safe building heights also result in the cases with extended plan layout proportions.

With reference to Table 5-23, in the numerical models analysed using 3Muri® with original plan layout proportions (with the exception of the cases which include a soft storey) the maximum height at which the average value of the reduction factor 'q_u' is lower than 4.5, is consistently higher than the building height at collapse resistance resulting from the corresponding numerical models analysed using ELS®, even though the latter represent a less severe limit state. This, therefore, suggests that the alternative capacity criterion considering the maximum building height at which an acceptable level of ductility demand is exhibited through the magnitude of reduction factor 'q_u' which is lower than the equivalent acceptable limit of 4.5 can only be used as an additional failure criterion in combination with the main criterion, which compares the capacity of the structure with the demand imposed by the earthquake through the comparison of the maximum displacement and the target displacement. Hence, while the option of altering the failure criterion to the maximum value of the reduction factor 'q_u' is available in 3Muri®, it is not advisable that this criterion is used in isolation as the only failure criterion in a seismic assessment of a structure.

Furthermore, Figures 5-30, 5-32 and 5-34 and Tables 5-17 to 5-24 indicate a number of cases[50], where the maximum building height at which the average magnitude of 'q_u' is lower than 4.5, is higher than the building height at which an adequate seismic resistance with respect to the positive verification of the maximum displacement to target displacement ratio was identified with respect to the limit state of Near Collapse. These results highlight the necessity of further investigations into the estimation of adequate maximum values for the behaviour factor 'q', overstrength factors, dispersion measures and hazard curve parameters (from which, more accurate estimates of the limits to the reduction factor 'q_u' can be derived) corresponding to the contemporary loadbearing URM building typology present in the Maltese Islands. Such investigations should include the variations in the limiting values of 'q_u' in the presence of particular construction materials (such as hollow concrete blockwork or softstone and the presence of a thick gauge polyethylene damp proof course), building characteristics (such as a soft storey or setbacks or double height spaces) or different subsoils. Furthermore, an investigation into

[50] This occurs in the numerical models with original plan proportions and including either setbacks at penthouse level or a double height space between levels 0 and 1 when analysed using 3Muri® on an upper coralline limestone and a clay subsoil; the control numerical models with extended plan layout proportions analysed using 3Muri® on upper coralline limestone and clay subsoils; and the control numerical models with a double height space between levels 0 and 1 and with extended plan layout proportions analysed using 3Muri® on a clay subsoil.

the influence of the effect of the unconservative assumption of full coupling between intersecting walls and the fixed restraints at slab boundaries on the overstrength ratio could improve the prediction of the seismic resistance of URM buildings using a non-linear static pushover analysis.

The building heights corresponding to an acceptable level of reduction factor 'q_u' of 4.5 refer to the limit state of Near Collapse and, hence, they should not really be compared to the building heights exhibiting an adequate seismic resistance with respect to the limit state of Significant Damage. However, as discussed in Section 5.2.1 of the present study, in the case of structures which do not exhibit major changes in lateral storey stiffness throughout their building height, the limit state of Near Collapse gives a more realistic estimate of the safe building height, compared to the less severe limit state of Significant Damage, in view of the over-estimation of the building seismic resistance resulting from the assumed full coupling between intersecting walls and the fixed restraint around slab boundaries, which are at the basis of the non-linear static pushover analysis procedure carried out using 3Muri®. Therefore, as proposed in Tables 5-23 and 5-24, in the absence of more accurate estimates of limits on behaviour factors 'q', overstrength factors and, hence, reduction factors 'q_u' with respect to the contemporary loadbearing URM building typology under study, in cases which have no or a low variation in lateral storey stiffness throughout their height, a conservative estimate of the safe building height with respect to the Near Collapse limit state should consider the lower maximum building height resulting from either:

a) the satisfaction of the failure criterion with respect to the maximum displacement to target displacement ratio, or
b) the ductility criterion with a maximum reduction factor 'q_u' of 4.5 (which may be updated following further research investigations).

In the case of structures, which include a soft storey at the lowermost level, by comparison to the building heights at which collapse resistance resulted in the corresponding numerical models analysed using ELS®, the limit state of Significant Damage results in a closer estimate of the seismic capacity of the structures. However, a larger dispersion in the range of values of the reduction factor 'q_u' resulting from the non-linear static pushover analyses was observed. Furthermore, the exceedance of the maximum limit on the reduction factor 'q_u' of 4.5 with respect to the limit state of Near Collapse even at a building height of one floor, when the failure criterion based on the ratio of maximum displacement to target displacement suggests that such structures with original plan layout proportions, as modelled in the present study, would have an acceptable seismic resistance at this building height, infers that, an unacceptable level of ductility demand might also result in this case with respect to the limit state of Significant Damage at the corresponding safe building heights identified with respect to the displacement capacity criterion.

Nevertheless, it must be acknowledged that the q-factor approach is empirically-based and assumes that the structure is approximately regular in order to ensure a relatively regular dissipation of energy throughout the building. This behaviour is, therefore, not applicable to structures, which include a soft storey at semi-basement level, where the significantly lower lateral storey stiffness of the soft storey leads to stress concentrations and to increased displacements at this level, thereby resulting in an

exhibited 'apparent ductility demand' which is much higher than indicated by the equivalent maximum value of the reduction factor 'q_u' of 4.5 for a regular masonry building. Hence, pending further investigations, the safe building heights resulting from the displacement capacity criterion with respect to the limit state of Significant Damage obtained from the non-linear static pushover analysis of structures which include a soft storey must be used with caution.

5.3 Summary and Conclusions

The preceding sections investigated the validity of a non-linear static pushover analysis for the prediction of the seismic response of the contemporary loadbearing unreinforced masonry (URM) building typology present in the Maltese Islands. This prediction was carried out through the numerical modelling, using the equivalent frame macro-element approach-based software package 3Muri®, of the control numerical models and control numerical models including only one additional building characteristic on upper coralline limestone and clay subsoils, that were previously analysed through a non-linear time-history analysis in the Applied Element Method-based software package ELS® (the results of which were discussed in Chapter 4).

The response parameters resulting from the ELS® analyses under the action of a simulated ground motion record for the Maltese Islands, whose maximum p.g.a. was in accordance with the requirements for a design seismic action with respect to the No Collapse Requirement (according to Eurocode 8: Part 1 [4]) and the corresponding response parameters resulting from the equivalent 3Muri® non-linear static pushover analyses with respect to the limit states of Significant Damage and Near Collapse (according to Eurocode 8: Part 3 [97]) were then compared. The response parameters considered were (i) the maximum overall building height at which the investigated cases exhibited an adequate resistance with respect to the design seismic action for the equivalent limit state, (ii) the natural frequency estimates for the first (fundamental) mode-type of vibration in the x- and y-plan directions of the numerical models, and (iii) the maximum displacement at the centroid of the storey where the control node was defined in 3Muri®, resulting from load distributions applied in the transverse x-x orientation of the 3Muri® numerical models (compared to the maximum relative x-displacement of an element in the left hand side party wall located at the same storey as the 3Muri® control node, in the corresponding ELS® numerical models which resulted in collapse). Furthermore, the maximum overall building height at which the control numerical models analysed on upper coralline limestone and clay subsoils using ELS® and 3Muri® resisted the design seismic action with respect to the No Collapse Requirement in the former case, and the limit states of Significant Damage and Near Collapse in the latter case, were compared to the maximum building heights at which collapse resistance was reported by Borg [20] for contemporary loadbearing unreinforced masonry structures with similar characteristics as the control numerical models and with plan length-to-width proportions of 2:1, 3:1 and 4:1, on equivalent subsoils and with respect to the No Collapse Requirement.

Moreover, in the case of the control numerical models with a double height space between Levels 0 and 1 and with the original plan length-to-width ratio of 2.75:1, the influence on the seismic resistance

of the building typology under study of a wider void at slab Level 1 encompassing the entire width of the structure between the longitudinal party walls, was studied by comparing the resulting response parameters to the equivalent case where the void for the double height space was of the same size as that originally modelled using ELS®. While only a marginal difference was noted between the two cases with respect to the natural frequency estimates for the fundamental modes of vibration and the maximum displacement resulting from load distributions in the x-direction, the case including the wider void resulted in a higher maximum overall building height at which an adequate seismic resistance was exhibited on an upper coralline limestone subsoil with respect to the limit state of Near Collapse. Though an increase in seismic resistance could be attributable to the shift in centre of mass in view of the widening of the void in the slab, which could lead to a reduced eccentricity with respect to the centre of stiffness, and hence, a decrease in torsional forces, it is highly unlikely that such a reduction can justify the difference of four storeys between the maximum building heights which resulted in this case. In addition, the reduction in seismic resistance resulting from the loss of restraint at slab level, and, therefore, the increased slenderness, of the party walls in the area of the floor void is not taken into account in the 3Muri® assessment of these two cases, since out-of-plane failure mechanisms are not considered in this method of analysis.

The study also investigated the influence of extended plan layout proportions on the seismic resistance of the URM building typology by comparing the response parameters resulting from the non-linear static pushover analysis of numerical models with the original length-to-width plan proportions of 2.75:1 to the those exhibited for the extended length-to-width plan proportions of 4:1, in the case of the control numerical models and the control numerical models which include either a soft storey at semi-basement level or a double height space between Levels 0 and 1. A lower natural frequency in the x-direction resulted in all cases, which include an extended plan layout. On the other hand, a lower seismic resistance was exhibited, in terms of the maximum building height for adequate seismic resistance with respect to the limit states of Significant Damage and Near Collapse in the extended plan layout cases of the control numerical models and in the control numerical models with a soft storey at semi-basement level on both upper coralline limestone and clay subsoils, than in the corresponding cases with original plan layout proportions. Conversely, the extended plan layout case with a double height space between Levels 0 and 1 resulted in a higher maximum overall building height for adequate seismic resistance with respect to the limit state of Near Collapse when analysed on an upper coralline limestone subsoil than the corresponding case with original plan layout proportions.

The seismic resistance exhibited in trial models, where different modes of vibration were chosen, suggest that 3Muri® takes into consideration all the modes of vibration selected by the user following a modal analysis of the structure, in the non-linear static pushover analysis considering uniform and modal force distributions. The default failure criterion in the 3Muri® pushover analysis is satisfied if the maximum displacement resulting from the non-linear static pushover analysis, with respect to a particular limit state (representing the displacement capacity of the structure) is higher than the target displacement for the same limit state (representing the displacement demand of the earthquake on

the structure). The maximum building height for adequate seismic resistance with respect to the limit State of Significant Damage resulting from the numerical models analysed using 3Muri®, which do not include major changes in lateral storey stiffness throughout their building height (such as the control numerical models and the control numerical models with a double height space between Levels 0 and 1) is significantly higher than the maximum building height for collapse resistance exhibited by the corresponding numerical models analysed using ELS® with respect to the No Collapse Requirement, for equivalent subsoils. On the other hand, closer correspondence with the ELS® outcomes is obtained when the 3Muri® assessment is carried out with respect to limit state of Near Collapse. Furthermore, in the case of the control numerical models with a soft storey at semi-basement level, where a significantly higher displacement results in the lowermost storey due to the reduced lateral storey stiffness of this level when compared to the overlying floors, the maximum building height for adequate seismic resistance with respect to the limit state of Significant Damage resulting from the 3Muri® analyses is more conservative, though still more comparable, to the building height at collapse resistance resulting from the corresponding numerical models analysed using ELS®. Moreover, the former cases result in higher natural frequency estimates with respect to the first (fundamental) mode of vibration in the x- and y-directions when compared to the corresponding models analysed using ELS®. Conversely, in the presence of a soft storey, the natural frequency for the fundamental mode of vibration in the x-direction estimated through 3Muri® is up to 31.1% higher than the corresponding ELS® estimate, whereas a significant reduction in the discrepancy between the 3Muri® and the ELS® natural frequency estimates is observed in the y-direction, in comparison with the investigated cases exhibiting a more regular distribution of lateral storey stffness.

The results obtained from the investigated cases, and their comparsion to the seismic response of corresponding numerical models analysed using ELS®, suggest that the main shortcoming of the use of the 3Muri® pushover method, for the seismic assessment of the contemporary loadbearing unreinforced masonry building typology present in the Maltese Islands can be attributed to the implicit assumption that the building seismic resistance is governed by their global response through the box-like structural behaviour through the full coupling between intersecting walls and the rigid connections with walls at slab boundaries. This assumption, therefore, disregards the possibility of occurrence of out-of-plane failure mechanisms and it assigns a higher stiffness to the structure than can be realistically attributed to the URM building typology under study (in view of the thin wall sections, the low mortar grade, the absence of mortar in the vertical joints of the wall construction, the frequent use of hollow concrete blockwork for the main loadbearing masonry structural system, resulting in a reduced contact area between overlying courses, and the long unrestrained lengths of walls in corridors, open plan areas and soft storeys). This, therefore results in an overall over-estimation of the building seismic resistance, particularly in cases where the relative displacement between overlying floors is comparable.

In view of the unrealistically high seismic resistance predicted by the 3Muri® numerical models of the URM building typology under study in cases which have a relatively regular lateral storey stiffness throughout their building height, the analysed numerical models were verified with respect to another

two possible failure criteria in order to determine whether these criteria could possibly constitute either valid alternatives to the main default displacement capacity criterion considered in 3Muri®, or whether, when considered in combination with the default 3Muri® criterion, a more realistic estimate of the seismic resistance of the building typology under study could be obtained. The first alternative considered consisted of the presence of shear failure in the longitudinal walls and the main transverse walls of the analysed numerical models at displacements, which are lower than the maximum displacement of the structure with respect to the limit state of Significant Damage. However, the results obtained suggest that the presence of shear failure in the main loadbearing walls of the numerical models is greatly affected by the ability of the structure to redistribute forces following the attainment of the limit in shear resistance in the first walls of the structure. The degree of coupling between intersecting walls and at wall-to-slab connections has a direct bearing on the ability of a structure to re-distribute the forces. Therefore, in structures where the degree of coupling assumed in the numerical models does not adequately reflect the level of restraint provided at these junctions in a real life scenario, the presence of shear failure in the main walls cannot be considered as a valid failure criterion in the context of a non-linear static pushover analysis.

The second alternative considered consisted of the overall building height at which the average value of the reduction factor 'q_u' is lower than the maximum equivalent limit of the reduction factor 'q_u' (derived in the present study with respect to the limit state of Near Collapse as 4.5 for masonry structures with irregular layouts and exhibiting a box-like behaviour). However, with the exception of the control numerical models which include a soft storey, the maximum overall building heights corresponding to the satisfaction of this criterion are higher than the maximum heights for collapse resistance resulting from the corresponding numerical models analysed using ELS®. Furthermore, a number of investigated cases also resulted in higher safe building heights than the corresponding maximum heights for adequate resistance with respect to the (same) limit state of Near Collapse resulting from the consideration of the displacement capacity criterion. These results, therefore, suggest that the building height corresponding to the equivalent maximum limit on the reduction factor 'q_u' can be considered as an additional failure criterion to be used in combination with the displacement capacity criterion, but not as its replacement.

Furthermore, the average value of reduction factor 'q_u' with respect to load distributions acting in the transverse x-x orientation of the analysed structures including a soft storey at semi-basement level, is higher than the equivalent maximum limit on 'q_u' of 4.5 even at an overall building height of one storey for both upper coralline limestone and clay subsoil cases. This, therefore implies that the maximum building height, at which the displacement criterion is satisfied with respect to the limit state of Near Collapse, results in a level of ductility demand, which is higher than the maximum allowable ductility demand in a masonry structure. This result highlights the extent to which the presence of a soft storey in a masonry structure, which is meant to resist seismic actions, is inadmissible even for structures located on an upper coralline limestone subsoil. Furthermore, while representing the response with respect to the limit state of Near Collapse, this result implies that, when a soft storey is present in a masonry structure, the building heights at which the displacement criterion is satisfied with respect to

the limit state of Significant Damage, should be accepted with caution in view of the excessive ductility demand resulting from the lower lateral storey stiffness at the soft storey level.

Therefore, on the basis the above arguments and pending further investigations with respect to the contemporary loadbearing URM building typology, the displacement capacity criterion should be used as the main failure criterion for the non-linear static assessment of this building typology for both the limit states of Significant Damage and Near Collapse, including due consideration of the maximum equivalent limit on the reduction factor 'q_u' in the latter limit state, and the lower resulting building height should be adopted. Furthermore, in the case of non-linear static assessments carried out with respect to the limit state of Significant Damage, in structures exhibiting a major change in lateral storey stiffness within their height, the displacement capacity criterion with respect to this limit state can be used. On the other hand, when a more regular lateral storey stiffness is present throughout the structure, the Near Collapse displacement capacity limits are more applicable, in order to compensate for the over-estimation in the seismic resistance due to the assumed coupling between respective walls and at slab boundaries, which is not representative of the characteristics of the building typology under investigation. Moreover, seismic assessments carried out through non-linear static pushover analysis methods must be verified with respect to realistic magnitudes of displacements, even in cases where the displacement capacity criterion is satisfied for all 24 load distributions. Furthermore, the additional confirmation of the adequacy of the seismic resistance of the structure for the reduction of a further storey, following the attainment of the satisfactory verification of the displacement capacity criterion, is advisable, in view of the influence of the non-linear analysis settings on the accuracy of the seismic assessment.

Chapter 6 CONCLUSIONS AND RECOMMENDATIONS FOR FUTURE RESEARCH WORK

6.1 Conclusions

The achievement of a sound understanding of the seismic response of a building typology which constitutes the major part of the newer developed urban areas in the Maltese Islands is of vital importance. Suggestions for retro-fitting strengthening measures of existing buildings and the drafting of regulations limiting the type of new constructions erected in particularly vulnerable areas can only be carried out after the vulnerability of this building typology to seismic actions is adequately assessed and the particular characteristics, which impair the seismic resistance of the contemporary loadbearing URM building typology, are identified.

6.1.1 Research objectives: summary of findings and conclusions

This research study was primarily aimed at the evaluation of the seismic vulnerability of the contemporary loadbearing URM building typology through the identification of the building characteristics, which alter the seismic response of this building typology and, the investigation of this seismic response through full non-linear dynamic analyses for the determination of the relative influence of the different characteristics investigated. The validity and limitations of a non-linear static pushover analysis method which assumes, by default, a box-like behaviour, for the seismic assessment of the URM building typology under study, was also investigated.

6.1.1.1 Development of the New Form and verification of its rating system

The 13 principal indicators, reproduced below from Sapiano et al. [148], which is due to be submitted for publication, form the basis of the developed rating system for the preliminary version of the New Form for the seismic viulnerability assessment of the URM building typology under study. References to the main published sources considered in the development of the rating system for every Section of the New Form are included in brackets next to the respective Section numbers.

i. Section 2 [16] [17]:
- number of storeys (vs. the type of underlying ground formation – rock or clay);
- presence of long and narrow plan layout;
- presence of a non-regular plan layout;

ii. Section 3 [27]:
- presence of a soft storey and/or vertical irregularity;
- presence of large openings;

- presence of double height spaces;
- presence of misalignment between the total number of floors of adjacent buildings (≥ 1 floor);

iii. Section 4 [26] [71] [75]:
- presence of lightweight (flexible) slab construction systems;
- presence of semi-rigid slab construction systems;
- presence of an inadequate / total absence of abutment in masonry arches or vaults;

iv. Section 5 [26] [71]:
- presence of minor, medium severity or severe cracks;

v. Section 6 [16] [17]:
- type of ground present (stable / gives rise to amplifications of seismic waves / unstable);

vi. Section 8:
- degree of availability of the internal plans (in full / in part/ not available).

The comparison of the seismic vulnerability ratings resulting from the assessment of 183 buildings in the Test Sites using the New Form, to the ratings obtained using other existing methods in use in other countries, suggested that the developed rating system:

a) results in more conservative estimates than the FEMA 154 (second edition) [27] and the GNDT level 2 [26] assessment methods. The higher ratings are mainly due to a more comprehensive consideration of the characteristics influencing the seismic response of this URM typology;
b) takes only very limited consideration of characteristics which influence the alteration of the seismic response of structures in view of their location within an aggregate (aggregate effect).

6.1.1.2 Statistical analysis

The three-stage statistical analysis of the data collected through the New Form for the 183 buildings in the Test Sites, and the corresponding seismic vulnerability ratings, resulted in 11 significant predictors which, are reproduced below, in the order of importance starting with the most significant:

i) total number of floors (Section 2, entry 26);
ii) presence of large openings on main façade 4 (Section 3, entry 76);
iii) presence of slabs spanning in one direction and not tied to each other / to walls parallel to their span (Section 4, entry 92);
iv) absence of intermediate walls in loadbearing masonry building in one or more storeys (Section 3, entry 65);
v) presence of double height spaces facing infrastructure for accessibility / connection (Section 3, entry 54);
vi) presence of long corridor / garage / other open plan space directly adjacent to party wall (Section 3, entry 63);
vii) evidence of shared party wall (Section 3, entry 62);
viii) presence of setbacks along main façade 3 at Level 1 (Section 3, entry 80b);
ix) presence of projecting rooms / balconies at two or three levels (Section 3, entry 82c);
x) proportions of building on plan at typical plan level (width : length) (Section 2, entry 33);
xi) vacant site directly adjacent to building (Section 3, entry 61).

The examination of the 11 significant predictors of the final seismic vulnerability ratings indicates:

a) a good correlation resulted between the significant predictors identified from Sections 2 and 3 of the New Form, and the building characteristics considered in the developed rating system for these Sections, suggesting the validity of the rating system for these two Sections;

b) that 8 out of the 11 significant predictors correspond with building characteristics recorded in Section 3 of the New Form, confirming the additional weighting attributed to this Section.

6.1.1.3 ELS® non-linear dynamic analyses: main outcomes

The parametric investigation of six building/ ground characteristics of the URM building typology under study, considered both individually and in combination, through a non-linear dynamic analysis using the software ELS® (Extreme Loading® for Structures by ASI, Version 3.1), and the detailed evaluation of the resulting dynamic properties and response parameters, resulted in the following conclusions.

i. Lack of clarity in a) the variation in seismic resistance resulting from numerical models, investigating the presence of two or three additional building characteristics in combination, and b) the relative influence of the building characteristics on the seismic response of the single building characteristic numerical models of the URM building typology under study at overall heights of six and five storeys, was very likely the consequence of complex interactions between the seismic responses resulting from the various building characteristics.

ii. The consistently lower maximum building heights for collapse resistance exhibited by numerical models analysed on clay-predominant subsoils, suggest that a higher seismic vulnerability can be associated with buildings erected on more flexible subsoils.

iii. The higher overall building height for collapse resistance exhibited by numerical models including setbacks at penthouse level, when compared to the other investigated cases, suggests that, for the proportions of the setbacks and the plan layout considered in the present study, a lower seismic vulnerability results in the presence of this characteristic.

iv. A higher seismic vulnerability linked to the presence of a soft storey is evidenced by: a) the higher reduction in natural frequency resulting at the end of the dynamic loading stage when compared to the natural frequency at the end of the static loading stage, b) the earlier start of failure, particularly, at a height of four storeys; and c) the higher relative x-displacement at slab over semi-basement level at the time of maximum x-displacement at the same position prior to the onset of failure, particularly, in the six- and four-storey cases.

v. The delay in the start of failure of the four-storey numerical model, which includes a double height space and, the higher relative x-displacement at slab over semi-basement level of this numerical model, at the time of the onset of failure at the same position in the corresponding control numerical model, suggests a higher relative ductility capacity in the former case.

vi. The close analysis times at the start of failure at slab over semi-basement level, exhibited by the two- and three-building aggregate control numerical models, suggests that, while an increase in seismic resistance is observed in both cases when compared to the single building control numerical model, no significant improvement is observed between the two- and the three-building cases.

vii. The study of the deformed shape of the analysed numerical models at the corresponding analysis time suggests that higher modes of vibration were exhibited in a number of cases.

viii. The order of relative influence of four of the investigated building characteristics, derived from the comparison of the extracted response parameters is as follows: 1) the number of storeys, 2) the

presence of a soft storey at lowest level, 3) the presence of a double height space between Levels 0 and 1, and 4) the presence of setbacks at penthouse level.

Pending results of further studies, seismic design code verifications are advisable, in the presence of a) an increased building height, b) a soft storey at the lowest level, and (c) a clay-predominant subsoil.

6.1.1.4 3Muri® non-linear static analyses: main outcomes

The main conclusions resulting from the comparison of the seismic response exhibited by numerical models analysed through a non-linear static analysis using the software 3Muri® (developed by by S.T.A. DATA srl, version 11.5.0.6) on upper coralline limestone and clay subsoils with respect to the limit states of Significant Damage and Near Collapse, to that of corresponding numerical models analysed through a non-linear dynamic analysis with respect to the No Collapse Requirement, on equivalent subsoils and for maximum seismic accelerations of equivalent magnitude, using ELS®, are listed below.

i) The box-like structural behaviour assumed in 3Muri® results in an incorrect representation of the wall-to-wall junctions and the slab boundary conditions when applied for the seismic evaluation of the contemporary loadbearing URM building typology under study. The assumed degree of coupling at these junctions is not present in practice, hence, leading to:
   a) an over-estimation of the seismic resistance of the analysed structures in terms of the maximum safe building height of structures exhibiting minor or no variation in the lateral storey stiffness throughout their height, when compared to ELS®, for the equivalent limit state, while a closer correlation resulted for a more severe limit state in 3Muri®;
   b) higher natural frequency estimates obtained using 3Muri® with respect to the control numerical models, and the control numerical models including either setbacks or a double height space, when compared to the corresponding ELS® estimates;
   c) closer estimates of the maximum safe building height using 3Muri® and ELS®, for the equivalent limit state, in structures which exhibit a major discrepancy in the lateral storey stiffness of overlying floors, as in the case of a soft storey, where, the over-estimation of the seismic resistance resulting from the assumed full coupling, is counteracted by the deleterious effect of the higher soft storey displacements;
   d) significantly lower natural frequency estimates, particularly in the transverse x-direction, in control numerical models which include a soft storey at the lowest level using 3Muri® when compared to ELS®, due to the limited number of walls influenced by the excessive stiffness of restraint assumed by 3Muri® at wall-to-wall intersections at soft storey level.
ii) The comparison of the maximum safe building heights for control numerical models analysed using 3Muri® and ELS® on upper coralline limestone and clay subsoils to the results obtained by Borg [20] through a modified 'Equivalent Frame Method' for corresponding structures with length-to-width plan ratios of 2:1, 3:1 and 4:1, suggests a more conservative estimate by Borg [20].
iii) The 3Muri® modal analysis of the investigated cases confirms that first, second, and torsional modes of vibration, and, to a lesser extent, third modes of vibration, contribute significantly to the seismic response of the URM building typology under study.

iv) The maximum horizontal sway displacements of the centroid of the storey at the level of the control node derived through a pushover analysis using 3Muri® were concluded not to be comparable to the maximum relative displacements of an element in the left hand side party wall of the same storey, in the equivalent ELS® analysed cases, and loading direction.

v) The presence of a double height space with a wider void resulted in a higher maximum safe building height with respect to the limit state of Near Collapse than the corresponding case with the original narrower size of void, when analysed using 3Muri®. Hence, only the improvement in seismic resistance arising from the reduction of torsional effects due to the more symmetrical mass distribution was considered, while the increased slenderness of the longitudinal party walls at the void position was overlooked in view of the disregard of out-of-plane failures.

The validity of the seismic resistance estimate for the URM building typology under study resulting from two alternative /additional failure criteria, which could lead to a more reliable seismic resistance estimate than is obtained using the 3Muri® default failure criterion, was investigated. These include:

a) the presence of shear failure in the walls before the attainment of the maximum displacement with respect to the limit state of Significant Damage: this failure criterion did not result in a reliable seismic resistance estimate since the results are significantly influenced by the ability of the structure to redistribute the forces and, hence, by the degree of coupling between intersecting walls;

b) the limit on the acceptable level of ductility demand for masonry structures: the comparison of the maximum safe building heights resulting from the derived equivalent maximum allowable value of reduction factor 'q_u' (of 4.5) with respect to the Near Collapse Limit state, to the maximum safe building heights obtained for equivalent numerical models analysed using ELS® and 3Muri® for the default displacement capacity criterion, suggest that this ductility criterion can be used in combination with the displacement capacity criterion but not as the main failure criterion in a seismic assessment of the building typology under study. In addition, in all analysed numerical control models, which include a soft storey, the average values for reduction factor 'q_u' corresponding to load distributions applied in the transverse x-direction of the numerical models, were higher than the equivalent maximum acceptable limit estimated for 'q_u' even at an overall height of one storey, highlighting the unacceptability of the excessive ductility demand resulting from the presence of this building characteristic.

Therefore, until more refined failure criteria are identified with respect to the local contemporary loadbearing URM building typology, based on the results obtained in this research study, an interim approximation is being proposed in order to partially make up for the over-estimation in seismic resistance resulting from the stiffer wall-to-wall and wall-to-slab junctions. For every verification that is intended to be carried out with respect to the limit state of Significant Damage, it is suggested that seismic assessments using non-linear static pushover analysis methods, are carried out:

a) with respect to the limit state of Near Collapse, if the lateral storey stiffness of the structure does not vary significantly throughout the height of the structure, by considering the lower allowable

height resulting from the displacement capacity criterion and the criterion based on the equivalent maximum value of 4.5 for reduction factor 'q_u'; and

b) if a soft storey or a change in construction method or material is present, which could result in a pronounced difference between the lateral storey stiffness of overlying floors, the non-linear static pushover seismic assessment can be carried out with respect to the limit state of Significant Damage, considering mainly the displacement capacity criterion. Nevertheless, a comparison of the maximum safe building height with respect to the displacement capacity criterion for the limit state of Near Collapse and the maximum safe building height corresponding to an equivalent maximum value of the reduction factor 'q_u' lower than the limit of 4.5, can provide the basis of an informed decision regarding the acceptance or otherwise of a lower overall safe building height for the limit state of Significant Damage.

Furthermore, based on a number of anomalous results observed in the numerical models analysed using 3Muri® in this research study, the following additional recommendations are being suggested:

a) the magnitude of the maximum displacements resulting from all 24 load distributions are to be checked, even if all the load distributions satisfy the displacement capacity criterion;
b) separate verifications with respect to out-of-plane failure mechanisms are required, particularly in walls with significant unrestrained lengths;
c) structures resulting in an adequate seismic resistance with respect to all 24 load distributions considered by 3Muri® are to be verified for a further reduction of one storey.

6.1.2 Limitations of study

i) Non-linear dynamic analyses carried out using ELS®:

a) Limitations included the limited constitutive material models available in Version 3.1 of the ELS® software program, particularly with respect to the representation of the behaviour of clay, and the limited information in the manuals of this program as regards to the modelling and analysis of masonry buildings and ground formation layers under seismic actions.
b) Significant time restrictions resulted due to the long analysis durations and the limited software licence period available, limiting the number of analyses which could be carried out, and conditioning the shortening of the simulated ground motion record applied as input seismic action in all analyses and the size of the analysed numerical models.
c) The inability to specify spring supports along the outer faces of the ground formation layers in order to represent the infinite extents of the ground led to concerns regarding the possible reflection of seismic vibrations at these faces and their influence on the seismic response of the analysed structures.
d) The partial correspondence of the simulated ground motion record used as input seismic action in all final numerical analyses carried out using ELS® with the Eurocode 8 Part 1 Type 1 elastic response spectrum for Type A ground [4], implies that the selected input accelerogram does not completely satisfy the recommendation in Clause 3.2.3.1.2(1)P of Eurocode 8 Part 1 [4] with respect to the full correspondence of artificial accelerograms to the elastic response

spectra for 5% damping defined in Clause 3.2.2.2 of the same code [4]. Nevertheless, in the context of the objectives of this research study, it is considered that this choice of input ground acceleration does not influence the validity of the main conclusions derived from this study.

ii) Non-linear static pushover analyses carried out using 3Muri®:

a) The anomalously high maximum safe building heights with respect to the limit state of Significant Damage resulting in the case of the control numerical models and the control numerical models including a double height space analysed on an upper coralline limestone subsoil were not representative of a realistic seismic resistance of loadbearing masonry structures, hence, necessitating the analysis of a number of investigated cases up to a lower building height. This precluded: i) the identification of the maximum safe building height with respect to the limit state of Significant Damage on an upper coralline limestone subsoil, and ii) a full comparison of the resulting response parameters with the corresponding control numerical model having the original plan layout proportions.

b) 3Muri® was not originally developed and verified on the basis of the contemporary loadbearing URM building typology in the Maltese Islands. It is not excluded that this software program results in a reliable estimate of the seismic capacity of building typologies, which conform with its background assumptions.

6.1.3 Sources of error

a) The main sources of error identified with respect to the numerical analyses carried out using ELS® are listed below.

i) Results from on-site investigations in the Maltese Islands reported by Farrugia et al. [191], suggest that the value of shear wave velocity corresponding to the material properties specified for upper coralline limestone in the numerical models analysed using ELS® in the present research study is excessive, resulting in a stiffer material represented in the numerical models. This observation, in addition to the 0 kg/m^3 density and the altered (increased) values of compressive strength, Young's Modulus of Elasticity and Shear Modulus of Elasticity specified for clay, while resulting in a subsoil scenario which is not representative of the Maltese Islands, could have also influenced the degree of amplification of seismic accelerations and the transmission of seismic vibrations, hence possibly affecting the building response.

ii) The unavailability of a constitutive material model using ELS®, which accurately represents the behaviour of clay, together with the inability to define an alternative material model for this ground layer within the limits of the available software licence, could have led to an imprecise representation of the variation of the Young's Modulus of Elasticity of clay in the three-dimensional blocks throughout the numerical analyses carried out using ELS®.

iii) In all numerical models analysed using ELS® the identification of the start and end of collapse was carried out through the examination of the x- and z-displacement behaviours, respectively, of the element in the left hand side party wall positioned directly below the slab over semi-basement level. The different stiffness and degree of restraint of the respective elements

from which the displacements were extracted from analysed numerical models which included or did not include a soft storey at semi-basement level, are likely to have introduced a margin of error in these results.

b) The main sources of error identified with respect to the numerical analyses carried out using 3Muri® are listed below.

i) As confirmed through trial models carried out in this research study, the selection of the control node at the penultimate level, when compared to the selection of the control node at the topmost storey, results in a lower number of unsatisfied verifications, which difference, though marginal, could have led to inaccurate estimates of the maximum building height for adequate seismic resistance for the different investigated cases.

ii) The increase in the self-weight setting precision from the default value used for the validation of the software program up to a maximum limit of 0.01, was considered acceptable by the S.T.A. DATA srl technical support in cases where unconvergence occurred in the first step of the analysis (Ing. Davide Seni, S.T.A. DATA srl technical support personal communication by email [219] davide.seni@stadata.com, 5th July 2018). However, the influence of the further increase of the self-weight setting precision and/or in the maximum iteration number from the default values due to lack of convergence of a number of numerical models (3M44, 3M45, 3M73, 3M79, 3M119, 3M126) on the validity of the seismic response could not be ascertained.

iii) The maximum displacement of the six-storey numerical models specified by the user in the 3Muri® non-linear static pushover analysis settings, was altered to correspond with 150% of the maximum relative x-displacement exhibited by the equivalent numerical models analysed using ELS® at roof level (Clause 4.3.3.4.2.3 (1) of Eurocode 8: Part 1 [4]). The number of substeps was also revised, keeping the default ratio between the maximum displacement and the number of substeps unchanged at a value of 1.2, since this ratio governs the rate of loading during the pushover analysis. The maximum displacement was, hence, increased or decreased in proportion to the overall building height of the numerical models at every change in building height, keeping the ratio of the maximum displacement to number of substeps constant at 1.2. This resulted in a discrepancy when compared to the default settings of structures with overall building heights which are lower or higher than six storeys since the default ratio of maximum displacement to number of substeps increases with increase in number of floors, as opposed to the constant ratio used in this study.

iv) While the K-Winkler subgrade reaction coefficient, the foundation materials and sizes specified in the cases of upper coralline limestone and clay subsoils differ, the maximum displacement resulting from corresponding numerical models analysed using 3Muri® on different subsoils are identical. The values of Young's Modulus of Elasticity, decreases rapidly with increased stress. Hence, unless a variable K-Winkler coefficient is used, the effect is not simulated correctly in the numerical model [220] (Perit Adrian Mifsud, Assistant Lecturer in Civil and Structural Engineering at the Faculty for the Built Environment of the University of Malta, personal communication by email, adrian.mifsud@um.edu.mt, 2nd November

2018). Questions to the technical support of S.T.A. DATA srl about the K-Winkler coefficient for subgrade reaction remained unanswered at the time of writing.

v) The smearing of the reduced shear capacity over the full height of the external walls at Level 0 for the representation of the presence of the damp proof course in the 3Muri® numerical models, when compared to the localised position of the damp proof course in a real life scenario, could have led to a higher detriment with respect to the seismic resistance of the structure than would be present in a real life scenario.

vi) While the modelling representation of the presence of a balcony or a room projecting outwards from the façade used in the present research study results in the consideration of an approximately correct seismic mass, the position of the mass corresponding to the facade projection is 'artificially' shifted inwards hence, introducing a marginal error in the resulting position of the centre of mass and the centre of stiffness of the storey.

6.1.4 Possible improvements

Possible improvements to the research work carried out, particularly with respect to the ELS® numerical analyses, are listed below. Further considerations are also included under Section 6.2.

a) Further ELS® numerical analyses using the actual compressive strength, Young's Modulus of Elasticity and Shear Modulus of Elasticity of clay for the Maltese Islands and the more gradual variation of these properties would have been advisable.

b) In the absence of a software package for the non-linear dynamic analysis of numerical models, which considers the shear wave velocity of subsoil materials, the density of the ground layers could be obtained from estimates of the shear wave velocity in the upper 30 m of ground, derived from in-situ passive seismic wave techniques (as in the study by Farrugia et al. [191]). It should be noted that the results obtained by Farrugia et al. [191]were not available at the time when the numerical modelling carried out in the present study using ELS® was under way.

6.2 Recommendations for Future Research Work

A number of additional studies which could develop from the research work presented in this thesis are presented below.

1) A study by Pulikanti et al. [221] reported the different rates of amplification affecting seismic accelerations resulting from different subsoil materials. A similar study of the amplification effect of the different ground formation materials present in the Maltese Islands and their thicknesses, on seismic excitations through the use of specialised numerical modelling software would provide an important background to seismic vulnerability assessments.

2) Extensive laboratory investigations on the strength and material properties of local building and ground materials for the accurate numerical modelling of buildings.

3) A study of the degree by which ground formation layers, modelled as three-dimensional blocks, should be extended away from the perimeter of a modelled structure in an ELS® numerical analysis, such that the infinite nature of the ground is adequately represented.

4) An investigation, using numerical modelling, on how changes in the stiffness of subsoil layers affect predominant frequencies of ground layers and the seismic response of overlying buildings, such that the effect of the stiffness of the ground on the transfer of seismic vibrations to and from the building can be adequately evaluated, particularly in the context of the ground formation layers present in the Maltese Islands.
5) The issue of a Draft Masterplan for Paceville [222] (subsequently withdrawn) proposing the development of structures with a maximum building height of fifteen storeys on reclaimed land suggests the need of the study of the seismic response of medium-to-high rise buildings on this subsoil scenario through numerical modelling.
6) The study of the influence of the position within the building (on plan: central, front, back; and throughout the height of the structure) of a plan or vertical irregularity on the seismic resistance of buildings, considering also the effect on the seismic resistance in the presence of an irregularity on more than one floor, as in the case of repeated setbacks in buildings.
7) A detailed investigation through non-linear dynamic analysis of the influence, which the location of a building in a two- and three-building aggregate has on its seismic resistance , with particular consideration of: a) the shared or non-shared common party walls and, hence, the possibility of pounding, b) the presence of adjacent buildings with different relative heights, c) the presence of staggered floors, d) the presence of adjacent buildings with lower or higher stiffness, and e) the position of the building within the building aggregate.
8) A study of the effect of retro-fitting strengthening measures on the seismic resistance of existing buildings, such as the reinforcement of masonry walls with fibre reinforced polymer materials, especially at the soft storey level.
9) The influence of extended plan layout proportions and of a wider double height space spanning the whole width of the structure between the longitudinal party walls on the seismic resistance of the URM building typology under study was investigated using 3Muri® in the present research study. In view of the limitations of the 3Muri® software in the context of the contemporary loadbearing URM building typology, an investigation into the influence of these characteristics on the seismic resistance of this building typology using ELS® is still advisable.
10) The study of the seismic resistance of a contemporary loadbearing unreinforced masonry building typology with hollow concrete blockwork longitudinal party walls.
11) The investigation of the seismic resistance of the contemporary loadbearing unreinforced masonry building typology through a non-linear static analysis using ELS®: a) with and without the presence of ring beams, b) with the representation of the wall-to-wall intersections as considered in the ELS® numerical models analysed in the present study, and the alternative of 'fused' wall-to-wall intersections at all wall intersections, and c) including the comparison to the corresponding seismic responses obtained using 3Muri® in the present research study.
12) The investigation of the seismic resistance of the contemporary loadbearing URM building typology for the same plan layouts with the original plan proportions as investigated in the present study, through a non-linear static pushover analysis using the research software TREMURI, that allows the definition of a link element between the walls [223] which ensures that no flexural or shear

coupling between the connected wall sections is present. The comparison of the response parameters resulting from the corresponding numerical models analysed using TREMURI and 3Muri® could give an insight into the associated 'margin of error' in the estimated seismic response when full coupling is assumed by default.

13) An investigation into the seismic response and the extent of shear failure in the loadbearing walls of the numerical models analysed using 3Muri® in the present research study in the case when a Turnšek-Cacovic shear failure criterion is specified (a) at all storeys, and (b) at all storeys except for Level 0.
14) A study on the estimation of the behaviour factor 'q', overstrength factor, dispersion measures and hazard curve parameters for the contemporary loadbearing URM building typology in the Maltese Islands, including the variation of these parameters in the presence of different construction materials, building characteristics and different subsoil types, in line with the studies carried out by Tomaževič et al. [216], Benedetti [217], Morandi [129] and Fajfar [218].
15) Experiimental verification through a shaking table study of the seismic response of the contemporary loadbearing URM building typology present in the Maltese Islands for the same plan layouts and building characteristics investigated using ELS®, as a direct verification of this numerical analysis method, particularly with respect to the building typology under study.
16) 3Muri® allows the alteration of the default failure criterion with respect to the limit state of Near Collapse (complying with Clause C.3.3(2) of Eurocode 8 Part 3 [97]), to the attainment of failure in the first element, thus eliminating or reducing significantly the consideration of the ability of the structure to dissipate forces. In the context of the contemporary loadbearing URM building typology under study, where the spatial and construction characteristics are unlikely to allow a high degree of dissipation of forces, while still retaining the structural integrity, an investigation into the adoption of this failure criterion with respect to the limit state of Near Collapse, while retaining the failure criterion of the limit state of Significant Damage at 75% of the limiting displacement corresponding to the Near Collapse limit state, could be an important verification.
17) The verification of ELS® and 3Muri® numerical seismic analysis methods through the comparison of the results obtained from experimental investigations on URM wall assemblages with numerical predictions obtained from these two methods.
18) With the availability of a seismic zonation map for the Maltese Islands, it would be possible to carry out regional seismic vulnerability assessments of URM buildings in different localities within the Maltese Islands.
19) The research study could be extended to carry out building loss assessment studies and also to derive analytical fragility curves for different URM buildings within the Maltese Islands subjected to seismic loading.

REFERENCES

1. Times of Malta. 3.6 Earthquake hits Malta - Sicily Channel. Times of Malta. 2016 August 18th: p. 3.

2. INGV. INGV terremoti. [Online].; 2016 [cited 2016 August 31st. Available from: https://ingvterremoti.wordpress.com/.

3. Galea P. Seismic history of the Maltese islands and considerations on seismic risk. Annals of geophysics. 2007 December; 50(6): p. 725-740.

4. CEN. Eurocode 8: Design of Structures for Earthquake Resistance – Part 1 – General Rules, Seismic Actions and Rules for Buildings (EN1998-1:2004) Brussels; 2004.

5. Torpiano A, Bonello MA, Borg RP, Sapiano P, Ellul AM. A methodology for the seismic vulnerability assessment of loadbearing masonry buildings in Malta. In: Cicero C, Lombardo G, editors. Establishment of an integrated Italy-Malta cross-border system of civil protection – Engineering aspects. SIMIT/3. Ariccia, Italy: ARACNE editrice int.le S.r.l.; 2015. p. 133-181.

6. Torpiano A, Bonello M, Borg RP, Sapiano P, Ellul AM. The development of a seismic vulnerability assessment methodology for contemporary loadbearing masonry buildings in the Maltese Islands. International Journal of Sustainable Materials and Structural Systems. 2016; 2(3/4): p. 283-307.

7. Camilleri DH. Vulnerability of buildings in Malta to earthquake, volcano and tsunami hazard. The Structural Engineer. 1999 November; 77: p. 25-31.

8. Pedley HM, House MR, Waugh B. The geology of the Pelagian block: the Maltese Islands. In: Nairn AEM, Kanes WH, Stehli FG, editors. The ocean basins and margins. Boston, MA: Springer; 1978. p. 417-433.

9. Pedley HM, Clarke MH. Limestone isles in a crystal sea: The Geology of the Maltese Islands. Publishers Enterprises Group; 2002.

10. Farrugia D, Paolucci E, D'Amico S, Galea P, Pace S, Panzera F, et al. Evaluation of seismic site response in the Maltese archipelago. In: Panzera F, Lombardo G, editors. Establishment of an integrated Italy-Malta cross-border system of civil protection: Geophysical aspects. Ariccia: ARACNE editrice int.le S.r.l.; 2015. p. 79-98.

11. D'Amico S, Galea P, Borg RP, Lotteri A. Earthquake ground-motion scenario: case study for the Xemjia Bay area, Malta. In: Proceedings of the international conference of European Council of Civil Engineers; 2011; Malta. p. 149-160.

12. Blackman JM. A study on the seismic risk of local buildings [B.E.& A. (Hons) Dissertation]. Malta: University of Malta, Faculty of Architecture and Civil Engineering; 2000.

13. Torpiano A. Seismic risk assessment in Malta. In: SeisMed Workshop III; 1991; Castelnuovo di Porto, Rome, Italy.

14. Galea J. Assessment of the seismic performance and retrofitting strengthening techniques of local heritage buildings [B.E.& A. (Hons) Dissertation]. Malta: University of Malta, Faculty of Architecture and Civil Engineering; 2013.

15. Mangion A. Seismic vulnerability of masonry heritage buildings in Malta [M.Sc. Dissertation]. Malta: University of Malta, Faculty for the Built Environment; 2015.

16. Farrugia J. Seismic vulnerability of local masonry building typologies [B. E. & A. (Hons) Dissertation]. Malta: University of Malta, Faculty of Architecture and Civil Engineering; 2002.

17. Galdes A. Vulnerability of local masonry buildings to seismic loading [B.E.&A. (Hons) Dissertation]. Malta: University of Malta, Faculty of Architecture and Civil Engineering; 2012.

18. Marmara' R. Seismic design of existing loadbearing unreinforced masonry buildings overlying open plan basements retrofitted with reinforced concrete plane frames [M.Eng Dissertation]. Malta: University of Malta, Faculty for the Built Environment; 2016.

19. Tong M. Seismic design of new loadbearing unreinforced masonry buildings overlying open plan basements employing structural steelwork plane frames [M.Eng Dissertation]. Malta: University of Malta, Faculty for the Built Environment; 2016.

20. Borg D. A parametric study of the effect of geometric proportions on the permissible height of local masonry buildings fitted with anti-seismic sway-resistant frames at basement level [M.Eng Dissertation].Malta:University of Malta,Faculty for the Built Environment; 2017.

21. Bonello E. A parametric study on the effect of plan typology on the seismic sway resistance of local unreinforced masonry buildings within an urban building aggregate [M.Eng. Dissertation]. Malta: University of Malta, Faculty for the Built Environment; 2018.

22. Zammit K. The effect of vertical building characteristics upon the seismic resistance of unreinforced masonry building aggregates [M.Eng. Dissertation]. Malta: University of Malta, Faculty for the Built Environment; 2018.

23. Azzopardi J. Structural assessment of the seismic sway resistance of local unreinforced masonry building aggregates with discontinuous internal masonry partition walls [M.Eng. Dissertation]. Malta: University of Malta, Faculty for the Built Environment; 2019.

24. Said N. A parametric study on the use of a local seismic risk assessment form to determine the seismic vulnerability of local unreinforced masonry buildings [M.Eng. Dissertation]. Malta: University of Malta, Faculty for the Built Environment; 2019.

25. Torpiano A, Bonello M, Borg RP, Sapiano P, Ellul AM. The development of a rapid empirical seismic vulnerability assessment methodology for contemporary loadbearing masonry buildings in the Maltese Islands. In: Galea P, Borg RP, Farrugia D, Agius MR, D'Amico S, Torpiano A, et al., editors. Proceedings of the international conference: Georisks in the Mediterranean and their mitigation; 2015; Valletta, Malta: Mistral Service sas. p. 272-275.

26. CNR-ITC, Regione Abruzzo. Manuale per il rilevamento della vulnerabilita' sismica degli edifici. Istruzione per la compilazione della scheda di secondo livello. Appendice n.1 alla pubblicazione 'Rischio sismico di edifici pubblici', Parte 1a Aspetti metodologici, GNDT, 1993 Roma; 2007.

27. Applied Technology Council (ATC). FEMA 154 Rapid visual screening of buildings for potential seismic hazards: A handbook. 2nd ed. Washington, DC.: Federal Emergency Management Agency (FEMA); 2002.

28. Formisano A, Mazzolani FM, Florio G, Landolfo R. A quick methodology for seismic vulnerability assessment of historical masonry aggregates. In: Mazzolani FM, editor. Proceedings of the COST action C26 final conference "Urban habitat constructions under catastrophic events"; 2010; Naples: CRC Press, Taylor and Francis Group. p. 577-582.

29. Formisano A, Florio G, Landolfo R, Mazzolani FF. Un metodo per la valutazione su larga scala della vulnerabilita' sismica degli aggregati storici. In XIV Convegno ANIDIS: L'ingegneria sismica in Italia; 2011; Bari.

30. Formisano A, Florio G, Landolfo R, Mazzolani FM. Numerical calibration of a simplified procedure for the seismic behaviour assessment of masonry building aggregates. In:

Proceedings of the thirteenth international conference on civil, structural and environmental engineering computing; 2011; Stirlingshire, UK: Civil-Comp Press.

31. Formisano A, Florio G, Landolfo R, Mazzolani FM. Numerical calibration of an easy method for seismic behaviour assessment on large scale of masonry building aggregates. Advances in Engineering Software. 2015 February; 80: p. 116-138.

32. Coburn A, Spence R. Earthquake protection. Chichester, England: John Wiley and Sons Ltd; 2002.

33. Karbassi A. Performance-based seismic vulnerability evaluation of existing buildings in old sectors of Quebec [Doctoral dissertation]. Canada: École de technologie supérieure, Montreal, Univeristé du Quebec. 2010..

34. Calvi GM, Pinho R, Magenes G, Bommer JJ, Restrepo-Vélez LF, Crowley H. Development of seismic vulnerability assessment methodologies over the past 30 years. ISET Journal of Earthquake Technology. 2006 September; 43(3): p. 75-104.

35. Valente M, Milani G. Non-linear dynamic and static analyses on eight historical masonry towers in the North-East of Italy. Engineering structures. 2016 May 1st; 117: p. 241-270.

36. Furukawa A, Kiyono J, Kenzo TO. Numerical simulation of the failure propagation of masonry buildings during an earthquake. Journal of Natural Disaster Science. 2012 June; 33(1): p. 11-36.

37. Casolo S. A three-dimensional model for vulnerability analysis of slender medieval masonry towers. Journal of Earthquake Engineering. 1998 October; 2(4): p. 487-512.

38. Karbassi A, Nollet MJ. Application of the Applied Element Method to the seismic vulnerability evaluation of existing buildings. In CSCE 2008 Annual Conference; 2008; Quebec, Canada. ST-401-1/10.

39. Karbassi A, Nollet MJ. Development of seismic vulnerability curves for masonry buildings using the Applied Element Method. In Goodno B, editor. Proceedings of the ATC and SEI 2009 Conference on improving the seismic performance of existing buildings and other structures; 2010; San Francisco: ASCE. p. 1353-1360.

40. Karbassi A, Nollet MJ. Performance-based seismic vulnerability evaluation of masonry buildings using Applied Element Method in a nonlinear dynamic-based analytical procedure. Earthquake Spectra. 2013 May; 29(2): p. 399-426.

41. Karbassi A, Lestuzzi P. Fragility analysis of existing unreinforced masonry buildings through a numerical-based methodology. The Open Civil Engineering Journal. 2012; 6 (Suppl 1-M2): p. 121-130.

42. Kappos AJ, Stylianidis KC, Pitilakis K. Development of seismic risk scenarios based on a hybrid method of vulnerability assessment. Natural Hazards. 1998 March 1st; 17(2): p. 177-192.

43. Chopra AK. Dynamics of structures (Theory and applications to earthquake engineering). New Jersey: Prentice Hall, Inc.; 1995.

44. Calvi GM, Pinho R, Crowley H. State-of-the-knowledge on the period of elongation of RC buildings during strong ground motion. In: Swiss Society for Earthquake Engineering and Structural Dynamics (SGEB), editor. Proceedings of the 1st European Conference of earthquake engineering and seismology, September 2006; 2006; Geneva, Switzerland. p. paper no. 1535.

45. Mucciarelli M, Masi A, Gallipoli MR, Harabaglia P, Vona M, Ponzo F, et al. Analysis of RC building response and soil-builiding resonance based on data recorded during a damaging earthquake (Molise, Italy, 2002). Bulletin of the Seismological Society of America. 2004; 94(5): p. 1943-1953.

46. Gueguen P, Bard PY, Oliveira CS. Experimental and numerical analysis of soil motions caused by free vibrations of a building model. Bulletin of the seismological society of America. 2000 December; 90(6): p. 1464-1479.

47. Lou M, Huaifeng W, Xi C, Yongmei Z. Structure-soil-structure interaction: Literature review. Soil dynamics and earthquake engineering. 2011 December; 31(12): p. 1724-1731.

48. Farghaly AA, Ahmed AH. Contribution of soil structure interaction to seismic response of buildings. Korean Society of Civil Engineers (KSCE) Journal of Civil Engineering. 2013 July; 17(5): p. 959-971.

49. Reza Tabatabaiefar SH, Fatahi B, Samali B. An empirical relationship to determine lateral seismic response of mid-rise building frames under influence of soil-structure interaction. The structural design of tall and special buildings. 2014 May; 23(7): p. 526-548.

50. Reza Tabatabaiefar SH, Fatahi B, Samali B. Seismic behaviour of building frames considering dynamic soil-structure interaction. International journal of geomechanics. 2012 August; 13(4): p. 409-420.

51. Xiong W, Jiang LZ, Li YZ. Influence of soil–structure interaction (structure-to-soil relative stiffness to mass ratio) on the fundamental period of buildings: experimental observation and analytical verification. Bulletin of earthquake engineering. 2016;(14): p. 139-160.

52. Gutenberg B. Effects of ground on earthquake motion. Bulletin of the Seismological Society of America. 1957 July 1; 47(3): p. 210-250.

53. Lang DH. Damage potential of seismic ground motion considering local site effects [Doctoral dissertation]. Germany: Bauhaus University, Weimar. 2004..

54. Murty CVR, Goswami R, Vijayanarayanan AR, Mehta VV. Some concepts in earthquake design of buildings. Gujarat: Gujarat State Disaster Management Authority, Government of Gujarat; 2013 [cited 2016 August 30]. Available from: http://www.iitk.ac.in/nicee/IITK-GSDMA/EBB_001_30May2013.pdf.

55. Arnold CH, Reitherman R. Building configuration and seismic design. New York: John Wiley & Sons, Inc.; 1982.

56. Guevara-Perez LT. "Soft storey" and "weak storey" in earthquake resistant design: A multidisciplinary approach. In: Sociedede Portuguesa de Engenharia Sismica (SPES), editor. 15th World Conference on Earthquake Engineering (15WCEE) 2012; 2012; Lisbon, Portugal: Curran Associates, Inc. p. 856-866.

57. FEMA. FEMA 454 - Designing for earthquakes: a manual for architects: Federal Emergency Management Agency (FEMA); 2006.

58. Al-Ansari LS. Calculating static deflection and natural frequency of stepped cantilever beam using modified Raleigh method. International Journal of Mechanical and Production Engineering Research and Development (IJMPERD). 2013 October; 3(4): p. 107-113.

59. Al-Ansari LS. Calculating natural frequency of stepping cantilevered beam. International Journal of Mechanical & Mechatronics Engineering IJMME-IJENS. 2012 October; 12(5): p. 59-68.

60. Parisi F. Nonlinear seismic analysis of masonry buildings [Doctoral dissertation]. Italy: Università degli Studi di Napoli Federico II, Department of Structural Engineering, Naples. 2010.

61. American Society of Civil Engineers, Structural Engineering Institute. ASCE/SEI 31-03: Seismic evaluation of existing buildings. Reston, Va.: American Society of Civil Engineers (ASCE); 2003.

62. Öztürk T. A study of the effects of slab gaps in buildings on seismic response according to three different codes. Scientific Research and Essays. 2011 September 8; 6(19): p. 3930-3941.

63. Anagnostopoulos SA. Pounding of buildings in series during earthquakes. Earthquake engineering and structural dynamics. 1988 April 1st; 16(3): p. 446-456.

64. Mahmoud S, Abd-Elhamed A, Jankowski R. Earthquake-induced pounding between equal height multi-storey buildings considering soil-structure interaction. Bulletin of Earthquake Engineering. 2013 Aug 1st; 11(4): p. 1021-1048.

65. D'Ayala DF. Force- and displacement-based vulnerability assessment for traditional buildings. Bulletin of Earthquake Engineering. 2005 Dec 11; 3(3): p. 235-265.

66. Ferreira T, Vicente R, Varum H. Vulnerability assessment of building aggregates: A macroseismic approach. In: Proceedings of the 15th world conference on earthquake engineering; 2012; Lisbon, Portugal. p. 18958-18966.

67. Parisi F, Augenti N. Seismic capacity of irregular unreinforced masonry walls with openings. Earthquake engineering and structural dynamics. 2013 Jan 1; 42(1): p. 101-121.

68. Parisi F, Sabella G, Augenti N. Seismic capacity prediction for irregular masonry walls with opening offsets. In: Kruis J, Tsompanakis Y, Topping BHV, editors. Proceedings of the 15th International Conference on Civil, Structural and Environmental Engineering Computing 2015; 2015; Prague: CIVIL COMP PRESS. p. Paper 63.

69. CNR-ITC , Regione Abruzzo. Manuale per il rilevamento della vulnerabilita' sismica degli edifici – Istruzione per la compilazione della scheda di I livello, Appendice n.1 alla pubblicazione 'Rischio sismico di edifici pubblici', Parte 1a Aspetti metodologici, GNDT, 1993 Roma; 2007.

70. Benedetti D, Petrini V. Sulla vulnerabilita' sismica di edifici in muratura: Un metodo di valutazione (A method for evaluating the seismic vulnerability of masonry buildings). L'industria delle costruzzioni. 1984; 149: p. 66-74.

71. Ferrini M, Melozzi A, Pagliazzi A, Scarparolo S. Rilevamento della vulnerabilita' sismica degli edifici in muratura. Manuale per la complilazione della scheda GNDT/CNR di II livello. Versione modificata dalla Regione Toscana. Italy, Direzione Generale delle Politiche Territoriali e Ambientali, settore: Servizio Sismico Regionale; 2003.

72. Cavaleri L, Di Trapani F, Macaluso G, Scaduto G. Assessment of vulnerability. In: Cicero C, Lombardo G, editors. Establishment of an integrated Italy-Malta cross-border system of civil

protection - Engineering aspects. First edition. Ariccia: Aracne editrice int.le S.r.l.; 2015. p. 97-102.

73. Lemme A, Miozzi C, Cifani G. 3H- Analisi dei costi di intervento e riduzione della vulnerabilita' sismica degli edifice residenziali. Modello di analisi. From: Repertorio dei meccanismi di danno, delle tecniche di intervento e dei relativi costi negli edifici in muratura. Regione Marche, UNIVAQ, CNR-ITC: Regione Molise; 2008.

74. Regione Toscana Giunta Regionale. Criteri per l'esecuzione delle indagini sugli edifici in muratura, la redazione della relazione tecnica e la compilazione della scheda di vulnerabilita' II liv. GNDT/CNR con riferimento alle nuove norme tecniche per le costruzioni (D.M. 14 gennaio 2008): Direzione Generale delle Politiche Territoriali, Ambientali e per la Mobilita': Coordinamento Regionale Prevenzione Sismica; 2012.

75. Ferrini M, Decanini L, Pagliazzi A, Scarparolo S. Edifici in muratura in zona sismica. Rilevamento delle carenze strutturali. Manuale per la compilazione della scheda delle carenze: Regione Toscana. Direzione generale delle politche territoriali e ambientali, settore: Servizio Sismico Regionale; 2004.

76. Zuccaro G, Cacace F, Rauci M. MEDEA: A multimedia and didactic handbook for structural damage and vulnerability assessment–L'Aquila Case Study. In: Mazzolani F, editor. Proceedings of COST Action C26-Final Conference Urban Habitat Constructions under Catastrophic Events; 2010. p. 747-754.

77. Borg RP, Indirli M, Rossetto T, Kouris LA. L'Aquila earthquake April 6th, 2009: The damage assessment methodologies. In Proceedings of the Final Conference of COST Action C26, Urban Habitat Constructions Under Catastrophic Events; 2010. p. 16-18.

78. Regione Marche , CNR-ITC , Universita' degli studi dell'Aquila. Repertorio dei meccanismi di danno, delle tecniche di intervento e dei relativi costi negli edifici in muratura: Sisma marche 1997 CNR-ITC (l'Aquila) , editor. Osimo: Tipografia Grafiche Scarponi s.r.l.; 2007.

79. Commissione Tecnica per la Microzonazione Sismica. Analisi della Condizione Limite per l'Emergenza (CLE) dell'insediamento urbano. Standard di rappresentazione e archiviazione informatica. 2nd ed. Rome; 2013.

80. Baggio C, Bernardini A, Colozza R, Corazza L, Della Bella M, Di Pasquale G, et al. Manuale per la compilazione della scheda di 1° livello di rilevamento danno, pronto intervento e agibilità per edifici ordinari nell'emergenza post-sismica (AeDES). 1st ed. Editrice Italiani nel mondo srl. , editor. Rome: Dipartimento della Protezione Civile; 2009.

81. Dolce M, Papa F, Pizza AG. Manuale per la compilazione della scheda di 1° livello di rilevamento danno, pronto intervento e agibilità per edifici ordinari nell'emergenza post-sismica (AeDES). 2nd ed. Dipartimento della Protezione Civile , editor.: Presidenza del Consiglio dei Ministri - Dipartimento della Protezione Civile; 2014.

82. Di Capua G, Peppoloni S, Pergalani F. Scheda per la valutazione qualitativa dei possibili effetti locali nei siti di ubicazione di edifice strategici e monumentali. GNDT, editor. 2001.

83. Di Capua G, Peppoloni S, Compagnoni M, Pergalani F. Una scheda "geologica" per la valutazione degli effetti sismici locali nei siti di ubicazione di edifici: primi risultati della sperimentazione. In: ANIDIS 2009-XIII Convegno nazionale "L'Ingegneria sismica in Italia"; 2009.

84. U.S. Geological Survey, Department of Interior USoA. USGS Science for a changing world. [Online].; 2017 [cited 2017 April 12]. Available from: ftp://hazards.cr.usgs.gov/web/nshm/conterminous/2014/2014pga10pct.pdf.

85. Southern California Earthquake Data Center. Southern California Earthquake Data Center. [Online].; 2013 [cited 2017 April 12]. Available from: http://scedc.caltech.edu/significant/northridge1994.html.

86. U.S. Geological Survey DoIUSoA. USGS Science for a changing world. [Online].; 2017 [cited 2017 April 12]. Available from: https://earthquake.usgs.gov/earthquakes/browse/specialstudies.php.

87. NIBS , FEMA. Multi-hazard loss estimation methodology earthquake model HAZUS-MH 2.1 Technical Manual Washington, DC: Federal Emergency Management Agency (FEMA).

88. Building Seismic Safety Council. FEMA 450-1 NEHRP recommended provisions for seismic regulations for new buildings or other structures, Part 1: Provisions, 2003 Edition. Washington D.C.: Federal Emergency Management Agency (FEMA); 2004.

89. Building Seismic Safety Council. FEMA 451 NEHRP Recommended provisions: design examples. Washington D.C.: Federal Emergency Management Agency (FEMA); 2006.

90. Applied Technology Council (ATC). FEMA P-58-1 Seismic performance assessment of buildings, Volume 1 - Methodology. Washington D.C.: Federal Emergency Management Agency (FEMA); 2012.

91. Applied Technology Council (ATC). FEMA P-58-2 Seismic performance assessment of buildings, Volume 2 - Implementation guide. Washington D.C.: Federal Emergency Management Agency (FEMA); 2012.

92. Applied Technology Council (ATC). FEMA P-154 Rapid visual screening of buildings for potential seismic hazards: A handbook. 3rd ed. Washington D.C.: Federal Emergency Management Agency (FEMA); 2015.

93. American Society of Civil Engineers, Structural Engineering Institute. ASCE/SEI 41-13 American Society of Civil Engineers: seismic evaluation and retrofit of existing buildings. Virginia: American Society of Civil Engineers (ASCE); 2014.

94. Pluss M, Zuzak C, Wright S, Kendro H. Using HAZUS for mitigation planning. Washington, DC: FEMA (Federal Emergency Management Agency); 2018.

95. Applied Technology Council (ATC). FEMA 155 Rapid visual screening of buildings for potential seismic hazards: Supporting documentation. 2nd ed. Washington D.C.: Federal Emergency Management Agency (FEMA); 2002.

96. Applied Technology Council (ATC). FEMA P-155 Rapid visual screening of buildings for potential seismic hazards: Supporting documentation. 3rd ed. Washington D.C.: Federal Emergency Management Agency (FEMA); 2015.

97. CEN. Eurocode 8: Design of structures for earthquake resistance - Part 3: Assessment and retrofitting of buildings. Brussels: CEN; 2005.

98. Swiss Re Zurich. Earthquake and Volcanic Eruptions: a handbook on risk assessment (in-house publication); 1992.

99. Giovinazzi S, Lagomarsino S. A macroseismic method for the vulnerability assessment of buildings. In: 13th world conference on earthquake engineering; 2004; Vancouver, BC, Canada. Paper no. 896.

100. Grunthal G. European Macroseismic Scale 1998 (EMS-98). Luxenburg: European Seismological Commission, Subcommission on Engineering Seismology, Working Group Macroseismic Scales. Conseil de l'Europe. Cahiers du Centre Européen de Géodynamique et de Séismologie; 1998.

101. D'Ayala D, Speranza E. An integrated procedure for the assessment of seismic vulnerability of historic buildings. In: 12th European Conference on earthquake engineering; 2002. Paper 561.

102. Lagomarsino S, Cattari S. PERPETUATE guidelines for seismic performance-based assessment of cultural heritage masonry structures. Bulletin of Earthquake Engineering. 2015 January; 13(1): p. 13-47.

103. Bhowmik A, Mohanty SP. Analysis and design of earthquake resistant masonry buildings [Bachelor of Technology in Civil Engineering Dissertation]: India: National Institute of Technology: Rourkela, Department of Civil Engineering; 2008.

104. Maio R, Vicente R, Formisano A, Varum H. Seismic vulnerability of building aggregates through hybrid and indirect assessment techniques. Bulletin of Earthquake Engineering. 2015 October 1st; 13(10): p. 2995-3014.

105. Vicente R, Parodi S, Lagomarsino S, Varum H, Mendes da Silva JAR. Seismic vulnerability assessment, damage scenarios and loss estimation: Case study of the old city centre of Coimbra, Portugal. In: Proceedings of the 14th world conference on earthquake engineering; 2008; Beijing, China.

106. Maio R, Vicente R, Formisano A, Varum H. Seismic vulnerability assessment of an old stone masonry building aggregate in San Pio delle Camere, Italy. In: Proceedings of the second European conference on earthquake engineering and seismology; 2014; Istanbul.

107. Marques RF, Vasconcelos G, Lourenco PB. Pushover analysis of a modern aggregate of masonry buildings through macro-element modelling. In: Ramos Roman H, Aris Parsekian G, editors. 15th International Brick and Block Masonry Conference 2012; 2012; Florianópolis, Brazil. p. Paper 3B2.

108. Senaldi I, Magenes G, Penna A. Numerical investigation of the seismic response of masonry building aggregates. Advanced materials research. 2010; 33: p. 715-720.

109. Rush A. Seismic evaluation of masonry building conglomerations of adjacent structures [Master's dissertation in earthquake engineering]. Pavia, Italy: University of Pavia; 2007.

110. Ramos LF, Lourenco PB. Modelling and vulnerability of historical city centers in seismic areas: a case study in Lisbon. Engineering structures. 2004 July 31st; 26(9): p. 1295-1310.

111. Munari M, Valluzzi MR, Saisi A, Cardani G, Modena C, Binda L. Limit analysis of macroelements in masonry aggregate buildings as a methodology for the seismic vulnerability study: An application to the umbrian city centres. In: 11th Canadian Masonry Symposium 2009; 2009; Toronto.

112. Munari M, Valluzzi MR, Cardani G, Anzani A, Binda L, Modena C. Seismic vulnerability analyses of masonry aggregate buildings in the historical centre of Sulmona (Italy). In: Proceedings of the 13th International Conference on Structural Faults and Repair; 2010.

113. Valluzzi MR, Munari M, Cardani G, Saisi A, Binda L, Modena C. Aggiornamento della vulnerabilità sismica del centro storico di Campi Alto di Norcia (PG). In: XIII Convegno ANIDIS "L'Ingegneria Sismica in Italia"; 2009; Bologna.

114. Munari M, da Porto F, Valluzzi MR, Modena C. Valutazione della vulnerabilita' sismica di edifici in aggregato. In: Convegno AIST; 2011; Bologna.

115. da Porto F, Munari M, Prota A, Modena C. Analysis and repair of clustered buildings: Case study of a block in the historic city centre of L'Aquila (Central Italy). Construction and building materials. 2013 January 31; 38: p. 1221-1237.

116. Craig RR. Structural dynamics: An introduction to computer methods. United States of America: John Wiley and Sons Inc.; 1981.

117. Meguro K, Tagel-Din H. Applied element method for structural analysis: theory and application for linear materials. Journal of mechanical earthquake engineering, JSCE. 2000 April; 17(1): p. 21-35.

118. Santos DBV, Bandeira AA. Numerical modeling of contact problems with the finite element method utilizing a B-Spline surface for contact surface smoothing. Latin American Journal of Solids and Structures. 2018; 15(8).

119. SAS IP Inc.. 1.3 Contact element capabilities (Ansys Fluent Manual). [cited 2019 July 12]. Available from: https://www.sharcnet.ca/Software/Ansys/17.0/en-us/help/ans_ctec/Hlp_ctec_anscon.html.

120. Betti M, Facchini L, Vignoli A. Time-history analysis of slender masonry towers: a simplified Bouc and Wen approach. In: XXII Congresso AIMETA; 2015; Genoa. p. 257-266.

121. Giordano A, Mele E, De Luca A. Modelling of historical masonry structures: comparison of different approaches through a case study. Engineering Structures. 2002 August 31st; 24(8): p. 1057-1069.

122. Lourenco PB. Structural masonry analysis: recent developments and prospects. In: 14th international brick and block masonry conference; 2008; Australia: University of Newcastle.

123. Lagomarsino S, Penna A, Galasco A, Cattari S. TREMURI program: an equivalent frame model for the nonlinear seismic analysis of masonry buildings. Engineering Structures. 2013 Nov 30;56:1787-99. 2013 November; 56: p. 1787-1799.

124. Magenes G. A method for pushover analysis in seismic assessment of masonry buildings. In: Proceedings of the 12th World conference on earthquake engineering; 2000; Auckland, New Zealand: New Zeland Society for Earthquake Engineerring.

125. Galasco A, Lagomarsino S, Penna A, Resemini S. Non-linear seismic analysis of masonry structures. In: Proceedings of the 13th World Conference on Earthquake Engineering; 2004; Vancouver, B.C., Canada.

126. Galasco A, Lagomarsino S, Penna A. On the use of pushover analysis for existing masonry buildings. In: Proceedings of the 1st European Conference on Earthquake Engineering and Seismology; 2006; Geneva, Switzerland.

127. Fajfar P. A non-linear analysis method for performance-based seismic design. Earhquake Spectra. 2000 August; 16(3): p. 573-592.

128. De Sutter J. Development of a software for the seismic verification of a masonry structure subject to earthquakes [Master of Science in Civil Engineering Dissertation]. Ghent: University of Ghent, Faculty of Engineering and Architecture; 2017.

129. Morandi P. Inconsistencies in codified procedures for seismic design of masonry buildings [Dissertation Masters in Earthquate Engineering]. Pavia: European School of Advanced Studies in Reduction of Seismic Risk,University of Pavia; 2006.

130. Lagomarsino S, Cattari S. Chapter 11 Seismic performance of historical masonry structures through pushover and nonlinear dynamic analyses. In: Ansal A, editor. Perspectives on european earthquake engineering and seismology - Volume 2.: Springer Open; 2015. p. 265-292.

131. Endo Y, Pela' L, Roca P. Review of different pushover analysis methods applied to masonry buildings and comparison with nonlinear dynamic analysis. Journal of earthquake engineering. 2017 November; 21(8).

132. Chopra AK, Goel RK. A modal pushover analysis procedure for estimating seismic demands for buildings. Earthquake engineering and structural dynamics. 2002 March; 31(3): p. 561-582.

133. Kreslin M, Fajfar P. The extended N2 method considering higher mode effects in both plan and elevation. Bulletin of earthquake engineering. 2012 April; 10(2): p. 695-715.

134. Aldemir A, Altuğ Erberik M, Demirel O, Sucuoğlu H. Seismic performance assessment of unreinforced masonry buildings with a hybrid modeling approach. Earthquake Spectra. 2013 February; 29(1): p. 33-57.

135. Chidiac SE, Rainer JH, Guan W, Lu Y, Razaqpur AG. A comparative study of modelling the dynamic characteristics of a solid-stone masonry tower. Transactions on the built environement. 1995; 15.

136. EL Shabrawi A, Verdel T. Modelling of ancient masonry structures by the Distint Element Method under dynamic loads. Transactions on the built environment. 1995; 15.

137. Al-Heib M. Distinct element method applied on old masonry structures. In: Miidla P, editor. Numerical Modelling: InTech; 2012. p. 303-328.

138. Lemos JV. Modelling stone masonry dynamics with 3DEC. In: Numerical modelling of discrete materials in geotechnical engineering, civil engineering and earth sciences: Proceedings of the first international UDEC/3DEC symposium; 2004; Bochum, Germany. p. 7-13.

139. Çaktı E, Oliveira CS, Lemos JV, Saygili O, Görk S, Zengin E. Earthquake behaviour of historical minarets in Istanbul. In: Papadrakakis M, Papadopoulo V, Plevris V, editors. 4th ECCOMAS thematic conference on computational methods in structural dynamics and earthquake engineering; 2013; Kos Island, Greece.

140. Roca P, Cervera M, Gariup G, Pela' L. Structural analysis of masonry historical constructions. Classical and advanced approaches. Archives of Computational Methods in Engineering. 2010 September; 17(3): p. 299-325.

141. Meguro K, Tagel-Din H. A new efficient technique for fracture analysis of structures. Bulletin of Earthquake Resistant Structure Research Center. 1997 March;(30): p. 103-116.

142. Tagel-Din H, Rahman NA. The Applied Element Method, the ultimate analysis of progressive collapse. Structure. 2006.

143. Rota M, Bracchi S, Penna A, Magenes G. Evaluation of the effect of modelling uncertainties on the seismic response of existing masonry buildings. In: Papadrakakis M, Papadopoulos V, Plevris V, editors. 4th ECCOMAS thematic conference on computational methods in structural dynamics and earthquake engineering; 2013; Kos Island, Greece.

144. Oil Exploration Directorate OotPMM. Geological map of the Maltese Islands Sheet 1: Malta. 1993.

145. Engineers Binnie, Deacon, Gourley. Report on geological investigation of the Bajada Ridge, Ghajn Tuffieha and Majesa carried out by the Soil Mechanics Department of Messrs. Richard Costain Ltd. Volume 69/167. London; 1958.

146. Oil Exploration Directorate, Office of the Prime Minister, Malta. Geological map of the Maltese Islands Sheet 2: Gozo and Comino. 1993.

147. Engineers Binnie DG. Report on geological investigation of the Nadur area carried out by the Soil Mechanics Department of Messrs. Richard Costain Ltd. Volume 69/167. London:; 1958.

148. Sapiano P, Camilleri L, Torpiano A, Bonello MA, Borg RP. Statistical sensitivity analysis of the main predictors to be included in a seismic vulnerability assessment method for buildings. (pending submission). .

149. Ballut Blocks Services Ltd.. Precast prestressed concrete panels - safe load tables. [Online]. [cited 2015 March 2nd]. Available from: http://www.ballutblocks.com.

150. Ballut Blocks Services Ltd.. Concrete blocks. [Online]. [cited 2015 February 25th]. Available from: http://www.ballutblocks.com.

151. Xuereb D. Elastic constants for globigerina limestone [B.E.&A. (Hons) Dissertation] Malta: University of Malta, Faculty of Architecture and Civil Engineering; 1991.

152. Cachia J. The mechanical and physical properties of the globigerina limestone as used in the local masonry construction. [B. E.&A. (Hons) Dissertation] Malta: University of Malta, Faculty of Architecture and Civil Engineering; 1985.

153. Buhagiar P. Structural masonry: Experimental determination of the compressive strength of a wall [B.E.&A. (Hons) Dissertation] Malta: University of Malta, Faculty of Architecture and Civil Engineering; 1985.

154. Debattista W. Masonry mortars [B.E.&A. (Hons) Dissertation]. Malta: University of Malta, Faculty of Architecture and Civil Engineering; 1985.

155. Bartolo IF. The strength of the mortar joint [B.E. & A. (Hons) Dissertation]. Malta: University of Malta, Faculty of Architecture and Civil Engineering. 1991..

156. CEN. Eurocode 2: Design of concrete structures. General rules and rules for buildings (EN 1992-1-1:2004). Brussels; 2004.

157. CEN. Eurocode 6. Design of masonry structures. General rules for reinforced and unreinforced masonry structures (EN 1996-1-1:2005). Brussels; 2005.

158. Barbosa CS, Hanai JB. Strength and deformability of hollow concrete blocks: correlation of block and cylindrical sample test results. Ibracon structures and materials journal. 2009 March; 2(1): p. 85-99.

159. Zhu T. Jackson school of Geosciences, University of Texas at Austin. [Online]. [cited 2015 August 17]. Available from: http://www.jsg.utexas.edu/tyzhu/files/Some-Useful-Numbers.pdf.

160. Bowles JE. Foundation analysis and design. 5th ed. Clark BJ, Kimbell KV, Morriss JM, editors. Singapore: McGraw-Hill; 1996.

161. Saliba S. The shear strength of the mortar joint: an investigation of the shear strength of masonry containing a damp proof course. [B.E. & A.(Hons.) Dissertation] Malta: University of Malta, Faculty of Architecture and Civil Engineering; 1993.

162. Helmy H. Consultation Department, Applied Science International, LLC, personal communications by email, huda@appliedscienceint.com, 9th September 2015..

163. Helmy H. Consultation Department, Applied Science International, LLC, personal communications by email, huda@appliedscienceint.com, 13th October 2015..

164. CEN. Eurocode. Basis of structural design (EN1990:2002). Brussels; 2002.

165. Motazedian D, Atkinson GM. Stochastic finite-fault modelling based on a dynamic corner frequency. Bulletin of the Seismological Society of America. 2005 June 1; 95(3): p. 995-1010.

166. Corchete V. Analysis of accelerograms for the earthquake resistant design of structures. International journal of geosciences. 2010; 1(01): p. 32-37.

167. European Facilities for Earthquake Hazard and Risk. [Image of EFEHR SHARE 2013 European Hazard Model for a probability of exceedance of 10% in 50 years and a 95% fractile]. [cited 2017 June 5]. Available from: http://www.efehr.org:8080/jetspeed/portal/HazardMaps.psml.

168. European Facilities for Earthquake Hazard and Risk. [Image of EFEHR SHARE 2013 European Hazard Model for a probability of exceedance of 10% in 50 years and a 50% fractile]. [cited 2017 June 5]. Available from: http://www.efehr.org:8080/jetspeed/portal/HazardMaps.psml.

169. European Facilities for Earthquake Hazard and Risk. [Image of EFEHR hazard curves for the Maltese Islands for a probability of exceedance of 10% in 50 years and a 95% or a 50% fractile]. [cited 2017 June 5]. Available from: http://www.efehr.org:8080/jetspeed/portal/HazardCurves2.psml.

170. Senaldi IE. Numerical investigation on the seismic response of masonry building aggregates [Dissertation for the Master of studies in Earthquake Engineering]] Pavia: University of Pavia, European school for advanced studies in reduction of seismic risk, Rose School; 2009.

171. Bommer JJ, Acevedo AB, Douglas J. The selection and scaling of real earthquake accelerograms for use in seismic design assessment. In: Proceedings of the ACI international conference on seismic bridge design; 2003; La Jolla, California: American Concrete Institute.

172. SM Working Group. Guidelines for seismic microzonation. Rome: Conference of Regions and Autonomous Provinces of Italy – Civil Protection Department; 2015.

173. Applied Science International. Extreme Loading for Structures theoretical manual. Durham, USA; 2013.

174. Ristic D, Yamada Y, Iemura H. Stress-strain based modelling of hysteretic structures under earthquake induced bending and varying axial loads, Research report No. 86-ST-01. Kyoto, Japan: Kyoto University, School of Civil Engineering; 1986.

175. Tagel-Din H, Meguro K. Applied element method for dynamic large deformation analysis of structures. Journal of mechanical earthquake engineering, JSCE. 2000 October; 17(2): p. 215-224.

176. Mifsud A. Assistant lecturer in civil and structural engineering at the Faculty for the Built Environment of the University of Malta, personal communication by email, adrian.mifsud@um.edu.mt, 8th June 2017..

177. Italian Ministry of Infrastructure and Transport. Aggiornamento delle norme techniche per le costruzioni (NTC 2018, in Italian). Decree 17-1-2018, Official Gazette of the Republic of Italy, Ordinary Supplement 42, 20-02-2018; 2018.

178. S.T.A. DATA srl. 3Muri Versione 11 (in Italian). S.T.A. DATA srl; 2017.

179. S.T.A. DATA srl. 3Muri User Manual Release 11.4.0. S.T.A. DATA srl.

180. Roberts J. Determination of normalised strength from the declared mean compressive strength of a masonry unit. [Online].; 2008 [cited 2018 March 8]. Available from: http://www.eurocode6.org/Published%20support%20material/Shape%20Factors.pdf.

181. Malta Competition and Consumer Affairs Authority. Malta National Annex to Eurocode 6: Design of masonry structures - Part 1-1: General rules for reinforced and unreinforced masonry structures. Malta Competition and Consumer Affairs Authority; 2013.

182. Tomaževič M. Shear resistance of masonry walls and Eurocode 6: shear versus tensile strength of masonry. Materials and structures. 2009 August; 42(7): p. 889-907.

183. European Facilities for Earthquake Hazard and Risk. [Image of the EFEHR SHARE 2013 European Hazard Model for a probability of exceedance of 2% in 50 years and a 95% fractile zoomed on the Maltese Islands]. [cited 2018 June 18]. Available from: http://www.efehr.org/en/hazard-data-access/hazard-maps/.

184. European Facilities for Earthquake Hazard and Risk. [Image of EFEHR hazard curve for the Maltese Islands for a 95% fractile]. [cited 2018 June 18]. Available from: http://www.efehr.org/en/hazard-data-access/hazard-curves/.

185. Sadrekarimi J, Akbarzad M. Comparative study of methods of determination of coefficient of subgrade reaction. Electronic Journal of Geotechnical Engineering. 2009 January; 14.

186. Sapiano P, Torpiano A, Bonello MA. A study of the variation in seismic response of a loadbearing masonry building typology over rock or clay subsoils through numerical modelling. In: D'Amico S, Galea P, Bozioneles G, Colica E, Farrugia D, Agius MR, editors. Book of Abstracts of the 36th General Assembly of the European Seismological Commission; 2018; Valletta, Malta: Mistral Services sas. p. 420-421.

187. Williams MS. Structural Analysis. In: Elghazouli AY, editor. Seismic design of buildings to Eurocode 8. Canada: Spon Press; 2009. p. 47-83.

188. Trifunac MD, Ivanovic SS, Todorovska MI. Apparent periods of a building. I: Fourier analysis. Journal of structural engineering. 2001 May; 127(5): p. 517-526.

189. Case J, Lord Chilver of Cranfield , Ross CTF. Strength of materials and structures. 4th ed. London: Arnold; 1999.

190. Wair BR, DeJong JT, Shantz T. Guidelines for estimation of shear wave velocity profiles (PEER Report 2012/08). California: Pacific Earthquake Engineering Research Centre, University of California; 2012.

191. Farrugia D, Paolucci E, D'Amico S, Galea P. Inversion of surface wave data for subsurface shear wave velocity profiles characterised by a thick buried low velocity layer. Geophysical Journal International. 2016 May;(206): p. 1221-1231.

192. Malta Environment and Planning Authority , Zammit A. Development control design policy, guidance and standards 2015. Malta: The Malta Environment and Planning Authority; 2015.

193. Gatti PL, Ferrari V. Applied structural and mechanical vibrations (Theory, methods and measuring instrumentation). 1st ed. London: E. & F.N. Spon; 1999.

194. Farrugia D. Ph.D. graduate, Department of Geosciences, Faculty of Science, University of Malta. Personal communication (by email), dfarrugia28@gmail.com, 29th September 2016..

195. Vella A, Galea P, D'Amico S. Site frequency response characterisation of the Maltese islands based on ambient noise H/V ratios. Engineering Geology. 2013 August; 163: p. 89-100.

196. Villaverde R. Methods to assess the seismic collapse capacity of building structures: state of the art. Journal of Structural Engineering. 2007 January; 133(1): p. 57-66.

197. Casolo S, Milani G, Uva G, Alessandri C. Comparative seismic vulnerability analysis on ten masonry towers in the coastal Po Valley in Italy. Engineering structures. 2013 April;(49): p. 465-490.

198. Helmy H. Consultation Department, Applied Science International, LLC. Personal communication by email, huda@appliedscienceint.com, 13th April 2016..

199. Uva G, Casolo S, Milani G, Acito M. An evaluation of the soil-structure interaction in the non-linear dynamic analysis of masonry towers. In: Proceedings of the 15th world conference on Earthquake Engineering, Lisbon. 2012 September 24-28; 36: p. 29207-29216.

200. Ulrich T, Gehl P, Negulescu C, Foerster E. Seismic Vulnerability assessment of masonry building aggregates. In: Proceedings of the 15th world conference on earthquake engineering; Lisbon, Portugal. p. 28269-28277.

201. Bernal D. Instability of buildings subjected to earthquakes. Journal of Structural Engineering. 1992 August; 118(8): p. 2239-2260.

202. Mendes N, Lourenco PB. Evaluation of the seismic performance of masonry buildings of the type “Gaioleiro”, Lisbon (Portugal). In: Santini A, Moraci N, editors. Proceedings of the 2008 seismic engineering conference commemorating the 1908 Messina and Reggio Calabria earthquake; 2008; Reggio Calabria, Italy: AIP. p. 1863-1870.

203. Betti M, Galano L, Vignoli A. Comparative analysis on the seismic behaviour of unreinforced masonry buildings with flexible diaphragms. Engineering structures. 2014 March;(61): p. 195-208.

204. Calio' I, Marletta M, Panto B. A discrete element approach for the evaluation of the seismic response of masonry buildings. In: Proceedings of the 14th world conference on earthquake engineering; 2008; Beijing, China.

205. Bilgin H, Korini O. Seismic capacity evaluation of unreinforced masonry residential buildings in Albania. Natural hazards and earth system sciences. 2012 December 19; 12(12): p. 3753-3764.

206. Alexandris A, Protopapa E, Psycharis I. Collapse mechanisms of masonry buildings derived by the distinct element method. In: Proceedings of the 13th world conference on earthquake engineering; 2004; Vancouver, Canada. p. 60.

207. Casolo S, Pena F. Dynamics of slender masonry towers considering hysteretic behaviour and damage. In: Papadrakakis M, Charmpis DC, Lagaros ND, Tsompanakis Y, editors. Proceedings of the ECCOMAS thematic conference on computational methods in structural dynamics and earthquake engineering; 2007; Rethymno, Crete, Greece.

208. Casolo S, Uva G. Seismic vulnerability assessment of masonry towers: full non-linear dynamics vs pushover analyses. In: Papadrakakis M, Fragiadakis, M, Plevris V, editors. Proceedings of COMPDYN 2011, 3rd ECCOMAS thematic conference on computational methods in structural dynamics and earthquake engineering; 2011; Corfu, Greece.

209. Park R. State of the art report: ductility evaluation from laboratory and analythical testing. In: Proceedings of Ninth World Conference on Earthquake Engineering; 1988; Tokyo-Kyoto, Japan. p. 609-616.

210. Priestley MJN, Calvi GM, Kowalsky MJ. Direct displacement-based design of structures. In: New Zealand Society for Earthquake Engineering Conference (keynote address, session 4); 2007; Palmerston North, New Zealand.

211. Priestley MJN. Seismic behaviour of unreinforced masonry walls. Bulletin of the New Zealand National Society for Earthquake Engineering. 1985 June; 18(2): p. 191-205.

212. Sucouglu H, Yazgan U. Simple survey procedures for seismic risk assessment in urban building stocks. In Wasti ST, Ozcebe G, editors. Seismic assessment and rehabilitation of existing buildings. Netherlands: Springer; 2003. p. 97-118.

213. Bolognini D, Braggio C, Magenes G, Gruppo nazionale per la difesa dai terremoti. Metodi semplificati per l'analisi nonlineare di edifici in muratura. CNR - Gruppo nazionale per la difesa dai terremoti; 2000.

214. Krawinkler H, Seneviratna GD. Pros and cons of a pushover analysis of seismic performance evaluation. Engineering structures. 1998 April; 20(4-6): p. 452-464.

215. Azizi-Bondarabadi H, Mendes N, Lourenco PB. Higher mode effects in pushover analysis of irregular masonry buildings. Journal of earthquake engineering. 2019 March; 9: p. 1-35.

216. Tomaževič M, Bosiljikov V, Weiss P. Structural behaviour factor for masonry structures. In: Proceedings of the 13th World Conference on Earthquake Engineering; 2004 August; Canada.

217. Benedetti D. Costruzioni in muratura: duttilità, norme ed esperienze. Ingegneria sismica. 2004;(3): p. 5-18.

218. Fajfar P. Analysis in seismic provisions for buildings: past, present and future. In: Pitilakis K, editor. Proceedings of the 16th European Conference on Earthquake Engineering - 2018: Recent Advances in Earthquake Engineering in Europe; 2018; Thessaloniki: Springer International Publishing. p. 1-49.

219. Seni D. S.T.A. DATA srl technical support personal communication by email, davide.seni@stadata.com, 5th July 2018..

220. Mifsud A. Assistant lecturer in civil and structural engineering at the Faculty for the Built Environment of the University of Malta, personal communication by email, adrian.mifsud@um.edu.mt, 2nd November 2018..

221. Pulikanti S, Hussain MA, Kumar RP. Amplification studies of local soils using Applied Element Method. International Journal of Earth Sciences and Engineering. 2010 August; 3(4): p. 475-486.

222. Mott Macdonald , BroadwayMalyan. Paceville – Malta: Malta's prime coastal location. Development Framework. Draft masterplan. Malta: Planning Authority; 2016.

223. Bracchi S, Rota M, Penna A, Magenes G. Consideration of modelling uncertainties in the seismic assessment of masonry buildings by equivalent-frame approach. Bulletin of Earthquake Engineering. 2015 November; 13(11): p. 3423-3448.

APPENDICES

Appendix A. FORM FOR THE SEISMIC VULNERABILITY ASSESSMENT OF INDIVIDUAL BUILDINGS DEVELOPED BY THE UNIVERSITY OF MALTA IN THIS STUDY

Seismic vulnerability assessment form for individual contemporary loadbearing masonry buildings in the Maltese Islands developed in this study

ALL TEXT TO BE ENTERED IN BLOCK LETTERS

SECTION 1

[1]Date (DD/MM/YY): [2]Name of assessor

[3]Reference no. for individual building: *4 digit [4]ID Ref of assessor *4 digit

[5a]Reference no. for block *3 digit

[5b]Reference no. for building aggregate *3 digit [6]ID Ref of assessing team *3 digit

[7]Form no. (for specific local council) *4 digit [8]Development Permit No. [9]Availability of plans Found Not Found Found in part

[10]Reference no. for Emergency area [11]Other permit nos. (additions / changes)

[12]Reference no. for infrastructure for accessibility/ connection a b c d

[13]Does building have a strategic function with respect to the emergency operations? Yes No

[14]Building typology Fully detached Semi-detached Terraced

[15a]Current property no. [15b]Current property name

[16a]Previous property no. [16b]Previous property name ([16] to be used only in case of change in no / name in post-earthquake case when pre-earthquake assessment had been carried out under different no. / name of same property) Not applicable

[17]Street:

[18]Town:

[19]Post code:

[20]Local Council:

[21]Location: Malta: Gozo:

[22]Site plan attached indicating site and façade nos. (Note: Façade nos. are to be assigned in a clockwise order starting from façade1 - street façade at entrance)

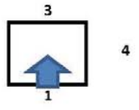

Figure 1 New Form developed in this study for the seismic vulnerability assessment of individual contemporary loadbearing masonry buildings: Section 1.

SECTION 2: GENERAL CHARACTERISTICS

[23]Position in block/aggregate ☐ Isolated ☐ In middle ☐ At edge ☐ At corner ☐ Individual building in block (i.e. not sharing party walls)

[24]Specialized structural form (characterized by large spans) ☐ Yes ☐ No [25]Type ☐ Church ☐ Theatre ☐ Tower/ belfry/chimney ☐ Other ☐ Not applicable

[26]Total no. of floors (incl. below street lev) ☐ [27]No. Of floors below street level ☐ 0 ☐ 1 ☐ 2 ☐ 3 ☐ 4 ☐ 5 ☐ 6 ☐ 7 ☐ 8 ☐ 9 ☐ 10

[28]Average storey height ☐ <=2.5m ☐ 2.5-3.5m ☐ 3.5-5m ☐ =>5m

[29]Height of roof above street level (m) (in case of varying ht, consider average) ☐ m

[30]Presence of front garden ☐ Yes ☐ No

[31]Length of façade facing infrastructure for accessibility /connection (m) ☐ m

[32a]Average area per floor (sq.m) ☐ sq.m [32b]Floor area at level 0 (excl. yards) (sq.m) ☐ sq.m

[33]Proportions of building on plan at typical plan level (W: L) ☐ 1:1<W:L<1:2 ☐ 1:2<W:L<1:3 ☐ 1:3<W:L<1:4 ☐ 1:4<W:L<1:5 ☐ W:L>1:5

[34]Plan regularity (overall shape, symmetry of layout, central position of stairwell) ☐ Yes ☐ Fair ☐ No ☐ Not identifiable

[35]Uniformity of plan in layout and room sizes ☐ Yes ☐ Fair ☐ No ☐ Not identifiable

[36]Proportions of building along narrowest elevation (H:W) ☐ =<1 ☐ 1<H:W<2 ☐ 2<H:W<3 ☐ H:W>3

Figure 2 New Form developed in this study for the seismic vulnerability assessment of individual contemporary loadbearing masonry buildings: Section 2.

SECTION 3A: VERTICAL STRUCTURAL SYSTEM - GENERAL CHARACTERISTICS

[37]Main loadbearing vertical structural system
☐ R.C. frame ☐ Steel frame ☐ Steel& R.C. ☐ Masonry walls ☐ Mixed: Masonry walls & R.C frame in same storey
☐ Mixed:Masonry walls above an R.C frame ☐ Two-leaf masonry walls with infill material in cavity ☐ Not identifiable

[38]Type of masonry wall construction ☐ Good ☐ Bad ☐ Not identifiable

[39]Tie beams /reinforcing ties in wall ☐ Yes ☐ No ☐ Not identifiable

[40]Confirmation by owners that strengthening measures with respect to the seismic response of the building have been effected ☐ Yes ☐ No

[41]Main type of masonry on façade 1 (street façade at entrance - as per attached site plan [22])
☐ Softstone ☐ HCB ☐ Not identifiable
☐ Reinforced HCB ☐ Strengthened:injected grout /fibre reinforcement /other ☐ Two leaf masonry walls with infill material in cavity

[42]Wall construction along façade 1 ☐ Double leaf ☐ Single leaf ☐ Not identifiable

[43]Main type of masonry on façade 2 (façade no. as per attached site plan [22])
☐ Softstone ☐ HCB ☐ Not identifiable ☐ Not applicable
☐ Reinforced HCB ☐ Strengthened:injected grout /fibre reinforcement /other ☐ Two leaf masonry walls with infill material in cavity

[44]Wall construction along façade 2 ☐ Double leaf ☐ Single leaf ☐ Not identifiable ☐ Not applicable

[45]Main type of masonry on façade 3 (façade no. as per attached site plan [22])
☐ Softstone ☐ HCB ☐ Not identifiable ☐ Not applicable
☐ Reinforced HCB ☐ Strengthened:injected grout /fibre reinforcement /other ☐ Two leaf masonry walls with infill material in cavity

[46]Wall construction along façade 3 ☐ Double leaf ☐ Single leaf ☐ Not identifiable ☐ Not applicable

[47]Main type of masonry on façade 4 (façade no. as per attached site plan [22])
☐ Softstone ☐ HCB ☐ Not identifiable ☐ Not applicable
☐ Reinforced HCB ☐ Strengthened:injected grout /fibre reinforcement /other ☐ Two leaf masonry walls with infill material in cavity

[48]Wall construction along façade 4 ☐ Double leaf ☐ Single leaf ☐ Not identifiable ☐ Not applicable

[49]Main type of masonry on left hand side party wall
☐ Softstone ☐ HCB ☐ Not identifiable ☐ Not applicable
☐ Reinforced HCB ☐ Strengthened:injected grout /fibre reinforcement /other ☐ Two leaf masonry walls with infill material in cavity

[50]Wall construction along left hand side party wall ☐ Double leaf ☐ Single leaf ☐ Not identifiable

[51]Main type of masonry on right hand side party wall
☐ Softstone ☐ HCB ☐ Not identifiable ☐ Not applicable
☐ Reinforced HCB ☐ Strengthened:injected grout /fibre reinforcement /other ☐ Two leaf masonry walls with infill material in cavity

[52]Wall construction along right hand side party wall ☐ Double leaf ☐ Single leaf ☐ Not identifiable

Figure 3 New Form developed in this study for the seismic vulnerability assessment of individual contemporary loadbearing masonry buildings: Section 3A.

SECTION 3B: VERTICAL STRUCTURAL SYSTEM - SEISMIC VULNERABILITY CHARACTERISTICS

[53]Presence of double height spaces ☐ Yes ☐ No ☐ Not identifiable

[54]Presence of double height spaces facing infrastructure for accessibility / connection ☐ Yes ☐ No ☐ Not identifiable ☐ Not applicable

[55a]Difference in level of topmost slab in adjacent building along **left** hand side party wall {in m}{+/- indicate adjacent building is higher/ lower respectively than building being assessed} ☐ Yes ☐ Left ☐ {+/-}m On left ☐ No ☐ Not applicable

[55b]Difference in level of topmost slab in adjacent building along **right** hand side party wall {in m}{+/- indicate adjacent building is higher/ lower respectively than building being assessed} ☐ Yes ☐ Right ☐ {+/-}m On right ☐ No ☐ Not applicable

[56a]Difference in level of floor slab at level +2 in adjacent building along **left** hand side party wall {in m}{+/- indicate slab level in adjacent building is higher/ lower respectively than building being assessed} ☐ Yes ☐ Left ☐ {+/-}m On left ☐ No ☐ Not applicable

[56b]Difference in level of floor slab at level +2 in adjacent building along **right** hand side party wall {in m}{+/- indicate slab level in adjacent building is higher/ lower respectively than building being assessed} ☐ Yes ☐ Right ☐ {+/-}m On right ☐ No ☐ Not applicable

[57a]Difference in plane of walls of **front** facade of adjacent building on **left** hand side of building being assessed {in m} {+/- indicate plane of façade of adjacent building is further towards street / towards back yard respectively than building being assessed} ☐ Yes ☐ Left ☐ {+/-}m Bldg on left ☐ No ☐ Not applicable

[57b]Difference in plane of walls of **front** facade of adjacent building on **right** hand side of building being assessed {in m} {+/- indicate plane of façade of adjacent building is further towards street / towards back yard respectively than building being assessed} ☐ Yes ☐ Right ☐ {+/-}m Bldg on right ☐ No ☐ Not applicable

[58a]Difference in plane of walls of **rear** facade of adjacent building on **left** hand side of building being assessed {in m} {+/- indicate plane of façade of adjacent building is further towards street / towards back yard respectively than building being assessed} ☐ Yes ☐ Left ☐ {+/-}m Bldg on left ☐ No ☐ Not applicable ☐ Not identifiable

[58b]Difference in plane of walls of **rear** facade of adjacent building on **right** hand side of building being assessed {in m} {+/- indicate plane of façade of adjacent building is further towards street / towards back yard respectively than building being assessed} ☐ Yes ☐ Right ☐ {+/-}m Bldg on right ☐ No ☐ Not applicable ☐ Not identifiable

[59]Difference in plane along front façade of building being assessed {in m} ☐ Yes ☐ m ☐ No

[60]Difference in plane along rear façade of building being assessed {in m} ☐ Yes ☐ m ☐ No ☐ Not identifiable

Figure 4 New Form developed in this study for the seismic vulnerability assessment of individual contemporary loadbearing masonry buildings: Section 3B part (i).

[61]Vacant site directly adjacent to building ☐ Yes ☐ Left ☐ Right ☐ No

[62]Evidence of shared party wall ☐ Yes ☐ Left ☐ Right ☐ No ☐ Not identifiable

[63]Presence of long corridor/garage/other open plan space directly adjacent to party wall (where L_{corr}>=50% L_{bldg}) ☐ Yes ☐ Left ☐ Right ☐ No ☐ Not identifiable

[64]Misalignment of the internal spaces of abutting properties ☐ Yes ☐ Left ☐ Right ☐ No ☐ Not applicable ☐ Not identifiable

[65]Absence of intermediate walls in loadbearing masonry building in 1 or more storeys ☐ Yes ☐ No ☐ Not Identifiable

[66]Storey level at which no intermediate walls are present (-1=semi/basement; 0=ground,...etc) ☐ Lev. ☐ Lev. ☐ Lev. ☐ Lev. ☐ Lev. ☐ Lev. ☐ Not Identifiable ☐ Not applicable

[67]Presence of open plan spaces without internal loadbearing walls over part of floor area ☐ Yes ☐ No ☐ Not Identifiable

[68]Average percentage area of open plan space to total area of floor ☐ % ☐ Not applicable

[69]Storey level at which open plan spaces without internal loadbearing walls over part of floor area are present (-1 = semi/basement; 0=ground,...etc) ☐ Lev. ☐ Lev. ☐ Lev. ☐ Lev. ☐ Lev. ☐ Lev. ☐ Not Identifiable ☐ Not applicable

[70]Max ratio of Area of discontinuous loadbearing walls (A_{disc})to Area of continuous loadbearing walls (A_{cont}) in building (where, 'discontinuous' refers to walls which do not reach up to foundation level but stop at a slab / beam)
☐ $A_{x,ydisc}$>=0.10$A_{x,ycont}$ ☐ 0.07$A_{x,ycont}$<=$A_{x,ydisc}$>=0.10$A_{x,ycont}$ ☐ 0.04$A_{x,ycont}$<=$A_{x,ydisc}$>=0.07$A_{x,ycont}$
☐ $A_{x,ydisc}$<=0.04$A_{x,ycont}$ ☐ Not applicable ☐ Not Identifiable

[71]Presence of inadequate or completely absent connection between perpendicular masonry walls (in whole building)
☐ 0%<=adequate connection <=20% ☐ 20%<adequate connection<60% ☐ No signs of inadequate connection between walls visible from exterior of building
☐ 60%<=adequate connection<100% ☐ adequate connection present throughout building (100%)

[72]Percentage evidence of inadequate or completely absent connection between loadbearing walls and slabs in whole building
☐ 0%<=adequate connection <=10% ☐ 10%<adequate connection<50% ☐ Not identifiable
☐ 50%<=adequate connection<100% ☐ adequate connection present throughout building (100%)

[73]Presence of large openings on main façade 1 (street façade at entrance - as per attached site plan [22]) (large openings > 50% of wall area) ☐ Yes ☐ No

[74]Presence of large openings on main façade 2 (façade no. as per attached site plan [22]) (large openings > 50% of wall area) ☐ Yes ☐ No ☐ Not identifiable

[75]Presence of large openings on main façade 3 (façade no. as per attached site plan [22]) (large openings> 50% of wall area) ☐ Yes ☐ No ☐ Not identifiable

Figure 5 New Form developed in this study for the seismic vulnerability assessment of individual contemporary loadbearing masonry buildings: Section 3B part (ii).

[76] Presence of large openings on main façade 4 (façade no. as per attached site plan [22]) (large openings> 50% of wall area) ☐ Yes ☐ No ☐ Not identifiable

[77] Irregular distribution or size of openings for windows/doors...etc on façade. (Note: 'irregular'=misaligned vertically/horizontally; located very close to perpendicular shear walls; or presence of very wide openings (W>4m) ☐ Yes ☐ No ☐ Not identifiable

[78] Presence of setbacks along main façade 1 (street façade at entrance - as per attached site plan [22]) ☐ [a]Yes ☐ [b]at 1 lev. ☐ [c]2 or 3 lev. ☐ [d]4 or 5 lev. ☐ [e]None ☐ [e]at >5 lev. ☐ [f]at penthouse lev.

[79] Presence of setbacks along main façade 2 (façade no. as per attached site plan [22]) ☐ [a]Yes ☐ [b]at 1 lev. ☐ [c]2 or 3 lev. ☐ [d]4 or 5 lev. ☐ [e]None ☐ [h]Not identifiable ☐ [e]at >5 lev. ☐ [f]at penthouse lev.

[80] Presence of setbacks along main façade 3 (façade no. as per attached site plan [22]) ☐ [a]Yes ☐ [b]at 1 lev. ☐ [c]2 or 3 lev. ☐ [d]4 or 5 lev. ☐ [e]None ☐ [h]Not identifiable ☐ [e]at >5 lev. ☐ [f]at penthouse lev.

[81] Presence of setbacks along main façade 4 (façade no. as per attached site plan [22]) ☐ [a]Yes ☐ [b]at 1 lev. ☐ [c]2 or 3 lev. ☐ [d]4 or 5 lev. ☐ [e]None ☐ [h]Not identifiable ☐ [e]at >5 lev. ☐ [f]at penthouse lev.

[82] Presence of projecting rooms / balconies ☐ [a]Yes ☐ [b]at 1 lev. ☐ [c]2 or 3 lev. ☐ [d]4 or 5 lev. ☐ [e]at >5 lev. ☐ [f]None

[83] Presence of masonry walls as infill panels in frame structure ☐ Yes ☐ No ☐ Not identifiable ☐ Not applicable

[84] Position of masonry walls relative to frame ☐ Concentric with columns ☐ Eccentric with respect to columns ☐ Not identifiable ☐ Not applicable

[85] Presence of isolated columns (not effectively tied to slab/beams) ☐ Yes ☐ No ☐ Not identifiable

[86] Open storey with just columns - no loadbearing/infill walls (*Italian: 'piano pilotis'*) ☐ Yes ☐ No ☐ Not identifiable

[87] Evidence of post-construction joining of originally separate individual buildings or post-construction additions in areas which were originally left as voids in building aggregate ☐ Yes ☐ No ☐ Not identifiable

[88a] Additional floors/ rooms over original construction ☐ Yes ☐ No ☐ Not identifiable

[88b] Number of additional floors from original permit ☐ No.

[89] Evidence of different construction system / materials for additional floors/rooms ☐ Yes ☐ No ☐ Not identifiable ☐ Not applicable

Figure 6 New Form developed in this study for the seismic vulnerability assessment of individual contemporary loadbearing masonry buildings: Section 3B part (iii).

SECTION 4A: HORIZONTAL STRUCTURAL SYSTEM - GENERAL CHARACTERISTICS

[90]Type of slab construction over semi/basement	☐	Precast prestressed hollow core planks	☐	Cast in-situ concrete slabs	☐ Predalle	☐	One of previous over R.C. beam system
	☐	Stone slabs over timber beams	☐	Stone slabs over steel beams	☐ R.C. slab over timber beams	☐	R.C. slab over steel beams
	☐	Stone slabs over stone arches	☐	Stone slabs over stone corbels	☐ Stone slab roofs	☐	timber panels over timber beams
	☐	Other ☐ Not identifiable	☐	Not applicable			
[91]Type of slab construction in other storeys	☐	Cast in-situ concrete slabs	☐	Predalle			
	☐	Stone slabs over timber beams	☐	Stone slabs over steel beams	☐ R.C. slab over timber beams	☐	R.C. slab over steel beams
	☐	Stone slabs over stone arches	☐	Stone slabs over stone corbels	☐ Stone slab roofs	☐	timber panels over timber beams
	☐	Other ☐ Not identifiable	☐	Not applicable			

SECTION 4B: HORIZONTAL STRUCTURAL SYSTEM - SEISMIC VULNERABILITY CHARACTERISTICS

[92]Presence of slabs spanning in one direction and not tied to each other / to walls parallel to their span	☐	Yes	☐	75%<spanning in one direction& not tied<=100%	☐ 50%<spanning in one direction & not tied<=75%	☐	No	☐ Not identifiable
			☐	25%<spanning in one direction & not tied<=50%	☐ 0%<spanning in one direction & not tied<=25%			
[93]Percentage occurrence of flexible slab construction systems in floors of **whole building** (e.g. in lightweight mezzanine structures)	☐	Yes	☐	75%<flexible systems <=100%	☐ 50%<flexible systems<=75%	☐	No	☐ Not identifiable
			☐	25%<flexible systems<=50%	☐ 0%<flexible systems<=25%			
[94]Presence of flexible slab construction systems at **floor level with maximum occurrence**	☐	[b]Level	☐	[a]75%<flexible systems <=100%	☐ [a]50%<flexible systems<=75%	☐	[a]No	☐ [a]Not identifiable
			☐	[a]25%<flexible systems<=50%	☐ [a]0%<flexible systems<=25%			
[95]Percentage occurrence of semi-rigid slab construction systems in floors of **whole building** (e.g. in xorok/beam floor systems..etc)	☐	Yes	☐	75%<semi-rigid systems <=100%	☐ 50%<semi-rigid systems<=75%	☐	No	☐ Not identifiable
			☐	25%<semi-rigid systems<=50%	☐ 0%<semi-rigid systems<=25%			
[96]Presence of semi-rigid slab construction systems at **floor level with maximum occurrence**	☐	[b]Level	☐	[a]75%<semi-rigid systems <=100%	☐ [a]50%<semi-rigid systems<=75%	☐	[a]No	☐ [a]Not identifiable
			☐	[a]25%<semi-rigid systems<=50%	☐ [a]0%<semi-rigid systems<=25%			
[97]Presence of vaults or arches	☐	Yes	☐	No	☐ Not Identifiable			
[98]Absence of or inadequte degree of abutment for arches or vaults	☐	Yes	☐	No	☐ Not Identifiable	☐	Not applicable	

Figure 7 New Form developed in this study for the seismic vulnerability assessment of individual contemporary loadbearing masonry buildings: Sections 4A and 4B.

SECTION 5A: CONDITION OF BUILDING - PRE-EARTHQUAKE

Not applicable (in case of post-earthquake assessment)

[99a]Pre-earthquake:Visible structural damage to external walls: Degree	☐ Severe	☐ Medium severity (1-10mm cracks)	☐ Minor (<=1mm)	☐ No damage	☐ Not identifiable	☐ Not applicable			
[99b]Pre-earthquake:Visible structural damage to external walls: Extent	☐ <=1/3 of building	☐ 1/3-2/3 of building	☐ =>2/3 of building	☐ Not applicable					
[100a]Pre-earthquake:Visible structural damage to internal walls: Degree	☐ Severe	☐ Medium severity (1-10mm cracks)	☐ Minor (<=1mm)	☐ No damage	☐ Not identifiable	☐ Not applicable	☐ Not probable		
[100b]Pre-earthquake:Visible structural damage to internal walls: Extent	☐ <=1/3 of building	☐ 1/3-2/3 of building	☐ =>2/3 of building	☐ Not applicable					
[101a]Pre-earthquake:Visible structural damage to horizontal loadbearing elements (slabs/beams): Degree	☐ Severe	☐ Medium severity Beams:<=5mm cracks)	☐ Minor (<=1mm)	☐ No damage	☐ Not identifiable	☐ Not applicable	☐ Not probable		
[101b]Pre-earthquake:Visible structural damage to horizontal loadbearing elements (slabs/beams): Extent	☐ <=1/3 of building	☐ 1/3-2/3 of building	☐ =>2/3 of building	☐ Not applicable					
[102a]Pre-earthquake:Visible structural damage to staircores: Degree	☐ Severe (>=5mm)	☐ Medium severity (1-2mm)	☐ Minor (<=1mm)	☐ No damage	☐ Not identifiable	☐ Not applicable	☐ Not probable		
[102b]Pre-earthquake:Visible structural damage to staircores: Extent	☐ <=1/3 of building	☐ 1/3-2/3 of building	☐ =>2/3 of building	☐ Not applicable					
[103]Degree of maintenance	☐ Lacking	☐ Sufficient	☐ Good						
Damages to non-structural elements (pre-earthquake assessment)[(104-106)] (due to settlement, explosion or war damage)	[104]Detachment of external render/pointing	☐ Yes	☐ No	☐ Not applicable					
	[105]Damages to parapet walls	☐ Yes	☐ No	☐ Not identifiable	☐ Not applicable				
	[106]Damages to internal plaster/false ceilings	☐ Yes	☐ No	☐ Not identifiable	☐ Not applicable	☐ Not probable			
[107]Evidence of failure of foundations / differential settlement (Pre-earthquake)	☐ Yes	☐ No	☐ Not identifiable	☐ Not applicable					
[108]Potential damage by building on infrastructure for accessibility / connection (Pre-earthquake) (arising from height of building> road width)	☐ Yes	☐ No	☐ Not applicable						
[109]Potential damage by building on infrastructure for accessibility/ connection (Pre-earthquake) (arising from falling secondary structural/non-structural components attached to projecting rooms and balconies)	☐ Yes	☐ No	☐ Not applicable						
Potential damage on building [(110-111)] (Pre-earthquake)	[110]From collapse/falling elements from nearby buildings	☐ Yes	☐ No						
	[111]From damage to access road	☐ Yes	☐ No						

Figure 8 New Form developed in this study for the seismic vulnerability assessment of individual contemporary loadbearing masonry buildings: Section 5A.

SECTION 5B: CONDITION OF BUILDING - POST-EARTHQUAKE

Not applicable (in case of pre-earthquake assessment)

[112a]Post-earthquake:Visible structural damage to external walls: Degree	☐ Severe	☐ Medium severity (1-10mm cracks)	☐ Minor (<=1mm)	☐ No damage	☐ Not identifiable	☐ Not applicable		
[112b]Post-earthquake:Visible structural damage to external walls: Extent	☐ <=1/3 of building	☐ 1/3-2/3 of building	☐ =>2/3 of building	☐ Not applicable				
[113a]Post-earthquake:Visible structural damage to internal walls: Degree	☐ Severe	☐ Medium severity (1-10mm cracks)	☐ Minor (<=1mm)	☐ No damage	☐ Not identifiable	☐ Not applicable	☐ Not probable	
[113b]Post-earthquake:Visible structural damage to internal walls: Extent	☐ <=1/3 of building	☐ 1/3-2/3 of building	☐ =>2/3 of building	☐ Not applicable				
[114a]Post-earthquake:Visible structural damage to horizontal loadbearing elements (slabs/beams): Degree	☐ Severe	☐ Medium severity Beams:<=5mm cracks)	☐ Minor (<=1mm)	☐ No damage	☐ Not identifiable	☐ Not applicable	☐ Not probable	
[114b]Post-earthquake:Visible structural damage to horizontal loadbearing elements (slabs/beams): Extent	☐ <=1/3 of building	☐ 1/3-2/3 of building	☐ =>2/3 of building	☐ Not applicable				
[115a]Post-earthquake:Visible structural damage to staircores: Degree	☐ Severe (>=5mm)	☐ Medium severity (1-2mm)	☐ Minor (<=1mm)	☐ No damage	☐ Not identifiable	☐ Not applicable	☐ Not probable	
[115b]Post-earthquake:Visible structural damage to staircores: Extent	☐ <=1/3 of building	☐ 1/3-2/3 of building	☐ =>2/3 of building	☐ Not applicable				
[116]Degree of maintenance	☐ Lacking	☐ Sufficient	☐ Good					
Damages to non-structural elements (pre-earthquake assessment)[117-119] (due to settlement, explosion or war damage)	[117]Detachment of external render/pointing	☐ Yes	☐ No	☐ Not applicable				
	[118]Damages to parapet walls	☐ Yes	☐ No	☐ Not identifiable	☐ Not applicable			
	[119]Damages to internal plaster/false ceilings	☐ Yes	☐ No	☐ Not identifiable	☐ Not applicable			
	[120]Damages to electrical system	☐ Yes	☐ No	☐ Not identifiable	☐ Not applicable			
	[121]Damages to fresh water supply/foul drainage system	☐ Yes	☐ No	☐ Not identifiable	☐ Not applicable			
[122]Evidence of failure of foundations / differential settlement (Post-earthquake)	☐ Yes	☐ No	☐ Not identifiable	☐ Not applicable				
[123]Potential damage by building on infrastructure for accessibility / connection (Post-earthquake) (arising from height of building> road width)	☐ Yes	☐ No	☐ Not applicable					
[124]Potential damage by building on infrastructure for accessibility/ connection (Post-earthquake) (arising from falling secondary structural/non-structural components attached to projecting rooms and balconies)	☐ Yes	☐ No	☐ Not applicable					
Potential damage on building [125-126] (Post-earthquake)	[125]From collapse/falling elements from nearby buildings	☐ Yes	☐ No					
	[126]From damage to access road	☐ Yes	☐ No					

Figure 9 New Form developed in this study for the seismic vulnerability assessment of individual contemporary loadbearing masonry buildings: Section 5B.

SECTION 6: GROUND CHARACTERISTICS

[127a]Ground morphology ☐ Flat (<15deg) ☐ With minor inclination (15-30deg.) ☐ With major inclination (30deg.) ☐ Abrupt drop in topogaphy

[127b]Height of abrupt drop (m) ☐ m ☐ Not applicable

[128]Stepping of foundation levels due to sloping ground ☐ Yes ☐ No ☐ Not identifiable ☐ Not applicable

[129]Location with respect to steep drop in landscape ☐ Directly below steep drop/slope in landscape ☐ Directly above steep drop ☐ Not applicable

Localized seismic characteristics of site [130-131]

[130]Microseismic rating of area (worst case): ☐ Stable ☐ Stable with amplifications ☐ Unstable

[131]Type of instability (if 'unstable' in [130]): ☐ Landslide ☐ Liquefaction ☐ Active fault ☐ Differential settlement ☐ Underground cavities ☐ Not applicable

Geology [132-136]:

[132]Topmost formation layer ☐ Upper Coralline Limestone ☐ Greensand ☐ Blue Clay ☐ Upper Globigerina Limestone ☐ Middle Globigerina Limestone ☐ Lower Globigerina Limestone ☐ Lower Coralline Limestone ☐ Made up land (eg. redaimed area)

[133]Thickness of topmost layer ☐ Thickness topmost layer <=15m ☐ Thickness topmost layer >=15m

[134]Second formation layer ☐ Upper Coralline Limestone ☐ Greensand ☐ Blue Clay ☐ Upper Globigerina Limestone ☐ Middle Globigerina Limestone ☐ Lower Globigerina Limestone ☐ Lower Coralline Limestone

[135]Thickness of second layer ☐ Thickness <=15m ☐ Thickness >=15m

[136]Localization of landslide ☐ Encroaching with building (ie building can be dragged down with landslide) ☐ Landslide positioned behind building ☐ Landslide positioned ahead of building ☐ Not applicable

Hydrology: [137]Risk of flooding ☐ Yes ☐ No

SECTION 7: BUILDING INFORMATION & USE

[138]Title of property ☐ Public ☐ Private

[139]Reference code for current use of building ☐

[140]Type and number of units corresponding with every use [a-g]

A ☐ [a]Residential (H ☐)
B ☐ [b]Commercial (I ☐)
C ☐ [c]Public service (J ☐)
D ☐ [d]Tourism (K ☐)
E ☐ [e]Production (L ☐)
F ☐ [f]Offices (M ☐)
G ☐ [g]Storage (N ☐)

[141]Year of construction and structural upgrade (if known) ☐ <=1919 ☐ 1919-1945 ☐ 1946-1961 ☐ 1962-1971 ☐ 1972-1981 ☐ 1982-1991 ☐ 1992-2001 ☐ =>2002

[142]Percentage of building in use ☐ >65% ☐ 30-65% ☐ <30% ☐ not in use ☐ under construction ☐ not complete ☐ abandoned

[143]Average no. of people using building (for residential or work purposes) ☐ No. ☐ Not identifiable ☐ Not applicable

Figure 10 New Form developed in this study for the seismic vulnerability assessment of individual contemporary loadbearing masonry buildings: Sections 6 and 7.

SECTION 8: ACCURACY OF ASSESSMENT

[144]Degree of accuracy of assessment

☐ Only inspected building externally
☐ Inspected building externally & partial internal inspection
☐ Exhaustive internal and external inspection to all levels
☐ Information regarding strengthening / renovation works obtained from owner

SECTION 9: POST-EARTHQUAKE ASSESSMENT OUTCOME ☐ Not applicable (in case of pre-earthquake assessment)

[145a]Post-earthquake assessment:
Emergency safety measures suggested

☐ Installation of supportive scaffolding to slabs/beams
☐ Installation of supportive scaffolding to walls
☐ Installation of supportive scaffolding to staircases
☐ Demolition / removal of damaged parapet walls, canopies, awnings...etc
☐ Removal of detached areas of render from walls
☐ Removal of damaged false ceilings

[145b]Other suggestions

[146]Post-earthquake assessment: Safety for use

☐ [a]No. of family units which are unsafe for use
☐ [b]No. of families evacuated
☐ [c]No. of persons evacuated

SECTION 10: DEGREE OF SEISMIC VULNERABILITY ☐ NOT APPLICABLE

[147]Summary of building assessment:

Level of seismic vulnerability	[a]Section 2 (General Characteristics)	[b]Section 3A & B (Vert. Struct. System & Characteristics)	[c]Section 4A & B (Horiz. Struct. System & Characteristics)	[d]Section 5 (Condition of building)	[e]Section 6 (Ground Characteristics)	[f]Section 8 (Accuracy of assessment)	[g]Degree of seismic vulnerability based on individual building
LOW							
MEDIUM-LOW							
MEDIUM							
MEDIUM-HIGH							
HIGH							

[148]**SECTION 11: NOTES & COMMENTS**

Figure 11 New Form developed in this study for the seismic vulnerability assessment of individual contemporary loadbearing masonry buildings: Sections 8 to 11.

Table 1 Comparison between the entries of Section 1 of the New Form and the corresponding entries in the main existing Italian seismic vulnerability assessment methods consulted in this study.

Developed methodology - Individual building form		**Reference methodologies**						
Entry No.	**Entry description in New Form for the seismic vulnerability assessment of the contemporary loadbearing building typology in the Maltese Islands**	**AeDES [80]**	**CLE v.2.0 (individual building form) [79]**	**GNDT 1st Level assessment form [69]**	**GNDT 2nd Level assessment form [26] [71]**	**Form for assessment of deficiencies [75]**	**Geological factors Form [82]**	**Characteristics of particular relevance in Maltese context**
SECTION 1								
1	Date (DD/MM/YY)	Section 1	US: Section1	Section 1 (11)		Entered at beginning of form	Entered at beginning of form	
2	Name of assessor	Entered at end of form					Entered at beginning of form	
3	Reference no. for individual building	Section 1	US: Section 1 (7)	Section 2		Entered at beginning of form		
4	ID Ref of assessor							
5a	Reference no. for block	Section 1	US: Section 1 (6)	Section 2		Entered at beginning of form		
5b	Reference no. for building aggregate							
6	ID Ref of assessing team	Section 1		Section 1 (17)				
7	Form no. (for specific local council)	Section 1		Section 1 (6)	6	Entered at beginning of form		
8	Development Permit No.							X
9	Availability of plans							X
10	Reference no. for Emergency area		US: Section 1 (8)					
11	Other permit nos. (additions / changes)							X
12	Reference no. for infrastructure for accessibility/connection		US: Section 1 (9)					
13	Does building have a strategic function with respect to the emergency operations?							
14	Building typology (fully detached/semi-detached/terraced)							X
15a/b	Current property no. / name	Section 1 (adapted)	US: Section 1 (1-5,10-11)	Section 2 (56)		Entered at beginning of form		
16a/b	Previous property no. / name							
17	Street			Section 2 (44)		Entered at beginning of form		
18	Town			Section 1 (adapted)	(1) adapted		Section 1	
19	Post code			Section 1 (adapted)				
20	Local Council			Section 1	(3) adapted		Section 1	
21	Location (Malta/Gozo)							
22	Site plan attached indicating site and façade nos.	Section 1	US: Section 1 (12)	Section 2 (22, 25, 28, 32, 34, 38) (adapted)			Section 3	

Table 2 Comparison between the entries of Section 2 of the New Form and the corresponding entries in the main existing Italian seismic vulnerability assessment methods consulted in this study.

Developed methodology - Individual building form		**Reference methodologies**						
Entry No.	**Entry description in New Form for the seismic vulnerability assessment of the contemporary loadbearing building typology in the Maltese Islands**	**AeDES [80]**	**CLE v.2.0 (individual building form) [79]**	**GNDT 1st Level assessment form [69]**	**GNDT 2nd Level assessment form [26] [71]**	**Form for assessment of deficiencies [75]**	**Geological factors Form [82]**	**Characteristics of particular relevance in Maltese context**
SECTION 2: GENERAL CHARACTERISTICS								
23	Position in block / aggregate	Section 1	US: Section 2 (13/14)					
24	Specialized structural form (characterized by large spans)		US: Section 2 (16)					
25	Type (of specialized structural form)		US: Section 2 (17)					
26	Total no. of floors (incl. below street lev)	Section 2	US: Section 2 (18)					
27	No. Of floors below street level	Section 2	US: Section 2 (19)					
28	Average storey height	Section 2	US: Section 2 (20)	Section 3 (83, 86, 89, 92, 95)				
29	Height of roof above street level (m)		US: Section 2 (21)	Section 3 (98/101) (adapted)				
30	Presence of front garden							X
31	Length of façade facing infrastructure for accessibility /connection (m)			Section 3 (104)				
32a	Average area per floor (m^2)	Section 2	US: Section 2 (23)	Section 3 (63, 68, 73, 78)				
32b	Floor area at level 0 (excl. yards) (m^2)							
33	Proportions of building on plan at typical plan level (W: L)				Section 6 (16) (adapted)	Section 3 (a & b) (adapted)		X
34	Plan regularity	Section 3						
35	Uniformity of plan in layout and room sizes							X
36	Proportions of building along narrowest elevation (H:W)							X

Table 3 Comparison between the entries of Section 3A of the New Form and the corresponding entries in the main existing Italian seismic vulnerability assessment methods consulted in this study.

Developed methodology - Individual building form		**Reference methodologies**						
Entry No.	**Entry description in New Form for the seismic vulnerability assessment of the contemporary loadbearing building typology in the Maltese Islands**	**AeDES [80]**	**CLE v.2.0 (individual building form) [79]**	**GNDT 1st Level assessment form [69]**	**GNDT 2nd Level assessment form [26] [71]**	**Form for assessment of deficiencies [75]**	**Geological factors Form [82]**	**Characteristics of particular relevance in Maltese context**
	SECTION 3A: VERTICAL STRUCTURAL SYSTEM - GENERAL CHARACTERISTICS							
37	Main loadbearing vertical structural system	Section 3 (adapted)	US: Section 2 (24) (adapted)	Section 7 (280, 281, 285, 289, 293, 297) (adapted)	Section 2 (12) (adapted)			
38	Type of masonry wall construction (Good/ bad)	Section 3 (adapted)	US: Section 2 (25)			Section 1 (a &b) (adapted)		
39	Tie beams /reinforcing ties in wall	Section 3 (adapted)	US: Section 2 (26)		Section 1 (11) (adapted)	Section 2 (b) (adapted)		
40	Confirmation by owners that strengthening measures with respect to the seismic response of the building have been effected							
41	Main type of masonry on façade 1	Section 3 (adapted)						
42	Wall construction along façade 1							
43	Main type of masonry on façade 2							
44	Wall construction along façade 2							
45	Main type of masonry on façade 3							
46	Wall construction along façade 3							
47	Main type of masonry on façade 4							
48	Wall construction along façade 4							
49	Main type of masonry on left hand side party wall							
50	Wall construction along left hand side party wall							
51	Main type of masonry on right hand side party wall							
52	Wall construction along right hand side party wall							

Table 4 Comparison between entries 53 to 71 of Section 3B of the New Form and the corresponding entries in the main existing Italian seismic vulnerability assessment methods consulted in this study.

Developed methodology - Individual building form		**Reference methodologies**						
Entry No.	**Entry description in New Form for the seismic vulnerability assessment of the contemporary loadbearing building typology in the Maltese Islands**	**AeDES [80]**	**CLE v.2.0 (individual building form) [79]**	**GNDT 1st Level assessment form [69]**	**GNDT 2nd Level assessment form [26] [71]**	**Form for assessment of deficiencies [75]**	**Geological factors Form [82]**	**Characteristics of particular relevance in Maltese context**
	SECTION 3B: VERTICAL STRUCTURAL SYSTEM - SEISMIC VULNERABILITY CHARACTERISTICS							
53	Presence of double height spaces				Section 7 (17) (adapted)	Section 3 (c) (adapted)		X
54	Presence of double height spaces facing infrastructure for accessibility / connection		US: Section 2 (22)					X
55a/b	Difference in level of topmost slab in adjacent building along left/right hand side party wall (in m)				Section 5 (15/62) (adapted)	Section 3 (h) simplified		
56a/b	Difference in level of floor slab at level +2 in adjacent building along left/right hand side party wall (in m)							
57a/b	Difference in plane of walls of front facade of adjacent building on left/right hand side of building being assessed (in m)							
58 a/b	Difference in plane of walls of rear facade of adjacent building on left/right hand side of building being assessed (in m)							
59	Difference in plane along front façade of building being assessed (in m)							X
60	Difference in plane along rear façade of building being assessed (in m)							X
61	Vacant site directly adjacent to building							X
62	Evidence of shared party wall							X
63	Presence of long corridor/garage/other open plan space directly adjacent to party wall (where $L_{corridor}$>=50% $L_{building}$)							X
64	Misalignment of the internal spaces of abutting properties							
65	Absence of intermediate walls in loadbearing masonry building in 1 or more storeys				Section 7 (17/79) & Section 8 (18) (adapted)	Section 1 (c) & 3 (c /d) (adapted)		X
66	Storey level at which no intermediate walls are present							X
67	Presence of open plan spaces without internal loadbearing walls over part of floor area				Section 7 (17/79) & Section 8 (18) (adapted)	Section 1 (c) & Section 3 (a, b, c) (adapted)		X
68	Average percentage area of open plan space to total area of floor							X
69	Storey level at which open plan spaces without internal loadbearing walls over part of floor area are present							X
70	Max ratio of Area of discontinuous loadbearing walls (Adisc)to Area of continuos loadbearing walls (Acont) in building					Section 3 (d) (simplified)		X
71	Presence of inadequate or completely absent connection between perpendicular masonry walls (in whole building)	Section 3 (adapted)			Section 1 (11) (adapted)	Section 2 (a) (simplified)		

Table 5 Comparison between entries 72 to 89 of Section 3B of the New Form and the corresponding entries in the main existing Italian seismic vulnerability assessment methods consulted in this study.

Developed methodology - Individual building form		**Reference methodologies**						
Entry No.	**Entry description in New Form for the seismic vulnerability assessment of the contemporary loadbearing building typology in the Maltese Islands**	**AeDES [80]**	**CLE v.2.0 (individual building form) [79]**	**GNDT 1st Level assessment form [69]**	**GNDT 2nd Level assessment form [26] [71]**	**Form for assessment of deficiencies [75]**	**Geological factors Form [82]**	**Characteristics of particular relevance in Maltese context**
	SECTION 3B: VERTICAL STRUCTURAL SYSTEM - SEISMIC VULNERABILITY CHARACTERISTICS							
72	Percentage evidence of inadequate or completely absent connection between loadbearing walls and slabs in whole building				Section 1 (11) (adapted)	Section 2(b) (simplified)		
73	Presence of large openings on main façade 1					Section 3(j) (simplified / adapted)		X
74	Presence of large openings on main façade 2							X
75	Presence of large openings on main façade 3							X
76	Presence of large openings on main façade 4							X
77	Irregular distribution or size of openings for windows/doors…etc on façade.					Section 3(j) (simplified)		
78	Presence of setbacks along main façade 1				Section 7 (17) (adapted)			X
79	Presence of setbacks along main façade 2							X
80	Presence of setbacks along main façade 3							X
81	Presence of setbacks along main façade 4							X
82	Presence of projecting rooms / balconies							X
83	Presence of masonry walls as infill panels in frame structure	Section 3 (adapted)						
84	Position of masonry walls relative to frame	Section 3 (adapted)						
85	Presence of isolated columns	Section 3 (adapted)	US: Section 2 (27)					
86	Open storey with just columns - no loadbearing/infill walls *(Italian: 'piano pilotis')*		US: Section 2 (28)					
87	Evidence of post-construction joining of originally separate individual buildings or post-construction additions in areas which were originally left as voids in building aggregate							
88a	Additional floors/ rooms over original construction		US: Section 2 (29)					
88b	Number of additional floors from original permit							X
89	Evidence of different construction system / materials for additional floors/rooms				Section 7 (17) (adapted)	Section 3(g) (simplified)		

Table 6 Comparison between the entries of Sections 4A and 4B of the New Form and the corresponding entries in the main existing Italian seismic vulnerability assessment methods consulted in this study.

Developed methodology - Individual building form		**Reference methodologies**						
Entry No.	**Entry description in New Form for the seismic vulnerability assessment of the contemporary loadbearing building typology in the Maltese Islands**	**AeDES [80]**	**CLE v.2.0 (individual building form) [79]**	**GNDT 1st Level assessment form [69]**	**GNDT 2nd Level assessment form [26] [71]**	**Form for assessment of deficiencies [75]**	**Geological factors Form [82]**	**Characteristics of particular relevance in Maltese context**
	SECTION 4A: HORIZONTAL STRUCTURAL SYSTEM - GENERAL CHARACTERISTICS							
90	Type of slab construction over semi/basement	Section 3 (adapted)		Section 7 (280, 281, 285, 289, 293, 297) (adapted)	Section 5 (adapted)			
91	Type of slab construction in other storeys							
	SECTION 4B: HORIZONTAL STRUCTURAL SYSTEM - SEISMIC VULNERABILITY CHARACTERISTICS							
92	Presence of slabs spanning in one direction and not tied to each other / to walls parallel to their span				Section 5 (15/63) (adapted)	Section 2 (d) (simplified)		
93	Percentage occurrence of flexible slab construction systems in floors of whole building	Section 3 (adapted)		Section 7 (280, 281, 285, 289, 293, 297) (adapted)	Section 5 (15, 63, 64) (adapted)	Section 2 (c) & Section 3 (i) (simplified)		
94	Presence of flexible slab construction systems at floor level with maximum occurrence							X
95	Percentage occurrence of semi-rigid slab construction systems in floors of whole building	Section 3 (adapted)		Section 7 (280, 281, 285, 289, 293, 297) (adapted)	Section 5 (15, 63, 64) (adapted)	Section 2 (c) & Section 3 (i) (simplified)		
96	Presence of semi-rigid slab construction systems at floor level with maximum occurrence							X
97	Presence of vaults or arches	Section 3 (adapted)						
98	Absence of or inadequte degree of abutment for arches or vaults	Section 3 (adapted)				Section 4 (a)		

Table 7 Comparison between the entries of Section 5A of the New Form and the corresponding entries in the main existing Italian seismic vulnerability assessment methods consulted in this study.

Developed methodology - Individual building form		**Reference methodologies**						
Entry No.	**Entry description in New Form for the seismic vulnerability assessment of the contemporary loadbearing building typology in the Maltese Islands**	**AeDES [80]**	**CLE v.2.0 (individual building form) [79]**	**GNDT 1st Level assessment form [69]**	**GNDT 2nd Level assessment form [26] [71]**	**Form for assessment of deficiencies [75]**	**Geological factors Form [82]**	**Characteristics of particular relevance in Maltese context**
SECTION 5A: CONDITION OF BUILDING - PRE-EARTHQUAKE								
99a/b	Pre-earthquake:Visible structural damage to external walls: Degree / Extent	Not applicable: AeDES is a post-earthquake assessment tool	US: Section 2 (30) (adapted)	Section 8 (308, 312, 316, 320, 324) (adapted)	Section 11 (21) (adapted)			
100a/b	Pre-earthquake:Visible structural damage to internal walls: Degree / Extent							
101a/b	Pre-earthquake:Visible structural damage to horizontal loadbearing elements (slabs/beams): Degree / Extent			Section 8 (328, 332, 336, 340, 344) (adapted)				
102a/b	Pre-earthquake:Visible structural damage to staircores: Degree / Extent			Section 8 (348, 352, 345, 360, 364) (adapted)				
103	Degree of maintenance		US: Section 2 (31)	Section 6 (273-279) (adapted)				
104	Damages to non-structural elements: Detachment of external render/pointing							
105	Damages to non-structural elements: Damages to parapet walls							
106	Damages to non-structural elements: Damages to internal plaster/false ceilings							
107	Evidence of failure of foundations / differential settlement (Pre-earthquake)					Section 5 (a)		X
108	Potential damage by building on infrastructure for accessibility / connection (Pre-earthquake) (H> W_{road})							
109	Potential damage by building on infrastructure for accessibility/ connection (Pre-earthquake) (falling secondary structural/non-structural components)				Section 10 (20)			
110	Potential damage on building: From collapse/falling elements from nearby buildings							
111	Potential damage on building: From damage to access road							

Table 8 Comparison between the entries of Section 5B of the New Form and the corresponding entries in the main existing Italian seismic vulnerability assessment methods consulted in this study.

Developed methodology - Individual building form		**Reference methodologies**						
Entry No.	**Entry description in New Form for the seismic vulnerability assessment of the contemporary loadbearing building typology in the Maltese Islands**	**AeDES [80]**	**CLE v.2.0 (individual building form) [79]**	**GNDT 1st Level assessment form [69]**	**GNDT 2nd Level assessment form [26] [71]**	**Form for assessment of deficiencies [75]**	**Geological factors Form [82]**	**Characteristics of particular relevance in Maltese context**
SECTION 5B: CONDITION OF BUILDING - POST-EARTHQUAKE								
112a/b	Post-earthquake:Visible structural damage to external walls: Degree / Extent	Section 4	US: Section 2 (30) (adapted)	Section 8 (308, 312, 316, 320, 324) (adapted)	Section 11 (21) (adapted)			
113a/b	Post-earthquake:Visible structural damage to internal walls: Degree / Extent	Section 4						
114a/b	Post-earthquake:Visible structural damage to horizontal loadbearing elements (slabs/beams): Degree / Extent	Section 4		Section 8 (328, 332, 336, 340, 344) (adapted)				
115a/b	Post-earthquake:Visible structural damage to staircores: Degree / Extent	Section 4		Section 8 (348, 352, 345, 360, 364) (adapted)				
116	Degree of maintenance		US: Section 2 (31)	Section 6 (273-279) (adapted)				
117	Damages to non-structural elements: Detachment of external render/pointing	Section 5						
118	Damages to non-structural elements: Damages to parapet walls	Section 5						
119	Damages to non-structural elements: Damages to internal plaster/false ceilings	Section 5						
120	Damages to non-structural elements: Damages to electrical system	Section 5						
121	Damages to non-structural elements: Damages to fresh water supply/foul drainage system	Section 5						
122	Evidence of failure of foundations / differential settlement (Post-earthquake)	Section 7				Section 5 (a)		X
123	Potential damage by building on infrastructure for accessibility / connection (Post-earthquake) (H> W_{road})							
124	Potential damage by building on infrastructure for accessibility/ connection (Post-earthquake) (falling secondary structural/non-structural components)				Section 10 (20)			
125	Potential damage on building: From collapse/falling elements from nearby buildings	Section 6						
126	Potential damage on building: From damage to access road	Section 6						

Table 9 Comparison between the entries of Sections 6 and 7 of the New Form and the corresponding entries in the main existing Italian seismic vulnerability assessment methods consulted in this study.

Developed methodology - Individual building form		**Reference methodologies**						
Entry No.	**Entry description in New Form for the seismic vulnerability assessment of the contemporary loadbearing building typology in the Maltese Islands**	**AeDES [80]**	**CLE v.2.0 (individual building form) [79]**	**GNDT 1st Level assessment form [69]**	**GNDT 2nd Level assessment form [26] [71]**	**Form for assessment of deficiencies [75]**	**Geological factors Form [82]**	**Characteristics of particular relevance in Maltese context**
SECTION 6: GROUND CHARACTERISTICS								
127a	Ground morphology	Section 7	US: Section 2 (34)		Section 4 (14/56) (adapted)		Section 2 (2) (adapted)	
127b	Height of abrupt drop (m)						Section 2 (3)	
128	Stepping of foundation levels due to sloping ground				Section 4 (14/56) (adapted)			X
129	Location with respect to steep drop in landscape	Section 7 (adapted)	US: Section 2 (35/36)					
130	Localized seismic characteristics of site: Microseismic rating		US: Section 2 (37)					
131	Localized seismic characteristics of site: Type of instability		US: Section 2 (38-42)					
132	Geology: Topmost formation layer				Section 4 (14/58) (adapted)		Section 2 (5) (adapted)	X
133	Geology: Thickness of topmost layer							X
134	Geology: Second formation layer							X
135	Geology:Thickness of second layer							X
136	Localization of landslide		US: Section 2 (43-45)				Section 2 (7) (adapted)	
137	Hydrology: Risk of flooding		US: Section 2 (46/47) adapted					X
SECTION 7: BUILDING INFORMATION AND USE								
138	Title of property (Public/private)	Section 2	US: Section 2 (32/33)	Section 4 (110) (adapted)				
139	Reference code for current use of building	Section 1	US: Section 3 (48)					
140	Type and number of units corresponding with every use	Section 2	US: Section 3 (49)	Section 4 (106, 112, 122,123) (adapted)				
141	Year of construction and structural upgrade	Section 2	US: Section 3 (50)	Section 5 (270-272) (adapted)				
142	Percentage of building in use	Section 2	US: Section 3 (51)	Section 4 (109, 113, 115, 116, 118, 119, 138-269) (adapted)				
143	Average no. of people using building (for residential or work purposes)	Section 2	US: Section 3 (52)					

Table 10 Comparison between the entries of Sections 8 to 11 of the New Form and the corresponding entries in the main existing Italian seismic vulnerability assessment methods consulted in this study.

Developed methodology - Individual building form		**Reference methodologies**						
Entry No.	**Entry description in New Form for the seismic vulnerability assessment of the contemporary loadbearing building typology in the Maltese Islands**	**AeDES [80]**	**CLE v.2.0 (individual building form) [79]**	**GNDT 1st Level assessment form [69]**	**GNDT 2nd Level assessment form [26] [71]**	**Form for assessment of deficiencies [75]**	**Geological factors Form [82]**	**Characteristics of particular relevance in Maltese context**
SECTION 8: ACCURACY OF ASSESSMENT								
144	Degree of accuracy of assessment	Section 8 (adapted)						
SECTION 9: POST-EARTHQUAKE ASSESSMENT OUTCOME								
145	Post-earthquake assessment: Emergency safety measures suggested	Section 8 (adapted)						
146	Post-earthquake assessment: Safety for use	Section 8						
SECTION 10: DEGREE OF SEISMIC VULNERABILITY								
147	Summary of building assessment:	Section 8 (adapted)						
SECTION 11: NOTES & COMMENTS		Section 9						

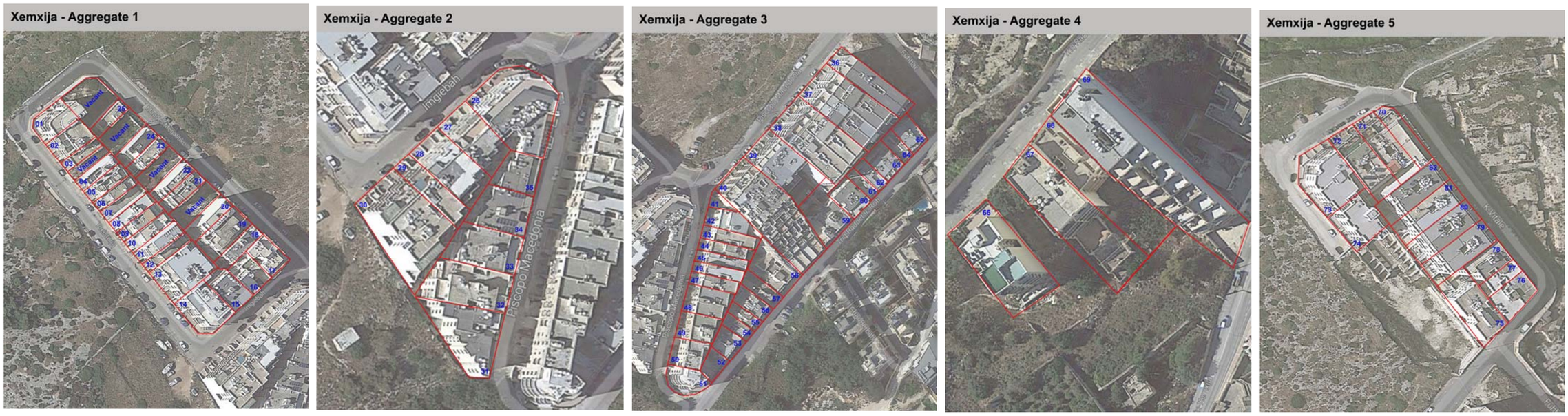

Figure 12 Building reference numbers for seismic vulnerability assessments carried out in Xemxija, Malta.

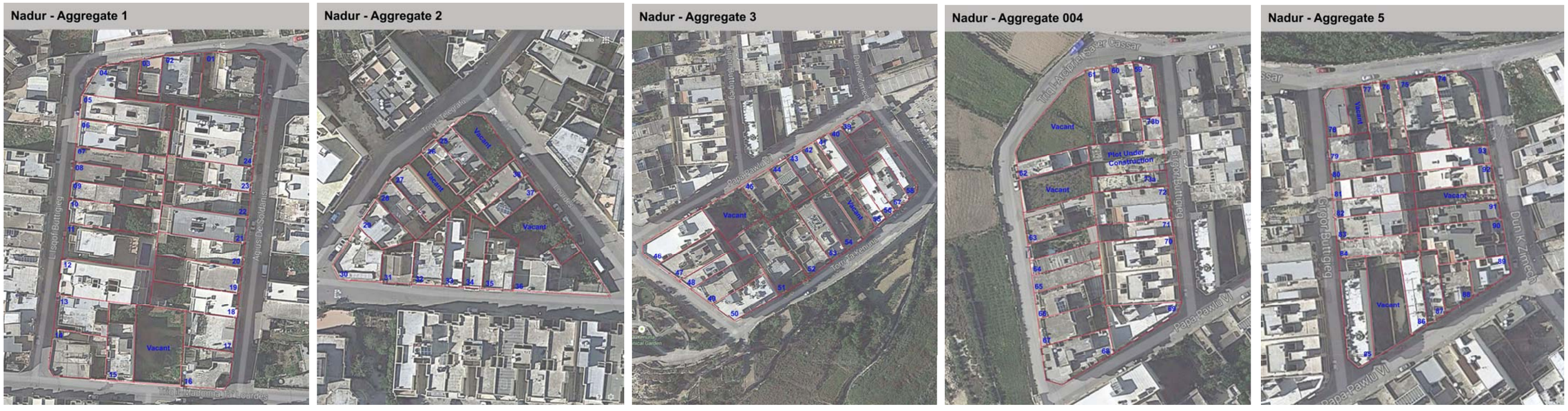

Figure 13 Building reference numbers for seismic vulnerability assessments carried out in Nadur, Gozo.

(a) (b) (c)

Figure 14 Comparison of the final seismic vulnerability ratings of the assessed buildings in Xemxija using (a) the GNDT level 2 method (24), (b) the additional parameters proposed by Formisano et al. (26) applied to the GNDT level 2 method, and (c) the New Form.

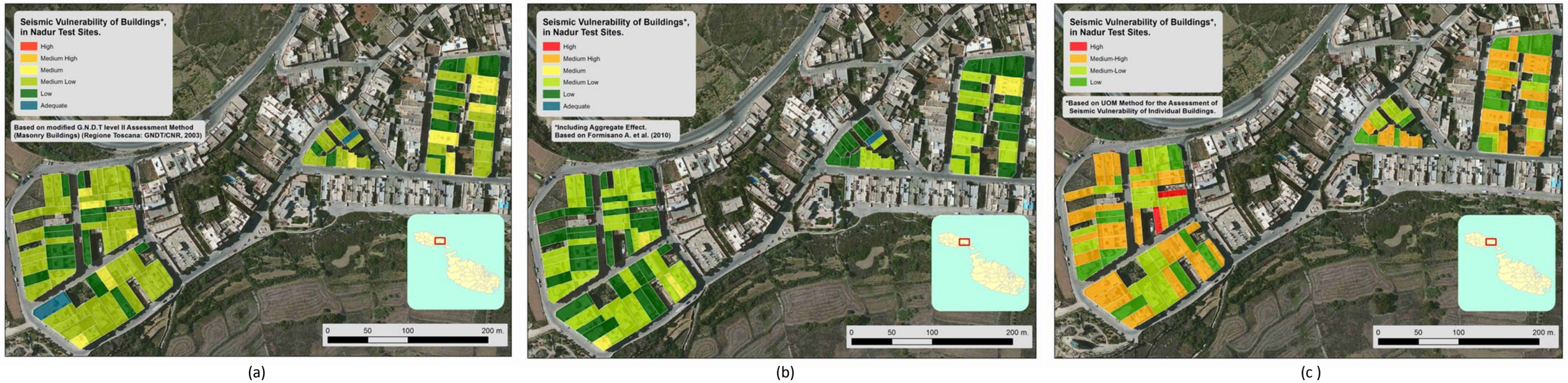

(a) (b) (c)

Figure 15 Comparison of the final seismic vulnerability ratings of the assessed buildings in Nadur using (a) the GNDT level 2 method (24), (b) the additional parameters proposed by Formisano et al. (26) applied to the GNDT level 2 method, and (c) the New Form.

Table 11 Comparison of the final seismic vulnerability ratings of assessed buildings numbers 0001 to 0014 in Xemxija using the original GNDT Level 2 method [26], the extended GNDT Level 2 method [28], and the New Form.

Count	Building number	Location	Aggregate number		(Original) GNDT Level 2 Normalised seismic vulnerability index [26] (using original maximum score (393.75))	(Original) GNDT Level 2 Seismic vulnerability rating [26] (for individual building assessment using revised ranges and original maximum score (393.75))	(Extended) GNDT Level 2 Normalised seismic vulnerability index including 'Aggregate effect' evaluation as proposed by Formisano et al. [28] (using revised maximum score (560.25))	(Extended) GNDT Level 2 Seismic vulnerability rating ('Aggregate effect' evaluation as proposed by Formisano et al. [28] applied to original GNDT Level 2 method [26])	Remarks on Extended GNDT Level 2 seismic vulnerability rating	New Form Seismic vulnerability rating
1	0001	Xemxija	001	n/a	0.39	Medium Low	0.24	Low	Left vacant. Right hand side party wall not shared, hence all entries 0 (since no aggregate effect) except for percentage openings which are similar therefore reducing the vulnerability index. Also, since most entries are 0, overall index is low compared to the revised maximum score.	Medium High
2	0002	Xemxija	001	n/a	0.47	Medium	0.37	Medium Low	Both party walls not shared. All entries 0 except for percentage openings, where there is a variation between the percentage area of openings of the assessed building building and those in building on right. Increase in seismic vulnerability results as decreased rating due to revised maximum score.	Medium High
3	0003	Xemxija	001	n/a	0.48	Medium	0.38	Medium Low	As Xemxija building 0002	Medium Low
4	0004	Xemxija	001	A	0.47	Medium	0.42	Medium Low	Vacant site on left and a lower building on right. Also a high number of staggered floors.	Medium High
5	0005	Xemxija	001	A	0.47	Medium	0.29	Low	High number of staggered floors but position of building in aggregate (middle) and difference in percentage area of openings compensate.	Medium High
6	0006	Xemxija	001	A	0.39	Medium Low	0.29	Low	Very low building on right and staggered floors increase seismic vulnerability but counteracted by similar sizes of openings on facades.	Medium High
7	0007	Xemxija	001	A	0.36	Medium Low	0.16	Low	Higher buildings on both sides; positioned in middle of aggregate; only 1 staggered pair of floors and similar size of openings, hence lower seismic vulnerability rating.	Medium High
8	0008	Xemxija	001	A	0.47	Medium	0.29	Low	Increase in seismic vulnerability caused by staggering of floors and one of adjacent buildings being lower. Counteracted in full by effect of similar percentage areas of openings on facades of adjacent buildings and position of building in middle of aggregate.	Medium High
9	0009	Xemxija	001	A	0.47	Medium	0.42	Medium Low	Unshared party wall on right and staggered floors increase seismic vulnerability rating but counteracted in part by presence of similar size of openings in adjacent buildings.	Medium Low
10	0010	Xemxija	001	B	0.47	Medium	0.36	Medium Low	Increase in seismic vulnerability due to a lower buildings on one side and staggering of floors is counteracted in part by similar size openings in adjacent buildings.	Medium High
11	0011	Xemxija	001	B	0.47	Medium	0.45	Medium	Increase in seismic vulnerability due to low buildings on both sides and staggered floors. Rest all 0 (no countereffect). Rating unchanged due to higher maximum score.	Medium High
12	0012	Xemxija	001	C	0.36	Medium Low	0.36	Medium Low	Increase in seismic vulnerability caused by left party wall not shared, staggering of floors, difference in area of openings. Rest all 0 (no countereffect). Rating unchanged due to higher maximum score.	Medium Low
13	0013	Xemxija	001	C	0.48	Medium	0.38	Medium Low	Increase in seismic vulnerability caused by lower building on left, staggering of floors, difference in area of openings. Counteracted in part by position of building in middle of aggregate. Lower overall rating due to higher maximum score.	Medium High
14	0014	Xemxija	001	C	0.39	Medium Low	0.40	Medium Low	Increase in seismic vulnerability caused by lower building on both sides, staggering of floors, difference in area of openings. Counteracted in part by position of building at corner of aggregate. Marginal increase in seismic vulnerability index which however does not result in a change in rating in view of the range of values corresponding to every rating class.	High

Table 12 Comparison of the final seismic vulnerability ratings of assessed buildings numbers 0015 to 0030 in Xemxija using the original GNDT Level 2 method [26], the extended GNDT Level 2 method [28], and the New Form.

Count	Building number	Location	Aggregate number		(Original) GNDT Level 2 Normalised seismic vulnerability index [26] (using original maximum score (393.75))	(Original) GNDT Level 2 Seismic vulnerability rating [26] (for individual building assessment using revised ranges and original maximum score (393.75))	(Extended) GNDT Level 2 Normalised seismic vulnerability index including 'Aggregate effect' evaluation as proposed by Formisano et al.[28] (using revised maximum score (560.25))	(Extended) GNDT Level 2 Seismic vulnerability rating ('Aggregate effect' evaluation as proposed by Formisano et al. [28] applied to original GNDT Level 2 method [26])	Remarks on Extended GNDT Level 2 seismic vulnerability rating	New Form Seismic vulnerability rating
15	0015	Xemxija	001	C	0.42	Medium Low	0.31	Medium Low	Increase in seismic vulnerability caused by staggering of floors, difference in area of openings. Counteracted in part by position of building in middle of aggregate. Lower overall rating due to higher maximum score.	Medium High
16	0016	Xemxija	001	C	0.38	Medium Low	0.24	Low	Increase in seismic vulnerability due to staggered floors. Counteracted in full by position of building in middle of aggregate.	Medium High
17	0017	Xemxija	001	C	0.42	Medium Low	0.42	Medium Low	Increase in seismic vulnerability caused by lower buildings on both sides, staggering of floors, difference in area of openings. Counteracted in part by position of building at corner of aggregate.	Medium High
18	0018	Xemxija	001	C	0.44	Medium Low	0.35	Medium Low	Increase in seismic vulnerability caused by lower building on right, staggering of floors, difference in area of openings. Counteracted in part by position of building in middle of aggregate.	Medium High
19	0019	Xemxija	001	C	0.47	Medium	0.36	Medium Low	Increase in seismic vulnerability caused by staggering of floors unshared party wall on right. Counteracted in part by similar percentage area of openings.	Medium High
20	0020	Xemxija	001	n/a	0.47	Medium	0.29	Low	Left party wall not shared, right vacant so isolated. Decrease in seismic vulnerability due to similar size of openings on adjacent facades.	Medium High
21	0021	Xemxija	001	D	0.47	Medium	0.36	Medium Low	Increase in seismic vulnerability caused by staggering of floors and vacant site on left. Counteracted in part by similar percentage area of openings.	Medium High
22	0022	Xemxija	001	D	0.47	Medium	0.42	Medium Low	Increase in seismic vulnerability caused by staggering of floors and vacant site on right. Counteracted in part by similar percentage area of openings.	Medium High
23	0023	Xemxija	001	E	0.47	Medium	0.42	Medium Low	Increase in seismic vulnerability caused by staggering of floors and vacant site on left. Counteracted in part by similar percentage area of openings.	Medium High
24	0024	Xemxija	001	E	0.47	Medium	0.36	Medium Low	Increase in seismic vulnerability caused by staggering of floors and vacant site on right. Counteracted in part by similar percentage area of openings.	Medium High
25	0025	Xemxija	001	n/a	0.25	Low	0.18	Low	Isolated - no change in seismic vulnerability.	Low
26	0026a	Xemxija	002	A	0.49	Medium	0.43	Medium Low	Increase in seismic vulnerability caused by lower building on left and difference in areas of openings. Counteracted in part by building's position at corner in aggregate.	Medium High
27	0026b	Xemxija	002	A	0.35	Medium Low	0.25	Low	Increase in seismic vulnerability caused by lower building on left and staggered floors. Counteracted in part by building's position in middle of aggregate.	Medium High
28	0027	Xemxija	002	A	0.41	Medium Low	0.33	Medium Low	Increase in seismic vulnerability caused by lower building on left, staggered floors and difference in percentage area of openings , Counteracted in part by building's position in middle of aggregate.	Medium High
29	0028	Xemxija	002	A	0.43	Medium Low	0.28	Low	Increase in seismic vulnerability caused by staggered floors. Counteracted in part by building's position in middle of aggregate.	Medium High
30	0029	Xemxija	002	A	0.47	Medium	0.44	Medium Low	Increase in seismic vulnerability caused by lower building on left, staggered floors and difference in percentage area of openings. Rest all 0 (no countereffect). Lower overall rating due to higher maximum score.	Medium High
31	0030	Xemxija	002	n/a	0.46	Medium	0.37	Medium Low	Right vacant. Left party wall not shared, hence all entries 0 since no aggregate effect except for percentage openings which increases seismic vulnerability, however seismic vulnerability rating lower due to higher maximum score.	Medium High

Table 13 Comparison of the final seismic vulnerability ratings of assessed buildings numbers 0031A to 0043 in Xemxija using the original GNDT Level 2 method [26], the extended GNDT Level 2 method [28], and the New Form.

Count	Building number	Location	Aggregate number		(Original) GNDT Level 2 Normalised seismic vulnerability index [26] (using original maximum score (393.75))	(Original) GNDT Level 2 Seismic vulnerability rating [26] (for individual building assessment using revised ranges and original maximum score (393.75))		(Extended) GNDT Level 2 Normalised seismic vulnerability index including 'Aggregate effect' evaluation as proposed by Formisano et al. [28] (using revised maximum score (560.25))	(Extended) GNDT Level 2 Seismic vulnerability rating ('Aggregate effect' evaluation as proposed by Formisano et al. [28] applied to original GNDT Level 2 method [26])	Remarks on Extended GNDT Level 2 seismic vulnerability rating		New Form Seismic vulnerability rating
32	0031A	Xemxija	002	B	0.49	Medium		0.46	Medium	Increase in seismic vulnerability caused by lower building on left, staggered floors and difference in percentage area of openings. Rest all 0 (no countereffect). Seismic vulnerability rating remains unchanged due to higher maximum score.		Medium High
33	0031B	Xemxija	002	B	0.5	Medium		0.46	Medium	Increase in seismic vulnerability caused by vacant site on left, staggered floors and difference in percentage area of openings. Rest all 0 (no countereffect). Rating remains unchanged due to higher maximum score.		Medium High
34	0032	Xemxija	002	A	0.47	Medium		0.40	Medium Low	Increase in seismic vulnerability caused by left party wall not shared and staggered floors. Rest all 0 (no countereffect). Lower overall rating due to higher maximum score.		Medium High
35	0033	Xemxija	002	A	0.46	Medium		0.32	Medium Low	Increase in seismic vulnerability caused by lower building on left and staggered floors. Counteracted in full by position of building in middle of aggregate.		Medium High
36	0034	Xemxija	002	A	0.41	Medium Low		0.29	Low	Increase in seismic vulnerability caused by lower building on left and staggered floors. Counteracted in full by position of building in middle of aggregate.		Medium High
37	0035	Xemxija	002	A	0.42	Medium Low		0.30	Low	Increase in seismic vulnerability caused by lower building on left and staggered floors. Counteracted in full by position of building in middle of aggregate.		Medium High
38	0036	Xemxija	003	n/a	0.42	Medium Low		0.30	Low	Left vacant, right party wall not shared so isolated. All entries 0 so overall index is lower compared to revised maximum score.		Medium High
39	0037	Xemxija	003	n/a	0.37	Medium Low		0.26	Low	Both party walls not shared so considered as isolated. All entries 0 so overall index is lower compared to revised maximum score.		Medium High
40	0038	Xemxija	003	n/a	0.44	Medium Low		0.39	Medium Low	Increase in seismic vulnerability due to different percentage area of openings in adjacent buildings. Rest all 0 since both party walls not shared (no countereffect).		Medium High
41	0039	Xemxija	003	n/a	0.37	Medium Low		0.34	Medium Low	Increase in seismic vulnerability due to different percentage area of openings in adjacent buildings. Rest all 0 since both party walls not shared.		Medium High
42	0040A	Xemxija	003	A	0.53	Medium		0.57	Medium	Increase in seismic vulnerability caused by left party wall not shared, staggered floors and difference in percentage area of openings. Rest 0 (no countereffect). Rating unchanged due to wide range of values corresponding to every rating class.		Medium High
43	0040b	Xemxija	003	B	0.53	Medium		0.57	Medium	Increase in seismic vulnerability caused by right party wall not shared, staggered floors and difference in percentage area of openings. Rest 0 (no countereffect). Rating unchanged due to wide range of values corresponding to every rating class.		Medium High
44	0041	Xemxija	003	A	0.24	Low		0.20	Low	Increase in seismic vulnerability caused by staggered floors and difference in percentage area of openings. Counteracted in part by position of building in middle of aggregate.		Low
45	0042	Xemxija	003	A	0.37	Medium Low		0.46	Medium	Increase in seismic vulnerability caused by lower building on right, staggered floors and difference in percentage area of openings. Counteracted in part by position of building in middle of aggregate.		Medium High
46	0043	Xemxija	003	A	0.45	Medium		0.36	Medium Low	Increase in seismic vulnerability caused by staggered floors and difference in percentage area of openings. Counteracted in part by position of building in middle of aggregate.		Medium High

Table 14 Comparison of the final seismic vulnerability ratings of assessed buildings numbers 0044 to 0057 in Xemxija using the original GNDT Level 2 method [26], the extended GNDT Level 2 method [28], and the New Form.

Count	Building number	Location	Aggregate number		(Original) GNDT Level 2 Normalised seismic vulnerability index [26] (using original maximum score (393.75))	(Original) GNDT Level 2 Seismic vulnerability rating [26] (for individual building assessment using revised ranges and original maximum score (393.75))	(Extended) GNDT Level 2 Normalised seismic vulnerability index including 'Aggregate effect' evaluation as proposed by Formisano et al. [28] (using revised maximum score (560.25))	(Extended) GNDT Level 2 Seismic vulnerability rating ('Aggregate effect' evaluation as proposed by Formisano et al. [28] applied to original GNDT Level 2 method [26])	Remarks on Extended GNDT Level 2 seismic vulnerability rating	New Form Seismic vulnerability rating
47	0044	Xemxija	003	A	0.28	Low	0.25	Low	Increase in seismic vulnerability caused by staggered floors and difference in percentage area of openings. Counteracted in part by position of building in middle of aggregate.	Low
48	0045	Xemxija	003	A	0.37	Medium Low	0.31	Medium Low	Increase in seismic vulnerability caused by staggered floors and difference in percentage area of openings. Counteracted in part by position of building in middle of aggregate.	Medium High
49	0046	Xemxija	003	A	0.42	Medium Low	0.43	Medium Low	Increase in seismic vulnerability caused by lower buildings on both sides, staggered floors and difference in percentage area of openings. Counteracted in part by position of building in middle of aggregate.	Medium High
50	0047	Xemxija	003	A	0.37	Medium Low	0.30	Medium Low	Increase in seismic vulnerability caused by lower building on right, staggered floors and difference in percentage area of openings. Counteracted in part by position of building in middle of aggregate.	Medium High
51	0048	Xemxija	003	A	0.37	Medium Low	0.30	Medium Low	Increase in seismic vulnerability caused by lower building on right, staggered floors and difference in percentage area of openings. Counteracted in part by position of building in middle of aggregate.	Medium High
52	0049	Xemxija	003	A	0.33	Medium Low	0.23	Low	Increase in seismic vulnerability caused by staggered floors. Counteracted in full by position of building in middle of aggregate.	Medium High
53	0050	Xemxija	003	A	0.36	Medium Low	0.32	Medium Low	Increase in seismic vulnerability caused by right party wall not shared and staggered floors. Rest all 0 (no countereffect).	Medium High
54	0051	Xemxija	003	B	0.48	Medium	0.54	Medium	Increase in seismic vulnerability caused by left party wall not shared, lower building on right, staggered floors and difference in areas of openings on adjacent facades. Rest all 0 (no countereffect). Increase in seismic vulnerability index is not reflected in an alteration in rating due to wide range of values corresponding to every rating class.	Medium High
55	0052	Xemxija	003	B	0.3	Medium Low	0.26	Low	Increase in seismic vulnerability caused by staggered floors and difference in areas of openings on adjacent facades. Counteracted in part by position of building in middle of aggregate.	Low
56	0053	Xemxija	003	B	0.25	Low	0.31	Medium Low	Increase in seismic vulnerability caused by presence of lower buildings on both sides, staggered floors and difference in areas of openings on adjacent facades. Counteracted in part by position of building in middle of aggregate.	Medium Low
57	0054	Xemxija	003	B	0.23	Low	0.18	Low	Increase in seismic vulnerability caused by staggered floors and difference in areas of openings on adjacent facades. Counteracted in part by position of building in middle of aggregate.	Low
58	0055	Xemxija	003	B	0.33	Medium Low	0.28	Low	Increase in seismic vulnerability caused by presence of lower building on left, staggered floors and difference in areas of openings on adjacent facades. Counteracted in part by position of building in middle of aggregate.	Low
59	0056	Xemxija	003	B	0.3	Medium Low	0.26	Low	Increase in seismic vulnerability caused by presence of lower buildings on both sides and staggered floors. Counteracted in part by position of building in middle of aggregate.	Medium High
60	0057	Xemxija	003	B	0.42	Medium Low	0.31	Medium Low	Increase in seismic vulnerability caused by staggered floors and difference in areas of openings on adjacent facades. Counteracted in part by position of building in middle of aggregate.	Medium Low

Table 15 Comparison of the final seismic vulnerability ratings of assessed buildings numbers 0058 to 0072 in Xemxija using the original GNDT Level 2 method [26], the extended GNDT Level 2 method [28], and the New Form.

Count	Building number	Location	Aggregate number		(Original) GNDT Level 2 Normalised seismic vulnerability index [26] (using original maximum score (393.75))	(Original) GNDT Level 2 Seismic vulnerability rating [26] (for individual building assessment using revised ranges and original maximum score (393.75))	(Extended) GNDT Level 2 Normalised seismic vulnerability index including 'Aggregate effect' evaluation as proposed by Formisano et al. [28] (using revised maximum score (560.25))	(Extended) GNDT Level 2 Seismic vulnerability rating ('Aggregate effect' evaluation as proposed by Formisano et al. [28] applied to original GNDT Level 2 method [26])	Remarks on Extended GNDT Level 2 seismic vulnerability rating	New Form Seismic vulnerability rating
61	0058	Xemxija	003	B	0.36	Medium Low	0.33	Medium Low	Increase in seismic vulnerability caused by presence of lower building on left, staggered floors and difference in areas of openings on adjacent facades. Counteracted in part by position of building in middle of aggregate.	Medium High
62	0059	Xemxija	003	C	0.31	Medium Low	0.37	Medium Low	Increase in seismic vulnerability caused by left party wall not shared, staggered floors and difference in areas of openings on adjacent facades. Rest all 0 (no countereffect). Increase in seismic vulnerability index is not reflected in an alteration in rating due to wide range of values corresponding to every rating class.	Medium High
63	0060	Xemxija	003	C	0.38	Medium Low	0.28	Low	Increase in seismic vulnerability caused by presence of lower building on left and staggered floors. Counteracted in part by position of building in middle of aggregate and similar areas of openings on adjacent facades.	Medium High
64	0061	Xemxija	003	C	0.33	Medium Low	0.25	Low	Increase in seismic vulnerability caused by staggered floors and difference in areas of openings on adjacent facades. Counteracted in part by position of building in middle of aggregate.	Low
65	0062	Xemxija	003	C	0.44	Medium Low	0.31	Medium Low	Increase in seismic vulnerability caused by presence of lower building on left and difference in areas of openings on adjacent facades. Counteracted in part by position of building in middle of aggregate.	Medium High
66	0063	Xemxija	003	C	0.36	Medium Low	0.35	Medium Low	Increase in seismic vulnerability caused by presence of lower buildings on both sides, staggered floors and difference in areas of openings on adjacent facades. Counteracted in part by position of building in middle of aggregate.	Medium High
67	0064	Xemxija	003	C	0.33	Medium Low	0.25	Low	Increase in seismic vulnerbility caused by staggered floors and difference in areas of openings on adjacent facades. Counteracted in part by position of building in middle of aggregate.	Medium Low
68	0065	Xemxija	003	C	0.36	Medium Low	0.34	Medium Low	Increase in seismic vulnerability caused by presence of lower building on left, a vacant site on right and staggered floors. Counteracted in part by similar areas of openings on adjacent facades.	Medium High
69	0066	Xemxija	004	n/a	0.52	Medium	0.37	Medium Low	Vacant site on both sides so isolated (hence, no aggregate effect). All entries 0 so overall index is lower due to revised maximum score.	Medium High
70	0067	Xemxija	004	A	0.48	Medium	0.46	Medium	Increase in seismic vulnerability caused by presence of lower building on left, a vacant site on right and staggered floors. Rest all 0 (no countereffect). Seismic vulnerability rating remains unchanged due to higher maximum score.	Medium High
71	0068	Xemxija	004	A	0.37	Medium Low	0.33	Medium Low	Increase in seismic vulnerability caused by left party wall not shared and staggered floors. Rest all 0 (no countereffect).	Medium High
72	0069	Xemxija	004	n/a	0.56	Medium	0.36	Medium Low	Left vacant, right party wall not shared so isolated. Increase in seismic resistance caused by similar areas of openings on adjacent facades. Lower rating due to higher maximum score.	Medium High
73	0070	Xemxija	005	B	0.43	Medium Low	0.29	Low	Increase in seismic vulnerability caused by lower building on right and staggered floors.Counteracted in part by position of building at corner of aggregate and similar areas of openings on adjacent facades.	Medium High
74	0071	Xemxija	005	B	0.49	Medium	0.21	Low	Seismic vulnerability of building decreased due to similar heights of adjacent buildings, middle position of building in aggregate and similar areas of openings.	Medium High
75	0072	Xemxija	005	B	0.49	Medium	0.42	Medium Low	Increase in seismic vulnerability caused by right party wall not shared and difference in areas of openings on adjacent facades. Rest all 0 (no countereffect). Seismic vulnerability rating results as lower due to higher maximum score.	Medium High

Table 16 Comparison of the final seismic vulnerability ratings of assessed buildings numbers 0073 to 0082 in Xemxija using the original GNDT Level 2 method [26], the extended GNDT Level 2 method [28], and the New Form.

Count	Building number	Location	Aggregate number		(Original) GNDT Level 2 Normalised seismic vulnerability index [26] (using original maximum score (393.75))	(Original) GNDT Level 2 Seismic vulnerability rating [26] (for individual building assessment using revised ranges and original maximum score (393.75))	(Extended) GNDT Level 2 Normalised seismic vulnerability index including 'Aggregate effect' evaluation as proposed by Formisano et al. [28] (using revised maximum score (560.25))	(Extended) GNDT Level 2 Seismic vulnerability rating ('Aggregate effect' evaluation as proposed by Formisano et al. [28] applied to original GNDT Level 2 method [26])	Remarks on Extended GNDT Level 2 seismic vulnerability rating	New Form Seismic vulnerability rating
76	0073	Xemxija	005	A	0.45	Medium	0.43	Medium Low	Increase in seismic vulnerability caused by left party wall not shared, staggered floors and difference in areas of openings on adjacent facades. Rest all 0 (no countereffect). Seismic vulnerability rating results as lower due to higher maximum score.	Medium High
77	0074	Xemxija	005	A	0.48	Medium	0.42	Medium Low	Increase in seismic vulnerability caused by lower building on left, vacant site on right and staggered floors. Counteracted in part by similar areas of openings on adjacent facades.	Medium High
78	0075	Xemxija	005	n/a	0.25	Low	0.18	Low	Left vacant and right party wall not shared so isolated. Percentage areas of openings on adjacent facades are similar. All values 0.	Medium High
79	0076	Xemxija	005	B	0.33	Medium Low	0.24	Low	Increase in seismic resistance due to presence of building of similar height on right.	Medium High
80	0077	Xemxija	005	B	0.33	Medium Low	0.09	Adequate	Increase in seismic resistance due to presence of buildings of similar height on both sides, position in middle of aggregate and similar percentage area of openings on adjacent facades.	Medium High
81	0078	Xemxija	005	B	0.3	Medium Low	0.26	Low	Increase in seismic vulnerability caused by staggered floors and difference in areas of openings on adjacent facades. Counteracted in part by position of building in middle of aggregate.	Medium High
82	0079	Xemxija	005	B	0.44	Medium Low	0.39	Medium Low	Increase in seismic vulnerability caused by presence of lower building on left, staggered floors and difference in areas of openings on adjacent facades. Counteracted in part by position of building in middle of aggregate.	Medium High
83	0080	Xemxija	005	B	0.44	Medium Low	0.25	Low	Increase in seismic vulnerability caused by staggered floors. Counteracted in full by position of building in middle of aggregate and similar percentage area of openings on adjacent facades.	Medium High
84	0081	Xemxija	005	B	0.53	Medium	0.34	Medium Low	Increase in seismic vulnerability caused by lower building on left and staggered floors. Counteracted in full by position of building in middle of aggregate and similar percentage area of openings on adjacent facades.	Medium High
85	0082	Xemxija	005	B	0.53	Medium	0.34	Medium Low	Right party wall not shared. Increase in seismic resistance due to similar openings on adjacent facades.	Medium High

Table 17 Comparison of the final seismic vulnerability ratings of assessed buildings numbers 0001 to 0014B in Nadur using the original GNDT Level 2 method [26], the extended GNDT Level 2 method [28], and the New Form.

Count	Building number	Location	Aggregate number		(Original) GNDT Level 2 Normalised seismic vulnerability index [26] (using original maximum score (393.75))	(Original) GNDT Level 2 Seismic vulnerability rating [26] (for individual building assessment using revised ranges and original maximum score (393.75))		(Extended) GNDT Level 2 Normalised seismic vulnerability index including 'Aggregate effect' evaluation as proposed by Formisano et al. [28] (using revised maximum score (560.25))	(Extended) GNDT Level 2 Seismic vulnerability rating ('Aggregate effect' evaluation as proposed by Formisano et al. [28] applied to original GNDT Level 2 method [26])	Remarks on Extended GNDT Level 2 seismic vulnerability rating		New Form Seismic vulnerability rating
86	0001	Nadur	001	n/a	0.23	Low		0.16	Low	Fully detached so isolated, hence no aggregate effect.		Low
87	0002	Nadur	001	n/a	0.3	Medium Low		0.29	Low	Semi-detached (left vacant and right party wall not shared so isolated). Increase in seismic vulnerability due tp different percentage area of openings on façade of adjacent building on right.		Low
88	0003	Nadur	001	A	0.39	Medium Low		0.43	Medium Low	Increase in seismic vulnerability caused by left party wall not shared and difference in percentage areas of openings on adjacent facade. Rest all 0 (no countereffect). Rating unchanged to the wide ranges of values applicable to every rating class.		Medium High
89	0004	Nadur	001	A	0.26	Low		0.29	Low	Increase in seismic vulnerabilty caused by Right party wall not shared, staggered floors and difference in percentage areas of openings on adjacent facade. Rest all 0 (no countereffect). Rating unchanged due to the wide ranges of values applicable to every rating class.		Low
90	0005	Nadur	001	n/a	0.47	Medium		0.37	Medium Low	Left and right party walls not shared so isolated. Increase in seismic vulnerability due to different percentage areas of openings on adjacent facades. Lower rating due to higher maximum score.		Medium High
91	0006	Nadur	001	B	0.33	Medium Low		0.41	Medium Low	Increase in seismic vulnerability caused by left party wall not shared, lower building on right, staggered floors and difference in percentage areas of openings on adjacent facade. Rest all 0 (no countereffect). Rating unchanged due to the wide range of values applicable to every rating class.		Medium High
92	0007	Nadur	001	B	0.36	Medium Low		0.29	Low	Increase in seismic vulnerability caused by staggered floors and difference in percentage areas of openings on adjacent facades. Counteracted in part by position of building in middle of aggregate.		Medium Low
93	0008	Nadur	001	B	0.44	Medium Low		0.36	Medium Low	Increase in seismic vulnerability caused by lower building on left, staggered floors and difference in percentage areas of openings on adjacent facades. Counteracted in part by position of building in middle of aggregate.		Medium High
94	0009	Nadur	001	B	0.42	Medium Low		0.27	Low	Increase in seismic vulnerability caused by difference in percentage areas of openings on adjacent facades. Counteracted in full by presence of buildings of similar height on both sides, position of building in middle of aggregate.		Medium High
95	0010	Nadur	001	B	0.47	Medium		0.44	Medium Low	Increase in seismic vulnerability caused by vacant site on right and difference in percentage areas of openings on adjacent facades. Rest all 0 (no countereffect). Rating unchanged due to the wide ranges of values applicable to every rating class.		Low
96	0011	Nadur	001	n/a	0.29	Low		0.20	Low	Fully detached so isolated, hence no aggregate effect.		Low
97	0012	Nadur	001	n/a	0.53	Medium		0.45	Medium	Left vacant and right party wall not shared so isolated. Increase in seismic vulnerability due to different percentage areas of openings on adjacent facades. This increase in the seismic vulnerability does not result in an increase in rating due to the higher maximum score.		Medium High
98	0013	Nadur	001	n/a	0.29	Low		0.28	Low	Left and right party walls not shared so isolated. Increase in seismic vulnerability due to different percentage areas of openings on adjacent facades. Lower rating due to higher maximum score.		Medium High
99	0014a	Nadur	001	n/a	0.21	Low		0.15	Low	Fully detached so isolated, hence no aggregate effect		Low
100	0014b	Nadur	001	C	0.28	Low		0.27	Low	Increase in seismic vulnerability caused by vacant site on left and difference in percentage areas of openings on adjacent facades. Rest all 0 (no countereffect). Increase in seismic vulnerability not detected due to higher maximum score.		Medium Low

Table 18 Comparison of the final seismic vulnerability ratings of assessed buildings numbers 0015 to 0028 in Nadur using the original GNDT Level 2 method [26], the extended GNDT Level 2 method [28], and the New Form.

Count	Building number	Location	Aggregate number		(Original) GNDT Level 2 Normalised seismic vulnerability index [26] (using original maximum score (393.75))	(Original) GNDT Level 2 Seismic vulnerability rating [26] (for individual building assessment using revised ranges and original maximum score (393.75))	(Extended) GNDT Level 2 Normalised seismic vulnerability index including 'Aggregate effect' evaluation as proposed by Formisano et al. [28] (using revised maximum score (560.25))	(Extended) GNDT Level 2 Seismic vulnerability rating ('Aggregate effect' evaluation as proposed by Formisano et al. [28] applied to original GNDT Level 2 method [26])	Remarks on Extended GNDT Level 2 seismic vulnerability rating	New Form Seismic vulnerability rating
101	0015	Nadur	001	C	0.25	Low	0.30	Medium Low	Increase in seismic vulnerability caused by lower building on left, vacant site on right and difference in percentage areas of openings on adjacent facades. Rest all 0 (no countereffect).	Medium High
102	0016	Nadur	001	n/a	0.34	Medium Low	0.32	Medium Low	Left vacant, right party wall not shared so isolated. Increase in seismic vulnerability caused difference in percentage areas of openings on adjacent facades. Rest all 0 (no countereffect).Rating unchanged to higher maximum score.	Medium High
103	0017	Nadur	001	n/a	0.21	Low	0.19	Low	Left and right party walls not shared so isolated. Increase in seismic vulnerability caused difference in percentage areas of openings on adjacent facades. Rest all 0 (no countereffect). Rating unchanged due to higher maximum score.	Medium Low
104	0018	Nadur	001	D	0.34	Medium Low	0.35	Medium Low	Increase in seismic vulnerability caused by unshared left party wall, staggered floors and difference in percentage areas of openings on adjacent facades. Rest all 0 (no countereffect).Rating unchanged due to higher maximum score and wide range of values associated with every rating class.	Medium High
105	0019	Nadur	001	D	0.34	Medium Low	0.34	Medium Low	Increase in seismic vulnerability caused by lower buildings on both sides, staggered floors and difference in percentage areas of openings on adjacent facades. Counteracted in part by position of building in middle of aggregate.	Medium High
106	0020	Nadur	001	D	0.19	Low	0.23	Low	Increase in seismic vulnerability caused by unshared right party wall, staggered floors and difference in percentage areas of openings on adjacent facades. Rest all 0 (no countereffect). Rating unchanged due to wide range of values associated with every rating class.	Low
107	0021	Nadur	001	n/a	0.48	Medium	0.38	Medium Low	Left and right party walls not shared so isolated. Increase in seismic vulnerability caused difference in percentage areas of openings on adjacent facades. Rest all 0 (no countereffect). Rating unchanged due to higher maximum score.	Medium High
108	0022	Nadur	001	n/a	0.37	Medium Low	0.34	Medium Low	Left and right party walls not shared so isolated. Increase in seismic vulnerability caused difference in percentage areas of openings on adjacent facades. Rest all 0 (no countereffect). Rating unchanged due to higher maximum score.	Medium Low
109	0023	Nadur	001	n/a	0.23	Low	0.24	Low	Left and right party walls not shared so isolated. Increase in seismic vulnerability caused difference in percentage areas of openings on adjacent facades. Rest all 0 (no countereffect). Rating unchanged due to wide range of values associated with every rating class.	Low
110	0024	Nadur	001	n/a	0.42	Medium Low	0.30	Low	Left party wall not shared, vacant site on right so isolated. Rest all 0 (no effect). Seismic vulnerability results as decreased due to higher maximum score.	Medium High
111	0025	Nadur	002	n/a	0.33	Medium Low	0.23	Low	Left vacant, unshared party wall on right, so isolated. Rest all 0 (no effect). Seismic vulnerability results as decreased due to higher maximum score.	Medium Low
112	0026	Nadur	002	n/a	0.33	Medium Low	0.23	Low	Left party wall not shared, vacant site on right, so isolated. Rest all 0 (no effect). Lower rating due to higher maximum score.	Medium Low
113	0027	Nadur	002	n/a	0.36	Medium Low	0.25	Low	Left vacant, unshared right party wall, so isolated. Rest all 0 (no effect). Lower rating due to higher maximum score.	Medium Low
114	0028	Nadur	002	n/a	0.33	Medium Low	0.20	Low	Both party walls not shared so isolated. Decrease in seismic vulnerability due to similar percentage area of openings on adjacent facades.	Medium Low

Table 19 Comparison of the final seismic vulnerability ratings of assessed buildings numbers 0029 to 0042 in Nadur using the original GNDT Level 2 method [26], the extended GNDT Level 2 method [28], and the New Form.

Count	Building number	Location	Aggregate number		(Original) GNDT Level 2 Normalised seismic vulnerability index [26] (using original maximum score (393.75))	(Original) GNDT Level 2 Seismic vulnerability rating [26] (for individual building assessment using revised ranges and original maximum score (393.75))	(Extended) GNDT Level 2 Normalised seismic vulnerability index including 'Aggregate effect' evaluation as proposed by Formisano et al. [28] (using revised maximum score (560.25))	(Extended) GNDT Level 2 Seismic vulnerability rating ('Aggregate effect' evaluation as proposed by Formisano et al. [28] applied to original GNDT Level 2 method [26])	Remarks on Extended GNDT Level 2 seismic vulnerability rating	New Form Seismic vulnerability rating
115	0029	Nadur	002	A	0.37	Medium Low	0.43	Medium Low	Increase in seismic vulnerability caused by unshared left party wall, lower building on right, staggered floors and difference in percentage areas of openings on adjacent facades. Rest all 0 (no countereffect). Rating unchanged in view of the wide range of values associated with every rating class.	Medium High
116	0030	Nadur	002	A	0.05	Adequate	0.05	Adequate	Increase in seismic vulnerability caused by staggered floors and difference in percentage areas of openings on adjacent facades. Counteracted in part by position of building at corner of aggregate.	Low
117	0031	Nadur	002	A	0.15	Low	0.13	Low	Increase in seismic vulnerabiltiy caused by lower left building, staggered floors and difference in percentage areas of openings on adjacent facades. Counteracted in part by position of building in middle of aggregate.	Low
118	0032	Nadur	002	A	0.36	Medium Low	0.27	Low	Increase in seismic vulnerability caused by lower buildings on left and right and staggered floors. Counteracted in part by position of building in middle of aggregate and similar percentage areas of openings on facades of adjacent buildings.	Medium High
119	0033	Nadur	002	A	0.36	Medium Low	0.22	Low	Increase in seismic vulnerability caused by lower right building and staggered floors. Counteracted in full by position of building in middle of aggregate and similar percentage areas of openings on facades of adjacent buildings.	Medium High
120	0034	Nadur	002	A	0.25	Low	0.11	Low	Increase in seismic vulnerability caused by staggered floors. Counteracted in full by position of building in middle of aggregate and similar percentage areas of openings on facades of adjacent buildings.	Low
121	0035	Nadur	002	A	0.42	Medium Low	0.31	Medium Low	Increase in seismic vulnerability caused by lower buildings on both sides and staggered floors. Counteracted in full by position of building in middle of aggregate and similar percentage areas of openings on facades of adjacent buildings.	Medium High
122	0036	Nadur	002	A	0.42	Medium Low	0.31	Medium Low	Increase in seismic vulnerability caused by vacant site on right and staggered floors. Counteracted in part by similar percentage areas of openings on facades of adjacent buildings.	Medium High
123	0037	Nadur	002	n/a	0.48	Medium	0.42	Medium Low	Vacant site on left and unshared party walls on right so isolated. Increase in seismic vulnerability due to different percentage areas of openings on adjacent facades. Lower ratings due to higher maximum score.	Low
124	0038	Nadur	002	n/a	0.36	Medium Low	0.33	Medium Low	Left party wall not shared and vacant site on right so isolated. Increase in seismic vulnerability due to different percentage areas of openings on adjacent facades. No increase in rating due to higher maximum score.	Medium Low
125	0039	Nadur	003	n/a	0.29	Low	0.2	Low	Isolated so no aggregate effect.	Medium High
126	0040	Nadur	003	A	0.07	Adequate	0.17	Low	Increase in seismic vulnerability caused by vacant site on left, staggered floors and different percentage area of openings on adjacent facades. Rest 0 (no countereffect).	Low
127	0041	Nadur	003	A	0.47	Medium	0.50	Medium	Increase in seismic vulnerability caused by lower building on left, recessed adjacent building on right (considered as vacant), staggered floors and different percentage area of openings on adjacent facades. Rest 0 (no countereffect).Rating unchanged due to the wide range of values associated with every rating class.	Medium High
128	0042	Nadur	003	A	0.34	Medium Low	0.32	Medium Low	Increase in seismic vulnerability caused by recessed adjacent building on left, staggered floors and different percentage area of openings on adjacent facades. Rest 0 (no countereffect). No change in rating due to higher maximum score.	Medium High

Table 20 Comparison of the final seismic vulnerability ratings of assessed buildings numbers 0043 to 0056 in Nadur using the original GNDT Level 2 method [26], the extended GNDT Level 2 method [28], and the New Form.

Count	Building number	Location	Aggregate number		(Original) GNDT Level 2 Normalised seismic vulnerability index [26] (using original maximum score (393.75))	(Original) GNDT Level 2 Seismic vulnerability rating [26] (for individual building assessment using revised ranges and original maximum score (393.75))	(Extended) GNDT Level 2 Normalised seismic vulnerability index including 'Aggregate effect' evaluation as proposed by Formisano et al. [28] (using revised maximum score (560.25))	(Extended) GNDT Level 2 Seismic vulnerability rating ('Aggregate effect' evaluation as proposed by Formisano et al. [28] applied to original GNDT Level 2 method [26])	Remarks on Extended GNDT Level 2 seismic vulnerability rating	New Form Seismic vulnerability rating
129	0043	Nadur	003	A	0.42	Medium Low	0.31	Medium Low	Increase in seismic vulnerability caused by staggered floors and different percentage area of openings on adjacent facades. Counteracted in part by position of building in middle of aggregate.	Medium High
130	0044	Nadur	003	A	0.39	Medium Low	0.41	Medium Low	Increase in seismic vulnerability caused by lower buildings on both sides, staggered floors and different percentage area of openings on adjacent facades. Counteracted in part by position of building in middle of aggregate. Rating unchanged due to the wide range of values associated with every rating class.	Medium Low
131	0045	Nadur	004	A	0.18	Low	0.25	Low	Increase in seismic vulnerability caused by vacant site on right, staggered floors and different percentage area of openings on adjacent facades. Rest all 0 (no countereffect). Rating unchanged due to the wide range of values associated with every rating class.	Medium Low
132	0046	Nadur	003	n/a	0.36	Medium Low	0.30	Low	Left vacant and unshared right party walls so isolated. Increase in seismic vulnerability due to different percentage areas of openings on adjacent facades. Increase in seismic vulnerability results as decreased due to higher maximum score.	Medium High
133	0047	Nadur	003	B	0.42	Medium Low	0.41	Medium Low	Increase in seismic vulnrability caused by unshared left party wall, staggered floors and different percentage area of openings on adjacent facades. Rest all 0 (no countereffect). No increase in seismic vulnerability rating due to higher maximum score.	Medium High
134	0048	Nadur	003	B	0.36	Medium Low	0.39	Medium Low	Increase in seismic vulnerability caused by lower buildings on both sides, staggered floors and different percentage area of openings on adjacent facades. Counteracted in part by position of building in middle of aggregate.Rating unchanged due to the wide range of values associated with every rating class.	Medium High
135	0049	Nadur	003	B	0.34	Medium Low	0.37	Medium Low	Increase in seismic vulnerability caused by unshared right party wall, staggered floors and different percentage area of openings on adjacent facades. Rest all 0 (no countereffect). Rating unchanged due to the wide range of values associated with every rating class.	Low
136	0050A	Nadur	003	D	0.31	Medium Low	0.24	Low	Increase in seismic vulnerability caused by unshared left party wall. Rest all 0 (no countereffect). Increase in seismic vulnerability results as decreased due to higher maximum score.	Medium High
137	0050B	Nadur	003	D	0.31	Medium Low	0.24	Low	Increase in seismic vulnerability caused by vacant site on right. Rest all 0 (no countereffect). Increase in seismic vulnerability results as decreased due to higher maximum score.	Medium High
138	0051	Nadur	003	n/a	0.47	Medium	0.33	Medium Low	Isolated so no aggregate effect. Seismic vulnerability results as lower due to higher maximum score.	Medium Low
139	0052	Nadur	003	n/a	0.22	Low	0.23	Low	Increase in seismic vulnerability caused by vacant site on left, unshared right party wall and difference in percentage area of openings on adjacent facades. Rest all 0 (no countereffect).Rating unchanged due to the wide range of values associated with every rating class.	Medium Low
140	0053	Nadur	003	n/a	0.37	Medium Low	0.34	Medium Low	Both party walls not shared so isolated.Increase in seismic vulnerability caused by difference in percentage area of openings on adjacent facades. Rest all 0 (no countereffect). No change in rating due to higher maximum score.	Medium High
141	0054	Nadur	003	n/a	0.36	Medium Low	0.22	Low	Left party wall not shared, right vacant, so isolated. All values 0 except percentage difference of areas of openings between adjacent facades which suggests an increase in resistance since percentage areas are similar.	Low
142	0055	Nadur	003	n/a	0.36	Medium Low	0.25	Low	Left vacant, right party wall not shared, so isolated. Rest all 0 (no effect). Lower seismic vulnerability rating due to higher maximum score.	Medium High
143	0056	Nadur	003	C	0.36	Medium Low	0.45	Medium	Increase in seismic vulnerability caused by unshared left party wall, lower building on right, staggered floors and different percentage area of openings on adjacent facades. Rest all 0 (no countereffect)	Medium High

Table 21 Comparison of the final seismic vulnerability ratings of assessed buildings numbers 0057 to 0070A in Nadur using the original GNDT Level 2 method [26], the extended GNDT Level 2 method [28], and the New Form.

Count	Building number	Location	Aggregate number		(Original) GNDT Level 2 Normalised seismic vulnerability index [26] (using original maximum score (393.75))	(Original) GNDT Level 2 Seismic vulnerability rating [26] (for individual building assessment using revised ranges and original maximum score (393.75))	(Extended) GNDT Level 2 Normalised seismic vulnerability index including 'Aggregate effect' evaluation as proposed by Formisano et al. [28] (using revised maximum score (560.25))	(Extended) GNDT Level 2 Seismic vulnerability rating ('Aggregate effect' evaluation as proposed by Formisano et al. [28] applied to original GNDT Level 2 method [26])	Remarks on Extended GNDT Level 2 seismic vulnerability rating	New Form Seismic vulnerability rating
144	0057	Nadur	003	C	0.33	Medium Low	0.31	Medium Low	Increase in seismic vulnerability caused by lower buildinh on right, staggered floors and different percentage area of openings on adjacent facades. Counteracted in part by position of building in middle of aggregate.	Low
145	0058	Nadur	003	C	0.42	Medium Low	0.34	Medium Low	Increase in seismic vulnerability caused by vacant site on right and staggered floors. Rest all 0 (no countereffect).	Medium High
146	0059	Nadur	004	A	0.33	Medium Low	0.25	Low	Increase in seismic vulnerability caused by staggered floors and different percentage area of openings on adjacent facades. Counteracted in part by similar height of adjacent buildings and position of building in middle of aggregate.	Medium High
147	0060	Nadur	004	A	0.33	Medium Low	0.21	Low	Increase in seismic vulnerability caused by staggered floors. Counteracted in full by position of building in middle of aggregate.	Medium High
148	0061	Nadur	004	A	0.33	Medium Low	0.35	Medium Low	Increase in seismic vulnerability caused by vacant site on right and staggered floors. Rest all 0 (no countereffect). IRating unchanged due to the wide range of values associated with every rating class.	Medium High
149	0062	Nadur	004	n/a	0.42	Medium Low	0.30	Low	Isolated so no aggregate effect. Lower seismic vulnerability due to higher maximum score.	Medium High
150	0063	Nadur	004	n/a	0.27	Low	0.19	Low	Isolated so no aggregate effect.	Medium High
151	0064	Nadur	004	n/a	0.36	Medium Low	0.33	Medium Low	Increase in seismic vulnerability caused by vacant site on left, unshared party wall on right party wall (so isolated) and different percentage area of openings on adjacent facades. Rest all 0 (no countereffect). No increase in rating due to high maximum score.	Medium Low
152	0065	Nadur	004	B	0.39	Medium Low	0.45	Medium Low	Increase in seismic vulnerability caused by unshared left party wall, lower building on right, staggered floors and different percentage area of openings on adjacent facades. Rest all 0 (no countereffect). Rating unchanged due to the wide range of values associated with every rating class.	Medium High
153	0066	Nadur	004	B	0.33	Medium Low	0.27	Low	Increase in seismic vulnerability caused by unshared right party wall and staggered floors. Rest all 0 (no countereffect). Lower rating due to higher maximum score.	Medium Low
154	0067	Nadur	004	C	0.33	Medium Low	0.34	Medium Low	Increase in seismic vulnerability caused by unshared left party wall, staggered floors and different percentage area of openings on adjacent facades. Rest all 0 (no countereffect).Rating unchanged due to the wide range of values associated with every rating class.	Medium High
155	0068	Nadur	004	C	0.33	Medium Low	0.36	Medium Low	Increase in seismic vulnerability caused by lower buildings on both sides, staggered floors and different percentage area of openings on adjacent facades. Counteracted in part by position of building at corner in aggregate. Rating unchanged due to the wide range of values associated with every rating class.	Low
156	0069	Nadur	004	C	0.25	Low	0.27	Low	Increase in seismic vulnerability caused by unshared right party wall, staggered floors and different percentage area of openings on adjacent facades. Rest all 0 (no countereffect).Rating unchanged due to the wide range of values associated with every rating class.	Low
157	0070A	Nadur	004	D	0.34	Medium Low	0.40	Medium Low	Increase in seismic vulnerability caused by unshared left party wall, lower building on right, staggered floors and different percentage area of openings on adjacent facades. Rest all 0 (no countereffect). Rating unchanged due to the wide range of values associated with every rating class.	Medium High

Table 22 Comparison of the final seismic vulnerability ratings of assessed buildings numbers 0070B to 0079 in Nadur using the original GNDT Level 2 method [26], the extended GNDT Level 2 method [28], and the New Form.

Count	Building number	Location	Aggregate number		(Original) GNDT Level 2 Normalised seismic vulnerability index [26] (using original maximum score (393.75))	(Original) GNDT Level 2 Seismic vulnerability rating [26] (for individual building assessment using revised ranges and original maximum score (393.75))		(Extended) GNDT Level 2 Normalised seismic vulnerability index including 'Aggregate effect' evaluation as proposed by Formisano et al. [28] (using revised maximum score (560.25))	(Extended) GNDT Level 2 Seismic vulnerability rating ('Aggregate effect' evaluation as proposed by Formisano et al. [28] applied to original GNDT Level 2 method [26])	Remarks on Extended GNDT Level 2 seismic vulnerability rating		New Form Seismic vulnerability rating
158	0070B	Nadur	004	D	0.34	Medium Low		0.35	Medium Low	Increase in seismic vulnerability caused by unshared right party wall, staggered floors and different percentage area of openings on adjacent facades. Rest all 0 (no countereffect). Rating unchanged due to the wide range of values associated with every rating class.		Medium High
159	0071	Nadur	004	E	0.2	Low		0.23	Low	Increase in seismic vulnerability caused by unshared left party wall, staggered floors and different percentage area of openings on adjacent facades. Rest all 0 (no countereffect). Rating unchanged due to the wide range of values associated with every rating class.		Low
160	0072A	Nadur	004	E	0.27	Low		0.26	Low	Increase in seismic vulnerability caused by lower left building, staggered floors and different percentage area of openings on adjacent facades. Counteracted in part by position of building in middle of aggregate.		Low
161	0072B	Nadur	004	E	0.36	Medium Low		0.32	Medium Low	Increase in seismic vulnerability caused by unshared right party wall, different percentage area of openings on adjacent facades. Rest all 0 (no countereffect).		Medium High
162	0073A	Nadur	004	n/a	0.28	Low		0.20	Low	Left party walls not shared, right vacant, so distinct. All parameters 0. No aggregate effect.		Medium Low
163	0073B	Nadur	004	A	0.13	Low		0.24	Low	Increase in seismic vulnerability caused by vacant site on left, staggered floors and different percentage area of openings on adjacent facades. Counteracted in part by position of building in middle of aggregate.		Low
164	0074	Nadur	005	A	0.23	Low		0.17	Low	Increase in seismic vulnerability caused by vacant site on left, staggered floors. Counteracted in part by similar percentage area of openings on adjacent facades.		Low
165	0075	Nadur	005	A	0.3	Medium Low		0.29	Low	Increase in seismic vulnerability caused by lower building on left, staggered floors, different percentage area of openings on adjacent facades. Counteracted in part by position of building in middle of aggregate.		Medium Low
166	0076	Nadur	005	A	0.44	Medium Low		0.39	Medium Low	Increase in seismic vulnerability caused by lower building on left, staggered floors and different percentage area of openings on adjacent facades. Counteracted in part by position of building in middle of aggregate. Rating unchanged due to higher maximum score.		Medium Low
167	0077	Nadur	005	A	0.42	Medium Low		0.48	Medium	Increase in seismic vulnrability caused by lower building on left, vacant site on right, staggered floors and different percentage area of openings on adjacent facades. Rest all 0 (no countereffect).		Medium Low
168	0078	Nadur	005	B	0.19	Low		0.25	Low	Increase in seismic vulnerability caused by vacant site on left, staggered floors and different percentage area of openings on adjacent facades. Rest all 0 (no countereffect). Rating unchanged due to the wide range of values associated with every rating class.		Low
169	0079	Nadur	005	B	0.30	Medium Low		0.34	Medium Low	Increase in seismic vulnerability caused by lower buildings on both sides, staggered floors and different percentage area of openings on adjacent facades. Counteracted in part by position of building in middle of aggregate. Rating unchanged due to the wide range of values associated with every rating class.		Medium High

Table 23 Comparison of the final seismic vulnerability ratings of assessed buildings numbers 0080 to 0093 in Nadur using the original GNDT Level 2 method [26], the extended GNDT Level 2 method [28], and the New Form.

Count	Building number	Location	Aggregate number		(Original) GNDT Level 2 Normalised seismic vulnerability index [26] (using original maximum score (393.75))	(Original) GNDT Level 2 Seismic vulnerability rating [26] (for individual building assessment using revised ranges and original maximum score (393.75))		(Extended) GNDT Level 2 Normalised seismic vulnerability index including 'Aggregate effect' evaluation as proposed by Formisano et al. [28] (using revised maximum score (560.25))	(Extended) GNDT Level 2 Seismic vulnerability rating ('Aggregate effect' evaluation as proposed by Formisano et al. [28] applied to original GNDT Level 2 method [26])	Remarks on Extended GNDT Level 2 seismic vulnerability rating		New Form Seismic vulnerability rating
170	0080	Nadur	005	B	0.37	Medium Low		0.28	Low	Increase in seismic vulnerability caused by staggered floors and different percentage area of openings on adjacent facades. Counteracted in part by position of building in middle of aggregate.		Medium Low
171	0081	Nadur	005	B	0.37	Medium Low		0.36	Medium Low	Increase in seismic vulnerability caused by lower buildings on both sides, staggered floors and different percentage area of openings on adjacent facades. Counteracted in part by position of building in middle of aggregate.		Medium High
172	0082	Nadur	005	B	0.37	Medium Low		0.30	Medium Low	Increase in seismic vulnerability caused by lower buillding on right, staggered floors and different percentage area of openings on adjacent facades. Counteracted in part by position of building in middle of aggregate.		Medium Low
173	0083	Nadur	005	B	0.37	Medium Low		0.30	Medium Low	Increase in seismic vulnerability caused by lower building on right, staggered floors and different percentage area of openings on adjacent facades. Counteracted in part by position of building in middle of aggregate.		Medium Low
174	0084	Nadur	005	B	0.29	Low		0.29	Low	Increase in seismic vulnrability caused by vacant site on right, staggered floors and different percentage area of openings on adjacent facades. Rest all 0 (no countereffect). Rating unchanged due to higher maximum score.		Medium Low
175	0085	Nadur	005	n/a	0.48	Medium		0.34	Medium Low	Isolated, hence no aggregate effect. Lower seismic vulnerability rating due to higher maximum score.		Medium High
176	0086	Nadur	005	n/a	0.36	Medium Low		0.25	Low	Left vacant, right party wall not shared, so isolated. Rest all 0 (no effect). Lower seismic vulnerability rating due to higher maximum score.		High
177	0087	Nadur	005	n/a	0.47	Medium		0.33	Medium Low	Both party walls not shared, so isolated. Rest all 0 (no effect). Lower seismic vulnerability rating due to higher maximum score.		Medium High
178	0088	Nadur	005	n/a	0.17	Low		0.12	Low	Both party walls not shared, so isolated. Rest all 0 (no countereffect).		Low
179	0089	Nadur	005	C	0.26	Low		0.31	Medium Low	Increase in seismic vulnerability caused by unshared left party wall, staggered floors and different percentage area of openings on adjacent facades. Rest all 0 (no countereffect).		Low
180	0090	Nadur	005	C	0.31	Medium Low		0.35	Medium Low	Increase in seismic vulnerability caused by lower buildings on both sides, staggered floors and different percentage area of openings on adjacent facades. Counteracted in part by position of building in middle of aggregate.Rating unchanged due to the wide range of values associated with every rating class.		Medium Low
181	0091	Nadur	005	C	0.48	Medium		0.42	Medium Low	Increase in seismic vulnerability caused by vacant site on right, staggered floors and different percentage area of openings on adjacent facades. Rest all 0 (no countereffect). Lower rating due to higher maximum score.		High
182	0092	Nadur	005	n/a	0.37	Medium Low		0.22	Low	Left vacant, right party wall not shared, so isolated. Seismic vulnerability reduced by presence of similar percentage areas of openings on facades of adjacent buildings.		Medium High
183	0093	Nadur	005	n/a	0.43	Medium Low		0.27	Low	Left party wall not shared, right vacant, so isolated. Seismic vulnerability reduced by presence of similar percentage areas of openings on facades of adjacent buildings.		Medium High

Appendix B. PUBLISHED STUDIES

i) Document (i): Chapter in the book which summarises the final outcomes of the different teams working on the engineering component of the SIMIT Project (Project code: B1-2.19/11). This chapter reports the work carried out by the author through her involvement as Research Support Officer I with the Faculty for the Built Environment of the University of Malta with respect to the deliverables of Work Package 2.1 of the SIMIT Project.
Reference: Torpiano A, Bonello MA, Borg RP, Sapiano P, Ellul AM. A methodology for the seismic vulnerability assessment of loadbearing masonry buildings in Malta. In: Cicero C, Lombardo G (eds.) *Establishment of an integrated Italy-Malta cross-border system of civil protection – Engineering aspects.* SIMIT/3. Ariccia, Italy: ARACNE editrice int.le S.r.l.; 2015. p. 133-181.
Status: published.

1. Introduction

Since the last major earthquake which hit the Maltese Islands on the 11th January 1693, significant urban areas have been built up. The urban environment consists of a large variety of building types, from different time periods, with varying characteristics. These characteristics contribute towards the vulnerability of the individual building and the aggregate of buildings in a block. Such characteristics, including materials, structural systems, building height and layout, position in a block and building - ground interface, all contribute to the structural performance of a building in case of an earthquake. The Faculty for the Built Environment at the University of Malta has carried out a thorough study of the identification and the definition of indicators based on the characteristics of the contemporary loadbearing masonry building typology present in the Maltese Islands, which can lead to an evaluation of the vulnerability of such structures and the built environment to seismic action in areas which have developed in the last 50 to 60 years, when such a building typology became prevalent. The methodology developed draws on other methodologies employed within other countries and on the experiences of regions with a high incidence of earthquakes, where such methodologies have been well-calibrated. However the methods employed in other countries cannot be directly transposed to the local building stock due to inherent variations in local building typologies which need to be taken into account. This, together with the knowledge that, in the vast majority of cases, residential buildings falling under this construction typology in the Maltese Islands, have not been constructed in accordance with any seismic design codes, in addition to the consideration of the high probability of occurrence of a major seismic event if a 475 year period is taken into account, stresses the necessity of the development of a seismic vulnerability assessment methodology for use in the case of contemporary loadbearing masonry buildings.

1.2. Structural Systems in the Maltese Islands

The loadbearing masonry building typologies present in the Maltese islands can be largely subdivided under two main types of construction, namely, traditional and contemporary construction.

Traditional loadbearing masonry buildings present in the Maltese islands typically consist of walls including two external leaves with infill material in between (Figure 1) and roofing systems composed of stone arches and stone slab roofs, stone slab roofs, stone slabs over timber beams or steel beams, and/ or timber panels over timber beams (not frequent) (Figure 2).

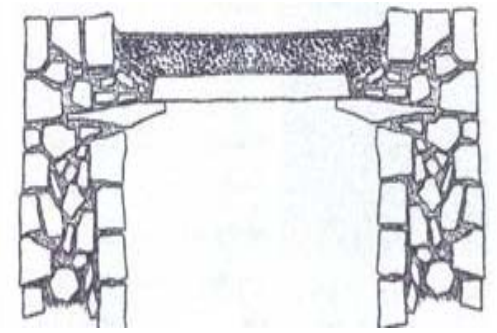

Figure 1. Typical traditional wall construction system.

http://markbiwwa.com/copywriting/the-times-property-and-construction/how-to-find-materials-to-renovate-a-house-of-character/

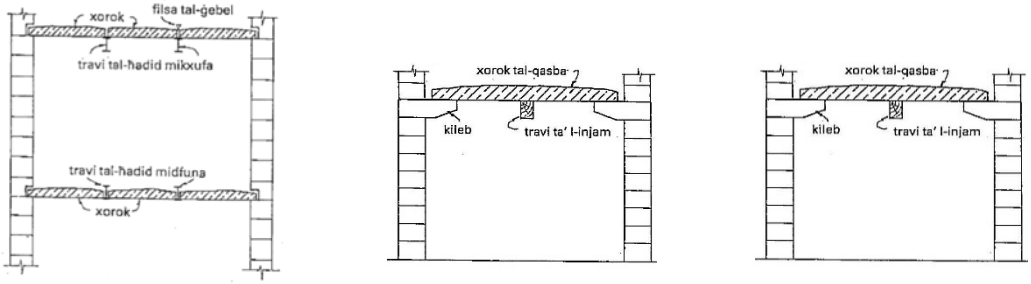

Sections through traditional roofs: 'Il- Bennej – taghlim dwar is-sengha tal-bini'. Malta Education Department.

Figure 2. Typical traditional roofing systems.

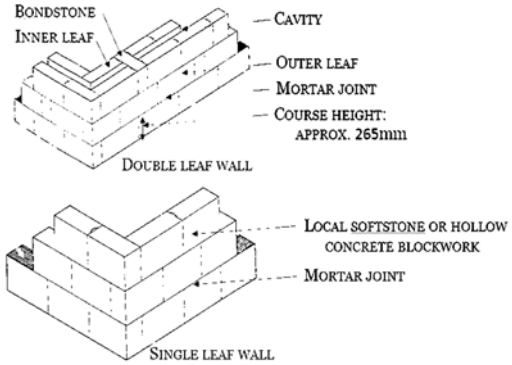

'Il- Bennej – taghlim dwar is-sengha tal-bini'. Malta Education Department.

Figure 3. Typical contemporary wall construction systems.

Contemporary loadbearing masonry buildings present in the Maltese islands mainly consist of loadbearing masonry (local softstone or concrete block) single or double leaf walls with a cavity or bondstones (Figure 3) and reinforced concrete cast in-situ or precast slab roofs (Figure 4). This is the main building typology used locally from around 1960 to the present day.

Figure 4. Typical contemporary roof construction systems.

This study has focused on the seismic vulnerability assessment of contemporary loadbearing masonry construction typology in the Maltese islands, with particular attention to specific structural systems. This building typology consists of blocks of residential apartments (flats) comprising:

- a semi-basement car park with no internal partition walls;
- generally roofed over by hollow-core precast-prestressed planks;
- usually 4 or more residential floors in addition to a penthouse level.

The additional characteristics, apart from the soft storey effect, which are particular to the building typology under investigation and which could cause an increase in the seismic vulnerability of these include (but are not limited to) (Figures 5a, 5b and 6):

i. narrow and long plan configurations and narrow and high elevation proportions arising from the typical plot proportions for the building typology under study;
ii. open plan spaces without loadbearing cross-walls (very often in more than one storey);
iii. shared or unshared party walls, where the party walls in general consist of single leaf 230mm thick unreinforced masonry walls;
iv. long corridors directly abutting party walls;
v. vacant sites, hence giving rise to unrestrained party walls;
vi. misalignment of intermediate slabs, roofs, front and rear facades and internal spaces;
vii. double height spaces;
viii. large openings on facades facing the view leaving a very small wall area constructed in masonry between openings;

ix. setbacks due to sloping sites (very often occurring on more than one floor);

x. the construction of additional floors due to changes in the regulations limiting the maximum building heights over the years;

xi. projecting rooms and balconies on more than one storey.

These characteristics are widespread throughout the Maltese Islands for the building typology under investigation.

(a) (b) (c)

Figure 5a: Examples of seismic vulnerability characteristics present in the contemporary loadbearing masonry building typology - 1:

a) double height spaces at lower levels due to commercial establishments;
b) adjacent buildings with different heights: unrestrained party walls and misaligned slab levels;
c) unrestrained party walls due to vacant sites.

(d) (e) (f)

(g) (h)

Figure 5b: Examples of seismic vulnerability characteristics present in the contemporary loadbearing masonry building typology - 2:

a) misalignment of slab levels within same individual buildings and between adjacent buildings;
b) misalignment between planes of facades of adjacent buildings;
c) setbacks – sloping sites;
d) projecting rooms;
e) large area of openings on façade.

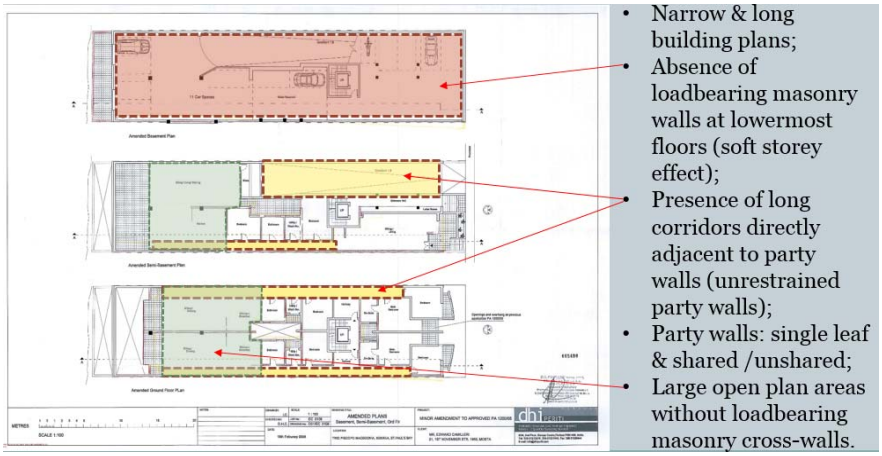

Figure 6: Examples of seismic vulnerability characteristics present in the contemporary loadbearing masonry building typology – 2.

1.3 Existing Seismic Vulnerability Assessment Methods

A detailed review of a number of existing first and second level vulnerability Italian assessment methods has been carried out not only with respect to the actual parameters listed in these existing forms but also with respect to the background principles affecting the seismic vulnerability of buildings as outlined in the manuals to these forms. The verification of the applicability of these existing assessment forms to the local contemporary loadbearing masonry building typologies in Malta & Gozo has also been carried out.

The existing assessment methods which have been reviewed and considered were the following:

a) AeDES (Agibilita' e Danno nell' Emergenza Sismica: Manuale per la compilazione, pronto intervento e agibilita' per edifici ordinari nell' emergenza post-sismica. Dipartimento della Protezione Civile, 2000). – AeDES;
b) CLE (Condizione Limite per l'Emergenza: Analisi della condizione limite per l'emergenza (CLE) nell'insediamento urbano. Version 2.0. Presidenza del Consiglio dei Ministri, Commissione Tecnica per la Microzonazione Sismica, October 2013) - CLE;
c) Manuale per il rilevamento della vulnerabilita' sismica degli edifici – Istruzione per la compilazione della scheda di I livello. (Regione Abruzzo: GNDT/CNR, 2007) .– Reg. Abruzzo GNDT 1st Level;
d) Rilevamento della vulnerabilita' sismica degli edifici in muratura. Manuale per la complilazione della scheda GNDT/CNR di II livello. Versione modificata dalla Regione Toscana. (Regione Toscana: GNDT/CNR, 2003). – Reg. Toscana GNDT 2nd Level;
e) Edifici in muratura in zona sismica – Rilevamento delle carenze strutturali. Manuale per la compilazione delle carenze. (Regione Toscana – Direzione generale delle politiche territoriali e ambientali, settore - Servizio Sismico Regionale, 2003) – Reg. Toscana (SSR) – Carenze;
f) Scheda per la valutazione qualitativa dei possibili effetti locali nei siti di ubicazione di edifici strategici e monumentali. (GNDT/INGV/DIS –Politecnico di Milano, Oct 2001)– GNDT 3 – Effetti Locali.

1.3.1 *The AeDES level I survey*

The AeDES level I survey of damage, emergency action and usability for ordinary buildings in the post-seismic event is intended for the post- earthquake intervention (GNDT). Its objectives include the collection of data regarding the damage in the structure and the determination of the emergency action required and the usability of the structure assessed. Hence, the form cannot be used to conclude a seismic vulnerability rating of the assessed buildings, however, the building characteristics listed in the form and the judgement of the assessor with respect to the evaluation of risk can be considered as indicative of the level of seismic vulnerability present. Nevertheless, in view of its intrinsic first level mode of assessment, any use of the AeDES form to interpret the seismic vulnerability of an isolated building, even though based on experience of building failures following a number of earthquakes which hit the Italian peninsula over the last forty years, would still retain a level of subjectivity if not backed by the necessary structural calculations or other system of calibration.

1.3.2 *CLE (Version 2.0, October 2013)*

The objective behind the CLE 'Condizione limite per l'emergenza dell' insediamento urbano' is the definition of the state which must be overcome following a seismic event where, even though physical and functional damages are suffered by the urban fabric and by its functions to such extent that most functions (including residential) are almost completely interrupted, the urban fabric is still capable of ensuring the uninterrupted operation of its emergency strategic functions, their accessibility and connection. The analysis of the CLE includes assessment forms for: strategic building (ES), emergency areas (AE), infrastructure for accessibility / connection (AC), aggregate of buildings (AS), individual building (US).

CLE forms are therefore only intended to be used in the pre-earthquake scenario by the entities which are responsible to coordinate the emergency operations. They are used at planning stage to identify problem areas (eg. inaccessibility of a strategic area/building due to the collapse of a building; or possible damage to a building which would have been identified for the execution of strategic emergency functions…etc.) in order to ensure that, in the case of a seismic event, the strategic areas / essential strategic buildings, and the main infrastructural routes remain in operation. Therefore, even though the forms for the Strategic buildings (ES), Individual buildings (US) and Building aggregates (AS) list a number of parameters/characteristics which are indicative of the seismic vulnerability of the building / group of buildings, their aim is not to be used for the assessment of seismic vulnerability as such but to assess their impact on the smooth running of emergency activities and to advise the local authorities (in Italian context) accordingly in the pre-earthquake planning stage. The CLE forms which have been referred to mainly during the development of the new seismic vulnerability assessment form for use in the Maltese Islands are those of the individual buildings (US) and the building aggregates (AS), however such reference has been restricted to the identification of characteristics which have a bearing on the seismic vulnerability of the building or the aggregate.

1.3.3 *GNDT Level I Assessment Form (Regione Abruzzo: GNDT/CNR, 2007)*

The data collected through the GNDT level I form provides information regarding the exposure and a first level seismic vulnerability assessment of residential buildings constructed in loadbearing masonry, reinforced concrete, steel or of mixed construction. In view of its first level of assessment nature, the information collected is very limited and must be statistically elaborated in order to evaluate the seismic vulnerability of the assessed building. The data recoded in this form includes: the floor area; the number of floors; the height of floors; the minimum and maximum height of the building; the height of the main building façade; the current state of repair of the building; how much of the building is in use; the uses; the potential number of people using building; the age of the building and the current state of finishes and services; the vertical and horizontal structural system present; the structural system of the roof and the stairs; and the degree and distribution of damages on all floors.

1.3.4 *GNDT Level II Assessment Form (Regione Toscana: GNDT/CNR, 2003)*

This second level assessment form reviews eleven parameters which have a bearing on the seismic vulnerability of individual masonry buildings and classifies such parameters under classes A to D, while also making the assessor record the degree of accuracy with which the parameter class is being established for every parameter. The eleven parameters include:

i. Parameter 1: Type and organization of structural system resisting seismic action;
ii. Parameter 2: Quality of structural system resisting seismic actions;
iii. Parameter 3: Seismic resistance of building;
iv. Parameter 4: Position of buildings and foundations;
v. Parameter 5: Slabs;
vi. Parameter 6: Plan configuration;
vii. Parameter 7: Configuration throughout the height of the building;
viii. Parameter 8: Maximum distance between main loadbearing walls;
ix. Parameter 9: Roofing system;
x. Parameter 10: Non-structural elements;
xi. Parameter 11: Current state of repair of building.

In the GNDT level II form class factors and parameter weightings can vary between GNDT level II forms used in different regions in Italy depending on the detailed characteristics of the parameters considered. In general, however the weightings take into account the relative importance which the different parameters have with respect to the seismic performance of the structure under assessment. The resulting vulnerability index is compared to existing ranges of values corresponding to the seismic vulnerability of building classes A to D for Adequate, Low, Medium-Low, Medium-High and High seismic vulnerability rating of the building being assessed.

1.3.5 *Scheda delle Carenze per Edifici in Muratura (Regione Toscana – Direzione generale delle politiche territoriali e ambientali, settore - Servizio Sismico Regionale, 2003)*

The form guides the assessor to establish the extent of deficiency in the structure of a masonry loadbearing building with respect to its resistance to seismic actions. The building is surveyed with respect to a list of possible deficiencies and the degree of every deficiency is rated A-D. Deficiencies considered by the form fall under 5 main sections:

a) deficiency in the seismic resistance of the masonry walls due to the wall construction typology;
b) deficiency in the tying action and the presence of flexible diaphragms;
c) the presence of irregularities;
d) the presence of side thrusts which are not resisted or eliminated;
e) serious deficiencies in the foundations.

The resulting overall deficiency of the building is rated as 'Low', 'Medium' or 'High' based on ranges of values for every category provided in the manual.

1.3.6 *Scheda per la valutazione qualitative dei possibili effetti locali nei siti di ubicazione di edifici strategici e monumentali. (GNDT/INGV/DIS –Politecnico di Milano, Oct 2001)*

The form reviews the parameters related to ground morphology of the area where the building is constructed and the site itself, the geology and the hydrology of the site and whether the site is susceptible to landslides, erosion due to watercourses or other. No weighting is given to the parameters and hence no degree of seismic vulnerability can be estimated through this form however it has been used as a reference with respect to the particular ground characteristics which could have a bearing on the seismic vulnerability of a building.

The study of the existing assessment forms has evidenced that, in general, the existing methods used in the Italian peninsula are more applicable for direct use in the Maltese Islands in the case of traditional masonry loadbearing construction in view of the similarities present between the wall and roof construction systems present in this building typology locally and those catered for by the manuals to the forms. The existing Italian methods would however need to be adapted prior to use on the contemporary loadbearing masonry building typology in view of the differences between the local contemporary construction methodologies and those covered by the existing Italian assessment forms, together with the absence of a number of seismic vulnerability characteristics which are present in the Maltese contemporary loadbearing masonry construction typology. A new vulnerability assessment form for use on the individual buildings in the Maltese Islands has therefore been developed in this study (hereafter referred to as 'New Form'). The main differences between the local construction methodologies and those catered for by the Italian assessment forms include:

i. local structural typologies exhibit additional characteristics which affect vulnerability and which are not catered for in the existing forms;
ii. local materials;

iii. local loadbearing masonry wall construction details;
iv. local site (plot) proportions in case of terraced development;
v. current local building regulations (building heights, setbacks and no restriction on floors without intermediate loadbearing walls at lowermost levels).

1.4 The Development of the Methodology

1.4.1 *The new seismic vulnerability assessment form for the individual building*

The new seismic vulnerability assessment form developed in this study has been based on the existing assessment methodologies in use in other countries, which, however, have been adapted to take into consideration of the different local construction methodology and building characteristics.

The New Form has first been tested on site in a Pilot Study on an aggregate consisting of 19 individual buildings in Msida close to the University of Malta. The test site included a large variety of building types with various parameters, and could therefore allow for the development of a method with a wide range of indicators for the seismic vulnerability of building stock in the Maltese Islands. Upon completion of this testing stage, the refined form has been used on a total of 183 buildings in the Xemxija (Malta) and Nadur Gozo Test Sites.

These Test Sites have been selected in view of their additional seismic vulnerability arising from the ground conditions. In both Test Sites a thick clay layer underlies the topmost layer which consists of upper coralline limestone. In Nadur the upper coralline limestone layer varies considerably in thickness however it has a minimum depth of 1-1.5 m and is extensively weathered and fractured. In Xemxija the upper coralline limestone layer is around 30 m thick. The geology of the Xemxija and Nadur test sites has been confirmed through reference to the 'Geological Map(s) for the Maltese Islands – Sheets 1 and 2' and borehole investigation results made available by the Malta Resources Authority.

Since the internal inspection of the buildings could not be carried out, MEPA (Malta Environment and Planning Authority) Development Permit Drawings have been used to obtain information with respect to the internal layouts such as overall floor areas, the presence and area of open plan spaces or levels without loadbearing walls, the percentage wall area which does not reach down to foundation level but stops at a slab or beam...etc. In the cases where the MEPA development permit drawings of the buildings were not available, or when they were available only in part, or when only an older version of the plans was available, the visual site assessment of external features, the use of aerial photographs of such buildings (MAPSERVER) and the use of photos submitted with building permit applications were the only means of data collection.

The New Form is divided into ten main sections together with a last section which records assumptions made or special features identified during the on-site survey. A brief description of the information recorded in the ten main sections follows below.

f) Section 1: this includes information regarding the general identification of the individual building being assessed (reference number, address, exact location of building indicated on a site plan which is to be attached to the form, reference numbers of emergency areas /

infrastructure for accessibility and list of development permit numbers) and a record of the inspection (date, name and identification reference of assessor and assessing team).

g) Section 2: this includes an overview of the general characteristics of the individual building being assessed, such as its position in the building aggregate (isolated/ in middle / at edge / at corner), whether it includes a specialized structural form, the total number of floors, the average storey height, the presence or otherwise of a front garden, the length of façade, the average floor area, the proportions of the building on plan and along its narrowest elevation and the uniformity / regularity of its plan layout. The subdivision of the aggregates has been based not only on the interruption of the cluster due to presence of vacant sites but also on the sharing or otherwise of the party walls between individual buildings.

h) Section 3 A&B: this includes the general and seismic vulnerability characteristics of the vertical structural system. The general characteristics include a record of the type of vertical structural system (reinforced concrete frame / steel frame / masonry walls / mixed construction with masonry walls and reinforced concrete frame in the same storey / mixed construction with masonry walls above a reinforced concrete frame / masonry walls with infill material in cavity); and the material (softstone / hollow concrete blockwork / reinforced concrete blockwork / strengthened wall construction), the type (double leaf / single leaf) of masonry wall construction present on every façade and the presence of tie beams or reinforcing ties in the walls. Even though the developed seismic vulnerability assessment form for the individual building is intended for the assessment of the contemporary loadbearing masonry construction typology, the option of the wall construction consisting of masonry walls with infill material in the cavity has been included as well in order to make the forms adequate even for use in the assessment of traditional construction typologies. The seismic vulnerability characteristics of the vertical structural system listed in the form include the most common characteristics present in the building typology under study in the Maltese islands which can have a bearing on the seismic performance of such building types. This section records:

- the presence of double height spaces – these occur most commonly at the lower-most storeys due to commercial establishments, however could be present even in the residential levels in the case of duplex apartments;
- difference in level of the topmost slab in the adjacent building along both party walls / difference in level of intermediate slabs along both party walls (checked at slab level +2 for consistency) / difference in plane of front and rear facades of adjacent buildings / the presence of vacant sites directly abutting the building / the evidence as to whether the party walls are shared / the presence of long corridors, garages or other open plan spaces adjacent to one or both party walls and the misalignment of internal spaces in abutting properties. These characteristics indicate the degree of restraint of the party walls;
- the complete absence of the intermediate walls in loadbearing masonry in one or more storeys and the level/s at which this occurs / the presence of open plan spaces without internal loadbearing walls over part of the floor area, the percentage open plan area and the level/s at which it occurs / the maximum ratio of discontinuous loadbearing walls to the area of

continuous loadbearing walls – these characteristics indicate the presence of a soft storey, the variation of mass throughout the height of the building and the degree of restraint of the party walls;

- the presence of an inadequate or completely absent connection between perpendicular masonry walls and between loadbearing walls and slabs in the whole building; the presence of large openings along the main facades, and the presence of an irregular distribution of openings on the facades – these factors indicate the degree of box-like behaviour which the building will exhibit and presence of direct load paths through the main shear walls to the foundations;
- the presence of setbacks, projecting rooms or balconies along the main facades - these factors indicate the degree of variation in mass throughout the height of the building;
- the presence of masonry walls as infill panels in a frame structure and the position of these walls relative to the frame therefore identifying whether the masonry walls will apply additional eccentric forces on the frame structure;
- the presence of isolated columns and open storeys – these factors also indicate the variation in mass throughout the height of the building;
- the evidence of post-construction joining of originally separate individual buildings or post-construction additions in areas which were originally left as voids in the building aggregate; the presence of additional floors or rooms over the original construction and the evidence of a different construction system present in the additional floors – these factors indicate a change in the load paths from the original construction, an increase in overall building mass at foundation level, a variation in the rigidity of the building throughout its height and structural discontinuity especially in the cases where any additions present have not been effectively tied to the underlying structure.

i) Section 4 A&B: this includes the general and seismic vulnerability characteristics of the horizontal structural system. The general characteristics include the type of slab construction over semi/basement and in the rest of the building. The slab construction systems considered include: precast hollow core planks, cast in-situ slabs, predalle, precast hollow core / cast in-situ / predalle over a reinforced concrete beam system, stone slabs over timber / steel beams, reinforced concrete slabs over timber/steel beams, stone slabs over stone arches/stone corbels, stone slab roofs, or timber panels over timber beams. It is to be noted that the stone and timber slab options have been included in order to make the developed seismic vulnerability assessment forms adequate even for the assessment of the traditional masonry construction typologies. The horizontal seismic vulnerability characteristics considered include the presence of slabs spanning in one direction and not tied to each other / or to walls parallel to their span and the occurrence of flexible and semi-rigid slab construction systems throughout the building. These characteristics indicate the degree of even distribution of seismic forces from the slab onto the walls and the diaphragm action provided by the slabs under such forces.

j) Section 5 A&B: records the condition of the building in the pre- and post-earthquake assessments. The degree of damages to external walls, internal walls, horizontal loadbearing elements and staircores are recorded. Damages to non-structural elements are also recorded, namely, the detachment of external render/pointing, damages to parapet walls, damages to internal plaster / false ceilings and, in the post-earthquake assessment case, damages to the electrical and fresh / foul water systems. This section also records any evidence of foundation failure or differential settlement, the potential damages by the building on the infrastructure for accessibility and connection arising from the collapse of the building onto the access road (if the height of the building above road level is greater than the width of the road) and the damages caused by falling secondary structural/non-structural components attached to projecting rooms / balconies. The potential damage on the building from collapse or falling elements from nearby buildings and the damage to the access road are also recorded.

k) Section 6: this includes information on the ground morphology, the position of the building relative to a steep drop in the landscape, the presence of stepped foundations. The seismic characteristics of the site, the type of instability (if applicable) and the localization of any landslide with respect to the position of the building (if applicable) are also recorded. The topmost and second rock formation layers are noted.

l) Section 7: this includes information regarding the title of the property (whether public or private), the reference code for the current use of the building, the number of units corresponding to particular uses, the year of construction and that of any structural upgrade, the percentage of the building in use and the average number of people using the building. Most of this information is more relevant with respect to the use of the forms in a post-earthquake assessment of the safety for use of the buildings rather than in determining its seismic vulnerability, however, this information has been included since the developed forms are even meant for this use. In the Italian forms, the year of construction and structural upgrade are required in order to identify the building construction regulations which were in effect at the time of construction / upgrade. In the local scene, the date of construction is more relevant in order to give an insight into the probable type of slab construction present or the construction material of the walls, where such information is not readily available. The information in this section is also relevant with respect to studying the exposure of the site.

m) Section 8 – This section includes the degree of accuracy on which the assessment was based by recording the extent of exhaustiveness of the building inspection.

n) Section 9 – This section is only applicable in the case of a post-earthquake assessment and includes the post-earthquake emergency safety measures suggested by the assessor and the number of units which are unsafe for use, hence, the number of persons/families which must be evacuated.

o) Section 10 – This section summarizes the seismic vulnerability ratings resulting from Sections 2-6 and Section 8 of the form in order to guide the assessor to determine an overall seismic vulnerability rating following a qualitative assessment of these ratings.

1.4.2 *The development of the rating system and its verification*

The intermediate slabs and roofing members of the contemporary loadbearing masonry building typology present in Malta and Gozo usually consist of flat cast in-situ concrete slabs or precast concrete slabs with a cast in-situ concrete topping. In general, therefore, a rigid diaphragm with an even distribution of forces from the slabs to the supporting walls is present at every storey level. Hence, the horizontal structural system is not typically one of the main contributors to the seismic vulnerability of this building typology, unless flexible diaphragms, such as lightweight mezzanine floors, are present in the building. This, however, is mainly limited to plan layouts which include a double height space either in the lower levels due to commercial establishments or at higher storeys where duplex apartments might be present. Therefore, the resulting reduced degree of restraint of the party walls at the storey levels where such flexible diaphragms are present and the increased slenderness of the walls would be taken into consideration in the assessment of the seismic vulnerability arising from the vertical structural system, which is covered by the third section of the New Form. Section 3 of the New Form also includes, amongst other factors, the presence and extent of soft storeys, double height spaces, long corridors adjacent to party walls, the sharing or un-sharing of party walls and their construction (in single or double wall thickness), the presence of setbacks, projecting rooms, balconies, large or irregularly distributed openings on facades, the presence of open plan spaces, the maximum ratio of discontinuous loadbearing walls to continuous loadbearing walls and the presence of additional floors over the original construction Hence, the evident major bearing which the characteristics of the vertical structural system recorded in Section 3 have on the seismic vulnerability rating of this building typology has been emphasized by the provision that the final rating cannot be less than that resulting from this section.

The detailed analysis of the existing literature and the relative weightings attributed to the seismic vulnerability characteristics in assessment methods which are currently in use in other countries together with a consideration of the outcomes of previous studies, has provided the background to the development of a rating system for the main sections of the New Form based on the relative importance of the more important characteristics identified in every section. A brief overview of the seismic vulnerability ratings attributed to every main sections of the New Form is outlined below.

1.4.2.1 *Section 2: General characteristics*

Previous studies on individual residential apartment blocks carried out by the University of Malta (Farrugia, 2002; Galdes, 2012) have shown that contemporary loadbearing masonry buildings, if considered in isolation, would survive a seismic event with a design peak ground acceleration of 0.1g if their overall height is not greater than 3 floors, if built on rock and, 2 floors, if built on clay. By reference to these results, the seismic vulnerability rating developed for Section 2 of the New Form is as follows:

- LOW: if the number of storeys are either less than or equal to 2 for a building constructed on clay,
  OR

Less than or equal to 3 for a building constructed on upper coralline limestone;

- MEDIUM: if the number of storeys are either less than or equal to 2 for a building constructed on clay,
  AND/OR
  the building has a long and narrow plan layout,
  AND/OR
  the building has a non-regular plan layout;
  OR
  if the number of storeys are less than or equal to 3 for a building constructed on upper coralline limestone,
  AND/OR
  the building has a long and narrow plan layout,
  AND/OR
  the building has a non-regular plan layout;
- HIGH: if all medium risk components described above are combined together.

1.4.2.2 *Section 3: Vertical structural system*

By reference to FEMA 154 (second edition), four characteristics of the vertical structural system which have a greater effect on the seismic vulnerability rating of the building under assessment have been identified thereby allowing for the formulation of a more refined rating for this section of the form. The four parameters and their relative weightings are as follows:

1. Soft Storey and/or vertical irregularity [x2 weighting];
2. Large Openings [x1 weighting];
3. Double Height Spaces [x1 weighting];
4. More than 1 floor higher than adjacent building and/or "Medium" result for Section 2 (relating to building height) [x1 weighting].

The consequent seismic vulnerability rating developed for Section 3 of the New Form is as follows:

- LOW: overall weighting of 1 i.e. if the building contains any one parameter out of the four listed above except for a Soft Storey/Vertical Irregularity;
- MEDIUM – LOW: overall weighting of 2 i.e. if the building contains a soft storey alone, or any other two parameters out of the four listed above;
- MEDIUM - HIGH: overall weighting of 3 i.e. if the building contains either a soft storey and one other parameter, or any other 3 parameters out of the four listed above;
- HIGH: overall weighting of 4 i.e. if the building contains either a soft storey and two other parameters, or three parameters out of the four listed above.

1.4.2.3 *Section 4: Horizontal structural system*

By reference to the categorisation of the seismic vulnerability classes considered in the corresponding parameters of the GNDT level II assessment and the Regione Toscana form for deficiencies in masonry buildings, the seismic vulnerability rating developed for this section of the New Form is as follows:

- LOW: if lightweight (flexible) roofing structures (e.g. in the case of mezzanine structures) are not present,
  AND/OR
  if semi-rigid slab construction systems are not present;

- MEDIUM: if lightweight (flexible) roofing structures are present,
  AND/OR
  if semi-rigid slab construction systems are present;

- HIGH: if an inadequate degree of abutment or a total absence of abutment is identified in the case that masonry arches or vaults are present.

1.4.2.4 *Section 5: Pre-/Post-earthquake condition of building*

The classes of the GNDT level II parameters which correspond to Section 5 of the New Form provided the background for the seismic vulnerability rating developed for this section. This consists of:

- LOW: if no damage is present;

- MEDIUM: if minor to medium severity cracks are present;

- HIGH: if severe cracks are present.

1.4.2.5 *Section 6: Ground conditions*

The studies carried out by the University of Malta (Farrugia, 2002; Galdes, 2012) on the seismic vulnerability of contemporary loadbearing masonry structures constructed on different ground conditions together with the consideration of the different ground conditions present on the Maltese Islands have led to the development of the following rating for this section:

- LOW: if stable ground is present;

- MEDIUM: if an upper coralline limestone layer over a clay layer is present (in view of the amplifications of the seismic waves through the clay layer);

- HIGH: if unstable ground is present.

1.4.2.6 *Section 8: Accuracy of assessment*

As the internal inspection of the buildings was not possible, the only source of information for the internal layouts of the buildings was through the sourcing of Development Permit Drawings from the Malta Environment and Planning Authority. Since not all permits could be traced, or in some cases, the permits sourced included only part of the plans of the building, and in view of the degree of uncertainty with respect to the assumptions which had to be made in such cases, the parameters governing the seismic vulnerability rating of this section have been established as follows:

- LOW: if all plans were available;

- MEDIUM: if plans were only found in part;

- HIGH: if plans were not available.

1.4.2.7 *Section 10: The overall seismic vulnerability rating*

The qualitative assessment of all the risk levels obtained in Sections 2, 3, 4, 5, 6 and 8 and the relative importance of the different parameters listed in these sections has indicated that the overall seismic vulnerability rating which must be determined in Section 10 of the New Form is dependent on the following:

- -LOW: if the majority of the seismic vulnerability results in Sections 2, 4, 5, 6 and 8 are LOW,
  AND
  the seismic vulnerability rating of Section 3 is LOW;

- MEDIUM-LOW: if the seismic vulnerability rating of Section 3 is MEDIUM-LOW;

- MEDIUM: if the number of MEDIUM seismic vulnerability results is
  ≥ the number of LOW seismic vulnerability results
  AND
  ≥ the number of HIGH seismic vulnerability results in Sections 2, 4, 5, 6 and 8
  AND
  the seismic vulnerability rating of Section 3 is not higher than MEDIUM-LOW;

- MEDIUM-HIGH: if the seismic vulnerability rating of Section 3 is MEDIUM-HIGH;

- HIGH: if the number of HIGH seismic vulnerability results is
  ≥ the number of LOW /MEDIUM–LOW/ MEDIUM / MEDIUM-HIGH seismic vulnerability results in Sections 2, 4, 5, 6 and 8
  AND/OR
  the seismic vulnerability rating of Section 3 is HIGH.

1.4.3 The verification of the rating system

The verification of these ratings has been carried out through the comparison of the seismic vulnerability outcome obtained using the newly developed form with that obtained from a GNDT level II assessment for all the 183 buildings under study in the Xemxija and Nadur Test Sites. It is to be noted that for parameters 5, 7, and 9 of the GNDT level II form, where varying weightings are allowed depending on the specific characteristics of the respective parameters in the building under evaluation, this study has always assumed the values which correspond to the worst case scenario. This was intended to cater in-part for the inability to take into account of the extent of the presence of one or more characteristics related to these parameters through the use of the GNDT level II form. The analysis of the seismic vulnerability outcomes obtained from these two methods has suggested that the original interval for the GNDT level II 'LOW' vulnerability rating was too small for the Xemxija and Nadur buildings assessed, since the rating of "LOW" was not used initially. The ratings resulting from the New Form included "LOW", "MEDIUM-LOW", "MEDIUM", "MEDIUM-HIGH" and "HIGH". Therefore, in order to carry out a comparison between the two systems, the 'LOW' range interval of the GNDT level II method has been increased in this study such that the buildings which were less

vulnerable according to this method could be identified. It is also worth noting that no rating larger or equal to 0.6 has been obtained for the Xemxija and Nadur assessments, therefore meaning that the 0-1.0 range provided by the GNDT level II method, was instead covered by the range 0-0.6 in the case of the Xemxija and Nadur buildings.

This has suggested the alteration of the vulnerability index intervals given in the GNDT document in order to ensure that the different classes of seismic vulnerability present in the case of the contemporary loadbearing masonry building typology are reflected in the outcome of the GNDT level II check. Table 1 below indicates the original GNDT level II ranges of seismic vulnerability ratings, and the corresponding altered ranges considered for the Xemxija and Nadur seismic vulnerability assessments.

Table 1: Original and altered GNDT level II ranges of seismic vulnerability ratings

Original GNDT level II intervals	Altered GNDT level 2 intervals for local case	Seismic Vulnerability Rating
0-0.1	0-0.1	Adequate
0.1-0.2	0.1-0.3	Low
0.2-0.4	0.3-0.45	Medium-Low
0.4-0.6	0.45-0.65	Medium
0.6-0.8	0.65-0.8	Medium-High
0.8-1.0	0.8-1.0	High

A FEMA 154 (second edition) check has also been carried out on the 183 buildings under assessment in the Xemxija and Nadur Test Sites, and the outcome from this check has been compared to the seismic vulnerability ratings obtained from the New Form and from the GNDT level II assessment. The results of this comparison are summarized in Figures 7-12. The 'Rapid Visual Screening of Buildings for Potential Seismic Hazards' - FEMA 154 (second edition) provides a rapid visual screening method for the determination of whether the assessed building is acceptable with respect to the risk to life safety or, if an overall score of 2 or less is obtained, whether it requires more detailed seismic design calculations in view of its potentially hazardous behaviour in an earthquake scenario. It has been assumed that the GNDT level II ratings 'ADEQUATE', 'LOW' OR 'MEDIUM-LOW' do not require detailed calculations[1]. Hence, for the graphical representation of this comparison, Table 2 below indicates the

[1] This decision was based on the definition of the construction scenarios corresponding to classes A to D given in Benedetti et al. (1984) and Lemme et al. (2008). These studies describe Class A as equivalent to a structure which is in accordance with current regulations, Class B as including deviations from seismic regulations which however do not result in a significant reduction in seismic resistance, whereas Classes C and D are associated with construction scenarios which include severe deviations from regulations which give rise to a significant increase in seismic vulnerability. Furthermore, the correlation between parameter classes and modified seismic vulnerability ratings given in Table 2 of Lemme et al. (2008) and reproduced in Section 2.3.1 of this thesis in Table 2-8 indicates that seismic vulnerability ratings of 'Adequate' to 'Medium-low' are associated with scenario classes A and B (hence, not requiring detailed seismic verifications) while ratings of 'Medium' to 'High' are associated with scenario classes C and D (where seismic verifications are required).

different weightings given to the overall seismic vulnerability ratings obtained for the 183 buildings under investigation using the GNDT level II assessment method, the new seismic vulnerability assessment form developed for the Maltese Islands, and the FEMA 154 check.

Table 2: Weightings given to the 3 methods for graphical representation of comparison of results

	GNDT level II	New Form	FEMA 154		
ADEQUATE	1	n/a	1	FEMA 4 to 5	no further checks required for results higher than 2
LOW	2	2	2	FEMA 3 to 4	
MEDIUM-LOW	3	3	3	FEMA 2 to 3	
MEDIUM	4	4	4	FEMA 1 to 2	further detailed checks required for a result of 2 or less
MEDIUM-HIGH	5	5	5		
HIGH	6	6	6	FEMA 0 to 1	

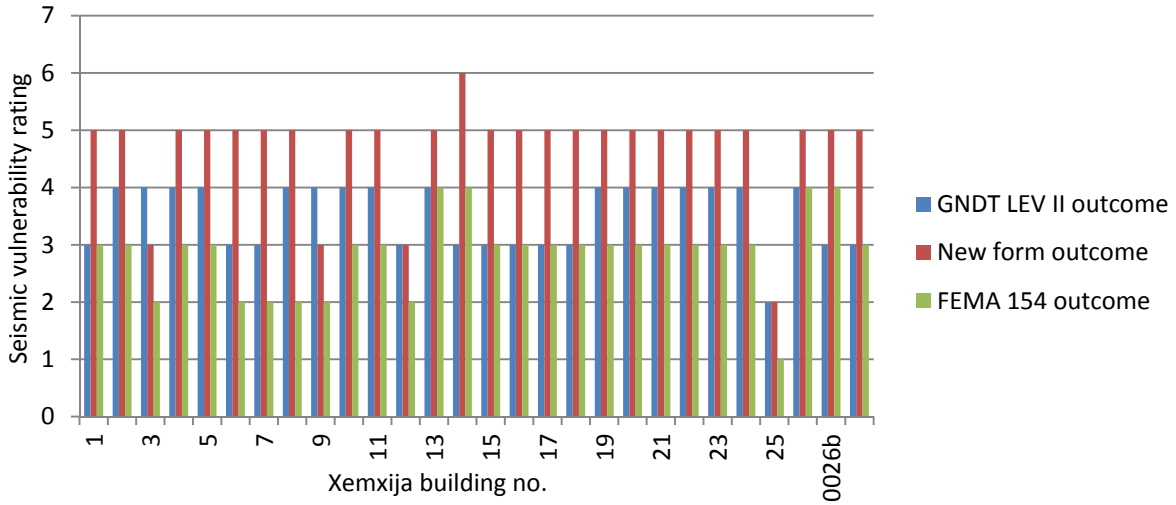

Figure 7: Comparison of the seismic vulnerability ratings obtained for the Xemxija building numbers 1-27 using the 3 methods.

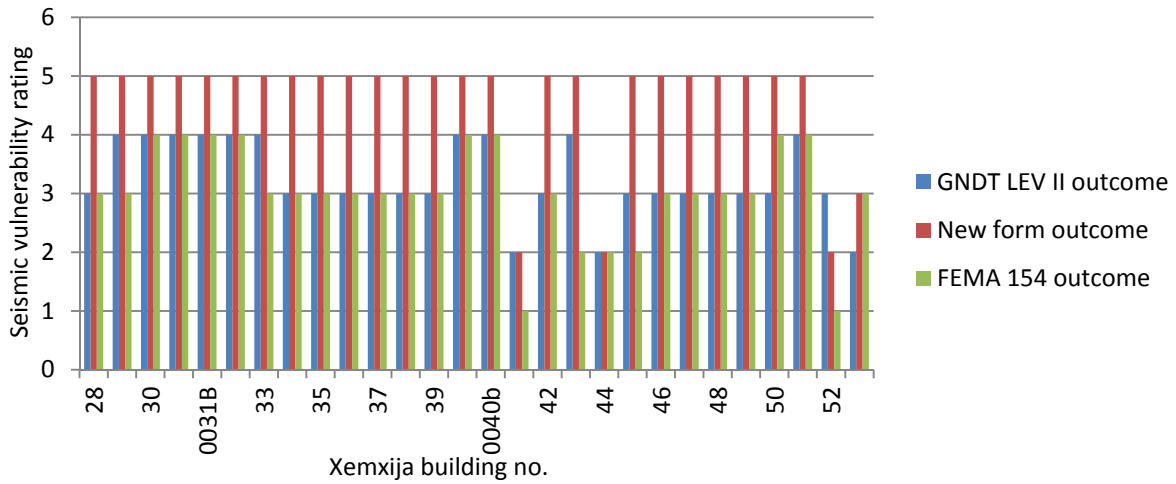

Figure 8: Comparison of the seismic vulnerability ratings obtained for the Xemxija building numbers 28-53 using the 3 methods.

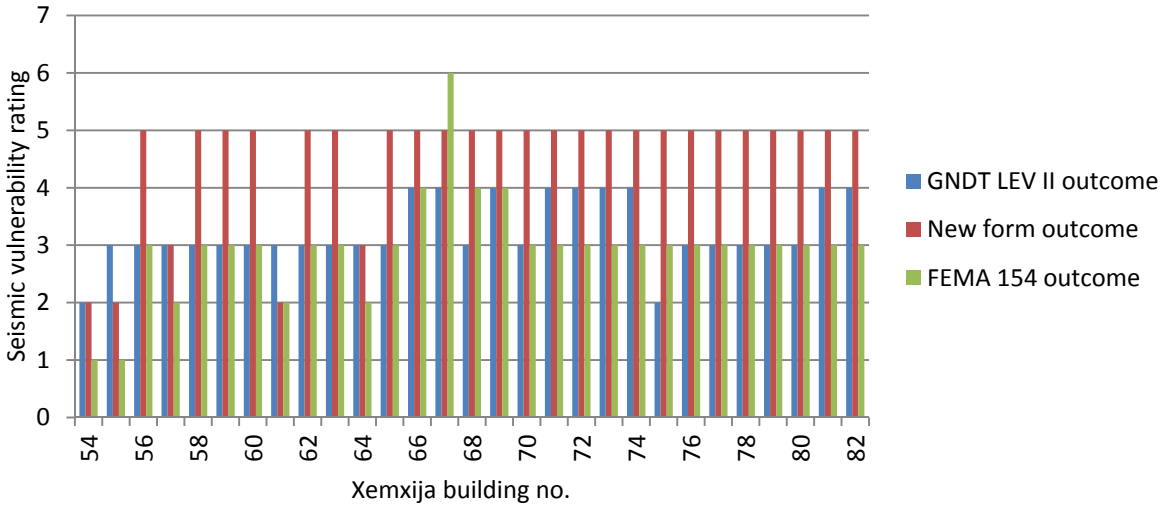

Figure 9: Comparison of the seismic vulnerability ratings obtained for the Xemxija building numbers 54-82 using the 3 methods.

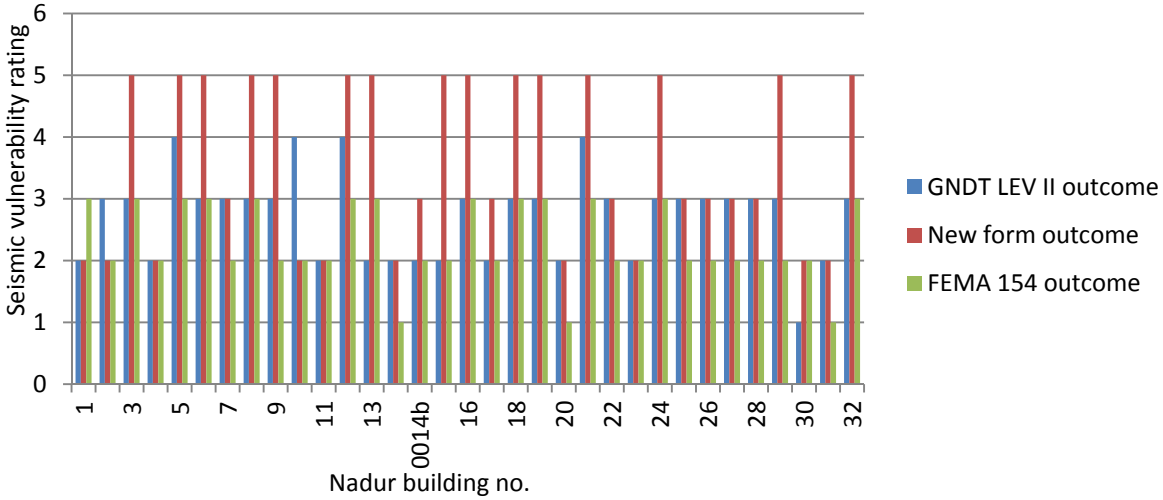

Figure 10: Comparison of the seismic vulnerability ratings obtained for the Nadur building numbers 1-32 using the 3 methods.

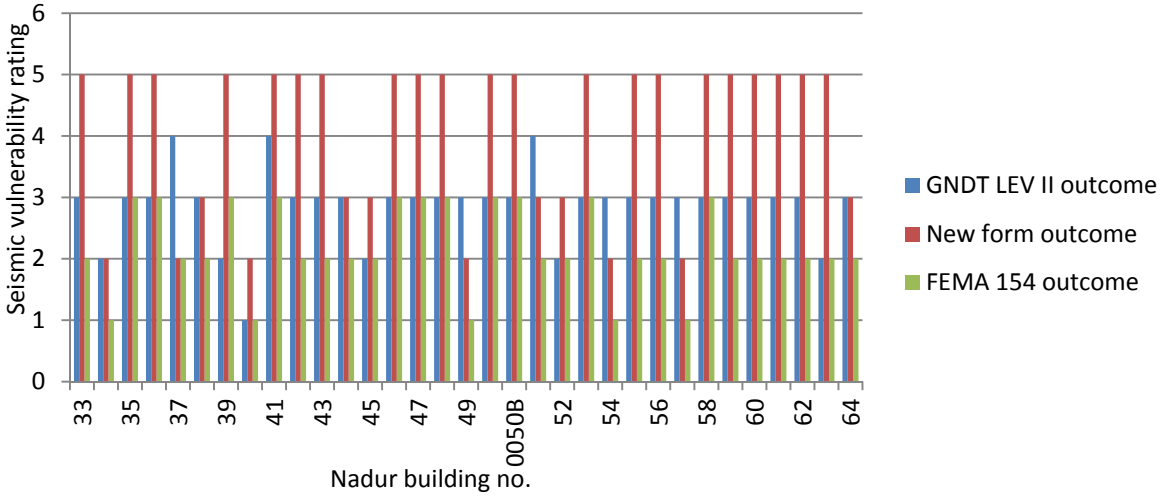

Figure 11: Comparison of the seismic vulnerability ratings obtained for the Nadur building numbers 33-64 using the 3 methods.

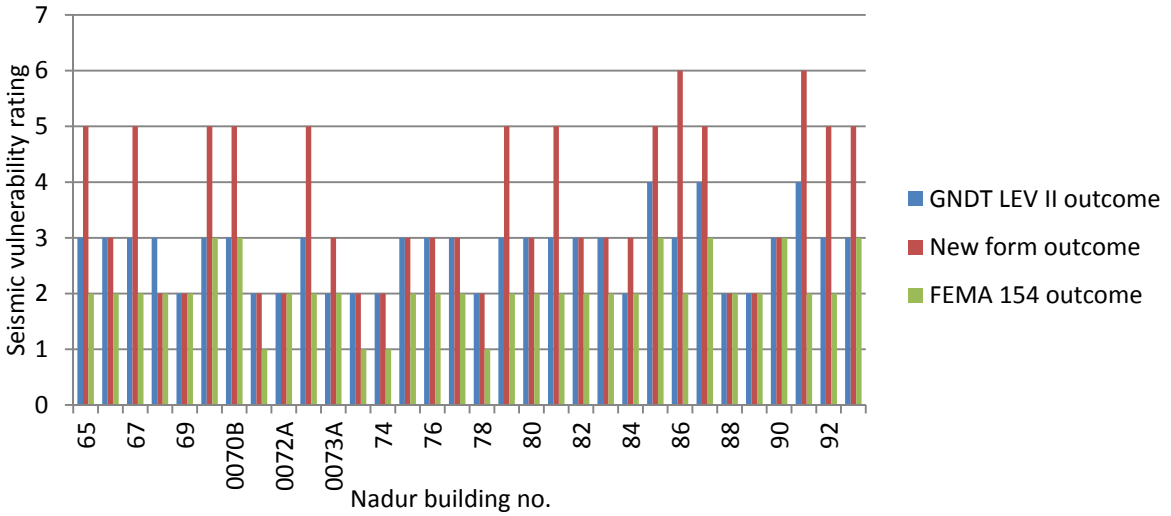

Figure 12: Comparison of the seismic vulnerability ratings obtained for the Nadur building numbers 65-93 using the 3 methods.

Table 3: GNDT level II parameters corresponding to every section of the New Form

Main sections of New form affecting seismic vulnerability rating	GNDT Level II Parameters										
	1. Organisation of the structural system	2. Quality of the structural system	3. Seismic resistance of the building	4. Position of building and foundations	5. Slabs	6. Plan configuration	7. Configuration throughout height	8. Maximum distance between main walls	9. Roofing system	10. Non-structural elements	11. Current state of repair of building
2. General characteristics			X	X		X					
3. Vertical structural system	X	X	X				X	X			
4. Horizontal structural system					X				X		
5. Pre- / post-earthquake condition of building										X	X
6. Ground characteristics				X							
8. Accuracy of assessment											

Most of the characteristics listed in the different sections of the New Form correspond to one or more parameters in the GNDT level II assessment. The additional comparison of the seismic vulnerability ratings obtained for the Xemxija and Nadur buildings from Sections 2, 3, 4, 5 and 6 of the New Form considered individually, to the corresponding parameters in the GNDT level II method presented in Figures 13-22 gives some insight into the validity of the developed ratings for the New Form. Table 3 summarises the GNDT level II parameters corresponding to the sections of the New Form upon which the seismic vulnerability rating is determined. A more detailed explanation of the reasons governing

the choice of GNDT level II Parameters which have been linked to the individual sections of the New Form follows hereunder.

a) Section 2: General characteristics. The main characteristics considered in this section of the New Form include the number of floors, average storey height, area, proportions, regularity and uniformity of plan. The corresponding GNDT level II parameters include:
   - Parameter 3: Seismic resistance of the building. This has a weighting of 1.5. It is dependent on the number of floors, average floor area, minimum area of walls (considering both orthogonal plan directions) and storey height. Therefore even though Section 2 of the New Form does not include the calculation of the seismic resistance, it indirectly takes into account of this parameter by including all the factors which are considered for its evaluation.
   - Parameter 4: Position of the building and foundations. This has a weighting of 0.75 and considers the underlying rock formation. Even though the underlying rock formation is not mentioned in Section 2 of the New Form, this parameter has still been considered as relevant since, especially in the case of the building typology considered in this study and the period of construction of most buildings, the type of rock formation would have affected the number of floors constructed in the area.
   - Parameter 6: Plan configuration. This has a weighting of 0.5. For the rectangular plan configuration, as is generally the case for the contemporary building typology under study, the narrower the plan layout with respect to its length, the lower the rating for this parameter, and hence the higher the seismic vulnerability. Therefore this parameter assesses the seismic vulnerability of the characteristic included in Section 2 of the New Form which deals with the plan proportions.

b) Section 3: Vertical structural system. The main parameters considered in this section of the New Form include: the type of vertical loadbearing system, seismic measures taken, wall construction, the presence of ties, the presence of double height spaces, the difference in slab level, the difference in façade planes, the presence of a long corridor, the absence of intermediate walls, the presence of a soft storey, connections between walls, the presence of large openings, setbacks and projecting rooms. The corresponding GNDT level II parameters are:
   - Parameter 1: Organisation of the structural system resisting seismic forces. This has a weighting of 1.0. This parameter assesses the degree of box-like behaviour based on presence and the adequacy of ties between perpendicular walls, regardless of material of the building blocks and the block distribution. In the GNDT level II check of the Xemxija and Nadur buildings under assessment, this parameter has always been considered as Class B, since it was safe to assume that the buildings in these Test Sites were not designed taking seismic forces into consideration. This parameter is therefore directly linked to the assessment of the degree of connection between perpendicular walls and the degree of connection between walls and slabs which are included in Section 3 of the New Form.

- Parameter 2: Quality of the structural system resisting seismic actions. This has a weighting of 0.25 and assesses the contribution to the seismic vulnerability of the building under evaluation which is due to the material of blocks making up walls, the layout of the blocks in the walls, the connection between different wall skins and the quality of mortar. In the GNDT level II assessment of the Xemxija and Nadur buildings, this parameter has always been assumed as Class A since the stone masonry considered in the buildings assessed consisted of homogeneous rectangular elements with good mortar joining, horizontal rows and staggering of joints. Furthermore, any double walls have been assumed as bonded through bondstones which extend from the outer face of one leaf to the other face of the connected leaf as is normal local practice. Therefore this parameter corresponds directly to the factors related to wall construction and wall material included under Section 3 of the New Form.
- Parameter 3: Seismic resistance of the building. The consideration of the minimum wall area for the calculation of the seismic resistance of the buildings is directly related to the presence of soft storeys and the presence of open plan spaces over part of the floor area which are covered in Section 3 of the New Form.
- Parameter 7: Configuration of building throughout its height. This parameter has a weighting of 1.0 and considers the degree of regularity of the built-up mass throughout the height of the building. This parameter is assessed as the ratio between the surface areas or masses of two consecutive floors and therefore corresponds directly to the presence of setbacks and projecting rooms which are identified in Section 3 of the New Form.
- Parameter 8: Maximum distance between main walls. This has a weighting of 1.0 and considers the seismic vulnerability which can be attributed to the increased slenderness of main loadbearing walls in view of the lack of restraint present in cases where intersecting perpendicular walls are positioned far apart. In the contemporary loadbearing masonry typology this seismic vulnerability characteristic is evident in the case of soft storeys with no intermediate walls, long corridors, and the presence of open plan spaces over part of the floor area, which characteristics are all considered in Section 3 of the New Form.

c) Section 4: Horizontal structural system. The main seismic vulnerability characteristics considered in this section of the New Form for the individual buildings include: the type of slab construction; whether flexible or semi-rigid slab construction are present and their extent throughout the building, and the presence of vaults or arches. The relevant corresponding GNDT level II Parameters are:

    - Parameter 5: Slabs. This has a weighting of 0.5 and assesses the level of seismic vulnerability arising from the degree of diaphragm effect, hence considering the presence of rigid or flexible slabs, with or without adequate connection between the adjacent slabs; and the misalignment between floors. This parameter has generally been rated as Class A in the Xemxija and Nadur GNDT level II assessments, as the

buildings considered have all been assumed to incorporate rigid slabs at every storey level and at roof level in view of the building typology present and the period of construction. The presence of staggered floors was only limited to a number of blocks which spanned along a sloping site and concerned a distinct portion of these blocks as opposed to a staggering of a limited number of floors throughout the building. Consequently, in the assessed buildings, such staggered portions have been treated as separate buildings. Staggered floors have therefore been considered as absent in the Test Sites. The characteristics covered by Parameter 5 of the GNDT level II assessment are therefore also included in Section 4 of the New Form.

- Parameter 9: Roofing system. This parameter has a weighting of 1.0 and assesses the seismic vulnerability based on the type of roof construction, whether it causes a side thrust, the presence of tie beams, the dead load on the roof, the length of supporting walls. All the Xemxija and Nadur buildings surveyed were given Class A since, all the buildings had flat roofs and from the period of construction, it was safe to assume that all roofs consisted of cast in situ concrete slabs, or alternatively, precast concrete slabs with a cast in-situ topping. This parameter is therefore linked to the following entries in the New Form: the type of slab construction above semi-/basement level, and presence of slabs spanning in 1 direction & not tied to each other or to walls.

d) Section 5: Pre- / Post-earthquake condition of building. The seismic vulnerability characteristics considered in this section of the New Form for the pre-earthquake case include: the visible structural damage to external, internal, horizontal elements, staircores; the degree of maintenance, and the potential damages. The corresponding GNDT level II Parameters are:

   - Parameter 10: Non-Structural Elements. This has a weighting of 0.25 and considers the presence of non-structural elements which can cause damage to people or other things in case of collapse or detachment, such as apertures, false ceilings, balconies (whose structure is not an integral part of the structure of the adjacent floor slab), shop signs…etc. All the Xemxija and Nadur buildings assessed have been rated as Class A or B, as they either had no projections, and / or any fixtures were well connected to the walls, and/or had balconies which were part of the floor slab. This parameter is therefore directly linked with the 'potential damages' considered under Section 5 of the New Form.
   - Parameter 11: Current state of repair of building. This has a weighting of 1.0 and assesses the seismic vulnerability associated with the state of repair of the building. In the case of the Xemxija and Nadur buildings under study, the buildings have been rated either class A or B in view of the complete absence of cracks or the presence of minor cracks visible on the facades of these buildings. This parameter is directly linked to the factors assessing the visible structural damage to the building elements included under Section 5 of the New Form.

e) Section 6: Ground characteristics. The main factors effecting the seismic vulnerability of buildings which are included in this section are ground morphology, the stepping of foundations, the microseismic rating of the site, the geology, the possibility of landslides and the risk of flooding. The corresponding GNDT level II Parameter is:

- Parameter 4: Position of the building and foundations. This parameter considers the underlying rock formation, the ground morphology and the presence of ground conditions which can cause a side thrust onto the building. The GNDT level II assessment method does not make any distinction with respect to the geology, the different rock formation layers and their thicknesses. This parameter is therefore linked in part with Section 6 of the New Form.

f) Section 8: Accuracy of assessment. This section records the level of reliability of the information recorded based on the completeness of the survey and the reliability of the information. There is no corresponding parameter in the GNDT level II assessment, however this assessment method requests the assessor to record the degree of reliability present in the determination of every Parameter class. Nevertheless, this degree of reliability is not taken into consideration in the determination of the seismic vulnerability rating of the building.

Figures 23 and 24 show GIS thematic maps indicating the distribution of the building heights, the number of floors, the presence of soft storeys, the presence of double height spaces and the overall seismic vulnerability rating of the individual buildings under evaluation in the Xemxija and Nadur Test Sites determined using the New Form. These images indicate that, while the Xemxija buildings evaluated in this study have a higher number of floors than the buildings assessed in the Nadur Test Site, soft storeys are widespread in both locations, and double height spaces are only present in a limited number of cases. The seismic vulnerability rating obtained following the assessment of the buildings in the Test Sites using the New Form is 'Medium-High' for most of the Xemxija buildings, whereas in the case of Nadur there is a more even distribution of 'Low', 'Medium-Low' and 'Medium-High' ratings. This variation is mostly related to the reduced height of the Nadur buildings and to other factors affecting the vertical structural system as can be confirmed from Figures 13-21.

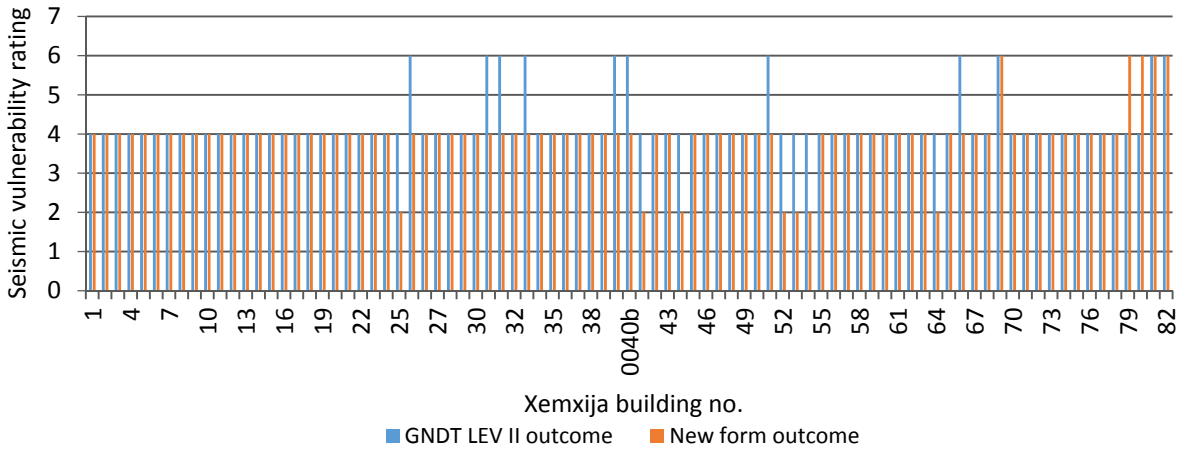

Figure 13: Comparison of the seismic vulnerability ratings obtained from Section 2 (General characteristics) of the New Form to those obtained from the corresponding GNDT level II parameters for the Xemxija building numbers 1-82.

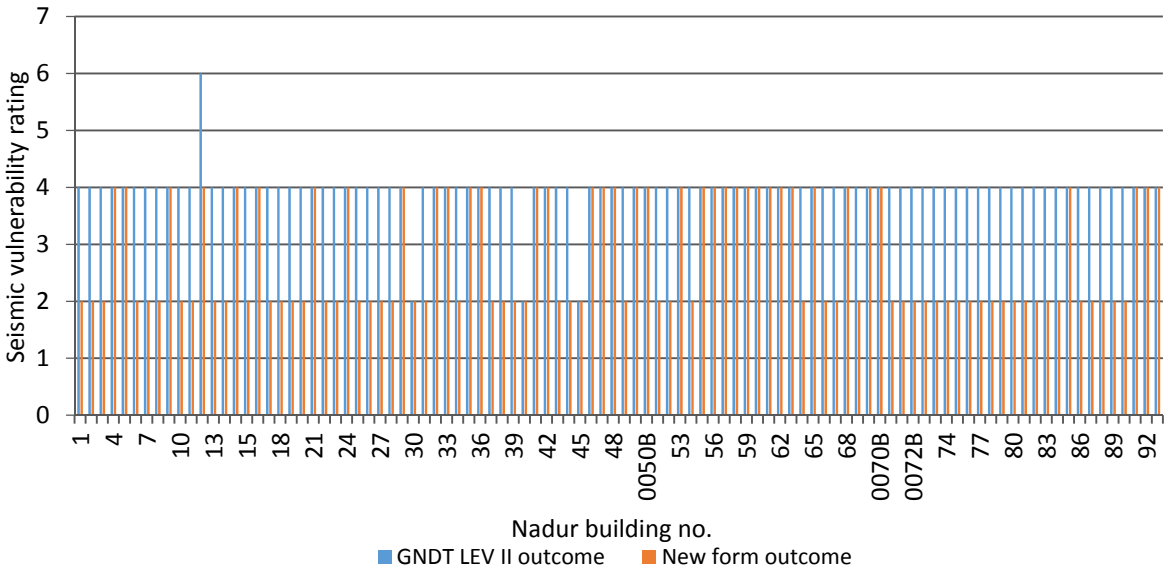

Figure 14: Comparison of the seismic vulnerability ratings obtained from Section 2 (General characteristics) of the New Form to those obtained from the corresponding GNDT level II parameters for the Nadur building numbers 1-93.

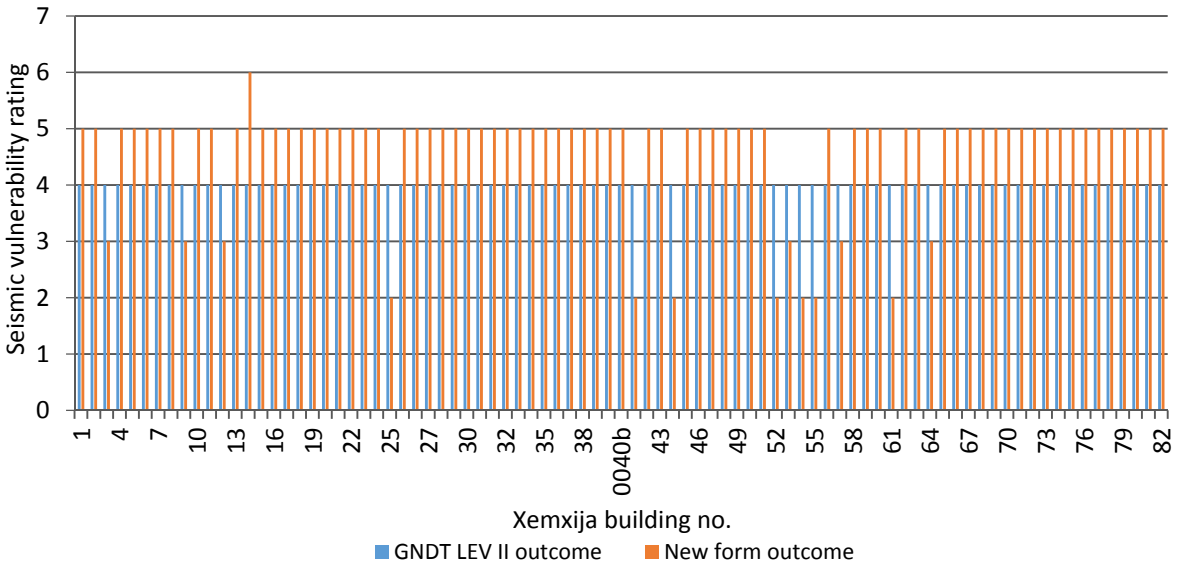

Figure 15: Comparison of the seismic vulnerability ratings obtained from Section 3 (Vertical structural system) of the New Form to those obtained from the corresponding GNDT level II parameters for the Xemxija building numbers 1-82.

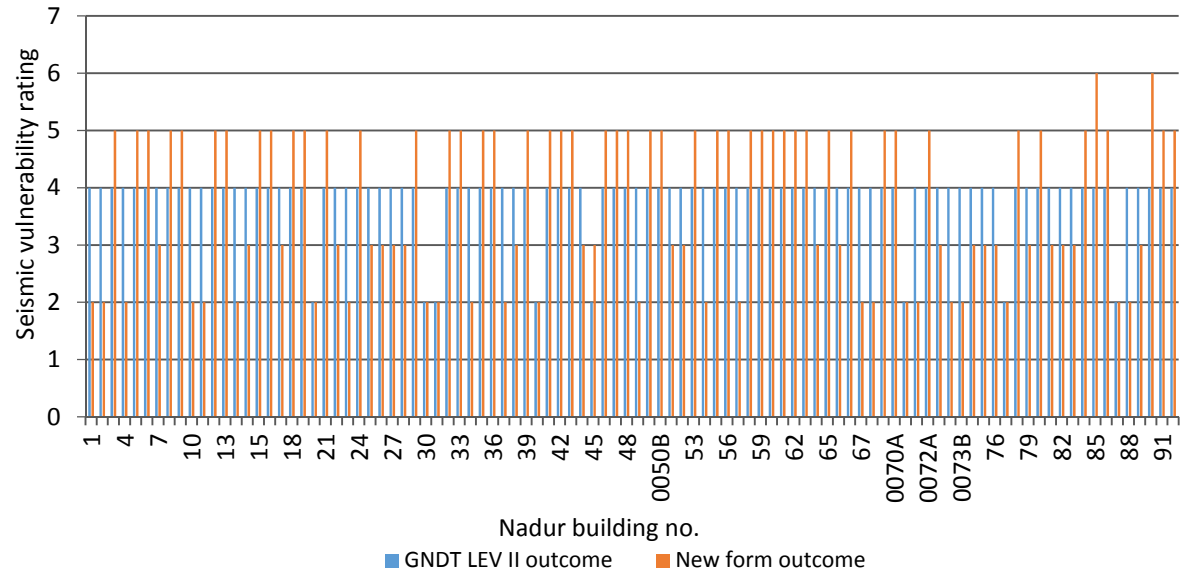

Figure 16: Comparison of the seismic vulnerability ratings obtained from Section 3 (Vertical structural system) of the New Form to those obtained from the corresponding GNDT level II parameters for the Nadur building numbers 1-93.

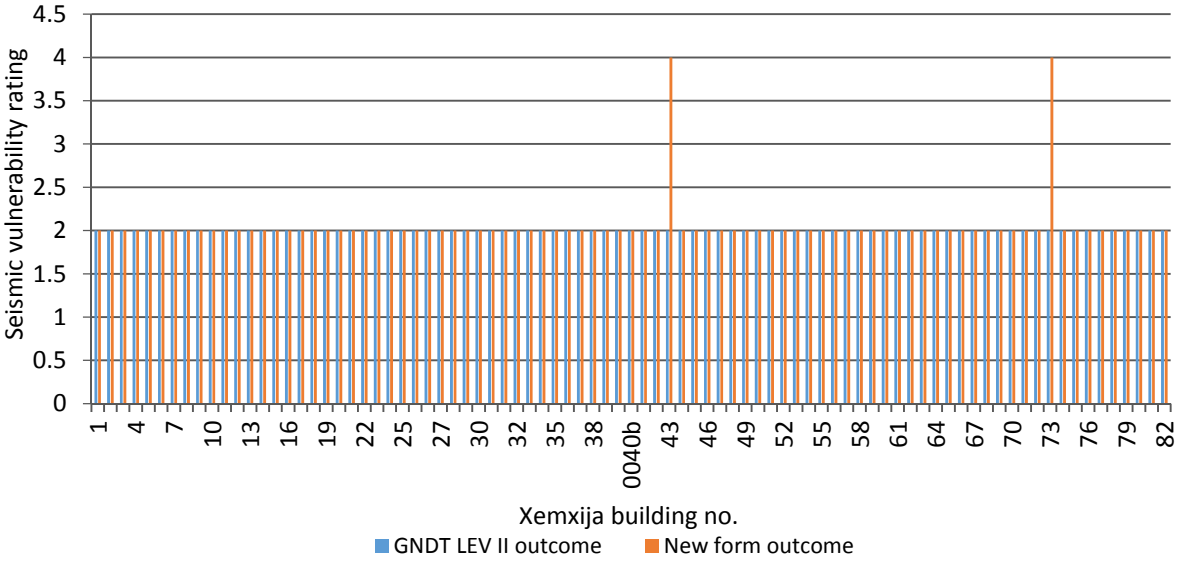

Figure 17: Comparison of the seismic vulnerability ratings obtained from Section 4 (Horizontal structural system) of the New Form to those obtained from the corresponding GNDT level II parameters for the Xemxija building numbers 1-82.

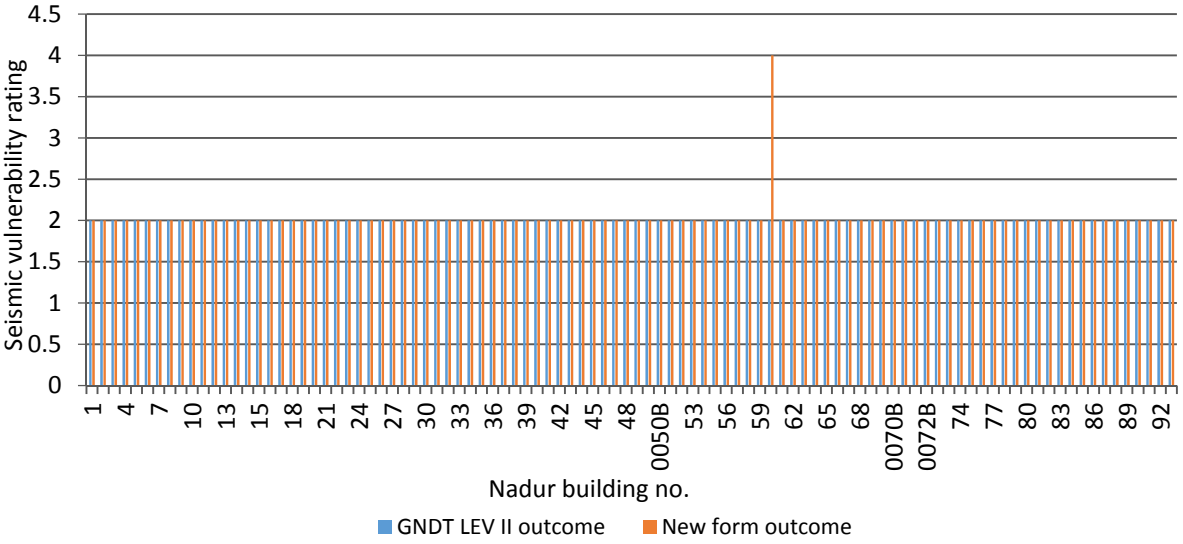

Figure 18: Comparison of the seismic vulnerability ratings obtained from Section 4 (Horizontal structural system) of the New Form to those obtained from the corresponding GNDT level II parameters for the Nadur building numbers 1-93.

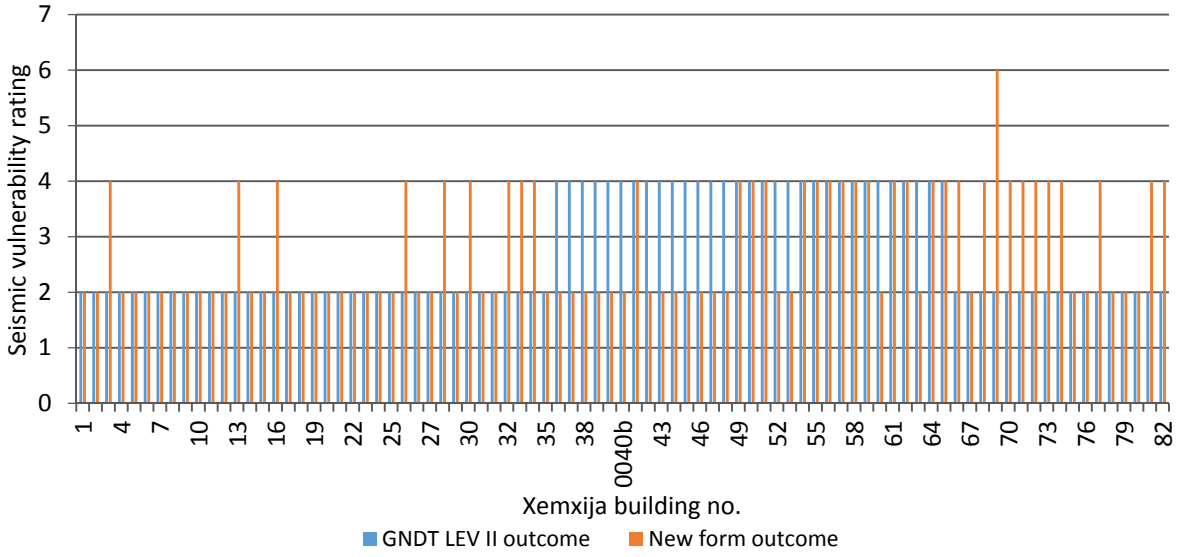

Figure 19: Comparison of the seismic vulnerability ratings obtained from Section 5 (Pre-/Post-earthquake condition) of the New Form to those obtained from the corresponding GNDT level II parameters for the Xemxija building numbers 1-82.

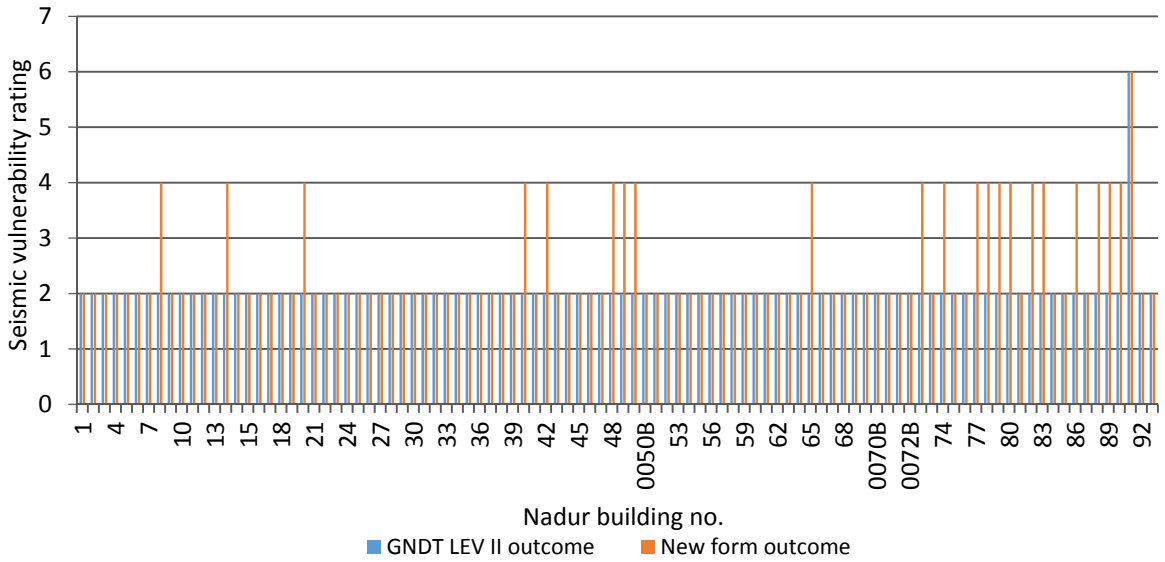

Figure 20: Comparison of the seismic vulnerability ratings obtained from Section 5 (Pre-/Post-earthquake condition) of the New Form to those obtained from the corresponding GNDT level II parameters for the Nadur building numbers 1-93.

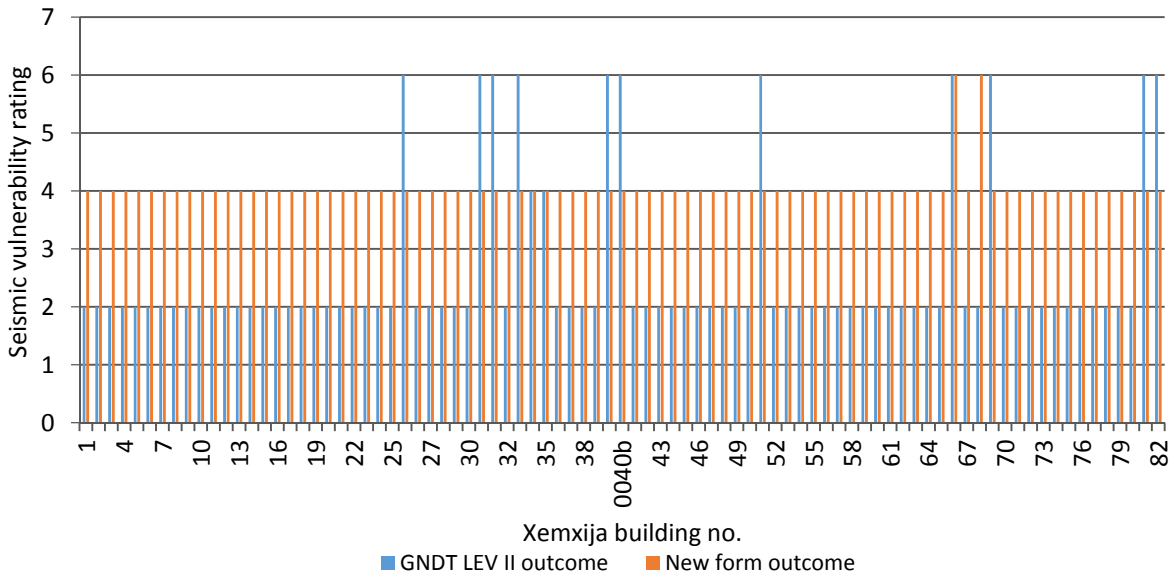

Figure 21: Comparison of the seismic vulnerability ratings obtained from Section 6 (Ground characteristics) of the New Form to those obtained from the corresponding GNDT level II parameters for the Xemxija building numbers 1-82.

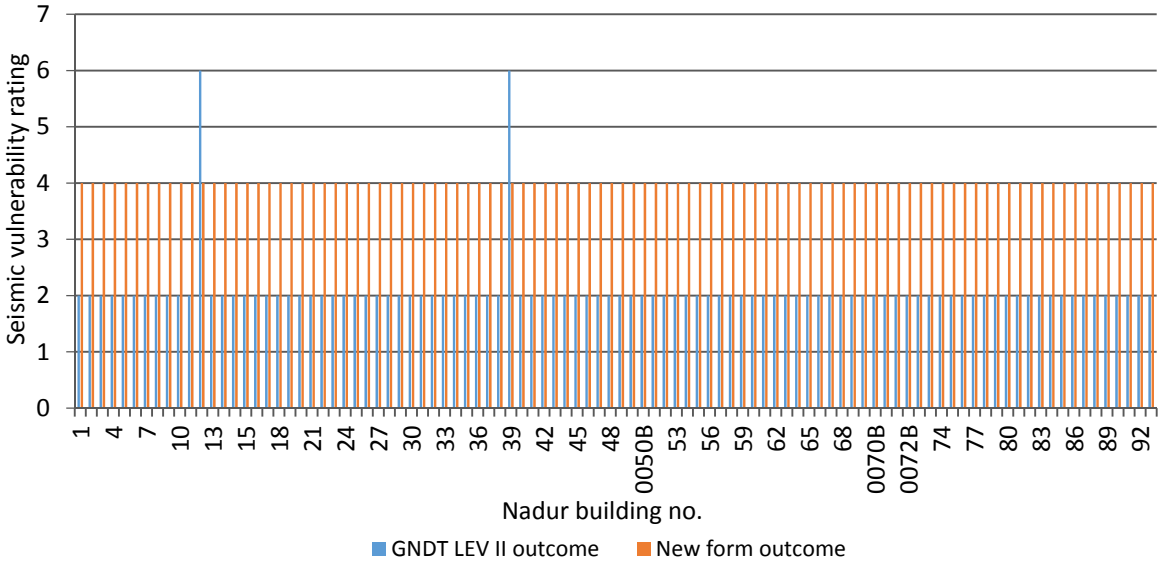

Figure 22: Comparison of the seismic vulnerability ratings obtained from Section 6 (Ground characteristics) of the New Form to those obtained from the corresponding GNDT level II parameters for the Nadur building numbers 1-93.

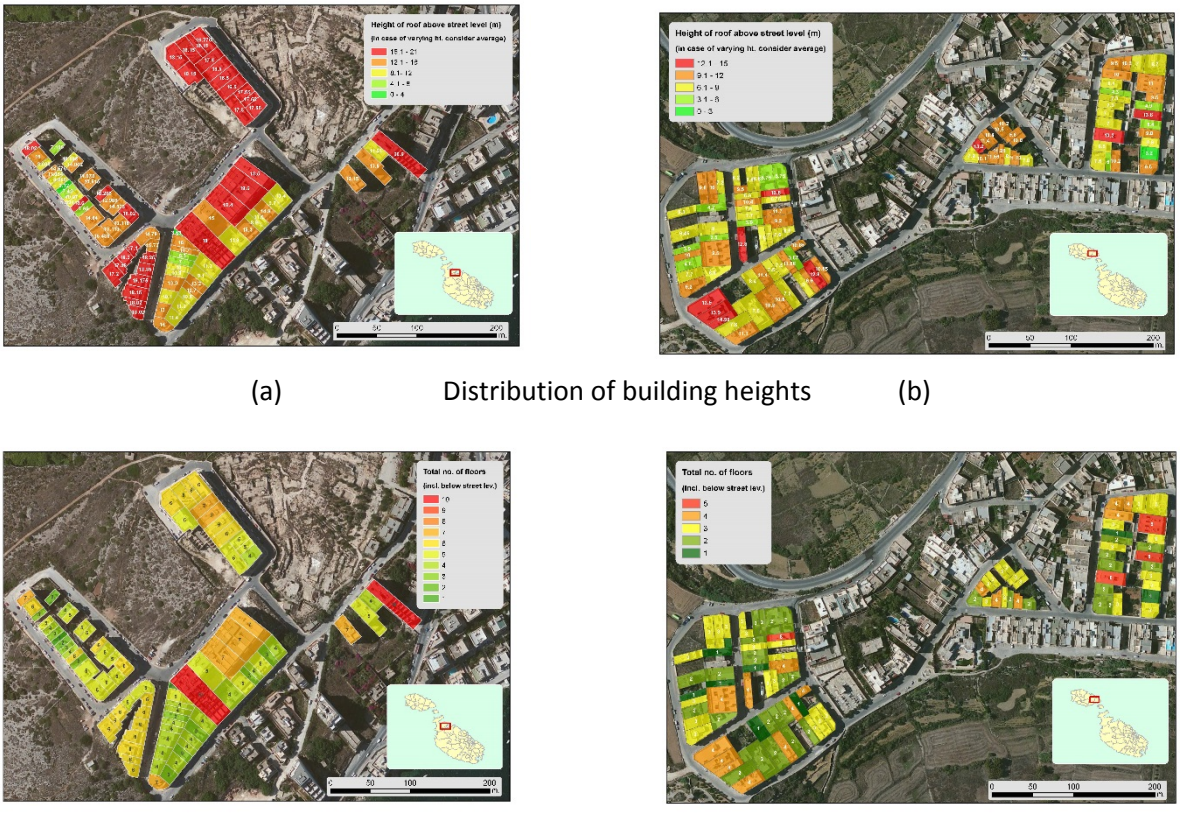

Figure 23a: GIS thematic maps for the Test Sites of Xemxija (a, c) and Nadur (b, d) respectively.

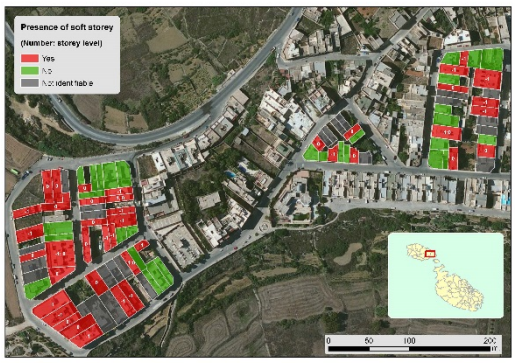

(e) Presence of soft storeys (f)

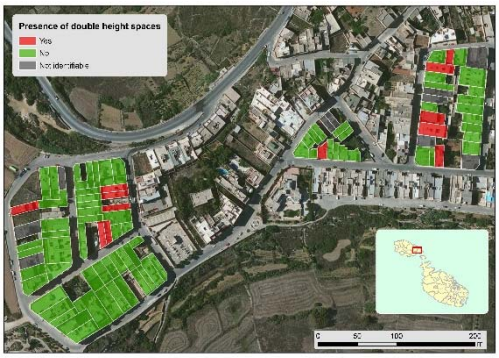

(g) Presence of double height spaces (h)

Figure 23b: GIS thematic maps for the Test Sites of Xemxija (e, g) and Nadur (f, h) respectively.

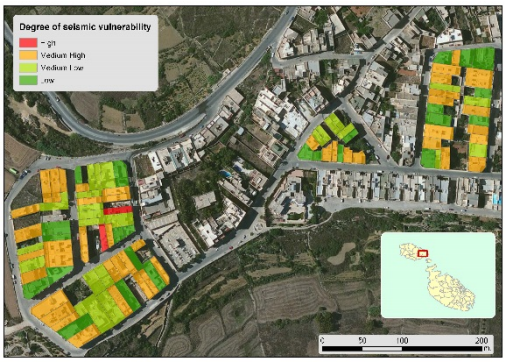

(a) (b)

Figure 24: GIS thematic maps indicating the overall seismic vulnerability rating based on New Form for the buildings under assessment in the Test Sites of Xemxija (a) and Nadur (b) respectively.

1.5 Conclusions

The development of a new seismic vulnerability assessment method for the contemporary loadbearing masonry building typology present in the Maltese Islands is the first study undertaken locally to focus on the evaluation of the seismic performance of this construction typology which constitutes the major portion of the local building stock. The external surveys and the analysis of the internal layouts carried out for the Msida Pilot Study and the 183 buildings selected for

evaluation in the Xemxija and Nadur Test Sites have provided a comprehensive inventory of the seismic vulnerability characteristics present in the building typology under study.

Existing seismic vulnerability assessment methods which are in use in other countries where the behaviour of buildings under seismic forces can be predicted from the experience gained through post-earthquake investigations provided the background to this study. The initial seismic vulnerability ratings proposed for the New Form were based on an in-depth study of the weightings attributed to the various building characteristics in these existing seismic vulnerability assessment methods.

The introduction of a 'Medium-Low' and 'Medium-High' rating for Section 3 of the New Form has resulted following the identification, through reference to FEMA 154 (second edition), of four main parameters which have a major bearing on the seismic vulnerability of buildings and the comparison of the ratings obtained using the New Form to those obtained from a GNDT level II check and the outcome of a FEMA 154 check. This comparison indicated that, while there is a closer correlation between the GNDT level II and the FEMA 154 results, the seismic vulnerability rating obtained through the use of the New Form is more conservative than the FEMA 154 assessment by one to three grades. FEMA 154 takes into account only four main parameters, namely the height of the building, the degree of vertical irregularity, the degree of plan irregularity and the soil type. It is to be noted that whereas the presence of a soft storey is considered in the vertical irregularity parameter, the plan irregularity parameter does not take into account of the increase in vulnerability of buildings having a long and narrow plan layout, as is typical in the contemporary loadbearing masonry building typology under study. Furthermore, in view of the limited number of parameters considered by FEMA 154, it does not take into account at all a number of seismic vulnerability characteristics which are present in the assessed buildings. Hence, before further checks are carried out, the additional degree of conservatism of the New Form which has been highlighted by this comparison does not necessarily imply that the ratings of the New Form must be amended.

The comparison also indicated that the New Form is more conservative by one to two grades than the GNDT level II assessment. It must be noted, however that, even though most of the main sections of the New Form which include the main parameters governing the seismic vulnerability rating correspond to one or more parameters in the GNDT level II method, the latter does not take into consideration the possibility that more than one seismic vulnerability characteristic can occur in the same building. An example of this can be obtained by considering a very typical apartment block which has a soft storey at the semi-basement level, an open plan ground floor due to a commercial establishment, and a long corridor adjacent to the party wall in addition to an open plan area in the front room at every level above the ground floor. Parameter 8 in the GNDT level II assessment classifies the degree of vulnerability of the building based on the maximum distance between loadbearing walls which are not restrained by perpendicular walls for the storey level representing the worst case scenario. Hence, in this example, the maximum distance between the walls at semi-basement level or at ground floor would be calculated. However, the GNDT level II

method would not take into consideration the added degree of vulnerability present in the building due to the presence of the second soft storey and the lack of restraint of the party walls together with the torsional effects caused by the presence of the long corridor next to the party wall and the open plan spaces occurring in the same building.

Furthermore, the study also included the comparison of the seismic vulnerability outcome obtained for the individual Section numbers 2, 3, 4, 5, and 6 of the New Form to that of the corresponding GNDT level II Parameters. This comparison indicated that in the case of Sections 4 (Horizontal structural system) and 5 (Pre- and post-earthquake condition) of the New Form there was a good correlation of outcomes from the two methods. In the case of Section 2 (General characteristics), the seismic vulnerability outcomes for the Xemxija buildings were also in agreement whereas those for Nadur indicated that the New Form gave lower ratings than the GNDT level II method by two grades. On the other hand, in the case of Sections 3 (Vertical structural system) and 6 (Ground Condition), the New Form gave higher ratings by 1 to 2 grades.

This variation in degree of correlation can be due to the extent of direct equivalence of the sections of the New Form to the GNDT level II parameters which have been selected as corresponding to these sections. As indicated in Table 3, every section which effects the seismic vulnerability rating in the New Form, with the exception of Section 8 (Accuracy of assessment), can be linked to one or a maximum of two parameters in the GNDT level II method. However, the different sections in the New Form include an inventory of all the seismic vulnerability characteristics identified during the study of the contemporary loadbearing masonry building typology present in the Maltese Islands. In most cases where complete correlation between the seismic vulnerability ratings obtained between the two methods was not achieved, the correspondence between the GNDT level II parameters and the main sections of the New Form is related only to a limited number of parameters in the New Form. This implies that in every assessment which has been carried out for the buildings in the Test Sites, a number of seismic vulnerability characteristics have been identified in the New method which have not been taken into account in the corresponding GNDT level II check. Moreover, if one had to consider the four parameters of the vertical structural system identified through reference to FEMA 154 (second edition) as having a major bearing on the seismic vulnerability rating of buildings, only the presence of the soft storey and the vertical irregularity are identified through the GNDT level II check. The presence of large openings, double height spaces and the presence of adjacent buildings which are lower than the building under assessment by more than one floor are not taken into account in the GNDT level II method. All these characteristics are commonly present in the contemporary loadbearing masonry typology present in Malta and Gozo. This could explain the increased level of conservativism of the seismic vulnerability ratings obtained for Sections 3 and 6 of the New Form when compared to the corresponding parameters of the GNDT level II method.

On the other hand the increased conservatism of the GNDT level II ratings obtained for the combination of Parameters 3, 4, and 6 when compared to the ratings obtained for Section 2 of the New Form for the buildings under assessment in Nadur could be due to the fact that Parameter 3

in the GNDT level II method takes into consideration the minimum area of walls in the test floor. Most of the buildings in Nadur have a soft storey, however the presence of the soft storey is recorded in Section 3 and not in Section 2 of the New Form. This, together with the high weighting attributed to this parameter in the GNDT level II method, might explain the discrepancy in seismic vulnerability ratings. It is interesting to note that in the case of the buildings investigated in Xemxija, a good correlation of seismic vulnerability ratings was obtained using the two systems for Section 2 of the form and the corresponding GNDT level II parameters. In Xemxija, however the presence of a higher number of floors, which is also taken into account in Parameter 3 of the GNDT level II method, is recorded under Section 2 of the New Form and has been attributed a high weighting in the seismic vulnerability rating of this section. Consequently, the presence of a higher number of floors in the case of Xemxija might have compensated for the missed detection of the soft storey in this comparison.

In the case of Sections 4 (Horizontal structural system) and 5 (Pre- and post-earthquake condition) of the New Form, where complete correlation of ratings has resulted, it is evident that the GNDT level II Parameters corresponding to these sections took into account of all the characteristics which were recorded through the use of the New Form in the Xemxija and Nadur assessments. It is to be noted that, while the presence of vaults or arches and their possible inadequate form of abutment is included in Section 4 of the New Form but not covered by the corresponding GNDT level II Parameters, this discrepancy did not cause a variation in the overall seismic vulnerability ratings because no vaults or arches were present in the assessed buildings.

The analysis of the comparison of the seismic vulnerability rating obtained for the individual main sections of the New Form to those obtained for the corresponding GNDT level II parameters gives a degree of confidence with respect to the validity of the developed ratings for the New Form. This, however, does not preclude the need of further investigations for the verification of the rating system and the calibration of the characteristics considered in every section of the form in order to ensure the correctness of the resulting ratings. The statistical analysis and the numerical modelling which are being carried out as a second stage to this study will be essential for the verification of these ratings, for the elimination of the need of additional calculations and, possibly, for the curtailment of the form.

Acknowledgements

This research study has been carried out under the SIMIT Project (Italia – Malta Operational Programme) (Project code: B1-2.19/11), Work Package 2.1.

The on-site assessments of the local building stock in the selected aggregates in Xemxija (Malta) and Nadur (Gozo) and the retrieval of the internal layouts of these buildings from the approved planning permits from the Malta Environment and Planning Authority have been carried out with the help of the following Research Support Officers on the SIMIT Project: Kim Cassar Torreggiani, Yanica Zammit, Charlo' Briguglio, Godwin Abela.

Furthermore, the following local entities are being gratefully acknowledged for their contributions to this research study:

- MEPA (Malta Environment and Planning Authority) for allowing access to the approved permit drawings of the buildings in the test sites of Msida and Xemxija (Malta), and Nadur (Gozo);
- MRA (Malta Resources Authority) for allowing access to reports on geological investigations carried out in Xemxija (Malta) and Nadur (Gozo);
- Institute for Climate Change and Sustainable Development - GIS Laboratory (University of Malta) for the elaboration of thematic maps based on the seismic vulnerability assessments carried out and the on-site data collected by the authors and the acknowledged Research Support Officers.

Bibliography

- AeDES, Scheda di 1° livello di rilevamento danno, pronto intervento e agibilità per edifici ordinari nell' emergenza post-sismica, Dipartimento della Protezione Civile (AeDES 05/2000).
- Borg R.P., Borg R.C., Borg Axisa G. (2008), The seismic risk of buildings in Malta. In Urban Habitat Constructions under Catastrophic events. Edited by Mazzolani .F et al, European Science Foundation, COST C26, University of Malta, Malta.
- Messrs Binnie, Deacon & Gourley (1958), "Report on Geological Investigation of Bajada Ridge, Ghajn Tuffieha and Majesa carried out by the Soil Mechanics Department of Messrs. Richard Costain Ltd.", Volume 69/167.
- Messrs Binnie, Deacon & Gourley (1958), "Report on Geological Investigation of the Nadur Area carried out by the Soil Mechanics Department of Messrs. Richard Costain Ltd.", Volume 69/167.
- Commissione Tecnica per la Microzonazione Sismica (2013) Analisi della Condizione Limite per l' Emergenza (CLE) dell' insediamento urbano. Version 2.0.
- Farrugia J. (2002) Seismic Vulnerability of Local Masonry Building Typologies, B.E. & A. Dissertation, University of Malta.
- FEMA (2002) "Rapid visual screening of buildings for potential seismic hazards: A handbook, FEMA 154". 2nd Edition.
- FEMA (2005) "Rapid visual screening of buildings for potential seismic hazards: Student Manual, FEMA 154 -SM". 2nd Edition.
- Galdes, A. (2012) Vulnerability of Local Masonry Buildings to Seismic Loading, B.E. & A. Dissertation, University of Malta.
- GNDT(INGV) / DIS (Politecnico di Milano) (2001) Scheda per la valutazione qualitativa dei possibili effetti locali nei siti di ubicazione di edifice strategici e monumentali.
- GNDT/CNR (2003) Regione Toscana: Rilevamento della vulnerabilita' sismica degli edifici in muratura. Manuale per la complilazione della scheda GNDT/CNR di II livello. Versione modificata Regione Toscana.

- GNDT/CNR (2007) Regione Abruzzo: Manuale per il rilevamento della vulnerabilita' sismica degli edifici – Istruzione per la compilazione della scheda di I livello.
- Regione Molise (2008) 3H- Analisi dei costi di intervento e riduzione della vulnerabilita' sismica degli edifice residenziali. Modello di analisi.
- Regione Toscana (2004) Edifici in muratura in zona sismica. Rilevamento delle carenze strutturali – Manuale per la compilazione della scheda delle carenze.

ii) Document (ii): Extended abstract of oral presentation at conference 'Geo-risks in the Mediterranean and their mitigation', 20-21st July 2015, Valletta, Malta.
Reference: Torpiano A, Bonello MA, Borg RP, Sapiano P, Ellul AM. The development of a rapid empirical seismic vulnerability assessment methodology for contemporary loadbearing masonry buildings in the Maltese Islands. In: Galea P, Borg RP, Farrugia D, Agius MR, D'Amico S, Torpiano A, Bonello M (eds.)*, 20-21 July 2015, Valletta, Malta*. Messina: Mistral Services sas; 2015. p. 272-275.
Status: published /presented.

Abstract

According to historical records, the last major earthquake reported to have caused extensive damage in the Maltese Islands dates back to 1693. It is not possible to assess the vulnerability of masonry structures to seismic action through post-earthquake damage assessments. Considering a return period of 475 years, the probability of occurrence of a major seismic event is quite high. This study is an attempt at addressing the issue of the seismic response of the building stock in Malta. It focuses on the typical contemporary load-bearing masonry building typology. This typology mainly consists of blocks of apartments including a semi-basement with no internal walls and, in most cases, roofed over by hollow core precast prestressed planks, and with around 4 overlying residential floors in addition to a penthouse level.

The methodology developed draws on other methodologies employed within other countries and on the experiences of regions with a high incidence of earthquakes, where such methodologies have been well-calibrated. In particular, reference is made to a number of first and second level pre- and post-earthquake assessment manuals and their corresponding forms, which have been developed in Italy over the past 40 years, not only with respect to the actual parameters listed but also with respect to the background principles affecting the seismic vulnerability of buildings as outlined in the manuals to these forms. These include the '*Analisi della Condizione Limite per l'Emergenza (CLE) dell' insediamento urbano*', the '*Agibilita' e Danno nell' Emergenza Sismica (AeDES)*' and '*Edifici in muratura in zona sismica. Rilevamento delle carenze strutturali – Manuale per la compilazione della scheda delle carenze*'. A number of GNDT manuals also provide an important background to this study. These include the '*Scheda per la valutazione qualitativa dei possibili effetti locali nei siti di ubicazione di edifici strategici e monumentali*', and the manuals and corresponding forms of the GNDT first and second level vulnerability assessment methods. Following the verification of the applicability of these assessment methods to the local contemporary load-bearing building typologies present in Malta and Gozo it is clear that the methods employed in other countries cannot be directly transposed to the local building stock due to inherent variations in local construction methods and materials and the presence of particular building characteristics. In addition the soft storey effect, could have a negative effect upon the seismic vulnerability of the building typology being considered and is, therefore, considered in more detail in the proposed method. The need for the development of a New seismic vulnerability assessment method for the seismic vulnerability assessment of individual buildings in the Maltese Islands is, therefore, evident. The newly-developed Form is based on the existing seismic

vulnerability assessment forms, but is further adapted to cater for the specific construction methods and materials and building characteristics present in the contemporary load-bearing masonry building typology present in Malta and Gozo.

The method was used in a Pilot study in Msida (Malta) and this allowed for the refinement of the Form prior to its use in the Test Sites, namely Xemxija (Malta) and Nadur (Gozo), where the seismic vulnerability assessment of a total of 183 individual buildings was carried out. The extensive field surveys of the buildings present in the Test Sites and in the Pilot Study, together with the extraction of parameters related to the internal layouts of buildings from the Malta Environment and Planning Authority (MEPA) Development Permit Drawings, allowed for the completion of an exhaustive and detailed database.

The method is based upon ten main areas and therefore the Form is likewise divided into ten sections including: general building identification, general characteristics, vertical and horizontal structural systems (general and seismic vulnerability characteristics), the pre- and post-earthquake condition of the building, ground characteristics, building information and use, accuracy of assessment, post-earthquake assessment outcome, and a final section with the degree of seismic vulnerability.

The last section of the Form summarizes the seismic vulnerability rating resulting from the relevant sections of the new assessment form, in order to establish a final rating following a qualitative assessment of the ratings concluded for these previous sections of the form which is based on the characteristics of the individual building under evaluation. By reference to FEMA 154, the study identifies 4 main parameters of the vertical structural system which are considered to have a greater bearing on the seismic vulnerability rating, thereby allowing for the formulation of a more refined rating for this section of the Form.

The study includes a FEMA 154 assessment and a GNDT Level II seismic vulnerability evaluation for all the 183 buildings assessed in the Test Sites. A refinement of the GNDT Level II ranges corresponding to the Low, Medium-Low, Medium and Medium-High seismic vulnerability ratings was carried out, in order to make it more applicable to the scenario of the Maltese Islands. A comparison of the results obtained using the different methods, was carried out. This was intended to assess the differences between the methods when these are applied to the typology analysed and also to assess the merits of the proposed new method developed for the Maltese Islands.

Acknowledgements

This research study has been carried out under the SIMIT Project (Italia – Malta Operational Programme) (Project code: B1-2.19/11), Work Package 2.1.

The on-site assessments of the local building stock in the selected aggregates in Xemxija (Malta) and Nadur (Gozo) and the retrieval of the internal layouts of these buildings from the approved development permits from the Malta Environment and Planning Authority (MEPA) has been carried

out with the help of the following Research Support Officers on the SIMIT Project: Godwin Abela, Charlo' Briguglio, Ann Marie Ellul, Kim Cassar Torreggiani and Yanica Zammit.

Furthermore, the following local entities are being gratefully acknowledged for their contributions to this research study:

- MEPA (Malta Environment and Planning Authority) for allowing access to the approved development permit drawings of the buildings in the Test Sites of Msida and Xemxija (Malta), and Nadur (Gozo);
- MRA (Malta Resources Authority) for allowing access to reports on geological investigations carried out in Xemxija (Malta) and Nadur (Gozo);
- Institute for Climate Change and Sustainable Development - GIS Laboratory (University of Malta) for the elaboration of thematic maps based on the seismic vulnerability assessments carried out and the on-site data collected by the authors and the acknowledged Research Support Officers.

References

- AeDES, Scheda di 1° livello di rilevamento danno, pronto intervento e agibilità per edifici ordinari nell' emergenza post-sismica, Dipartimento della Protezione Civile (AeDES 05/2000).
- Commissione Tecnica per la Microzonazione Sismica (2013), Analisi della Condizione Limite per l' Emergenza (CLE) dell' insediamento urbano, Version 2.0.
- FEMA (2002), Rapid visual screening of buildings for potential seismic hazards: A handbook, FEMA 154. 2nd Edition.
- FEMA (2005), Rapid visual screening of buildings for potential seismic hazards: Student Manual, FEMA 154 -SM. 2nd Edition.
- GNDT(INGV) / DIS (Politecnico di Milano) (2001), Scheda per la valutazione qualitativa dei possibili effetti locali nei siti di ubicazione di edifice strategici e monumentali.
- GNDT/CNR (2003), Regione Toscana: Rilevamento della vulnerabilita' sismica degli edifici in muratura. Manuale per la complilazione della scheda GNDT/CNR di II livello. Versione modificata Regione Toscana.
- GNDT/CNR (2007) Regione Abruzzo: Manuale per il rilevamento della vulnerabilita' sismica degli edifici – Istruzione per la compilazione della scheda di I livello.
- Regione Molise (2008) 3H- Analisi dei costi di intervento e riduzione della vulnerabilita' sismica degli edifice residenziali. Modello di analisi.
- Regione Toscana (2004), Edifici in muratura in zona sismica. Rilevamento delle carenze strutturali – Manuale per la compilazione della scheda delle carenze.

iii) Document (iii): Paper published in the International Journal of Sustainable Materials and Structural Systems. This paper includes the main work carried out in this thesis with respect to the development of the New Form and the corresponding rating system, in addition to the comparisons of the seismic vulnerability ratings resulting from the use of the New Form on a total of 183 buildings in the test sites of Xemxija (Malta) and Nadur (Gozo) to the outcomes of a FEMA 154 check (second edition) and a GNDT second level assessment on the same buildings. Furthermore, the seismic vulnerability ratings resulting from Sections 2, 3, 4, 5 and 6 of the New Form are compared to the ratings obtained from the corresponding GNDT second level parameters.

Reference: Torpiano A, Bonello M, Borg RP, Sapiano P, Ellul AM. The development of a seismic vulnerability assessment methodology for contemporary loadbearing masonry buildings in the Maltese Islands. International Journal of Sustainable Materials and Structural Systems. 2016;2(3-4):283-307. DOI http://dx.doi.org/10.1504/IJSMSS.2016.078729.

Status: published.

Abstract

This study focuses on the development of a seismic vulnerability assessment method adapted for use on the contemporary loadbearing masonry building typology present in the Maltese Islands. This assessment methodology refers to existing vulnerability assessment methodologies, pre- and post-earthquake survey methods and manuals developed for different Italian regions. The methodology refers to seismic vulnerability characteristics present in the building typology under study. The Method was tested in a pilot study in Msida and then in the test sites of Xemxija and Nadur covering 183 individual buildings. The assessment was carried out through site surveys and information extracted from the Development Permit Drawings. FEMA 154 and a GNDT level II seismic vulnerability evaluation were carried out to assess the differences between the methods when these are applied to the typology analysed and also to assess the merits of the proposed new method developed for the Maltese Islands.

Keywords: seismic vulnerability, loadbearing masonry, assessment.

1. Introduction

In the Maltese context, the assessment of the effect which the different characteristics have on the overall seismic vulnerability of the individual buildings and on the aggregate as a whole cannot be obtained from the historical experience of the performance of similar buildings under seismic forces since the last major earthquake dates back to 1693. The direct application of existing methodologies and forms in use in other countries for the assessment of the seismic vulnerability of contemporary loadbearing masonry buildings present in the Maltese Islands would ignore the differences in the

construction methods and materials and the particular characteristics present in this building typology and not catered for in the available forms.

The contemporary loadbearing masonry building typology, present in the Maltese Islands since the 1960s and considered in this study, consists of loadbearing masonry (local softstone or hollow concrete blockwork) single leaf or double leaf walls with a cavity and including the presence of bondstones tying the two skins. The slabs and roofs usually consist of reinforced cast in-situ concrete or precast slabs. The building typology under study mainly includes blocks of flats with a semi-basement with no internal walls and, in most cases, roofed over by hollow core precast prestressed planks, and around 4 residential floors in addition to a penthouse level. Even though Malta can be considered to be located in an area of low - moderate seismicity, with a peak ground acceleration of around 0.10g, and Eurocode 8 (CEN 2004) allows the use of reduced or simplified procedures in such cases, it is safe to assume that, in the majority of cases, no seismic design considerations have been made in the structural design of the residential buildings constructed to date in the Maltese Islands.

The high probability of a major seismic event occurring when considering a return period of 475 years, the absence of earthquake resistant design, the inability of applying directly an existing seismic vulnerability assessment method, together with the awareness that certain construction characteristics which are typical of the building typology under study have a negative effect on the seismic resistance of the buildings, all emphasise the urgent need for the development of a customised seismic vulnerability assessment method for the Maltese Islands.

2. The development of the methodology

2.1 The background to the development of the new form for the seismic vulnerability assessment of the individual building

The study started off with the identification of additional characteristics, apart from the soft storey effect, which could have a negative effect upon the seismic vulnerability of the building typology being considered. Such characteristics include (but are not limited to):

a) narrow and long plan configurations and narrow and high elevation proportions arising from the typical plot proportions for the building typology under study;
b) open plan spaces without loadbearing cross-walls (very often in more than one storey);
c) shared or unshared party walls, where the party walls in general consist of single leaf 230mm thick unreinforced masonry walls;
d) long corridors directly abutting party walls;
e) vacant sites, hence giving rise to unrestrained party walls;
f) misalignment of intermediate slabs, roofs, front and rear facades and internal spaces;
g) double height spaces;
h) large openings on facades with very small masonry pilasters constructed between openings;
i) setbacks due to sloping sites (very often occurring on more than one floor);
j) construction of additional floors due to changes in the regulations limiting the maximum building heights over the years;

k) projecting rooms and balconies on more than one storey.

These characteristics are evident in the building typology under study throughout Malta and Gozo. Figures 1 and 2 show examples of seismic vulnerability characteristics of the contemporary loadbearing masonry building typology which can be identified in the buildings of the Msida pilot study and the Test Sites of Xemxija and Nadur. Borg et al. (2008) discuss the effect which a number of common seismic vulnerability characteristics have upon the seismic resistance of buildings. Some of the effects which would apply to the contemporary loadbearing masonry typology include: the development of high stresses and torsion caused in buildings with irregular plans and elevations, the out-of-plane action of horizontal diaphragms on party walls in cases where the floors of adjacent buildings sharing the same party wall are not aligned, the inadequate shear transfer of loads to foundations in cases where the party wall thickness varies throughout its height, the effect of pounding in cases where the (unshared) party walls in adjacent buildings are almost touching and the reduction of lateral stiffness in soft storeys. Additional causes of seismic vulnerability could also arise due to lack of continuity in detailing between parallel spans of one-way spanning cast in-situ slabs and the inadequate shear transfer together with the varying building stiffness throughout the building height in the case of structures with projecting rooms and/ or setbacks.

Figure 1: Examples of seismic vulnerability characteristics present in the contemporary loadbearing masonry building typology -1: (a) double height spaces at lower levels due to commercial establishments; (b) adjacent buildings with different heights: unrestrained party walls and misaligned slab levels; (c) unrestrained party walls due to vacant sites; (d) misalignment of slab levels within same individual buildings and between adjacent buildings; (e) misalignment between planes of facades of adjacent buildings; (f) setbacks – sloping sites; (g) projecting rooms; (h) large area of openings on façade.

Figure 2: Examples of seismic vulnerability characteristics present in the contemporary loadbearing masonry building typology – 2. (Downloaded from the Malta Environment and Planning Authority Mapserver).

'The data collection methods concerning damage of structures can be classified in accordance with the scope of the survey, the discipline considered, the time of data collection, the accuracy of data collection, and the amount of the data collected. Many of the above are correlated, and the damage assessment methods can be classified with respect to the scope, the discipline and the time of data collection (Goretti A. et al., 2002). Systematic typological, dimensional and functional data collection of buildings can be conducted, and result in an inventory based on technical information on buildings on a regional or national level'.[2]

For the data to be reliable, it has to be objective and therefore, clear methods, unambiguous data collection forms, and well-trained inspectors are required. The data collection forms are required to be detailed and easy to compile.

'In the data collection, the assessment of component performance is preferred to the component description. The accuracy of the data is related to the accuracy of the inspection and it is recommended that buildings should not be inspected only from the exterior. The processing should allow for checks on the data collected'.[3]

The management of the data is an important consideration, and includes the data processing, the validation of the data input and maintenance. In this regard, the data collected is processed using appropriate tools. The use of GIS systems and pre-event databases help to accelerate the damage

[2] Borg RP, Indirli M, Rossetto T, Kouris LA. L'Aquila earthquake April 6th, 2009: The damage assessment methodologies. In: Proceedings of the Final Conference of COST Action C26, Urban Habitat Constructions Under Catastrophic Events 2010 Dec 1 (pp. 16-18).

[3] Borg et al. (2010).

assessment, the processing and the validation of the data. Dissemination and access to the data are important considerations, and depend on the users, including researchers, the purpose of use of the data, and the type of data required.

A thorough study of a number of first and second level pre- and post-earthquake assessment manuals and their corresponding forms which have developed in the Italy over the past 40 years has been carried out. In view of the intrinsic differences present in the construction system and the particular building characteristics in the Maltese scenario, special consideration has been given to the listed parameters and the underlying principles which govern the increase in the seismic vulnerability of buildings as outlined in the manuals to these forms. The main forms and manuals referenced include the '*Analisi della Condizione Limite per l' Emergenza (CLE) dell' insediamento urbano*' (Commissione Tecnica per la Microzonazione Sismica, 2013), the AeDES – '*Agibilita' e Danno nell' Emergenza Sismica*' (Baggio et al., 2000) and '*Edifici in muratura in zona sismica. Rilevamento delle carenze strutturali – Manuale per la compilazione della scheda delle carenze*' (Ferrini et al., 2004). A number of GNDT manuals have also provided an important background to this study. These include the '*Scheda per la valutazione qualitativa dei possibili effetti locali nei siti di ubicazione di edifici strategici e monumentali*' (Di Capua et al., 2001), and the manuals and corresponding forms of the GNDT first and second level vulnerability assessment methods (Ferrini et al., 2003, GNDT/CNR, 2007, Lemme et al., 2008). From this study of the existing seismic vulnerability assessment methods, in the Maltese Islands, the existing methods have generally resulted as being more directly applicable to the case of traditional and vernacular masonry loadbearing construction, where the walls usually consist of two leaves constructed out of local stone blocks with infill material in between and the roofing systems are composed of stone slab roofs, stone arches supporting stone slab roofs, stone slabs over timber beams or steel beams, and/ or timber panels over timber beams (not frequent). It was evident, however, that these methods, could not be directly applied to the assessment of the contemporary loadbearing masonry building typology under study without any adaptation. This was mainly due to the inherent variations in the local construction methods and materials, and the presence of particular building characteristics, in addition to the soft storey effect as indicated in Figures 1 and 2, which increase the seismic vulnerability of the building typology being considered and which are not catered for in these existing assessment methods. If the classification of the construction materials and roofing / wall construction systems within the categories covered by the GNDT level II assessment method (Ferrini et al., 2003) were to be adopted, even though most of the characteristics identified in the local building typology under study could be linked to one or more corresponding parameters in the GNDT level II manual (Ferrini et al., 2003), this manual does not take into consideration the extent of the occurrence of these parameters throughout the height of the building and the possibility that, in Malta, one parameter could be present in various forms, and at more than one level throughout the same building. The need for the development of a new assessment form for use within the Maltese Islands for the seismic vulnerability assessment of individual buildings is, therefore, evident. Notwithstanding, the influence which these existing methods have had upon the development of the local seismic vulnerability assessment method is hereby being acknowledged, especially with respect to the

identification of the seismic vulnerability characteristics particular to the local building typology under study and in the relative weightings attributed to the various parameters.

Calvi et al. (2006) identified three main types of seismic vulnerability assessment methods, namely empirical, hybrid and analytical. The empirical methods are based upon post-earthquake surveys, as in the case of rapid screening methods and the vulnerability index method, or past post-earthquake survey data available in national databases, as in the case of damage probability matrices and continuous vulnerability curves. In analytical methods, the damage scale is related to the limit-state behaviour of buildings. Numerical analysis can be used for the derivation of seismic vulnerability curves and damage probability matrices. Hybrid methods involve the combined use of the empirical and the analytical procedures, especially in areas where no or limited past earthquake data is available, as in the case of the Maltese Islands. In view of the difficulty of predicting the behaviour of the contemporary loadbearing masonry building typology in the Maltese Islands under seismic actions, the development of a customized rapid seismic vulnerability assessment method for the local building typology under investigation and its rating system are being presented in this study. The verification of the rating system carried out by means of statistical analysis and numerical modelling as well as the calibration of the relative weightings which should be attributed to the most important seismic vulnerability characteristics in the assessment form, will be published separately.

The assigned weightings of the ten seismic vulnerability parameters which were identified by Benedetti and Petrini (1984) in their proposal of the vulnerability index method and which formed the basis of the GNDT level II assessment, have been based upon the different importance levels which every parameter has with respect to the seismic resistance of the buildings. The parameters have been split into three main categories, namely, elements of primary importance (such as the distribution of load-resisting elements on plan), important elements (such as the organisation of the vertical structural system, the location of the building and type of foundations, the current state of repair of the building, the regularity of the plan and the regularity of the building throughout its height) and secondary elements (such as the type of vertical loadbearing system and the presence of non-structural elements attached to the facades).

Athmani et al. (2015) proposed an amendment of the GNDT level II assessment method for Annaba city (Algeria) through the consideration of additional parameters which take into account the building characteristics which are particular to Annaba city and which include the typology of the structural resisting system with reference to the EMS-98 macro-seismic intensity scale, the number of floors, the position of the building in the aggregate and its interaction, and the effect of structural interventions. The modification of the method included also the determination of a fixed vulnerability class for the GNDT level II Parameter 2 (Organisation of vertical resisting system) in accordance with the general characteristics identified in the study area, and also for GNDT level II Parameter 3 (Conventional seismic resistance), since this parameter required information with respect to the structural plans and material properties which were not available for Annaba City. The parameters which were considered to have the highest bearing upon the seismic vulnerability assessment were the ‘type of resisting system’, the ‘organisation of the resisting system’, the ‘conventional strength’, the ‘horizontal

diaphragms' and the 'general state of preservation', with weightings ranging between 1.0 and 2.5. The study also involved a comparison of the seismic vulnerability ratings obtained using this modified GNDT level II assessment with those obtained from a 'macro-seismic method' based upon the EMS 98 which was developed in the European Project RISK-UE.

A similar modification of the GNDT level II assessment method had also been used by Vicente et al. (2011) in the seismic vulnerability assessment of the historic city centre of Coimbra in Portugal. As in the case of Annaba city, the modified assessment method for Portuguese city was also based upon a list of 14 parameters with the main differences lying in the exclusion of the parameter assessing the effect of structural interventions and the introduction of a parameter which takes into consideration the effect on the seismic vulnerability of the degree of alignment of openings on façade. No fixed vulnerability classes were specified in this case and the weightings attributed to the different parameters were particular to the Portuguese scenario. The parameters with the highest weightings were the 'conventional strength', the 'number of floors' and the 'aggregate position and interaction'. The authors noted, however, that in the case of the assessments carried out in Coimbra, the parameters recording the 'maximum distance between walls', the 'fragilities and conservation state' and the 'wall façade openings and alignments' had a high bearing upon the seismic vulnerability rating, even though they had been assigned lower weightings (0.50-0.75) in view of their low scores (C to D).

Indirli et al. (2013) used a 2006 Italian official datasheet for post-earthquake damage assessments, in addition to MEDEA (Manuale di Esercitazioni sul Danno ed Agibilità 2005) and AEDES (Agibilità e Danno nell'Emergenza Sismica 2010) damage assessment methods in the immediate post-earthquake assessment of L'Aquila and the village of Castelvecchio Subequo following the 2009 Abruzzo earthquake in Italy. The MEDEA assessment method has also been used in the study for the determination of the collapse mechanisms present in the damaged structures.

2.2 The new form for the seismic vulnerability assessment of the individual building

A new form has been developed, based upon the existing seismic vulnerability assessment forms, however adapted to cater for the specific construction methods, materials and building characteristics present in the contemporary loadbearing masonry building typology present in Malta and Gozo. The form is divided into ten main sections, namely:

1) general building identification;
2) general characteristics;
3) vertical structural system (general and seismic vulnerability characteristics);
4) horizontal structural system (general and seismic vulnerability characteristics);
5) pre- and post-earthquake condition of the building;
6) ground characteristics;
7) building information and use;
8) accuracy of assessment;
9) post-earthquake assessment outcome; and
10) degree of seismic vulnerability.

Section 1 includes general information on the building under assessment and the assessing team, mainly for identification and reference purposes. Section 7 records general information about the use of the building and the year of construction and structural upgrade and the number of people using the building. This information is required for studies related to exposure. Section 9 includes any emergency safety measures suggested by the assessor in the case that the form is used for a post-earthquake assessment.

Section 2 records general information about the building under assessment, such as, the number of storeys, the average floor area, the plan and elevation proportions, the uniformity and regularity of the plan, etc. The information on the vertical structural system documented in Section 3 includes mainly the type of wall construction on every façade of the building, the material in which the facades are constructed and the presence of a number of seismic vulnerability characteristics which mainly affect the degree of restraint of the party walls, the variation in mass throughout the height of the building, the degree of box-like behaviour which the building will exhibit during a seismic event and the presence of direct load paths through the main walls up to foundation level. Examples of these building characteristics are the presence of soft storeys, double height spaces, open plan areas, long corridors directly abutting party walls, setbacks, large areas of openings on facades, projecting rooms, the presence of vacant sites directly adjacent to the buildings under assessment, the presence of lower adjacent buildings and the misalignment of slab levels in adjacent buildings and misaligned facades. Section 4 records the type of slab construction systems present together with a number of seismic vulnerability characteristics of the horizontal structural system such as, the presence of flexible and semi-rigid slab construction systems, and the presence of vaults or arches with inadequate abutments. The degree and extent of damages, in the form of cracks present in the external walls, internal walls, horizontal loadbearing elements, staircores and non-structural elements, together with the current condition of the building are recorded in Section 5. This section also takes note of any evidence of foundation failure, differential settlement and the potential damages caused to the building. The ground morphology, the micro-seismic rating of the site and the type and thickness of the topmost and second ground formation layers are recorded in Section 6. The degree of exhaustiveness of the assessment, which is related to whether only an external inspection was carried out or whether the building could be partially or completely inspected internally, is recorded in Section 8.

Therefore, only Sections 2, 3, 4, 5, 6 and 8 record information which has a direct bearing upon the final seismic vulnerability assessment of the building, which is carried out in Section 10. This last section of the form summarizes the seismic vulnerability rating resulting from Sections 2, 3, 4, 5, 6, and 8 of the new assessment form, based upon the characteristics of the individual building under evaluation that would be identified during the on-site external survey and the information on the internal layouts obtained from the Development Permit Drawings, in order to establish a final rating following a qualitative assessment of these ratings. The developed form includes a total of 146 entries, which include a comprehensive record of the characteristics of the building under evaluation and upon which the overall seismic vulnerability rating must be based. This new assessment form for the Maltese

Islands was first tested upon a building aggregate in Msida (Malta) and, following refinement, it was then applied to a total of 183 buildings in Xemxija (Malta) and Nadur (Gozo).

2.3 The development of the rating system

In the contemporary loadbearing masonry building typology present in the Maltese Islands, the roofs are generally flat and the slab construction system mainly consists of cast in-situ concrete or precast concrete elements with a cast in-situ concrete topping. Hence, in general, diaphragms can be considered to be rigid and provide an even distribution of forces from the slabs onto the walls. The main characteristics of this building typology which govern the final seismic vulnerability rating are, therefore, found in the Section 3 of the assessment form, where, amongst other factors, the presence and extent of soft storeys, double height spaces, long corridors adjacent to party walls, the sharing or un-sharing of party walls and their construction (in single or double wall thickness), the presence of setbacks, projecting rooms, balconies, large or irregularly-distributed openings on facades, the presence of open plan spaces, the maximum ratio of discontinuous loadbearing walls to continuous loadbearing walls and the presence of additional floors over the original construction, are listed. Section 3 has, therefore, been given a greater bearing in the final seismic vulnerability rating of the building under evaluation than the other sections in the assessment form by stipulating that the final seismic vulnerability rating of the building cannot be less than the rating obtained in Section 3.

The developed rating system for every main section of the assessment form, based upon the existing research literature, the relative weightings attributed to the seismic vulnerability characteristics in assessment methods which are currently in use in other countries, together with a consideration of the outcomes of previous research studies, is summarised below.

- Section 2: General characteristics

Studies on individual residential apartment blocks carried out by the University of Malta (Farrugia, 2002; Galdes, 2012) have shown that isolated contemporary loadbearing unreinforced masonry buildings, would not be damaged by an earthquake with a design peak ground acceleration of 0.10g if their overall height is not greater than 3 floors, if built on rock and, 2 floors, if built on clay. These results suggested the following seismic vulnerability rating for Section 2 of the new form:

- LOW: if the number of storeys is either less than or equal to 2 for a building constructed on clay,
  OR
  Less than or equal to 3 for a building constructed on upper coralline limestone;
- MEDIUM: for a building constructed on clay, if the number of storeys is either less than or equal to 2,
  AND/OR
  the building has a long and narrow plan layout,
  AND/OR

the building has a non-regular plan layout;
OR
for a building constructed on upper coralline limestone, if the number of storeys is less than or equal to 3,
AND/OR
the building has a long and narrow plan layout,
AND/OR
the building has non-regular plan layout;

- HIGH: if all medium risk components described above are combined together.

- Section 3: Vertical structural system

With reference to FEMA 154, the present study has identified four main parameters of the vertical structural system (Section 3 of the assessment form) which are considered to have a greater influence on the seismic vulnerability rating thereby allowing for the formulation of a more refined rating for this section of the form. The four parameters together with their relative weightings are listed below:

1. Soft storey and/or a vertical irregularity [x2 weighting];
2. Large openings [x1 weighting];
3. Double height spaces [x1 weighting];
4. More than 1 floor higher than adjacent building and/or "Medium" rating for Section 2 (relating to building height) [x1 weighting].

Hence, the resulting seismic vulnerability rating for Section 3 is obtained as follows:

- LOW: overall weighting of 1 i.e. if the building contains any one parameter out of the four listed above except for a soft storey and/or a vertical irregularity;
- MEDIUM-LOW: overall weighting of 2 i.e. if the building contains a soft storey and/or a vertical irregularity alone, or else any other two parameters listed above;
- MEDIUM-HIGH: overall weighting of 3 i.e. if the building contains a soft storey and/or a vertical irregularity together with any one other parameter, or else the other three parameters listed above;
- HIGH: overall weighting of 4 i.e. if the building contains a soft storey and/or a vertical irregularity together with any two other parameters listed above.

- Section 4: Horizontal structural system

The seismic vulnerability classes of the equivalent parameters of the GNDT level II method and the Regione Toscana form for the identification of structural deficiencies of masonry buildings have provided the basis for the development of the seismic vulnerability rating for this section of the new form. This rating consists of:

- LOW: if there is no presence of lightweight (flexible) roofing structures (e.g. in the case of mezzanine structures),
  AND/OR
  if there is no presence of semi-rigid slab construction systems;
- MEDIUM: if lightweight (flexible) roofing structures are present,
  AND/OR
  if semi-rigid slab construction systems are present;
- HIGH: if an inadequate degree of abutment or a total absence of abutment is identified in the case that masonry arches or vaults are present.

- Section 5: Pre- / Post-earthquake condition of building

The rating of Section 5 of the new form has been developed with reference to the categorisation of the damage classes present in the GNDT level II parameters which correspond to this section. This includes:

- LOW: if no damage is present;
- MEDIUM: if minor to medium severity cracks are present;
- HIGH: if severe cracks are present.

- Section 6: Ground conditions

The rating of Section 6 has been based on the results of previous studies carried out by the University of Malta (Farrugia, 2002; Galdes, 2012) on the seismic vulnerability of contemporary loadbearing unreinforced masonry building typologies and by taking account of the geology and the different ground conditions of the Maltese Islands. The rating of this section consists of:

- LOW: if stable ground is present;
- MEDIUM: if an upper coralline limestone layer over a clay layer is present (in view of the amplifications of the seismic waves through the clay layer);
- HIGH: if unstable ground is present.

- Section 8: Accuracy of assessment

In view of the difficulty in sourcing the Development Permit Drawings from the Malta Environment and Planning Authority due to cases where the permit drawings were either not available at all, or were only available in part, a number of assumptions with respect to the characteristics of the internal layouts had to be made in such cases. The ratings for this section, therefore, consists of:

- LOW: if all plans were available;
- MEDIUM: if plans were only found in part;
- HIGH: if plans were not available.

The qualitative assessment of all the risk levels obtained in Sections 2, 3, 4, 5, 6 and 8 of the form for the determination of the overall seismic vulnerability (i.e. the ratings of LOW, MEDIUM–LOW, MEDIUM, MEDIUM-HIGH and HIGH) of the individual building under evaluation, resulting from the relative importance of the different parameters listed in the separate sections of the assessment form, has indicated that the overall seismic vulnerability rating may be determined as follows:

- LOW: if the majority of the seismic vulnerability results in Sections 2, 4, 5, 6 and 8 are LOW
  AND
  the seismic vulnerability rating of Section 3 is LOW;
- MEDIUM-LOW: if the seismic vulnerability rating of Section 3 is MEDIUM-LOW;
- MEDIUM: if the number of MEDIUM seismic vulnerability results is
  ≥ the number of LOW seismic vulnerability results
  AND
  ≥ the number of HIGH seismic vulnerability results in Sections 2, 4, 5, 6 and 8
  AND
  the seismic vulnerability rating of Section 3 is not higher than MEDIUM-LOW;
- MEDIUM-HIGH: if the seismic vulnerability rating of Section 3 is MEDIUM-HIGH;
- HIGH: if the number of HIGH seismic vulnerability results is
  ≥ the number of LOW / MEDIUM–LOW / MEDIUM / MEDIUM HIGH seismic vulnerability results in Sections 2, 4, 5, 6 and 8
  AND/OR
  the seismic vulnerability rating of Section 3 is HIGH.

These ratings have been verified following the comparison of the seismic vulnerability outcome obtained using the new assessment form with that obtained from a GNDT level II assessment for all the 183 buildings under study in the Xemxija and Nadur Test Sites. In the case of the GNDT level II Parameters 5, 7 and 9, where a range of weightings is allowed depending on the specific characteristics of the parameter for the building under evaluation, the values which have been assumed for the assessments of the surveyed buildings in Xemxija and Nadur were taken to correspond to the worst case scenario. This assumption was made in order to partially cater for the inability to take explicit account of the extent of the presence of one or more characteristics related to these three parameters in the new assessment form. In general, it was observed that buildings assessed using the Maltese assessment form resulted in a higher seismic vulnerability than that obtained using the GNDT level II method. In fact, the seismic vulnerability ratings obtained for the Xemxija and Nadur buildings assessed using the GNDT level II method varied between 0.00-0.60, that is, from 'ADEQUATE' to 'MEDIUM', while the corresponding ratings obtained using the Maltese assessment form varied from 'LOW' to 'HIGH'. It was also observed that the original interval corresponding to the GNDT level II 'LOW' seismic vulnerability rating was too narrow when applied to the Xemxija and Nadur buildings assessed and, therefore, the 'LOW' interval range was widened in order to improve the correlation between the ratings obtained from the two assessment methods (vide Table 1). Consequently, the

interval ranges for the 'MEDIUM-LOW', 'MEDIUM' and 'MEDIUM-HIGH' seismic vulnerability ratings were adjusted as shown in Table 1, while the original interval ranges for the 'ADEQUATE' and 'HIGH' seismic vulnerability ratings were retained.

Following this comparison of the seismic vulnerability ratings obtained using the new seismic vulnerability assessment form developed in this study with those obtained using the GNDT level II assessment form, the vulnerability index intervals given in the GNDT document were altered in order to reflect better the different classes of seismic vulnerability for the contemporary loadbearing unreinforced masonry building typology in the Maltese Islands Table 1 provides the original GNDT level II ranges of seismic vulnerability ratings, and the corresponding altered ranges considered for the Xemxija and Nadur seismic vulnerability assessments.

Table 1: Original and altered GNDT level II ranges of seismic vulnerability ratings.

Original GNDT level II intervals	Altered GNDT level 2 intervals for local use	Seismic Vulnerability Rating
0.00-0.10	0.00-0.10	Adequate
0.10-0.20	0.10-0.30	Low
0.20-0.40	0.30-0.45	Medium-Low
0.40-0.60	0.45-0.65	Medium
0.60-0.80	0.65-0.80	Medium-High
0.80-1.00	0.80-1.00	High

The seismic vulnerability ratings for the buildings under investigation in the Xemxija and Nadur Test Sites obtained using the GNDT level II assessment with the altered seismic vulnerability ranges and using the newly-developed form for the contemporary loadbearing unreinforced masonry buildings were compared with the outcome of a seismic check using FEMA 154. The results of these comparisons for the Xemxija and Nadur buildings under investigation are summarized in Figures 3 to 8. The 'Rapid Visual Screening of Buildings for Potential Seismic Hazards' - FEMA 154 is aimed at providing a rapid visual screening method to establish whether buildings are acceptable with respect to the risk to life safety or, if an overall score of 2 or less is obtained, whether they are potentially-hazardous in an earthquake scenario and, therefore, require detailed seismic design calculations. It has been assumed that no detailed seismic calculations are necessary in buildings with an 'ADEQUATE', 'LOW' OR 'MEDIUM-LOW' seismic vulnerability rating. Hence, for the graphical representation of this comparison, Table 2 provides the different weightings given to the overall seismic vulnerability ratings obtained for the 183 buildings under investigation using the GNDT level II assessment method and the new assessment form developed for the Maltese Islands, together with the weightings given to the outcome of the seismic check using FEMA 154.

Table 2: Weightings given to the 3 methods for graphical comparison of results.

	GNDT level II	New Form	FEMA 154		
ADEQUATE	1	n/a	1	FEMA 4 to 5	no further checks required for results higher than 2
LOW	2	2	2	FEMA 3 to 4	
MEDIUM-LOW	3	3	3	FEMA 2 to 3	
MEDIUM	4	4	4	FEMA 1 to 2	further detailed checks required for a result of 2 or less
MEDIUM-HIGH	5	5	5		
HIGH	6	6	6	FEMA 0 to 1	

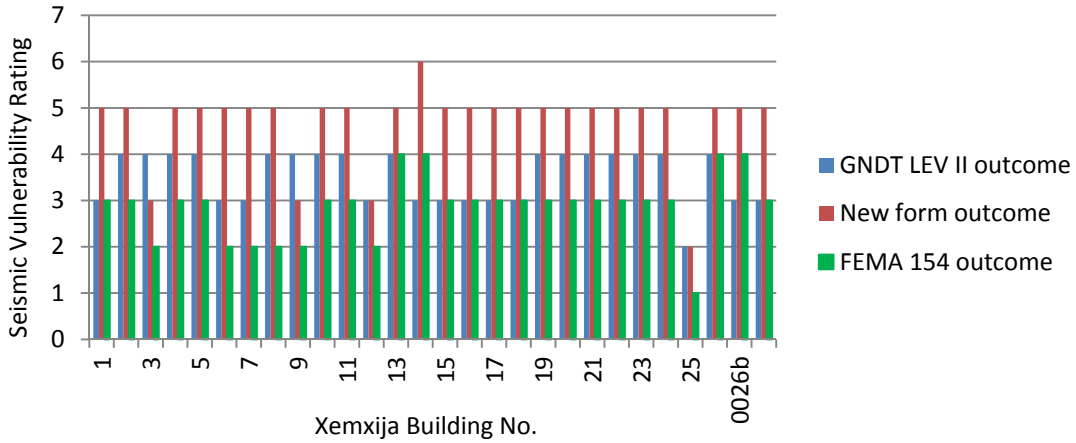

Figure 3: Comparison of the seismic vulnerability ratings obtained for the Xemxija Building Nos. 1-27 using the 3 methods.

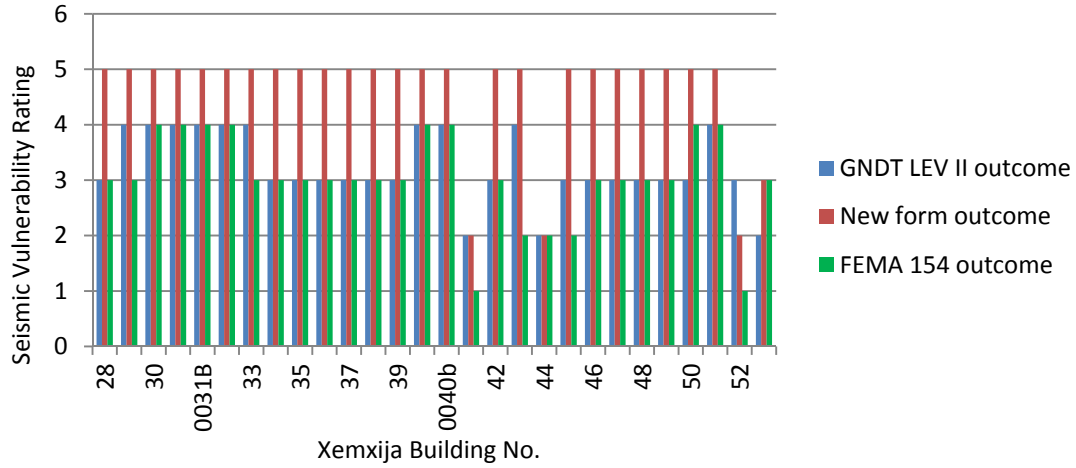

Figure 4: Comparison of the seismic vulnerability ratings obtained for the Xemxija Building Nos. 28-53 using the 3 methods.

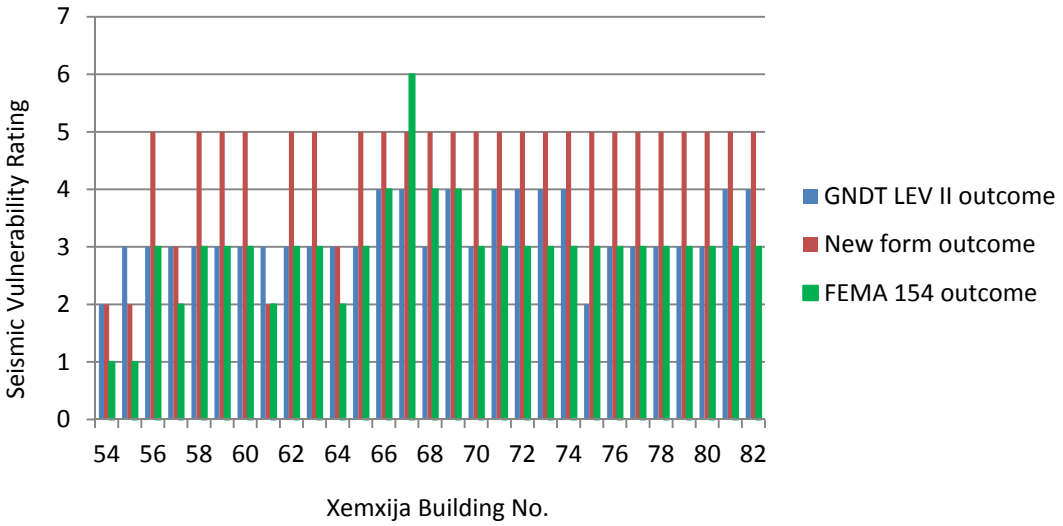

Figure 5: Comparison of the seismic vulnerability ratings obtained for the Xemxija Building Nos. 54-82 using the 3 methods.

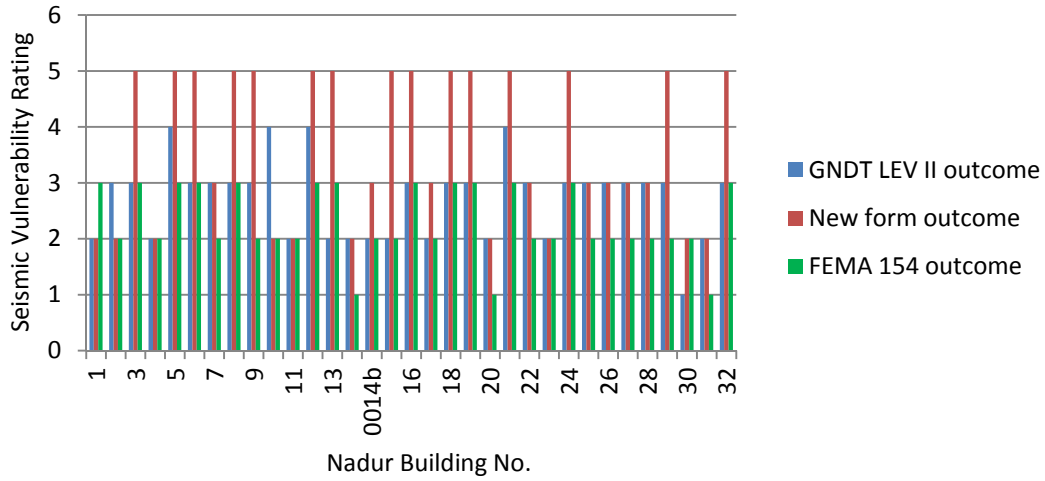

Figure 6: Comparison of the seismic vulnerability ratings obtained for the Nadur Building Nos. 1-32 using the 3 methods.

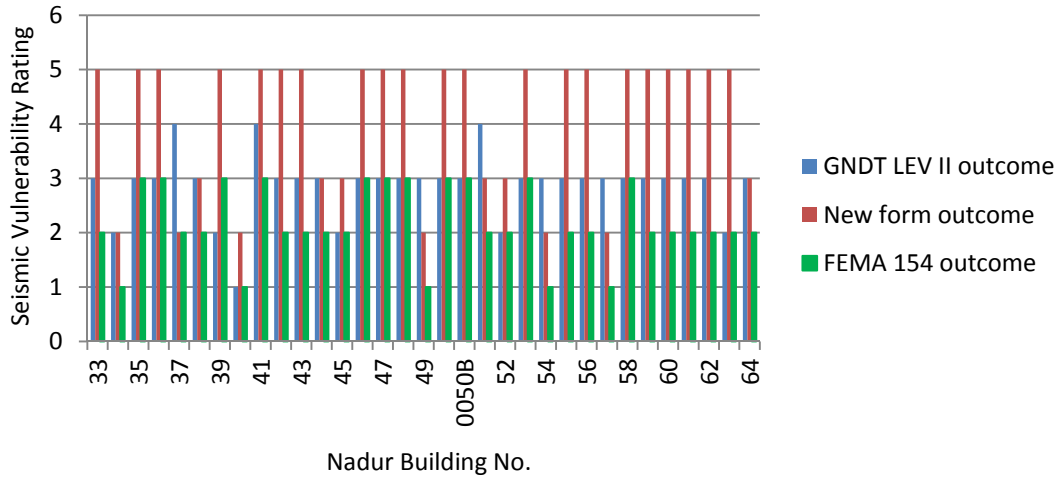

Figure 7: Comparison of the seismic vulnerability ratings obtained for the Nadur Building Nos. 33-64 using the 3 methods.

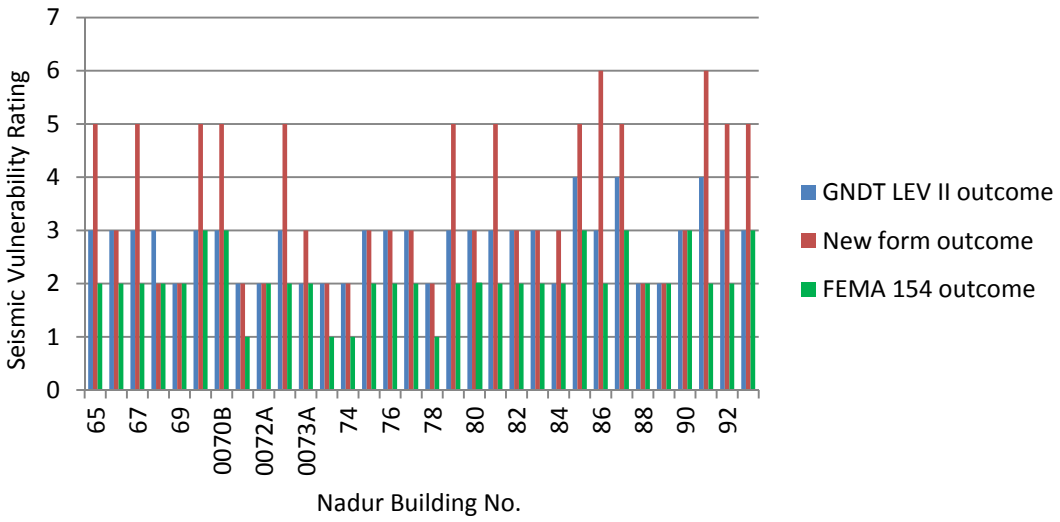

Figure 8: Comparison of the seismic vulnerability ratings obtained for the Nadur Building Nos. 65-93 using the 3 methods.

Table 3: GNDT level II parameters corresponding to every section of the new form.

Main sections of new form affecting seismic vulnerability rating	GNDT Level II Parameters										
	1. Organisation of the structural system	2. Quality of the structural system	3. Seismic resistance of the building	4. Position of building and foundations	5. Slabs	6. Plan configuration	7. Configuration throughout height	8. Maximum distance between main walls	9. Roofing system	10. Non-structural elements	11. Current state of repair of building
2. General characteristics			X	X		X					
3. Vertical structural system	X	X	X				X	X			
4. Horizontal structural system					X				X		
5. Pre- / post-earthquake condition of building										X	X
6. Ground characteristics				X							
8. Accuracy of assessment											

The developed ratings for the new seismic vulnerability assessment form for individual buildings were further verified through a comparison of the seismic vulnerability ratings obtained for Sections 2, 3, 4, 5 and 6 of the new form considered individually, with the rating obtained for the corresponding GNDT level II Parameters. Table 3 summarises the GNDT level II Parameters corresponding to every section of the new form upon which the overall seismic vulnerability rating is based, while Figures 9 to 14 show

the comparison of the seismic vulnerability outcome obtained in the case of Section 3 for the Xemxija and Nadur buildings using the new form to that obtained from the corresponding parameters of the GNDT level II assessment. Similar comparisons were also carried out with respect to Sections 2, 4, 5, 6 and 8 and their corresponding GNDT level II parameters. However the results of these comparisons have not been included within this paper for brevity. Full details of the outcomes of these comparisons have been published separately (Torpiano et al., 2015).

GIS thematic maps indicating the resulting distribution of the seismic vulnerability of the individual buildings under evaluation in the Xemxija and Nadur Test Sites that were determined using the new form together with the legend of the seismic vulnerability ratings have been included in Figure 15.

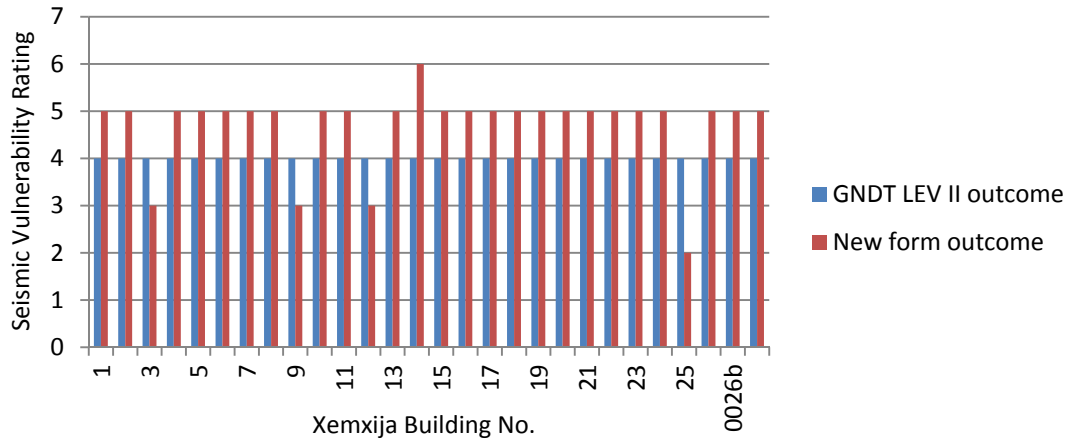

Figure 9: Comparison of the seismic vulnerability ratings obtained for Section 3 of the new form with those obtained from the corresponding GNDT level II parameters for the Xemxija Building Nos. 1-27.

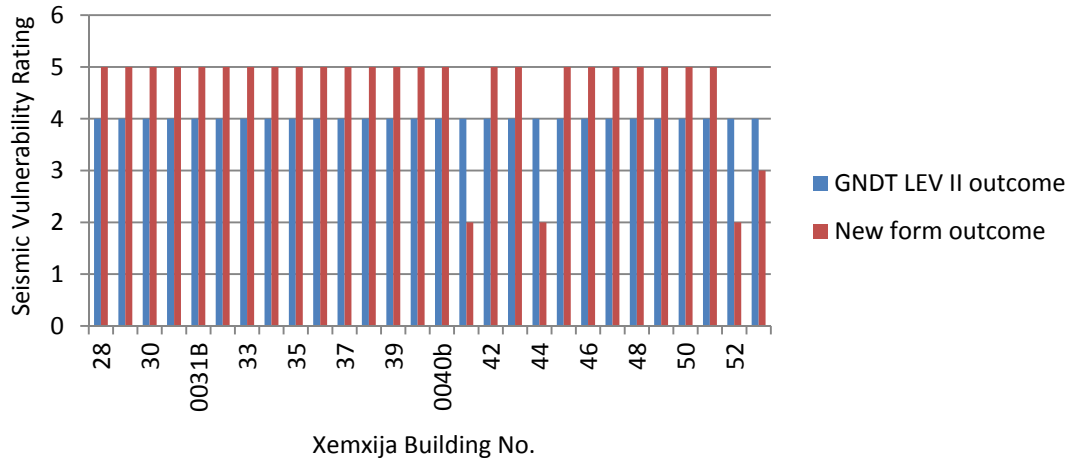

Figure 10: Comparison of the seismic vulnerability ratings obtained for Section 3 of the new form with those obtained from the corresponding GNDT level II parameters for the Xemxija Building Nos. 28-53.

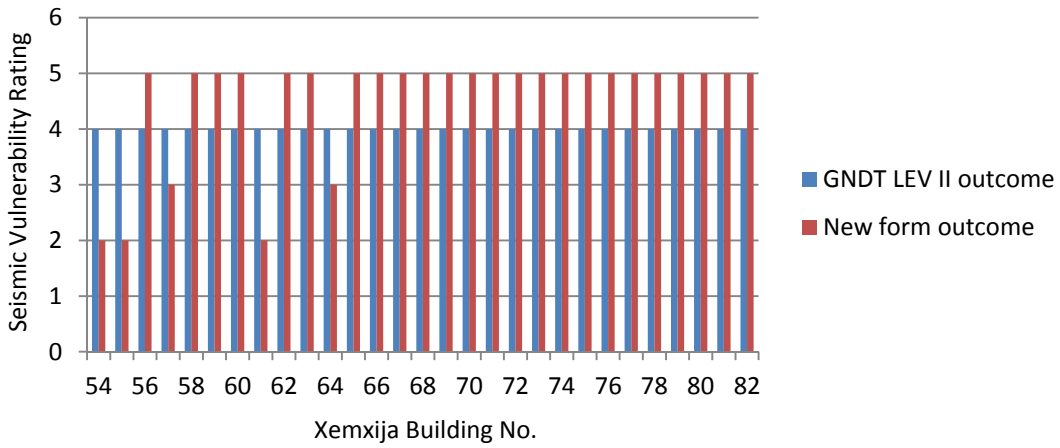

Figure 11: Comparison of the seismic vulnerability ratings obtained for Section 3 of the new form with those obtained from the corresponding GNDT level II parameters for the Xemxija Building Nos. 54-82.

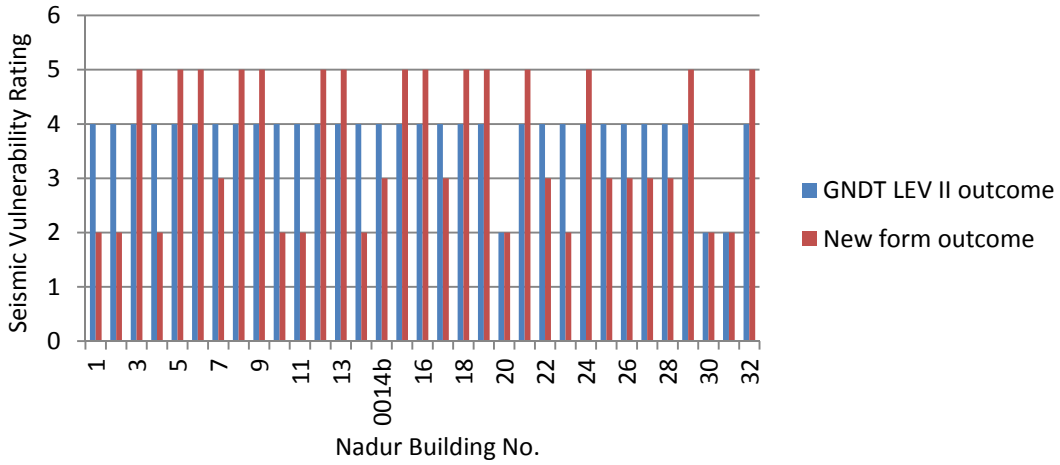

Figure 12: Comparison of the seismic vulnerability ratings obtained for Section 3 of the new form with those obtained from the corresponding GNDT level II parameters for the Nadur Building Nos. 1-32.

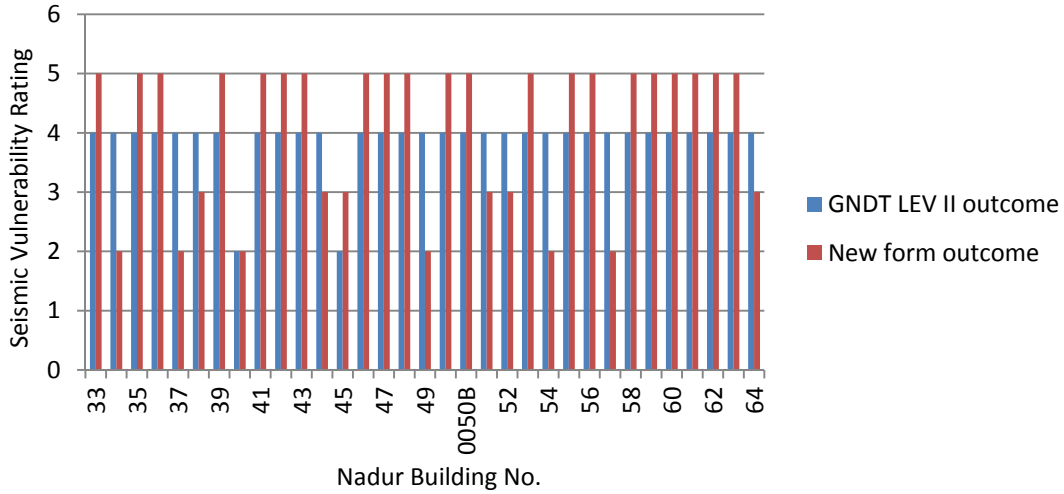

Figure 13: Comparison of the seismic vulnerability ratings obtained for Section 3 of the new form to those obtained from the corresponding GNDT level II parameters for the Nadur Building Nos. 33-64.

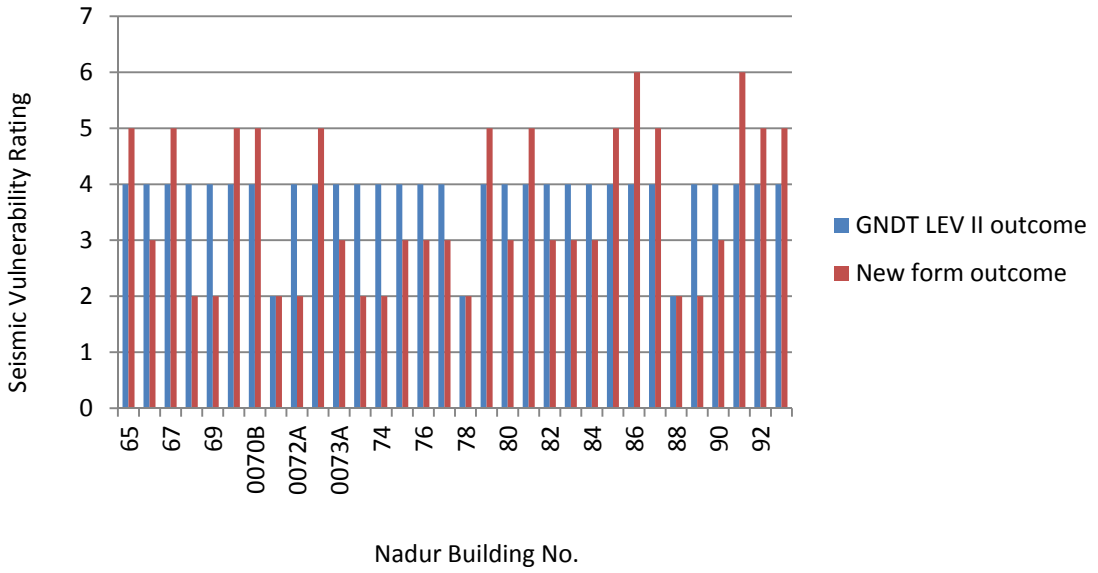

Figure 14: Comparison of the seismic vulnerability ratings obtained for Section 3 of the new form to those obtained from the corresponding GNDT level II parameters for the Nadur Building Nos. 65-93.

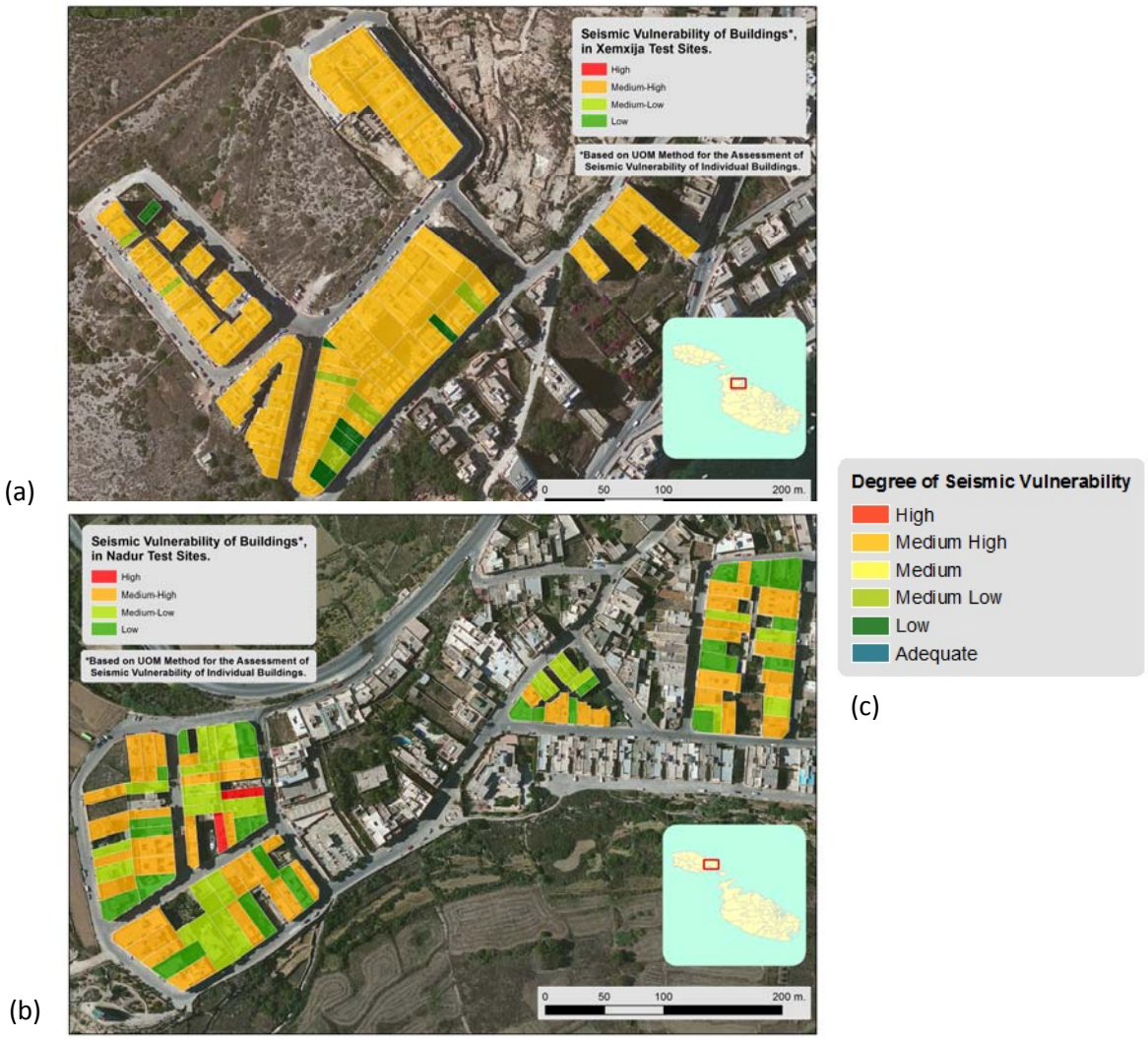

Figure 15: GIS thematic maps of the seismic vulnerability rating obtained using the new form for the 183 buildings under investigation in: (a) Xemxija, and (b) Nadur, together with (c) a legend indicating seismic vulnerability ratings.

3. Conclusions and discussion

The developed seismic vulnerability assessment form for the Maltese Islands is a first attempt in the Maltese scenario at addressing the issue of seismic response of the contemporary building stock. This study involved a very detailed investigation of the seismic vulnerability characteristics present in the contemporary loadbearing unreinforced masonry building typology present throughout the Maltese Islands. The new assessment form was first tested in a pilot study at Msida (Malta) and then it was used for the assessment of 183 buildings in the Xemxija (Malta) and Nadur (Gozo) Test Sites. Such evaluations have not been limited to the information which is readily available from a visual screening exercise of the exterior of the buildings, but it also included the consideration of the seismic vulnerability parameters present in the plan layouts, which were obtained from the Development Permit Drawings, whenever this information was available.

The initial seismic vulnerability ratings proposed for this form were based upon a thorough study of the experience gained in other countries where earthquake damage data of masonry buildings is available as well as the distribution of the relative weightings in the Italian GNDT level II method. A refinement exercise was carried out on these seismic vulnerability ratings through a comparison of the outcome of the new assessment form with that obtained using the GNDT level II method and the FEMA 154 seismic check. The results, which are summarized in Figures 3 to 8, together with a consideration of the main parameters identified in FEMA 154, which have the greatest bearing upon the seismic vulnerability of unreinforced masonry buildings, have suggested the introduction of a 'Medium-Low' and a 'Medium-High' seismic vulnerability rating for Section 3 of the new form developed in this study for the seismic vulnerability assessment of individual buildings in the Maltese Islands. The comparison of these three assessment methods suggests that the seismic vulnerability rating obtained using the new assessment form is more conservative by one to three grades than the FEMA 154 assessment form. However, this does not necessarily mean that the rating of the new assessment form should be altered. In view of the limited number of parameters considered by the FEMA 154 form, a number of seismic vulnerability characteristics which are present in the Maltese scenario are not explicitly taken into consideration in the FEMA 154 seismic check.

This additional degree of conservatism is also evidenced when comparing the seismic vulnerability ratings obtained using the new assessment form for the individual buildings to those obtained using the GNDT Level II assessment form. Whereas there is correspondence between the seismic vulnerability parameters listed in the GNDT Level II assessment and the new assessment form for the individual buildings, the GNDT Level II method does not take into consideration the simultaneous occurrence of characteristics detrimental to the seismic resistance of buildings, such as the occurrence of a soft storey and a double height space and an open plan area, etc. in the same building, which is very common in the local building typology under study.

The present study also included a more detailed comparison of the seismic vulnerability ratings resulting from Sections 2, 3, 4, 5, and 6 of the new assessment form, considered individually, with the corresponding parameters in the GNDT level II method. The seismic vulnerability ratings obtained for Section 4 (Horizontal structural system) and Section 5 (Pre-and post-earthquake condition) of the new

assessment form were in agreement with those of the corresponding GNDT level II parameters. The assessments which were carried out on the Xemxija buildings indicate that this correlation of seismic vulnerability ratings was also obtained for Section 2. However, in the case of the Nadur buildings, the ratings resulting from Section 2 of the new assessment form were lower by two grades compared to those obtained from the GNDT level II evaluation. In the case of Section 3 (Vertical structural system) and Section 6 (Ground conditions), the ratings obtained from the new assessment form for both the Xemxija and Nadur Test Sites were one to two grades higher than those of the corresponding GNDT level II parameters.

The variation in the degree of agreement of the ratings resulting from these two methods could be due to the level of direct correspondence between the sections of the new assessment form and their GNDT level II counterparts. In most cases where correlation between the ratings obtained from both methods was lacking, the GNDT level II Parameters only include one or two of the characteristics recorded in the corresponding section of the new assessment form. Moreover, important characteristics which have been given a major weighting in the ratings of the new assessment form, such as the presence of large openings, double height spaces and the presence of adjacent buildings which are more than one floor lower than the building under assessment, are not taken into account at all in the GNDT level II method.

The discrepancy observed between the degree of correlation obtained in the Xemxija and Nadur building ratings for Section 2 of the new assessment form compared with the corresponding GNDT level II Parameters could be due to the fact that the 'Presence of soft stories' is recorded in Parameter 3 of the GNDT level II method, whereas this characteristic is recorded in Section 3 and not in Section 2 of the new assessment form. In addition, the high weighting attributed to Parameter 3 in the GNDT level II method could have caused the GNDT level II rating (obtained from Parameters 3, 4, and 6) to be higher than the rating of Section 2 of the new assessment form. It is worth noting that, in the case of the Xemxija building assessments, the discrepancy between Section 2 of the new assessment form and the GNDT level II rating was lower than that observed for the Nadur building assessments. This trend may be attributed to the higher number of storeys present in the Xemxija buildings compared to the Nadur buildings. The 'number of storeys' are recorded in both Section 2 of the new assessment form and Parameter 3 of the GNDT level II method, and hence this characteristic could have compensated for the discrepancy in the ratings resulting from the 'Presence of soft stories' in the case of the Xemxija building assessments.

The excellent correlation observed between the seismic vulnerability ratings obtained from Section 4 (Horizontal structural system) and Section 5 (Pre- / Post-earthquake condition of the building) compared with the corresponding GNDT level II ratings could be due to the presence of the same characteristics found in both assessment methods.

The analysis of the comparison of the ratings obtained for the main sections of the new assessment form with the corresponding parameters of the GNDT level II method suggests that the developed seismic vulnerability ratings for the new assessment form have a satisfactory degree of validity. However, further investigations are necessary in order to verify whether the additional degree of

conservatism resulting from the new assessment form is justified for the case of the local building typology under study. The assumptions made in the development of the seismic vulnerability ratings must be verified and the parameters listed in the assessment form need to be calibrated in order to eliminate the need of additional seismic calculations on the assessed buildings and to have a sound scientific background to the resulting ratings. Hence, a statistical analysis of the parameters in the assessment form and the numerical modelling of the local building typology during an earthquake event, which will be carried out following the present study, would be essential for the confirmation or otherwise of the relative weightings attributed to the parameters in the assessment form and for the assessment of the effect of the building aggregate on the behaviour of masonry structures under seismic forces. These additional calibration tools could possibly lead to a curtailment in the number of parameters included in the new assessment form, thereby simplifying the assessment process even further.

4. Acknowledgements

This research study has been carried out under the SIMIT Project (Italia – Malta Operational Programme) (Project Code: B1-2.19/11), Work Package 2.1.

The on-site assessments of the local building stock in the selected aggregates in Xemxija (Malta) and Nadur (Gozo) and the retrieval of the internal layouts of these buildings from the approved planning permits from the Malta Environment and Planning Authority have been carried out with the help of the following Research Support Officers on the SIMIT Project: Godwin Abela, Charlo' Briguglio, Kim Cassar Torreggiani and Yanica Zammit.

Furthermore, the following local entities are being gratefully acknowledged for their contributions to this research study:

- MEPA (Malta Environment and Planning Authority) for allowing access to the approved permit drawings of the buildings in the test sites of Msida and Xemxija (Malta), and Nadur (Gozo);
- MRA (Malta Resources Authority) for allowing access to reports on geological investigations carried out in Xemxija (Malta) and Nadur (Gozo);
- Institute for Climate Change and Sustainable Development - GIS Laboratory (University of Malta) for the elaboration of thematic maps based on the seismic vulnerability assessments carried out and the on-site data collected by the authors and the acknowledged Research Support Officers.

5. References

- Athmani, A. E., Gouasmi, A., Ferreira, T.M., Vicente, R. & Khemis, A. (2015). "Seismic vulnerability assessment of historical masonry buildings located in Annaba city (Algeria) using non ad-hoc data survey", Bulletin of Earthquake Engineering, vol.13, pp. 2283–2307. DOI 10.1007/s10518-014-9717-7.
- Baggio, C., Bernardini, A., Colozza, R., Corazza, L., Della Bella, M., Di Pasquale, G., Dolce, M., Goretti, A., Martinelli, A., Orsini, G., Papa, F. & Zuccaro, G. (2000). "AeDES, Scheda di 1° livello

di rilevamento danno, pronto intervento e agibilità per edifici ordinari nell' emergenza post-sismica", Dipartimento della Protezione Civile. Editrice Italiani nel Mondo srl., Roma.

- Benedetti, D. & Petrini, V. (1984). "Sulla vulnerabilita' sismica di edifici in muratura: Un metodo di valutazione (A method for evaluating the seismic vulnerability of masonry buildings)". L'industria delle costruzioni vol. 149, pp. 66-74.
- Borg R.P., Borg R.C. & Borg Axisa G. (2008), "The seismic risk of buildings in Malta". Editor: F. Mazzolani et al., in: Urban Habitat Constructions under Catastrophic events. European Science Foundation, COST C26, University of Malta, Malta.
- Calvi, G.M., Pinho, R., Magenes, G., Bommer, J.J., Restrepo-Vélez, L.F. & Crowley, H. (2006), "Development of seismic vulnerability assessment methodologies over the past 30 years", ISET Journal of Earthquake Technology, paper no. 472, vol.43, no.3, pp. 75-104.
- CEN (2004), "Eurocode 8: Design of structures for earthquake resistance – Part 1- General rules, seismic actions and rules for buildings".
- Commissione Tecnica per la Microzonazione Sismica (2013), "Analisi della Condizione Limite per l' Emergenza (CLE) dell' insediamento urbano". Version 2.0.
- Di Capua G., Peppoloni S. & Pergalani F. (2001), "Scheda per la valutazione qualitativa dei possibili effetti locali nei siti di ubicazione di edifice strategici e monumentali".
- Farrugia J. (2002), "Seismic Vulnerability of Local Masonry Building Typologies", B.E. & A. Dissertation, University of Malta.
- FEMA (2002), "Rapid visual screening of buildings for potential seismic hazards: A handbook, FEMA 154". Federal Emergency Management Agency, Washington, DC. 2nd Edition.
- FEMA (2005), "Rapid visual screening of buildings for potential seismic hazards: Student Manual, FEMA 154 -SM". Federal Emergency Management Agency, Washington, DC. 2nd Edition.
- Ferrini, M., Decanini, L., Pagliazzi, A. & Scarparolo, S. (2004), "Edifici in muratura in zona sismica. Rilevamento delle carenze strutturali – Manuale per la compilazione della scheda delle carenze. Regione Toscana".
- Ferrini, M., Melozzi, A., Pagliazzi, A. & Scarparolo, S. (2003), "Rilevamento della vulnerabilita' sismica degli edifici in muratura. Manuale per la complilazione della scheda GNDT/CNR di II livello. Versione modificata dalla Regione Toscana".
- Galdes, A. (2012), "Vulnerability of Local Masonry Buildings to Seismic Loading", B.E. & A. Dissertation, University of Malta.
- GNDT/CNR (2007), "Regione Abruzzo: Manuale per il rilevamento della vulnerabilita' sismica degli edifici – Istruzione per la compilazione della scheda di I livello. Appendice n.1 alla pubblicazione "Rischio sismico di edifici pubblici" Parte Ia Aspetti metodologici Del GNDT" - Gruppo Nazionale per la Difesa dai terremoti, 1993 Roma.
- Goretti A. & Di Pasquale G. (2002), "An Overview of Post-Earthquake Damage Assessment in Italy", EERI International Workshop.
- Indirli, M., Kouris, L. A. S., Formisano, A., Borg, R.P. & Mazzolani, F. (2013), "Seismic damage assessment of unreinforced masonry structures after the Abruzzo 2009 earthquake: the case

study of the historical centres of L'Aquila and Castelvecchio Subequo" International Journal of Architectural Heritage, vol. 7, pp. 536-578. Taylor & Francis Group, LLC. DOI: 10.1080/15583058.2011654050.

- Lemme, A., Miozzi, C. & Cifani, G. (2008), "3H-Analisi dei costi di intervento e riduzione della vulnerabilita' sismica degli edifice residenziali. Modello di analisi. Regione Molise". (Estratto da: "Repertorio dei Meccanismi di danno, delle tecniche di intervento e dei relativi costi negli edifici in muratura", Regione Marche, Università degli Studi dell'Aquila e CNR-ITC).
- Torpiano, A., Bonello, M.A., Borg, R. P., Sapiano, P. & Ellul, A.M., (2015), "Methodology for the seismic vulnerability assessment of load–bearing masonry buildings in Malta", Editors: C.Cicero, G.Lombardo, in: Establishment of an integrated Italy–Malta cross–border system of civil protection Engineering aspects, Aracne Editrice S.r.l., Ariccia, Italy.
- Vicente, R., Parodi, S., Lagomarsino, S., Varum, H. & Mendes Silva, J. A. R. (2011). "Seismic vulnerability and risk assessment: case study of historic city centre of Coimbra, Portugal". Bulletin of Earthquake Engineering, vol.9, pp. 1067–1096. DOI 10.1007/s10518-010-9233-3.

iv) Document (iv): Paper prepared for submission to a peer-reviewed journal. This includes the work carried out for this thesis with respect to the statistical analysis of the data collected in the seismic vulnerability assessments of the 183 buildings of the Xemxija (Malta) and Nadur (Gozo) Test Sites through the New Form for the identification of the parameters which are significant predictors of the final seismic vulnerability rating.
Reference: Sapiano P, Camilleri L, Torpiano A, Bonello MA, Borg RP. Statistical sensitivity analysis of the main predictors to be included in a seismic vulnerability assessment method for buildings.
Status: pending submission.

Abstract

This study investigates the building and construction characteristics identified in a total of 183 buildings surveyed in Xemxija, Malta and Nadur, Gozo in order to establish, through statistical analysis, those parameters which have a major bearing on the seismic vulnerability of the contemporary loadbearing masonry building typology present in the Maltese Islands and their order of significance. All surveys have been carried out using a new seismic vulnerability assessment form for individual buildings (hereafter referred to as the 'New Form') which has been developed by the authors (Torpiano et al. 2015, 2016). This form has been based on existing seismic vulnerability assessment methods, pre-earthquake survey methods for the planning of civil protection activities and post-earthquake surveys for the determination of safety for use of buildings which are in use in other countries. The identification of the most significant building characteristics is considered an important step in the verification of the main seismic vulnerability parameters which have been considered in the rating system which was developed by the authors for the New Form and the determination of the building characteristics which will be investigated through numerical modelling in the subsequent phase of this study in order to finally obtain a calibrated survey form with a curtailed list of parameters. Univariate analysis of the 143 parameters considered, followed by multivariate analyses, result in a total of eleven most important predictors with respect to the final seismic vulnerability rating. A comparison of this outcome to the rating system developed for the new seismic vulnerability assessment form is carried out.

Keywords: seismic vulnerability assessment; loadbearing; masonry; predictors; statistical analysis.

1.0 Introduction

The contemporary loadbearing masonry construction typology emerged in the Maltese Islands around 40 years ago following the introduction of precast prestressed concrete planks in the local construction industry which allowed the roofing of larger spans without the need of intermediate points of support (Camilleri 1999) and has, since then, become the most widespread construction typology present in the newer developed urban areas of the islands of Malta and Gozo. It includes, in general, apartment

blocks consisting of a semi-basement level with no internal walls and, in most cases, roofed over by hollow core precast prestressed planks, and around 4 residential floors in addition to a penthouse level. Since no major earthquake has occurred in the Maltese Islands in the last 40-60 years, the seismic resistance of this construction typology and the effect of building characteristics particular to this typology on its seismic resistance cannot be predicted from experience.

The in-depth study of existing first and second level pre- and post- earthquake assessment manuals and their forms which have been developed in Italy in the last 40 years suggested that, in view of the differences in the construction methods and materials together with the particular building characteristics present in the contemporary loadbearing building typology in the Maltese Islands, a new seismic vulnerability assessment form was required. The thorough study of the seismic vulnerability parameters listed in a number of existing methods (Commissione Tecnica per la Microzonazione Sismica 2013; Baggio et al. 2000; Ferrini et al. 2004; Di Capua et al. 2001; CNR –ITC 2007a,b; Ferrini et al. 2003; ATC 2002) and the underlying principles, together with an exhaustive review of the building characteristics which are present in the contemporary loadbearing masonry typology in the Maltese Islands have led to the formulation of a survey form with 147 entries, which has been used in the seismic vulnerability assessment of 183 buildings of this typology. The work presented in this paper forms part of a larger study consisting of three main stages. The development of the New Form and the rating system based on existing literature and results from previous local studies (which work has been published by the authors, Torpiano et al. (2015, 2016)) together with the identification of the most significant parameters affecting the seismic vulnerability of the contemporary loadbearing masonry typology under investigation through statistical analysis are intended to provide the groundwork for the third stage of the study which will consist of the calibration of the main seismic vulnerability parameters through numerical modelling. The results of the latter study will be published separately. Hence, this paper focuses on the statistical analysis of the results obtained from the use of the New Form in the seismic vulnerability assessment of the buildings in the Test sites for the identification of the parameters which have the greatest bearing on the seismic vulnerability outcome, therefore serving as a verification of the main parameters considered in the developed rating system for the New Form. The determination of which characteristics must be considered in a rapid assessment method, the number of characteristics considered and the estimation of the relative bearing which the considered characteristics have on the final seismic vulnerability evaluation, all have a direct consequence on the accuracy of the proposed method and the time and degree of expertise required for the assessment.

The effect which particular building characteristics have on the seismic behaviour of structures has been a widely researched subject in the international scene. Whereas a building typology which is specifically present in a country might exhibit certain characteristics which are the direct consequence of the construction methods and materials and the planning regulations in force in the country, the structural behaviour triggered by the presence of particular seismic vulnerability characteristics on the seismic response of structures is very likely to be observed throughout all building typologies. While the increase in flexibility and mass of a uniform structure resulting from an increase in the number of

storeys can explain the longer fundamental periods and consequent lower seismic resistance of structures consisting of a higher number of storeys, the presence of particular characteristics such as a soft storey in the lowermost floor of the buildings or a double height space can give rise to stress concentrations which exceed the member capacities. Arnold and Reitherman (1982) attribute the earlier failure of reinforced concrete structures where the shear walls do not reach up to the foundations but are stopped above the first floor slab to overstressed members which result due to the discontinuity in load paths. Guevara-Perez (2015) gives a similar explanation for the failure of the walls of the lowermost storey when a soft storey is present at this level. The otherwise gradual distribution of relative displacements throughout the floors of a uniform building is altered if a soft storey is present since the reduced stiffness, and hence the higher flexibility of this level when compared to the rest of the building, results in the attraction of a higher amount of earthquake forces towards the walls of this storey, hence resulting in higher displacements which could lead to collapse. Similarly, the larger displacements reported by Öztürk (2011) in the presence of large voids in reinforced concrete structures without frame continuity can be approximated to the effects caused by the presence of double height spaces.

Furthermore, the effect of the presence of pre-existent damages on the seismic resistance of buildings was investigated by Mucciarelli et al. (2004). The study reported the reduction in the natural frequency of a four-storey building following a magnitude 5.3 earthquake which occurred just one day after the occurrence of another seismic event of similar magnitude. Since the overall mass of the building did not suffer any alterations, the resulting reduction in natural frequency was interpreted by the authors as arising due to the reduction in the stiffness of the building caused by the formation of cracks, hence suggesting that a building which incorporates pre-existent cracks would have a higher seismic vulnerability.

Moreover, the presence of ground formations exhibiting a reduced stiffness have been demonstrated to have a significant bearing on the seismic response of buildings by causing an elongation of the natural period of the buildings in proportion to the relative stiffness of the ground and that of the overlying structures (Trifunac et al. 2001) and in view of the complex interchange of vibrations between the ground and the overlying buildings caused by soil-structure interaction effects (Gueguen et al. 2000, Lou et al. 2011). In this regard, local studies carried out by Farrugia (2002) and Galdes (2012) have reported that isolated contemporary loadbearing masonry buildings would withstand a seismic event with a peak ground acceleration of 0.1g if their overall height does not exceed three floors, if constructed on rock, and two floors, if constructed on clay.

Whereas the current study presented herein proposes the use of statistical tools for the identification of the most relevant building characteristics which can be considered to predict the outcome of a rapid seismic vulnerability assessment for a particular building typology and their respective order of significance in order to assess the validity of the rating system developed by the authors for the New Form, international studies have tackled this issue in a number of alternate ways which do not always make use of more advanced statistical tools. The main seismic vulnerability characteristics identified in these studies, and where available, their order of significance however still present a relevant basis

of comparison to the eleven significant predictors resulting from the present study. A number of studies have focused on the estimation of the seismic vulnerability of urban areas based on the frequency of occurrence of particular seismic vulnerability characteristics. Ahmed et al. (2014) proposed a seismic vulnerability assessment method for the city of Cox's Bazar, Bangladesh, involving an external survey of the buildings. The seismic vulnerability characteristics identified in this study in order of frequency of occurrence were: buildings with heavy overhangs, the absence of a basement, the possibility of pounding due to the close proximity of adjacent buildings, plan irregularities, the presence of a soft storey, the presence of a soft underlying soil, the asymmetric location of the water tanks, the poor quality of construction and the presence of vertical irregularities.

The determination of the relative weightings to be assigned to the various seismic vulnerability parameters considered in a seismic vulnerability assessment is a crucial component in the validity of the method. Benedetti and Petrini (1984), in their proposal of the method which formed the background of the GNDT second level assessment method (Ferrini et al. 2003, CNR-ITC 2007b), identified ten parameters which affect the seismic vulnerability of masonry buildings and attributed different weightings to the separate parameters depending on the different degree of importance which the parameters have with respect to the seismic resistance of buildings. The parameters considered were (a) the 'organisation of the vertical structural system', (b) the 'nature of vertical structural system', (c) the 'location of the building and type of foundation', (d) the 'distribution of load resisting elements on plan', (e) 'plan regularity', (f) the 'regularity of the building throughout its height', (g) 'diaphragms', (h) 'roofing system', (i) 'elements attached to the façade' and (j)'current state'. Three groups of parameters were considered, namely 'elements of primary importance' to which a weighting of 1.5 was attributed (parameter (d)), 'important elements' with a weighting between 0.5 and 1 (parameters (a), (c), (e), (f), (g), (h) and (j))), and 'secondary elements' which were assigned weightings lower than 0.5 (parameters (b) and (i)). The weightings were calibrated using the post-earthquake survey data of a number of earthquakes which had occurred on the Italian peninsula in the recent past at the time of writing of the paper and for which accurate documentation was available in the Italian databases. The subsequently developed GNDT second level assessment method (Ferrini et al. 2003, CNR-ITC 2007b) retained the basic structure of the Benedetti and Petrini method, the parameters and the relative weightings, however, apart from presenting the parameters in a different sequence, included an additional parameter which considered the maximum distance between transverse intersecting walls as an 'important' parameter with a corresponding weighting of 1.0 and considered different criteria in the evaluation of the class distribution for the 'roofing system' and the 'location of the building and type of foundation'. Furthermore, in the GNDT second level assessment method, the class factors and parameter weightings of a number of parameters can vary depending on the detailed characteristics of the respective parameters in the region where the method is applied.

Formisano et al. (2010[a], 2010[b], 2011, 2015) proposed an extension of the Benedetti and Petrini form through the addition of five parameters to include the consideration of the aggregate effect in the estimate of the seismic Vulnerability Index of the assessed buildings. The five parameters included the 'presence of adjacent buildings with different heights', the 'position of the building in the aggregate',

the ‘number of staggered floors’, the ‘effect of structural or typological heterogeneity between adjacent structural units’ and the ‘percentage difference of opening areas between adjacent units’. The scores (A-D) and the weights for every parameter were determined following pushover analyses using 3MURI numerical software in the longitudinal and transverse directions. The scores were defined for every class of every parameter in proportion to the difference between the mechanical vulnerability indexes (IM) obtained in the most unfavourable direction. The overall weightings for every parameter were first defined considering the difference between the values of IM for the various classes, and subsequently weightings were assigned in proportion to the influence which every parameter has on the seismic behaviour of the building.

Furthermore, the different approaches adopted in international studies to carry out sensitivity analyses for the identification of the degree by which uncertainties in the modelling of structures or in the main input parameters have a direct bearing on the structural behaviour are also of particular interest since these methods can also be applied to similar studies as the one presented herein. An example is the study presented by Porter et al. (2002) which included a sensitivity study with respect to the sources of uncertainty which would have the highest bearing on the seismic response of a structure and hence on the costs of its repairs in the eventuality of an earthquake. Three categories of parameters were studied, namely parameters which correspond to the seismic accelerations such as the spectral acceleration; parameters related to the structure, such as its mass, damping, force-deformation behaviour; and parameters which are dependent on the contractor carrying out the repairs, such as the contractor’s costs, overheads and profit margin. The proposed procedure involves the evaluation of the absolute difference in output (‘the swing’) obtained when input variables are defined, one at a time, at their extreme (highest, corresponding to the 90th percentile, and lowest, corresponding to the 10th percentile) values, whereas the rest of the input variables are defined at their best-estimate (median) values. The variables resulting in a higher swing are indicative of a higher level of associated uncertainty. Another study by Celarec et al. (2013) investigated the uncertainties in the modelling parameters on the seismic response of an older reinforced concrete frame and two more recent concrete buildings. The modelling parameters investigated were the concrete and steel strength, the mass of the structure, the effective slab width, the rotation in columns and beams at yield and the ultimate column and beam rotation (in the formation of plastic hinges), whereas the near collapse limit state (corresponding to the seismic response) parameters were the peak ground acceleration, determined through the N2 method, and the top displacement, determined through a pushover analysis. The method proposed by the authors consisted of the study of the variation in the structural response parameter results obtained from the deterministic methods, where all modelling parameters were specified at their best-estimate (median) values, to those obtained when one modelling parameter at a time was set at its 16^{th} or 84^{th} fractile value while all the rest were kept at the median values. As in the case of the study carried out by Porter et al. (2002), the absolute difference in the results obtained for the two input extremes of every modelling parameter is interpreted as a measure of the impact which the parameter has on the seismic response of the structure. The outcome of this sensitivity study resulted in the ranking of the modelling parameters depending on their degree of bearing on the seismic response. In all three structures investigated the

uncertain modelling parameters were demonstrated to effect the seismic response significantly however the parameter to influence most the seismic behaviour of the structures varied from one structure to another since this depended on the collapse mechanism of the structure which in turn was dependent on the design.

A number of studies, have also adopted a statistical approach to carry out sensitivity analyses with the aim of determining seismic vulnerability weightings, the probability of structural failure and the identification of an in-situ investigation protocol prior to the numerical modelling of historic structures. A survey procedure considering eight main characteristics has been proposed by Sucouglu and Yazgan (2003) for the prediction of seismic risk of reinforced concrete buildings. The eight characteristics considered include: the 'number of storeys above ground', the 'presence of a soft storey', the 'presence of heavy overhangs', the 'quality of the building construction', the 'presence of short columns', the 'possibility of pounding', 'local soil conditions' and 'topographic effects'. In addition, the degree of regularity on plan, the redundancy (with respect to the number of spans present in a continuous concrete frame) and the calculation of the lateral strength of the buildings in the form of a 'strength index' are evaluated following an internal inspection of the ground floor and the basement level. The weightings for every parameter in the evaluation of the seismic resistance were determined from the statistical correlation obtained through a multiple linear regression analysis of the characteristics present in a number of damaged buildings out of a total of 477 buildings surveyed following the 1999 Düzce earthquake and the respective parameter variations with increase in number of storeys. The weightings resulting from this study were assigned to the parameters in the following order starting with the highest: the presence of a soft storey, heavy overhangs and quality of construction, which were all attributed the same weightings, followed by the strength index, the redundancy, the presence of short columns, the presence of plan irregularities and topographic effects. Except in the case of the presence of short columns, all other parameters were assigned increasing weightings corresponding to increasing number of storeys.

The statistical analysis of seismic vulnerability characteristics of reinforced concrete buildings was also carried out by Yakut et al. (2004). The study involved the investigation of the correlations, through discriminant analysis using SPSS software, between six building characteristics and the degree of damage observed in 484 surveyed low-to-medium-rise reinforced concrete buildings which were damaged following the same 1999 Düzce earthquake. The six characteristics include the 'number of storeys above ground *(n)*', the 'minimum normalised lateral stiffness index *(mnlstfi)*', the 'minimum normalized lateral strength index *(mnlsi)*', the 'normalised redundancy index *(nrs)*', the 'soft storey index *(ssi)*' and the 'overhang ratio *(or)*'. The survey data obtained for the 484 buildings was used to estimate the unstandardized (raw) discriminant functions based on the six parameters for both the 'Life Safety Performance Classification' (LSPC) and the 'Immediate Occupancy Performance Classification' (IOPC) damage states given in Equations 1 and 2 below respectively. The structure coefficients in the discriminant functions for each damage state give an indication of the weighting which every variable has in the formation of the respective discriminant function.

$$DI_{LSPC}=0.620n-0.246mnlstfi-0.182mnlsi-0.699nrs+3.269ssi+2.728or-4.905 \quad (1)$$

$$DI_{IOPC}=0.808n-0.334mnlstfi-0.107mnlsi-0.687nrs+0.508ssi+3.884or-2.868 \quad (2)$$

Since the number of storeys resulted as being the most significant characteristic, cut-off values were selected according to this parameter through the derivation of a functional relationship between the cut-off values and the number of storeys, therefore resulting in the cut-off functions given in Equations (3) and (4).

$$CF\ (LSPC) = -0.090n^3+1.498n^2-7.518n+11.885 \quad (3)$$

$$CF\ (IOPC) = -0.085n^3+1.416n^2-6.951n+9.979 \quad (4)$$

An indicator variable of '0' or '1' was assigned following the comparison of the damage scores with the cut-off values for both damage states. The evaluation of the rating of the indicator variable for both damage states led to the determination of a 'safe' (corresponding to 'none or slight damage'), 'unsafe' (corresponding to 'severe damage or collapse') or 'intermediate' (meaning that more detailed evaluation was required) building rating.

Lijie et al. (2014) proposed a method based on the probability density function evolution method (PDEM) and the Copula transformation to solve two new probabilistic importance measures (PIMs) which were defined in order to quantify the influence of input variables on the output performance function and the probability of failure of a structure. Cattari et al. (2015) proposed a procedure for the use of sensitivity analysis in the definition of Confidence Factors (CF) with respect to the determination of the required in-situ investigations and surveys for the acquisition of information regarding geometry of structural elements, foundations, material properties, historical data on alterations / past damage…etc. prior to numerical modelling during the seismic vulnerability assessment of cultural heritage buildings in order to avoid unnecessary invasive testing as part of the PERPETUATE Project. The procedure is summarised in flowchart format in Figure 1.

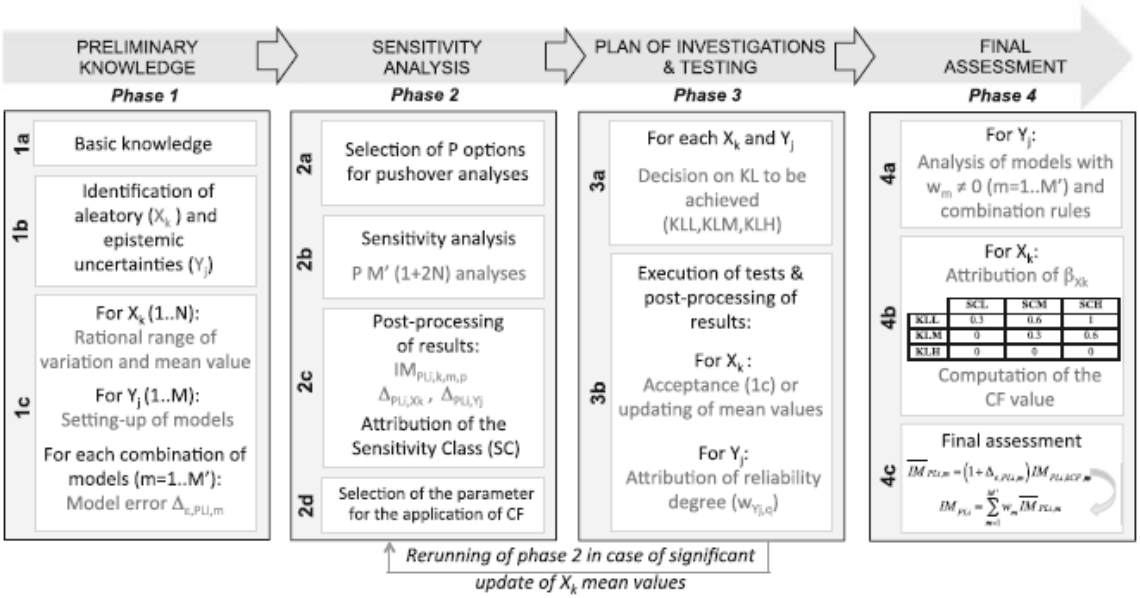

Figure 1: Flowchart for use of sensitivity analysis in the definition of the investigation protocol and Confidence Factor (Cattari et al. 2015).

The method defined a Knowledge Level for every parameter and uses the maximum Intensity measure for every performance level (IMPLi) as the Structural Performance Indicator. The IMPLi is achieved

through the use of mean values for all parameters and the CF takes into consideration the uncertainties and the dispersion in the values. The definition of aleatory and epistemic uncertainties and the minimum and maximum value for every parameter lead to the determination of the 'plausible mean value' and f_k (the ratio of the difference between the minimum and maximum values of the variable to their summation), which is, in turn, used in the definition of the Confidence Factor. The sensitivity analysis used consists of a non-linear static pushover analysis considering various combinations of options (with respect to direction of footprint, load pattern, accidental eccentricity and control node). For a given Performance Level, the resulting maximum and minimum intensity measure of every m-th model and p-th option would be:

$$IM_{PLi,k\text{-min}} = \min(IM_{PLi,k\text{-}low}, IM_{PLi,k\text{-}up}, IM_{PLi,mean}) \quad (5)$$

$$IM_{PLi,k\text{-max}} = \max(IM_{PLi,k\text{-}low}, IM_{PLi,k\text{-}up}, IM_{PLi,mean}) \quad (6)$$

The sensitivity to variables X_k is derived from Equation 7 and the sensitivity class (SC) for each k-th parameter and j-th factor is attributed according to a set of rules. The parameter to which the Confidence Factor is to be assigned is selected from those which fall under the 'high' sensitivity class.

$$\Delta PLi, Xk = 2\,\frac{IMPLi,k-\max - IMPLi,k-min}{IMPLi,k-\max + IMPLi,k-min} \quad (7)$$

Hence, in the planning of the investigation protocol, a different knowledge level associated to its particular sensitivity class is attributed to every parameter.

The studies mentioned above present different techniques which can be used to determine the degree of significance of particular parameters on the building response and which can also be used to determine the relative weightings to be attributed to the respective parameters. The present study proposes alternative statistical techniques to determine the most significant parameters which affect the seismic vulnerability of the contemporary loadbearing masonry building typology, where eleven most significant parameters are identified out of a total of 143 initial parameters following a three-stage analysis which takes into consideration not only the significance of every parameter in isolation when compared to the overall seismic vulnerability rating but also their significance in relation to all the other parameters.

2.0 Seismic vulnerability evaluation of the contemporary loadbearing masonry construction typology

2.1 Seismic vulnerability characteristics

The contemporary loadbearing masonry buildings present in the Maltese Islands mainly consists of loadbearing masonry (local softstone or concrete block) single or double leaf walls with a cavity or bondstones and reinforced concrete cast in-situ or precast slab roofs. Following an in-depth study of the contemporary loadbearing building typology, apart from the soft storey effect, a number of characteristics which could have a negative bearing upon the seismic vulnerability of this building typology have been identified (Figures 2 and 3). Such characteristics include (but are not limited to):

i. narrow and long plan configurations and narrow and high elevation proportions arising from the typical plot proportions for the building typology under study;
ii. open plan spaces without loadbearing cross-walls (very often in more than one storey);
iii. shared or unshared party walls, where the party walls, in general, consist of single leaf 230mm thick unreinforced masonry walls;
iv. long corridors directly abutting party walls;
v. vacant sites, hence giving rise to unrestrained party walls;
vi. misalignment of intermediate slabs, roofs, front and rear facades and internal spaces;
vii. double height spaces;
viii. large openings on facades with very small masonry pilasters constructed between openings;
ix. setbacks due to sloping sites (very often occurring on more than one floor);
x. construction of additional floors due to changes in the regulations limiting the maximum building heights over the years;
xi. projecting rooms and balconies on more than one storey.

a) Double height spaces at lower levels;
b) Adjacent buildings with different heights;
c) Unrestrained party walls – vacant sites;

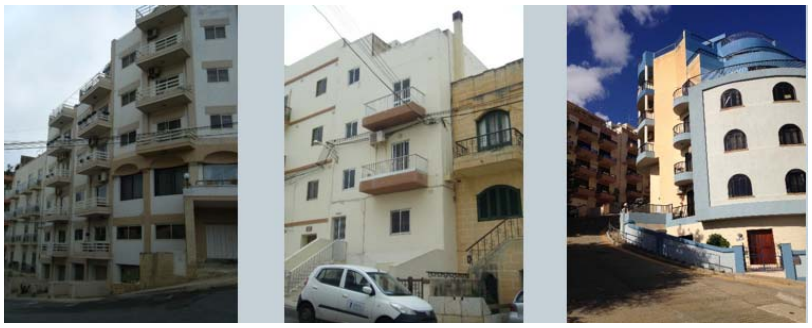

d) Misalignment of slab levels;
e) Misalignment between planes of facade;
f) Setbacks – sloping sites;

g) Projecting rooms;
h) Large areas of openings on facades.

Figure 2: Examples of seismic vulnerability characteristics present in the contemporary loadbearing building typology present in the Maltese Islands (Torpiano et al. 2016).

Figure 3: Examples of seismic vulnerability characteristics identifiable on plan in the contemporary loadbearing building typology present in the Maltese Islands (Malta Environment and Planning Authority Mapserver https://www.mepa.org.mt/mepa-mapserver).

2.2 The new seismic vulnerability assessment form for the individual building

The new seismic vulnerability assessment form developed in the first stage of this study included an initial set of 147 entries covering the seismic vulnerability characteristics present in this building typology in the Maltese Islands. The form is divided into 10 main sections, which include:

1.) general building identification;

2.) general characteristics;

3.) vertical structural system (general and seismic vulnerability characteristics);

4.) horizontal structural system (general and seismic vulnerability characteristics);

5.) pre- and post-earthquake condition of the building;

6.) ground characteristics;

7.) building information and use;

8.) accuracy of assessment;

9.) post-earthquake assessment outcome; and

10.) degree of seismic vulnerability.

The first section of the form records information related to the general identification of the building and the assessment / assessing team. Section 7 includes information regarding the occupancy and use of the buildings which is required for studies of exposure, whereas Section 9 records any suggestions made by the assessor with respect to necessary emergency measures in the case of the use of the form for a post-earthquake assessment. Therefore, only data recorded in Sections 2, 3, 4, 5, 6 and 8 is considered in the determination of the degree of seismic vulnerability which is carried out in Section

10 through the qualitative assessment of the risk levels resulting from the on-site surveys and the study of the internal layouts of the buildings. A brief overview of the building characteristics recorded in the main sections which lead to the determination of the final seismic vulnerability rating is included below:

a) Section 2: the characteristics which are recorded in this section of the New Form include the position of the building under assessment in the building aggregate, whether it includes a specialized structural form, the total number of floors, the average storey height, the presence or otherwise of a front garden, the length of façade, the average floor area, the proportions of the building on plan and along its narrowest elevation and the uniformity / regularity of its plan layout. The subdivision of the aggregates has been based not only on the interruption of the cluster due to presence of vacant sites but also on the sharing or otherwise of the party walls between individual buildings.

b) Sections 3A and 3B: this section includes an overview of the type of vertical structural system including, in the case of a loadbearing masonry structural system, the material and the type of wall construction, together with the vertical seismic vulnerability characteristics particular to the building typology under study. The latter include (a) characteristics which affect the degree of restraint of party walls and the variation in mass throughout the height of the building such as the presence of double height spaces, the difference in level of the topmost slab in adjacent buildings, the difference in the level of intermediate slabs along both party walls, the difference in plane of front and rear facades of adjacent buildings, the presence of vacant sites directly abutting the building, the sharing / unsharing of party walls, the presence of long corridors, garages or other open plan spaces adjacent to one or both party walls, the presence of soft storeys and open plan spaces, the presence of isolated columns and open storeys, the presence of setbacks, projecting rooms and balconies; (b) the degree of box-like behaviour which the building will exhibit and the presence of direct load paths through the main walls up to foundation level such as: the presence of an adequate connection between perpendicular masonry walls and slabs, the presence of large /irregularly-distributed openings on the facades, the evidence of post-construction joining of originally separate individual buildings or post-construction additions in areas which were originally left as voids in the building aggregate; the presence of additional floors or rooms over the original construction and the evidence of a different construction system present in the additional floors / rooms.

c) Sections 4A and 4B: this section reviews the type and materials of the slab construction over semi/basement and in the rest of the building together with horizontal seismic vulnerability characteristics which could affect the degree of even distribution of seismic forces from the slabs onto the walls and the diaphragm action provided by the slabs under such forces. The characteristics considered include the presence of slabs spanning in one direction and not tied to each other or to walls parallel to their span, the occurrence of flexible and semi-rigid slab construction systems throughout the building and the presence of vaults or arches with an inadequate abutment.

d) Sections 5A and 5B: this section records the degree and extent of damages to external walls, internal walls, horizontal loadbearing elements, staircores and non-structural elements. The evidence of foundation failure or differential settlement, the potential damages by the building on the infrastructure for accessibility and connection arising from the collapse of the building onto the access road and the potential damages caused by falling secondary structural/non-structural components attached to projecting rooms / balconies and the potential damage on the building from collapse or falling elements from nearby buildings and the potential damage to the access road are also recorded.

e) Section 6: this section includes information on the ground morphology, the position of the building relative to a steep drop in the landscape, the presence of stepped foundations, the seismic characteristics of the site, the type of instability (if applicable) and the localization of any landslide with respect to the position of the building (if applicable). The topmost and second rock formation layers are also noted.

f) Section 8 – this section records the degree of accuracy on which the assessment was based by recording the extent of exhaustiveness of the building inspection.

The developed rating system for the New Form has been based on the outcome of previous studies carried out by the Faculty for the Built Environment of the University of Malta (Farrugia 2002; Galdes 2012) together with the consideration of the relative weightings which have been attributed to seismic vulnerability characteristics in existing methods (Ferrini et al. 2003, Ferrini et al. 2004, ATC 2002). The parameters which have been identified as having a major bearing on the seismic vulnerability of the individual buildings in the developed rating system for the New Form are listed below whereas the main sources of reference for the development of the rating of every particular section have been indicated next to the respective section number:

i. Section 2 (Farrugia 2002; Galdes 2012):
   - The number of storeys (vs. the type of underlying ground formation – rock or clay);
   - The presence of long and narrow plan layout;
   - The presence of a non-regular plan layout;

ii. Section 3 (ATC 2002):
   - The presence of a soft storey and/or vertical irregularity;
   - The presence of large openings;
   - The presence of double height spaces;
   - The presence of a misalignment between the total number of floors of adjacent buildings such that the individual building under assessment results as being more than 1 floor higher than its adjacent building;

iii. Section 4 (Ferrini et al. 2003, Ferrini et al. 2004):
   - The presence of lightweight (flexible) slab construction systems;
   - The presence of semi-rigid slab construction systems;
   - The presence of an inadequate degree of abutment or a total absence of abutment is identified in the case that masonry arches or vaults;

iv. Section 5 (Ferrini et al. 2003):
    - The presence of minor, medium severity or severe cracks;
v. Section 6 (Farrugia 2002; Galdes 2012):
    - The type of ground present (stable/ gives rise to amplifications of seismic waves / unstable) ;
vi. Section 8:
    - The degree of availability of the internal plans (in full / in part/ not available).

Full details of the development of the form and its rating system together with the studies which have been carried out for the verification of this rating system through comparisons with the GNDT second level assessment method (Ferrini et al. 2003, CNR-ITC 2007b) and FEMA 154 (ATC 2002) have been published by Torpiano et al. (2015, 2016). The final rating for Sections 2, 4, 6 and 8 consists of a 'Low', 'Medium' or 'High' seismic vulnerability rating, whereas that for Section 3 involves a broader range of ratings, namely: 'Low', 'Medium-Low', 'Medium-High' and 'High'. A more refined rating has been developed for Section 3 in view of the consideration that most of the seismic vulnerability parameters identified for the building typology under study fall under this section of the form. The major bearing which this section has on the final overall seismic vulnerability rating of the building has been further emphasised by the provision that the final rating cannot be lower than the rating of this section. The final rating for Section 10, therefore, consists of a 'Low', 'Medium-Low', 'Medium', 'Medium-High' or 'High' seismic vulnerability rating for the building under assessment.

3.0 Statistical analysis

3.1 Methodology and Results

The New Form has been used in the seismic vulnerability assessment of 183 buildings in Xemxija (Malta) and Nadur (Gozo). The assessments have been carried out by a team of 6 assessors. The subjective human element may have somewhat contributed to a degree of variation in the data collected and, perhaps, some of the site surveys would have to be repeated in order to ensure consistent criteria of assessment. However, at the same time, this degree of variation also gives validity to the decision of choosing a statistical tool for the analysis of the data.

IBM SPSS Statistics Version 23 software has been used to carry out the statistical analysis of the data obtained from the seismic vulnerability assessments. The statistical analysis has been carried out in three stages. The first stage included a univariate analysis of the individual parameters in the main sections of the New Form (Sections 2, 3, 4, 5, 6 and 8) for the identification of the variables which are significant predictors of the final rating of their particular section in the New Form. Non-parametric tests were employed since the seismic vulnerability rating scores have an ordinal scale. The Kruskal Wallis Test has been used to compare mean rating scores provided for seismic vulnerability across the levels of a categorical seismic vulnerability parameter. The null hypothesis specifying no difference in the mean seismic vulnerability rating scores across the parameter categories is accepted if the p-value exceeds the 0.05 level of significance. The Spearman Correlation Test has been used to assess the significance of the relationship between seismic vulnerability and a continuous seismic vulnerability

parameter. The null hypothesis specifying no relationship between seismic vulnerability rating scores and a continuous seismic vulnerability parameter is accepted if the p-value exceeds the 0.05 level of significance. For both tests, the alternative hypothesis specifying significant difference/relationship is accepted if the p-value is less than the 0.05 criterion. The results of the univariate analyses of Sections 2, 3, 4, 5, 6 and 8 are summarised in Tables 1 to 6 respectively. Significant results having p-values less than the 0.05 criterion are marked bold. In a few tests, the p-value could not be computed either because seismic vulnerability rating scores were all identical or the seismic parameter had less than two categories.

Table 1: Summary of results for Section 2 of the New Form from univariate analysis.

Entry No. (Section 2 of the New Form)	P-value
(23) Position in block/aggregate	0.694
(24) Specialized structural form	/
(25) Type of specialised structural form	/
(26) Total no. of floors (including below street level)	< **0.001**
(27) Number of floors below street level	< **0.001**
(28) Average storey height	**0.038**
(29) Height of roof above street level (m)	< **0.001**
(30) Presence of front garden	< **0.001**
(31) Length of façade facing infrastructure for accessibility /connection (m)	0.092
(32a) Average area per floor (sq.m)	**0.004**
(32b) Floor area at Level 0	**0.008**
(33) Proportions of building on plan at typical plan level (W: L)	0.228
(34) Plan regularity	< **0.001**
(35) Uniformity of plan in layout & room sizes	**0.007**
(36) Proportions of building along narrowest elevation (H:W)	< **0.001**

Table 2 (Part 1): Summary of results for Section 3 of the New Form from univariate analysis.

Entry No. (Section 3 A&B of the New Form)	P-value
(37) Main loadbearing vertical structural system	0.446
(38) Type of masonry wall construction	0.506
(39) Tie beams /reinforcing ties in wall	0.477
(40) Confirmation by owners that strengthening measures with respect to the seismic response of the building have been effected	/
(41) Main type of masonry on Façade 1	0.063
(42) Wall construction along Façade 1	**0.004**
(43) Main type of masonry on Façade 2	0.074
(44) Wall construction along Façade 2	0.822
(45) Main type of masonry on Façade 3	0.243
(46) Wall construction along Façade 3	0.241
(47) Main type of masonry on Façade 4	0.460

Table 2 (Part 2): Summary of results for Section 3 of the New Form from univariate analysis.

Entry No. (Section 3 A&B of the New Form)	P-value
(48) Wall construction along Façade 4	0.538
(49) Main type of masonry on left hand side party wall	0.052
(50) Wall construction along left hand side party wall	0.246
(51) Main type of masonry on right hand side party wall	0.050
(52) Wall construction along right hand side party wall	0.198
(53) Presence of double height spaces	0.061
(54) Presence of double height spaces facing infrastructure for accessibility / connection	**0.023**
(55a) Presence of difference in level of topmost slab in adjacent building along left hand side party wall	**0.036**
(55b) Presence of difference in level of topmost slab in adjacent building along right hand side party wall	0.262
(56a) Presence of difference in level of floor slab at Level +2 in adjacent building along left hand side party wall	**0.005**
(56b) Presence of difference in level of floor slab at Level +2 in adjacent building along right hand side party wall	**0.023**
(57a) Presence of difference in plane of walls of front facade of adjacent building on left hand side of building being assessed	0.185
(57b) Presence of difference in plane of walls of front facade of adjacent building on right hand side of building being assessed	0.737
(58a) Presence of difference in plane of walls of rear facade of adjacent building on left hand side of building being assessed	0.065
(58b) Presence of difference in plane of walls of rear facade of adjacent building on right hand side of building being assessed	0.975
(59) Presence of difference in plane along front façade of building being assessed	**0.002**
(60) Presence of difference in plane along rear façade of building being assessed	0.730
(61) Vacant site directly adjacent to building	0.699
(62) Evidence of shared party wall	0.246
(63) Presence of long corridor/garage/other open plan space directly adjacent to party wall	< **0.001**
(64) Misalignment of the internal spaces of abutting properties	0.771
(65) Absence of intermediate walls in loadbearing masonry building in 1 or more storeys	< **0.001**
(66) Storey level at which no intermediate walls are present	< **0.001**
(67) Presence of open plan spaces without internal loadbearing walls over part of floor area	< **0.001**
(68) Average percentage area of open plan space to total area of floor	< **0.001**
(69) Storey level at which open plan spaces without internal loadbearing walls over part of floor area are present	0.145
(70) Maximum ratio of Area of discontinuous loadbearing walls (Adisc) to Area of continuous loadbearing walls (Acont) in building	< **0.001**
(71) Presence of inadequate or completely absent connection between perpendicular masonry walls	/
(72) Evidence of inadequate or completely absent connection between loadbearing walls and slabs in whole building	0.511

Table 2 (Part 3): Summary of results for Section 3 of the New Form from univariate analysis.

Entry No. (Section 3 A&B of the New Form)	P-value
(73) Presence of large openings on Main Façade 1	0.503
(74) Presence of large openings on Main Façade 2	0.366
(75) Presence of large openings on Main Façade 3	**0.028**
(76) Presence of large openings on Main Façade 4	**0.045**
(77) Irregular distribution or size of openings for windows/doors etc on façade.	**0.023**
(78a) Presence of setbacks along Main Façade 1	< **0.001**
(78b) Presence of setbacks along Main Façade 1 at 1 level	0.069
(78c) Presence of setbacks along Main Façade 1 at 2 or 3 levels	0.501
(78d) Presence of setbacks along Main Façade 1 at 4 or 5 levels	/
(78e) Presence of setbacks along Main Façade 1 at more than 5 levels	0.511
(78f) Presence of setbacks along Main Façade 1 at penthouse level	< **0.001**
(79a) Presence of setbacks along Main Façade 2	0.375
(79b) Presence of setbacks along Main Façade 2 at 1 level	0.801
(79c) Presence of setbacks along Main Façade 2 at 2 or 3 levels	0.511
(79d) Presence of setbacks along Main Façade 2 at 4 or 5 levels	/
(79e) Presence of setbacks along Main Façade 2 at more than 5 levels	/
(79f) Presence of setbacks along Main Façade 2 at penthouse level	0.228
(80a) Presence of setbacks along Main Façade 3	<**0.001**
(80b) Presence of setbacks along Main Façade 3 at 1 level	**0.036**
(80c) Presence of setbacks along Main Façade 3 at 2 or 3 levels	0.329
(80d) Presence of setbacks along Main Façade 3 at 4 or 5 levels	0.252
(80e) Presence of setbacks along Main Façade 3 at more than 5 levels	/
(80f) Presence of setbacks along Main Façade 3 at penthouse level	**0.004**
(81a) Presence of setbacks along Main Façade 4	0.082
(81b) Presence of setbacks along Main Façade 4 at 1 level	0.251
(81c) Presence of setbacks along Main Façade 4 at 2 or 3 levels	0.252
(81d) Presence of setbacks along Main Façade 4 at 4 or 5 levels	/
(81e) Presence of setbacks along Main Façade 4 at more than 5 levels	/
(81f) Presence of setbacks along Main Façade 4 at penthouse level	0.204
(82a) Presence of projecting rooms / balconies	0.062
(82b) Presence of projecting rooms / balconies at 1 level	0.235
(82c) Presence of projecting rooms / balconies at 2 or 3 levels	**0.049**
(82d) Presence of projecting rooms / balconies at 4 or 5 levels	**0.001**
(82e) Presence of projecting rooms / balconies at more than 5 levels	0.252
(83) Presence of masonry walls as infill panels in frame structure	0.720
(84) Position of masonry walls relative to frame	0.053
(85) Presence of isolated columns (not effectively-tied to slab/beams)	**0.030**
(86) Open storey with just columns - no loadbearing/infill walls	0.684

Table 2 (Part 4): Summary of results for Section 3 of the New Form from univariate analysis.

Entry No. (Section 3 A&B of the New Form)	P-value
(87) Evidence of post-construction joining of originally-separate individual buildings or post-construction additions in areas which were originally left as voids in building aggregate	0.161
(88a) Additional floors/ rooms over original construction	**0.001**
(88b) Number of additional floors from original building permit	**0.001**
(89) Evidence of different construction system / materials for additional floors/rooms	**0.046**

Table 3: Summary of results for Section 4 of the New Form from univariate analysis.

Entry No. (Section 4 A&B of the New Form)	P-value
(90) Type of slab construction over semi/basement	0.564
(91) Type of slab construction in other storeys	0.972
(92) Presence of slabs spanning in one direction and not tied to each other / to walls parallel to their span	< **0.001**
(93) Presence of flexible slab construction systems in floors of whole building	0.812
(94) Presence of flexible slab construction systems at floor level with maximum occurrence	0.812
(95) Presence of semi-rigid slab construction systems in floors of whole building	/
(96a) Presence of semi-rigid slab construction systems at floor level with maximum occurrence	/
(97) Presence of vaults or arches	/
(98) Absence of or inadequate degree of abutment for arches or vaults	/

Table 4: Summary of results for Section 5 of the New Form from univariate analysis.

Entry No. (Section 5 of the New Form)	P-value
(99a) Visible structural damage to external walls: Degree	< **0.001**
(99b) Visible structural damage to external walls: Extent	< **0.001**
(100a) Visible structural damage to internal walls: Degree	< **0.001**
(100b) Visible structural damage to internal walls: Extent	< **0.001**
(101a) Visible structural damage to horizontal loadbearing elements (slabs/beams): Degree	< **0.001**
(101b) Visible structural damage to horizontal loadbearing elements (slabs/beams): Extent	< **0.001**
(102a) Visible structural damage to staircores: Degree	< **0.001**
(102b) Visible structural damage to staircores: Extent	< **0.001**
(103) Degree of maintenance	< **0.001**
(104) Damages to non-structural elements: Detachment of external render/pointing	< **0.001**
(105) Damages to non-structural elements: Damages to parapet walls	0.089
(106) Damages to non-structural elements: Damages to internal plaster/false ceilings	< **0.001**
(107) Evidence of failure of foundations / differential settlement	< **0.001**
(108) Potential damage by building on infrastructure for accessibility / connection (arising from height of building> road width)	0.290
(109) Potential damage by building on infrastructure for accessibility/connection (from falling secondary structural/non-structural components attached to projecting rooms balconies)	**0.043**
(110) Potential damage on building: From collapse/falling elements from nearby buildings	0.361
(111) Potential damage on building: From damage to access road	**0.004**

Table 5: Summary of results for Section 6 of the New Form from univariate analysis.

Entry No. (Section 6 of the New Form)	P-value
(127a) Ground morphology	**0.008**
(127b) Height of abrupt drop (m)	0.080
(128) Stepping of foundation levels due to sloping ground	0.128
(129) Location with respect to steep drop in landscape	**0.026**
(130) Microseismic rating of area	1.000
(131) Type of instability	1.000
(132) Topmost formation layer	< **0.001**
(133) Thickness of topmost formation layer	**0.046**
(134) Second formation layer	< **0.001**

Table 6: Summary of results for Section 8 of the New Form from univariate analysis.

Entry No. (Section 8 of New Form)	P-value
(144) Degree of accuracy of assessment	/
(9) Availability of plans (from Section 1)	< **0.001**

It is worth noting that the major limitation of the Kruskal Wallis and Spearman Correlation tests is that they investigate solely the relationship between seismic vulnerability and one seismic parameter. However, the goal of many research studies is to estimate collectively the quantitative effect of all the seismic parameters impacting the seismic vulnerability rating scores. It is well known that, in the presence of collinearity, a lone seismic parameter could be rendered a very important contributor in explaining variations in the seismic vulnerability rating scores, but would be rendered unimportant in the presence of other predictors. On the other hand, an insignificant predictor could be rendered important in a particular combination of predictors. The multivariate analysis carried out in the second stage of this study resolved this problem by conducting Ordinal Logistic regression analysis. Besides being the appropriate model to analyse ordinally-scaled seismic vulnerability rating scores, this model analyses all seismic parameters collectively, identifies the significant ones and ranks them by their contribution in explaining variation in the seismic vulnerability rating scores. By using a backward elimination procedure, the weaker parameters were removed in turn until the parsimonious model included solely significant parameters. An Ordinal Logistic model was then fitted for each section considering only those entries which were identified as significant predictors in the univariate analysis. Table 7 displays the results of this multivariate analysis for each section of the New Form separately.

Table 7: Multivariate analysis using Ordinal Logistic Regression Analysis for each section of the New Form.

Section No.	Description	P-value
Section 2	(26) Total no. of floors (including below street level)	< **0.001**
	(29) Height of roof above street level (m)	**0.013**
	(34) Plan regularity (overall shape, symmetry of layout, central position of stairwell)	**0.013**
Section 3	(51) Main type of masonry on right hand side party wall	**0.002**
	(54) Presence of double height spaces facing infrastructure for accessibility/ connection	< **0.001**
	(55a) Difference in level of topmost slab in adjacent building along left hand side party wall (in m)	**0.009**
	(61) Vacant site directly adjacent to building	< **0.001**
	(62) Evidence of shared party wall	**0.010**
	(63) Presence of long corridor/garage/other open plan space directly adjacent to party wall	**0.040**
	(67) Presence of open plan spaces without internal loadbearing walls over part of floor area	**0.024**
	(70) Maximum ratio of Area of discontinuous loadbearing walls (Adisc) to Area of continuous loadbearing walls (Acont) in building	< **0.001**
	(75) Presence of large openings on Main Façade 3	**0.011**
	(76) Presence of large openings on Main Façade 4	< **0.001**
	(80b) Presence of setbacks along Main Façade 3 at 1 level	**0.007**
	(82c) Presence of projecting rooms / balconies at 2 or 3 levels	**0.006**
	(82d) Presence of projecting rooms / balconies (at 4 or 5 levels)	**0.001**
	(85) Presence of isolated columns (not effectively tied to slab/beams)	**0.003**
	(88b) Number of additional floors from original building permit	**0.003**
Section 4	(92) Presence of slabs spanning in one direction and not tied to each other / to walls parallel to their span	**0.003**
Section 5	(99a) Pre-earthquake: Visible structural damage to external walls: Degree	< **0.001**
	(103) Degree of maintenance	**0.005**
Section 6	N/A	/
Section 8	(9) Availability of plans	< **0.001**

Finally, in the third stage of this study, all the significant predictors resulting from the multivariate analysis of every section of the New Form were refitted in a final Ordinal Logistic model using the overall seismic vulnerability rating scores as the dependent variable. The merit of this model is that the significant predictors can be ranked by their contribution in explaining variations in the overall seismic vulnerability rating scores. The predictor (seismic parameter) with the lowest p-value is the most significant one. Table 8 summarizes the significant predictors resulting from this multivariate analysis and lists these predictors in order of importance.

Table 8: Multivariate analysis using Ordinal Logistic Regression Analysis for all sections of the New Form in combination.

Rank	Description	Section No.	P-value
1	(26) Total number of floors (including below street level)	Section 2	< **0.001**
2	(76) Presence of large openings on Main Façade 4	Section 3	< **0.001**
3	(92) Presence of slabs spanning in one direction and not tied to each other / to walls parallel to their span	Section 4	**0.001**
4	(65) Absence of intermediate walls in loadbearing masonry building in 1 or more storeys	Section 3	**0.002**
5	(54) Presence of double height spaces facing infrastructure for accessibility / connection	Section 3	**0.002**
6	(63) Presence of long corridor/garage/other open plan space directly adjacent to party wall	Section 3	**0.004**
7	(62) Evidence of shared party wall	Section 3	**0.019**
8	(80b) Presence of setbacks along Main Façade 3 at 1 level	Section 3	**0.031**
9	(82c) Presence of projecting rooms / balconies at 2 or 3 levels	Section 3	**0.033**
10	(33) Proportions of building on plan at typical plan level (W: L)	Section 2	**0.035**
11	(61) Vacant site directly adjacent to building	Section 3	**0.039**

3.2 Discussion and Conclusions

To identify the most significant predictors for every section of the New Form, an Ordinal Logistic Regression model was fitted for each section to relate the rating scores provided for a particular section with all corresponding predictors. This multivariate analysis identifies significant predictors of the overall rating scores corresponding to Sections 2, 3, 4, 5, 6 and 8.

The second stage multivariate analysis for Section 2 (General characteristics) of the New Form identified three main predictors in the following order of importance with respect to the final rating of this section, namely, the total number of floors (entry 26) , the plan regularity (entry 34) and the height of roof above street level (entry 29). The main parameters for this section in the developed rating system for the New Form consist of the number of floors considered in conjunction with the type of underlying ground formation, and the presence of a long and narrow plan configuration and an irregular plan layout. Since the seismic vulnerability effect of entry 29 is covered by entry 26, almost complete correlation between the two methods can be concluded in the case of Section 2. Entry 33 (Proportions of building on plan at typical plan level, W: L) has, however, still been included in the third stage multivariate analysis as a verification of the developed rating system for the New Form.

The univariate analysis of the parameters in Section 3 (Vertical structural system) resulted in a number of borderline cases (with p-values ranging between 0.05 and 0.10). This suggests that the mean rating score for seismic vulnerability varies considerably between the levels of these seismic predictors. However, the difference is not significant at the 0.05 level of significance. A number of these

characteristics had been identified in other research literature as having a major bearing in the seismic vulnerability of buildings and hence these parameters had been included as main indicators in the developed rating system for the New Form. Undoubtedly, the p-value is affected by the sample size. By increasing the sample size, it is more likely to identify significant predictors, particularly borderline cases. Moreover, the univariate analysis results might have been affected by a number of factors, such as the lack of information on the internal layouts due to the number of cases where either only part of the Development Permit Drawings had been traced, or where none of the plans had been found, and the limited presence of certain characteristics in the test sites. The resulting 'bias' in the outcome had to be corrected in order to ensure that the New Form could be applied to the contemporary loadbearing building typology in all localities of the Maltese Islands. An overview of the borderline cases and of other entries consisting of parameters which have been identified in literature as having a substantial bearing on the seismic vulnerability of buildings has therefore been carried out. This discrepancy has been identified in the following entries:

a) Entry 53 (p-value 0.061) - Presence of double height spaces: It is to be noted that, whereas this entry has not been identified as a significant predictor through univariate analysis, entry 54 (Presence of double height spaces facing infrastructure for accessibility and connection) has resulted as a significant predictor. Following the consideration of the minimal difference between the number of cases which have a double height space and those where the double height space faces the road together with the high vulnerability associated with this characteristic in the developed rating system, this parameter has not been included in the second stage multivariate analysis in addition to entry 54 as the close correlation of the two entries could lead to multi-collinearity problems and the model fit would not produce robust parameter estimates.
b) Entry 58a (p-value 0.065) Presence of difference in plane of walls of rear façade of adjacent building on left hand side of building being assessed: This parameter indicates the presence of a reduced restraint to party walls and hence, has been included in the multivariate analysis of Section 3 in view of its potential bearing on the seismic vulnerability of buildings.
c) Entry 78b (p-value 0.069) Presence of setbacks along Main Façade 1 at 1 level: This parameter indicates a vertical irregularity and the presence of vertical irregularities has been identified as a main seismic vulnerability characteristic in the developed rating system. However since entries 78a (Presence of setbacks on Main Façade 1) and 78f (Presence of setbacks on Main Façade 1 at penthouse level) have resulted as significant predictors of the final seismic vulnerability rating for Section 3 from univariate analysis, it was not considered necessary to include even entry 78b in the multivariate analysis of this section.
d) Entry 81a (p-value 0.082) Presence of setbacks on Main Façade 4: In the loadbearing masonry terraced building typology which has been investigated in this study, setbacks typically occur along façade 1 and 3 (the façade facing the street and the rear façade respectively). Setbacks along facades 2 and 4 are not typical and only occur in cases of corner sites or when only half the site is constructed at the topmost floor level. Entries 78a (Presence of setbacks along Main Façade 1 – general), 78f (Presence of setbacks along main façade 1 at penthouse level), 80a

(general presence of setbacks along Main Façade 3), 80b (Presence of setbacks along Main Façade 3 at 1 level) and 80f (Presence of setbacks along main façade 3 at penthouse level) have been identified as significant predictors of the final rating for Section 3 from the univariate analysis of this section. Hence, the consideration of entry 81a in addition to these parameters in the multivariate analysis of Section 3 has therefore not been considered as necessary.

e) Entry 82a (p-value 0.062) Presence of balcony or projecting room: Even this parameter indicates the presence of a vertical irregularity however since the entries identifying the presence of projecting rooms at 2 or 3 levels (entry 82c) and at 4 or 5 levels (entry 82d) have resulted as significant predictors from the univariate analysis, this entry has not been included in the second stage multivariate analysis for Section 3 as its inclusion could cause collinearity problems as explained in the case of entry 53 in (a) above in view of its close correlation with entries 82c and 82d.

Apart from the above, entries 41 (Main type of masonry on façade 1), 43 (Main type of masonry on façade 2), 49 (Main type of masonry on left hand side party wall) and 84 (Position of masonry walls relative to frame) also resulted in borderline p-values (0.063, 0.074, 0.052 and 0.053 respectively). These entries, however, have not been included in the second stage multivariate analysis because, in the case of entries 41 and 43, none of the entries recording the type of masonry walls on the four building facades have been identified as significant predictors of the final rating, whereas with respect to entry 49, the corresponding entry identifying the main type of masonry on the right hand side party wall (entry 51) had resulted as a significant predictor of the final rating of Section 3 from the univariate analysis of the parameters of this section. In the case of entry 84, the frame structure with infill masonry walls is not typical of the contemporary loadbearing masonry building typology under study. On the other hand, entries 61 (Presence of vacant site) and 62 (Presence of shared party walls) have been included in the second stage multivariate analysis in view of the negative effect of these characteristics on the seismic vulnerability of buildings due to their influence on the degree of restraint of party walls.

The parsimonious model resulting from the second stage multivariate analysis of Section 3 of the New Form is moderately well-related with the characteristics which have been identified as main seismic vulnerability parameters in the developed seismic vulnerability rating for this section. The fifteen parameters which have been identified as significant predictors of the final rating from the statistical analysis consist of, in order of importance,

- the presence of large openings on Main Façade 4 (entry 76),
- the presence of a vacant site directly adjacent to the building (entry 61),
- the presence of double height spaces facing infrastructure for accessibility / connection (entry 54),
- the maximum ratio of the area of discontinuous loadbearing walls (A_{disc}) to the area of continuous loadbearing walls (A_{cont}) in the building (entry 70),
- the presence of projecting rooms or balconies at 4 or 5 levels (entry 82d),

- the main type of masonry in which the right hand side party wall is constructed (entry 51),
- the number of additional floors constructed from the original building permit (entry 88b),
- the presence of isolated columns which are not effectively tied to slabs or beams (entry 85),
- the presence of projecting rooms or balconies at 2 or 3 levels (entry 82c),
- the presence of setbacks along Main Façade 3 at 1 level (entry 80b),
- the presence of a difference in the level of the topmost slab in the adjacent building along the left hand side party wall (entry 55a),
- the presence of large openings on Main Façade 3 (entry 75),
- the presence of open plan spaces without internal loadbearing walls over part of the floor area (entry 67) and
- the presence of a long corridor, garage or other open plan space directly adjacent to a party wall (entry 63).

The presence of a soft storey and/ or other form of vertical irregularity has been associated with a high seismic vulnerability in the developed rating system. This characteristic is directly linked with entries 63, 67, 70, 80b, 82c, 82d and 85. In addition, with respect to the remaining three main seismic vulnerability characteristics identified in the developed rating system, the presence of double height spaces is associated with entry 54, entries 75 and 76 identify the presence of large openings, whereas the difference in height with respect to adjacent buildings is linked to entries 55a and 61, since the presence of a vacant site can be considered an extreme case of misalignment between roof slabs of adjacent buildings. In view of the widespread occurrence of soft storeys in the loadbearing masonry building typology under study and based on available literature, this parameter has been identified as one of the main parameters affecting the seismic vulnerability of masonry buildings in the developed rating system for the New Form. Hence in order to verify this rating system, entry 65 (Absence of intermediate walls in loadbearing masonry building in 1 or more storeys) has been included in the third stage multivariate analysis even though it didn't result as a significant predictor of the final rating of Section 3 from the second stage multivariate analysis.

The univariate analysis of Section 4 (Horizontal structural system) of the New Form identified only entry 92 (Presence of slabs spanning in one direction and not tied to each other/to walls parallel to their span) as a significant predictor of the seismic vulnerability rating for the horizontal structural system. Since the main parameters considered to have a bearing on the seismic vulnerability of this section in the developed rating system included the presence of flexible or semi-rigid slab construction systems and the presence of an inadequate abutment or the absence of an abutment in the case of vaults or arches, entries 90, 91, 93 and 94 have still been included in the second stage multivariate analysis. This second stage analysis however, re-confirmed entry 92 as the sole significant predictor of the final rating scores for Section 4 in the parsimonious model. The developed rating system for this section of the form did not consider the tying action between slabs and between slabs and walls because the roofing structures in the construction typology under study generally include cast in-situ concrete slabs or precast slabs which, in most cases, have a cast in-situ concrete topping. Hence, slabs

spanning in one direction and not tied to each other or to walls parallel to their span are not generally present if adequate detailing has been carried out (which, however, cannot be verified without more intrusive testing and, hence, it has been assumed as present). On the other hand, the presence of lightweight (flexible) or semi-rigid roofing structures or the presence of an inadequate or the complete absence of an abutment in the case of vaults or arches could be present and would have a negative effect on the seismic resistance of the horizontal structural system (Section 4). Since none of the buildings in the Test Sites exhibited any of these characteristics, the importance of these parameters with respect to the final rating scores of this section could not be identified through the statistical check. Entries 93 (Percentage occurrence of flexible slab construction systems in floors of whole building) and 96a (Presence of semi-rigid slab construction systems at the floor level with maximum occurrence) have, therefore, been included in the third stage multivariate analysis.

The parsimonious model obtained from the second stage multivariate analysis of Section 5 (Pre- and post-earthquake condition of building) of the New Form identified two significant predictors of the seismic vulnerability rating for this section, namely, entry 99a (Visible structural damage to external walls) and entry 103 (Degree of maintenance). This result is in agreement with the parameters which have been considered to have the highest effect on the seismic vulnerability of the building in the rating system developed by the Faculty for the Built Environment at the University of Malta, where the degree of damages (in the form of cracks) has been considered as the main indicator of seismic vulnerability for this section. Since an internal inspection of the buildings could not be carried out, only the damages on the exterior envelope could be ascertained. The degree of damages present on the exterior envelope has been assumed to be similar to the damages present in the other structural elements inside the buildings.

The univariate analysis of the parameters included under Section 6 (Ground characteristics) of the New Form discarded entries 127b (Height of abrupt drop (m)), 128 (Stepping of foundation levels due to sloping ground), 130 (Microseismic rating of area) and 131 (Type of instability) from the list of significant predictors of the final rating for this section. However, no significant predictor of the final rating scores for Section 6 resulted from the second stage multivariate analysis of this section therefore no parsimonious model was found. Following reference to the results obtained in previous studies which had been carried out at the University of Malta (Farrugia 2002; Galdes 2012), the rating system developed for the New Form considered the type of underlying rock formations, and hence, the resulting ground stability, as the main parameters which affect the seismic vulnerability rating of this section. Therefore, entry 134 (Second formation layer) has still been included in the third stage multivariate analysis with respect to the overall final rating of the New Form.

In the case of Section 8 (Accuracy of assessment) of the New Form, since only an external inspection of the buildings in the Test sites could be carried out and information regarding the internal layouts could only be obtained from Development Permit Drawings, when these were available, entry 9 (Availability of plans) has been included in the statistical check of this section even though this entry falls under Section 1 of the New Form. Entry 9 has been considered as the main parameter which affects the seismic vulnerability rating for Section 8 in the developed rating system of the New Form

for the case when internal inspections are not possible. This result was confirmed by the univariate analysis and re-confirmed in the second stage multivariate analysis for this section. This result is in agreement with the rating system developed for this section of the form. The statistical check in the case of entry 144 (Degree of accuracy of assessment) could not be carried out since all the buildings in the Test Sites had the same result as only an external inspection of the buildings was possible.

The third stage multivariate analysis of all the significant predictors identified from the multivariate analyses of all the separate sections of the New Form with respect to their seismic vulnerability rating (including a number of additional parameters which have been considered as important seismic vulnerability characteristics in the developed rating system) with respect to the overall seismic vulnerability rating of the New Form resulting from Section 10 resulted in a parsimonious model consisting of eleven significant predictors in the order of importance as listed in Table 8. The most significant predictors for Sections 2 and 3 resulting from this third stage of the statistical analysis can be concluded to be overall in agreement with the developed rating system for the New Form. These include entries 26 (Total number of floors), 76 (Presence of large openings on Main Façade 4), 65 (Absence of intermediate walls in loadbearing masonry building in 1 or more storeys), 54 (Presence of double height spaces facing infrastructure for accessibility / connection), 63 (Presence of long corridor/garage/other open plan space directly adjacent to party wall), 62 (Evidence of shared party wall), 80b (Presence of setbacks along Main Façade 3 at 1 level), 82c (Presence of projecting rooms / balconies at 2 or 3 levels), 33 (Proportions of building on plan at typical plan level (W: L)), and 61 (Vacant site directly adjacent to building). In the case of Section 2, two out of the three parameters which have been considered to have the greatest effect on the seismic resistance of buildings have resulted as significant predictors of the final rating, namely, the total number of storeys present (entry 26) and the proportions of the building on plan (entry 33). Even though the entry which records the presence of an irregular plan layout (entry 34) has not resulted as a significant predictor of the final overall seismic vulnerability rating, entry 63 (Presence of long corridor/garage/other open plan space directly adjacent to party wall) from Section 3 which indicates a very typical case of plan irregularity in the loadbearing masonry building typology, has resulted as a significant predictor. Furthermore, eight out of the eleven most significant predictors result from Section 3. This confirms the greater bearing which the parameters which are recorded in Section 3 have on the overall seismic vulnerability rating of the surveyed buildings, as identified by the developed rating system for the New Form and emphasized by the provision that the final seismic vulnerability rating cannot be lower than the rating obtained for Section 3. It is to be noted that five out of the eight entries from Section 3 which resulted as significant with respect to the final overall seismic vulnerability rating obtained from the New Form correspond to the main parameters identified in the developed rating system for this section. Entry 65 (Absence of intermediate walls in loadbearing masonry building in 1 or more storeys) indicates the presence of a soft storey whereas, entries 80b (Presence of setbacks along Main Façade 3 at 1 level) and 82c (Presence of projecting rooms / balconies at 2 or 3 levels) indicate the presence of other forms of vertical irregularity. Entry 76 (Presence of large openings on Main Façade 4) identifies the presence of large openings whereas entry 54 (Presence of double height spaces facing infrastructure for accessibility / connection) identifies the presence of double height spaces. Entry 61 (Vacant site

directly adjacent to building) represents an extreme case of unrestraint of the party wall due to a lower (in this case, missing) adjacent building.

The identification of the presence of a soft storey and that of a double height space as significant predictors of the final seismic vulnerability rating is in line with the structural behaviour explained by Arnold and Reitherman (1982) and the results reported by Guevara-Perez (2015) and Öztürk (2011). Furthermore, while different building characteristics have been investigated in this study from the ones studied by Sucouglu and Yazgan (2003), it is still pertinent to remark that the presence of entries corresponding to the total number of floors (entry 26), the absence of intermediate walls in one or more storeys, which corresponds to the presence of a soft storey (entry 65), and the presence of plan irregularities such as the presence of a long corridor (entry 63), setbacks (entry 80b), projecting rooms or balconies (entry 82c) and the plan proportions of the building (entry 33), in the final set of eleven most significant predictors of the seismic vulnerability rating is in accordance with the results of their study.

GIS thematic maps indicating the distribution of the number of storeys, soft storeys and double height spaces in the 183 buildings of the Test Sites of Xemxija and Nadur which have been considered in this study together with the overall seismic vulnerability rating of these buildings are shown in Figures 4 to 7.

The most significant predictor resulting for Section 4, entry 92 (Presence of slabs spanning in one direction and not tied to each other / to walls parallel to their span) is, however, not in agreement with the developed rating system. As explained in the case of the outcome from the second stage multivariate analysis of Section 4, the rating system developed for the New Form has been based on the premise that this tying action between slabs and between slabs and walls is provided by the cast in-situ slabs in the contemporary loadbearing building typology. On the other hand, the presence of flexible and semi-rigid slab construction system which occur, for example, in cases of lightweight mezzanine structures or when horizontal structural systems such as stone slabs over timber or steel beams are present, have been considered to have a higher negative bearing on the seismic vulnerability of this building typology. Lightweight mezzanine structures are more frequent especially when the buildings under assessment are located on a main road, hence giving rise to the presence of commercial establishments at the lower levels. Semi-rigid slab construction systems such as stone slabs over timber or steel beams could be present if the building under assessment was constructed at an earlier date than that considered for the contemporary loadbearing building typology but was altered and extended to include additional floors in the last 40-60 years. These two parameters, however, could not result as significant parameters from the statistical analysis in this study since they were not present in any of the buildings in the Test sites. On the other hand, the presence of a double height space (which has been identified as a significant predictor of the final rating) can be considered as an extreme case of the reduction in the restraint to the party wall which would occur when a flexible slab construction and, to a lesser extent, when a semi rigid slab construction are present, therefore confirming the impact which such characteristics have on the seismic vulnerability of this building typology, as taken into account in the developed rating system of the New Form. Therefore, even

though the developed rating system for Section 4 of the New Form for the individual building has not, and could not, be verified through the statistical analysis of the data recorded in the Xemxija and Nadur Test sites, the presence of flexible and semi-rigid slab construction systems are still being considered as more relevant predictors with respect to the seismic vulnerability rating of individual buildings in view of the reduced restraint provided by these horizontal structural systems to the main loadbearing walls.

Similarly, the third stage multivariate analysis did not identify any parameters from Sections 5, 6 and 8 as significant predictors of the final seismic vulnerability rating. This is not in agreement with the rating system developed for the New Form however this statistical result can be explained in view of the characteristics present or the lack of variations in the corresponding building characteristics identified in the Test sites. The presence of an inadequate degree of abutment or a total absence of abutment in the case of masonry arches or vaults and the presence of pre-existent damages in the buildings could not result as significant predictors from the statistical analysis since none of the buildings in the Test sites had horizontal structural systems supported on arches or vaults and only a very limited number of the surveyed buildings included visible damages. Moreover, all the assessed buildings were located in areas which generally have the same upper and lower ground formation layers consisting of a relatively hard fractured upper rock layer overlying a clay layer (though present in different thicknesses and resulting in only localised variations due to the 'loss' of the rock layer along slopes). Hence, the lack of variation in the overall geology of the analysed buildings resulted in this parameter not being identified as statistically significant with respect to the final seismic vulnerability rating even though a large number of international studies such as the ones mentioned earlier (Gueguen et al. 2000, Trifunac et al. 2001, Lou et al. 2011), in addition to local studies (Farrugia 2002; Galdes 2012) have confirmed the impact of this parameter on the seismic response of buildings. The authors therefore propose that a more extensive survey which includes buildings in areas with more differing geologies would very likely result in the identification of this parameter as one of the significant predictors of the final seismic vulnerability rating.

In the case of Section 8, since the internal inspections of the buildings in the Test Sites could not be carried out, the availability of the Development Permit Drawings determined the level of accuracy of the assessment as well as the extent to which certain assumptions have been made with respect to the presence of certain characteristics. Furthermore, since the on-site surveys of the 183 buildings in the Test sites have been carried out by 6 different assessors, there is an inevitable variation in the degree of assumptions made (due to the subjective human element) in the cases when the internal layouts were either not available at all or available only in part.

(a) (b)

Figure 4: GIS thematic maps indicating the total number of floors in (a) Xemxija and (b) Nadur Test sites.

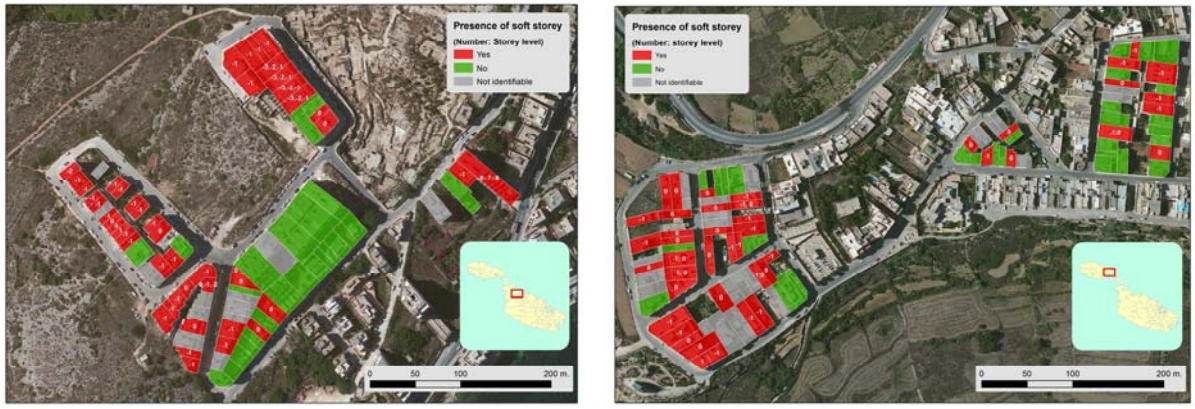

(a) (b)

Figure 5: GIS thematic maps indicating the presence of soft storeys in (a) Xemxija and (b) Nadur Test sites.

(a) (b)

Figure 6: GIS thematic maps indicating the presence of double height spaces in (a) Xemxija and (b) Nadur Test sites.

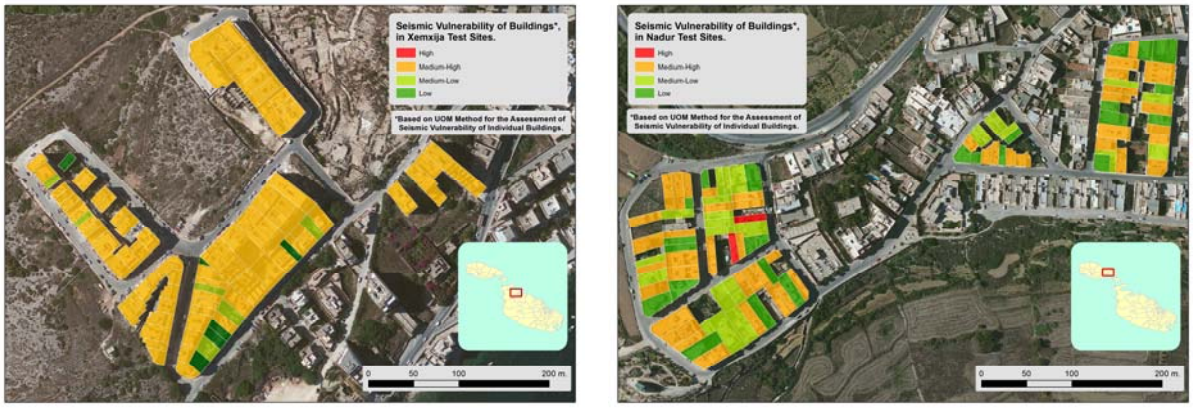

(a) (b)

Figure 7: GIS thematic maps indicating the seismic vulnerability rating of the buildings in (a) Xemxija and (b) Nadur Test sites.

While strong statistical relationships have been identified between the rating system developed for the New Form and the outcome of the second stage multivariate analyses with respect to the seismic vulnerability ratings of the separate sections of the New Form, the third stage multivariate analysis confirmed, as significant predictors of the final rating score, only the parameters of Sections 2 and 3, which also happen to be the sections which have the major bearing on the seismic vulnerability outcome, and, by extrapolation, the parameters of Section 4, when considering the similarity of their effect on the structural response to that resulting from the presence of double height spaces. On the other hand, none of the characteristics identified from Sections 5 and 6 in the developed rating system for the New Form were identified as significant predictors of the final rating through the statistical analysis. Hence, the effect which the parameters which resulted as significant predictors of the final rating and those considered in the developed rating system have on the seismic behaviour of the building typology under study will need to be confirmed in more detail by means of numerical modelling.

4.0 References

- Ahmed M M, Jahan I, Alam J (2014). Earthquake vulnerability assessment of existing buildings in Cox's Bazar using field survey & GIS. International Journal of Engineering Research and Technology (IJERT) 3:1147-1156.
- Arnold CH, Reitherman R. (1982). Building configuration and seismic design, John Wiley & Sons, Inc. New York.
- Applied Technology Council (ATC). (2002) FEMA 154 Rapid visual screening of buildings for potential seismic hazards: A handbook. Federal Emergency Management Agency (FEMA), Washington, DC. 2nd Edition.
- Baggio C, Bernardini A, Colozza R, Corazza L, Della Bella M, Di Pasquale G, Dolce M, Goretti A, Martinelli A, Orsini G, Papa F, Zuccaro G (2000). AeDES, Scheda di 1° livello di rilevamento danno, pronto intervento e agibilità per edifici ordinari nell' emergenza post-sismica. Dipartimento della Protezione Civile. Editrice Italiani nel Mondo srl., Roma.

- Benedetti D, Petrini V (1984). Sulla vulnerabilita' sismica di edifici in muratura: Un metodo di valutazione (A method for evaluating the seismic vulnerability of masonry buildings). L'industria delle costruzioni 149: 66-74.
- Camilleri D H (1999). Vulnerability of buildings in Malta to earthquake, volcano and tsunami hazard. The Structural Engineer 77: 25-31.
- Cattari S, Lagomarsino S, Bosiljkov V, D'Ayala D (2015). Sensitivity analysis for setting up the investigation protocol and defining proper confidence factors for masonry buildings. Bulletin of Earthquake Engineering 13:129-151. doi 10.1007/s10518-014-9648-3.
- Celarec D, Dolšek M (2013). The impact of modelling uncertainties on the seismic performance assessment of reinforced concrete frame buildings. Engineering structures 52: 340-354.
- CNR-ITC (2007a). Regione Abruzzo: Manuale per il rilevamento della vulnerabilita' sismica degli edifici – Istruzione per la compilazione della scheda di I livello. Appendice n.1 alla pubblicazione "Rischio sismico di edifici pubblici" Parte I a Aspetti metodologici Del GNDT - Gruppo Nazionale per la Difesa dai terremoti, 1993 Roma.
- CNR-ITC (2007b). Regione Abruzzo: Manuale per il rilevamento della vulnerabilita' sismica degli edifici. Istruzione per la compilazione della scheda di secondo livello. Appendice n.1 alla pubblicazione 'Rischio sismico di edifici pubblici', Parte 1a Aspetti metodologici, GNDT, 1993 Roma.
- Commissione Tecnica per la Microzonazione Sismica (2013). Analisi della Condizione Limite per l' Emergenza (CLE) dell' insediamento urbano. Version 2.0.
- Di Capua G, Peppoloni S, Pergalani F (2001). Scheda per la valutazione qualitativa dei possibili effetti locali nei siti di ubicazione di edifice strategici e monumentali.
- Farrugia J (2002). Seismic Vulnerability of Local Masonry Building Typologies. Dissertation, University of Malta.
- Formisano A, Mazzolani F M, Florio G, Landolfo R (2010a). A quick methodology for seismic vulnerability assessment of historic aggregates'. In: Mazzolani F M (ed) Proceedings of the COST Action 26 Final Conference "Urban habitat constructions under catastrophic events". CRC Press Taylor & Francis Group, London, pp 577-582.
- Formisano A, Florio G, Landolfo R, Mazzolani F M (2010b). Un metodo per la valutazione su larga scala della vulnerabilita sismica degli aggregati storici. Proceedings of the Workshop Wondermasonry "Design for Rehabilitation of Masonry Structures", Ischia.
- Formisano A, Florio G, Landolfo R, Mazzolani F M (2011). Numerical calibration of a simplified procedure for the seismic behaviour of masonry aggregates. In: Topping B H V, Tsompanakis Y (ed) Proceedings of the 13th International Conference on Civil, Structural and Environmental Engineering Computing. Civil-Comp Press, Stirlingshire, Scotland.
- Formisano A, Florio G, Landolfo R, Mazzolani F M (2015). Numerical calibration of an easy method for seismic behaviour assessment on large scale of masonry building aggregates. Advances in Engineering Software 80:116-138.

- Ferrini M, Decanini L, Pagliazzi A, Scarparolo S (2004). Edifici in muratura in zona sismica. Rilevamento delle carenze strutturali – Manuale per la compilazione della scheda delle carenze. Regione Toscana.
- Ferrini M, Melozzi A, Pagliazzi A, Scarparolo S (2003). Rilevamento della vulnerabilita' sismica degli edifici in muratura. Manuale per la complilazione della scheda GNDT/CNR di II livello. Versione modificata dalla Regione Toscana.
- FEMA (2005) "Rapid visual screening of buildings for potential seismic hazards: Student Manual, FEMA 154 -SM". Federal Emergency Management Agency, Washington, DC. 2nd Edition.
- Galdes A (2012). Vulnerability of Local Masonry Buildings to Seismic Loading. Dissertation, University of Malta.
- Gueguen P, Bard P Y, Oliveira C S (2000). Experimental and numerical analysis of soil motions caused by free vibrations of a building model. Bulletin of the Seismological Society of America 90(6):1464-79.
- Guevara-Perez L T (2012). "Soft storey" and "weak storey" in earthquake resistant design: A multidisciplinary approach. Proceedings of the 15th World Conference on Earthquake Engineering (15WCEE) (Lisbon, Portugal), 856-866.
- Lijie C, Zhenzhou L, Changcong Z (2014). Probabilistic importance analysis of the input variables in structural systems. Structural Safety 51:13-22.
- Lou M, Wang H, Chen X, Zhai Y (2011). Structure–soil–structure interaction: literature review. Soil Dynamics and Earthquake Engineering 31(12):1724-31.
- Mucciarelli, M, Masi, A, Gallipoli M R, Harabaglia P, Vona M, Ponzo, F, Dolce M (2004). Analysis of RC building response and soil-building resonance based on data recorded during a damaging earthquake (Molise, Italy, 2002). Bulletin of the Seismological Society of America 94 (5):1943-1953.
- Öztürk T (2011). A study of the effects of slab gaps in buildings on seismic response according to three different codes, Scientific Research and Essays, 6(19):3930-3941, DOI: 10.5897/SRE10.076, ISSN 1992-2248.
- Porter K A, Beck J L, Shaikhutdinov R V (2002). Sensitivity of building loss estimates to major uncertain variables. Earthquake Spectra 18(4):719-43.
- Sucouglu H, Yazgan U (2003). Simple survey procedures for seismic risk assessment in urban building stocks. Seismic Assessment & Rehabilitation of Existing Buildings. Klawer Academic Publisher, Netherlands.
- Torpiano A., Bonello M A, Borg R P, Sapiano P, Ellul A M (2015). Methodology for the seismic vulnerability assessment of loadbearing masonry buildings in Malta. In: Cicero C, Lombardo G (ed) Establishment of an integrated Italy-Malta cross-border system of civil protection, Engineering aspects. Aracne Editrice srl., Rome, Italy, 133-186.
- Torpiano A, Bonello M A, Borg R P, Sapiano P, Ellul A M (2016). The development of a seismic vulnerability assessment methodology for contemporary loadbearing masonry buildings in the

Maltese Islands. International Journal of Sustainable Materials and Structural Systems, Vol 2, Nos. 3/4: 283-307.

- Trifunac MD, Ivanovic SS, Todorovska MI (2001). Apparent periods of a building. I: Fourier analysis. Journal of Structural Engineering 127(5):517-26.
- Yakut A, Ozcebe G, Yucemen M S (2004). A statistical procedure for the assessment of seismic performance of existing reinforced concrete buildings in Turkey. 13th World Conference on Earthquake Engineering, Vancouver B.C., Canada, paper 687.

Acknowledgements

This research study has been carried out under the SIMIT Project (Italia – Malta Operational Programme) (Project code: B1-2.19/11), Work Package 2.1.

The on-site assessments of the local building stock in the selected aggregates in Xemxija (Malta) and Nadur (Gozo) and the retrieval of the internal layouts of these buildings from the approved planning permits from the Malta Environment and Planning Authority have been carried out with the help of the following Research Support Officers on the SIMIT Project: Ann Marie Ellul, Kim Cassar Torreggiani, Yanica Zammit, Charlo' Briguglio, Godwin Abela.

Furthermore, the following local entities are being gratefully acknowledged for their contributions to this research study:

- MEPA (Malta Environment and Planning Authority) for allowing access to the approved permit drawings of the buildings in the test sites of Msida and Xemxija (Malta), and Nadur (Gozo);
- Institute for Climate Change and Sustainable Development - GIS Laboratory (University of Malta) for the elaboration of thematic maps based on the seismic vulnerability assessments carried out and the on-site data collected by the authors and the acknowledged Research Support Officers.

v) Document (v): Abstract of oral presentation at conference '36th General Assembly of the European Seismological Commission', 2-7th September 2018, Valletta, Malta.
Reference: Sapiano P, Torpiano A, Bonello MA, A Study of the Variation in Seismic Response of a Loadbearing Masonry Building Typology over Rock or Clay Subsoils through Numerical Modelling. In: D'Amico S, Galea P, Bozionelos G, Colica E, Farrugia D, Agius MR, (eds.), *Book of Abstracts of the 36th General Assembly of the European Seismological Commission, 2-7th September 2018, Valletta, Malta*. Messina: Mistral Services sas; 2018. p. 420-421; ISBN: 978-88-98161-12-6. Presentation number: ESC2018-S29-341.
Status: published / presented.

Abstract

The absence of earthquakes in Malta causing significant structural damages in the last century led to an unjustified complacency in the construction methods used for loadbearing masonry structures (Galea, 2007). The Maltese Islands are associated with a low-to-moderate seismicity and a design peak ground acceleration of 0.10g. This study focuses upon the seismic vulnerability of the contemporary loadbearing unreinforced masonry (URM) building typology, consisting of apartment blocks in row developments, typically including four to five residential levels overlying an open plan basement. The URM building typology under study includes a number of typical construction characteristics. In addition to the soft storey at the lowermost level, this typology could also include setbacks, voids in slabs, pounding problems and large openings, all of which impair the seismic resistance of such buildings.

The geology of the Maltese Islands varies from lower coralline limestone or globigerina limestone in most of the Eastern part of Malta to the presence of upper coralline limestone outcrops over blue clay in the Western part of Malta and most of Gozo. To date, there is no regulated restriction on the overall safe building heights nor on the structural characteristics of buildings erected in the Maltese Islands, with the only restrictions being stipulated in the local planning building height regulations, irrespective of the site geology. While studies carried out at the University of Malta on the URM building typology under investigation showed that the investigated structures resist collapse at a lower overall number of storeys if erected on clay when compared to a rock subsoil (Borg, 2017), published literature also suggests that the presence of flexible subsoils can considerably impair the seismic resistance of buildings due to a number of factors, including the higher displacements resulting in structures with a lower number of floors, and the amplification of seismic accelerations leading to increased structural damage.

This study investigates the variation in response of the URM building typology in a seismic event for six different ground formations and ground modelling scenarios through the non-linear time-history analysis (using the software package Extreme Loading® for Structures) of a loadbearing masonry building, where the typical plan layout is repeated on every floor. For every ground formation case studied, the numerical model was analysed starting with a height of six floors and re-analysed following

the reduction of one floor at a time, until collapse was resisted. The ground formation scenarios investigated included:

i. A single 30 m thick upper coralline limestone layer (modelled as a three-dimensional block);
ii. Upper coralline limestone specified as the material of the ground at the numerical model's Minimum Z-position;
iii. A 30 m thick upper coralline limestone layer overlying a 30 m thick clay layer (both layers modelled as three-dimensional blocks);
iv. A 1.5 m thick upper coralline limestone layer overlying a 60 m thick clay layer (both layers modelled as three-dimensional blocks);
v. A single 60 m thick clay layer (modelled as a three-dimensional block);
vi. Clay specified as the ground material at the model's Minimum Z position.

A simulated ground motion record for the Maltese Islands (similar to the last major earthquake, which hit the Maltese Islands, on the 11th January 1693) for a magnitude 7.6 earthquake with a hypocentral distance of 170.3 km to the North-East of Malta (obtained from the database of the Seismic Monitoring and Research Unit of the University of Malta) was applied in the transverse X-direction in all analysed numerical models, and corresponded to a design peak ground acceleration of 0.10g.

The main response parameters investigated included the:

1) Comparison of the overall building height at which collapse was resisted;
2) Comparison of the natural frequency under static and dynamic loads in the two main orthogonal directions of the numerical models and for two main subsoil cases considered;
3) Comparison of the predominant frequencies in the acceleration spectrum of the ground layers to the predominant frequencies of the simulated ground motion record;
4) Variation of a wide range of structural response parameters.

The study of the variation in the response parameters extracted from the analysed numerical models suggests that the resistance of the contemporary loadbearing URM building typology in Malta is severely impaired with increased overall building height and when erected over a clay subsoil as opposed to a predominantly rock subsoil. These results, therefore, suggest that maximum height limitations for URM building typologies and the consideration of seismic actions in the design of new URM buildings or in the alteration of existing URM buildings in the Maltese Islands should be regulated, particularly taking into consideration the different geological scenarios present and the seismicity of the region.

References

- Borg D., A Parametric Study of the Effect of Geometric Proportions on the Permissible Height of Local Masonry Buildings Fitted with Anti-Seismic Sway-Resistant Frames at Basement Level. *M.Eng Dissertation. University of Malta*, Malta, 2017.
- Galea P., Seismic History of the Maltese Islands and Considerations on Seismic Risk. *Annals of Geophysics.* 2007 December; 50(6): pp. 725-740.

Appendix C. **NUMERICAL MODELS**

Table 24 Material properties specified in full scale numerical models analysed using ELS®.

Material properties	Concrete	Hollow concrete blockwork (153 mm thick)	Hollow concrete blockwork (228 mm thick, double density)	Globigerina limestone masonry	Mortar	Mortar for 153 mm thick HCB walls	Mortar for 228 mm thick HCB, double density walls	Mortar for 153 mm thick HCB walls at DPM	Mortar for 228 mm thick HCB (double density) walls at DPM	Mortar for 228 mm thick globigerina limestone walls at DPM	Steel reinforce-ment	Upper coralline limestone	Clay	Upper coralline limestone (ground interface material)	Clay (ground interface material)
Young's modulus (N/mm^2)	33000 [1]	33000 [1]	33000 [1]	21000 [7]	8000	8000	8000	8000	8000	8000	200000	55000 [14]	204.3*[17]	55000 [14]	204.3*[17]
Shear modulus (N/mm^2)	13750 [2]	13200 [4]	13200 [4]	8400 [4]	3077 [11]	3077 [11]	3077 [11]	3077 [11]	3077 [11]	3077 [11]	76923	22000 [15]	68.1*[18]	22000 [15]	68.1*[18]
Tensile strength (N/mm^2)	3.8 [3]	1.59 [5]	2.65 [5]	3 [8]	0	0	0	0	0	0	n/a	3	0	3	0
Tensile yield stress (N/mm^2)	n/a	n/a	n/a	n/a	n/a	n/a	n/a	n/a	n/a	n/a	410 [13]	n/a	n/a	n/a	n/a
Compressive strength (N/mm^2)	30	4.838	5.385	17.5 [9]	2	1.29	1.436	1.29	1.436	2	n/a	30	4.903*	30	4.903*
Separation strain	0.1	0.1	0.1	0.1	0.1	0.1	0.1	0.1	0.1	0.1	n/a	0.1	0.1	0.1	0.1
Ultimate strain	n/a	n/a	n/a	n/a	n/a	n/a	n/a	n/a	n/a	n/a	0.05	n/a	n/a	n/a	n/a
Ultimate strength/Tensile yield stress	n/a	n/a	n/a	n/a	n/a	n/a	n/a	n/a	n/a	n/a	1.08	n/a	n/a	n/a	n/a
Friction coefficient	0.4	0.258	0.287	0.4	0.4	0.258	0.287	0.1899	0.2114	0.2944	1	0.4	0.85	1*	1*
External damping ratio	0	0	0	0	0	0	0	0	0	0	0	6	6	6	6
Specific weight (kg/m^3)	2400	1220 [6]	1336 [6]	1726 [10]	1760	1135.2	1263.7	1135.2	1263.7	1760	7850	2059 [16]	0*[19]	2059 [16]	0*[19]
Normal contact stiffness factor	0.0001	0.0001	0.0001	0.0001	0.0001	0.0001	0.0001	0.0001	0.0001	0.0001	0.0001	0.0001	0.0001	0.0001	0.0001
Shear contact stiffness factor	0.00001	0.00001	0.00001	0.00001	0.00001	0.00001	0.00001	0.00001	0.00001	0.00001	0.00001	0.00001	0.00001	0.00001	0.00001
Contact upon loading stiffness factor	10	10	10	10	10	10	10	10	10	10	10	10	10	10	10
Post yield stiffness ratio	n/a	n/a	n/a	n/a	n/a	n/a	n/a	n/a	n/a	n/a	0.01	n/a	n/a	n/a	n/a

Table 25 Notes to material properties reported in Table 24.

Reference number (superscript)	Material	Property	Source / background information
*	Clay; Clay (ground interface material); Upper coralline limestone (ground interface material)	Young's modulus, Shear modulus, compressive strength, density, friction coefficient	Altered material properties due to stability failures in the static loading stage during numerical analysis of test models
(1)	Young's modulus	Concrete	For C25/30 concrete from Table 3.1 in Eurocode 2 [156]
(2)	Shear modulus	Concrete	From corresponding Young's modulus and Poisson's ratio of 0.2
(3)	Tensile strength	Concrete	For C25/30 concrete and 95% factile from Table 3.1 in Eurocode 2 [156]
(4)	Shear modulus	All masonry walls	0.4*E (Clause 3.7.3 (1), Eurocode 6 [157])
(5)	Tensile strength	All HCB walls	Scaled values from Barbosa et al. [158] for actual web area and compressive strength
(6)	Specific weight	All HCB walls	Data sheet for concrete blocks produced by Ballut Blocks Services Ltd. (http://www.ballutblocks.com, downloaded 25-02-2015) [150]. Revised by author in view of modelling as solid blocks
(7)	Young's modulus	Globigerina limestone	Results reported by Xuereb [151]
(8)	Tensile strength	Globigerina limestone	Results obtained by Cachia (131), as reported in Buhagiar [153]
(9)	Compressive strength	Globigerina limestone	Results reported by Xuereb [151]
(10)	Specific weight	Globigerina limestone	Average value between results reported by Cachia [152] and Xuereb [151]
(11)	Shear modulus	Mortar	From corresponding Young's modulus and Poisson's ratio of 0.3
(12)	Compressive strength	Mortar	Result reported by Debattista [154] for mortar used in the Maltese Islands
(13)	Tensile yield stress	Steel reinforcement	Value of tensile yield stress for steel was selected based on the age of a large part of the building stock forming part of the contemporary loadbearing masonry building typology present in the Maltese Islands
(14)	Young's modulus	Upper coralline limestone	Based on upper-bound valure for limestones reported by Zhu (http://www.jsg.utexas.edu/tyzhu/files/Some-Useful-Numbers.pdf, downloaded 17-06-2015) [159]
(15)	Shear modulus	Upper coralline limestone	From corresponding Young's modulus and Poisson's ratio of 0.25
(16)	Specific weight	Upper coralline limestone	Average value from the results reported by Bartolo [155]
(17)	Young's modulus (original value)	Clay	Original value (50 N/sq.mm) corresponds to lower-bound value reported by Bowles [160] for stiff clay (Table 2-8)
(18)	Shear modulus	Clay	From corresponding Young's modulus and Poisson's ratio of 0.5
(19)	Specific weight (original value)	Clay	Orignial value (1800 kg/m^3) reported by for 'clayey soil' by Zhu (http://www.jsg.utexas.edu/tyzhu/files/Some-Useful-Numbers.pdf, downloaded 17-06-2015) [159]

Table 26 Maximum shear force results reported by Saliba [161] on masonry triplets including no or different types of damp proof courses for three different levels of pre-compression stress.

Test settings			Case 1: no damp proof course			Case 2: L.D.P.E. as damp proof course			Case 3: bitumen damp proof course (Lead core/ fibre based)			Case 4: Hot bitumen (pitch asphalt) damp proof course		
Test number	Pre-compression (N/mm^2)	Mortar	DPC	Maximum shear force (kN)	Average (maximum) shear force (kN) per pre-compression stress case	DPC	Maximum shear force (kN)	Average (maximum) shear force (kN) per pre-compression stress	DPC	Maximum shear force (kN)	Average (maximum) shear force (kN) per pre-compression stress	DPC	Maximum shear force (kN)	Average (maximum) shear force (kN) per pre-compression stress
1	0.25	1:2:10	n/a	16.923	18.615	L.D.P.E.	10.564	10.659	Bitumen dpc	14.138	13.138	Hot bitumen	14.000	14.855
2	0.25	1:2:10	n/a	19.385		L.D.P.E.	11.622		Bitumen dpc	13.027		Hot bitumen	14.690	
3	0.25	1:2:10	n/a	19.538		L.D.P.E.	9.792		Bitumen dpc	12.250		Hot bitumen	15.875	
4	0.5	1:2:10	n/a	26.905	27.070	L.D.P.E.	21.163	21.512	Bitumen dpc	19.269	19.938	Hot bitumen	30.156	29.140
5	0.5	1:2:10	n/a	28.056		L.D.P.E.	21.744		Bitumen dpc	19.846		Hot bitumen	29.474	
6	0.5	1:2:10	n/a	26.250		L.D.P.E.	21.628		Bitumen dpc	20.698		Hot bitumen	27.791	
7	0.75	1:2:10	n/a	42.857	43.901	L.D.P.E.	33.333	32.871	Bitumen dpc	26.686	25.752	Hot bitumen	41.207	39.635
8	0.75	1:2:10	n/a	44.231		L.D.P.E.	31.842		Bitumen dpc	28.243		Hot bitumen	40.769	
9	0.75	1:2:10	n/a	44.615		L.D.P.E.	33.438		Bitumen dpc	22.326		Hot bitumen	36.930	
10	1	1:2:10	n/a	58.571	53.579	L.D.P.E.	45.865	46.927	Bitumen dpc	28.784	27.303	Hot bitumen	46.154	49.161
11	1	1:2:10	n/a	54.474		L.D.P.E.	47.788		Bitumen dpc	27.500		Hot bitumen	51.860	
12	1	1:2:10	n/a	47.692		L.D.P.E.	47.128		Bitumen dpc	25.625		Hot bitumen	49.468	

Table 27 Comparison of average maximum shear force attained during the testing of the masonry triplets by Saliba [161].

Test numbers	Case 2 vs. Case 1	Case 3 vs. Case 1	Case 4 vs. Case 1
1 to 3	0.573	0.706	0.798
4 to 6	0.795	0.737	1.076
7 to 9	0.749	0.587	0.903
10 to 12	0.876	0.510	0.918

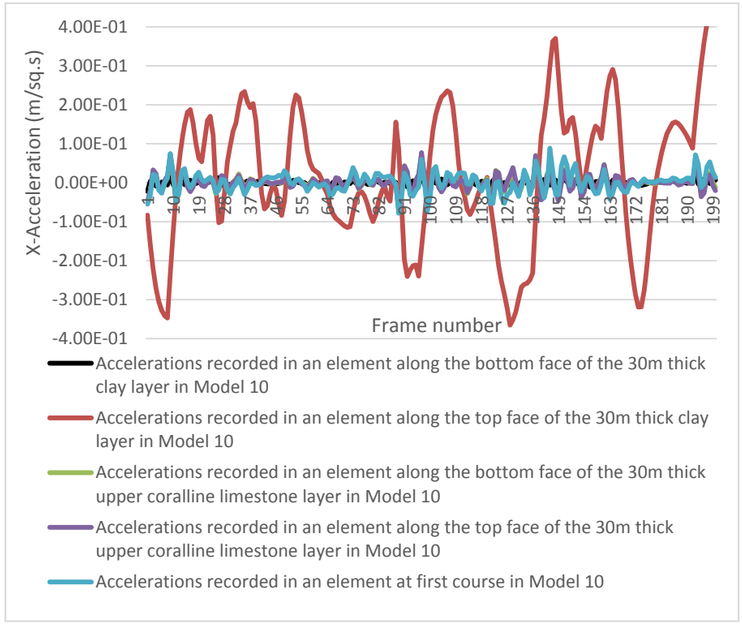

(a)

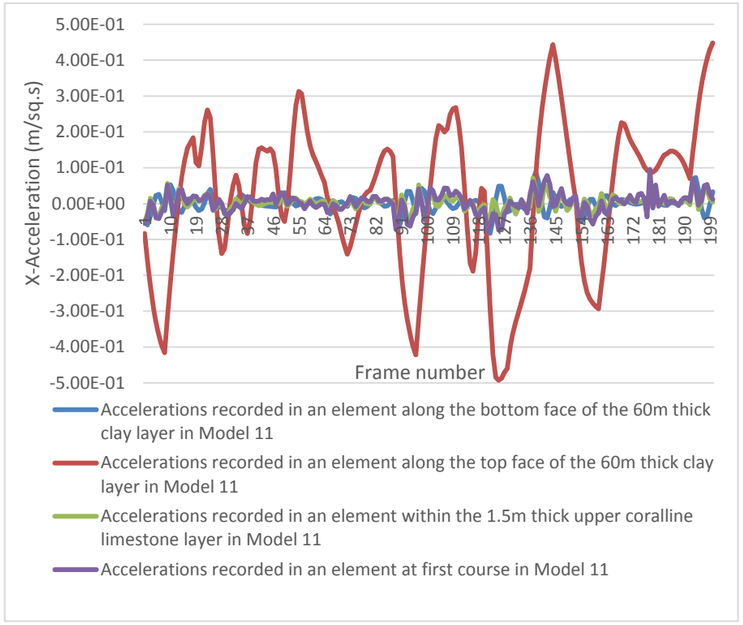

(b)

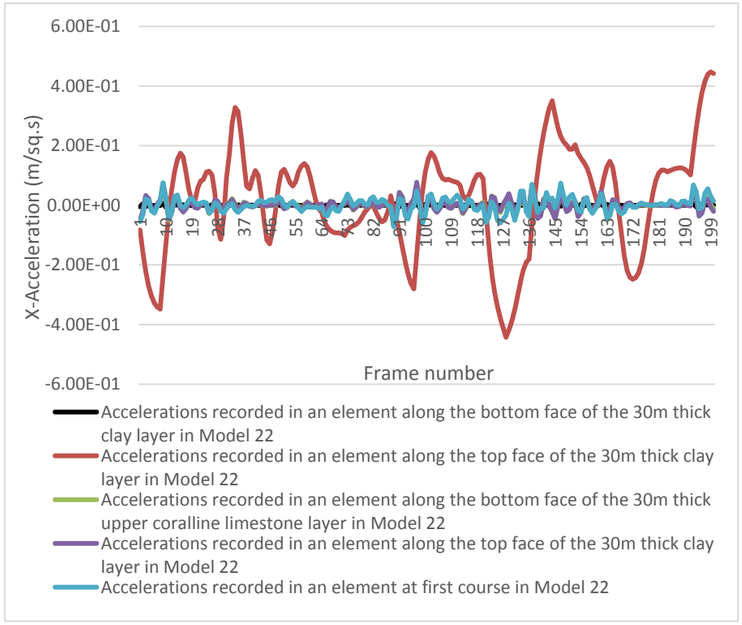

(c)

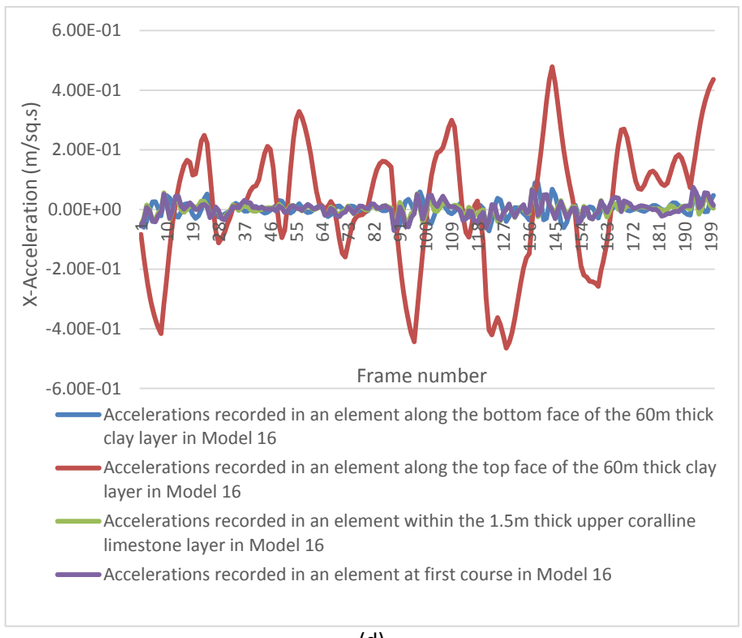

(d)

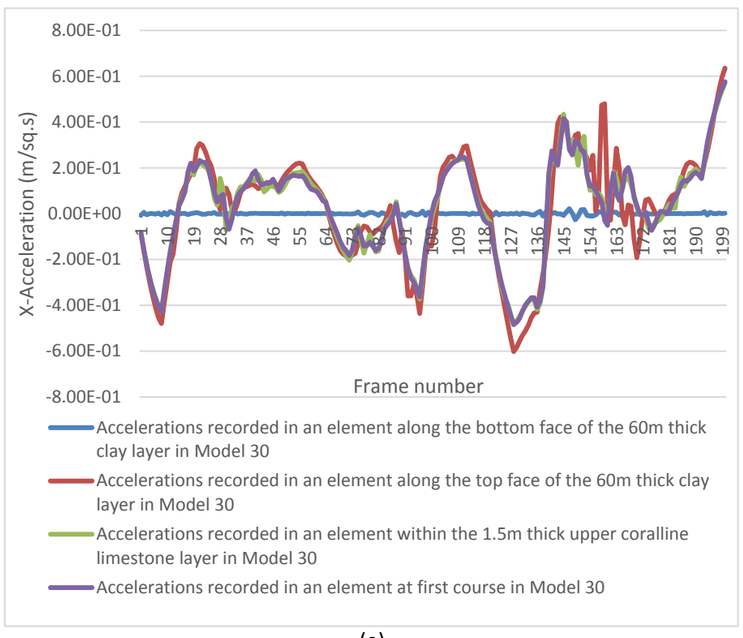

(e)

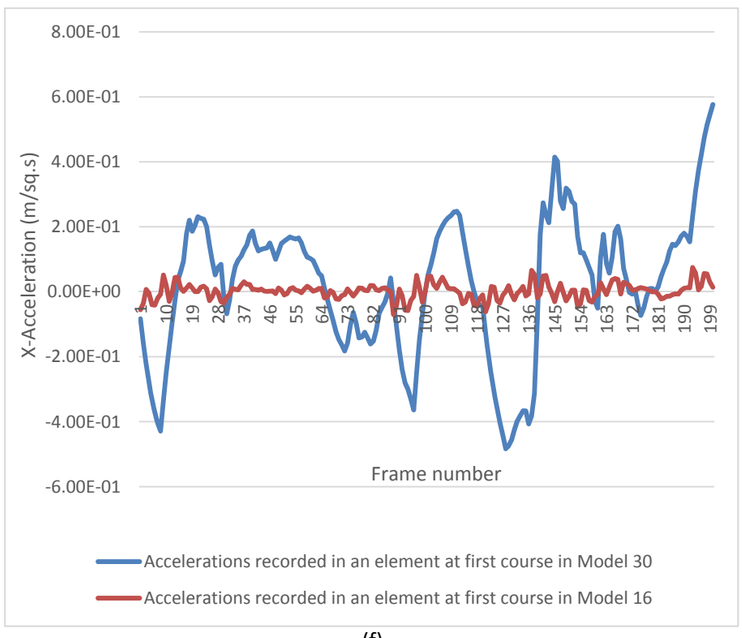

(f)

Figure 16 Comparison of x-accelerations recorded at the first 200 frames of dynamic loading in elements located in the ground layers and at first course in trial Models (a) 10, (b) 11, (c) 22, (d) 16, (e) 30.(f) x-accelerations at first course in Models 30 and 16.

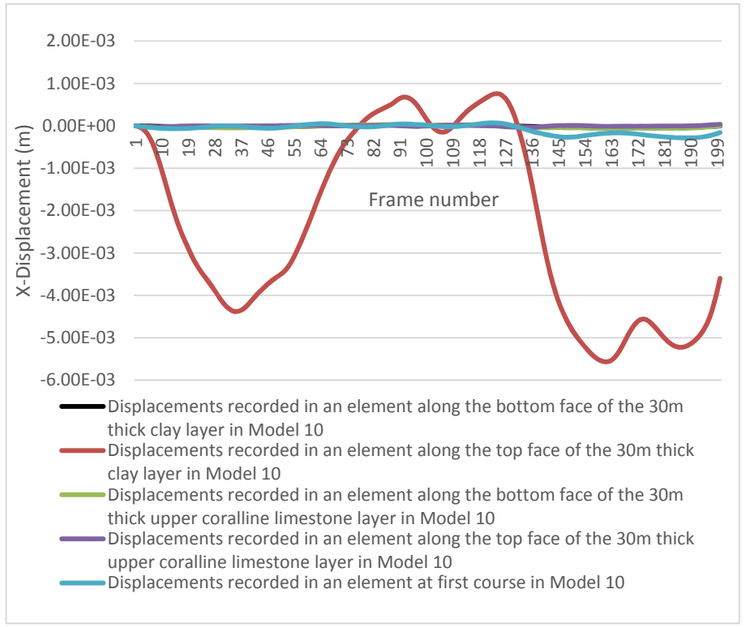

(a)

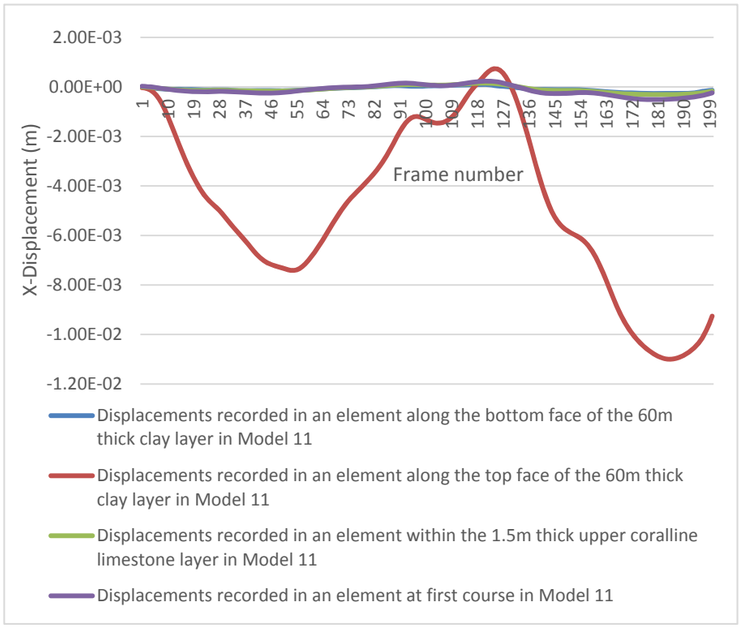

(b)

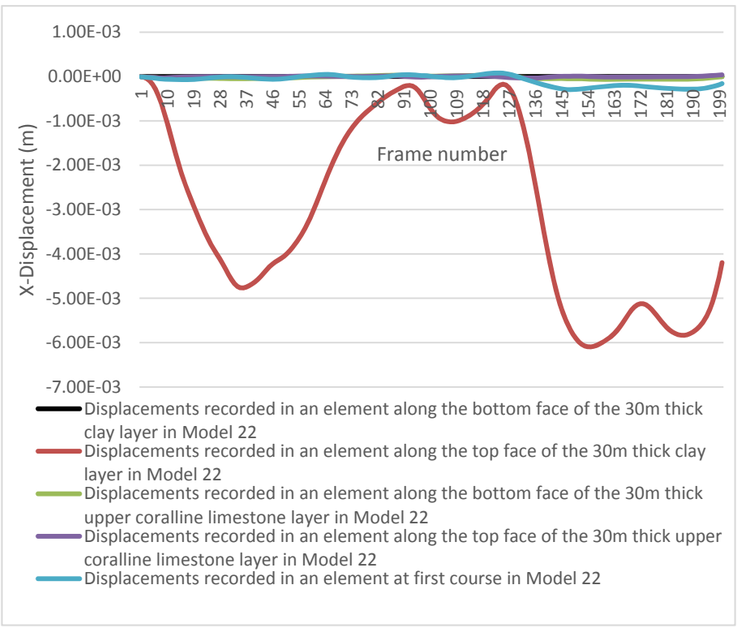

(c)

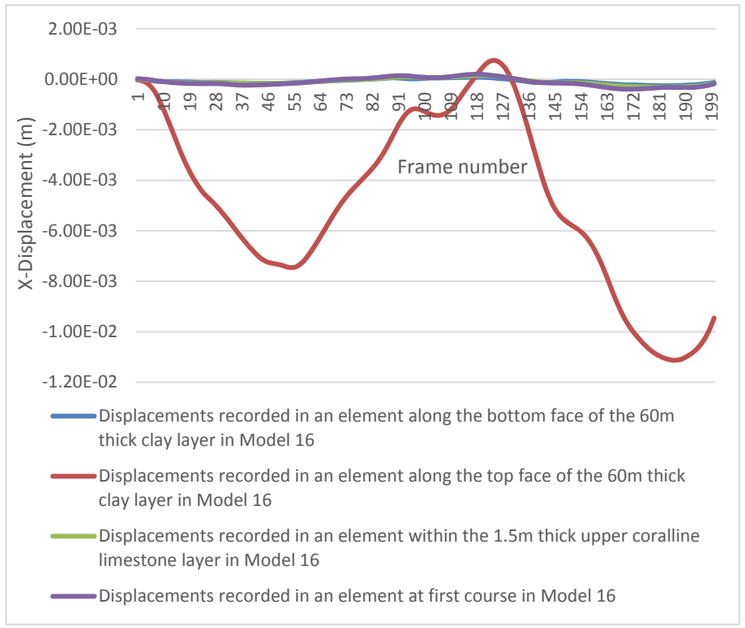

(d)

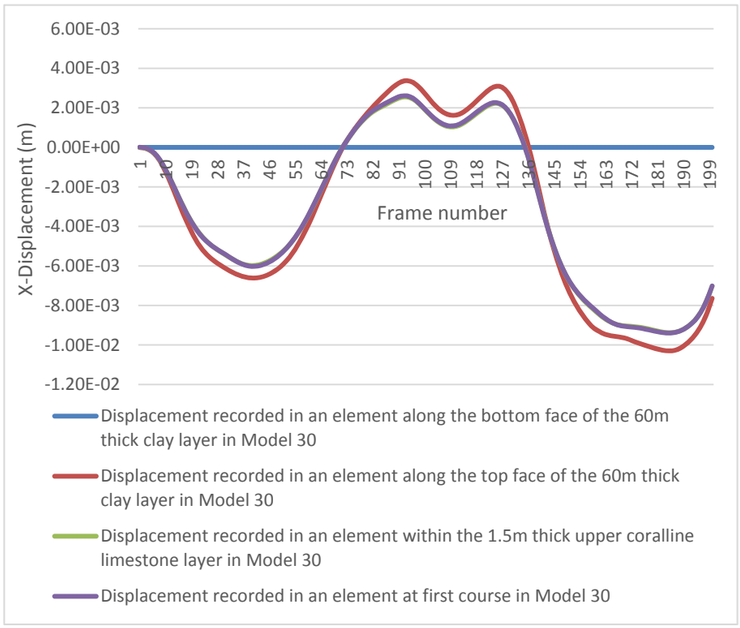

(e)

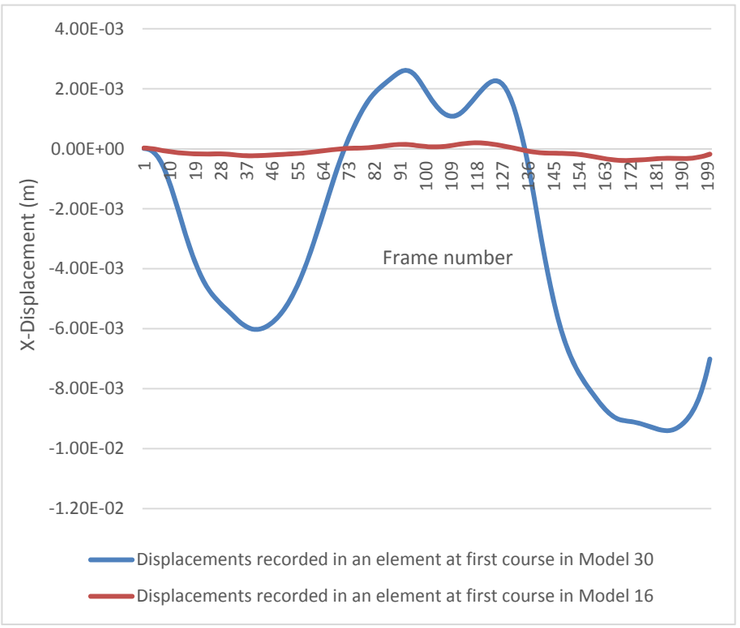

(f)

Figure 17Comparison of x-displacements recorded at the first 200 frames of dynamic loading in elements located in the ground layers and at first course in trial Models (a) 10, (b) 11, (c) 22, (d) 16, (e) 30.(f) x-displacements at first course in Models 30 and 16.

Apartment levels:

Permanent Loads				
Tiles + buildup (115 mm overall thickness)	2.3	kN/m² =	234.535	kgf/m²
Variable Loads (to be included with revised self-weight of slabs)				
1.5kN/m² *0.3*0.5=	0.225	kN/m² =	22.944	kgf/m²
TOTAL PERMANENT AND VARIABLE	2.525	kN/m² =	257.478	kgf/m²

Revised slab densities: APARTMENT LEVELS

Slab thickness (mm)	Revised density	
150	4163.841	kgf/m³
175	3918.624	kgf/m³
200	3734.711	kgf/m³
250	3477.232	kgf/m³
50mm topping	7596.886	kgf/m³

ROOF: in area with services:

Permanent Loads				
Tiles + build-up (150 mm overall)	3	kN/m² =	305.915	kgf/m²
Concrete screed (75 mm)	1.8	kN/m² =	183.549	kgf/m²
Services	5	kN/m² =	509.858	kgf/m²
Total permanent loads (including services)	9.8	kN/m² =	999.322	kgf/m²
Variable loads for area with services (to be included with revised self-weight of slabs)				
0kN/m² *0.3*1.0 =	0	kN/m² =	0	kgf/m²
TOTAL PERMANENT AND VARIABLE	9.8	kN/m² =	999.322	kgf/m²

Revised slab densities: ROOF LEVEL IN AREA FOR SERVICES

Slab thickness (mm)	Revised density	
150	9109.465	kgf/m³

ROOF: in area without services:

Permanent Loads				
Tiles + buildup (150 mm overall)	3	kN/m² =	305.915	kgf/m²
Concrete screed (75 mm)	1.8	kN/m² =	183.549	kgf/m²
Total permanent loads (excluding services)	4.8	kN/m² =	489.464	kgf/m²
Variable loads for area without services (to be included with revised self-weight of slabs)				
0.75 kN/m² *0.3*1.0=	0.225	kN/m² =	22.9436	kgf/m²
TOTAL PERMANENT AND VARIABLE	5.025	kN/m² =	512.407	kgf/m²

Revised slab densities: ROOF LEVEL (no services)

Slab thickness (mm)	Revised density	
150	5863.368	kgf/m³
175	5375.361	kgf/m³
200	5009.356	kgf/m³
250	4496.948	kgf/m³
275	4310.619	kgf/m³

Figure 18 Revised slab densities to include superimposed permanent and variable loads with self-weight of slabs.

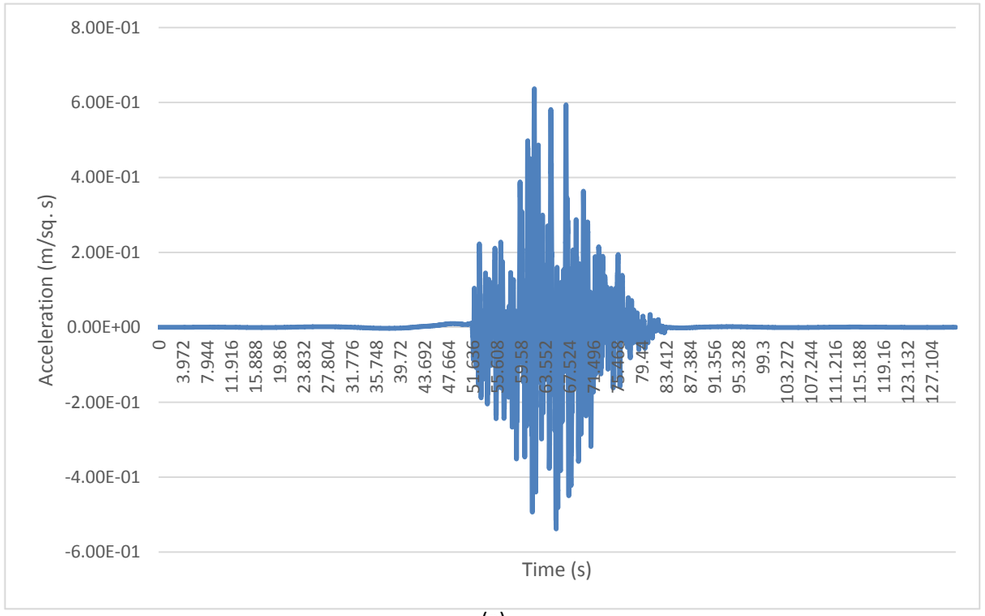

(a)

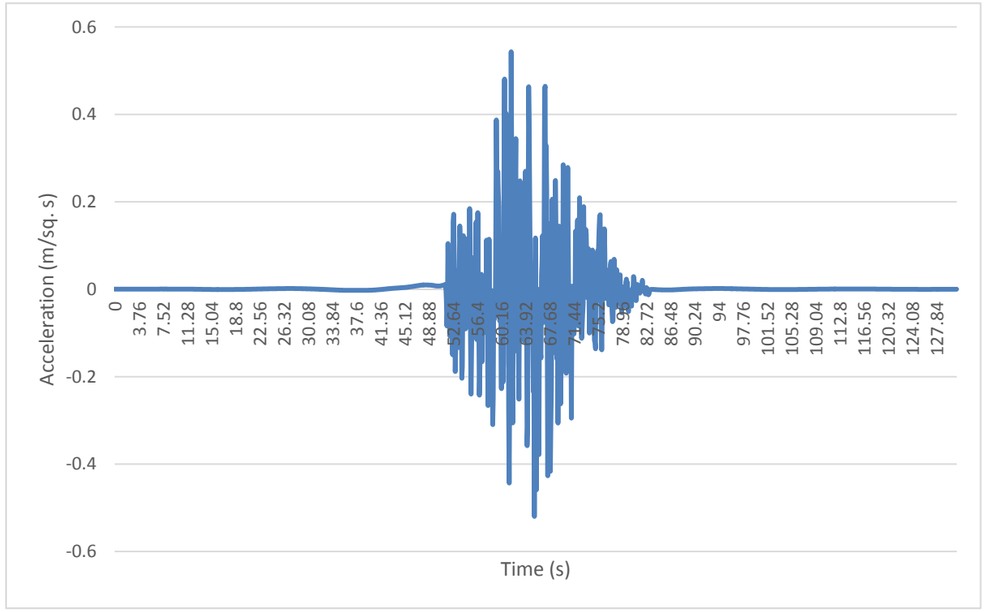

(b)

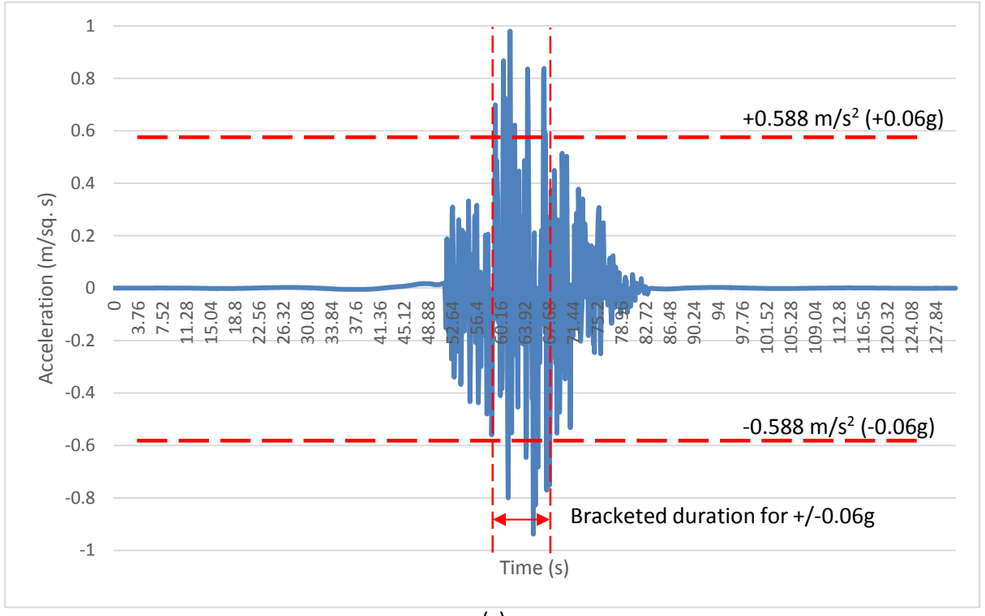

(c)

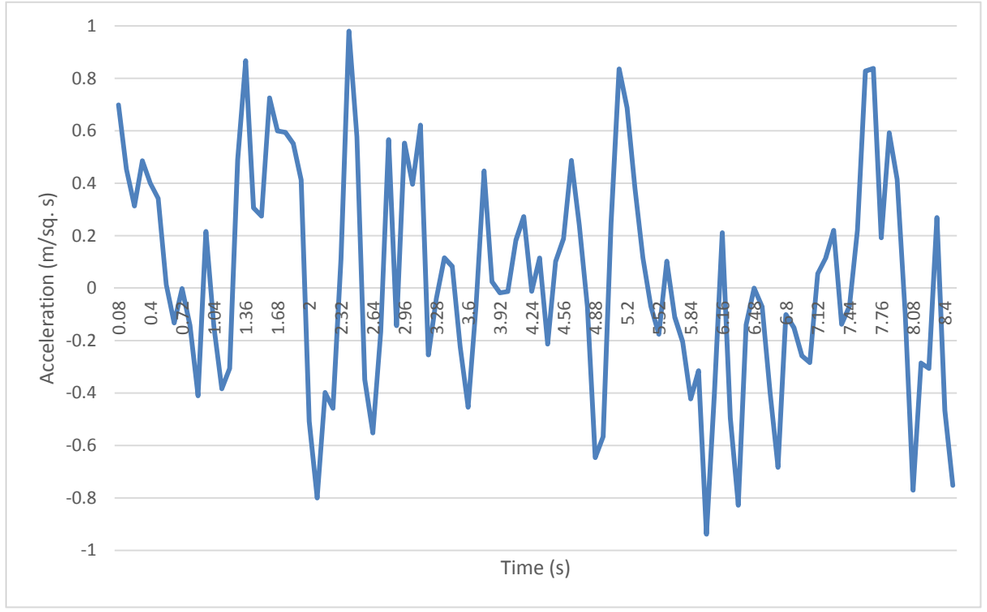

(d)

Figure 19 Magnitude 7.6 simulated ground motion record with hypocentral distance 170.30 km and epicentral distance 139.91 km used in the numerical analyses carried out using ELS®: a)original record with 0.002 s time step, 0.065g maximum pga, record length 131.07 s; (b)revised time step to 0.08 s; (c)scaled maximum pga to 0.1g; (d)bracketed duration +/-0.06g.

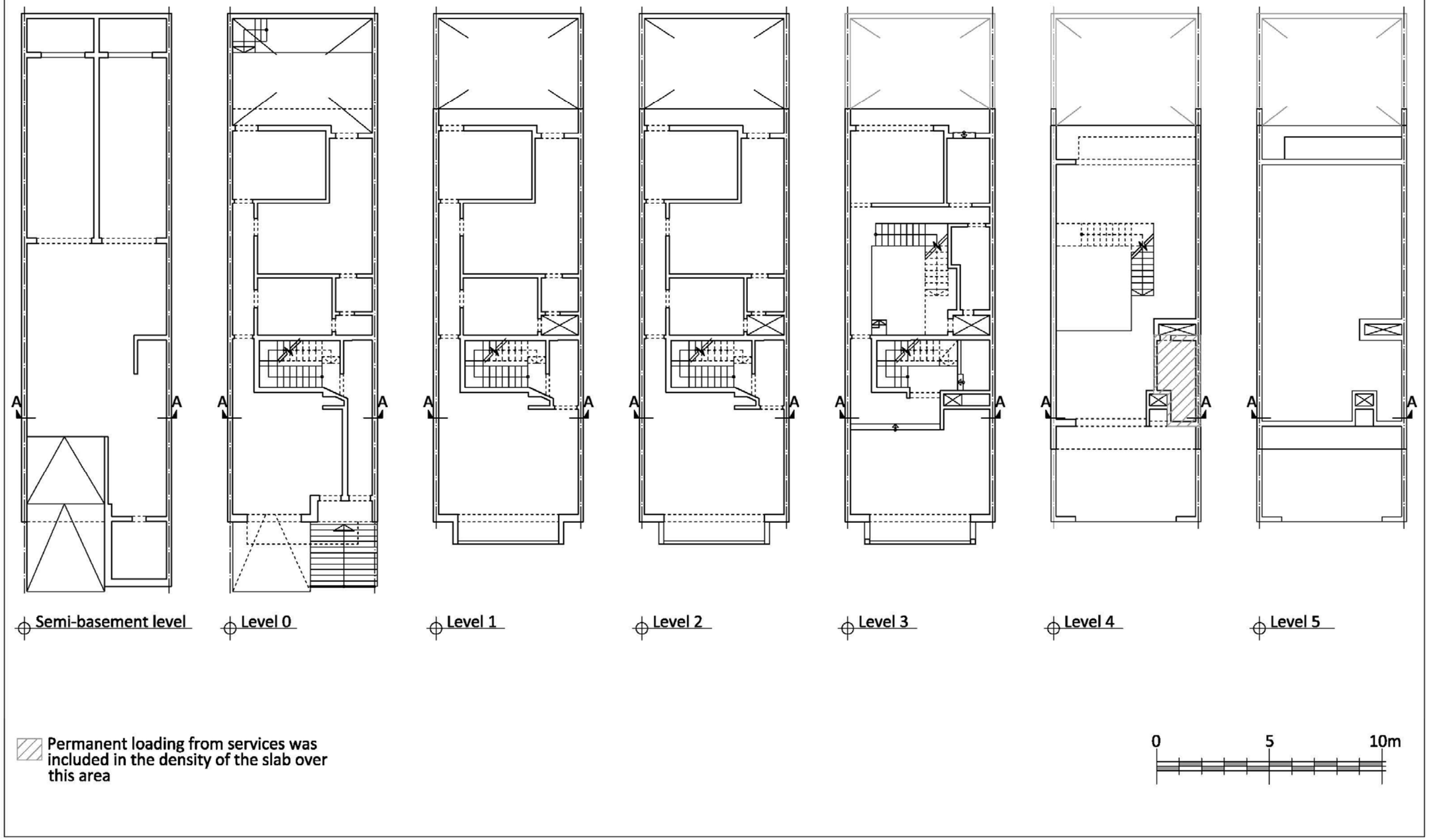

Figure 20 Plan layouts at all levels of Xemxija Building Number 0011 (from Development Permit Drawings).

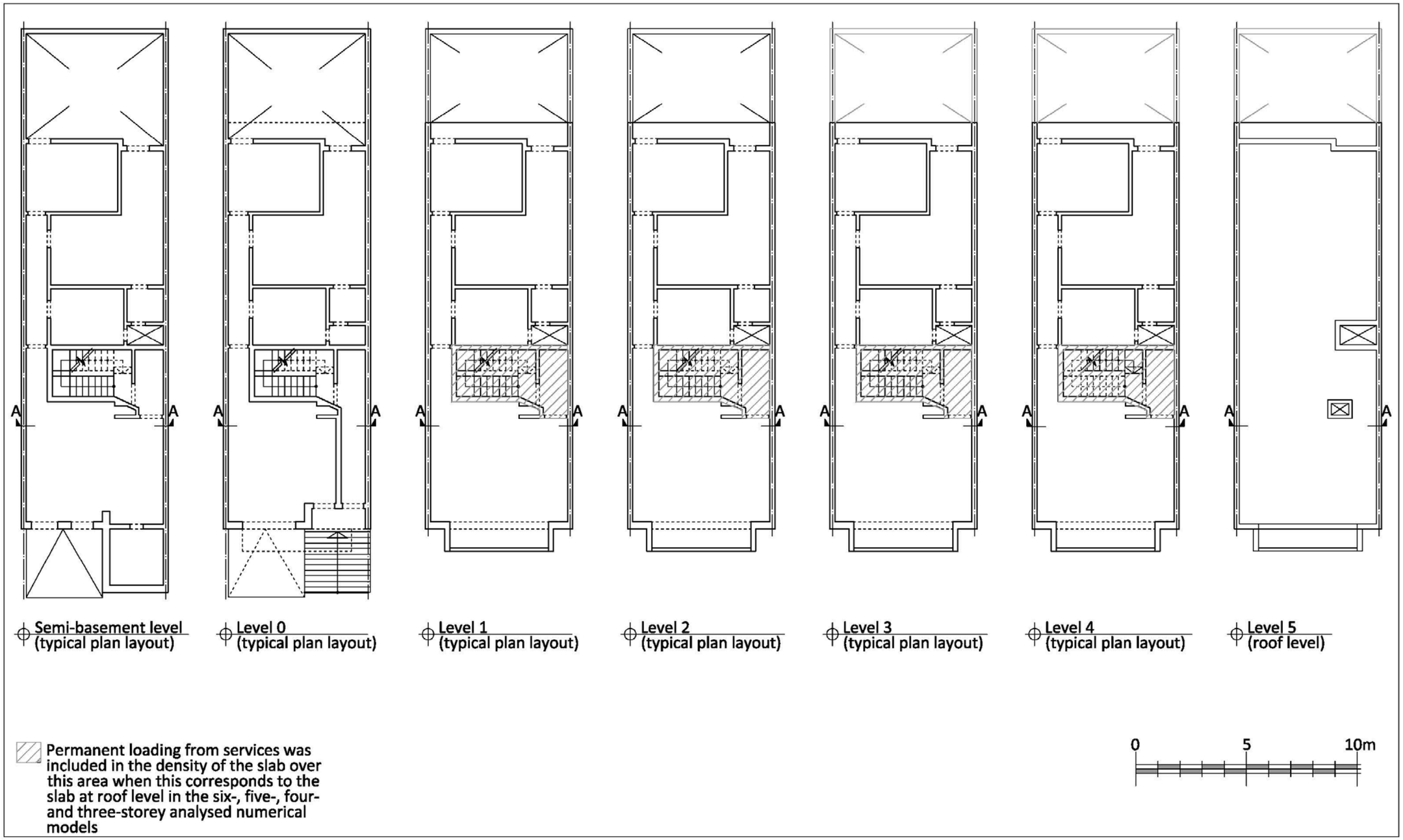

Figure 21 Plan layouts at all levels for analysed single building six-storey control numerical models (plan length-to-width ratio 2.75:1).

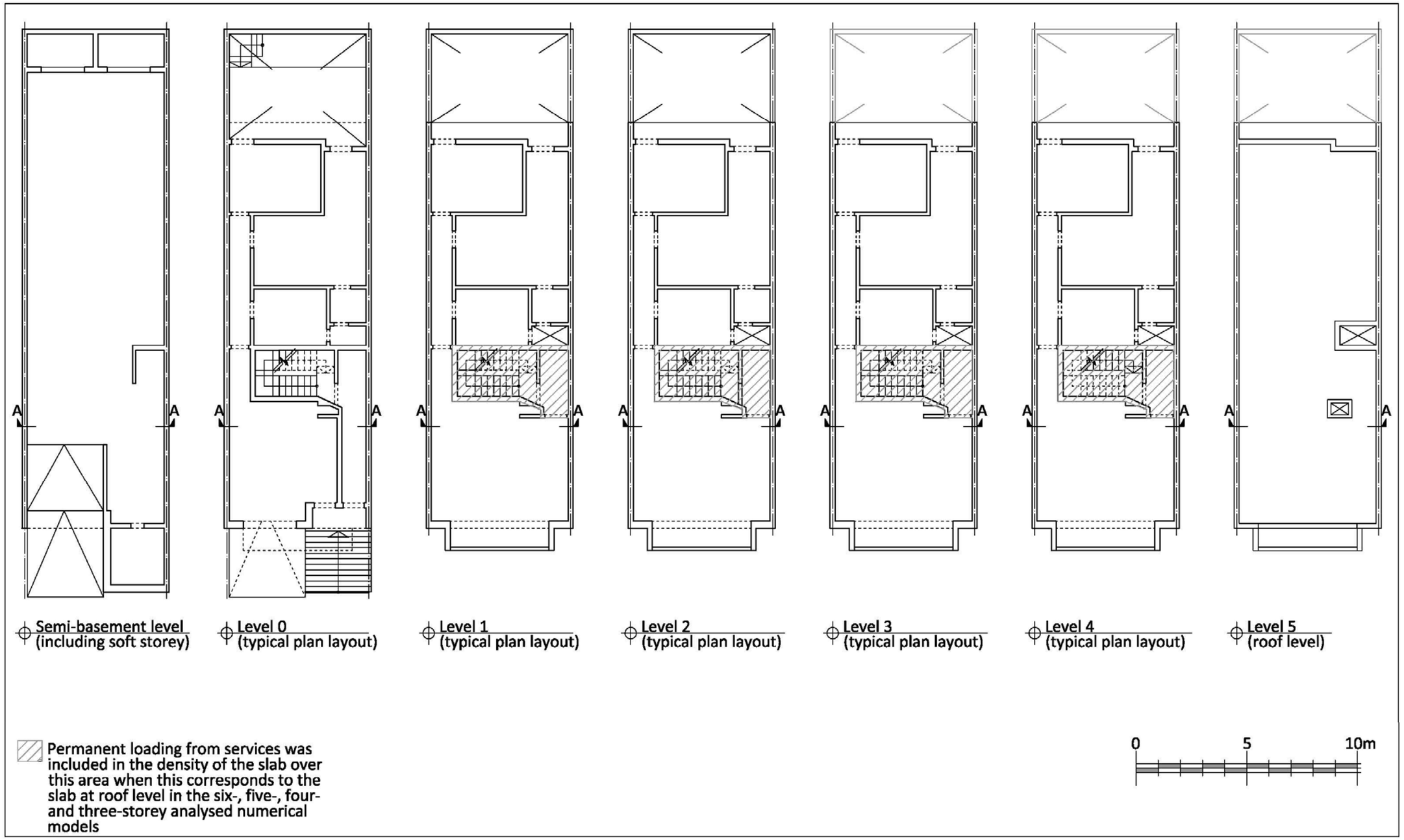

Figure 22 Plan layouts at all levels for analysed single building numerical models including a soft storey at semi-basement level (plan length-to-width ratio 2.75:1).

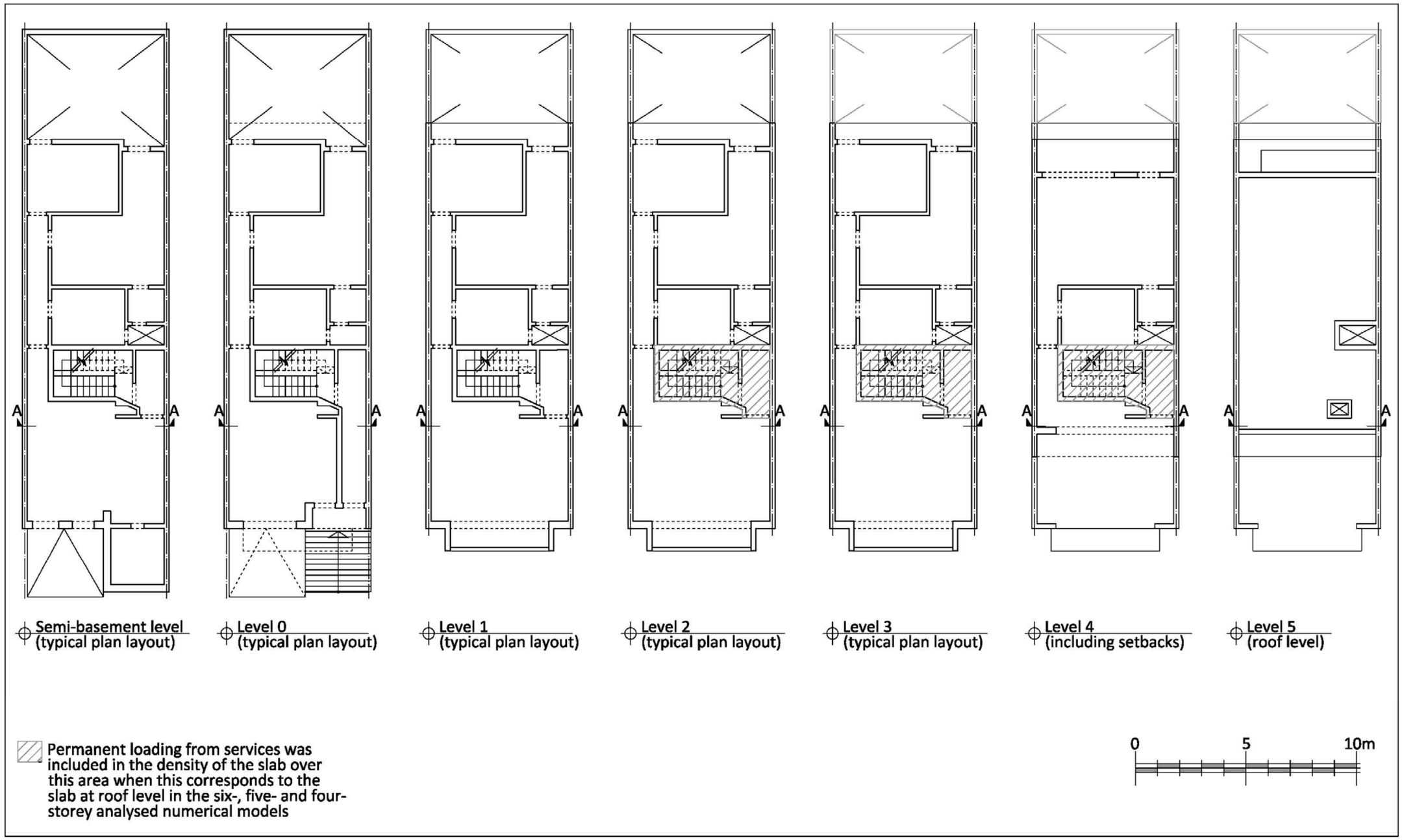

Figure 23 Plan layouts at all levels for analysed single building numerical models including setbacks at penthouse level (plan length-to-width ratio 2.75:1).

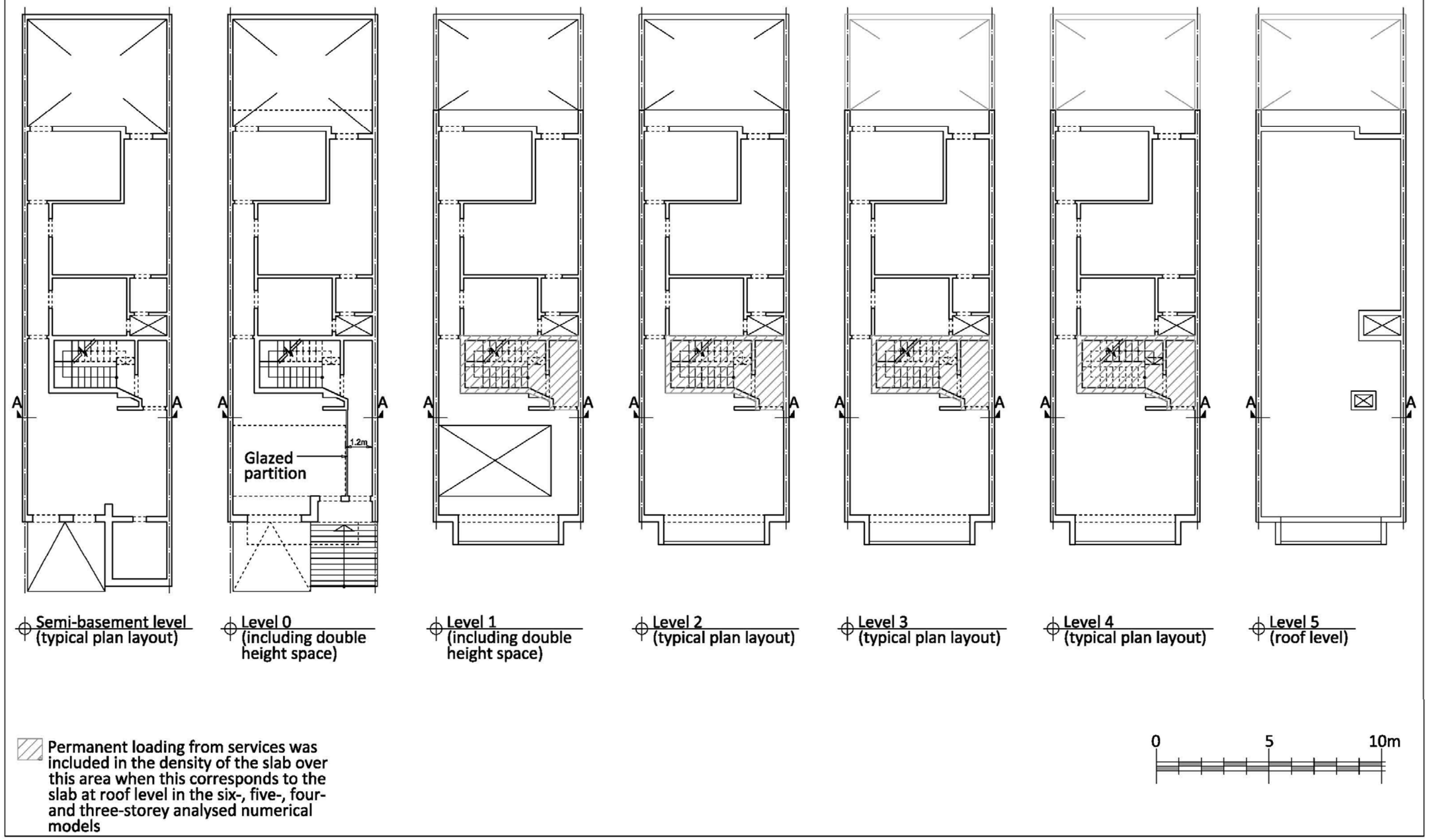

Figure 24 Plan layouts at all levels for analysed single building numerical models including a double height space between Levels 0 and 1 (plan length-to-width ratio 2.75:1).

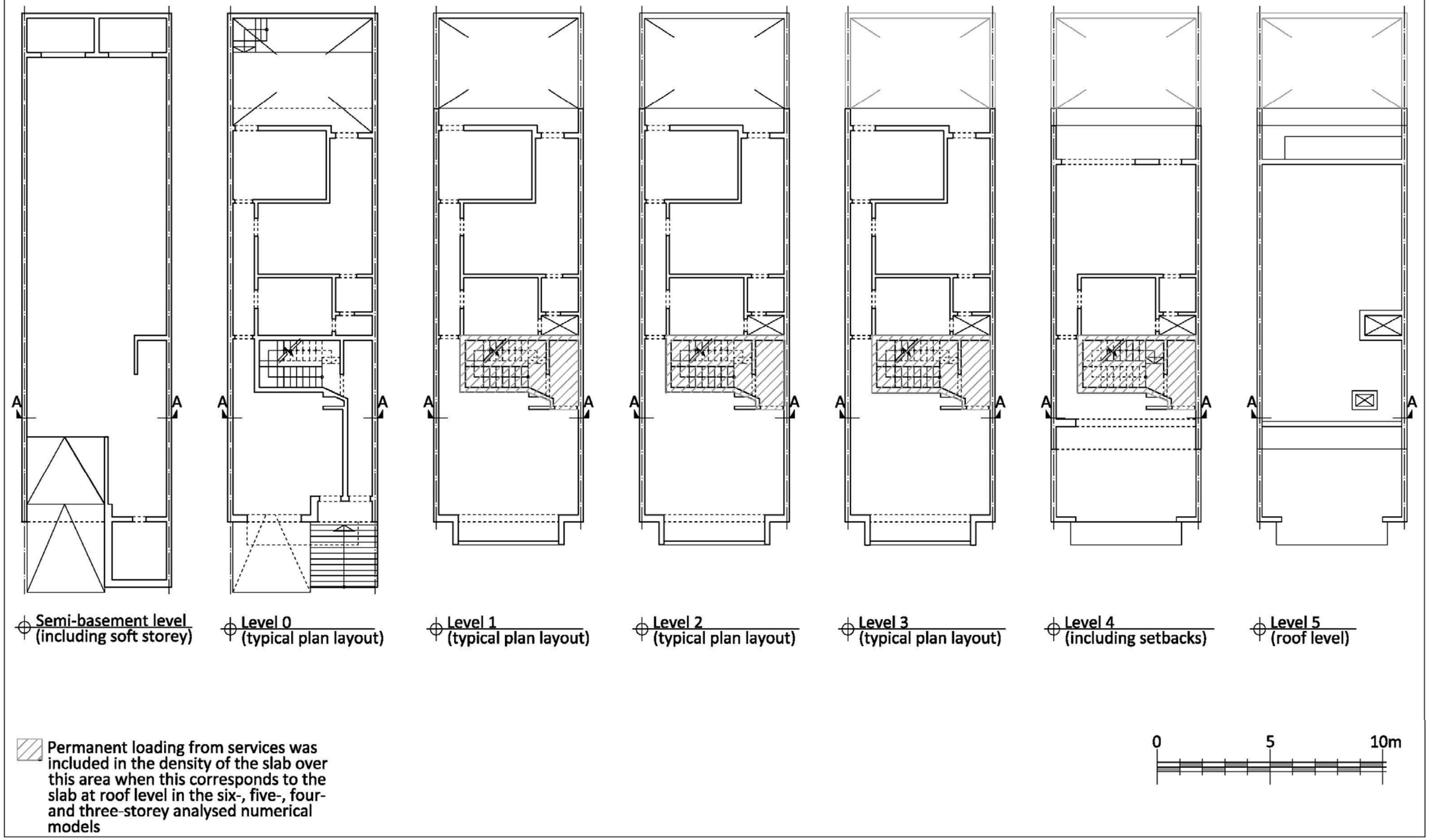

Figure 25 Plan layouts at all levels for analysed single building numerical models including a soft storey at semi-basement level and setbacks at penthouse level (plan length-to-width ratio 2.75:1).

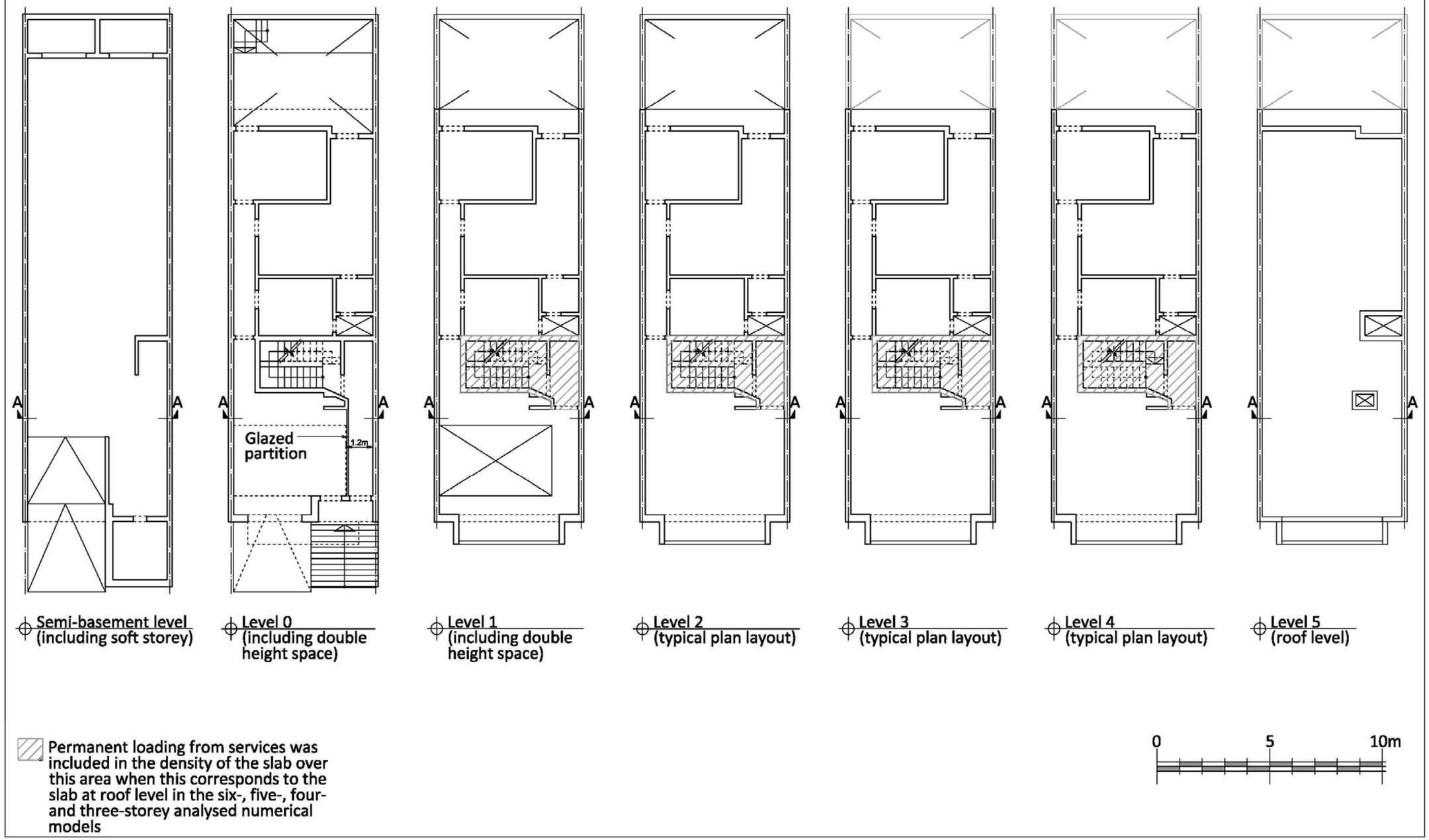

Figure 26 Plan layouts at all levels for analysed single building numerical models including a soft storey at semi-basement level and a double height space between Levels 0 and 1 (plan length-to-width ratio 2.75:1).

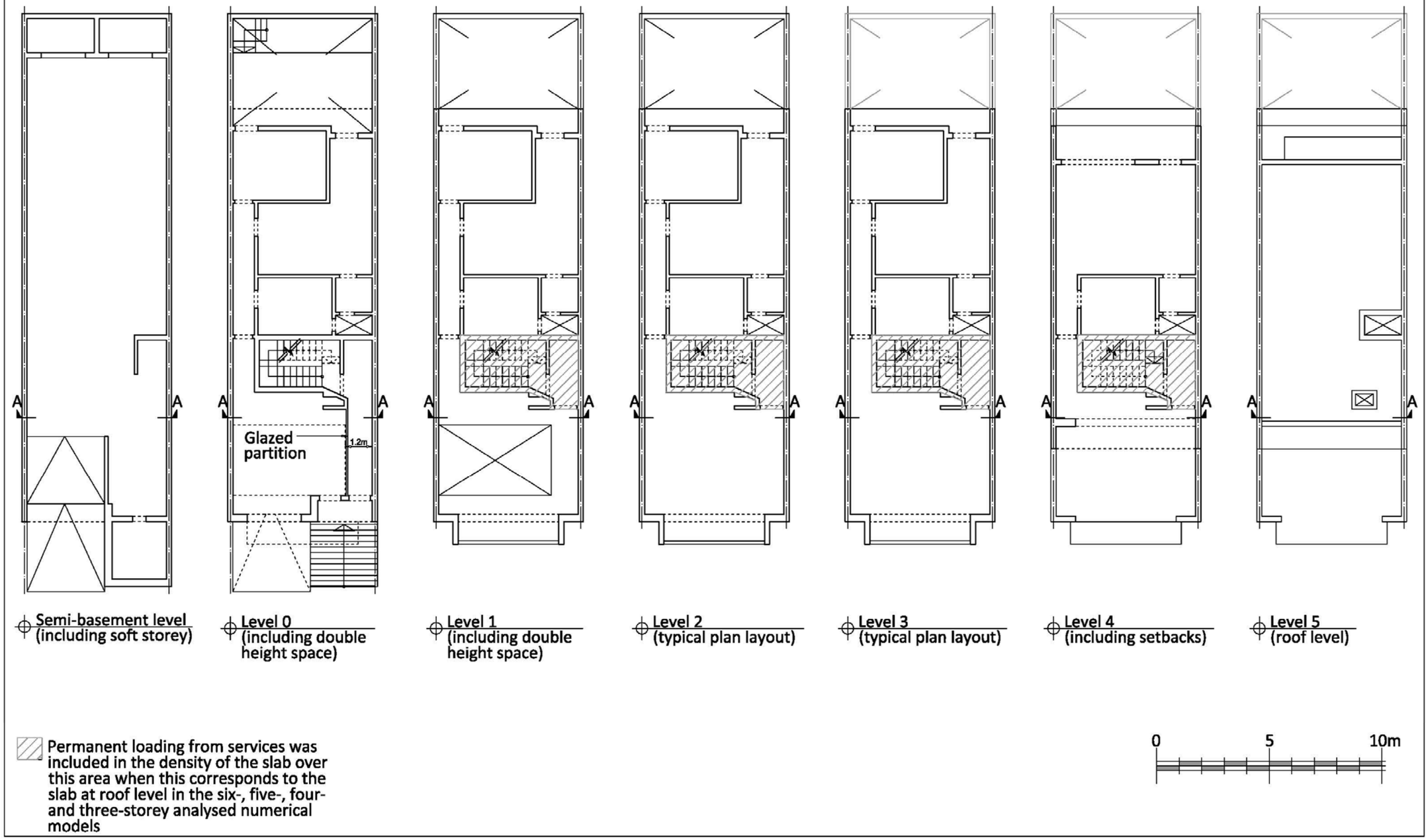

Figure 27 Plan layouts at all levels for analysed single building numerical models including a soft storey at semi-basement level, setbacks at penthouse level and a double height space between Levels 0 and 1 (plan length-to-width ratio 2.75:1).

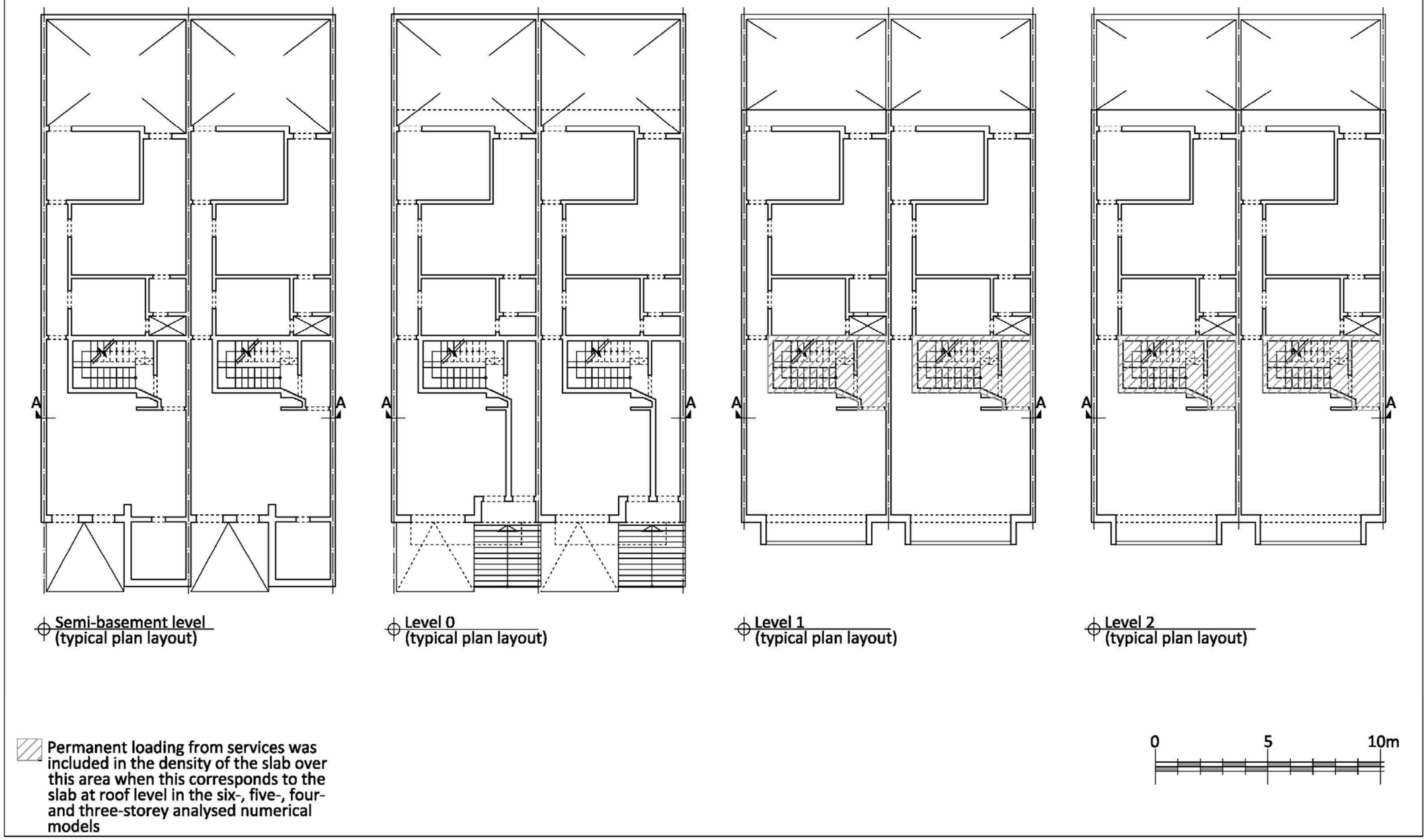

Figure 28 Plan layouts at semi-basement level and Levels 0 to 2 for analysed two-building control numerical models (plan length-to-width ratio 1.37:1).

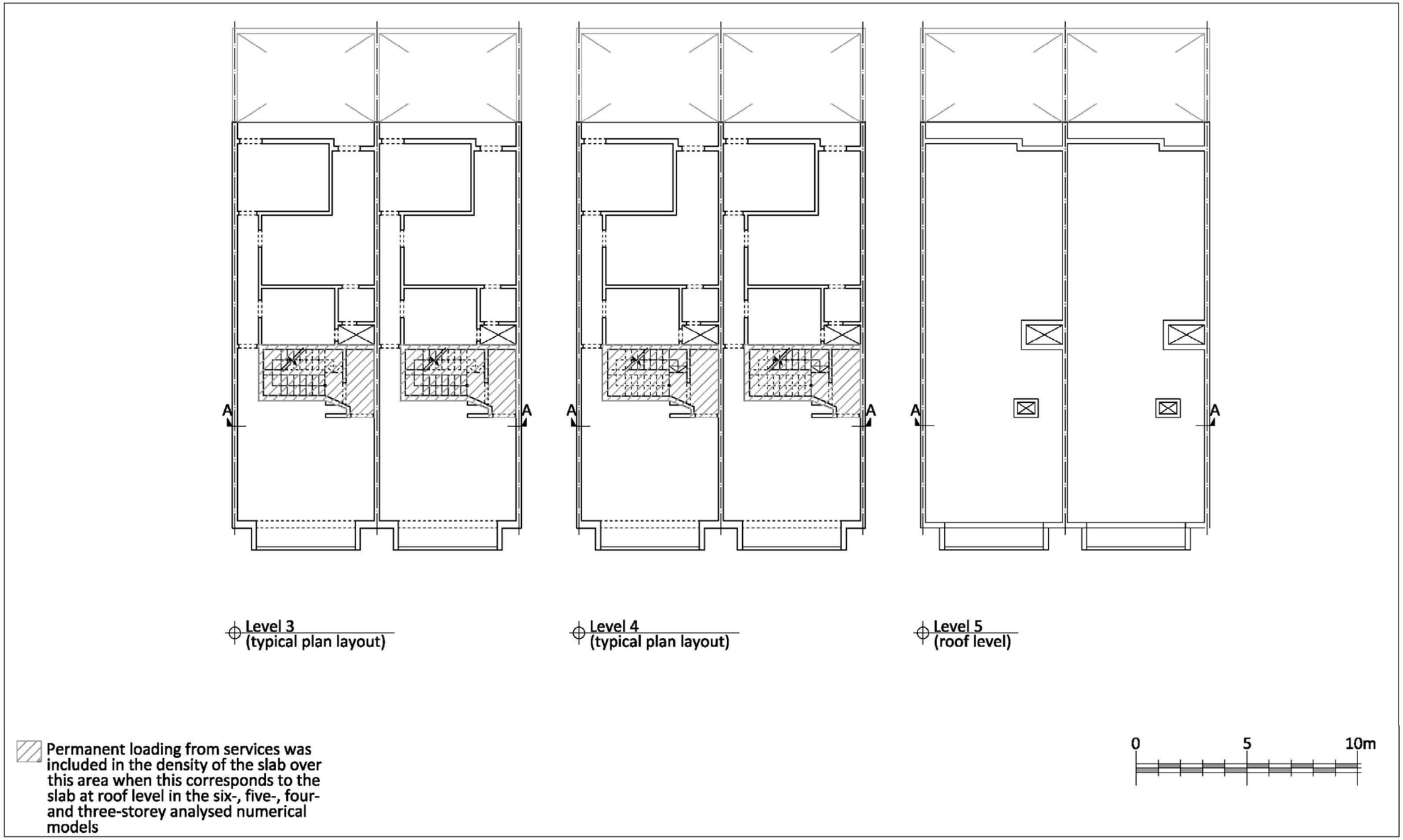

Figure 29 Plan layouts at Levels 3 to 5 for analysed two-building control numerical models (plan length-to-width ratio 1.37:1).

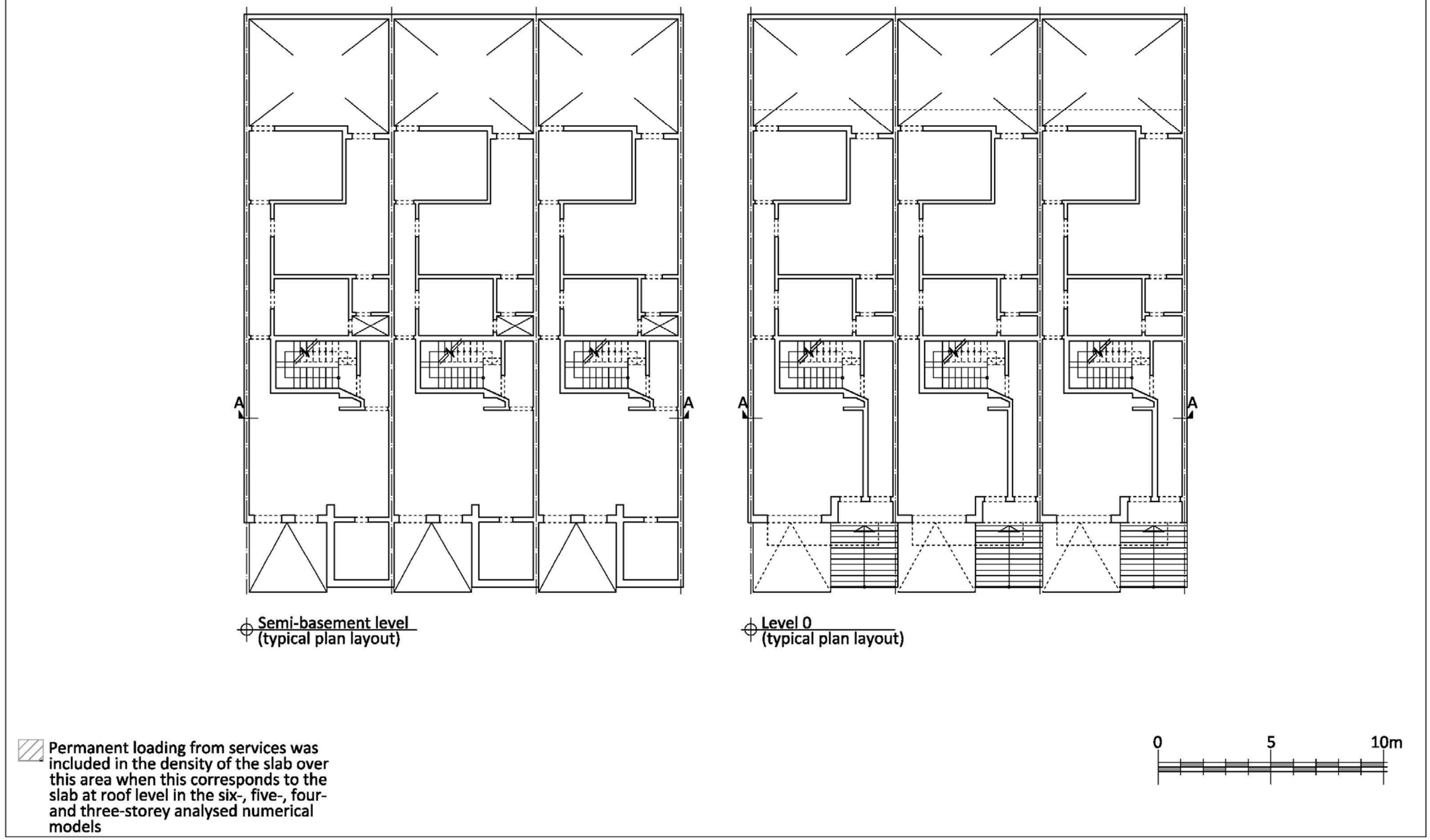

Figure 30 Plan layouts at semi-basement level and Level 0 for analysed three-building control numerical models (plan length-to-width ratio 0.92:1).

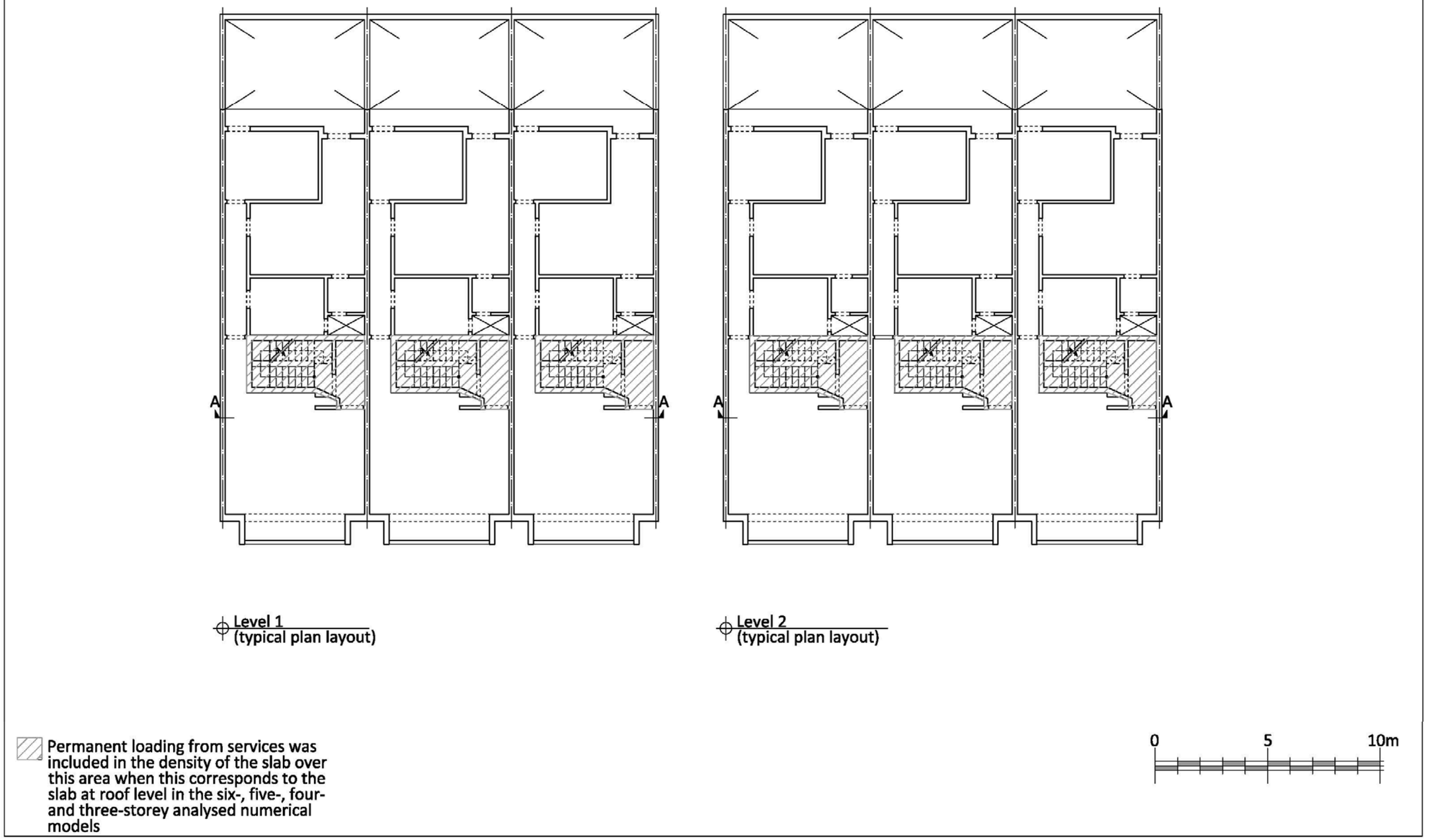

Figure 31 Plan layouts at Levels 1 and 2 for analysed three-building control numerical models (plan length-to-width ratio 0.92:1).

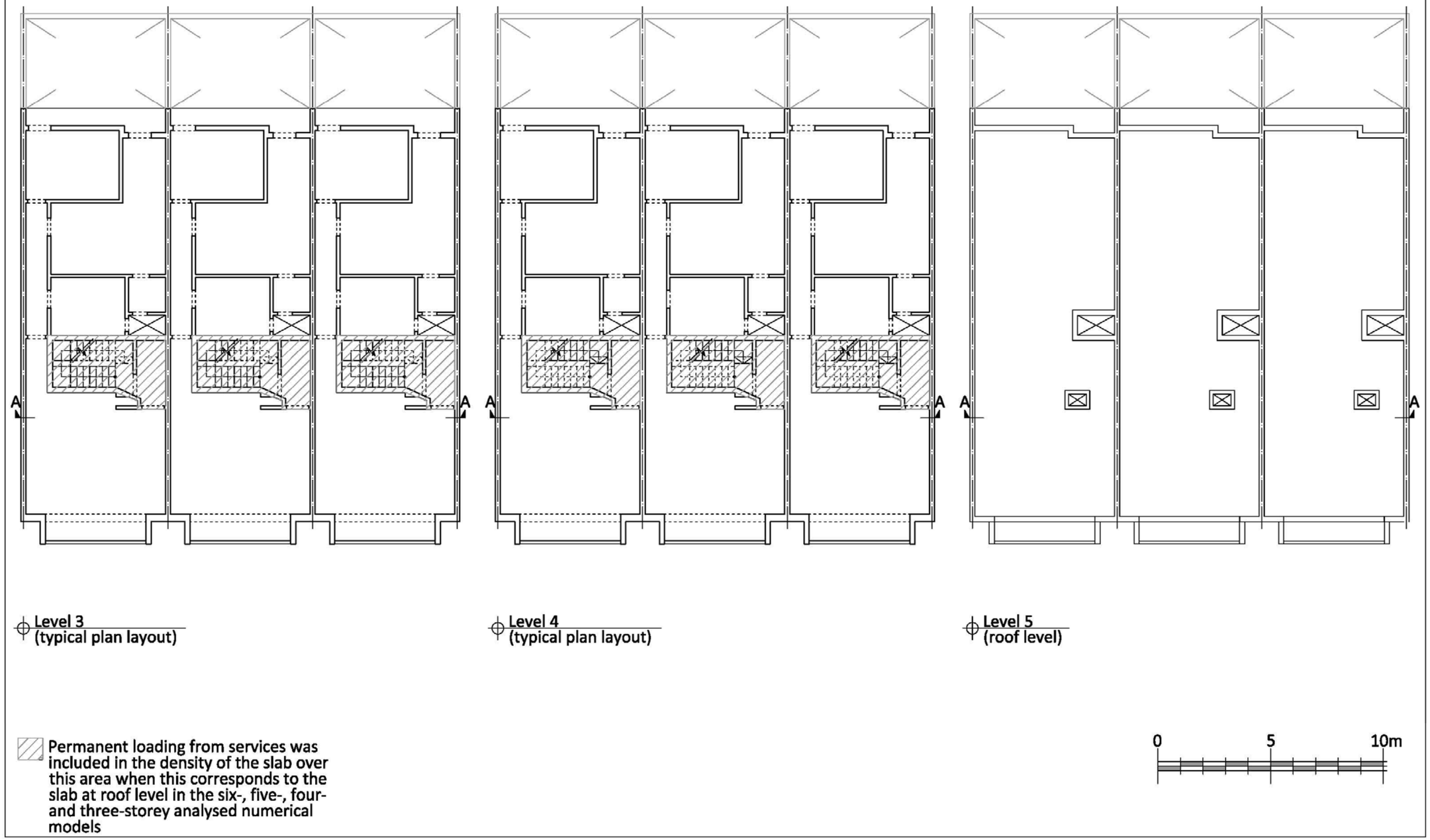

Figure 32 Plan layouts at Levels 3 to 5 for analysed three-building control numerical models (plan length-to-width ratio 0.92:1).

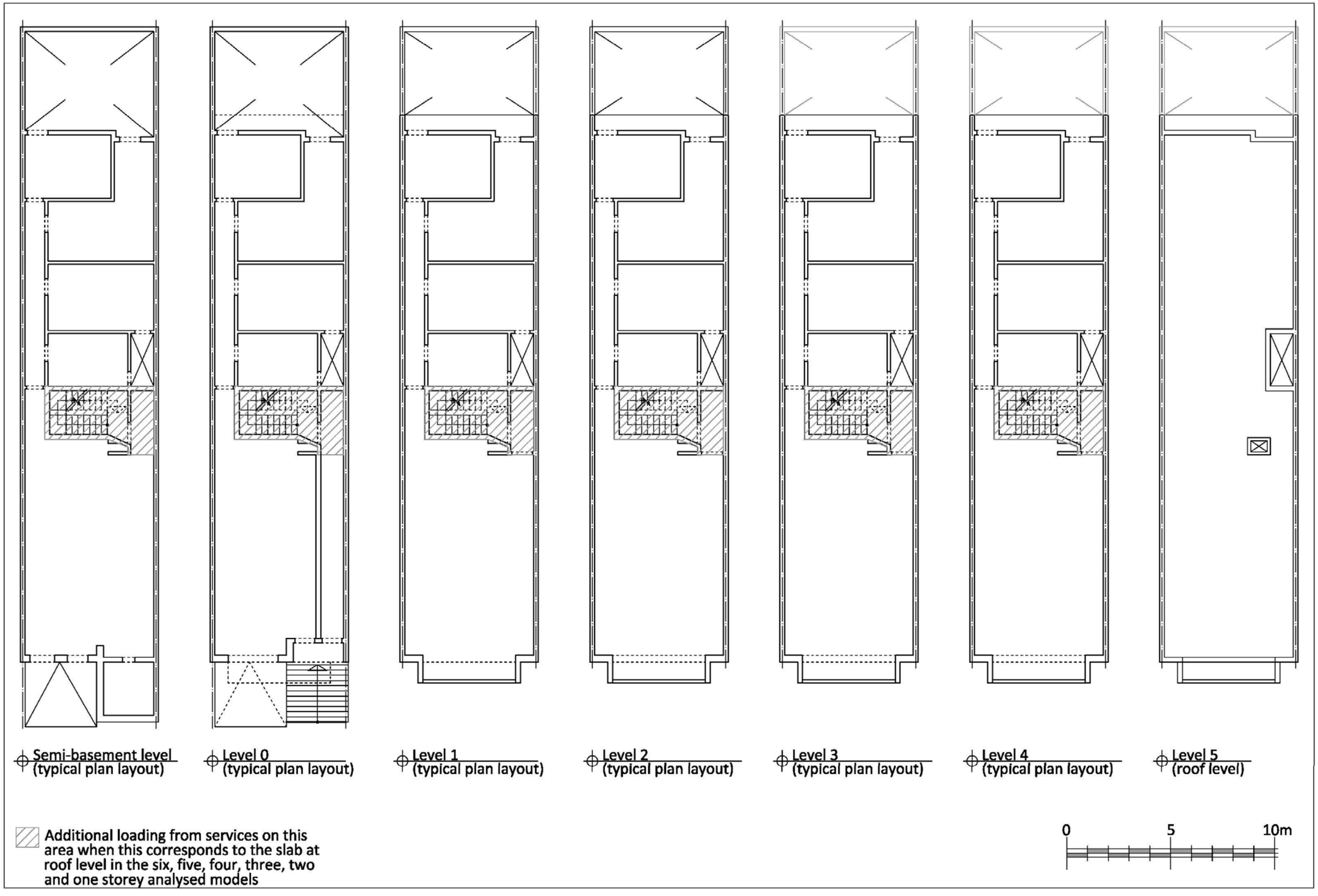

Figure 33 Plan layouts at all levels for analysed single building control numerical models with extended plan layout proportions (plan length-to-width ratio 4:1).

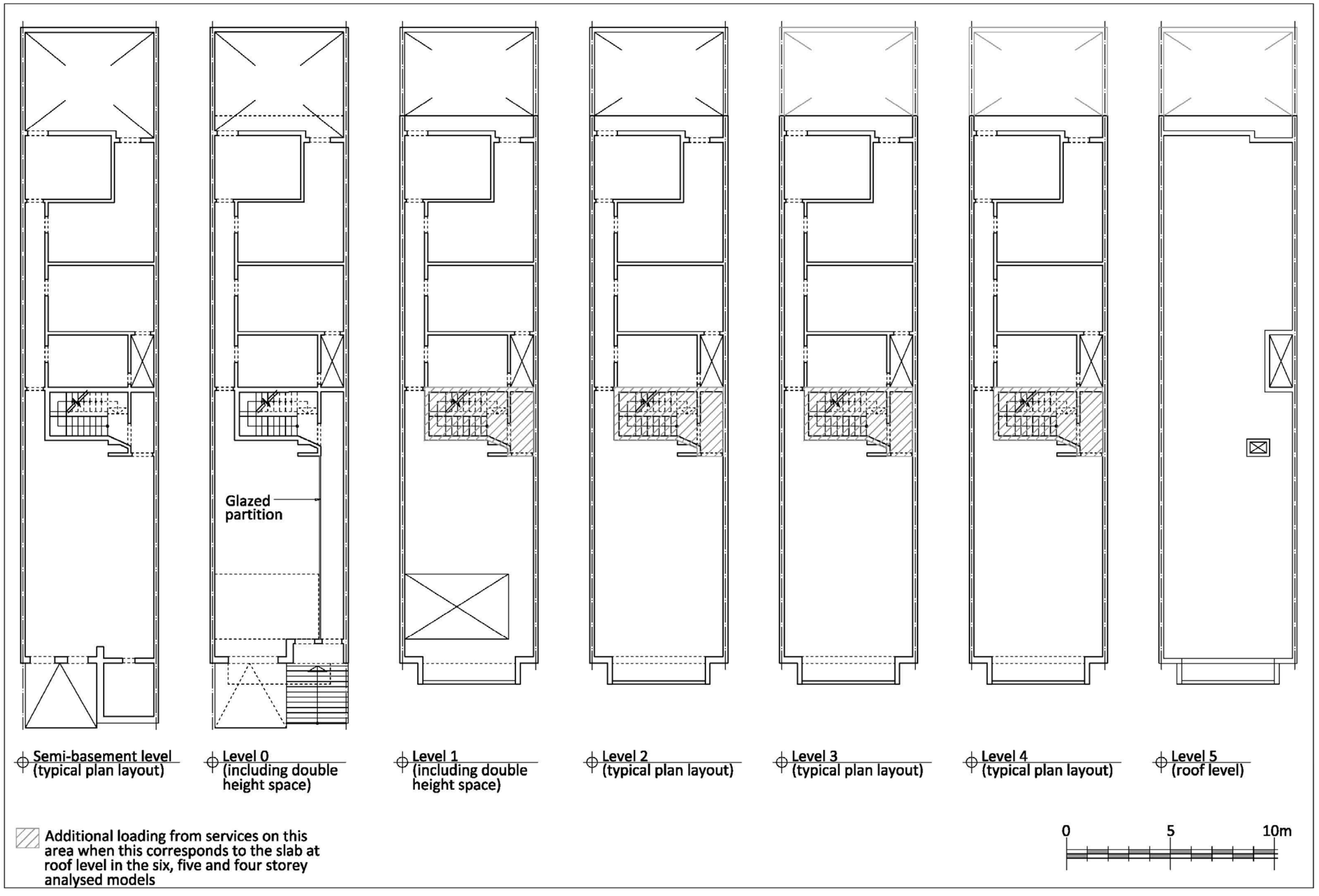

Figure 34 Plan layouts at all levels for analysed single building numerical models including a double height space between Levels 0 and 1 and with extended plan layout proportions (plan length-to-width ratio 4:1).

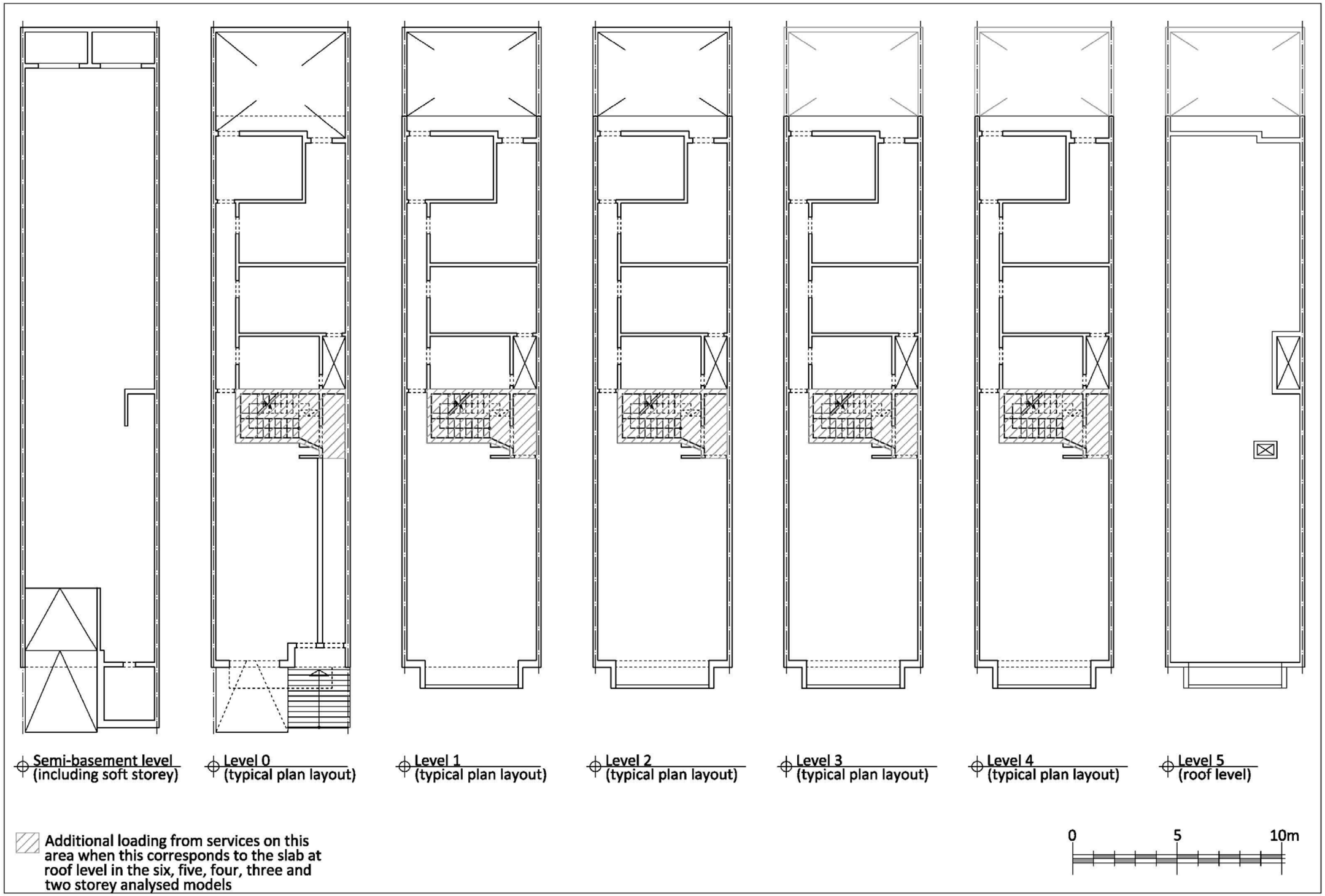

Figure 35 Plan layouts at all levels for analysed single building numerical models including a soft storey at semi-basement level and with extended plan layout proportions (plan length-to-width ratio 4:1).

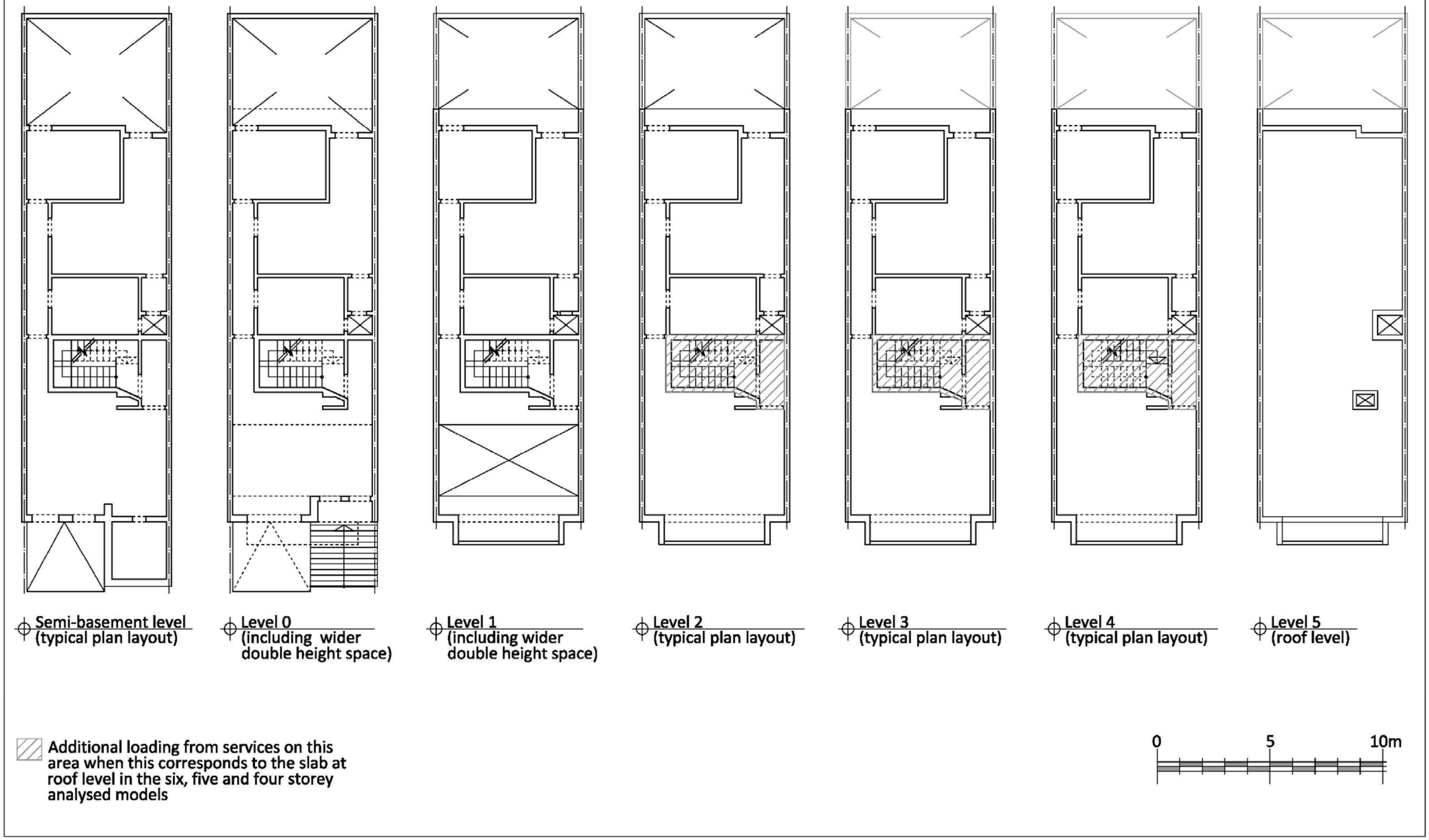

Figure 36 Plan layouts at all levels for analysed single building numerical models including a wider double height space between Levels 0 and 1 spanning the whole width between party walls (plan length-to-width ratio 2.75:1).

Table 28 Wall material properties specified in full scale numerical models analysed using 3Muri®.

	Globigerina limestone masonry (without damp proof course)	Globigerina limestone masonry (with damp proof course)	Hollow concrete blockwork (153 mm thick; without damp proof course)	Hollow concrete blockwork (153 mm thick; with damp proof course)	Hollow concrete blockwork (153 mm - 25 mm gap - 153 mm thick double wall modelled as equivalent 306 mm thick single wall; without damp proof course)	Hollow concrete blockwork (153 mm - 25 mm gap - 153 mm thick double wall modelled as equivalent 306 mm thick single wall; with damp proof course)	Hollow concrete blockwork (228 mm thick, double density; without damp proof course)	Hollow concrete blockwork (228 mm thick, double density; with damp proof course)
Young's Modulus 'E' (N/mm^2)	21000	21000	33000	33000	33000	33000	33000	33000
Shear Modulus 'G' (N/mm^2)	8400	8400	13200	13200	13200	13200	13200	13200
Self-weight 'W' (kg/m^3)	17.260	17.260	12.200	12.200	12.200	12.200	13.360	13.360
Mean compressive strength 'f_m' (N/mm^2)	17.500	17.500	4.838	4.838	4.838	4.838	5.385	5.385
Shear strength limit 'f_{vlim}' (N/mm^2)	0.752	0.554	0.293	0.215	0.293	0.215	0.289	0.213
Characteristic compressive strength of masonry 'f_k' (N/mm^2)	3.978	3.978	2.054	2.054	2.054	2.054	2.038	2.038
Confidence factor 'CF'	1.350	1.350	1.350	1.350	1.350	1.350	1.350	1.350
Partial safety factor for materials 'γ_m'	2.000	2.000	2.000	2.000	2.000	2.000	2.000	2.000
Drift Shear limit	0.0053	0.0053	0.0053	0.0053	0.0053	0.0053	0.0053	0.0053
Drift Bending limit	0.0107	0.0107	0.0107	0.0107	0.0107	0.0107	0.0107	0.0107
Final creep coefficient '$\phi \infty$'	$1x10^{-6}$	$1x10^{-6}$	1.500	1.500	1.500	1.500	1.500	1.500

Table 29 Material properties of concrete and reinforcing steel specified in full scale numerical models analysed using 3Muri®.

Material properties	Concrete grade C25/30	Reinforcing steel in concrete members
Young's Modulus 'E ' (N/mm^2)	33000	200000
Shear Modulus 'G' (N/mm^2)	13750	76923
Self-weight 'W' (kg/m^3)	24	78.50
Mean value of concrete cylinder compressive strength 'f_{cm}' (N/mm^2)	33	
Characteristic compressive cylinder strength of concrete at 28 days 'f_{ck}' (N/mm^2)	25	
Coefficient taking account of long term effects on the compressive strength and of unfavourable effect due to application of load 'α_{cc}'	1	
Mean yield strength of steel reinforcement 'f_{ym}' (N/mm^2)		455.56
Characteristic yield strength of steel reinforcement 'f_{yk}' (N/mm^2)		410.00
Confidence Factor 'CF'	1.35	1.35
Partial safety factor for concrete 'γ_c' or steel reinforcement 'γ_s'	1.50	1.15

Appendix D. RESULTS FROM ELS® NUMERICAL ANALYSIS

Table 30 List of numerical models analysed using ELS® under dynamic loading including the seismic vulnerability characteristics, number of storeys and type of ground formations modelled.

Count	Model reference number	ELS® model name	Building characteristics investigated								Lower ground formation layer			Upper ground formation layer		Ground specified as upper coralline limestone (friction coefficient 1.0) at Minimum Z		Ground specified as clay (friction coefficient 1.0) at Minimum Z	Interface material between ground formation layers
			Number of storeys	Control	Soft storey at semi-basement level	Setbacks at penthouse level	Double height space between Levels 0 and +1	Other (including description)	Single building	2-building aggregate	3-building aggregate	30 m thick upper coralline limestone	30 m thick clay	60 m thick clay	30 m thick upper coralline limestone	1.5 m thick upper coralline limestone	As only ground formation specification	Beneath ground formation layers modelled as 3-dimensional elements	As only ground formation specification	Clay with friction coefficient 1.0
1	42v2	42v2_CTRLa_30rk_ 6flrs_LIVE_accA_REV	6	X					X			X						X		
2	43v2	43v2_CTRLa_rk minz_ 6flrs_INCL LIVE_accA_REV	6	X					X								X			
3	44v2	44v2_CTRLb_30rk on 30 cly_ 6flrs_LIVE_accA_REV	6	X					X				X		X			X		X
4	45v2	45v2_CTRLc_thn rk on cly_ 6flrs_INCL LIVE_accA	6	X					X					X		X		X		X
5	46	46CTRLd_60cly only_ 6flrs_INCL LIVE_accA_RAFT	6	X					X					X				X		
6	47	47CTRLd_cly min z_6flrs_INCL LIVE_accA	6	X					X										X	
7	48	48_CTRLa_30rk only_ 5flrs_LIVE_accA	5	X					X			X						X		
8	49	49_CTRLa_rk minz_ 5flrs_LIVE_accA	5	X					X								X			
9	50	50_CTRLb_30rk 30cly_ 5flrs_LIVE_accA	5	X					X				X		X			X		X
10	51	51_CTRLc_thn rk on cly_ 5flrs_LIVE_accA	5	X					X					X		X		X		X
11	52	52_CTRLd_60cly only_ 5flrs_LIVE_accA	5	X					X					X				X		
12	53	53_CTRLd_CLy minz_ 5flrs_LIVE_accA	5	X					X										X	
13	57	57_CTRLc_thn rk on cly_ 4flrs_LIVE_accA	4	X					X					X		X		X		X
14	58	58_CTRLd_60cly only_ 4flrs_LIVE_accA	4	X					X					X				X		
15	59	59_CTRLd_cly minz_ 4flrs_LIVE_accA	4	X					X										X	
16	63	63_CTRLc_thn rk on cly_3flrs_LIVE_accA	3	X					X					X		X		X		X
17	64	64_CTRLd_60cly only_3flrs_LIVE_accA	3	X					X					X				X		
18	69	69_CTRL wt SSTRYc_thn rk on cly_ 6flrs_LIVE_accA	6	X	X				X					X		X		X		X
19	71	71_CTRL wt SSTRYc_thn rk on cly_ 5flrs_LIVE_accA	5	X	X				X					X		X		X		X
20	73	73_CTRL wt SSTRYc_thn rk on cly_ 4flrs_LIVE_accA	4	X	X				X					X		X		X		X
21	75	75_CTRL wt SSTRYc_thn rk on cly_ 3flrs_LIVE_accA	3	X	X				X					X		X		X		X
22	79	79_CTRL wt STBKc_thn rk on cly_6flrs_LIVE_accA	6	X		X			X					X		X		X		X
23	81	81_CTRL wt STBKc_thn rk on cly_5flrs_LIVE_accA	5	X		X			X					X		X		X		X

Key:

Collapse
No collapse
30m thick upper coralline limestone
Upper coralline limestone at minimum z
30m thick upper coralline limestone on 30m thick clay
1.5m thick upper coralline limestone on 60m thick clay
60m thick clay
clay at minimum z

Table 30 List of numerical models analysed using ELS® under dynamic loading including the seismic vulnerability characteristics, number of storeys and type of ground formations modelled (continued).

Count	Model reference number	ELS® model name	Building characteristics investigated									Lower ground formation layer			Upper ground formation layer		Ground specified as upper coralline limestone (friction coefficient 1.0) at Minimum Z		Ground specified as clay (friction coefficient 1.0) at Minimum Z	Interface material between ground formation layers
			Number of storeys	Control	Soft storey at semi-basement level	Setbacks at penthouse level	Double height space between Levels 0 and +1	Other (including description)	Single building	2-building aggregate	3-building aggregate	30 m thick upper coralline limestone	30 m thick clay	60 m thick clay	30 m thick upper coralline limestone	1.5 m thick upper coralline limestone	As only ground formation specification	Beneath ground formation layers modelled as 3-dimensional elements	As only ground formation specification	Clay with friction coefficient 1.0
24	83	83_CTRL wt STBKc_thn rk on cly_4flrs_LIVE_accA	4	X		X			X					X		X		X		X
25	89	89_CTRL_STBK_SSTRYc_thn rk on cly_6flrs_LIVE_accA	6	X	X	X			X					X		X		X		X
26	91	91_CTRL_STBK_SSTRYc_thn rk on cly_5flrs_LIVE_accA	5	X	X	X			X					X		X		X		X
27	93	93_CTRL_STBK_SSTRYc_thn rk on cly_4flrs_LIVE_accA	4	X	X	X			X					X		X		X		X
28	95	95_CTRL_STBK_SSTRYc_thn rk on cly_3flrs_LIVE_accA	3	X	X	X			X					X		X		X		X
29	99	99_CTRL_DHTc_thn rk on cly_ 6flrs_INCL LIVE_accA	6	X			X		X					X		X		X		X
30	101	101_CTRL_DBL HTc_thn rk on cly_ 5flrs_LIVE_accA	5	X			X		X					X		X		X		X
31	103	103_CTRL_DBL HTc_thn rk on cly_4flrs_LIVE_accA	4	X			X		X					X		X		X		X
32	105	105_CTRL_DBL HTc_thn rk on cly_3flrs_LIVE_accA	3	X			X		X					X		X		X		X
33	109	109_CTRL_SSTRY_D_HTc_thnRKonCY_6flrs_LIVE_accA	6	X	X		X		X					X		X		X		X
34	111	111_CTRL_SSTRY_D_HTc_thnRKonCY_5flrs_LIVE_accA	5	X	X		X		X					X		X		X		X
35	113	113_CTRL_ SSTRY_D_HTc_thn rk on cly_ 4flrs_LIVE_accA	4	X	X		X		X					X		X		X		X
36	115	115_CTRL _SSTRY_D HTc_thnRKonCY_3flrs_LIVE_accA	3	X	X		X		X					X		X		X		X
37	119	119_CTRL_STBK_SSTRY_DHTc_thnRK_CY_6fls_LV_accA	6	X	X	X	X		X					X		X		X		X
38	121	121_CTRL_STBK_SSTRY_DHTc_thnRK_CY_5fls_LV_accA	5	X	X	X	X		X					X		X		X		X
39	123	123_CTRL_STBK_SSTRY_DHTc_thnRK_CY_4fls_LV_accA	4	X	X	X	X		X					X		X		X		X
40	125	125_CTRL_STBK_SSTRY_DHTc_thnRK_CY_3fls_LV_accA	3	X	X	X	X		X					X		X		X		X
41	128	128X11_01c_ThnRk_CY_accA6flrs_InclLIVE_incl Bsmt wlls	6					Exist-ing	X					X		X		X		X
42	129	129X11_01b_30Rk30CY_accA6flrs_InclLIVE_incl Bsmt wlls	6					Exist-ing	X				X		X			X		X
43	130	130_CTRLx2AGG_c_thnRK_CY_6flrs_LIVE_accA	6	X						X				X		X		X		X
44	132	132_CTRLx2AGG_c_thnRK_CY_5flrs_LIVE_accA	5	X						X				X		X		X		X
45	134	134_CTRLx2AGG_c_thnRK_CY_4flrs_LIVE_accA	4	X						X				X		X		X		X
46	136	136_CTRLx2AGG_c_thnRK_CY_3flrs_LIVE_accA	3	X						X				X		X		X		X
47	138	138_CTRLx3AGG_c_thnRK_CY_6flrs_LIVE_accA	6	X							X			X		X		X		X
48	140	140_CTRLx3AGG_c_thnRK_CY_5flrs_LIVE_accA	5	X							X			X		X		X		X
49	142	142_CTRLx3AGG_c_thnRK_CY_4flrs_LIVE_accA	4	X							X			X		X		X		X
50	144	144_CTRLx3AGG_c_thnRK_CY_3flrs_LIVE_accA	3	X							X			X		X		X		X

Key:

Collapse
No collapse
30m thick upper coralline limestone
Upper coralline limestone at minimum z
30m thick upper coralline limestone on 30m thick clay
1.5m thick upper coralline limestone on 60m thick clay
60m thick clay
clay at minimum z

Table 31 Summary of natural frequency results of analysed models.

Modelling of ground	Loading stage	Single building control models Investigated parameters: building height / geology								Existing Xemxija building (XMX 0011)	
		6- storeys		5- storeys		4- storeys		3-storeys		6-storeys	
		Transverse direction	Longitudinal direction	Transverse direction	Longitudinal direction	Transverse direction	Longitudinal direction	Transverse direction	Longitudinal direction	Transverse direction	Longitudinal direction
Ground defined as upper coralline limestone with a friction coefficient of 1.0 at Minimum Z	At end of static loading stage	Model 43v2		Model 49 (no collapse)		Model 55		Model 61		Model X127 (Incl. Live) 2 Modes	
		3.882 Hz	6.579 Hz	5.067 Hz	7.951 Hz	6.744 Hz	9.757 Hz	9.218 Hz	9.856 Hz	3.804 Hz	7.413 Hz
	At end of dynamic loading stage	Model 43v2b (collapse)		Model 49b (no collapse)		Model 55b (no collapse)		Model 61b (no collapse)		Model X127b (collapse)	
		0.771 Hz	0.726 Hz	4.829 Hz	7.409 Hz	6.419 Hz	9.216 Hz	9.066 Hz	9.637 Hz	0.392 Hz	0.855 Hz
Natural frequency at end of the dynamic loading stage as a percentage of that at the end of the static loading stage		19.9%	11.0%	95.3%	93.2%	95.2%	94.5%	98.4%	97.8%	10.3%	11.5%
Ground defined as clay with a friction coefficient of 1.0 at Minimum Z	At end of static loading stage	Model 47c (collapse)		Model 49c (collapse)		Model 59b (no collapse)		Model 64c (no collapse)		Model X127c (collapse)	
		2.623 Hz	5.487 Hz	3.341 Hz	6.500 Hz	5.309 Hz	8.593 Hz	5.904 Hz	9.311 Hz	2.589 Hz	5.727 Hz
	At end of dynamic loading stage	0.712 Hz	1.501 Hz	1.163 Hz	2.329 Hz	5.131 Hz	8.059 Hz	5.673 Hz	8.822 Hz	1.227 Hz	2.813 Hz
Natural frequency at end of the dynamic loading stage as a percentage of that at the end of the static loading stage		27.1%	27.4%	34.8%	35.8%	96.6%	93.8%	96.1%	94.7%	47.4%	49.1%
Natural frequency at end of the static loading stage stage when analysed on clay at Minimum Z as a percentage of that obtained when analysed on UCL at Minimum Z		67.6%	83.4%	65.9%	81.8%	78.7%	88.1%	64.0%	94.5%	68.1%	77.3%
Natural frequency at end of the dynamic loading stage stage when analysed on clay at Minimum Z as a percentage of that obtained when analysed on UCL at Minimum Z		92.3%	206.7%	23.5%	31.4%	79.9%	87.4%	62.6%	91.5%	313.0%	329.0%

Table 31 Summary of natural frequency results of analysed models (continued).

Modelling of ground	Loading stage	Single building control models with a soft storey at semi-basement level							
		6-storeys		5-storeys		4-storeys		3-storeys	
		Transverse direction	Longitudinal direction	Transverse direction	Longitudinal direction	Transverse direction	Longitudinal direction	Transverse direction	Longitudinal direction
Ground defined as upper coralline limestone with a friction coefficient of 1.0 at Minimum Z	At end of static loading stage	Model 70v2		Model 72		Model 74		Model 76	
		3.539 Hz	6.708 Hz	4.513 Hz	8.144 Hz	5.798 Hz	10.131 Hz	7.593 Hz	13.109 Hz
	At end of dynamic loading stage	Natural frequency at the end of the dynamic stage was not estimated for these models		Natural frequency at the end of the dynamic stage was not estimated for these models		Natural frequency at the end of the dynamic stage was not estimated for these models		Model 76b (no collapse)	
								6.259 Hz	11.643 Hz
Natural frequency at end of the dynamic loading stage as a percentage of that at the end of the static loading stage		N/A	N/A	N/A	N/A	N/A	N/A	82.4%	88.8%
Ground defined as clay with a friction coefficient of 1.0 at Minimum Z	At end of static loading stage	Model 70v2d (collapse)		Model 72d (collapse)		Model 74d (collapse)		Model 76c (no collapse)	
		2.416 Hz	5.167 Hz	3.019 Hz	6.742 Hz	3.848 Hz	8.658 Hz	5.038 Hz	11.022 Hz
	At end of dynamic loading stage	Natural frequency at the end of the dynamic stage was not estimated for these models		Natural frequency at the end of the dynamic stage was not estimated for these models		Natural frequency at the end of the dynamic stage was not estimated for these models		3.522 Hz	8.129 Hz
Natural frequency at end of the dynamic loading stage as a percentage of that at the end of the static loading stage		N/A	N/A	N/A	N/A	N/A	N/A	69.9%	73.8%
Natural frequency at end of the static loading stage stage when analysed on clay at Minimum Z as a percentage of that obtained when analysed on UCL at Minimum Z		68.3%	77.0%	66.9%	82.8%	66.4%	85.5%	66.4%	84.1%
Natural frequency at end of the dynamic loading stage stage when analysed on clay at Minimum Z as a percentage of that obtained when analysed on UCL at Minimum Z		N/A	N/A	N/A	N/A	N/A	N/A	56.3%	69.8%

Table 31 Summary of natural frequency results of analysed models (continued).

Modelling of ground	Loading stage	Single building control models with setbacks at penthouse level					
		6-storeys		5-storeys		4-storeys	
		Transverse direction	Longitudinal direction	Transverse direction	Longitudinal direction	Transverse direction	Longitudinal direction
Ground defined as upper coralline limestone with a friction coefficient of 1.0 at Minimum Z	At end of static loading stage	Model 80		Model 82		Model 84	
		4.167 Hz	7.224 Hz	5.478 Hz	8.945 Hz	7.331 Hz	9.768 Hz
	At end of dynamic loading stage	Natural frequency at the end of the dynamic stage was not estimated for these models		Natural frequency at the end of the dynamic stage was not estimated for these models		Model 84b (no collapse)	
						7.086 Hz	9.427 Hz
Natural frequency at end of the dynamic loading stage as a percentage of that at the end of the static loading stage		N/A	N/A	N/A	N/A	96.7%	96.5%
Ground defined as clay with a friction coefficient of 1.0 at Minimum Z	At end of static loading stage	Model 80d (collapse)		Model 82d (collapse)		Model 84c (no collapse)	
		2.782 Hz	5.874 Hz	3.579 Hz	7.262 Hz	4.697 Hz	8.672 Hz
	At end of dynamic loading stage	Natural frequency at the end of the dynamic stage was not estimated for these models		Natural frequency at the end of the dynamic stage was not estimated for these models		4.548 Hz	8.306 Hz
Natural frequency at end of the dynamic loading stage as a percentage of that at the end of the static loading stage		N/A	N/A	N/A	N/A	96.8%	95.8%
Natural frequency at end of the static loading stage stage when analysed on clay at Minimum Z as a percentage of that obtained when analysed on UCL at Minimum Z		66.9%	81.3%	65.3%	81.2%	64.1%	88.8%
Natural frequency at end of the dynamic loading stage stage when analysed on clay at Minimum Z as a percentage of that obtained when analysed on UCL at Minimum Z		N/A	N/A	N/A	N/A	64.2%	88.1%

Table 31 Summary of natural frequency results of analysed models (continued).

Modelling of ground	Loading stage	Single building control models with a double height space between Levels 0 and +1							
		6-storeys		5-storeys		4-storeys		3-storeys	
		Transverse direction	Longitudinal direction	Transverse direction	Longitudinal direction	Transverse direction	Longitudinal direction	Transverse direction	Longitudinal direction
Ground defined as upper coralline limestone with a friction coefficient of 1.0 at Minimum Z	At end of static loading stage	Model 100		Model 102		Model 104		Model 106	
		3.784 Hz	6.549 Hz	5.058 Hz	7.906 Hz	6.727 Hz	9.709 Hz	9.254 Hz	9.855 Hz
	At end of dynamic loading stage	Natural frequency at the end of the dynamic stage was not estimated for these models		Natural frequency at the end of the dynamic stage was not estimated for these models		Natural frequency at the end of the dynamic stage was not estimated for these models		Model 106b (no collapse)	
								9.097 Hz	9.623 Hz
Natural frequency at end of the dynamic loading stage as a percentage of that at the end of the static loading stage		N/A	N/A	N/A	N/A	N/A	N/A	98.3%	97.6%
Ground defined as clay with a friction coefficient of 1.0 at Minimum Z	At end of static loading stage	Model 100d (collapse)		Model 102d (collapse)		Model 104d (collapse)		Model 106c (no collapse)	
		2.624 Hz	5.494 Hz	3.347 Hz	6.497 Hz	4.390 Hz	7.803 Hz	5.952 Hz	9.013 Hz
	At end of dynamic loading stage	Natural frequency at the end of the dynamic stage was not estimated for these models		Natural frequency at the end of the dynamic stage was not estimated for these models		Natural frequency at the end of the dynamic stage was not estimated for these models		5.715 Hz	8.784 Hz
Natural frequency at end of the dynamic loading stage as a percentage of that at the end of the static loading stage		N/A	N/A	N/A	N/A	N/A	N/A	96.0%	97.5%
Natural frequency at end of the static loading stage stage when analysed on clay at Minimum Z as a percentage of that obtained when analysed on UCL at Minimum Z		69.3%	83.9%	66.2%	82.2%	65.3%	80.4%	64.3%	91.5%
Natural frequency at end of the dynamic loading stage stage when analysed on clay at Minimum Z as a percentage of that obtained when analysed on UCL at Minimum Z		N/A	N/A	N/A	N/A	N/A	N/A	62.8%	91.3%

Table 31 Summary of natural frequency results of analysed models (continued).

Modelling of ground	Loading stage	Single building control models with a soft storey at semi-basement level and setbacks at penthouse level								Single building control models with a soft storey at semi-basement level and a double height space between Levels 0 and +1							
		6-storeys		5-storeys		4-storeys		3-storeys		6-storeys		5-storeys		4-storeys		3-storeys	
		Transverse direction	Longitudinal direction	Transverse direction	Longitudinal direction	Transverse direction	Longitudinal direction	Transverse direction	Longitudinal direction	Transverse direction	Longitudinal direction	Transverse direction	Longitudinal direction	Transverse direction	Longitudinal direction	Transverse direction	Longitudinal direction
Ground defined as upper coralline limestone with a friction coefficient of 1.0 at Minimum Z	At end of static loading stage	Model 90		Model 92		Model 94		Model 96		Model 110		Model 112		Model 114		Model 116	
		3.773 Hz	7.346 Hz	4.831 Hz	9.149 Hz	6.206 Hz	11.593 Hz	8.207 Hz	15.049 Hz	3.528 Hz	6.660 Hz	4.511 Hz	8.086 Hz	5.808 Hz	10.027 Hz	7.641 Hz	12.825 Hz
	At end of dynamic loading stage	Natural frequency at the end of the dynamic stage was not estimated for these models		Natural frequency at the end of the dynamic stage was not estimated for these models		Natural frequency at the end of the dynamic stage was not estimated for these models		Model 96b (no collapse)		Natural frequency at the end of the dynamic stage was not estimated for these models		Natural frequency at the end of the dynamic stage was not estimated for these models		Natural frequency at the end of the dynamic stage was not estimated for these models		Model 116b (no collapse)	
								6.864 Hz	13.025 Hz							6.351 Hz	11.454 Hz
Natural frequency at end of the dynamic loading stage as a percentage of that at the end of the static loading stage		N/A	N/A	N/A	N/A	N/A	N/A	83.6%	86.6%	N/A	N/A	N/A	N/A	N/A	N/A	83.1%	89.3%
Ground defined as clay with a friction coefficient of 1.0 at Minimum Z	At end of static loading stage	Model 90d (collapse)		Model 92d (collapse)		Model 94d (collapse)		Model 96c (no collapse)		Model 110d (collapse)		Model 112d (collapse)		Model 114d (collapse)		Model 116c (no collapse)	
		2.556 Hz	5.626 Hz	3.221 Hz	7.241 Hz	4.144 Hz	9.300 Hz	5.494 Hz	11.011 Hz	2.408 Hz	5.325 Hz	3.026 Hz	6.757 Hz	3.876 Hz	8.656 Hz	5.110 Hz	10.968 Hz
	At end of dynamic loading stage	Natural frequency at the end of the dynamic stage was not estimated for these models		Natural frequency at the end of the dynamic stage was not estimated for these models		Natural frequency at the end of the dynamic stage was not estimated for these models		4.038 Hz	8.587 Hz	Natural frequency at the end of the dynamic stage was not estimated for these models		Natural frequency at the end of the dynamic stage was not estimated for these models		Natural frequency at the end of the dynamic stage was not estimated for these models		3.58 9Hz	8.203 Hz
Natural frequency at end of the dynamic loading stage as a percentage of that at the end of the static loading stage		N/A	N/A	N/A	N/A	N/A	N/A	73.5%	78.0%	N/A	N/A	N/A	N/A	N/A	N/A	70.2%	74.8%
Natural frequency at end of the static loading stage stage when analysed on clay at Minimum Z as a percentage of that obtained when analysed on UCL at Minimum Z		67.7%	76.6%	66.7%	79.1%	66.8%	80.2%	66.9%	73.2%	68.3%	80.0%	67.1%	83.6%	66.7%	86.3%	66.9%	85.5%
Natural frequency at end of the dynamic loading stage stage when analysed on clay at Minimum Z as a percentage of that obtained when analysed on UCL at Minimum Z		N/A	N/A	N/A	N/A	N/A	N/A	58.8%	65.9%	N/A	N/A	N/A	N/A	N/A	N/A	56.5%	71.6%

Table 31 Summary of natural frequency results of analysed models (continued).

Modelling of ground	Loading stage	Single building control models with a soft storey at semi-basement level, setbacks at penthouse level and a double height space between Levels 0 and +1							
		6-storeys		5-storeys		4-storeys		3-storeys	
		Transverse direction	Longitudinal direction	Transverse direction	Longitudinal direction	Transverse direction	Longitudinal direction	Transverse direction	Longitudinal direction
Ground defined as upper coralline limestone with a friction coefficient of 1.0 at Minimum Z	At end of static loading stage	Model 120		Model 122		Model 124		Model 126	
		3.764 Hz	7.298 Hz	4.827 Hz	9.089 Hz	6.230 Hz	11.509 Hz	8.291 Hz	15.075 Hz
	At end of dynamic loading stage	Natural frequency at the end of the dynamic stage was not estimated for these models		Natural frequency at the end of the dynamic stage was not estimated for these models		Natural frequency at the end of the dynamic stage was not estimated for these models		Model 126b (no collapse)	
								6.967 Hz	13.132 Hz
Natural frequency at end of the dynamic loading stage as a percentage of that at the end of the static loading stage		N/A	N/A	N/A	N/A	N/A	N/A	84.0%	87.1%
Ground defined as clay with a friction coefficient of 1.0 at Minimum Z	At end of static loading stage	Model 120d (collapse)		Model 122d (collapse)		Model 124d (collapse)		Model 126c (no collapse)	
		2.554 Hz	5.677 Hz	3.234 Hz	7.230 Hz	4.180 Hz	9.322 Hz	5.586 Hz	11.167 Hz
	At end of dynamic loading stage	Natural frequency at the end of the dynamic stage was not estimated for these models		Natural frequency at the end of the dynamic stage was not estimated for these models		Natural frequency at the end of the dynamic stage was not estimated for these models		4.314 Hz	8.570 Hz
Natural frequency at end of the dynamic loading stage as a percentage of that at the end of the static loading stage		N/A	N/A	N/A	N/A	N/A	N/A	77.2%	76.7%
Natural frequency at end of the static loading stage stage when analysed on clay at Minimum Z as a percentage of that obtained when analysed on UCL at Minimum Z		67.9%	77.8%	67.0%	79.5%	67.1%	81.0%	67.4%	74.1%
Natural frequency at end of the dynamic loading stage stage when analysed on clay at Minimum Z as a percentage of that obtained when analysed on UCL at Minimum Z		N/A	N/A	N/A	N/A	N/A	N/A	61.9%	65.3%

Table 31 Summary of natural frequency results of analysed models (continued).

Modelling of ground	Loading stage	2-building control models								3-building control models							
		6-storeys		5-storeys		4-storeys		3-storeys		6-storeys		5-storeys		4-storeys		3-storeys	
		Transverse direction	Longitudinal direction	Transverse direction	Longitudinal direction	Transverse direction	Longitudinal direction	Transverse direction	Longitudinal direction	Transverse direction	Longitudinal direction	Transverse direction	Longitudinal direction	Transverse direction	Longitudinal direction	Transverse direction	Longitudinal direction
Ground defined as upper coralline limestone with a friction coefficient of 1.0 at Minimum Z	At end of static loading stage	Model 131		Model 133		Model 135		Model 137		Model 139		Model 141		Model 143		Model 145	
		4.793 Hz	6.759 Hz	6.033 Hz	8.788 Hz	7.766 Hz	9.448 Hz	9.559 Hz	10.399 Hz	5.151 Hz	6.501 Hz	6.393 Hz	8.632 Hz	8.120 Hz	10.041 Hz	9.937 Hz	10.728 Hz
	At end of dynamic loading stage	Natural frequency at the end of the dynamic stage was not estimated for these models		Natural frequency at the end of the dynamic stage was not estimated for these models		Natural frequency at the end of the dynamic stage was not estimated for these models		Model 137b (no collapse)		Natural frequency at the end of the dynamic stage was not estimated for these models		Natural frequency at the end of the dynamic stage was not estimated for these models		Natural frequency at the end of the dynamic stage was not estimated for these models		Model 145b (no collapse)	
								9.541 Hz	10.194 Hz							9.567 Hz	10.542 Hz
Natural frequency at end of the dynamic loading stage as a percentage of that at the end of the static loading stage		N/A	N/A	N/A	N/A	N/A	N/A	99.8%	98.0%	N/A	N/A	N/A	N/A	N/A	N/A	96.3%	98.3%
Ground defined as clay with a friction coefficient of 1.0 at Minimum Z	At end of static loading stage	Model 131d (collapse)		Model 133d (collapse)		Model 135d (collapse)		Model 137c (no collapse)		Model 139d (collapse)		Model 141d (collapse)		Model 143d (collapse)		Model 145c (no collapse)	
		3.437 Hz	4.945 Hz	4.271 Hz	6.531 Hz	5.408 Hz	8.329 Hz	7.011 Hz	8.534 Hz	3.836 Hz	4.714 Hz	4.707 Hz	6.298 Hz	5.852 Hz	8.450 Hz	7.438 Hz	9.250 Hz
	At end of dynamic loading stage	Natural frequency at the end of the dynamic stage was not estimated for these models		Natural frequency at the end of the dynamic stage was not estimated for these models		Natural frequency at the end of the dynamic stage was not estimated for these models		6.642 Hz	8.312 Hz	Natural frequency at the end of the dynamic stage was not estimated for these models		Natural frequency at the end of the dynamic stage was not estimated for these models		Natural frequency at the end of the dynamic stage was not estimated for these models		7.070 Hz	8.826 Hz
Natural frequency at end of the dynamic loading stage as a percentage of that at the end of the static loading stage		N/A	N/A	N/A	N/A	N/A	N/A	94.70%	97.40%	N/A	N/A	N/A	N/A	N/A	N/A	95.10%	95.40%
Natural frequency at end of the static loading stage stage when analysed on clay at Minimum Z as a percentage of that obtained when analysed on UCL at Minimum Z		71.7%	73.2%	70.8%	74.3%	69.6%	88.2%	73.3%	82.1%	74.5%	72.5%	73.6%	73.0%	72.1%	84.2%	74.9%	86.2%
Natural frequency at end of the dynamic loading stage stage when analysed on clay at Minimum Z as a percentage of that obtained when analysed on UCL at Minimum Z		N/A	N/A	N/A	N/A	N/A	N/A	69.6%	81.6%	N/A	N/A	N/A	N/A	N/A	N/A	73.9%	83.7%

Table 32 Percentage increase in natural frequency under static loading in the transverse direction with every reduction in number of floors.

	6-5 storeys				5-4 storeys				4-3 storeys			
	Average percentage increase in natural frequency throughout all analysed cases (%)	Average percentage increase in natural frequency in control models, and models which include setbacks or double height spaces as the only additional seismic vulnerability characteristic (%)	Average percentage increase in natural frequency in models which include a soft storey at semi-basement level as the only additional seismic vulnerability characteristic or in combination with setbacks and/ or double height spaces (%)	Average percentage increase in natural frequency in models which consist of 2- or 3-control building aggregates (%)	Average percentage increase in natural frequency throughout all analysed cases (%)	Average percentage increase in natural frequency in control models, and models which include setbacks or double height spaces as the only additional seismic vulnerability characteristic (%)	Average percentage increase in natural frequency in models which include a soft storey at semi-basement level as the only additional seismic vulnerability characteristic or in combination with setbacks and/ or double height spaces (%)	Average percentage increase in natural frequency in models which consist of 2- or 3-control building aggregates (%)	Average percentage increase in natural frequency throughout all analysed cases (%)	Average percentage increase in natural frequency in control models, and models which include setbacks or double height spaces as the only additional seismic vulnerability characteristic (%)	Average percentage increase in natural frequency in models which include a soft storey at semi-basement level as the only additional seismic vulnerability characteristic or in combination with setbacks and/ or double height spaces (%)	Average percentage increase in natural frequency in models which consist of 2- or 3-control building aggregates (%)
Structural models analysed on upper coralline limestone at Minimum Z	28.589	31.885	27.917	24.991	30.046	33.307	28.688	27.870	30.945	36.025	31.961	22.732
Structural models analysed on clay at Minimum Z	25.979	27.858	25.816	23.486	31.745	40.435	28.364	25.473	29.063	26.009	32.244	28.372

Table 33 Percentage increase in natural frequency under static loading in the longitudinal direction with every reduction in number of floors.

	6-5 storeys				5-4 storeys				4-3 storeys			
	Average percentage increase in natural frequency throughout all analysed cases (%)	Average percentage increase in natural frequency in control models, and models which include setbacks or double height spaces as the only additional seismic vulnerability characteristic (%)	Average percentage increase in natural frequency in models which include a soft storey at semi-basement level as the only additional seismic vulnerability characteristic or in combination with setbacks and/ or double height spaces (%)	Average percentage increase in natural frequency in models which consist of 2- or 3-control building aggregates (%)	Average percentage increase in natural frequency throughout all analysed cases (%)	Average percentage increase in natural frequency in control models, and models which include setbacks or double height spaces as the only additional seismic vulnerability characteristic (%)	Average percentage increase in natural frequency in models which include a soft storey at semi-basement level as the only additional seismic vulnerability characteristic or in combination with setbacks and/ or double height spaces (%)	Average percentage increase in natural frequency in models which consist of 2- or 3-control building aggregates (%)	Average percentage increase in natural frequency throughout all analysed cases (%)	Average percentage increase in natural frequency in control models, and models which include setbacks or double height spaces as the only additional seismic vulnerability characteristic (%)	Average percentage increase in natural frequency in models which include a soft storey at semi-basement level as the only additional seismic vulnerability characteristic or in combination with setbacks and/ or double height spaces (%)	Average percentage increase in natural frequency in models which consist of 2- or 3-control building aggregates (%)
Structural models analysed on upper coralline limestone at Minimum Z	24.456	21.799	22.976	31.399	20.033	18.240	25.435	11.917	17.190	1.259	29.524	8.454
Structural models analysed on clay at Minimum Z	26.606	20.116	28.359	32.837	27.479	23.906	28.473	30.850	15.999	11.931	23.051	5.964

Table 34 Predominant frequencies in acceleration spectrum within main energy range of input ground motion record and energy distribution of frequency spectrum at 4 positions in every analysed model.

			Mid-depth through of clay layer			Mid-depth of upper coralline limestone layer or whole thickness in case of 1.5 m thick layer			First course			Slab over semi-basement level			Possibility of resonant behaviour in subsoil layers (not pure resonance) (Y/N)	
Count	Model reference number	ELS® Model Name	Peak frequency (Hz)	Secondary frequencies within main energy range of input ground motion record (Hz)	Energy distribution of frequency spectrum	Peak frequency (Hz)	Secondary frequencies within main energy range of input ground motion record (Hz)	Energy distribution of frequency spectrum	Peak frequency (Hz)	Secondary frequencies within main energy range of input ground motion record (Hz)	Energy distribution of frequency spectrum	Peak frequency (Hz)	Secondary frequencies within main energy range of input ground motion record (Hz)	Energy distribution of frequency spectrum	Mid-depth of clay	Mid-depth of upper coralline limestone (or whole thickness in 1.5 m thick case)
1	42v2	42v2_CTRLa_30rk_6flrs_LIVE_accA_REV	N/A	N/A	N/A	27.93	2.93, 6.54	Distributed in four main zones throughout frequency range. Highest energy content between 27.93-34.18 Hz	45.61	6.05	Increasing energy content in higher frequencies. Highest energy content between 45.61-48.93 Hz	46.39	4.69	Almost even distribution throughout most of frequency range	N/A	Y
2	43v2	43v2_CTRLa_rk minz_6flrs_INCLLIVE_accA_REV	N/A	N/A	N/A	N/A	N/A	N/A	46.78	N/A	Main energy content between 46.78 -49.71 Hz	36.04	N/A	Almost even distribution throughout most of frequency range. Highest energy content between 31.84 -36.04 Hz	N/A	N/A
3	44v2	44v2_CTRLb_30rk on 30 cly_6flrs_LIVE_accA_REV	49.8	2.15, 5.96	Main energy content between 42.58-49.80 Hz	1.86	5.96	Main energy content between 1.00-3.00 Hz	41.21	2.05, 4.00	Increasing energy content in higher frequencies. Highest energy content between 35.35-47.75 Hz	33.69	2.83	Almost even distribution throughout most of frequency range	Y	Y
4	45v2	45v2_CTRLc_thn rk on cly_6flrs_INCLLIVE_accA	47.66	3.52	Main energy content between 46.00-49.50 Hz	2.93	5.96	Main energy content between 2.93 - 4.00 Hz	21.58	2.93, 5.57	Main energy distributed between 17.50 -48.83 Hz	31.5	1.75, 6.5	Most energy content distributed between 27.50-42.00 Hz	N	Y
5	46	46CTRLd_60cly only_6flrs_INCLLIVE_accA_RAFT	45.3	N/A	Main energy content between 48.73-50.00 Hz	N/A	N/A	N/A	30.08	0.78, 6.45	Almost even distribution throughout frequency range	33.3	3.52	Almost even distribution throughout frequency range. Higher energy content around 27.44 Hz, 33.30 Hz and between 38.5-47.5 Hz	N	N/A
6	47	47CTRLd_cly minz_6flrs_INCLLIVE_accA	N/A	N/A	N/A	N/A	N/A	N/A	41.99	2.93, 6.54	Almost even distribution throughout frequency range	38.96	2.05	Main energy distributed between 31.00-40.00 Hz	N/A	N/A

Key:

Possibility of resonant behaviour

Resonant behaviour unlikely

Table 34 Predominant frequencies in acceleration spectrum within main energy range of input ground motion record and energy distribution of frequency spectrum at 4 positions in every analysed model (continued).

Count	Model reference number	ELS® Model Name	Mid-depth through of clay layer			Mid-depth of upper coralline limestone layer or whole thickness in case of 1.5 m thick layer			First course			Slab over semi-basement level			Possibility of resonant behaviour in subsoil layers (not pure resonance) (Y/N)	
			Peak frequency (Hz)	Secondary frequencies within main energy range of input ground motion record (Hz)	Energy distribution of frequency spectrum	Peak frequency (Hz)	Secondary frequencies within main energy range of input ground motion record (Hz)	Energy distribution of frequency spectrum	Peak frequency (Hz)	Secondary frequencies within main energy range of input ground motion record (Hz)	Energy distribution of frequency spectrum	Peak frequency (Hz)	Secondary frequencies within main energy range of input ground motion record (Hz)	Energy distribution of frequency spectrum	Mid-depth of clay	Mid-depth of upper coralline limestone (or whole thickness in 1.5 m thick case)
7	48	48_CTRLa_30rk only_5flrs_LIVE_accA	N/A	N/A	N/A	27.93	2.93, 6.54	Distributed in four main zones throughout frequency range. Highest energy content between 27.93-32.00 Hz	3.43	6.54	Main energy content around 3.43 Hz and between 18.50 and 31.50 Hz	3.42	5.96	Main energy content around 3.43 Hz	N/A	Y
8	49	49_CTRLa_rk minz_5flrs_LIVE_accA	N/A	N/A	N/A	N/A	N/A	N/A	4.59	N/A	Main energy content around 4.59 Hz and between 44.24 - 47.07 Hz	4.79	N/A	Main energy content around 4.79 Hz	N/A	N/A
9	50	50_CTRLb_30rk 30cly_5flrs_LIVE_accA	47.75	2.15, 5.96	Main energy content between 44.50-50.00Hz. Significant energy content also between 2.15-3 Hz	1.86	5.96	Main energy content between 0.80-3.00 Hz	1.86	5.96	Main energy content between 0.80-3.00 Hz	1.86	5.96	Main energy content between 0.80-3.00 Hz	Y	Y
10	51	51_CTRLc_thn rk on cly_5flrs_LIVE_accA	49.02	2.93	Main energy content between 46.88-49.02 Hz	2.93	5.96	Main energy content between 2.93-4.00 Hz	39.06	2.83	Main energy content between 22.5-23.34 Hz and between 34.47-40.80 Hz	39.36	1.07, 2.93, 5.18	Increasing energy content in higher frequencies. Highest energy content between 32.52-49.80 Hz	Y	Y
11	52	52_CTRLd_60cly only_5flrs_LIVE_accA	48.54	N/A	Main energy content between 44.50-48.54 Hz	N/A	N/A	N/A	37.7	4.39	Main energy content between 34.5-42.194 Hz	31.74	4.00	Increasing energy content in higher frequencies. Highest energy content between 29.80-34.50 Hz	N	N

Key:

Possibility of resonant behaviour

Resonant behaviour unlikely

Table 34 Predominant frequencies in acceleration spectrum within main energy range of input ground motion record and energy distribution of frequency spectrum at 4 positions in every analysed model (continued).

Count	Model reference number	ELS® Model Name	Mid-depth through of clay layer			Mid-depth of upper coralline limestone layer or whole thickness in case of 1.5 m thick layer			First course			Slab over semi-basement level			Possibility of resonant behaviour in subsoil layers (not pure resonance) (Y/N)	
			Peak frequency (Hz)	Secondary frequencies within main energy range of input ground motion record (Hz)	Energy distribution of frequency spectrum	Peak frequency (Hz)	Secondary frequencies within main energy range of input ground motion record (Hz)	Energy distribution of frequency spectrum	Peak frequency (Hz)	Secondary frequencies within main energy range of input ground motion record (Hz)	Energy distribution of frequency spectrum	Peak frequency (Hz)	Secondary frequencies within main energy range of input ground motion record (Hz)	Energy distribution of frequency spectrum	Mid-depth of clay	Mid-depth of upper coralline limestone (or whole thickness in 1.5 m thick case)
12	53	53_CTRLd_CLy minz_5flrs_LIVE_accA	N/A	N/A	N/A	N/A	N/A	N/A	7.23	1.76	Main energy content between 5.00 - 9.004 Hz. Almost even distribution throughout rest of frequency range.	33.69	1.66, 5.86	Increasing energy content in higher frequencies. Highest energy content between 23.00 -33.69 Hz. Significant peaks also at 37.79 Hz, 41.89 Hz, 46.29 Hz	N/A	N/A
13	57	57_CTRLc_thn rk on cly_4flrs_LIVE_accA	47.85	2.93	Main energy content between 44.00-50.00 Hz	2.93	6.54	Main energy content between 2.93-3.50 Hz	49.51	4.69	Increasing energy content in higher frequencies. Highest energy content between 47.00-49.51 Hz	35.35	3.71	Almost even distribution throughout most of frequency range.	Y	Y
14	58	58_CTRLd_60cly only_4flrs_LIVE_accA	49.22	N/A	Main energy content between 44.00-50.00 Hz	N/A	N/A	N/A	25.39	2.83	Almost even distribution throughout most of frequency range.	47.95	3.13	Increasing energy content in higher frequencies. Highest energy content between 45.50-50.00 Hz	N	N/A
15	59	59_CTRLd_cly minz_4flrs_LIVE_accA	N/A	N/A	N/A	N/A	N/A	N/A	4.98	N/A	Main energy content around 4.98 Hz	4.98	N/A	Main energy content around 4.98 Hz	N/A	N/A
16	63	63_CTRLc_thn rk on cly_3flrs_LIVE_accA	49.61	2.93	Main energy content between 46.00-49.61 Hz. Significant energy content also between 2.93-3.50 Hz	2.93	5.96	Main energy content between 2.93-3.90 Hz	2.93	5.96	Main energy content between 2.93-3.90 Hz	2.93	5.96	Main energy content between 2.93-3.90 Hz	Y	Y
17	64	64_CTRLd_60cly only_3flrs_LIVE_accA	44.73	3.22, 6.15	Main energy content between 44.73 - 47.50 Hz.	N/A	N/A	N/A	3.22	N/A	Main energy content around 3.22 Hz	3.22	N/A	Main energy content around 3.22 Hz	N	N/A

Key:
Possibility of resonant behaviour
Resonant behaviour unlikely

Table 34 Predominant frequencies in acceleration spectrum within main energy range of input ground motion record and energy distribution of frequency spectrum at 4 positions in every analysed model (continued).

Count	Model reference number	ELS® Model Name	Mid-depth through of clay layer			Mid-depth of upper coralline limestone layer or whole thickness in case of 1.5 m thick layer			First course			Slab over semi-basement level			Possibility of resonant behaviour in subsoil layers (not pure resonance) (Y/N)	
			Peak frequency (Hz)	Secondary frequencies within main energy range of input ground motion record (Hz)	Energy distribution of frequency spectrum	Peak frequency (Hz)	Secondary frequencies within main energy range of input ground motion record (Hz)	Energy distribution of frequency spectrum	Peak frequency (Hz)	Secondary frequencies within main energy range of input ground motion record (Hz)	Energy distribution of frequency spectrum	Peak frequency (Hz)	Secondary frequencies within main energy range of input ground motion record (Hz)	Energy distribution of frequency spectrum	Mid-depth of clay	Mid-depth of upper coralline limestone (or whole thickness in 1.5 m thick case)
18	69	69_CTRL wt S_STORYc_ thn rk on cly_ 6flrs_LIVE_ accA	48.34	2.93, 6.25	Main energy content between 46.00-49.50 Hz	2.93	6.54	Main energy content between 2.93-3.50 Hz	35.45	2.93, 6.64	Increasing energy content in higher frequencies. Highest energy content between 35.45-45.80 Hz	45.31	3.03	Almost even distribution throughout most of frequency range	Y	Y
19	71	71_CTRL wt S_STORYc_ thn rk on cly_ 5flrs_LIVE_ accA	49.12	2.93	Main energy content between 47.00-49.12 Hz	2.93	5.96	Main energy content between 2.93-3.25 Hz	47.27	2.83	Almost even distribution throughout most of frequency range except for marked increase in energy at peak frequency	1.17	3.22, 6.64	Almost even distribution throughout most of frequency range except for higher energy content around 1.17 Hz and 49.71 Hz	Y	Y
20	73	73_CTRL wt S_STORYc_ thn rk on cly_ 4flrs_LIVE_ accA	47.95	2.93	Main energy content between 47.00-47.95 Hz	2.93	5.96	Main energy content around 2.93 Hz	39.06	2.93	Increasing energy content in higher frequencies. Highest energy content between 33.20-43.07 Hz	1.37	N/A	Almost even distribution throughout most of frequency range except for higher energy content around 1.37 Hz, 39.75 Hz and 46.78 Hz	Y	Y
21	75	75_CTRL wt S_STORYc_ thn rk on cly_ 3flrs_LIVE_ accA	49.32	2.93, 6.25	Main energy content between 45.50-49.32 Hz	2.93	5.96	Main energy content between 2.93-3.90 Hz	2.93	5.96	Main energy content between 2.93-3.90 Hz	3.22	4.59, 6.54	Main energy content between 2.50-3.22 Hz.	Y	Y
22	79	79_CTRL wt STBKc_thn rk on cly_6flrs_ LIVE_accA	49.12	3.52	Main energy content between 48.50-49.12 Hz	2.93	5.96	Main energy content between 2.93-3.50 Hz	3.32	N/A	Increasing energy content in higher frequencies. Highest energy content between 42.58-48.82 Hz	21.09	2.83	Almost even distribution throughout most of frequency range. Highest energy content around 21.09 Hz	N	Y

Key:
Possibility of resonant behaviour
Resonant behaviour unlikely

Table 34 Predominant frequencies in acceleration spectrum within main energy range of input ground motion record and energy distribution of frequency spectrum at 4 positions in every analysed model (continued).

			Mid-depth through of clay layer			Mid-depth of upper coralline limestone layer or whole thickness in case of 1.5 m thick layer			First course			Slab over semi-basement level			Possibility of resonant behaviour in subsoil layers (not pure resonance) (Y/N)	
Count	Model reference number	ELS® Model Name	Peak frequency (Hz)	Secondary frequencies within main energy range of input ground motion record (Hz)	Energy distribution of frequency spectrum	Peak frequency (Hz)	Secondary frequencies within main energy range of input ground motion record (Hz)	Energy distribution of frequency spectrum	Peak frequency (Hz)	Secondary frequencies within main energy range of input ground motion record (Hz)	Energy distribution of frequency spectrum	Peak frequency (Hz)	Secondary frequencies within main energy range of input ground motion record (Hz)	Energy distribution of frequency spectrum	Mid-depth of clay	Mid-depth of upper coralline limestone (or whole thickness in 1.5 m thick case)
23	81	81_CTRL wt STBKc_thn rk on cly_5flrs_ LIVE_accA	48.93	2.93	Main energy content between 42.97-48.93 Hz	2.93	5.96	Main energy content between 2.93-3.50 Hz	44.63	2.93	Increasing energy content in higher frequencies. Highest energy content between 44.63-48.05 Hz. A significant peak is also present at 29.98 Hz	41.99	N/A	Increasing energy content in higher frequencies. Highest energy content between 38.48-47.17 Hz. A significant peak is also present at 33.01 Hz	Y	Y
24	83	83_CTRL wt STBKc_thn rk on cly_4flrs_ LIVE_accA	49.61	2.93	Main energy content between 43.36-49.61 Hz	2.93	5.96	Main energy content between 2.93-3.50 Hz	2.93	5.96	Main energy content between 2.93-3.50 Hz	2.93	5.96	Main energy content between 2.93-3.50 Hz	Y	Y
25	89	89_CTRL_ STBK_SSTRY c_thn rk on cly_6flrs_ LIVE_accA	48.83	3.42	Main energy content between 47.50-49.80 Hz	3.42	5.96	Main energy content between 3.00-3.42 Hz	29.59	3.52	Increasing energy content in higher frequencies. Highest energy content between 29.59-31.00 Hz. Significant energy is also present between 37.50-43.36 Hz	2.34	6.64	Almost even distribution throughout most of frequency range except for higher energy content between 1.90-2.34 Hz and between 49.50-49.90 Hz	N	Y
26	91	91_CTRL_ STBK_SSTRY c_thn rk on cly_5flrs_ LIVE_accA	49.41	3.52	Main energy content between 46.50-49.41 Hz	2.93	6.54	Main energy content between 2.93-3.50 Hz	30.86	3.32	Main energy content between 28.03-39.00 Hz	1.37	N/A	Energy distributed in three zones: between 1.37-2.00 Hz, 22.27-24.22 Hz and 41.21-49.99 Hz	N	Y
27	93	93_CTRL_ STBK_SSTRY c_thn rk on cly_4flrs_ LIVE_accA	47.85	2.93	Main energy content between 46.50-49.90 Hz	2.93	5.96	Main energy content between 2.93-3.90 Hz	38.57	N/A	Main energy content between 36.52-47.95 Hz	1.46	3.22	Almost even distribution throughout most of frequency range except for higher energy content between 1.10-3.22 Hz	Y	Y

Key:

Possibility of resonant behaviour

Resonant behaviour unlikely

Table 34 Predominant frequencies in acceleration spectrum within main energy range of input ground motion record and energy distribution of frequency spectrum at 4 positions in every analysed model (continued).

Count	Model reference number	ELS® Model Name	Mid-depth through of clay layer			Mid-depth of upper coralline limestone layer or whole thickness in case of 1.5 m thick layer			First course			Slab over semi-basement level			Possibility of resonant behaviour in subsoil layers (not pure resonance) (Y/N)	
			Peak frequency (Hz)	Secondary frequencies within main energy range of input ground motion record (Hz)	Energy distribution of frequency spectrum	Peak frequency (Hz)	Secondary frequencies within main energy range of input ground motion record (Hz)	Energy distribution of frequency spectrum	Peak frequency (Hz)	Secondary frequencies within main energy range of input ground motion record (Hz)	Energy distribution of frequency spectrum	Peak frequency (Hz)	Secondary frequencies within main energy range of input ground motion record (Hz)	Energy distribution of frequency spectrum	Mid-depth of clay	Mid-depth of upper coralline limestone (or whole thickness in 1.5 m thick case)
28	95	95_CTRL_STBK_SSTRYc_thn rk on cly_3flrs_LIVE_accA	48.14	2.93, 6.25	Main energy content between 45.50-49.00 Hz	2.93	5.96	Main energy content between 2.93-3.50 Hz	2.93	5.96	Main energy content between 2.93-3.90 Hz	2.93	4.59, 5.27	Main energy content between 2.93-3.50 Hz	Y	Y
29	99	99_CTRL_DHTc_thn rk on cly_6flrs_INCL LIVE_accA	48.24	2.93	Main energy content between 47.00-49.50 Hz	2.93	5.96	Main energy content between 2.93-3.90 Hz	32.13	3.91	Increasing energy content in higher frequencies. Highest energy content between 32.13-38.00 Hz	31.25	1.86, 5.08	Almost even distribution throughout most of frequency range. Highest energy content around 31.25 Hz	Y	Y
30	101	101_CTRL_DBL HTc_thn rk on cly_5flrs_LIVE_accA	48.44	2.93	Main energy content between 47.00-49.50 Hz	2.93	5.96	Main energy content between 2.93-3.50 Hz	34.08	2.15, 6.25	Increasing energy content in higher frequencies. Highest energy content between 33.00-35.94 Hz and between 39.94-42.19 Hz	33.59	2.93, 5.57	Almost even distribution throughout most of frequency range. Highest energy content between 25.39-42.68 Hz	Y	Y
31	103	103_CTRL_DBL HTc_thn rk on cly_4flrs_LIVE_accA	47.95	3.52	Main energy content between 43.50-50.00 Hz	2.93	5.96	Main energy content between 2.93-3.90 Hz	28.71	4.98	Increasing energy content in higher frequencies. Highest energy content around 28.71 Hz.	30.86	1.27, 4.00, 6.25	Increasing energy content towards middle of frequency range. Highest energy content around 22.46 Hz and 30.86 Hz	N	Y
32	105	105_CTRL_DBL HTc_thn rk on cly_3flrs_LIVE_accA	48.63	2.93, 5.86	Main energy content between 45.12-48.63 Hz	2.93	5.96	Main energy content between 2.93-3.90 Hz	2.93	5.96	Main energy content between 2.93-3.90 Hz	2.93	4.79, 5.96	Main energy content between 2.93-3.90 Hz	Y	Y

Key:
Possibility of resonant behaviour
Resonant behaviour unlikely

Table 34 Predominant frequencies in acceleration spectrum within main energy range of input ground motion record and energy distribution of frequency spectrum at 4 positions in every analysed model (continued).

			Mid-depth through of clay layer			Mid-depth of upper coralline limestone layer or whole thickness in case of 1.5 m thick layer			First course			Slab over semi-basement level			Possibility of resonant behaviour in subsoil layers (not pure resonance) (Y/N)	
Count	Model reference number	ELS® Model Name	Peak frequency (Hz)	Secondary frequencies within main energy range of input ground motion record (Hz)	Energy distribution of frequency spectrum	Peak frequency (Hz)	Secondary frequencies within main energy range of input ground motion record (Hz)	Energy distribution of frequency spectrum	Peak frequency (Hz)	Secondary frequencies within main energy range of input ground motion record (Hz)	Energy distribution of frequency spectrum	Peak frequency (Hz)	Secondary frequencies within main energy range of input ground motion record (Hz)	Energy distribution of frequency spectrum	Mid-depth of clay	Mid-depth of upper coralline limestone (or whole thickness in 1.5 m thick case)
33	109	109_CTRL_S_STRY_D_HTc_thnRKonCY_6flrs_LIVE_accA	49.61	3.52, 5.66	Main energy content between 45.70-49.61 Hz	2.93	6.54	Main energy content between 2.93-3.50 Hz	29.79	4.00	Increasing energy content in higher frequencies. Highest energy content between 29.79-37.40 Hz. Significant energy also around 20.70 Hz and between 47.75-48.93 Hz	49.32	1.86, 6.45	Almost even distribution throughout most of frequency range. Highest energy content between 48.15-49.32 Hz. Significant peaks present also between 6.45-14.26 Hz	N	Y
34	111	111_CTRL_S_STRY_D_HTc_thnRKonCY_5flrs_LIVE_accA	49.41	3.03	Main energy content between 47.50-49.41 Hz	2.93	5.96	Main energy content between 2.93-3.90 Hz	46.09	N/A	Increasing energy content in higher frequencies. Highest energy content around 46.09 Hz Significant energy also present around 30.86 Hz and between 37.50-43.50 Hz	34.08	2.83	Almost even distribution throughout most of frequency range. Highest energy content between 34.08-36.43 Hz and around 47.65 Hz	Y	Y
35	113	113_CTRL_S_STRY_D_HTc_thnrk on cly_4flrs_LIVE_accA	48.24	2.93	Main energy content between 47.00-49.00 Hz	2.93	5.96	Main energy content between 2.93-3.90 Hz	33.01	3.32	Increasing energy content in higher frequencies. Highest energy content between 32.00-34.96 Hz. Significant energy also present between 41.00 - 43.90 Hz	1.37	N/A	Main energy content around 1.37 Hz. A lower gradual increase in energy towards end of frequency range is also present.	Y	Y
36	115	115_CTRL_S_STRY_DHTc_thnRKonCY_3flrs_LIVE_accA	49.02	2.93	Main energy content between 46.00-49.02 Hz	2.93	5.96	Main energy content between 2.93-3.90 Hz	3.32	5.96	Main energy content between 3.32-3.90 Hz	3.22	4.59, 6.54	Main energy content between 2.90-3.22 Hz	Y	Y

Key:
Possibility of resonant behaviour
Resonant behaviour unlikely

Table 34 Predominant frequencies in acceleration spectrum within main energy range of input ground motion record and energy distribution of frequency spectrum at 4 positions in every analysed model (continued).

Count	Model reference number	ELS® Model Name	Mid-depth through of clay layer			Mid-depth of upper coralline limestone layer or whole thickness in case of 1.5 m thick layer			First course			Slab over semi-basement level			Possibility of resonant behaviour in subsoil layers (not pure resonance) (Y/N)	
			Peak frequency (Hz)	Secondary frequencies within main energy range of input ground motion record (Hz)	Energy distribution of frequency spectrum	Peak frequency (Hz)	Secondary frequencies within main energy range of input ground motion record (Hz)	Energy distribution of frequency spectrum	Peak frequency (Hz)	Secondary frequencies within main energy range of input ground motion record (Hz)	Energy distribution of frequency spectrum	Peak frequency (Hz)	Secondary frequencies within main energy range of input ground motion record (Hz)	Energy distribution of frequency spectrum	Mid-depth of clay	Mid-depth of upper coralline limestone (or whole thickness in 1.5 m thick case)
37	119	119_CTRL_STBK_SSTRY_DHTc_thnRK_CY_6fls_LV_accA	49.51	2.93, 5.66	Main energy content between 44.90-49.51 Hz	2.93	5.96	Main energy content between 2.93-3.50 Hz	45.51	6.84	Increasing energy content in higher frequencies. Highest energy content between 39.94-49.61 Hz. Significant energy also present between 32.71 - 34.10 Hz	44.14	3.32, 5.86	Main energy content between 41.21-47.07 Hz. A significant (lower) energy content is also present between 2.00-10.50 Hz. Almost even distributiion in between these zones	Y	Y
38	121	121_CTRL_STBK_SSTRY_DHTc_thnRK_CY_5fls_LV_accA	47.95	2.93	Main energy content between 46.25-49.00 Hz	2.93	5.96	Main energy content between 2.93-3.90 Hz	44.04	3.32, 5.18	Increasing energy content in higher frequencies. Highest energy content between 37.50-44.75 Hz. Significant energy also present between 27.50-31.50 Hz	41.7	1.86, 4.49	Almost even distribution throughout most of frequency range. Highest energy content between 41.70-50.00 Hz	Y	Y
39	123	123_CTRL_STBK_SSTRY_DHTc_thnRK_CY_4fls_LV_accA	47.36	3.52, 5.66	Main energy content between 44.10-48.90 Hz	2.93	5.96	Main energy content between 2.93-3.90 Hz	28.71	4.49, 6.45	Higher energy content in upper half of frequency range. Highest energy content between 26.46-33.69 Hz. Significant energy also present around 42.58 Hz	1.27	N/A	Main energy content between 1.27-4.5 Hz. Almost even distributiion in the rest of the frequency range.	N	Y
40	125	125_CTRL_STBK_SSTRY_DHTc_thnRK_CY_3fls_LV_accA	49.80	2.93	Main energy content between 44.90-49.80 Hz	2.93	5.96	Main energy content between 2.93-3.90 Hz	2.93	5.96	Main energy content between 2.93-3.90 Hz	2.93	4.59, 6.54	Main energy content between 2.93-3.50 Hz	Y	Y

Key:
Possibility of resonant behaviour
Resonant behaviour unlikely

Table 34 Predominant frequencies in acceleration spectrum within main energy range of input ground motion record and energy distribution of frequency spectrum at 4 positions in every analysed model (continued).

			Mid-depth through of clay layer			Mid-depth of upper coralline limestone layer or whole thickness in case of 1.5 m thick layer			First course			Slab over semi-basement level			Possibility of resonant behaviour in subsoil layers (not pure resonance) (Y/N)	
Count	Model reference number	ELS® Model Name	Peak frequency (Hz)	Secondary frequencies within main energy range of input ground motion record (Hz)	Energy distribution of frequency spectrum	Peak frequency (Hz)	Secondary frequencies within main energy range of input ground motion record (Hz)	Energy distribution of frequency spectrum	Peak frequency (Hz)	Secondary frequencies within main energy range of input ground motion record (Hz)	Energy distribution of frequency spectrum	Peak frequency (Hz)	Secondary frequencies within main energy range of input ground motion record (Hz)	Energy distribution of frequency spectrum	Mid-depth of clay	Mid-depth of upper coralline limestone (or whole thickness in 1.5 m thick case)
41	128	128X11_01c_ThnRk_CY_accA6flrs_InclLIVE_incl Bsmt wlls	46.78	2.15, 5.76	Main energy content between 45.50-50.00 Hz. A significant (lower) peak in energy content is also present between 2.15-3.00 Hz	2.15	5.96	Main energy content between 2.15-3.00 Hz	32.91	4.20	Increasing energy content in higher frequencies. Highest energy content between 27.64-36.50 Hz. Significant energy also present between 43.36-48.80 Hz	42.29	2.25	Main energy content between 35.50-49.50 Hz. Almost even distributiion in the rest of the frequency range.	N	Y
42	129	129X11_01b_30Rk30CY_accA6flrs_InclLIVE_incl Bsmt wlls	47.95	1.86, 5.96	Main energy content is distributed in two main zones: between 40.92-49 Hz, and a lower energy zone between 1.86-3.00 Hz	1.86	5.96	Main energy content between 1.00-3.00 Hz	45.02	2.15, 6.25	Increasing energy content in higher frequency range. Highest energy content between 38.00-45.10 Hz	10.25	1.56	Main energy content between 4.70-12.90 Hz. A significant lower energy content is also present between 44.00-49.00 Hz	Y	Y
43	130	130_CTRLx2AGG_c_thnRK_CY_6flrs_LIVE_accA	47.85	3.52	Main energy content between 47.85-50.00 Hz	3.52	5.96	Main energy content between 2.90-4.00 Hz	45.31	3.52	Increasing energy content in higher frequencies. Highest energy content between 44.00-50.00 Hz. Significant (lower) peaks also present around 31.93 Hz and between 38.67-40.00 Hz	32.03	N/A	Higher energy content in upper half of frequencies. Highest energy content between 31.90-33.00 Hz. Significant (lower) energy also present around 41.90-45.10 Hz	N	Y
44	132	132_CTRLx2AGG_c_thnRK_CY_5flrs_LIVE_accA	44.73	2.93	Main energy content between 47.30-49.90 Hz. Significant (lower) energy content is present between 44.10-46.30 Hz	3.52	5.96	Main energy content between 2.90-4.00 Hz	39.26	3.32, 6.74	Increasing energy content in higher frequencies. Highest energy content between 36.90-41.10 Hz. Significant (lower) energy content also present between 30.50-34.10 Hz	21.97	2.73, 6.35	Almost even distribution throughout most of frequency range. Highest energy content between 21.97-23.30 Hz and, to a lesser degree, around 35.16 Hz	Y	Y

Key:

Possibility of resonant behaviour

Resonant behaviour unlikely

Table 34 Predominant frequencies in acceleration spectrum within main energy range of input ground motion record and energy distribution of frequency spectrum at 4 positions in every analysed model (continued).

Count	Model reference number	ELS® Model Name	Mid-depth through of clay layer			Mid-depth of upper coralline limestone layer or whole thickness in case of 1.5 m thick layer			First course			Slab over semi-basement level			Possibility of resonant behaviour in subsoil layers (not pure resonance) (Y/N)	
			Peak frequency (Hz)	Secondary frequencies within main energy range of input ground motion record (Hz)	Energy distribution of frequency spectrum	Peak frequency (Hz)	Secondary frequencies within main energy range of input ground motion record (Hz)	Energy distribution of frequency spectrum	Peak frequency (Hz)	Secondary frequencies within main energy range of input ground motion record (Hz)	Energy distribution of frequency spectrum	Peak frequency (Hz)	Secondary frequencies within main energy range of input ground motion record (Hz)	Energy distribution of frequency spectrum	Mid-depth of clay	Mid-depth of upper coralline limestone (or whole thickness in 1.5 m thick case)
45	134	134_CTRLx2 AGG_c_thn RK_CY_4flrs _LIVE_accA	49.61	3.32, 5.96	Main energy content between 45.50-50.00 Hz	3.52	5.96	Main energy content between 2.90-4.00 Hz	40.53	3.32, 5.96	Main energy content between 40.53-42.50 Hz. Significant (lower) energy content is present between 47.00-49.50 Hz	34.38	2.44, 5.18	Almost even distribution throughout most of frequency range. Highest energy content between 34.38-35.90 Hz and, to a lesser degree, around 21.80-33.00 Hz and 42.90-44.04 Hz	Y	Y
46	136	136_CTRLx2 AGG_c_thn RK_CY_3flrs _LIVE_accA	48.14	3.52	Main energy content between 47.50-49.25 Hz. A significant (lower) energy content is present between 45.41-46.25 Hz	2.93	5.96	Main energy content between 2.93-3.90 Hz	2.93	5.96	Main energy content between 2.93-3.50 Hz	3.52	4.59, 5.96	Main energy content between 2.90-4.00 Hz	N	Y
47	138	138_CTRLx3 AGG_c_thn RK_CY_6flrs _LIVE_accA	49.32	2.93	Main energy content between 49.32-50.00 Hz. A significant (lower) energy content is present between 44.04-45.00 Hz	2.93	4.49, 5.96	Main energy content between 2.93-3.90 Hz	47.56	2.93, 6.54	Increasing energy content in higher frequencies. Highest energy content between 43.16-49.50 Hz. Significant (lower) energy content also present between 37.00-37.60 Hz	38.09	4.88	Main energy content is concentrated in three zones in the second half of the frequency range: 36.50-39.80 Hz, and to a marginally lower extent, 27.90-29.10 Hz and 48.00-50.00 Hz. Almost even distribution throughout rest of frequency range	Y	Y

Key:

Possibility of resonant behaviour

Resonant behaviour unlikely

Table 34 Predominant frequencies in acceleration spectrum within main energy range of input ground motion record and energy distribution of frequency spectrum at 4 positions in every analysed model (continued).

			Mid-depth through of clay layer			Mid-depth of upper coralline limestone layer or whole thickness in case of 1.5 m thick layer			First course			Slab over semi-basement level			Possibility of resonant behaviour in subsoil layers (not pure resonance) (Y/N)	
Count	Model reference number	ELS® Model Name	Peak frequency (Hz)	Secondary frequencies within main energy range of input ground motion record (Hz)	Energy distribution of frequency spectrum	Peak frequency (Hz)	Secondary frequencies within main energy range of input ground motion record (Hz)	Energy distribution of frequency spectrum	Peak frequency (Hz)	Secondary frequencies within main energy range of input ground motion record (Hz)	Energy distribution of frequency spectrum	Peak frequency (Hz)	Secondary frequencies within main energy range of input ground motion record (Hz)	Energy distribution of frequency spectrum	Mid-depth of clay	Mid-depth of upper coralline limestone (or whole thickness in 1.5 m thick case)
48	140	140_CTRLx3 AGG_c_thn RK_CY_5flrs _LIVE_accA	49.8	2.93	Main energy content between 45.02-49.80 Hz	2.93	6.15	Main energy content between 2.93-3.50 Hz	46.09	4.79	Almost constant distribution of energy in upper half of frequency range	30.08	2.93	Main energy content is concentrated in three zones in the second half of the frequency range: 30.08-31 Hz, and to a marginally lower extent, 36.50-38.50 Hz and 47.36-49.51 Hz. Almost even distribution throughout rest of frequency range.	Y	Y
49	142	142_CTRLx3 AGG_c_thn RK_CY_4flrs _LIVE_accA	48.93	3.52, 5.96	Main energy content between 46.80-49.90 Hz	2.93	4.49, 5.96	Main energy content between 2.93-3.90 Hz	49.51	2.93, 4.98	Increasing energy content in higher frequencies. Highest energy content around 49.51 Hz. Significant (marginally lower) energy content also present between 34.50-44.00 Hz	44.63	5.96	Increasing energy content in higher frequencies. Highest energy content between 43.10-47.10 Hz. Significant (marginally lower) energy content also present between 36.90-41.00 Hz and 48.10-49.90 Hz	Y	Y
50	144	144_CTRLx3 AGG_c_thn RK_CY_3flrs _LIVE_accA	48.54	2.93, 5.94	Main energy content between 45.00-49.50 Hz. A significant (lower) energy content is present between 2.93-3.90 Hz	2.93	5.96	Main energy content between 2.93-3.90 Hz	2.93	5.96	Main energy content between 2.93-3.90 Hz	2.93	5.96	Main energy content between 2.93-3.90 Hz	Y	Y

Key:
Possibility of resonant behaviour
Resonant behaviour unlikely

Table 35 Analysis time, frame number and displacement at slab over semi-basement level at onset of failure and complete collapse in single building control models. Collapse duration also included.

	Parameters investigated from Sections 2 and 3 of New Form Variations: building height, geology checks																
	Geology type (a): Models analysed on a **30 m thick layer of upper coralline limestone** modelled as a three dimensional block. Ground material at Minimum Z defined as upper coralline limestone		Geology type (b): Models analysed on ground specified as **upper corolline limestone at Minimum Z**		Geology type (c): Models analysed on a **30 m thick upper coralline limestone layer which overlies a 30 m thick layer of clay** (Xemxija case), both modelled as three dimensional blocks.Ground material at Minimum Z defined as upper coralline limestone		Geology type (d): Models analysed on a **1.5 m thick upper coralline limestone layer which overlies a 60 m thick layer of clay** (Nadur case), both modelled as three dimensional blocks. Ground material at Minimum Z defined as upper coralline limestone				Geology type (e): Models analysed on a **60 m thick layer of clay** modelled as a three dimensional block. Ground material at Minimum Z defined as upper coralline limestone				Geology type (f): Models analysed on ground specified as **clay at Minimum Z**		
	6- storeys	5- storeys	6- storeys	5- storeys	6- storeys	5- storeys	6- storeys	5- storeys	4- storeys	3- storeys	6- storeys	5- storeys	4- storeys	3- storeys	6- storeys	5- storeys	4- storeys
Model Number; collapse/ no collapse	Model 42v2; collapse		Model 43v2; collapse		Model 44v2; collapse		Model 45v2; collapse	Model 51; collapse	Model 57; collapse		Model 46; collapse	Model 52; collapse	Model 58; collapse		Model 47; collapse	Model 53; collapse	
Onset of failure in x-direction at slab over semi-basement level: frame number (analysis time)	frame 257 (1.56 s)		frame 375 (2.74 s)		frame 359 (2.58 s)		frame 128 0.27 s)	frame 170 (0.69 s)	frame 375 (2.74 s)		frame 110 (0.09 s)	frame 144 (0.43 s)	frame 397 (2.96 s)		frame 236 (1.35 s)	frame 466 (3.65 s)	
Relative x-displacement at start of failure at slab over semi-basement level with respect to displacement at first course in every respective model *(ratio to relative displacement at same position at start of failure in corresponding control model)*	-2.57×10^{-3} m *(N/A: control model)*	Model 48; no collapse	-2.16×10^{-3} m *(N/A: control model)*	Model 49; no collapse	-7.76×10^{-3} m *(N/A: control model)*	Model 50; no collapse	-9.53×10^{-4} m *(N/A: control model)*	-9.99×10^{-4} m *(N/A: control model)*	-6.56×10^{-4} m *(N/A: control model)*	Model 63; no collapse	-1.04×10^{-3} m *(N/A: control model)*	-1.49×10^{-3} m *(N/A: control model)*	-3.97×10^{-3} m *(N/A: control model)*	Model 64; no collapse	-7.52×10^{-3} m *(N/A: control model)*	7.24×10^{-5} m *(N/A: control model)*	Model 59; no collapse
Collapse duration (frame number, analysis time (model direction where collapse was determined))	1.25 s (frame 382, 2.81 s (z))		1.3 s (frame 435, 3.34 s (z))		0.86 s (frame 445, 3.44 s (z))		1.52 s (frame 280, 1.79 s (z))	1.66 s (frame 336, 2.35 s (z))	2.22 s (frame 597, 4.96 s (z))		1.38 s (frame 248, 1.47 s (z))	1.93 s (frame 318, 2.17 s (z))	1.43 s (frame 540, 4.39 s (z))		1.12 s (frame 348, 2.47 s (z)	1.89 s (frame 655, 5.54 s (z))	
Model behaviour prior to onset of collapse	Type C		Type C		Type C		Type A	Type A	Type C		Type A	Type A	Type C		Type A	Type C	

Key:

Models which resisted collapse

Models which resulted in collapse

Table 36 Analysis time, frame number, displacement at slab over semi-basement level at onset of failure / complete collapse and collapse duration in single building control models including one additional seismic vulnerability characteristic and existing building.

	Parameters investigated from Sections 2 and 3 of New Form												
	Geology type (d): Models analysed on a **1.5 m thick upper coralline limestone layer which overlies a 60 m thick layer of clay** (Nadur case), both modelled as three dimensional blocks. Ground material at Minimum Z defined as upper coralline limestone											Geology type (d): **1.5 m thick upper coralline limestone on 60 m thick clay**	Geology type (c) (actual scenario): **30 m thick upper coralline limestone on 30 m thick clay**
	Single building control model with soft storey at semi-basement level				Single building control model with setbacks at penthouse level			Single building control model with double height space between levels 0 and +1				Existing Xemxija building (single building) (XMX 0011)	
	Variations: presence of soft storey at semi-basement level, building height.				Variations: presence of setbacks at penthouse level, building height.			Variations: presence of a double height space between Levels 0 and +1, building height.				Seismic vulnerability characteristics in addition to those present in control models: discontinuous loadbearing walls at slab over semi-basememt level, large open plan at semi-basement level without intermediate walls, setbacks at penthouse level , double height space between levels +5 and +6 (penthouse level) towards middle of plan layout in longitudinal direction	
	6- storeys	5- storeys	4- storeys	3- storeys	6- storeys	5- storeys	4- storeys	6- storeys	5- storeys	4- storeys	3- storeys	6- storeys	6- storeys
Model Number; collapse/ no collapse	Model 69; collapse	Model 71; collapse	Model 73; collapse		Model 79; collapse	Model 81; collapse		Model 99; collapse	Model 101; collapse	Model 103; collapse		Model 128; collapse	Model 129; collapse
Onset of failure in x-direction at slab over semi-basement level: frame number (analysis time)	frame 147 (0.46 s)	frame 230 (1.29 s)	frame 361 (2.60 s)		frame 146 (0.45 s)	frame 256 (1.55 s)		frame 140 (0.39 s)	frame 233 (1.32 s)	frame 536 (4.35 s)		frame 177 (0.76 s)	frame 302 (2.01 s)
Relative x-displacement at start of failure at slab over semi-basement level in every respective model with respect to displacement at first course *(ratio to equivalent relative displacement at start of failure in corresponding control model)*	-5.39×10^{-4} m *(0.566)*	5.72×10^{-3} m *(5.728)*	-1.36×10^{-2} m *(20.755)*	Model 75; no collapse	-1.76×10^{-3} m *(1.847)*	-1.35×10^{-3} m *(1.347)*	Model 83; no collapse	-3.31×10^{-3} m *(3.472)*	-7.92×10^{-4} m *(0.793)*	5.71×10^{-3} m *(8.710)*	Model 105; no collapse	-3.04×10^{-3} m *(3.191)*	-1.49×10^{-3} m *(0.192)*
Relative x-displacement at time of start of failure at slab over semi-basement level in corresponding control model with respect to displacement at first course, (*ratio to relative displacement at start of failure in corresponding control model*, (frame number)	-2.40×10^{-3} m, *(2.522),* (frame 128)	2.36×10^{-4} m, *(0.236),* (frame 170)	1.57×10^{-2} m, *(24.016),* (frame 375)		-1.15×10^{-3} m, *(1.203),* (frame 128)	3.12×10^{-4} m, *(0.312),* (frame 170)		-8.74×10^{-4} m, *(0.917),* (frame 128)	-1.25×10^{-4} m, *(0.125),* frame 375	6.73×10^{-4} m, *(1.026),* (frame 375)		-1.64×10^{-3} m, *(1.720),* (frame 128)	2.49×10^{-2} m, *(3.208),* (frame 340)
Collapse duration (frame number, analysis time (model direction where collapse was determined))	1.63 s (frame 310, 2.09 s (z))	1.39 s (frame 369, 2.68 s (z))	1.19 s (frame 480, 3.79 s (z))		1.28 s (frame 274, 1.73 s (z))	1.45 s (frame 401, 3.00 s (z))		1.23 s (frame 263, 1.62 s (z))	1.11 s (frame 344, 2.43 s (z))	1.94 s (frame 730, 6.29 s (z))		1.24 s (frame 301, 2.00 s (z))	1.28 s (frame 431, 3.30 s (z))
Model behaviour prior to onset of collapse	Type B	Type B	Type B		Type A	Type C		Type A	Type C	Type C		Type B	Type B

Key:

Models which resisted collapse

Models which resulted in collapse

Table 37 Analysis time, frame number and displacement at slab over semi-basement level at onset of failure and complete collapse in single building control models including 2 or 3 additional seismic vulnerability characteristics. Collapse duration also included.

	Parameters investigated from Sections 2 and 3 of New Form											
	Geology type (d): Models analysed on a **1.5 m thick upper coralline limestone layer which overlies a 60 m thick layer of clay** (Nadur case), both modelled as three dimensional blocks. Ground material at Minimum Z defined as upper coralline limestone.											
	Single building control model with soft storey at semi-basement level and setbacks at penthouse level				Single building control model with soft storey at semi-basement level and double height space between Levels 0 and +1				Single building control model with setbacks at penthouse level, soft storey at semi-basement level and double height space between Levels 0 and +1			
	Variations: presence of soft storey at semi-basement level in conjunction with setbacks at penthouse level, building height.				Variations: presence of soft storey at semi-basement level in conjunction with double height space between Levels 0 and +1, building height.				Variations: presence of soft storey at semi-basement level in conjunction with setbacks at penthouse level and double height space between Levels 0 and +1, building height.			
	6- storeys	5- storeys	4- storeys	3-storeys	6- storeys	5- storeys	4- storeys	3-storeys	6- storeys	5- storeys	4- storeys	3-storeys
Model Number; collapse/ no collapse	Model 89; collapse	Model 91; collapse	Model 93; collapse	Model 95; no collapse	Model 109; collapse	Model 111; collapse	Model 113; collapse	Model 115; no collapse	Model 119; collapse	Model 121; collapse	Model 123; collapse	Model 125; no collapse
Onset of failure in x-direction at slab over semi-basement level: frame number (analysis time)	frame 176 (0.75 s)	frame 292 (1.91 s)	frame 678 (5.77 s)		frame 139 (0.38 s)	frame 299 (1.98 s)	frame 359 (2.58 s)		frame 177 (0.76 s)	frame 442 (3.41 s)	frame 671 (5.70 s)	
Relative x-displacement at start of failure at slab over semi-basement level in every respective model with respect to displacement at first course *(ratio to equivalent relative displacement at start of failure in corresponding control model)*	-6.94×10^{-5} m *(0.073)*	-5.73×10^{-3} m *(5.739)*	-2.05×10^{-2} m *(31.251)*		6.16×10^{-3} m *(6.459)*	1.27×10^{-2} m *(12.742)*	-1.23×10^{-2} m *(18.796)*		7.52×10^{-3} m *(7.891)*	2.04×10^{-3} m *(2.044)*	-4.67×10^{-3} m *(7.121)*	
Relative x-displacement at time of start of failure at slab over semi-basement level in corresponding control model with respect to displacement at first course, (*ratio to relative displacement at start of failure in corresponding control model*, (frame number)	-2.25×10^{-3} m, *(2.362),* (frame 128)	9.07×10^{-4} m, *(0.908),* (frame 170)	4.27×10^{-3} m, *(6.520),* frame 375		-1.57×10^{-3} m, *(1.642),* (frame 128)	2.34×10^{-4} m, *(0.234)* (frame 170)	4.68×10^{-3} m, *(7.145),* (frame 375)		-2.66×10^{-3} m, *(2.785),* (frame 128)	9.12×10^{-4} m, *(0.913),* (frame 170)	5.54×10^{-3} m, *(8.448),* (frame 375)	
Collapse duration (frame number, analysis time (model direction where collapse was determined))	0.72 s (frame 248, 1.47 s (z))	1.19 s (frame 411, 3.10 s (z))	1.12 s (frame 790, 6.89 s (z))		1.62 s (frame 301, 2.00 s (z))	0.65 s (frame 364, 2.63 s (z))	1.24 s (frame 483, 3.82 s (z))		0.68 s (frame 245, 1.44 s (z))	1.32 s (frame 574, 4.73 s (z))	1.04 s (frame 775, 6.74 s (z))	
Model behaviour prior to onset of collapse	Type C	Type B	Type B		Type B	Type B	Type B		Type B	Type C	Type C	

Key: Models which resisted collapse; Models which resulted in collapse

Table 38 Analysis time, frame number and displacement at slab over semi-basement level at onset of failure and complete collapse in single building, 2-, and 3-building control models analysed on geology type (d). Collapse duration also included.

	Parameters investigated from Sections 2 and 3 of New Form											
	Geology type (d): Models analysed on a **1.5 m thick upper coralline limestone layer which overlies a 60 m thick layer of clay** (Nadur case), both modelled as three dimensional blocks. Ground material at Minimum Z defined as upper coralline limestone.											
	Single building control model				2-building control model sharing party wall				3-building control model sharing party walls			
	Variations: building height				Variations: aggregate effect, building height.				Variations: aggregate effect, building height.			
	6- storeys	5- storeys	4- storeys	3-storeys	6- storeys	5- storeys	4- storeys	3-storeys	6- storeys	5- storeys	4- storeys	3-storeys
Model Number; collapse/ no collapse	Model 45v2; collapse	Model 51; collapse	Model 57; collapse	Model 63; no collapse	Model 130; collapse	Model 132; collapse	Model 134; collapse	Model 136; no collapse	Model 138; collapse	Model 140; collapse	Model 142; collapse	Model 144; no collapse
Onset of failure in x-direction at slab over semi-basement level: frame number (analysis time)	frame 128 (0.27 s)	frame 170 (0.69 s)	frame 375 (2.74 s)		Right hand side building: frame 190 (0.89 s)	Right hand side building: frame 194 (0.93 s)	Right hand side building: frame 580 (4.79 s)		Middle building: frame 185 (0.84 s)	Middle building: frame 214 (1.13 s)	Middle building: frame 582 (4.81 s)	
Relative x-displacement at start of failure at slab over semi-basement level in every respective model with respect to displacement at first course *(ratio to equivalent relative displacement at start of failure in corresponding control model)*	$-9.53x10^{-4}$ m *(N/A: control model)*	$-9.99x10^{-4}$ m *(N/A: control model)*	$-6.56x10^{-4}$ m *(N/A: control model)*		$-1.54x10^{-2}$ m *(16.181)*	$-4.09x10^{-3}$ m *(4.095)*	$-9.80x10^{-4}$ m *(1.495)*		$-1.77x10^{-3}$ m *(1.853)*	$-1.46x10^{-2}$ m *(14.658)*	$1.77x10^{-2}$ m *(27.014)*	
Relative x-displacement at time of start of failure at slab over semi-basement level in corresponding control model with respect to displacement at first course, (*ratio to relative displacement at start of failure in corresponding control model*, (frame number)	N/A (control model)	N/A (control model)	N/A (control model)		$-2.48x10^{-3}$ m, *(2.606),* (frame 128)	$-6.21x10^{-3}$ m, *(6.221),* (frame 170)	$-9.06x10^{-6}$ m, *(0.014),* (frame 375)		$-1.51x10^{-3}$ m, *(1.583),* (frame 128)	$-9.47x10^{-3}$ m, *(9.480),* (frame 170)	-6.57x10-6 m, *(0.010),* (frame 375)	
Collapse duration (frame number, analysis time (model direction where collapse was determined))	1.52 s (frame 280, 1.79 s (z))	1.66 s (frame 336, 2.35 s (z))	2.22 s (frame 597, 4.96 s (z))		0.87 s (frame 277, 1.76 s (z))	1.52 s (frame 346, 2.45 s (z))	2.17 s (frame 797, 6.96 s (z))		0.75 s (frame 260, 1.59 s (z))	1.17 s (frame 331, 2.30 s (z))	1.55 s (frame 737, 6.36 s (z))	
Model behaviour prior to onset of collapse	Type A	Type A	Type C		Type B	Type B	Type C		Type B	Type B	Type C	

Key: Models which resisted collapse; Models which resulted in collapse

Table 39 Maximum x-acceleration in subsoil layers, first course and slab over semi-basement level prior to the start of failure at slab over semi-basement level.

Model details	Geology	Model reference number	ELS® model name	Time (frame no.) of 1st sign of failure at slab over semi-basement level; orientation	Direction (frame no., time (s)) of maximum x-acceleration before start of failure at slab over semi-basement level (m/s^2): **Bottom clay**; ratio to maximum input p.g.a. prior to start of failure	Direction (frame no., time (s)) of maximum x-acceleration before start of failure at slab over semi-basement level (m/s^2): **Middle clay**; ratio to maximum input p.g.a. prior to start of failure	Direction (frame no., time (s)) of maximum x-acceleration before start of failure at slab over semi-basement level (m/s^2): **Top clay**; ratio to maximum input p.g.a .prior to start of failure	Direction (frame no., time (s)) of maximum x-acceleration before start of failure at slab over semi-basement level (m/s^2): **Bottom UCL**; ratio to maximum input p.g.a. prior to start of failure	Direction (frame no., time (s)) of maximum x-acceleration before start of failure at slab over semi-basement level (m/s^2): **Middle UCL**; ratio to maximum input p.g.a. prior to start of failure	Direction (frame no., time (s)) of maximum x-acceleration before start of failure at slab over semi-basement level (m/s^2): **Top UCL**; ratio to maximum input p.g.a. prior to start of failure	Direction (frame no., time (s)) of maximum x-acceleration before start of failure at slab over semi-basement level (m/s^2): **Thin (1.5m thick) UCL**; ratio to maximum input p.g.a. prior to start of failure	Direction (frame no., time (s)) of maximum x-acceleration before start of failure at slab over semi-basement level (m/s^2)**: 1st course**; ratio to maximum input p.g.a. prior to start of failure	Direction (frame no., time (s)) of maximum x-acceleration before start of failure at slab over semi-basement level (m/s^2): **Slab over semi-basement**; ratio to maximum input p.g.a. prior to start of failure
Single building control models analysed on 'rock' subsoil cases	Geology type (a): Models analysed on a **30 m thick layer of upper coralline limestone** modelled as a three dimensional block.	42v2	42v2_CTRLa_30rk_ 6flrs_LIVE_accA_ REV	1.56 s (257); x				x (198, 0.97 s) $1.77x10^{-2}$ m/s^2 0.020	x (238, 1.37 s) $4.61x10^{-2}$ m/s^2 0.053	x (238, 1.37 s) $5.73x10^{-2}$ m/s^2 0.066		x (254, 1.53 s) $-1.58x10^{-1}$ m/s^2 0.182	x (255, 1.54 s) -1.63 m/s^2 1.876
		48	48_CTRLa_30rk only_ 5flrs_LIVE_accA	N / A (no collapse)					N / A (no collapse)			N / A (no collapse)	N / A (no collapse)
	Geology type (b): Models analysed on ground specified as **upper corolline limestone at Minimum Z**	43v2	43v2_CTRLa_rk minz_ 6flrs_INCL LIVE_accA_REV	2.74 s (375); x								x (374, 2.73 s) $-9.69x10^{-3}$ m/s^2 0.010	x (374, 2.73 s) 1.93 m/s^2 1.969
		49	49_CTRLa_rk minz_ 5flrs_LIVE_accA	N / A (no collapse)								N / A (no collapse)	N / A (no collapse)
	Geology type (c): Models analysed on a **30 m thick upper coralline limestone layer which overlies a 30 m thick layer of clay** (Xemxija case), both modelled as three dimensional blocks.	44v2	44v2_CTRLb_30rk on 30 cly_ 6flrs_LIVE_accA_ REV	2.58 s (359); x	x (243, 1.42 s) $-4.23x10^{-3}$ m/s^2 0.004	x (315, 2.14 s) 2.61 m/s^2 2.659	x (319, 2.18 s) -3.29 m/s^2 3.359	x (341, 2.40 s) $-9.33x10^{-1}$ m/s^2 0.952	x (341, 2.40 s) -1.05 m/s^2 1.068	x (341, 2.40 s) -1.16 m/s^2 1.183		x (345, 2.44 s) -5.59 m/s^2 5.700	x (342, 2.41 s) $1.15x10^{2}$ m/s^2 117.389
		50	50_CTRLb_30rk 30cly_ 5flrs_LIVE_accA	N / A (no collapse)		N / A (no collapse)			N / A (no collapse)			N / A (no collapse)	N / A (no collapse)

Table 39 Maximum x-acceleration in subsoil layers, first course and slab over semi-basement level prior to the start of failure at slab over semi-basement level (continued).

Model details	Geology	Model reference number	ELS® model name	Time (frame no.) of 1st sign of failure at slab over semi-basement level; orientation	Direction (frame no., time (s)) of maximum x-acceleration before start of failure at slab over semi-basement level (m/s^2): **Bottom clay**; ratio to maximum input p.g.a. prior to start of failure	Direction (frame no., time (s)) of maximum x-acceleration before start of failure at slab over semi-basement level (m/s^2): **Middle clay**; ratio to maximum input p.g.a. prior to start of failure	Direction (frame no., time (s)) of maximum x-acceleration before start of failure at slab over semi-basement level (m/s^2): **Top clay**; ratio to maximum input p.g.a. prior to start of failure	Direction (frame no., time (s)) of maximum x-acceleration before start of failure at slab over semi-basement level (m/s^2): **Bottom UCL**; ratio to maximum input p.g.a. prior to start of failure	Direction (frame no., time (s)) of maximum x-acceleration before start of failure at slab over semi-basement level (m/s^2): **Middle UCL**; ratio to maximum input p.g.a. prior to start of failure	Direction (frame no., time (s)) of maximum x-acceleration before start of failure at slab over semi-basement level (m/s^2): **Top UCL**; ratio to maximum input p.g.a. prior to start of failure	Direction (frame no., time (s)) of maximum x-acceleration before start of failure at slab over semi-basement level (m/s^2): **Thin (1.5m thick) UCL**; ratio to maximum input p.g.a. prior to start of failure	Direction (frame no., time (s)) of maximum x-acceleration before start of failure at slab over semi-basement level (m/s^2): **1st course**; ratio to maximum input p.g.a. prior to start of failure	Direction (frame no., time (s)) of maximum x-acceleration before start of failure at slab over semi-basement level (m/s^2): **Slab over semi-basement**; ratio to maximum input p.g.a. prior to start of failure
Single building control models analysed on 'clay' subsoil cases	Geology type (d): Models analysed on a **1.5 m thick upper coralline limestone layer which overlies a 60 m thick layer of clay** (Nadur case), both modelled as three dimensional blocks	45v2	45v2_CTRLc_thn rk on cly_ 6flrs_INCL LIVE_accA	0.27 s (128);x	x (111, 0.10 s) $-9.00x10^{-5}$ m/s² 0.0001	x (113, 0.12 s) $6.02x10^{-1}$ m/s² 0.862	x (116, 0.15 s) $3.93x10^{-1}$ m/s² 0.563				x (115, 0.14 s) $4.42x10^{-1}$ m/s² 0.633	x (115, 0.14 s) $4.52x10^{-1}$ m/s² 0.647	x (116, 0.15 s) 1.00 m/s² 1.434
		51	51_CTRLc_thn rk on cly_ 5flrs_LIVE_accA	0.69 s (170); x		x (129, 0.28 s) -1.92 m/s² 2.742					x (114, 0.13 s) $4.41x10^{-1}$ m/s² 0.632	x (116, 0.15 s) $4.38\ x10^{-1}$ m/s² 0.626	x (168, 0.67 s) -2.52 m/s² 3.612
		57	57_CTRLc_thn rk on cly_ 4flrs_LIVE_accA	2.74 s (375); x		x (359, 2.58 s) 2.71 m/s² 2.762					x (348, 2.47 s) $9.16x10^{-1}$ m/s² 0.935	x (348, 2.47 s) $8.82x10^{-1}$ m/s² 0.900	x (373, 2.72 s) -1.55 m/s² 1.578
		63	63_CTRLc_thn rk on cly_3flrs_LIVE_accA	N / A (no collapse)		N / A (no collapse)					N / A (no collapse)	N / A (no collapse)	N / A (no collapse)
	Geology type (e): Models analysed on a **60 m thick layer of clay** modelled as a three dimensional block	46	46CTRLd_60cly only_ 6flrs_INCL LIVE_accA_RAFT	0.09 s (110); x	x (103, 0.02 s) $-5.92\ x10^{-5}$ m/s² 0.0001	x (104, 0.03 s) $-6.20x10^{-2}$ m/s² 0.089	x (108, 0.07 s) $2.48x10^{-1}$ m/s² 0.355					x (105, 0.04 s) $-2.29x10^{-1}$ m/s² 0.327	x (107, 0.06 s) $-9.49x10^{-1}$ m/s² 1.359
		52	52_CTRLd_60cly only_ 5flrs_LIVE_accA	0.43 s (144); x		x (131, 0.30 s) -2.91 m/s² 4.169						x (133, 0.32 s) 2.58 m/s² 3.689	x (139, 0.38 s) 86.80 m/s² 124.297
		58	58_CTRLd_60cly only_ 4flrs_LIVE_accA	2.96 s (397); x		x (247, 1.46 s) $7.18x10^{-1}$ m/s² 0.733						x (384, 2.83 s) 2.15 m/s² 2.191	x (377, 2.76 s) -59.30 m/s² 60.544
		64	64_CTRLd_60cly only_3flrs_LIVE_accA	N / A (no collapse)		N / A (no collapse)						N / A (no collapse)	N / A (no collapse)
	Geology type (f): Models analysed on ground specified as **clay at Minimum Z**	47	47CTRLd_cly min z_6flrs_INCL LIVE_accA	1.35 s (236); x								x (232, 1.31 s) 1.34 m/s² 1.543	x (231, 1.30 s) -13.20 m/s² 15.170
		53	53_CTRLd_CLy minz_ 5flrs_LIVE_accA	3.65 s (466); x								x (361, 2.60 s) -6.85 x10^-2 m/s² 0.070	x (464, 3.63 s) -2.34 m/s² 2.387
		59	59_CTRLd_cly minz_ 4flrs_LIVE_accA	N / A (no collapse)								N / A (no collapse)	N / A (no collapse)

Table 39 Maximum x-acceleration in subsoil layers, first course and slab over semi-basement level prior to the start of failure at slab over semi-basement level (continued).

Model details	Geology	Model reference number	ELS® model name	Time (frame no.) of 1st sign of failure at slab over semi-basement level; orientation	Direction (frame no., time (s)) of maximum x-acceleration before start of failure at slab over semi-basement level (m/s^2): **Bottom clay**; ratio to maximum input p.g.a. prior to start of failure	Direction (frame no., time (s)) of maximum x-acceleration before start of failure at slab over semi-basement level (m/s^2): **Middle clay**; ratio to maximum input p.g.a. prior to start of failure	Direction (frame no., time (s)) of maximum x-acceleration before start of failure at slab over semi-basement level (m/s^2): **Top clay**; ratio to maximum input p.g.a. prior to start of failure	Direction (frame no., time (s)) of maximum x-acceleration before start of failure at slab over semi-basement level (m/s^2): **Bottom UCL**; ratio to maximum input p.g.a. prior to start of failure	Direction (frame no., time (s)) of maximum x-acceleration before start of failure at slab over semi-basement level (m/s^2): **Middle UCL**; ratio to maximum input p.g.a. prior to start of failure	Direction (frame no., time (s)) of maximum x-acceleration before start of failure at slab over semi-basement level (m/s^2): **Top UCL**; ratio to maximum input p.g.a. prior to start of failure	Direction (frame no., time (s)) of maximum x-acceleration before start of failure at slab over semi-basement level (m/s^2): **Thin (1.5m thick) UCL**; ratio to maximum input p.g.a. prior to start of failure	Direction (frame no., time (s)) of maximum x-acceleration before start of failure at slab over semi-basement level (m/s^2): **1st course**; ratio to maximum input p.g.a. prior to start of failure	Direction (frame no., time (s)) of maximum x-acceleration before start of failure at slab over semi-basement level (m/s^2): **Slab over semi-basement**; ratio to maximum input p.g.a. prior to start of failure
Single building control model with soft storey at semi-base-ment level	Geology type (d): Models analysed on a **1.5 m thick upper coralline limestone layer which overlies a 60 m thick layer of clay** (Nadur case), both modelled as three dimensional blocks	69	69_CTRL wt S_STORYc_thn rk on cly_ 6flrs_LIVE_accA	0.46 s (147); x		x (145, 0.44 s) $-8.13x10^{-1}$ m/s² 1.164					x (140, 0.39 s) $4.88x10^{-1}$ m/s² 0.698	x (144, 0.43 s) 3.21 m/s² 4.597	x (139, 0.38 s) 6.42 m/s² 9.195
		71	71_CTRL wt S_STORYc_thn rk on cly_ 5flrs_LIVE_accA	1.29 s (230); x		x (113, 0.12 s) 1.09 m/s² 1.561					x (206, 1.05s) $6.56x10^{-1}$m/s² 0.940	x (228, 1.27 s) -1.54 m/s² 2.202	x (228, 1.27 s) -2.35 m/s² 3.359
		73	73_CTRL wt S_STORYc_thn rk on cly_ 4flrs_LIVE_accA	2.60 s (361); x		x (126, 0.25 s) -1.51 m/s² 1.544					x (348, 2.47s) $9.38x10^{-1}$m/s² 0.957	x (351, 2.50 s) $9.82x10^{-1}$ m/s² 1.002	x (359, 2.58 s) 1.81 m/s² 1.844
		75	75_CTRL wt S_STORYc_thn rk on cly_ 3flrs_LIVE_accA	N / A (no collapse)		N / A (no collapse)					N / A (no collapse)	N / A (no collapse)	N / A (no collapse)
Single building control model with setbacks at pent-house level		79	79_CTRL wt STBKc_thn rk on cly_6flrs_LIVE_accA	0.45 s (146); x		x (127, 0.26 s) 1.64 m/s² 2.342					x (116, 0.15s) $4.44x10^{-1}$m/s² 0.636	x (115, 0.14 s) $4.96x10^{-1}$ m/s² 0.710	x (144, 0.43 s) -6.47 m/s² 9.260
		81	81_CTRL wt STBKc_thn rk on cly_5flrs_LIVE_accA	1.55 s (256); x		x (127, 0.26 s) 2.03 m/s² 2.338					x (202, 1.01s) $4.78x10^{-1}$m/s² 0.551	x (202, 1.01 s) $4.48x10^{-1}$ m/s² 0.517	x (253, 1.52 s) -1.12 m/s² 1.288
		83	83_CTRL wt STBKc_thn rk on cly_4flrs_LIVE_accA	N / A (no collapse)		N / A (no collapse)					N / A (no collapse)	N / A (no collapse)	N / A (no collapse)
Single building control model with a double height space bet-ween Levels 0 and +1		99	99_CTRL_DHTc_thn rk on cly_ 6flrs_INCL LIVE_accA	0.39 s (140); x		x (124, 0.23 s) $-7.75x10^{-1}$ m/s² 1.109					x (114, 0.13s) $4.65x10^{-1}$m/s² 0.665	x (138, 0.37 s) $5.41x10^{-1}$ m/s² 0.774	x (136, 0.35 s) 5.34 m/s² 7.639
		101	101_CTRL_DBL HTc_thn rk on cly_ 5flrs_LIVE_accA	1.32 s (233); x		x (127, 0.26 s) -1.45 m/s² 1.672					x (194, 0.93s) $-5.24x10^{-1}$m/s² 0.604	x (228, 1.27 s) 2.60 m/s² 3.003	x (205, 1.04 s) -84.70 m/s² 97.714
		103	103_CTRL_DBL HTc_thn rk on cly_4flrs_LIVE_accA	4.35 s (536); x		x (125, 0.24 s) 2.11 m/s² 2.153					x (348, 2.47s) $9.39x10^{-1}$m/s² 0.958	x (532, 4.31 s) -2.75 m/s² 2.807	x (533, 4.32 s) 53.30 m/s² 54.424
		105	105_CTRL_DBL HTc_thn rk on cly_3flrs_LIVE_accA	N / A (no collapse)		N / A (no collapse)					N / A (no collapse)	N / A (no collapse)	N / A (no collapse)

Table 39 Maximum x-acceleration in subsoil layers, first course and slab over semi-basement level prior to the start of failure at slab over semi-basement level (continued).

Model details	Geology	Model reference number	ELS® model name	Time (frame no.) of 1st sign of failure at slab over semi-basement level; orientation	Direction (frame no., time (s)) of maximum x-acceleration before start of failure at slab over semi-basement level ($m/m/s^2$): **Bottom clay**; ratio to maximum input p.g.a. prior to start of failure	Direction (frame no., time (s)) of maximum x-acceleration before start of failure at slab over semi-basement level (m/s^2): **Middle clay**; ratio to maximum input p.g.a. prior to start of failure	Direction (frame no., time (s)) of maximum x-acceleration before start of failure at slab over semi-basement level (m/s^2): **Top clay**; ratio to maximum input p.g.a. prior to start of failure	Direction (frame no., time (s)) of maximum x-acceleration before start of failure at slab over semi-basement level (m/s^2): **Bottom UCL**; ratio to maximum input p.g.a. prior to start of failure	Direction (frame no., time (s)) of maximum x-acceleration before start of failure at slab over semi-basement level (m/s^2): **Middle UCL**; ratio to maximum input p.g.a. prior to start of failure	Direction (frame no., time (s)) of maximum x-acceleration before start of failure at slab over semi-basement level (m/s^2): **Top UCL**; ratio to maximum input p.g.a. prior to start of failure	Direction (frame no., time (s)) of maximum x-acceleration before start of failure at slab over semi-basement level (m/s^2): **Thin (1.5m thick) UCL**; ratio to maximum input p.g.a. prior to start of failure	Direction (frame no., time (s)) of maximum x-acceleration before start of failure at slab over semi-basement level (m/s^2): **1st course**; ratio to maximum input p.g.a. prior to start of failure	Direction (frame no., time (s)) of maximum x-acceleration before start of failure at slab over semi-basement level (m/s^2): **Slab over semi-basement**; ratio to maximum input p.g.a. prior to start of failure
Single building control model with soft storey at semi-basement level and setbacks at penthouse level	Geology type (d): Models analy-sed on a **1.5 m thick upper coralline lime-stone layer which overlies a 60 m thick layer of clay** (Nadur case), both modelled as three dimen-sional blocks	89	89_CTRL_STBK_SSTRYc_thn rk on cly_6flrs_LIVE_accA	0.75 s (176); x		x (165, 0.64 s) $6.30x10^{-1}$ m/s² 0.902					x (166, 0.65 s) $-7.54x10^{-1}$ m/s² 1.079	x (175, 0.74 s) -47.10 m/s² 67.375	x (157, 0.56 s) 3.94 m/s² 5.636
		91	91_CTRL_STBK_SSTRYc_thn rk on cly_5flrs_LIVE_accA	1.91 s (292); x		x (246, 1.45 s) -1.88 m/s² 2.163					x (202, 1.01 s) $5.0\ x10^{-1}$ m/s² 0.578	x (115, 0.14 s) $4.40x10^{-1}$ m/s² 0.507	x (260, 1.59 s) $-7.78x10^{-1}$ m/s² 0.897
		93	93_CTRL_STBK_SSTRYc_thn rk on cly_4flrs_LIVE_accA	5.77 s (678); x		x (124, 0.23 s) -2.46 m/s² 2.508					x (348, 2.47 s) $9.21x10^{-1}$ m/s² 0.940	x (676, 5.75 s) 3.64 m/s² 3.714	x (657, 5.56 s) -5.74 m/s² 5.856
		95	95_CTRL_STBK_SSTRYc_thn rk on cly_3flrs_LIVE_accA	N / A (no collapse)		N / A (no collapse)					N / A (no collapse)	N / A (no collapse)	N / A (no collapse)
Single building control model with soft storey at semi-basement level and double height space between Levels 0 and +1		109	109_CTRL_S_STRY_D_HTc_thnRK onCY_6flrs_LIVE_accA	0.38 s (139); x		x (130, 0.29 s) $-4.34x10^{-1}$ m/s² 0.622					x (137, 0.36 s) $5.09x10^{-1}$ m/s² 0.729	x (130, 0.29 s) 5.11 m/s² 7.313	x (133, 0.32 s) 4.53 m/s² 6.488
		111	111_CTRL_S_STRY_D_HTc_thnRK onCY_5flrs_LIVE_accA	1.98 s (299); x		x (201, 1.00 s) 1.13 m/s² 1.303					x (270, 1.69 s) $6.39x10^{-1}$ m/s² 0.737	x (294, 1.93 s) -87.10 m/s² 100.488	x (268, 1.67 s) 3.48 m/s² 4.008
		113	113_CTRL_ S_STRY_D_HTc_thn rk on cly_ 4flrs_LIVE_accA	2.58 s (359); x		x (125, 0.24 s) 2.69 m/s² 2.750					x (348, 2.47 s) $9.51x10^{-1}$ m/s² 0.970	x (349, 2.48 s) 1.13 m/s² 1.156	x (358, 2.57 s) 1.70 m/s² 1.730
		115	115_CTRL _S_STRY_D HTc_thnRKonCY_3flrs_LIVE_accA	N / A (no collapse)		N / A (no collapse)					N / A (no collapse)	N / A (no collapse)	N / A (no collapse)
Single building control model with soft storey, double height space and setbacks		119	119_CTRL_STBK_SSTRY_DHTc_th nRK_CY_6fls_LV_accA	0.76 s (177); x		x (123, 0.22 s) -2.11 m/s² 3.025					x (115, 0.14 s) $4.46x10^{-1}$ m/s² 0.638	x (172, 0.71 s) -67.20 m/s² 96.140	x (151, 0.50 s) -6.68 m/s² 9.559
		121	121_CTRL_STBK_SSTRY_DHTc_th nRK_CY_5fls_LV_accA	3.41 s (442); x		x (364, 2.63 s) -2.54 m/s² 2.588					x (286, 2.85 s) 1.15 m/s² 1.173	x (414, 3.13 s) 9.06 m/s² 9.246	x (381, 2.80 s) -6.45 m/s² 6.581
		123	123_CTRL_STBK_SSTRY_DHTc_th nRK_CY_4fls_LV_accA	5.70 s (671); x		x (125, 0.24 s) 2.17 m/s² 2.218					x (660, 5.59 s) 1.02 m/s² 1.040	x (659, 5.58 s) -2.23 m/s² 2.272	x (656, 5.55 s) -7.03 m/s² 7.176
		125	125_CTRL_STBK_SSTRY_DHTc_th nRK_CY_3fls_LV_accA	N / A (no collapse)		N / A (no collapse)					N / A (no collapse)	N / A (no collapse)	N / A (no collapse)

Table 39 Maximum x-acceleration in subsoil layers, first course and slab over semi-basement level prior to the start of failure at slab over semi-basement level (continued).

Model details	Geology	Model reference number	ELS® model name	Time (frame no.) of 1st sign of failure at slab over semi-basement level; orientation	Direction (frame no., time (s)) of maximum x-acceleration before start of failure at slab over semi-basement level (m/s^2): **Bottom clay**; ratio to maximum input p.g.a. prior to start of failure	Direction (frame no., time (s)) of maximum x-acceleration before start of failure at slab over semi-basement level (m/s^2): **Middle clay**; ratio to maximum input p.g.a. prior to start of failure	Direction (frame no., time (s)) of maximum x-acceleration before start of failure at slab over semi-basement level (m/s^2): **Top clay**; ratio to maximum input p.g.a. prior to start of failure	Direction (frame no., time (s)) of maximum x-acceleration before start of failure at slab over semi-basement level (m/s^2): **Bottom UCL**; ratio to maximum input p.g.a. prior to start of failure	Direction (frame no., time (s)) of maximum x-acceleration before start of failure at slab over semi-basement level (m/s^2): **Middle UCL**; ratio to maximum input p.g.a. prior to start of failure	Direction (frame no., time (s)) of maximum x-acceleration before start of failure at slab over semi-basement level (m/s2): **Top UCL**; ratio to maximum input p.g.a. prior to start of failure	Direction (frame no., time (s)) of maximum x-acceleration before start of failure at slab over semi-basement level (m/s^2): **Thin (1.5m thick) UCL**; ratio to maximum input p.g.a. prior to start of failure	Direction (frame no., time (s)) of maximum x-acceleration before start of failure at slab over semi-basement level (m/s^2): **1st course**; ratio to maximum input p.g.a. prior to start of failure	Direction (frame no., time (s)) of maximum x-acceleration before start of failure at slab over semi-basement level (m/s^2): **Slab over semi-basement**; ratio to maximum input p.g.a. prior to start of failure
2-building control model	Geology type (d): Models analysed on a **1.5 m thick upper coralline limestone layer which overlies a 60 m thick layer of clay** (Nadur case), both modelled as three dimensional blocks	130	130_CTRLx2AGG_c_thnRK_CY_6flrs_LIVE_accA	0.89 s (190); x		x (122, 0.21 s) -1.16 m/s^2 1.661					x (189, 0.88 s) -7.01×10^{-1} m/s^2 1.004	x (173, 0.72 s) 2.61 m/s^2 3.740	x (128, 0.27 s) -90.60 m/s^2 129.732
		132	132_CTRLx2AGG_c_thnRK_CY_5flrs_LIVE_accA	0.93 s (194); x		x (149, 0.48 s) -1.37 m/s^2 1.967					x (116, 0.15 s) 4.70×10^{-1} m/s^2 0.672	x (157, 0.56 s) 1.32 m/s^2 1.896	x (163, 0.62 s) 45.00 m/s^2 64.418
		134	134_CTRLx2AGG_c_thnRK_CY_4flrs_LIVE_accA	4.79 s (580); x		x (356, 2.55 s) -2.35 m/s^2 2.400					x (395, 2.94 s) -8.25×10^{-1} m/s^2	x (407, 3.06 s) 1.61 m/s^2 1.643	x (413, 3.12 s) -56.60 m/s^2 57.724
		136	136_CTRLx2AGG_c_thnRK_CY_3flrs_LIVE_accA	N / A (no collapse)		N / A (no collapse)					N / A (no collapse)	N / A (no collapse)	N / A (no collapse)
3-building control model		138	138_CTRLx3AGG_c_thnRK_CY_6flrs_LIVE_accA	0.84 s (185); x		x (158, 0.57 s) -3.27×10^{-1} m/s^2 0.468					x (178, 0.77 s) -6.41×10^{-1} m/s^2 0.918	x (124, 0.23 s) -3.33 m/s^2 4.769	x (166, 0.65 s) -100.00 m/s^2 143.344
		140	140_CTRLx3AGG_c_thnRK_CY_5flrs_LIVE_accA	1.13 s (214); x		x (201, 1.00 s) 4.83×10^{-1} m/s^2 0.691					x (139, 0.38 s) 9.91×10^{-1} m/s^2 1.418	x (184, 0.838 s) 2.65 m/s^2 3.791	x (213, 1.12 s) 68.40 m/s^2 97.958
		142	142_CTRLx3AGG_c_thnRK_CY_4flrs_LIVE_accA	4.81 s (582); x		x (358, 2.57 s) -1.88 m/s^2 1.923					x (313, 2.12 s) -8.86×10^{-1} m/s^2 0.904	x (434, 3.33 s) -1.88 m/s^2 1.920	x (498, 3.97 s) -91.90 m/s^2 93.736
		144	144_CTRLx3AGG_c_thnRK_CY_3flrs_LIVE_accA	N / A (no collapse)		N / A (no collapse)					N / A (no collapse)	N / A (no collapse)	N / A (no collapse)
Existing Xemxija building (XMX 0011)	Geology type (d): **1.5 m thick upper coralline limestone on 60 m thick clay**	128	128X11_01c_ThnRk_CY_accA6flrs_InclLIVE_incl Bsmt wlls	0.76 s (177); x		x (102, 0.01 s) -5.40×10^{-1} m/s^2 0.773					x (109, 0.08 s) -4.23×10^{-1} m/s^2 0.606	x (109, 0.08 s) -4.21×10^{-1} m/s^2 0.602	x (175, 0.74 s) 2.65 m/s^2 3.791
	Geology type (c) (actual scenario): **30 m thick upper coralline limestone on 30 m thick clay**	129	129X11_01b_30Rk30CY_accA6flrs_InclLIVE_incl Bsmt wlls	2.01 s (302); x		x (245, 1.44 s) 1.45 m/s^2 1.667			x (301, 2.00 s) 7.44×10^{-1} m/s^2 0.858			x (299, 1.98 s) 7.61 m/s^2 8.772	x (296, 1.95 s) 5.79 m/s^2 6.675

Table 40 X-displacement (m) at analysis time corresponding to start of failure at different positions throughout the height of analysed models.

Model details	Geology	Model reference number	Direction (frame number, analysis time) at first sign of failure at **penthouse roof slab**, corresponding x-displacement (m)	Direction (frame number, analysis time) at first sign of failure at **penthouse floor slab**, corresponding x-displacement (m)	Direction (frame number, analysis time) at first sign of failure at **slab over 1st floor level**, corresponding x-displacement (m)	Direction (frame number, analysis time) at first sign of failure at **slab over level 0**, corresponding x-displacement (m)	Direction (frame number, analysis time) at first sign of failure in **element above DPM**, corresponding x-displacement (m)	Direction (frame number, analysis time) at first sign of failure in **element below DPM**, corresponding x-displacement (m)	Direction (frame number, analysis time) at first sign of failure at **slab over semi-basement level**, corresponding x-displacement (m)	Direction (frame number, analysis time) at first sign of failure at **1st course**, corresponding x-displacement (m)	Direction (frame number, analysis time) at slab over semi-basement level, corresponding x-displacement (m) at **top of clay layer**	Direction (frame number, analysis time) at slab over semi-basement level, corresponding x-displacement (m) at **middle of clay layer**	Direction (frame number, analysis time) at slab over semi-basement level, corresponding x-displacement (m) at **bottom of clay layer**	Direction (frame number, analysis time) at slab over semi-basement level, corresponding x-displacement (m) at **top of UCL layer**	Direction (frame number, analysis time) at slab over semi-basement level, corresponding x-displacement (m) at **middle of UCL layer**	Direction (frame number, analysis time) at slab over semi-basement level, corresponding x-displacement (m) at **bottom of UCL layer**	Direction (frame number, analysis time) at slab over semi-basement level, corresponding x-displacement (m) at **thin (1.5 m thick) UCL layer**
Single building control models	Geology type (a): Models analysed on a **30 m thick layer of upper coralline limestone** modelled as a three dimensional block	42v2	x(234, 1.33 s) -5.94×10^{-4}	x(234, 1.33 s) -4.85×10^{-4}	x(234, 1.33 s) -3.53×10^{-4}	x(233, 1.32 s) -6.36×10^{-5}	x(259, 1.59 s) 1.33×10^{-5}	x(259, 1.59 s) -2.46×10^{-3}	x(257, 1.56 s) -2.60×10^{-3}	x(227, 1.26 s) -3.84×10^{-6}				x(257, 1.56 s) -1.35×10^{-5}	x(257, 1.56 s) -1.08×10^{-5}	x(257, 1.56 s) -3.83×10^{-6}	
		48	N / A (no collapse)	N / A (no collapse)	N / A (no collapse)	N / A (no collapse)			N / A (no collapse)	N / A (no collapse)					N / A (no collapse)		
	Geology type (b): Models analysed on ground specified as **upper corolline limestone at Minimum Z**	43v2	x(410, 3.09 s) 9.59×10^{-4}	x(406, 3.05 s) 5.22×10^{-4}	x(385, 2.84 s) 2.13×10^{-4}	x(377, 2.76 s) 2.18×10^{-4}			x(375, 2.74 s) -2.17×10^{-3}	Not identifiable							
		49	N / A (no collapse)	N / A (no collapse)	N / A (no collapse)	N / A (no collapse)			N / A (no collapse)	N / A (no collapse)							
	Geology type (c): Models analysed on a **30 m thick upper coralline limestone layer which overlies a 30 m thick layer of clay** (Xemxija case), both modelled as three dimensional blocks	44v2	x(322, 2.21 s) 7.52×10^{-4}	x(325, 2.24 s) 6.80×10^{-3}	x(410, 3.09 s) -5.07×10^{-3}	x(390, 2.89 s) 2.89×10^{-3}			x(359, 2.58 s) -1.03×10^{-2}	x(362, 2.61 s) -2.13×10^{-3}	x(359, 2.58 s) -3.27×10^{-3}	x(359, 2.58 s) -1.79×10^{-3}	x(359, 2.58 s) -9.16×10^{-7}	x(359, 2.58 s) -2.04×10^{-3}	x(359, 2.58 s) -2.73×10^{-3}	x(359, 2.58 s) -2.04×10^{-3}	
		50	N / A (no collapse)	N / A (no collapse)	N / A (no collapse)	N / A (no collapse)			N / A (no collapse)	N / A (no collapse)		N / A (no collapse)			N / A (no collapse)		

Table 40 X-displacement (m) at analysis time corresponding to start of failure at different positions throughout the height of analysed models (continued).

Model details	Geology	Model reference number	Direction (frame number, analysis time) at first sign of failure at **penthouse roof slab**, corresponding x-displacement (m)	Direction (frame number, analysis time) at first sign of failure at **penthouse floor slab**, corresponding x-displacement (m)	Direction (frame number, analysis time) at first sign of failure at **slab over 1st floor level**, corresponding x-displacement (m)	Direction (frame number, analysis time) at first sign of failure at **slab over level 0**, corresponding x-displacement (m)	Direction (frame number, analysis time) at first sign of failure in **element above DPM**, corresponding x-displacement (m)	Direction (frame number, analysis time) at first sign of failure in **element below DPM**, corresponding x-displacement (m)	Direction (frame number, analysis time) at first sign of failure at s**lab over semi-basement level**, corresponding x-displacement (m)	Direction (frame number, analysis time) at first sign of failure at **1st course**, corresponding x-displac-ment (m)	Direction (frame number, analysis time) at slab over semi-basement level, corresponding x-displacement (m) at **top of clay layer**	Direction (frame number, analysis time) at slab over semi-basement level, corresponding x-displacement (m) at **middle of clay layer**	Direction (frame number, analysis time) at slab over semi-basement level, corresponding x-displacement (m) at **bottom of clay layer**	Direction (frame number, analysis time) at slab over semi-basement level, corresponding x-displacement (m) at **top of UCL laye**r	Direction (frame number, analysis time) at slab over semi-basement level, corresponding x-displacement (m) at **middle of UCL laye**r	Direction (frame number, analysis time) at slab over semi-basement level, corresponding x-displacement (m) at **bottom of UCL layer**	Direction (frame number, analysis time) at slab over semi-basement level, corresponding x-displacement (m) at **thin (1.5 m thick) UCL layer**
Single building control models	Geology type (d): Models analysed on a **1.5 m thick upper coralline limestone layer which overlies a 60 m thick layer of clay** (Nadur case), both modelled as three dimensional blocks	45v2	x(130,0.29 s) $-1.32x10^{-2}$	x(125,0.24 s) $-8.04x10^{-3}$	x(110,0.09 s) $-1.07x10^{-3}$	x(110,0.09 s) $-1.01x10^{-3}$			x(128,0.27 s) $-9.99x10^{-4}$	x(253,1.52 s) $2.91x10^{-4}$	x(128,0.27 s) $-2.64x10^{-4}$	x(128,0.27 s) $1.40x10^{-5}$	x(128,0.27 s) $3.05x10^{-8}$				x(128,0.27 s) $-1.55x10^{-4}$
		51	x(243,1.42 s) $-9.90x10^{-5}$	x(245,1.44 s) $-9.14x10^{-4}$	x(219,1.18 s) $2.21x10^{-4}$	x(224,1.23 s) $1.22x10^{-4}$			x(170,0.69 s) $-7.30x10^{-4}$	x(352,2.51 s) $9.06x10^{-5}$		x(170,0.69 s) $-1.49x10^{-6}$					x(170,0.69 s) $1.36x10^{-4}$
		57	x(383,2.82 s) $-4.44x10^{-4}$	x(380,2.79 s) $-1.97x10^{-4}$	refer to penthouse floor slab	x(379,2.78 s) $-2.27x10^{-4}$			x(375,2.74 s) $-4.48x10^{-4}$	x(569,4.68 s) $-3.36x10^{-3}$		x(375,2.74 s) $2.46x10^{-4}$					x(375,2.74 s) $1.35x10^{-4}$
		63	N / A (no collapse)	N / A (no collapse)	N / A (no collapse)	N / A (no collapse)			N / A (no collapse)	N / A (no collapse)		N / A (no collapse)					N / A (no collapse)
	Geology type (e): Models analysed on a **60 m thick layer of clay** modelled as a three dimensional block	46	x(125,0.24 s) $-1.31x10^{-2}$	x(120,0.19 s) $-7.81x10^{-3}$	x(110,0.09 s) $-1.45x10^{-3}$	x(106,0.05 s) $-6.35x10^{-4}$			x(110,0.09 s) $-1.63x10^{-3}$	x(133,0.32 s) $-9.01x10^{-4}$	x(110,0.09 s) $-6.09x10^{-5}$	x(110,0.09 s) $-1.42x10^{-4}$	x(110,0.09 s) $-8.05x10^{-9}$				
		52	x(200,0.90 s) $-1.35x10^{-2}$	x(150,0.49 s) $-1.94x10^{-3}$	x(149,0.48 s) $-1.81x10^{-3}$	x(147,0.46 s) $-1.61x10^{-3}$			x(144,0.43 s) $-2.23x10^{-3}$	x(167,0.66 s) $-6.42x10^{-4}$		x(144,0.43 s) $-8.75 x10^{-5}$					
		58	x(396,2.95 s) $-1.59x10^{-2}$	x(382,2.81s) $-8.07x10^{-4}$	refer to penthouse floor slab	x(395,2.94 s) $3.21x10^{-3}$			- x(397,2.96 s) $5.25x10^{-3}$	- x(409,3.08 s) $3.43x10^{-3}$		x(397,2.96 s) $-4.99x10^{-5}$					
		64	N / A (no collapse)	N / A (no collapse)	N / A (no collapse)	N / A (no collapse)			N / A (no collapse)	N / A (no collapse)		N / A (no collapse)					
	Geology type (f): Models analysed on ground specified as **clay at Minimum Z**	47	x(255,1.54 s) $-1.36x10^{-2}$	x(250,1.49 s) $-5.32x10^{-3}$	x(245,1.44 s) $-1.21x10^{-3}$	x(210,1.09 s) $1.12x10^{-3}$			x(236,1.35 s) $-8.15x10^{-3}$	x(295,1.94 s) $-6.15x10^{-4}$							
		53	x(520,4.19 s) $-6.31x10^{-3}$	x(517,4.16 s) $-5.64x10^{-4}$	x(518,4.17 s) $-2.39x10^{-4}$	x(521,4.20 s) $-8.30x10^{-5}$			x(466,3.65 s) $-2.91x10^{-5}$	x(508,4.07 s) $-3.16x10^{-3}$							
		59	N / A (no collapse)	N / A (no collapse)	N / A (no collapse)	N / A (no collapse)			N / A (no collapse)	N / A (no collapse)							

Table 40 X-displacement (m) at analysis time corresponding to start of failure at different positions throughout the height of analysed models (continued).

Model details	Geology	Model reference number	Direction (frame number, analysis time) at first sign of failure at **penthouse roof slab**, corresponding x-displacement (m)	Direction (frame number, analysis time) at first sign of failure at **penthouse floor slab**, corresponding x-displacement (m)	Direction (frame number, analysis time) at first sign of failure at **slab over 1st floor level**, corresponding x-displacement (m)	Direction (frame number, analysis time) at first sign of failure at **slab over level 0**, corresponding x-displacement (m)	Direction (frame number, analysis time) at first sign of failure in **element above DPM**, corresponding x-displacement (m)	Direction (frame number, analysis time) at first sign of failure in **element below DPM**, corresponding x-displacement (m)	Direction (frame number, analysis time) at first sign of failure at **slab over semi-basement level**, corresponding x-displacement (m)	Direction (frame number, analysis time) at first sign of failure at **1st course**, corresponding x-displacement (m)	Direction (frame number, analysis time) at slab over semi-basement level, corresponding x-displacement (m) at **top of clay layer**	Direction (frame number, analysis time) at slab over semi-basement level, corresponding x-displacement (m) at **middle of clay layer**	Direction (frame number, analysis time) at slab over semi-basement level, corresponding x-displacement (m) at **bottom of clay layer**	Direction (frame number, analysis time) at slab over semi-basement level, corresponding x-displacement (m) at **top of UCL layer**	Direction (frame number, analysis time) at slab over semi-basement level, corresponding x-displacement (m) at **middle of UCL layer**	Direction (frame number, analysis time) at slab over semi-basement level, corresponding x-displacement (m) at **bottom of UCL layer**	Direction (frame number, analysis time) at slab over semi-basement level, corresponding x-displacement (m) at **thin (1.5 m thick) UCL layer**
Single building control model with soft storey at semi-basement level	Geology type (d): Models analysed on a **1.5 m thick upper coralline limestone layer which overlies a 60 m thick layer of clay** (Nadur case), both modelled as three dimensional blocks	69	x(140,0.39 s) -2.51×10^{-2}	x(114,0.13 s) -3.31×10^{-3}	x(110,0.09 s) -1.40×10^{-3}	x(105,0.04 s) -3.89×10^{-4}			x(147,0.46 s) -1.08×10^{-3}	x(181,0.80 s) -1.40×10^{-4}		x(147,0.46 s) -3.16×10^{-5}					x(147, 0.46 s) -4.96×10^{-4}
		71	x(206,1.05 s) -2.76×10^{-3}	x(206,1.05 s) -4.91×10^{-3}	x(221,1.20 s) -5.84×10^{-3}	x(229,1.28 s) -3.66×10^{-4}			x(230,1.29 s) 5.35×10^{-3}	x(304,2.03 s) -3.05×10^{-3}		X(230,1.29 s) -1.60×10^{-4}					x(230,1.29 s) -6.98×10^{-4}
		73	x(365,2.64 s) -1.65×10^{-2}	x(344,2.43 s) -5.68×10^{-5}	refer to penthouse floor slab	x(400,2.99 s) -6.80×10^{-3}			x(361,2.60 s) -1.32×10^{-2}	x(380,2.79 s) 5.81×10^{-4}		x(361,2.60 s) 4.73×10^{-4}					x(361,2.60 s) 1.50×10^{-3}
		75	N / A (no collapse)	N / A (no collapse)	N / A (no collapse)	N / A (no collapse)			N / A (no collapse)	N / A (no collapse)		N / A (no collapse)					N / A (no collapse)
Single building control model with setbacks at penthouse level		79	x(151,0.50 s) -1.85×10^{-2}	x(145,0.44 s) -1.09×10^{-2}	x(110,0.09 s) -1.18×10^{-3}	x(108,0.07 s) -6.47×10^{-4}			x(146,0.45 s) -2.26×10^{-3}	x(276,1.7 5s) -3.82×10^{-4}		x(146,0.45 s) -1.85×10^{-4}					x(146,0.45 s) -6.16×10^{-4}
		81	x(277,1.76 s) -1.75×10^{-2}	x(280,1.79 s) -1.87×10^{-2}	x(260,1.59 s) -2.30×10^{-3}	x(259,1.58 s) -1.70×10^{-3}			x(256,1.55 s) -1.47×10^{-3}	x(254,1.53 s) -3.23×10^{-6}		x(256,1.55 s) -2.22×10^{-4}					x(256,1.55 s) -2.55×10^{-4}
		83	N / A (no collapse)	N / A (no collapse)	N / A (no collapse)	N / A (no collapse)			N / A (no collapse)	N / A(no collapse)		N / A (no collapse)					N / A (no collapse)
Single building control model with a double height space between Levels 0 and +1		99	x(134,0.33 s) -1.41×10^{-2}	x(130,0.29 s) -9.16×10^{-3}	x(140,0.39 s) -9.81×10^{-3}	x(110,0.09 s) -9.46×10^{-4}			x(140,0.39 s) -4.22×10^{-3}	x(220,1.19 s) 9.17×10^{-4}		x(140,0.39 s) -2.77×10^{-4}					x(140,0.39 s) -9.89×10^{-4}
		101	x(240,1.39 s) -1.23×10^{-2}	x(240,1.39 s) -1.04×10^{-2}	x(225,1.24 s) -8.79×10^{-4}	x(227,1.26 s) 2.38×10^{-3}			x(233,1.32 s) -2.80×10^{-3}	x(219,1.18 s) 9.72×10^{-4}		x(233,1.32 s) -3.97×10^{-4}					x(233,1.32 s) -1.28×10^{-3}
		103	x(400,2.99 s) -9.63×10^{-3}	x(400,2.99 s) -7.18×10^{-3}	refer to penthouse floor slab	x(372,2.71 s) 5.36×10^{-3}			x(536,4.35 s) 6.04×10^{-3}	x(814,7.13 s) 3.55×10^{-3}		x(536,4.35 s) -1.72×10^{-4}					x(536,4.35 s) 1.72×10^{-4}
		105	N / A (no collapse)	N / A (no collapse)	N / A (no collapse)	N / A (no collapse)			N / A (no collapse)	N / A (no collapse)		N / A (no collapse)					N / A (no collapse)

Table 40 X-displacement (m) at analysis time corresponding to start of failure at different positions throughout the height of analysed models (continued).

Model details	Geology	Model reference number	Direction (frame number, analysis time) at first sign of failure at **penthouse roof slab**, corresponding x-displacement (m)	Direction (frame number, analysis time) at first sign of failure at **penthouse floor slab**, corresponding x-displacement (m)	Direction (frame number, analysis time) at first sign of failure at **slab over 1st floor level**, corresponding x-displacement (m)	Direction (frame number, analysis time) at first sign of failure at **slab over level 0**, corresponding x-displacement (m)	Direction (frame number, analysis time) at first sign of failure in **element above DPM**, corresponding x-displacement (m)	Direction (frame number, analysis time) at first sign of failure in **element below DPM**, corresponding x-displacement (m)	Direction (frame number, analysis time) at first sign of failure at **slab over semi-basement level**, corresponding x-displacement (m)	Direction (frame number, analysis time) at first sign of failure at **1st course**, corresponding x-displacement (m)	Direction (frame number, analysis time) at slab over semi-basement level, corresponding x-displacement (m) at **top of clay layer**	Direction (frame number, analysis time) at slab over semi-basement level, corresponding x-displacement (m) at **middle of clay layer**	Direction (frame number, analysis time) at slab over semi-basement level, corresponding x-displacement (m) at **bottom of clay layer**	Direction (frame number, analysis time) at slab over semi-basement level, corresponding x-displacement (m) at **top of UCL layer**	Direction (frame number, analysis time) at slab over semi-basement level, corresponding x-displacement (m) at **middle of UCL layer**	Direction (frame number, analysis time) at slab over semi-basement level, corresponding x-displacement (m) at **bottom of UCL layer**	Direction (frame number, analysis time) at slab over semi-basement level, corresponding x-displacement (m) at **thin (1.5 m thick) UCL layer**
Single building control model with a soft storey and setbacks		89	x(157,0.56 s) -3.53×10^{-2}	x(145,0.44 s) -1.22×10^{-2}	x(145,0.44 s) -5.62×10^{-3}	x(146,0.45 s) -2.57×10^{-3}			x(176,0.75 s) 4.01×10^{-3}	x(169,0.68 s) 5.18×10^{-4}		x(176,0.75 s) -6.75×10^{-5}					x(176,0.75 s) -3.32×10^{-5}
		91	x(333,2.32 s) -2.73×10^{-2}	x(340,2.39 s) -1.41×10^{-2}	x(349,2.48 s) -7.88×10^{-4}	x(307,2.06 s) 4.27×10^{-5}			x(292,1.91 s) -7.2×10^{-3}	x(340,2.39 s) -2.68×10^{-5}		x(292,1.91 s) -4.04×10^{-4}					x(292,1.91 s) -1.13×10^{-3}
		93	x(608,5.07s) 1.19×10^{-2}	x(608,5.07 s) 1.15×10^{-2}	refer to penthouse floor slab	x(608,5.07 s) 1.11×10^{-2}			x(678,5.77 s) -2.03×10^{-2}	x(700,5.99 s) 2.67×10^{-3}		x(678,5.77 s) -1.38×10^{-4}					x(678,5.77 s) 9.64×10^{-5}
		95	N / A (no collapse)	N / A (no collapse)	N / A (no collapse)	N / A (no collapse)			N / A (no collapse)	N / A (no collapse)		N / A (no collapse)					N / A (no collapse)
Single building control model with a soft storey and a double height space	Geology type (d): Models analysed on a **1.5 m thick upper coralline limestone layer which overlies a 60 m thick layer of clay** (Nadur case), both modelled as three dimensional blocks	109	x(135,0.34 s) -2.31×10^{-2}	x(135,0.34 s) -1.87×10^{-2}	x(110,0.09 s) -1.43×10^{-3}	x(140,0.39 s) -7.85×10^{-3}			x(139,0.38 s) 5.44×10^{-3}	x(193,0.92 s) 4.88×10^{-4}		x(139,0.38 s) -1.56×10^{-4}					x(139,0.38 s) -8.91×10^{-4}
		111	x(340,1.39 s) -1.26×10^{-2}	x(227,1.26 s) -1.62×10^{-3}	x(227,1.26 s) -3.93×10^{-3}	x(238,1.37 s) -7.00×10^{-3}			x(299,1.98 s) -7.36×10^{-3}	x(286,1.85 s) -4.05×10^{-3}		x(299,1.98 s) -1.64×10^{-4}					x(299,1.98 s) -5.87×10^{-4}
		113	x(375,2.74 s) -5.77×10^{-3}	x(379,2.78 s) -1.54×10^{-3}	refer to penthouse floor slab	x(410,3.09 s) -4.44×10^{-3}			x(359,2.58 s) -1.22×10^{-2}	x(403,3.02 s) 2.20×10^{-3}		x(359,2.58 s) 1.40×10^{-4}					x(359,2.58 s) 9.56×10^{-4}
		115	N / A (no collapse)	N / A (no collapse)	N / A (no collapse)	N / A (no collapse)			N / A (no collapse)	N / A (no collapse)		N / A (no collapse)					N / A (no collapse)
Single building control model with a soft storey, a double height space and setbacks		119	x(147,0.46 s) -1.48×10^{-2}	x(145,0.44 s) -9.48×10^{-3}	x(138,0.37 s) -3.66×10^{-3}	x(152,0.51 s) -5.67×10^{-3}			x(177,0.76 s) -2.86×10^{-3}	x(141,0.40 s) -9.20×10^{-4}		x(177,0.76 s) -4.80×10^{-5}					x(177,0.76 s) -8.78×10^{-5}
		121	x(325,2.24 s) 1.36×10^{-2}	x(325,2.24 s) 1.30×10^{-2}	x(326,2.25 s) 1.24×10^{-2}	x(362,2.61 s) -1.50×10^{-2}			x(442,3.41 s) 1.38×10^{-3}	x(453,3.52 s) 3.53×10^{-4}		x(442,3.41 s) -2.21×10^{-4}					x(442,3.41 s) -8.56×10^{-4}
		123	x(607,5.06 s) 1.18×10^{-2}	x(607,5.06 s) 1.14×10^{-2}	refer to penthouse floor slab	x(654,5.53 s) -1.61×10^{-2}			x(671,5.70 s) -5.14×10^{-3}	x(734,6.33 s) 5.02×10^{-4}		x(671,5.70 s) -2.53×10^{-4}					x(671,5.70 s) -3.57×10^{-4}
		125	N / A (no collapse)	N / A (no collapse)	N / A (no collapse)	N / A (no collapse)			N / A (no collapse)	N / A (no collapse)		N / A (no collapse)					N / A (no collapse)

Table 40 X-displacement (m) at analysis time corresponding to start of failure at different positions throughout the height of analysed models (continued).

Model details	Geology	Model reference number	Direction (frame number, analysis time) at first sign of failure at **penthouse roof slab**, corresponding x-displacement (m)	Direction (frame number, analysis time) at first sign of failure at **penthouse floor slab**, corresponding x-displacement (m)	Direction (frame number, analysis time) at first sign of failure at **slab over 1st floor level**, corresponding x-displacement (m)	Direction (frame number, analysis time) at first sign of failure at **slab over level 0**, corresponding x-displacement (m)	Direction (frame number, analysis time) at first sign of failure in **element above DPM**, corresponding x-displacement (m)	Direction (frame number, analysis time) at first sign of failure in **element below DPM**, corresponding x-displacement (m)	Direction (frame number, analysis time) at first sign of failure at **slab over semi-basement level**, corresponding x-displacement (m)	Direction (frame number, analysis time) at first sign of failure at **1st course**, corresponding x-displacement (m)	Direction (frame number, analysis time) at slab over semi-basement level, corresponding x-displacement (m) at **top of clay layer**	Direction (frame number, analysis time) at slab over semi-basement level, corresponding x-displacement (m) at **middle of clay layer**	Direction (frame number, analysis time) at slab over semi-basement level, corresponding x-displacement (m) at **bottom of clay layer**	Direction (frame number, analysis time) at slab over semi-basement level, corresponding x-displacement (m) at **top of UCL layer**	Direction (frame number, analysis time) at slab over semi-basement level, corresponding x-displacement (m) at **middle of UCL layer**	Direction (frame number, analysis time) at slab over semi-basement level, correspond-ding x-displacement (m) at **bottom of UCL layer**	Direction (frame number, analysis time) at slab over semi-basement level, corresponding x-displacement (m) at **thin (1.5 m thick) UCL layer**
2-building control model	Geology type (d): Models analysed on a **1.5 m thick upper coralline limestone layer which overlies a 60 m thick layer of clay** (Nadur case), both modelled as three dimensional blocks	130	x(127,0.26 s) -1.83×10^{-2}	x(125,0.24 s) -1.29×10^{-2}	x(110,0.09 s) -1.08×10^{-3}	x(105,0.04 s) -1.16×10^{-4}			x(190,0.89 s) -1.46×10^{-2}	x(264,1.63 s) -1.03×10^{-3}		x(190,0.89 s) 2.07×10^{-4}					x(190,0.89 s) 9.89×10^{-4}
		132	x(161,0.60 s) -2.74×10^{-2}	x(165,0.64s) -2.58×10^{-2}	x(157,0.56 s) -1.14×10^{-2}	x(131,0.30 s) -8.65×10^{-4}			x(194,0.93 s) -3.00×10^{-3}	x(322,2.21 s) 7.36×10^{-4}		x(194,0.93 s) 4.43×10^{-4}					x(194,0.93 s) 9.96×10^{-4}
		134	x(437,3.36 s) -2.70×10^{-2}	x(418,3.17 s) -5.15×10^{-3}	refer to penthouse floor slab	x(411,3.10 s) -4.60×10^{-4}			x(580,4.79 s) -5.41×10^{-4}	Not identifiable		x(580,4.79 s) 3.07×10^{-4}					x(580,4.79 s) 4.95×10^{-4}
		136	N / A (no collapse)	N / A (no collapse)	N / A (no collapse)	N / A (no collapse)			N / A (no collapse)	N / A (no collapse)		N / A (no collapse)					N / A (no collapse)
3-building control model		138	x(123,0.22 s) -1.49×10^{-2}	x(123,0.22 s) -1.30×10^{-2}	x(110,0.09 s) -2.08×10^{-3}	x(107,0.06 s) -1.11×10^{-3}			x(185,0.84 s) -1.44×10^{-3}	x(243,1.42 s) -1.30×10^{-3}		x(185,0.84 s) 1.26×10^{-5}					x(185,0.84 s) 2.47×10^{-4}
		140	x(145,0.44 s) -1.90×10^{-2}	x(142,0.41 s) -1.13×10^{-2}	x(135,0.34 s) -4.23×10^{-3}	x(131,0.30 s) -1.82×10^{-3}			x(214,1.13 s) -1.39×10^{-2}	x(325,2.24 s) -2.08×10^{-4}		x(214,1.13 s) 1.35×10^{-4}					x(214,1.13 s) 8.43×10^{-4}
		142	x(444,3.43 s) -1.26×10^{-2}	x(442,3.41 s) -4.71×10^{-3}	refer to penthouse floor slab	x(441,3.40 s) 7.77×10^{-4}			x(582,4.81 s) 1.78×10^{-2}	Not identifiable		x(582,4.81 s) -6.04×10^{-5}					x(582,4.81 s) 1.04×10^{-4}
		144	N / A (no collapse)	N / A (no collapse)	N / A (no collapse)	N / A (no collapse)			N / A (no collapse)	N / A (no collapse)		N / A (no collapse)					N / A (no collapse)
Existing Xemxija building (XMX 0011)	Geology type (d): **1.5 m thick upper coralline limestone on 60 m thick clay**	128	x(230,1.29 s) -5.59×10^{-2}	x(230,1.29 s) -4.14×10^{-2}	x(148,0.47 s) -1.73×10^{-3}	x(252,1.51 s) 2.26×10^{-4}			x(177,0.76 s) -2.35×10^{-3}	x(200,0.99 s) 3.47×10^{-3}		x(177,0.76 s) 1.08×10^{-4}					x(177,0.76 s) 7.78×10^{-4}
	Geology type (c) (actual scenario): **30 m thick upper coralline limestone on 30 m thick clay**	129	x(280,1.79 s) -4.15×10^{-2}	x(278,1.77 s) -3.42×10^{-2}	x(227,1.26 s) 7.56×10^{-3}	x(226,1.25 s) 7.46×10^{-3}			x(302,2.01 s) -1.69×10^{-2}	x(360,2.59 s) -3.30×10^{-3}		x(302,2.01 s) -3.92×10^{-3}			x(302, 2.01 s) -1.26×10^{-2}		

Table 41 Maximum x-displacement (m) during dynamic stage prior to the onset of collapse at every position throughout the height of the analysed models.

Model details	Geology	Model reference number	Direction (frame number, analysis time) at maximum x-displacement at **penthouse roof slab level** prior to start of failure at this position; Maximum x-displacement (m)	Direction (frame number, analysis time) at maximum x-displacement at **penthouse floor slab level** prior to start of failure at this position; Maximum x-displacement (m)	Direction (frame number, analysis time) at maximum x-displacement at **slab over 1st floor** prior to start of failure at this position; Maximum x-displacement (m)	Direction (frame number, analysis time) at maximum x-displacement at **slab over level 0** prior to start of failure at this position; Maximum x-displacement (m)	Direction (frame number, analysis time) at maximum x-displacement in **element above DPM** prior to start of failure at this position; Maximum x-displacement (m)	Direction (frame number, analysis time) at maximum x-displacement in **element below DPM** prior to start of failure at this position; Maximum x-displacement (m)	Direction (frame number, analysis time) at maximum x-displacement at **slab over semi-basement level** prior to start of failure at this position; Maximum x-displacement (m)	Direction (frame number, analysis time) at maximum x-displacement at **first course** prior to start of failure at this position; Maximum x-displacement (m)
Single building control models	Geology type (a): Models analysed on a **30 m thick layer of upper coralline limestone** modelled as a three dimensional block	42v2	x (119, 0.18 s) -4.09×10^{-3}	x (119, 0.18 s) -3.34×10^{-3}	x (119, 0.18 s) -1.88×10^{-3}	x (119, 0.18 s) -1.21×10^{-3}	x (256, 1.55 s) -1.17×10^{-3}	x (258, 1.57 s) -1.59×10^{-3}	x (256, 1.55 s) -2.55×10^{-3}	x (119, 0.18 s) -5.13×10^{-5}
		48	N / A (No collapse)	N / A (No collapse)	N / A (No collapse)	N / A (No collapse)			N / A (No collapse)	N / A (No collapse)
	Geology type (b): Models analysed on ground specified as **upper corolline limestone at Minimum Z**	43v2	x (396, 2.95 s) 1.16×10^{-2}	x (387, 2.86 s) 6.79×10^{-3}	x (353, 2.52 s) -2.80×10^{-3}	x (353, 2.52s) -1.52×10^{-3}			x (374, 2.73 s) -1.79×10^{-3}	Not identifiable
		49	N / A (No collapse)	N / A (No collapse)	N / A (No collapse)	N / A (No collapse)			N / A (No collapse)	N / A (No collapse)
	Geology type (c): Models analysed on a **30 m thick upper coralline limestone layer which overlies a 30 m thick layer of clay** (Xemxija case), both modelled as three dimensional blocks	44v2	x (286, 1.85 s) -2.79×10^{-2}	x (286, 1.85 s) -2.60×10^{-2}	x (346, 2.45 s) 3.09×10^{-2}	x (343, 2.42s) 2.76×10^{-2}			x (286, 1.85 s) -1.96×10^{-2}	x (287, 1.86 s) -1.82×10^{-2}
		50	N / A (No collapse)	N / A (No collapse)	N / A (No collapse)	N / A (No collapse)			N / A (No collapse)	N / A (No collapse)
	Geology type (d): Models analysed on a **1.5 m thick upper coralline limestone layer which overlies a 60 m thick layer of clay** (Nadur case), both modelled as three dimensional blocks	45v2	x (129, 0.28 s) -1.25×10^{-2}	x (124, 0.23 s) -7.56×10^{-3}	x (109, 0.08 s) -8.35×10^{-4}	x (109, 0.08 s) -8.05×10^{-4}			x (116, 0.15 s) -2.26×10^{-3}	x (244, 1.43 s) -2.03×10^{-3}
		51	x (230, 1.29 s) 1.11×10^{-2}	x (232, 1.31 s) 9.14×10^{-3}	x (183, 0.82 s) -4.52×10^{-3}	x (184, 0.83 s) -3.15×10^{-3}			x (117, 0.16 s) -1.74×10^{-3}	x (325, 2.24 s) 3.17×10^{-3}
		57	x (318, 2.17 s) 1.01×10^{-2}	x (317, 2.16 s) 7.40×10^{-3}	refer to penthouse floor slab	x (316, 2.15 s) 5.30×10^{-3}			x (349, 2.48 s) -3.20×10^{-3}	x (568, 4.67 s) -2.88×10^{-3}
		63	N / A (No collapse)	N / A (No collapse)	N / A (No collapse)	N / A (No collapse)			N / A (No collapse)	N / A (No collapse)
	Geology type (e): Models analysed on a **60 m thick layer of clay** modelled as a three dimensional block	46	x (124, 0.23 s) -1.22×10^{-2}	x (119, 0.18 s) -7.07×10^{-3}	x (109, 0.08 s) -1.20×10^{-3}	x (105, 0.04 s) -5.38×10^{-4}			x (109, 0.08 s) -1.41×10^{-3}	x (122, 0.21 s) -9.21×10^{-4}
		52	x (199, 0.98 s) -1.32×10^{-2}	x (126, 0.25 s) -7.50×10^{-3}	x (126, 0.25 s) -5.79×10^{-3}	x (126, 0.25 s) -4.11×10^{-3}			x (132, 0.31 s) -2.82×10^{-3}	x (123, 0.22 s) -1.21×10^{-3}
		58	x (315, 2.14 s) 1.60×10^{-2}	x (315, 2.14 s) 1.21×10^{-2}	refer to penthouse floor slab	x (314, 2.13 s) 8.52×10^{-3}			x (380, 2.79 s) -1.31×10^{-2}	x (408, 3.07 s) -3.04×10^{-3}
		64	N / A (No collapse)	N / A (No collapse)	N / A (No collapse)	N / A (No collapse)			N / A (No collapse)	N / A (No collapse)
	Geology type (f): Models analysed on ground specified as **clay at Minimum Z**	47	x (254, 1.53 s) -1.16×10^{-2}	x (230, 1.29 s) 7.54×10^{-3}	x (233, 1.32 s) 6.27×10^{-3}	x (120, 1.90 s) -1.28×10^{-3}			x (235, 1.34 s) -5.99×10^{-3}	x (262, 1.61 s) -1.13×10^{-2}
		53	x (479, 3.78 s) 1.00×10^{-2}	x (478, 3.77 s) 8.12×10^{-3}	x (477, 3.76 s) 6.19×10^{-3}	x (477, 3.76 s) 4.32×10^{-3}			x (366, 2.65 s) 1.16×10^{-3}	x (507, 4.06 s) -2.51×10^{-3}
		59	N / A (No collapse)	N / A (No collapse)	N / A (No collapse)	N / A (No collapse)			N / A (No collapse)	N / A (No collapse)

Table 41 Maximum x-displacement (m) during dynamic stage prior to the onset of collapse at every position throughout the height of the analysed models (continued).

Model details	Geology	Model reference number	Direction (frame number, analysis time) at maximum x-displacement at **penthouse roof slab level** prior to start of failure at this position; Maximum x-displacement (m)	Direction (frame number, analysis time) at maximum x-displacement at **penthouse floor slab level** prior to start of failure at this position; Maximum x-displacement (m)	Direction (frame number, analysis time) at maximum x-displacement at **slab over 1st floor** prior to start of failure at this position; Maximum x-displacement (m)	Direction (frame number, analysis time) at maximum x-displacement at **slab over level 0** prior to start of failure at this position; Maximum x-displacement (m)	Direction (frame number, analysis time) at maximum x-displacement in **element above DPM** prior to start of failure at this position; Maximum x-displacement (m)	Direction (frame number, analysis time) at maximum x-displacement in **element below DPM** prior to start of failure at this position; Maximum x-displacement (m)	Direction (frame number, analysis time) at maximum x-displacement at **slab over semi-basement level** prior to start of failure at this position; Maximum x-displacement (m)	Direction (frame number, analysis time) at maximum x-displacement at **first course** prior to start of failure at this position; Maximum x-displacement (m)
Single building control model with soft storey at semi-basement level	Geology type (d): Models analysed on a **1.5 m thick upper coralline limestone layer which overlies a 60 m thick layer of clay** (Nadur case), both modelled as three dimensional blocks	69	x (139, 0.38 s) -2.40×10^{-2}	x (113, 0.12 s) -2.85×10^{-3}	x (109, 0.08 s) -1.13×10^{-3}	x (104, 0.03 s) -3.28×10^{-4}			x (124, 0.23 s) -3.44×10^{-3}	x (116, 0.15 s) -1.29×10^{-3}
		71	x (122, 0.21 s) -5.46×10^{-3}	x (122, 0.21 s) -4.58×10^{-3}	x (210, 1.09 s) -7.69×10^{-3}	x (208, 1.07 s) -9.21×10^{-3}			x (229, 1.28 s) 5.41×10^{-3}	x (303, 2.02 s) -3.63×10^{-3}
		73	x (361, 2.60 s) -1.64×10^{-2}	x (325, 2.14 s) 1.18×10^{-2}	refer to penthouse floor slab	x (360, 2.59 s) -1.44×10^{-2}			x (360, 2.59 s) -1.32×10^{-2}	x (349, 2.48 s) -2.55×10^{-3}
		75	N / A (No collapse)	N / A (No collapse)	N / A (No collapse)	N / A (No collapse)			N / A (No collapse)	N / A (No collapse)
Single building control model with setbacks at penthouse level		79	x (150, 0.49 s) -1.75×10^{-2}	x (144, 0.43 s) -1.02×10^{-2}	x (109, 0.08 s) -9.31×10^{-4}	x (107, 0.06 s) -4.89×10^{-4}			x (118, 0.17 s) -1.97×10^{-3}	x (268, 1.67 s) -3.69×10^{-3}
		81	x (276, 1.75 s) -1.59×10^{-2}	x (279, 1.78 s) -1.72×10^{-2}	x (245, 1.44 s) -5.49×10^{-3}	x (244, 1.43 s) -3.74×10^{-3}			x (242, 1.41 s) -2.79×10^{-3}	x (239, 1.38 s) -1.70×10^{-3}
		83	N / A (No collapse)	N / A (No collapse)	N / A (No collapse)	N / A (No collapse)			N / A (No collapse)	N / A (No collapse)
Single building control model with a double height space between Levels 0 and +1		99	x (133, 0.32 s) -1.32×10^{-2}	x (129, 0.28 s) -8.74×10^{-3}	x (139, 0.38 s) -9.01×10^{-3}	x (109, 0.08 s) -7.35×10^{-4}			x (139, 0.38 s) -3.62×10^{-3}	x (115, 0.14 s) -1.17×10^{-3}
		101	x (239, 1.38 s) -1.14×10^{-2}	x (239, 1.38 s) -9.44×10^{-3}	x (120, 0.19 s) -3.04×10^{-3}	x (208, 1.07 s) -3.06×10^{-3}			x (224, 1.23 s) 6.55×10^{-3}	x (115, 0.14 s) -1.18×10^{-3}
		103	x (374, 2.73 s) 1.11×10^{-2}	x (373, 2.72 s) 7.88×10^{-3}	refer to penthouse floor slab	x (371, 2.70 s) 5.42×10^{-3}			x (535, 4.34 s) 7.25×10^{-3}	x (813, 7.12 s) 3.94×10^{-3}
		105	N / A (No collapse)	N / A (No collapse)	N / A (No collapse)	N / A (No collapse)			N / A (No collapse)	N / A (No collapse)

Table 41 Maximum x-displacement (m) during dynamic stage prior to the onset of collapse at every position throughout the height of the analysed models (continued).

Model details	Geology	Model reference number	Direction (frame number, analysis time) at maximum x-displacement at **penthouse roof slab level** prior to start of failure at this position; Maximum x-displacement (m)	Direction (frame number, analysis time) at maximum x-displacement at **penthouse floor slab level** prior to start of failure at this position; Maximum x-displacement (m)	Direction (frame number, analysis time) at maximum x-displacement at **slab over 1st floor** prior to start of failure at this position; Maximum x-displacement (m)	Direction (frame number, analysis time) at maximum x-displacement at **slab over level 0** prior to start of failure at this position; Maximum x-displacement (m)	Direction (frame number, analysis time) at maximum x-displacement in **element above DPM** prior to start of failure at this position; Maximum x-displacement (m)	Direction (frame number, analysis time) at maximum x-displacement in **element below DPM** prior to start of failure at this position; Maximum x-displacement (m)	Direction (frame number, analysis time) at maximum x-displacement at **slab over semi-basement level** prior to start of failure at this position; Maximum x-displacement (m)	Direction (frame number, analysis time) at maximum x-displacement at **first course** prior to start of failure at this position; Maximum x-displacement (m)
Single building control model with a soft storey and setbacks	Geology type (d): Models analysed on a **1.5 m thick upper coralline limestone layer which overlies a 60 m thick layer of clay** (Nadur case), both modelled as three dimensional blocks	89	x (156, 0.55 s) -3.35×10^{-2}	x (144, 0.43 s) -1.11×10^{-2}	x (144, 0.43 s) -5.27×10^{-3}	x (122, 0.21 s) -3.48×10^{-3}			x (175, 0.74 s) 3.77×10^{-3}	x (116, 0.15 s) -1.26×10^{-3}
		91	x (332, 2.31 s) -2.69×10^{-2}	x (339, 2.38 s) -1.35×10^{-2}	x (291, 1.90 s) -8.59×10^{-3}	x (291, 1.90 s) -7.78×10^{-3}			x (291, 1.90 s) -7.21×10^{-3}	x (312, 2.11 s) 2.68×10^{-3}
		93	x (356, 2.55 s) -1.28×10^{-2}	x (356, 2.55 s) -1.21×10^{-2}	refer to penthouse floor slab	x (356, 2.55 s) -1.13×10^{-2}			x (677, 5.76 s) -2.05×10^{-2}	x (699, 5.98 s) 2.72×10^{-3}
		95	N / A (No collapse)	N / A (No collapse)	N / A (No collapse)	N / A (No collapse)			N / A (No collapse)	N / A (No collapse)
Single building control model with a soft storey and a double height space		109	x (134, 0.33 s) -2.09×10^{-2}	x (134, 0.33 s) -1.69×10^{-2}	x (109, 0.08 s) -1.15×10^{-3}	x (139, 0.38 s) -7.15×10^{-3}			x (138, 0.37 s) 5.60×10^{-3}	x (116, 0.15 s) -1.30×10^{-3}
		111	x (239, 1.38 s) -1.07×10^{-2}	x (122, 0.21 s) -4.53×10^{-3}	x (216, 1.15 s) -4.41×10^{-3}	x (228, 1.27 s) -7.04×10^{-3}			x (298, 1.97 s) -7.41×10^{-3}	x (285, 1.84 s) -4.17×10^{-3}
		113	x (358, 2.57 s) -1.49×10^{-2}	x (358, 2.57s) -1.41×10^{-2}	refer to penthouse floor slab	x (358, 2.57 s) -1.32×10^{-2}			x (358, 2.57 s) -1.22×10^{-2}	x (397, 2.96 s) 3.78×10^{-3}
		115	N / A (No collapse)	N / A (No collapse)	N / A (No collapse)	N / A (No collapse)			N / A (No collapse)	N / A (No collapse)
Single building control model with a soft storey, a double height space and setbacks		119	x (146, 0.45 s) -1.31×10^{-2}	x (144, 0.43 s) -8.43×10^{-3}	x (125, 0.24 s) -4.50×10^{-3}	x (151, 0.50 s) -5.21×10^{-3}			x (152, 0.51 s) 4.74×10^{-3}	x (116, 0.15 s) -1.26×10^{-3}
		121	x (324, 2.23 s) 1.36×10^{-2}	x (324, 2.23 s) 1.30×10^{-2}	x (325, 2.24 s) 1.24×10^{-2}	x (361, 2.60 s) -1.51×10^{-2}			x (360, 2.59 s) -1.30×10^{-2}	x (349, 2.48 s) -2.53×10^{-3}
		123	x (355, 2.54 s) -1.19×10^{-2}	x (606, 5.05 s) 1.14×10^{-2}	refer to penthouse floor slab	x (641, 5.40 s) -1.99×10^{-2}			x (638, 5.37 s) -1.78×10^{-2}	x (349, 2.48 s) -2.72×10^{-3}
		125	N / A (No collapse)	N / A (No collapse)	N / A (No collapse)	N / A (No collapse)			N / A (No collapse)	N / A (No collapse)

Table 41 Maximum x-displacement (m) during dynamic stage prior to the onset of collapse at every position throughout the height of the analysed models (continued).

Model details	Geology	Model reference number	Direction (frame number, analysis time) at maximum x-displacement at **penthouse roof slab level** prior to start of failure at this position; Maximum x-displacement (m)	Direction (frame number, analysis time) at maximum x-displacement at **penthouse floor slab level** prior to start of failure at this position; Maximum x-displacement (m)	Direction (frame number, analysis time) at maximum x-displacement at **slab over 1st floor** prior to start of failure at this position; Maximum x-displacement (m)	Direction (frame number, analysis time) at maximum x-displacement at **slab over level 0** prior to start of failure at this position; Maximum x-displacement (m)	Direction (frame number, analysis time) at maximum x-displacement in **element above DPM** prior to start of failure at this position; Maximum x-displacement (m)	Direction (frame number, analysis time) at maximum x-displacement in **element below DPM** prior to start of failure at this position; Maximum x-displacement (m)	Direction (frame number, analysis time) at maximum x-displacement at **slab over semi-basement level** prior to start of failure at this position; Maximum x-displacement (m)	Direction (frame number, analysis time) at maximum x-displacement at **first course** prior to start of failure at this position; Maximum x-displacement (m)
2-building control model	Geology type (d): Models analysed on a **1.5 m thick upper coralline limestone layer which overlies a 60 m thick layer of clay** (Nadur case), both modelled as three dimensional blocks	130	x (126, 0.25 s) -1.69×10^{-2}	x (124, 0.23 s) -1.18×10^{-2}	x (109, 0.08 s) -7.79×10^{-4}	x (102, 0.01 s) 1.67×10^{-4}			x (189, 0.88 s) -1.48×10^{-2}	x (215, 1.14 s) 1.54×10^{-3}
		132	x (160, 0.59 s) -2.61×10^{-2}	x (164, 0.63 s) -2.45×10^{-2}	x (156, 0.55 s) -1.06×10^{-2}	x (117, 0.16 s) -1.88×10^{-3}			x (167, 0.66 s) -6.46×10^{-3}	x (310, 2.09 s) 2.11×10^{-3}
		134	x (436, 3.35 s) -2.56×10^{-2}	x (368, 2.67 s) 6.81×10^{-3}	refer to penthouse floor slab	x (367, 2.66 s) 4.70×10^{-3}			x (520, 4.19 s) -4.07×10^{-3}	Not identifiable
		136	N / A (No collapse)	N / A (No collapse)	N / A (No collapse)	N / A (No collapse)			N / A (No collapse)	N / A (No collapse)
3-building control models		138	x (122, 0.21 s) -1.34×10^{-2}	x (122, 0.21 s) -1.18×10^{-2}	x (109, 0.08 s) -1.75×10^{-3}	x (106, 0.05 s) -9.68×10^{-4}			x (166, 0.65 s) 1.31×10^{-2}	x (242, 1.41 s) -1.86×10^{-3}
		140	x (144, 0.44 s) -1.74×10^{-2}	x (141, 0.40 s) -1.04×10^{-2}	x (134, 0.33 s) -3.84×10^{-3}	x (119, 0.18 s) -2.41×10^{-3}			x (213, 1.12 s) -1.62×10^{-2}	x (313, 2.12 s) 1.93×10^{-3}
		142	x (443, 3.42 s) -1.14×10^{-2}	x (421, 3.20 s) -6.81×10^{-3}	refer to penthouse floor slab	x (421, 3.20 s) -6.56×10^{-3}			x (579, 4.78 s) 1.94×10^{-2}	Not Identifiable
		144	N / A (No collapse)	N / A (No collapse)	N / A (No collapse)	N / A (No collapse)			N / A (No collapse)	N / A (No collapse)
Existing Xemxija building (XMX 0011)	Geology type (d): **1.5 m thick upper coralline limestone on 60 m thick clay**	128	x (229, 1.28 s) -5.42×10^{-2}	x (229, 1.28 s) -4.02×10^{-2}	x (126, 0.25 s) -5.91×10^{-3}	x (178, 0.77 s) -1.07×10^{-2}			x (125, 0.24 s) -5.00×10^{-3}	x (199, 0.98 s) 3.71×10^{-3}
	Geology type (c) (actual scenario): **30 m thick upper coralline limestone on 30 m thick clay**	129	x (279, 1.78 s) -3.92×10^{-2}	x (277, 1.76 s) -3.28×10^{-2}	x (151, 0.50 s) -1.55×10^{-2}	x (151, 0.50 s) -1.46×10^{-2}			x (275, 1.74 s) -2.25×10^{-2}	x (285, 1.84 s) -1.82×10^{-2}

Table 42 Relative x-displacement (m) at different positions throughout the height of the analysed models with respect to the x-displacement at first course at the time of the maximum x-displacement at slab over semi-basement level prior to the onset of failure.

Model details	Geology	Model reference number	X- Relative displacement at **penthouse roof slab level** to displacement at 1st course (m); ratio to relative displacement at same position in corresponding control model of single building modelled on 1.5 m rock over 60 m clay	X- Relative displacement at **penthouse floor slab level** to displacement at 1st course (m); ratio to relative displacement at same position in corresponding control model of single building modelled on 1.5 m rock over 60 m clay	X- Relative displacement at level of **slab over 1st floor** to displacement at 1st course (m); ratio to relative displacement at same position in corresponding control model of single building modelled on 1.5 m rock over 60 m clay	X- Relative displacement at **level of slab over level 0** to displacement at 1st course (m); ratio to relative displacement at same position in corresponding control model of single building modelled on 1.5 m rock over 60 m clay	X- Relative displace-ment in **element above DPM** to displace-ment at 1st course (m)	X- Relative displace-mentin **element below DPM** to displace-ment at 1st course (m)	(Analysis frame number, analysis time at maximum x-displacement at slab over semi-basement level prior to start of failure) X- Relative displacement at **level of slab over semi-basement** to displacement at 1st course (m); ratio to relative displacement at same position in corresponding control model of single building modelled on 1.5 m rock over 60 m clay	X- Displacement at **first course** (m); ratio to displacement at same position in corresponding control model of single modelled on 1.5 m rock over 60 m clay
Single building control models	Geology type (a): Models analysed on a **30 m thick layer of upper coralline limestone** modelled as a three dimensional block	42v2	-1.68×10^{-2} 5.423	-1.36×10^{-2} 5.427	-7.24×10^{-3} 4.776	-4.07×10^{-3} 3.797	-1.06×10^{-3}	-1.27×10^{-3}	x (256, 1.55s) -2.44×10^{-3} 2.227	-1.12×10^{-4} 0.096
		48	N / A (No collapse)	N / A (No collapse)	N / A (No collapse)	N / A (No collapse)			N / A (No collapse)	N / A (No collapse)
	Geology type (b): Models analysed on ground specified as **upper corolline limestone at Minimum Z**	43v2	4.49×10^{-3} 1.450	3.72×10^{-3} 1.485	1.85×10^{-3} 1.222	7.33×10^{-4} 0.684			x (374, 2.73s) -1.79×10^{-3} 1.634	-5.23×10^{-6} 1.209
		49	N / A (No collapse)	N / A (No collapse)	N / A (No collapse)	N / A (No collapse)			N / A (No collapse)	N / A (No collapse)
	Geology type (c): Models analysed on a **30 m thick upper coralline limestone layer which overlies a 30 m thick layer of clay** (Xemxija case), both modelled as three dimensional blocks	44v2	-9.69×10^{-3} 3.132	-7.86×10^{-3} 3.142	-4.38×10^{-3} 2.886	-2.68×10^{-3} 2.504			x (286, 1.85s) -1.44×10^{-3} 1.316	-1.82×10^{-2} 15.569
		50	N / A (No collapse)	N / A (No collapse)	N / A (No collapse)	N / A (No collapse)			N / A (No collapse)	N / A (No collapse)
	Geology type (d): Models analysed on a **1.5 m thick upper coralline limestone layer which overlies a 60 m thick layer of clay** (Nadur case), both modelled as three dimensional blocks	45v2	-3.09×10^{-3}	-2.50×10^{-3}	-1.52×10^{-3}	-1.07×10^{-3}			x (116, 0.15s) -1.10×10^{-3}	-1.17×10^{-3}
		51	-3.03×10^{-3}	-2.36×10^{-3}	-1.78×10^{-3}	-1.19×10^{-3}			x (117, 0.16s) -6.14×10^{-4}	-1.13×10^{-3}
		57	-1.61×10^{-3}	-1.21×10^{-3}	refer to penthouse floor slab	-7.85×10^{-4}			x (349, 2.48s) -9.02×10^{-4}	-2.30×10^{-3}
		63	N / A (No collapse)	N / A (No collapse)	N / A (No collapse)	N / A (No collapse)			N / A (No collapse)	N / A (No collapse)
	Geology type (e): Models analysed on a **60 m thick layer of clay** modelled as a three dimensional block	46	-1.16×10^{-3} 0.375	-9.55×10^{-4} 0.381	-6.67×10^{-4} 0.440	-5.74×10^{-4} 0.536			x (109, 0.08) -8.73×10^{-4} 0.797	-5.37×10^{-4} 0.460
		52	-7.10×10^{-3} 2.344	-5.49×10^{-3} 2.321	-4.02×10^{-3} 2.254	-2.56×10^{-3} 2.159			x (132, 0.31s) -1.64×10^{-3} 2.675	-1.18×10^{-3} 1.041
		58	-3.69×10^{-3} 2.296	-5.17×10^{-4} 0.428	refer to penthouse floor slab	2.99×10^{-3} 3.807			x (380, 2.79s) -1.26×10^{-2} 14.017	-4.49×10^{-4} 0.196
		64	N / A (No collapse)	N / A (No collapse)	N / A (No collapse)	N / A (No collapse)			N / A (No collapse)	N / A (No collapse)
	Geology type (f): Models analysed on ground specified as **clay at Minimum Z**	47	7.44×10^{-3} 2.406	7.17×10^{-3} 2.866	6.47×10^{-3} 4.266	6.28×10^{-3} 5.862			x (235, 1.34s) -5.50×10^{-3} 5.020	-4.89×10^{-4} 0.418
		53	6.36×10^{-3} 2.098	4.95×10^{-3} 2.095	3.67×10^{-3} 2.061	2.42×10^{-3} 2.037			x (366, 2.65s) 1.11×10^{-3} 1.806	4.79×10^{-5} 0.042
		59	N / A (No collapse)	N / A (No collapse)	N / A (No collapse)	N / A (No collapse)			N / A (No collapse)	N / A (No collapse)

Table 42 Relative x-displacement (m) at different positions throughout the height of the analysed models with respect to the x-displacement at first course at the time of the maximum x-displacement at slab over semi-basement level prior to the onset of failure (continued).

Model details	Geology	Model reference number	X- Relative displacement at **penthouse roof slab level** to displacement at 1st course (m); ratio to relative displacement at same position in corresponding control model of single building modelled on 1.5 m rock over 60 m clay	X- Relative displacement at **penthouse floor slab level** to displacement at 1st course (m); ratio to relative displacement at same position in corresponding control model of single building modelled on 1.5 m rock over 60 m clay	X- Relative displacement at **level of slab over 1st floor** to displacement at 1st course (m); ratio to relative displacement at same position in corresponding control model of single building modelled on 1.5 m rock over 60 m clay	X- Relative displacement at **level of slab over level 0** to displacement at 1st course (m); ratio to relative displacement at same position in corresponding control model of single building modelled on 1.5 m rock over 60 m clay	X- Relative displace-ment in **element above DPM** to displace-ment at 1st course (m)	X- Relative displace-ment in **element below DPM** to displace-ment at 1st course (m)	(Analysis frame number, analysis time at maximum x-displacement at slab over semi-basement level prior to start of failure) X- Relative displacement at **level of slab over semi-basement** to displacement at 1st course (m); ratio to relative displacement at same position in corresponding control model of single building modelled on 1.5 m rock over 60 m clay	X- Displacement at **first course** (m); ratio to displacement at same position in corresponding control model of single modelled on 1.5 m rock over 60 m clay
Single building control model with soft storey at semi-basement level	Geology type (d): Models analysed on a **1.5 m thick upper coralline limestone layer which overlies a 60 m thick layer of clay** (Nadur case), both modelled as three dimensional blocks	69	-8.78×10^{-3} 2.840	-7.51×10^{-3} 3.001	-5.04×10^{-3} 3.321	-3.72×10^{-3} 3.468			x (124, 0.23s) -2.94×10^{-3} 2.683	-5.00×10^{-4} 0.428
		71	-2.58×10^{-2} 8.518	-1.72×10^{-2} 7.273	-8.62×10^{-3} 4.835	-2.07×10^{-4} 0.174			x (229, 1.28s) 5.56×10^{-3} 9.067	-1.59×10^{-4} 0.141
		73	-1.68×10^{-2} 10.447	-1.58×10^{-2} 13.126	refer to penthouse floor slab	-1.48×10^{-2} 18.879			x (360, 2.59s) -1.36×10^{-2} 15.079	4.40×10^{-4} 0.192
		75	N / A (No collapse)	N / A (No collapse)	N / A (No collapse)	N / A (No collapse)			N / A (No collapse)	N / A (No collapse)
Single building control model with setbacks at penthouse level		79	-4.26×10^{-3} 1.378	-3.64×10^{-3} 1.454	-2.15×10^{-3} 1.420	-1.42×10^{-3} 1.324			x (118, 0.17s) -9.27×10^{-4} 0.846	-1.05×10^{-3} 0.896
		81	-5.76×10^{-3} 1.901	-4.72×10^{-3} 1.995	-3.45×10^{-3} 1.938	-2.13×10^{-3} 1.789			x (242, 1.41s) -1.32×10^{-3} 2.158	-1.46×10^{-3} 1.293
		83	N / A (No collapse)	N / A (No collapse)	N / A (No collapse)	N / A (No collapse)			N / A (No collapse)	N / A (No collapse)
Single building control model with a double height space between Levels 0 and +1		99	-1.90×10^{-2} 6.127	-1.54×10^{-2} 6.139	-8.13×10^{-3} 5.358	-4.33×10^{-3} 4.045			x (139, 0.38s) -2.73×10^{-3} 2.496	-8.89×10^{-4} 0.761
		101	-7.77 x10^-3 2.564	-4.37 x10^-3 1.850	-1.08 x10^-3 0.608	2.11 x10^-3 1.780			x (224, 1.23s) 6.34×10^{-3} 10.328	2.17×10^{-4} 0.192
		103	-2.81×10^{-1} 174.609	-1.79×10^{-1} 148.386	refer to penthouse floor slab	-7.70×10^{-2} 98.179			x (535, 4.34s) 6.90×10^{-3} 7.647	3.55×10^{-4} 0.155
		105	N / A (No collapse)	N / A (No collapse)	N / A (No collapse)	N / A (No collapse)			N / A (No collapse)	N / A (No collapse)

Table 42 Relative x-displacement (m) at different positions throughout the height of the analysed models with respect to the x-displacement at first course at the time of the maximum x-displacement at slab over semi-basement level prior to the onset of failure (continued).

Model details	Geology	Model reference number	X- Relative displacement at **penthouse roof slab level** to displacement at 1st course (m); ratio to relative displacement at same position in corresponding control model of single building modelled on 1.5 m rock over 60 m clay	X- Relative displacement at **penthouse floor slab level** to displacement at 1st course (m); ratio to relative displacement at same position in corresponding control model of single building modelled on 1.5 m rock over 60 m clay	X- Relative displacement at **level of slab over 1st floor** to displacement at 1st course (m); ratio to relative displacement at same position in corresponding control model of single building modelled on 1.5 m rock over 60 m clay	X- Relative displacement at **level of slab over level 0** to displacement at 1st course (m); ratio to relative displacement at same position in corresponding control model of single building modelled on 1.5 m rock over 60 m clay	X- Relative displace-ment in **element above DPM** to displace-ment at 1st course (m)	X- Relative displace-ment in **element below DPM** to displace-ment at 1st course (m)	(Analysis frame number, analysis time at maximum x-displacement at slab over semi-basement level prior to start of failure) X- Relative displacement at **level of slab over semi-basement** to displacement at 1st course (m); ratio to relative displacement at same position in corresponding control model of single building modelled on 1.5 m rock over 60 m clay	X- Displacement at **first course** (m); ratio to displacement at same position in corresponding control model of single modelled on 1.5 m rock over 60 m clay
Single building control model with a soft storey and setbacks	Geology type (d): Models analysed on a **1.5 m thick upper coralline limestone layer which overlies a 60 m thick layer of clay** (Nadur case), both modelled as three dimensional blocks	89	-8.06×10^{-2} 26.048	-6.68×10^{-2} 26.703	-3.91×10^{-2} 25.780	-2.51×10^{-2} 23.409			x (175, 0.74s) -3.98×10^{-3} 3.630	7.74×10^{-3} 6.630
		91	-8.55×10^{-3} 2.824	-7.90×10^{-3} 3.343	-7.13×10^{-3} 3.999	-6.32×10^{-3} 5.318			x (291, 1.90) -5.75×10^{-3} 9.369	-1.46×10^{-3} 1.293
		93	-1.06×10^{-1} 65.758	-7.36×10^{-2} 60.987	refer to penthouse floor slab	-4.79×10^{-2} 61.022			x (677, 5.76) -2.02×10^{-2} 22.402	-3.02×10^{-4} 0.132
		95	N / A (No collapse)	N / A (No collapse)	N / A (No collapse)	N / A (No collapse)			N / A (No collapse)	N / A (No collapse)
Single building control model with a soft storey and a double height space		109	-3.01×10^{-2} 9.720	-2.40×10^{-2} 9.605	-1.18×10^{-2} 7.814	-5.91×10^{-3} 5.512			x (138, 0.37s) 6.26×10^{-3} 5.720	-6.66×10^{-4} 0.571
		111	-2.54×10^{-1} 83.833	-1.90×10^{-1} 80.276	-1.26×10^{-1} 70.484	-6.91×10^{-2} 58.157			x (298, 1.97s) 1.31×10^{-2} 21.338	-2.05×10^{-2} 18.136
		113	-1.48×10^{-2} 9.174	-1.39×10^{-2} 11.518	refer to penthouse floor slab	-1.30×10^{-2} 16.596			x (358, 2.57s) -1.20×10^{-2} 13.339	-1.71×10^{-4} 0.074
		115	N / A (No collapse)	N / A (No collapse)	N / A (No collapse)	N / A (No collapse)			N / A (No collapse)	N / A (No collapse)
Single building control model with a soft storey, a double height space and setbacks		119	-2.58×10^{-2} 8.324	-2.07×10^{-2} 8.277	-1.07×10^{-2} 7.058	-5.83×10^{-3} 5.436			x (152, 0.51s) 4.58×10^{-3} 4.184	1.54×10^{-4} 0.131
		121	-1.94×10^{-2} 6.389	-1.81×10^{-2} 7.667	-1.68×10^{-2} 9.432	-1.54×10^{-2} 12.943			x (360, 2.59s) -1.34×10^{-2} 21.910	4.07×10^{-4} 0.360
		123	-2.11×10^{-2} 13.120	-1.97×10^{-2} 16.336	refer to penthouse floor slab	-1.83×10^{-2} 23.306			x (638, 5.37s) -1.67×10^{-2} 18.459	-1.15×10^{-3} 0.502
		125	N / A (No collapse)	N / A (No collapse)	N / A (No collapse)	N / A (No collapse)			N / A (No collapse)	N / A (No collapse)

Table 42 Relative x-displacement (m) at different positions throughout the height of the analysed models with respect to the x-displacement at first course at the time of the maximum x-displacement at slab over semi-basement level prior to the onset of failure (continued).

Model details	Geology	Model reference number	X- Relative displacement at **penthouse roof slab level** to displacement at 1st course (m); ratio to relative displacement at same position in corresponding control model of single building modelled on 1.5 m rock over 60 m clay	X- Relative displacement at **penthouse floor slab level** to displacement at 1st course (m); ratio to relative displacement at same position in corresponding control model of single building modelled on 1.5 m rock over 60 m clay	X- Relative displacement at **level of slab over 1st floor** to displacement at 1st course (m); ratio to relative displacement at same position in corresponding control model of single building modelled on 1.5 m rock over 60 m clay	X- Relative displacement at **level of slab over level 0** to displacement at 1st course (m); ratio to relative displacement at same position in corresponding control model of single building modelled on 1.5 m rock over 60 m clay	X- Relative displace-ment in **element above DPM** to displace-ment at 1st course (m)	X- Relative displace-ment in **element below DPM** to displace-ment at 1st course (m)	(Analysis frame number, analysis time at maximum x-displacement at slab over semi-basement level prior to start of failure) X- Relative displacement at **level of slab over semi-basement** to displacement at 1st course (m); ratio to relative displacement at same position in corresponding control model of single building modelled on 1.5 m rock over 60 m clay	X- Displacement at **first course** (m); ratio to displacement at same position in corresponding control model of single modelled on 1.5 m rock over 60 m clay
2-building control model	Geology type (d): Models analysed on a **1.5 m thick upper coralline limestone layer which overlies a 60 m thick layer of clay** (Nadur case), both modelled as three dimensional blocks	130	-2.67×10^{-1} 86.272	-2.15×10^{-1} 85.702	-1.10×10^{-1} 72.354	-5.75×10^{-2} 53.697			x (189, 0.88s) -1.56×10^{-2} 14.213	7.45×10^{-4} 0.638
		132	-3.90×10^{-2} 12.865	-2.91×10^{-2} 12.298	-1.91×10^{-2} 10.718	-9.25×10^{-3} 7.789			x (167, 0.66s) -7.08×10^{-3} 11.538	6.21×10^{-4} 0.549
		134	-2.43×10^{-1} 150.921	-1.66×10^{-1} 137.449	refer to penthouse floor slab	-8.93×10^{-2} 113.762			x (520, 4.19s) -4.29×10^{-3} 4.751	2.17×10^{-4} 0.095
		136	N / A (No collapse)	N / A (No collapse)	N / A (No collapse)	N / A (No collapse)			N / A (No collapse)	N / A (No collapse)
3-building control model		138	-1.45×10^{-1} 46.899	-1.19×10^{-1} 47.514	-6.66×10^{-2} 43.944	-4.06×10^{-2} 37.933			x (166, 0.65s) 1.27×10^{-2} 11.610	3.94×10^{-4} 0.338
		140	-1.78×10^{-1} 58.815	-1.35×10^{-1} 57.010	-9.13×10^{-2} 51.234	-4.81×10^{-2} 40.522			x (213, 1.12s) -1.68×10^{-2} 27.408	5.90×10^{-4} 0.522
		142	-2.97×10^{-1} 184.540	-2.07×10^{-1} 171.322	refer to penthouse floor slab	-1.16×10^{-1} 148.459			x (579, 4.78s) 1.98×10^{-2} 21.928	-3.37×10^{-4} 0.147
		144	N / A (No collapse)	N / A (No collapse)	N / A (No collapse)	N / A (No collapse)			N / A (No collapse)	N / A (No collapse)
Existing Xemxija building (XMX 0011)	Geology type (d): **1.5 m thick upper coralline limestone on 60 m thick clay**	128	-3.91×10^{-3} 1.264	-3.23×10^{-3} 1.291	-2.37×10^{-3} 1.566	-1.92×10^{-3} 1.787			x (125, 0.24s) -1.49×10^{-3} 1.356	-3.51×10^{-3} 3.007
	Geology type (c) (actual scenario): **30 m thick upper coralline limestone on 30 m thick clay**	129	-1.53×10^{-2} 1.575	-1.34×10^{-2} 1.704	-9.47×10^{-3} 2.165	-7.38×10^{-3} 2.750			x (275, 1.74s) -5.39×10^{-3} 3.736	-1.71×10^{-2} 0.939

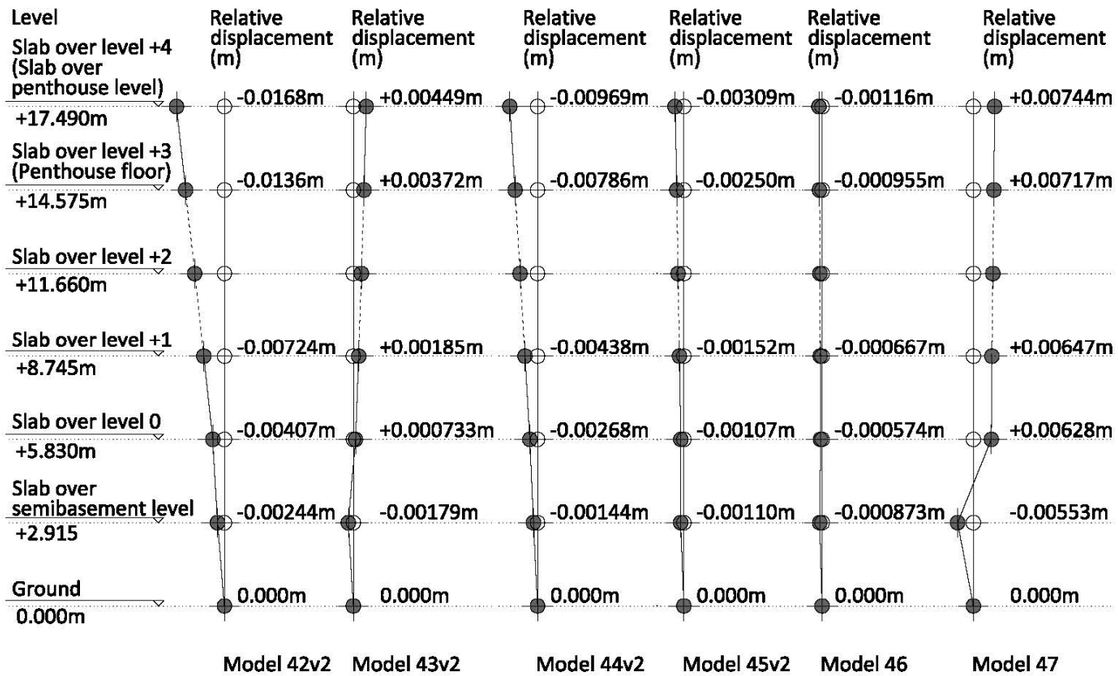

Figure 37 Comparison of the x-displacement mode throughout the 6-storey single building control models at the analysis times corresponding to the maximum x-displacement at slab over semi-basement level before the start of failure in the same position.

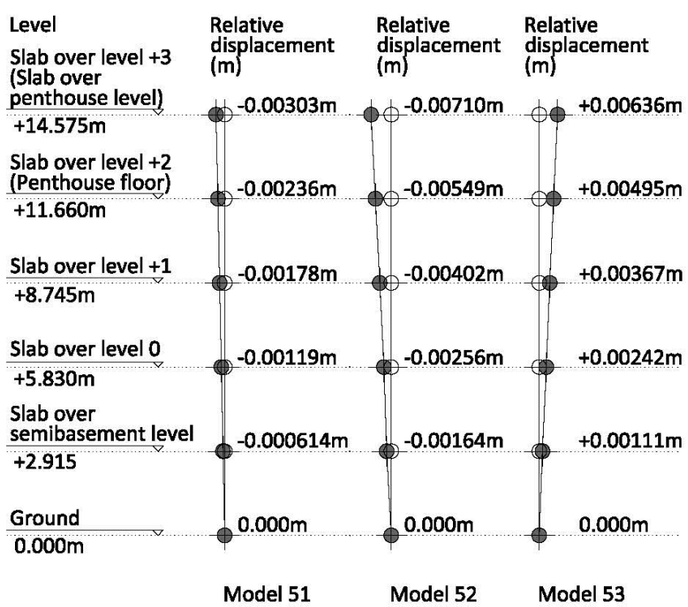

Figure 38 Comparison of the x-displacement mode throughout the 5-storey single building control models at the analysis times corresponding to the maximum x-displacement at slab over semi-basement level before the start of failure in the same position.

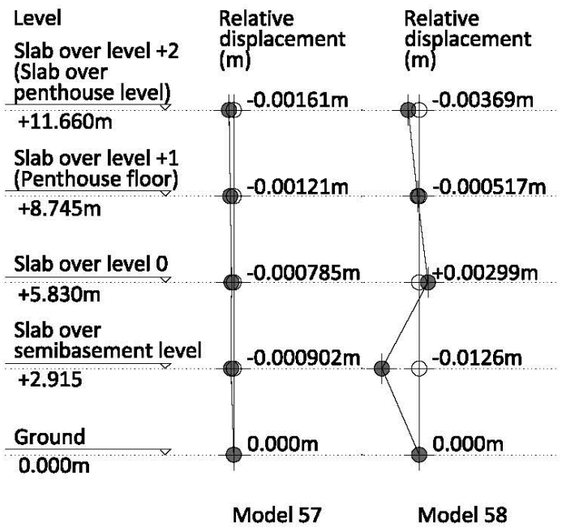

Figure 39 Comparison of the x-displacement mode throughout the 4-storey single building control models at the analysis times corresponding to the maximum x-displacement at slab over semi-basement level before the start of failure in the same position.

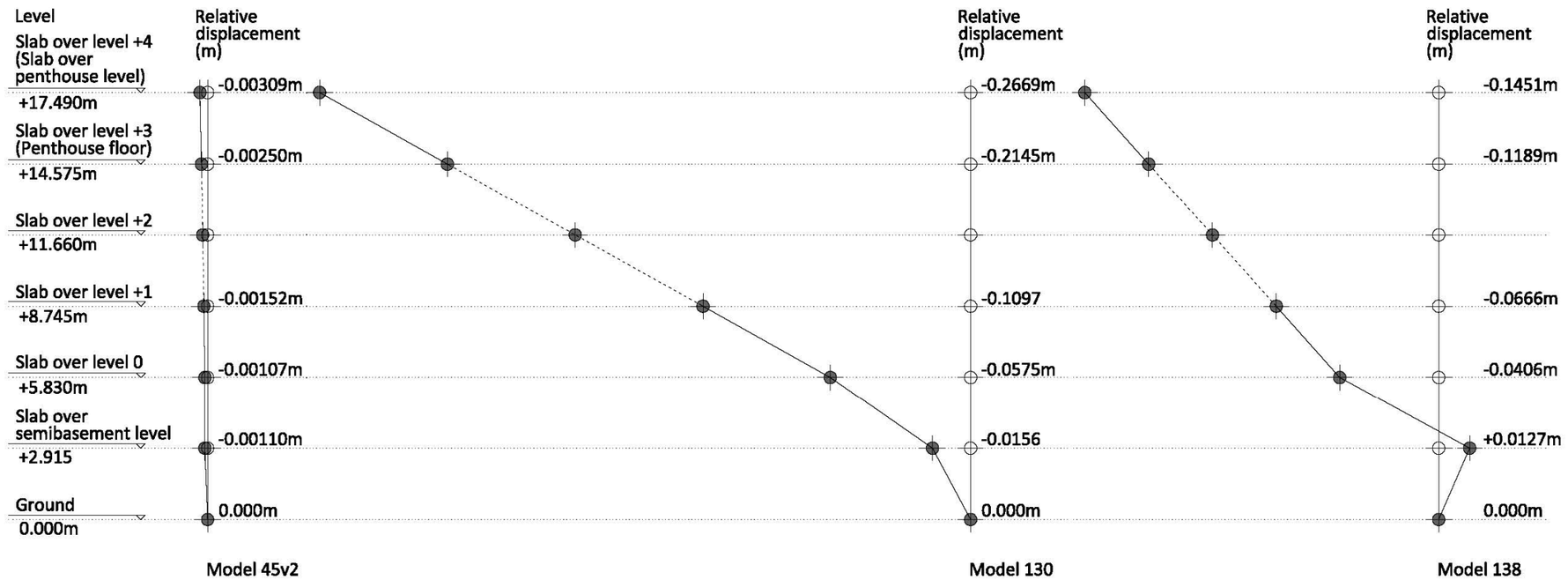

Figure 40 Comparison of the x-displacement mode throughout the 6-storey single,two- and three-building control models at the analysis times corresponding to the maximum x-displacement at slab over semi-basement level before the start of failure in the same position.

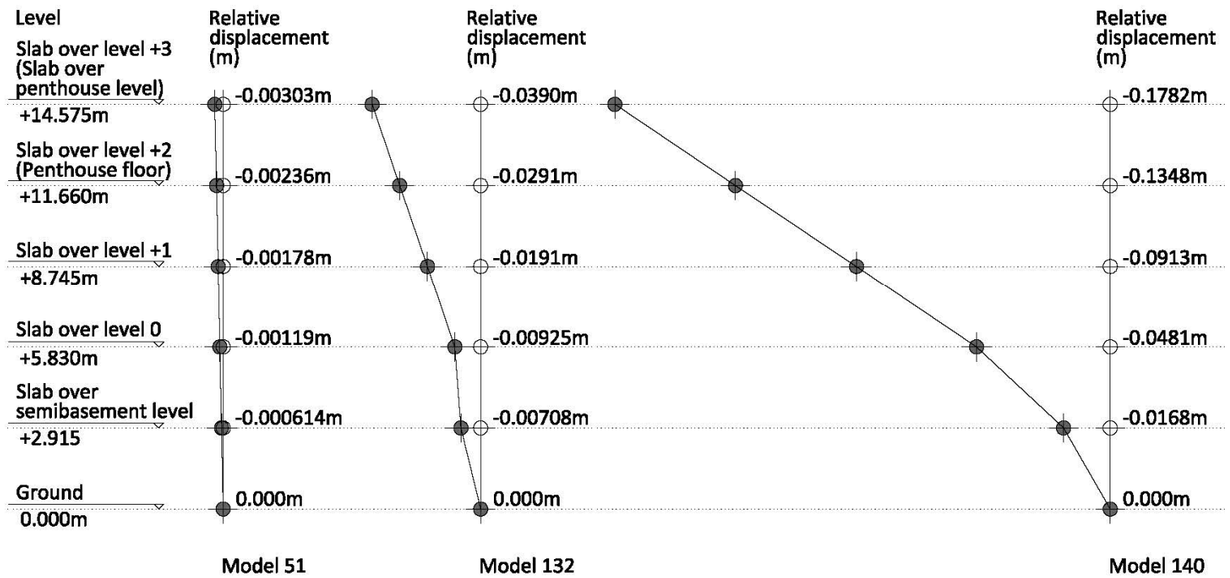

Figure 41 Comparison of the x-displacement mode throughout the 5-storey single, two- and three-building control models at the analysis times corresponding to the maximum x-displacement at slab over semi-basement level before the start of failure in the same position.

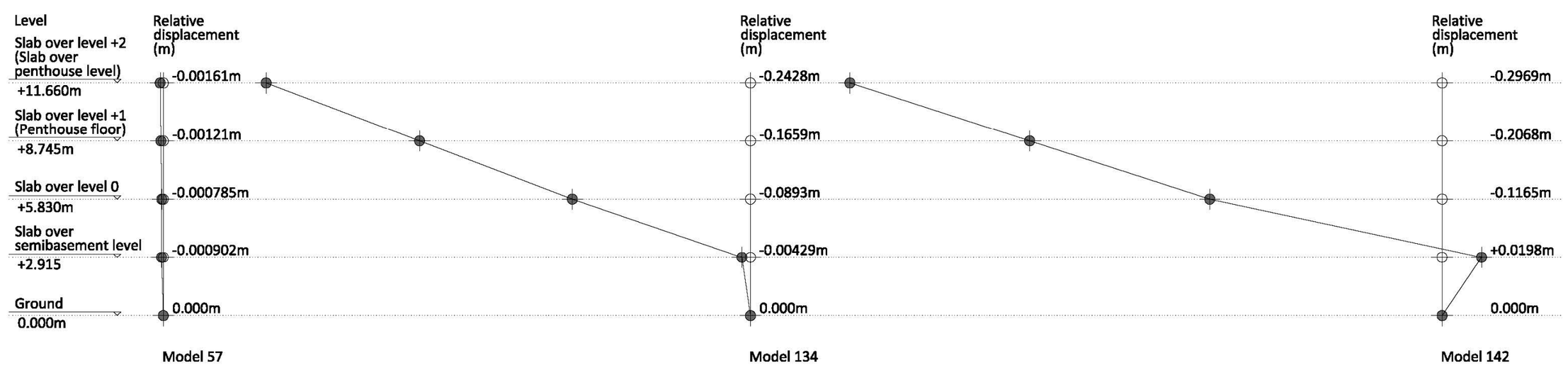

Figure 42 Comparison of the x-displacement mode throughout the 4-storey single, two- and three-building control models at the analysis times corresponding to the maximum x-displacement at slab over semi-basement level before the start of failure in the same position.

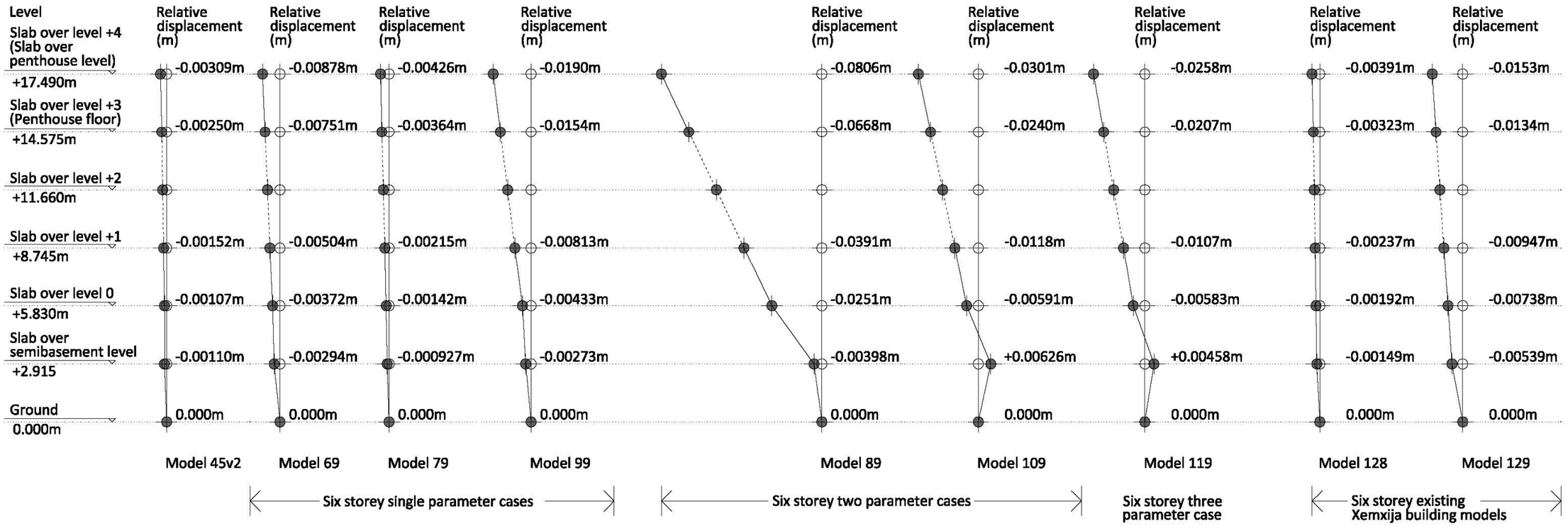

Figure 43 Comparison of the x-displacement mode throughout the 6-storey single building control models with 1-3 additional parameters at the time of the maximum x-displacement at slab over semi-basement level before the start of failure in the same position.

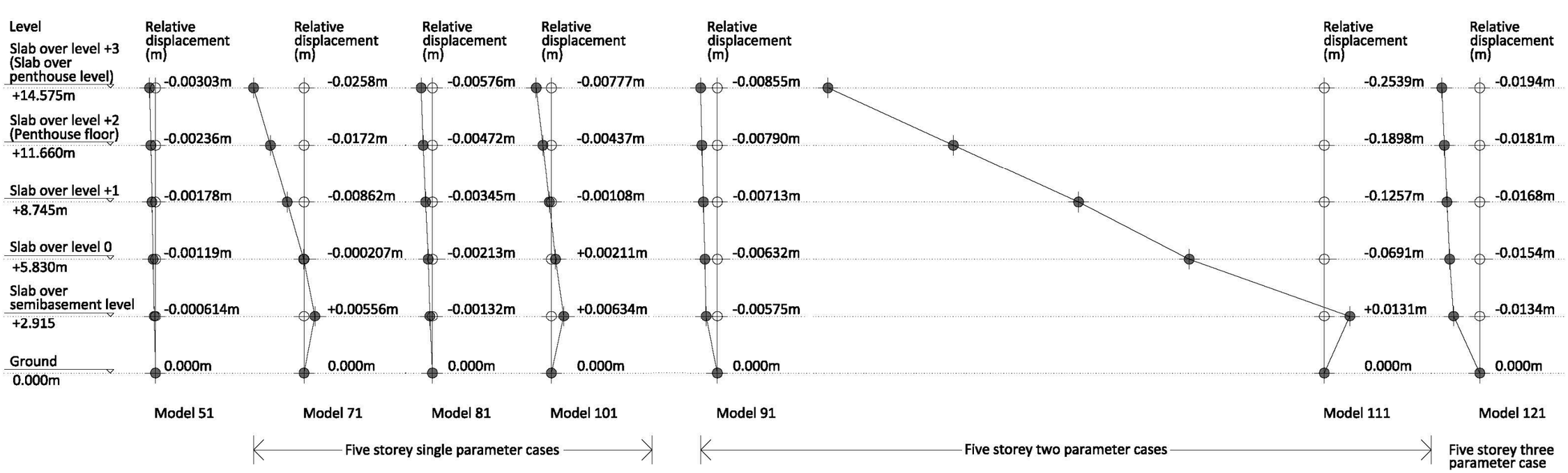

Figure 44 Comparison of the x-displacement mode throughout the 5-storey single building control models with 1-3 additional parameters at the time of the maximum x-displacement at slab over semi-basement level before the start of failure in the same position.

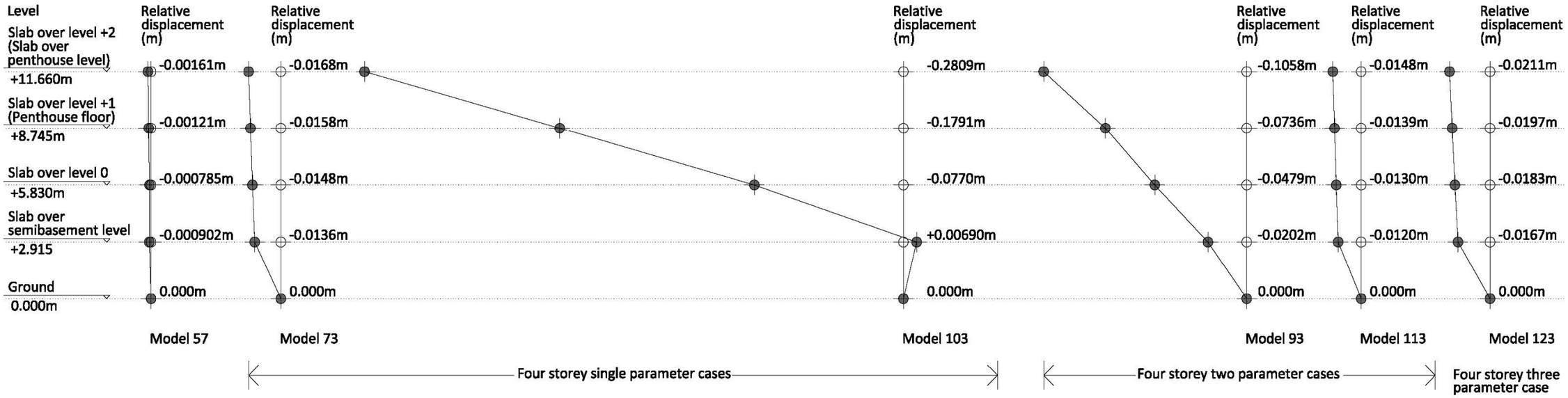

Figure 45 Comparison of the x-displacement mode throughout the 4-storey single building control models with 1-3 additional parameters at the time of the maximum x-displacement at slab over semi-basement level before the start of failure in the same position.

Appendix E. RESULTS FROM 3MURI® NUMERICAL ANALYSIS

Table 43 List of numerical models analysed using 3Muri® including the seismic vulnerability characteristics, number of storeys, type of subsoil and the main results from the non-linear static pushover analyses.

Count	Model reference number	3Muri® model name	Subsoil material		Building characteristics investigated							Non-linear static analysis pushover results for main capacity criterion (maximum displacement to target displacement ratio)					Alpha ratio (maximum accerleration in pushover to maximum p.g.a.)			
			Rock	Clay	Number of storeys	Control	Soft storey at semi-basement level	Double height space (level)	Setbacks	Length: width plan proportions 2.75 : 1	Length: width plan proportions 4:1	Number of 'unsatisfied verifications': limit state of Significant Damage (load distribution numbers)	Number of 'unsatisfied verifications': limit state of Near Collapse (load distribution numbers)	Number of 'unsatisfied verifications': limit state of Damage Limitation (load distribution numbers)	All pushover curves bilinear? (Y/N)	Average number of steps in pushover curves	Minimum Alpha ratio: limit state of Significant Damage	Load distribution number resulting in minimum Alpha ratio for limit state of Significant Damage	Minimum Alpha ratio: limit state of Near Collapse	Load distribution number resulting in minimum Alpha ratio for limit state of Near Collapse
1	3M44	3M_44_F_XMX011_a1R_6flrs_N_ rock ELS	X	N/A	6	X	X	X (3/4)	X	X	N/A	0 (N/A)	3 (6; 10; 14)	12(1-4; 9-16)	N	26	1.258	14	0.699	14
2	3M45	3M_45_F_XMX011_b2C_6flrs_N_ clay ELS	N/A	X	6	X	X	X (3/4)	X	X	N/A	1 (14)	11 (2-3; 6; 9-11; 13-16)	12(1-4; 9-16)	N	26	0.839	14	0.466	14
3	3M57	3M_57_F_CTRL_a1R_15flrs_N	X	N/A	15	X	N/A	N/A	N/A	X	N/A	1 (16)	6 (3-4; 13-16)	12 (1-4; 9-16)	Y	51	0.988	16	0.549	16
4	3M56	3M_56_F_CTRL_a1R_14lrs_N	X	N/A	14	X	N/A	N/A	N/A	X	N/A	0 (N/A)	6 (3-4; 13-16)	12 (1-4; 9-16)	Y	51	1.203	3	0.668	3
5	3M53	3M_53_F_CTRL_a1R_13flrs_N	X	N/A	13	X	N/A	N/A	N/A	X	N/A	0 (N/A)	4 (3; 4; 13; 16)	12 (1-4; 9-16)	Y	49	1.594	13	0.886	13
6	3M52	3M_52_F_CTRL_a1R_12flrs_N	X	N/A	12	X	N/A	N/A	N/A	X	N/A	0 (N/A)	1 (15)	12 (1-4; 9-16)	Y	46	1.719	15	0.955	15
7	3M51	3M_51_F_CTRL_a1R_11flrs_N	X	N/A	11	X	N/A	N/A	N/A	X	N/A	0 (N/A)	3 (4; 13; 15)	12 (1-4; 9-16)	Y	37	1.572	15	0.874	15
8	3M50	3M_50_F_CTRL_a1R_10flrs_N	X	N/A	10	X	N/A	N/A	N/A	X	N/A	0 (N/A)	7 (1-2; 4; 10;12;15-16)	12 (1-4; 9-16)	Y	33	1.545	15	0.858	15
9	3M49	3M_49_F_CTRL_a1R_9flrs_N	X	N/A	9	X	N/A	N/A	N/A	X	N/A	0 (N/A)	5 (1; 10; 12; 15-16)	12 (1-4; 9-16)	Y	31	1.594	15	0.885	15
10	3M48	3M_48_F_CTRL_a1R_8flrs_N	X	N/A	8	X	N/A	N/A	N/A	X	N/A	0 (N/A)	2 (10; 12)	12 (1-4; 9-16)	Y	27	1.712	10	0.943	10
11	3M47v2	3M_47v2_F_CTRL_a1R_7flrs_N	X	N/A	7	X	N/A	N/A	N/A	X	N/A	0 (N/A)	3 (4; 15-16)	12 (1-4; 9-16)	Y	22	1.720	4	0.937	4
12	3M46	3M_46_F_CTRL_a1R_6flrs_N	X	N/A	6	X	N/A	N/A	N/A	X	N/A	0 (N/A)	0 (N/A)	12 (1-4; 9-16)	Y	19	2.039	4	1.103	4
13	3M54	3M_54_F_CTRL_a1R_5flrs_N	X	N/A	5	X	N/A	N/A	N/A	X	N/A	0 (N/A)	0 (N/A)	10 (1-2; 4; 9-12; 14-16)	Y	17	2.425	16	1.308	16
14	3M55	3M_55_F_CTRL_a1R_4flrs_N	X	N/A	4	X	N/A	N/A	N/A	X	N/A	0 (N/A)	0 (N/A)	0 (N/A)	Y	14	2.864	14	1.526	14

Key

No unsatisfied verifications: limit state of Significant Damage

No unsatisfied verifications: limit state of Near Collapse

Rock subsoil

Clay subsoil

Table 43 List of numerical models analysed using 3Muri® including the seismic vulnerability characteristics, number of storeys, type of subsoil and the main results from the non-linear static pushover analyses (continued).

Count	Model reference number	3Muri® model name	Subsoil material		Building characteristics investigated							Non-linear static analysis pushover results for main capacity criterion (maximum displacement to target displacement ratio)					Alpha ratio (maximum acceleration in pushover to maximum p.g.a.)			
			Rock	Clay	Number of storeys	Control	Soft storey at semi-basement level	Double height space (level)	Setbacks	Length: width plan proportions 2.75 : 1	Length: width plan proportions 4:1	Number of 'unsatisfied verifications': limit state of Significant Damage (load distribution numbers)	Number of 'unsatisfied verifications': limit state of Near Collapse (load distribution numbers)	Number of 'unsatisfied verifications': limit state of Damage Limitation (load distribution numbers)	All pushover curves bilinear? (Y/N)	Average number of steps in pushover curves	Minimum Alpha ratio: limit state of Significant Damage	Load distribution number resulting in minimum Alpha ratio for limit state of Significant Damage	Minimum Alpha ratio: limit state of Near Collapse	Load distribution number resulting in minimum Alpha ratio for limit state of Near Collapse
15	3M168	3M_168_F_CTRL_a1R_3flrs_N	X	N/A	3	X	N/A	N/A	N/A	X	N/A	0 (N/A)	0 (N/A)	0 (N/A)	Y	12	2.366	23	1.219	19
16	3M169	3M_169_F_CTRL_a1R_2flrs_N	X	N/A	2	X	N/A	N/A	N/A	X	N/A	0 (N/A)	0 (N/A)	0 (N/A)	Y	20	3.415	13	1.813	13
17	3M170	3M_170_F_CTRL_a1R_1flr_N	X	N/A	1	X	N/A	N/A	N/A	X	N/A	0 (N/A)	2 (14; 16)	0 (N/A)	Y	19	1.395	14	0.657	14
18	3M69	3M_69_F_CTRL_b2C_15flrs_N	N/A	X	15	X	N/A	N/A	N/A	X	N/A	6 (3-4; 13-16)	23 (1-16; 18-24)	18 (1-4; 7-16; 21-24)	Y	51	0.659	16	0.366	16
19	3M68	3M_68_F_CTRL_b2C_14flrs_N	N/A	X	14	X	N/A	N/A	N/A	X	N/A	5 (3; 13-16)	21 (1-5; 7-16; 18; 20-24)	18 (1-4; 7-16; 21-24)	Y	51	0.802	3	0.446	3
20	3M67	3M_67_F_CTRL_b2C_13flrs_N	N/A	X	13	X	N/A	N/A	N/A	X	N/A	0 (N/A)	16 (1-4; 8-16; 21-23)	18 (1-4; 7-16; 21-24)	Y	49	1.063	13	0.590	13
21	3M66	3M_66_F_CTRL_b2C_12flrs_N	N/A	X	12	X	N/A	N/A	N/A	X	N/A	0 (N/A)	12 (1-4; 9-13; 15; 21; 23)	12 (1-4; 9-16)	Y	46	1.146	15	0.637	15
22	3M65	3M_65_F_CTRL_b2C_11flrs_N	N/A	X	11	X	N/A	N/A	N/A	X	N/A	0 (N/A)	13 (1-4; 9-16; 21)	13 (1-4; 9-16; 23)	Y	37	1.048	15	0.582	15
23	3M64	3M_64_F_CTRL_b2C_10flrs_N	N/A	X	10	X	N/A	N/A	N/A	X	N/A	0 (N/A)	12 (1-4; 9-16)	12 (1-4; 9-16)	Y	33	1.045	15	0.578	15
24	3M63	3M_63_F_CTRL_b2C_9flrs_N	N/A	X	9	X	N/A	N/A	N/A	X	N/A	0 (N/A)	9 (1-2; 4; 9-12; 15-16)	12 (1-4; 9-16)	Y	31	1.130	15	0.619	15
25	3M62	3M_62_F_CTRL_b2C_8flrs_N	N/A	X	8	X	N/A	N/A	N/A	X	N/A	0 (N/A)	11 (1-4; 9-12; 14-16)	12 (1-4; 9-16)	Y	27	1.218	10	0.661	10
26	3M61v2	3M_61v2_F_CTRL_b2C_7flrs_N	N/A	X	7	X	N/A	N/A	N/A	X	N/A	0 (N/A)	11 (1-4; 9-12; 14-16)	12 (1-4; 9-16)	Y	22	1.224	16	0.658	4
27	3M58	3M_58_F_CTRL_b2C_6flrs_N	N/A	X	6	X	N/A	N/A	N/A	X	N/A	0 (N/A)	11 (1-4; 9-12; 14-16)	12 (1-4; 9-16)	Y	19	1.446	4	0.771	4
28	3M59	3M_59_F_CTRL_b2C_5flrs_N	N/A	X	5	X	N/A	N/A	N/A	X	N/A	0 (N/A)	7 (2-4; 12; 14-16)	12 (1-4; 9-16)	Y	17	1.709	16	0.91	16
29	3M60	3M_60_F_CTRL_b2C_4flrs_N	N/A	X	4	X	N/A	N/A	N/A	X	N/A	0 (N/A)	0 (N/A)	12 (1-4; 9-16)	Y	14	2.033	14	1.069	14

Key

No unsatisfied verifications: limit state of Significant Damage

No unsatisfied verifications: limit state of Near Collapse

Rock subsoil

Clay subsoil

Table 43 List of numerical models analysed using 3Muri® including the seismic vulnerability characteristics, number of storeys, type of subsoil and the main results from the non-linear static pushover analyses (continued).

Count	Model reference number	3Muri® model name	Subsoil material		Building characteristics investigated							Non-linear static pushover analysis results for main capacity criterion (maximum displacement to target displacement ratio)					Alpha ratio (maximum accerleration in pushover to maximum p.g.a.)			
			Rock	Clay	Number of storeys	Control	Soft storey at semi-basement level	Double height space (level)	Setbacks	Length: width plan proportions 2.75 : 1	Length: width plan proportions 4:1	Number of 'unsatisfied verifications': limit state of Significant Damage (load distribution numbers)	Number of 'unsatisfied verifications': limit state of Near Collapse (load distribution numbers)	Number of 'unsatisfied verifications': limit state of Damage Limitation (load distribution numbers)	All pushover curves bilinear? (Y/N)	Average number of steps in pushover curves	Minimum Alpha ratio: limit state of Significant Damage	Load distribution number resulting in minimum Alpha ratio for limit state of Significant Damage	Minimum Alpha ratio: limit state of Near Collapse	Load distribution number resulting in minimum Alpha ratio for limit state of Near Collapse
30	3M70	3M_70_F_CTRL_SSTRY_a1R_6flrs_N	X	N/A	6	X	X	N/A	N/A	X	N/A	5 (1-2;10-11; 15)	13 (1-4; 9-16; 23)	12 (1-4; 9-16)	N	23	0.118	1	0.066	1
31	3M71	3M_71_F_CTRL_SSTRY_a1R_5flrs_N	X	N/A	5	X	X	N/A	N/A	X	N/A	4 (1; 10-11; 23)	13 (1-4; 8-11; 13; 15-16; 23-24)	12 (1-4; 9-16)	N	30	0.807	10	0.448	10
32	3M72	3M_72_F_CTRL_SSTRY_a1R_4flrs_N	X	N/A	4	X	X	N/A	N/A	X	N/A	5 (3-4; 13; 15-16)	9 (2-4; 9;11; 13-16)	10 (2-4; 9-12; 14-16)	N	59	0.606	13	0.337	13
33	3M73	3M_73_F_CTRL_SSTRY_a1R_3flrs_N	X	N/A	3	X	X	N/A	N/A	X	N/A	12 (1-4; 9-16)	12 (1-4; 9-16)	12 (1-4; 9-16)	N	13	0.386	12	0.215	12
34	3M74	3M_74_F_CTRL_SSTRY_a1R_2flrs_N	X	N/A	2	X	X	N/A	N/A	X	N/A	0 (N/A)	10 1; 3-4; 9-10; 12-16)	12 (1-4; 9-16)	Y	21	1.009	16	0.561	16
35	3M75	3M_75_F_CTRL_SSTRY_a1R_1flr_N	X	N/A	1	X	X	N/A	N/A	X	N/A	0 (N/A)	0 (N/A)	12 (1-4; 9-16)	Y	20	2.632	19	1.375	19
36	3M76	3M_76_F_CTRL_SSTRY_b2C_6flrs_N	N/A	X	6	X	X	N/A	N/A	N/A	N/A	8 (1-2; 4; 10-12; 15-16)	13 (1-4; 9-16; 23)	12 (1-4; 9-16)	N	23	0.079	1	0.044	1
37	3M77	3M_77_F_CTRL_SSTRY_b2C_5flrs_N	N/A	X	5	X	X	N/A	N/A	N/A	N/A	5 (1-2; 10-11; 23)	15 (1-4; 8-16; 23-24)	12 (1-4; 9-16)	N	30	0.538	10	0.299	10
38	3M78	3M_78_F_CTRL_SSTRY_b2C_4flrs_N	N/A	X	4	X	X	N/A	N/A	X	N/A	9 (2-4; 9; 11; 13-16)	9 (2-4; 9; 11; 13-16)	11 (2-4; 9-16)	N	59	0.404	13	0.225	13
39	3M79	3M_79_F_CTRL_SSTRY_b2C_3flrs_N	N/A	X	3	X	X	N/A	N/A	X	N/A	12 (1-4; 9-16)	12 (1-4; 9-16)	12 (1-4; 9-16)	Y	13	0.210	4	0.117	4
40	3M80	3M_80_F_CTRL_SSTRY_b2C_2flrs_N	N/A	X	2	X	X	N/A	N/A	X	N/A	6 (3-4; 13-16)	12 (1-4; 9-16)	12 (1-4; 9-16)	Y	21	0.673	16	0.374	16
41	3M81	3M_81_F_CTRL_SSTRY_b2C_1flr_N	N/A	X	1	X	X	N/A	N/A	X	N/A	0 (N/A)	0 (N/A)	12 (1-4; 9-16)	Y	20	2.047	19	1.038	19

Key

No unsatisfied verifications: limit state of Significant Damage

No unsatisfied verifications: limit state of Near Collapse

Rock subsoil

Clay subsoil

Table 43 List of numerical models analysed using 3Muri® including the seismic vulnerability characteristics, number of storeys, type of subsoil and the main results from the non-linear static pushover analyses (continued).

Count	Model reference number	3Muri® model name	Subsoil material		Building characteristics investigated							Non-linear static pushover analysis results for main capacity criterion (maximum displacement to target displacement ratio)					Alpha ratio (maximum accerleration in pushover to maximum p.g.a.)			
			Rock	Clay	Number of storeys	Control	Soft storey at semi-basement level	Double height space (level)	Setbacks	Length: width plan proportions 2.75 : 1	Length: width plan proportions 4:1	Number of 'unsatisfied verifications': limit state of Significant Damage (load distribution numbers)	Number of 'unsatisfied verifications': limit state of Near Collapse (load distribution numbers)	Number of 'unsatisfied verifications': limit state of Damage Limitation (load distribution numbers)	All pushover curves bilinear? (Y/N)	Average number of steps in pushover curves	Minimum Alpha ratio: limit state of Significant Damage	Load distribution number resulting in minimum Alpha ratio for limit state of Significant Damage	Minimum Alpha ratio: limit state of Near Collapse	Load distribution number resulting in minimum Alpha ratio for limit state of Near Collapse
42	3M159	3M_159_F_CTRL_STBCK_a1R_6Flrs_N	X	N/A	6	X	N/A	N/A	X	X	N/A	0 (N/A)	0 (N/A)	12 (1-4; 9-16)	Y	19	2.236	11	1.205	11
43	3M161	3M_161_F_CTRL_STBCK_a1R_5Flrs_N	X	N/A	5	X	N/A	N/A	X	X	N/A	0 (N/A)	0 (N/A)	8 (2; 9-12; 14-16)	Y	17	2.538	16	1.362	16
44	3M162	3M_162_F_CTRL_STBCK_a1R_4Flrs_N	X	N/A	4	X	N/A	N/A	X	X	N/A	0 (N/A)	2 (4; 15)	1(16)	Y	14	1.139	15	0.577	15
45	3M163	3M_163_F_CTRL_STBCK_a1R_3Flrs_N	X	N/A	3	X	N/A	N/A	X	X	N/A	0 (N/A)	0 (N/A)	0 (N/A)	Y	15	3.723	6	1.995	9
46	3M167	3M_167_F_CTRL_STBCK_b2C_6Flrs_N	N/A	X	6	X	N/A	N/A	X	X	N/A	0 (N/A)	8 (1-2; 4; 9-12; 16)	12 (1-4; 9-16)	Y	19	1.59	11	0.845	11
47	3M166	3M_166_F_CTRL_STBCK_b2C_5Flrs_N	N/A	X	5	X	N/A	N/A	X	X	N/A	0 (N/A)	2 (12; 16)	12 (1-4; 9-16)	Y	17	1.799	16	0.952	16
48	3M165	3M_165_F_CTRL_STBCK_b2C_4Flrs_N	N/A	X	4	X	N/A	N/A	X	X	N/A	2 (4;15)	3 (4; 15-16)	12 (1-4; 9-16)	Y	14	0.877	15	0.434	15
49	3M164	3M_164_F_CTRL_STBCK_b2C_3Flrs_N	N/A	X	3	X	N/A	N/A	X	X	N/A	0 (N/A)	0 (N/A)	0 (N/A)	Y	15	2.628	9	1.391	9
50	3M93	3M_93_F_CTRL_DHT_a1R_15flrs_N	X	N/A	15	X	N/A	X (0/1)	N/A	X	N/A	1 (16)	7 (3-4; 13-16; 19)	12 (1-4; 9-16)	Y	51	0.986	16	0.548	16
51	3M92	3M_92_F_CTRL_DHT_a1R_14flrs_N	X	N/A	14	X	N/A	X (0/1)	N/A	X	N/A	0 (N/A)	6 (3-4; 13-16)	12 (1-4; 9-16)	Y	51	1.232	3	0.684	3
52	3M91	3M_91_F_CTRL_DHT_a1R_13flrs_N	X	N/A	13	X	N/A	X (0/1)	n/a	X	N/A	0 (N/A)	4 (3-4; 13; 16)	12 (1-4; 9-16)	Y	49	1.603	13	0.890	13
53	3M90	3M_90_F_CTRL_DHT_a1R_12flrs_N	X	N/A	12	X	N/A	X (0/1)	N/A	X	N/A	0 (N/A)	1 (15)	12 (1-4; 9-16)	Y	47	1.770	15	0.983	15
54	3M89	3M_89_F_CTRL_DHT_a1R_11flrs_N	X	N/A	11	X	N/A	X (0/1)	N/A	X	N/A	0 (N/A)	2 (4, 15)	12 (1-4; 9-16)	Y	40	1.571	15	0.873	15
55	3M88	3M_88_F_CTRL_DHT_a1R_10flrs_N	X	N/A	10	X	N/A	X (0/1)	N/A	X	N/A	0 (N/A)	4 (1; 10; 12; 15)	12 (1-4; 9-16)	Y	36	1.580	15	0.878	15

Key

No unsatisfied verifications: limit state of Significant Damage

No unsatisfied verifications: limit state of Near Collapse

Rock subsoil

Clay subsoil

Table 43 List of numerical models analysed using 3Muri® including the seismic vulnerability characteristics, number of storeys, type of subsoil and the main results from the non-linear static pushover analyses (continued).

Count	Model reference number	3Muri® model name	Subsoil material		Building characteristics investigated							Non-linear static pushover analysis results for main capacity criterion (maximum displacement to target displacement ratio)					Alpha ratio (maximum accerleration in pushover to maximum p.g.a.)			
			Rock	Clay	Number of storeys	Control	Soft storey at semi-basement level	Double height space (level)	Setbacks	Length: width plan proportions 2.75 : 1	Length: width plan proportions 4:1	Number of 'unsatisfied verifications': limit state of Significant Damage (load distribution numbers)	Number of 'unsatisfied verifications': limit state of Near Collapse (load distribution numbers)	Number of 'unsatisfied verifications': limit state of Damage Limitation (load distribution numbers)	All pushover curves bilinear? (Y/N)	Average number of steps in pushover curves	Minimum Alpha ratio: limit state of Significant Damage	Load distribution number resulting in minimum Alpha ratio for limit state of Significant Damage	Minimum Alpha ratio: limit state of Near Collapse	Load distribution number resulting in minimum Alpha ratio for limit state of Near Collapse
56	3M87	3M_87_F_CTRL_DHT_a1R_9flrs_N	X	N/A	9	X	N/A	X (0/1)	N/A	X	N/A	0 (N/A)	3 (10; 12; 16)	12 (1-4; 9-16)	Y	33	1.648	15	0.915	15
57	3M86	3M_86_F_CTRL_DHT_a1R_8flrs_N	X	N/A	8	X	N/A	X (0/1)	N/A	X	N/A	0 (N/A)	1 (10)	12 (1-4; 9-16)	Y	28	1.734	10	0.955	10
58	3M85	3M_85_F_CTRL_DHT_a1R_7flrs_N	X	N/A	7	X	N/A	X (0/1)	N/A	X	N/A	0 (N/A)	3 (4; 15-16)	12 (1-4; 9-16)	Y	22	1.694	16	0.925	16
59	3M82	3M_82_F_CTRL_DHT_a1R_6Flrs_N	X	N/A	6	X	N/A	X (0/1)	N/A	X	N/A	0 (N/A)	0 (N/A)	12 (1-4; 9-16)	Y	19	2.051	4	1.109	4
60	3M83	3M_83_F_CTRL_DHT_a1R_5flrs_N	X	N/A	5	X	N/A	X (0/1)	N/A	X	N/A	0 (N/A)	1 (14)	9 (1-2; 4; 9-12; 15-16)	Y	17	1.866	14	0.987	14
61	3M84	3M_84_F_CTRL_DHT_a1R_4flrs_N	X	N/A	4	X	N/A	X (0/1)	N/A	X	N/A	0 (N/A)	0 (N/A)	0 (N/A)	Y	13	2.367	8	1.229	8
62	3M107	3M_107_F_CTRL_DHT_a1R_3flrs_N	X	N/A	3	X	N/A	X (0/1)	N/A	X	N/A	0 (N/A)	0 (N/A)	0 (N/A)	Y	14	2.995	14	1.577	14
63	106	3M_106_F_CTRL_DHT_b2C_15flrs_N	N/A	X	15	X	N/A	X (0/1)	N/A	X	N/A	6 (3-4; 13-16)	23 (1-16; 18-24)	18 (1-4; 7-16; 21-24)	Y	51	0.657	16	0.365	16
64	105	3M_105_F_CTRL_DHT_b2C_14flrs_N	N/A	X	14	X	N/A	X (0/1)	N/A	X	N/A	4 (3-4; 13-14)	21 (1-5; 7-16; 18; 21-24)	1-4; 7-16; 21-24)	Y	51	0.821	3	0.456	3
65	3M104	3M_104_F_CTRL_DHT_b2C_13flrs_N	N/A	X	13	X	N/A	X (0/1)	N/A	X	N/A	0 (N/A)	17 (1-4; 7; 9-16; 21-24)	18 (1-4; 7-16; 21-24)	Y	49	1.069	13	0.594	13
66	3M103	3M_103_F_CTRL_DHT_b2C_12flrs_N	N/A	X	12	X	N/A	X (0/1)	N/A	X	N/A	0 (N/A)	13 (1-4; 9-15; 21; 23)	12 (1-4; 9-16)	Y	47	1.180	15	0.655	15
67	3M102	3M_102_F_CTRL_DHT_b2C_11flrs_N	N/A	X	11	X	N/A	X (0/1)	N/A	X	N/A	0 (N/A)	14 (1-4;6; 9-16; 19)	15 (1-4; 8-16; 23-24)	Y	40	1.047	15	0.582	15
68	3M101	3M_101_F_CTRL_DHT_b2C_10flrs_N	N/A	X	10	X	N/A	X (0/1)	N/A	X	N/A	0 (N/A)	11 (1-4; 9-13; 15-16)	12 (1-4; 9-16)	Y	36	1.068	15	0.591	15
69	3M100	3M_100_F_CTRL_DHT_b2C_9flrs_N	N/A	X	9	X	N/A	X (0/1)	N/A	X	N/A	0 (N/A)	9 (1-2; 4; 9-12; 15-16)	12 (1-4; 9-16)	Y	33	1.167	15	0.639	15
70	3M99	3M_99_F_CTRL_DHT_b2C_8flrs_N	N/A	X	8	X	N/A	X (0/1)	N/A	X	N/A	0 (N/A)	11 (1-4; 9-12; 14-16)	12 (1-4; 9-16)	Y	28	1.233	10	0.669	10

Key

No unsatisfied verifications: limit state of Significant Damage

No unsatisfied verifications: limit state of Near Collapse

Rock subsoil

Clay subsoil

Table 43 List of numerical models analysed using 3Muri® including the seismic vulnerability characteristics, number of storeys, type of subsoil and the main results from the non-linear static pushover analyses (continued).

Count	Model reference number	3Muri® model name	Subsoil material		Building characteristics investigated							Non-linear static pushover analysis results for main capacity criterion (maximum displacement to target displacement ratio)					Alpha ratio (maximum accerleration in pushover to maximum p.g.a.)			
			Rock	Clay	Number of storeys	Control	Soft storey at semi-basement level	Double height space (level)	Setbacks	Length: width plan proportions 2.75 : 1	Length: width plan proportions 4:1	Number of 'unsatisfied verifications': limit state of Significant Damage (load distribution numbers)	Number of 'unsatisfied verifications': limit state of Near Collapse (load distribution numbers)	Number of 'unsatisfied verifications': limit state of Damage Limitation (load distribution numbers)	All pushover curves bilinear? (Y/N)	Average number of steps in pushover curves	Minimum Alpha ratio: limit state of Significant Damage	Load distribution number resulting in minimum Alpha ratio for limit state of Significant Damage	Minimum Alpha ratio: limit state of Near Collapse	Load distribution number resulting in minimum Alpha ratio for limit state of Near Collapse
71	3M98	3M_98_F_CTRL_DHT_b2C_7flrs_N	N/A	X	7	X	N/A	X (0/1)	N/A	X	N/A	0 (N/A)	11 (1-4; 9-12; 14-16)	12 (1-4; 9-16)	Y	22	1.204	16	0.648	16
72	3M94	3M_94_F_CTRL_DHT_b2C_6Flrs_N	N/A	X	6	X	N/A	X (0/1)	N/A	X	N/A	0 (N/A)	11 (1-4; 9-12; 14-16)	12 (1-4; 9-16)	Y	19	1.455	4	0.776	4
73	3M95	3M_95_F_CTRL_DHT_b2C_5flrs_N	N/A	X	5	X	N/A	X (0/1)	N/A	X	N/A	0 (N/A)	4 (4; 14-16)	12 (1-4; 9-16)	Y	17	1.360	14	0.706	14
74	3M96	3M_96_F_CTRL_DHT_b2C_4flrs_N	N/A	X	4	X	N/A	X (0/1)	N/A	X	N/A	0 (N/A)	3 (8; 14; 23)	10 (1-3; 9-15)	Y	13	1.794	14	0.912	8
75	3M97	3M_97_F_CTRL_DHT_b2C_3flrs_N	N/A	X	3	X	N/A	X (0/1)	N/A	X	N/A	0 (N/A)	0 (N/A)	0 (N/A)	Y	14	2.155	14	1.117	14
76	3M156	3M_156_F_CTRL_DHT_WtoW_a1R_10Flrs_N	X	N/A	10	X	N/A	X (0/1)	N/A	X	N/A	0 (N/A)	4 (10; 12; 15-16)	12 (1-4; 9-16)	Y	35	0.883	15	0.883	15
77	3M155	3M_155_F_CTRL_DHT_WtoW_a1R_9Flrs_N	X	N/A	9	X	N/A	X (0/1)	N/A	X	N/A	0 (N/A)	4 (10; 12; 15-16)	12 (1-4; 9-16)	Y	33	1.711	10	0.950	10
78	3M154	3M_154_F_CTRL_DHT_WtoW_a1R_8Flrs_N	X	N/A	8	X	N/A	X (0/1)	N/A	X	N/A	0 (N/A)	3 (1; 10; 12)	12 (1-4; 9-16)	Y	28	1.727	12	0.953	12
79	3M153	3M_153_F_CTRL_DHT_WtoW_a1R_7Flrs_N	X	N/A	7	X	N/A	X (0/1)	N/A	X	N/A	0 (N/A)	0 (N/A)	12 (1-4; 9-16)	Y	21	1.959	10	1.068	10
80	3M152	3M_152_F_CTRL_DHT_WtoW_a1R_6Flrs_N	X	N/A	6	X	N/A	X (0/1)	N/A	X	N/A	0 (N/A)	0 (N/A)	12 (1-4; 9-16)	Y	19	2.190	12	1.186	12
81	3M157	3M_157_F_CTRL_DHT_WtoW_a1R_5Flrs_N	X	N/A	5	X	N/A	X (0/1)	N/A	X	N/A	0 (N/A)	0 (N/A)	3 (1; 9-10)	Y	14	1.900	14	1.006	14
82	3M158	3M_158_F_CTRL_DHT_WtoW_a1R_4Flrs_N	X	N/A	4	X	N/A	X (0/1)	N/A	X	N/A	0 (N/A)	0 (N/A)	0 (N/A)	Y	13	2.063	8	1.033	20
83	3M121	3M_121_F_CTRL_EXTNDD_a1R_7flrs_N	X	N/A	7	X	N/A	N/A	N/A	N/A	X	0 (N/A)	3 (2; 11-12)	12 (1-4; 9-16)	Y	34	1.109	12	0.610	12

Key

No unsatisfied verifications: limit state of Significant Damage

No unsatisfied verifications: limit state of Near Collapse

Rock subsoil

Clay subsoil

Table 43 List of numerical models analysed using 3Muri® including the seismic vulnerability characteristics, number of storeys, type of subsoil and the main results from the non-linear static pushover analyses (continued).

Count	Model reference number	3Muri® model name	Subsoil material		Building characteristics investigated							Non-linear static pushover analysis results for main capacity criterion (maximum displacement to target displacement ratio)					Alpha ratio (maximum accerleration in pushover to maximum p.g.a.)			
			Rock	Clay	Number of storeys	Control	Soft storey at semi-basement level	Double height space (level)	Setbacks	Length: width plan proportions 2.75 : 1	Length: width plan proportions 4:1	Number of 'unsatisfied verifications': limit state of Significant Damage (load distribution numbers)	Number of 'unsatisfied verifications': limit state of Near Collapse (load distribution numbers)	Number of 'unsatisfied verifications': limit state of Damage Limitation (load distribution numbers)	All pushover curves bilinear? (Y/N)	Average number of steps in pushover curves	Minimum Alpha ratio: limit state of Significant Damage	Load distribution number resulting in minimum Alpha ratio for limit state of Significant Damage	Minimum Alpha ratio: limit state of Near Collapse	Load distribution number resulting in minimum Alpha ratio for limit state of Near Collapse
84	3M116	3M_116_F_CTRL_EXTNDD_a1R_6flrs_N	X	N/A	6	X	N/A	N/A	N/A	N/A	X	1 (2)	4 (2; 11-12; 16)	12 (1-4; 9-16)	Y	28	0.982	2	0.524	2
85	3M117	3M_117_F_CTRL_EXTNDD_a1R_5flrs_N	X	N/A	5	X	N/A	N/A	N/A	N/A	X	0 (N/A)	0 (N/A)	12 (1-4; 9-16)	Y	27	3.857	11	2.104	11
86	3M118	3M_118_F_CTRL_EXTNDD_a1R_4flrs_N	X	N/A	4	X	N/A	N/A	N/A	N/A	X	0 (N/A)	1 (13)	9 (1-3; 9-12; 14; 16)	Y	24	1.651	13	0.856	13
87	3M119	3M_119_F_CTRL_EXTNDD_a1R_3flrs_N	X	N/A	3	X	N/A	N/A	N/A	N/A	X	0 (N/A)	0 (N/A)	0 (N/A)	Y	26	5.758	11	3.142	11
88	3M122	3M_122_F_CTRL_EXTNDD_b2C_7flrs_N	N/A	X	7	X	N/A	N/A	N/A	N/A	X	1 (12)	4 (2; 10-12)	12 (1-4; 9-16)	Y	34	0.808	12	0.435	12
89	3M123	3M_123_F_CTRL_EXTNDD_b2C_6flrs_N	N/A	X	6	X	N/A	N/A	N/A	N/A	X	3 (2; 11-12)	5 (2; 4; 11-12; 16)	12 (1-4; 9-16)	Y	28	0.736	2	0.383	2
90	3M124	3M_124_F_CTRL_EXTNDD_b2C_5flrs_N	N/A	X	5	X	N/A	N/A	N/A	N/A	X	0 (N/A)	0 (N/A)	12 (1-4; 9-16)	Y	27	2.662	11	1.441	11
91	3M125	3M_125_F_CTRL_EXTNDD_b2C_4flrs_N	N/A	X	4	X	N/A	N/A	N/A	N/A	X	0 (N/A)	1 (13)	12 (1-4; 9-16)	Y	24	0.620	13	0.620	13
92	3M126	3M_126_F_CTRL_EXTNDD_b2C_3flrs_N	N/A	X	3	X	N/A	N/A	N/A	N/A	X	0 (N/A)	0 (N/A)	4 (2;9;11-12)	Y	26	3.971	11	2.150	11
93	3M140	3M_140_F_CTRL_SSTRY_EXTNDD_a1R_6flrs_N	X	N/A	6	X	X	N/A	N/A	N/A	X	12 (1-4; 9-16)	12 (1-4; 9-16)	12 (1-4; 9-16)	N	17 (wide range)	0.025	1	0.014	1
94	3M141	3M_141_F_CTRL_SSTRY_EXTNDD_a1R_5flrs_N	X	N/A	5	X	X	N/A	N/A	N/A	X	10 (1-2; 4; 9-13; 15-16)	12 (1-4; 9-16)	12 (1-4; 9-16)	N	18 (wide range)	0.022	11	0.012	11

Key

No unsatisfied verifications: limit state of Significant Damage

No unsatisfied verifications: limit state of Near Collapse

Rock subsoil

Clay subsoil

Table 43 List of numerical models analysed using 3Muri® including the seismic vulnerability characteristics, number of storeys, type of subsoil and the main results from the non-linear static pushover analyses (continued).

Count	Model reference number	3Muri® model name	Subsoil material		Building characteristics investigated							Non-linear static pushover analysis results for main capacity criterion (maximum displacement to target displacement ratio)					Alpha ratio (maximum accerleration in pushover to maximum p.g.a.)			
			Rock	Clay	Number of storeys	Control	Soft storey at semi-basement level	Double height space (level)	Setbacks	Length: width plan proportions 2.75 : 1	Length: width plan proportions 4:1	Number of 'unsatisfied verifications': limit state of Significant Damage (load distribution numbers)	Number of 'unsatisfied verifications': limit state of Near Collapse (load distribution numbers)	Number of 'unsatisfied verifications': limit state of Damage Limitation (load distribution numbers)	All pushover curves bilinear? (Y/N)	Average number of steps in pushover curves	Minimum Alpha ratio: limit state of Significant Damage	Load distribution number resulting in minimum Alpha ratio for limit state of Significant Damage	Minimum Alpha ratio: limit state of Near Collapse	Load distribution number resulting in minimum Alpha ratio for limit state of Near Collapse
95	3M142	3M_142_F_CTRL_SSTRY_EXTNDD_a1R_4flrs_N	X	N/A	4	X	X	N/A	N/A	N/A	X	11 (1-3; 9-13; 16; 19-20)	14 (1-4; 9-16; 19-20)	13 (1-4; 9-16; 20)	N	17 (wide range)	0.118	12	0.065	12
96	3M143	3M_143_F_CTRL_SSTRY_EXTNDD_a1R_3flrs_N	X	N/A	3	X	X	N/A	N/A	N/A	X	9 (1-3; 9-12; 14; 20)	11 (1-3;6; 9-12; 14; 19-20)	8 (3-4; 11-16)	N	25 (wide range)	0.124	3	0.069	3
97	3M144	3M_144_F_CTRL_SSTRY_EXTNDD_a1R_2flrs_N	X	N/A	2	X	X	N/A	N/A	N/A	X	6 (3-4; 13-16)	8 (2-4; 11; 13-16)	9 (1-3; 9-14)	N	22	0.550	13	0.305	13
98	3M145	3M_145_F_CTRL_SSTRY_EXTNDD_a1R_1flr_N	X	N/A	1	X	X	N/A	N/A	N/A	X	0 (N/A)	2 (4; 10)	12 (1-4; 9-16)	N	25	1.541	10	0.856	10
99	3M146	3M_146_F_CTRL_SSTRY_EXTNDD_b2C_6flrs_N	N/A	X	6	X	X	N/A	N/A	N/A	X	12 (1-4; 9-16)	12 (1-4; 9-16)	12 (1-4; 9-16)	N	17 (wide range)	0.017	1	0.009	1
100	3M147	3M_147_F_CTRL_SSTRY_EXTNDD_b2C_5flrs_N	N/A	X	5	X	X	N/A	N/A	N/A	X	12 (1-4; 9-16)	12 (1-4; 9-16)	12 (1-4; 9-16)	N	18 (wide range)	0.015	11	0.008	11
101	3M148	3M_148_F_CTRL_SSTRY_EXTNDD_b2C_4flrs_N	N/A	X	4	X	X	N/A	N/A	N/A	X	14 (1-4; 9-16; 19-20)	14 (1-4; 9-16; 19-20)	15 (1-4; 6; 9-16; 19-20)	N	17 (wide range)	0.079	12	0.044	12
102	3M149	3M_149_F_CTRL_SSTRY_EXTNDD_b2C_3flrs_N	N/A	X	3	X	X	N/A	N/A	N/A	X	9 (1-3; 9-12; 14; 16)	15 (1-4; 6; 9-16; 19-20)	10 (3-4; 6; 11-16; 20)	N	25 (wide range)	0.083	3	0.046	3
103	3M150	3M_150_F_CTRL_SSTRY_EXTNDD_b2C_2flrs_N	N/A	X	2	X	X	N/A	N/A	N/A	X	6 (3-4; 13-16)	12 (1-4; 9-16)	12 (1-4; 9-16)	N	22	0.367	13	0.204	13
104	3M151	3M_151_F_CTRL_SSTRY_EXTNDD_b2C_1flrs_N	N/A	X	1	X	X	N/A	N/A	N/A	X	0 (N/A)	7 (1; 3-4; 9-10; 12; 16)	12 (1-4; 9-16)	N	25	1.027	10	0.571	10
105	3M133	3M_133_F_CTRL_DHT_EXTNDD_a1R_8flrs_N	X	N/A	8	X	N/A	X (0/1)	N/A	N/A	X	0 (N/A)	0 (N/A)	12 (1-4; 9-16)	Y	37	2.390	10	1.328	10

Key

No unsatisfied verifications: limit state of Significant Damage

No unsatisfied verifications: limit state of Near Collapse

Rock subsoil

Clay subsoil

Table 43 List of numerical models analysed using 3Muri® including the seismic vulnerability characteristics, number of storeys, type of subsoil and the main results from the non-linear static pushover analyses (continued).

Count	Model reference number	3Muri® model name	Subsoil material		Building characteristics investigated							Non-linear static pushover analysis results for main capacity criterion (maximum displacement to target displacement ratio)					Alpha ratio (maximum accerleration in pushover to maximum p.g.a.)			
			Rock	Clay	Number of storeys	Control	Soft storey at semi-basement level	Double height space (level)	Setbacks	Length: width plan proportions 2.75 : 1	Length: width plan proportions 4:1	Number of 'unsatisfied verifications': limit state of Significant Damage (load distribution numbers)	Number of 'unsatisfied verifications': limit state of Near Collapse (load distribution numbers)	Number of 'unsatisfied verifications': limit state of Damage Limitation (load distribution numbers)	All pushover curves bilinear? (Y/N)	Average number of steps in pushover curves	Minimum Alpha ratio: limit state of Significant Damage	Load distribution number resulting in minimum Alpha ratio for limit state of Significant Damage	Minimum Alpha ratio: limit state of Near Collapse	Load distribution number resulting in minimum Alpha ratio for limit state of Near Collapse
106	3M128	3M_128_F_CTRL_DHT_EXTNDD_a1 R_7flrs_N	X	N/A	7	X	N/A	X (0/1)	N/A	N/A	X	0 (N/A)	0 (N/A)	12 (1-4; 9-16)	Y	32	2.185	11	1.194	11
107	3M129	3M_129_F_CTRL_DHT_EXTNDD_a1 R_6flrs_N	X	N/A	6	X	N/A	X (0/1)	N/A	N/A	X	0 (N/A)	3 (2; 11-12)	12 (1-4; 9-16)	Y	30	1.365	12	0.742	12
108	3M130	3M_130_F_CTRL_DHT_EXTNDD_a1 R_5flrs_N	X	N/A	5	X	N/A	X (0/1)	N/A	N/A	X	0 (N/A)	0 (N/A)	12 (1-4; 9-16)	Y	28	4.230	12	2.317	12
109	3M131	3M_131_F_CTRL_DHT_EXTNDD_a1 R_4flrs_N	X	N/A	4	X	N/A	X (0/1)	N/A	N/A	X	0 (N/A)	0 (N/A)	2 (3; 14)	Y	24	1.932	13	1.010	13
110	3M132	3M_132_F_CTRL_DHT_EXTNDD_a1 R_3flrs_N	X	N/A	3	X	N/A	X (0/1)	N/A	N/A	X	0 (N/A)	0 (N/A)	3 (4; 15-16)	Y	26	3.770	19	1.991	19
111	3M134	3M_134_F_CTRL_DHT_EXTNDD_b2 C_8flrs_N	N/A	X	8	X	N/A	X (0/1)	N/A	N/A	X	0 (N/A)	2 (1; 10)	12 (1-4; 9-16)	Y	37	1.647	10	0.908	10
112	3M135	3M_135_F_CTRL_DHT_EXTNDD_b2 C_7flrs_N	N/A	X	7	X	N/A	X (0/1)	N/A	N/A	X	0 (N/A)	1 (11)	12 (1-4; 9-16)	Y	32	1.535	11	0.829	11
113	3M136	3M_136_F_CTRL_DHT_EXTNDD_b2 C_6flrs_N	N/A	X	6	X	N/A	X (0/1)	N/A	N/A	X	1 (12)	5 (2; 4; 11-12; 16)	12 (1-4; 9-16)	Y	30	0.991	12	0.528	12
114	3M137	3M_137_F_CTRL_DHT_EXTNDD_b2 C_5flrs_N	N/A	X	5	X	N/A	X (0/1)	N/A	N/A	X	0 (N/A)	0 (N/A)	12 (1-4; 9-16)	Y	28	2.911	12	1.583	12
115	3M138	3M_138_F_CTRL_DHT_EXTNDD_b2 C_4flrs_N	N/A	X	4	X	N/A	X (0/1)	N/A	N/A	X	0 (N/A)	1 (13)	12 (1-4; 9-16)	Y	24	1.411	13	0.725	13
116	3M139	3M_139_F_CTRL_DHT_EXTNDD_b2 C_3flrs_N	N/A	X	3	X	N/A	X (0/1)	N/A	N/A	X	0 (N/A)	0 (N/A)	6 (2; 4; 11-12; 15-16)	Y	26	2.916	19	1.495	19

Key

No unsatisfied verifications: limit state of Significant Damage

No unsatisfied verifications: limit state of Near Collapse

Rock subsoil

Clay subsoil

Table 44 Summary of maximum building height for adequate seismic resistance resulting from cases analysed using 3Muri® and the corresponding cases analysed using ELS®.

Case	3Muri®: Upper coralline limestone subsoil			3Muri®: Clay subsoil			ELS®: 'rock subsoil' cases			ELS®: 'clay subsoil' cases		
	Range of overall heights analysed (number of storeys)	Maximum height for no 'unsatisfied verifications': limit state of Significant Damage (3Muri® model reference number)	Maximum height for no 'unsatisfied verifications': limit state of Near Collapse (3Muri® model reference number)	Range of overall heights analysed (number of storeys)	Maximum height for no 'unsatisfied verifications': limit state of Significant Damage (3Muri® model reference number)	Maximum height for no 'unsatisfied verifications': limit state of Near Collapse (3Muri® model reference number)	Range of overall heights analysed (number of storeys)	Maximum height for collapse resistance (ELS® model reference number)	Ground formations	Range of overall heights analysed (number of storeys)	Maximum height for collapse resistance (ELS® model reference number)	Ground formations
Control (length : width plan proportions 2.75:1)	1 to 15	14 (3M56)	6 (3M46)	4 to 15	13 (3M67)	4 (3M60)	5 to 6	5 (48, 49, 50)	All 'rock subsoil' cases	3 to 6	3 (63, 64)	1.5 m thick upper coralline limestone over 60 m thick clay; 60 m thick clay
											4 (59)	Clay specified at Minimum Z
Control with a soft storey at lowest level (length : width plan proportions 2.75:1)	1 to 6	2 (3M74)	1 (3M75)	1 to 6	1 (3M81)	1 (3M81)	Case not investigated	N/A	N/A	3 to 6	3 (75)	1.5 m thick upper coralline limestone over 60 m thick clay
Control with setbacks at penthouse level (length : width plan proportions 2.75:1)	3 to 6	=>6 (Maximum height not identified within investigated range)	3 (3M163)	3 to 6	3 (3M164)	3 (3M164)	Case not investigated	N/A	N/A	4 to 6	4 (83)	1.5 m thick upper coralline limestone over 60 m thick clay
Control with a double height space between levels 0 and 1 (length : width plan proportions 2.75:1)	3 to 15	14 (3M92)	4 (3M84)	3 to 15	13 (3M104)	3 (3M97)	Case not investigated	N/A	N/A	3 to 6	3 (105)	1.5 m thick upper coralline limestone over 60 m thick clay
Control with a wider double height space over whole width of structure between levels 0 and 1 (length : width plan proportions 2.75:1)	4 to 10	=>10 (Maximum height not identified within investigated range)	7 (3M153)	Case not investigated	N/A	N/A	Case not investigated	N/A	N/A	Case not investigated	N/A	N/A
Control (length : width plan proportions 4:1)	3 to 7	5 (3M117)	3 (3M119)	3 to 7	5 (3M124)	3 (3M126)	Case not investigated	N/A	N/A	Case not investigated	N/A	N/A
Control with a soft storey at lowest level (length : width plan proportions 4:1)	1 to 6	1 (3M145)	<1 (3M145 results in 2 unsatisfied verifications)	1 to 6	1 (3M151)	<1 (3M151 results in 7 unsatisfied verifications)	Case not investigated	N/A	N/A	Case not investigated	N/A	N/A
Control with a double height space between levels 0 and 1 (length : width plan proportions 4:1)	3 to 8	=>8 (Maximum height not identified within investigated range)	5 (3M130)	3 to 8	5 (3M137)	3 (3M139)	Case not investigated	N/A	N/A	Case not investigated	N/A	N/A

Key

Numerical models with a higher number of floors resulted in no unsatisfied verifications for the limit state under consideration. In such cases, the number of storeys indicated is the lowest height of the structure before the first case of unsatisfied verification occured

Unsatisfied verifications resulted for the limit state under consideration even at the lowest height at which case was investigated

Maximum height for no unsatisfied verifications with respect to the limit state under consideration not identified within the range of overall building heights investigated for this case

Table 45 Summary of modal analyses results obtained using 3Muri® for analysed cases on an upper coralline limestone subsoil and natural frequencies in the x- and y-directions for the first mode of vibration in corresponding numerical models analysed using ELS®.

Model reference number	3Muri® model name		3Muri®: Natural frequency (Hz) in x-direction (for mass contribution ≥ 5%)				ELS®: Natural frequency (Hz): first mode of vibration in x-direction	3Muri®: Natural frequency (Hz) in y-direction (for mass contribution ≥ 5%)				ELS®: Natural frequency (Hz): first mode of vibration in y-direction	3Muri®: Natural frequency (Hz) in z-direction (for mass contribution ≥ 5%)						Displacement profile: modal analysis			
			Natural frequency (Hz) in x-direction (mode number, mass contribution)	Natural frequency (Hz) in x-direction (mode number, mass contribution)	Natural frequency (Hz) in x-direction (mode number, mass contribution)	Natural frequency (Hz) in x-direction (mode number, mass contribution)		Natural frequency (Hz) in y-direction (mode number, mass contribution)	Natural frequency (Hz) in y-direction (mode number, mass contribution)	Natural frequency (Hz) in y-direction (mode number, mass contribution)	Natural frequency (Hz) in y-direction (mode number, mass contribution)		Natural frequency (Hz) in z-direction (mode number, mass contribution)	Natural frequency (Hz) in z-direction (mode number, mass contribution)	Natural frequency (Hz) in z-direction (mode number, mass contribution)	Natural frequency (Hz) in z-direction (mode number, mass contribution)	Natural frequency (Hz) in z-direction (mode number, mass contribution)	Natural frequency (Hz) in z-direction (mode number, mass contribution)	Displacement profile: modes of vibration in x-direction	Displacement profile: modes of vibration in y-direction	Box-like behaviour from deformed plan shapes (Y/N)	Modes of vibration where box-like behaviour not present (main modes of vibration only considered)
3M44	3M_44_F_XMX 011_ a1R_6flrs_N_rock ELS		3.493 (1, 77.18%)	9.895 (4, 16.26%)	N/A	N/A	3.804	7.935 (3, 67.49%)	19.157 (8, 12.87%)	20.657 (9, 5.57%)	N/A	7.413	19.157 (8, 28.27%)	20.657 (9, 47.57%)	N/A	N/A	N/A	N/A	1,2	1,2	N	All main
3M57	3M_57_F_CTRL_a1R_15flrs_N		0.996 (1, 65.49%)	4.306 (4, 20.07%)	8.998 (7, 5.10%)	N/A	N/A	1.918 (2, 57.68%)	2.215 (3, 7.16%)	7.331 (6, 17.91%)	14.910 (11, 5.55%)	N/A	10.208 (8, 80.99%)	N/A	N/A	N/A	N/A	N/A	1,2,3	1,2,3, T	N	Modes 4, 6, 7, 11
3M56	3M_56_F_CTRL_a1R_14lrs_N		1.123 (1, 65.82%)	4.742 (4, 19.88%)	9.789 (7, 4.88%)	N/A	N/A	2.136 (2, 52.43%)	2.403 (3, 12.82%)	7.966 (6, 18.49%)	16.100 (11, 5.48%)	N/A	10.913 (8, 80.71%)	N/A	N/A	N/A	N/A	N/A	1,2,3	1,2,3, T	N	Modes 4, 7, 11
3M53	3M_53_F_CTRL_a1R_13flrs_N		1.276 (1, 66.18%)	5.250 (4, 19.64%)	10.695 (7, 4.64%)	N/A	N/A	2.383 (2, 42.68%)	2.637 (3, 23.05%)	8.696 (6, 18.88%)	17.440 (11, 5.36%)	N/A	11.725 (8, 80.29%)	N/A	N/A	N/A	N/A	N/A	1,2,3	1,2,3	N	Modes 4,6,7,11
3M52	3M_52_F_CTRL_a1R_12flrs_N		1.460 (1, 66.57%)	5.848 (4, 19.32%)	N/A	N/A	N/A	2.656 (2, 29.39%)	2.935 (3, 36.93%)	9.543 (6, 19.09%)	18.943 (6, 5.15%)	N/A	12.668 (8, 79.67%)	N/A	n/a	N/A	N/A	N/A	1,2	1, 2, 3, T	N	Modes 6, 11
3M51	3M_51_F_CTRL_a1R_11flrs_N		1.686 (1, 66.98%)	6.562 (4, 18.91%)	N/A	N/A	N/A	2.961 (2, 17.97%)	3.320 (3, 49.05%)	10.535 (6, 19.11%)	N/A	N/A	13.776 (8, 78.75%)	N/A	N/A	N/A	N/A	N/A	1, 2	1,2,T	N	Modes 4, 6
3M50	3M_50_F_CTRL_a1R_10flrs_N		1.967 (1, 67.40%)	7.425 (4, 18.39%)	N/A	N/A	N/A	3.315 (2, 10.95%)	3.811 (3, 56.92%)	11.712 (6, 18.91%)	N/A	N/A	15.088 (8, 77.32%)	N/A	N/A	N/A	N/A	N/A	1, 2	1. 2 , T	N	Modes 4, 6
3M49	3M_49_F_CTRL_a1R_9flrs_N		2.321 (1, 67.80%)	8.486 (4, 17.74%)	N/A	N/A	N/A	3.743 (2, 7.05%)	4.434 (3, 61.87%)	13.127 (6, 18.43%)	N/A	N/A	13.127 (6, 4.27%)	16.711 (8, 75.05%)	N/A	N/A	N/A	N/A	1, 2	1. 2 , T	N	Mode 4
3M48	3M_48_F_CTRL_a1R_8flrs_N		2.779 (1, 68.15%)	9.819 (4, 16.92%)	N/A	N/A	N/A	4.284 (2, 4.81%)	5.234 (3, 65.44%)	14.863 (6, 17.59%)	N/A	N/A	14.863 (6, 6.42%)	18.723 (8, 71.84%)	N/A	N/A	N/A	N/A	1, 2	1. T	N	Modes 4, 6
3M47v2	3M_47v2_F_CTRL_a1R_7flrs_N		3.372 (1, 68.36%)	11.586 (4, 15.96%)	N/A	N/A	N/A	6.322 (3, 69.97%)	17.164 (6, 16.28%)	N/A	N/A	N/A	17.164 (6, 7.55%)	21.349 (8, 69.63%)	N/A	N/A	N/A	N/A	1,2	1,2	N	Modes 4, 6

Table 45 Summary of modal analyses results obtained using 3Muri® for analysed cases on an upper coralline limestone subsoil and natural frequencies in the x- and y-directions for the first mode of vibration in corresponding numerical models analysed using ELS® (continued).

Model reference number	3Muri® model name	3Muri®: Natural frequency (Hz) in x-direction (for mass contribution ≥ 5%)				ELS®: Natural frequency (Hz): first mode of vibration in x-direction	3Muri®: Natural frequency (Hz) in y-direction (for mass contribution ≥ 5%)				ELS®: Natural frequency (Hz): first mode of vibration in y-direction	3Muri®: Natural frequency (Hz) in z-direction (for mass contribution ≥ 5%)						Displacement profile: modal analysis			
		Natural frequency (Hz) in x-direction (mode number, mass contribution)	Natural frequency (Hz) in x-direction (mode number, mass contribution)	Natural frequency (Hz) in x-direction (mode number, mass contribution)	Natural frequency (Hz) in x-direction (mode number, mass contribution)		Natural frequency (Hz) in y-direction (mode number, mass contribution)	Natural frequency (Hz) in y-direction (mode number, mass contribution)	Natural frequency (Hz) in y-direction (mode number, mass contribution)	Natural frequency (Hz) in y-direction (mode number, mass contribution)		Natural frequency (Hz) in z-direction (mode number, mass contribution)	Natural frequency (Hz) in z-direction (mode number, mass contribution)	Natural frequency (Hz) in z-direction (mode number, mass contribution)	Natural frequency (Hz) in z-direction (mode number, mass contribution)	Natural frequency (Hz) in z-direction (mode number, mass contribution)	Natural frequency (Hz) in z-direction (mode number, mass contribution)	Displacement profile: modes of vibration in x-direction	Displacement profile: modes of vibration in y-direction	Box-like behaviour from deformed plan shapes (Y/N)	Modes of vibration where box-like behaviour not present (main modes of vibration only considered)
3M46	3M_46_F_CTRL_a1R_6flrs_N	4.212 (1, 68.47%)	13.852 (4, 14.69%)	N/A	N/A	3.882	7.726 (3, 72.91%)	20.064 (6, 14.64%)	N/A	N/A	6.579	20.064 (6, 10.19%)	24.673 (8, 62.06%)	26.911 (9, 5.85%)	N/A	N/A	N/A	1,2	1,2	N	Modes 4, 6
3M54	3M_54_F_CTRL_a1R_5flrs_N	5.384 (1, 66.35%)	7.374 (2, 5.86%)	16.912 (4, 12.97%)	N/A	5.067	9.668 (3, 76.38%)	24.010 (6, 12.38%)	N/A	N/A	7.951	24.010 (6, 13.5%)	29.053 (8, 36.57%)	30.276 (9, 25.3%)	N/A	N/A	N/A	1,2, T	1,2	N	Modes 4, 6
3M55	3M_55_F_CTRL_a1R_4flrs_N	7.155 (1, 68.16%)	9.437 (2, 8.31%)	21.169 (4, 10.6%)	26.205 (5, 5.14%)	6.744	12.492 (3, 80.75%)	29.780 (6, 9.38%)	N/A	N/A	9.757	29.780 (6, 17.11%)	36.311 (9, 51.80%)	42.427 (11, 7.62%)	N/A	N/A	N/A	1,2	1,2	N	All main except 1,2
3M168	3M_168_F_CTRL_a1R_3flrs_N	10.080 (1, 68.45%)	12.791 (2, 11.07%)	27.525 (4, 7.69%)	34.083 (5, 5.96%)	9.218	16.855 (3, 86.31%)	39.185 (6, 5.66%)	N/A	N/A	9.856	39.185 (6, 23.07%)	45.893 (9, 31.33%)	50.942 (11, 16.76%)	N/A	N/A	N/A	1,2,T	1,2	N	All main except 2
3M169	3M_169_F_CTRL_a1R_2flrs_N	15.657 (1, 71.25%)	18.918 (2, 11.98%)	36.640 (4, 6.53%)	46.125 (6, 6.64%)	N/A	24.301 (3, 91.95%)	61.125 (9, 4.91%)	N/A	N/A	N/A	48.996 (7, 16.36%)	64.767 (10, 32.24%)	71.531 (13, 10.88%)	N/A	N/A	N/A	1,2,T	1,2	N	All main except 2
3M170	3M_170_F_CTRL_a1R_1flr_N	28.273 (1, 77.68%)	33.400 (2, 17.46%)	N/A	N/A	N/A	39.888 (3, 97.55%)	N/A	N/A	N/A	N/A	94.607 (9, 28.28%)	96.993 (10, 7.52%)	99.900 (12, 14.75%)	110.865 (15, 8.71%)	N/A	N/A	1, T	1	N	All main
3M70	3M_70_F_CTRL_SSTRY_a1R_6flrs_N	2.916 (1, 81.57%)	8.812 (4, 11.26%)	N/A	N/A	3.539	6.637 (3, 74.92%)	16.359 (6, 18.43%)	N/A	N/A	6.708	15.696 (5, 6.06%)	16.359 (6, 7.79%)	17.337 (7, 69.13%)	N/A	N/A	N/A	1,2	1,2	N	All main
3M71	3M_71_F_CTRL_SSTRY_a1R_5flrs_N	3.475 (1, 83.28%)	10.428 (4, 8.77%)	N/A	N/A	4.513	8.213 (3, 78.78%)	19.051 (6, 13.84%)	N/A	N/A	8.144	17.473 (5, 11.24%)	19.051 (5, 14.77%)	19.814 (7, 56.88%)	N/A	N/A	N/A	1,2	1,2	N	All main
3M72	3M_72_F_CTRL_SSTRY_a1R_4flrs_N	4.209 (1, 84.95%)	8.573 (2, 4.68%)	12.697 (4, 6.41%)	N/A	5.798	10.365 (3, 83.95%)	23.010 (3, 6.77%)	N/A	N/A	10.131	19.223 (5, 15.27%)	22.650 (6, 58.54%)	N/A	N/A	N/A	N/A	1,2,T	1, T	N	All main

Table 45 Summary of modal analyses results obtained using 3Muri® for analysed cases on an upper coralline limestone subsoil and natural frequencies in the x- and y-directions for the first mode of vibration in corresponding numerical models analysed using ELS® (continued).

Model reference number	3Muri® model name	3Muri®: Natural frequency (Hz) in x-direction (for mass contribution ≥ 5%)				ELS®: Natural frequency (Hz): first mode of vibration in x-direction	3Muri®: Natural frequency (Hz) in y-direction (for mass contribution ≥ 5%)				ELS®: Natural frequency (Hz): first mode of vibration in y-direction	3Muri®: Natural frequency (Hz) in z-direction (for mass contribution ≥ 5%)						Displacement profile: modal analysis			
		Natural frequency (Hz) in x-direction (mode number, mass contribution)	Natural frequency (Hz) in x-direction (mode number, mass contribution)	Natural frequency (Hz) in x-direction (mode number, mass contribution)	Natural frequency (Hz) in x-direction (mode number, mass contribution)		Natural frequency (Hz) in y-direction (mode number, mass contribution)	Natural frequency (Hz) in y-direction (mode number, mass contribution)	Natural frequency (Hz) in y-direction (mode number, mass contribution)	Natural frequency (Hz) in y-direction (mode number, mass contribution)		Natural frequency (Hz) in z-direction (mode number, mass contribution)	Natural frequency (Hz) in z-direction (mode number, mass contribution)	Natural frequency (Hz) in z-direction (mode number, mass contribution)	Natural frequency (Hz) in z-direction (mode number, mass contribution)	Natural frequency (Hz) in z-direction (mode number, mass contribution)	Natural frequency (Hz) in z-direction (mode number, mass contribution)	Displacement profile: modes of vibration in x-direction	Displacement profile: modes of vibration in y-direction	Box-like behaviour from deformed plan shapes (Y/N)	Modes of vibration where box-like behaviour not present (main modes of vibration only considered)
3M73	3M_73_F_CTRL_SSTRY_a1R_3flrs_N	5.233 (1, 86.38%)	11.364 (2, 5.63%)	16.013 (4, 4.63%)	N/A	7.593	13.362 (3, 90.58%)	N/A	N/A	N/A	13.109	20.825 (5, 18.90%)	25.961 (6, 47.30%)	44.131 (14, 5.36%)	N/A	N/A	N/A	1, 2, T	1	N	All main
3M74	3M_74_F_CTRL_SSTRY_a1R_2flrs_N	6.866 (1, 87.54%)	15.818 (2, 5.91%)	N/A	N/A	N/A	17.677 (3, 95.56%)	N/A	N/A	N/A	N/A	22.994 (5, 23.22%)	27.322 (6, 22.22%)	N/A	N/A	N/A	N/A	1, T	1	N	All main
3M75	3M_75_F_CTRL_SSTRY_a1R_1flr_N	10.033 (1, 88.74%)	22.406 (6, 9.17%)	N/A	N/A	N/A	24.988 (7, 5.52%)	25.246 (8, 76.56%)	26.420 (9, 12.82%)	N/A	N/A	13.693 (2, 12.53%)	15.454 (4, 9.3%)	22.406 (5, 12.35%)	N/A	N/A	N/A	1, T	1	N	All main
3M159	3M_159_F_CTRL_STBCK_a1R_6Flrs_N	4.471 (1, 71.00%)	14.440 (4, 16.51%)	N/A	N/A	4.167	8.006 (3, 71.26%)	20.683 (6, 16.55%)	N/A	N/A	7.224	25.056 (8, 67.26%)	N/A	N/A	N/A	n/a	N/A	1, 2	1, 2	N	Modes 4, 6
3M161	3M_161_F_CTRL_STBCK_a1R_5Flrs_N	5.769 (1, 72.33%)	17.683 (4, 15.48%)	N/A	N/A	5.478	10.054 (3, 74.80%)	24.752 (6, 15.33%)	N/A	N/A	8.945	29.464 (8, 64.35%)	30.609 (9, 4.86%)	32.541 (10, 5.12%)	N/A	N/A	N/A	1, 2	1, 2	N	Modes 4, 6
3M162	3M_162_F_CTRL_STBCK_a1R_4Flrs_N	7.748 (1, 74.41%)	22.124 (4, 14.91%)	N/A	N/A	7.331	13.019 (3, 78.87%)	30.497 (6, 13.69%)	N/A	N/A	9.768	35.971 (8, 60.48%)	37.258 (9, 8.65%)	38.476 (10, 4.86%)	N/A	N/A	N/A	1, 2	1, 2	N	All main
3M163	3M_163_F_CTRL_STBCK_a1R_3Flrs_N	10.958 (1, 76.52%)	28.868 (5, 10.51%)	N/A	N/A	N/A	17.495 (3, 82.89%)	38.685 (6, 11.97%)	N/A	N/A	N/A	45.188 (8, 9.52%)	46.147 (9, 52.8%)	46.882 (10, 11.49%)	N/A	N/A	N/A	1, 2	1, 2	N	All main
3M93	3M_93_F_CTRL_DHT_a1R_15flrs_N	0.996 (1, 65.66%)	4.306 (4, 20.01%)	9.013 (7, 5.00%)	N/A	N/A	1.912 (2, 57.86%)	2.216 (3, 7.27%)	7.334 (6, 17.51%)	14.905 (11, 5.42%)	N/A	10.202 (8, 81.10%)	N/A	N/A	N/A	N/A	N/A	1, 2, 3	1, 2, 3, T	N	Modes 4, 7, 11
3M92	3M_92_F_CTRL_DHT_a1R_14flrs_N	1.123 (1, 66.00%)	4.743 (4, 19.80%)	9.810 (7, 4.77%)	N/A	N/A	2.129 (2, 53.73%)	2.405 (3, 12.83%)	7.967 (6, 18.10%)	16.098 (11, 5.33%)	N/A	10.906 (8, 80.83%)	N/A	N/A	N/A	N/A	N/A	1, 2, 3	1, 2, 3, T	N	Modes 4, 7, 11

Table 45 Summary of modal analyses results obtained using 3Muri® for analysed cases on an upper coralline limestone subsoil and natural frequencies in the x- and y-directions for the first mode of vibration in corresponding numerical models analysed using ELS® (continued).

Model reference number	3Muri® model name		3Muri®: Natural frequency (Hz) in x-direction (for mass contribution ≥ 5%)				ELS®: Natural frequency (Hz): first mode of vibration in x-direction	3Muri®: Natural frequency (Hz) in y-direction (for mass contribution ≥ 5%)				ELS®: Natural frequency (Hz): first mode of vibration in y-direction	3Muri®: Natural frequency (Hz) in z-direction (for mass contribution ≥ 5%)						Displacement profile: modal analysis			
			Natural frequency (Hz) in x-direction (mode number, mass contribution)	Natural frequency (Hz) in x-direction (mode number, mass contribution)	Natural frequency (Hz) in x-direction (mode number, mass contribution)	Natural frequency (Hz) in x-direction (mode number, mass contribution)		Natural frequency (Hz) in y-direction (mode number, mass contribution)	Natural frequency (Hz) in y-direction (mode number, mass contribution)	Natural frequency (Hz) in y-direction (mode number, mass contribution)	Natural frequency (Hz) in y-direction (mode number, mass contribution)		Natural frequency (Hz) in z-direction (mode number, mass contribution)	Natural frequency (Hz) in z-direction (mode number, mass contribution)	Natural frequency (Hz) in z-direction (mode number, mass contribution)	Natural frequency (Hz) in z-direction (mode number, mass contribution)	Natural frequency (Hz) in z-direction (mode number, mass contribution)	Natural frequency (Hz) in z-direction (mode number, mass contribution)	Displacement profile: modes of vibration in x-direction	Displacement profile: modes of vibration in y-direction	Box-like behaviour from deformed plan shapes (Y/N)	Modes of vibration where box-like behaviour not present (main modes of vibration only considered)
3M91	3M_91_F_CTRL_DHT_a1R_13flrs_N		1.275 (1, 66.36%)	5.252 (4, 19.54%)	10.725 (7, 4.53%)	N/A	N/A	2.374 (2, 43.40%)	2.638 (3, 22.66%)	8.697 (6, 18.49%)	17.443 (11, 5.2%)	N/A	11.716 (8, 80.42%)	N/A	N/A	N/A	N/A	N/A	1, 2, 3	1, 2, 3, T	N	Modes 4, 7, 11
3M90	3M_90_F_CTRL_DHT_a1R_12flrs_N		1.460 (1, 66.76%)	5.852 (4, 19.19%)	N/A	N/A	N/A	2.647 (2, 30.67%)	2.936 (3, 35.99%)	9.550 (6, 18.69%)	18.950 (11, 4.97%)	N/A	12.658 (8, 79.81%)	N/A	N/A	N/A	N/A	N/A	1,2	1,2, 3, T	N	Mode 4, 11
3M89	3M_89_F_CTRL_DHT_a1R_11flrs_N		1.686 (1, 67.17%)	6.569 (4, 18.76%)	N/A	N/A	N/A	2.952 (2, 19.38%)	3.318 (3, 48.00%)	10.537 (6, 18.70%)	N/A	N/A	13.765 (8, 78.90%)	N/A	N/A	N/A	N/A	N/A	1,2	1,2,T	N	Mode 4
3M88	3M_88_F_CTRL_DHT_a1R_10flrs_N		1.966 (1, 67.59%)	7.437 (4, 18.22%)	N/A	N/A	N/A	3.306 (2, 12.16%)	3.806 (3, 56.10%)	17.164 (6, 18.48%)	N/A	N/A	15.088 (8, 77.47%)	N/A	N/A	N/A	N/A	N/A	1,2	1,2,T	N	Mode 4
3M87	3M_87_F_CTRL_DHT_a1R_9flrs_N		2.321 (1, 67.98%)	8.507 (4, 17.55%)	N/A	N/A	N/A	3.735 (2, 8.02%)	4.426 (3, 61.03%)	13.134 (6, 17.99%)	N/A	N/A	13.134 (6, 4.61%)	16.700 (8, 75.09%)	N/A	N/A	N/A	N/A	1,2	1,2,T	N	Modes 4,6
3M86	3M_86_F_CTRL_DHT_a1R_8flrs_N		2.779 (1, 68.30%)	9.855 (4, 16.73%)	N/A	N/A	N/A	4.276 (2, 5.61%)	5.221 (3, 65.04%)	14.877 (6, 17.14%)	N/A	N/A	14.877 (6, 6.29%)	18.716 (8, 71.68%)	N/A	N/A	N/A	N/A	1,2	1,2,T	N	Modes 4,6
3M85	3M_85_F_CTRL_DHT_a1R_7flrs_N		3.386 (1, 68.46%)	11.659 (4, 15.80%)	N/A	N/A	N/A	6.302 (3, 69.79%)	17.182 (6, 15.86%)	N/A	N/A	N/A	17.182 (6, 7.36%)	21.349 (8, 69.52%)	N/A	N/A	N/A	N/A	1,2	1,2	N	Modes 4,6
3M82	3M_82_F_CTRL_DHT_a1R_6Flrs_N		4.213 (1, 68.5%)	13.974 (4, 14.62%)	N/A	N/A	3.784	7.698 (3, 72.72%)	20.101 (6, 14.27%)	N/A	N/A	6.549	20.101 (6, 9.9%)	24.691 (8, 62.41%)	26.954 (9, 5.12%)	N/A	N/A	N/A	1,2	1,2	N	All main
3M83	3M_83_F_CTRL_DHT_a1R_5flrs_N		5.391 (1, 68.33%)	7.376 (2, 5.96%)	17.082 (4, 12.95%)	N/A	5.058	9.631 (3, 76.08%)	24.079 (6, 12.15%)	N/A	N/A	7.906	24.079 (6, 12.99%)	29.087 (8, 39.54%)	30.130 (9, 19.41%)	N/A	N/A	N/A	1,2,T	1, 2	N	All main modes except mode 2

Table 45 Summary of modal analyses results obtained using 3Muri® for analysed cases on an upper coralline limestone subsoil and natural frequencies in the x- and y-directions for the first mode of vibration in corresponding numerical models analysed using ELS® (continued).

Model reference number	3Muri® model name	3Muri®: Natural frequency (Hz) in x-direction (for mass contribution ≥ 5%)				ELS®: Natural frequency (Hz): first mode of vibration in x-direction	3Muri®: Natural frequency (Hz) in y-direction (for mass contribution ≥ 5%)				ELS®: Natural frequency (Hz): first mode of vibration in y-direction	3Muri®: Natural frequency (Hz) in z-direction (for mass contribution ≥ 5%)						Displacement profile: modal analysis			
		Natural frequency (Hz) in x-direction (mode number, mass contribution)	Natural frequency (Hz) in x-direction (mode number, mass contribution)	Natural frequency (Hz) in x-direction (mode number, mass contribution)	Natural frequency (Hz) in x-direction (mode number, mass contribution)		Natural frequency (Hz) in y-direction (mode number, mass contribution)	Natural frequency (Hz) in y-direction (mode number, mass contribution)	Natural frequency (Hz) in y-direction (mode number, mass contribution)	Natural frequency (Hz) in y-direction (mode number, mass contribution)		Natural frequency (Hz) in z-direction (mode number, mass contribution)	Natural frequency (Hz) in z-direction (mode number, mass contribution)	Natural frequency (Hz) in z-direction (mode number, mass contribution)	Natural frequency (Hz) in z-direction (mode number, mass contribution)	Natural frequency (Hz) in z-direction (mode number, mass contribution)	Natural frequency (Hz) in z-direction (mode number, mass contribution)	Displacement profile: modes of vibration in x-direction	Displacement profile: modes of vibration in y-direction	Box-like behaviour from deformed plan shapes (Y/N)	Modes of vibration where box-like behaviour not present (main modes of vibration only considered)
3M84	3M_84_F_CTRL_DHT_a1R_4flrs_N	7.184 (1, 68.27%)	9.452 (2, 8.16%)	21.200 (4, 10.14%)	26.185 (5, 5.42%)	6.727	12.446 (3, 80.19%)	29.833 (6, 8.59%)	N/A	N/A	9.709	29.833 (6, 16.89%)	34.674 (9, 9.39%)	36.430 (10, 20.55%)	37.313 (11, 23.63%)	42.337 (12, 7.34%)	N/A	1,2,T	1, 2	N	All main modes except mode 2
3M107	3M_107_F_CTRL_DHT_a1R_3flrs_N	10.202 (1, 69.64%)	12.858 (2, 9.67%)	26.652 (4, 5.80%)	34.048 (6, 7.72%)	9.254	16.821 (3, 85.27%)	N/A	N/A	N/A	9.855	40.355 (8,, 16.70%)	45.558 (10, 11.70%)	46.083 (11, 6.57%)	48.263 (12, 6.47%)	49.702 (13, 28.88%)	N/A	1,2, T	1	N	All main
3M156	3M_156_F_CTRL_DHT_WtoW_a1R_10Flrs_N	1.966 (1, 67.66%)	7.446 (4, 18.13%)	N/A	N/A	N/A	3.305 (2, 12.17%)	3.805 (3, 56.13%)	11.725 (6, 18.48%)	N/A	N/A	15.085 (8, 76.87%)	N/A	N/A	N/A	N/A	N/A	1, 2	1, 2, T	N	Modes 2, 4, 6
3M155	3M_155_F_CTRL_DHT_WtoW_a1R_9Flrs_N	2.320 (1, 68.02%)	8.521 (4, 17.48%)	N/A	N/A	N/A	3.735 (2, 8.00%)	4.425 (3, 61.36%)	13.144 (6, 17.99%)	N/A	N/A	13.144 (6, 4.68%)	16.700 (8, 74.77%)	N/A	N/A	N/A	N/A	1, 2	1, 2, T	N	All main modes except 3
3M154	3M_154_F_CTRL_DHT_WtoW_a1R_8Flrs_N	2.778 (1, 68.31%)	9.869 (4, 16.69%)	N/A	N/A	N/A	4.276 (2, 5.57%)	5.221 (3, 65.09%)	14.888 (6, 17.18%)	N/A	N/A	14.888 (6, 6.36%)	18.716 (8, 72.44%)	N/A	N/A	N/A	N/A	1, 2	1, 2, T	N	All main modes except 3
3M153	3M_153_F_CTRL_DHT_WtoW_a1R_7Flrs_N	3.382 (1, 68.41%)	11.562 (4, 15.52%)	N/A	N/A	N/A	6.260 (3, 68.27%)	17.059 (6, 15.69%)	N/A	N/A	N/A	17.059 (6, 7.84%)	21.290 (8, 68.78%)	N/A	N/A	N/A	N/A	1, 2	1, 2	N	All main
3M152	3M_152_F_CTRL_DHT_WtoW_a1R_6Flrs_N	4.206 (1, 68.24%)	13.563 (4, 12.75%)	N/A	N/A	N/A	7.654 (3, 71.42%)	19.956 (7, 12.53%)	N/A	N/A	N/A	19.956 (7, 11.37%)	24.679 (8, 62.35%)	N/A	N/A	N/A	N/A	1, 2	1, 2	N	All main
3M157	3M_157_F_CTRL_DHT_WtoW_a1R_5Flrs_N	5.390 (1, 68.19%)	7.384 (2, 6.03%)	16.661 (4, 11.44%)	20.623 (5, 5.14%)	N/A	9.638 (3, 76.12%)	23.652 (6, 6.64%)	24.516 (7, 5.89%)	N/A	N/A	23.652 (6, 4.92%)	24.516 (7, 8.89%)	29.036 (8, 32.16%)	30.257 (8, 29.74%)	N/A	N/A	1, 2, T	1, 2(T)	N	All main modes except 2)
3M158	3M_158_F_CTRL_DHT_WtoW_a1R_4Flrs_N	7.201 (1, 68.23%)	9.471 (2, 8.03%)	19.257 (4, 5.87%)	25.394 (5, 9.87%)	N/A	12.473 (3, 80.18%)	30.451 (7, 7.51%)	N/A	N/A	N/A	30.451 (7, 15.70%)	36.684 (10, 50.90%)	42.553 (11, 7.21%)	N/A	N/A	N/A	1, 2, T	1, 2	N	All main modes except 2)

Table 45 Summary of modal analyses results obtained using 3Muri® for analysed cases on an upper coralline limestone subsoil and natural frequencies in the x- and y-directions for the first mode of vibration in corresponding numerical models analysed using ELS® (continued).

Model reference number	3Muri® model name	3Muri®: Natural frequency (Hz) in x-direction (for mass contribution ≥ 5%)				ELS®: Natural frequency (Hz): first mode of vibration in x-direction	3Muri®: Natural frequency (Hz) in y-direction (for mass contribution ≥ 5%)				ELS®: Natural frequency (Hz): first mode of vibration in y-direction	3Muri®: Natural frequency (Hz) in z-direction (for mass contribution ≥ 5%)						Displacement profile: modal analysis			
		Natural frequency (Hz) in x-direction (mode number, mass contribution)	Natural frequency (Hz) in x-direction (mode number, mass contribution)	Natural frequency (Hz) in x-direction (mode number, mass contribution)	Natural frequency (Hz) in x-direction (mode number, mass contribution)		Natural frequency (Hz) in y-direction (mode number, mass contribution)	Natural frequency (Hz) in y-direction (mode number, mass contribution)	Natural frequency (Hz) in y-direction (mode number, mass contribution)	Natural frequency (Hz) in y-direction (mode number, mass contribution)		Natural frequency (Hz) in z-direction (mode number, mass contribution)	Natural frequency (Hz) in z-direction (mode number, mass contribution)	Natural frequency (Hz) in z-direction (mode number, mass contribution)	Natural frequency (Hz) in z-direction (mode number, mass contribution)	Natural frequency (Hz) in z-direction (mode number, mass contribution)	Natural frequency (Hz) in z-direction (mode number, mass contribution)	Displacement profile: modes of vibration in x-direction	Displacement profile: modes of vibration in y-direction	Box-like behaviour from deformed plan shapes (Y/N)	Modes of vibration where box-like behaviour not present (main modes of vibration only considered)
3M121	3M_121_F_CTRL_EXTNDD_a1R_7flrs_N	2.874 (1, 55.92%)	4.424 (2, 14.89%)	9.251 (4, 11.24%)	15.375 (6, 5.44%)	N/A	6.704 (3, 73.09%)	15.825 (7, 11.97%)	21.186 (10, 4.68%)	N/A	N/A	15.825 (7, 23.36%)	21.186 (10, 49.08%)	26.219 (12, 10.13%)	N/A	N/A	N/A	1, 2, 3, T	1, 2	N	Modes 4,6,7,10
3M116	3M_116_F_CTRL_EXTNDD_a1R_6flrs_N	3.506 (1, 52.91%)	5.362 (2, 19.28%)	10.837 (4, 10.14%)	17.609 (6, 7.31%)	N/A	8.091 (3, 75.07%)	18.146 (7, 10.02%)	24.667 (10, 5.37%)	N/A	N/A	18.146 (7, 24.70%)	24.667 (10, 44.61%)	29.403 (13, 13.58%)	N/A	N/A	N/A	1, 2, 3, T	1, 2	N	Modes 4,6,7,10
3M117	3M_117_F_CTRL_EXTNDD_a1R_5flrs_N	4.396 (1, 49.73%)	6.712 (2, 24.21%)	12.865 (4, 8.79%)	20.877 (6, 8.89%)	N/A	10.013 (3, 77.70%)	21.295 (7, 7.96%)	29.412 (11, 5.90%)	N/A	N/A	21.295 (7, 25.83%)	29.412 (11, 38.99%)	33.223 (12, 8.30%)	33.772 (13, 10.42%)	N/A	N/A	1, 2,2/3, T	1, 2	N	Modes 4,6,7,11
3M118	3M_118_F_CTRL_EXTNDD_a1R_4flrs_N	5.741 (1, 49.78%)	8.761 (2, 29.44%)	15.497 (4, 7.00%)	25.589 (6, 7.40%)	N/A	12.819 (3, 81.35%)	36.337 (11, 6.22%)	N/A	N/A	N/A	25.589 (6, 7.44%)	25.981 (7, 20.54%)	33.807 (10, 6.67%)	36.337 (11, 22.58%)	38.491 (12, 5.55%)	39.841 (13, 19.62%)	1, 2,2/3, T	1, 2	N	All main modes except 2
3M119	3M_119_F_CTRL_EXTNDD_a1R_3flrs_N	7.982 (1, 44.30%)	12.093 (2, 35.09%)	19.357 (4, 4.58%)	33.659 (7, 4.90%)	N/A	17.197 (3, 86.59%)	N/A	N/A	N/A	N/A	30.769 (6, 16.36%)	33.659 (7, 6.63%)	34.566 (8, 7.06%)	46.642 (13, 26.27%)	48.216 (14, 6.45%)	51.177 (15, 12.21%)	1, 1/2, T	1	N	All main modes except 2
3M140	3M_140_F_CTRL_SSTRY_EXTNDD_a1R_6flrs_N	2.489 (1, 77.92%)	4.679 (2, 9.57%)	7.491 (4, 6.70%)	N/A	N/A	7.012 (3, 63.59%)	7.491 (4, 15.74%)	15.825 (7, 11.87%)	N/A	N/A	15.253 (6, 6.95%)	15.825 (7, 15.57%)	17.209 (8, 63.43%)	N/A	N/A	N/A	1, 2, T	1,2 , 2(T)	N	All main
3M141	3M_141_F_CTRL_SSTRY_EXTNDD_a1R_5flrs_N	2.941 (1, 79.70%)	5.662 (2, 10.64%)	N/A	N/A	N/A	8.449 (3, 50.13%)	8.901 (4, 33.43%)	18.159 (7, 8.70%)	N/A	N/A	18.159 (7, 24.23%)	19.135 (8, 52.41%)	N/A	N/A	N/A	N/A	1, T	1, 2	N	All main
3M142	3M_142_F_CTRL_SSTRY_EXTNDD_a1R_4flrs_N	3.541 (1, 81.93%)	7.077 (2, 11.02%)	N/A	N/A	N/A	10.416 (3, 38.16%)	10.886 (4, 50.62%)	N/A	N/A	N/A	20.206 (6, 14.73%)	20.627 (7, 39.53%)	21.664 (8, 6.10%)	24.010 (9, 16.66%)	N/A	N/A	1, T	1	N	All main
3M143	3M_143_F_CTRL_SSTRY_EXTNDD_a1R_3flrs_N	4.385 (1, 84.40%)	9.236 (2, 10.63%)	N/A	N/A	N/A	13.344 (3, 53.94%)	13.738 (4, 40.25%)	N/A	N/A	N/A	20.872 (6, 25.15%)	24.050 (8, 18.80%)	29.240 (9, 17.01%)	N/A	N/A	N/A	1, T	1	N	All main

Table 45 Summary of modal analyses results obtained using 3Muri® for analysed cases on an upper coralline limestone subsoil and natural frequencies in the x- and y-directions for the first mode of vibration in corresponding numerical models analysed using ELS® (continued).

Model reference number	3Muri® model name	3Muri®: Natural frequency (Hz) in x-direction (for mass contribution ≥ 5%)				ELS®: Natural frequency (Hz): first mode of vibration in x-direction	3Muri®: Natural frequency (Hz) in y-direction (for mass contribution ≥ 5%)				ELS®: Natural frequency (Hz): first mode of vibration in y-direction	3Muri®: Natural frequency (Hz) in z-direction (for mass contribution ≥ 5%)						Displacement profile: modal anlysis			
		Natural frequency (Hz) in x-direction (mode number, mass contribution)	Natural frequency (Hz) in x-direction (mode number, mass contribution)	Natural frequency (Hz) in x-direction (mode number, mass contribution)	Natural frequency (Hz) in x-direction (mode number, mass contribution)		Natural frequency (Hz) in y-direction (mode number, mass contribution)	Natural frequency (Hz) in y-direction (mode number, mass contribution)	Natural frequency (Hz) in y-direction (mode number, mass contribution)	Natural frequency (Hz) in y-direction (mode number, mass contribution)		Natural frequency (Hz) in z-direction (mode number, mass contribution)	Natural frequency (Hz) in z-direction (mode number, mass contribution)	Natural frequency (Hz) in z-direction (mode number, mass contribution)	Natural frequency (Hz) in z-direction (mode number, mass contribution)	Natural frequency (Hz) in z-direction (mode number, mass contribution)	Natural frequency (Hz) in z-direction (mode number, mass contribution)	Displacement profile: modes of vibration in x-direction	Displacement profile: modes of vibration in y-direction	Box-like behaviour from deformed plan shapes (Y/N)	Modes of vibration where box-like behaviour not present (main modes of vibration only considered)
3M144	3M_144_F_CTRL_SSTRY_EXTNDD_a1R_2flrs_N	5.739 (1, 87.18%)	12.868 (2, 9.13%)	N/A	N/A	N/A	17.590 (3, 95.87%)	N/A	N/A	N/A	N/A	19.623 (5, 14.19%)	20.292 (6, 14.91%)	25.681 (7, 17.58%)	N/A	N/A	N/A	1, T	1	N	All main
3M145	3M_145_F_CTRL_SSTRY_EXTNDD_a1R_1flr_N	8.163 (1, 88.57%)	18.285 (6, 9.38%)	N/A	N/A	N/A	24.783 (9, 96.18%)	N/A	N/A	N/A	N/A	13.799 (2, 8.40%)	14.118 (3, 13.20%)	15.652 (5, 10.80%)	29.682 (12, 4.97%)	N/A	N/A	1, T	1	N	All main
3M133	3M_133_F_CTRL_DHT_EXTNDD_a1R_8flrs_N	2.402 (1, 58.47%)	3.743 (2, 11.36%)	8.025 (4, 12.14%)	12.180 (6, 5.65%)	N/A	5.646 (3, 71.70%)	14.019 (8, 13.56%)	N/A	N/A	N/A	14.019 (8, 20.54%)	18.546 (11, 48.43%)	23.798 (14, 4.87%)	N/A	N/A	N/A	1, 2, T	1, 2	N	All main modes except 2, 3
3M128	3M_128_F_CTRL_DHT_EXTNDD_a1R_7flrs_N	2.872 (1, 55.84%)	4.423 (2, 15.11%)	9.315 (5, 10.65%)	14.150 (6, 5.59%)	N/A	6.681 (3, 73.27%)	15.835 (8, 11.24%)	N/A	N/A	N/A	15.835 (8, 21.24%)	21.169 (11, 48.83%)	26.247 (13, 10.19%)	N/A	N/A	N/A	1, 2, 2(T), T	1, 2	N	All main modes except 2
3M129	3M_129_F_CTRL_DHT_EXTNDD_a1R_6flrs_N	3.504 (1, 52.81%)	5.362 (2, 19.57%)	10.965 (5, 10.10%)	17.816 (7, 5.55%)	N/A	8.057 (3, 75.12%)	18.202 (8, 9.04%)	24.661 (11, 5.08%)	N/A	N/A	18.202 (8, 21.77%)	24.661 (11, 44.38%)	29.446 (14, 12.93%)	N/A	N/A	N/A	1, 2, 3, T	1, 2, 2 (T)	N	All main modes except 2, 3
3M130	3M_130_F_CTRL_DHT_EXTNDD_a1R_5flrs_N	4.395 (1, 49.64%)	6.714 (2, 24.55%)	13.153 (5, 8.88%)	20.912 (7, 8.64%)	N/A	9.966 (4, 77.85%)	21.445 (8, 7.37%)	29.455 (12, 5.57%)	N/A	N/A	21.455 (8, 23.53%)	29.455 (12, 38.53%)	33.647 (13, 17.65%)	N/A	N/A	N/A	1, 2,2/3 (T), T	1, 2	N	All main modes except 2, 4
3M131	3M_131_F_CTRL_DHT_EXTNDD_a1R_4flrs_N	5.752 (1, 46.82%)	8.767 (2, 29.48%)	16.077 (5, 7.29%)	25.694 (7, 8.15%)	N/A	12.740 (4, 81.65%)	26.420 (8, 4.58%)	36.284 (11, 6.44%)	N/A	N/A	26.420 (8, 21.68%)	36.284 (11, 29.68%)	39.620 (14, 21.65%)	N/A	N/A	N/A	1, 2,2/3 (T), T	1, 2	N	All main modes except 2, 4
3M132	3M_132_F_CTRL_DHT_EXTNDD_a1R_3flrs_N	8.065 (1, 45.06%)	12.124 (3, 34.55%)	20.157 (5, 5.01%)	N/A	N/A	17.074 (4, 86.60%)	47.059 (15, 5.12%)	N/A	N/A	N/A	33.014 (7, 7.07%)	34.435 (8, 8.51%)	36.324 (9, 11.72%)	46.882 (14, 22.93%)	47.059 (15, 16.43%)	N/A	1, 2, T	1, 2	N	All main modes except 2

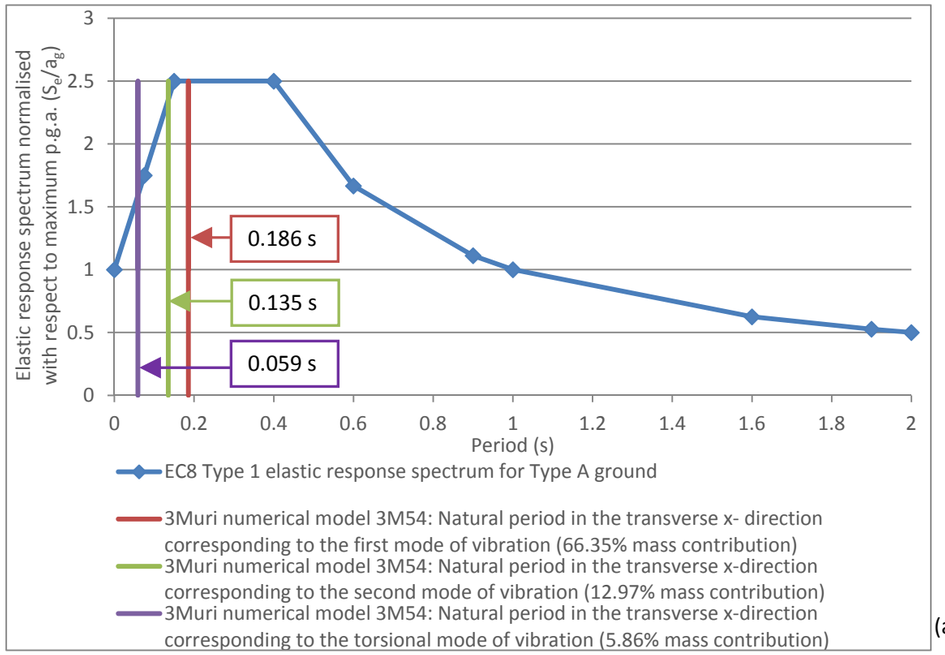

(a)

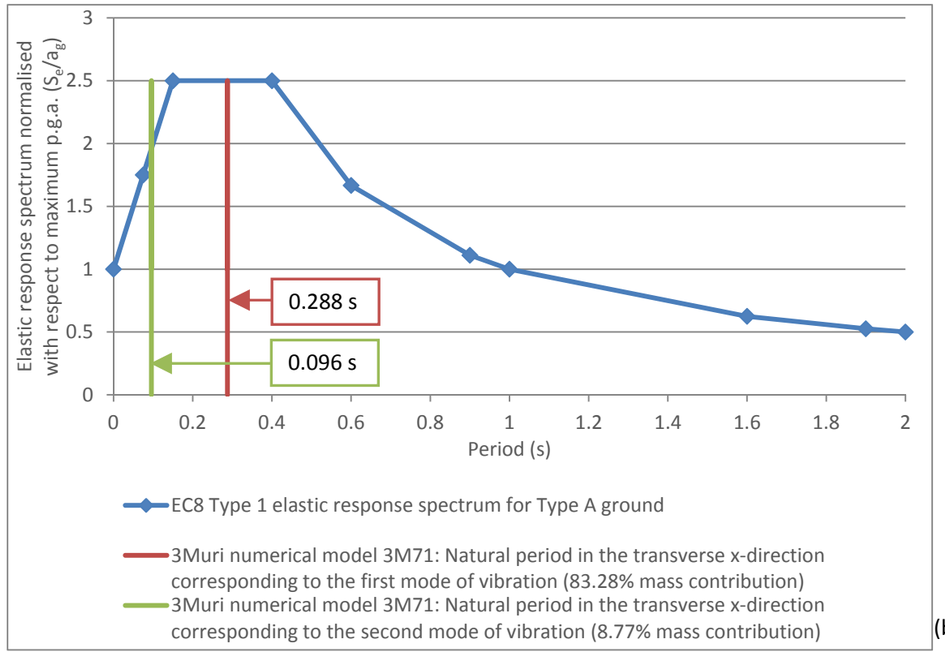

(b)

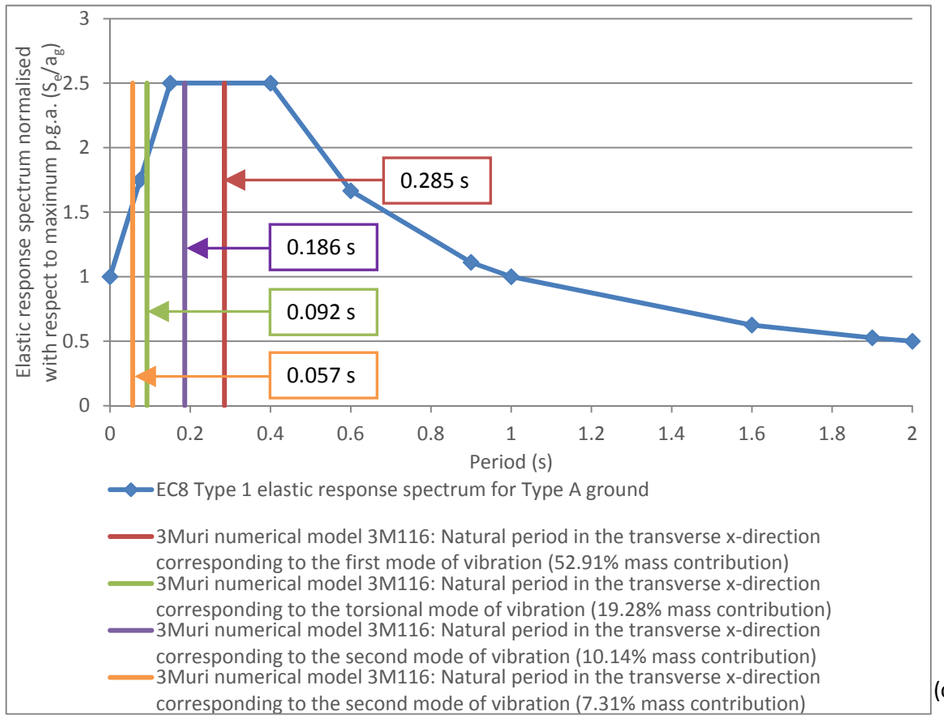

(c)

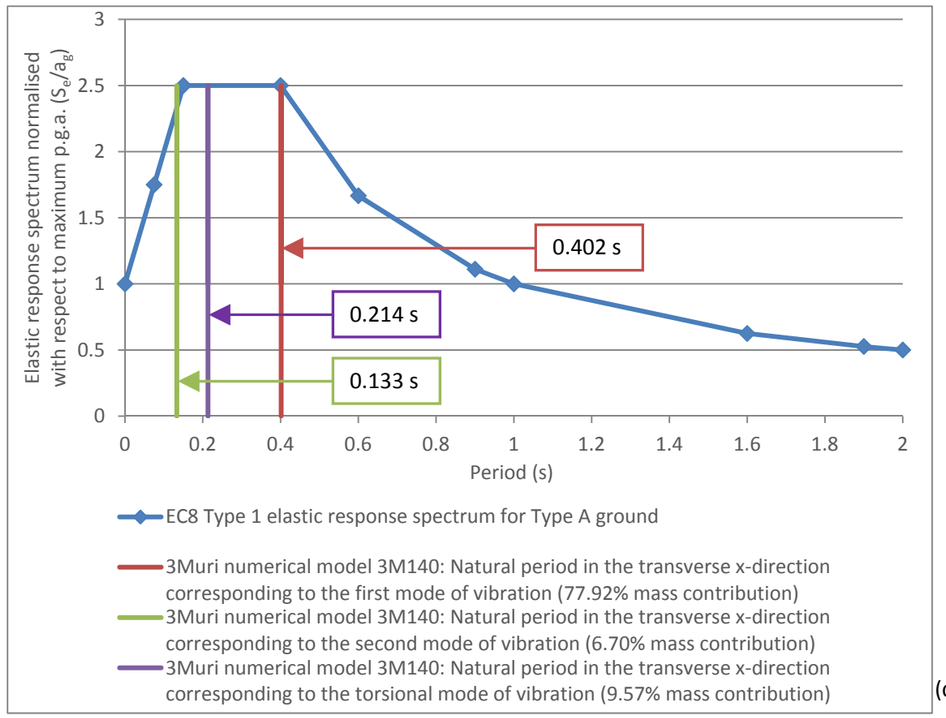

(d)

Description of 3Muri® numerical models represented in (a) to (d):

(a) 3M54: 5 storey control numerical model (L:W 2.75:1) analysed on UCL;
(b) 3M71: 5 storey control numerical model with a soft storey at semi-basement level (L:W 2.75:1) analysed on UCL;
(c) 3M116: 6 storey control numerical model (L:W 4:1) analysed on UCL;
(d) 3M140: 6 storey control numerical model with soft storey at semi-basement level (L:W 4:1) analysed on UCL.

Figure 46 Comparison of the natural period estimates of the main modes of vibration in the transverse x-direction of 3Muri® numerical models (a) 3M54 (b) 3M71, (c) 3M 116 and (d) 3M 140 to the Eurocode 8 Type 1 elastic response spectrum for ground Type A [4].

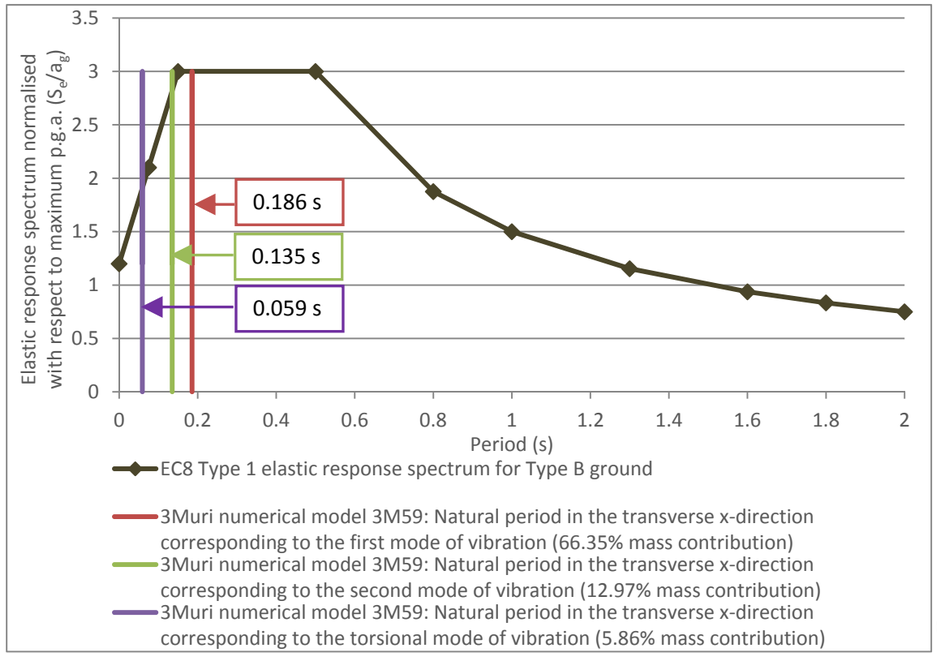

(a)

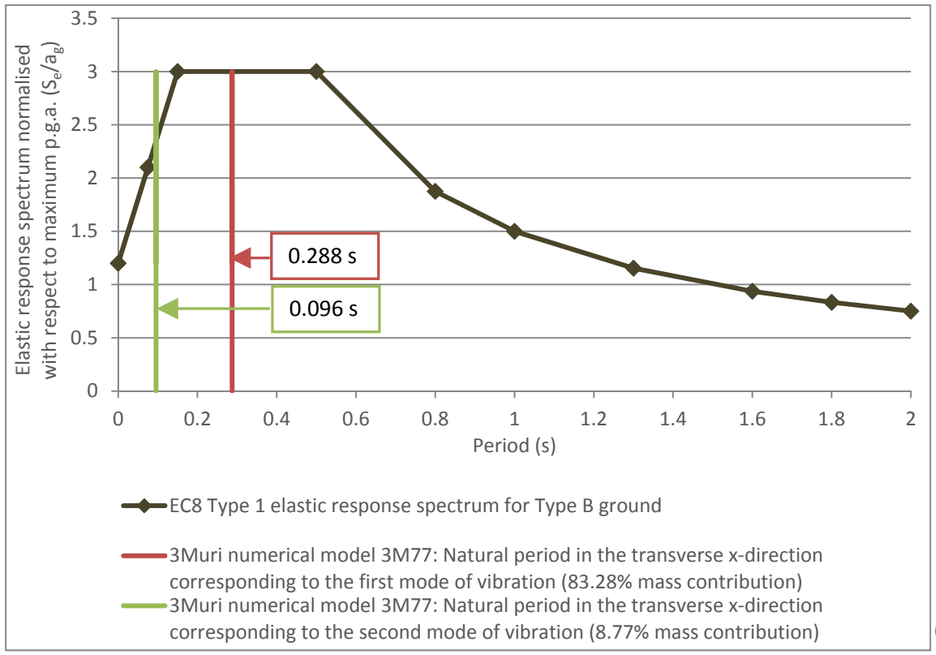

(b)

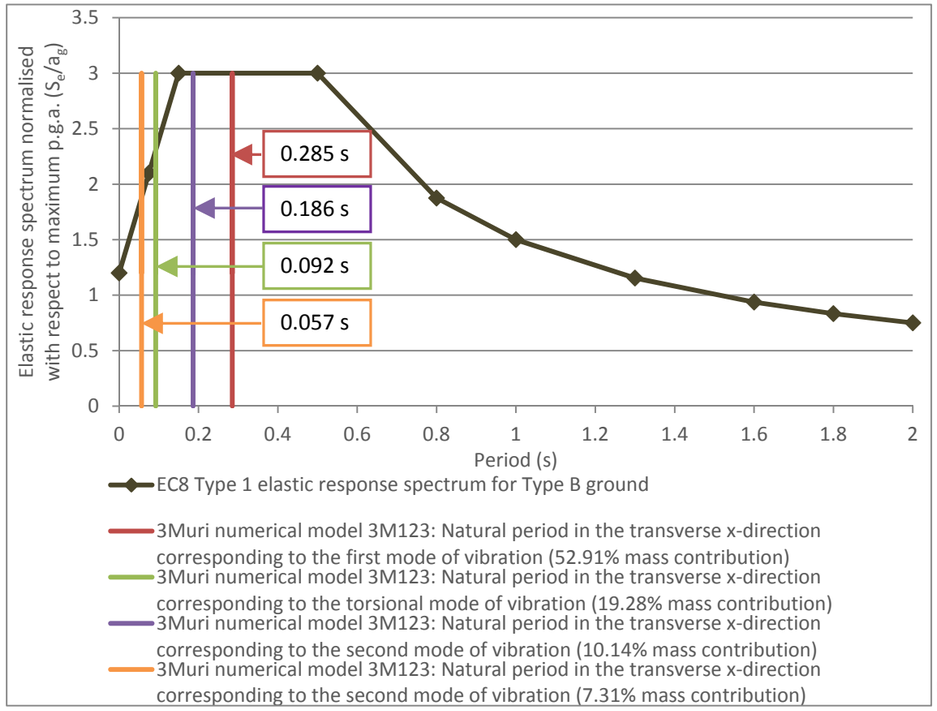

(c)

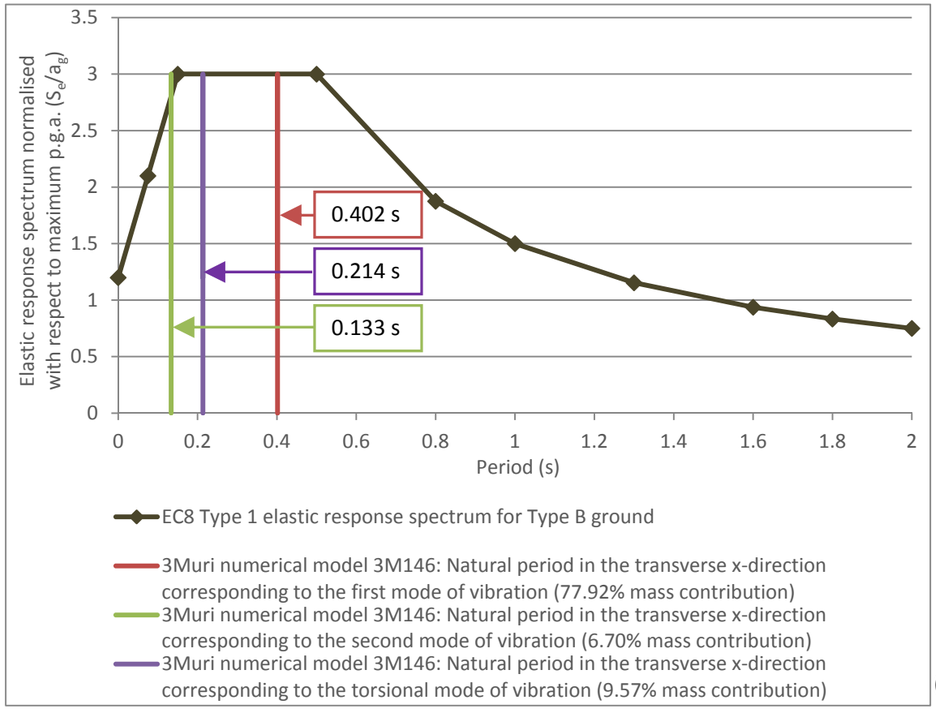

(d)

Description of 3Muri® numerical models represented in (a) to (d):

(a) 3M59: 5 storey control numerical model (L:W 2.75:1) analysed on clay;

(b) 3M77: 5 storey control numerical model with a soft storey at semi-basement level (L:W 2.75:1) analysed on clay;

(c) 3M123: 6 storey control numerical model (L:W 4:1) analysed on clay;

(d) 3M146: 6 storey control numerical model with soft storey at semi-basement level (L:W 4:1) analysed on clay.

Figure 47 Comparison of the natural period estimates of the main modes of vibration in the transverse x-direction of 3Muri® numerical models (a) 3M59 (b) 3M77, (c) 3M 123 and (d) 3M 146 to the Eurocode 8 Type 1 elastic response spectrum for ground Type B [4].